THE HONG KONG
POLYTECHNIC UNIVERSITY
香港理工大學
Pao Yue-kong Library
包玉剛圖書館

Copyright Undertaking

This thesis is protected by copyright, with all rights reserved.

By reading and using the thesis, the reader understands and agrees to the following terms:

1. The reader will abide by the rules and legal ordinances governing copyright regarding the use of the thesis.
2. The reader will use the thesis for the purpose of research or private study only and not for distribution or further reproduction or any other purpose.
3. The reader agrees to indemnify and hold the University harmless from and against any loss, damage, cost, liability or expenses arising from copyright infringement or unauthorized usage.

IMPORTANT

If you have reasons to believe that any materials in this thesis are deemed not suitable to be distributed in this form, or a copyright owner having difficulty with the material being included in our database, please contact lbsys@polyu.edu.hk providing details. The Library will look into your claim and consider taking remedial action upon receipt of the written requests.

Pao Yue-kong Library, The Hong Kong Polytechnic University, Hung Hom, Kowloon, Hong Kong

http://www.lib.polyu.edu.hk

EXPLORATION OF REGIO- & STEREO-CONTROLLED INTRAMOLECULAR AMIDATION OF CARBON (SP^2/SP^3) – HYDROGEN BONDS BY IRON AND COPPER-MEDIATED DECOMPOSITION OF 1,4,2-DIOXAZOL-5-ONES TOWARDS THE DEVELOPMENT OF LIGAND-CONTROLLED REGIOSELECTIVE SYNTHESIS OF γ-/δ- LACTAMS

AU CHI MING

PhD

The Hong Kong Polytechnic University

2025

The Hong Kong Polytechnic University

Department of Applied Biology and Chemical Technology

Exploration of Regio- & Stereo-Controlled Intramolecular Amidation of Carbon (sp^2/sp^3) – Hydrogen Bonds by Iron and Copper-Mediated Decomposition of 1,4,2-Dioxazol-5-ones towards the Development of Ligand-Controlled Regioselective Synthesis of γ-/δ- Lactams

Au Chi Ming

A thesis submitted in partial fulfillment

of the requirements for the degree of

Doctor of Philosophy

December 2024

CERTIFICATE OF ORIGINALITY

I hereby declare that this thesis is my own work and that, to the best of my knowledge and belief, it reproduces no material previously published or written, nor material that has been accepted for the award of any other degree or diploma, except where due acknowledgement has been made in the text.

AU Chi Ming

ABSTRACT

Abstract of the thesis entitled

Exploration of Regio- & Stereo-Controlled Intramolecular Amidation of Carbon (sp^2/sp^3) – Hydrogen Bonds by Iron and Copper-Mediated Decomposition of 1,4,2-Dioxazol-5-ones towards the Development of Ligand-Controlled Regioselective Synthesis of γ-/δ- Lactams

Submitted by Au Chi Ming

for the degree of Doctor of Philosophy

at The Hong Kong Polytechnic University in December 2024

Amide bonds are prevalent motifs in many bioactive natural products, pharmaceuticals, and synthetic intermediates. Transition metal-catalyzed direct C–H amidation via metal-nitrenoid transfer offers a straightforward approach for amide bond formation in an atom- and step-economical manner. In recent decades, noble metals (e.g. Pd, Rh, Ir, Ru) have been extensively studied as catalysts for direct C–H amidations. Yet, owing to the natural abundance and environmental sustainability,

attention is increasingly drawn to developing earth-abundant metals as catalysts for selective C–H amidation. This research aims to develop catalytic systems based on earth-abundant metals such as iron and copper for catalytic regio- and stereo-controlled direct C–H amidations.

Our investigation began with developing ferrocenium complexes as a new class of catalysts for nitrene transfer reactions. Being a first-row metal, Fe complexes often exist as high-spin complexes, and this poses enormous challenges to catalyst stability due to high lability. In this work, we employed strong-field cyclopentadiene (Cp) ligand to stabilize low-spin Fe center for enhanced catalyst stabilization. With 1,4,2-dioxazol-5-ones derived from arylpropanoic acids as substrate, the ferrocenium $[Cp_2Fe(III)]^+$ complex (10 mol%) in CH_2Cl_2 solvent was found to catalyze decomposition of the dioxazolones to afford 3,4-dihydroquinolin-2(1*H*)-ones in up to 97% yields. The reaction formally proceeds as regioselective intramolecular acylnitrenoid *ortho*-C(sp^2)–H bond insertion and the competing Curtius-type rearrangement is largely suppressed. Our combined experimental and computational analysis revealed that the intramolecular C(sp^2)–H amidation should occur by electrophilic arene addition by reactive Fe(IV)-amidyl radical intermediates. Consistent with the mechanistic study, the regioselectivity (*ipso*- versus *ortho*-amidyl radical addition) is influenced by the electronic character on the arenes. The *ipso*-amidyl radical addition pathway should

afford an azaspirocyclohexadienyl radical intermediate. Subsequent radical-polar crossover and 1,2-alkyl migration followed by rearomatization would produce the skeletal rearranged dihydroquinolinone lactams. Our ferrocenium catalysts have been successfully grafted on commercial silica gel to become recyclable heterogeneous catalysts. Conventional construction of 3,4-dihydroquinolin-2(1*H*)-ones that constitute a unique scaffold in many pharmaceuticals and bioactive compounds are commonly prepared by using stoichiometric toxic reagents with forcing experimental conditions. Our ferrocenium-based catalysis should provide a greener and milder route to this medicinally valuable class of molecules.

Catalyst-controlled regioselective C(sp^3)–H functionalization is a topic of fundamental significance. Considerable progress has been made in designing transition metal catalysts to target benzylic or tertiary C–H bonds, in which the target C–H bonds are differentiated by their bond dissociation and steric properties. However, effective differentiation of the methylene C–H bonds on the same hydrocarbon skeleton with similar bond dissociation energies and the steric environment remains a formidable challenge. Our next goal is to develop a catalytic system capable for differentiating γ- and δ- methylene C–H bonds for direct amidation to form γ- or δ-lactams. We found that 1,4,2-dioxazol-5-ones derived from carboxylic acids reacted with $[Cu(MeCN)_4]BF_4$ (2.5 mol%) and 2-bromo-1,10-phenanthroline (3.0 mol%) in a HFIP-

toluene (4:1) solvent would give the corresponding δ-lactams (up to 75% yields and >20:1 regioselectivities) via the entropically disfavored 1,6-hydrogen atom transfer (HAT) pathway. Yet, employing 2,9-diphenyl-1,10-phenanthroline as ligand in the NFTB-toluene (4:1) solvent (NFTB= 1,1,1,3,3,3-Hexafluoro-2-trifluoromethyl-2-propanol), γ-lactams (up to 62% yields and >10:1 regioselectivities) was produced via the 1,5-HAT at the γ-C–H bonds selectively. It was found that the regioselectivity is largely influenced by the size of the ligand and the substrates. Different solvent systems seem to enhance the regioselectivity via modulating the conformations of the acylnitrene ligand. Radical trapping and Hammett correlation studies suggest that the Cu-nitrenoid intermediate can be best formulated as amidyl radical species. For instance, the 1,n-HAT (n = 5 or 6) afforded the benzyl radicals, which can be trapped by 2,2,6,6-tetramethylpiperidinyloxy (TEMPO). The Cu-catalyzed regioselective C–H amidation should provide insights for the development of regiocontrolled amidation of methylene C–H bonds.

Regiocontrolled alkene difunctionalization is a versatile synthetic route for constructing two different C(sp^3)–X bonds (X = C, N, O etc.) within a single operation for forging functionally diversified skeletons. Recently, Chang and co-workers have successfully extended the pentamethylcyclopentadiene (Cp*) Ir-nitrenoid chemistry to stereoselective olefin difunctionalization to synthesize γ-lactams. With an interest in

exploring earth-abundant metal-based nitrenoid chemistry, we have extended our study to the Cu-catalyzed stereoselective alkene carboxyamidation. Reacting 1,4,2-dioxazol-5-ones derived from 5-alkenyl carboxylic acids as substrate with $[Cu(MeCN)_4]BF_4$ (10 mol%), (4*S*,4'*S*)-2,2'-(propane-2,2-diyl)bis(4-(tert-butyl)-4,5-dihydrooxazole) (12 mol%) and benzoic acid (3.0 equiv) in 1,1,1,3,3,3-hexafluoroisopropanol (HFIP) afforded oxy-γ-lactams up to 96% yields with *threo*: *erthyro* >20:1 selectivity. Consistent with our earlier study, the Cu-nitrene intermediate could be formulated as Cu-amidyl radical. The oxylactamization can be rationalized by the electrophilic radical addition to the C=C bond by the Cu-amidyl radical intermediate via *5-exo-trig* cyclization to afford the benzyl radicals. Subsequent radical-polar crossover of the benzyl radicals, followed by nucleophile addition, produced the oxylactam products. The Cu-catalyzed lactamization exhibits excellent functional group tolerance, and nucleophiles derived from pharmaceuticals and bioactive natural products are successfully coupling partners to afford the *threo*-lactams in >20:1 diastereoselectivities.

PUBLICATIONS

Sun, W.; Ling, C.-H.; **Au, C.-M.**; Yu, W.-Y. "Ruthenium-Catalyzed Intramolecular Arene C(sp^2)−H Amidation for Synthesis of 3,4-Dihydroquinolin-2(1*H*)-ones" *Organic Letters*, **2021**, *23*, 3310–3314.

Du, B.; Chan, C.-M.; **Au, C.-M.**; Yu, W.-Y. "Transition Metal-Catalyzed Regioselective Direct C–H Amidation: Interplay between Inner- and Outer-Sphere Pathways for Nitrene Cross-Coupling Reactions" *Accounts of Chemical Research*, **2022**, *55*, 2123–2137.

Sun, W.; **Au, C.-M.**; Wong, K.-W.; Chan, K.-L.; Ngai, C.-K.; Lee, H.-K.; Lin, Z.; Yu W.-Y. "Intramolecular Arene C(sp^2)–H Amidation Enabled by Ferrocenium-Mediated Decomposition of 1,4,2-Dioxazol-5-ones as Amidyl Radical Precursors" *ACS Catalysis*, **2023**, *13*, 11389−11398.

Sun, W.; Pang, H.; Khan, S. U.; Yang, R.; Wu, Q.; Ma, H.; **Au, C.-M.**; Sun, W.; Wang, X.; Yang, G.; Yu, W.-Y. "Highly Efficient Photocatalysts: Polyoxometalate Synthons

Enable Tailored CdS–MoS_2 Morphologies and Enhanced H_2 Evolution" *ACS Applied Materials & Interfaces,* **2023**, *15*, 35611–35621.

Fu, S.; Ullah Khan, S.; Yang, R.; Pang, H.; **Au, C.-M.**; Ma, H.; Wang, X.; Yang, G.; Sun, W.; Yu, W.-Y. "High-performance heterometallic photocatalysts afforded by polyoxometalate synthons for efficient H_2 production" *Journal of Colloid and Interface Science*, **2024**, *666*, 469–504.

Xin, J.; Pang, H.; Gómez-García, C. J.; Sun, W.; Wu, Q.; **Au, C.-M.**; Ma, H.; Wang, X.; Yang, G.; Yu, W.-Y. "One-Step Synthesis of Hollow CoS_2 Spheres Derived from Polyoxometalate-Based Metal–Organic Frameworks with Peroxidase-like Activity" *Inorganic Chemistry,* **2024,** *63*, 860–869.

Xin, J.; Pang, H.; Gómez-García, C. J.; Jin, Z.; Wang, Y.; **Au, C.-M.**; Ma, H.; Wang, X.; Yang, G.; Yu, W.-Y. "Nitrogen doped 1 T/2H mixed phase MoS_2/CuS heterostructure nanosheets for enhanced peroxidase activity" *Journal of Colloid and Interface Science*, **2024,** *659*, 312–319.

CONFERENCES & SYMPOSIUMS

Au, C.-M.; Sun, W.; Wong, K.-W.; Ngai, C.-K.; Lee, H.-K.; Lin, Z.; Yu W.-Y. "Intramolecular Arene C(sp^2)–H Amidation Enabled by Ferrocenium-Mediated Decomposition of 1,4,2-Dioxazol-5-ones as Amidyl Radical Precursors" *23rd Tetrahedron Symposium*, June 2023, Gothenburg, Sweden. (Poster presentation)

Au, C.-M.; Yu W.-Y. "Regio- and Stereocontrolled C–H Amidation Enabled by Earth Abundant Metal-Mediated Decomposition of 1,4,2-Dioxazol-5-ones as Amidyl Radical Precursors" *The International Young Scholars Academic Forum of Institute of Zhejiang University-Quzhou*, May 2024, Quzhou, China. (Oral and poster presentation; Best Poster Award)

Au, C.-M.; Sun, W.; Ling, C.-H.; Yu, W.-Y. "Ruthenium-Catalyzed Intramolecular Arene C(sp^2)–H Amidation for Synthesis of 3,4-Dihydroquinolin-2(1*H*)-ones" The 28th Symposium on Chemistry Postgraduate Research in Hong Kong, November 2021, Hong Kong. (Poster presentation)

Au, C.-M.; Yu, W.-Y. "Recent Development in Transition Metal Catalyzed Regio- and Stereo-controlled Direct Amidation of Unactivated C–H Bonds" The 30th Symposium on Chemistry Postgraduate Research in Hong Kong, April 2024, Hong Kong. (Oral presentation)

ACKNOWLEDGEMENTS

I wish to express my heartfelt thanks to my chief supervisor, Professor Wing-Yiu Yu, Michael, for his steadfast support and patient guidance throughout my BSc and PhD studies. I first knew Michael when taking his course in my second year as an undergraduate, and his teaching made a profound and motivating impact on me. Instead of just sharing knowledge, he inspired me to think critically and understand the science behind the concepts. Learning from him prepared me for my academic path and enriched my life in many ways. Michael has been much more than just an instructor; he has been a mentor and a father figure to me. His guidance has fostered my growth into an independent researcher and has greatly enhanced my confidence. His support and encouragement were pivotal in completing my PhD studies.

I am also grateful to the members of Yu's group. I want to thank Dr. Chun-Ming Chan and Dr. Bingnan Du for teaching me basic laboratory techniques and for sharing their insights on postgraduate study when I was a student helper. Additionally, I would like to express my gratitude to Dr. Wenlong Sun, Dr. Yiu-Wai Yeung, Dr. Ka-Wa Wong, Mr. Yip-Chi Chow, Mr. Sing-Fung Hung, Mr. Ming-Kit Lin, Mr. Hon-Lam Au, and Mr. Marco Chan for the inspiring discussions and for exchanging research ideas. Other members in W707, including Dr. Qi Xing, Dr. Pui-Yiu Lee, Dr. Cho-Hon Ling,

Mr. Yu-Ting Chen, Mr. Wai-Hin Chung, Mr. Chun-To Wong, and Mr. Ting Zhang, also provided support that made this journey memorable.

I would also like to acknowledge the financial support provided by PolyU. Additionally, I am grateful to the staff and technicians of the Department of Applied Biology and Chemical Technology, particularly Dr. Kwong-Chak Cheung, Dr. Kenneth Yan, Dr. Pui-Kin So, and Mr. Wing-Kong Kwan, for their assistance support.

I must also thank our collaborators for providing me opportunities to appreciate the beauty of chemistry across different fields. Professor Zhenyang Lin from HKUST for the DFT calculations, Professor Hung Kay Lee from CUHK for EPR studies, and Professor Yixin Lu from NUS for offering a research attachment opportunity. Your support and encouragement have been instrumental in completing this work.

Most importantly, I wish to express my deep love for my parents and Nichole. During my postgraduate studies, my parents continually motivated me to take care of my health, providing an abundance of meals. While they might not fully grasp the intricacies of my research, their warmth and support have always been palpable. As a research postgraduate, I spend most of my time working in the lab, yet Nichole never complains. Her unwavering love, support and encouragement are my greatest sources of strength.

Table of Contents

Chapter 1 Introduction..... 1

1.1 General Background..... 1

1.2 Transition Metal-Catalyzed C(sp^3)–N Cross-Coupling Reactions..... 6

1.2.1 Metallonitrenoid and Its Reactivity..... 7

1.2.2 Pioneering Works Inspired by the Cytochrome P450..... 11

1.2.3 Rhodium-Catalyzed C(sp^3)–H Aminations..... 13

1.2.3.1 Seminal Works of [$Rh_2(OAc)_4$]-Catalyzed C(sp^3)–H Aminations..... 13

1.2.3.2 Chemoselectivity Issue of Dirhodium Catalysts..... 14

1.2.3.3 Ligand-Enabled Regioselective C(sp^3)–H Amidation Reactions 15

1.2.4 Silver-Catalyzed Nitrene Transfer Reactions..... 17

1.2.4.1 Chemoselective Nitrene Transfer Reactions..... 18

1.3 Catalytic Acylnitrene Transfer Reactions..... 19

1.3.1 Pioneering Work of Transition-Metal-Catalyzed Acylnitrene Transfer Reactions..... 20

1.3.2 Asymmetric Carbonyl Nitrene Transfer Reactions..... 21

1.4 Earth-abundant Metal-Catalyzed C(sp^3)–H Amidations 22

1.4.1 Copper-Catalyzed Nitrene C(sp^3)–H Insertion Reactions 22

1.4.2 Iron-Catalyzed Nitrene C(sp^3)–H Insertion Reactions 24

1.4.2.1 Biocatalytic C(sp^3)–H Amination by Recombinant P450 Enzymes 25

1.4.2.2 Non-Heme-Type Iron-Catalyzed C(sp^3)–H Aminations 26

1.5 Concluding Summary 28

Chapter 2 Intramolecular Arene C(sp2)—H Amidation Enabled by Ferrocenium-Mediated Decomposition of 1,4,2-Dioxazol-5-ones as Amidyl Radical Precursors 29

2.1 Introduction 29

2.2 Results and Discussion 33

2.2.1 Reaction Development 33

2.2.2 Substrate Scope Studies 39

2.2.2.1 *para*-Substituted Aryl 1,4,2-Dioxazol-5-ones 39

2.2.2.2 *ortho*-/*meta*-/ Polysubstituted Aryl 1,4,2-Dioxazol-5-ones 42

2.3 Mechanistic Studies 49

2.3.1 Probing the Nature of the Reactive Intermediate: Trapping Study .49

2.3.2 Physical Study and Hammett Correlation Study 53

2.3.3 Computational Study 55

2.4 Immobilization of Ferrocene on Silica Support 63

2.5 Concluding Summary.....68

2.6 Experimental Section 69

2.6.1 General Experimental Section 69

2.6.2 Experimental Procedures and Physical Characterizations.....72

2.6.2.1 General Procedure for the Preparation of Alkenoic Acid.....72

2.6.2.2 General Procedure for the Preparation of 1,4,2-Dioxazol-5-ones 74

2.6.2.3 Physical Characterization of Dioxazolones 83

2.6.3 Preparation and Physical Characterization of Catalysts and Additives 115

2.6.3.1 Procedures for Preparation of (4-Fluorophenyl)ferrocene.....115

2.6.3.2 Preparation of Ferrocenium Hexafluorophosphate.....120

2.6.3.3 Preparation of Ferrocenium Tetrafluoroborate 120

2.6.3.4 Preparation of Aryldiazonium Tetrafluoroborates and Aryldiazonium Hexafluorophosphates 121

2.6.3.5 Preparation of Silica-APTES-ferrocene 125

2.6.4 Experimental Procedures for Ferrocenium-Catalyzed Reactions .. 132

2.6.5 Mechanistic Studies 164

2.6.5.1 Hammett Correlation Study 164

2.6.5.2 EPR Study 166

2.6.5.3 ESI-MS Study 168

Chapter 3 Ligand-Promoted Copper-Catalyzed Regioselective Nitrene Transfer Reactions Towards Synthesis of γ- / δ-Lactams 169

3.1 Introduction 169

3.2 Results and Discussion 173

3.2.1 Reaction Development 173

3.2.1.1 Cu-Catalyzed Decomposition of 1,4,2-Dioxazol-5-ones for γ-Lactam Synthesis by Direct C(sp^3)–H Amidation 173

3.2.1.2 Substrate Scope Studies 177

3.3 Mechanistic Studies 180

3.3.1 Mechanistic Probe Experiments 180

3.3.2 Kinetic Isotope Effect Study 183

3.3.3 Hammett Correlation Study 184

3.4 Study on Ligand-Modulated Selective γ- and δ-C(sp^3)–H Amidation.....

..... 186

3.4.1 Reaction Development for Selective δ-C–H Amidation 186

3.4.2 Substrate Scope Studies of the δ-Selective C–H Amidation 189

3.4.3 Reaction Development for Selective γ-C–H Amidation 192

3.4.4 Substrate Scope Studies of the γ-Selective C–H Amidation 201

3.5 Concluding Summary 204

3.6 Experimental Section 205

3.6.1 General Experimental Section 205

3.6.2 Experimental Procedures and Physical Characterization 206

3.6.2.1 General Procedure for the Preparation of 1,4,2-Dioxazol-5-ones

..... 206

3.6.2.2 Physical Characterization of Substrates 211

3.6.3 Experimental Procedures for Cu(I)-Catalyzed C(sp^3)–H Amidation .. 222

3.6.4 Physical Characterization of Products 224

3.6.5. Mechanistic Studies 252

3.6.5.1 Kinetic Isotope Effect Study 252

3.6.5.2 Hammett Correlation Study 259

3.6.5.3 Radical Trapping Experiment 261

Chapter 4 Stereocontrolled γ-Lactams Synthesis by Copper-Nitrenoid Mediated Intramolecular Oxyamidation of Alkenes 263

4.1 Introduction 263

4.2 Results and Discussion 266

4.2.1 Reaction Development 266

4.2.1.1 Cu-Catalyzed Oxyamidation of Alkenes for γ-Lactams Synthesis 266

4.2.1.2 Substrate Scope Studies 271

4.3 Mechanistic Studies 277

4.4 Concluding Summary 280

4.5 Experimental Section 281

4.5.1 General Experimental Section 281

4.5.2 Experimental Procedures and Physical Characterization 282

4.5.2.1 General Procedure for the Preparation of Alkenoic Acids 282

4.5.2.2 General Procedure for the Preparation of 1,4,2-Dioxazol-5-ones 284

4.5.2.3 Physical Characterization of Substrates 287

4.5.3 Experimental Procedure for Cu(I)-Catalyzed Oxyamidation 290

4.5.4 Physical Characterization of Products 291

4.5.5 Mechanistic Studies 315

4.5.5.1 Stereoconvergent Study 315

4.5.6 Single Crystal X-Ray Diffraction Data 316

Chapter 5 Conclusion 322

Appendices 324

A.1 Supplementary Information of Chapter 2 324

A.2 NMR Spectra of Chapter 2 329

A.4 Supplementary Information of Chapter 3 489

A.4 NMR Spectra of Chapter 3 500

A.5 Supplementary Information of Chapter 4 594

A.6 NMR Spectra of Chapter 4 598

References 640

ABBRIEVIATION AND SYMBOLS

Ac	Acetyl
AcOH	Acetic acid
Ad	Adamantyl
Ar	Aryl
aq	Aqueous
BDE	Bond dissociation energy
BHT	Butylated hydroxytoluene
BINAP	2,2′-Bis-1,1′-binaphthalene
bpy	2,2′-Bipyridine
Bz	Benzoyl
BzOH	Benzoic acid
CDI	Carbonyldiimidazole
Cp*	1,2,3,4,5-Penyamethylcyclopentadienyl
DCE	1,2-Dichloroethane
DCM	Dichloromethane
DMF	*N*,*N*-Dimethylformamide
DMSO	Dimethyl sulfoxide
dr	Diastereomeric ratio
ee	Enantiomeric excess
equiv	Equivalent
esp	α,α,α′,α′-tetramethyl-1,3-benzenedipropionate
ESI	Electrospray ionization

GC-MS	Gas chromatography–mass spectrometry
HAT	Hydrogen atom transfer
HFIP	Hexafluoroisopropanol
HRMS	High resolution mass spectrometry
KIE	Kinetic isotope effect
LG	Leaving group
LUMO	Lowest unoccupied molecular orbital
m/z	Mass-to-charge ratio
n.d.	Not detected
NFTB	Nonafluoro-tert-butyl alcohol
NMR	Nuclear magnetic resonance
NEt_3	Triethylamine
OAc	Acetyl
phen	1,10-Phenyanthroline
rr	Regiomeric ratio
rt	Room temperature
tBu	*tert*-butyl
TBDPS	*tert*-Butyldiphenylsilyl
TBS	*tert*-Butyldimethylsilyl
TEMPO	(2,2,6,6-Tetramethylpiperidin-1-yl)oxyl
TFE	Trifluroethanol
TON	Turnover number
Tp	Trispyrazolylborate
TPP	Tetraphenylporphyrin
Ts	*p*-Toluenesulfonyl

Å	Angstrom
s	Singlet
d	Doublet
q	Quartet
m	Multiplet
J	Coupling constant
κ	Denticity
ρ	Hammett rho value
R_f	Retention value

LIST OF FIGURES

Figure 2.1 ESI-MS Spectrum of Reaction Crude After 12 Hours of Reaction ... 35

Figure 2.2. Simulated Isotopic Distribution Pattern of Ferrocenium ($C_{10}H_{10}Fe^{+}$) Complex ... 35

Figure 2.3 Molecular Structure of 2a (CCDC: 2143908) ... 45

Figure 2.4 Molecular Structure of 2ze (CCDC: 2143909) ... 47

Figure 2.5 X-band EPR Spectrum of the "$[Cp_2Fe(III)]BF_4$ + 1a" Reaction Mixture ... 54

Figure 2.6 Hammett Plot of $\log(k_Y/k_H)$ versus σ_{para} ... 55

Figure 2.7 Energy Profile Calculated for the Reaction of *para*-MeO-Substituted Aryl Dioxazolone 1v Catalyzed by $[Cp_2Fe(III)]^{+}$ (A); Formation of the Fe-Amidyl Radical Complex (B) ... 57

Figure 2.8 (a) Electronic Properties and (b) Spin Natural Orbital Calculated for the Fe(IV)-Amidyl Radical Complex (B) ... 57

Figure 2.9 Energy Profiles Calculated for the Reaction of *para*-MeO-Substituted Aryl Dioxazolone 1v Catalyzed by $[Cp_2Fe(III)]^{+}$ (A); Pathway Selectivity of *ipso* versus *ortho* Amidyl Radical Addition Starting from the Fe-Amidyl Radical Complex (B) ... 59

Figure 2.10 (a) Reflectance UV-Vis Spectra of SiO_2-APTES and SiO_2-APTES-Fc (b) FT-IR Spectra of SiO_2-APTES and SiO_2-APTES-Fc (c) TGA Spectrum of SiO_2-APTES (d) TGA Spectrum of SiO_2-APTES-Fc 66

Figure 2.11 Molecular Structure of (4-Fluorophenyl)ferrocene (CCDC: 2143911) 117

Figure 2.12 UV-Vis Spectrum of SiO_2-APTES and SiO_2-APTES-Ferrocene 126

Figure 2.13 FT-IR Spectrum of SiO_2-APTES, SiO_2-APTES-Ferrocene before 1st Cycle and after 5th Cycle..... 127

Figure 2.14 TGA Profile of Silica-APTES..... 128

Figure 2.15 TGA Profile of Silica-APTES-Ferrocene 129

Figure 2.16 XPS Spectrum Silica-APTES-Ferrocene 130

Figure 2.17 SEM Images of SiO_2-APTES-Fc (a) before 1st Run (b) after 5th Run 131

Figure 2.18 Hammett Plot of $\log(k_Y/k_H)$ versus σ_{para} 165

Figure 2.19 X-band EPR Spectrum of The "$[Cp_2Fe(III)]BF_4$ + 1a" Reaction Mixture 167

Figure 3.1 LFER Study of Regioselective Lactamization with Different Phenanthroline Ligands using the modified Taft Equation 200

Figure 4.1 ^{1}H NMR Analysis (Reaction Crude) for Diastereomeric *threo*- Versus *erythro*-2a Oxylactams.....269

Figure 4.2 Molecular Structure of 2q (CCDC 2226006).....270

Figure 4.3 Plausible Mechanistic Cycle 279

Figure 4.4 Molecular Structure of 2q 316

LIST OF SCHEMES

Scheme 1.1 Selected Examples of Amide Containing Molecules 1

Scheme 1.2 Examples of Conventional C–H Amination Reactions 2

Scheme 1.3 Ullmann–Goldberg Amination & Buchwald–Hartwig Amination 3

Scheme 1.4 Mechanism and Ligand Examples of Buchwald–Hartwig Amination. 4

Scheme 1.5 Selected Examples of Electrophilic Aminating Reagents 5

Scheme 1.6 General Approaches for Metal-Catalyzed C(sp^3)–H Aminations 7

Scheme 1.7 Generation of Metallonitrenoid & Its Oxidation-state Formalism 8

Scheme 1.8 Synthesis of [Ru(VI)(tpp)$(NTs)_2$] & Its Nitrenoid Transfer Reactions 9

Scheme 1.9 Synthesis of Binuclear Copper(II) Imido Complex [$(Me_3NN)Cu)_2$ (μ-NAd)] 10

Scheme 1.10 Synthesis of Terminal Copper Nitrene Complexes 11

Scheme 1.11 Cytochrome P-450 Inspired C(sp^3)–H Amdiations 12

Scheme 1.12 [$Rh_2(OAc)_2$]-Catalyzed Intramolecular C(sp^3)–H Amidations/ Aminations 14

Scheme 1.13 Synthetic Protocol for [$Rh_2(esp)_2$] Complex 14

Scheme 1.14 Competitive Aziridination of Rh-catalyzed C–H Amidations 15

Scheme 1.15 [Rh_2(*S*-nta)$_4$]-Catalyzed Chemoselective C(sp^3)–H Amidations 15

Scheme 1.16 Ligand-Enabled [Rh_2(*S*-tfpttl)$_4$]-Catalyzed Regioselective C(sp^3)–H Amidations 17

Scheme 1.17 Examples of Ag-Catalyzed C–H Amination and Aziridinations 18

Scheme 1.18 Ag-Catalyzed Chemoselective Aminations 19

Scheme 1.19 Curtius-Type Rearrangement of Metal-Carbonylnitrene to Isocyanates 20

Scheme 1.20 Ir(III)-Catalyzed C(sp^3)–H Amidation for γ-Lactam Synthesis 21

Scheme 1.21 Ru(II)/ Ir(III)-Catalyzed Enantioselective C(sp^3)–H Amidations 22

Scheme 1.22 Examples of Cu-Catalyzed C(sp^3)–H Aminations 23

Scheme 1.23 Cu-Catalyzed Chemoselective Allylic C–H Aminations 24

Scheme 1.24 Iron(III) Phthalocyanines-Catalyzed C(sp^3)–H bonds Amidation 25

Scheme 1.25 Heme-Containing Enzymes Catalyzed Intramolecular C(sp^3)–H Aminations 26

Scheme 1.26 Intramolecular C–H Amination of Fe-Dipyrromethene Complexes .. 27

Scheme 2.1. Selected Examples of Amidyl Radical Precursors 30

Scheme 2.2 Mechanistic Rationale for the Ferrocenium-Catalyzed Arene C–H Amidation via Amidyl Radicals..... 32

Scheme 2.3 Trapping of the Azaspirocyclohexadienyl Intermediate by Dearomative Spirolactamization..... 51

Scheme 2.4 Trapping of the Ferrocenium(IV)-Amidyl Radicals by Alkenes: Oxyamidation of Alkenes 52

Scheme 2.5 Immobilization of Ferrocenecarboxylic Acid onto Silica Gel 60 65

Scheme 3.1 Examples of γ-/ δ- Lactams as Scaffolds of Bioactive Compounds and Mechanistic Hypothesis for Catalytic Reactions for γ-Lactam Formation..... 171

Scheme 3.2 Postulated Mechanism and Mechanistic Probe Experiments..... 182

Scheme 3.3 Kinetic Isotope Effect Studies..... 183

Scheme 3.4 Hammett Correlation Study 185

Scheme 3.5 Postulated Transition State Models for 1,5- / 1,6-HAT 198

Scheme 3.6 Experimental δ- versus γ-Lactams Selectivity with Different Phenanthroline Ligands and Solvents..... 199

Scheme 4.1 Examples of Transition-metal Catalyzed Alkene Oxyamidation..... 265

Scheme 4.2 Possible Reaction Mechanism and Stereoconvergent Lactamization 278

Scheme 4.3 Proposed Transition State for the Diastereoselectivity Towards threo-Isomer 279

LIST OF TABLES

Table 2.1. Catalyst Structure-Activities Study 34

Table 2.2 Effect of Solvents 37

Table 2.3 Effect of Oxidant 38

Table 2.4 Substrate Scope Studies of Ferrocenium-Catalyzed C(sp^2)–H Amidation of *para*-Substituted Aryl 1,4,2-dioxazol-5-ones 41

Table 2.5 Substrate Scope Studies of the Ferrocenium-Catalyzed C(sp^2)–H Amidation of *ortho*-/*meta*-/ Polysubstituted Aryl 1,4,2-dioxazol-5-ones 44

Table 2.6 Crystal Data and Structure Refinement of 2a. 46

Table 2.7. Crystal Data and Structure Refinement of 2ze. 48

Table 2.8 Relative Free Energies among the Corresponding Five Transition States Calculated for Different Monosubstituted Aryl Dioxazolones, and Comparison between the Calculated and Experimental Ratios of the *ortho* and *ipso* Amidation Products 62

Table 2.9 SiO_2-APTES-Fc-Catalyzed Heterogeneous C(sp^2)–H Amidations 67

Table 2.10 Crystal Data and Structure Refinement of (4-Fluorophenyl)ferrocene 118

Table 2.11 Elemental Analysis of SiO_2-APTES-Fc before 1st Run by SEM-EDX 131

Table 2.12 Elemental Analysis of SiO_2-APTES-Fc after 5th Run by SEM-EDX 131

Table 3.1 Effect of Solvents and Copper Catalyst Precursors 175

Table 3.2 Effect of Ligands 176

Table 3.3 Substrate Scope for the Cu-Catalyzed γ-C(sp^3)–H Amidation 179

Table 3.4 Effect of Substituents on the Phenanthroline Ligands 188

Table 3.5 Substrate Scope of δ-C(sp^3)–H Selective Amidation 191

Table 3.6 Effect of Solvents on the δ: γ Regioselectivity 197

Table 3.7 Substrate Scope of γ-C(sp^3)–H Selective Amidation 203

Table 4.1 Effect of Solvents 268

Table 4.2 Substrate Scope for the Cu-Catalyzed Intramolecular Alkene Oxyamidation via 5- and 6-exo trig Cyclization 274

Table 4.3 Substrate Scope for the Cu-Catalyzed Intramolecular Alkene Oxyamidation Involving Nucleophiles Derived from Bioactive Molecules 276

Table 4.4 Crystal Data and Structure Refinement for 2q 317

Table 4.5 Fractional Atomic Coordinates and Equivalent Isotropic Displacement Parameters ($Å^2$) for 2q. 318

Table 4.6 Anisotropic Displacement Parameters ($Å^2$) for 2q. 319

Table 4.7 Bond Lengths for 2q 320

Table 4.8 Bond Angles for 2q 320

Table 4.9 Hydrogen Atom Coordinates (Å) and Isotropic Displacement Parameters (Å2) for 2q 321

Table A1 Optimization of Ferrocene-Catalyzed Arene C–H Amidation 325

Table A2 Catalyst Screening 326

Table A3 Ferrocene Derivatives Screening 327

Table A4 Effects of Anion of Fe-Catalyzed C–H Amidation 328

Table A5 Effect of Solvents 490

Table A6 Effect of Solvents and Temperature 491

Table A7 Effect of Copper Salt 492

Table A8 Effect of Ligands 493

Table A9 Effect of Ligands 494

Table A10 Effect of Catalyst Loading 495

Table A11 Effect of Ligands on δ- versus γ-Lactamization Regioselectivity 497

Table A12 Effect of Solvents on δ- versus γ-Lactamization Regioselectivity Using 2-Bromophenanthroline Ligand 498

Table A13 Effect of Solvents on δ- versus γ-Lactamization Regioselectivity Using 2,9-Diphenylphenanthroline Ligand 499

Table A14 Effect of Solvent with tBuBOX Ligand 595

Table A15 Effect of Catalyst Loading 596

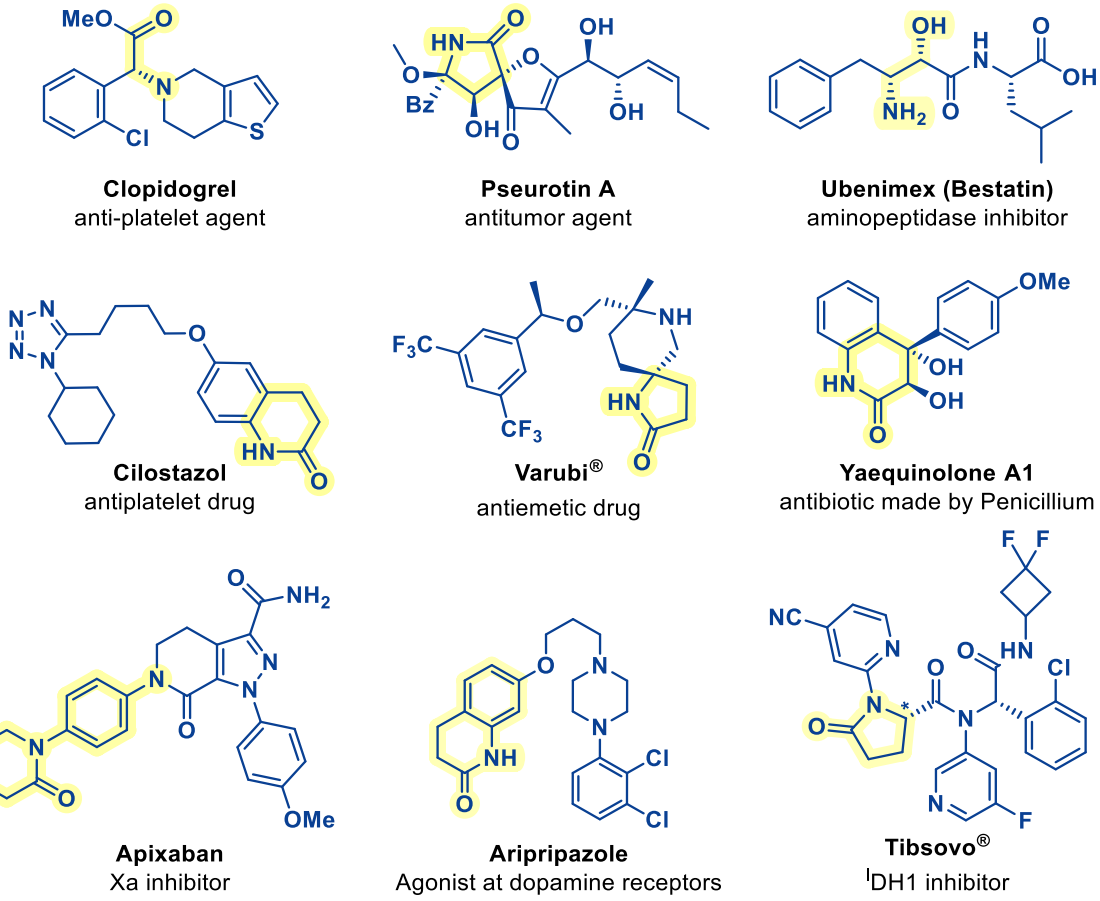
Table A16 Effect of Solvents with 2,9-*n*-Butylphenanthroline Ligand 597

Chapter 1 Introduction

1.1 General Background

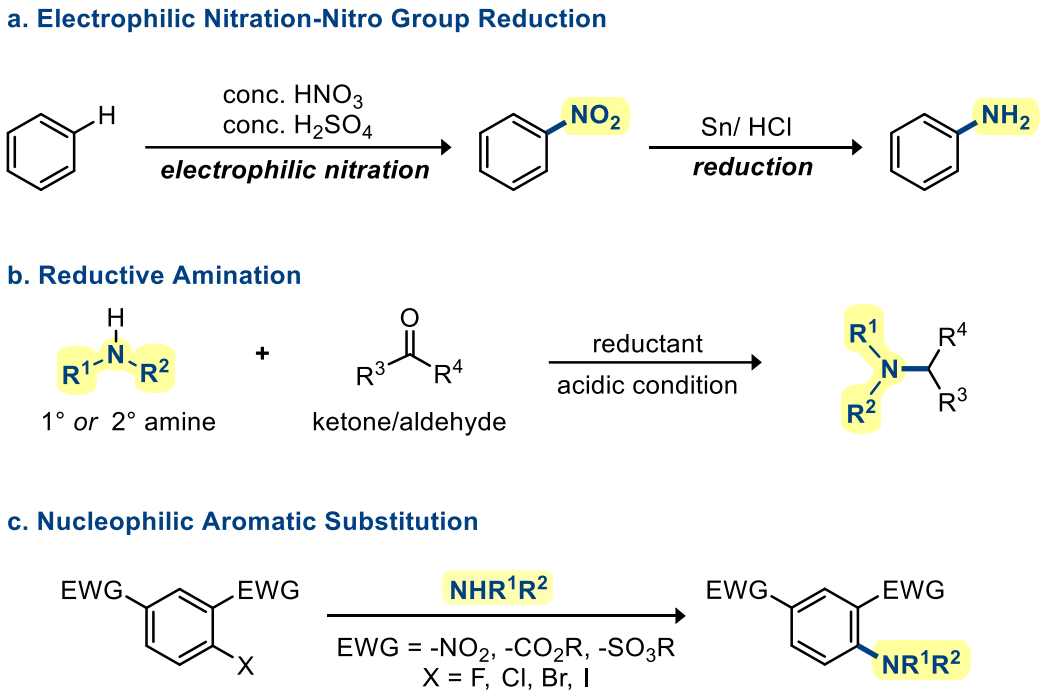
Amide bonds are common elements in numerous pharmaceuticals, bioactive natural products, and synthetic intermediates (Scheme 1.1)[1] These amide bond-forming reactions account for about 25% of the reactions utilized in the pharmaceutical sector.[2] Current research is focused on developing reactions that facilitate selective amide bond formations.

Scheme 1.1 Selected Examples of Amide Containing Molecules



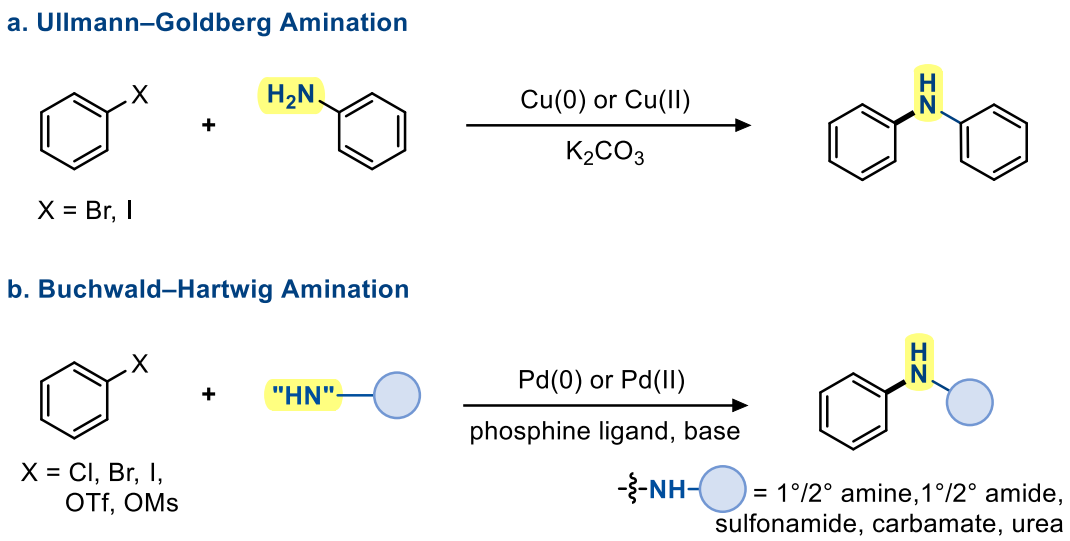
Conventional synthetic routes for constructing C–N bonds (e.g., reductive amination, nucleophilic aromatic substitutions, etc.) often require harsh conditions such as high temperatures and laborious synthetic steps (Scheme 1.2).[3] Reactions utilizing

Scheme 1.2 Examples of Conventional C–H Amination Reactions



transition metal catalysts offer an alternative with improved efficiency and selectivity. Pioneering work by Ullmann and Goldberg in 1903 utilized copper as catalyst for the synthesis of arylamines (Scheme 1.3a).[4] Breakthrough was accomplished by Buchwald and Hartwig independently in 1994 (Scheme 1.3b).[5] The Buchwald-Hartwig amination involves the use palladium complex with the use of phosphine ligands and sterically bulky bases. The oxidative addition of the Pd(0) to aryl halide would give the aryl-palladium(II)-halide complex followed by the amine coordination to the palladium. The coordination to metal center further polarized the N–H bond and increased the

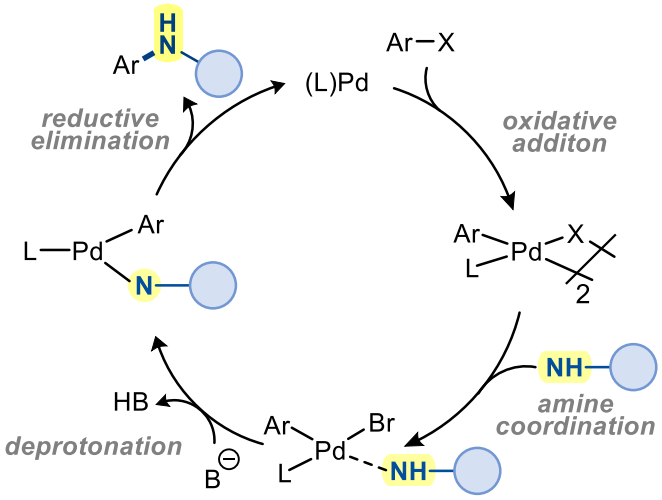
Scheme 1.3 Ullmann–Goldberg Amination & Buchwald–Hartwig Amination



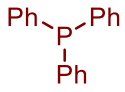
acidity of amine. A rapid deprotonation by the base (e.g. NaO*t*Bu) would then give the amido-palladium(II)-aryl complex followed by reductive elimination to give the arylamine product (Scheme 1.4a). Significant advances have been made in the ligand design supported by extensive mechanistic studies. For instance, a highly robust catalyst system (TON >1,000; catalyst loading <0.001 mol%) has been developed by introducing sterically encumbered biarylphosphine-type ligands.[6] In later years, phosphine ligands acquiring different alkyl or aryl groups have been developed to expand the amine scope and enable the Ar-Cl as substrate.[7] Selected examples of the most frequently used ligands in Buchwald-Hartwig amination are shown in Scheme 1.4b.[6] The Buchwald-Hartwig amination reaction has significantly advanced the catalytic amination field and inspired researchers to design reaction manifolds for novel amination reactions.

Scheme 1.4 Mechanism and Ligand Examples of Buchwald–Hartwig Amination

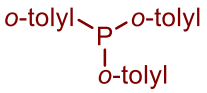
a. Mechanism of Buchwald–Hartwig Amination



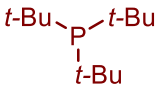
b. Selected Examples of Phosphine Ligands



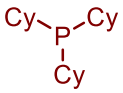
PPh_3



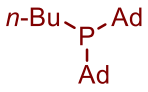
P(*o*-tolyl)$_3$



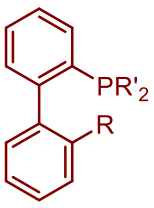
P(*t*-Bu)$_3$



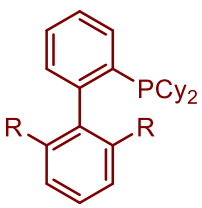
PCy_3



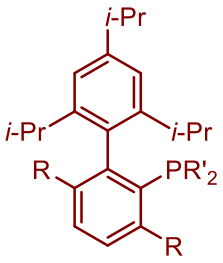
***n*-BuP(Ad)$_2$**



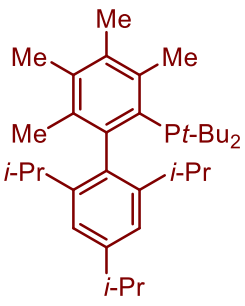
JohnPhos
(R = H; R' = *t*-Bu)
CyJohnPhos
(R = H; R' = Cy)
DavePhos
(R = NMe_2; R' = Cy)



RuPhos
(R = O*i*-Pr)
SPhos
(R = OMe)

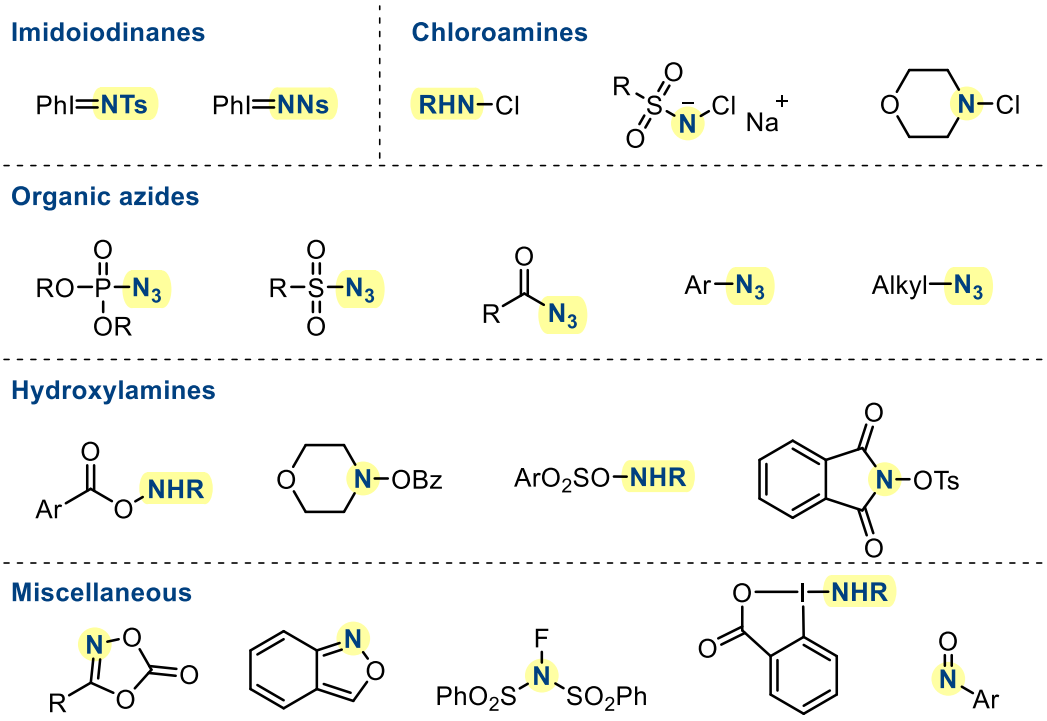


XPhos
(R= H; R' = Cy)
BrettPhos
(R= OMe; R' = Cy)
***t*-BuXPhos**
(R = H; R' = *t*-Bu)
***t*-BuBrettPhos**
(R = OMe; R' = *t*-Bu)



Me_4*t*-BuXPhos

Scheme 1.5 Selected Examples of Electrophilic Aminating Reagents



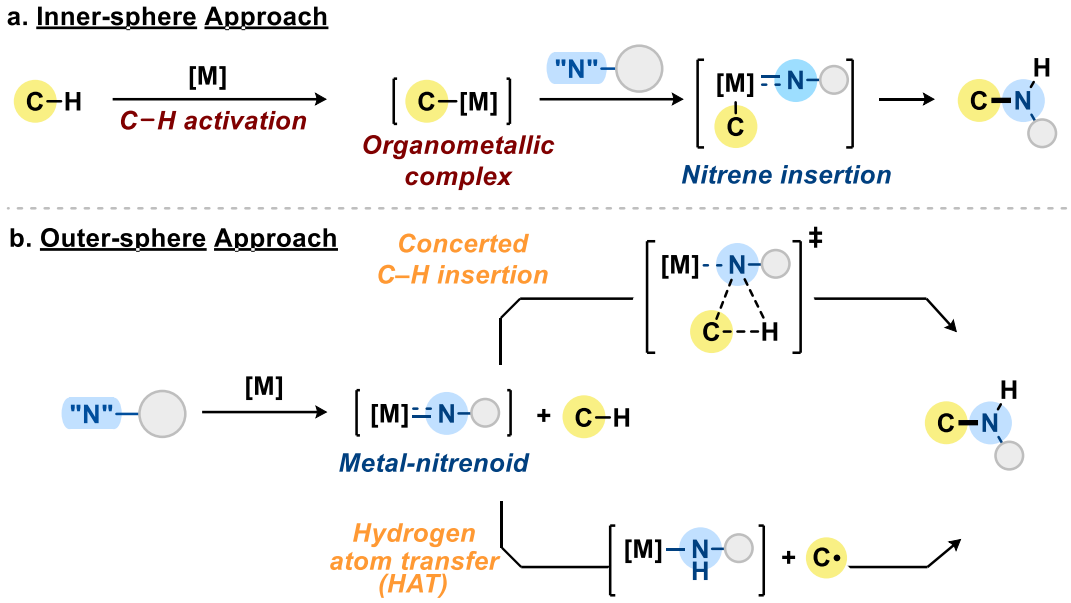
Despite the success of the transition-metal-catalyzed C–H amination reactions, the reaction requires pre-activation of the arene C–H bond (BDE = 465 kJ mol^{-1}) to aryl halides or pseudohalides (BDE = 276 – 400 kJ mol^{-1}). Indeed, direct C–H amidations offer an atom-economical and step-efficient approach for constructing C–N bonds.[8] However, the high bond dissociation energy and pKa values of the C–H bond lead to its chemical inertness. The cross-dehydrogenative C(aryl)–N coupling reactions are thermodynamically uphill as it involves breaking the strong C(aryl)–H (BDE = 465 kJ mol^{-1}) and N–H (BDE = 386 kJ mol^{-1}) bonds and forming weaker H–H (BDE = 436 kJ mol^{-1}) and C(aryl)–N bonds (BDE = 305 kJ mol^{-1}).[9] To this end, introducing electrophilic aminating reagents (Scheme 1.5) with a weaker N–X bond (X = leaving

group) would lower the energy demand for bond breaking, and the X–H bond formation also provides a stronger driving force for C–N bond formation.

1.2 Transition Metal-Catalyzed C(sp^3)–N Cross-Coupling Reactions

The transition metal-catalyzed C(sp^3)–N cross-coupling reactions can be achieved via inner-sphere and outer-sphere pathways.[1b, 10] The inner-sphere pathway involves organometallic intermediates derived from oxidation addition, electrophilic metalation or concerted metalation deprotonation to the C(sp^3)–H bond. These organometallic intermediates would then react with electrophilic aminating reagents to give the amination products (Scheme 1.6a). Unlike the inner-sphere pathway, the outer-sphere pathway is where the transition metal first reacts with the electrophilic aminating reagents to give the reactive metallonitrenoid species followed by concerted C–H insertion *or* hydrogen atom abstraction to the targeted (usually the weakest) C–H bond affording the C(sp^3)–N bond product (Scheme 1.6b). The outer-sphere metallonitrenoid insertion pathway usually exhibits a reactivity signature of 3° C–H bond > 2° C–H bond >> 1° C–H bond.[11] Therefore, designing catalytic systems (catalyst, ligands, etc.) that would selectively functionalize different C–H bonds of the same molecule is a formidable challenge. Against this background, this chapter will present an overview of the different strategies to achieve catalytic selective C(sp^3)–N bond formation.

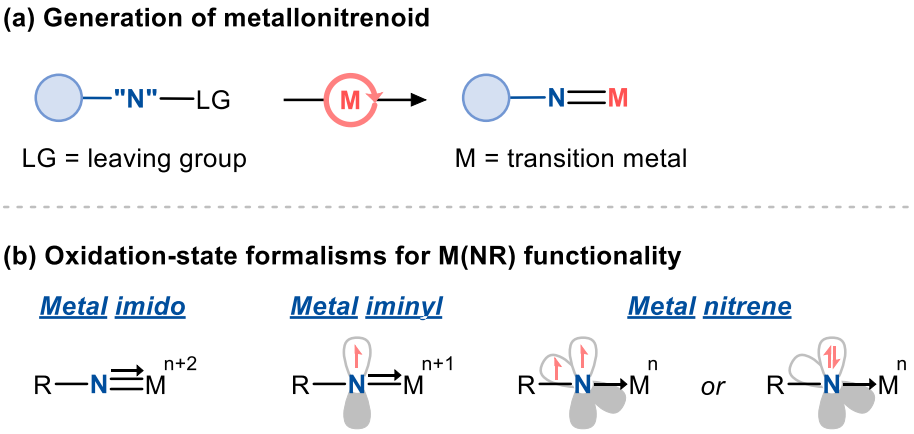
Scheme 1.6 General Approaches for Metal-Catalyzed C(sp^3)–H Aminations



1.2.1 Metallonitrenoid and Its Reactivity

Metallonitrenoid refers to a species in which the nitrene ligand is bonded to and stabilized by a metal center. This species is typically generated through the reaction of the metal catalyst with electrophilic aminating reagents (nitrene precursors). It can be classified into three different types: (1) metal imido, (2) metal iminyl, and (3) metal nitrene (Scheme 1.7). Due to its inherent instability, examples of isolated and characterized metallonitrenoids are sparse in the literature. The first example is reported by Che and co-workers, by treating the [Ru(tpp)(CO)(MeOH)] (tpp = dianionic of 5,10,15,20-tetraphenylporphyrin) with [(*N*-tosylimino)iodo]benzene (PhI=NTs) as nitrene source in DCM at room temperature for 5 minutes would afford the bis(tosyl)imidoruthenium(VI)porphyrin [Ru(VI)(tpp)$(NTs)_2$] complex **1** in 60%

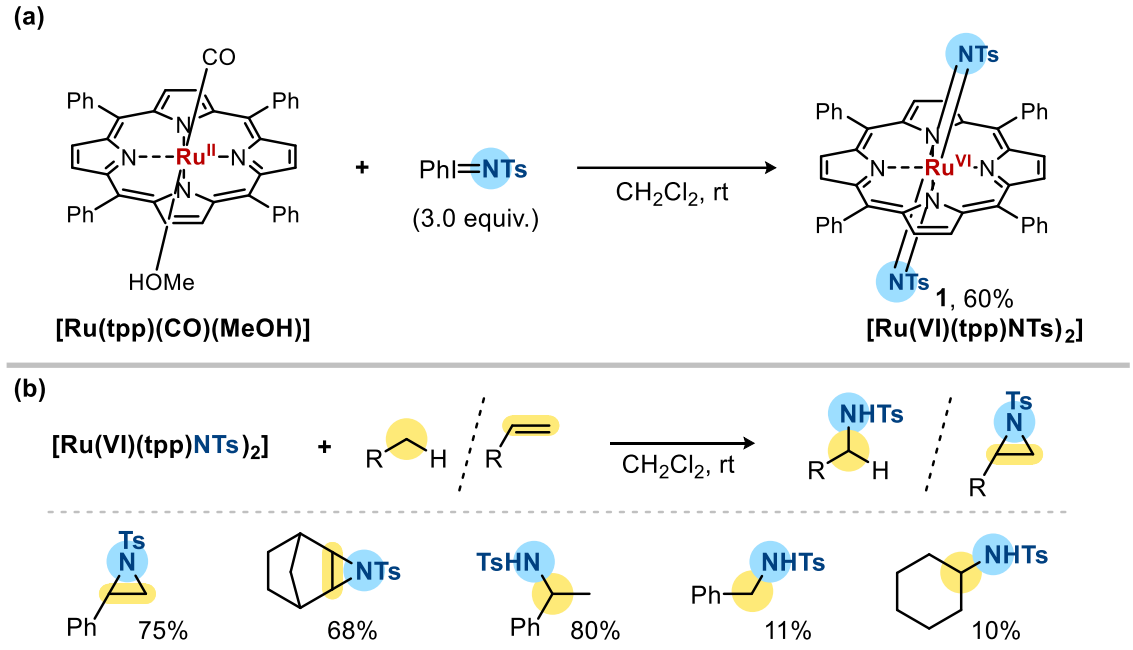
Scheme 1.7 Generation of Metallonitrenoid & Its Oxidation-state Formalism



(Scheme 1.8a).[12] Notably, this isolated Ru(VI) complex is stable at -20 °C for days, and can be kept for a few hours at room temperature. The Ru(VI) complex **1** reacts to alkene to give the aziridine product. Later, the same group reported that complex **1** can mediate the nitrene transfer reaction into activated C(sp^3)–H bonds such as benzylic, allylic, tertiary C–H bonds, etc (Scheme 1.8b).[13] The nitrene transfer by complex **1** to unactivated secondary C–H bond is less favorable, and the reaction of cyclohexane with complex **1** only affords 10% of the amidation product. The kinetic isotope effect study of k_H/k_D = 11 indicates that the C–H bond breaking is the rate-limiting step. The authors suggest the C–N bond formation is via a hydrogen atom abstraction followed by a radical rebound of the carboradical to give the amidation products. Noted that the formation of bisimidoruthenium complex involves oxidation of the Ru center. Therefore, a strong field ligand (e.g. porphyrin or salen) is required to stabilize the high oxidation state of Ru. Surprisingly, the same group found that Ru complex bearing non-

porphyrin ligand [Ru(III)(Me$_3$tacn)(CF$_3$CO$_2$)$_3$·H$_2$O][14] (Me$_3$tacn = N, N′, N″-trimethyl-1,4,7-triazacyclononane) & *cis*-[Ru(II)(6,6′-Cl$_2$bpy)$_2$Cl$_2$][15] (6,6′-Cl$_2$bpy = 6,6′-dichloro-2,2′-bipyridine) can also mediate the C–H amidation with the use of PhI=NTs as nitrene source.

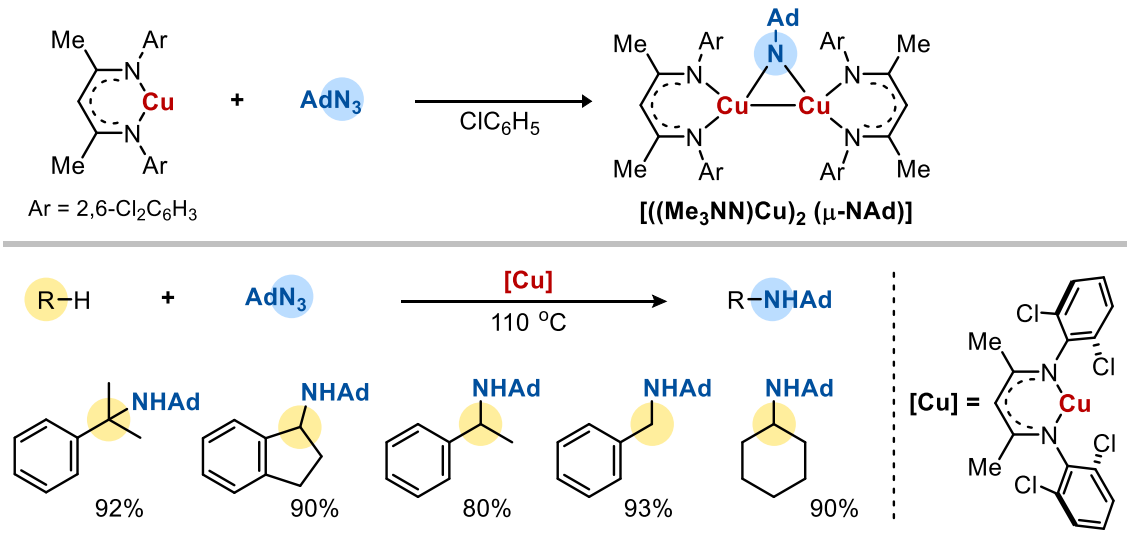
Scheme 1.8 Synthesis of [Ru(VI)(tpp)(NTs)$_2$] & Its Nitrenoid Transfer Reactions



Following the pioneering work by Che, the metal-imido and iminyl complexes (early and mid-transition metals) have been extensively studied.[16] For first-row late transition metal featuring a high d-count and displaying a poor spatial overlap between metal and nitrogen atom, it is possible that their metallonitrenoid bonding may be described by inverted ligand field.[17] For example, the copper–nitrenoid has been proposed as the key intermediate for the catalytic C–H amidation. In 2006, Warren and

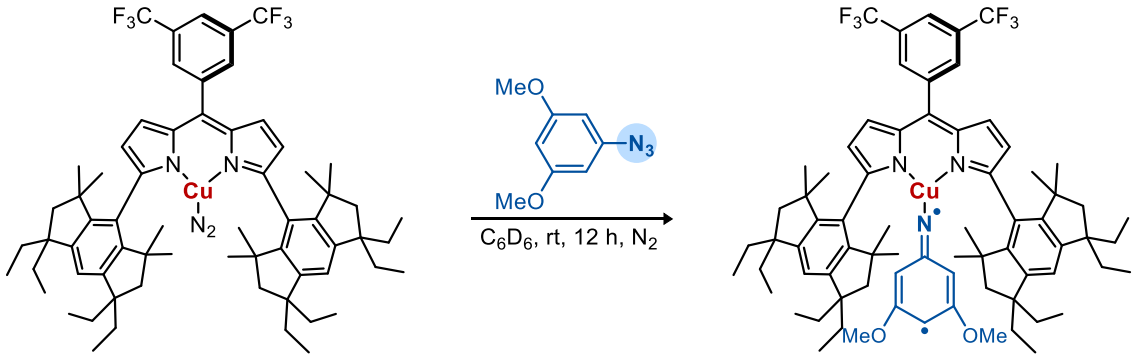
co-workers successfully isolated a stable binuclear copper(II)-imido complex [((Cl$_2$NN)Cu)$_2$ (μ-NAd)] (Ad= adamantyl) (Scheme 1.9).[18] By treating [(Cl$_2$NN)Cu]$_2$·C$_6$H$_6$ and adamantyl azide as nitrene source in chlorobenzene affords the binuclear copper(II)-imido complex in 63% yield. Upon thermal treatment, the dicopper(II) imido complexes would give some terminal nitrene-Cu complexes for C–H amination reaction.[19] The mechanistic studies revealed that the reaction proceeded in a non-concerted manifold and involved the generation of carbon radical.[20] While different groups (Ray[21], Bertrand[22], etc.) reported using different spectroscopic and theoretical characterization of the terminal copper-nitrenoid, the isolation of an authentic terminal copper–nitrenoid complex was unprecedented.

Scheme 1.9 Synthesis of Binuclear Copper(II) Imido Complex [((Me$_3$NN)Cu)$_2$ (μ-NAd)]



A breakthrough was made by Betley in 2019, a near linear terminal copper nitrene complex with short Cu–N bonds (1.745-1.759 Å) has been isolated (Scheme 1.10).[23] Combined with X-ray absorption spectroscopy and computational analysis revealed that the copper(I) nitrene complex can be formulated as a triplet nitrene adduct to copper(I), indicating the absence of Cu–N multiple bond character. The terminal triplet copper–nitrenoid species can undergo facile C–H amination or C=C aziridination, consistent with its involvement in the Cu-catalyzed C–N coupling reactions.

Scheme 1.10 Synthesis of Terminal Copper Nitrene Complexes

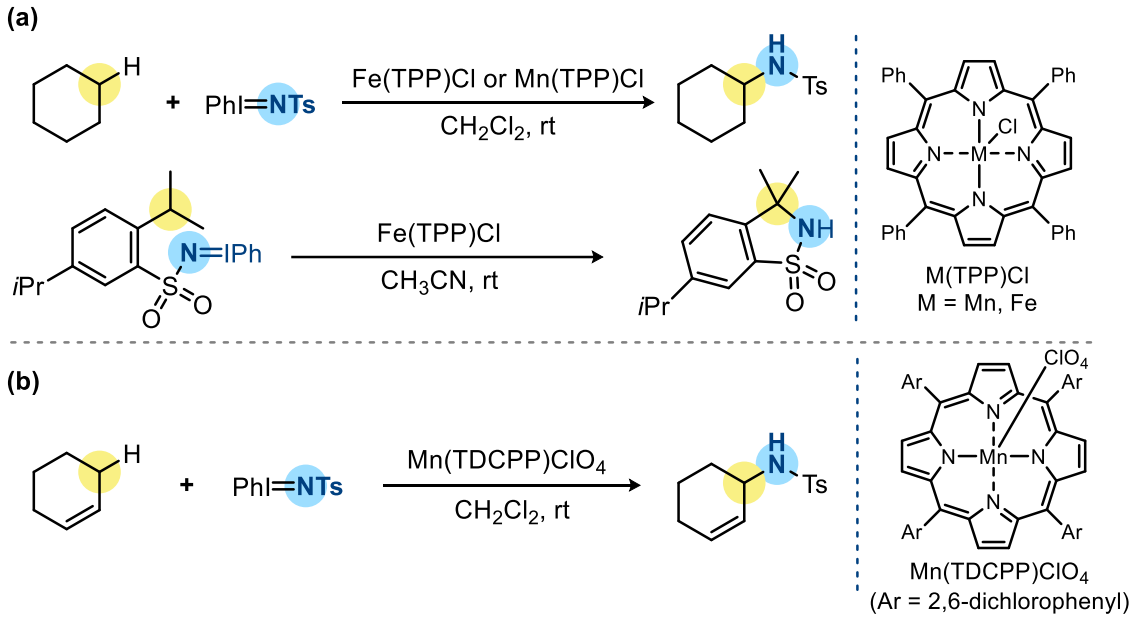


1.2.2 Pioneering Works Inspired by the Cytochrome P450

A pioneering example of catalytic nitrene transfer reaction was reported by Breslow in 1982. Inspired by the cytochrome P450-catalyzed C–H oxidation, Breslow's group reported that metalloporphyrins [M(TPP)Cl] [M = Mn(III) or Fe(III] can catalyze direct C–H amidation of cyclohexane with [(*N*-tosylimino)iodo]benzene (PhI=NTs) as the nitrogen source (Scheme 1.11a top).[11a] A year later, the same group developed the [Fe(TPP)Cl]-mediated intramolecular C(sp^3)–H amidation for the synthesis of cyclic

sulfonamide in up to 85% yield (Scheme 1.11a below).[11b] In 1988, Mansuy reported a more efficient Mn(III) porphyrin-catalyzed intermolecular allylic C–H amidation. Using PhI=NTs and cyclohexene as substrates, the combination of [Mn(TDCPP)]ClO_4 (1.0 mol%) in DCM solvent successfully mediated the C–H amidation reaction, yielding 3-tosylamidocyclohexene at 70% efficiency (Scheme 1.11b).[11c] Notably, the reaction involving *trans*-hex-2-ene produced a mixture of allylic tosylamides. These results may suggest that the Mn–nitrenoid species undergoes hydrogen atom abstraction to form an allylic radical, which then undergoes radical rebound to afford the amidation product.

Scheme 1.11 Cytochrome P-450 Inspired C(sp^3)–H Amdiations

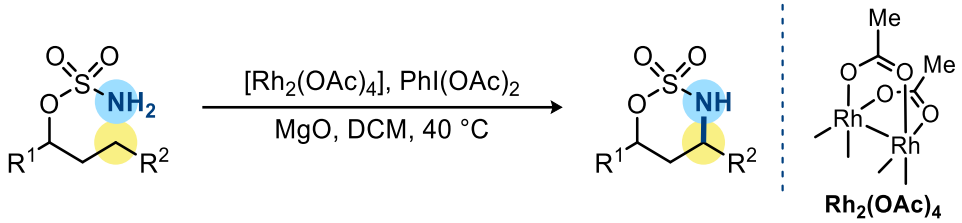


1.2.3 Rhodium-Catalyzed C(sp^3)–H Aminations

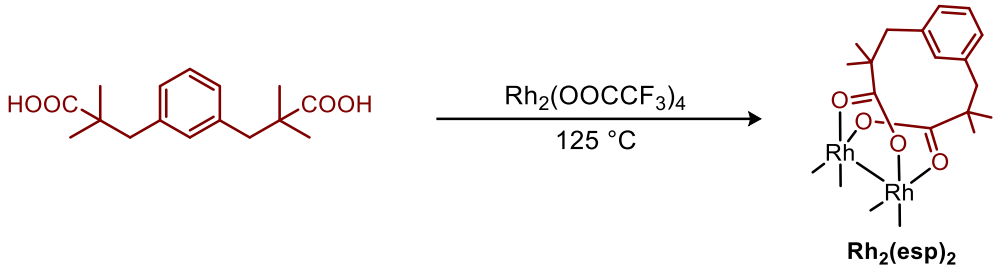
1.2.3.1 Seminal Works of [$Rh_2(OAc)_4$]-Catalyzed C(sp^3)–H Aminations

Following the pioneering work of Breslow and Mansuy, the use of the benchtop unstable iminoiodinane reagents remains problematic. A significant breakthrough was achieved by Du Bois' group in 2001 (Scheme 1.12).[24] With [$Rh_2(OAc)_4$] as the catalyst, treating sulfonamide and $PhI(OAc)_2$ as the oxidant would generate the corresponding iminoiodinane species *in situ*. This *in-situ* protocol practically extends the nitrene sources beyond sulfonamides, enabling carbamates, sulfamates, and sulfamides to be viable coupling partners for C(sp^3)–H amination reactions without the need to isolate the iminoiodinane reagents.[25] Mechanistic and computational analyses indicated that the dirhodium-catalyzed amidation likely occurs via a concerted C–H insertion pathway (Scheme 1.6b top).[26] While this research advanced practical applications for synthetic chemists, the involvement of hypervalent iodine could lead to undesirable ligand exchange and catalyst degradation. Later, in 2004, Du Bois and co-workers introduced a more stable dirhodium catalyst, [$Rh_2(esp)_2$], featuring a strap-type ligand [α,α,α′,α′-tetramethyl-1,3-benzenedipropionate] (Scheme 1.13).[27] The [$Rh_2(esp)_2$] catalyst displayed improved catalytic activity (TON > 600) and expanded substrate scope for C–H amidations.

Scheme 1.12 [$Rh_2(OAc)_2$]-Catalyzed Intramolecular C(sp^3)–H Amidations/ Aminations



Scheme 1.13 Synthetic Protocol for [$Rh_2(esp)_2$] Complex



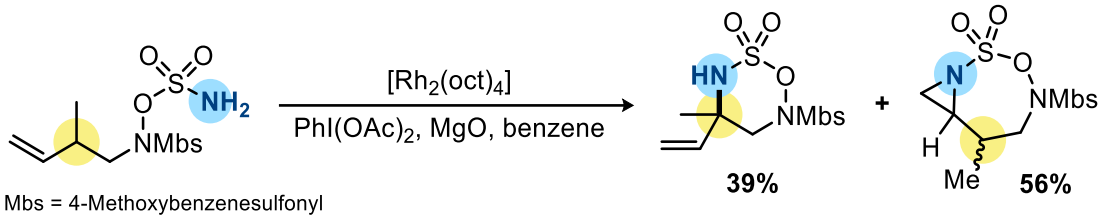
1.2.3.2 Chemoselectivity Issue of Dirhodium Catalysts

Yet, the dirhodium-catalyzed C–H amination reaction is limited by the chemoselectivity issue when utilizing alkene substrates (aziridination versus C–H amidation).[25a, 28] For instance, the [$Rh_2(oct)_4$]-catalyzed intramolecular allylic C–H amidation of 4-methoxy-*N*-(2-methylbut-3-en-1-yl)-*N*-(sulfamoyloxy)benzene-sulfonamide afforded only the C–H amidation product in 39% yield along with the aziridination product (56% yield) (Scheme 1.14).

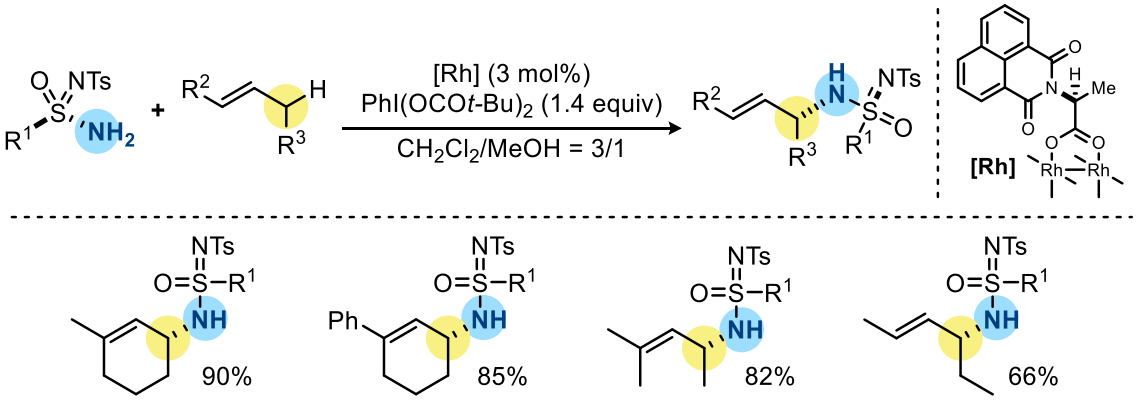
The C–H amidation reaction rate following the reactivity order: tertiary > α-ethereal, α-aminal, benzylic > secondary >> primary C–H bonds, consistent with the electronic influence of the C–H bonds.[29] To address the selectivity issue of the

dirhodium catalysts, Dauban's group discovered that the dirhodium catalyst [Rh_2(*S*)-nta$_4$], derived from alanine, can chemoselectively couple the sulfonimidamide with different C(sp^3)–H bonds (Scheme 1.15).[30] Significantly, amidation reactions for substrates with various allylic C–H bonds occur at the least hindered site, with no competing aziridination detected. The authors indicated that the notable stereo- and chemo-selectivities are attributed to the cooperative interactions between the dirhodium catalyst and the sulfonimidamide.

Scheme 1.14 Competitive Aziridination of Rh-catalyzed C–H Amidations



Scheme 1.15 [Rh_2(*S*-nta)$_4$]-Catalyzed Chemoselective C(sp^3)–H Amidations



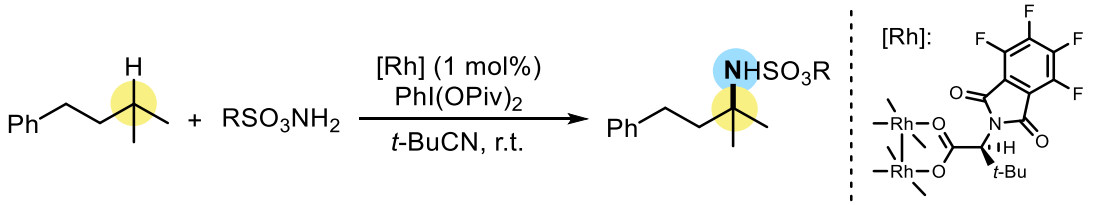
1.2.3.3 Ligand-Enabled Regioselective C(sp^3)–H Amidation Reactions

Building on the advancements made by Du Bois and Dauban, the range of the dirhodium-catalyzed nitrene transfer reaction has significantly expanded. However,

moderating the catalyst to effect functionalization at the stronger C–H bonds rather than the weaker ones (e.g., tertiary vs. benzylic) remains a paramount challenge.[31] Recently, Dauban's group made a breakthrough in ligand-controlled regioselective amidation at the tertiary C–H bond (BDE = 395 kJ mol^{-1}) compared to the weaker benzylic C–H bond (BDE = 356 kJ mol^{-1}).[32] Through comprehensive design and evaluation, it was revealed that the [Rh_2(*S*-tfpttl)$_4$] complex features a distinct catalytic pocket capable of selectively functionalizing the tertiary C–H bond using *tert*-butylphenol sulfamate (see Scheme 1.16). This dirhodium catalyst demonstrates remarkable stability, allowing successful gram-scale reactions to produce amidation products with just 0.01 mol% of the catalyst. To account for the regioselectivity, the [Rh_2(*S*-tfpttl)$_4$] catalyst would afford an all-up conformation (i.e., the four phthalimido groups pointing on the same side), thereby creating a pocket for the *tert*-butyl groups in the nitrene precursor. This would lead to the nitrene binding occurring at the "all-up" face of the rhodium catalyst. There are additional interactions between the fluorine atoms at the phthalimido group with the carbonyl group of the nitrene and the α-protons to the carboxylic acid function. Therefore, the benzylic C–H bonds became poorly accessible by the rhodium–nitrenoid species due to the steric effect, resulting in a selectivity disfavoring the weaker benzylic C–H bond. Notably, in 2024 the same group reported a homobenzylic C–H selective

amination reaction by alternating the nitrene source from *tert*-butylphenol sulfamate to 2,6-dibromocresolsulfonamide.[33]

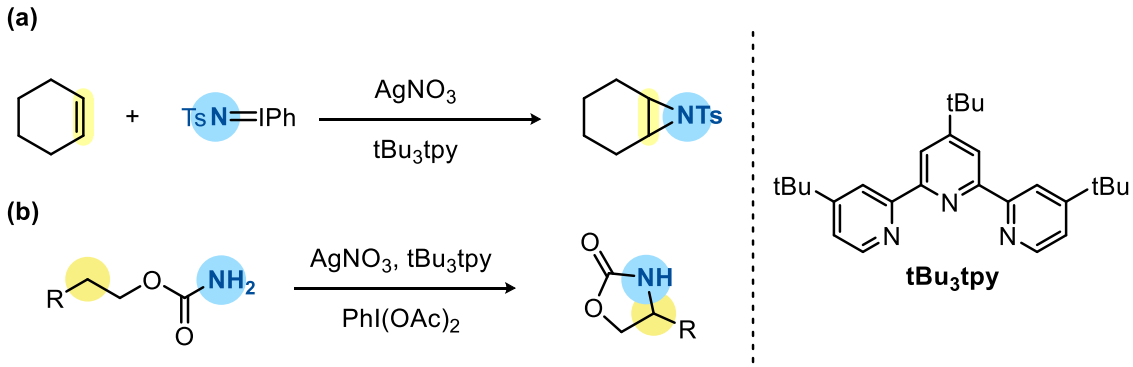
Scheme 1.16 Ligand-Enabled [Rh_2(*S*-tfpttl)$_4$]-Catalyzed Regioselective C(sp^3)–H Amidations



1.2.4 Silver-Catalyzed Nitrene Transfer Reactions

By taking advantage of the diverse range of coordination geometries (such as seesaw, tetrahedral, linear, etc.) of Ag(I) complexes with nitrogen-donor ligands, the steric and electronic characteristics of the catalytic system can be tuned independently, thereby creating an avenue for catalyst-controlled selective C–N reaction formation.[34] He and co-workers established the pioneering Ag-catalyzed C(sp^3)–N coupling.[35] In the presence of Ag(I) salt and terpyridine (tpy) type ligands, aziridination of alkene was observed chemoselectively without the competing allylic C(sp^3)–H amination (Scheme 1.17a).[35a] Notably, the same catalytic system can undergo facile intramolecular C–H amidation of alkyl carbamates to give oxazolidin-2-ones (Scheme 1.17b).[35b] Later, Pérez developed an Ag-catalyzed regioselective alkene aziridination of allylic alcohols with trispyrazolylborate (Tp) as ligand.[36]

Scheme 1.17 Examples of Ag-Catalyzed C–H Amination and Aziridinations



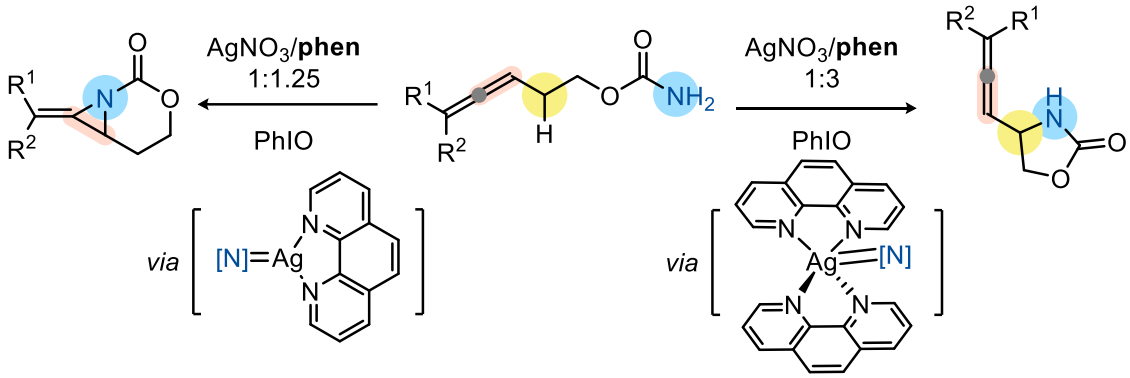
1.2.4.1 Chemoselective Nitrene Transfer Reactions

As shown in 1.2.3.2, dirhodium catalysts frequently encounter chemoselectivity issues with substrates containing C=C bonds, resulting in competing aziridination versus C–H amidation. Despite Dauban's notable progress, the range of substrates applicable for [Rh_2(*S*)-nta$_4$]-catalyzed chemoselective C(sp^3)–H amidation is still restricted, as the selectivity relies on the synergistic interaction between the catalyst and sulfonimidamide.

Schomaker and co-workers reported that varying the Ag to ligand ratio would produce silver complexes of different molecular geometry (linear, square planar tetrahedral, etc). Harnessing the unique reactivity profile of the Ag complexes, Schomaker has developed a toolbox for chemodivergent nitrene transfer reactions.[37] By reacting 25 mol% of 1,10-phenanthroline as ligand and 20 mol% of AgOTf as catalyst with the homoallenic carbamate in the presence of $PhI(OAc)_2$ would afford a trigonal planar [(phen)Ag–nitrene] intermediate. This [(phen)Ag–nitrene] species will undergo

intramolecular aziridination chemoselectively over the C–H insertion (Scheme 1.18 left). On the other hand, increasing the ligand/Ag ratio to 3:1 would give the tetrahedral [Ag(phen)$_2$]OTf as the active catalyst. The [Ag(phen)$_2$]OTf then reacts with the nitrene precursor to give a distorted square pyramidal [(phen)$_2$Ag–nitrene], which promotes intramolecular C–H insertion while suppressing aziridination (Scheme 1.18 right). The authors revealed the chemodivergence is owing to the difference in the steric environment between Ag(L) and Ag(L)$_2$. The kinetic studies show that the rate of aziridination using Ag(L)$_2$ as catalyst is much slower as the steric congestion increased while the rate of C–H insertion decreased slightly using Ag(L) vs Ag(L)$_2$.

Scheme 1.18 Ag-Catalyzed Chemoselective Aminations

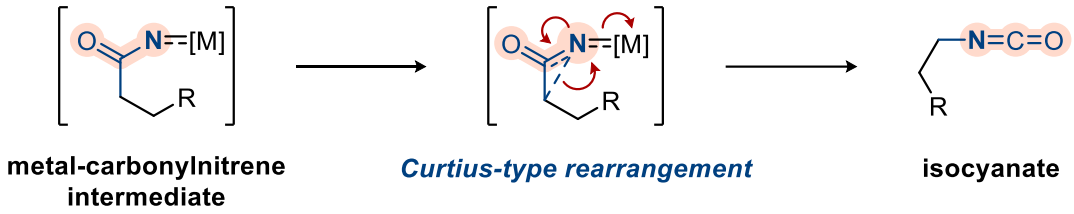


1.3 Catalytic Acylnitrene Transfer Reactions

Direct amidation of the C(sp^3)–H bond via carbonylnitrene transfer offers a simple pathway to produce carboxamides, including lactams. Although the dirhodium/silver method has substantially broadened the range of substrates applicable for C–H amidation reactions using carbamate or sulfonyl-based nitrene reagents, nitrene

precursors derived from carboxamides are ineffective as reagents. The inherent instability of carbonylnitrene leads to a competing Curtius-type rearrangement that primarily produces isocyanate instead of the target C–H amidation product. (Scheme 1.19).[38]

Scheme 1.19 Curtius-Type Rearrangement of Metal-Carbonylnitrene to Isocyanates

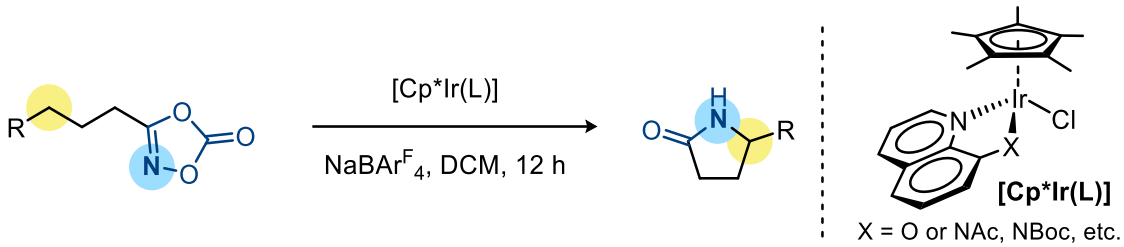


1.3.1 Pioneering Work of Transition-Metal-Catalyzed Acylnitrene Transfer Reactions

Recently, Chang and co-workers revealed that the Cp*Rh(III) complex bearing a σ-donating 2-arylpyridine ligand can decompose 1,4,2-dioxazol-5-ones to generate reactive carbonylnitrene species. These species subsequently undergo migratory nitrene insertion into aryl–Rh bond. [39] Later, Chang's team developed a Cp*Ir(III) complex featuring a σ-donating bidentate carboxamidoquinoline ligand. This complex effectively catalyzes intramolecular C(sp^3)–H amidation of 3-(3-alkylpropyl)-1,4,2-dioxazol-5-one to afford *γ*-lactams without any isocyanate formation (Scheme 1.20).[40] Notably, 1,4,2-dioxazol-5-ones, can be readily synthesized from carboxylic acids

through a two-step process. A combined computational and experimental study suggests that strong σ-donating ligands enhance the electron density on the Ir(III) center, leading to increased π-back bonding. This π-interaction from the metal center to the acylnitrene raises the barrier of Curtius-type rearrangement.

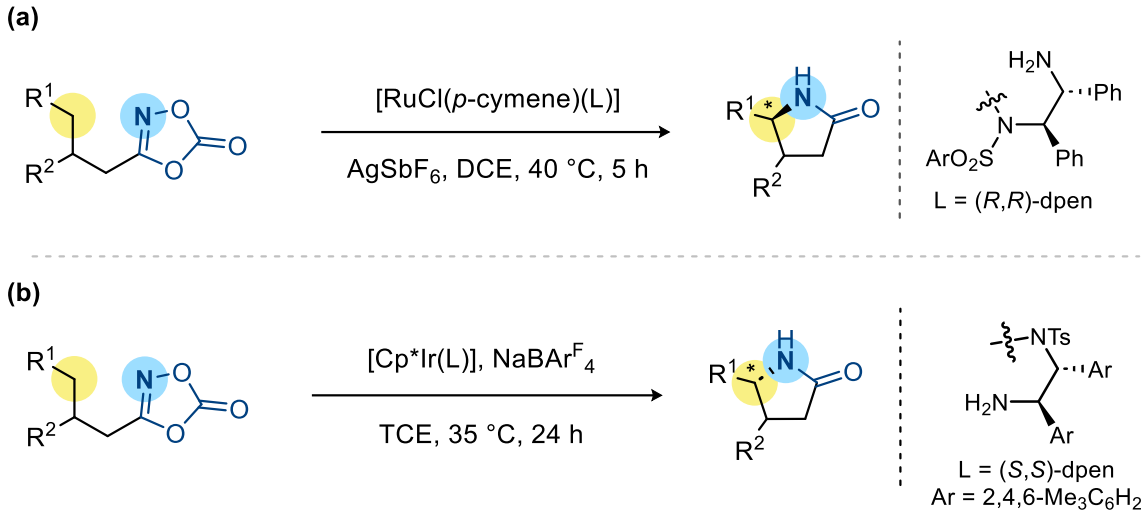
Scheme 1.20 Ir(III)-Catalyzed C(sp^3)–H Amidation for γ-Lactam Synthesis



1.3.2 Asymmetric Carbonyl Nitrene Transfer Reactions

Inspired by this work, Yu and Chang's group independently reported the use of Ru(II)[41] and Ir(III)[42] for catalytic asymmetric intramolecular C(sp^3)–H amidation reaction (Scheme 1.21). As anticipated, the π-basic d^6 metal centers successfully suppressed the Curtius-type rearrangement, and enantioselective γ-lactam synthesis has been accomplished by using chiral 1,2-diphenylethylene diamine (dpen) ligands. Both groups proposed that the transition state of N–H formation is a hydrogen bond-stabilized transition state. The observed enantioselectivity can be attributed to the steric interaction between the aryl group on the ligand and the R group on the substrate.

Scheme 1.21 Ru(II)/ Ir(III)-Catalyzed Enantioselective C(sp^3)–H Amidations



1.4 Earth-abundant Metal-Catalyzed C(sp^3)–H Amidations

The catalytic C–H amination/amidation systems based on earth-abundant metals such as Fe, Co, Ni, and Cu are attracting attention for enhanced sustainable industrial applications. This section will discuss the development in Cu and Fe-catalyzed nitrene transfer reactions for direct C(sp^3)–H amidation/amination.

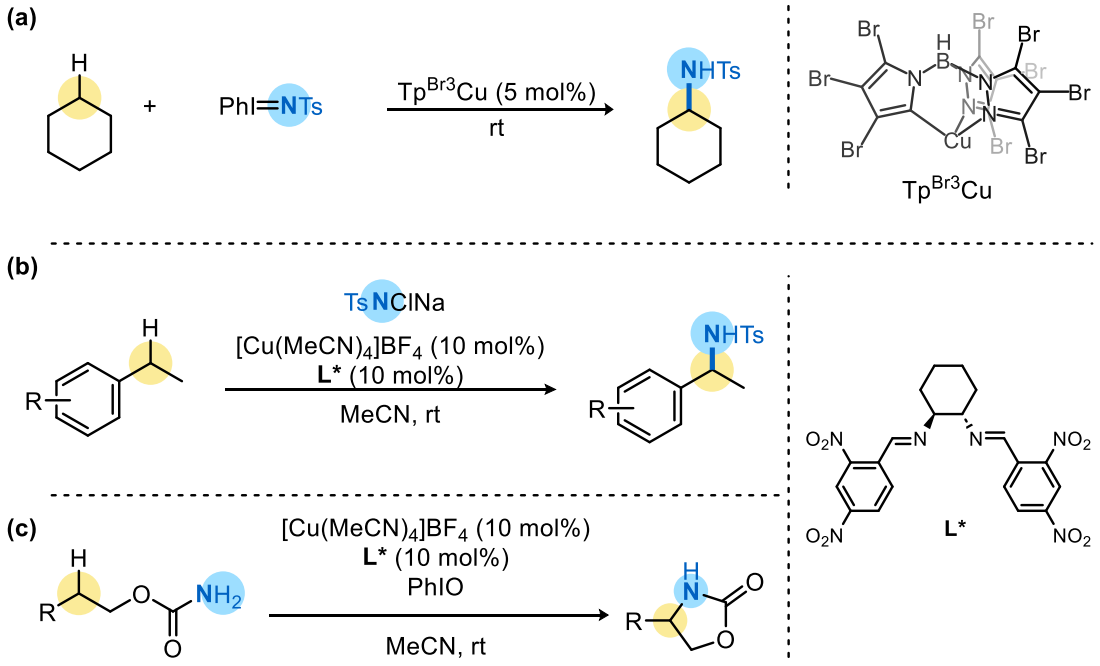
1.4.1 Copper-Catalyzed Nitrene C(sp^3)–H Insertion Reactions

The use of Cu for C–H amination dates back to a report by Kwart and Khan published in 1967. The reaction protocol employed benzenesulfonyl azide as the reagent and cyclohexene as substrate in the presence of copper powder, and aziridine (15%) was obtained as a primary product.[43] The corresponding C–H amination yielded only 3%. The author suggests that Cu–nitrene is the crucial intermediate for both aziridination and C–H amination processes. This proposal is supported by the finding

that the putative nitrene species can be trapped by DMSO to afford $Me_2S(O)(=NTs)$ in 50% yield. Later, Turner reported a similar C–H amination of dioxane utilizing copper powder and chloramine-T (TsNClNa) as reagent,[44] and the corresponding C–H amination product was obtained in 70% yield. Soon later, Pérez and co-workers demonstrated the intermolecular C–H amination of cyclohexanes and benzenes using molecularly defined copper complexes of trispyrazolylborate (Tp) (Scheme 1.22a).[45]

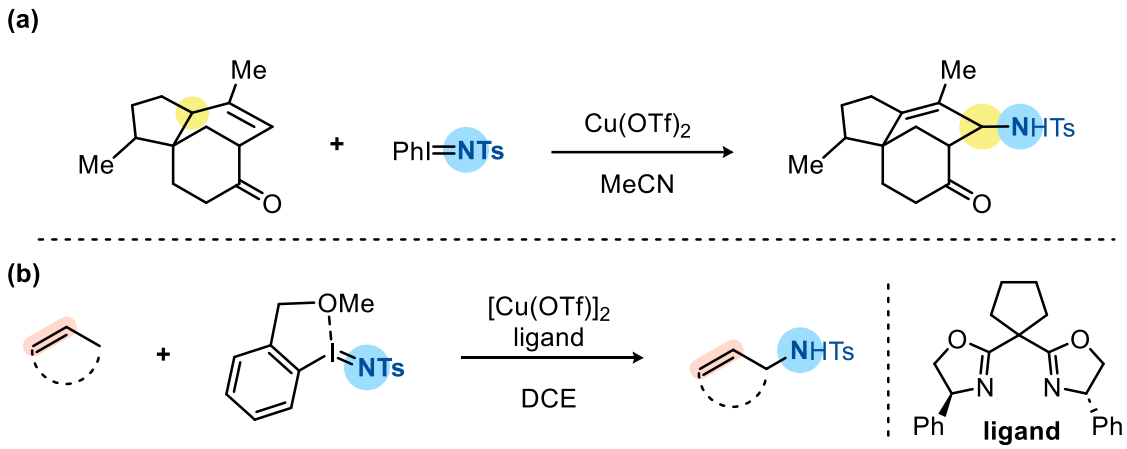
Inspired by these pioneering works, the catalytic enantioselective C–H amination mediated by chiral copper complexes has been pursued. For instance, Nicholas and co-workers reported intramolecular[46] and intermolecular[47] C–H amination by employing chiral C2-symmetric diamine ligands (Scheme 1.22b & c). The corresponding amination products were obtained in ca. 70% yield, albeit in <40% *ee*.

Scheme 1.22 Examples of Cu-Catalyzed C(sp^3)–H Aminations



Competing aziridination has been a problematic issue in Cu-catalyzed C–H amination.[48] In this regard, Overman and co-workers accomplished early success of Cu-catalyzed allylic C–H amination during the total synthesis of hispidospermidin.[49] The allylic C–H amination takes place in preference to aziridination when the C=C bond becomes hindered (Scheme 1.23a). Recently, Zhu and co-workers developed a Cu-catalyzed chemoselective nitrene transfer for late-stage amination of natural products (Scheme 1.23b).[50] Using C2-symmetric bisoxazoline as ligand, the allylic C–H amination of cyclohexene with *ortho*-methoxymethyl iminoiodinanes occurs over the aziridination.

Scheme 1.23 Cu-Catalyzed Chemoselective Allylic C–H Aminations

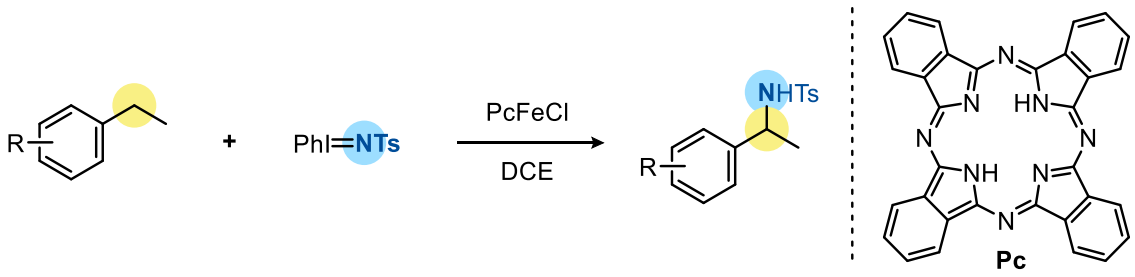


1.4.2 Iron-Catalyzed Nitrene C(sp^3)–H Insertion Reactions

As discussed in 1.2.2, the cytochrome P450 chemistry has inspired the seminal work on biomimetic Fe-catalyzed C–H amination by Breslow, Mansuy, and Gellman in the 1980s.[51] In 2006, Zhou and co-workers utilized iron(III) phthalocyanines

complex [Fe(Pc)Cl] for the nitrene transfer of tosyliminoiodane and hydrocarbons. The amination selectively targets the weakest C–H bond on the hydrocarbon chain (Scheme 1.24).[52] In 2010, Che and co-workers reported that [Fe(F_{20}-TPP)Cl] can affect catalytic alkene aziridination with sulfonyl azide as a nitrene source. Yet, the catalyst is inactive for C–H amination.[53] However, when 4-nitrophenyl azide was employed as the nitrene reagent, the [Fe(F_{20}-TPP)Cl]-catalyzed C–H amination can forge C–N at the benzylic C–H bonds of alkylbenzenes and the methylene positions of the cycloalkanes in moderate-to-good yields. This study shows that the reactivity of the nitrene transfer can be tuned by the electronic or steric characteristics of the nitrene or the porphyrin ligand.

Scheme 1.24 Iron(III) Phthalocyanines-Catalyzed C(sp^3)–H bonds Amidation

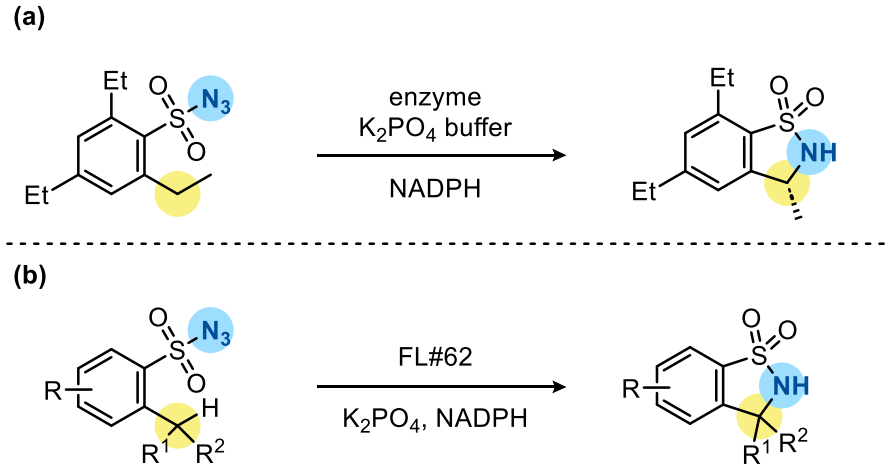


1.4.2.1 Biocatalytic C(sp^3)–H Amination by Recombinant P450 Enzymes

In 2013, Arnold found that $P450_{BM3}$ exhibited a high reactivity towards intramolecular C–H amination of aryl sulfonyl azides with a high total turnover number (TTN) and enantioselectivity (Scheme 1.25a).[54] The $P450_{BM3}$ mainly reduces the sulfonyl azide to sulfonyl amide under anaerobic and reducing conditions. After several examinations, Arnold found that $P450_{BM3}$-C400S-CIS-T438S could catalyze the C–H

amination with TTN of 383 along with 73% *ee*. Notably, the enzymatic C–H amination can be preserved *in vivo*. Intact *E. coli* cells expressing $P411_{BM3}$-CIS have demonstrated the capability to support C–H amination, achieving a TTN of 690 and 60 % *ee*. Notably, in 2014, Fasan parallelly showcased cysteine-ligated hemoproteins that could facilitate intramolecular C–H amination reaction (Scheme 1.25b).[55] They examined a series of $P450_{BM3}$ variants and found that the variant FL#62 is capable of α-C–H amination with a TON of 388.

Scheme 1.25 Heme-Containing Enzymes Catalyzed Intramolecular C(sp^3)–H Aminations



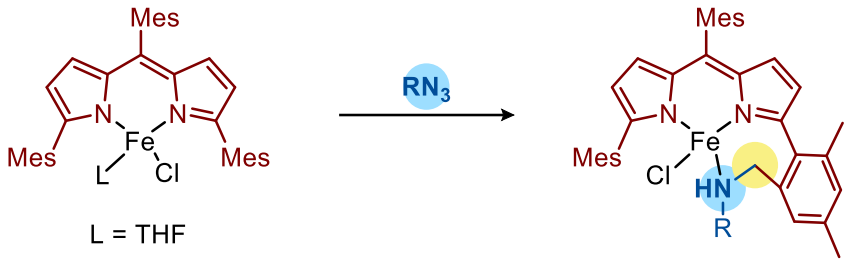
1.4.2.2 Non-Heme-Type Iron-Catalyzed C(sp^3)–H Aminations

Parallel with the biomimetic approaches for catalyst development, the non-heme type ligands are attractive candidates for developing successful C(sp^3)–H amination catalysts.[56] Che and co-workers reported intramolecular C–H amidation can be achieved using $[Fe(Cl_3terpy)_2]^{2+}$ (Cl_3terpy = 4,4′,4″-trichloroterpyridine) as a catalyst.[57]

The Fe-imido intermediate has been spectroscopically characterized by ESI-MS analysis. The catalytic reaction displayed a kinetic H/D isotope effect of 4.4, and a non-concerted radical pathway was proposed.

In 2009, Betley reported that [FeCl(dipyrromethene)] complex would undergo intramolecular C–H amination upon treatment with adamantyl azide to give an iron(III)-amido products (Scheme 1.26).[58] A reactive iron-imido was proposed as the key intermediate; however, no successful isolation of the iron-imido complex was achieved. In 2011, Betley achieved a significant breakthrough by successfully isolating a terminal imido-iron (III) complex.[58b, 59] Reacting *para*-*t*BuC$_6$H$_4$N$_3$ with [(^{Ar}L)FeCl] led to the formation of a high-spin (S = 2) [(^{Ar}L)FeCl(N(*para*-*t*BuC$_6$H$_4$)),] complex as determined by NMR, X-ray crystallography and ^{57}Fe Mössbauer spectroscopy.

Scheme 1.26 Intramolecular C–H Amination of Fe-Dipyrromethene Complexes



1.5 Concluding Summary

Transition metal-catalyzed C–N coupling reactions via reactive metallonitrene complexes are powerful tools for organic synthesis. Since Breslow's pioneering works, the field has undergone enormous development. New catalyst systems utilizing second and third-row late transition metals like Ru, Rh, and Ir have notably enhanced catalyst stability and achieved ligand-tunable selectivity for benzylic and tertiary C–H bonds. The introduction of second and third-row metal catalysts has increased the synthetic value of catalytic C–H amidation in practical organic synthesis. Despite these advances, there is a demand for developing earth-abundant metal catalysts due to increasing environmental concerns. Unlike the second-/third-row metals, the first-row metals do not form strong bonds with nitrene ligand due to poor 3d-2p orbital overlap, implying a potential problem of poor reactivity control of the first-row metal-nitrene species. Furthermore, regioselective functionalization of methylene C–H bonds has been a formidable challenge. The strategy successfully targeting benzylic versus tertiary C–H bond amidation relies on electronic and steric tuning of the auxiliary ligands. Yet, a similar strategy is not applicable for regioselective methylene C–H bonds. The subsequent sections of this thesis will detail our exploration of metal-amidyl radicals as promising active reagents for regiocontrolled C–H transformations functionalization.

Chapter 2 Intramolecular Arene C(sp2)—H Amidation Enabled by Ferrocenium-Mediated Decomposition of 1,4,2-Dioxazol-5-ones as Amidyl Radical Precursors

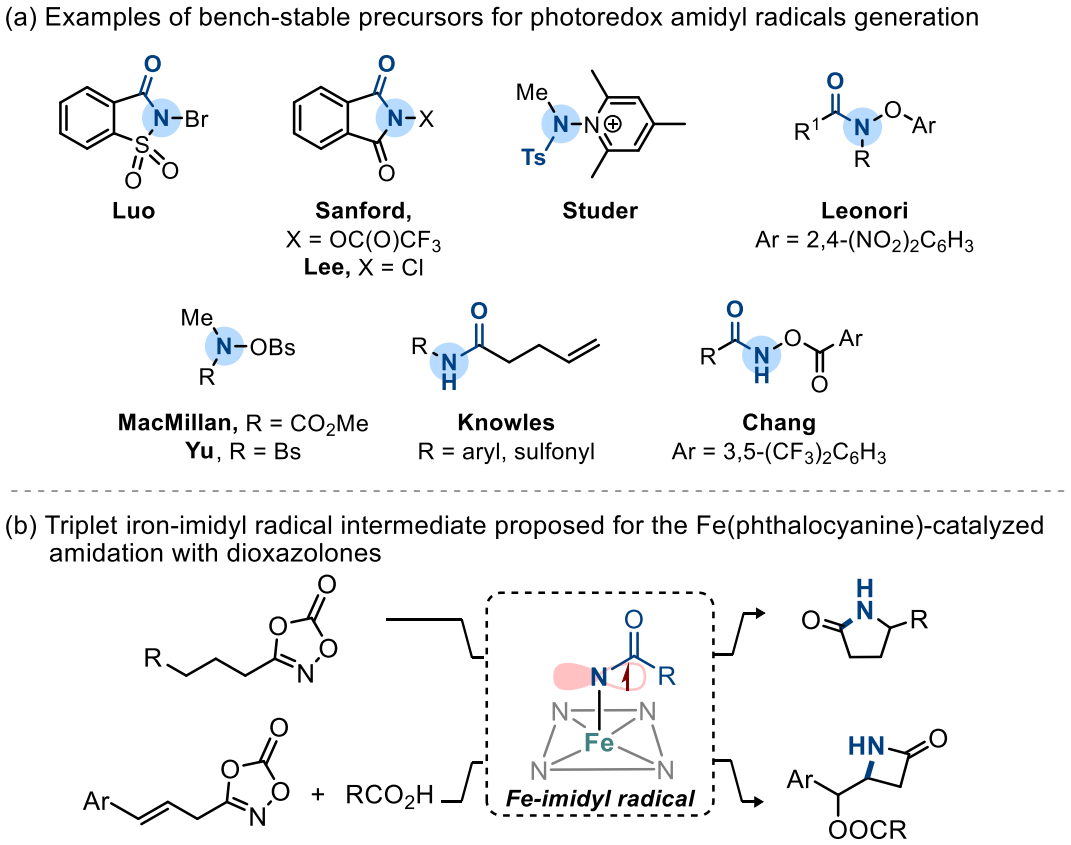
2.1 Introduction

Arylamines are prevalent scaffolds in pharmaceuticals, agrochemicals, and electronic materials; developing new atom-economical and step-efficient methodologies for C–N bond formations is of great interest.[60] Due to the broad application of amides and carbamates, direct arene C–N coupling by amidyl radicals is attracting current interest because of an expanded arene scope and promising regioselectivity.[61] Recent advancement of photocatalysis has enabled effective amidyl radical generation from some bench-stable precursors, including *N*-acyloxy(halo)phthalimides,[62] *N*-aminopyridinium salts[63] and hydroxylamides[64] (Scheme 2.1a). Employing hydroxyamide reagents bearing bis-3,5-(trifluoromethyl)benzoate leaving group, Chang and co-workers developed the photocatalytic generation of amidyl radicals for intramolecular amidation of alkanes[64d] and arenes[64e].

Late transition metals (e.g. Rh, Ru, Ir, Ni, Cu)[65] are known to mediate productive acylnitrene group transfer to hydrocarbons with dioxazolones as precursors.[41-42, 66] Currently, research effort is directed to the development of catalytic C–H amidation

involving earth-abundant 3d metals such as Fe as catalysts.[59, 67] However, being weaker π-donors, the use of 3d metal as catalysts for dioxazolone decomposition is potentially problematic due to the competing Curtius-type rearrangement. Yet, Chang's group recently reported the Fe(III) phthalocyanine catalyzed intramolecular acylnitrene C(sp^3)–H amidation with dioxazolones as reagents to afford γ-lactams.[67k, l] Some reactive triplet Fe-imidyl radical intermediates have been proposed (Scheme 2.1b).

Scheme 2.1. Selected Examples of Amidyl Radical Precursors

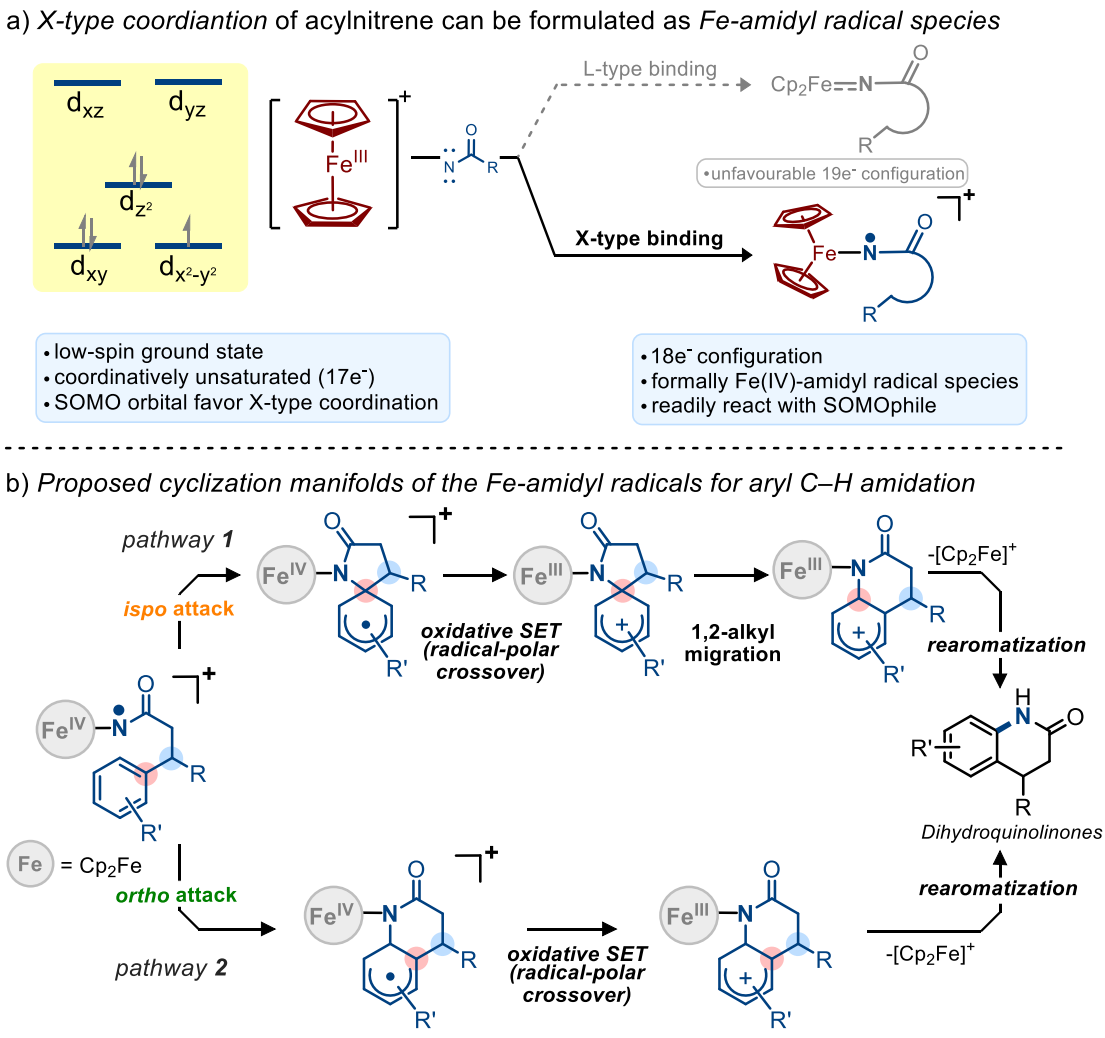


Encouraged by our previous successes on the arene-ruthenium(II)-catalyzed direct aliphatic[41] and arene[66c] C–H amidation, we hypothesized that the related CpFe unit may share similar nitrene transfer reactivities. Unlike most Fe(II/III) complexes, low-spin

configuration[68] of ferrocenes renders stronger metal-ligand interaction, thereby enabling its reversible redox properties. By simple 18-electron rule argument, we surmised that X-type coordination of a triplet nitrene ligand to the 17-electron ferrocenium $[Cp_2Fe(III)]^+$ can be formulated as Fe(IV)-amidyl radical species[69] which would be reactive toward C–H amidation reactions. (Scheme 2.2) Ferrocenes are well-known for electron-transfer catalysis;[70] however, their activity to mediate nitrene transfer to hydrocarbons is unprecedented.[71] Here we present that the $[Cp_2Fe(III)]^+$ complex serves as an effective catalyst for intramolecular electrophilic amidyl radical addition to arenes to form 3,4-dihydroquinolin-2(1*H*)-ones. Unlike most reported Fe complexes involving chelating nitrogen-based ligands, ferrocenium complexes represent a new class of catalysts for C–H amidations.

We hypothesized that the Fe-amidyl radical-mediated intramolecular C–H amidation would proceed[64e] via two plausible pathways: (1) *ipso* and (2) *ortho* amidyl radical addition at the arene moiety. The *ipso*-addition should afford an azaspirocyclohexadienyl radical intermediate. Notably, the *ipso*-addition pathway is expected to furnish the dihydroquinolinone with rearranged skeleton since the spirocarbenium ion intermediate would undergo facile 1,2-alkyl migration.

Scheme 2.2 Mechanistic Rationale for the Ferrocenium-Catalyzed Arene C–H Amidation via Amidyl Radicals



2.2 Results and Discussion

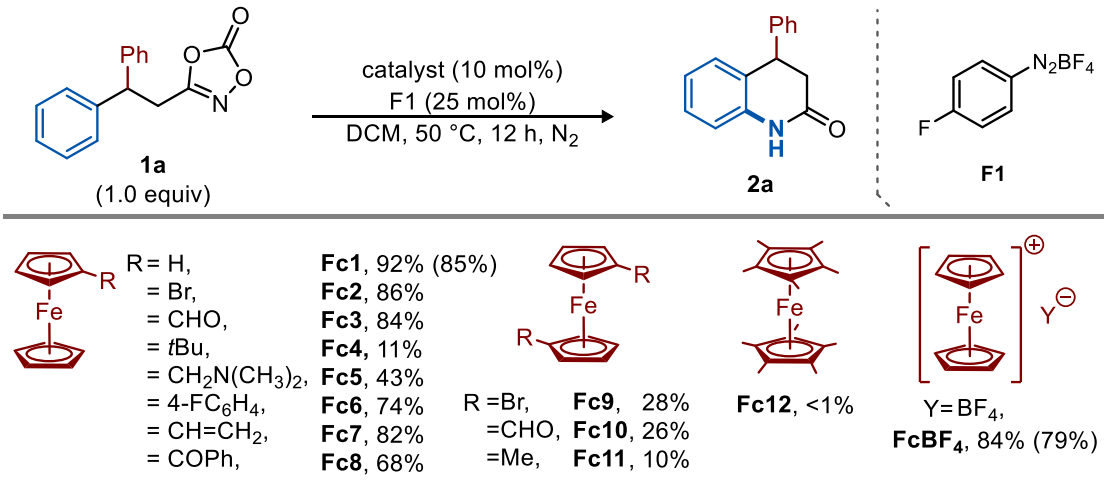
2.2.1 Reaction Development

We initiated our study by examining the reactivity of $[Cp_2Fe(III)]^+$ for catalytic nitrene transfer reactions using 3-(2,2-diphenylethyl)-1,4,2-dioxazol-5-one (**1a**) as the model substrate. The ferrocenium complex was prepared *in situ* by treating $[Cp_2Fe(II)]$ (10 mol%) with $[4\text{-}F\text{-}C_6H_4N_2]BF_4$ (**F1**; 25 mol%) as oxidant in DCM (2 mL). The ferrocenium complex formation is featured by an immediate color change from pale yellow to dark olive green. Reacting dioxazolone **1a** (0.2 mmol) with the $[Cp_2Fe(III)]^+$ (10 mol%) at 50 °C for 12 h afforded 4-phenyl-3,4-dihydroquinolin-2(1*H*)-one (**2a**) in 85% isolated yield (Table 2.1). The arenediazonium salt **F1** should serve as a single-electron oxidant for the $[Cp_2Fe(III)]^+$ generation from $[Cp_2Fe(II)]$ *in situ*.[72] As expected, the pre-formed $[Cp_2Fe(III)]^+BF_4$ gives a comparable results in **2a** (79%) formation. To verify the structural integrity of the ferrocenium complex during the catalytic reaction, the reaction mixture was analyzed by ESI-MS. A prominent molecular ion cluster peak at m/z = 186 was observed, and it can be assigned as the ferrocenium complex based on mass value and the agreement between the experimental and simulated mass spectra (Figures 2.1 & 2.2).

Next, we turned to study the substituent effect on the ferrocene derivatives. Different *mono*- or *disubstituted* ferrocenes derivatives were synthesized and employed

to the standard reaction condition. We found that the reactivity of the ferrocene derivatives is not sensitive to the electronic perturbation. For instance, bromo-substituted ferrocene (**Fc2**) and formyl-substituted ferrocene (**Fc3**) promoted the formation of dihydroquinolinone (**2a**) in ca. 85% yield. Apparently, a bulkier substituent would produce lower yield of **2a** [**Fc4**: 11%; **Fc5**: 43%]. In general, the *monosubstituted* ferrocenes showed higher activities than those *disubstituted* derivatives [compare results: **Fc2**: 86% vs **Fc9**: 28%]. Notably, the [Cp*$_2$Fe] exhibits negligible activity with full substrate recovery.

Table 2.1. Catalyst Structure-Activities Study[a-c]



[a]Reaction conditions: **1a** (0.2 mmol), ferrocene derivatives (10 mol%), **F1** oxidant (25 mol%), DCM (2 mL) at 50 °C for 12 h under N_2; [b]^{1}H NMR yield using CH_2Br_2 as the internal standard; [c]Isolated yield in parentheses

Figure 2.1 ESI-MS Spectrum of Reaction Crude After 12 Hours of Reaction

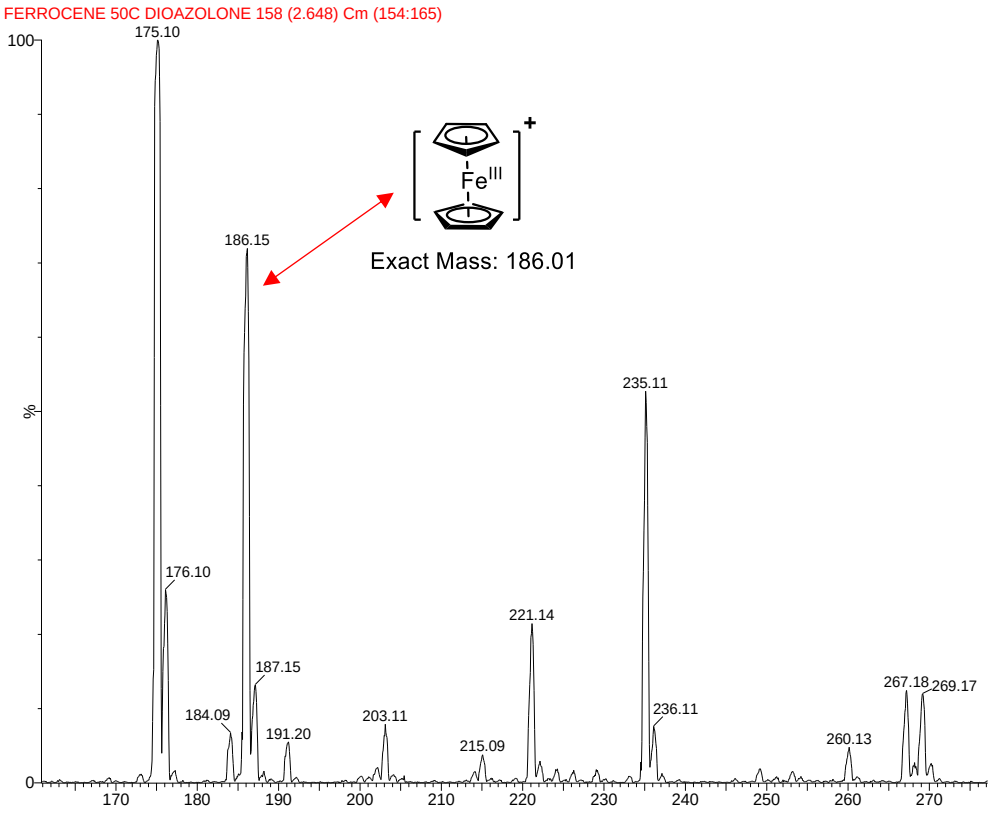
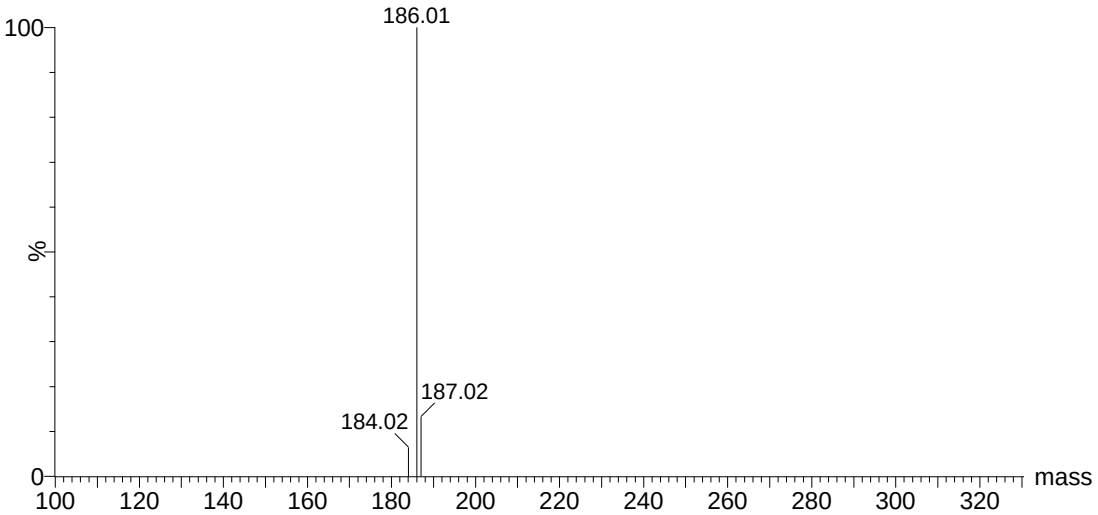


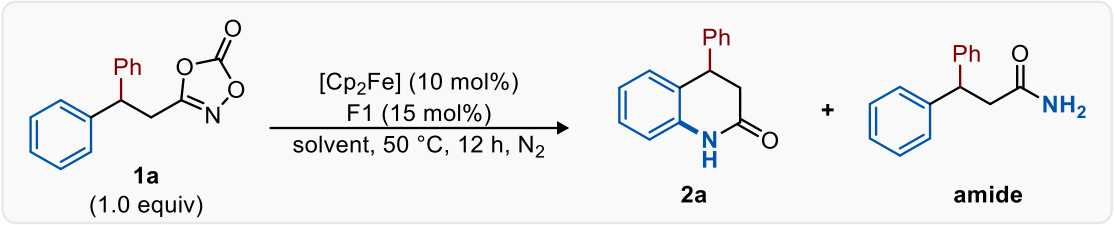
Figure 2.2. Simulated Isotopic Distribution Pattern of Ferrocenium ($C_{10}H_{10}Fe^{+}$) Complex



Prior to the investigation of solvent effect, control experiments confirmed that ferrocene (**Fc**) and oxidant (**F1**) are crucial for effective amidation. As anticipated, **1a** was fully recovered unchanged in the absence of either **Fc** or **F1**. As shown in Table 2.2, several common solvents were tested; the use of halogenated solvents such as DCM (74%), DCE (67%), and $CHCl_3$ (65%) gave better results than other polar solvents acetone (n.d.), DMA (n.d.), MeCN (n.d.), THF (16%), TFE (31%) and HFIP (n.d.) (entries 1 – 10). It is noteworthy that a significant formation of 3,3-diphenylpropanamide was detected. There is no formation of **2a** when toluene was employed as solvent with full substrate recovery (entry 11). Obviously, the co-solvent system does not improve the yield of **2a** (entries 11 – 12).

Different common oxidants such as $Cu(OAc)_2$, AgOAc, NFSI, I_2, Selectflour, and 1-fluoropyridin-1-iums are ineffective for the transformation (Table 2.3; entries 1-5, 10-12). Several *para*-substituted arenediazoniums salts (**F2**–**F4**) displayed comparable activities to initiate the amidation (Table 2.3; entries 7 – 9). Changing the quantities (15 and 50 mol%) of **F1** led to a slightly lower **2a** yield (ca. 75%) (entries 13 and 14).

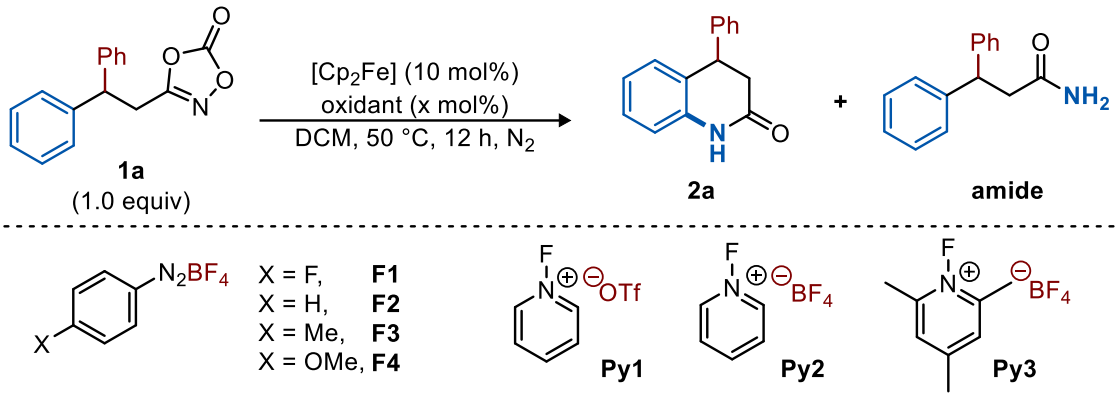
Table 2.2 Effect of Solvents[a]



entry	solvent	yield of **2a** (%)[b]	yield of amide(%)[b]
1	THF	16	<5
2	DCE	67	12
3	$CHCl_3$	65	14
4	**DCM**	**74**	**15**
5	TFE	31	<10
6	HFIP	n.d.	n.d.
7	Acetone	n.d.	n.d.
8	DMA	n.d.	n.d.
9	MeCN	n.d.	n.d.
10	toluene	n.d.	n.d.
11	DCM/TFE (1:1)	n.d.	n.d.
12	DCE/TFE (1:1)	n.d.	n.d.

[a]Reaction conditions: **1a** (0.2 mmol), ferrocene (10 mol%), **F1** (15 mol%) in solvent (2 mL) at 50 °C for 12 h under N_2; [b]^{1}H NMR yield using CH_2Br_2 as the internal standard

Table 2.3 Effect of Oxidant



entry	oxidant (x mol%)	yield of **2a** (%)[b]	yield of amide(%)[b]
1	$Cu(OAc)_2$ (25)	n.d.	n.d.
2	AgOAc (25)	n.d.	n.d.
3	I_2 (25)	n.d.	n.d.
4	NFSI (25)	n.d.	n.d.
5	Selectfluor® (25)	44	22
6	**F1 (25)**	**92**	**<5**
7	F2 (25)	84	<10
8	F3 (25)	75	<10
9	F4 (25)	85	<10
10	Py1 (25)	10	<5
11	Py2 (25)	5	<5
12	Py3 (25)	43	<10
13	F1 (15)	74	15
14	F1 (50)	77	<5

[a]Reaction conditions: **1a** (0.2 mmol), ferrocene (10 mol%), oxidant (x mol%) in solvent (2 mL) at 50 °C for 12 h under N_2; [b1]H NMR yield using CH_2Br_2 as the internal standard

2.2.2 Substrate Scope Studies

2.2.2.1 *para*-Substituted Aryl 1,4,2-Dioxazol-5-ones

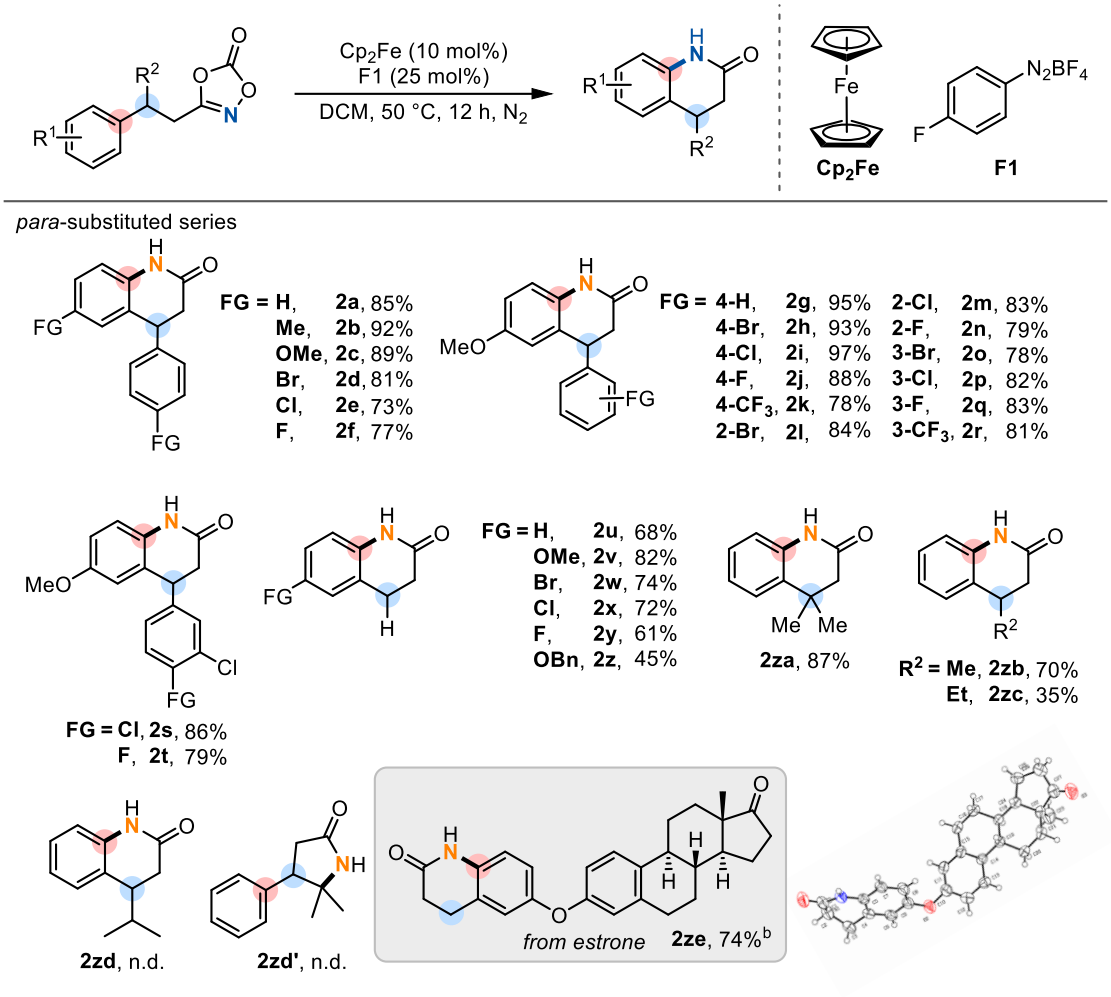
We began our scope study by examining the intramolecular C(sp^2)–H amidations of the *para*-substituted aryl 1,4,2-dioxazol-5-ones (Table 2.4). Reacting the *symmetrically* substituted-diaryl dioxazolones with Cp_2Fe (10 mol%) and **F1** (25 mol%) in DCM at 50 °C, their corresponding dihydroquinolin-2-ones **2a** – **2f** were obtained in up to 90% yields. While skeletal rearrangement may not be apparent for **2a**, all the other *para*-substituted aryl dioxazolones were transformed selectively to skeletal-rearranged dihydroquinolinones **2b** – **2f** and confirmed by ^{1}H NMR and X-ray crystallographic analysis in agreement with the reported result of the Cp*Ir(X)-catalyzed condition[73].

The amidation of the *unsymmetrically* substituted aryl dioxazolones occurred exclusively at the more electron-rich MeO-substituted aryl group (**2g** – **2t:** 78–97%), consistent with the electrophilic nature of the putative amidyl radical intermediates. It should be noted that the Fe-amidyl radical intermediate can react with the less electron-rich arene motifs. For instance, the monosubstituted aryl dioxazolone series bearing the *para*-substituents (OMe, Br, Cl, F, H, and OBn) can be transformed to their corresponding dihydroquinolinones in good yields (**2u** – **2z**). The more electron-rich MeO-substituted dioxazolones reacted to give **2v** in higher yield (82%), compared with the analogous reactions of the chloro-/fluoro-substituted derivatives (ca. 60%). As

expected, the estrone-derived dihydroquinolinone **2ze** can be obtained in 74% yield with the ferrocenium-catalyzed protocol.

Any competitive aryl versus C(sp^3)–H amidation has been assessed by employing aryl dioxazolone substrates bearing isopropyl and ethyl substituents. Under the catalytic conditions, all the cases studied gave exclusively the arene amidation products (**2az** – **2zc**).

Table 2.4 Substrate Scope Studies of Ferrocenium-Catalyzed C(sp^2)–H Amidation of *para*-Substituted Aryl 1,4,2-dioxazol-5-ones[a]



[a]Reaction conditions: dioxazolones (0.2 mmol), Cp_2Fe (10 mol%), **F1** (25 mol%), DCM (2 mL) at 50 °C for 12 h under N_2; Isolated yields. [b]24 h instead.

2.2.2.2 *ortho*-/*meta*-/ Polysubstituted Aryl 1,4,2-Dioxazol-5-ones

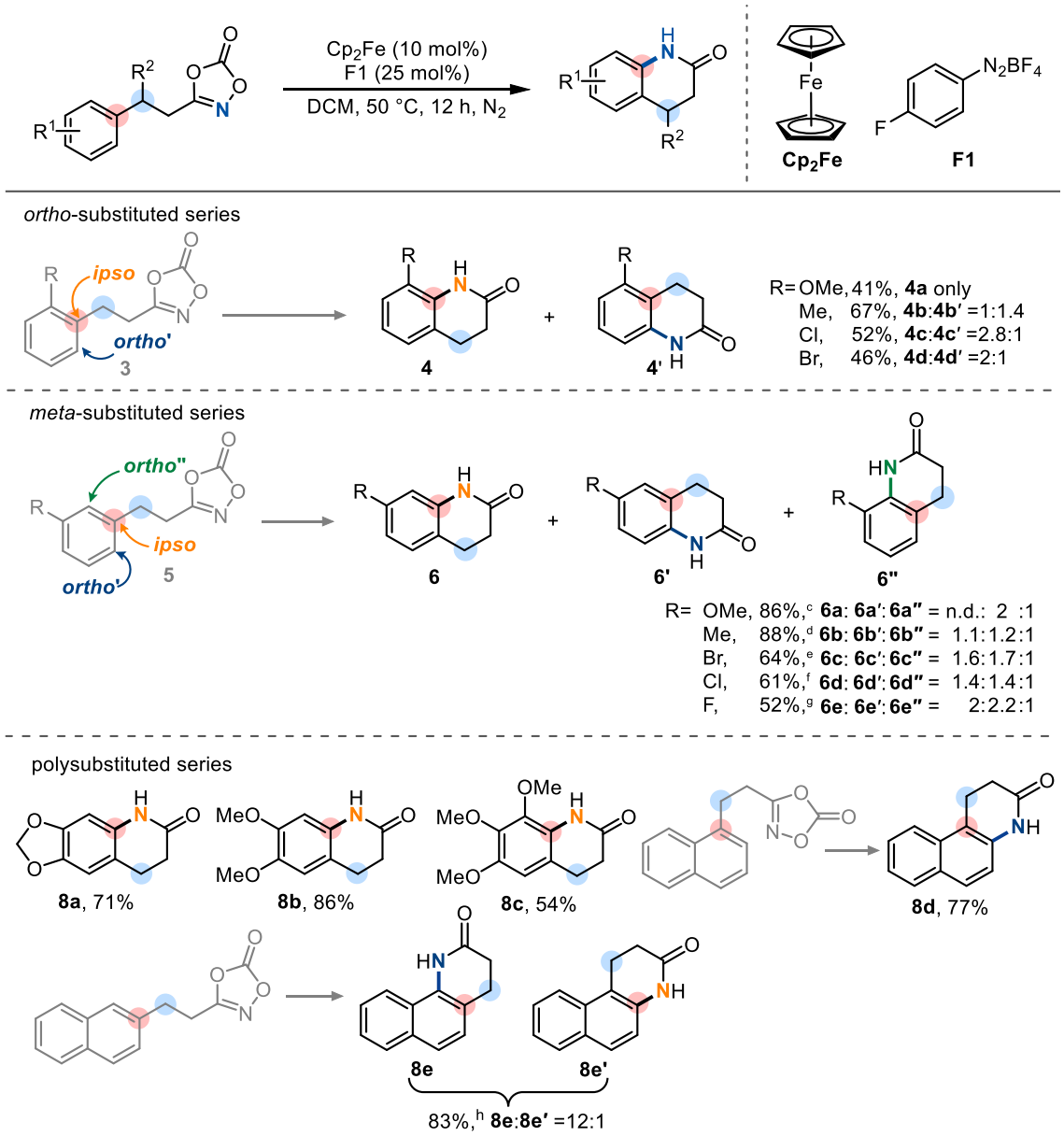
Considering the electrophilic nature of the amidyl radical, we have explored the *ortho*- and *meta*-substituted aryl dioxazolone series for a unique pattern of the *ipso* versus *ortho* selectivity. As shown in Table 2.5, the *ortho*-OMe substituted aryl dioxazolones were transformed entirely to the skeletal rearranged dihydroquinolinone product **4a** characteristic of the *ipso* addition selectivity. Those dioxazolones bearing the weakly electron-releasing Me to electron-withdrawing Cl and Br groups reacted with a lower preference for the *ipso* cyclization, and *both* the skeletal *rearranged* and *unrearranged* dihydroquinolinone products (ca. 2:1) were obtained. Plausibly the unrearranged dihydroquinolinones **4a′** – **4d′** are produced by the *ortho* cyclization pathway.

Notably, the reaction of the *meta*-methoxy substituted aryl dioxazolones *exclusively* furnished the *unrearranged* dihydroquinolinone products **6a′** and **6a″** via *ortho*- amidyl radical addition. The observed regioselectivity (**6a′**:**6a″** = 2:1) may be attributed to steric factors. Meanwhile those aryl dioxazolones bearing the weakly electron-releasing Me and the electron-withdrawing Br, Cl and F groups exhibit lower *ortho* selectivity. The *meta*-directing halogen groups would apparently favor *ipso* amidyl radical attack to afford the rearranged dihydroquinolinones **6c** – **6e**. The analogous reactions involving dioxazolones bearing polyoxygenated aryl groups

proceeded selectively by the *ortho* amidyl radical addition, and the *unrearranged* dihydroquinolinones were formed in good-to-moderate yields (**8a**: 71%; **8b**: 86%; **8c**: 54%).

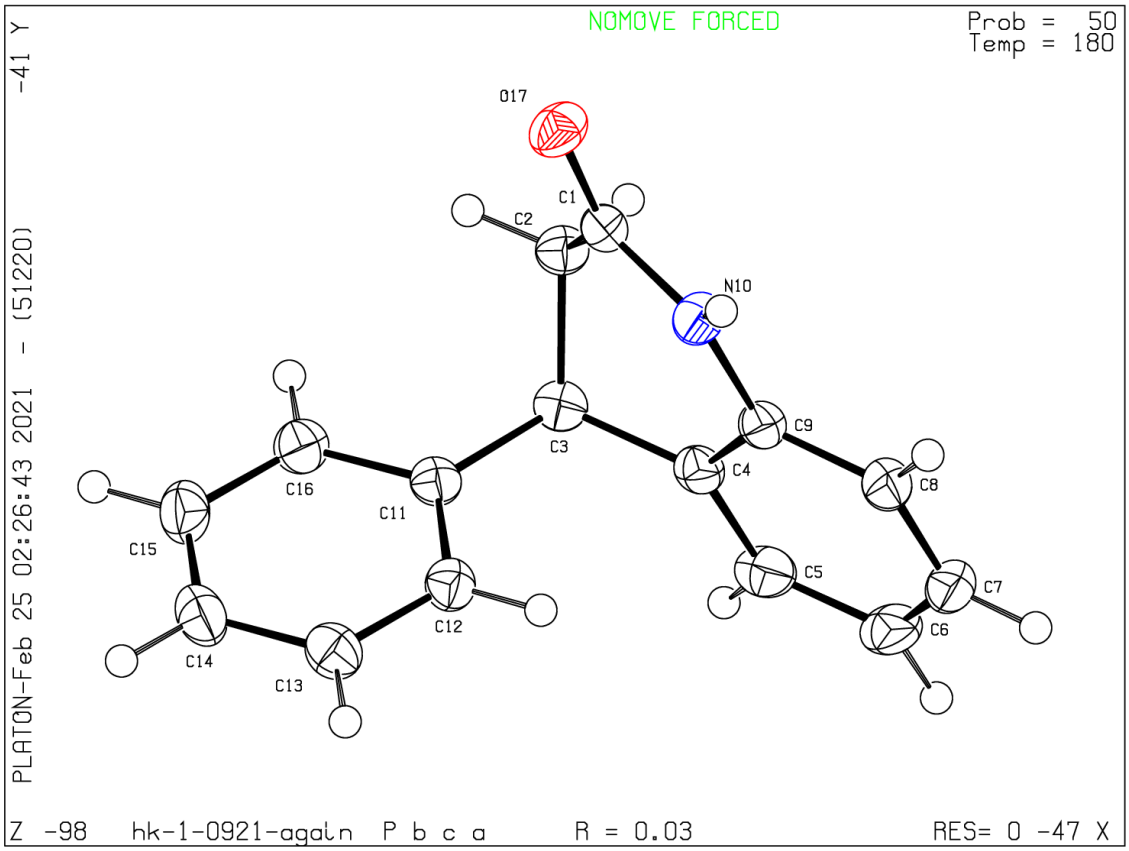
With ferrocenium as catalyst, 3-(2-(naphthalen-1-yl)ethyl)-1,4,2-dioxazol-5-one was transformed to 1,4-dihydrobenzo[*f*]quinolin-3(2*H*)-one (**8d**) in 77% yield. The **8d** formation should occur via the *ortho* amidyl radical addition to the naphthalene. Similar transformation of 3-(2-(naphthalen-2-yl)ethyl)-1,4,2-dioxazol-5-one was also observed with 3,4-dihydrobenzo[*h*]quinolin-2(1*H*)-one (**8e**) being isolated in 83% yield (**8e**:**8e′** = 12:1).

Table 2.5 Substrate Scope Studies of the Ferrocenium-Catalyzed C(sp^2)–H Amidation of *ortho*-/*meta*-/ Polysubstituted Aryl 1,4,2-dioxazol-5-ones[a]



[a]Reaction conditions: dioxazolones (0.2 mmol), Cp_2Fe (10 mol%), **F1** (25 mol%), DCM (2 mL) at 50 °C for 12 h under N_2; Isolated yields. [b]24 h instead. [c]**6a′**=**2v**; **6a″**=**4a**. [d]**6b″**=**4b**. [e]**6c′**=**2w**; **6c″**=**4d**. [f]**6d′**=**2x**; **6d″**=**4c**. [g]**6e′**=**2y**. [h]**8e′**=**8d**.

Figure 2.3 Molecular Structure of 2a (CCDC: 2143908)

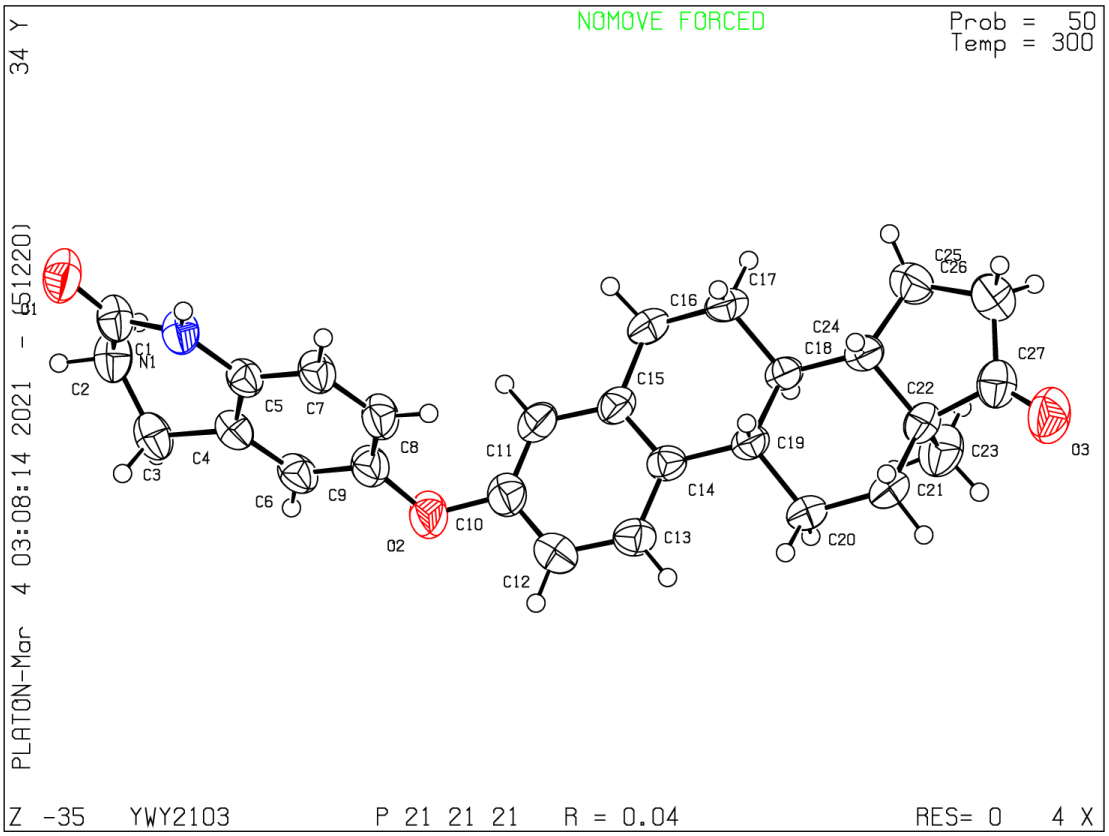


A single crystal of $C_{15}H_{13}NO$ **2a** was obtained by recrystallization over DCM/Et_2O.

Table 2.6 Crystal Data and Structure Refinement of 2a.

Compound	**2a** (**CCDC:** 2143908**)**
Formula	$C_{15}H_{13}NO$
$D_{calc.}$/ g cm^{-3}	1.324
μ/mm^{-1}	0.655
Formula Weight	223.26
T/K	180(2)
Crystal System	orthorhombic
Space Group	*Pbca*
a/Å	10.5128(4)
b/Å	7.6660(6)
c/Å	27.7880(12)
α/°	90
β/°	90
γ/°	90
V/Å^3	2239.5(2)
Z	8
Wavelength/Å	1.54184
Radiation type	CuK
Θ_{min}/°	3.181
Θ_{max}/°	77.243
F(000)	944
Measured Refl.	7513
Independent Refl.	2281
Reflections with I > 2(I)	2122
R_{int}	0.0170
Parameters	155
Restraints	0
Largest Peak	0.223
Deepest Hole	-0.178
Goodness-of-Fit	1.038
wR_2 (all data)	0.0895
wR_2	0.0880
R_1 (all data)	0.0350
R_1	0.0331

Figure 2.4 Molecular Structure of 2ze (CCDC: 2143909)



A single crystal of $C_{27}H_{29}NO_3$ **2ze** was obtained by recrystallization over DCM/Et_2O.

Table 2.7. Crystal Data and Structure Refinement of 2ze.

Compound	**2ze** (**CCDC:** 2143909)
Formula	$C_{27}H_{29}NO_3$
$D_{calc.}$/ g cm^{-3}	1.281
μ/mm^{-1}	0.656
Formula weight	415.51
T/K	300(2) K
Crystal system	Orthorhombic
space group	P 21 21 21
a/Å	7.23650(10)
b/Å	7.75950(10)
c/Å	38.3701(7)
α/°	90
β/°	90
γ/°	90
V/Å^3	2154.54(6)
Z	4
Wavelength/Å	1.54178
Radiation type	CuK
Θ_{min}/°	2.30
Θ_{max}/°	71.91
F(000)	888
Measured Refl.	9927
Independent Refl.	4224
Reflections with I > 2(I)	3860
R_{int}	0.0520
Parameters	280
Restraints	0
Largest Peak	0.154
Deepest Hole	-0.146
Goodness-of-Fit	1.052
wR_2 (all data)	0.1101
wR_2	0.1060
R_1 (all data)	0.0447
R_1	0.0397

2.3 Mechanistic Studies

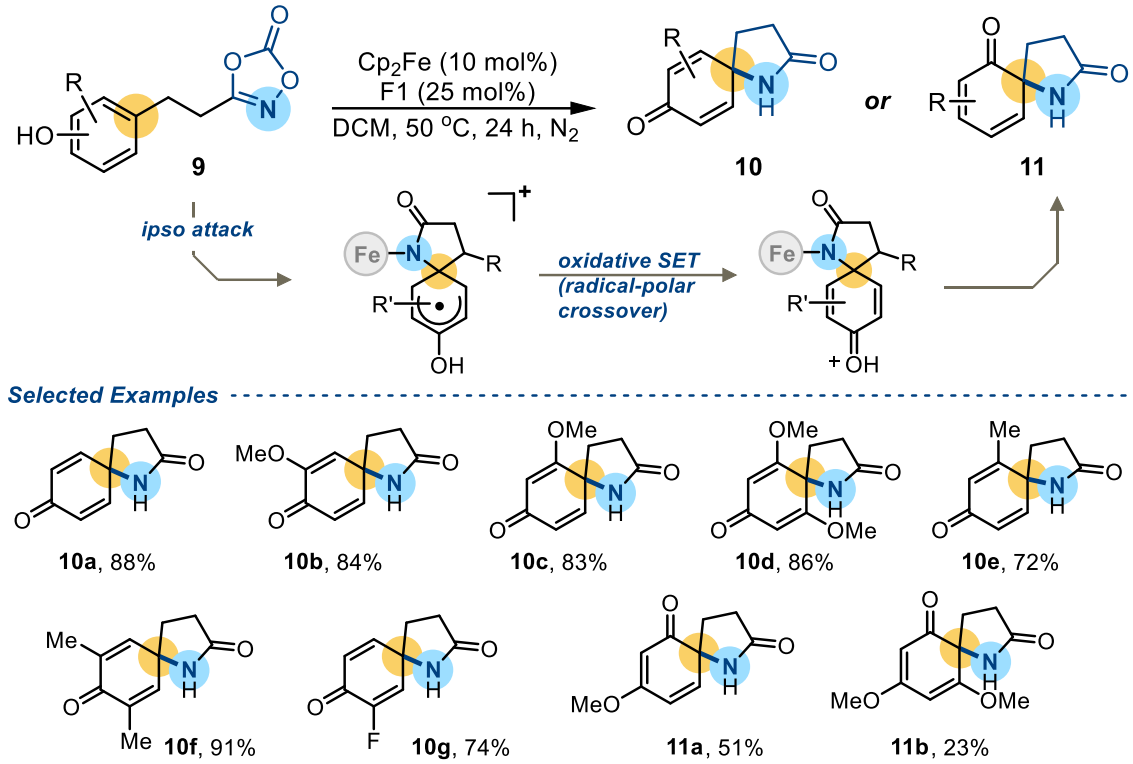
2.3.1 Probing the Nature of the Reactive Intermediate: Trapping Study

To account for the formation of the skeletal rearranged lactams, the putative amidyl radical should undergo the *ipso*-addition to the arene to give the azaspirocyclohexadienyl radical intermediate. Single-electron oxidation of the azaspirocyclohexadienyl radical intermediate should produce an arenium ion (*radical-polar crossover*), which then undergoes spontaneous 1,2-alkyl migration, followed by rearomatization to afford the rearranged dihydroquinolinone. Consistent with this mechanistic hypothesis, the spirobicyclic intermediate can be trapped using 3-(4-hydroxyphenethyl)-1,4,2-dioxazol-5-one (**9a**) as substrate. Subjecting **9a** to the ferrocenium-catalyzed conditions furnished the expected azaspiro[4.5]deca-6,9-diene-2,8-dione (**10a**) in 88% yield. Similar dearomative spirolactamization was achieved for other phenol-based dioxazolone derivatives bearing *ortho*- and *meta*- substituents. (Scheme 2.3)

Further to developing the arene C(sp^2)–H amidation reaction, we have probed the reactivity of the putative Fe(IV)-amidyl radical intermediate. According to Chang and co-workers, the related Fe(III)-amidyl radicals derived from metallophthalocyanine would undergo electrophilic addition to alkene π-bonding.[67k] In this work, when **12a** was treated with ferrocene (10 mol%), **F1** (25 mol%) and benzoic acid (3.0 equiv) in

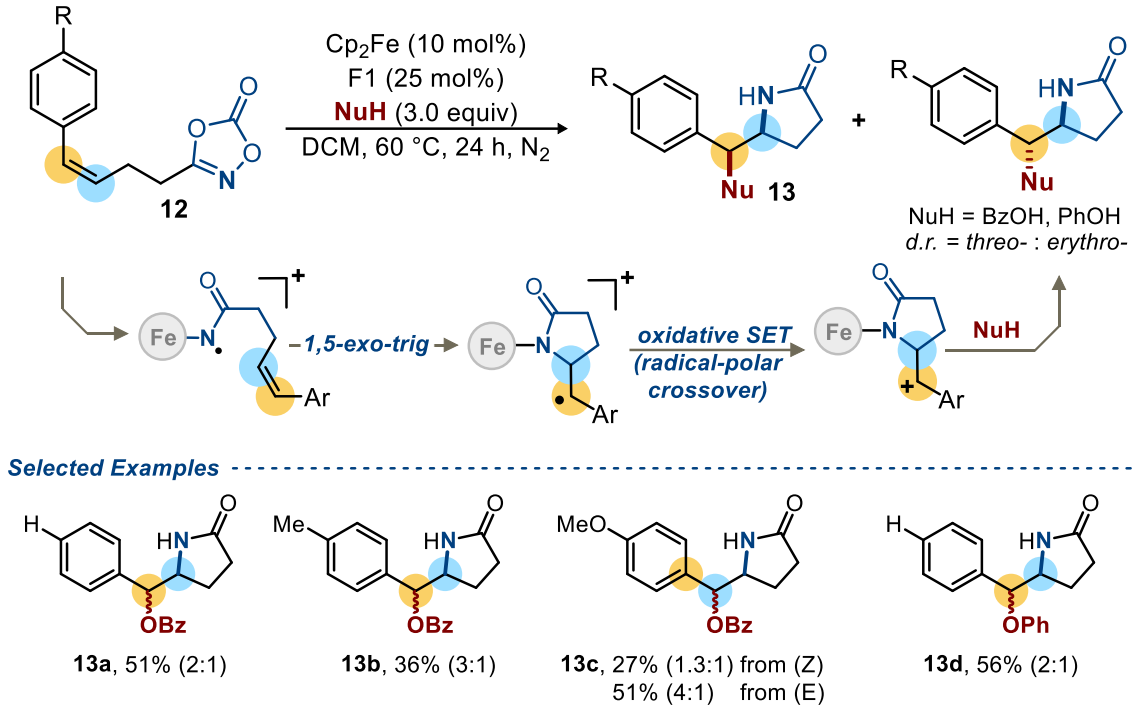
CH_2Cl_2 at 60 °C, γ-oxylactam **13a** was obtained as a mixture of *threo* and *erythro* isomers. (Scheme 2.4) By means of ^1H NMR, the major diastereomer was assigned to *threo*-configuration.[67k] Notably, when the (*Z*)-allyl dioxazolone containing a 4-methoxyphenyl substituent was treated with benzoic acid in the presence of the ferrocenium catalyst, an equimolar mixture of *threo*- and *erythro*-γ-oxylactam products **13c** was obtained. Yet, the analogous reaction of the (*E*)-allyl dioxazolone afforded the *threo*-**13c** as the major isomer (*threo*: *erthyro*= 4: 1). As anticipated, phenol effectively coupled with allyl dioxazolone to furnish the corresponding phenoxy γ-lactam in 56% yield. The observed oxyamidation results are compatible with the non-concerted electrophilic addition of the putative Fe(IV)-amidyl radical to the alkene π-bond via *5-exo-trig* cyclization. A subsequent radical-polar crossover should generate a carbocation for further nucleophilic functionalization.

Scheme 2.3 Trapping of the Azaspirocyclohexadienyl Intermediate by Dearomative Spirolactamization[a]



[a]Reaction conditions: **9** (0.2 mmol), Cp_2Fe (10 mol%), **F1** (25 mol%), DCM (2 mL) at 50 °C for 24 h under N_2; Isolated yields.

Scheme 2.4 Trapping of the Ferrocenium(IV)-Amidyl Radicals by Alkenes: Oxyamidation of Alkenes[a]



[a]Reaction conditions: **12** (0.2 mmol), Cp_2Fe (10 mol%), **F1** (25 mol%), nucleophile (3.0 equiv.) DCM (2 mL) at 60 °C for 24 h under N_2; Isolated yields; d.r. were determined by ^1H NMR of the crude reaction mixture.

2.3.2 Physical Study and Hammett Correlation Study

Apart from the trapping studies, we turned to record an X-band EPR spectrum of the "[$Cp_2Fe(III)$]BF_4 + **1a**" reaction mixture in DCM at 12 K (Figure 2.5). The spectrum displayed signals at $g_{//} \sim 2.14$ and $g_{\perp} \sim 1.88$, which are assigned to the $[Cp_2Fe]^+$ cation. Therefore, $[Cp_2Fe(III)]^+$ should be the resting state. Indeed, related Fe-amidyl radical species have been proposed recently by the Chang[67k, l] and Arnold[74] groups in their studies on the catalytic acylnitrene C(sp^3)–H amidation.

The nature of the amidyl radical-formation step was probed by Hammett correlation study employing a series of 4-substituted dioxazolones **1-Y** (Y = OMe, Me, H, F and Cl). Plotting the log k_Y/k_H (Y = OMe, Me, F and Cl) versus Hammett constant σ_{para} afforded a straight line (R^2 = 0.991) with slope (ρ) = -0.55 (Figure 2.6). The negative ρ value is consistent with electrophilic nature of the putative amidyl radical intermediate.

Figure 2.5 X-band EPR Spectrum of the "[$Cp_2Fe(III)]BF_4$ + 1a" Reaction Mixture

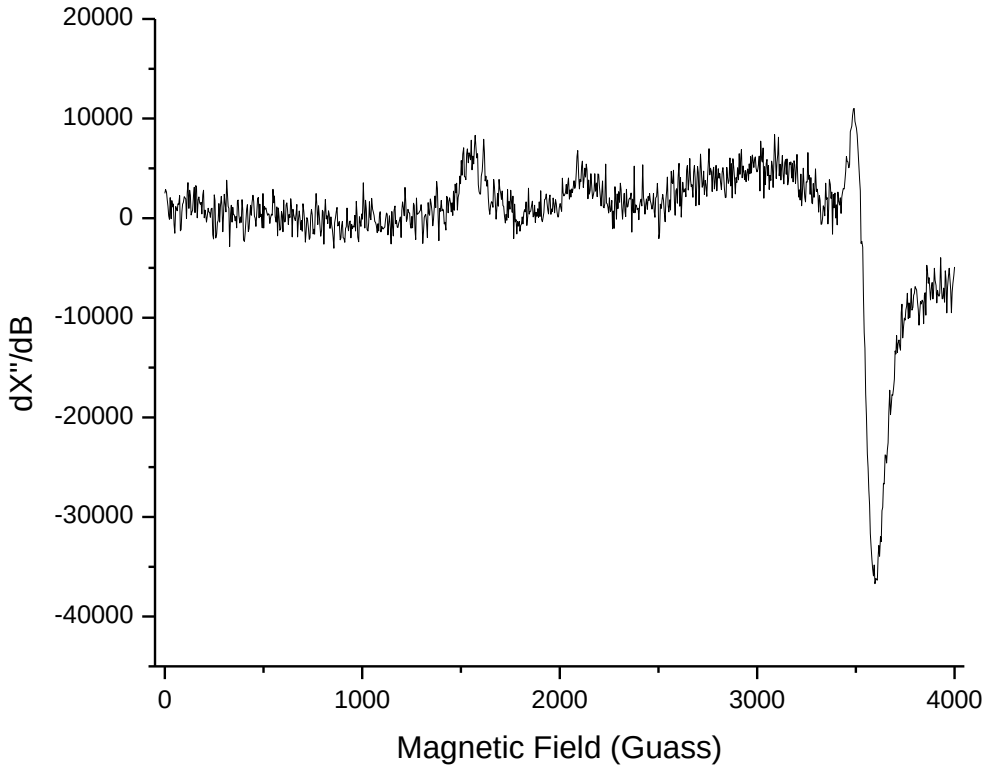
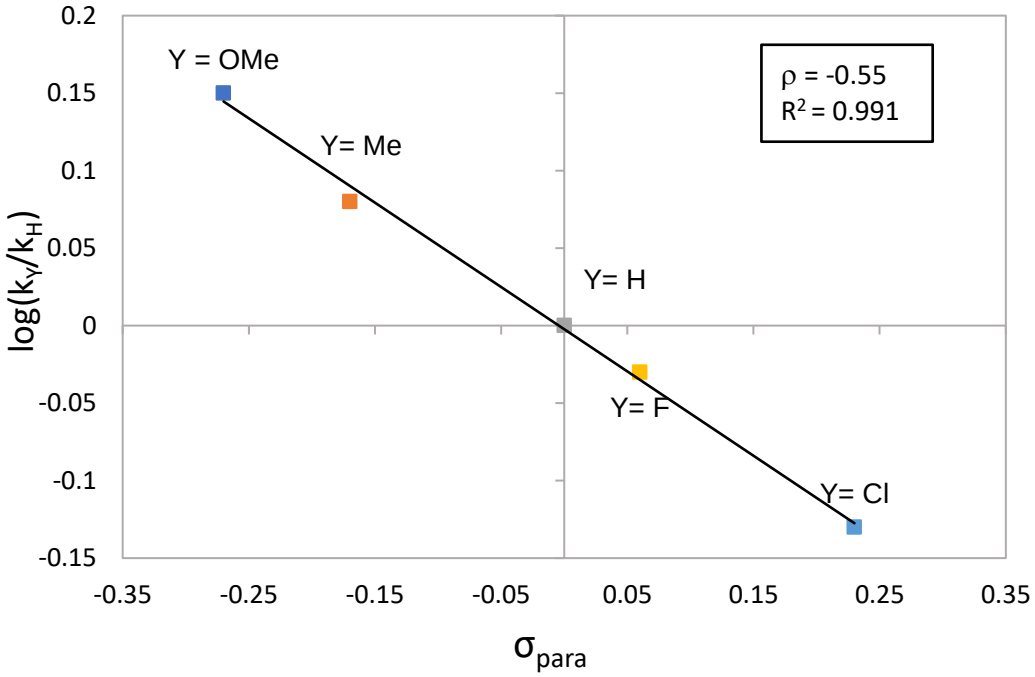


Figure 2.6 Hammett Plot of log(k_Y/k_H) versus σ_{para}



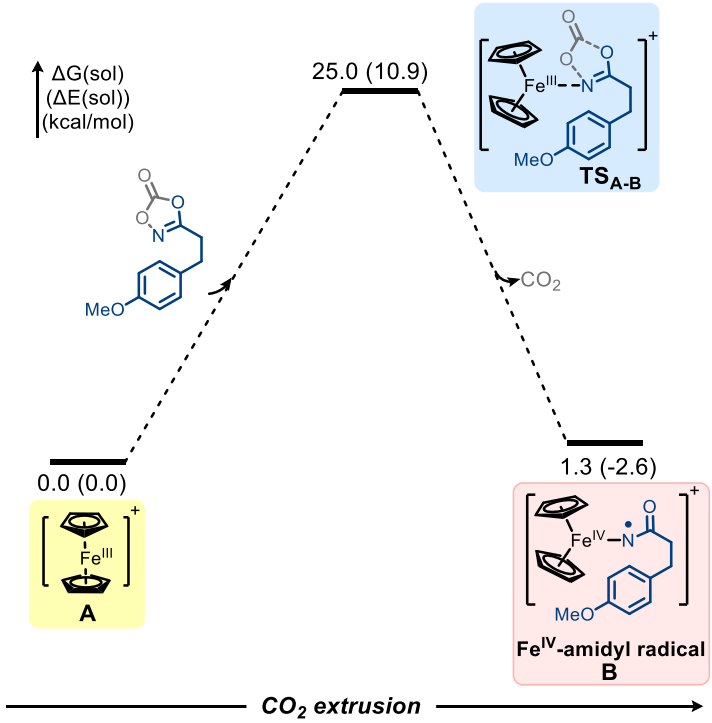
2.3.3 Computational Study

The computational study was performed by Prof. Zhenyang Lin (HKUST) and Dr. Ka-Wa Wong (PolyU). To advance a better mechanistic understanding of the amidation reaction, we pursued a computational study to address two important issues: (1) nature of the reactive nitrene species, and (2) the selectivity of *ipso* versus *ortho* arene amidation using density-functional theory (DFT) calculations at the TPSS/def2-ZTVP (Fe)/6-311++G(d,p) level of theory. Our DFT study selected the *para*-MeO-substituted aryl dioxazolone **1v** as the model substrate for simplicity.

As described in **2.3.1** & **2.3.2**, $[Cp_2Fe(III)]^+$ (**A**), generated *in situ* by single-electron oxidation of $Cp_2Fe(II)$, is the active species. Thus, we commenced our study by

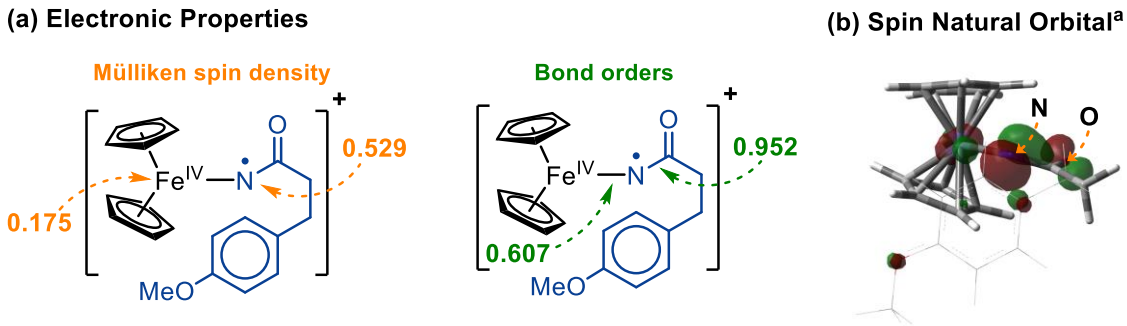
examining the reaction of $[Cp_2Fe(III)]^+$ (**A**) with the dioxazolone **1v**. As revealed in figure 2.7, the formation of the Fe-amidyl radical complex (**B**) was found to be a single-step process involving the coordination of the dioxazolone followed by the extrusion of carbon dioxide. The barrier for this process was calculated to be 25.0 kcal mol^{-1}, which is the highest among other processes in the whole catalytic cycle (*vide infra*). This result is consistent with the experimental observation that $[Cp_2Fe(III)]^+$ (**A**) is the resting state. To delineate the nature of (**B**), significant spin density was characterized at the N atom (Figure 2a): calculated Mülliken spin densities have been evaluated for the Fe center (0.175), N (0.529) and O (0.198). Based on the spin natural orbital and bond orders, the species **B** is best assigned as an Fe(IV)-amidyl radical with the sp^2-hybridized orbital of the N atom being the radical center (Figure 2.8b).

Figure 2.7 Energy Profile Calculated for the Reaction of *para*-MeO-Substituted Aryl Dioxazolone 1v Catalyzed by $[Cp_2Fe(III)]^+$ (A); Formation of the Fe-Amidyl Radical Complex (B)



[a]Relative free energies and electronic energies (in parentheses) are given in kcal/mol.

Figure 2.8 (a) Electronic Properties and (b) Spin Natural Orbital Calculated for the Fe(IV)-Amidyl Radical Complex (B)

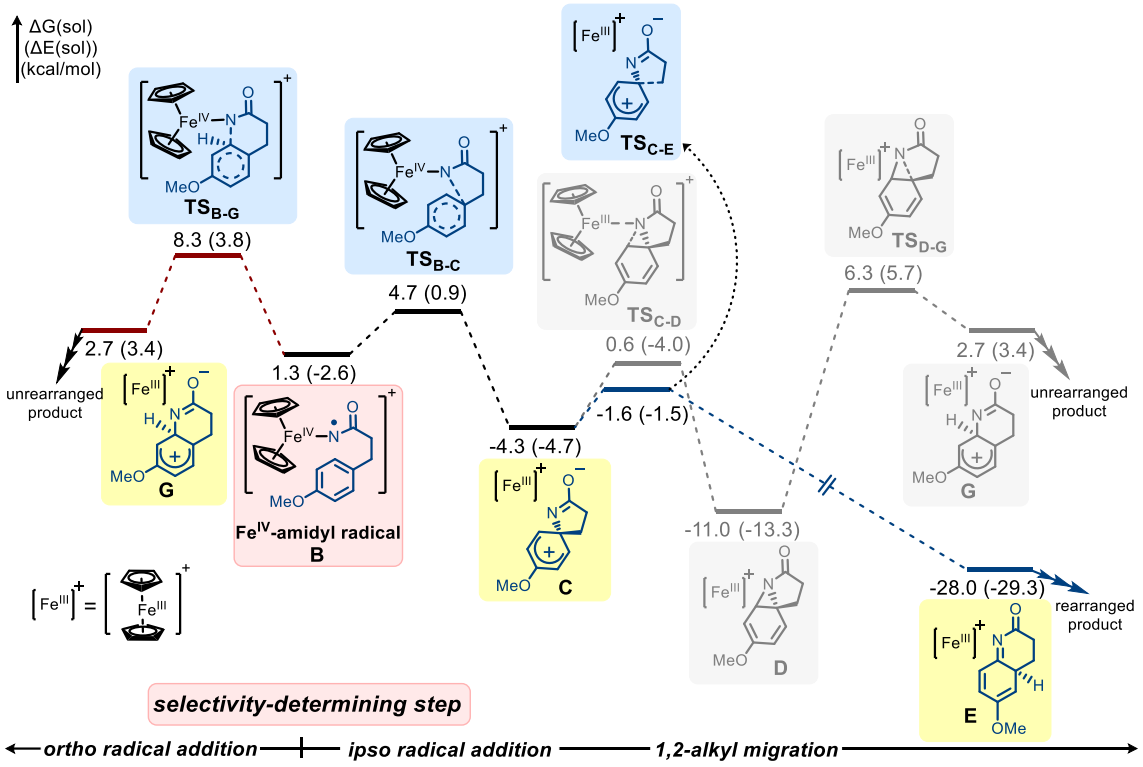


[a]The aryl group is displayed in a wireframe style.

Having established the Fe(IV)-amidyl radical as intermediate, we turned to examine the *ipso* versus *ortho* cyclization pathway selectivity (Figure 2.9). The *ortho* amidyl radical addition to the arene gives the intermediate **G** via $\mathbf{TS_{B\text{-}G}}$, followed by rearomatization via the facile BF_4^--assisted 1,2-proton migration. The *ortho*-addition pathway should produce the *unrearranged* dihydroquinolinone, the *ortho* amidation product.

Instead, the *ipso* amidyl radical addition gives an azaspirocyclohexadienyl intermediate **C** via a spirocyclic $\mathbf{TS_{B\text{-}C}}$ transition state. **C** may undergo either 1,2-N–C or 1,2-alkyl migration. Our computation showed that the 1,2-alkyl migration should be a single-step process through $\mathbf{TS_{C\text{-}E}}$, resulting in the alkyl rearranged intermediate **E**. Notably, our study revealed that the 1,2-N–C migration should be a two-step process to form an aziridinium intermediate **D**, followed by a ring-opening process to give **G**. This route should afford the unrearranged *ortho* amidation products. We thus considered that 1,2-alkyl migration should be more favorable than the analogous N–C migration. The intermediate **E** derived from the 1,2-alkyl migration would easily re-aromatize via proton migration to give *the skeletal rearranged* amidation products.

Figure 2.9 Energy Profiles Calculated for the Reaction of *para*-MeO-Substituted Aryl Dioxazolone 1v Catalyzed by $[Cp_2Fe(III)]^+$ (A); Pathway Selectivity of *ipso* versus *ortho* Amidyl Radical Addition Starting from the Fe-Amidyl Radical Complex (B)



[a]Relative free energies and electronic energies (in parentheses) are given in kcal mol^{-1}.

As revealed earlier, the *para*- (**1v**) and *ortho*-MeO-substituted (**3a**) aryl dioxazolones would favor *ipso* amidyl radical addition rather than the *ortho*-addition. Yet, the *meta*-MeO-substituted analogue reacts via *ortho*-addition to give the corresponding unrearranged dihydroquinolinone **6a′** and **6a″**. The strong electron-releasing MeO substituent appears to exert an important influence on the observed preference of the *ipso versus ortho*-addition.

To gain a deeper insight into the regioselectivity, we have performed a computational analysis of the reaction pathways for a series of aryl-substituted dioxazolones. Our computational study revealed that the arene amidation of the unsubstituted dioxazolone **1u** should afford the desired dihydroquinoline via the *ipso*- and *ortho*-amidyl radical attack with similar preference. As shown in Table 2.8, the transition state energies associated with the *ipso* (10.5 kcal mol^{-1}) and *ortho* (10.0 kcal mol^{-1}) attack of the amidyl radical are comparable.

For the analogous intramolecular arene amidations of the *para*- and *ortho*-MeO-substituted aryl dioxazolones, the amidyl radical addition was found to be predominantly biased toward the *ipso*-selectivity. Detailed analysis of the reaction landscape of the *para*- and *ortho*-MeO substituted aryl dioxazolones revealed that the rate-limiting *ipso*-addition transition states $\mathbf{TS_{B\text{-}C}}$ are particularly stabilized by the electron-releasing MeO group versus the *ortho*-addition $\mathbf{TS_{B\text{-}G}}$. Consistent with the

experimental findings, the arene amidation for the *meta*-MeO-substituted analogue would preferentially proceed via the *ortho*-addition, in which case the transition state **TS$_{B\text{-}G}$** becomes more stabilized.

For the *ortho*-X-substituted (X = Cl, Br, Me) aryl dioxazolones, the intramolecular amidations evidently exhibit a weaker preference for either *ipso*- or *ortho*-addition pathway, which contrasts with the MeO-substituted derivatives. The lack of selectivity is manifested by the comparable transition state energies associated with the *ipso*- and *ortho*-addition. The ratios of the calculated transition state energies are in good agreement with the experimental selectivity.

Regarding the product formation, rearomatization of the arenium intermediate should be critical. Based on our computational study, the BF_4^- is believed to mediate the rearomatization via proton transfer. Consistent with this finding, changing BF_4^- to PF_6^- as the counterion led to lower product yields. For instance, the reaction of **1a** with Cp_2Fe and [**F1**]BF_4 afforded **2a** in 85% yield. However, when [**F1**]PF_6 was employed as oxidant, the analogous reaction gave **2a** in 29% yield. This is attributed to the better proton-accepting properties of BF_4^- anion for promoting reversible proton transfer of the arenium ions.

Table 2.8 Relative Free Energies among the Corresponding Five Transition States Calculated for Different Monosubstituted Aryl Dioxazolones, and Comparison between the Calculated and Experimental Ratios of the *ortho* and *ipso* Amidation Products

	ΔG (kcal mol^{-1})		**Amidation product ratio *ipso* : *ortho***	
Mono-substituted aryl dioxazolone	*ipso* addition (**TS$_{B-C}$**); *1,2-alkyl* migration (**TS$_{C-E}$**)	*ortho* addition (**TS$_{B-G}$**)	DFT	Experiments
Unsubstituted	10.0; **10.5**	**10.0**	N.A.	N.A.
ortho-Cl	10.9; **11.1**	**11.2**	**1.2**:1	**2.8**:1
ortho-Br	11.0; **11.0**	**11.0**	**1**:1	**2.0**:1
ortho-Me	**10.3**; 7.6	**9.2**	1:**6.4**	1:**1.4**
ortho-MeO	**6.5**; 0.5	10.6	>200:1	*ipso* only
meta-MeO	9.7; 11.3	**6.1**	1:>200	*ortho* only
para-MeO	**4.7**; -1.6	8.3	>200:1	*ipso* only

2.4 Immobilization of Ferrocene on Silica Support

Ferrocenes are known to exhibit robust redox properties due to its structural integrity being maintained by the strong Cp–Fe bonding. By virtue of the stabilizing effect of the Cp ligand, we were prompted to examine the robustness of the ferrocene catalyst for the amidation reaction. In this regard, we prepared a heterogenous ferrocene catalyst by grafting ferrocenecarboxylic acid complex into silica gel 60 modified with (3-aminopropyl)triethoxysilane (APTES) for easy recycling of the ferrocene after the amidation.

In brief, commercial silica gel 60 (230-400 mesh) was treated with APTES in chloroform at ambient temperature for 8–12 h with vigorous stirring (Scheme 2.5). Afterwards, any unreacted silanols site on the channel wall are then covered by the treatment with hexamethyldisilazane (HMDS) in toluene for 24 h to give SiO_2-APTES, which was isolated by filtration. After washing thoroughly with toluene and hexane, the SiO_2-APTES was dried in vacuum. The heterogenous ferrocene complex was prepared by reacting SiO_2-APTES ferrocenecarboxylic acid, O-(7-azabenzotriazol-1-yl)-*N*,*N*,*N*,*N*-tetramethyluronium hexafluorophosphate (HATU) and N(Et)iPr_2 in a CH_2Cl_2 solution at room temperature for 12 h. The SiO_2-APTES-Fc was then isolated by filtration, followed by washing with CH_2Cl_2, DMF and acetone, and dried in a vacuum. The success of the grafting process is confirmed by physical analysis, such as FT-IR,

UV/vis spectroscopy and TGA, where the peaks corresponding to the ferrocene moiety are conspicuously characterized (Figure 2.10). The Fe content in the SiO_2-APTES-Fc was estimated to be 2.41 wt% by Energy Dispersive X-ray analysis (SEM-EDX).

When dioxazolone **1c** (0.2 mmol) was treated with SiO_2-APTES-Fc (24 mg) in CH_2Cl_2 in the presence of [F1]BF_4 (25 mol%) at 60 °C for 24 h, the desired dihydroquinolinone **2c** was obtained in 83% yield. For a library of representative dioxazolone substrates (Table 2.9), comparable results were obtained for the heterogeneous ferrocene catalyst.

The SiO_2-APTES-Fc catalyst has been recycled for five successive reactions with **1c** as the model substrate. For catalyst recycling, the silica-immobilized ferrocene catalyst was first isolated by filtration, followed by washing with CH_2Cl_2 and EtOAc prior to each reuse. As revealed by the product yield (ca. 80%), the activity of the catalyst sustains for at least four cycles while the significant drop in product yield (61%) was registered after the 5th reaction run. A total cumulative catalyst turnover of 333 was attained for consecutive five reaction runs.

It was noted that the product yields dropped substantially after the fifth run. A sample of the recycled catalyst after the fifth run was analyzed by SEM-EDX. The Fe content of the recycled Si-APTES-Fc is only 1.39 wt%. This result suggests that the loss of catalyst activity may be attributed to leaching or catalyst deactivation. An

ongoing study is underway to improve the robustness and activity of the immobilized ferrocene catalysts.

Scheme 2.5 Immobilization of Ferrocenecarboxylic Acid onto Silica Gel 60[75]

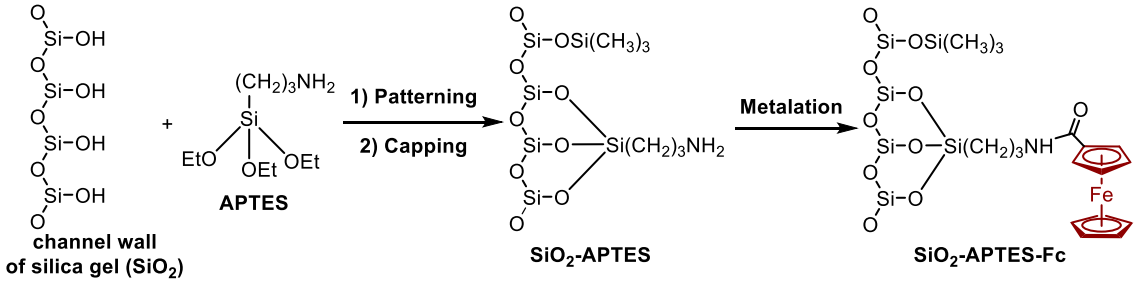


Figure 2.10 (a) Reflectance UV-Vis Spectra of SiO_2-APTES and SiO_2-APTES-Fc (b) FT-IR Spectra of SiO_2-APTES and SiO_2-APTES-Fc (c) TGA Spectrum of SiO_2-APTES (d) TGA Spectrum of SiO_2-APTES-Fc

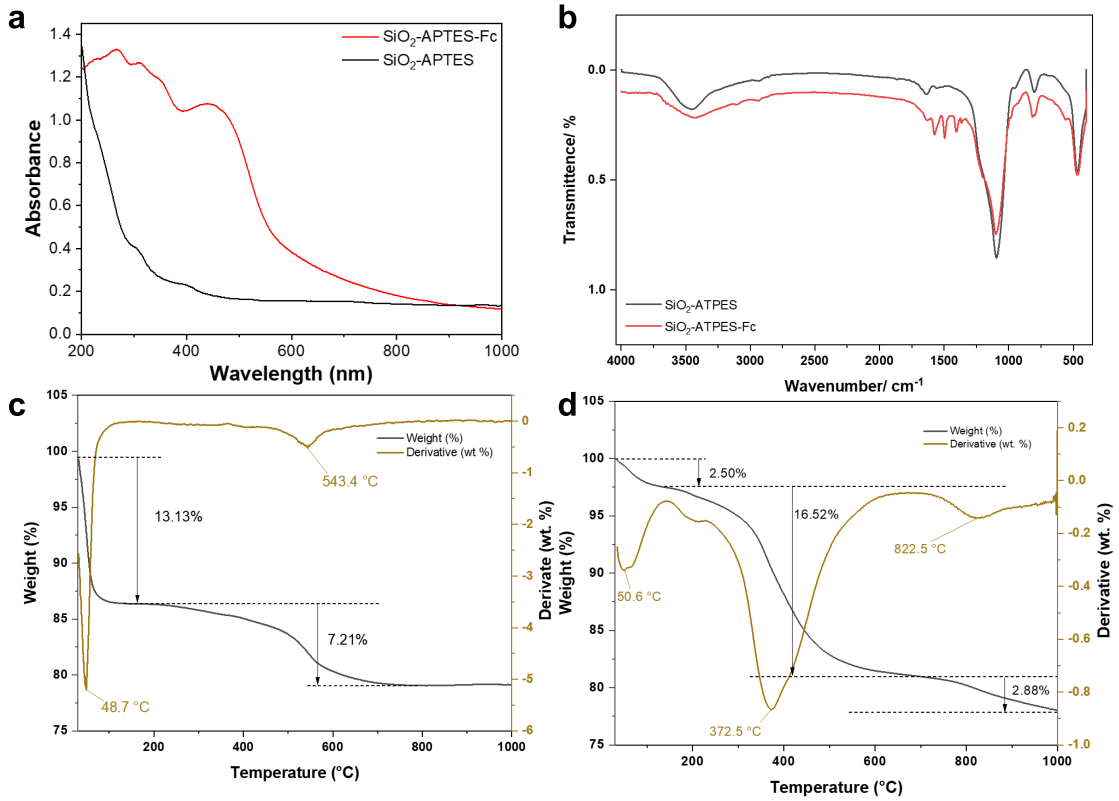
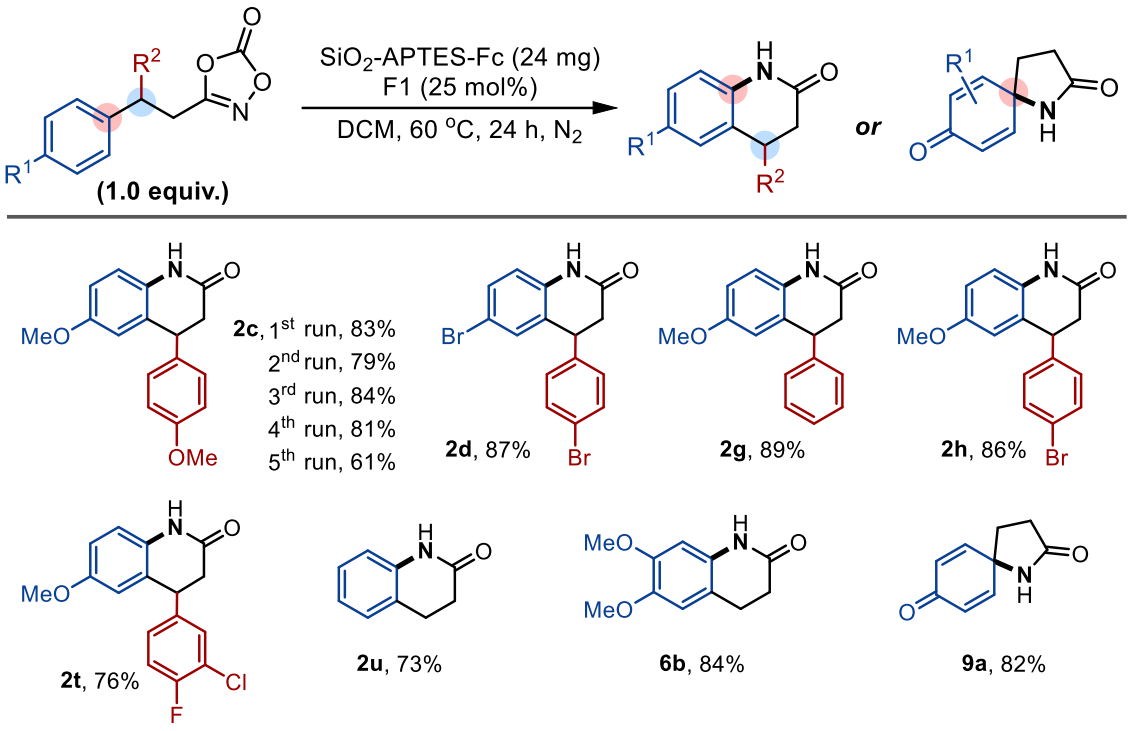


Table 2.9 SiO_2-APTES-Fc-Catalyzed Heterogeneous C(sp^2)–H Amidations [a]



[a]Reaction conditions: Dioxazolone (0.2 mmol), SiO_2-APTES-Fc (24 mg), **F1** (25 mol%), DCM (2 mL) at 60 °C for 24 h under N_2; Isolated yields.

2.5 Concluding Summary

In conclusion, we have developed ferrocenium complexes as a new class of catalysts for intramolecular arene C–H amidation using 1,4,2-dioxazol-5-ones as amidyl radical precursors. The ferrocenium-catalyzed reactions furnished dihydroquinolinones in excellent yields and selectivity. The Cp ligands render a low-spin Fe(III) configuration conducive for effective amidyl radical formation. As revealed by computational study, the amidation should be mediated by the Fe(IV)-amidyl radical intermediate. Subjecting to electronic control, the amidyl radical addition would occur by *ipso*- or *ortho*-selectivity. A heterogenous ferrocene catalyst was also prepared by simple grafting of the ferrocene onto commercially available silica; up to TON = 333 have been accomplished. We anticipate that ferrocenium would be a promising base metal catalyst for harnessing the amidyl radical reactivity for selective amide bond formation.

2.6 Experimental Section

2.6.1 General Experimental Section

All the solvents and reagents were obtained from commercial sources and used without purification unless stated otherwise. All glassware were dried overnight at 150 °C prior to use. DCM was dried with activated 3Å molecular sieves (heated at 500 °C before use) and stored in a sealed tube with N_2 protection.

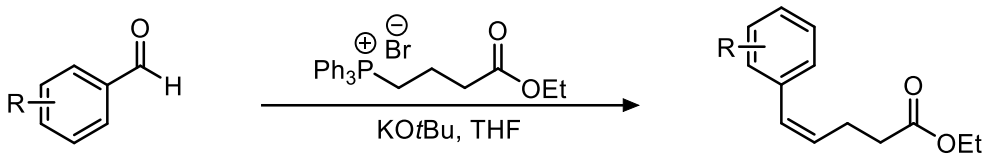
Analytical thin layer chromatography (TLC) was performed on precoated silica gel plates with aluminum backing. Visualization on TLC was achieved using UV light (254 nm) or treatment with potassium permanganate solution followed by heating. Flash column chromatography was performed on a silica gel (Merck, 230-400 mesh) column. ^{1}H, ^{13}C, ^{19}F, and ^{31}P NMR spectra were recorded on a Brüker DPX-400 MHz spectrometer. The chemical shift (δ) values were given in ppm and are referenced to residual solvent peaks; carbon multiplicities were determined by DEPT-135 experiments. Coupling constants (*J*) were reported in hertz (Hz). The NMR yields were determined using dibromomethane as internal standard unless stated otherwise. Mass spectra and high-resolution mass spectra (HRMS) were obtained on a VG MICROMASS Fison VG platform, a Finnigan Model Mat 95 ST instrument, or a Bruker APEX 47e FT-ICR mass spectrometer, or Waters Acquity UPLC H-Class-QDa System. Single Crystal Data collection was performed by a Bruker-AXS diffractometer

(see crystallographic section for details). The structure was solved by SHELXT and refined by the full-matrix least-squares (SHELXL) method. The thermogravimetric analysis (TGA) measurements of as-synthesized samples were performed in N_2 (250 mL min^{-1}) from 30 °C to 1000 °C (10 K min^{-1}) using Thermogravimetric analyzer /Differential Scanning Calorimeter (Mettler Toledo TGA/DSC^{3+}). The Fourier-Transform infrared spectroscopy (FT-IR) data measurements in an attenuated total reflection (ATR) mode was recorded using Thermo Scientific Nicolet iS50 FTIR spectrometer equipped with a single bounce diamond crystal and a deuterated triglycine sulfate (DTGS) detector. The scanning electron microscopy (SEM) images were obtained by TESCAN MIRA LMS (Brno, Czech Republic) for surface morphology study. Before scanning, the samples were coated with a thin layer of gold and then inspected with an accelerating voltage of 5 keV. The Ultraviolet-Visible-Near-Infrared diffuse reflectance spectroscopy (UV-vis-NIR DRS) measurements were carried out with the obtained samples using PerkinElmer Lambda 1050-UV-Vis-NIR spectrophotometer with an Integrating Sphere-150 mm UVvis-NIR (InGaAs) Module. The equipment was calibrated using Spectralon standard and the reflectance was measured in the 200-2500 nm range at an interval of 1 nm. The X-ray photoelectron spectroscopy (XPS) measurements were performed using a Thermo Fisher Scientific K-Alpha spectrometer (Al Kα radiation, hν = 1486.6 eV). The XPS spectra were

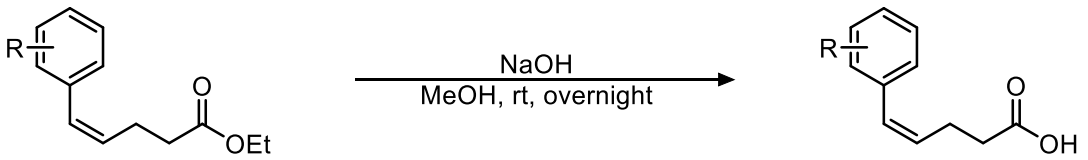
obtained at approximately 20 nm depth intervals. The raw data were corrected for substrate charging with the binding energy of the C 1s peak at 284.5 eV.

2.6.2 Experimental Procedures and Physical Characterizations

2.6.2.1 General Procedure for the Preparation of Alkenoic Acid

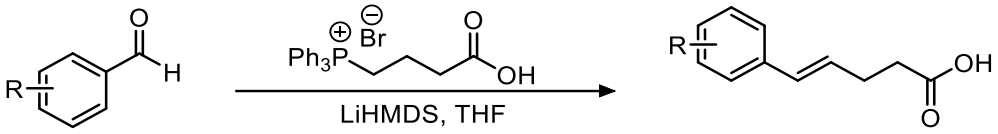


A mixture of (4-ethoxy-4-oxobutyl)triphenylphosphonium bromide (4.3 g, 9.5 mmol) and potassium tert-butoxide (1.1 g, 9.5 mmol) in THF (20 mL) was stirred at 0 ℃ for 30 min. The resulting mixture was allowed to warm to ambient temperature and stirred for additional 1 h. The solution was again cooled to 0 ℃, and 4-substituted-benzaldehyde (7.9 mmol) was added dropwise. The solution was stirred at ambient temperature for 5 h. The resulting mixture was quenched with H_2O, and then the aqueous layers were extracted with Et_2O (20 mL×3). The organic layers were washed with brine, dried over Na_2SO_4, and concentrated *in vacuo*. Evaporation followed by column chromatography afforded ethyl (*Z*)-5-(substituted-phenyl)pent-4-enoate (Z: E = >20: 1).



A mixture of ethyl (*Z*)-5-(substituted-phenyl)pent-4-enoate (2 mmol) and NaOH (0.2 g, 5 mmol) in MeOH (20 mL) was stirred at room temperature for overnight. The solvent was removed by under rotatory evaporation. H_2O (50 mL) was added to the

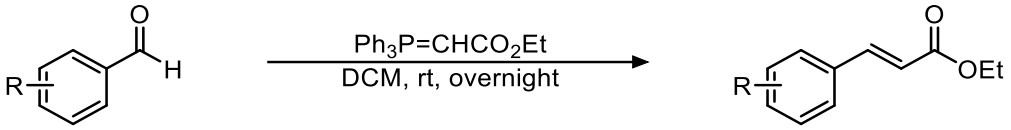
residue and the aqueous layer was extracted with EtOAc (3 x 50 mL). The ethyl acetate layers were discarded while the H_2O layer was acidified to pH 1 using HCl (1.0 M). The acidified aqueous layer was further extracted with ethyl acetate (3 x 20 mL). The combined organic extracts were dried with $MgSO_4$ and concentrated to dryness to give the corresponding carboxylic acid, which was used for the next step without further purification.



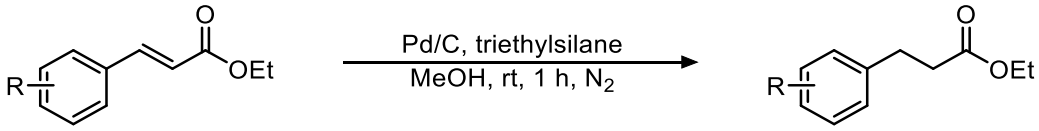
(3-Carboxypropyl)triphenylphosphonium bromide (10.8 mmol, 1.08 equiv) was first suspended in THF (40 mL) at -20 °C. LiHMDS (20.16 mmol, 2.16 equiv) was added into the suspension in dropwise manner and further stirred for 20 min. The mixture was then cooled to -78 °C and the corresponding aldehyde (10 mmol, 1.0 equiv) was added. After stirred for 18 hours, the solvent was removed *in vacuo*. H_2O (80 mL) was added to the residue and extracted with ethyl acetate (3 x 20 mL). The organic layers were discarded, and the aqueous layer was acidified to pH 2 using HCl (1.0 M). The acidified aqueous layer was further extracted with ethyl acetate (3 x 20 mL). The combined organic extracts were dried with $MgSO_4$ and concentrated to dryness. The crude mixture was purified by flash chromatography (n-hexane/EtOAc = 1:1) to obtain corresponding (*E*)-alkenoic acid (E: Z = >20: 1).

2.6.2.2 General Procedure for the Preparation of 1,4,2-Dioxazol-5-ones

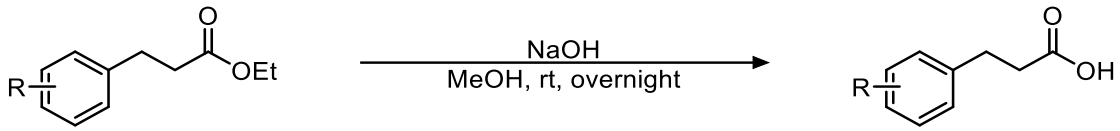
Method A:



To a solution of benzaldehyde (10 mmol) in DCM (50 mL) was added ethyl (triphenylphosphoranylidene) acetate (5.015 g, 1.5 equiv) at 0 °C in several batches. The reaction mixture was stirred at room temperature overnight. To work-up, the solvent was removed by rotatory evaporation, and the residue was purified by flash chromatography to obtain the desired ethyl cinnamate products (E: Z = 10: 1).

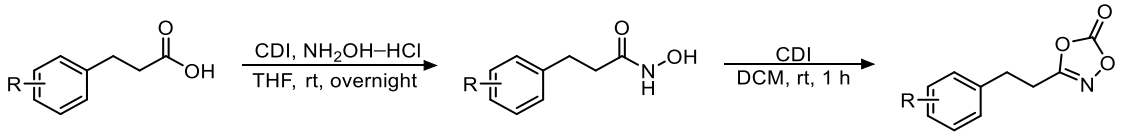


To a suspension of ethyl cinnamates (1.2 mmol) and 10 % Pd/C (100 mg) in MeOH (5 mL) was added triethylsilane (1.8 mL, 11.7 mmol) in a dropwise manner under an N_2 atmosphere. After the addition, the reaction mixture was stirred at room temperature for 1 h. The reaction crude mixture was filtered through Celite® and concentrated by rotatory evaporation. The desired ethyl ester products were purified by short silica gel column chromatography.



The ethyl esters (2 mmol) and NaOH (0.2 g, 5 mmol) were dissolved in MeOH (20 mL) and then stirred at room temperature. After standing for overnight, the solvent was

removed by under rotatory evaporation. Water was added to the residue and then 1M HCl was added to the mixture until pH = 1 being reached. The aqueous layer was extracted with EtOAc (3 x 50 mL) and the combined organic extracts were dried with $MgSO_4$. The solvent was removed by rotatory evaporation to give the corresponding carboxylic acid, which can be used for next step without further purification.

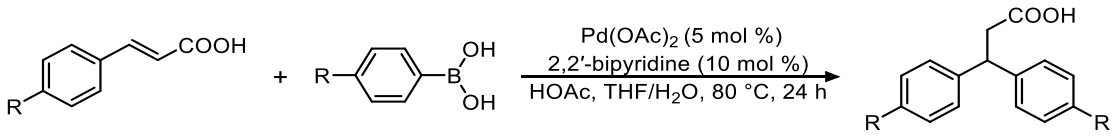


To a solution of corresponding carboxylic acid (2 mmol) in dry THF (15 mL) was added CDI (486.45 mg, 1.5 equiv). The reaction mixture was stirred at room temperature for 1 h. After 1 h, hydroxylamine hydrochloride (4 mmol) was added into reaction mixture. The resulting mixture was stirred at room temperature overnight. The reaction was quenched by 5 % $KHSO_4$(aq) (20 mL). The aqueous layer was extracted with EtOAc (3 x 50 mL). The combined organic extract was washed with brine (20 mL) and dried with $MgSO_4$. The organic extract was filtered and concentrated by rotatory evaporation to obtain the corresponding hydroxamic acid which was used without further purification.

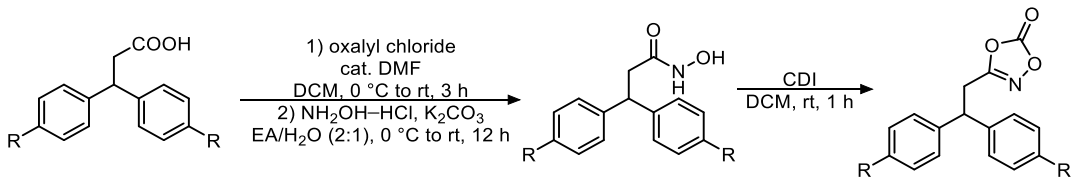
The hydroxamic acid (2 mmol) and CDI (356.8 mg, 1.1 equiv) were dissolved in DCM (20 mL) and stirred at room temperature for 30 min. Then, 1M HCl (3 mL) was added into reaction mixture and stirred at room temperature for another 1 h. After that, the organic layer was separated, and the aqueous phase was extracted with DCM (3 x

20 mL). The combined organic extracts were dried by $MgSO_4$ and concentrated under rotatory evaporation. The crude mixture was purified by flash chromatography (n-hexane/EtOAc = 2:1) to obtain 3-substituted-aryl-1,4,2-dioxazol-5-ones.[2-4]

Method B:



Cinnamic acids (5 mmol), arylboronic acids (2.0 equiv), $Pd(OAc)_2$ (56.1 mg, 5 mol %) and 2,2′-bipyridine (78.1 mg, 10 mol %) were mixed in HOAc (5 mL), THF (10 mL) and H_2O (3 mL) and stirred at 80 °C for 24 h. THF and HOAc were removed under vacuum at 100 °C after the reaction. The reaction crude was cooled to 60 °C and then H_2O (5 mL) was added into the reaction crude at 60 °C. After cooling to room temperature, the aqueous layer was extracted by chloroform. The combined organic layer was dried with $MgSO_4$. After removal of the solvent, the products were purified by flash chromatography (n-hexane/EtOAc = 7:3, R_f = 0.3) and the spectral characterization data are consistent with the reported literature data.

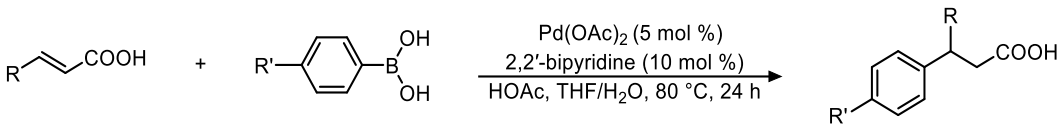


To a DCM (30 mL) solution of carboxylic acid (2 mmol) was added oxalyl chloride (0.34 mL, 2.0 equiv) at 0 °C in a dropwise manner, and DMF (0.2 mL) was added to the mixture. After stirring the mixture at room temperature for 3 h, the solvent

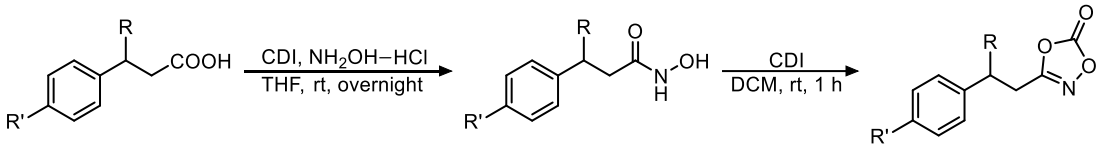
and excess oxalyl chloride were removed by vacuum distillation. K_2CO_3 (2.0 equiv, 552.8 mg) was dissolved in EtOAc/H_2O = 2:1 (16 mL of EtOAc and 8 mL of H_2O) and then cooled to 0 °C. The hydroxylamine hydrogen chloride (1.2 equiv, 166.8 mg) was added into the K_2CO_3 solution. The corresponding unpurified acid chloride obtained were dissolved in DCM (5 mL) and was transferred to the reaction mixture. The reaction mixture was stirred at room temperature for overnight. To work-up, the distillated water (30 mL) was added into reaction mixture and the organic layer was separated. The aqueous phase was extracted with EtOAc (3 x 50 mL) and the combined organic extracts were dried with $MgSO_4$. The solvent was evaporated by rotatory evaporation to obtain the corresponding hydroxamic acid which was used without further purification.

The hydroxamic acid (2 mmol) and CDI (1.1 equiv, 356.8 mg) were dissolved in DCM (20 mL) and stirred at room temperature for 30 min. Then, 1M HCl (3 mL) was added to the reaction mixture and stirred at room temperature for another 1 h. After that, the organic layer was separated, and the aqueous phase was extracted with DCM (3 x 20 mL). The combined organic extracts were dried over anhydrous $MgSO_4$ and concentrated by rotatory evaporation. The crude mixture was purified by flash chromatography (n-hexane/EtOAc = 9:1) to obtain 3-substituted-(2,2-diarylethyl)-1,4,2-dioxazol-5-ones.

Method C



Carboxylic acids (5 mmol), arylboronic acids (2.0 equiv), $Pd(OAc)_2$ (56.1 mg, 5 mol %) and 2,2′-bipyridine (78.1 mg, 10 mol %) were mixed in HOAc (5 mL), THF (10 mL) and H_2O (3 mL) and stirred at 80 °C for 24 h. THF and HOAc were removed under vacuum at 100 °C after the reaction. The reaction crude was cooled to 60 °C and then of H_2O (5 mL) was added to the reaction crude at 60 °C. After cooling to room temperature, the aqueous layer was extracted by chloroform. The combined organic layer was dried with $MgSO_4$. After removal of the solvent, the products were purified by flash chromatography (n-hexane/EtOAc = 7:3, R_f = 0.3) and the spectral characterization data are consistent with the reported literature data.

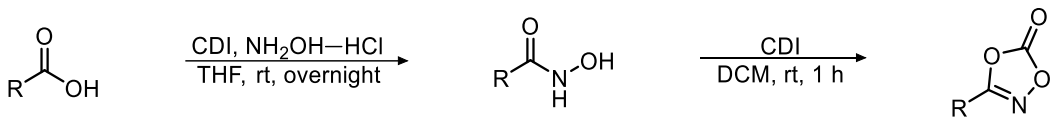


To a solution of corresponding carboxylic acid (2 mmol) in dry THF (15 mL) was added CDI (486.45 mg, 1.5 equiv). The reaction mixture was stirred at room temperature for 1 h. After 1 h, hydroxylamine hydrochloride (4 mmol) was added to the reaction mixture. The resulting mixture was stirred at room temperature overnight. The reaction was quenched by 5 % $KHSO_4$(aq) (20 mL). The aqueous layer was extracted with EtOAc (3 x 50 mL). The combined organic extract was washed with

brine (20 mL) and dried with $MgSO_4$. The organic extract was filtered, and the volume was concentrated by rotatory evaporation to obtain the corresponding hydroxamic acid for use without further purification.

The hydroxamic acid (2 mmol) and CDI (1.1 equiv, 356.8 mg) were dissolved in DCM (20 mL), and the mixture was stirred at room temperature for 30 min. After 30 min, 1M HCl (3 mL) was added to the reaction mixture and stirred at room temperature for another 1 h. After that, the organic layer was separated, and the aqueous phase was extracted with DCM (3 x 20 mL). The combined organic extracts were dried by $MgSO_4$ and were concentrated by rotatory evaporation. The crude mixture was purified by flash chromatography (n-hexane/EtOAc = 9:1) to obtain 3-substitutedaryl-1,4,2-dioxazol-5-ones.

Method D

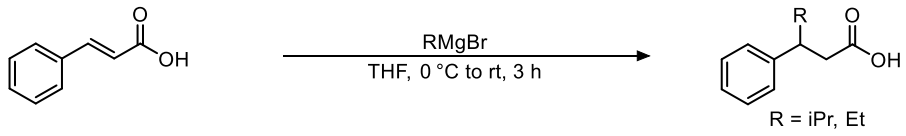


To a solution of corresponding carboxylic acids (2 mmol) in dry THF (15 mL) was added CDI (486.45 mg, 1.5 equiv). The reaction mixture was stirred at room temperature for 1 h. After stirring for 1 h, hydroxylamine hydrochloride (4 mmol) was added to the reaction mixture. The resulting mixture was stirred at room temperature for overnight. The reaction was quenched by 5 % $KHSO_4$(aq) (20 mL). The aqueous layer was extracted with EtOAc (3 x 50 mL). The combined organic extracts were

washed with brine (20 mL) and dried with $MgSO_4$. The organic extract was filtered, and the volume was concentrated by rotatory evaporation to obtain the corresponding hydroxamic acid for use without further purification.

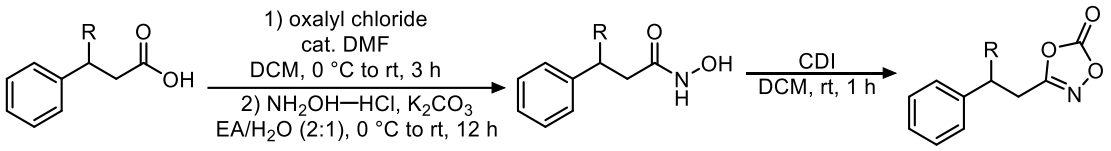
The hydroxamic acid (2 mmol) and CDI (356.8 mg, 1.1 equiv) were dissolved in DCM (20 mL), and the mixture was stirred at room temperature for 30 min. After addition of 1 M HCl (3 mL), the reaction mixture was stirred at room temperature for another 1 h. After that, the organic layer was separated, and the aqueous phase was extracted with DCM (3 x 20 mL). The combined organic extracts were dried by $MgSO_4$, and the volume was concentrated by rotatory evaporation. The crude mixture was purified by flash chromatography (n-hexane/EtOAc = 1:9) to obtain 3-substituted aryl-1,4,2-dioxazol-5-ones.

Method E



To a solution of cinnamic acid (2 mmol) in dry THF (2 mL) was cooled to 0 °C. The EtMgBr (3.0 M in THF, 2 mL, 6 mmol) or *i*PrMgCl (2.0 M in THF, 3 mL, 6 mmol) was then transferred to the reaction mixture in a dropwise manner at 0 °C. After that, the reaction crude was allowed to stand at room temperature and stirred for addition 3 h. After 3 h, 6M HCl (1.5 mL) was added to the reaction mixture at 0 °C. The aqueous layer was extracted with diethyl ether (2 x 10 mL) and the combined organic extracts

were dried over anhydrous $MgSO_4$. The solution was concentrated by rotatory evaporation, and the residue was used without further purification.

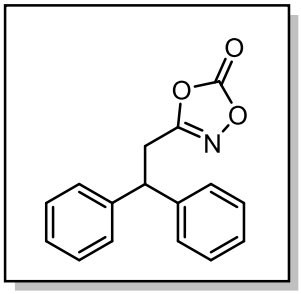


To a solution of carboxylic acid (2 mmol) in DCM (30 mL) was cooled to 0 °C. Oxalyl chloride (2.0 equiv, 0.34 mL) was then transferred to the reaction mixture in a dropwise manner at 0 °C. Subsequently, DMF (0.2 mL) was added to the mixture, and the reaction mixture was allowed to stir for 3 h at room temperature. Then, the solvent and the excess oxalyl chloride were removed by vacuum distillation. K_2CO_3 (2.0 equiv, 552.8 mg) was then dissolved in EtOAc/H_2O = 2:1 (16 mL of EtOAc and 8 mL of H_2O) and then cooled to 0 °C. Hydroxylamine hydrogen chloride (1.2 equiv, 166.8 mg) was added to the K_2CO_3 solution. The corresponding crude acyl chloride obtained was dissolved in DCM (5 mL) and transferred to the reaction mixture. The reaction mixture was allowed to stir for overnight at room temperature. To work-up, distillated water (30 mL) was added to the reaction mixture and the organic layer was collected. The aqueous phase was extracted with EtOAc (3 x 50 mL), and the combined organic extracts were dried over anhydrous $MgSO_4$. The solvent was removed by rotatory evaporation to obtain the crude hydroxamic acid, which was used without further purification.

The hydroxamic acid (2 mmol) and CDI (1.1 equiv, 356.8 mg) were dissolved in DCM (20 mL) and stirred at room temperature for 30 min. Then, 1M HCl (3 mL) was added into the reaction mixture, which was then stirred for an additional 1 h. To work-up, the organic layer was collected by separation, and the aqueous phase was extracted with DCM (3 x 20 mL). The combined organic extracts were dried over anhydrous $MgSO_4$, and the solvent was removed by rotatory evaporation. The crude residue was purified by flash chromatography (n-hexane/EtOAc = 9:1).

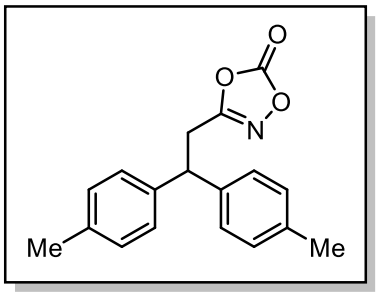
2.6.2.3 Physical Characterization of Dioxazolones

3-(2,2-Diphenylethyl)-1,4,2-dioxazol-5-one (1a)[66c]–Prepared by Method B



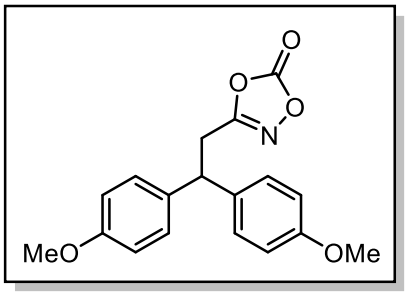
White solid; ^{1}H NMR (400 MHz, CD_2Cl_2) δ 7.39 – 7.32 (m, 4H), 7.32 – 7.24 (m, 6H), 4.51 (t, *J* = 8.2 Hz, 1H), 3.44 – 3.40 (m, 2H). ^{13}C NMR (101 MHz, CD_2Cl_2) δ 165.3, 153.9, 141.6, 128.9, 127.4, 127.3, 46.7, 31.0.

3-(2,2-Di-*p*-tolylethyl)-1,4,2-dioxazol-5-one (1b)[66c]–Prepared by Method B



White solid; ^{1}H NMR (400 MHz, $CDCl_3$) δ 7.12 (s, 8H), 4.40 (t, *J* = 8.2 Hz, 1H), 3.32 (d, *J* = 8.2 Hz, 2H), 2.31 (s, 6H). ^{13}C NMR (101 MHz, $CDCl_3$) δ 165.2, 153.9, 138.5, 137.0, 129.6, 127.2, 46.0, 31.3, 21.0.

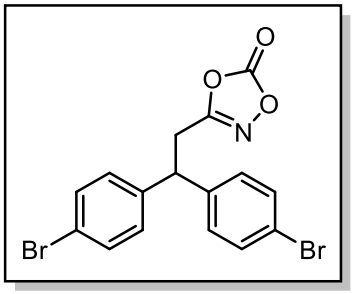
3-(2,2-Bis(4-methoxyphenyl)ethyl)-1,4,2-dioxazol-5-one (1c)[66c]–Prepared by Method B



White solid; ^{1}H NMR (400 MHz, $CDCl_3$) δ 7.13 (d, *J* = 8.7 Hz, 4H), 6.85 (d, *J* = 8.7 Hz, 4H), 4.38 (t, *J* = 8.2 Hz, 1H), 3.78 (s, 6H), 3.29 (d, *J* = 8.3 Hz, 2H).

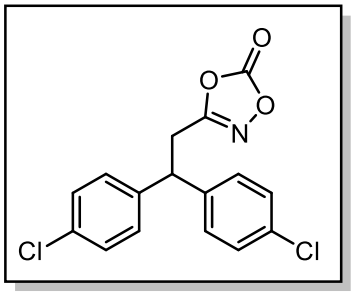
^{13}C NMR (101 MHz, $CDCl_3$) δ 165.2, 158.7, 153.9, 133.7, 128.4, 114.3, 55.3, 45.2, 31.6.

3-(2,2-Bis(4-bromophenyl)ethyl)-1,4,2-dioxazol-5-one (1d)[66c]–Prepared by Method B



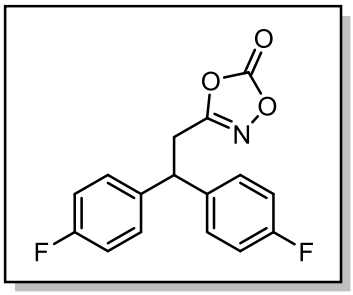
White solid; ^{1}H NMR (400 MHz, $CDCl_3$) δ 7.46 (d, *J* = 8.4 Hz, 4H), 7.09 (d, *J* = 8.4 Hz, 4H), 4.41 (t, *J* = 8.2 Hz, 1H), 3.31 (d, *J* = 8.2 Hz, 2H). ^{13}C NMR (101 MHz, $CDCl_3$) δ 164.4, 153.5, 139.7, 132.3, 129.0, 121.7, 45.5, 30.8.

3-(2,2-Bis(4-chlorophenyl)ethyl)-1,4,2-dioxazol-5-one (1e)[66c]–Prepared by Method B



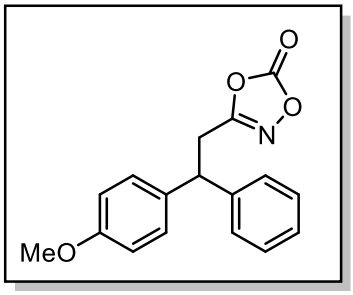
White solid; ^{1}H NMR (400 MHz, $CDCl_3$) δ 7.31 (d, *J* = 8.5 Hz, 4H), 7.15 (d, *J* = 8.4 Hz, 4H), 4.44 (t, *J* = 8.2 Hz, 1H), 3.32 (d, *J* = 8.2 Hz, 2H). ^{13}C NMR (101 MHz, $CDCl_3$) δ 164.5, 153.5, 139.2, 133.6, 129.3, 128.7, 45.4, 31.0.

3-(2,2-Bis(4-fluorophenyl)ethyl)-1,4,2-dioxazol-5-one (1f)[66c]–Prepared by Method B



White solid; ^{1}H NMR (400 MHz, $CDCl_3$) δ 7.23 – 7.14 (m, 4H), 7.08 – 6.98 (m, 4H), 4.46 (t, *J* = 8.2 Hz, 1H), 3.32 (d, *J* = 8.2 Hz, 2H). ^{13}C NMR (101 MHz, $CDCl_3$) δ 164.7, 163.2, 160.8, 153.6, 136.8, 136.8, 129.0, 128.9, 116.1, 115.9, 45.2, 31.4. ^{19}F NMR (376 MHz, $CDCl_3$) δ -114.6.

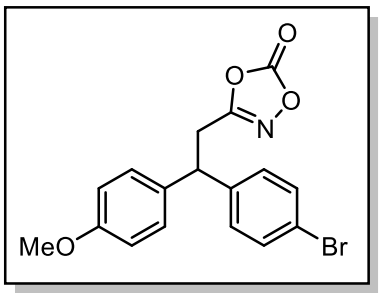
3-(2-(4-Methoxyphenyl)-2-phenylethyl)-1,4,2-dioxazol-5-one (1g)[66c]–Prepared by Method C



Colorless oil; ^{1}H NMR (400 MHz, $CDCl_3$) δ 7.33 (t, *J* = 7.4 Hz, 2H), 7.24 (t, *J* = 7.7 Hz, 3H), 7.16 (d, *J* = 8.6 Hz, 2H), 6.86 (d, *J* = 8.7 Hz, 2H), 4.43 (t, *J* = 8.2 Hz, 1H), 3.78 (s, 3H), 3.33 (d, *J* = 8.2 Hz, 2H). ^{13}C NMR (101 MHz, $CDCl_3$) δ 165.1, 158.8, 153.9, 141.7, 133.2, 129.0, 128.5, 127.3, 114.4, 55.3, 46.0, 31.4.

3-(2-(4-Bromophenyl)-2-(4-methoxyphenyl)ethyl)-1,4,2-dioxazol-5-one (1h)–

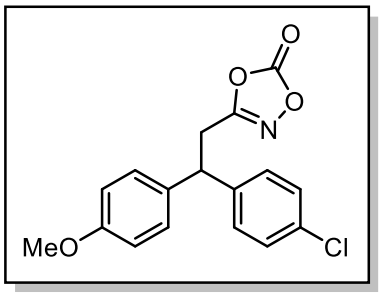
Prepared by Method C



White solid; ^{1}H NMR (400 MHz, $CDCl_3$) δ 7.45 (d, *J* = 8.5 Hz, 2H), 7.11 (dd, *J* = 8.5, 6.5 Hz, 4H), 6.86 (d, *J* = 8.7 Hz, 2H), 4.39 (t, *J* = 8.2 Hz, 1H), 3.78 (s, 3H), 3.30 (d, *J* = 8.2 Hz, 2H). ^{13}C NMR (101 MHz, $CDCl_3$) δ 164.8, 158.9, 153.7, 140.7, 132.6, 132.1, 129.1, 128.4, 121.3, 114.5, 55.3, 45.4, 31.2. HRMS (ESI) m/z: calcd for $C_{17}H_{15}BrNO_4$ [M + H], 376.0184; found, 376.0181.

3-(2-(4-Chlorophenyl)-2-(4-methoxyphenyl)ethyl)-1,4,2-dioxazol-5-one (1i)–

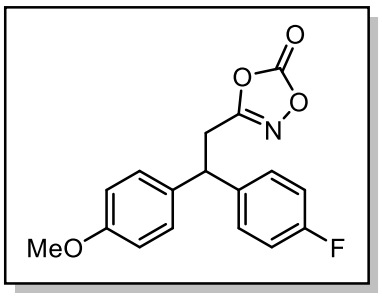
Prepared by Method C



White solid; ^{1}H NMR (400 MHz, $CDCl_3$) δ 7.33 – 7.27 (m, 2H), 7.19 – 7.09 (m, 4H), 6.89 – 6.83 (m, 2H), 4.41 (t, *J* = 8.2 Hz, 1H), 3.78 (s, 3H), 3.31 (d, *J* = 8.2 Hz, 2H). ^{13}C NMR (101 MHz, $CDCl_3$) δ 164.8, 158.9, 153.7, 140.1, 133.2, 132.7, 129.2, 128.7, 128.4, 114.5, 55.3, 45.3, 31.3. HRMS (ESI) m/z: calcd for $C_{17}H_{15}ClNO_4$ [M + H], 332.0690 ; found, 332.0692.

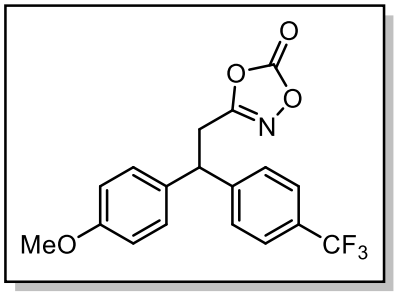
3-(2-(4-Fluorophenyl)-2-(4-methoxyphenyl)ethyl)-1,4,2-dioxazol-5-one (1j)–

Prepared by Method C



Yellow oil; ^{1}H NMR (400 MHz, $CDCl_3$) δ 7.23 – 7.10 (m, 4H), 7.05 – 6.97 (m, 2H), 6.90 – 6.82 (m, 2H), 4.42 (t, *J* = 8.2 Hz, 1H), 3.78 (s, 3H), 3.34 – 3.28 (m, 2H). ^{13}C NMR (101 MHz, $CDCl_3$) δ 164.9, 163.1, 160.7, 158.9, 153.8, 137.5, 137.4, 133.0, 129.0, 128.9, 128.4, 116.0, 115.8, 114.4, 55.3, 45.2, 31.5. ^{19}F NMR (376 MHz, $CDCl_3$) δ -115.1. HRMS (ESI) m/z: calcd for $C_{17}H_{15}FNO_4$ [M + H], 316.0985; found, 316.0983.

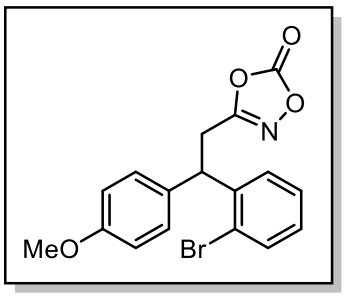
3-(2-(4-Methoxyphenyl)-2-(4-(trifluoromethyl)phenyl)ethyl)-1,4,2-dioxazol-5-one (1k)–Prepared by Method C



Yellow oil; ^{1}H NMR (400 MHz, $CDCl_3$) δ 7.58 (d, *J* = 8.1 Hz, 2H), 7.35 (d, *J* = 8.1 Hz, 2H), 7.13 (d, *J* = 8.6 Hz, 2H), 6.86 (d, *J* = 8.6 Hz, 2H), 4.49 (t, *J* = 8.2 Hz, 1H), 3.77 (s, 3H), 3.34 (d, *J* = 8.2 Hz, 2H). ^{13}C NMR (101 MHz, $CDCl_3$) δ 164.7, 159.1, 153.7, 145.7, 132.2, 129.8, 129.5, 128.5, 127.8, 126.0, 125.3, 122.6, 114.6, 55.3, 45.7, 31.1. ^{19}F NMR (376 MHz, $CDCl_3$) δ -62.6. HRMS (ESI) m/z: calcd for $C_{18}H_{15}F_3NO_4$ [M + H], 366.0953; found, 366.0957

3-(2-(2-Bromophenyl)-2-(4-methoxyphenyl)ethyl)-1,4,2-dioxazol-5-one (1l)–

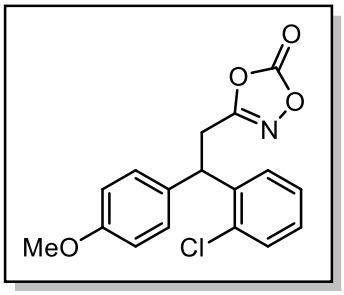
Prepared by Method C



White solid; ^{1}H NMR (400 MHz, $CDCl_3$) δ 7.57 (d, *J* = 7.9 Hz, 1H), 7.27 (dd, *J* = 14.9, 7.5 Hz, 1H), 7.21 – 7.15 (m, 3H), 7.11 (t, *J* = 7.6 Hz, 1H), 6.85 (d, *J* = 8.7 Hz, 2H), 4.95 (t, *J* = 8.1 Hz, 1H), 3.77 (s, 3H), 3.29 (dd, *J* = 8.0, 2.0 Hz, 2H). ^{13}C NMR (101 MHz, $CDCl_3$) δ 164.8, 158.9, 153.8, 140.8, 133.6, 131.6, 129.0, 128.9, 128.3, 128.0, 124.6, 114.4, 55.3, 44.6, 30.7. HRMS (ESI) m/z: calcd for $C_{17}H_{15}BrNO_4$ [M + H], 376.0184; found, 376.0180.

3-(2-(2-Chlorophenyl)-2-(4-methoxyphenyl)ethyl)-1,4,2-dioxazol-5-one (1m)–

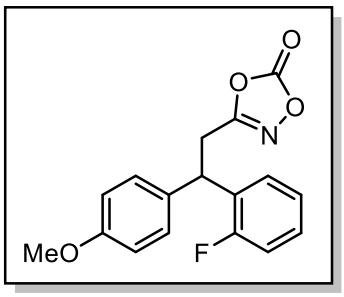
Prepared by Method C



White solid; ^{1}H NMR (400 MHz, $CDCl_3$) δ 7.41 – 7.35 (m, 1H), 7.25 – 7.15 (m, 5H), 6.85 (d, *J* = 8.7 Hz, 2H), 4.95 (t, *J* = 8.1 Hz, 1H), 3.77 (s, 3H), 3.33 – 3.28 (m, 2H). ^{13}C NMR (101 MHz, $CDCl_3$) δ 164.9, 158.9, 153.8, 139.1, 133.8, 131.6, 130.3, 128.9, 128.6, 128.1, 127.4, 114.4, 55.3, 42.0, 30.5. HRMS (ESI) m/z: calcd for $C_{17}H_{15}ClNO_4$ [M + H], 332.0690; found, 332.0695.

3-(2-(2-Fluorophenyl)-2-(4-methoxyphenyl)ethyl)-1,4,2-dioxazol-5-one (1n)–

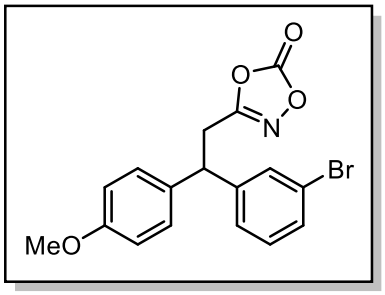
Prepared by Method C



Yellow oil; ^{1}H NMR (400 MHz, $CDCl_3$) δ 7.26 – 7.15 (m, 4H), 7.12 – 7.00 (m, 2H), 6.85 (d, *J* = 8.7 Hz, 2H), 4.70 (t, *J* = 8.2 Hz, 1H), 3.77 (s, 3H), 3.37 – 3.32 (m, 2H). ^{13}C NMR (101 MHz, $CDCl_3$) δ 164.9, 161.6, 159.2, 158.9, 153.8, 131.8, 129.2, 129.1, 128.8, 128.6, 128.6, 128.4, 128.4, 124.6, 124.6, 116.2, 116.0, 114.4, 55.3, 39.8, 39.8, 30.2, 30.2. ^{19}F NMR (376 MHz, $CDCl_3$) δ -117.0. HRMS (ESI) m/z: calcd for $C_{17}H_{15}FNO_4$ [M + H], 316.0985; found, 316.0987.

3-(2-(3-Bromophenyl)-2-(4-methoxyphenyl)ethyl)-1,4,2-dioxazol-5-one (1o)–

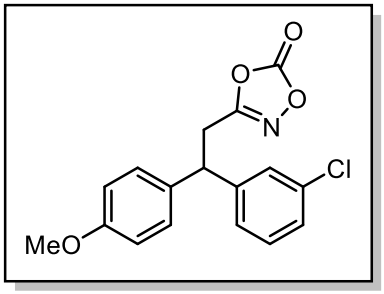
Prepared by Method C



Yellow oil; ^{1}H NMR (400 MHz, $CDCl_3$) δ 7.36 (dd, *J* = 7.2, 1.0 Hz, 2H), 7.21 – 7.09 (m, 4H), 6.85 (d, *J* = 8.7 Hz, 2H), 4.38 (t, *J* = 8.2 Hz, 1H), 3.77 (s, 3H), 3.30 (d, *J* = 8.3 Hz, 2H). ^{13}C NMR (101 MHz, $CDCl_3$) δ 164.8, 159.0, 153.7, 144.1, 132.4, 130.5, 130.5, 128.5, 126.0, 123.1, 114.5, 55.3, 45.6, 31.2. HRMS (ESI) m/z: calcd for $C_{17}H_{15}BrNO_4$ [M + H], 376.0184; found, 376.0187.

3-(2-(3-Chlorophenyl)-2-(4-methoxyphenyl)ethyl)-1,4,2-dioxazol-5-one (1p) –

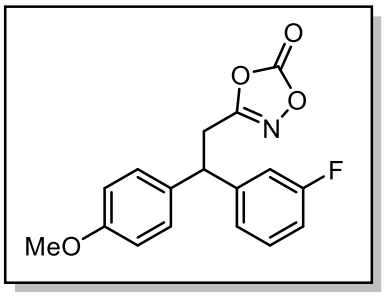
Prepared by Method C



White solid; ^{1}H NMR (400 MHz, $CDCl_3$) δ 7.26 – 7.18 (m, 3H), 7.16 – 7.08 (m, 3H), 6.86 (t, *J* = 5.8 Hz, 2H), 4.39 (t, *J* = 8.2 Hz, 1H), 3.77 (s, 3H), 3.30 (d, *J* = 8.2 Hz, 2H). ^{13}C NMR (101 MHz, $CDCl_3$) δ 164.8, 159.0, 153.8, 143.8, 134.8, 132.4, 130.3, 128.5, 127.6, 125.5, 114.5, 55.3, 45.6, 31.2. HRMS (ESI) m/z: calcd for $C_{17}H_{15}ClNO_4$ [M + H], 332.0690; found, 332.0693.

3-(2-(3-Fluorophenyl)-2-(4-methoxyphenyl)ethyl)-1,4,2-dioxazol-5-one (1q)–

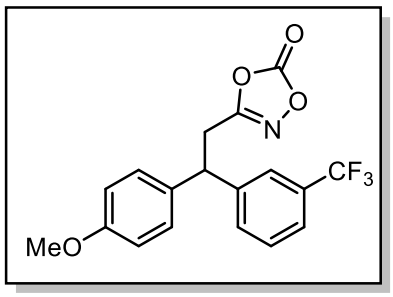
Prepared by Method C



Yellow oil; ^{1}H NMR (400 MHz, $CDCl_3$) δ 7.32 – 7.23 (m, 1H), 7.13 (d, *J* = 8.5 Hz, 2H), 7.01 (d, *J* = 7.6 Hz, 1H), 6.96 – 6.82 (m, 4H), 4.41 (t, *J* = 8.2 Hz, 1H), 3.77 (s, 3H), 3.30 (d, *J* = 8.2 Hz, 2H). ^{13}C NMR (101 MHz, $CDCl_3$) δ 164.8, 164.3, 161.8, 159.0, 153.8, 144.3, 144.2, 132.5, 130.6, 130.5, 128.5, 123.0, 123.0, 114.5, 114.5, 114.4, 114.3, 114.2, 55.3, 45.6, 45.6, 31.2. ^{19}F NMR (376 MHz, $CDCl_3$) δ -111.9. HRMS (ESI) m/z: calcd for $C_{17}H_{15}FNO_4$ [M + H], 316.0985; found, 316.0988.

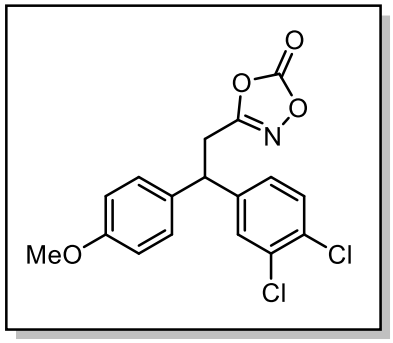
3-(2-(4-Methoxyphenyl)-2-(3-(trifluoromethyl)phenyl)ethyl)-1,4,2-dioxazol-5-one

(1r) –Prepared by Method C



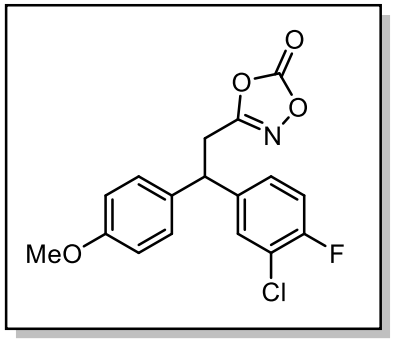
Yellow oil; ^{1}H NMR (400 MHz, $CDCl_3$) δ 7.54 – 7.38 (m, 4H), 7.13 (d, *J* = 8.7 Hz, 2H), 6.86 (d, *J* = 8.7 Hz, 2H), 4.49 (t, *J* = 8.2 Hz, 1H), 3.78 (s, 3H), 3.34 (dd, *J* = 8.2, 1.8 Hz, 2H). ^{13}C NMR (101 MHz, $CDCl_3$) δ 164.7, 159.1, 153.7, 142.8, 132.2, 131.5, 131.2, 130.8, 130.7, 129.5, 128.5, 125.2, 124.3, 124.3, 124.1, 124.0, 122.5, 114.6, 55.3, 45.7, 31.2. ^{19}F NMR (376 MHz, $CDCl_3$) δ -62.6. HRMS (ESI) m/z: calcd for $C_{18}H_{15}F_3NO_4$ [M + H], 366.0953; found, 366.0958.

3-(2-(3,4-Dichlorophenyl)-2-(4-methoxyphenyl)ethyl)-1,4,2-dioxazol-5-one (1s) – Prepared by Method C



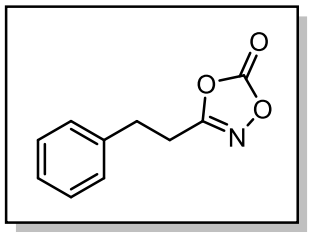
Yellow oil; ^{1}H NMR (400 MHz, $CDCl_3$) δ 7.38 (d, *J* = 8.3 Hz, 1H), 7.30 (d, *J* = 2.0 Hz, 1H), 7.16 – 7.03 (m, 3H), 6.86 (d, *J* = 8.7 Hz, 2H), 4.38 (t, *J* = 8.2 Hz, 1H), 3.77 (s, 3H), 3.34 – 3.24 (m, 2H). ^{13}C NMR (101 MHz, $CDCl_3$) δ 164.6, 159.1, 153.7, 142.0, 133.1, 132.0, 131.5, 130.9, 129.4, 128.4, 126.7, 114.6, 55.3, 45.1, 31.1. HRMS (ESI) m/z: calcd for $C_{17}H_{14}Cl_2NO_4$ [M + H], 366.0300; found, 366.0302.

3-(2-(3-Chloro-4-fluorophenyl)-2-(4-methoxyphenyl)ethyl)-1,4,2-dioxazol-5-one (1t) –Prepared by Method C



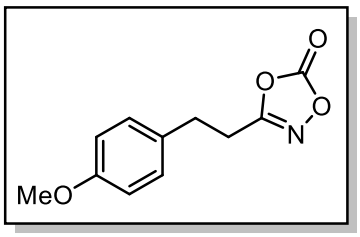
White solid; ^{1}H NMR (400 MHz, $CDCl_3$) δ 7.28 – 7.21 (m, 1H), 7.09 (dd, *J* = 12.0, 6.0 Hz, 4H), 6.86 (d, *J* = 8.6 Hz, 2H), 4.38 (t, *J* = 8.2 Hz, 1H), 3.78 (s, 3H), 3.29 (dd, *J* = 8.2, 2.3 Hz, 2H). ^{13}C NMR (101 MHz, $CDCl_3$) δ 164.6, 159.1, 158.5, 153.0, 153.7, 138.9, 138.9, 132.2, 129.6, 128.4, 127.1, 127.0, 121.6, 121.4, 117.1, 116.9, 114.6, 55.3, 45.0, 31.3. ^{19}F NMR (376 MHz, $CDCl_3$) δ -117.1. HRMS (ESI) m/z: calcd for $C_{17}H_{14}ClFNO_4$ [M + H], 350.0595; found, 350.0597.

3-Phenethyl-1,4,2-dioxazol-5-one (**1u**)[73]–Prepared by Method D



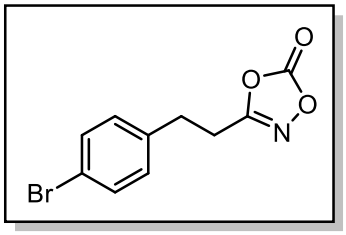
White solid; ^{1}H NMR (400 MHz, $CDCl_3$) δ 7.34 (t, *J* = 7.3 Hz, 2H), 7.31 – 7.24 (m, 1H), 7.21 (d, *J* = 7.2 Hz, 2H), 3.08 – 3.01 (m, 2H), 2.94 (dd, *J* = 11.4, 4.5 Hz, 2H). ^{13}C NMR (101 MHz, $CDCl_3$) δ 165.9, 154.0, 138.0, 129.0, 128.2, 127.2, 30.5, 26.7.

3-(4-Methoxyphenethyl)-1,4,2-dioxazol-5-one (**1v**)[73]–Prepared by Method D



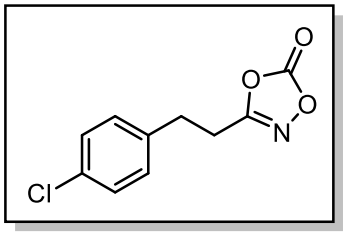
White solid; ^{1}H NMR (400 MHz, $CDCl_3$) δ 7.12 (d, *J* = 8.6 Hz, 2H), 6.86 (d, *J* = 8.6 Hz, 2H), 3.80 (s, 3H), 2.99 (dd, *J* = 11.4, 4.5 Hz, 2H), 2.93 – 2.87 (m, 2H). ^{13}C NMR (101 MHz, $CDCl_3$) δ 165.9, 158.7, 154.1, 130.0, 129.2, 114.3, 55.3, 29.7, 27.0.

3-(4-Bromophenethyl)-1,4,2-dioxazol-5-one (**1w**)[66c]–Prepared by Method D



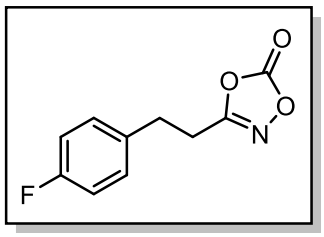
White solid; ^{1}H NMR (400 MHz, $CDCl_3$) δ 7.45 (dd, *J* = 6.2, 4.5 Hz, 2H), 7.09 (d, *J* = 8.3 Hz, 2H), 3.01 (dd, *J* = 11.6, 4.6 Hz, 2H), 2.95 – 2.89 (m, 2H). ^{13}C NMR (101 MHz, $CDCl_3$) δ 165.5, 153.9, 136.9, 132.1, 130.0, 121.1, 29.8, 26.5.

3-(4-Chlorophenethyl)-1,4,2-dioxazol-5-one (1x)[73]–Prepared by Method D



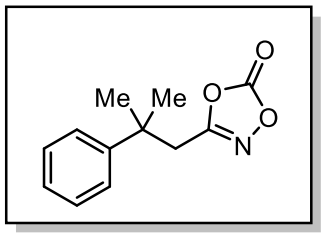
Colorless oil; ^{1}H NMR (400 MHz, $CDCl_3$) δ 7.31 (d, *J* = 8.3 Hz, 2H), 7.14 (d, *J* = 8.3 Hz, 2H), 3.02 (dd, *J* = 11.1, 4.0 Hz, 2H), 2.96 – 2.90 (m, 2H). ^{13}C NMR (101 MHz, $CDCl_3$) δ 165.6, 153.9, 136.4, 133.1, 129.6, 129.1, 29.8, 26.5.

3-(4-Fluorophenethyl)-1,4,2-dioxazol-5-one (1y)[66c]–Prepared by Method D



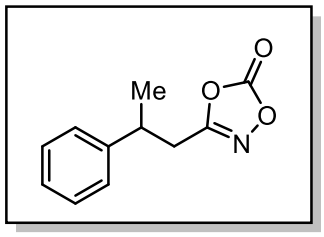
Colorless oil; ^{1}H NMR (400 MHz, $CDCl_3$) δ 7.21 – 7.13 (m, 2H), 7.07 – 6.97 (m, 2H), 3.01 (dd, *J* = 11.7, 4.6 Hz, 2H), 2.93 (ddd, *J* = 8.6, 5.6, 1.7 Hz, 2H). ^{13}C NMR (101 MHz, $CDCl_3$) δ 165.7, 163.2, 160.7, 153.9, 133.7, 133.7, 129.8, 129.7, 115.9, 115.7, 29.7, 26.8, 26.8. ^{19}F NMR (376 MHz, $CDCl_3$) δ -115.4.

3-(2-Methyl-2-phenylpropyl)-1,4,2-dioxazol-5-one (1za)–Prepared by Method D



Colorless oil; ^{1}H NMR (400 MHz, $CDCl_3$) δ 7.36 (d, *J* = 4.3 Hz, 4H), 7.29 – 7.23 (m, 1H), 2.92 (s, 2H), 1.51 (s, 6H). ^{13}C NMR (101 MHz, $CDCl_3$) δ 165.0, 154.0, 145.7, 128.7, 126.9, 125.3, 39.2, 37.7, 28.7. HRMS (ESI) m/z: calcd for $C_{12}H_{14}NO_3$ [M + H], 220.0974; found, 220.0977.

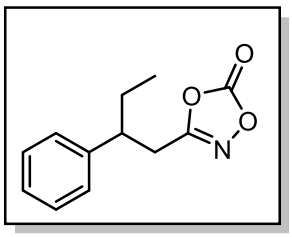
3-(2-Phenylpropyl)-1,4,2-dioxazol-5-one (1zb)–Prepared by Method D



Colorless oil; ^{1}H NMR (400 MHz, $CDCl_3$) δ 7.33 (t, *J* = 7.4 Hz, 2H), 7.25 (dd, *J* = 8.5, 6.1 Hz, 1H), 7.20 (d, *J* = 7.2 Hz, 2H), 3.31 – 3.17 (m, 1H), 2.96 – 2.80 (m, 2H), 1.39 (d, *J* = 7.0 Hz, 3H). ^{13}C NMR (101 MHz, $CDCl_3$) δ 165.4, 154.0, 143.2, 129.0, 127.4, 126.5,

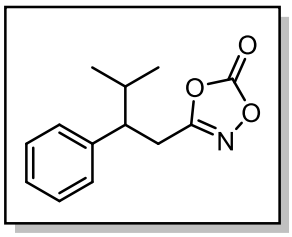
36.4, 33.3, 21.6. HRMS (ESI) m/z: calcd for $C_{11}H_{12}NO_3$ [M + H], 206.0817; found, 206.0815.

3-(2-Phenylbutyl)-1,4,2-dioxazol-5-one (1zc)[66c]–Prepared by Method E



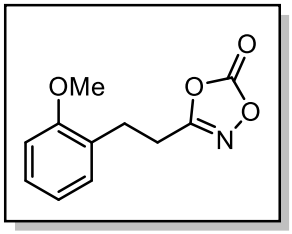
Pale yellow liquid; ^{1}H NMR (400 MHz, $CDCl_3$) δ 7.32 (dd, *J* = 10.1, 4.5 Hz, 2H), 7.27 – 7.22 (m, 1H), 7.19 – 7.11 (m, 2H), 3.02 – 2.77 (m, 3H), 1.75 (qdd, *J* = 21.4, 7.8, 6.1 Hz, 2H), 0.88 – 0.77 (m, 3H). ^{13}C NMR (101 MHz, $CDCl_3$) δ 165.5, 154.0, 141.3, 128.9, 127.4, 127.3, 43.7, 31.8, 29.0, 11.8.

3-(3-Methyl-2-phenylbutyl)-1,4,2-dioxazol-5-one (1zd)[66c]–Prepared by Method E



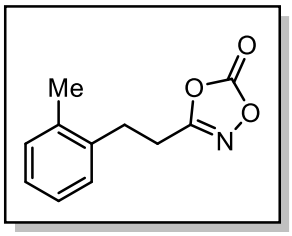
Yellow liquid; ^{1}H NMR (400 MHz, CD_2Cl_2) δ 7.30 (t, *J* = 7.3 Hz, 2H), 7.24 (m, 1H), 7.13 (d, *J* = 7.1 Hz, 2H), 3.08 (dd, *J* = 15.1, 4.7 Hz, 1H), 2.90 (dd, *J* = 15.1, 10.8 Hz, 1H), 2.84 – 2.74 (m, 1H), 1.94 (dq, *J* = 13.6, 6.8 Hz, 1H), 1.00 (d, *J* = 6.7 Hz, 3H), 0.77 (d, *J* = 6.7 Hz, 3H). ^{13}C NMR (101 MHz, CD_2Cl_2) δ 166.6, 154.5, 140.9, 128.9, 128.5, 127.6, 49.2, 33.6, 29.4, 20.7, 20.3.

3-(2-Methoxyphenethyl)-1,4,2-dioxazol-5-one (3a)[66c]–Prepared by Method D



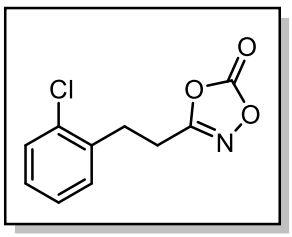
White solid; ^{1}H NMR (400 MHz, $CDCl_3$) δ 7.30 – 7.23 (m, 1H), 7.13 (dd, *J* = 7.4, 1.4 Hz, 1H), 6.90 (dd, *J* = 16.2, 8.0 Hz, 2H), 3.83 (s, 3H), 3.02 (t, *J* = 7.2 Hz, 2H), 2.91 (dd, *J* = 11.2, 4.1 Hz, 2H). ^{13}C NMR (101 MHz, $CDCl_3$) δ 166.4, 157.4, 154.3, 130.1, 128.7, 126.4, 120.8, 110.5, 55.2, 26.3, 25.1.

3-(2-Methylphenethyl)-1,4,2-dioxazol-5-one (3b)[73]–Prepared by Method D



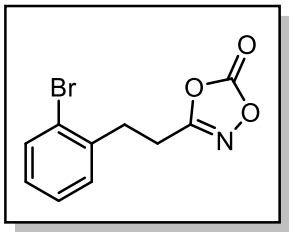
White solid; ^{1}H NMR (400 MHz, $CDCl_3$) δ 7.21 – 7.11 (m, 4H), 3.04 (dd, *J* = 8.9, 6.6 Hz, 2H), 2.93 – 2.87 (m, 2H), 2.35 (s, 3H). ^{13}C NMR (101 MHz, $CDCl_3$) δ 166.0, 154.0, 136.3, 135.8, 130.8, 128.5, 127.3, 126.5, 28.0, 25.4, 19.2.

3-(2-Chlorophenethyl)-1,4,2-dioxazol-5-one (3c) –Prepared by Method D



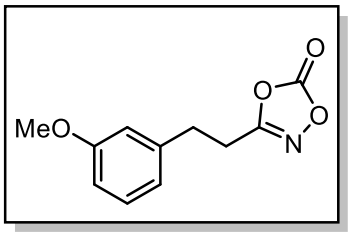
White solid; ^{1}H NMR (400 MHz, $CDCl_3$) δ 7.42 – 7.31 (m, 1H), 7.26 – 7.15 (m, 3H), 3.15 (t, *J* = 7.6 Hz, 2H), 2.96 (t, *J* = 7.6 Hz, 2H). ^{13}C NMR (101 MHz, $CDCl_3$) δ 165.7, 154.0, 135.7, 133.9, 130.5, 130.0, 128.9, 127.4, 28.7, 24.9. HRMS (ESI) m/z: calcd for $C_{10}H_9ClNO_3$ [M + H], 226.0271; found, 226.0275.

3-(2-Bromophenethyl)-1,4,2-dioxazol-5-one (3d)[73]–Prepared by Method D



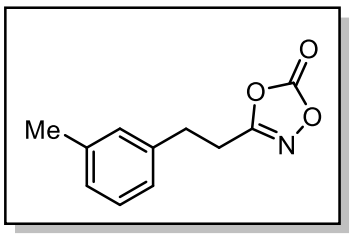
White solid; ^{1}H NMR (400 MHz, $CDCl_3$) δ 7.58 (d, *J* = 7.8 Hz, 1H), 7.32 – 7.22 (m, 2H), 7.15 (td, *J* = 7.8, 1.9 Hz, 1H), 3.17 (t, *J* = 7.6 Hz, 2H), 2.98 (t, *J* = 7.6 Hz, 2H). ^{13}C NMR (101 MHz, $CDCl_3$) δ 165.6, 154.0, 137.4, 133.3, 130.5, 129.1, 128.0, 124.2, 31.2, 25.1.

3-(3-Methoxyphenethyl)-1,4,2-dioxazol-5-one (5a)[73]–Prepared by Method D



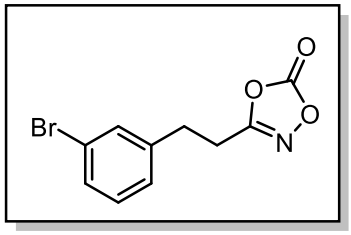
White solid; ^{1}H NMR (400 MHz, $CDCl_3$) δ 7.25 (dd, *J* = 9.8, 6.0 Hz, 1H), 6.83 – 6.72 (m, 3H), 3.80 (s, 3H), 3.02 (dd, *J* = 11.6, 4.6 Hz, 2H), 2.97 – 2.91 (m, 2H). ^{13}C NMR (101 MHz, $CDCl_3$) δ 165.9, 160.0, 154.0, 139.6, 130.0, 120.4, 114.1, 112.3, 55.2, 30.5, 26.6.

3-(3-Methylphenethyl)-1,4,2-dioxazol-5-one(5b)[66c]–Prepared by Method D



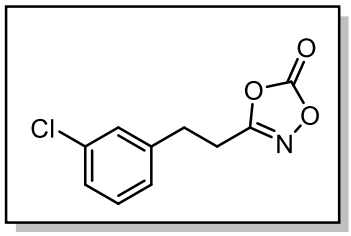
White solid; ^{1}H NMR (400 MHz, $CDCl_3$) δ 7.23 (t, *J* = 7.5 Hz, 1H), 7.09 (d, *J* = 7.6 Hz, 1H), 7.01 (d, *J* = 11.4 Hz, 2H), 3.04 – 2.97 (m, 2H), 2.93 (ddd, *J* = 9.1, 5.5, 1.7 Hz, 2H), 2.35 (s, 3H). ^{13}C NMR (101 MHz, $CDCl_3$) δ 165.9, 154.1, 138.6, 138.0, 129.0, 128.8, 127.9, 125.2, 30.4, 26.7, 21.4.

3-(3-Bromophenethyl)-1,4,2-dioxazol-5-one (5c)[66c]–Prepared by Method D



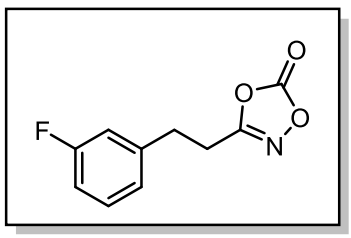
White solid; ^{1}H NMR (400 MHz, $CDCl_3$) δ 7.44 – 7.34 (m, 2H), 7.21 (t, *J* = 7.8 Hz, 1H), 7.14 (d, *J* = 7.7 Hz, 1H), 3.05 – 2.99 (m, 2H), 2.97 – 2.91 (m, 2H). ^{13}C NMR (101 MHz, $CDCl_3$) δ 165.5, 153.9, 140.3, 131.3, 130.5, 130.4, 126.9, 122.9, 30.0, 26.4.

3-(3-Chlorophenethyl)-1,4,2-dioxazol-5-one (5d) –Prepared by Method D



White solid; ^{1}H NMR (400 MHz, $CDCl_3$) δ 7.30 – 7.16 (m, 3H), 7.08 (d, *J* = 6.3 Hz, 1H), 3.01 (dd, *J* = 11.4, 4.5 Hz, 2H), 2.96 – 2.89 (m, 2H). ^{13}C NMR (101 MHz, $CDCl_3$) δ 165.5, 153.9, 140.0, 134.7, 130.2, 128.4, 127.5, 126.4, 30.0, 26.4. HRMS (ESI) m/z: calcd for $C_{10}H_9ClNO_3$ [M + H], 226.0271; found, 226.0274.

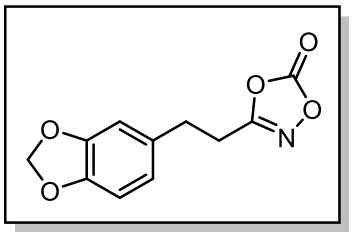
3-(3-Fluorophenethyl)-1,4,2-dioxazol-5-one (5e) –Prepared by Method D



Colorless oil; ^{1}H NMR (400 MHz, $CDCl_3$) δ 7.28 (dt, *J* = 13.3, 6.7 Hz, 1H), 7.03 – 6.83 (m, 3H), 3.07 – 2.99 (m, 2H), 2.93 (dd, *J* = 11.3, 4.3 Hz, 2H). ^{13}C NMR (101 MHz, $CDCl_3$) δ 165.6, 164.2, 161.8, 153.9, 140.5, 140.4, 130.5, 130.5, 123.9, 123.9, 115.3,

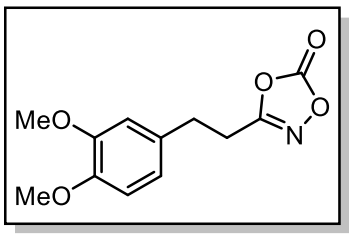
115.1, 114.3, 114.1, 30.1, 30.0, 26.4. ^{19}F NMR (376 MHz, $CDCl_3$) δ -112.5. HRMS (ESI) m/z: calcd for $C_{10}H_9FNO_3$ [M + H], 210.0566; found, 210.0569.

3-(2-(Benzo[d][1,3]dioxol-5-yl)ethyl)-1,4,2-dioxazol-5-one (7a) – Prepared by Method D



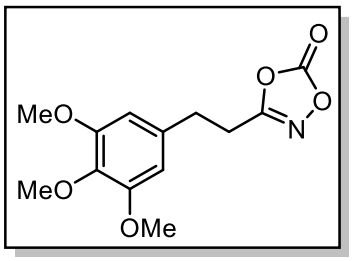
White solid; ^{1}H NMR (400 MHz, $CDCl_3$) δ 6.74 (d, *J* = 7.9 Hz, 1H), 6.67 – 6.61 (m, 2H), 5.93 (s, 2H), 2.97 – 2.91 (m, 2H), 2.90 – 2.85 (m, 2H). ^{13}C NMR (101 MHz, $CDCl_3$) δ 165.8, 154.0, 148.1, 146.7, 131.7, 121.2, 108.6, 108.6, 101.1, 30.3, 27.0. HRMS (ESI) m/z: calcd for $C_{11}H_{10}NO_5$ [M + H], 236.0559; found, 236.0554.

3-(3,4-Dimethoxyphenethyl)-1,4,2-dioxazol-5-one (7b)[76]–Prepared by Method D



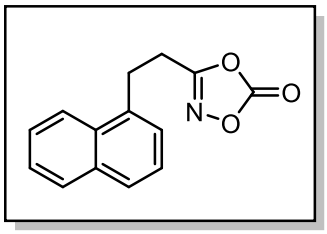
White solid; ^{1}H NMR (400 MHz, $CDCl_3$) δ 6.82 (d, *J* = 8.1 Hz, 1H), 6.77 – 6.68 (m, 2H), 3.87 (d, *J* = 3.2 Hz, 6H), 3.02 – 2.95 (m, 2H), 2.95 – 2.89 (m, 2H). ^{13}C NMR (101 MHz, $CDCl_3$) δ 165.9, 154.0, 149.2, 148.2, 130.5, 120.2, 111.6, 111.5, 55.9, 55.9, 30.2, 26.9.

3-(3,4,5-Trimethoxyphenethyl)-1,4,2-dioxazol-5-one (7c)[76]–Prepared by Method D



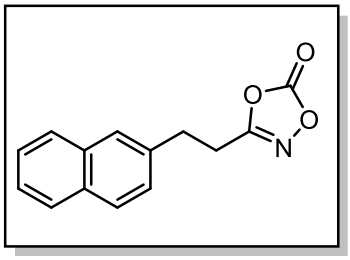
White solid; ^{1}H NMR (400 MHz, $CDCl_3$) δ 6.40 (s, 2H), 3.85 (s, 6H), 3.83 (s, 3H), 3.00 – 2.91 (m, 4H). ^{13}C NMR (101 MHz, $CDCl_3$) δ 165.8, 154.0, 153.6, 137.1, 133.7, 105.2, 60.9, 56.2, 30.9, 26.8.

3-(2-(Naphthalen-1-yl)ethyl)-1,4,2-dioxazol-5-one (7d)[73]–Prepared by Method D



White solid; ^{1}H NMR (400 MHz, $CDCl_3$) δ 7.94 (d, *J* = 8.3 Hz, 1H), 7.89 (d, *J* = 7.9 Hz, 1H), 7.79 (d, *J* = 8.2 Hz, 1H), 7.60 – 7.48 (m, 2H), 7.45 – 7.38 (m, 1H), 7.34 (d, *J* = 6.9 Hz, 1H), 3.53 – 3.46 (m, 2H), 3.11 – 3.02 (m, 2H). ^{13}C NMR (101 MHz, $CDCl_3$) δ 166.0, 154.0, 134.0, 131.2, 129.2, 128.1, 126.7, 126.4, 126.0, 125.6, 122.6, 27.8, 26.0.

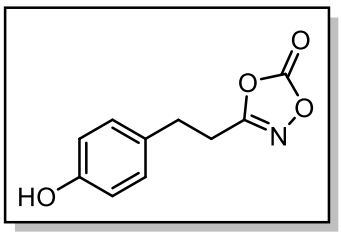
3-(2-(Naphthalen-2-yl)ethyl)-1,4,2-dioxazol-5-one (7e) – Prepared by Method D



White solid; ^{1}H NMR (400 MHz, $CDCl_3$) δ 7.80 (dd, *J* = 12.0, 7.9 Hz, 3H), 7.65 (s, 1H), 7.52 – 7.43 (m, 2H), 7.31 (dd, *J* = 8.4, 1.5 Hz, 1H), 3.19 (t, *J* = 7.7 Hz, 2H), 3.02 (t, *J* = 7.7 Hz, 2H). ^{13}C NMR (101 MHz, $CDCl_3$) δ 165.8, 154.0, 135.4, 133.5, 132.5, 128.8,

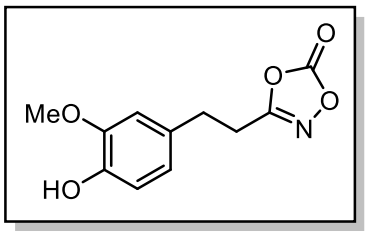
127.7, 127.6, 126.8, 126.5, 126.3, 126.0, 30.6, 26.6. HRMS (ESI) m/z: calcd for $C_{14}H_{12}NO_3$ [M + H], 242.0817; found, 242.0819.

3-(4-Hydroxyphenethyl)-1,4,2-dioxazol-5-one (9a)[73] –Prepared by Method A



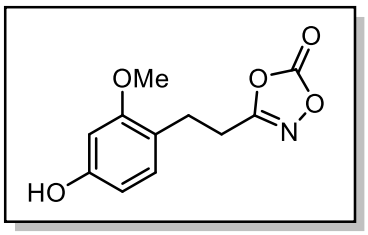
White solid; ^{1}H NMR (400 MHz, $CDCl_3$) δ 7.06 (d, *J* = 8.4 Hz, 2H), 6.85 – 6.72 (m, 2H), 5.00 (s, 1H), 3.00 – 2.94 (m, 2H), 2.93 – 2.87 (m, 2H). ^{13}C NMR (101 MHz, $CDCl_3$) δ 165.9, 154.7, 154.1, 130.1, 129.4, 115.8, 29.7, 27.0.

3-(4-Hydroxy-3-methoxyphenethyl)-1,4,2-dioxazol-5-one (**9b**)[73]–Prepared by Method A



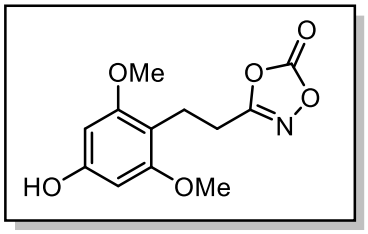
White solid; ^{1}H NMR (400 MHz, $CDCl_3$) δ 6.86 (d, *J* = 7.8 Hz, 1H), 6.69 (d, *J* = 8.1 Hz, 2H), 5.56 (s, 1H), 3.88 (s, 3H), 3.00 – 2.94 (m, 2H), 2.90 (dd, *J* = 11.0, 4.5 Hz, 2H). ^{13}C NMR (101 MHz, $CDCl_3$) δ 165.9, 154.0, 146.7, 144.8, 129.9, 120.9, 114.7, 110.8, 56.0, 30.3, 27.0.

3-(4-Hydroxy-2-methoxyphenethyl)-1,4,2-dioxazol-5-one (**9c**)[73] – Prepared by Method A



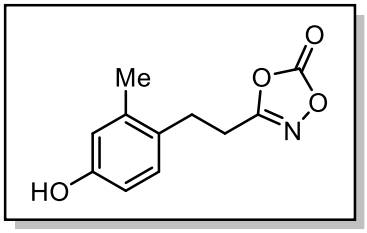
White solid; ^{1}H NMR (400 MHz, $CDCl_3$) δ 6.94 (d, *J* = 8.0 Hz, 1H), 6.43 – 6.29 (m, 2H), 5.03 (s, 1H), 3.78 (s, 3H), 2.98 – 2.90 (m, 2H), 2.86 (t, *J* = 6.7 Hz, 2H).^{13}C NMR (101 MHz, $CDCl_3$) δ 166.7, 158.7, 156.4, 154.7, 130.8, 118.6, 107.1, 99.2, 55.4, 25.8, 25.5.

3-(4-Hydroxy-2,6-dimethoxyphenethyl)-1,4,2-dioxazol-5-one (9d)[66c]–Prepared by Method A



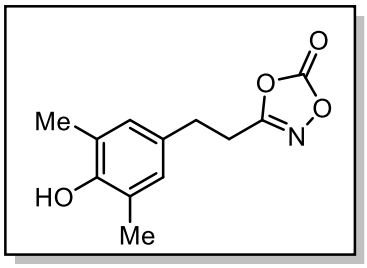
White solid; ^{1}H NMR (400 MHz, $CDCl_3$) δ 6.05 (s, 2H), 4.80 (s, 1H), 3.75 (s, 6H), 2.97 (t, *J* = 7.0 Hz, 2H), 2.72 (t, *J* = 7.0 Hz, 2H). ^{13}C NMR (101 MHz, $CDCl_3$) δ 166.9, 158.9, 156.2, 154.7, 106.6, 91.7, 55.6, 24.7, 18.6.

3-(4-Hydroxy-2-methylphenethyl)-1,4,2-dioxazol-5-one (9e) –Prepared by Method A



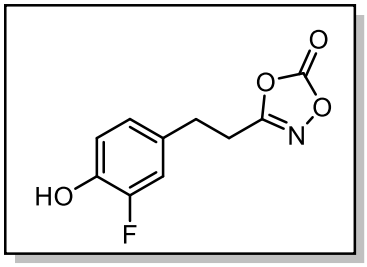
White solid; ^{1}H NMR (400 MHz, $CDCl_3$) δ 6.97 (d, *J* = 8.2 Hz, 1H), 6.69 – 6.59 (m, 2H), 4.93 (s, 1H), 2.97 – 2.90 (m, 2H), 2.87 – 2.80 (m, 2H), 2.26 (s, 3H). ^{13}C NMR (101 MHz, $CDCl_3$) δ 166.0, 154.6, 154.1, 137.5, 129.8, 128.5, 117.5, 113.2, 27.3, 25.7, 19.3. HRMS (ESI) m/z: calcd for $C_{11}H_{12}NO_4$ [M + H], 222,0766; found, 222,0769.

3-(4-Hydroxy-3,5-dimethylphenethyl)-1,4,2-dioxazol-5-one (9f)[73]–Prepared by Method A



White solid; ^{1}H NMR (400 MHz, $CDCl_3$) δ 6.80 (s, 2H), 4.59 (s, 1H), 2.89 (s, 4H), 2.23 (s, 6H). ^{13}C NMR (101 MHz, $CDCl_3$) δ 166.0, 154.1, 151.2, 129.6, 128.3, 123.5, 29.7, 27.0, 15.9.

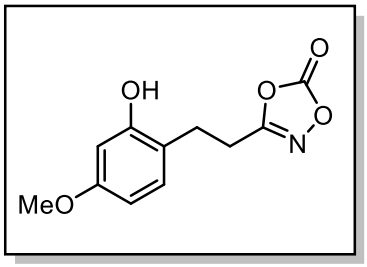
3-(3-Fluoro-4-hydroxyphenethyl)-1,4,2-dioxazol-5-one (9g) –Prepared by Method A



White solid; ^{1}H NMR (400 MHz, $CDCl_3$) δ 6.97 – 6.87 (m, 2H), 6.84 (d, *J* = 8.3 Hz, 1H), 5.43 (s, 1H), 2.97 – 2.91 (m, 2H), 2.91 – 2.85 (m, 2H). ^{13}C NMR (101 MHz, $CDCl_3$) δ 165.7, 154.1, 152.2, 149.8, 142.7, 142.5, 130.8, 130.8, 124.6, 124.5, 117.7,

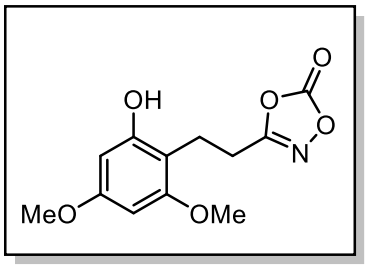
117.7, 115.5, 115.3, 29.5, 29.5, 26.7. ^{19}F NMR (376 MHz, $CDCl_3$) δ -139.6. HRMS (ESI) m/z: calcd for $C_{10}H_9FNO_4$ [M + H], 226.0516; found, 226.0517.

3-(2-Hydroxy-4-methoxyphenethyl)-1,4,2-dioxazol-5-one (9h)[73]–Prepared by Method A



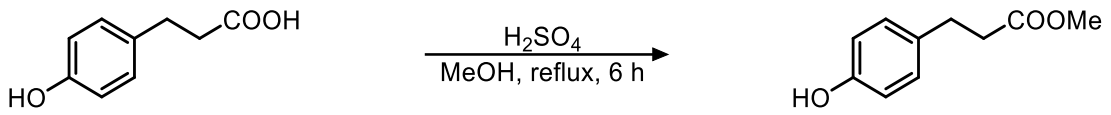
White solid; ^{1}H NMR (400 MHz, $CDCl_3$) δ 6.99 (d, *J* = 8.3 Hz, 1H), 6.43 (dd, *J* = 8.3, 2.4 Hz, 1H), 6.31 (d, *J* = 2.3 Hz, 1H), 5.23 (s, 1H), 3.75 (s, 3H), 2.99 – 2.93 (m, 2H), 2.93 – 2.88 (m, 2H). ^{13}C NMR (101 MHz, $CDCl_3$) δ 166.4, 159.9, 154.4, 154.4, 131.1, 117.1, 106.0, 102.2, 55.4, 25.4, 25.3.

3-(2-Hydroxy-4,6-dimethoxyphenethyl)-1,4,2-dioxazol-5-one (9i) –Prepared by Method A

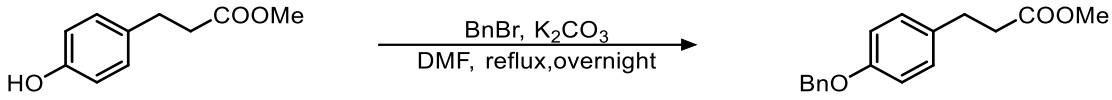


White solid; ^{1}H NMR (400 MHz, $CDCl_3$) δ 6.06 (d, *J* = 2.1 Hz, 1H), 6.00 (d, *J* = 2.1 Hz, 1H), 3.76 (s, 3H), 3.73 (s, 3H), 2.98 (t, *J* = 6.9 Hz, 2H), 2.79 (t, *J* = 6.9 Hz, 2H). ^{13}C NMR (101 MHz, $CDCl_3$) δ 167.1, 159.9, 159.3, 155.3, 154.7, 105.6, 93.9, 91.0, 55.5, 55.3, 24.7, 18.5. HRMS (ESI) m/z: calcd for $C_{12}H_{14}NO_6$ [M + H], 268.0821; found, 268.0825.

Preparation of 3-(4-(benzyloxy)phenethyl)-1,4,2-dioxazol-5-one (1z)

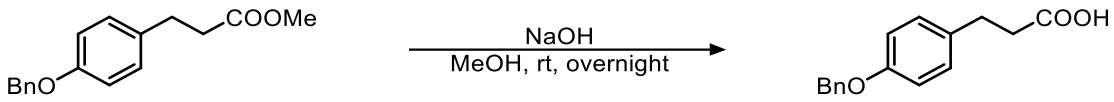


3-(4-Hydroxyphenyl)propanoic acid (20 mmol) was dissolved in methanol (40 mL), and sulfuric acid (concentrated, 0.4 mL) was added. The reaction mixture was heated to reflux for 6 h until full conversion. Solid $NaHCO_3$ was added to neutralize the solution. After filtration, the slightly yellow solution was evaporated to dryness. The residue was dissolved in ethyl acetate and washed with saturated sodium bicarbonate solution and saturated sodium chloride solution. The organic layer was dried and concentrated to give methyl ester.

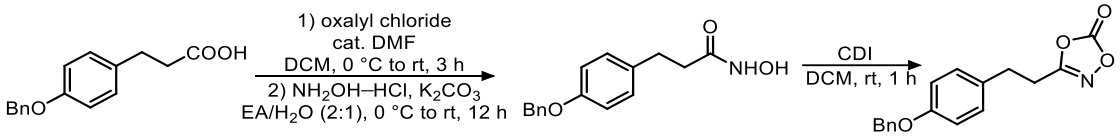


A Schlenk tube equipped with a magnetic stir bar was charged with K_2CO_3 (40 mmol), methyl 3-(4-hydroxyphenyl)propanoate (10 mmol), and (bromomethyl)benzene (BnBr) (12 mmol) in DMF (30 mL) under an N_2 atmosphere. The reaction mixture was heated to reflux overnight. The mixture was cooled to room temperature and diluted with EtOAc (20 mL). The resulting suspension was directly filtered through a pad of Celite®, and the filtrate was washed with brine (20 mL) and dried over anhydrous Na_2SO_4. The organic phase was concentrated, and the crude

mixtures were purified by column chromatography on silica gel (300–400 mesh) using n-hexane/EtOAc solvent mixture as the eluent.



To a solution of methyl 3-(4-(benzyloxy)phenyl)propanoate (5 mmol) in methanol (40 mL) was added sodium hydroxide (15 mmol) in one portion. Then, the mixture was stirred at room temperature for overnight. After the reaction, methanol was removed by rotatory evaporation, and water (20 mL) was added. Then, 1 N HCl was added to adjust the pH of the mixture to 1−2, and the mixture was extracted with ethyl acetate. The combined organic phases were collected and concentrated by rotatory evaporation give the crude product that was used for the next step without further purification.

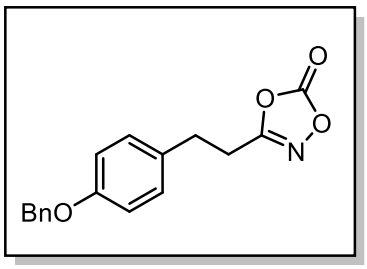


To a DCM (30 mL) solution of 3-(4-(benzyloxy)phenyl)propanoic acid (2 mmol) was added oxalyl chloride (2.0 equiv, 0.34 mL) at 0 °C in a dropwise manner, and DMF (0.2 mL) was added to the mixture. After stirring the mixture at room temperature for 3 h, the solvent and excess oxalyl chloride were removed by vacuum distillation. K_2CO_3 (2.0 equiv, 552.8 mg) was dissolved in EtOAc/H_2O = 2:1 (16 mL of EtOAc and 8 mL of H_2O) and then cooled to 0 °C. The hydroxylamine hydrogen chloride (1.2 equiv, 166.8 mg) was added to the K_2CO_3 solution. The corresponding unpurified acid

chloride obtained was dissolved in DCM (5 mL) and was transferred to the reaction mixture. The reaction mixture was stirred at room temperature for overnight. To work-up, the distillated water (30 mL) was added to the reaction mixture and the organic layer was separated. The aqueous phase was extracted with EtOAc (3 x 50 mL) and the combined organic extracts were dried with $MgSO_4$. The solvent was evaporated by rotatory evaporation to obtain the corresponding 3-(4-(benzyloxy)phenyl)-N-hydroxypropanamide for use without further purification.

The 3-(4-(benzyloxy)phenyl)-N-hydroxypropanamide (2 mmol) and CDI (1.1 equiv, 356.8 mg) were dissolved in DCM (20 mL) and stirred at room temperature for 30 min. Then, 1M HCl (3 mL) was added to the reaction mixture and stirred at room temperature for another 1 h. After that, the organic layer was separated, and the aqueous phase was extracted with DCM (3 x 20 mL). The combined organic extracts were dried by $MgSO_4$ and concentrated by rotatory evaporation. The crude mixture was purified by flash chromatography (n-hexane/EtOAc = 5:1) to obtain 3-(4-(benzyloxy)phenethyl)-1,4,2-dioxazol-5-one.

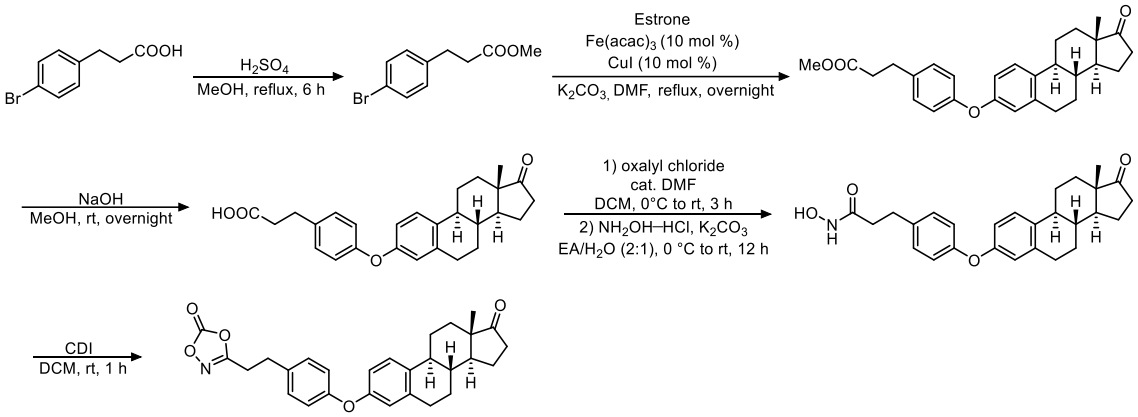
3-(4-(Benzyloxy)phenethyl)-1,4,2-dioxazol-5-one (1z)[66c]



White solid; ^1H NMR (400 MHz, $CDCl_3$) δ 7.48 – 7.27 (m, 5H), 7.10 (d, *J* = 8.6 Hz, 2H), 6.93 (dd, *J* = 6.6, 4.8 Hz, 2H), 5.04 (s, 2H), 2.97 (dd, *J* = 11.5, 4.6 Hz, 2H),

2.93 – 2.86 (m, 2H). ^{13}C NMR (101 MHz, $CDCl_3$) δ 165.9, 157.9, 154.1, 136.9, 130.3, 129.3, 128.6, 128.0, 127.5, 115.3, 70.1, 29.7, 27.0.

Preparation of 3-(4-(((8*R*,9*S*,13*S*,14*S*)-13-methyl-17-oxo-7,8,9,11,12,13,14,15,16,17-decahydro-6H-cyclopenta[a]phenanthren-3-yl)oxy)phenethyl)-1,4,2-dioxazol-5-one (1ze)



3-(4-Bromophenyl)propanoic acid (20 mmol) was dissolved in methanol (40 mL), and sulfuric acid (concentrated, 0.4 mL) was added. The reaction mixture was heated to reflux for 6 h until full conversion. Solid $NaHCO_3$ was added to neutralize the solution. After filtration, the slightly yellow solution was evaporated to dryness. The residue was dissolved in ethyl acetate (40 mL) and washed with saturated sodium bicarbonate solution (20 mL) and saturated sodium chloride solution. The organic layer was dried and concentrated to give the methyl ester.

A Schlenk tube equipped with a magnetic stir bar was charged with K_2CO_3 (40 mmol), Estrone (10 mmol), methyl 3-(4-bromophenyl)propanoate (12 mmol), $Fe(acac)_3$ (10 mol %), CuI (10 mol %) in DMF (30 mL) under an N_2 atmosphere. The reaction mixture was heated to reflux overnight. The mixture was cooled to room temperature and diluted with EtOAc (20 mL). The resulting suspension was directly

filtered through a pad of Celite®, and the filtrate was washed with brine (20 mL) and dried over anhydrous Na_2SO_4. The organic phase was concentrated, and the crude mixtures were purified by column chromatography on silica gel (300–400 mesh) using n-hexane/EtOAc solvent mixture as the eluent.

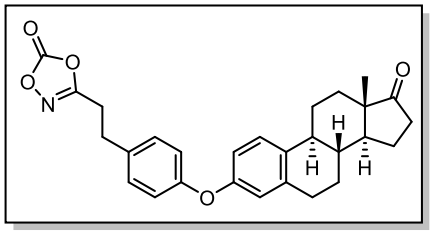
To a solution of the methyl ester (5 mmol) in methanol (40 mL) was added sodium hydroxide (15 mmol) in one portion. Then, the mixture was stirred at room temperature for overnight. After the reaction, methanol was removed by a rotatory evaporation, and water (20 mL) was added. Then, 1 N HCl was added to the mixture until pH = 1−2 being reached, and the mixture was extracted with ethyl acetate(20 mL x 3). The combined organic phase was collected and concentrated to give the crude product that was used for the next step without further purification.

To a DCM (30 mL) solution of corresponding carboxylic acid (2 mmol) was added oxalyl chloride (2.0 equiv, 0.34 mL) at 0 ˚C in a dropwise manner, and DMF (0.2 mL) was added to the mixture. After stirring the mixture at room temperature for 3 h, the solvent and excess oxalyl chloride were removed by vacuum distillation. K_2CO_3 (552.8 mg, 2.0 equiv) was dissolved in EtOAc/H_2O = 2:1 (16 mL of EtOAc and 8 mL of H_2O) and then cooled to 0 ˚C. The hydroxylamine hydrogen chloride (166.8 mg, 1.2 equiv) was added into the K_2CO_3 solution. The corresponding unpurified acyl chloride obtained was dissolved in DCM (5 mL) and was transferred to the reaction mixture.

The reaction mixture was stirred at room temperature for overnight. To work-up, the distillated water (30 mL) was added to the reaction mixture and the organic layer was separated. The aqueous phase was extracted with EtOAc (50 mL x 3) and the combined organic extracts were dried with $MgSO_4$. The solvent was removed by rotatory evaporation to obtain the corresponding hydroxamic acid for use without further purification.

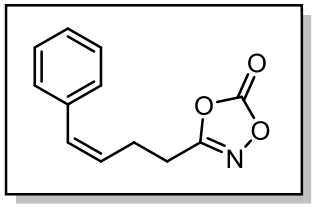
The corresponding hydroxamic acid (2 mmol) and CDI (1.1 equiv, 356.8 mg) were dissolved in DCM (20 mL) and stirred at room temperature for 30 mins. Then, 1M HCl (3 mL) was added to the reaction mixture, and the mixture was stirred at room temperature for another 1 h. After that, the organic layer was separated and the aqueous phase was extracted with DCM (3 x 20 mL). The combined organic extracts were dried by $MgSO_4$ and concentrated by rotatory evaporation. The crude mixture was purified by flash chromatography (n-hexane/EtOAc = 4:1) to obtain corresponding 3-(4-(((8*R*,9*S*,13*S*,14*S*)-13-methyl-17-oxo-7,8,9,11,12,13,14,15,16,17-decahydro-6H-cyclopenta[a]phenanthren-3-yl)oxy)phenethyl)-1,4,2-dioxazol-5-one.

3-(4-(((8*R*,9*S*,13*S*,14*S*)-13-methyl-17-oxo-7,8,9,11,12,13,14,15,16,17-decahydro-6H-cyclopenta[a]phenanthren-3-yl)oxy)phenethyl)-1,4,2-dioxazol-5-one (1ze)



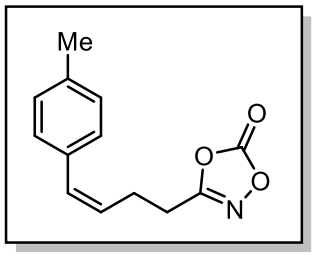
White solid; ^{1}H NMR (400 MHz, $CDCl_3$) δ 7.23 (d, *J* = 9.0 Hz, 1H), 7.13 (d, *J* = 8.4 Hz, 2H), 6.94 (d, *J* = 8.5 Hz, 2H), 6.78 (dd, *J* = 8.5, 2.4 Hz, 1H), 6.73 (d, *J* = 2.1 Hz, 1H), 3.05 – 2.96 (m, 2H), 2.97 – 2.81 (m, 4H), 2.50 (dd, *J* = 18.8, 8.6 Hz, 1H), 2.40 (dd, *J* = 12.9, 4.5 Hz, 1H), 2.26 (dd, *J* = 13.7, 7.1 Hz, 1H), 2.20 – 1.91 (m, 4H), 1.69 – 1.36 (m, 6H), 0.91 (s, 3H). ^{13}C NMR (101 MHz, $CDCl_3$) δ 165.8, 156.7, 154.8, 154.0, 138.4, 135.0, 132.4, 129.5, 126.7, 119.1, 119.0, 116.5, 50.4, 48.0, 44.1, 38.2, 35.9, 31.6, 29.8, 29.5, 26.8, 26.5, 25.9, 21.6, 13.9. HRMS (ESI) m/z: calcd for $C_{28}H_{30}NO_5$ [M + H], 460.2124; found, 460.2126.

(Z)-3-(4-Phenylbut-3-en-1-yl)-1,4,2-dioxazol-5-one (12a)[66k]–Prepared by Method D



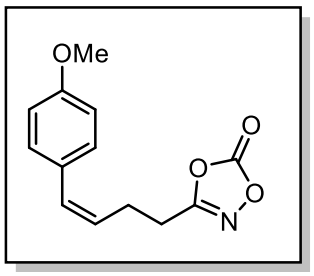
Colorless liquid; ^{1}H NMR (400 MHz, $CDCl_3$) δ 7.34 (t, *J* = 7.5 Hz, 2H), 7.23 (dd, *J* = 18.1, 7.5 Hz, 3H), 6.57 (d, *J* = 11.5 Hz, 1H), 5.66 – 5.54 (m, 1H), 2.76 – 2.65 (m, 4H). ^{13}C NMR (101 MHz, $CDCl_3$) δ 166.1, 154.1, 136.5, 132.1, 128.6, 128.5, 127.6, 127.3, 25.0, 23.48.

(*Z*)-3-(4-(*p*-Tolyl)but-3-en-1-yl)-1,4,2-dioxazol-5-one (12b)[66k]–Prepared by Method D



Colorless liquid; ^{1}H NMR (400 MHz, $CDCl_3$) δ 7.19 (q, *J* = 8.2 Hz, 4H), 6.59 (d, *J* = 11.5 Hz, 1H), 5.67 – 5.53 (m, 1H), 2.81 – 2.71 (m, 4H), 2.40 (s, 3H).^{13}C NMR (101 MHz, $CDCl_3$) δ 166.1, 154.1, 137.1, 133.7, 132.0, 129.2, 128.5, 126.9, 25.1, 23.5, 21.2.

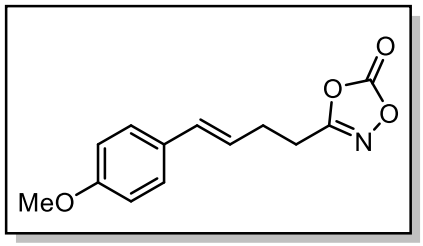
(*Z*)-3-(4-(4-Methoxyphenyl)but-3-en-1-yl)-1,4,2-dioxazol-5-one ((*Z*)-12c) Prepared by Method D



Yellow liquid; ^{1}H NMR (400 MHz, $CDCl_3$) δ 7.16 (d, *J* = 8.7 Hz, 2H), 6.90 – 6.81 (m, 2H), 6.49 (d, *J* = 11.4 Hz, 1H), 5.53 – 5.42 (m, 1H), 3.79 (s, 3H), 2.76 – 2.64 (m, 4H). ^{13}C NMR (101 MHz, $CDCl_3$) δ 166.1, 158.8, 154.1, 131.4, 129.9, 129.1, 126.1, 113.9, 55.3, 25.1, 23.5. HRMS (ESI) m/z: calcd for $C_{13}H_{14}NO_4$ [M + H], 248.0923; found, 248.0928.

(*E*)-3-(4-(4-Methoxyphenyl)but-3-en-1-yl)-1,4,2-dioxazol-5-one ((E)-12c)[66k]–

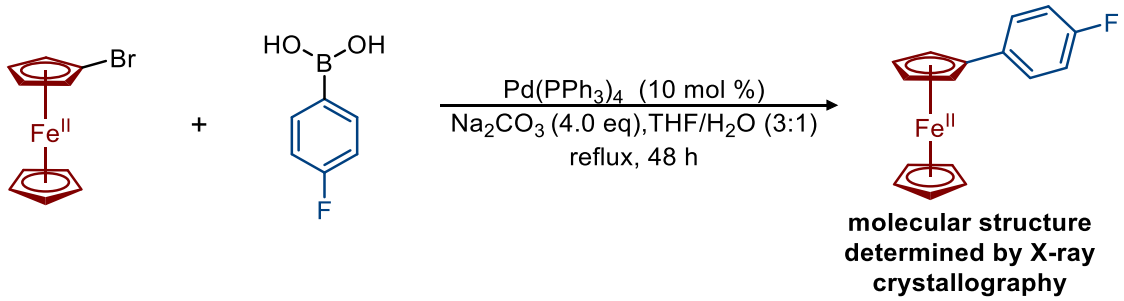
Prepared by Method D



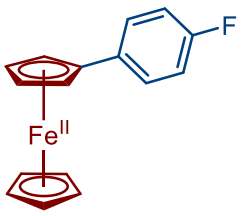
White solid; ^{1}H NMR (400 MHz, $CDCl_3$) δ 7.27 (d, *J* = 8.8 Hz, 2H), 6.84 (d, *J* = 8.8 Hz, 2H), 6.43 (d, *J* = 15.8 Hz, 1H), 6.00 (dt, *J* = 15.7, 6.9 Hz, 1H), 3.80 (s, 3H), 2.79 (t, *J* = 7.4 Hz, 2H), 2.61 (q, *J* = 7.1 Hz, 2H). ^{13}C NMR (101 MHz, $CDCl_3$) δ 166.2, 159.5, 154.3, 132.4, 129.5, 127.5, 123.4, 114.2, 55.5, 28.0, 25.2.

2.6.3 Preparation and Physical Characterization of Catalysts and Additives

2.6.3.1 Procedures for Preparation of (4-Fluorophenyl)ferrocene



To a 50 mL three-necked round-bottom flask equipped with a reflux condenser were added bromoferrocene (0.53 g, 2 mmol), 4-fluorophenylboronic acid (0.56 g, 4 mmol), $Pd(PPh_3)_4$, (0.23 g, 0.2 mmol), and Na_2CO_3 (0.85 g, 8 mmol) in a degassed mixture of THF/water (3:1 v/v, 20 mL). The mixture was allowed to reflux for 48 h under an argon atmosphere. The solvents were evaporated, and the black-brown residue was extracted with ethyl acetate (200 mL) followed by washing with water (3 x 120 mL), then with brine. The organic phase was dried over $MgSO_4$, concentrated under reduced pressure. The residue was then purified by silica gel column chromatography.



Yellow solid; mp 101−102 °C; ^{1}H NMR (400 MHz, $CDCl_3$) δ 7.45 – 7.38 (m, 2H), 7.01 – 6.92 (m, 2H), 4.57 (t, *J* = 1.8 Hz, 2H), 4.31 – 4.27 (m, 2H), 4.02 (s, 5H). ^{13}C NMR (101 MHz, $CDCl_3$) δ 127.5,

127.4, 115.3, 115.1, 69.6, 68.9, 66.4. ^{19}F NMR (376 MHz, $CDCl_3$) δ -117.1. HRMS (ESI) m/z: calcd for $C_{16}H_{14}FFe$ [M + H], 281.0429; found, 281.0381.

Figure 2.11 Molecular Structure of (4-Fluorophenyl)ferrocene (CCDC: 2143911)

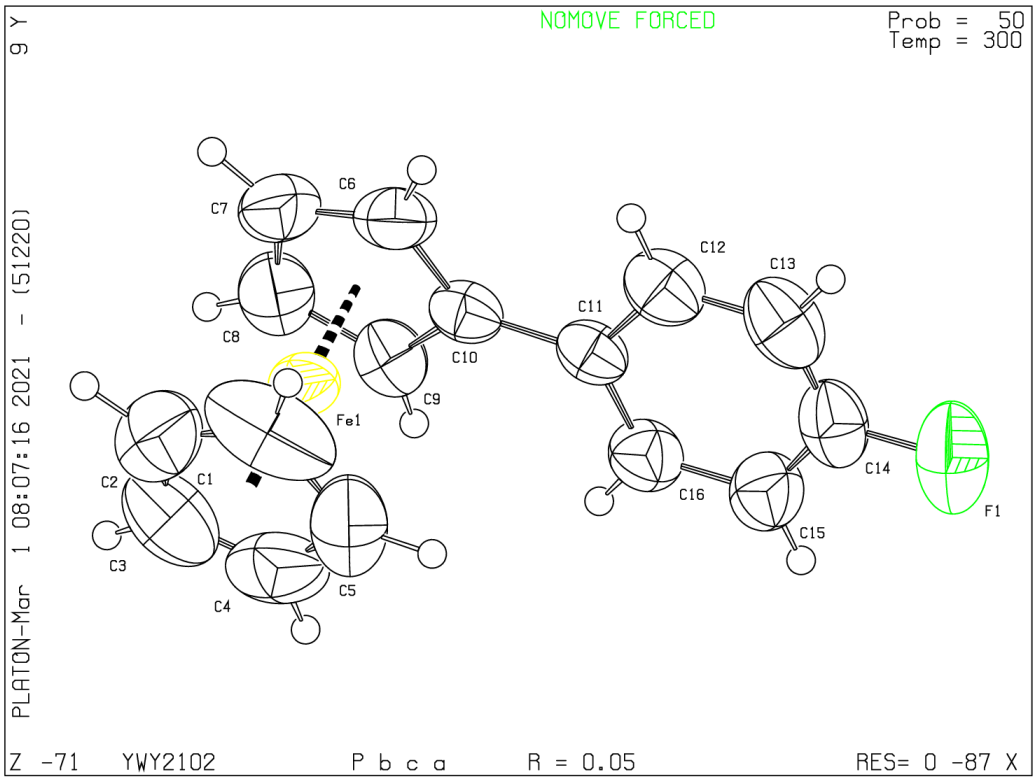
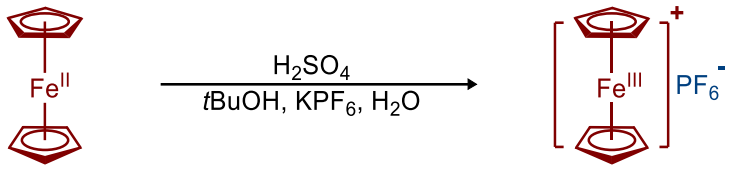


Table 2.10 Crystal Data and Structure Refinement of (4-Fluorophenyl)ferrocene

Compound	(4-Fluorophenyl)ferrocene **(CCDC:** 2143911**)**
Formula	$C_{16}H_{13}FFe$
$D_{calc.}$/ g cm^{-3}	1.480
μ/mm^{-1}	1.188
Formula weight	280.11
T/K	300(2)
Crystal system	Orthorhombic
space group	Pbca
a/Å	10.4854(9)
b/Å	7.8452(7)
c/Å	30.5606(25)
α/°	90
β/°	90
γ/°	90
V/Å^3	2513.9(4)
Z	8
Wavelength/Å	0.71073
Radiation type	MoK
Θ_{min}/°	2.36
Θ_{max}/°	27.473
F(000)	1152
Measured Refl.	9922
Independent Refl.	2859
Reflections with I > 2(I)	2433
R_{int}	0.0328
Parameters	163
Restraints	6
Largest Peak	0.720
Deepest Hole	-0.391
Goodness-of-Fit	1.050
wR_2 (all data)	0.1400

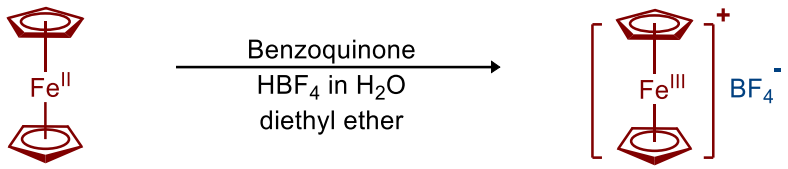
wR_2	0.1340
R_1 (all data)	0.0566
R_1	0.0498

2.6.3.2 Preparation of Ferrocenium Hexafluorophosphate[77]



Ferrocene (5.58 g, 30.0 mmol) was added to concentrated H_2SO_4 (10 mL) and the mixture was stirred for 45 min. The blue-black reaction mixture was slowly added to a solution of *t*BuOH (5.00 g) in H_2O (170 mL), stirred for 15 min, and filtered. At 0 °C, KPF_6 (11.00 g, 60.0 mmol), dissolved in H_2O (235 mL), was added to the filtrate and the mixture was stirred for 60 min at 0 °C. The blue precipitate was filtered, washed twice with 40 mL ice-cold H_2O, 50 mL EtOH, and diethyl ether. Drying the solid for 12 h in vacuum. Yield: 8.46 g (85%); Blue solid; HRMS (ESI) m/z: calcd for $C_{10}H_{10}Fe^+$, 186.0132; found, 186.0127. elemental analysis calcd (%) for $C_{10}H_{10}F_6FeP$ (331.00) : C, 36.29; H, 3.05; found: C, 36.15; H, 3.12.

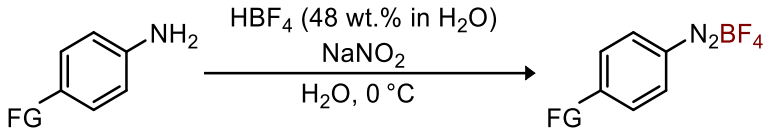
2.6.3.3 Preparation of Ferrocenium Tetrafluoroborate[78]



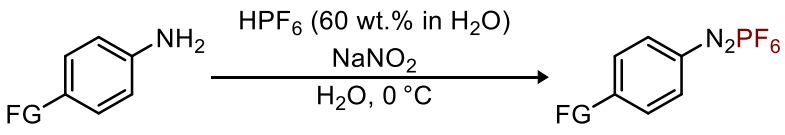
Benzoquinone (0.5 mmol) was added to ferrocene (1.0 mmol) in diethyl ether (20 mL) at room temperature. The reaction mixture was stirred for 10 min. Then HBF_4 (48 wt% solution in H_2O, 2.0 mmol) was added at 0 °C. A blue solid was formed, which was filtered through a sintered glass funnel and washed with ice-cold ether until the

ether solution became colorless to give products. Blue solid; HRMS (ESI) m/z: calcd for $C_{10}H_{10}Fe^{+}$, 186.0132; found, 186.0129. elemental analysis calcd (%) for $C_{10}H_{10}BF_4Fe$ (272.84) : C, 44.02; H, 3.69; found: C, 44.13; H, 3.63.

2.6.3.4 Preparation of Aryldiazonium Tetrafluoroborates and Aryldiazonium Hexafluorophosphates[79]



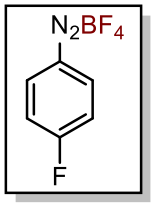
To a solution of aniline (10 mmol) in distilled water (6 mL) was added tetrafluoroboric acid solution (48 wt.% in H_2O, 26 mmol) at 0 °C. Sodium nitrite (0.7 g, 10 mmol) in distilled water (2 mL) was added dropwise and allowed to stir for 1 h at 0 °C. A thick precipitate was collected by filtration, followed by washing with diethyl ether (40 mL). The resulting precipitate was further purified by recrystallization with acetonitrile/diethyl ether to give the desired aryldiazonium tetrafluorborate as a white solid.



To a solution of aniline (10 mmol) in distilled water (6 mL) was added HPF_6 (60 wt.% in H_2O, 26 mmol) at 0 °C. Sodium nitrite (0.7 g, 10 mmol) in distilled water (2

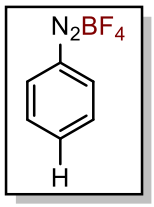
mL) was added dropwise and allowed to stir for 1 h at 0 °C. A thick precipitate was collected by filtration, followed by washing with diethyl ether (40 mL). The resulting precipitate was further purified by recrystallization with acetone/diethyl ether to give the title product as a white solid.

4-Fluorobenzenediazonium tetrafluoroborate (F1)



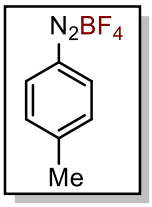
White solid; mp 147−148 °C; ^{1}H NMR (400 MHz, DMSO) δ 8.83 – 8.70 (m, 2H), 7.86 (dd, *J* = 12.1, 5.5 Hz, 2H). ^{13}C NMR (101 MHz, DMSO) δ 170.2, 167.5, 137.5, 137.4, 120.0, 119.7, 112.3. ^{19}F NMR (376 MHz, DMSO) δ -87.2, -148.1, -148.2. HRMS (ESI) m/z: calcd for $C_6H_4F^+$, 95.0297; found, 95.0298.

Benzenediazonium tetrafluoroborate (F2)



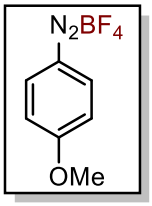
White solid; mp 95−96 °C; ^{1}H NMR (400 MHz, DMSO) δ 8.63 (d, *J* = 8.0 Hz, 2H), 8.22 (t, *J* = 7.6 Hz, 1H), 7.95 (t, *J* = 8.1 Hz, 2H). ^{13}C NMR (101 MHz, DMSO) δ 141.3, 133.1, 131.7, 116.5. ^{19}F NMR (376 MHz, DMSO) δ -148.1, -148.2. HRMS (ESI) m/z: calcd for $C_6H_5^+$, 77.0391; found, 77.0388.

4-Methylbenzenediazonium tetrafluoroborate (F3)



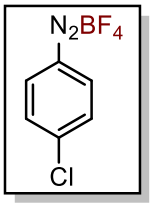
White solid; mp 103−104 °C; ^{1}H NMR (400 MHz, DMSO) δ 8.51 (d, *J* = 8.7 Hz, 2H), 7.76 (d, *J* = 8.6 Hz, 2H), 2.54 (s, 3H). ^{13}C NMR (101 MHz, DMSO) δ 154.4, 133.1, 132.2, 112.4, 22.3. ^{19}F NMR (376 MHz, DMSO) δ -148.1, -148.2. HRMS (ESI) m/z: calcd for $C_7H_7^+$, 91.0548; found, 91.0547.

4-Methoxybenzenediazonium tetrafluoroborate (F4)



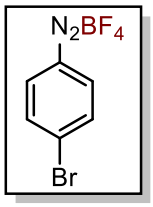
White solid; mp 139−140 °C; ^{1}H NMR (400 MHz, DMSO) δ 8.58 (d, *J* = 9.3 Hz, 2H), 7.45 (d, *J* = 9.4 Hz, 2H), 4.01 (s, 3H). ^{13}C NMR (101 MHz, DMSO) δ 169.2, 136.6, 117.7, 103.8, 57.9. ^{19}F NMR (376 MHz, DMSO) δ -148.2, -148.2. HRMS (ESI) m/z: calcd for $C_7H_7O^+$, 107.0497; found, 107.0492.

4-Chlorobenzenediazonium tetrafluoroborate (F5)



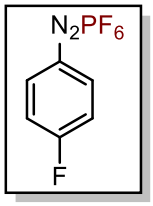
White solid; mp 134−135 °C; ^{1}H NMR (400 MHz, DMSO) δ 8.65 (d, *J* = 9.0 Hz, 2H), 8.08 (d, *J* = 9.0 Hz, 2H). ^{13}C NMR (101 MHz, DMSO) δ 147.0, 134.9, 132.1, 115.2. ^{19}F NMR (376 MHz, DMSO) δ -148.1, -148.2. HRMS (ESI) m/z: calcd for $C_6H_4Cl^+$, 111.0002; found, 110.9995.

4-Bromobenzenediazonium tetrafluoroborate (F6)



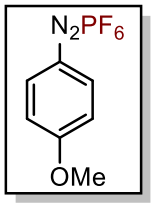
White solid; mp 140−141 °C; ^{1}H NMR (400 MHz, DMSO) δ 8.54 (d, *J* = 9.0 Hz, 2H), 8.22 (d, *J* = 9.0 Hz, 2H). ^{13}C NMR (101 MHz, DMSO) δ 137.0, 135.0, 134.4, 115.6. ^{19}F NMR (376 MHz, DMSO) δ -148.1, -148.2. HRMS (ESI) m/z: calcd for $C_6H_4Br^+$, 154.9496; found, 154.9489.

4-Fluorobenzenediazonium hexafluorophosphate (F7)



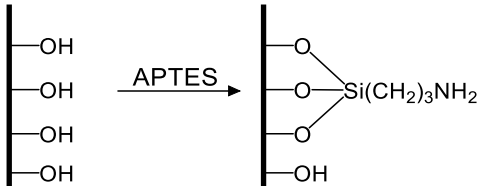
White solid; mp 125−126 °C; ^{1}H NMR (400 MHz, DMSO) δ 8.84 – 8.71 (m, 2H), 7.86 (dd, *J* = 14.6, 5.9 Hz, 2H). ^{13}C NMR (101 MHz, DMSO) δ 170.2, 167.5, 137.5, 137.4, 120.0, 119.7, 112.3, 112.3. ^{19}F NMR (376 MHz, DMSO) δ -69.2, -71.0, -87.2. ^{31}P NMR (162 MHz, DMSO) δ -144.2. HRMS (ESI) m/z: calcd for $C_6H_4F^+$, 95.0297; found, 95.0295.

4-Methoxybenzenediazonium hexafluorophosphate (F8)

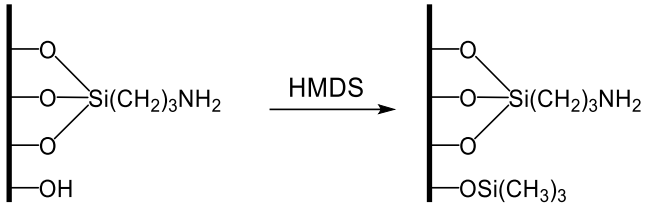


White solid; mp 149−150 °C; ^{1}H NMR (400 MHz, DMSO) δ 8.58 (d, *J* = 9.3 Hz, 2H), 7.45 (d, *J* = 9.3 Hz, 2H), 4.01 (s, 3H). ^{13}C NMR (101 MHz, DMSO) δ 169.2, 136.6, 117.7, 103.8, 57.9. ^{19}F NMR (376 MHz, DMSO) δ -69.2, -71.1. ^{31}P NMR (162 MHz, DMSO) δ -144.2. HRMS (ESI) m/z: calcd for $C_7H_7O^+$, 107.0497; found, 107.0492.

2.6.3.5 Preparation of Silica-APTES-ferrocene

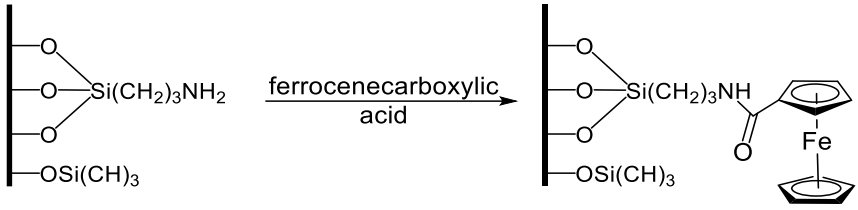


Patterning: Silica gel 60 (230-400 mesh) (2 g) was suspended in a chloroform solution of APTES (0.05 M, 22 mL) at room temperature for 8-12 h with stirring. The solid product was collected by filtration, washed with chloroform, and then dried in a vacuum at room temperature overnight, and then stored in a dry box.



Silanol Capping Reaction:

Silica–APTES was then contacted with a large excess of hexamethyldisilazane in anhydrous toluene at room temperature under argon for 24 h. The resulting solid was filtered and washed with toluene and hexane in a dry box, dried under vacuum at room temperature overnight, and then stored in a dry box.



Metalation:

Silica–APTES–TMS was suspended in a DCM solution (0.1 M, 50 mL) of ferrocene carboxylic acid, (5.5 mmol) O-(7-Azabenzotriazol-1-yl)-N,N,N,N-tetramethyluronium hexafluorophosphate (HATU) and (5.5 mmol) N,N-diisopropylethylamine at room temperature for 12 h with stirring. The yellow solid product was collected by filtration, washed with DCM (40 mL x 3), DMF (40 mL x 3) and Acetone (40mL x 3), and then dried in a vacuum at room temperature overnight, and then stored in a dry box.

Figure 2.12 UV-Vis Spectrum of SiO_2-APTES and SiO_2-APTES-Ferrocene

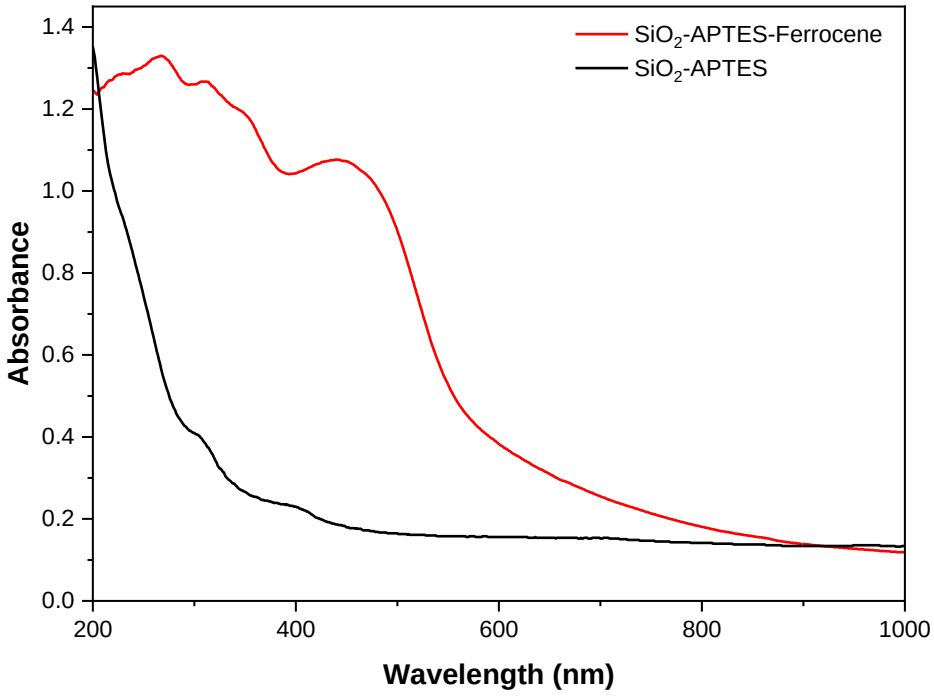


Figure 2.13 FT-IR Spectrum of SiO_2-APTES, SiO_2-APTES-Ferrocene before 1st Cycle and after 5th Cycle

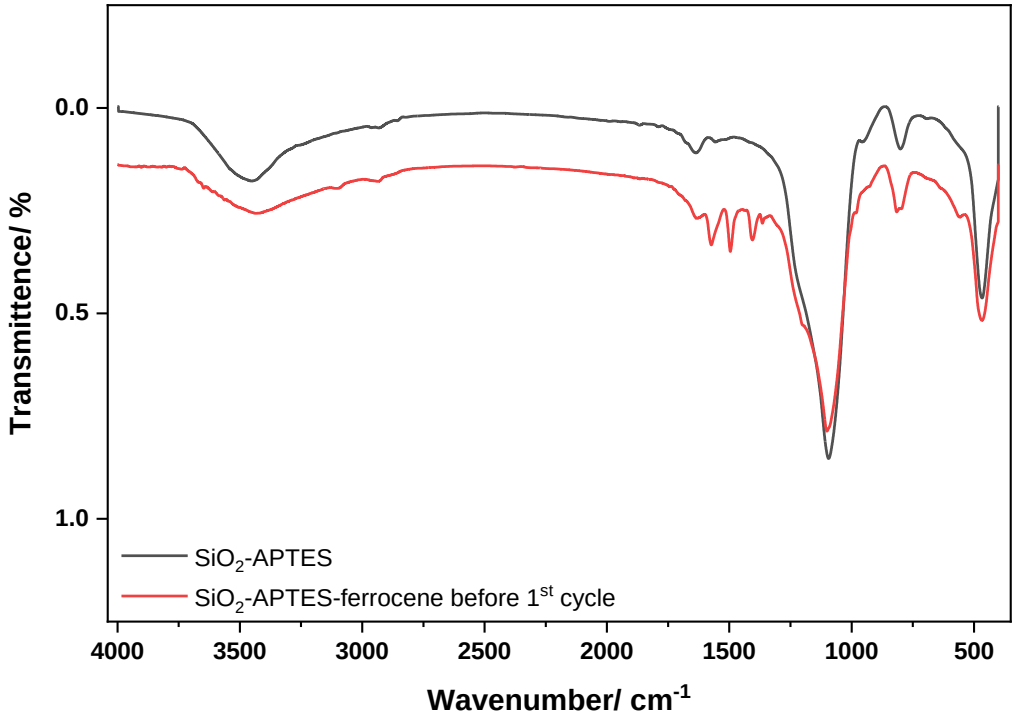


Figure 2.14 TGA Profile of Silica-APTES

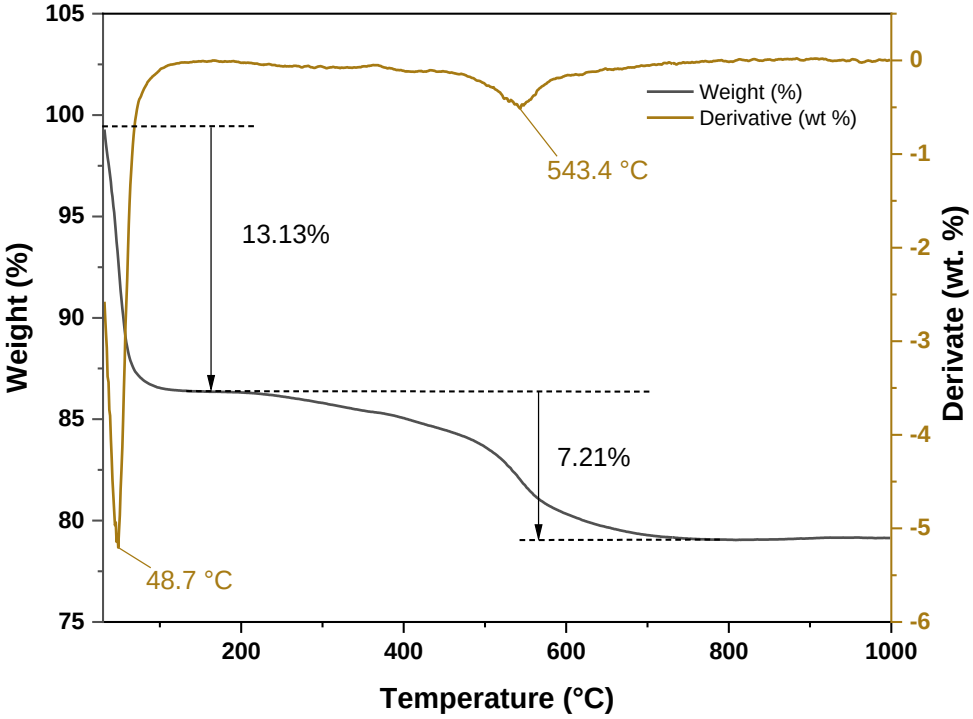


Figure 2.15 TGA Profile of Silica-APTES-Ferrocene

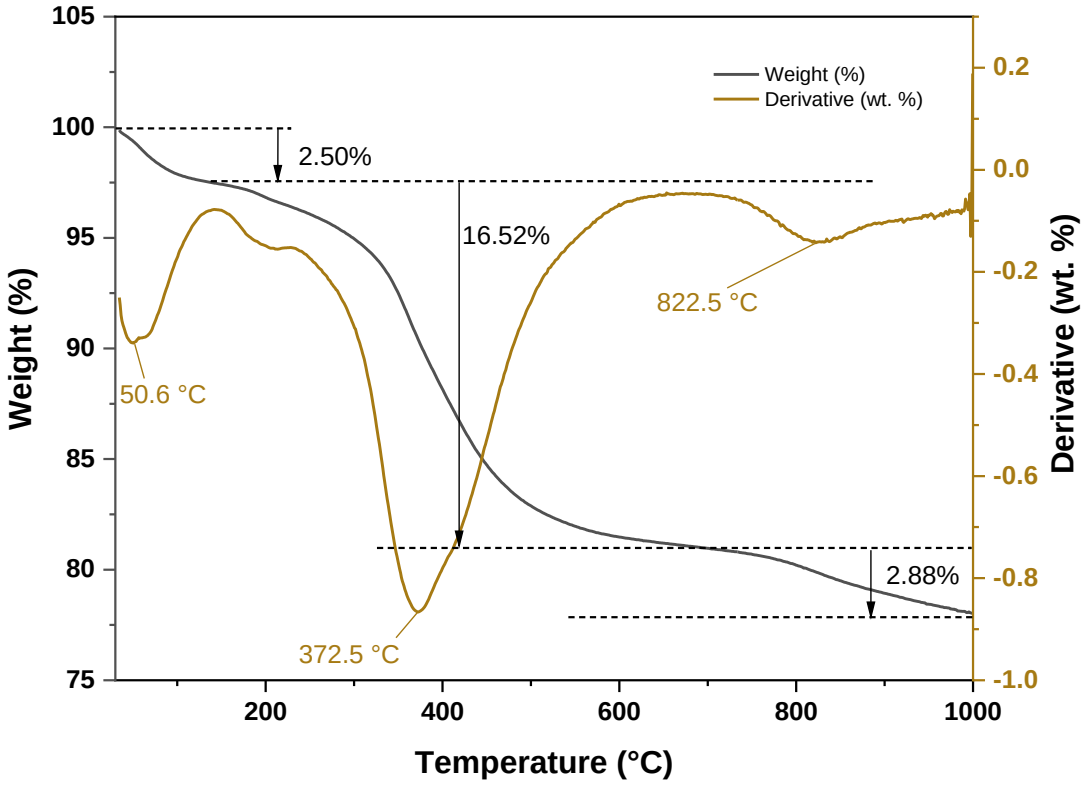


Figure 2.16 XPS Spectrum Silica-APTES-Ferrocene

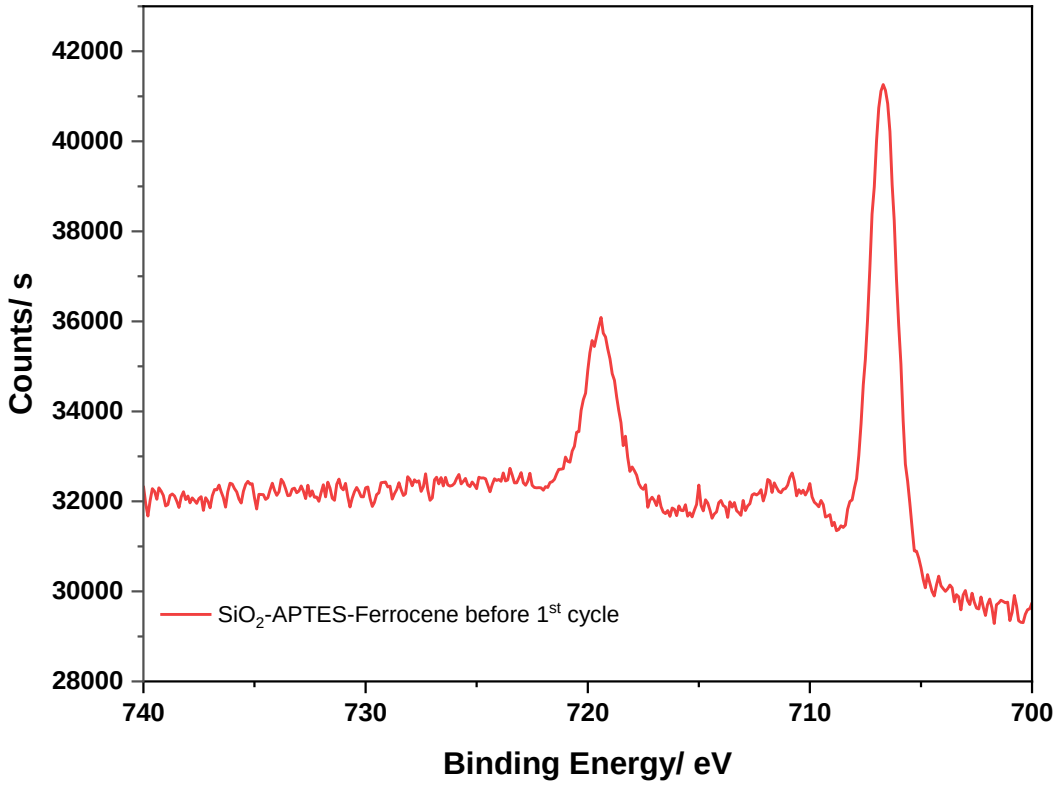


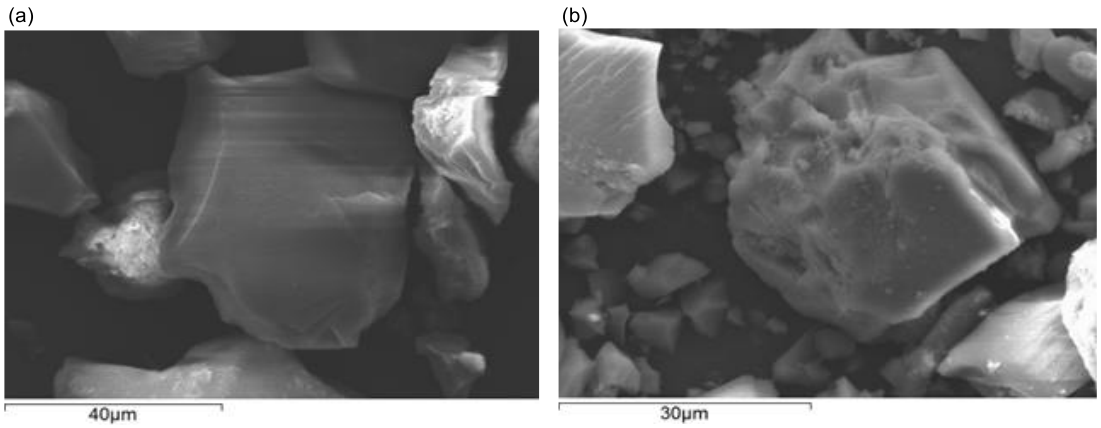
Table 2.11 Elemental Analysis of SiO_2-APTES-Fc before 1st Run by SEM-EDX

No.	Element	Weight%	Atomic%
1	C	15.38	22.42
2	N	2.98	3.73
3	O	50.33	55.08
4	Si	28.89	18.01
5	Fe	2.41	0.76

Table 2.12 Elemental Analysis of SiO_2-APTES-Fc after 5th Run by SEM-EDX

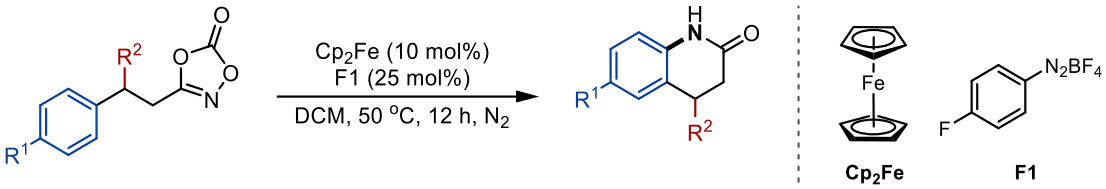
No.	Element	Weight%	Atomic%
1	C	36.02	46.63
2	N	14.85	12.16
3	O	34.41	33.45
4	Si	13.32	7.38
5	Fe	1.39	0.39

Figure 2.17 SEM Images of SiO_2-APTES-Fc (a) before 1st Run (b) after 5th Run



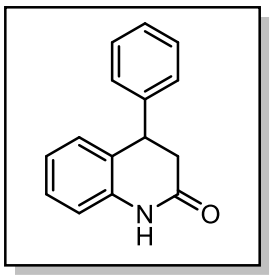
2.6.4 Experimental Procedures for Ferrocenium-Catalyzed Reactions

General Procedures for Fe-Catalyzed Intramolecular C(sp^2)-H Bond Amidation



In a glove box, ferrocene (3.72 mg, 10 mol%) and 4-fluorobenzenediazonium tetrafluoroborate (10.5 mg, 25 mol%) were added into an 8 mL-vial A. Dry DCM (1 mL) was added to the 8 mL-vial. The reaction was stirred at room temperature for 15 min. The dioxazolones (0.2 mmol) was added into another 4 mL-vial B and dissolved in dry DCM (1 mL). The dioxazolones solution was transferred from vial B to vial A. The reaction in vial A was sealed and stirred at 50 °C for 12 h. After 12 h, the reaction crude mixture was evaporated to dryness under vacuum, and the residue was passed through the Celite® eluted with EtOAc (25 mL). The solvent was moved by vacuum and the products were purified by preparative flash column chromatography.

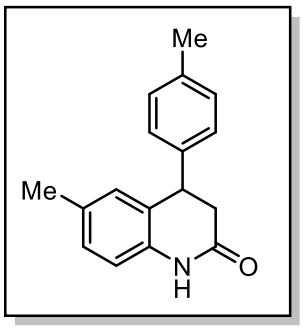
4-Phenyl-3,4-dihydroquinolin-2(1H)-one (2a)



White solid; mp 176−177 °C; ^{1}H NMR (400 MHz, $CDCl_3$) δ 8.68 (s, 1H), 7.32 (t, *J* = 7.3 Hz, 2H), 7.28 – 7.23 (m, 1H), 7.19 (t, *J* = 6.6 Hz, 3H), 6.93 (dt, *J* = 14.8, 7.4 Hz, 2H), 6.85 (d, *J* = 7.9 Hz, 1H), 4.29 (t, *J* = 7.4 Hz, 1H), 2.99 – 2.86 (m, 2H). ^{13}C NMR (101 MHz, $CDCl_3$) δ 170.7, 141.5, 137.1, 128.9, 128.4, 128.0, 127.8, 127.3, 126.7,

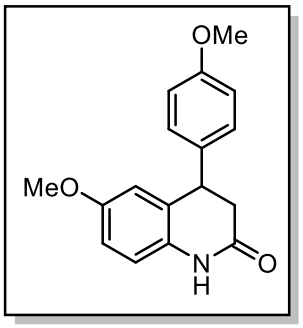
123.4, 115.7, 42.0, 38.4. HRMS (ESI) m/z: calcd for $C_{15}H_{14}NO$ [M + H], 224.1075; found, 224.1075.

6-Methyl-4-(p-tolyl)-3,4-dihydroquinolin-2(1H)-one (2b)



White solid; mp 179−180 °C; ^{1}H NMR (400 MHz, $CDCl_3$) δ 8.41 (s, 1H), 7.13 (d, *J* = 8.0 Hz, 2H), 7.06 (d, *J* = 8.1 Hz, 2H), 6.98 (d, *J* = 8.0 Hz, 1H), 6.75 – 6.68 (m, 2H), 4.20 (t, *J* = 7.3 Hz, 1H), 2.93 – 2.81 (m, 2H), 2.32 (s, 3H), 2.20 (s, 3H). ^{13}C NMR (101 MHz, $CDCl_3$) δ 171.2, 138.7, 136.8, 134.7, 132.9, 129.6, 128.9, 128.4, 127.7, 126.7, 115.7, 41.7, 38.6, 21.1, 20.8. HRMS (ESI) m/z: calcd for $C_{17}H_{18}NO$ [M + H], 252.1388; found, 252.1383.

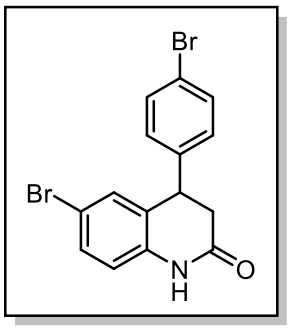
6-Methoxy-4-(4-methoxyphenyl)-3,4-dihydroquinolin-2(1H)-one (2c)



White solid; mp 154−155 °C; ^{1}H NMR (400 MHz, $CDCl_3$) δ 8.55 (s, 1H), 7.09 (d, *J* = 8.6 Hz, 2H), 6.88 – 6.82 (m, 2H), 6.74 (dt, *J* = 8.6, 5.6 Hz, 2H), 6.46 (d, *J* = 2.4 Hz, 1H), 4.24 – 4.14 (m, 1H), 3.78 (s, 3H), 3.68 (s, 3H), 2.91 – 2.77 (m, 2H). ^{13}C NMR (101 MHz, $CDCl_3$) δ 171.0, 158.7, 155.8, 133.3, 130.7, 128.8, 128.5,

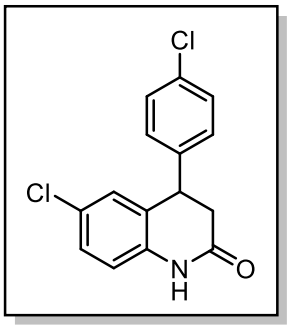
116.6, 114.3, 112.7, 55.5, 55.3, 41.5, 38.5. HRMS (ESI) m/z: calcd for $C_{17}H_{18}NO_3$ [M + H], 284.1287; found, 284.1283.

6-Bromo-4-(4-bromophenyl)-3,4-dihydroquinolin-2(1H)-one (2d)



White solid; mp 257−258 °C; ^{1}H NMR (400 MHz, $CDCl_3$) δ 8.25 (s, 1H), 7.47 (d, *J* = 8.3 Hz, 2H), 7.32 (dd, *J* = 8.3, 1.7 Hz, 1H), 7.11 – 6.97 (m, 3H), 6.71 (d, *J* = 8.4 Hz, 1H), 4.27 – 4.15 (m, 1H), 2.86 (qd, *J* = 16.3, 7.5 Hz, 2H). ^{13}C NMR (101 MHz, $CDCl_3$) δ 169.5, 139.5, 136.1, 132.3, 131.2, 131.2, 129.4, 128.2, 121.6, 117.2, 116.0, 41.4, 38.0. HRMS (ESI) m/z: calcd for $C_{15}H_{12}Br_2NO$ [M + H], 379.9286; found, 379.9278.

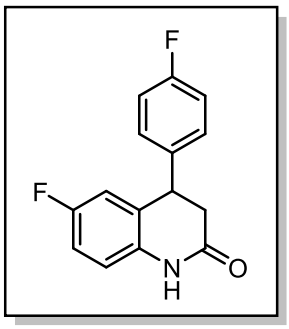
6-Chloro-4-(4-chlorophenyl)-3,4-dihydroquinolin-2(1H)-one (2e)



White solid; mp 234−235 °C; ^{1}H NMR (400 MHz, $CDCl_3$) δ 8.66 (s, 1H), 7.33 (d, *J* = 8.3 Hz, 2H), 7.19 (d, *J* = 8.3 Hz, 1H), 7.12 (d, *J* = 8.2 Hz, 2H), 6.88 (s, 1H), 6.80 (d, *J* = 8.4 Hz, 1H), 4.29 – 4.19 (m, 1H), 2.88 (qd, *J* = 16.3, 7.5 Hz, 2H). ^{13}C NMR (101 MHz, $CDCl_3$) δ 170.0, 139.0, 135.6, 133.5, 129.3, 129.1, 128.6, 128.3, 127.9,

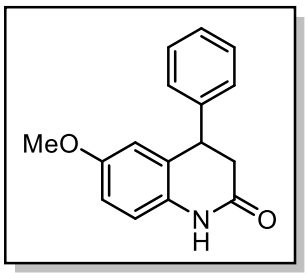
116.9, 41.4, 38.0. HRMS (ESI) m/z: calcd for $C_{15}H_{12}Cl_2NO$ [M + H], 292.0296; found, 292.0291.

6-Fluoro-4-(4-fluorophenyl)-3,4-dihydroquinolin-2(1H)-one (2f)



White solid; mp 211−212 °C; ^{1}H NMR (400 MHz, $CDCl_3$) δ 9.07 (s, 1H), 7.21 – 7.09 (m, 2H), 7.08 – 6.98 (m, 2H), 6.90 (td, *J* = 8.3, 2.7 Hz, 1H), 6.83 (dd, *J* = 8.6, 4.8 Hz, 1H), 6.59 (dd, *J* = 8.9, 2.6 Hz, 1H), 4.25 (dd, *J* = 8.6, 6.6 Hz, 1H), 2.87 (qd, *J* = 16.2, 7.7 Hz, 2H). ^{13}C NMR (101 MHz, $CDCl_3$) δ 170.8, 163.3, 160.9, 160.1, 157.7, 136.4, 133.2, 129.3, 128.4, 117.0, 116.1, 115.9, 115.3, 115.0, 114.7, 41.4, 38.2. ^{19}F NMR (376 MHz, $CDCl_3$) δ -114.8, -119.1. HRMS (ESI) m/z: calcd for $C_{15}H_{12}F_2NO$ [M + H], 260.0887; found, 260.0884.

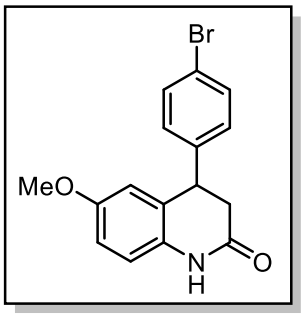
6-Methoxy-4-phenyl-3,4-dihydroquinolin-2(1H)-one (2g)



White solid; mp 153−154 °C; ^{1}H NMR (400 MHz, $CDCl_3$) δ 9.04 (s, 1H), 7.32 (t, *J* = 7.3 Hz, 2H), 7.25 (dd, *J* = 8.4, 6.1 Hz, 1H), 7.18 (d, *J* = 7.1 Hz, 2H), 6.81 (d, *J* = 8.6 Hz, 1H), 6.73 (dd, *J* = 8.6, 2.7 Hz, 1H), 6.46 (d, *J* = 2.6 Hz, 1H), 4.24 (t, *J* = 7.4 Hz, 1H), 3.67 (s, 3H), 2.96 – 2.82 (m, 2H). ^{13}C NMR (101 MHz, $CDCl_3$) δ 171.0, 155.8, 141.4, 130.8,

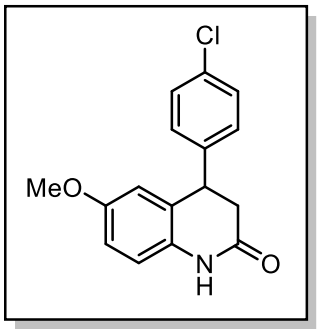
128.9, 128.0, 127.8, 127.3, 116.7, 114.4, 112.8, 55.5, 42.3, 38.4. HRMS (ESI) m/z: calcd for $C_{16}H_{16}NO_2$ [M + H], 254.1181; found, 254.1179.

4-(4-Bromophenyl)-6-methoxy-3,4-dihydroquinolin-2(1H)-one (2h)



White solid; mp 180−181 °C; ^{1}H NMR (400 MHz, $CDCl_3$) δ 8.28 (s, 1H), 7.49 – 7.38 (m, 2H), 7.05 (d, *J* = 8.4 Hz, 2H), 6.81 – 6.71 (m, 2H), 6.45 (d, *J* = 2.0 Hz, 1H), 4.24 – 4.16 (m, 1H), 3.69 (s, 3H), 2.85 (qd, *J* = 16.1, 7.3 Hz, 2H). ^{13}C NMR (101 MHz, $CDCl_3$) δ 170.2, 155.9, 140.4, 132.1, 130.6, 129.5, 127.4, 121.2, 116.7, 114.3, 113.1, 55.6, 41.8, 38.2. HRMS (ESI) m/z: calcd for $C_{16}H_{15}BrNO_2$ [M + H], 332.0286; found, 332.0284.

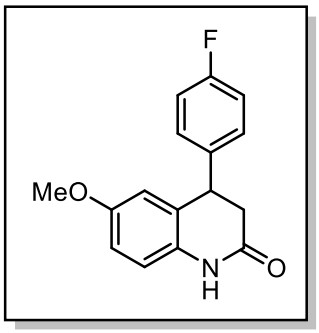
4-(4-Chlorophenyl)-6-methoxy-3,4-dihydroquinolin-2(1H)-one (2i)



White solid; mp 172−173 °C; ^{1}H NMR (400 MHz, $CDCl_3$) δ 8.98 (s, 1H), 7.27 (t, *J* = 9.3 Hz, 2H), 7.10 (d, *J* = 8.2 Hz, 2H), 6.86 – 6.69 (m, 2H), 6.45 (s, 1H), 4.22 (t, *J* = 7.1 Hz, 1H), 3.69 (s, 3H), 2.85 (qd, *J* = 16.1, 7.2 Hz, 2H). ^{13}C NMR (101 MHz, $CDCl_3$) δ 170.6, 155.9, 139.9, 133.1, 130.7, 129.2, 129.1, 127.4, 116.9,

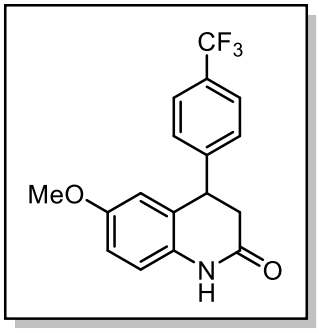
114.3, 113.0, 55.6, 41.7, 38.3. HRMS (ESI) m/z: calcd for $C_{16}H_{15}ClNO_2$ [M + H], 288.0791; found, 288.0788.

4-(4-Fluorophenyl)-6-methoxy-3,4-dihydroquinolin-2(1H)-one (2j)



White solid; mp 169−170 °C; ^{1}H NMR (400 MHz, $CDCl_3$) δ 9.00 (s, 1H), 7.19 – 7.08 (m, 2H), 7.00 (t, *J* = 8.3 Hz, 2H), 6.77 (dd, *J* = 30.3, 7.8 Hz, 2H), 6.45 (s, 1H), 4.23 (t, *J* = 6.8 Hz, 1H), 3.69 (s, 3H), 2.86 (qd, *J* = 16.1, 7.3 Hz, 2H). ^{13}C NMR (101 MHz, $CDCl_3$) δ 170.2, 163.2, 160.7, 155.9, 137.0, 137.0, 130.5, 129.4, 129.3, 127.9, 116.6, 115.9, 115.7, 114.3, 112.9, 55.5, 41.6, 38.5. ^{19}F NMR (376 MHz, $CDCl_3$) δ -115.4. HRMS (ESI) m/z: calcd for $C_{16}H_{15}FNO_2$ [M + H], 272.1087; found, 272.1085.

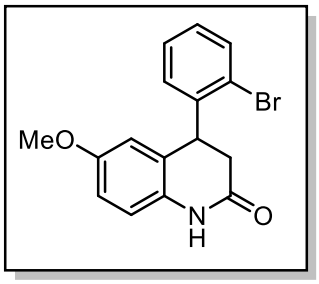
6-Methoxy-4-(4-(trifluoromethyl)phenyl)-3,4-dihydroquinolin-2(1H)-one (2k)



White solid; mp 223−224 °C; ^{1}H NMR (400 MHz, $CDCl_3$) δ 9.11 (s, 1H), 7.57 (d, *J* = 8.0 Hz, 2H), 7.29 (d, *J* = 8.0 Hz, 2H), 6.84 (d, *J* = 8.6 Hz, 1H), 6.76 (dd, *J* = 8.6, 1.9 Hz, 1H), 6.46 (s, 1H), 4.31 (t, *J* = 7.0 Hz, 1H), 3.69 (s, 3H), 2.90 (ddd, *J* = 24.0, 16.2, 7.1 Hz, 2H). ^{13}C NMR (101 MHz, $CDCl_3$) δ 170.0, 155.9, 145.5, 130.6, 129.8, 129.5, 128.2, 126.9, 126.0, 126.0, 125.9, 125.9, 125.4, 122.7, 116.9, 114.4, 113.2,

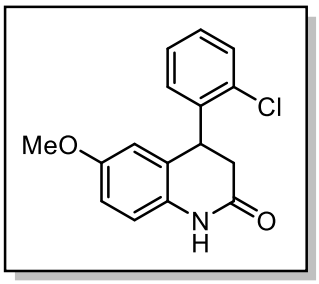
55.6, 42.2, 38.2. ^{19}F NMR (376 MHz, $CDCl_3$) δ -62.6. HRMS (ESI) m/z: calcd for $C_{17}H_{15}F_3NO_2$ [M + H], 322.1055; found, 322.1051.

4-(2-Bromophenyl)-6-methoxy-3,4-dihydroquinolin-2(1H)-one (2l)



White solid; mp 220−221 °C; ^{1}H NMR (400 MHz, $CDCl_3$) δ 9.27 (s, 1H), 7.60 (d, *J* = 7.9 Hz, 1H), 7.20 (t, *J* = 7.4 Hz, 1H), 7.10 (t, *J* = 7.1 Hz, 1H), 6.95 (d, *J* = 7.5 Hz, 1H), 6.85 (d, *J* = 8.6 Hz, 1H), 6.76 (dd, *J* = 8.6, 2.4 Hz, 1H), 6.48 (d, *J* = 1.9 Hz, 1H), 4.77 (t, *J* = 6.9 Hz, 1H), 3.68 (s, 3H), 2.96 – 2.83 (m, 2H). ^{13}C NMR (101 MHz, $CDCl_3$) δ 170.2, 156.0, 140.5, 133.3, 131.1, 129.1, 128.8, 128.1, 126.6, 124.4, 116.8, 114.2, 113.4, 55.6, 41.4, 37.0. HRMS (ESI) m/z: calcd for $C_{16}H_{15}BrNO_2$ [M + H], 332.0286; found, 332.0281.

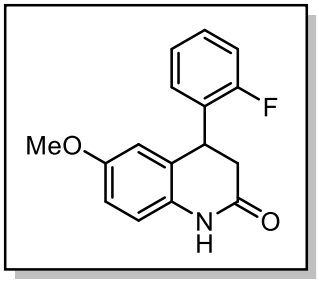
4-(2-Chlorophenyl)-6-methoxy-3,4-dihydroquinolin-2(1H)-one (2m)



White solid; mp 207−208 °C; ^{1}H NMR (400 MHz, $CDCl_3$) δ 9.53 (s, 1H), 7.41 (d, *J* = 7.6 Hz, 1H), 7.16 (td, *J* = 13.7, 6.7 Hz, 2H), 6.93 (d, *J* = 7.2 Hz, 1H), 6.86 (d, *J* = 8.6 Hz, 1H), 6.75 (dd, *J* = 8.6, 2.3 Hz, 1H), 6.48 (s, 1H), 4.78 (t, *J* = 6.8 Hz, 1H), 3.68 (s, 3H), 2.96 – 2.85 (m, 2H). ^{13}C NMR (101 MHz, $CDCl_3$) δ 170.5,

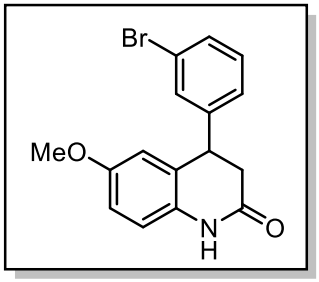
156.0, 138.8, 133.7, 131.1, 130.0, 129.0, 128.5, 127.4, 126.5, 116.8, 114.1, 113.4, 55.5, 38.8, 36.8. HRMS (ESI) m/z: calcd for $C_{16}H_{15}ClNO_2$ [M + H], 288.0791; found, 288.0788.

4-(2-Fluorophenyl)-6-methoxy-3,4-dihydroquinolin-2(1H)-one (2n)



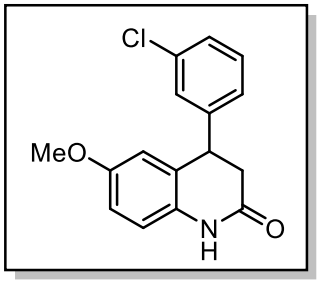
White solid; mp 139−140 °C; ^{1}H NMR (400 MHz, $CDCl_3$) δ 9.52 (s, 1H), 7.22 (dd, *J* = 11.3, 4.3 Hz, 1H), 7.02 (ddd, *J* = 26.5, 16.3, 8.5 Hz, 3H), 6.85 (d, *J* = 8.6 Hz, 1H), 6.74 (dd, *J* = 8.5, 2.0 Hz, 1H), 6.51 (s, 1H), 4.59 (t, *J* = 6.9 Hz, 1H), 3.68 (s, 3H), 2.90 (d, *J* = 7.0 Hz, 2H). ^{13}C NMR (101 MHz, $CDCl_3$) δ 170.7, 161.8, 159.4, 155.9, 130.9, 129.1, 129.1, 129.0, 128.9, 128.4, 128.3, 126.4, 124.6, 124.6, 116.8, 115.9, 115.7, 114.0, 113.2, 55.5, 37.0, 35.7, 35.6. ^{19}F NMR (376 MHz, $CDCl_3$) δ -117.1. HRMS (ESI) m/z: calcd for $C_{16}H_{15}FNO_2$ [M + H], 272.1087; found, 272.1084.

4-(3-Bromophenyl)-6-methoxy-3,4-dihydroquinolin-2(1H)-one (2o)



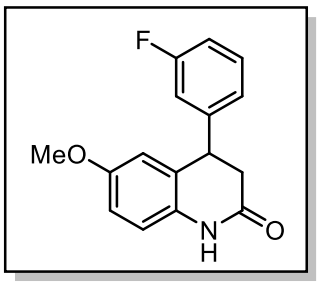
White solid; mp 153−154 °C; ^{1}H NMR (400 MHz, $CDCl_3$) δ 8.82 (s, 1H), 7.39 (d, *J* = 7.8 Hz, 1H), 7.31 (s, 1H), 7.18 (t, *J* = 7.8 Hz, 1H), 7.09 (d, *J* = 7.7 Hz, 1H), 6.77 (dt, *J* = 8.6, 5.6 Hz, 2H), 6.46 (d, *J* = 2.2 Hz, 1H), 4.21 (t, *J* = 7.2 Hz, 1H), 3.70 (s, 3H), 2.87 (qd, *J* = 16.2, 7.2 Hz, 2H). ^{13}C NMR (101 MHz, $CDCl_3$) δ 170.0, 155.9, 143.7, 130.9, 130.6, 130.5, 130.5, 127.1, 126.4, 123.0, 116.7, 114.4, 113.1, 55.6, 42.0, 38.3. HRMS (ESI) m/z: calcd for $C_{16}H_{15}BrNO_2$ [M + H], 332.0286; found, 332.0279.

4-(3-Chlorophenyl)-6-methoxy-3,4-dihydroquinolin-2(1H)-one (2p)



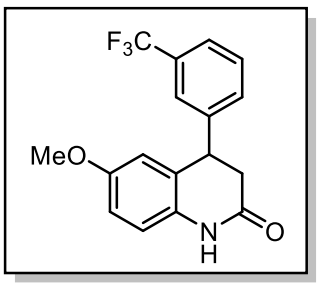
White solid; mp 139−140 °C; ^{1}H NMR (400 MHz, $CDCl_3$) δ 9.47 (s, 1H), 7.23 (d, *J* = 5.8 Hz, 2H), 7.15 (s, 1H), 7.05 (dd, *J* = 5.6, 2.3 Hz, 1H), 6.84 (d, *J* = 8.6 Hz, 1H), 6.74 (dd, *J* = 8.6, 2.7 Hz, 1H), 6.46 (d, *J* = 2.4 Hz, 1H), 4.21 (t, *J* = 7.2 Hz, 1H), 3.69 (s, 3H), 2.87 (qd, *J* = 16.2, 7.2 Hz, 2H). ^{13}C NMR (101 MHz, $CDCl_3$) δ 170.5, 155.9, 143.5, 134.7, 130.7, 130.2, 128.0, 127.5, 127.0, 126.0, 116.9, 114.3, 113.1, 55.6, 42.0, 38.2. HRMS (ESI) m/z: calcd for $C_{16}H_{15}ClNO_2$ [M + H], 288.0791; found, 288.0788.

4-(3-Fluorophenyl)-6-methoxy-3,4-dihydroquinolin-2(1H)-one (2q)



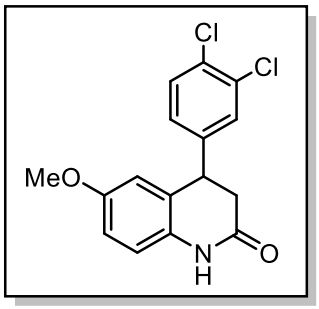
White solid; mp 136−137 °C; ^{1}H NMR (400 MHz, $CDCl_3$) δ 9.52 (s, 1H), 7.27 (dd, *J* = 14.2, 7.8 Hz, 1H), 7.02 – 6.80 (m, 4H), 6.74 (dd, *J* = 8.5, 2.2 Hz, 1H), 6.47 (d, *J* = 1.3 Hz, 1H), 4.23 (t, *J* = 7.0 Hz, 1H), 3.69 (s, 3H), 2.88 (qd, *J* = 16.1, 7.2 Hz, 2H). ^{13}C NMR (101 MHz, $CDCl_3$) δ 170.5, 164.3, 161.9, 155.9, 144.1, 144.0, 130.7, 130.5, 130.4, 127.2, 123.5, 123.5, 116.9, 114.9, 114.7, 114.3, 114.1, 113.1, 55.5, 42.0, 38.2. ^{19}F NMR (376 MHz, $CDCl_3$) δ -112.2. HRMS (ESI) m/z: calcd for $C_{16}H_{15}FNO_2$ [M + H], 272.1087; found, 272.1084.

6-Methoxy-4-(3-(trifluoromethyl)phenyl)-3,4-dihydroquinolin-2(1H)-one (2r)



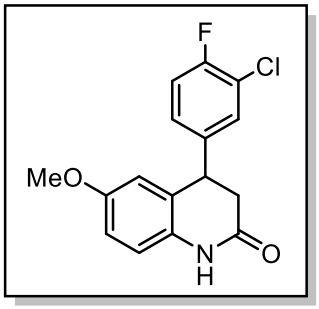
White solid; mp 138−139 °C; ^{1}H NMR (400 MHz, $CDCl_3$) δ 9.26 (s, 1H), 7.52 (d, *J* = 7.6 Hz, 1H), 7.48 – 7.39 (m, 2H), 7.34 (d, *J* = 7.6 Hz, 1H), 6.85 (d, *J* = 8.6 Hz, 1H), 6.76 (d, *J* = 8.6 Hz, 1H), 6.43 (s, 1H), 4.31 (t, *J* = 7.1 Hz, 1H), 3.68 (s, 3H), 2.90 (ddd, *J* = 24.3, 16.1, 7.2 Hz, 2H). ^{13}C NMR (101 MHz, $CDCl_3$) δ 170.2, 155.9, 142.5, 131.4, 131.2, 131.1, 130.7, 129.5, 126.9, 125.3, 124.7, 124.7, 124.3, 124.3, 122.6, 116.9, 114.3, 113.2, 55.6, 42.2, 38.3. ^{19}F NMR (376 MHz, $CDCl_3$) δ -62.6. HRMS (ESI) m/z: calcd for $C_{17}H_{15}F_3NO_2$ [M + H], 322.1055; found, 322.1051.

4-(3,4-Dichlorophenyl)-6-methoxy-3,4-dihydroquinolin-2(1H)-one (2s)



White solid; mp 191−192 °C; ^{1}H NMR (400 MHz, $CDCl_3$) δ 9.60 (s, 1H), 7.36 (d, *J* = 8.3 Hz, 1H), 7.24 (d, *J* = 1.9 Hz, 1H), 7.00 (dd, *J* = 8.3, 1.8 Hz, 1H), 6.85 (d, *J* = 8.6 Hz, 1H), 6.75 (dd, *J* = 8.6, 2.6 Hz, 1H), 6.45 (d, *J* = 2.3 Hz, 1H), 4.19 (t, *J* = 7.0 Hz, 1H), 3.70 (s, 3H), 2.91 (dd, *J* = 16.1, 6.3 Hz, 1H), 2.79 (dd, *J* = 16.2, 7.8 Hz, 1H). ^{13}C NMR (101 MHz, $CDCl_3$) δ 170.2, 155.9, 141.8, 133.0, 131.4, 130.9, 130.6, 129.8, 127.1, 126.5, 117.1, 114.3, 113.3, 55.6, 41.5, 38.2. HRMS (ESI) m/z: calcd for $C_{16}H_{14}Cl_2NO_2$ [M + H], 322.0402; found, 322.0400.

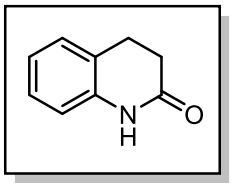
4-(3-Chloro-4-fluorophenyl)-6-methoxy-3,4-dihydroquinolin-2(1H)-one (2t)



White solid; mp 174−175 °C; ^{1}H NMR (400 MHz, $CDCl_3$) δ 9.43 (s, 1H), 7.18 (dd, *J* = 6.8, 1.5 Hz, 1H), 7.12 – 6.99 (m, 2H), 6.84 (d, *J* = 8.6 Hz, 1H), 6.75 (dd, *J* = 8.6, 2.5 Hz, 1H), 6.45 (d, *J* = 2.1 Hz, 1H), 4.20 (t, *J* = 6.9 Hz, 1H), 3.70 (s, 3H), 2.91 (dd, *J* = 16.1, 6.2 Hz, 1H), 2.79 (dd, *J* = 16.1, 7.8 Hz, 1H). ^{13}C NMR (101 MHz, $CDCl_3$) δ 170.2, 158.5, 156.0, 155.9, 138.5, 138.5, 130.6, 129.9, 127.5, 127.4, 126.9, 121.5, 121.3, 117.1, 117.0, 116.9, 114.3, 113.2, 55.6, 41.4, 38.4. ^{19}F NMR (376

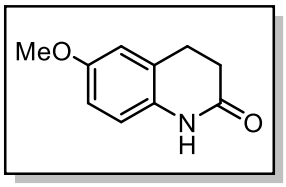
MHz, $CDCl_3$) δ -117.4. HRMS (ESI) m/z: calcd for $C_{16}H_{14}ClFNO_2$ [M + H], 306.0697; found, 306.0692.

3,4-Dihydroquinolin-2(1H)-one (2u)



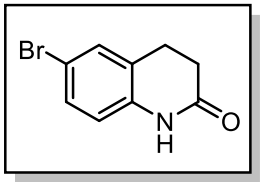
White solid; mp 158−159 °C; ^{1}H NMR (400 MHz, $CDCl_3$) δ 8.76 (s, 1H), 7.16 (t, *J* = 8.0 Hz, 2H), 6.97 (t, *J* = 7.4 Hz, 1H), 6.80 (d, *J* = 7.7 Hz, 1H), 2.96 (t, *J* = 7.5 Hz, 2H), 2.69 – 2.57 (m, 2H). ^{13}C NMR (101 MHz, $CDCl_3$) δ 172.1, 137.3, 127.9, 127.5, 123.7, 123.1, 115.5, 30.7, 25.3. HRMS (ESI) m/z: calcd for $C_9H_{10}NO$ [M + H], 148.0762; found, 148.0757.

6-Methoxy-3,4-dihydroquinolin-2(1H)-one (2v)



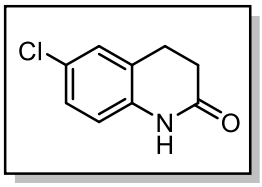
White solid; mp 139−140 °C; ^{1}H NMR (400 MHz, $CDCl_3$) δ 8.39 (s, 1H), 6.71 (d, *J* = 2.7 Hz, 3H), 3.76 (s, 3H), 2.95 – 2.89 (m, 2H), 2.60 (dd, *J* = 8.4, 6.7 Hz, 2H). ^{13}C NMR (101 MHz, $CDCl_3$) δ 171.8, 155.6, 130.9, 125.0, 116.3, 113.8, 112.4, 55.6, 30.6, 25.7. HRMS (ESI) m/z: calcd for $C_{10}H_{12}NO_2$ [M + H], 178.0868; found, 178.0863.

6-Bromo-3,4-dihydroquinolin-2(1H)-one (2w)



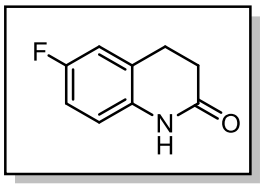
White solid; mp 159−160 °C; ^{1}H NMR (400 MHz, $CDCl_3$) δ 8.85 (s, 1H), 7.35 – 7.21 (m, 2H), 6.69 (d, *J* = 8.1 Hz, 1H), 2.94 (t, *J* = 7.5 Hz, 2H), 2.62 (t, *J* = 7.5 Hz, 2H). ^{13}C NMR (101 MHz, $CDCl_3$) δ 172.0, 136.4, 130.8, 130.4, 125.7, 117.1, 115.5, 30.3, 25.1. HRMS (ESI) m/z: calcd for C_9H_9BrNO [M + H], 225.9868; found, 225.9866.

6-Chloro-3,4-dihydroquinolin-2(1H)-one (2x)



White solid; mp 160−161 °C; ^{1}H NMR (400 MHz, $CDCl_3$) δ 8.80 (s, 1H), 7.13 (d, *J* = 7.6 Hz, 2H), 6.73 (d, *J* = 8.3 Hz, 1H), 2.94 (t, *J* = 7.5 Hz, 2H), 2.66 – 2.57 (m, 2H). ^{13}C NMR (101 MHz, $CDCl_3$) δ 172.1, 136.0, 128.0, 127.9, 127.5, 125.3, 116.7, 30.3, 25.2. HRMS (ESI) m/z: calcd for C_9H_9ClNO [M + H], 182.0373; found, 182.0369.

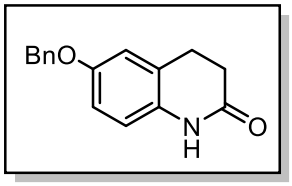
6-Fluoro-3,4-dihydroquinolin-2(1H)-one (2y)



White solid; mp 171−172 °C; ^{1}H NMR (400 MHz, $CDCl_3$) δ 8.98 (s, 1H), 6.86 (t, *J* = 8.0 Hz, 2H), 6.76 (dd, *J* = 8.2, 4.8 Hz, 1H), 2.94 (t, *J* = 7.5 Hz, 2H), 2.65 – 2.58 (m, 2H). ^{13}C NMR (101 MHz, $CDCl_3$) δ 171.8, 159.9, 157.5, 133.5, 133.4, 125.5, 125.4, 116.5, 116.4, 115.0,

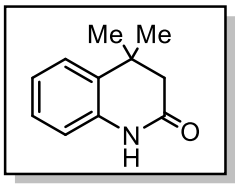
114.8, 114.2, 113.9, 30.3, 25.4, 25.4. ^{19}F NMR (376 MHz, $CDCl_3$) δ -120.2. HRMS (ESI) m/z: calcd for C_9H_9FNO [M + H], 166.0668; found, 166.0670.

6-(Benzyloxy)-3,4-dihydroquinolin-2(1H)-one (2z)



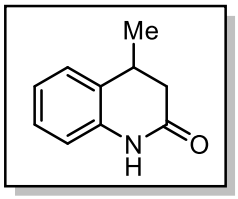
White solid; mp 158−159 °C; ^{1}H NMR (400 MHz, $CDCl_3$) δ 8.83 (s, 1H), 7.48 – 7.27 (m, 5H), 6.82 – 6.70 (m, 3H), 5.01 (s, 2H), 2.92 (t, *J* = 7.5 Hz, 2H), 2.64 – 2.56 (m, 2H). ^{13}C NMR (101 MHz, $CDCl_3$) δ 171.7, 154.8, 137.0, 131.1, 128.6, 128.0, 127.5, 125.1, 116.3, 114.9, 113.5, 70.5, 30.6, 25.7. HRMS (ESI) m/z: calcd for $C_{16}H_{16}NO_2$ [M + H], 254.1181; found, 254.1179.

4,4-Dimethyl-3,4-dihydroquinolin-2(1H)-one (2za)



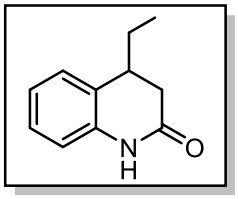
White solid; mp 110−111 °C; ^{1}H NMR (400 MHz, $CDCl_3$) δ 8.59 (s, 1H), 7.28 (d, *J* = 7.7 Hz, 1H), 7.17 (td, *J* = 7.6, 1.3 Hz, 1H), 7.04 (td, *J* = 7.5, 1.0 Hz, 1H), 6.80 (dd, *J* = 7.8, 1.0 Hz, 1H), 2.48 (s, 2H), 1.32 (s, 6H). ^{13}C NMR (101 MHz, $CDCl_3$) δ 171.4, 135.9, 132.5, 127.5, 124.4, 123.6, 115.9, 45.3, 33.9, 27.7. HRMS (ESI) m/z: calcd for $C_{11}H_{14}NO$ [M + H], 176.1075; found, 176.1070.

4-Methyl-3,4-dihydroquinolin-2(1H)-one (2zb)



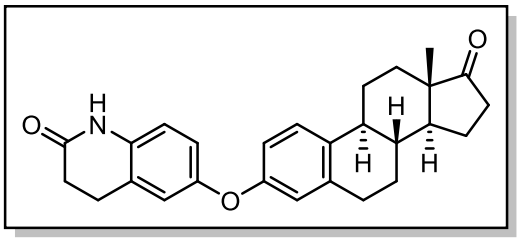
White solid; mp 88−89 °C; ^{1}H NMR (400 MHz, $CDCl_3$) δ 8.22 (s, 1H), 7.17 (dd, *J* = 11.0, 7.6 Hz, 2H), 7.01 (t, *J* = 7.3 Hz, 1H), 6.77 (d, *J* = 7.7 Hz, 1H), 3.12 (d, *J* = 6.3 Hz, 1H), 2.80 – 2.61 (m, 1H), 2.49 – 2.31 (m, 1H), 1.30 (dd, *J* = 6.9, 2.4 Hz, 3H). ^{13}C NMR (101 MHz, $CDCl_3$) δ 171.2, 136.4, 128.8, 127.5, 126.6, 123.4, 115.5, 38.4, 30.8, 19.8. HRMS (ESI) m/z: calcd for $C_{10}H_{12}NO$ [M + H], 162.0919; found, 162.0915.

4-Ethyl-3,4-dihydroquinolin-2(1H)-one (2zc)



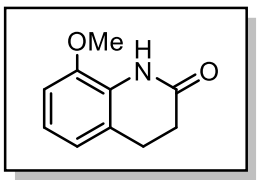
White solid; mp 128−129 °C; ^{1}H NMR (400 MHz, $CDCl_3$) δ 7.74 (s, 1H), 7.16 (dd, *J* = 11.6, 7.5 Hz, 2H), 7.00 (t, *J* = 7.5 Hz, 1H), 6.73 (d, *J* = 7.8 Hz, 1H), 2.89 – 2.79 (m, 1H), 2.75 (dd, *J* = 16.1, 6.2 Hz, 1H), 2.55 (dd, *J* = 16.1, 3.8 Hz, 1H), 1.63 (ddd, *J* = 21.4, 14.0, 7.2 Hz, 2H), 0.92 (t, *J* = 7.4 Hz, 3H). ^{13}C NMR (101 MHz, $CDCl_3$) δ 171.1, 136.4, 128.1, 127.5, 127.5, 123.0, 115.6, 37.9, 35.8, 27.0, 11.4. HRMS (ESI) m/z: calcd for $C_{11}H_{14}NO$ [M + H], 176.1075; found, 176.1073.

6-(((8*R*,9*S*,13*S*,14*S*)-13-Methyl-17-oxo-7,8,9,11,12,13,14,15,16,17-decahydro-6H-cyclopenta[a]phenanthren-3-yl)oxy)-3,4-dihydroquinolin-2(1H)-one (2ze)



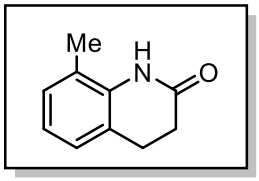
White solid; mp 231-232 °C; ^{1}H NMR (400 MHz, $CDCl_3$) δ 9.16 (s, 1H), 7.21 (d, *J* = 8.5 Hz, 1H), 6.80 (dt, *J* = 9.4, 4.7 Hz, 3H), 6.74 (dd, *J* = 8.5, 2.4 Hz, 1H), 6.69 (d, *J* = 2.0 Hz, 1H), 2.97 – 2.80 (m, 4H), 2.67 – 2.57 (m, 2H), 2.49 (dd, *J* = 18.9, 8.6 Hz, 1H), 2.43 – 2.34 (m, 1H), 2.25 (dd, *J* = 13.5, 7.0 Hz, 1H), 2.04 (dddd, *J* = 20.3, 17.7, 14.8, 9.0 Hz, 4H), 1.66 – 1.36 (m, 6H), 0.90 (s, 3H). ^{13}C NMR (101 MHz, $CDCl_3$) δ 171.9, 155.7, 152.7, 138.3, 134.5, 133.0, 126.6, 125.2, 118.9, 118.3, 118.2, 116.5, 115.7, 50.4, 48.0, 44.1, 38.2, 35.9, 31.6, 30.5, 29.5, 26.5, 25.9, 25.5, 21.6, 13.9. HRMS (ESI) m/z: calcd for $C_{27}H_{30}NO_3$ [M + H], 416.2226; found, 416.2228.

8-Methoxy-3,4-dihydroquinolin-2(1H)-one (4a)



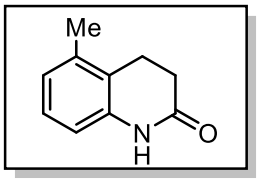
White solid; mp 140−141 °C; ^{1}H NMR (400 MHz, $CDCl_3$) δ 7.80 (s, 1H), 6.93 (t, *J* = 7.9 Hz, 1H), 6.77 (dd, *J* = 7.8, 2.5 Hz, 2H), 3.86 (s, 3H), 2.96 (t, *J* = 7.5 Hz, 2H), 2.65 – 2.59 (m, 2H). ^{13}C NMR (101 MHz, $CDCl_3$) δ 170.3, 145.8, 126.5, 124.0, 122.7, 120.0, 109.0, 55.8, 30.7, 25.4. HRMS (ESI) m/z: calcd for $C_{10}H_{12}NO_2$ [M + H], 178.0868; found, 178.0860.

8-Methyl-3,4-dihydroquinolin-2(1H)-one (4b)



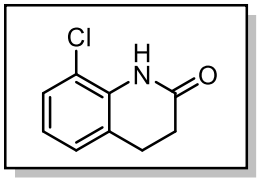
White solid; mp 160−161 °C; ^{1}H NMR (400 MHz, $CDCl_3$) δ 7.55 (s, 1H), 7.02 (d, *J* = 6.6 Hz, 2H), 6.89 (t, *J* = 7.5 Hz, 1H), 2.98 – 2.90 (m, 2H), 2.65 – 2.58 (m, 2H), 2.22 (s, 3H). ^{13}C NMR (101 MHz, $CDCl_3$) δ 171.4, 135.5, 129.0, 125.8, 123.7, 122.7, 122.6, 30.8, 25.7, 16.7. HRMS (ESI) m/z: calcd for $C_{10}H_{12}NO$ [M + H], 162.0919; found, 162.0916.

5-Methyl-3,4-dihydroquinolin-2(1H)-one (4b')



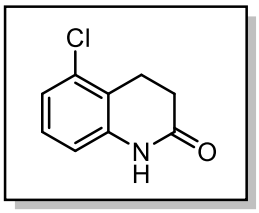
White solid; mp 126−127 °C; ^{1}H NMR (400 MHz, $CDCl_3$) δ 8.57 (s, 1H), 7.07 (t, *J* = 7.7 Hz, 1H), 6.86 (d, *J* = 7.5 Hz, 1H), 6.66 (d, *J* = 7.9 Hz, 1H), 2.92 (t, *J* = 7.6 Hz, 2H), 2.64 (t, *J* = 7.6 Hz, 2H), 2.29 (s, 3H). ^{13}C NMR (101 MHz, $CDCl_3$) δ 171.6, 137.2, 136.1, 127.1, 125.0, 122.0, 113.5, 30.4, 22.0, 19.4. HRMS (ESI) m/z: calcd for $C_{10}H_{12}NO$ [M + H], 162.0919; found, 162.0915.

8-Chloro-3,4-dihydroquinolin-2(1H)-one (4c)



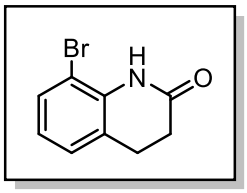
White solid; mp 105−106 °C; ^{1}H NMR (400 MHz, $CDCl_3$) δ 7.78 (s, 1H), 7.22 (s, 1H), 7.07 (d, *J* = 7.4 Hz, 1H), 6.92 (t, *J* = 7.8 Hz, 1H), 3.04 – 2.94 (m, 2H), 2.64 (dd, *J* = 8.3, 6.7 Hz, 2H). ^{13}C NMR (101 MHz, $CDCl_3$) δ 170.5, 134.0, 127.7, 126.5, 125.4, 123.3, 119.6, 30.5, 25.8. HRMS (ESI) m/z: calcd for C_9H_9ClNO [M + H], 182.0373; found, 182.0372.

5-Chloro-3,4-dihydroquinolin-2(1H)-one (4c')



White solid; mp 103−104 °C; ^{1}H NMR (400 MHz, $CDCl_3$) δ 8.37 (s, 1H), 7.16 – 6.96 (m, 2H), 6.68 (d, *J* = 7.6 Hz, 1H), 3.08 (t, *J* = 7.7 Hz, 2H), 2.64 (t, *J* = 7.7 Hz, 2H). ^{13}C NMR (101 MHz, $CDCl_3$) δ 171.6, 138.6, 133.5, 128.3, 124.0, 121.7, 114.0, 29.9, 22.6. HRMS (ESI) m/z: calcd for C_9H_9ClNO [M + H], 182.0373; found, 182.0375.

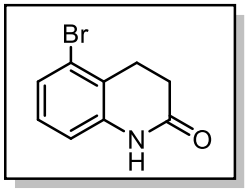
8-Bromo-3,4-dihydroquinolin-2(1H)-one (4d)



White solid; mp 166−167 °C; ^{1}H NMR (400 MHz, $CDCl_3$) δ 7.78 (s, 1H), 7.39 (d, *J* = 8.0 Hz, 1H), 7.10 (d, *J* = 7.4 Hz, 1H), 6.86 (t, *J* = 7.8 Hz, 1H), 3.02 – 2.95 (m, 2H), 2.67 – 2.60 (m, 2H). ^{13}C

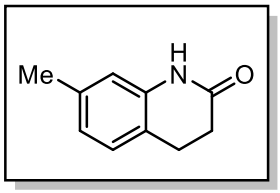
NMR (101 MHz, $CDCl_3$) δ 170.6, 135.2, 130.9, 127.2, 125.6, 123.8, 109.6, 30.6, 26.0. HRMS (ESI) m/z: calcd for C_9H_9BrNO [M + H], 225.9868; found, 225.9871.

5-Bromo-3,4-dihydroquinolin-2(1H)-one (4d')



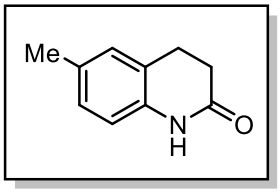
White solid; mp 114−115 °C; ^{1}H NMR (400 MHz, $CDCl_3$) δ 7.88 (s, 1H), 7.22 (d, *J* = 8.4 Hz, 1H), 7.02 (t, *J* = 7.9 Hz, 1H), 6.68 (d, *J* = 7.9 Hz, 1H), 3.08 (t, *J* = 7.6 Hz, 2H), 2.67 – 2.60 (m, 2H). ^{13}C NMR (101 MHz, $CDCl_3$) δ 171.5, 138.4, 128.6, 127.2, 123.8, 123.5, 114.7, 30.1, 25.5. HRMS (ESI) m/z: calcd for C_9H_9BrNO [M + H], 225.9868; found, 225.9864.

7-Methyl-3,4-dihydroquinolin-2(1H)-one (6b)



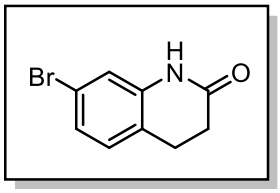
White solid; mp 134−135 °C; ^{1}H NMR (400 MHz, $CDCl_3$) δ 8.05 (s, 1H), 7.03 (d, *J* = 7.6 Hz, 1H), 6.79 (d, *J* = 7.5 Hz, 1H), 6.57 (s, 1H), 2.91 (t, *J* = 7.5 Hz, 2H), 2.65 – 2.57 (m, 2H), 2.29 (s, 3H). ^{13}C NMR (101 MHz, $CDCl_3$) δ 171.7, 137.5, 137.1, 127.8, 123.8, 120.7, 115.9, 31.0, 25.0, 21.1. HRMS (ESI) m/z: calcd for $C_{10}H_{12}NO$ [M + H], 162.0919; found, 162.0917.

6-Methyl-3,4-dihydroquinolin-2(1H)-one (6b')



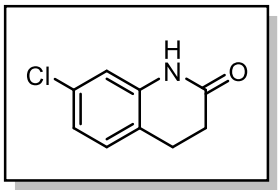
White solid; mp 145−146 °C; ^{1}H NMR (400 MHz, $CDCl_3$) δ 8.11 (s, 1H), 6.97 (d, *J* = 6.0 Hz, 2H), 6.66 (d, *J* = 8.5 Hz, 1H), 2.93 (t, *J* = 7.5 Hz, 2H), 2.66 – 2.55 (m, 2H), 2.29 (s, 3H).^{13}C NMR (101 MHz, $CDCl_3$) δ 171.5, 134.7, 132.7, 128.7, 127.9, 123.6, 115.2, 30.8, 25.4, 20.7. HRMS (ESI) m/z: calcd for $C_{10}H_{12}NO$ [M + H], 162.0919; found, 162.0917.

7-Bromo-3,4-dihydroquinolin-2(1H)-one (6c)



White solid; mp 137−138 °C; ^{1}H NMR (400 MHz, $CDCl_3$) δ 8.07 (s, 1H), 7.10 (dd, *J* = 8.0, 1.7 Hz, 1H), 7.02 (d, *J* = 8.0 Hz, 1H), 6.91 (d, *J* = 1.6 Hz, 1H), 2.91 (t, *J* = 7.5 Hz, 2H), 2.62 (dd, *J* = 9.9, 5.1 Hz, 2H). ^{13}C NMR (101 MHz, $CDCl_3$) δ 171.8, 138.6, 129.3, 126.0, 122.6, 120.7, 118.3, 30.5, 24.9. HRMS (ESI) m/z: calcd for C_9H_9BrNO [M + H], 225.9868; found, 225.9866.

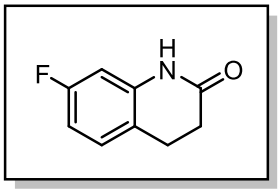
7-Chloro-3,4-dihydroquinolin-2(1H)-one (6d)



White solid; mp 176−177 °C; ^{1}H NMR (400 MHz, $CDCl_3$) δ 8.84 (s, 1H), 7.07 (d, *J* = 8.0 Hz, 1H), 6.94 (dd, *J* = 8.0, 1.4 Hz, 1H), 6.82 (s, 1H), 2.93 (t, *J* = 7.5 Hz, 2H), 2.63 (t, *J* = 7.5 Hz,

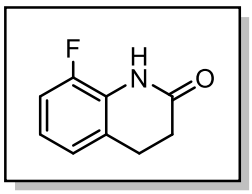
2H). ^{13}C NMR (101 MHz, $CDCl_3$) δ 171.8, 138.4, 133.0, 129.0, 123.0, 122.1, 115.5, 30.5, 24.9. HRMS (ESI) m/z: calcd for C_9H_9ClNO [M + H], 182.0373; found, 182.0370.

7-Fluoro-3,4-dihydroquinolin-2(1H)-one (6e)



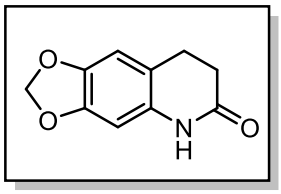
White solid; mp 181−182 °C; ^{1}H NMR (400 MHz, $CDCl_3$) δ 9.01 (s, 1H), 7.07 (s, 1H), 6.66 (t, *J* = 8.3 Hz, 1H), 6.56 (d, *J* = 9.2 Hz, 1H), 2.92 (t, *J* = 6.9 Hz, 2H), 2.62 (t, *J* = 6.7 Hz, 2H). ^{13}C NMR (101 MHz, $CDCl_3$) δ 172.1, 163.3, 160.9, 138.6, 138.5, 129.1, 129.0, 119.2, 119.2, 109.6, 109.4, 103.2, 102.9, 30.7, 24.7. ^{19}F NMR (376 MHz, $CDCl_3$) δ -114.7 (d, *J* = 0.7 Hz). HRMS (ESI) m/z: calcd for C_9H_9FNO [M + H], 166.0668; found, 166.0672.

8-Fluoro-3,4-dihydroquinolin-2(1H)-one (6e'')



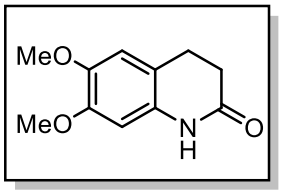
White solid; mp 136−137 °C; ^{1}H NMR (400 MHz, $CDCl_3$) δ 7.94 (s, 1H), 7.01 – 6.86 (m, 3H), 3.02 – 2.96 (m, 2H), 2.65 (dd, *J* = 8.3, 6.8 Hz, 2H). ^{13}C NMR (101 MHz, $CDCl_3$) δ 170.3, 151.0, 148.6, 125.8, 125.8, 125.7, 125.6, 123.2, 123.2, 122.9, 122.9, 113.9, 113.7, 30.6, 25.3, 25.3. ^{19}F NMR (376 MHz, $CDCl_3$) δ -135.7. HRMS (ESI) m/z: calcd for C_9H_9FNO [M + H], 166.0668; found, 166.0668.

7,8-Dihydro-[1,3]dioxolo[4,5-g]quinolin-6(5H)-one (8a)



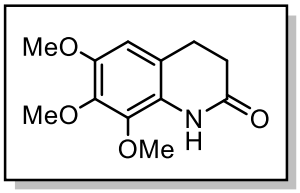
White solid; mp 231−232 °C; ^{1}H NMR (400 MHz, $CDCl_3$) δ 8.31 (s, 1H), 6.61 (s, 1H), 6.34 (s, 1H), 5.89 (s, 2H), 2.84 (t, *J* = 7.5 Hz, 2H), 2.61 – 2.53 (m, 2H). ^{13}C NMR (101 MHz, $CDCl_3$) δ 171.8, 146.8, 143.3, 131.4, 116.0, 108.1, 101.2, 97.8, 30.8, 25.3. HRMS (ESI) m/z: calcd for $C_{10}H_{10}NO_3$ [M + H], 192.0661; found, 192.0659.

6,7-Dimethoxy-3,4-dihydroquinolin-2(1H)-one (8b)



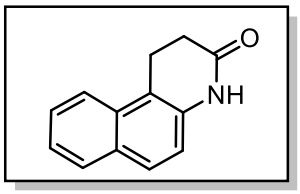
White solid; mp 130−131 °C; ^{1}H NMR (400 MHz, $CDCl_3$) δ 8.18 (s, 1H), 6.67 (s, 1H), 6.33 (s, 1H), 3.84 (d, *J* = 3.2 Hz, 6H), 2.92 – 2.84 (m, 2H), 2.60 (dd, *J* = 8.4, 6.7 Hz, 2H). ^{13}C NMR (101 MHz, $CDCl_3$) δ 172.2, 148.4, 144.8, 130.7, 114.8, 111.7, 100.5, 56.4, 56.2, 30.9, 25.0. HRMS (ESI) m/z: calcd for $C_{11}H_{14}NO_3$ [M + H], 208.0974; found, 208.0969.

6,7,8-Trimethoxy-3,4-dihydroquinolin-2(1H)-one (8c)



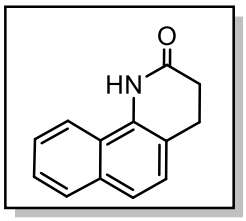
White solid; mp 119−120 °C; ^{1}H NMR (400 MHz, $CDCl_3$) δ 7.67 (s, 1H), 6.46 (s, 1H), 3.90 (s, 3H), 3.83 (d, *J* = 11.9 Hz, 6H), 2.89 (t, *J* = 7.5 Hz, 2H), 2.59 (t, *J* = 7.5 Hz, 2H). ^{13}C NMR (101 MHz, $CDCl_3$) δ 170.1, 148.8, 140.9, 140.2, 124.1, 118.3, 106.8, 61.1, 61.0, 56.4, 30.8, 25.6. HRMS (ESI) m/z: calcd for $C_{12}H_{16}NO_4$ [M + H], 238.1079; found, 238.1074.

1,2-Dihydrobenzo[f]quinolin-3(4H)-one (8d)



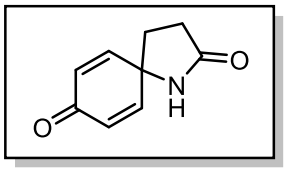
White solid; mp 235−236 °C; ^{1}H NMR (400 MHz, $CDCl_3$) δ 8.64 (s, 1H), 7.89 (d, *J* = 8.5 Hz, 1H), 7.79 (d, *J* = 8.1 Hz, 1H), 7.71 (d, *J* = 8.6 Hz, 1H), 7.52 (t, *J* = 7.5 Hz, 1H), 7.39 (t, *J* = 7.4 Hz, 1H), 7.02 (d, *J* = 8.6 Hz, 1H), 3.35 (t, *J* = 7.8 Hz, 2H), 2.79 (t, *J* = 7.8 Hz, 2H). ^{13}C NMR (101 MHz, $CDCl_3$) δ 171.8, 134.5, 131.5, 130.5, 128.8, 128.3, 127.0, 124.3, 122.6, 116.7, 116.1, 30.3, 21.1. HRMS (ESI) m/z: calcd for $C_{13}H_{12}NO$ [M + H], 198.0919; found, 198.0914.

3,4-Dihydrobenzo[h]quinolin-2(1H)-one (8e)



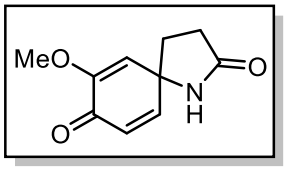
White solid; mp 192−193 °C;^{1}H NMR (400 MHz, $CDCl_3$) δ 8.86 (s, 1H), 7.90 (d, *J* = 8.5 Hz, 1H), 7.82 (d, *J* = 8.1 Hz, 1H), 7.51 (dq, *J* = 21.9, 7.5 Hz, 3H), 7.29 (d, *J* = 8.3 Hz, 1H), 3.16 – 3.08 (m, 2H), 2.80 – 2.72 (m, 2H). ^{13}C NMR (101 MHz, $CDCl_3$) δ 172.2, 133.1, 132.0, 128.6, 126.5, 126.1, 125.8, 123.0, 122.5, 119.5, 31.0, 26.0. HRMS (ESI) m/z: calcd for C_{13}H12NO [M + H], 198.0919; found, 198.0916.

1-Azaspiro[4.5]deca-6,9-diene-2,8-dione (10a)



White solid; mp 177−178 °C; ^{1}H NMR (400 MHz, $CDCl_3$) δ 6.82 (d, *J* = 10.0 Hz, 2H), 6.29 (s, 1H), 6.22 (d, *J* = 10.0 Hz, 2H), 2.54 (t, *J* = 8.1 Hz, 2H), 2.25 (t, *J* = 8.1 Hz, 2H). ^{13}C NMR (101 MHz, $CDCl_3$) δ 184.4, 177.6, 149.4, 128.8, 57.5, 32.2, 29.5. HRMS (ESI) m/z: calcd for $C_9H_{10}NO_2$ [M + H], 164.0712; found, 164.0708.

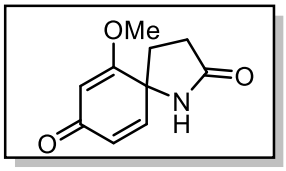
7-Methoxy-1-azaspiro[4.5]deca-6,9-diene-2,8-dione (10b)



White solid; mp 221−222 °C; ^{1}H NMR (400 MHz, $CDCl_3$) δ 6.81 (dd, *J* = 9.9, 2.7 Hz, 1H), 6.42 (s, 1H), 6.20 (d, *J* = 9.9 Hz, 1H), 5.69 (d, *J* = 2.6 Hz, 1H), 3.66 (s, 3H), 2.59 – 2.45 (m, 2H), 2.35 – 2.19 (m, 2H).

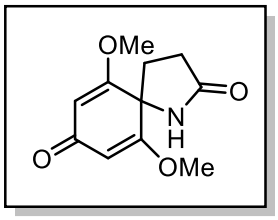
^{13}C NMR (101 MHz, $CDCl_3$) δ 179.9, 177.1, 150.7, 149.8, 127.7, 116.5, 59.1, 55.1, 33.4, 29.6. HRMS (ESI) m/z: calcd for $C_{10}H_{12}NO_3$ [M + H], 194.0817; found, 194.0815.

6-Methoxy-1-azaspiro[4.5]deca-6,9-diene-2,8-dione (10c)



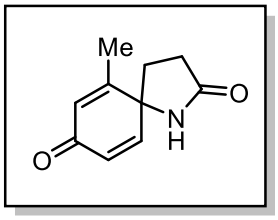
White solid; mp 213−214 °C; ^{1}H NMR (400 MHz, $CDCl_3$) δ 6.54 (d, *J* = 9.8 Hz, 1H), 6.19 (s, 1H), 6.14 (dd, *J* = 9.8, 1.2 Hz, 1H), 5.50 (s, 1H), 3.75 (s, 3H), 2.65 (dt, *J* = 17.2, 9.4 Hz, 1H), 2.43 (ddd, *J* = 17.0, 10.1, 3.7 Hz, 1H), 2.32 (ddd, *J* = 13.5, 9.9, 3.7 Hz, 1H), 2.23 – 2.13 (m, 1H). ^{13}C NMR (101 MHz, $CDCl_3$) δ 186.5, 178.6, 174.6, 145.9, 128.2, 101.5, 58.8, 56.2, 32.2, 29.8. HRMS (ESI) m/z: calcd for $C_{10}H_{12}NO_3$ [M + H], 194.0817; found, 194.0814.

6,10-Dimethoxy-1-azaspiro[4.5]deca-6,9-diene-2,8-dione (10d)



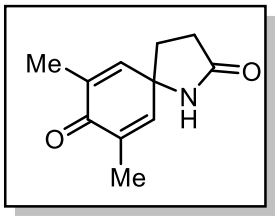
White solid; mp 252−253 °C; ^{1}H NMR (400 MHz, $CDCl_3$) δ 5.46 (s, 1H), 5.44 (s, 2H), 3.74 (s, 6H), 2.58 – 2.52 (m, 2H), 2.38 (t, *J* = 8.2 Hz, 2H). ^{13}C NMR (101 MHz, $CDCl_3$) δ 186.5, 179.1, 171.0, 100.9, 60.9, 56.4, 31.4, 29.9, 29.7. HRMS (ESI) m/z: calcd for $C_{11}H_{14}NO_4$ [M + H], 224.0923; found, 224.0918.

6-Methyl-1-azaspiro[4.5]deca-6,9-diene-2,8-dione (10e)



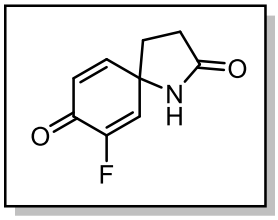
White solid; mp 161−162 °C; ^{1}H NMR (400 MHz, $CDCl_3$) δ 6.95 (s, 1H), 6.81 (d, *J* = 9.9 Hz, 1H), 6.14 (d, *J* = 9.9 Hz, 1H), 6.06 (s, 1H), 2.54 (dd, *J* = 12.5, 5.0 Hz, 2H), 2.18 (dtd, *J* = 16.4, 13.9, 8.7 Hz, 2H), 1.99 (s, 3H). ^{13}C NMR (101 MHz, $CDCl_3$) δ 185.0, 178.2, 158.9, 150.7, 127.9, 127.6, 59.9, 31.2, 29.8, 18.5. HRMS (ESI) m/z: calcd for $C_{10}H_{12}NO_2$ [M + H], 178.0868; found, 178.0864.

7,9-Dimethyl-1-azaspiro[4.5]deca-6,9-diene-2,8-dione (10f)



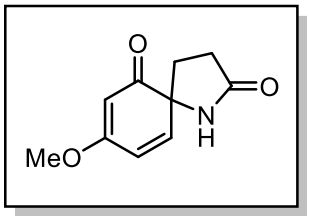
White solid; mp 179−180 °C; ^{1}H NMR (400 MHz, $CDCl_3$) δ 6.56 (s, 2H), 6.29 (s, 1H), 2.51 (t, *J* = 8.1 Hz, 2H), 2.18 (t, *J* = 8.1 Hz, 2H), 1.87 (s, 6H). ^{13}C NMR (101 MHz, $CDCl_3$) δ 185.9, 177.8, 144.5, 135.1, 57.7, 32.5, 29.7, 15.9. HRMS (ESI) m/z: calcd for $C_{11}H_{14}NO_2$ [M + H], 192.1025; found, 192.1024.

7-Fluoro-1-azaspiro[4.5]deca-6,9-diene-2,8-dione (10g)



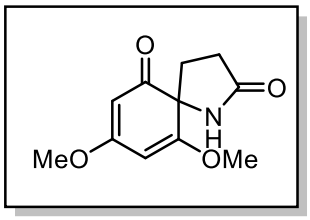
White solid; mp 174−175 °C; ^{1}H NMR (400 MHz, $CDCl_3$) δ 6.84 (dd, *J* = 9.9, 2.7 Hz, 1H), 6.55 (s, 1H), 6.38 (dd, *J* = 11.8, 2.8 Hz, 1H), 6.24 (dd, *J* = 9.9, 7.2 Hz, 1H), 2.55 (t, *J* = 8.1 Hz, 2H), 2.32 (t, *J* = 8.1 Hz, 2H). ^{13}C NMR (101 MHz, $CDCl_3$) δ 177.7, 177.5, 177.5, 154.4, 151.7, 150.4, 150.4, 127.5, 127.4, 125.4, 125.3, 59.4, 59.4, 32.3, 32.3, 29.4. ^{19}F NMR (376 MHz, $CDCl_3$) δ -128.5. HRMS (ESI) m/z: calcd for $C_9H_9FNO_2$ [M + H], 182.0617; found, 182.0613.

8-Methoxy-1-azaspiro[4.5]deca-7,9-diene-2,6-dione (11a)



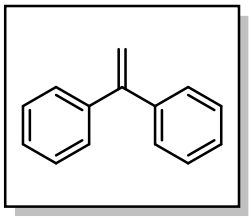
White solid; mp 133−134 °C; ^{1}H NMR (400 MHz, $CDCl_3$) δ 6.37 (d, *J* = 10.0 Hz, 1H), 6.23 (s, 1H), 6.10 (dd, *J* = 10.0, 2.2 Hz, 1H), 5.40 (d, *J* = 2.2 Hz, 1H), 3.77 (s, 3H), 2.64 (dt, *J* = 16.8, 9.4 Hz, 1H), 2.38 – 2.19 (m, 2H), 1.99 (dt, *J* = 12.9, 9.5 Hz, 1H). ^{13}C NMR (101 MHz, $CDCl_3$) δ 199.6, 179.5, 170.5, 143.4, 122.9, 97.7, 64.2, 56.2, 32.3, 28.4. HRMS (ESI) m/z: calcd for $C_{10}H_{12}NO_3$ [M + H], 194.0817; found, 194.0814.

8,10-Dimethoxy-1-azaspiro[4.5]deca-7,9-diene-2,6-dione (11b)



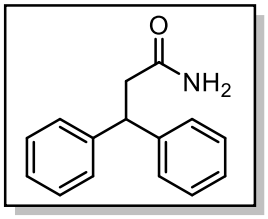
White solid; mp 218−219 °C; ^{1}H NMR (400 MHz, $CDCl_3$) δ 5.56 (s, 1H), 5.30 (d, *J* = 1.8 Hz, 1H), 5.18 (d, *J* = 1.7 Hz, 1H), 3.79 (s, 3H), 3.73 (s, 3H), 2.55 (ddd, *J* = 16.6, 9.8, 6.8 Hz, 1H), 2.49 – 2.39 (m, 1H), 2.32 (ddd, *J* = 12.6, 9.9, 5.9 Hz, 1H), 2.25 – 2.15 (m, 1H). ^{13}C NMR (101 MHz, $CDCl_3$) δ 196.9, 179.5, 173.9, 168.6, 93.2, 93.0, 65.9, 56.3, 33.4, 29.7, 29.0. HRMS (ESI) m/z: calcd for $C_{11}H_{14}NO_4$ [M + H], 224.0923; found, 224.0918.

1,1-Diphenyl ethylene



Colourless oil; ^{1}H NMR (400 MHz, $CDCl_3$) δ 7.33 (d, *J* = 5.9 Hz, 10H), 5.45 (s, 2H). ^{13}C NMR (101 MHz, $CDCl_3$) δ 150.1, 141.5, 128.3, 128.2, 127.7, 114.3. HRMS (ESI) m/z: calcd for $C_{14}H_{13}$ [M + H], 181.1017; found, 181.1018.

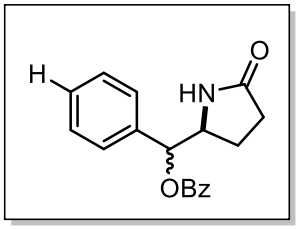
3,3-Diphenylpropanamide



White solid; mp 98−99 °C; ^{1}H NMR (400 MHz, $CDCl_3$) δ 7.33 – 7.25 (m, 5H), 7.19 (dd, *J* = 15.5, 8.5 Hz, 5H), 5.22 (s, 2H), 4.55 (t, *J* = 7.7 Hz, 1H), 2.94 (d, *J* = 7.7 Hz, 2H). ^{13}C NMR (101

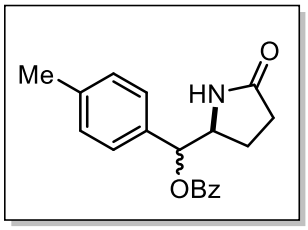
MHz, $CDCl_3$) δ 173.3, 143.5, 128.7, 127.7, 126.7, 47.2, 42.5. HRMS (ESI) m/z: calcd for $C_{15}H_{16}NO$ [M + H], 226.1232; found, 226.1230.

(5-Oxopyrrolidin-2-yl)(phenyl)methyl benzoate (13a)



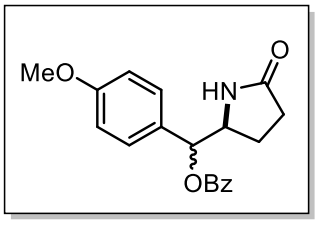
Colorless solid; ^1H NMR spectroscopic analysis of the unpurified reaction mixture Indicated = 2:1 d.r.; ***threo*** **diastereomer:** ^1H NMR (400 MHz, $CDCl_3$); δ 8.06 (d, *J* = 7.32 Hz, 2H), 7.59 – 7.52 (m, 1H), 7.48 – 7.42 (m, 2H), 7.42 – 7.35 (m, 5H), 6.43 (s, 1H), 5.85 (d, *J* = 6.7 Hz, 1H), 4.12 (m, 1H), 2.37 – 2.15 (m, 2H), 2.11 – 2.02 (m, 1H), 1.94 – 1.85 (m, 1H); ^{13}C NMR (151 MHz, $CDCl_3$) δ 178.2, 165.4, 136.8, 133.5, 129.7, 129.2, 129.0, 128.9, 128.6, 127.5, 78.9, 57.8, 29.7, 23.5 ***erythro*** **diastereomer:** ^1H NMR (400 MHz, $CDCl_3$) δ 8.06 (d, *J* = 7.32 Hz, 2H), 7.59 – 7.52 (m, 1H), 7.48 – 7.42 (m, 2H), 7.42 – 7.35 (m, 5H), 6.33 (s, 1H), 5.96 (d, *J* = 8.1 Hz, 1H), 4.13 (m, 1H), 2.37 – 2.15 (m, 2H), 2.11 – 2.02 (m, 1H), 1.94 – 1.85 (m, 1H). ^{13}C NMR (151 MHz, $CDCl_3$) 178.0, 165.5, 136.3, 133.5, 129.6, 129.2, 129.0, 128.8, 128.6, 127.1, 77.4, 58.0, 29.5, 23.0

(5-Oxopyrrolidin-2-yl)(p-tolyl)methyl benzoate (13b)



Colorless solid; ^{1}H NMR spectroscopic analysis of the unpurified reaction mixture Indicated = 3:1 d.r.; ***threo*** **diastereomer:** ^{1}H NMR (400 MHz, $CDCl_3$) δ 8.07 (m, 2H), 7.59 (m, 1H), 7.46 (m, 2H), 7.31 (m, 2H), 7.19 (m, 2H), 6.17 (s, 1H), 5.81 (d, *J* = 6.8 Hz, 1H), 4.15 (m, 1H), 2.35 – 2.33 (m, 3H), 2.11 (m, 3H), 1.95 (m, 1H); ***erythro*** **diastereomer:** ^{1}H NMR (400 MHz, $CDCl_3$) δ 8.07 (m, 2H), 7.59 (m, 1H), 7.46 (m, 2H), 7.31 (m, 2H), 7.19 (m, 2H), 6.28 (s, 1H), 5.91 (d, *J* = 6.8 Hz, 1H), 4.15 (m, 1H), 2.35 – 2.33 (m, 3H), 2.11 (m, 3H), 1.95 (m, 1H). **^{13}C NMR of diastereomeric mixture** (101 MHz, $CDCl_3$) ^{13}C NMR (151 MHz, $CDCl_3$) δ 178.0, 165.4, 138.8, 133.7, 133.5, 129.7, 129.6, 128.6, 126.6, 78.9, 58.1, 29.7, 23.5, 21.2.

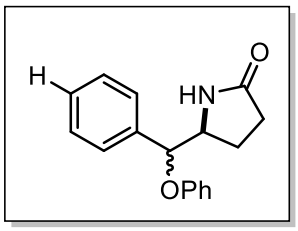
(4-Methoxyphenyl)(5-oxopyrrolidin-2-yl)methyl benzoate (13c)



Colorless resin;^{1}H NMR spectroscopic analysis of the unpurified reaction mixture Indicated = 1.3:1 d.r.; ***threo*** **diastereomer:** ^{1}H NMR (400 MHz, $CDCl_3$) δ 8.06 (dd, *J* = 7.1, 4.5 Hz, 2H), 7.58 (t, *J* = 7.4 Hz, 1H), 7.45 (t, *J* = 7.6 Hz, 2H), 7.35 (t, *J* = 8.4 Hz, 2H), 6.95 – 6.82 (m, 2H), 6.21 (s, 1H), 5.78 (d, *J* = 7.0 Hz, 1H), 4.13 (dd, *J* = 12.2, 7.1 Hz, 1H), 3.79 (s, 3H), 2.29 (ddd, *J* = 14.0, 12.5, 6.5 Hz, 2H), 2.12 – 2.02 (m, 1H), 1.90

(dt, *J* = 20.7, 10.2 Hz, 1H). ***erythro* diastereomer:** ^{1}H NMR (400 MHz, $CDCl_3$) δ 8.06 (dd, *J* = 7.1, 4.5 Hz, 2H), 7.58 (t, *J* = 7.4 Hz, 1H), 7.45 (t, *J* = 7.6 Hz, 2H), 7.35 (t, *J* = 8.4 Hz, 2H), 6.95 – 6.82 (m, 2H), 6.00 (s, 1H), 5.88 (d, *J* = 5.9 Hz, 1H), 4.13 (dd, *J* = 12.2, 7.1 Hz, 1H), 3.79 (s, 3H), 2.29 (ddd, *J* = 14.0, 12.5, 6.5 Hz, 2H), 2.12 – 2.02 (m, 1H), 1.90 (dt, *J* = 20.7, 10.2 Hz, 1H). **^{13}C NMR of diastereomeric mixture** (101 MHz, $CDCl_3$) δ 178.3, 178.1, 165.5, 165.4, 160.0, 159.9, 133.4, 133.4, 129.8, 129.7, 129.7, 129.7, 128.7, 128.6, 128.5, 128.2, 128.2, 114.3, 114.3, 78.9, 77.3, 58.0, 57.7, 55.3, 29.7, 29.2, 23.5, 23.1. HRMS (ESI) m/z: calcd for $C_{19}H_{20}NO_4$ [M + H], 326.1392; found, 326.1397.

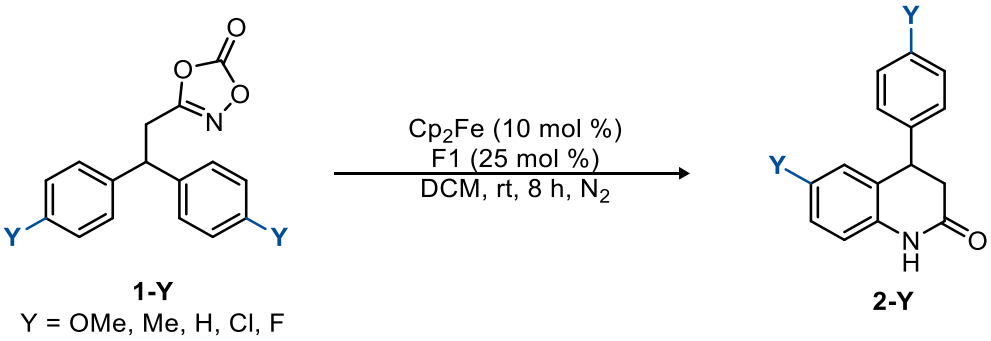
5-(Phenoxy(phenyl)methyl)pyrrolidin-2-one (13d)



Yellowish solid; ^{1}H NMR spectroscopic analysis of the unpurified reaction mixture Indicated = 2:1 d.r.; ***threo*** **diastereomer:** ^{1}H NMR (400 MHz, $CDCl_3$) δ 7.37 – 7.36 (m, 5H), 7.19 – 7.16 (m, 2H), 6.91 – 6.89 (m, 1H), 6.82 – 6.80 (m, 2H), 6.24 (s, 1H), 4.92 (d, *J* = 6.0 Hz, 1H), 4.14 – 4.04 (m, 1H), 2.42 – 2.36 (m, 2H), 2.20 – 2.16 (m, 1H), 2.07 – 1.93 (m, 1H). ^{13}C NMR (101 MHz, $CDCl_3$) δ 177.89, 157.40, 137.28, 129.44, 128.97, 128.62, 126.76, 121.36, 115.94, 82.10, 58.89, 29.34, 23.20. ^{13}C NMR (151 MHz, $CDCl_3$) δ 178.48, 157.50, 137.47, 129.44, 128.64, 121.41, 115.95, 83.49, 59.51, 29.99, 23.38. ***erythro*** **diastereomer:** ^{1}H NMR (600 MHz, $CDCl_3$) δ 7.37 – 7.36 (m, 5H), 7.19 – 7.16 (m, 2H), 6.91 – 6.89 (m, 1H), 6.82 – 6.80 (m, 2H), 5.94 (s, 1H) , 5.00 (d, *J* = 7.0 Hz, 1H), 4.14 – 4.04 (m, 1H) 2.42 – 2.36 (m, 2H), 2.20 – 2.16 (m, 1H), 2.07 – 1.93 (m, 1H). ^{13}C NMR (151 MHz, $CDCl_3$)178.0, 157.4, 137.3, 129.0, 128.6, 127.6, 126.8, 121.3, 115.9, 82.0, 59.0, 29.4, 23.0. **HRMS** (ESI) m/z calcd. for $C_{17}H_{17}NO_2$ $[M+Na]^+$: 290.1157, found: 290.1159.

2.6.5 Mechanistic Studies

2.6.5.1 Hammett Correlation Study



1-Y
Y = OMe, Me, H, Cl, F

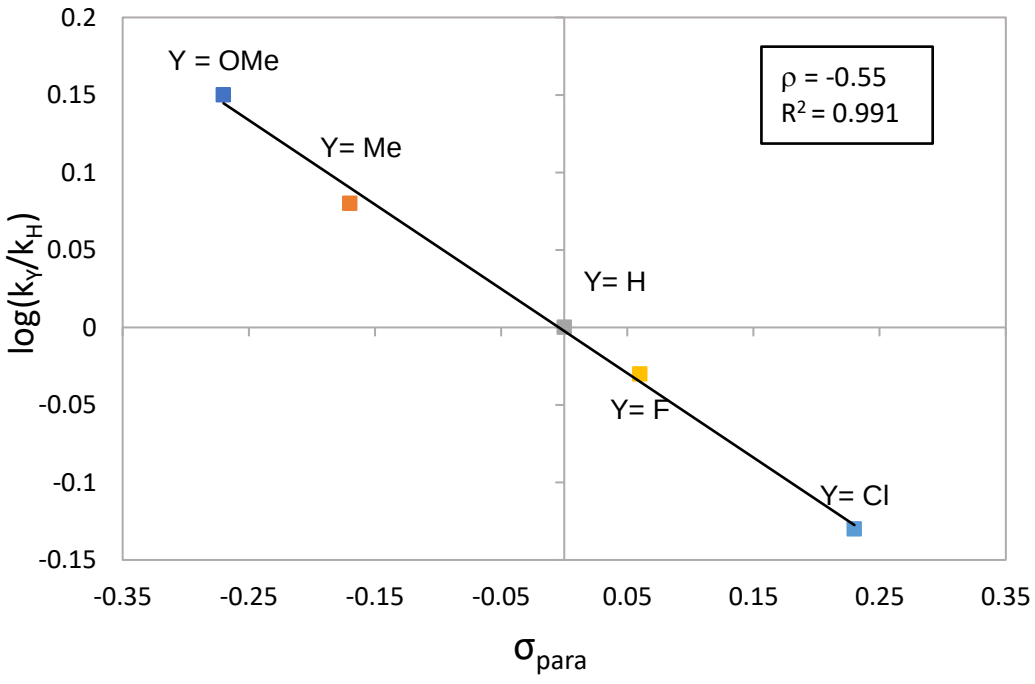
2-Y

In a glove box, ferrocene (3.72 mg, 10 mol%) and 4-fluorobenzenediazonium tetrafluoroborate (10.5 mg, 25 mol%) were added into 8 mL vial A. The dry DCM (1 mL) was added to the 8 mL-vial. The reaction was stirred at room temperature for 30 min. The *para*-substituted dioxazolones **1-Y** (0.2 mmol) was added into another 4 mL-vial B and dissolved in dry solvent (1 mL). The dioxazolones solution was transferred from vial B to vial A. The reaction vial A was sealed and stirred at room temperature for 8 h. After 8 h, the reaction crude mixture was evaporated to dryness under vacuum, and the residue was passed through preparative thin layer chromatography (n-hexane/EtOAc = 1:1; 40 mL). The yield of products **2-Y** formation was determined based on the integration ratios of the triplet C–H signal (δ_H 4.3 ppm). The reactions were run in triplicate, and an average value of the yields of products **2-Y** formation was obtained (dibromomethane (0.025 mmol, 1.74 µL) was added as internal standard).The

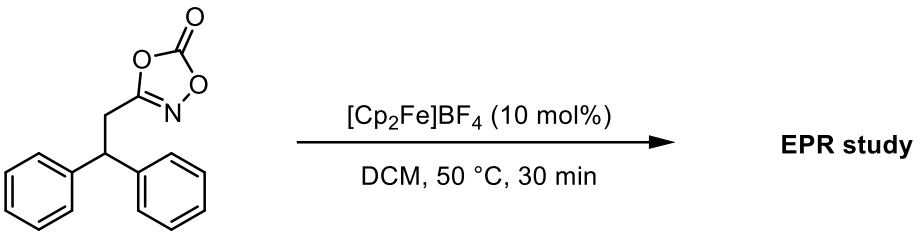
initial rate k_Y/k_H was calculated and the graph k_Y/k_H against σ_{para} was plotted. A straight line (R^2 =0.99) with ρ = -0.55 was obtained from the graph.

Y	yield 1 (x10^2)	yield 2 (x10^2)	yield 3 (x10^2)	average yield (x10^2)	log(k_Y/k_H)	σ_{para}
OMe	0.1710	0.1854	0.1756	0.1773	0.15	-0.27
Me	0.1405	0.1469	0.1584	0.1486	0.08	-0.17
H	0.1192	0.1224	0.1312	0.1242	0	0
F	0.1101	0.1239	0.1170	0.1170	-0.03	0.06
Cl	0.0917	0.0873	0.0957	0.0915	-0.13	0.23

Figure 2.18 Hammett Plot of log(k_Y/k_H) versus σ_{para}

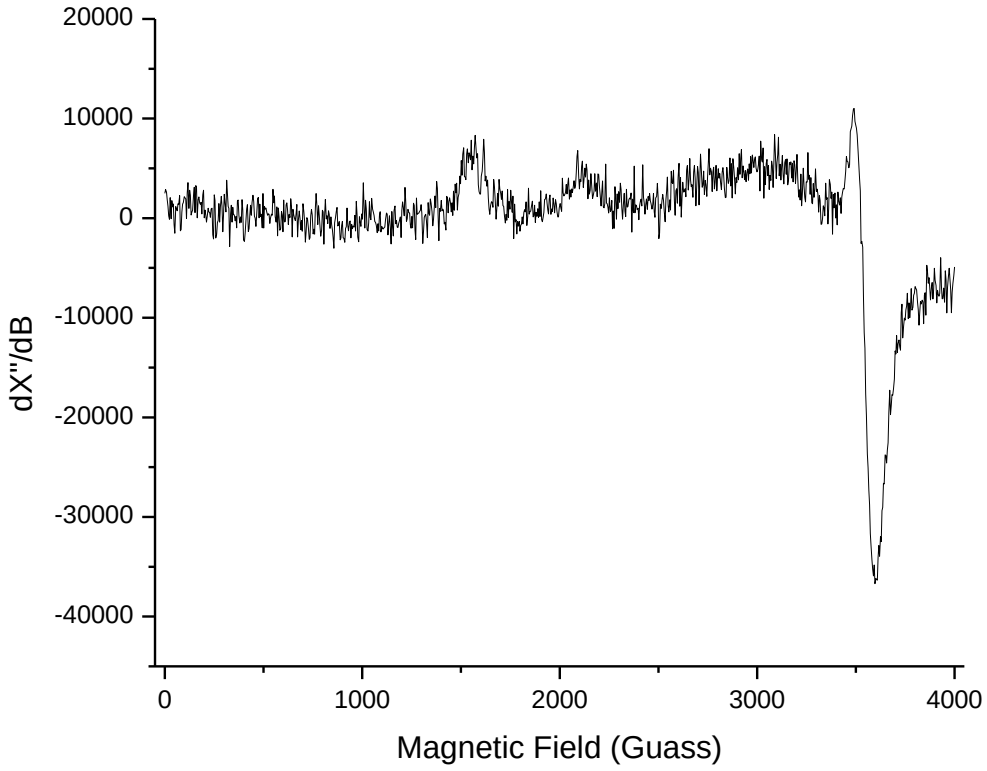


2.6.5.2 EPR Study

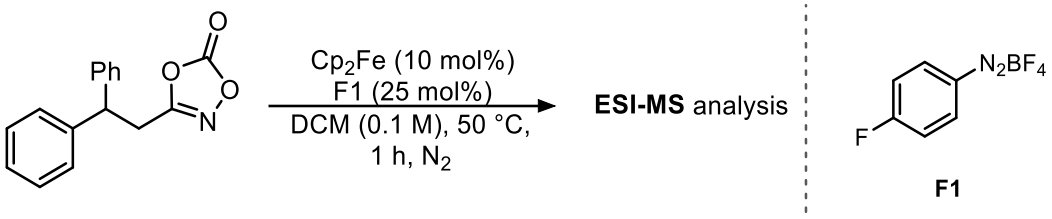


To a solution of $[Cp_2Fe(III)]BF_4$ (0.02 mmol) in DCM (2.0 mL) was added **1a** (0.2 mmol) under a nitrogen atmosphere. The reaction mixture was stirred at 50 °C for 30 min. A portion of the reaction mixture (0.10 mL) was then transferred into a quartz EPR tube and then froze at 77 K (liquid nitrogen). An X-band EPR spectrum of this sample solution was measured at 12 K with the following experimental parameters: microwave frequency: 9.370 GHz; microwave power: 2 mW; modulation frequency: 100 kHz; modulation amplitude: 2 G; time constant: 5.12 ms; conversion time: 20.5 ms. EPR spectral simulation was performed using the Brüker program SimFonia. The strong signal with $g_{//} \sim 2.14$ and $g_{\perp} \sim 1.88$ is attributed to the ferrocenium cation, and the signal at ~1600 Gauss (g~4.3) is attributed to some Fe(III) species of unknown identities.

Figure 2.19 X-band EPR Spectrum of The "[$Cp_2Fe(III)$]BF_4 + 1a" Reaction Mixture



2.6.5.3 ESI-MS Study



In a glove box, ferrocene (3.72 mg, 10 mol%) and 4-fluorobenzenediazonium tetrafluoroborate (10.5 mg, 25 mol%) were added into an 8 mL-vial A. Dry DCM (1 mL) was added to the 8 mL-vial. The reaction mixture was stirred at room temperature for 15 min. **1a** (0.2 mmol) was added into another 4 mL-vial B and dissolved in dry DCM (1 mL). The dioxazolone solution was transferred from vial B to vial A. The reaction in vial A was sealed and stirred at 50 °C for 1 h. After 1 h, aliquot was taken and diluted with MeOH (500:1). The diluted aliquot was analyzed by ESI-MS. A prominent molecular ion cluster peaks at m/z = 186 was observed, and it can be assigned as the ferrocenium complex based on mass value and the agreement between the experimental and simulated mass spectra (see figure 2.1 & 2.2).

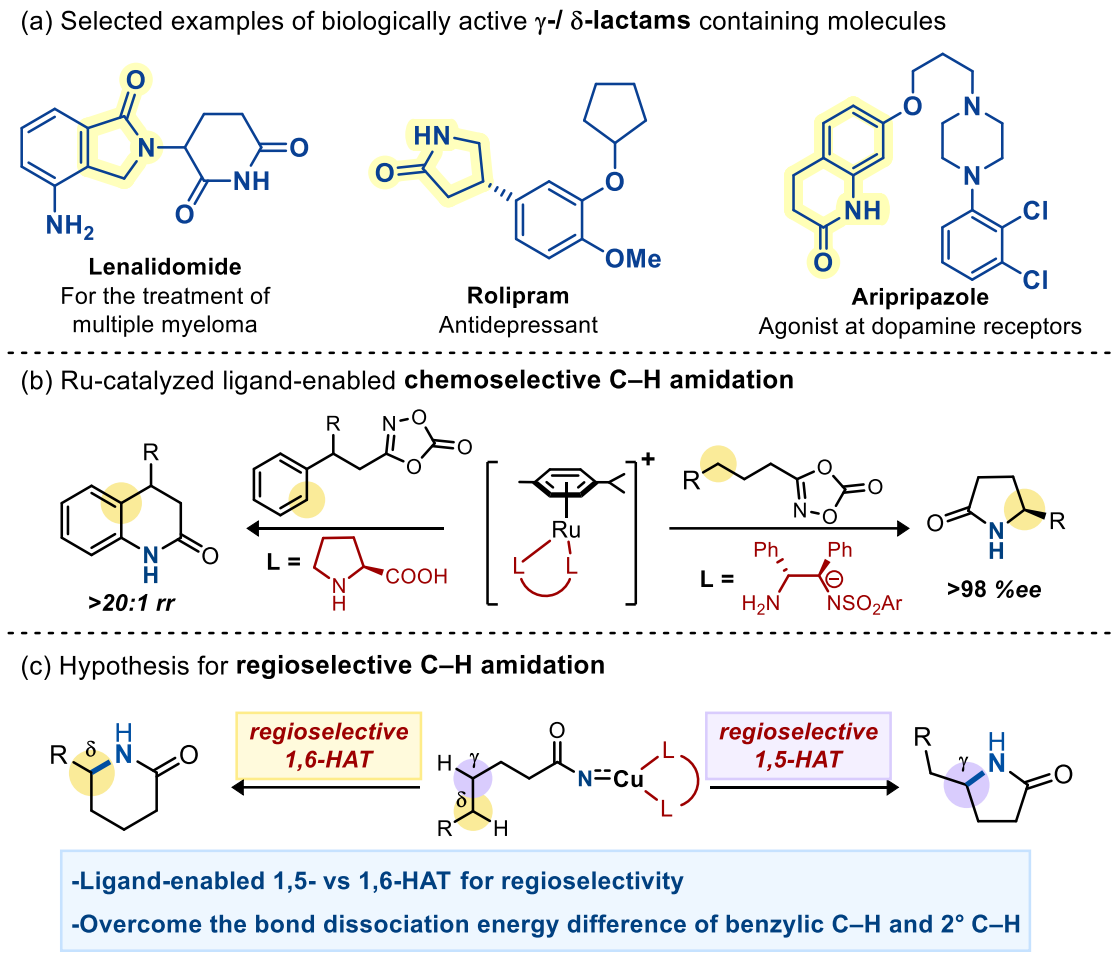
Chapter 3 Ligand-Promoted Copper-Catalyzed Regioselective Nitrene Transfer Reactions Towards Synthesis of γ- / δ-Lactams

3.1 Introduction

γ-/ δ-Lactams are privileged scaffolds in medicinal chemistry and drug development (Scheme 3.1a).[80] Transition metal-catalyzed intramolecular acyl nitrene insertion to C–H bonds is the most straightforward approach to regiocontrolled lactam synthesis.[8, 60c, 61b, 65b, 81] Pioneered by Chang's group, extensive study is directed to noble transition metal-catalyzed (e.g. Rh[16a, 66d, e, 82], Ir[42a, 66h-k, 66p, 83], Ag[84], and Ru[41, 66a-c, 85]) decomposition of 1,4,2-dioxazol-5-ones to afford reactive metal-acylnitrene complexes. With strong σ-donor ligands, the competing Curtius-type rearrangement can be suppressed, and intramolecular acylnitrene C–H bond insertion can become favorable to afford γ-lactams products with remarkable regio- and chemoselectivities. The research groups of Chang and Yu independently showed that the π-arene-metal complexes of Ir(III)[42a, 66j] and Ru(II)[41] bearing chiral diamine ligands can effect catalytic enantioselective intramolecular acylnitrene insertion to γ-C(sp^3)–H bond to furnish the chiral γ-lactams in >95% *ee*. Notably, We previously showed that the catalytic activities of the π-arene-Ru complex can be switched toward targeting arene C(sp^2)–H by employing proline as ligand (Scheme 3.1b).[66c]

Yet, designing catalysts capable of differentiating C–H sites of different reactivities for nitrene insertion remains a formidable challenge.[86] It is established that the site-selectivity of nitrene insertion to C(sp^3)–H bonds can be modulated by electronic and steric factors.[32-33, 87] For instance, Chang's group reported that using $[CpRu(II)]^+$ complexes bearing 5-nitro-1,10-phenanthroline as ligand can bring about preferential intramolecular amidation at the benzylic C–H bond (BDE = 356 kJ mol^{-1}) over the tertiary C–H bond (BDE = 395 kJ mol^{-1}).[66a] Yet, the selectivity principle for nitrene insertion toward methylene C–H bonds is underdeveloped. Recently, Schomaker's group reported the ligand-enabled Ag-catalyzed intramolecular regioselective C–H amidation for the synthesis of β- and γ-amino alcohols with carbamate ester as the nitrogen source.[34, 37a, 88]

Scheme 3.1 Examples of *γ*-/ *δ*- Lactams as Scaffolds of Bioactive Compounds and Mechanistic Hypothesis for Catalytic Reactions for *γ*-Lactam Formation



Nitrogen-centered radicals are gaining attention for advancing regioselective C(sp^3)–H reactions amination. It is long established that nitrogen-centered radicals would undergo 1,5-hydrogen atom transfer (HAT) reaction (Hoffman-Löffler-Fretag reaction) due to favorable chair-like transition state.[89] Recently, Nagib and co-workers reported a new Cu-catalyzed strategy to generate iminyl radicals, which undergo regioselective 1,5-HAT at unactivated *γ*-methylene C–H bonds to afford secondary carboradical intermediates.[90] Effective capture of the carboradicals via

organocopper(III) intermediate results in pyrrolidine formation. With our long-standing interest in developing regiocontrolled metal-nitrene C–H bond insertion, we are attracted to the works by Warren[18, 91]and Betley[23] that mononuclear copper-nitrene complexes derived from aryl azides can be formulated as open-shell copper-imidyl radical complexes. Recently, Chang's group reported an enantioselective copper(I)-bisoxazoline catalyzed δ–C–H amidation of 1,4,2-dioxazol-5-ones derived from pentanoic acid, and the reaction is believed to involve triplet Cu(II)-amidyl radical intermediates.[92] Inspired by these precedents, we aspire to develop a catalytic regiocontrolled γ- or δ-lactams synthesis system by differentiating γ- and δ- methylene C–H bonds for direct amidation (Scheme 3.1c). Herein we describe our study on the copper-catalyzed regioselective nitrene C(sp^3)–H insertion to afford γ- or δ-lactams with 1,4,2-dioxazol-5-ones as nitrene source. With different phenanthroline ligands, the copper catalysts can differentiate between γ- or δ- bonds, overriding the reaction at a weaker C–H bond in favor of a stronger C–H bond with remarkable functional group tolerance without the apparent Curtius-type rearrangement.

3.2 Results and Discussion

3.2.1 Reaction Development

3.2.1.1 Cu-Catalyzed Decomposition of 1,4,2-Dioxazol-5-ones for γ-Lactam Synthesis by Direct C(sp^3)–H Amidation

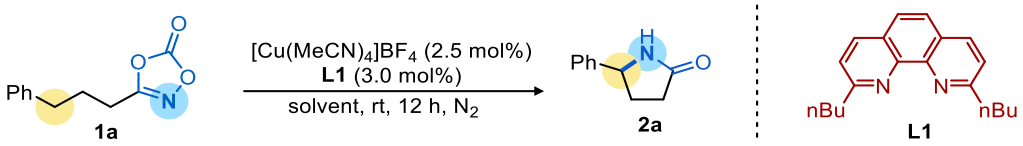
We initiated our study by examining the conditions for facile the γ-C–H amidation. By treating 1,4,2-dioxazol-5-one **1a** (0.2 mmol) with $[Cu(MeCN)_4]BF_4$ (2.5 mol%) and 2,9-di-*n*-butylphenanthroline (3.0 mol%) at room temperature in hexafluoro-2-propanol (HFIP; 2 mL) for 12 h afforded **2a** in 97% yield (Table 3.1, entry 1). No desired product was obtained in the absence of the copper catalyst or the ligand (entries 2 – 3). While the reaction with $[Cu(OTf)]_2•C_6H_6$ as catalyst afforded **2a** in comparable yield (87%), the analogous CuCN catalyst failed to effect significant transformation with full recovery of the starting dioxazolone (entries 4 – 5).

We found that common organic solvents such as dichloromethane (DCM), chlorobenzene (PhCl), and toluene gave inferior results compared to HFIP (entries 6 – 8). Notably, comparable results (**2a**: 90%; entry 9) were obtained with 1,1,1-trifluoroethanol (TFE) as solvent. However, employing nonafluoro-tert-butyl alcohol (NFTB) as solvent led to significant (*E*)-4-phenylbut-3-enamide formation (30%) due to dehydrogenation (entry 10). A similar dehydrogenation reaction in NFTB solvent with Ir-catalysts was reported by Chang's group.[93] The dehydrogenation product

formation may imply a non-concerted nitrene C–H insertion reaction (see later section). Increasing the catalyst loading to 10 mol% did not give a better yield (entry 11).

Compared to **L1**, tridentate and tetradentate ligands such as **L2** and **L3** are ineffective ligands for the amidation reaction (Table 3.2). Yet, bidentate ligand **L4** promotes moderate **2a** (51%) formation (entry 14). Notably, comparing a series of phenanthroline ligands, **L5**, **L6** and **L7** would afford lower lactam yields, suggesting that the substitution at the 2- and 9-positions are critical for catalyst activities. Notably, **L1** containing the n-butyl substituents seems to be the optimized ligands compared to those bearing the methyl- (**L8**) and the phenyl- (**L9**) substituents.

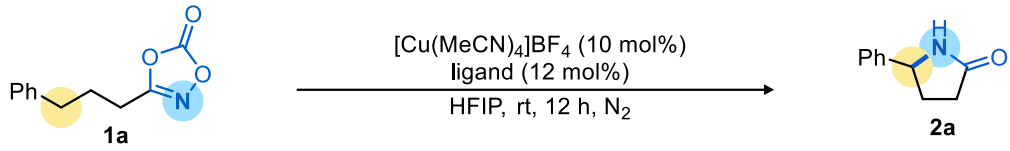
Table 3.1 Effect of Solvents and Copper Catalyst Precursors[a]

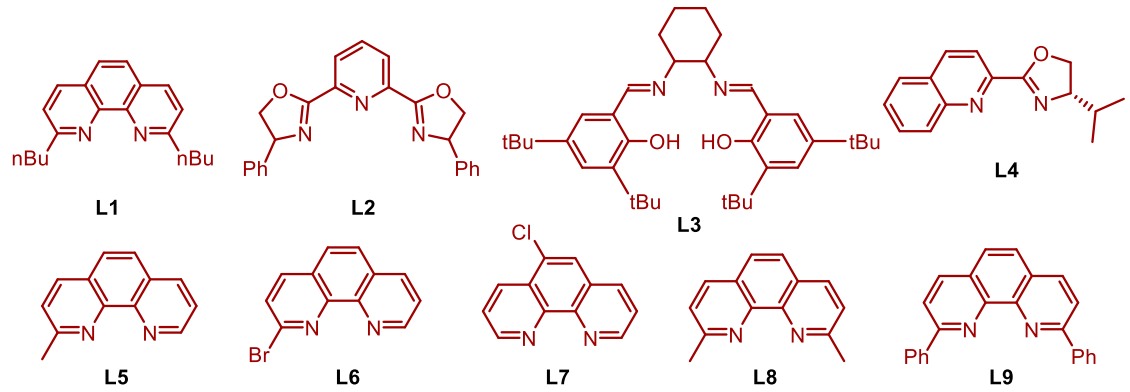


entry	[Cu] catalyst (mol%)	solvent	yield of **2a** (%)[b]
1	**[Cu(MeCN)$_4$]BF$_4$ (2.5)**	**HFIP**	**99 (97)**
2	–	HFIP	n.d.
3	[Cu(MeCN)$_4$]BF$_4$ (10)	HFIP	n.d.[c]
4	[Cu(OTf)]$_2$•C$_6$H$_6$ (10)	HFIP	87
5	[CuCN] (10)	HFIP	n.d.
6	[Cu(MeCN)$_4$]BF$_4$ (2.5)	DCM	40
7	[Cu(MeCN)$_4$]BF$_4$ (2.5)	toluene	<10
8	[Cu(MeCN)$_4$]BF$_4$ (2.5)	PhCl	<10
9	[Cu(MeCN)$_4$]BF$_4$ (2.5)	TFE	90
10	[Cu(MeCN)$_4$]BF$_4$ (2.5)	NFTB	60
11	[Cu(MeCN)$_4$]BF$_4$ (10)	HFIP	93

[a]Reaction conditions: **1a** (0.2 mmol), Cu catalyst (2.5 mol%), and **L1** (3.0 mol%) in solvent under N_2 for 12 hours at room temperature. [b] ^{1}H NMR yield (internal standard: dibromomethane); Isolated yield in parentheses. [c]Reaction run without ligand.

Table 3.2 Effect of Ligands[a-b]





entry	ligand	yield of **2a** (%)[b]
1	**L1**	**99 (97)**
2	L2	n.d.
3	L3	n.d.[c]
4	L4	51
5	L5	46
6	L6	54
7	L7	26
8	L8	55
9	L9	60

[a]Reaction conditions: **1a** (0.2 mmol), [Cu(MeCN)4BF4] (10 mol%), and ligand (12 mol%) in HFIP under N_2 for 12 hours at room temperature. [b]^{1}H NMR yield (internal standard: dibromomethane); Isolated yield in parentheses.

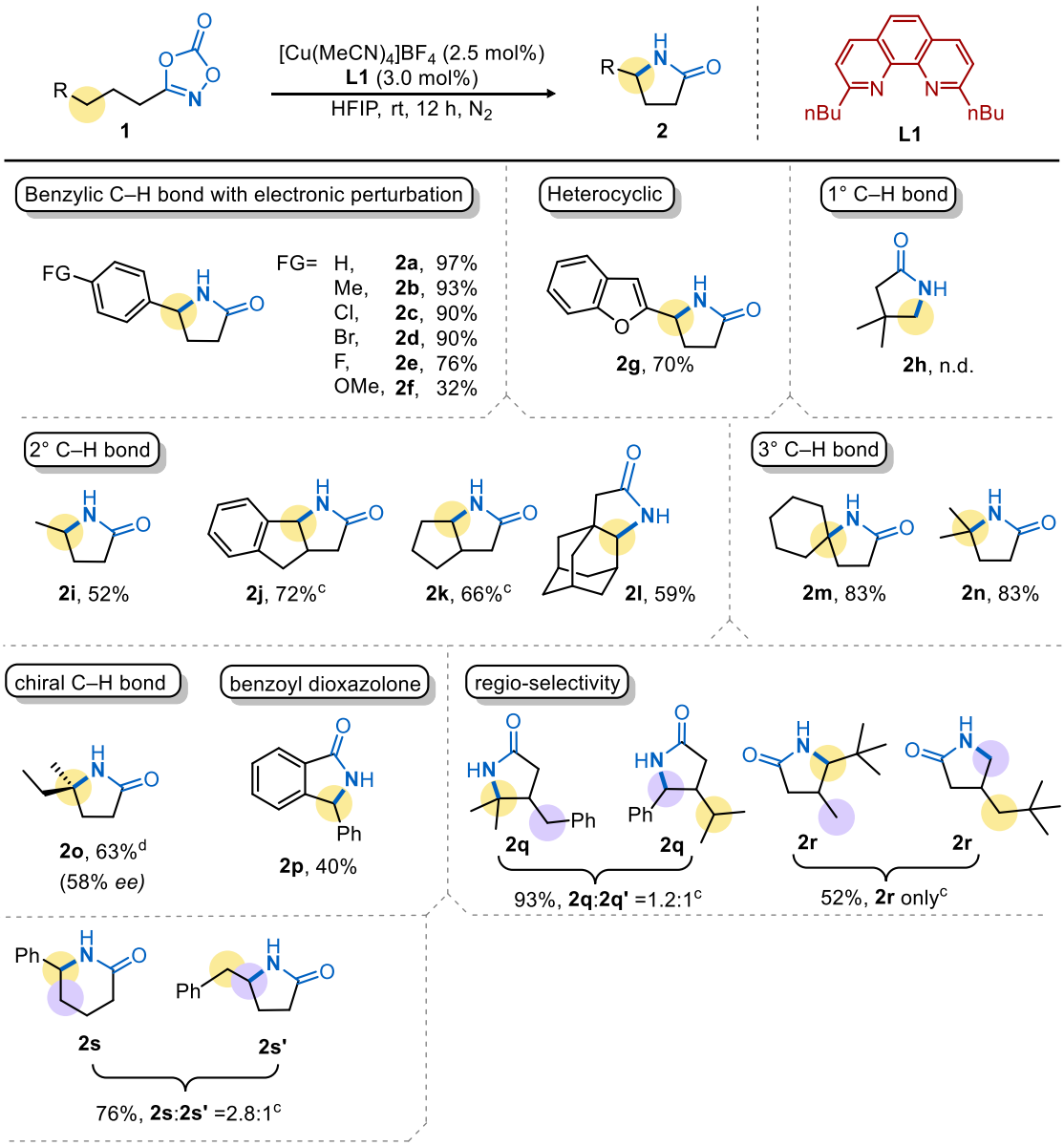
3.2.1.2 Substrate Scope Studies

With the optimized condition in hand, we turned to examine the generality of the copper-catalyzed γ-C–H amidation. We began with the dioxazolones containing benzylic C–H bond with different electronic perturbations at the aryl moiety. The corresponding γ-lactams were successfully obtained in ca. 90% yield (**2a** – **2e**; Table 3.3). Apparently, the reaction involving the dioxazolone bearing an electron releasing -OMe group afforded the lactam **2f** in only 32% yield. In this case, an HFIP-ethereal adduct **2f′**, 4-((1,1,1,3,3,3-hexafluoropropan-2-yl)oxy)-4-(4-methoxyphenyl)butanamide, was obtained in 60% yield. The ethereal adduct formation may be indicative of a carbocation intermediate during the amidation (see later section). Nevertheless, the analogous transformations involving dioxazolones containing benzofuranyl and indanyl moieties afforded their corresponding γ-lactams **2g** (70%) and **2j** (72%) without the HFIP-ethereal adduct being obtained.

For a series of dioxazolones involving amidation of aliphatic C(sp^3)–H bonds, the reaction exhibits a reactivity characteristic: benzylic C–H ≈ tertiary C–H > secondary C–H >> primary C–H. For instance, the amidations at the tertiary C–H bonds afforded the lactams **2m** – **2n** in 83% yield. Yet, the analogous amidations involving secondary C–H bonds produced **2i** – **2l** in lower yields (ca. 60%). The attempt to obtain lactams **2h** by direct amidation of primary C–H bonds was unsuccessful.

Intramolecular competitive experiments were performed to examine the relative reactivity of the C(sp^3)–H bonds toward the Cu-catalyzed amidation. For instance, the lactamization of the substrate containing benzylic and tertiary C–H bonds displayed poor site-differentiation (**2q**: **2q′** = 1.2: 1). On the other hand, the amidation exclusively occurred at the secondary C–H bonds in the presence of competing primary C–H bonds (**2r**). Yet, the lactamization is preferred at the benzylic δ-C–H site over the secondary γ-C–H site, manifested by the selectivity of the six- versus five-membered lactam formation (**2s**: **2s′** = 2.8: 1).

Table 3.3 Substrate Scope for the Cu-Catalyzed γ-C(sp^3)–H Amidation[a-b]



[a]Reaction conditions: **1** (0.2 mmol), $[Cu(MeCN)_4]BF_4$ (2.5 mol%), and **L1** (3.0 mol%) in HFIP under N_2 for 12 hours at room temperature. [b]Isolated yield. [c]Diastereoselectivity (*dr*) & regioselectivity (*rr*) were determined by ^{1}H NMR of the crude reaction mixture [d]Enantiomeric excess (*ee*) was determined by chiral HPLC analysis.

3.3 Mechanistic Studies

3.3.1 Mechanistic Probe Experiments

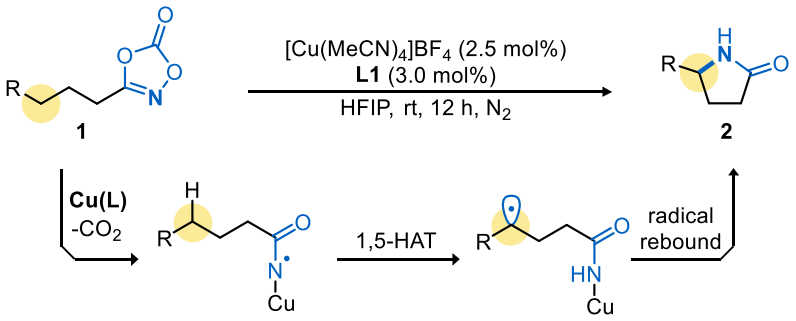
Before this study, there were several reports on copper–nitrenoid transfer reactions, and the copper–nitrenoid species can be understood as reactive nitrogen radicals.[18, 23, 91b, 92] The direct C–H amidation mediated by reactive nitrogen radicals may proceed through a non-concerted pathway involving the hydrogen atom abstraction, followed by radical rebound reactions (Scheme 3.2a). To verify the involvement of radical intermediate, a γ-chiral dioxazolones **1o** (>99% *ee*) derived from enantiopure (*S*)-(+)-4-methyl-1-hexanol was subjected to the Cu-catalyzed conditions, and the expected lactam **2o** was formed with enantiopurity of 58% *ee*. The partial racemization of the stereogenic center is consistent with a non-concerted mechanism (Scheme 3.2b).

In support of the carboradical intermediates, the Cu-catalyzed amidation reaction was found to be suppressed by the presence of a radical scavenger 2,2,6,6-tetramethylpiperidinooxy (TEMPO, 3.0 equiv), and the γ-lactam **2a** formation was diminished to 58% yield. The corresponding TEMPO adduct (23%) has been isolated and spectroscopically characterized (Scheme 3.2c). The isolation of the TEMPO adduct strongly supports a carboradical intermediate, which is plausibly generated by hydrogen atom abstraction by reactive Cu-nitrene species.

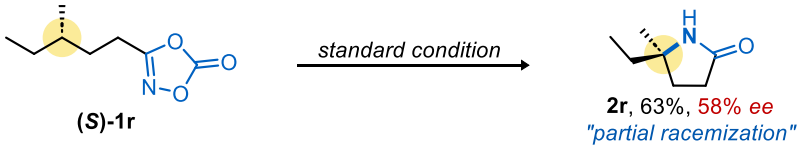
Consistent with the non-concerted mechanism, the reaction of **1f** produced the HFIP-adduct **2f′** as the primary product (60%). The HFIP-adduct formation can be attributed to the nucleophilic solvent attack on a carbocation intermediate, derived from a carboradical intermediate via a radical-polar crossover. The radical-polar crossover becomes a dominant reaction for the dioxazolone substrates bearing the electron-releasing -OMe substituent in the arene.

Scheme 3.2 Postulated Mechanism and Mechanistic Probe Experiments

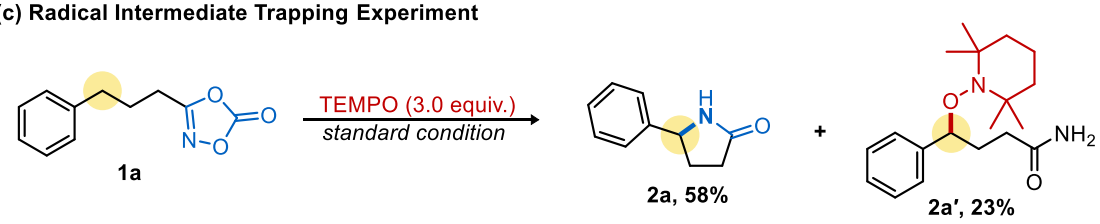
(a) Postulated Mechanism



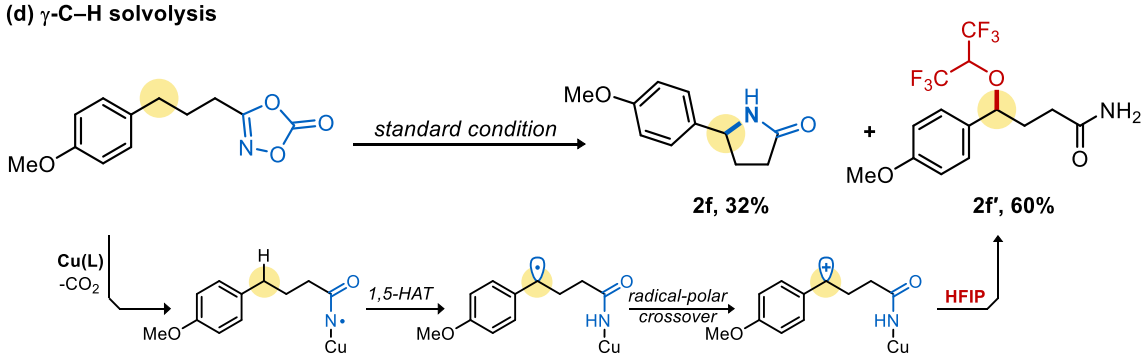
(b) Racemization of Chiral Substrate



(c) Radical Intermediate Trapping Experiment



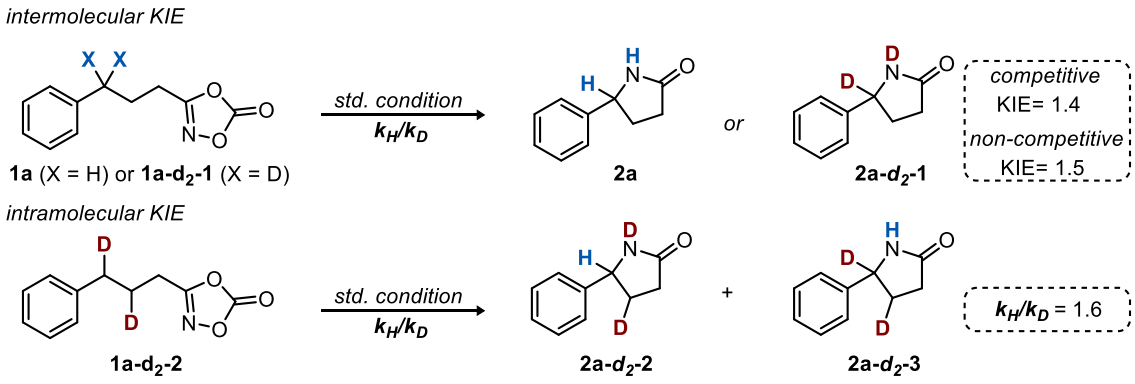
(d) γ-C–H solvolysis



3.3.2 Kinetic Isotope Effect Study

We have conducted a primary H-D kinetic isotope effect study to examine whether the rate-determining step would involve substantial C–H bond cleavage (Scheme 3.3). In this work, the KIE studies were first performed under non-competitive conditions. By comparing the initial rates of the two independent reactions involving **1a** and **1a-d**$_2$, the k_H/k_D value = 1.5 was obtained. Furthermore, an intramolecular KIE study was also performed, and a comparable k_H/k_D value (1.6) was registered. Based on these KIE results, the C–H bond cleavage is unlikely to be involved in the rate-determining step. Given that the Cu-nitrene C–H insertion likely occurs through a non-concerted mechanism, the low k_H/k_D value suggests that the formation of the reactive Cu-nitrene complexes may be the rate-limiting step.

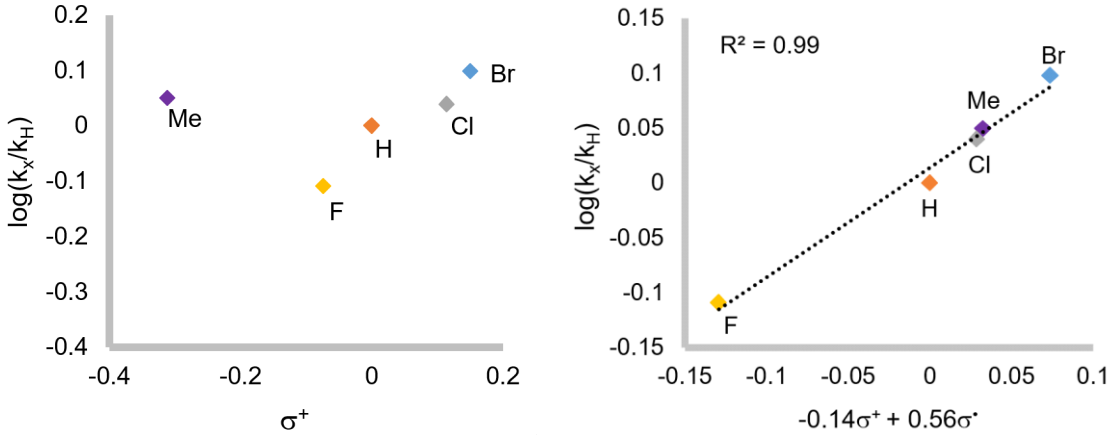
Scheme 3.3 Kinetic Isotope Effect Studies



3.3.3 Hammett Correlation Study

Noted that the Cu-nitrene formation is turnover-limiting, the nature of the nitrene intermediate has been probed by Hammett correlation study employing a series of *para*-substituted dioxazolones **1-X** (X = Me, F, H, Cl, Br). By plotting the log k_x/k_H versus the Hammett constant σ_p or σ^+, a non-linear correlation was observed. The deviation from the expected linear correlation led us to consider the spin-delocalization substituent constants $\sigma\bullet$ as a possibility for some radical intermediates. After testing several spin delocalization scales reported in the literature[94], the $\sigma^{\bullet}$ scale developed by Fischer and co-workers gave the best linearity fit. As shown in Scheme 3.4, the log k_x/k_H versus (σ^+, $\sigma^{\bullet}$) plot afforded a linear fit (R^2= 0.99) by considering both the polar and spin delocalization effects. The multiple linear regression for the dual parameter equation gives the value of σ^+ and $\sigma^{\bullet}$ of -0.14 and 0.56, respectively. With the small $|\sigma^+/\sigma^{\bullet}|$ ratio of 0.25, the observed stronger influence of spin-delocalization effect may imply a dominant radical character of the Cu-nitrene intermediate.

Scheme 3.4 Hammett Correlation Study



3.4 Study on Ligand-Modulated Selective γ- and δ-C(sp^3)–H Amidation

3.4.1 Reaction Development for Selective δ-C–H Amidation

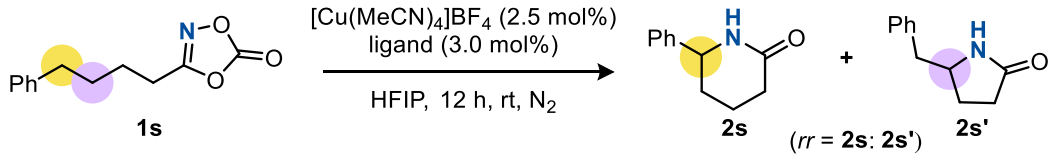
Our earlier study shows that the γ-lactamization of the dioxazolones derived from 4-phenylbutanoic acid should proceed by regioselective 1,5-hydrogen atom transfer (HAT) involving reactive Cu-amidyl radical intermediates. Our competitive experiments further revealed that benzylic C–H bonds (BDE = 356 kJ mol^{-1}) are more reactive than methylene C–H bonds (BDE = 410 kJ mol^{-1}). Compatible with this finding, Chang and co-workers reported the Cu-amidyl radical-mediated formation of δ-lactam from the dioxozalones derived from 5-phenylpentanoic acid. According to Chang's report, the δ-lactam formation occurs via the less favorable 1,6-HAT process that targets exclusively the benzylic C–H bonds.

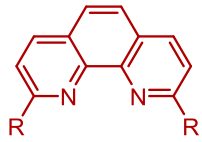
In this work, when we reacted the 3-(4-phenylbutyl)-1,4,2-dioxazol-5-one **1s** under our Cu-catalyzed conditions with **L1** as the ligand, a mixture of δ- and γ-lactams (**2s: 2s′** = 2.8: 1) was furnished. Notably, the exclusive preference toward the δ-benzylic C–H bond amidation by 1,6-HAT was not observed. Instead, the 1,5-HAT involving activating the stronger methylene C–H appeared competitive. We surmised that the preference for 1,6-HAT is likely to be enthalpy-driven, whereas the 1,5-HAT would be entropic-driven. As 1,6-HAT should occur in the preferred linear transition state (N–H–C angle close to 180°), we postulated that the subtle interplay between the enthalpy and

entropy through ligand modulation may influence the preference of 1,5- versus 1,6-HAT processes. For instance, smaller substituents on the ligand would accommodate a larger 7-membered cyclic transition state for *δ*-C–H amidation.

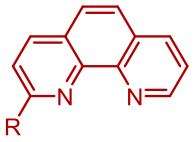
To achieve regioselective *δ*-lactamization, we initiated a ligand screening exercise using phenanthroline ligands with smaller 2,9-substituents (e.g., Me, Cl). With HFIP solvent, the Cu-catalyzed lactamization of **1s** displayed higher regioselectivity towards the *δ*-benzylic C–H bonds activation, albeit the yield remained 20 – 30% (Table 3.4). We observed that the 2-bromophenanthroline ligand (**L6**) provided the most favorable *δ*-regioselectivity (δ: γ = 7.5: 1) and a higher yield of 50%. Additional screening revealed that a mixed solvent system of HFIP and toluene (4: 1) significantly enhanced the *δ*-lactam yield to 75%, achieving a δ: γ regioselectivity of 18: 1.

Table 3.4 Effect of Substituents on the Phenanthroline Ligands[a-c]

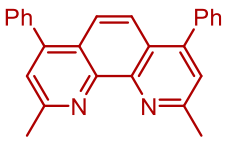




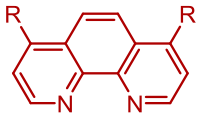
R = nBu, 80(76)%, 2.8:1
R = sBu, 10%, 1.7:1
R = Me, 20%, 7.7:1
R = Cl, 25%, 5.0:1
R = Br, 10%, 5.7:1
R = tBu, 30%, 3.5:1
R = Ph, 32%[d], 1.2:1



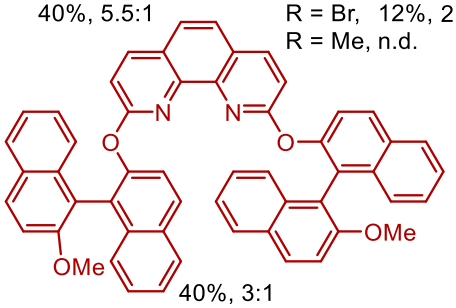
R = Br, 50%, 7.5:1
R = Cl, 25%, 9.8:1
R = Br, 80(75)%[e], 18:1



40%, 5.5:1



R = Br, 12%, 2.7:1
R = Me, n.d.



40%, 3:1

[a]Reaction conditions: **1s** (0.2 mmol), $[Cu(MeCN)_4]BF_4$ (2.5 mol%), and ligand (3.0 mol%) in HFIP under N_2 for 12 hours at room temperature. [b] ^1H NMR yield; Isolated yield in parentheses; Combined yield of **2** and **2′**. [c]Regioselectivity (*rr*) were determined by ^1H NMR of the crude reaction mixture. [d]Reaction run in 10 mol% catalyst and 12 mol% ligand. [e]Reaction run in HFIP: toluene = 4: 1.

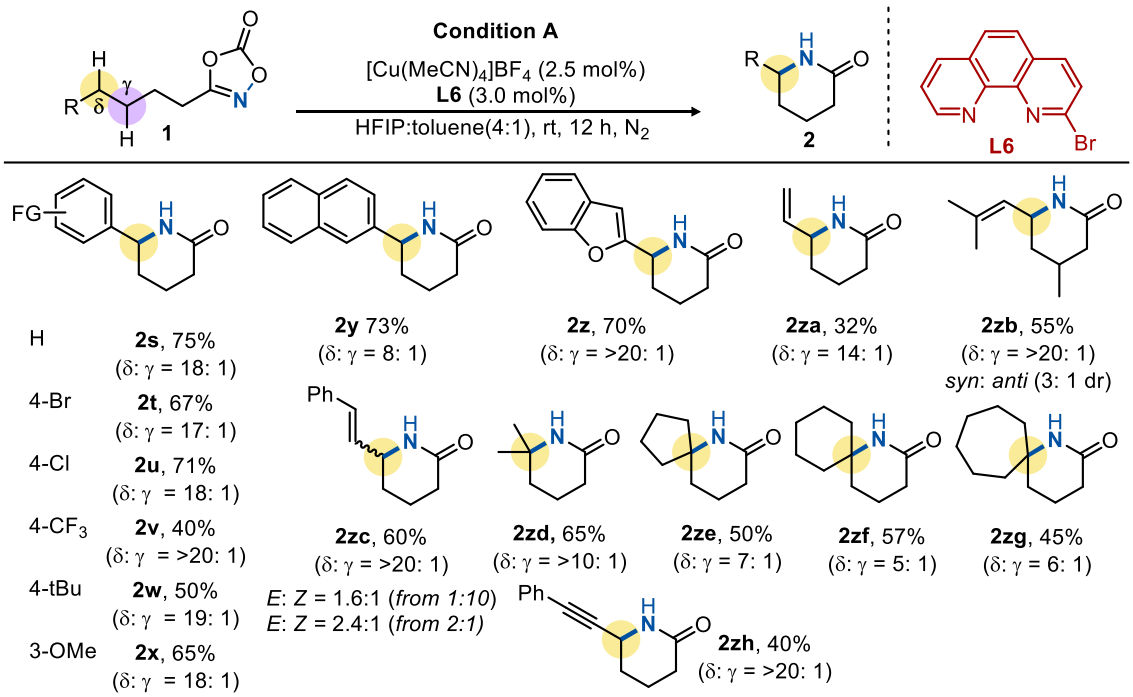
3.4.2 Substrate Scope Studies of the δ-Selective C–H Amidation

Having optimized the conditions for the δ-selective amidation, we turned to scope study by employing a HFIP: toluene (4: 1) co-solvent system and 2-bromophenanthroline (**L6**) as ligand. As depicted in Table 3.5, a range of dioxazolones (**1s** – **1x**) containing competing benzylic δ-C–H and γ-methylene C–H bonds was competent under condition A, affording the δ-lactam in regioselectivity δ: γ = >17: 1 in ca. 70% yields (**2s** – **2x**). Apparently, the substrate bearing an electron-withdrawing CF_3 substituent gives a less satisfactory yield (**2v**: 40%). For dioxazolone containing 2-naphthyl group corresponding δ-lactam was successfully obtained with acceptable yields (**2y**: 73%) while the regioselectivity is less satisfactory (8: 1 *rr*). The substrate containing benzofuran moiety was also amenable to afford the δ-lactam product in good yield (**2z**: 70%, >20: 1 *rr*).

Under condition A, the alkenyl dioxazolones were also successfully converted to corresponding δ-lactam under the mixed-solvent protocol (**2za – 2zc**). Notably, the lactamization was observed to be stereoconvergent which is consistent with the non-concerted mechanism. When (*E*)-alkenyl dioxazolone **1zh** (*Z*: *E* = 1: >10) was employed to condition A, an isomeric mixture of δ-lactams **2zh** (*Z*: *E* = 1.6: 1) were obtained in good yield with excellent regioselectivity (60%, >20: 1 *rr*). For substrate bearing secondary and tertiary C–H bond also gives the corresponding δ-lactam (**2zd** –

2zg) in moderate to good yield (45 – 65%) with remarkable regioselectivity (>10: 1 *rr*). Notably, corresponding azaspirocyclic lactams were successfully obtained with substrate containing cyclic moiety at δ-site (**2ze** – **2zg**). In addition, the propargylic δ-lactam was obtained in excellent regioselectivity with remarkable yield (**2zh**: 40%, >20: 1 *rr*).

Table 3.5 Substrate Scope of δ-C(sp^3)–H Selective Amidation[a-c]



[a]Reaction conditions: (Condition A) **1** (0.2 mmol), $[Cu(MeCN)_4]BF_4$ (2.5 mol%), and **L6** (3.0 mol%) in HFIP: toluene 4: 1 under N_2 for 12 hours at room temperature. [b]Isolated yield; Combined yield of **2** and **2′**. [c]Regioselectivity (*rr*) and diastereoselectivity (*dr*) were determined by ^{1}H NMR of the crude reaction mixture.

3.4.3 Reaction Development for Selective *γ*-C–H Amidation

Having established the reaction condition favoring the 1,6-HAT, we turned to search for a protocol that brings about the *γ*-methylene C–H bond amidation selectively. As depicted in Table 3.4, the preference for the *δ*-lactam versus the *γ*-lactam apparently decreases with larger substituents on the ligand. For instance, with 2,6-dichlorophenanthroline as ligand, the Cu-catalyzed lactamization of **1s** in HFIP solvent afforded a mixture of *δ*- and *γ*-lactams in 5: 1 (*rr*). Yet, when 2,9-diphenylphenanthroline was employed as ligand, an equimolar amount of *γ*- and *δ*-lactams (1.2: 1 = δ: γ) was obtained. In contrast, the binaphthyl-substituted phenanthroline fails to give a better selectivity (3: 1 = δ: γ), plausibly the freely rotating C–O–C linkages resulting in a less rigid transition state for 1,5-HAT. Based on the above results, 2,9-diphenylphenanthroline was selected as the model ligand for more screening.

With 2,9-diphenylphenanthroline as ligand and **1s** as substrate, we then examined the solvent effect on the regioselectivity. Notably, the reaction in chlorinated solvents such as DCM and PhCl failed to afford any lactams formation, and dioxazolone **1s** was converted to 4-phenylbutylamide (Table 3.6; entries 1 – 2). To our surprise, the reactions conducted in dioxane or MeCN registered production of the *δ*-lactam almost exclusively in ca. 15% yield (δ: γ = >20: 1; entries 3 – 4) even with 2,9-

diphenylphenathroline as the ligand. After several trials, the yield and preference for the γ-lactam formation improved gradually when polar fluorinated alcohol solvents were employed as the solvents (TFE, HFIP; entries 5 – 6).

Several literature reported that the ability of strong hydrogen-bond donor (α_{HFIP} = 1.96, α_{TFE} = 1.51)[95] makes the fluorinated solvent itself a good candidate in C–H activation reactions.[96] We hypothesized that the H-bonding with the solvent coordinated to the Cu(II) center may favor the transition state for 1,5-HAT (Scheme 3.5 bottom). By inspection, the hydrogen bonding interaction may "lock" the Cu–amidyl radical intermediate favoring conformation A in which the substrate's skeleton would become closer in contact with the auxiliaries of the phenanthroline ligand. Thus, we surmised that solvents with different hydrogen bonding donor acidity (α) should influence the susceptibility of the transition states towards the steric environment imposed by the ligand, thereby affecting the δ: γ-regioselectivity.[97]

Several solvents of different hydrogen-bond donor acidity (α) were tested for the Cu-catalyzed γ-selective amidation with 2,9-diphenylphenanthroline as the ligand. It was found that the preference to γ-lactams decreases in the solvents with low α values (e.g. dioxane, MeCN) (Table 3.6; entries 3–4). Notably, as the hydrogen-bond donor acidity (α) of the solvent rises from 1.51 (TFE) to 1.96 (HFIP), the δ: γ-selectivity

changes from 3: 1 to 1: 1, showing an improved preference for the *γ*-lactam. This result implies that H-bonding may favor the transition state for 1,5-HAT.

Despite the improved selectivity towards *γ*-C–H bond, the *δ*-lactams remained the major product. Notably, when we switched to a more acidic solvent (NFTB) the regioselectivity reversed in favor of the *γ*-C–H bond (3.1: 1 = γ: δ). While there are no reports on the hydrogen bond acidity of NFTB, the relative acidity can be measured by comparing the difference (Δλ) of the infrared stretching frequencies of unbonded -OH in CCl_4 with the bonded frequencies in THF. The larger difference in the stretching frequency ($\Delta\lambda_{HFIP}$ = 0.35; $\Delta\lambda_{NFTB}$= 0.5) indicates that NFTB should be more acidic.[98] To support our analysis, we employed polar aprotic donor solvents (e.g. DMSO, DMF, NMP) as co-solvents for the lactamization reaction. As anticipated, employing these non-hydrogen bonding donor solvents would favor the conformation for the *δ*-lactams formation where the 1,6-HAT occurs at the space away from the ligand auxiliaries (Table 3.6; entries 8 – 10).

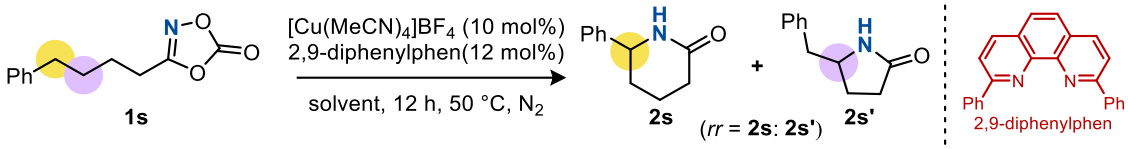
To verify the effect of hydrogen bonding of the solvents on the transition state, we further examined the reaction of dioxazolone **1s** with different sizes of ligand substituent (2-bromo, 2,9-di-*n*-butyl, 2,9-diphenyl) in different perfluorinated alcohol solvents with increasing hydrogen bonding donor acidity (TFE, HFIP, NFTB). The γ: δ-regioselectivity was found to increase with the higher solvent acidity. As expected, the

γ-regioselectivity is further increased with larger sizes of the substituent (Scheme 3.6). To our delight, the co-solvent system of NFTB and toluene (1: 1) gave a comparable yield of **2s** and **2s′** in 55% with regioselectivity favoring the *γ*-C–H bond (3.1: 1 = γ: δ). Notably, if aprotic donor solvents such as MeCN was employed as solvent, the reaction of **1s** afforded exclusively *δ*-lactams across all substituted phenanthroline ligands.

To investigate the steric effect of ligands on the regioselectivity, we performed a linear free-energy correlation study using steric parameters (ν). The parameters are defined based on the steric effects on the rates of acid-catalyzed esterification, and the modified Taft equation ($\log[k/k_0] = \psi\nu$) was adopted for our correlation study.[99] In this work, using **1s** as substrate, the relative rates of the δ- versus γ-C–H lactamization were obtained from the δ- : γ-lactam product ratios for a series of 2,9-disubstituted (R = Me, n-Bu, s-Bu, t-Bu, and Ph) phenanthroline ligands. As depicted in Figure 3.1, a plot of $\log (k_\delta/k_\gamma)$ versus steric parameters (ν) exhibits a linear free-energy relationship (R^2 = 0.9581) with a slope (ψ) value being -0.97. The rather large and negative ψ value implies that the γ-lactam formation is favored by larger substituents of the phenanthroline ligands. Noted that the reactions conducted in the NFTB solvent would afford better γ-regioselectivity, the observed linear free-energy relationship with the

steric parameters seems to agree with higher steric sensitivity in the γ-lactamization transition state in the NFTB solvent due to stronger hydrogen bonding.

Table 3.6 Effect of Solvents on the δ: γ Regioselectivity[a]



entry	solvent	hydrogen-bond donor acidity (α)	combined yield[b] (%)	δ vs γ[c]
1	DCM	0.00	n.d.	-
2	PhCl	0.00	n.d.	-
3	dioxane	0.00	17	>20: 1
4	MeCN	0.19	12	>20: 1
5	TFE	1.51	40	3.2: 1
6	HFIP	1.96	32	1.2: 1
7	NFTB	-	40	1: 3.1
8	NFTB: DMSO (1: 1)	-	20	>20: 1
9	NFTB: NMP (1: 1)	-	15	>20: 1
10	NFTB: DMF (1: 1)	-	16	>20: 1
11	**NFTB: toluene (1: 1)**	-	**55(51)[d]**	**1: 3.6**
12	NFTB: toluene (4: 1)	-	35[d]	1: 5.2

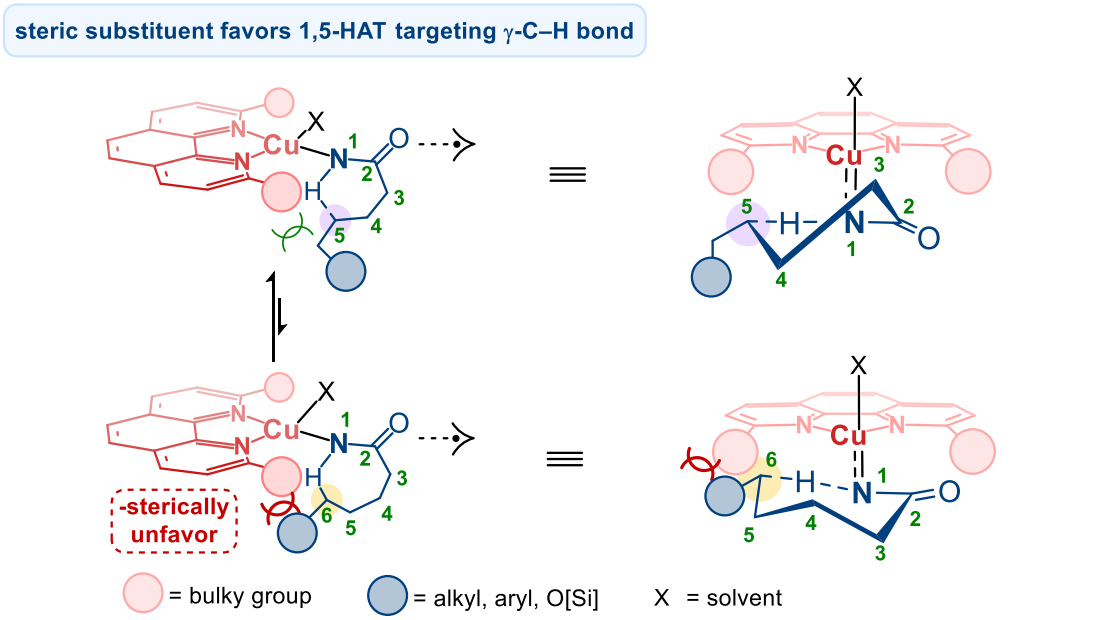
[a]Reaction conditions: **1s** (0.2 mmol), $[Cu(MeCN)_4]BF_4$ (10 mol%), and 2,9-diphenylphenanthroline (12 mol%) in specified solvent under N_2 for 12 hours at 50 °C.

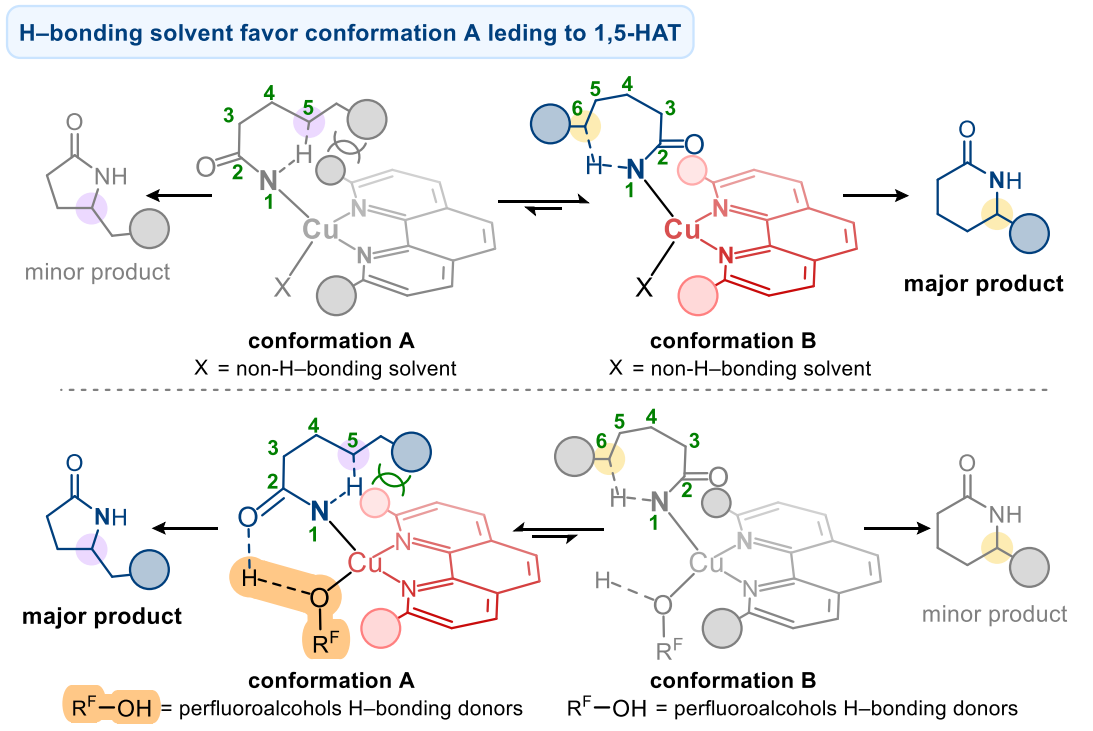
[b] ^{1}H NMR yield; Isolated yield in parentheses; Combined yield of **2s** and **2s′**.

[c]Regioselectivity (*rr*) was determined by ^{1}H NMR of the crude reaction mixture.

[d]Reaction run at room temperature.

Scheme 3.5 Postulated Transition State Models for 1,5- / 1,6-HAT





Scheme 3.6 Experimental *δ*- versus *γ*-Lactams Selectivity with Different Phenanthroline Ligands and Solvents

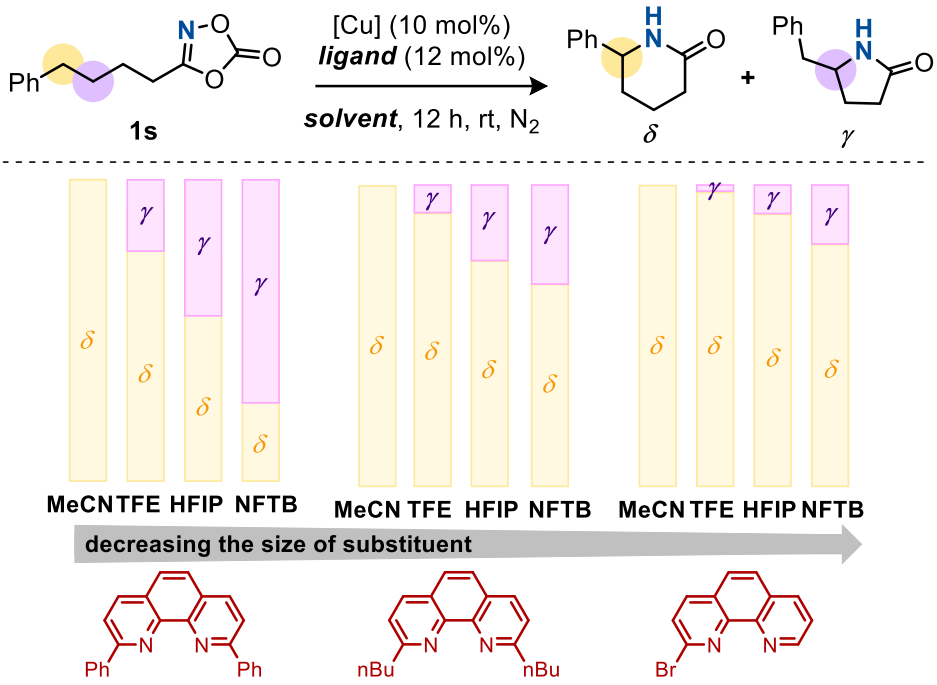
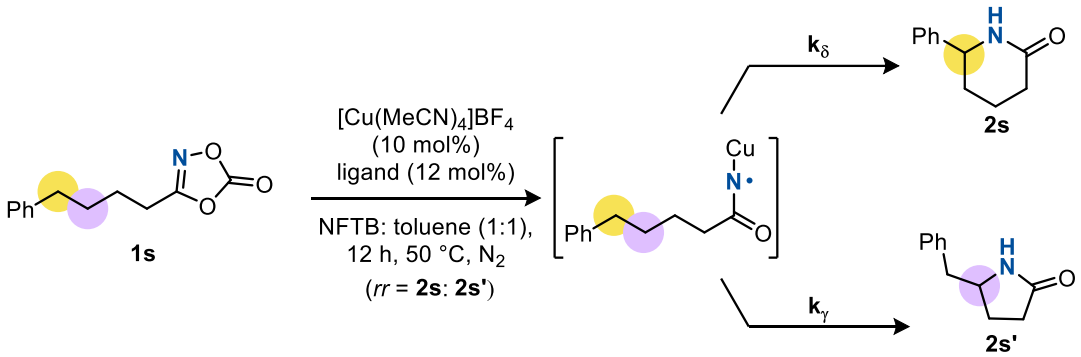
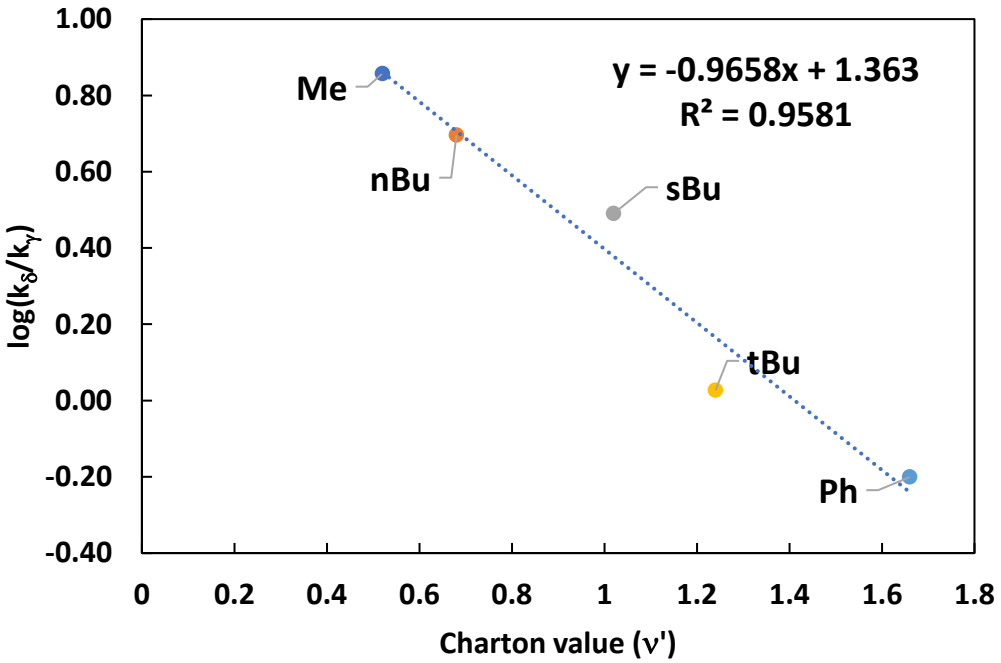


Figure 3.1 LFER Study of Regioselective Lactamization with Different Phenanthroline Ligands using the modified Taft Equation





R	ν'	Entry1 δ/γ	Entry2 δ/γ	Entry3 δ/γ	Average of 3 entries	log(kδ/kγ)
Me	**0.52**	7.90	7.90	5.80	**7.20**	**0.86**
nbu	**0.68**	4.90	5.40	4.60	**4.97**	**0.70**
sBu	**1.02**	2.80	3.18	3.30	**3.09**	**0.49**
tbu	**1.24**	0.98	0.98	1.23	**1.06**	**0.03**
Ph	**1.66**	0.63	0.62	0.64	**0.63**	**-0.20**

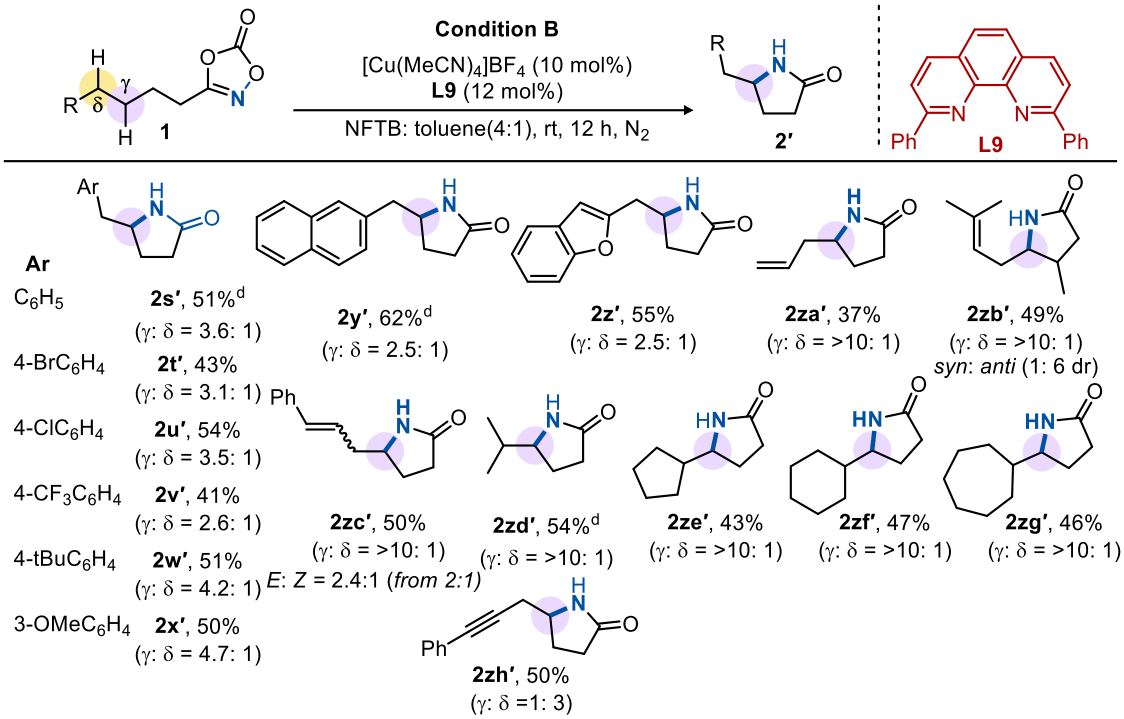
3.4.4 Substrate Scope Studies of the *γ*-Selective C–H Amidation

Next, we conducted the scope study of the Cu-catalyzed *γ*-lactamization using 2,9-diphenylphenanthroline (**L9**) and NFTB-toluene as solvent system (**condition B**). As shown in Table 3.7, employing condition B resulted in successful amidation of the inert *γ*-homobenzylic C–H bonds while overriding the preference for activated *δ*-benzylic C–H bond; the corresponding *γ*-lactams (**2s′ – 2x′**) were obtained with moderate regioselectivity (γ: δ = 4: 1). Less satisfactory regioselectivity (2.5: 1 *rr*) were obtained for the substrates containing benzofuran and naphthalene moiety with ca. 60% yield (**2y′ – 2z′**).

The olefin group was compatible with condition B, and the corresponding *γ*-lactams (**2za′ – 2zc′**) were formed with excellent regioselectivity (>10: 1). Substantial hept-6-enamide was obtained in the reaction of **1za** owing to the direct reduction of the copper-nitrenoid. Notably, stereoconvergent lactamization was also observed in the reaction involving (*E*)-alkenyl dioxazolone **1zc** (*Z*: *E* = 1: 2), an isomeric mixture of *γ*-lactams **2zc′** were obtained in 50% yield with good regioselectivity (>10: 1 *rr*). Excellent *γ*-selectivity (>10: 1 *rr*) were also achieved for the substrate bearing tertiary and secondary C–H bonds, and their *γ*-lactams **2zd′** – **2zg′** were obtained in ca. 50%. For the reaction of the dioxazolone derived from 7-phenylhept-6-ynoic acid, a mixture of *δ*-(13%) and *γ*-lactam (37%) (γ: δ = 1: 3) was obtained. As expected, the analogous

reaction conducted in condition A (**L6**; HFIP: toluene = 4: 1) afforded the δ-lactam in 40% yield with δ: γ selectivity being >20: 1. The observed insensitivity of the linear propargylic moiety is consistent with our proposed steric-driven regioselectivity in condition B.

Table 3.7 Substrate Scope of γ-C(sp^3)–H Selective Amidation[a-c]



[a]Reaction conditions: (Condition B) **1** (0.2 mmol), $[Cu(MeCN)_4]BF_4$ (10 mol%), and **L9** (12 mol%) in NFTB: toluene = 4: 1 under N_2 for 12 hours at room temperature. [b]Isolated yield; Combined yield of **2** and **2′**. [c]Regioselectivity (*rr*) and diastereoselectivity (*dr*) were determined by ^{1}H NMR of the crude reaction mixture. [d]Reaction run in NFTB: toluene = 1: 1.

3.5 Concluding Summary

We have developed a copper-catalyzed, ligand-enabled method for achieving highly regioselective synthesis of γ- and δ-lactams. The lactamization involves intramolecular nitrenoid-mediated C(sp^3)–H abstraction, using tethered 1,4,2-dioxazol-5-ones as the nitrene precursor. Our experimental and mechanistic studies highlight that a reactive copper-amidyl radical is likely to be involved in the regio-determining step of lactam formation (1,5-HAT versus 1,6-HAT). Consistent with other reports on base-metal catalysis, we have demonstrated precise control over the regioselectivity of carboradical formation using open-shell copper-nitrene radicals. The selectivity principle appears to arise from the steric environment established by the ligand. We anticipate that this study offers significant insights for developing new base metal-catalyzed regioselective C–N cross-coupling reactions by harnessing the unique reactivity of radicals.

3.6 Experimental Section

3.6.1 General Experimental Section

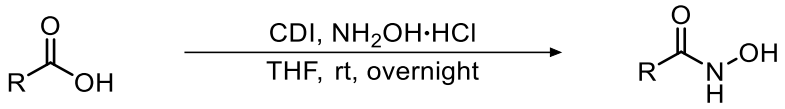
All the solvents and reagents were obtained from commercial sources and used without purification unless stated otherwise. HFIP was dried with activated 3Å molecular sieves (heated at 500 °C before use) and stored in a sealed tube with N_2 protection. All glassware was dried overnight at 150 °C prior to use. Analytical thin layer chromatography (TLC) was performed on precoated silica gel plates with aluminum backing. Preparative TLC was performed on 20 × 20 cm precoated silica gel with layer thickness of 0.5 mm. Visualization on TLC was achieved using UV light (254 nm) or treatment with an aqueous potassium permanganate solution followed by heating. Flash column chromatography was performed on a silica gel (Merck, 230-400 mesh) column. ^{1}H and ^{13}C NMR spectra were recorded on a Brüker DPX-400 MHz spectrometer or Brüker DPX-600 MHz spectrometer. The chemical shift (δ) values were given in ppm and are referenced to residual solvent peaks; carbon multiplicities were determined by DEPT-135 experiments. Coupling constants (*J*) were reported in hertz (Hz). The NMR yields were determined using dibromomethane or 1,1,2,2-tetrachloroethane as internal standard. Mass spectra and high-resolution mass spectra (HRMS) were obtained on a VG MICROMASS Fison VG platform, a Finnigan Model Mat 95 ST instrument, or a Bruker APEX 47e FT-ICR mass spectrometer.

High performance liquid chromatography (HPLC) was carried out on (Waters semi-preparative high performance liquid chromatography system with 2535 quaternary gradient module, 2707 autosampler, 2998 photodiode array detector) equipped with a Chiralpak IC column (4.6 mm φ × 250 mmL) (UV detection at 210, 230, 250, 254 and 280 nm).

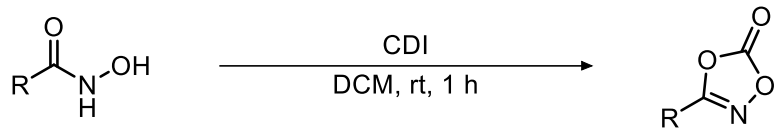
3.6.2 Experimental Procedures and Physical Characterization

3.6.2.1 General Procedure for the Preparation of 1,4,2-Dioxazol-5-ones[41, 66i, 100]

Method A:

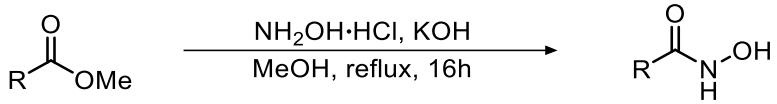


To a round bottom flask equipped with a magnetic stir bar, a solution of corresponding carboxylic acids (2 mmol) in dry THF (20 mL) was added. CDI (3 mmol) was then added to the solution, and the resulting mixture was stirred at room temperature. After stirring for 1 h, hydroxylamine hydrochloride (4 mmol) was added to the reaction mixture. The resulting mixture was then stirred at room temperature for overnight and quenched by 5% $KHSO_4$(aq) (20 mL). The aqueous layer was extracted with EtOAc (3 x 20 mL). The combined organic extracts were dried over $MgSO_4$ and concentrated under vacuo to obtain the corresponding hydroxamic acid for use without further purification.

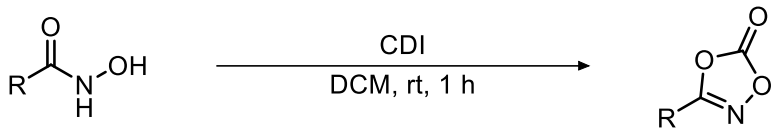


The crude hydroxamic acid and CDI (1.1 equiv) were dissolved in DCM (20 mL) and stirred at room temperature for 1 h. The mixture was quenched with 1 M HCl (20 mL), and the aqueous layer was extracted with DCM (3 x 10 mL). The combined organic extracts were dried over $MgSO_4$ and concentrated under vacuo. The crude mixture was purified by flash chromatography (n-hexane/EtOAc = 10:1 to 8:2) to obtain corresponding 1,4,2-dioxazol-5-ones.

Method B:

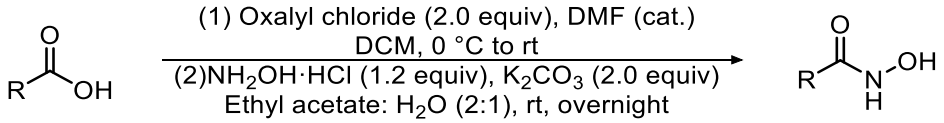


To a round bottom flask equipped with a magnetic stir bar, a solution of corresponding ester (2.0 mmol) in dry MeOH (20 mL) was added. KOH (12.0 mmol) and hydroxylamine hydrochloride (6.0 mmol) were then added to the solution, and the resulting mixture was stirred under reflux and N_2 atmosphere for 16 h. The reaction mixture was then cooled to room temperature and acidified with 1 N HCL to pH 4. The resultant liquid was then extracted with EtOAc (10 mL x 3). The combined organic layer was dried over $MgSO_4$ and concentrated under vacuo to obtain the corresponding hydroxamic acid for use without further purification.



The crude hydroxamic acid and CDI (1.1 equiv) were dissolved in DCM (20 mL) and stirred at room temperature for 1 h. The mixture was quenched with 1 M HCl (20 mL), and the aqueous layer was extracted with DCM (3 x 10 mL). The combined organic extracts were dried over $MgSO_4$ and concentrated under vacuum. The crude mixture was purified by flash chromatography (n-hexane/EtOAc = 10:1 to 8:2) to obtain corresponding 1,4,2-dioxazol-5-ones.

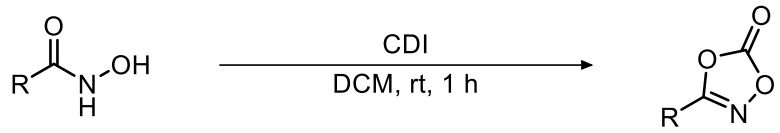
Method C:



(1) To a round bottom flask equipped with a magnetic stir bar, carboxylic acid (2 mmol) was dissolved in DCM (25 mL) with 0.2 mL DMF. Oxalyl chloride was added to the mixture dropwise at 0 °C under an N_2 atmosphere. The reaction mixture was then allowed to stir at room temperature for 4 hours and concentrated under reduced pressure. The crude product (acyl chloride) was used directly without further purification.

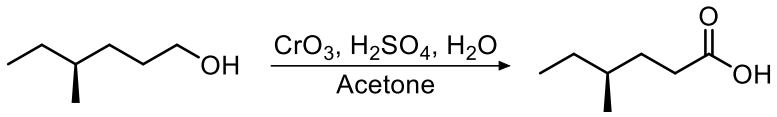
(2) To another round bottom flask equipped with a magnetic stir bar, K_2CO_3 (4 mmol, 2 equiv) was dissolved in a solution of EtOAc (16 mL) and H_2O (8 mL). $NH_2OH{\cdot}HCl$ (2.4 mmol) was then added to the mixture and cooled to 0 °C. The acyl chloride was

dissolved in EtOAc (2 mL) and then added dropwise to the solution under an N_2 atmosphere. The reaction mixture was stirred at room temperature for 12 h. Distilled water was added to the resulting liquid and extracted with EtOAc (3 x 15 mL). The combined organic extracts were dried with $MgSO_4$ and concentrated under vacuo. The crude product was used for the next step without further purification.



The crude hydroxamic acid and CDI (1.1 equiv) were dissolved in DCM (20 mL) and stirred at room temperature for 1 h. The mixture was quenched with 1 M HCl (20 mL), and the aqueous layer was extracted with DCM (3 x 10 mL). The combined organic extracts were dried over $MgSO_4$ and concentrated under vacuo. The crude mixture was purified by flash chromatography (n-hexane/EtOAc = 10:1 to 8:2) to obtain corresponding 1,4,2-dioxazol-5-ones.

Preparation of (*S*)-4-methylhexanoic acid[66i]

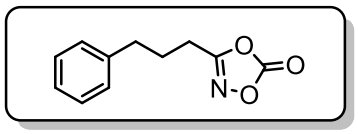


Preparation of Jones Reagent: The Jones reagent is prepared by dissolving chromium trioxide (5 g) in water (30 mL) and concentrated sulfuric acid (4.3 mL) were added slowly at 0°C.

To a round bottom flask equipped with a magnetic stir bar, a solution of (*S*)-4-methylhexan-1-ol (10 mmol) in acetone (60 mL) was added under nitrogen and cooled to 0 °C. The Jones reagent (12 mL) was added over a period of 30 min until an orange tint persisted in the reaction mixture. The mixture is allowed to stir for 1 h at room temperature and isopropyl alcohol (20 mL) is added to destroy the excess Jones reagent. The aqueous layer was extracted twice with diethyl ether (2 x 50 mL), and the combined organic extracts were washed with brine, dry over $MgSO_4$ and concentrated under vacuo. The crude mixture was purified by flash chromatography (DCM: MeOH = 95:5) to obtain (*S*)-4-methylhexanoic acid (0.94 g, 72%) as colorless liquid.

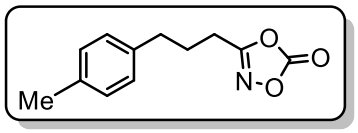
3.6.2.2 Physical Characterization of Substrates

3-(3-Phenylpropyl)-1,4,2-dioxazol-5-one[41]



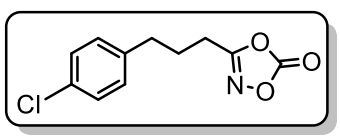
Prepared according to method **A**. Colorless liquid (68%); ^{1}H NMR (400 MHz, $CDCl_3$); δ 7.36 – 7.27 (m, 3H), 7.25 – 7.20 (m, 2H), 2.76 (t, *J* = 7.4 Hz, 2H), 2.63 (t, *J* = 7.4 Hz, 2H), 2.12 – 2.04 (m, 2H); ^{13}C NMR (151 MHz, $CDCl_3$); δ 166.8, 154.4, 140.3, 128.8, 128.7, 126.7, 34.7, 26.0, 24.1.

3-(3-(p-Tolyl)propyl)-1,4,2-dioxazol-5-one[41]



Prepared according to method **A**. White solid (65%); ^{1}H NMR (400 MHz, $CDCl_3$); δ 7.12 (d, *J* = 8.0 Hz, 2H), 7.06 (d, *J* = 8.0 Hz, 2H), 2.70 (t, *J* = 7.4 Hz, 2H), 2.61 (t, *J* = 7.6 Hz, 2H), 2.33 (s, 3H), 2.08-2.00 (m, 2H); ^{13}C NMR (151 MHz, $CDCl_3$); δ 166.6, 154.2, 136.7, 136.1, 129.4, 128.4, 34.1, 26.0, 24.0, 21.0.

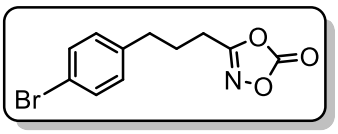
3-(3-(4-Chlorophenyl)propyl)-1,4,2-dioxazol-5-one[41]



Prepared according to method **A**. White solid (86%); ^{1}H NMR (400 MHz, $CDCl_3$); δ 7.31 (d, *J* = 8.4 Hz, 2H), 7.14 (d, *J* = 8.4 Hz, 2H), 2.74 (t, *J* = 7.4 Hz, 2H), 2.65 (t, *J* = 7.4 Hz, 2H), 2.11 – 2.03 (m,

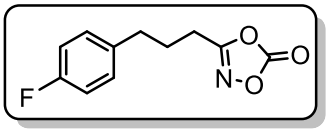
2H); ^{13}C NMR (151 MHz, $CDCl_3$); δ 166.4, 154.1, 138.4, 132.4, 129.9, 128.9, 33.9, 25.8, 24.0.

3-(3-(4-Bromophenyl)propyl)-1,4,2-dioxazol-5-one [41]



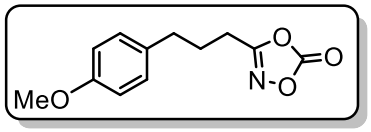
Prepared according to method **A**. White solid (87%); ^{1}H NMR (400 MHz, $CDCl_3$); δ 7.46 (d, *J* = 8.4 Hz, 2H), 7.09 (d, *J* = 8.4 Hz, 2H), 2.72 (t, *J* = 7.6 Hz, 2H), 2.64 (t, *J* = 7.4 Hz, 2H), 2.10 – 2.03 (m, 2H); ^{13}C NMR (151 MHz, $CDCl_3$); δ 166.3, 154.0, 138.8, 131.8, 130.2, 120.4, 33.9, 25.7, 24.0.

3-(3-(4-Fluorophenyl)propyl)-1,4,2-dioxazol-5-one[66i]



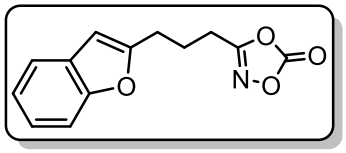
Prepared according to method **A**. Colorless liquid (63%); ^{1}H NMR (400 MHz, $CDCl_3$); δ 7.17 – 7.14 (m, 2H), 6.99 (t, *J* = 8.7 Hz, 2H), 2.72 (t, *J* = 7.5 Hz, 2H), 2.62 (t, *J* = 7.5 Hz, 2H), 2.03 (p, *J* = 7.5 Hz, 2H). ^{13}C NMR (151 MHz, $CDCl_3$); δ 166.4, 162.9, 160.4, 154.1, 135.6, 135.6, 130.0, 129.9, 115.6, 115.4, 33.8, 26.0, 24.0. ^{19}F NMR (565 MHz, CDCl3) δ -117.6.

3-(3-(4-Methoxyphenyl)propyl)-1,4,2-dioxazol-5-one[41]



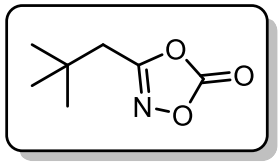
Prepared according to method **A**. Colorless liquid (61%); ^{1}H NMR (400 MHz, $CDCl_3$); δ 7.09 (d, *J* = 8.4 Hz, 2H), 6.85 (d, *J* = 8.0 Hz, 2H), 3.80 (s, 3H), 2.68 (t, *J* = 7.2 Hz, 2H), 2.60 (t, *J* = 7.6 Hz, 2H), 2.07 – 1.99 (m, 2H); ^{13}C NMR (151 MHz, $CDCl_3$) δ 166.6, 158.3, 154.2, 131.9, 129.5, 114.1, 55.3, 33.7, 26.2, 24.0.

3-(3-(Benzofuran-2-yl)propyl)-1,4,2-dioxazol-5-one[41]



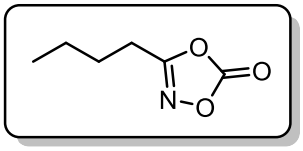
Prepared according to method **B**. White solid (50%); ^{1}H NMR (400 MHz, $CDCl_3$); δ 7.57 – 7.54 (m, 1H), 7.50 – 7.48 (m, 1H), 7.31 – 7.24 (m, 2H), 6.49 (s, 1H), 2.91 – 2.87 (m, 2H), 2.64 (t, *J* = 7.5 Hz, 2H), 2.15 (p, *J* = 7.4 Hz, 2H); ^{13}C NMR (151 MHz, $CDCl_3$); δ 166.4, 156.9, 154.9, 154.3, 128.7, 123.8, 122.9, 120.6, 111.0, 103.3, 27.3, 24.0, 22.5.

3-neopentyl-1,4,2-dioxazol-5-one[41]



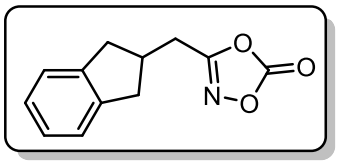
Prepared according to method **A**. Colorless liquid (52%); ^{1}H NMR (400 MHz, $CDCl_3$); δ 2.51 (s, 2H), 1.07 (s, 9H); ^{13}C NMR (151 MHz, $CDCl_3$); δ 165.7, 154.3, 38.4, 31.4, 29.4.

3-Butyl-1,4,2-dioxazol-5-one[41]



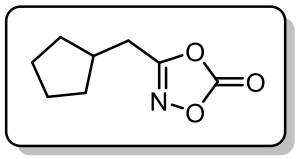
Prepared according to method **A**. Pale yellow liquid (40%); ^{1}H NMR (400 MHz, $CDCl_3$); δ 2.62 (t, *J* = 7.5 Hz, 2H), 1.69 (p, *J* = 7.5 Hz, 2H), 1.42 (h, *J* = 7.4 Hz, 2H), 0.94 (t, *J* = 7.4 Hz, 3H); ^{13}C NMR (151 MHz, $CDCl_3$); δ 166.8, 154.3, 26.5, 24.5, 21.9, 13.4.

3-((2,3-Dihydro-1H-inden-2-yl)methyl)-1,4,2-dioxazol-5-one[41]



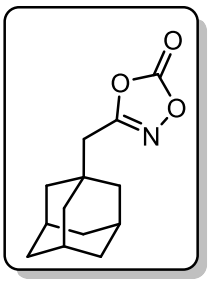
Prepared according to method **A**. White Solid (63%); ^{1}H NMR (400 MHz, $CDCl_3$) δ 7.26 – 7.18 (m, 4H), 3.24 (dd, *J* = 15.6, 7.6 Hz, 2H), 2.99 – 2.88 (m, 1H), 2.82 – 2.75 (m, 4H). ^{13}C NMR (151 MHz, $CDCl_3$); δ 165.9, 154.1, 141.4, 126.8, 124.7, 38.7, 35.5, 30.3.

3-(Cyclopentylmethyl)-1,4,2-dioxazol-5-one[66i]



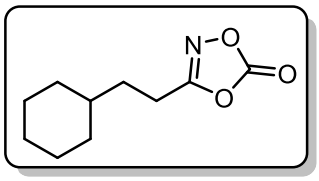
Prepared according to method **A**. Colorless liquid (63%);^{1}H NMR (400 MHz, $CDCl_3$) δ 2.61 (d, *J* = 7.4 Hz, 2H), 2.22 (dq, *J* = 15.5, 7.8 Hz, 1H), 1.94 – 1.81 (m, 2H), 1.74 – 1.52 (m, 4H), 1.31 – 1.17 (m, 2H). ^{13}C NMR (151 MHz, $CDCl_3$) δ 166.5, 154.3, 36.0, 32.3, 30.5, 24.9.

3-(((3r,5r,7r)-Adamantan-1-yl)methyl)-1,4,2-dioxazol-5-one[41]



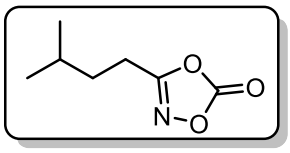
Prepared according to method **A**. White solid (63%); ^{1}H NMR (400 MHz, $CDCl_3$); δ 2.37 (s, 2H), δ 2.03 (s, 3H), δ 1.75 – 1.72 (m, 3H), 1.65 – 1.61 (m, 2H), 1.60 (s, 7H); ^{13}C NMR (151 MHz, $CDCl_3$); δ 165.1, 154.4, 42.2, 38.9, 36.4, 33.2, 28.4.

3-(2-Cyclohexylethyl)-1,4,2-dioxazol-5-one[41]



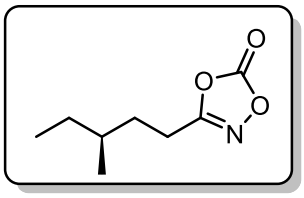
Prepared according to method **A**. Colorless liquid (60%); ^{1}H NMR (400 MHz, $CDCl_3$); δ 2.65 – 2.61 (m, 2H), 1.75 – 1.63 (m, 5H), 1.61 – 1.57 (m, 2H), 1.33 – 1.13 (m, 4H), 0.97 – 0.83 (m, 2H); ^{13}C NMR (151 MHz, $CDCl_3$); δ 167.0, 154.2, 36.8, 32.7, 31.7, 26.3, 26.0, 22.4.

3-Isopentyl-1,4,2-dioxazol-5-one[41]



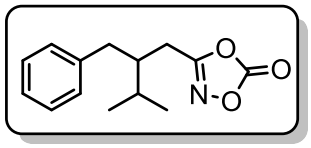
Prepared according to method **A**. Colorless liquid (73%); ^{1}H NMR (400 MHz, $CDCl_3$); δ 2.62 (t, *J* = 7.6 Hz, 2H), 1.70 – 1.57 (m, 3H), 0.95 (d, *J* = 6.4 Hz, 6H); ^{13}C NMR (151 MHz, $CDCl_3$); δ 166.9, 154.3, 26.5, 24.5, 21.9, 13.4.

(*S*)-3-(3-Methylpentyl)-1,4,2-dioxazol-5-one[67l]



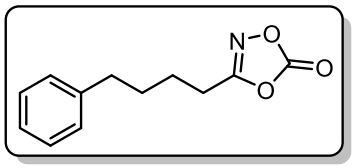
Prepared according to method **A**. Colorless liquid (67%); ^{1}H NMR (400 MHz, $CDCl_3$); δ 2.65 – 2.59 (m, 2H), 1.76 – 1.70 (m, 1H), 1.57 –1.48 (m, 1H), 1.46 – 1.34 (m, 2H), 1.25 – 1.18 (m, 1H), 0.93 – 0.89 (m, 6H); ^{13}C NMR (151 MHz, $CDCl_3$); δ 167.1, 154.3, 33.8, 31.1, 29.0, 22.7, 18.6, 11.2.

3-(2-Benzyl-3-methylbutyl)-1,4,2-dioxazol-5-one[66a]



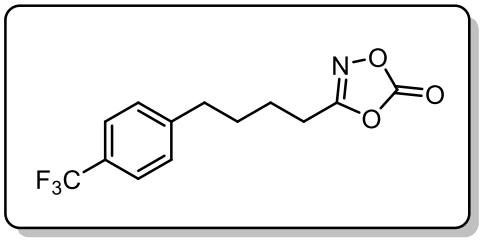
Prepared according to method **B**. Colorless liquid (87%); ^{1}H NMR (400 MHz, $CDCl_3$); δ 7.27 (m, 2H), 7.15 (m, 3H), 2.86 (dd, *J* = 13.9, 5.3 Hz, 1H), 2.60 – 2.41 (m, 3H), 2.13 (td, *J* = 10.4, 9.5, 5.7 Hz, 1H), 1.82 (pd, *J* = 6.9, 3.9 Hz, 1H), 1.00 (dd, *J* = 19.4, 6.9 Hz, 6H). ^{13}C NMR (151 MHz, $CDCl_3$) δ 166.6, 154.2, 139.5, 129.2, 128.8, 126.7, 43.0, 36.9, 29.9, 26.3, 19.0, 18.9.

3-(4-Phenylbutyl)-1,4,2-dioxazol-5-one[67l]



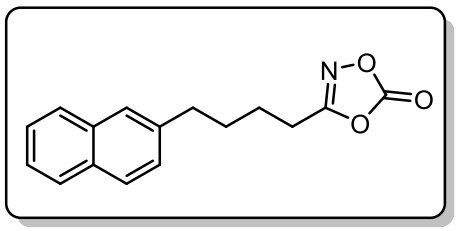
Prepared according to method **A**. Colorless liquid (80%); ^{1}H NMR (400 MHz, $CDCl_3$) δ 7.40 – 7.25 (m, 5H), 2.77 – 2.70 (m, 4H), 1.86 – 1.82 (m, 4H). ^{13}C NMR (151 MHz, $CDCl_3$) δ 166.6, 154.3, 141.3, 128.7, 128.5, 126.3, 35.3, 30.5, 24.8, 24.2.

3-(4-(4-(Trifluoromethyl)phenyl)butyl)-1,4,2-dioxazol-5-one[92]



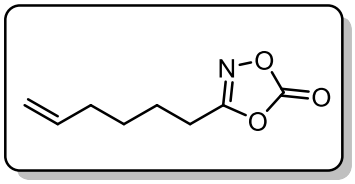
Prepared according to method **A**. Colorless liquid (73%); ^{1}H NMR (400 MHz, $CDCl_3$) δ 7.55 (d, *J* = 7.9 Hz, 2H), 7.28 (d, *J* = 7.9 Hz, 2H), 2.73 (q, *J* = 5.1, 3.5 Hz, 2H), 2.70 – 2.60 (m, 2H), 1.82 – 1.70 (m, *J* = 4.5 Hz, 4H).

3-(4-(Naphthalen-2-yl)butyl)-1,4,2-dioxazol-5-one[92]



Prepared according to method **A**. White solid (78%); ^{1}H NMR (600 MHz, $CDCl_3$) δ 7.83 – 7.77 (m, 3H), 7.61 (s, 1H), 7.50 – 7.41 (m, 2H), 7.31 (dd, *J* = 8.4, 1.7 Hz, 1H), 2.84 (t, *J* = 7.2 Hz, 2H), 2.66 (t, *J* = 7.2 Hz, 2H), 1.88 – 1.75 (m, 4H). ^{13}C NMR (151 MHz, $CDCl_3$) δ 166.5, 154.1, 138.6, 133.6, 132.1, 128.2, 127.7, 127.4, 127.0, 126.5, 126.1, 125.4, 35.3, 30.2, 24.7, 24.0.

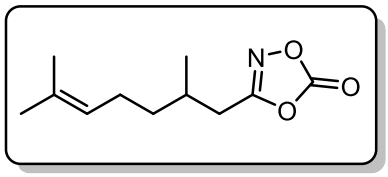
3-(Hex-5-en-1-yl)-1,4,2-dioxazol-5-one[92]



Prepared according to method **A**. Colorless liquid (80%); ^{1}H NMR (600 MHz, $CDCl_3$) δ 5.81 – 5.74 (m, 1H), 5.07 – 4.97 (m, 2H), 2.64 (t, *J* = 7.6 Hz, 2H), 2.15 – 2.08 (m,

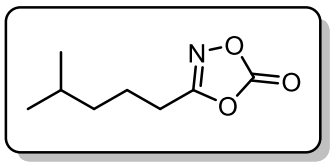
2H), 1.75 (p, *J* = 7.6 Hz, 2H), 1.56 – 1.48 (m, 2H). ^{13}C NMR (151 MHz, $CDCl_3$) δ 166.6, 154.2, 137.5, 115.5, 33.0, 27.8, 24.6, 23.9.

3-(2,6-dimethylhept-5-en-1-yl)-1,4,2-dioxazol-5-one[66i]



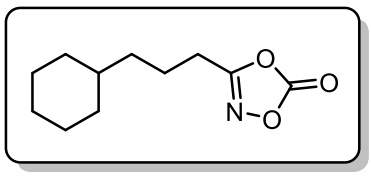
Prepared according to method **A**. Colorless liquid (70%); ^{1}H NMR (400 MHz, $CDCl_3$) δ 5.09 (t, *J* = 7.1 Hz, 1H), 2.64 (dd, *J* = 15.2, 5.8 Hz, 1H), 2.47 (dd, *J* = 15.2, 8.0 Hz, 1H), 2.03 (ddt, *J* = 32.0, 14.0, 7.0 Hz, 3H), 1.72 (s, 3H), 1.63 (s, 3H), 1.51 – 1.39 (m, 1H), 1.42 – 1.24 (m, 1H), 1.05 (d, *J* = 6.7 Hz, 3H). ^{13}C NMR (151 MHz, $CDCl_3$) δ 166.3, 154.4, 132.5, 123.5, 36.4, 31.9, 30.5, 29.9, 25.9, 25.3, 19.4, 17.8.

3-(4-Methylpentyl)-1,4,2-dioxazol-5-one[92]



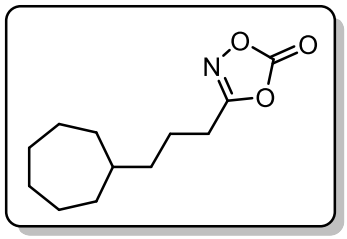
Prepared according to method **A**. Colorless liquid (62%); ^{1}H NMR (600 MHz, $CDCl_3$); δ 2.61 (t, J =7.5 Hz, 2H), 1.75–1.70 (m, 2H), 1.63– 1.56 (m, 1H), 1.33–1.27 (m, 2H), 0.90 (d, J = 6.6 Hz, 6H); ^{13}C NMR (151 MHz, $CDCl_3$) δ 166.7, 154.2, 37.9, 27.6, 25.0, 22.5, 22.3.

3-(3-Cyclohexylpropyl)-1,4,2-dioxazol-5-one



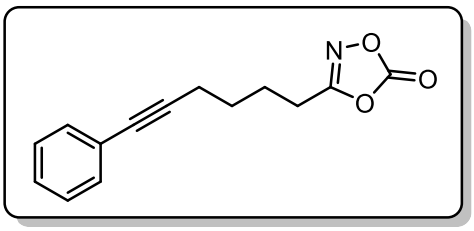
Prepared according to method **A**. Colorless liquid (83%); ^{1}H NMR (600 MHz, $CDCl_3$) δ 2.60 (t, *J* = 7.6 Hz, 2H), 1.77 – 1.63 (m, 7H), 1.31 – 1.09 (m, 6H), 0.93 – 0.86 (m, 2H). ^{13}C NMR (151 MHz, $CDCl_3$) δ 166.8, 154.3, 37.1, 36.4, 33.1, 26.5, 26.2, 25.1, 22.0.

3-(3-Cycloheptylpropyl)-1,4,2-dioxazol-5-one



Prepared according to method **A**. Colorless liquid (87%); ^{1}H NMR (400 MHz, $CDCl_3$) δ 2.60 (t, *J* = 7.5 Hz, 2H), 1.76 – 1.64 (m, 5H), 1.63 – 1.57 (m, 3H), 1.51 – 1.37 (m, 5H), 1.35 – 1.29 (m, 2H), 1.22 – 1.12 (m, 2H). ^{13}C NMR (151 MHz, $CDCl_3$) δ 166.8, 154.3, 38.8, 37.1, 34.4, 28.4, 26.4, 25.0, 22.5.

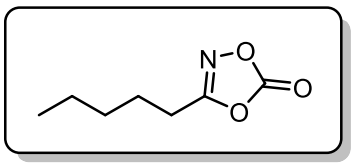
3-(6-Phenylhex-5-yn-1-yl)-1,4,2-dioxazol-5-one[92]



Prepared according to method **C**. White solid (62%); ^{1}H NMR (600 MHz, $CDCl_3$) δ 7.41 – 7.35 (m, 2H), 7.31 – 7.24 (m, 3H), 2.64 (t, *J* = 7.5 Hz, 2H), 2.46 (t, *J* = 7.0 Hz, 2H), 1.88 (p, *J* = 7.6 Hz, 2H), 1.68 (dt, *J* = 14.3, 7.0 Hz, 2H)

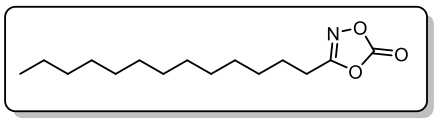
^{13}C NMR (151 MHz, $CDCl_3$) δ 166.5, 154.2, 131.6, 128.3, 127.9, 123.6, 88.7, 81.5, 27.6, 24.4, 23.6, 18.9.

3-Pentyl-1,4,2-dioxazol-5-one[92]



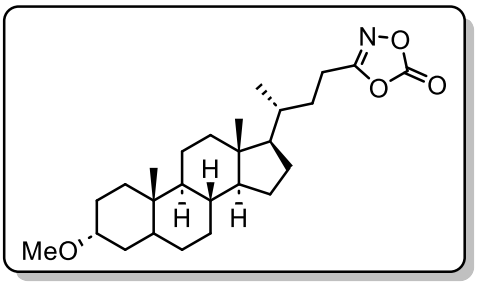
Prepared according to method **A**. Colorless liquid (52%); ^{1}H NMR (600 MHz, $CDCl_3$); δ 2.62 (t, *J* = 7.5 Hz, 2H), 1.73 (p, *J* = 7.2 Hz, 2H), 1.40– 1.35 (m, 4H), 0.92 (t, *J* = 6.6 Hz, 3H); ^{13}C NMR (151 MHz, $CDCl_3$) δ 166.7, 154.3, 30.8, 24.7, 24.2, 22.0, 13.8.

3-Tridecyl-1,4,2-dioxazol-5-one[66i]



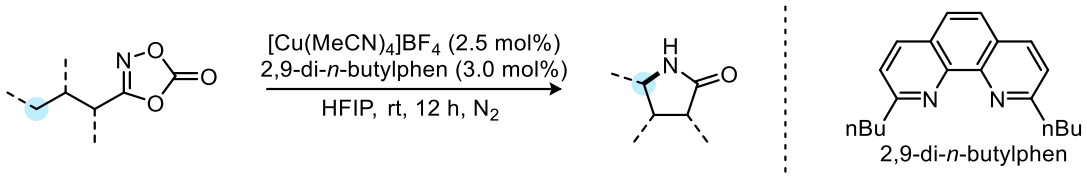
Prepared according to method **A**. Colorless liquid (50%); ^{1}H NMR (600 MHz, $CDCl_3$) δ 2.62 (t, *J* = 7.5 Hz, 2H), 1.72 (p, *J* = 7.5 Hz, 2H), 1.43-1.26 (m, 20H), 0.88 (t, *J* = 6.6 Hz, 3H). ^{13}C NMR (151 MHz, $CDCl_3$) δ 166.7, 154.3, 31.9, 29.7, 29.6, 29.6, 29.4, 29.3, 28.9, 28.7, 24.8, 24.5, 22.7, 14.1

3-((3*R*)-3-((3*R*,8*R*,9*S*,10*S*,13*R*,14*S*,17*R*)-3-Methoxy-10,13-dimethylhexadecahydro-1H-cyclopenta[a]phenanthren-17-yl)butyl)-1,4,2-dioxazol-5-one[66i]



Prepared according to method **A**. White solid (88%); ^{1}H NMR (600 MHz, $CDCl_3$) δ 3.27 (s, 3H), 3.09 (tt, *J* = 10.9, 4.6 Hz, 1H), 2.60 (ddd, *J* = 15.4, 10.4, 4.7 Hz, 1H), 2.46 (ddd, *J* = 15.9, 9.9, 6.4 Hz, 1H), 1.88 (dt, *J* = 12.4, 3.2 Hz, 1H), 1.83 – 1.66 (m, 5H), 1.61 (td, *J* = 12.9, 11.0 Hz, 1H), 1.56 – 1.47 (m, 2H), 1.46 – 1.26 (m, 7H), 1.22 – 1.12 (m, 5H), 1.04 (dddd, *J* = 35.3, 17.9, 12.2, 6.3 Hz, 5H), 0.90 (d, *J* = 6.4 Hz, 3H), 0.85 (s, 3H), 0.58 (s, 3H). ^{13}C NMR (151 MHz, $CDCl_3$) δ 166.2, 153.2, 79.3, 55.4, 54.6, 54.5, 41.8, 41.0, 39.3, 39.1, 34.8, 34.3, 34.2, 33.9, 31.7, 29.6, 27.2, 26.3, 25.8, 25.4, 23.2, 22.4, 20.8, 19.8, 17.1, 11.0.

3.6.3 Experimental Procedures for Cu(I)-Catalyzed C(sp^3)–H Amidation



General procedure A: All reactions were performed in the glovebox under an N_2 atmosphere. Cu catalyst (2.5 mol%) and 2,9-di-*n*-butylphenanthroline (3.0 mol%) were added to an oven-dried 8 mL vial equipped with a magnetic stir bar. HFIP (2 mL) was added, and the mixture was stirred at room temperature for 3 min. 1,4,2-Dioxazol-5-one **1** (0.2 mmol) was added to the mixture, and the vial was capped. The reaction was at room temperature for 12 hours. After that, the reaction mixture was filtered through a pad of silica gel and washed with EtOAc (2 mL × 3). The filtrate was concentrated under vacuum, and the residue was purified by flash column chromatography (eluent: 10: 10: 1 hexane/EtOAc/MeOH) to obtain the desired product.

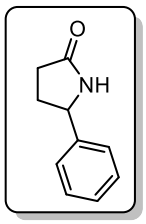
General procedure B: All reactions were performed in the glovebox under N_2 atmosphere. Cu catalyst (2.5 mol%) and 2-bromophenanthroline (3.0 mol%) were added to an oven-dried 8 mL vial equipped with a magnetic stir bar. HFIP: toluene = 4: 1 (2 mL) was added, and the mixture was stirred at room temperature for 3 min. 1,4,2-Dioxazol-5-one **1** (0.2 mmol) was added to the mixture, and the vial was capped. The reaction was stirred at room temperature for 12 hours. After that, the reaction mixture was filtered through a pad of silica gel and washed with EtOAc (2 mL × 3). The filtrate

was concentrated under vacuum, and the residue was purified by flash column chromatography (eluent: 100: 1: 0.1 EtOAc/MeOH/NH_4OH) to obtain the δ-lactam product.

General procedure C: All reactions were performed in the glovebox under an N_2 atmosphere. Cu catalyst (10 mol%) and 2,9-diphenylphenanthroline (12 mol%) were added to an oven-dried 8 mL vial equipped with a magnetic stir bar. NFTB: toluene = 4: 1 (2 mL) was added, and the mixture was stirred at room temperature for 3 min. 1,4,2-Dioxazol-5-one **1** (0.2 mmol) was added to the mixture, and the vial was capped. The reaction was stirred at room temperature for 12 hours. After that, the reaction mixture was filtered through a pad of silica gel and washed with EtOAc (2 mL × 3). The filtrate was concentrated under vacuum, and the residue was purified by flash column chromatography (eluent: 100: 1: 0.1 EtOAc/MeOH/NH_4OH) to obtain the γ-lactam product.

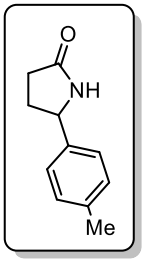
3.6.4 Physical Characterization of Products

5-Phenylpyrrolidin-2-one[41]–prepared using procedure A



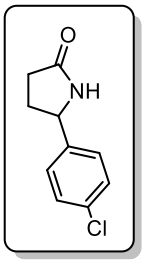
White solid (97%); ^{1}H NMR (400 MHz, $CDCl_3$); δ 7.39 – 7.32 (m, 2H), 7.31 – 7.26 (m, 3H), 6.26 (s, 1H), 4.75 (t, *J* = 7.2 Hz, 1H), 2.59 – 2.43 (m, 1H), 2.40 – 2.38 (m, 2H), 2.02 – 1.94 (m, 1H); ^{13}C NMR (101 MHz, $CDCl_3$); δ 178.7, 142.6, 129.1, 128.1, 125.8, 58.2, 31.5, 30.4.

5-(4-Tolyl)pyrrolidin-2-one[41]–prepared using procedure A



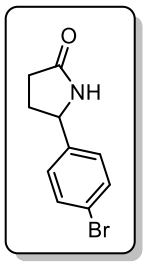
White solid (93%); ^{1}H NMR (400 MHz, $CDCl_3$); δ 7.18 (s, 4H), 6.12 (s, 1H), 4.71 (t, *J* = 7.0 Hz, 1H), 2.62 – 2.49 (m, 2H), 2.34 (s, 3H), 2.00 – 1.91 (m, 1H); ^{13}C NMR (101 MHz, $CDCl_3$); δ 178.5, 139.6, 137.9, 129.7, 125.7, 58.0, 31.6, 30.5, 21.2.

5-(4-Chlorophenyl)pyrrolidin-2-one[41]–prepared using procedure A



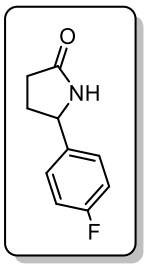
White solid (90%); ^{1}H NMR (400 MHz, $CDCl_3$); δ 7.33 (d, *J* = 8.4 Hz, 2H), 7.23 (d, *J* = 8.0 Hz, 2H), 6.65 (s, 1H), 4.73 (t, *J* = 7.0 Hz, 1H), 2.60 – 2.44 (m, 1H), 2.43 – 2.35 (m, 2H), 1.96 – 1.87 (m, 1H); ^{13}C NMR (101 MHz, $CDCl_3$); δ 178.7, 141.2, 133.8, 129.2, 127.1, 57.6, 31.4, 30.4.

5-(4-Bromophenyl)pyrrolidin-2-one[41]–prepared using procedure A



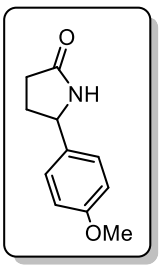
White solid (90%); ^{1}H NMR (400 MHz, $CDCl_3$); δ 7.49 (d, *J* = 8.0 Hz, 2H), 7.17 (d, *J* = 8.4 Hz, 2H), 6.44 (s, 1H), 4.72 (t, *J* = 7.0 Hz, 1H), 2.61 – 2.44 (m, 1H), 2.44 – 2.35 (m, 2H), 1.96 – 1.87 (m, 1H); ^{13}C NMR (101 MHz, $CDCl_3$); δ 178.6, 141.7, 132.2, 127.5, 121.9, 57.7, 31.4, 30.3.

5-(4-Fluorophenyl)pyrrolidin-2-one[41]–prepared using procedure A



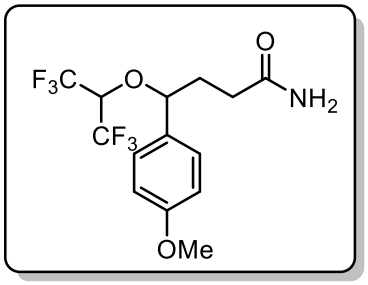
White solid (76%); ^{1}H NMR (400 MHz, $CDCl_3$) δ 7.31 – 7.24 (m, 2H), 7.06 (t, *J* = 8.6 Hz, 2H), 6.03 (s, 1H), 4.75 (t, *J* = 7.1 Hz, 1H), 2.69 – 2.36 (m, 3H), 2.01 – 1.88 (m, 1H). ^{13}C NMR (101 MHz, $CDCl_3$) δ 179.0, 163.6, 161.1, 138.4, 127.4, 127.3, 115.9, 115.7, 57.7, 31.4, 30.5. ^{19}F NMR (565 MHz, CDCl3) δ -114.67.

5-(4-Methoxyphenyl)pyrrolidin-2-one[41]–prepared using procedure A



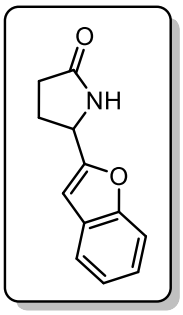
White solid (32%); ^{1}H NMR (400 MHz, $CDCl_3$) δ 7.21 (d, *J* = 8.5 Hz, 2H), 6.89 (d, *J* = 8.5 Hz, 2H), 5.79 (s, 1H), 4.70 (t, *J* = 7.1 Hz, 1H), 3.81 (s, 3H), 2.56 –2.39 (m, 3H), 2.00 –1.93 (m, 1H). ^{13}C NMR (101 MHz, $CDCl_3$) δ 178.4, 159.3, 134.4, 126.9, 114.3, 57.7, 55.4, 31.6, 30.5.

4-((1,1,1,3,3,3-Hexafluoropropan-2-yl)oxy)-4-(4-methoxyphenyl)butanamide – prepared using procedure A



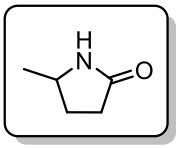
Yellow liquid (60%); ^{1}H NMR (400 MHz, $CDCl_3$) δ 7.27 (d, *J* = 8.4 Hz, 2H), 6.93 (d, *J* = 8.5 Hz, 2H), 5.65 (d, *J* = 75.1 Hz, 2H), 4.79 – 4.58 (m, 1H), 4.00 (p, *J* = 5.8 Hz, 1H), 3.84 (s, 3H), 2.43 – 2.24 (m, 3H), 2.09 (dq, *J* = 14.2, 9.0, 7.4 Hz, 1H). ^{13}C NMR (101 MHz, $CDCl_3$) δ 174.6, 160.5, 129.7, 129.3, 114.4, 84.0, 72.7, 72.3, 72.0, 55.4, 32.8, 31.7. ^{19}F NMR (565 MHz, $CDCl_3$) δ -72.39 (q, *J* = 9.3 Hz), -73.59 (q, *J* = 9.3 Hz). **HRMS** (ESI) m/z calcd. for $C_{14}H_{15}F_6NO_3$ $[M+H]^+$: 360.1029, found: 360.1033.

5-(Benzofuran-2-yl)pyrrolidin-2-one[41]–prepared using procedure A



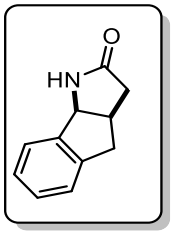
White solid (70%); ^{1}H NMR (400 MHz $CDCl_3$,); δ 7.55 (d, *J* = 7.4 Hz, 1H), 7.46 (d, *J* = 8.3 Hz, 1H), 7.32 – 7.24 (m, 1H), 7.2 – 7.22 (m, 1H), 6.63 (s, 1H), 6.40 (s, 1H), 4.92 (dd, *J* = 8.3, 4.3 Hz, 1H), 2.64 – 2.54 (m, 2H), 2.49 – 2.33 (m, 2H); ^{13}C NMR (101 MHz, $CDCl_3$); δ 178.4, 157.2, 155.2, 128.0, 124.6, 123.2, 121.2, 111.4, 103.0, 51.9, 29.5, 27.0.

5-Methylpyrrolidin-2-one[66i]–prepared using procedure A



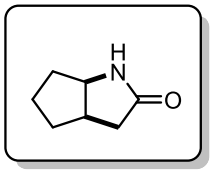
White solid (52%); ^{1}H NMR (400 MHz, $CDCl_3$); δ 6.28 (s, 1H), 3.82 – 3.75 (m, 1H), 2.41 – 2.22 (m, 3H), 1.70 – 1.61 (m, 1H), 1.22 (d, *J* = 6.4 Hz, 3H); ^{13}C NMR (101 MHz, $CDCl_3$); δ 178.3, 50.1, 30.6, 29.3, 22.3.

***cis*-3,3a,4,8b-Tetrahydroindeno[1,2-b]pyrrol-2(1H)-one[41]–prepared using procedure A**



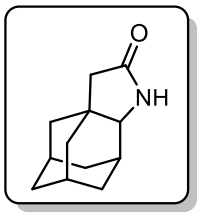
White solid (72%); ^{1}H NMR (400 MHz, $CDCl_3$); δ 7.44 (s, 1H), 7.42 – 7.14 (m, 4H), 5.02 (d, *J* = 6.8 Hz, 1H), 3.33 – 3.24 (m, 2H), 2.88 – 2.81 (m, 1H), 2.70 (dd, *J* = 17.3, 8.7 Hz, 1H), 2.20 (dd, *J* = 17.5, 4.6 Hz, 1H); ^{13}C NMR (101 MHz, $CDCl_3$); δ 177.9, 142.6, 141.8, 128.8, 127.4, 125.5, 125.0, 63.6, 38.7, 37.7, 37.6.

***cis*-Hexahydrocyclopenta[b]pyrrol-2(1H)-one[66i]–prepared using procedure A**



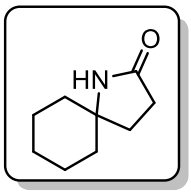
White solid (66%); ^{1}H NMR (400 MHz, $CDCl_3$); δ 5.82 (s, 1H), 4.11 (m, 1H), 2.87 – 2.81 (m, 1H), 2.63 (dd, *J* = 17.7, 10.3 Hz, 1H), 2.06 (dd, *J* = 17.7, 3.5 Hz, 1H), 1.83 – 1.74 (m, 1H), 1.71 – 1.62 (m, 4H), 1.54 – 1.26 (m, 1H); ^{13}C NMR (101 MHz, $CDCl_3$); δ 178.4, 59.3, 38.0, 37.4, 34.7, 34.5, 23.9.

(3ar,5*R*,7*S*,9s)-Octahydro-3a,7:5,9-dimethanocycloocta[b]pyrrol-2(3*H*)-one[41]–prepared using procedure A



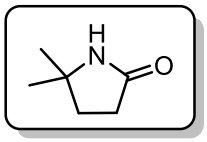
White solid (59%); ^{1}H NMR (400 MHz, $CDCl_3$); δ 5.72 (s, 1H), 3.46 (s, 1H), 2.10 – 1.81 (m, 3H), 1.79 – 1.74 (m, 6H), 1.73 – 1.58 (m, 5H), 1.44 – 1.39 (m, 1H); ^{13}C NMR (101 MHz, $CDCl_3$); δ 179.4, 64.1, 46.4, 40.0, 38.6, 37.2, 37.1, 36.8, 29.5, 29.5, 29.0, 27.4.

1-Azaspiro[4.5]decan-2-one[66i]–prepared using procedure A



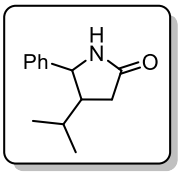
White solid (83%); ^{1}H NMR (400 MHz, $CDCl_3$); δ 6.90 (s, 1H), 2.36 (t, *J* = 8.0 Hz, 2H), 11.88 (t, *J* = 8.0 Hz, 2H), 1.54 – 1.47 (m, 8H), 1.42 – 1.39 (d, *J* = 4.0 Hz, 2H); ^{13}C NMR (101 MHz, $CDCl_3$); δ 177.5, 59.4, 38.4, 32.7, 30.1, 25.2, 23.0.

5,5-Dimethylpyrrolidin-2-one[66i]–prepared using procedure A



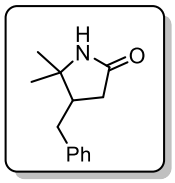
White solid (83%); ^{1}H NMR (400 MHz, $CDCl_3$); δ 5.64 (s, 1H), 2.42 (t, J = 8.0 Hz, 2H), 1.94 (t, *J* = 8.0 Hz, 2H), 1.29 (s, 6H); ^{13}C NMR (101 MHz, $CDCl_3$); δ 176.9, 56.6, 35.5, 30.7, 29.4.

4-Isopropyl-5-phenylpyrrolidin-2-one[66a]–prepared using procedure A



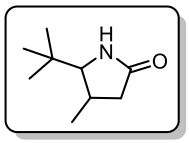
White solid (42%); ^{1}H NMR (400 MHz, $CDCl_3$); δ 7.35 (t, *J* = 7.2 Hz, 2H), 7.30 – 7.28 (m, 3H), 6.42 (s, 1H), 4.43 (d, *J* = 5.6 Hz, 1H), 2.52 – 2.44 (m, 1H), 2.23 – 2.16 (m, 2H), 1.84 – 1.76 (m, 1H), 0.95 (d, *J* = 6.8 Hz, 3H), 0.86 (d, *J* = 6.4 Hz, 3H); ^{13}C NMR (101 MHz, $CDCl_3$); δ 177.6, 142.6, 128.9, 128.0, 126.5, 61.8, 50.9, 33.1, 30.3, 20.9, 18.9.

4-Benzyl-5,5-dimethylpyrrolidin-2-one[66a]–prepared using procedure A



White solid (51%); ^{1}H NMR (400 MHz, $CDCl_3$); δ 7.31 – 7.26 (m, 2H), 7.23 – 7.16 (m, 3H), 6.66 (s, 1H), 2.84 – 2.79 (q, *J* = 5.87 Hz, 1H), 2.52 (t, *J* = 11.8 Hz, 1H), 2.43 – 2.34 (m, 1H), 2.27 – 2.13 (m, 2H), 1.24 (d, *J* = 16.8 Hz, 6H); ^{13}C NMR (101 MHz, $CDCl_3$); δ 176.0, 139.9, 128.8, 128.7, 126.5, 59.0, 47.7, 36.6, 36.0, 28.5, 23.7.

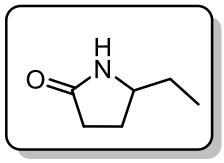
5-(Tert-butyl)-4-methylpyrrolidin-2-one –prepared using procedure A



White solid (52%); ^{1}H NMR (400 MHz, $CDCl_3$); δ 6.71 (s, 1H), 2.91 (dd, *J* = 3.0, 1.1 Hz, 1H), 2.58 (dd, *J* = 17.4, 9.4 Hz, 1H), 2.29 (dtd, *J* = 11.7, 6.1, 5.2, 2.8 Hz, 1H), 1.92 (dd, *J* = 17.4, 3.7 Hz, 1H), 1.16 (d, *J* = 7.0 Hz, 3H), 0.91 (s, 9H); ^{13}C NMR (101 MHz, $CDCl_3$); δ 177.9, 71.8, 38.8, 34.7, 29.4, 25.5, 23.1.

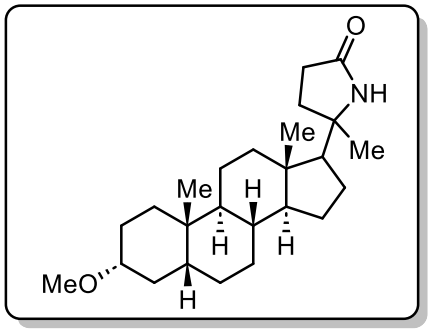
HRMS (ESI) m/z calcd. for $C_9H_{17}NO$ $[M+H]^+$: 156.1383, found: 156.1391.

5-Ethylpyrrolidin-2-one[66i]–prepared using procedure A



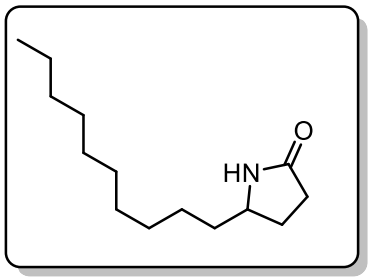
White solid (43%); ^{1}H NMR (400 MHz, $CDCl_3$); δ 5.97 (s, 1H), 3.58 (p, *J* = 6.6 Hz, 1H), 2.43 – 2.27 (m, 2H), 2.31 – 2.15 (m, 1H), 1.79 – 1.67 (m, 1H), 1.64 – 1.43 (m, 2H), 0.94 (t, *J* = 7.4 Hz, 3H). ^{13}C NMR (101 MHz, $CDCl_3$) δ 178.2, 55.8, 30.2, 29.5, 26.9, 10.0.

5-((3*R*,5*R*,8*R*,9*S*,10*S*,13*S*,14*S*)-3-Methoxy-10,13-dimethylhexadecahydro-1H-cyclopenta[a]phenanthren-17-yl)-5-methylpyrrolidin-2-one[66i]–prepared using procedure A



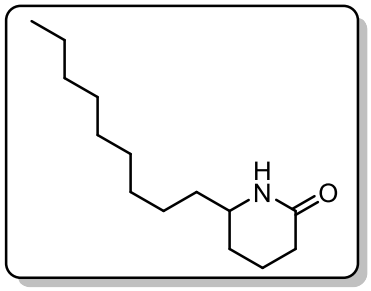
White solid (31%); ^{1}H NMR (600 MHz, $CDCl_3$) δ 5.54 (s, 1H), 3.36 (s, 3H), 3.16 (tt, *J* = 10.9, 4.5 Hz, 1H), 2.41 – 2.31 (m, 1H), 2.31 – 2.21 (m, 1H), 2.11 – 1.99 (m, 2H), 1.90 – 1.81 (m, 1H), 1.81 – 1.75 (m, 2H), 1.75 – 1.63 (m, 3H), 1.61 – 1.54 (m, 1H), 1.43 – 1.26 (m, 10H), 1.24 – 1.04 (m, 8H), 0.99 – 0.90 (m, 4H), 0.73 (s, 3H). ^{13}C NMR (151 MHz, $CDCl_3$) δ 177.6, 80.3, 61.7, 59.6, 56.4, 55.6, 43.5, 41.9, 40.2, 35.3, 35.2, 34.9, 34.9, 32.8, 29.7, 29.1, 28.7, 27.2, 26.8, 26.2, 23.7, 23.4, 23.0, 20.6, 13.6.

5-Decylpyrrolidin-2-one–prepared using procedure A



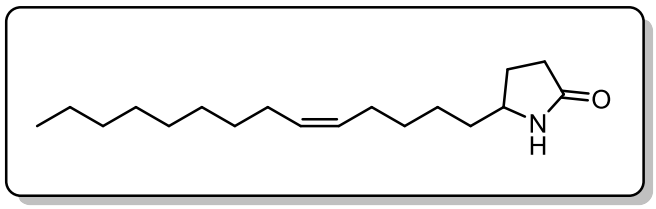
White solid (47%); ^{1}H NMR (400 MHz, $CDCl_3$) δ 6.39 (s, 1H), 3.62 (p, *J* = 6.7 Hz, 1H), 2.42 – 2.17 (m, 3H), 1.76 – 1.59 (m, 1H), 1.56 – 1.42 (m, 2H), 1.32 – 1.26 (m, 16H), 0.88 (t, *J* = 6.7 Hz, 3H). ^{13}C NMR (101 MHz, $CDCl_3$) δ 178.3, 54.6, 36.8, 31.9, 30.2, 29.6, 29.6, 29.5, 29.3, 27.3, 25.9, 22.7, 14.1.

6-Nonylpiperidin-2-one–prepared using procedure A



White solid (13%); ^{1}H NMR (400 MHz, $CDCl_3$) δ 6.06 (s, 1H), 3.34 (dt, *J* = 10.0, 3.1 Hz, 1H), 2.42 – 2.17 (m, 3H), 1.76 – 1.59 (m, 1H), 1.56 – 1.42 (m, 2H), 1.32-1.26 (m, 16H), 0.88 (t, *J* = 6.7 Hz, 3H).^{13}C NMR (101 MHz, $CDCl_3$) δ 172.5, 53.2, 37.0, 31.9, 29.7, 29.6, 29.5, 29.4, 29.3, 28.5, 25.3, 19.8, 14.1.

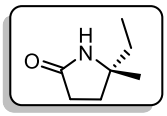
(*Z*)-5-(Tetradec-5-en-1-yl)pyrrolidin-2-one–prepared using procedure A



White solid (39%); ^{1}H NMR (400 MHz, $CDCl_3$) δ 6.62 (s, 1H), 5.32 (tp, *J* = 11.3, 6.4, 5.9 Hz, 2H),

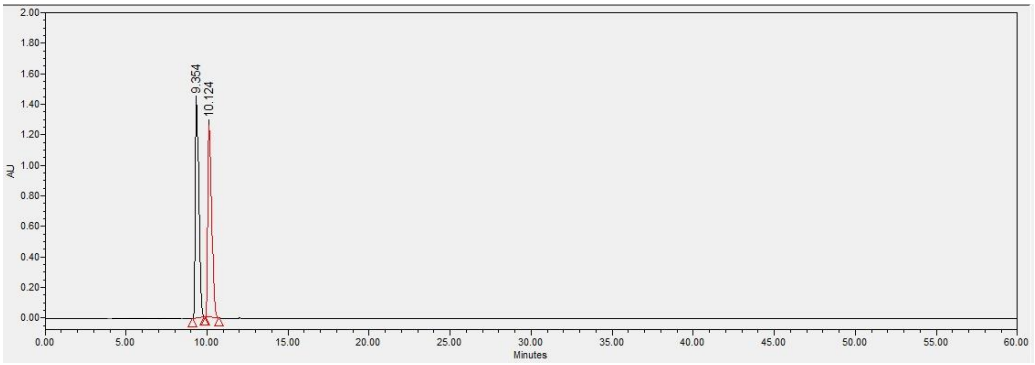
3.60 (p, *J* = 6.6 Hz, 1H), 2.42 – 2.10 (m, 3H), 2.11 – 1.92 (m, 4H), 1.73 – 1.25 (m, 20H), 0.85 (t, *J* = 6.7 Hz, 3H). ^{13}C NMR (101 MHz, $CDCl_3$) δ 178.7, 130.5, 129.3, 54.9, 36.7, 32.0, 30.4, 29.9, 29.8, 29.7, 29.7, 29.5, 27.4, 27.3, 27.1, 25.6, 22.8, 14.2.

(*R*)-5-Ethyl-5-methylpyrrolidin-2-one[66i]–prepared using procedure A



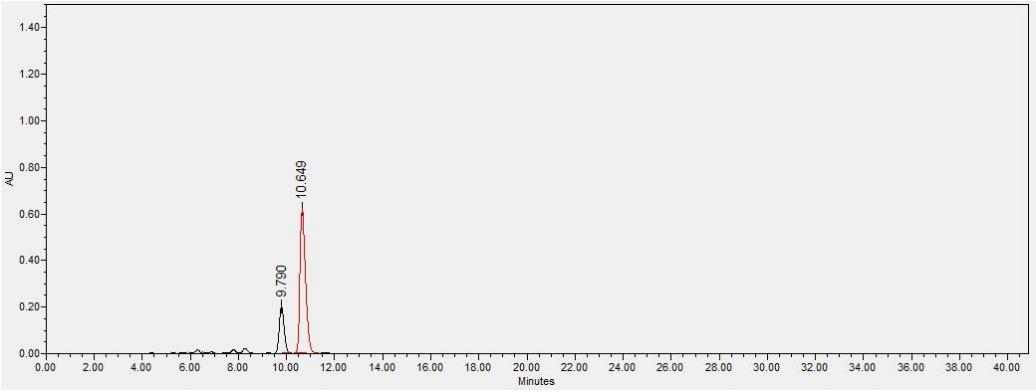
White solid (63%); ^{1}H NMR (400 MHz, $CDCl_3$); δ 6.16 (s, 1H), 2.41 (m, 2H), 2.04 – 1.81 (m, 2H), 1.57 (qd, *J* = 7.5, 2.4 Hz, 2H), 1.26 (s, 3H), 0.93 (t, *J* = 7.5 Hz, 3H); ^{13}C NMR (101 MHz, $CDCl_3$); δ 177.4, 59.6, 34.8, 33.1, 30.7, 26.9, 8.7. HPLC (Chiralpak IC, 50% IPA/Hexane, 0.7 mL/min, 210 nm) tr(minor) = 9.790 min, tr(major) = 10.649 min

racemic compound



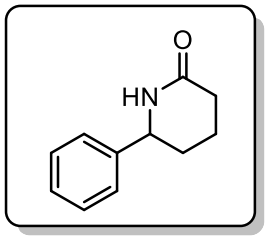
	Sample Name	Vial	Inj	Retention Time (min)	Area	% Area	Height
1	Achiral 7ra1	1:A,1	1	10.124	21738890	50.52	1253297
2	Achiral 7ra1	1:A,1	1	9.354	21292081	49.48	1417131
Mean				9.739			
Std. Dev.				0.545			

chiral compound



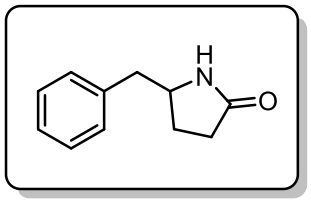
	Sample Name	Vial	Inj	Retention Time (min)	Area	% Area	Height
1	Chiral 7ra1	1:A,2	1	10.649	10206821	78.90	620641
2	Chiral 7ra1	1:A,2	1	9.790	2728892	21.10	201731
Mean				10.219			
Std. Dev.				0.607			

6-Phenylpiperidin-2-one[92]–prepared using procedure B



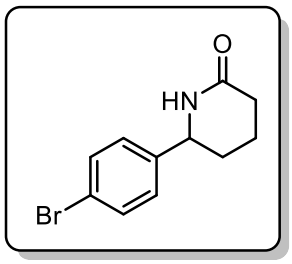
White solid (75%, 18: 1 *rr*); ^{1}H NMR (600 MHz, $CDCl_3$) δ 7.37 (t, *J* = 7.5 Hz, 2H), 7.34 – 7.28 (m, 3H), 5.95 (s, 1H), 4.55 (dd, *J* = 9.2, 4.6 Hz, 1H), 2.46 (m, 2H), 2.15 – 2.08 (m, 1H), 1.92 (m, 1H), 1.86 – 1.75 (m, 1H), 1.69 (mz, 1H). ^{13}C NMR (151 MHz, $CDCl_3$) δ 172.4, 142.5, 128.9, 128.0, 126.1, 57.8, 32.2, 31.3, 19.7.

5-Benzylpyrrolidin-2-one[67l]–prepared using procedure C



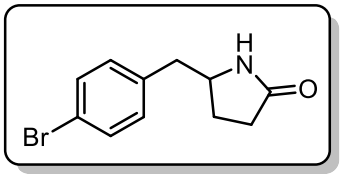
White solid (51%, 3.6: 1 *rr*); ^{1}H NMR (400 MHz, $CDCl_3$) δ 7.42 – 7.27 (m, 3H), 7.26 – 7.15 (m, 2H), 5.53 (s, 1H), 3.88 (p, *J* = 6.0 Hz, 1H), 2.87 (dd, *J* = 13.4, 5.3 Hz, 1H), 2.69 (dd, *J* = 13.4, 8.6 Hz, 1H), 2.37 – 2.17 (m, 3H), 1.99 – 1.75 (m, 1H). ^{13}C NMR (151 MHz, $CDCl_3$) δ 177.6, 137.6, 129.0, 129.0, 126.9, 55.7, 43.2, 30.0, 27.1.

6-(4-Bromophenyl)piperidin-2-one[92]–prepared using procedure B



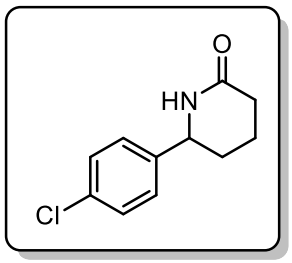
Colorless liquid (67%, 17: 1 *rr*); ^{1}H NMR (400 MHz, $CDCl_3$) δ 7.49 (d, *J* = 8.4 Hz, 2H), 7.18 (d, *J* = 8.4 Hz, 2H), 6.12 (s, 1H), 4.53 (dd, *J* = 9.0, 4.7 Hz, 1H), 2.53 – 2.35 (m, 2H), 2.15 – 2.02 (m, 1H), 1.94 – 1.85 (m, 1H), 1.84 – 1.73 (m, 1H), 1.68 – 1.59 (m, 1H).

5-(4-Bromobenzyl)pyrrolidin-2-one–prepared using procedure C



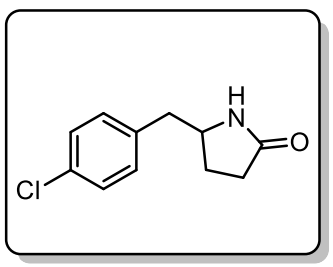
Colorless liquid (43%, 3.1: 1 *rr*); ^{1}H NMR (400 MHz, $CDCl_3$) δ 7.45 (d, *J* = 8.3 Hz, 2H), 7.06 (d, *J* = 8.3 Hz, 2H), 5.66 (s, 1H), 3.86 (q, *J* = 6.9 Hz, 1H), 2.80 (dd, *J* = 13.6, 5.5 Hz, 1H), 2.68 (dd, *J* = 13.5, 8.1 Hz, 1H), 2.37 – 2.20 (m, 3H), 1.92 – 1.77 (m, 1H). **HRMS** (ESI) m/z calcd. for $C_{11}H_{12}BrNO$ $[M+Na]^+$: 275.9994, found: 275.9996.

6-(4-Chlorophenyl)piperidin-2-one[92]–prepared using procedure B



White solid (71%, 18: 1 *rr*); ^{1}H NMR (400 MHz, $CDCl_3$) δ 7.34 (d, *J* = 8.3 Hz, 2H), 7.24 (d, *J* = 8.3 Hz, 2H), 6.14 (s, 1H), 4.55 (dd, *J* = 9.0, 4.7 Hz, 1H), 2.54 – 2.34 (m, 2H), 2.13 –2.06 (m, 1H), 1.97 – 1.72 (m, 2H), 1.68 – 1.59 (m, 1H). ^{13}C NMR (151 MHz, $CDCl_3$, *two carbon signals were merged together*) δ 172.3, 141.1, 133.7, 129.0, 127.5, 57.1, 32.1, 19.6.

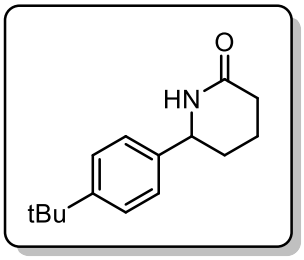
5-(4-Chlorobenzyl)pyrrolidin-2-one –prepared using procedure C



Colorless liquid (54%, 3.5: 1 *rr*); ^{1}H NMR (400 MHz, $CDCl_3$) 7.30 (d, *J* = 8.3 Hz, 2H), 7.11 (d, *J* = 8.2 Hz, 2H), 5.50 (s, 1H), 3.86 (p, *J* = 6.6 Hz, 1H), 2.83 (dd, *J* = 13.5,

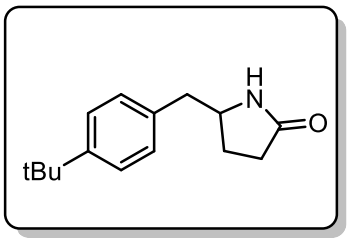
5.4 Hz, 1H), 2.68 (dd, *J* = 13.6, 8.4 Hz, 1H), 2.38 – 2.21 (m, 3H), 1.93 – 1.78 (m, 1H). ^{13}C NMR (151 MHz, $CDCl_3$) δ 177.6, 135.9, 132.9, 130.3, 129.0, 55.4, 42.5, 29.9, 27.0. **HRMS** (ESI) m/z calcd. for $C_{11}H_{12}ClNO$ $[M+Na]^+$: 232.0500, found: 232.0510.

6-(4-(*tert*-Butyl)phenyl)piperidin-2-one –prepared using procedure B



White solid (50%, 19: 1 *rr*); ^{1}H NMR (400 MHz, $CDCl_3$) δ 7.39 (d, *J* = 8.4 Hz, 2H), 7.22 (d, *J* = 8.4 Hz, 2H), 5.80 (s, 1H), 4.53 (dd, *J* = 9.1, 4.6 Hz, 1H), 2.52 – 2.39 (m, 2H), 2.12 – 2.05 (m, 1H), 1.98 – 1.88 (m, 1H), 1.87 – 1.73 (m, 1H), 1.72 – 1.64 (m, 1H), 1.32 (s, 9H). ^{13}C NMR (151 MHz, $CDCl_3$) δ 172.4, 151.1, 139.4, 125.8, 125.8, 57.6, 32.2, 31.3, 31.3, 29.7, 19.8. **HRMS** (ESI) m/z calcd. for $C_{15}H_{21}NO$ $[M+Na]^+$: 254.1515, found: 254.1523.

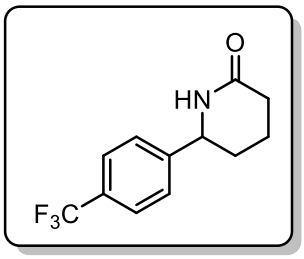
5-(4-(*tert*-Butyl)benzyl)pyrrolidin-2-one –prepared using procedure C



White solid (51%, 4.2: 1 *rr*); ^{1}H NMR (400 MHz, $CDCl_3$) δ 7.34 (d, *J* = 8.2 Hz, 2H), 7.11 (d, *J* = 8.2 Hz, 2H), 5.58 (s, 1H), 3.92 – 3.81 (m, 1H), 2.84 (dd, *J* = 13.5, 5.2 Hz, 1H), 2.65 (dd, *J* = 13.5, 8.7 Hz, 1H), 2.40 – 2.22 (m, 3H), 1.96 – 1.75 (m, 1H), 1.31 (s, 9H). ^{13}C NMR (151 MHz, $CDCl_3$) δ 177.7, 149.8, 134.5, 128.7, 125.8, 55.8, 42.6, 34.5,

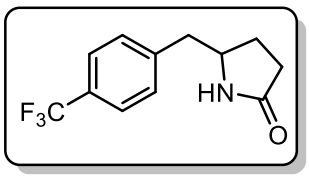
31.4, 30.1, 27.2. **HRMS** (ESI) m/z calcd. for $C_{15}H_{21}NO$ $[M+Na]^+$: 254.1515, found: 254.1528.

6-(4-(Trifluoromethyl)phenyl)piperidin-2-one[92]–prepared using procedure B



Colorless liquid (40%, >20: 1 *rr*); ^{1}H NMR (600 MHz, $CDCl_3$) δ 7.64 (d, *J* = 8.0 Hz, 2H), 7.43 (d, *J* = 8.0 Hz, 2H), 5.97 (s, 1H), 4.65 (dd, *J* = 9.1, 4.8 Hz, 1H), 2.54 – 2.42 (m, 2H), 2.17 – 2.13 (m, 1H), 1.95 – 1.89 (m, 1H), 1.86 – 1.79 (m, 1H), 1.73 – 1.66 (m, 1H). ^{13}C NMR (151 MHz, $CDCl_3$) δ 172.3, 146.5, 130.7, 130.4, 130.2, 130.0, 126.6, 126.5, 126.0, 125.9, 125.9, 125.9, 124.8, 123.0, 121.2, 57.4, 32.1, 31.3, 19.5.^{19}F NMR (565 MHz, $CDCl_3$) δ -62.6.

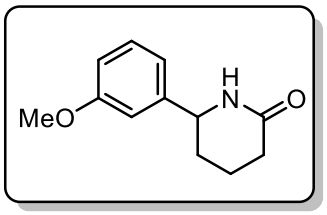
5-(4-(Trifluoromethyl)benzyl)pyrrolidin-2-one –prepared using procedure C



Colorless liquid (41%, 2.6: 1 *rr*); ^{1}H NMR (400 MHz, $CDCl_3$) δ 7.59 (d, *J* = 7.9 Hz, 2H), 7.31 (d, *J* = 7.9 Hz, 2H), 5.66 (s, 1H), 3.95 – 3.87 (m, 1H), 2.91 (dd, *J* = 13.5, 5.6 Hz, 1H), 2.80 (dd, *J* = 13.4, 8.1 Hz, 1H), 2.38 – 2.24 (m, 3H), 1.96 – 1.78 (m, 1H). ^{13}C NMR (151 MHz, $CDCl_3$) δ 177.7, 141.6, 129.4, 126.5, 126.4, 125.8, 125.8, 125.8, 125.7,

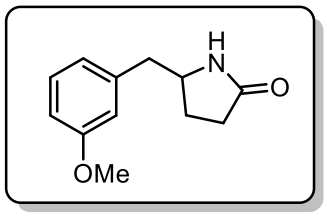
125.0, 123.2, 121.4, 55.3, 42.9, 29.8, 27.0. ^{19}F NMR (565 MHz, $CDCl_3$) δ -62.50. **HRMS** (ESI) m/z calcd. for $C_{12}H_{12}F_3NNaO$ $[M+Na]^+$: 266.0763, found: 266.0768.

6-(3-Methoxyphenyl)piperidin-2-one –prepared using procedure B



Colorless oil (65%, 18: 1 *rr*);^{1}H NMR (400 MHz, $CDCl_3$) δ 7.32 – 7.24 (m, 1H), 6.91 – 6.80 (m, 3H), 6.00 (s, 1H), 4.52 (dd, *J* = 9.1, 4.6 Hz, 1H), 3.81 (s, 3H), 2.54 – 2.36 (m, 2H), 2.16 – 2.05 (m, 1H), 1.98 – 1.86 (m, 1H), 1.86 – 1.61 (m, 2H). ^{13}C NMR (151 MHz, $CDCl_3$) δ 172.4, 160.0, 144.2, 129.9, 129.9, 118.4, 113.2, 111.7, 57.7, 55.3, 32.1, 31.3, 19.7. **HRMS** (ESI) m/z calcd. for $C_{12}H_{15}NO_2$ $[M+Na]^+$: 228.0995, found: 228.1004.

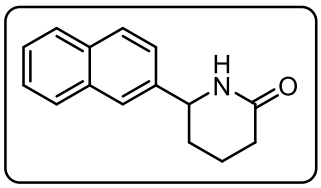
5-(3-Methoxybenzyl)pyrrolidin-2-one –prepared using procedure C



Yellow oil (50%, 4.7: 1 *rr*); ^{1}H NMR (600 MHz, $CDCl_3$) δ 7.24 (t, *J* = 7.9 Hz, 1H), 6.82 – 6.70 (m, 3H), 5.58 (s, 1H), 3.88 (dt, *J* = 13.4, 6.3 Hz, 1H), 3.81 (s, 3H), 2.84 (dd, *J* = 13.4, 5.2 Hz, 1H), 2.66 (dd, *J* = 13.4, 8.7 Hz, 1H), 2.39 – 2.26 (m, 3H), 1.87 – 1.85 (m, 1H). ^{13}C NMR (151 MHz, $CDCl_3$) δ 177.7, 159.9, 139.2, 129.9, 121.2, 114.8, 112.0,

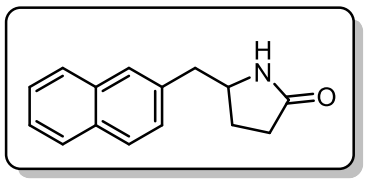
55.6, 55.2, 43.2, 30.1, 27.1. **HRMS** (ESI) m/z calcd. for $C_{12}H_{15}NO_2$ $[M+Na]^+$: 228.0995, found: 228.1001.

6-(Naphthalen-2-yl)piperidin-2-one[92]–prepared using procedure B



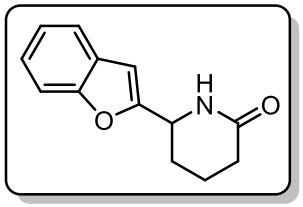
White solid (73%, 8: 1 *rr*); ^{1}H NMR (600 MHz, CD_2Cl_2) δ 7.89 (m, 3H), 7.81 (s, 1H), 7.56 – 7.50 (m, 2H), 7.46 (d, *J* = 8.5, 1H), 6.11 (s, 1H), 4.75 (dd, *J* = 8.4, 4.7 Hz, 1H), 2.51 – 2.42 (m, 2H), 2.22 – 2.18 (m, 1H), 1.98 – 1.90 (m, 1H), 1.87 – 1.78 (m, 2H). ^{13}C NMR (151 MHz, CD_2Cl_2) δ 172.0, 140.4, 133.3, 133.0, 128.5, 127.8, 127.6, 126.4, 126.1, 124.8, 124.3, 57.8, 32.0, 31.4, 19.7.

5-(Naphthalen-2-ylmethyl)pyrrolidin-2-one–prepared using procedure C



White solid (62%, 2.5: 1 *rr*); ^{1}H NMR (600 MHz, $CDCl_3$) δ 7.88 – 7.77 (m, 3H), 7.63 (s, 1H), 7.54 – 7.44 (m, 2H), 7.30 (dd, *J* = 8.3, 1.7 Hz, 1H), 5.63 (s, 1H), 3.98 (p, *J* = 6.2 Hz, 1H), 3.02 (dd, *J* = 13.5, 5.3 Hz, 1H), 2.87 (dd, *J* = 13.5, 8.6 Hz, 1H), 2.42 – 2.32 (m, 2H), 2.32 – 2.16 (m, 2H). ^{13}C NMR (151 MHz, $CDCl_3$) δ 177.7, 135.1, 133.5, 132.3, 128.6, 127.7, 127.6, 127.5, 127.1, 126.4, 125.8, 55.6, 43.3, 30.0, 27.1.

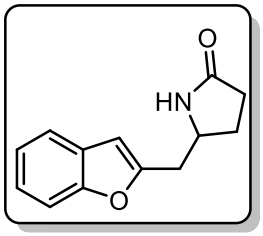
6-(Benzofuran-2-yl)piperidin-2-one –prepared using procedure B



White solid (70%, >20: 1 *rr*); ^{1}H NMR (600 MHz, $CDCl_3$) δ 7.54 (ddd, *J* = 7.7, 1.4, 0.7 Hz, 1H), 7.44 (dq, *J* = 8.2, 0.9 Hz, 1H), 7.31 – 7.26 (m, 1H), 7.23 (td, *J* = 7.5, 1.0 Hz, 1H), 6.63 (t, *J* = 0.9 Hz, 1H), 6.13 (s, 1H), 4.81 – 4.76 (m, 1H), 2.46 (t, *J* = 6.7 Hz, 2H), 2.22 (dddd, *J* = 13.5, 8.4, 5.1, 3.2 Hz, 1H), 2.08 (dddd, *J* = 13.5, 9.1, 7.0, 3.1 Hz, 1H), 1.94 (dddd, *J* = 12.8, 8.5, 6.4, 3.1 Hz, 1H), 1.88 – 1.78 (m, 1H). ^{13}C NMR (151 MHz, $CDCl_3$) δ 171.9, 157.3, 154.9, 127.9, 124.5, 123.0, 121.1, 111.2, 103.1, 51.3, 31.5, 27.3, 18.8.

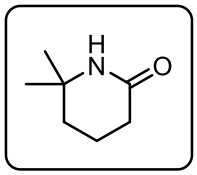
HRMS (ESI) m/z calcd. for $C_{13}H_{13}NO_2$ $[M+Na]^+$: 238.0838, found: 238.0843.

5-(Benzofuran-2-ylmethyl)pyrrolidin-2-one –prepared using procedure C



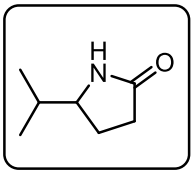
Yellow liquid (55%, 2.5: 1 *rr*); ^{1}H NMR (600 MHz, $CDCl_3$) 7.51 (d, *J* = 7.6 Hz, 1H), 7.42 (d, *J* = 8.1 Hz, 1H), 7.31 – 7.19 (m, 2H), 6.49 (s, 1H), 5.82 (s, 1H), 4.06 (p, *J* = 5.8 Hz, 1H), 3.01 (dd, *J* = 14.9, 4.8 Hz, 1H), 2.91 (dd, *J* = 14.9, 8.5 Hz, 1H), 2.43 – 2.32 (m, 3H), 1.98 – 1.89 (m, 1H). ^{13}C NMR (151 MHz, $CDCl_3$) δ 177.5, 157.3, 154.8, 128.3, 124.0, 122.9, 120.6, 111.0, 104.2, 53.2, 35.9, 29.8, 27.1. **HRMS** (ESI) m/z calcd. for $C_{13}H_{13}NO_2$ $[M+Na]^+$: 238.0838, found: 238.0845.

6,6-Dimethylpiperidin-2-one[92]–prepared using procedure B



White solid (65%, >10: 1 *rr*); ^{1}H NMR (400 MHz, $CDCl_3$) δ 5.55 (s, 1H), 2.30 (t, *J* = 6.6 Hz, 2H), 1.87 – 7.82 (m, 2H), 1.67 – 1.62 (m, 2H), 1.25 (s, 6H). ^{13}C NMR (151 MHz, $CDCl_3$) δ 171.7, 52.6, 35.3, 30.9, 30.7, 17.7.

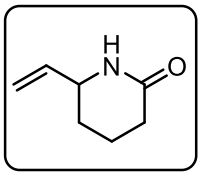
5-Isopropylpyrrolidin-2-one –prepared using procedure C



White solid (54%, >10: 1 *rr*); ^{1}H NMR (600 MHz, $CDCl_3$) δ 6.01 (s, 1H), 3.38 (q, *J* = 7.0 Hz, 1H), 2.36 – 2.30 (m, 2H), 2.18 (dq, *J* = 12.1, 7.5 Hz, 1H), 1.83 – 1.74 (m, 1H), 1.63 (dt, *J* = 13.5, 6.8 Hz, 1H), 0.94

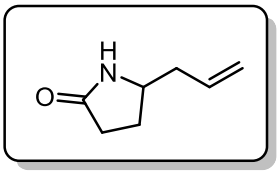
(d, *J* = 6.7 Hz, 3H), 0.90 (d, *J* = 6.8 Hz, 3H). ^{13}C NMR (151 MHz, $CDCl_3$) δ 178.3, 60.4, 33.5, 30.4, 24.8, 18.8, 18.1. **HRMS** (ESI) m/z calcd. for $C_7H_{13}NO$ $[M+H]^+$: 128.1070, found: 128.1077.

6-Vinylpiperidin-2-one –prepared using procedure B



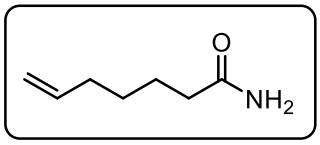
Colorless liquid (32%, 14: 1 *rr*);^{1}H NMR (600 MHz, $CDCl_3$) δ 5.79 (ddd, *J* = 16.9, 10.3, 6.5 Hz, 1H), 5.67 (s, 1H), 5.25 – 5.15 (m, 2H), 3.96 (q, *J* = 6.4, 6.0 Hz, 1H), 2.43 – 2.25 (m, 2H), 1.98 – 1.93 (m, 1H), 1.92 – 1.86 (m, 1H), 1.76 – 1.69 (m, 1H), 1.56 – 1.50 (m, 1H). ^{13}C NMR (151 MHz, $CDCl_3$) δ 172.1, 138.9, 116.1, 55.7, 31.3, 28.7, 19.1. **HRMS** (ESI) m/z calcd. for $C_7H_{11}NO$ $[M+H]^+$: 126.0913, found: 129.0918.

5-Allylpyrrolidin-2-one –prepared using procedure C



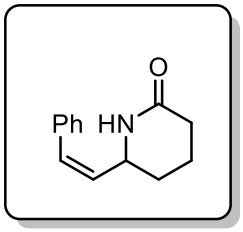
White solid (37%, >10: 1 *rr*);^{1}H NMR (600 MHz, $CDCl_3$) δ 5.75 (dtd, *J* = 17.6, 8.5, 6.2 Hz, 1H), 5.57 (s, 1H), 5.14 (d, *J* = 11.9 Hz, 2H), 3.71 (p, *J* = 6.5 Hz, 1H), 2.38 – 2.22 (m, 4H), 2.22 – 2.16 (m, 1H), 1.83 – 1.74 (m, 1H). **HRMS** (ESI) m/z calcd. for $C_7H_{11}NO$ $[M+H]^+$: 126.0913, found: 129.0920.

Hept-6-enamide



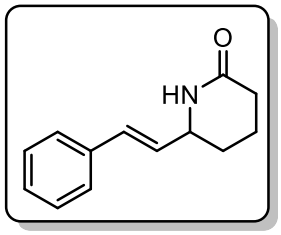
Yellow liquid; ^{1}H NMR (600 MHz, $CDCl_3$) δ 5.80 (ddt, *J* = 17.0, 10.2, 6.7 Hz, 1H), 5.39 (s, 2H), 5.06 – 4.93 (m, 2H), 2.24 (t, *J* = 7.6 Hz, 2H), 2.12 – 2.05 (m, 2H), 1.73 – 1.62 (m, 2H), 1.47 – 1.42 (m, 2H). ^{13}C NMR (151 MHz, $CDCl_3$) δ 175.3, 138.4, 114.8, 35.7, 33.4, 28.4, 25.0.

(*Z*)-6-Styrylpiperidin-2-one[92] –prepared using procedure B



White solid (60%, 20: 1 *rr*); ^{1}H NMR (400 MHz, $CDCl_3$) δ 7.37 – 7.35 (m, 2H), 7.31 – 7.30 (m, 1H), 7.23 – 7.16 (m, 2H), 6.61 (d, *J* = 11.4 Hz, 1H), 5.66 (s, 1H), 5.59 (dd, *J* = 11.5, 9.7 Hz, 1H), 4.41 (td, *J* = 9.7, 4.1 Hz, 1H), 2.46 – 2.25 (m, 2H), 2.03 – 1.90 (m, 2H), 1.74 (tdd, *J* = 13.1, 9.4, 4.0 Hz, 1H), 1.60 – 1.53 (m, 1H). ^{13}C NMR (151 MHz, $CDCl_3$) δ 171.9, 135.9, 132.1, 132.1, 128.6, 128.5, 127.6, 50.9, 31.1, 29.2, 19.9.

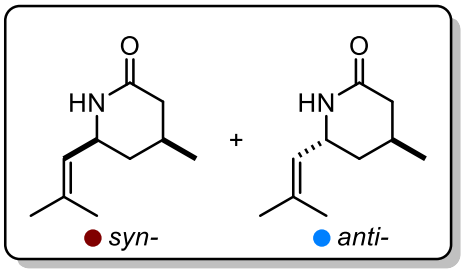
(*E*)-6-styrylpiperidin-2-one[92]–prepared using procedure B



White solid (60%, 20: 1 *rr*);^{1}H NMR (600 MHz, $CDCl_3$) δ 7.39 – 7.31 (m, 4H), 7.30 – 7.23 (m, 1H), 6.55 (d, *J* = 15.8 Hz, 1H), 6.13 (dd, *J* = 15.8, 7.1 Hz, 1H), 5.76 (s, 1H), 4.14 (q, *J* = 6.9 Hz, 1H), 2.47 – 2.31 (m, 2H), 2.05 – 1.99 (m, 1H), 1.98 – 1.89 (m, 1H), 1.80 – 1.74 (m,

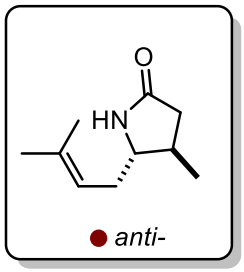
1H), 1.66 – 1.58 (m, 1H). ^{13}C NMR (151 MHz, $CDCl_3$) δ 172.1, 136.0, 131.4, 130.1, 128.7, 128.1, 126.5, 55.5, 31.3, 29.1, 19.2.

4-Methyl-6-(2-methylprop-1-en-1-yl)piperidin-2-one[92]–prepared using procedure B



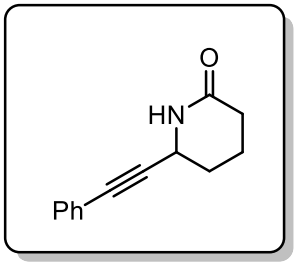
White solid (55%, >20: 1 *rr*); A 3:1 mixture of ***syn***- and ***anti***- isomers were obtained and the ratio was determined by ^{1}H NMR spectroscopic analysis of the reaction crude;^{1}H NMR (400 MHz, $CDCl_3$) δ 5.60 (s, 0.26H), 5.46 (s, 0.71H), 5.22 – 5.14 (dp, *J* = 9.0, 1.5 Hz, 0.22H), 5.02 (dp, *J* = 9.0, 1.5 Hz, 0.71H), 4.29 – 4.22 (m, 0.23H), 4.14 (m, 0.75H), 2.47 – 2.40 (m, 1H), 2.18 – 1.75 (m, 3H), 1.72 – 1.71 (m, 3H), 1.67 – 1.66 (m, 3H), 1.17 – 1.07 (m, 1H), δ 1.05 (d, *J* = 6.8 Hz, 0.70H), 1.02 (d, *J* = 6.2 Hz, 2.22H). ***anti***-^{13}C NMR (151 MHz, $CDCl_3$) δ171.8, 134.8, 126.2, 48.3, 39.0, 35.8, 29.7, 24.4, 20.3, 17.9. ***syn***- ^{13}C NMR (151 MHz, $CDCl_3$) δ 172.1, 135.9, 125.6, 51.3, 39.4, 37.9, 27.8, 25.7, 21.5, 18.0.

(±)-trans-4-Methyl-5-(3-methylbut-2-en-1-yl)pyrrolidin-2-one –prepared using procedure C



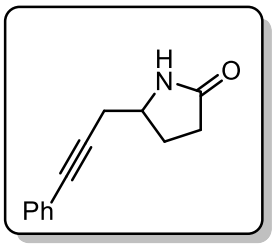
White solid (49%, >10: 1 *rr*); A 6: 1 mixture of ***anti***- and ***syn***-isomers were obtained and the ratio was determined by ^{1}H NMR spectroscopic analysis of the reaction crude; ^{1}H NMR (400 MHz, $CDCl_3$) δ 5.51 (s, 1H), 5.09 (t, *J* = 7.7 Hz, 1H), 3.18 (dt, *J* = 8.0, 5.4 Hz, 1H), 2.52 (dd, *J* = 16.6, 8.3 Hz, 1H), 2.28 – 2.18 (m, 1H), 2.20 – 2.06 (m, 2H), 2.07 – 1.94 (m, 1H), 1.72 (s, 3H), 1.63 (s, 3H), 1.13 (d, *J* = 6.7 Hz, 3H). ^{13}C NMR (101 MHz, $CDCl_3$) δ 176.9, 135.5, 119.5, 61.9, 38.8, 35.5, 33.8, 25.9, 18.9, 18.0. **HRMS** (ESI) m/z calcd. for $C_{10}H_{17}NO$ $[M+Na]^+$: 190.1202, found: 190.1211.

6-(Phenylethynyl)piperidin-2-one[92] –prepared using procedure B



White solid (40%, >20: 1 *rr*); ^{1}H NMR (600 MHz, $CDCl_3$) δ 7.44 – 7.38 (m, 2H), 7.36 – 7.28 (m, 3H), 5.99 (s, 1H), 4.52 – 4.50 (m, 1H), 2.48 – 2.34 (m, 2H), 2.15 – 2.06 (m, 2H), 2.03 – 1.91 (m, 1H), 1.86 – 1.79 (m, 1H). ^{13}C NMR (151 MHz, $CDCl_3$) δ 171.3, 131.7, 128.7, 128.4, 122.2, 87.8, 83.8, 45.2, 31.3, 29.2, 19.2.

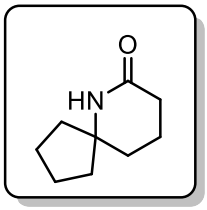
5-(3-Phenylprop-2-yn-1-yl)pyrrolidin-2-one –prepared using procedure C



White solid (50%, 1: 3 *rr*); ^{1}H NMR (600 MHz, $CDCl_3$) δ 7.40 – 7.37 (m, 2H), 7.33 – 7.28 (m, 3H), 5.47 (s, 1H), 4.02 – 3.80 (m, 1H), 2.65 (dd, *J* = 16.7, 5.3 Hz, 1H), 2.57 (dd, *J* = 16.7, 7.1 Hz, 1H), 2.39 – 2.35 (m, 1H), 2.15 – 2.12 (m, 2H), 1.75 – 1.70 (m, 1H). ^{13}C NMR (151 MHz, $CDCl_3$) δ 177.7, 131.6, 128.4, 128.2, 122.9, 85.2, 82.9, 53.2, 29.9, 27.5, 26.5.

HRMS (ESI) m/z calcd. for $C_{13}H_{13}NO$ $[M+Na]^+$: 222.0889, found: 222.0894.

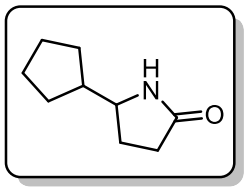
6-Azaspiro[4.5]decan-7-one –prepared using procedure B



White solid (50%, 7: 1 *rr*); ^{1}H NMR (400 MHz, $CDCl_3$) δ 5.88 (s, 1H), 2.34 (t, *J* = 6.6 Hz, 2H), 1.87 – 1.77 (m, 2H), 1.79 – 1.60 (m,

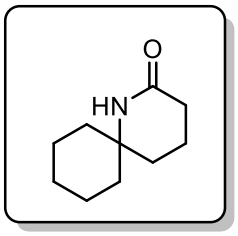
10H). ^{13}C NMR (151 MHz, $CDCl_3$) δ 171.8, 63.5, 40.5, 33.6, 31.2, 23.0, 18.6. **HRMS** (ESI) m/z calcd. for $C_9H_{15}NO$ $[M+Na]^+$: 176.1046, found: 176.1050.

5-Cyclopentylpyrrolidin-2-one –prepared using procedure C



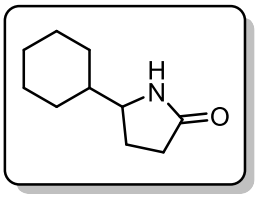
White solid (43%, >10: 1 *rr*); ^{1}H NMR (400 MHz, $CDCl_3$) δ 6.21 (s, 1H), 3.45 (q, *J* = 7.2 Hz, 1H), 2.36 – 2.29 (m, 2H), 2.28 – 2.15 (m, 1H), 1.95 – 1.73 (m, 4H), 1.71 – 1.50 (m, 4H), 1.25 – 1.09 (m, 2H). ^{13}C NMR (151 MHz, $CDCl_3$) δ 178.4, 59.4, 46.1, 30.4, 29.8, 28.8, 26.5, 25.5, 25.3. **HRMS** (ESI) m/z calcd. for $C_9H_{15}NO$ $[M+Na]^+$: 176.1046, found: 176.1056.

1-Azaspiro[5.5]undecan-2-one –prepared using procedure B



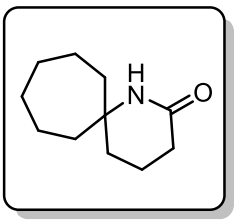
White solid (57%, 5: 1 *rr*); ^{1}H NMR (600 MHz, $CDCl_3$) δ 5.92 (s, 1H), 2.33 (t, *J* = 6.6 Hz, 2H), 1.84 – 1.75 (m, 2H), 1.74 – 1.65 (m, 4H), 1.56 – 1.51 (m, 6H), 1.45 – 1.40 (m, 2H). ^{13}C NMR (151 MHz, $CDCl_3$) δ 172.0, 54.0, 39.0, 26.3, 25.8, 25.8, 25.4, 25.0, 21.9, 17.0. **HRMS** (ESI) m/z calcd. for $C_{10}H_{17}NO$ $[M+Na]^+$: 190.1202, found: 190.1205.

5-Cyclohexylpyrrolidin-2-one –prepared using procedure C



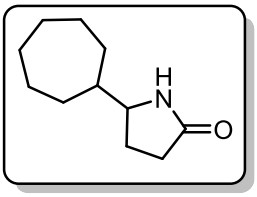
White solid (47%, >10: 1 *rr*); ^{1}H NMR (400 MHz, $CDCl_3$) δ 5.96 (s, 1H), 3.37 (q, *J* = 7.0 Hz, 1H), 2.31 (dd, *J* = 9.4, 7.2 Hz, 2H), 2.18 (dq, *J* = 12.7, 7.3 Hz, 1H), 1.87 – 1.66 (m, 6H), 1.37 – 1.08 (m, 4H), 1.05 – 0.83 (m, 2H). ^{13}C NMR (151 MHz, $CDCl_3$) δ 178.3, 59.5, 43.4, 30.3, 29.4, 28.7, 26.3, 25.8, 25.8, 25.0. **HRMS** (ESI) m/z calcd. for $C_{10}H_{17}NO$ $[M+Na]^+$: 190.1202, found: 190.1214.

1-Azaspiro[5.6]dodecan-2-one –prepared using procedure B



White solid (45%, 6: 1 *rr*); ^{1}H NMR (400 MHz, Methylene Chloride-d_2) δ 5.73 (s, 1H), 2.14 (t, *J* = 6.6 Hz, 2H), 1.70 – 1.60 (m, 4H), 1.58 – 1.51 (m, 4H), 1.50 – 1.28 (m, 8H). ^{13}C NMR (101 MHz, CD_2Cl_2) δ 171.4, 58.0, 42.5, 34.6, 30.4, 28.8, 28.4, 27.2, 27.0, 22.7, 17.7. **HRMS** (ESI) m/z calcd. for $C_{11}H_{19}NO$ $[M+Na]^+$: 204.1359, found: 204.1366.

5-Cycloheptylpyrrolidin-2-one –prepared using procedure C



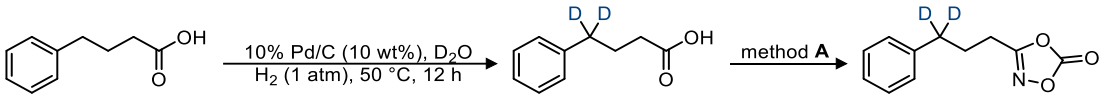
White solid (46%, >10: 1 *rr*); ^{1}H NMR (600 MHz, $CDCl_3$) δ 5.98 (s, 1H), 3.51 (q, *J* = 6.9 Hz, 1H), 2.36 – 2.28 (m, 2H), 2.17 (dq, *J* = 14.4, 7.4 Hz, 1H), 1.83 – 1.75 (m, 1H), 1.70 – 1.65 (m, 2H),

1.63 – 1.36 (m, 7H), 1.28 – 1.15 (m, 3H).^{13}C NMR (151 MHz, $CDCl_3$) δ 178.3, 59.7, 44.5, 30.7, 30.4, 29.5, 28.4, 27.9, 26.8, 26.6, 24.7. **HRMS** (ESI) m/z calcd. for $C_{11}H_{19}NO$ $[M+Na]^+$: 204.1359, found: 204.1368.

3.6.5. Mechanistic Studies

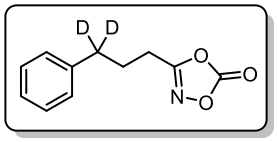
3.6.5.1 Kinetic Isotope Effect Study

Preparation of 3-(3-phenylpropyl)-1,4,2-dioxazol-5-one-d$_2$ (1a-*d$_2$*-1)[41]



To a round bottom flask equipped with a magnetic stir bar, a solution of 4-phenylbutyric acid (1.5 mmol, 246 mg), Pd/C (10 wt% of the substrate, 24.6 mg) in D_2O (3 mL) was stirred under H_2 atmosphere for 12 h at 50 °C. The reaction mixture was then cooled to room temperature and Et_2O (20 mL) was then added, and the resultant mixture was filtered through a pad of Celite. The filtrate was then extracted with Et_2O (20 mL × 2) and the combined organic layer was dried over $MgSO_4$ and concentrated under vacuo and purified by flash chromatography (eluent: 85:15 DCM/Acetone) to give the corresponding deuterated product in 84% yield.[41, 101] The deuterated acid was subsequently converted to the corresponding dioxazolone **1a-*d$_2$*-1** using general method **A** in 66% yield.

3-(3-Phenylpropyl)-1,4,2-dioxazol-5-one-d$_2$ (1a-*d$_2$*-1)

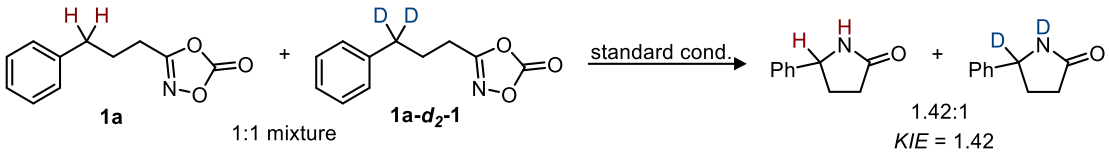


^{1}H NMR (400 MHz, $CDCl_3$) δ 7.36 – 7.27 (m, 2H), 7.27 – 7.18 (m, 1H), 7.21 – 7.14 (m, 2H), 2.62 (t, *J* = 7.5 Hz, 2H), 2.05 (t,

J = 7.5 Hz, 2H). ^{13}C NMR (101 MHz, $CDCl_3$) δ 166.6, 154.2, 139.9, 128.8, 128.6, 126.7, 25.9, 24.1.

Intermolecular KIE experiment

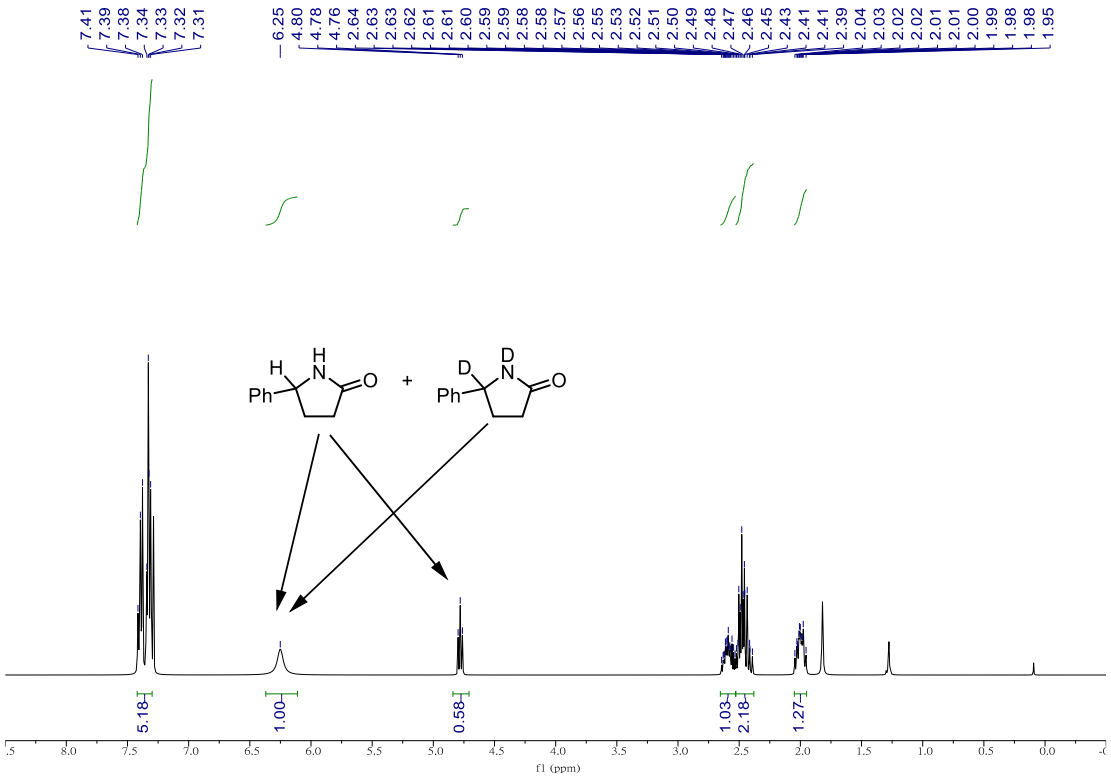
KIE experiment (competitive)



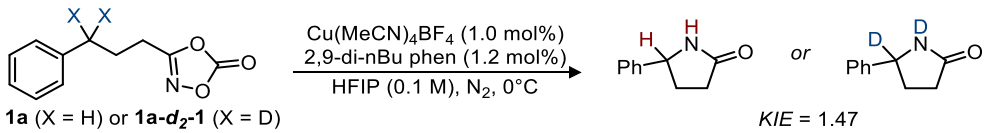
Procedures: In a glovebox, $[Cu(MeCN)_4]BF_4$ (2.5 mol%), 2,9-di-*n*Bu-phenanthroline (3.0 mol%) and HFIP (1.0 mL) were added to an oven-dried 8 mL vial. The resultant mixture was stirred at room temperature for 2 min and a solution of 3-(3-phenylpropyl)-1,4,2-dioxazol-5-one **1a** (20.6 mg, 0.1 mmol) and 3-(3-phenylpropyl-3,3-d_2)-1,4,2-dioxazol-5-one **1a-*d*$_2$-1** (20.7 mg, 0.1 mmol) in HFIP (1.0 mL) was added to the vial. The reaction mixture was allowed to stir at room temperature for 1 hour (<30% conv.), monitored by ^{1}H NMR, the C–H amidation product was isolated. ^{1}H NMR analysis showed that a ratio **2a:2a-*d*$_2$-1** of 1.42:1. (Both **2a** and **2a-*d*$_2$-1** have the same signal at 6.25 ppm while only **2a** has the signal at 4.78 ppm)

Summary of intermolecular kinetic isotope effect and error analysis

	Repeat 1	Repeat 2	Repeat 3	Average	Stdev
KIE value	1.44	1.42	1.40	1.42	±0.02


7.41
7.39
7.38
7.34
7.33
7.32
7.31
6.25
4.80
4.78
4.76
2.64
2.63
2.63
2.62
2.61
2.61
2.60
2.59
2.59
2.58
2.58
2.57
2.56
2.55
2.53
2.52
2.51
2.50
2.49
2.48
2.47
2.46
2.45
2.43
2.41
2.41
2.39
2.04
2.03
2.02
2.02
2.01
2.01
2.00
1.99
1.98
1.98
1.95
H
N
O
Ph
+
D
N
O
Ph
5.18
1.00
0.58
1.03
2.18
1.27
f1 (ppm)

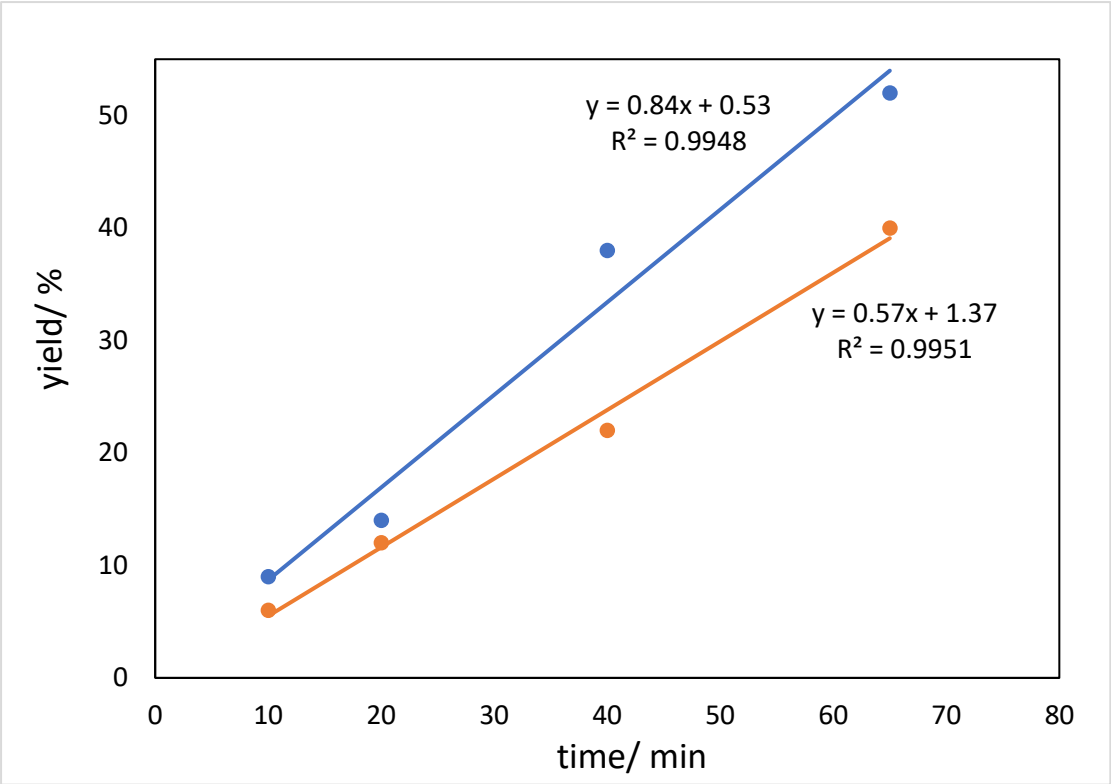
KIE experiment (non-competitive)



1a (X = H) or **1a-*d*$_2$-1** (X = D)

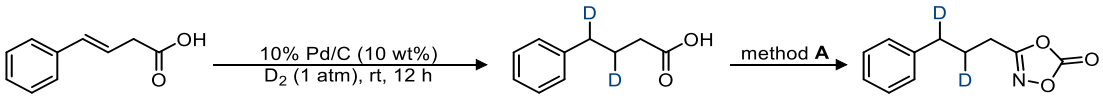
KIE = 1.47

Procedures: **1a** and **1a-*d*$_2$-1** were separated as individual reactions. In a glovebox, [Cu(MeCN)$_4$]BF$_4$ (1.0 mol%), 2,9-di-*n*Bu-phenanthroline (1.2 mol%), $Cl_2CHCHCl_2$ (10.6 mL, 0.1 mmol) and HFIP (1.0 mL) were added to an oven-dried 8 mL vial. The resultant mixture was stirred at room temperature for 2 min and a solution of **1a** (20.6 mg, 0.1 mmol) or **1a-*d*$_2$-1** (20.7 mg, 0.1 mmol) in HFIP (1.0 mL) was added to the vial. The reaction mixture was allowed to stir at 0 °C. Aliquots were taken at time intervals as indicated in the figure below. The aliquot was analyzed by ^{1}H NMR for the formation of C–H amidation product.



Intramolecular KIE experiment

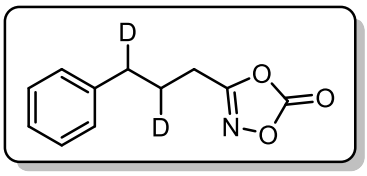
Preparation of 3-(3-phenylpropyl)-1,4,2-dioxazol-5-one-d$_2$ (1a-*d*$_2$-2)[66i]



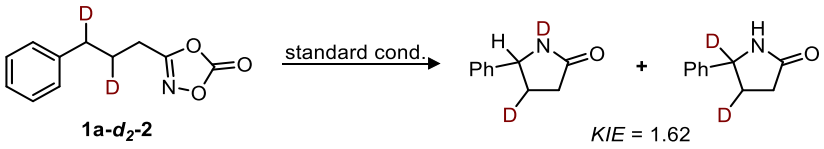
To a round bottom flask equipped with a magnetic stir bar, a solution of (*E*)-4-phenylbut-3-enoic acid (1.5 mmol, 243 mg), Pd/C (10 wt% of the substrate, 24.3 mg) in MeOH (5 mL) was stirred under D_2 atmosphere for 12 hours at room temperature. After 12 hours, the resultant mixture was filtered through a pad of Celite. The filtrate was then extracted with Et_2O (20 mL × 2) and the combined organic layer was dried over $MgSO_4$ and concentrated under vacuo and purified by flash chromatography (eluent: 85:15 DCM/Acetone) to give the corresponding deuterated product in 79%

yield. The deuterated acid was subsequently converted to the corresponding dioxazolone **1a-*d*$_2$-2** using general method **A** in 57% yield.

3-(3-Phenylpropyl)-1,4,2-dioxazol-5-one-d$_2$ (1a-*d*$_2$-2)



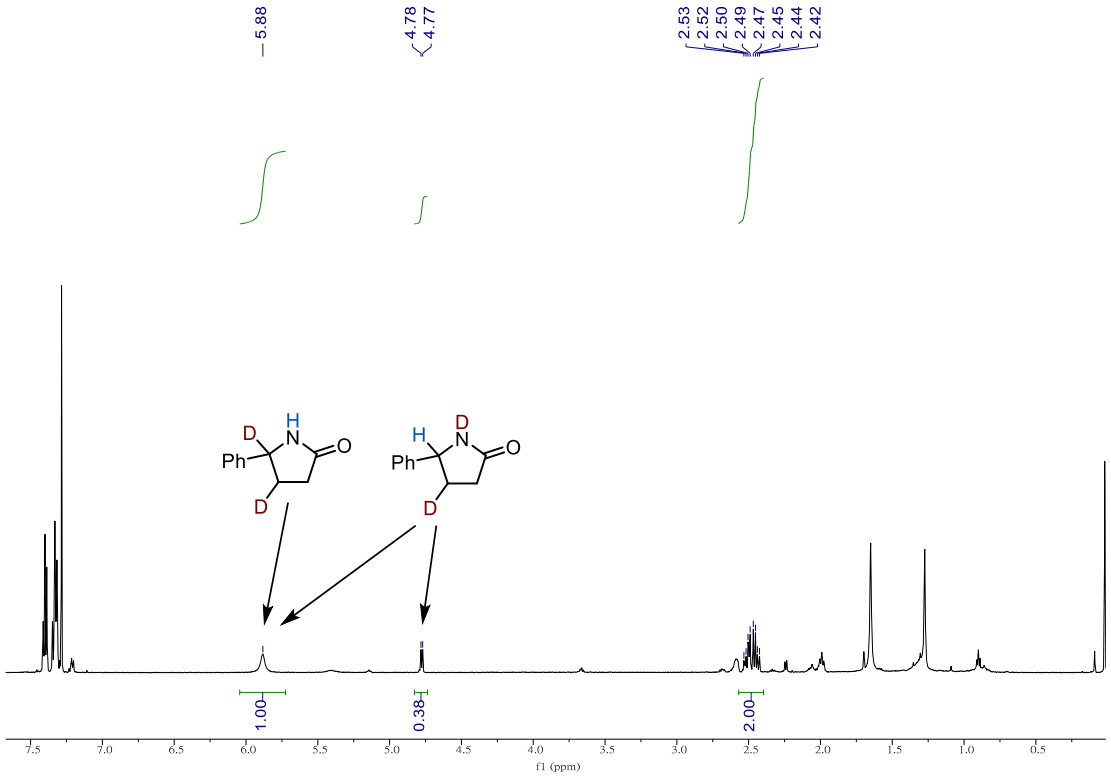
^{1}H NMR (400 MHz, $CDCl_3$) δ 7.34 (t, *J* = 7.3 Hz, 2H), 7.24 (m, 3H), 2.76 (m, 1H), 2.64 (d, *J* = 7.4 Hz, 2H), 2.13 – 1.99 (m, 1H).^{13}C NMR (101 MHz, $CDCl_3$) δ 166.6, 154.2, 139.9, 128.8, 128.6, 126.7, 34.6–34.1 (m), 26.0–25.4 (m), 24.1.



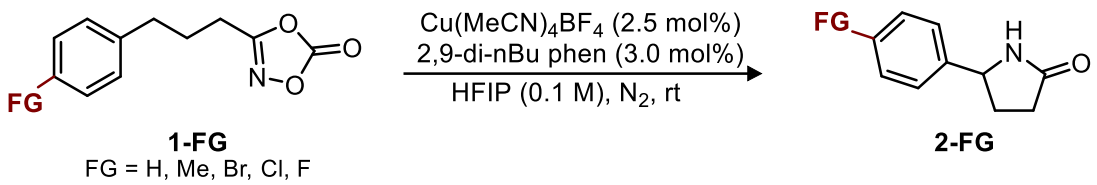
Procedures: In a glovebox, $[Cu(MeCN)_4]BF_4$ (2.5 mol%), 2,9-di-*n*Bu-phenanthroline (3.0 mol%) and HFIP (1.0 mL) were added to an oven-dried 8 mL vial. The resultant mixture was stirred at room temperature for 2 min and a solution of **1a-*d*$_2$-2** (20.7 mg, 0.1 mmol) in HFIP (1.0 mL) was added to the vial. The reaction mixture was allowed to stir at room temperature for 1 hour (<30% conv.), monitored by ^{1}H NMR, the C–H amidation product was isolated. KIE value (P_H/P_D = 1.62 ±0.005) was determined by the ratio of C–H inserted product to C–D inserted product.

Summary of intramolecular kinetic isotope effect and error analysis

	Repeat 1	Repeat 2	Repeat 3	Average	Stdev
KIE value	1.62	1.63	1.62	1.62	±0.005



3.6.5.2 Hammett Correlation Study



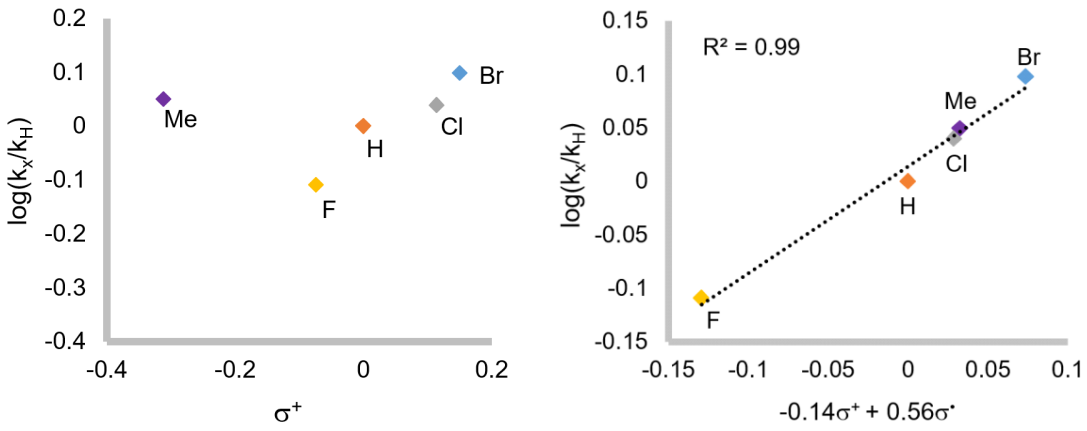
1-FG
FG = H, Me, Br, Cl, F

2-FG

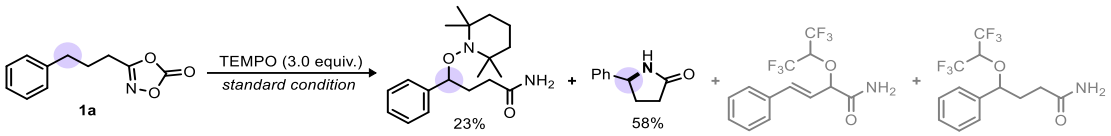
Procedure: In a glovebox, $[Cu(MeCN)_4]BF_4$ (2.5 mol%), 2,9-di-*n*Bu-phenanthroline (3.0 mol%) and HFIP (1.0 mL) were added to an oven-dried 8 mL vial. The resultant mixture was stirred at room temperature for 2 min and a solution of *para*-substitued-1,4,2-dioxazol-5-one **1-FG** (0.2 mmol) in HFIP (1.0 mL) was added to the vial. The reaction mixture was allowed to stir at room temperature for 25 min. The reaction mixture was then quenched with silica and subjected to a short-packed column with silica gel (ethyl acetate: n-hexane = 1:1 as eluent) to afford a crude mixture. The mixture was then analyzed with ^1H NMR, with CH_2Br_2 as internal standard to calculate the substrate conversion. The reactions were run in triplicate and, an average value of conversion was obtained. The initial rate k_{FG}/k_H was given by the substrate conversion (FG)/ substrate conversion(H) and Hammett substituent constant (log k_{FG}/k_H vs σ^+) was plotted. A non-linear curve was obtained. This result indicates that the spin-delocalization effect should exist.[102] A multiple linear regression for the dual-parameter equation were employed and gives the values of σ^+ and $\sigma^\bullet$ of -0.14 and 0.56 respectively.

$$\log \frac{k_{FG}}{k_H} = \rho^{+}\sigma^{+} + \rho^{\bullet}\sigma^{\bullet}$$

entry	FG	σ^{+}	$\sigma^{\bullet}$	conversion	k_{FG}/k_H	$\log (k_{FG}/k_H)$
1	Me	-0.311	-0.02	43	1.12	0.0491
2	H	0	0	38	1.00	0
3	Cl	0.114	0.08	41	1.09	0.0390
4	F	-0.073	-0.25	30	0.78	-0.1098
5	Br	0.15	0.17	48	1.25	0.0975

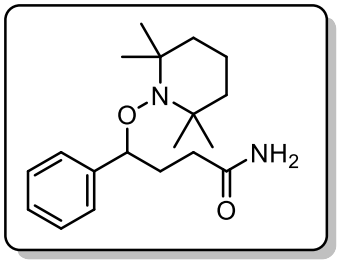


3.6.5.3 Radical Trapping Experiment



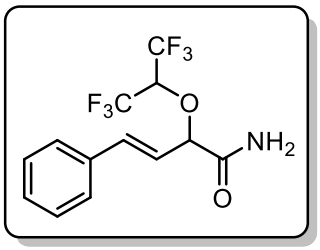
Procedure: In a glovebox, $[Cu(MeCN)_4]BF_4$ (2.5 mol%), 2,9-di-*n*Bu-phenanthroline (3.0 mol%) and HFIP (1.0 mL) were added to an oven-dried 8 mL vial. The resultant mixture was stirred at room temperature for 2 min and a solution of **1a** (0.2 mmol) amd TEMPO (3.0 equiv.) in HFIP (1.0 mL) was added to the vial. The reaction mixture was allowed to stir at room temperature for 12 hours. After stirring at room temperature for 12 h, the reaction mixture was filtered through a pad of silica gel and washed with EtOAc (2 mL × 3). The filtrate was concerned under vacuum and purified by flash column chromatography (eluent: 8: 2 to 1: 1 Hexane/EtOAc).

4-Phenyl-4-((2,2,6,6-tetramethylpiperidin-1-yl)oxy)butanamide



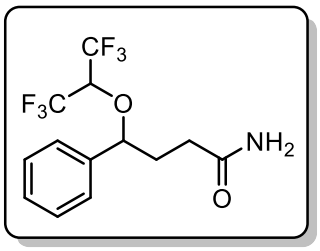
^{1}H NMR (600 MHz, $CDCl_3$) δ 7.33 – 7.30 (m, 2H), δ 7.30 – 7.28 (m, 2H), δ 7.28 – 7.25 (m, 1H), 5.20 (d, *J* = 20.9 Hz, 2H), 4.68 (dd, *J* = 9.5, 4.0 Hz, 1H), 2.46 – 2.41 (m, 1H), 2.28 – 2.11 (m, 1H), 2.03 – 1.91 (m, 2H), 1.48 (s, 3H), 1.32 – 1.29 (m, 6H), 1.17 (s, 3H), 1.00 (s, 3H), 0.57 (s, 3H). ^{13}C NMR (151 MHz, $CDCl_3$) δ 175.00, 142.65, 128.10, 127.63, 127.33, 86.25, 60.18, 59.76, 40.35, 34.38, 33.91, 31.58, 31.36, 20.40, 20.33, 17.14. **HRMS** (ESI) m/z calcd. for $C_{19}H_{30}N_2O_2$ $[M+H]^+$: 319.2380, found: 319.2382.

(*E*)-2-((1,1,1,3,3,3-Hexafluoropropan-2-yl)oxy)-4-phenylbut-3-enamide



^{1}H NMR (600 MHz, $CDCl_3$) δ 7.45 – 7.35 (m, 3H), 7.35 – 7.30 (m, 2H), 6.90 (dd, *J* = 15.4, 5.0 Hz, 1H), 6.19 (dd, *J* = 15.3, 1.7 Hz, 1H), 5.53 (d, *J* = 25.1 Hz, 2H), 5.36 – 5.32 (m, 1H), 4.10 (p, *J* = 5.9 Hz, 1H). ^{13}C NMR (151 MHz, $CDCl_3$) δ 166.31, 141.86, 137.69, 135.23, 129.81, 129.18, 128.20, 123.25, 83.14, 72.85, 72.64, 72.42, 72.23, 71.99. ^{19}F NMR (565 MHz, $CDCl_3$) -72.73 (q, *J* = 9.2 Hz), -73.45 (q, *J* = 9.2 Hz) **HRMS** (ESI) m/z calcd. for $C_{13}H_{11}F_6NO_2$ $[M+Na]^+$: 350.0592, found: 350.0593.

4-((1,1,1,3,3,3-Hexafluoropropan-2-yl)oxy)-4-phenylbutanamide



^{1}H NMR (600 MHz, $CDCl_3$) δ 7.45 – 7.35 (m, 3H), 7.35 – 7.30 (m, 2H), 5.41 (s, 1H), 4.74 (dd, *J* = 8.9, 4.6 Hz, 1H), 3.99 (p, *J* = 5.8 Hz, 1H), 2.41 – 2.34 (m, 2H), 2.26 (dq, *J* = 15.0, 7.8 Hz, 1H), 2.12 (dt, *J* = 13.9, 6.6 Hz, 1H). ^{13}C NMR (151 MHz, $CDCl_3$) δ 166.3, 141.9, 129.3, 128.9, 127.6, 123.2, 84.2, 72.9, 72.6, 72.4, 72.2, 72.0, 32.7, 31.3. ^{19}F NMR (565 MHz, $CDCl_3$) δ -72.34 (q, *J* = 9.3 Hz), -73.51 (q, *J* = 9.3 Hz).

HRMS (ESI) m/z calcd. for $C_{13}H_{13}F_6NO_2$ $[M+Na]^+$: 352.0748, found: 352.0746.

Chapter 4 Stereocontrolled γ-Lactams Synthesis by Copper-Nitrenoid Mediated Intramolecular Oxyamidation of Alkenes

4.1 Introduction

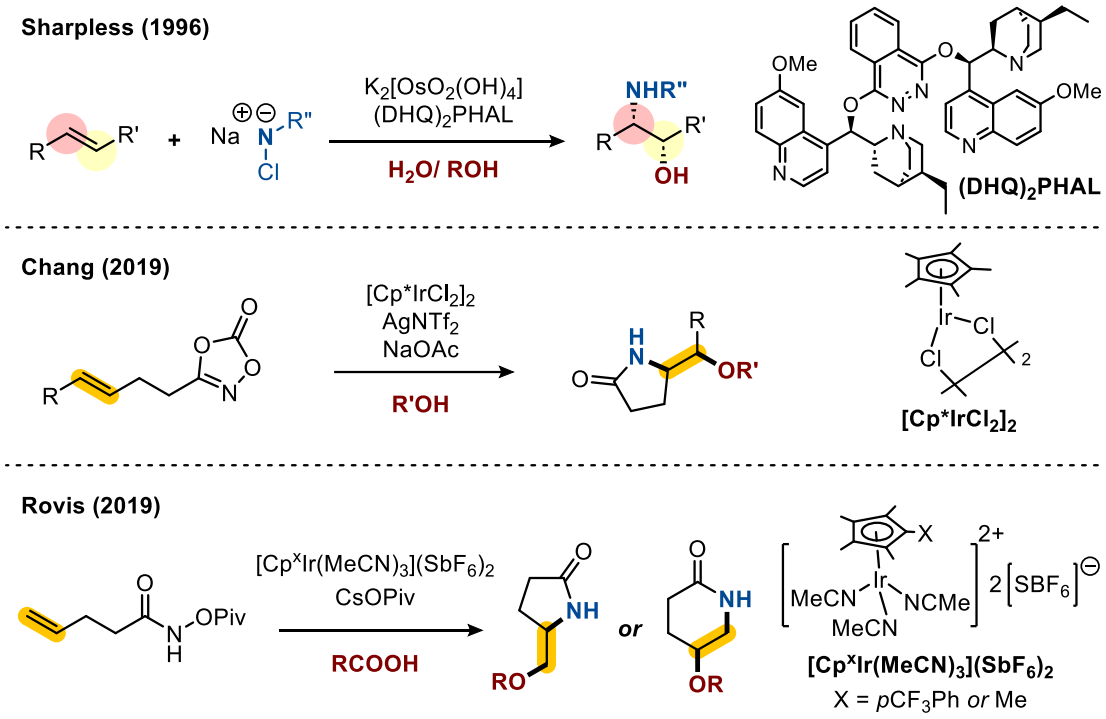
Regio- and stereocontrolled oxyamination of alkenes[103] offers a straightforward approach to access vicinal amino alcohols, which are widely abundant in biologically active natural products and pharmaceuticals.[81d, 104] The pioneering works by Sharpless in Os-catalyzed asymmetric aminohydroxylations have inspired an extensive effort in developing regio- and stereoselective alkene oxyaminations by other transition metal catalysts.[105]

In 2019, Chang developed the Cp*Ir-catalyzed stereocontrolled oxyamidation reaction of alkenyl 1,4,2-dixoazol-5-ones for the synthesis of lactams.[106] Computational studies revealed that the putative Ir-nitrenoid serves as 1,3-dipole to enable stereocontrolled *syn*-addition to the alkene analogous to (3+2) cycloaddition. In the same year, Rovis reported the Cp^XIr-catalyzed intramolecular regiodivergent oxyamination of alkenes to afford γ- and δ-lactams.[97d, 107] Assuming reactive Ir-nitrene intermediates, the regioselectivity is probably controlled by the electronically tunable cyclopentadienyl Ir(III) complexes via either *5-exo-trig* or *6-endo-trig* pathway. Indeed, several reports emerged concerning the catalytic synthesis of lactams and

oxazolidinones via *5-exo-trig* cyclization involving reactive metal-nitrene species of noble metals (Ag[37b], Ir[97d, 108], Os[109]).

As discussed earlier, ferrocenium $[Cp_2Fe(III)]^+$ complex can mediate intramolecular *5-exo-trig* nitrenoid cyclization to alkenes to afford γ-lactam. With benzoic acids as nucleophiles, effective oxyamidation of some alkenyl dioxazolones has been accomplished, albeit with poor stereocontrol manifested by equimolar of *threo*- and *erthyro*- isomers formation. Our computational study showed that the Fe(IV)-amidyl radical is the plausible intermediate for the oxyamidation reaction.[100] In the previous chapters, we showed that the Cu(I)-catalyzed decomposition of 1,4,2-dioxazol-5-ones would produce reactive Cu-amidyl radicals for regiocontrolled intramolecular 1,5 and 1,6-HAT reactions. Here we successfully extended the reaction scope of the Cu-amidyl radicals for stereocontrolled intramolecular oxyamidation of alkenes by harnessing the electrophilicity of the Cu-amidyl radicals for via *5-exo-trig* pathway.

Scheme 4.1 Examples of Transition-metal Catalyzed Alkene Oxyamidation



4.2 Results and Discussion

4.2.1 Reaction Development

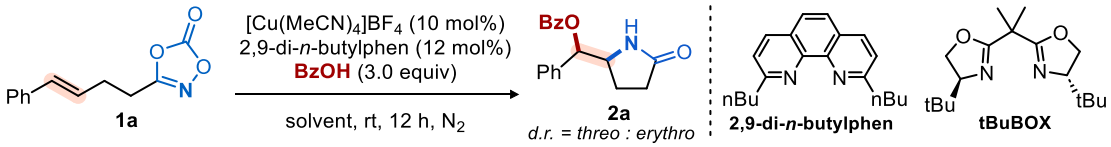
4.2.1.1 Cu-Catalyzed Oxyamidation of Alkenes for γ-Lactams Synthesis

Prompted by the successful development of the Cu-nitrene radical-mediated C–H amidation reaction in Chapter 3, we envisioned that facile interaction of the nitrene-centered SOMO with the alkene π-bonding can be exploited for regiocontrolled γ-lactam synthesis via *5-exo-trig* cyclization of allyl dioxazolones. We hypothesized that intramolecular electrophilic nitrene radical attack on the C=C bond should afford a carboradical intermediate. A subsequent radical polar crossover should generate a carbocation and proceed to nucleophilic functionalization.

We initiated our study with the use of (*E*)-3-(4-phenylbut-3-en-1-yl)-1,4,2-dioxazol-5-one **1a** and benzoic acid as model substrate. By treating dioxazolone **1a** (0.1 mmol) and benzoic acid (0.3 mmol) with $[Cu(MeCN)_4]BF_4$ (10.0 mol%) and 2,9-di-*n*-butylphenanthroline (12.0 mol%) at room temperature in DCM for 12 h afforded **2a** in 47% yield with 2: 1 *threo* versus *erthro* diastereoselectivity (Table 4.1, entry 1). Similar result was obtained in DCE as solvent (38%, 2: 1 *d.r.*; entry 2). No desired product was obtained in MeCN and PhCl as solvent (entries 3–4). Less satisfactory results were obtained in trifluorotoluene, toluene and TFE as solvent (entries 5–7). It is noteworthy that ca. 70% of 5-(phenyl(2,2,2-trifluoroethoxy)methyl)pyrrolidin-2-one (10: 1 *d.r.*)

was obtained indicating that the solvent would compete with the BzOH. Employing less nucleophilic HFIP as solvent affords **2a** in 80% yield (17: 1 *d.r.*) without significant competing solvent addition (entry 8). As expected, running the reactions without BzOH afforded the solvent adduct in 90% yield. The major diastereomer was assigned to be *threo*-configuration and confirmed by ^{1}H NMR and X-ray crystallographic analysis in agreement with the reported spectral data.[106a] After several trials, we found that the catalyst system with $[Cu(MeCN)_4]BF_4$ (10.0 mol%) and tBuBOX (12.0 mol%) furnished the desired five-membered lactam **4a** in 92% isolated yield with excellent *threo: erythro* selectivity (>20: 1).

Table 4.1 Effect of Solvents[a]



entry	solvent	yield of **2a** (%)[b]	d.r.[c]
1	DCM	47	2:1
2	DCE	38	2:1
3	MeCN	n.d.	-
4	PhCl	n.d.	-
5	$PhCF_3$	22	1:1
6	toluene	17	1.3:1
7	TFE	18	10:1
8	HFIP	80	17:1
9	HFIP	n.d.[d]	-
10[e]	**HFIP**	**96(92)**	**>20:1 (30% *ee*)**
11	HFIP:DCM 1:1	84(80)	>10:1

[a]Reaction conditions: **1a** (0.1 mmol), BzOH (3.0 equiv), Cu catalyst (10 mol%), and 2,9-di-*n*-butylphenanthroline (12 mol%) in solvent under N_2 for 12 hours at room temperature. [b]^{1}H NMR yield (internal standard: dibromomethane), isolated yield in parentheses. [c]d.r. were determined by ^{1}H NMR of the crude reaction mixture. [d]Reaction

run without Cu catalyst. [e]Reaction run with tBuBOX as ligand; *threo*-**2a** was enantioenriched with the use of the chiral ligand tBuBOX.

Figure 4.1 ^{1}H NMR Analysis (Reaction Crude) for Diastereomeric *threo*-Versus *erythro*-2a Oxylactams

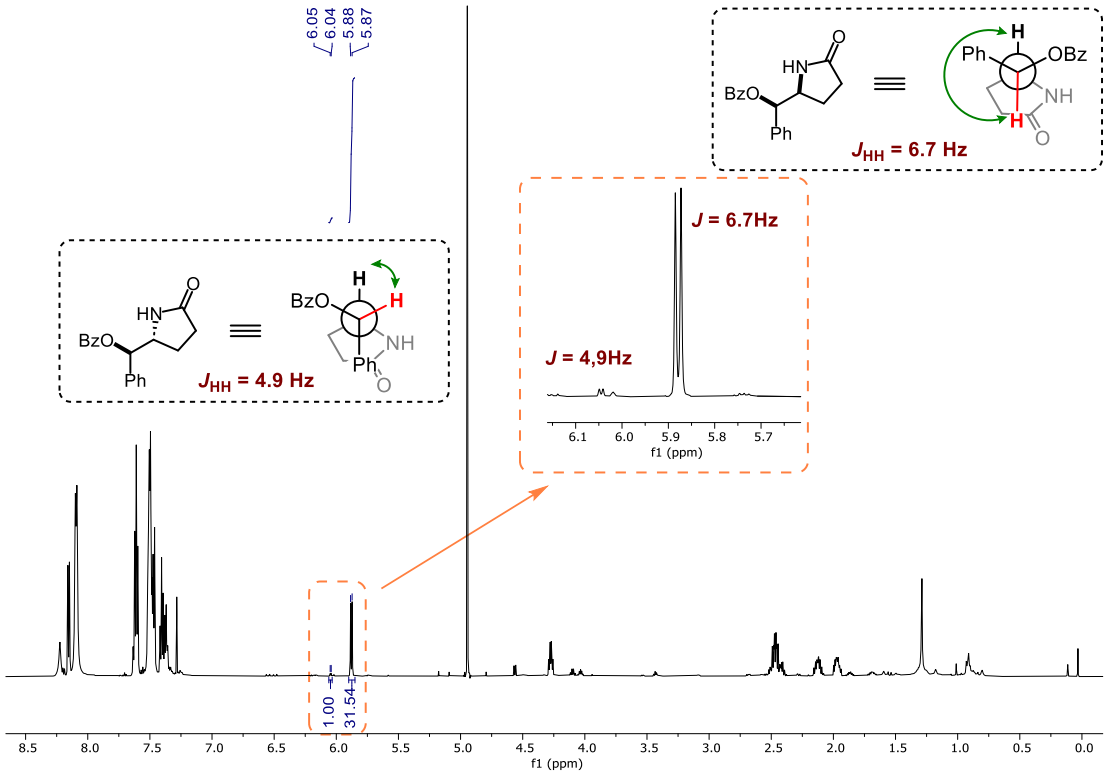
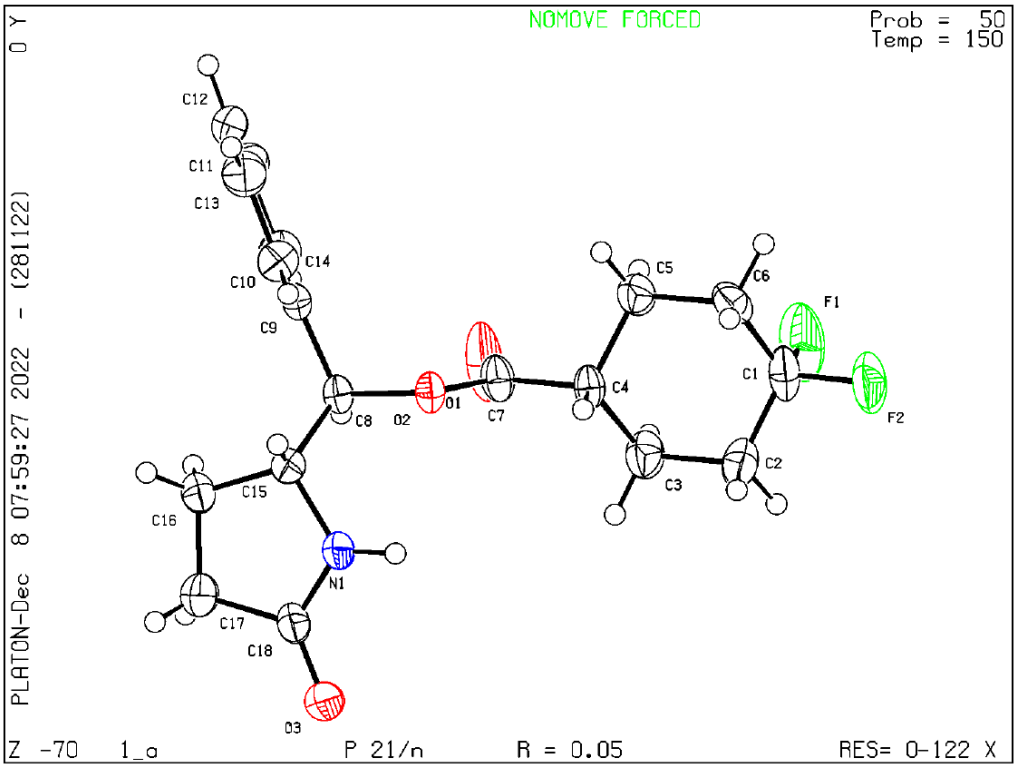


Figure 4.2 Molecular Structure of 2q (CCDC 2226006)



4.2.1.2 Substrate Scope Studies

Employing the standard reaction conditions: [$Cu(MeCN)_4BF_4$] (10 mol%), tBuBOX (12 mol%), and nucleophile (3.0 equiv) in HFIP, several dioxazolones bearing electron-releasing and -withdrawing para-substituents at the aryl moiety were smoothly converted to the corresponding *threo*-lactams (**2a** – **2d**) in good-to-excellent yields (76-96%) (Table 4.2). In all cases, excellent *threo*-selectivities (>20: 1) were registered. While the allyl dioxazolones bearing a naphthalene group gave **2e** in 80% yield with >20: 1 *d.r.*, the analogous reactions with the furan-substituted derivative afforded lactam **2f** in only 3: 1 *d.r.*

Without the carboxylic acid nucleophiles, the Cu-catalyzed lactamization of **1a** took place to afford the corresponding lactams **2g** – **2i** in >70% yields with solvent (e.g. HFIP, TFE, H_2O) adduct formation, albeit in less favorable diastereoselectivities. Next, we investigated the scope of carboxylic acid nucleophiles for the lactamization reaction. For instance, employing α-naphthyl acetic acid as nucleophile, the lactamization of **1a** proceeded to give the corresponding *threo*- **2j** in 74% yield with >10: 1 *d.r*. Likewise, the analogous reaction with *N*-phthalimidyl glycine effectively afforded the desired *threo*-lactam **2k** in 68% yield. Notably, facile coupling of some carboxylic acids containing strained carbocycles were also accomplished with the corresponding lactams (**2l – 2o**) being obtained in ca. 70% yields and >20: 1 diastereoselectivity. A

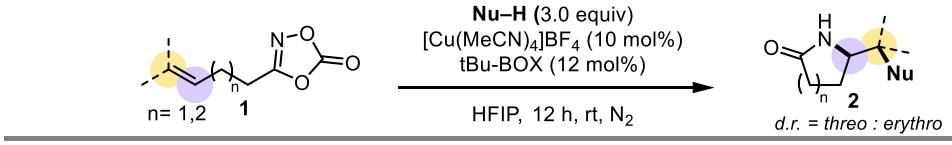
series of highly branched aliphatic carboxylic acids are effective coupling partners. For instance, the reactions of **1a** with adamantyl carboxylic acid and difluorocyclohexane carboxylic acid furnished the desired *threo*-lactams **2p** and **2q** in 52 and 64% yields respectively. Notably, carboxylic acid containing alkene such as cinnamic acid were tolerated under the standard conditions with the corresponding lactam **2r** being obtained in 70% yield. Nevertheless, alcohols nucleophile like phenol was successful coupling partners to afford the corresponding lactams (**2s**) with poor (*threo*: *erythro* = 1: 1.3) diastereoselectivity.

To assess the functional group tolerance, bioactive compounds such as indomethacin, fenbufen, gemfibofil, citronellic acid and lithocholic acid were reacted with **1a** under the Cu-catalyzed conditions, the corresponding *threo*-lactams **2t** – **2x** were furnished in 48–70% yields with >20: 1 diastereoselectivities (Table 4.3). While coupling of the carboxylic acids containing asymmetric carbon centers (e.g., lexoprofen and cholesterol) proceeded effectively to their γ-lactams **2y** and **2z** in 70–50% yields despite the rather poor diastereoselectivies.

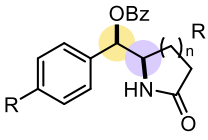
Having established the reaction conditions toward the γ-lactams synthesis, we anticipated that the Cu-amidyl radical intermediate should undergo facile *6-exo-trig* cyclization to form the δ-lactam. To our delight, when reacting the analogous (*E*)-3-(5-phenylpent-4-en-1-yl)-1,4,2-dioxazol-5-one **1a'** and benzoic acid (3.0 equiv) under our

optimized conditions afforded the corresponding δ-lactam **2a'** in 40%. By comparing the ^{1}H NMR spectral characteristics of the *threo*- (δ_H 5.76 ppm) and *erythro*- (δ_H 5.82 ppm) isomers, the diastereoselectivity (*threo*: *erythro*) >10:1 *d.r.* was registered. To showcase the generality of the δ-lactamization, we pursued the coupling reactions of **1a'**with a scope of nucleophiles (e.g. indomethacin, phenol etc). Under the standard conditions, the corresponding δ-lactams (**2g'**, **2s'**, **2t'**, **2u'** & **2x'**) were obtained in ca. 35% yield with good-to-less satisfactory diastereoselectivities (>10: 1 to 1: 1.3 *d.r.*).

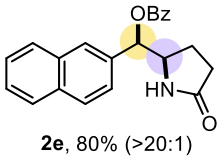
Table 4.2 Substrate Scope for the Cu-Catalyzed Intramolecular Alkene Oxyamidation via 5- and 6-exo trig Cyclization[a-c]



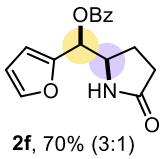
Variation of Dioxazolone (Nu–H = BzOH)



R = H, **2a**, 92% (>20:1) n=1; **2a′**, 40% (>10:1) n=2
OMe, **2b**, 96% (>20:1) *from E-alkene*; 94% (>10:1) *from Z-alkene*
Me, **2c**, 90% (>20:1)
Cl, **2d**, 76% (>20:1)

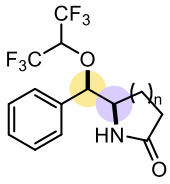


2e, 80% (>20:1)

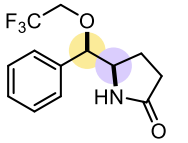


2f, 70% (3:1)

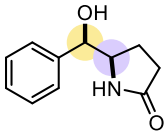
Variation of Nucleophile



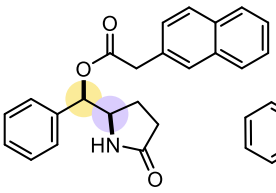
2g, n=1, 90%[d] (>20:1)
2g′, n=2, 70%[d] (5:1)



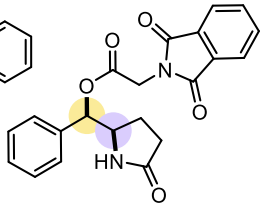
2h, 78%[d,e] (4.5:1)



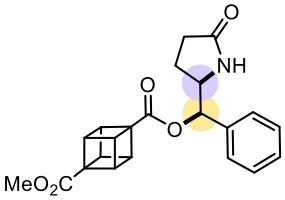
2i, 70%[d,f] (9:1)



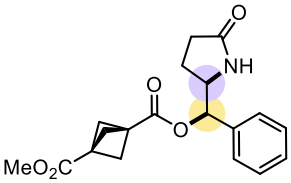
2j, 74% (>10:1)



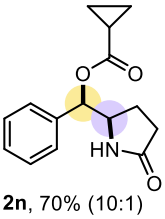
2k, 68% (10:1)



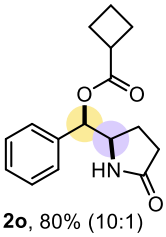
2l, 62% (>20:1)



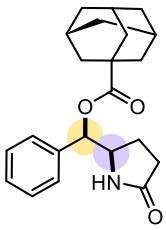
2m, 63% (>20:1)



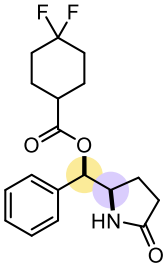
2n, 70% (10:1)



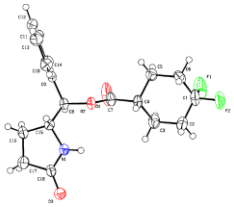
2o, 80% (10:1)

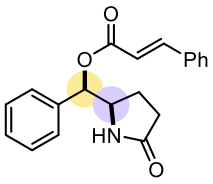


2p, 52% (>20:1)

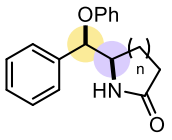


2q, 64% (>20:1)





2r, 70% (>20:1)

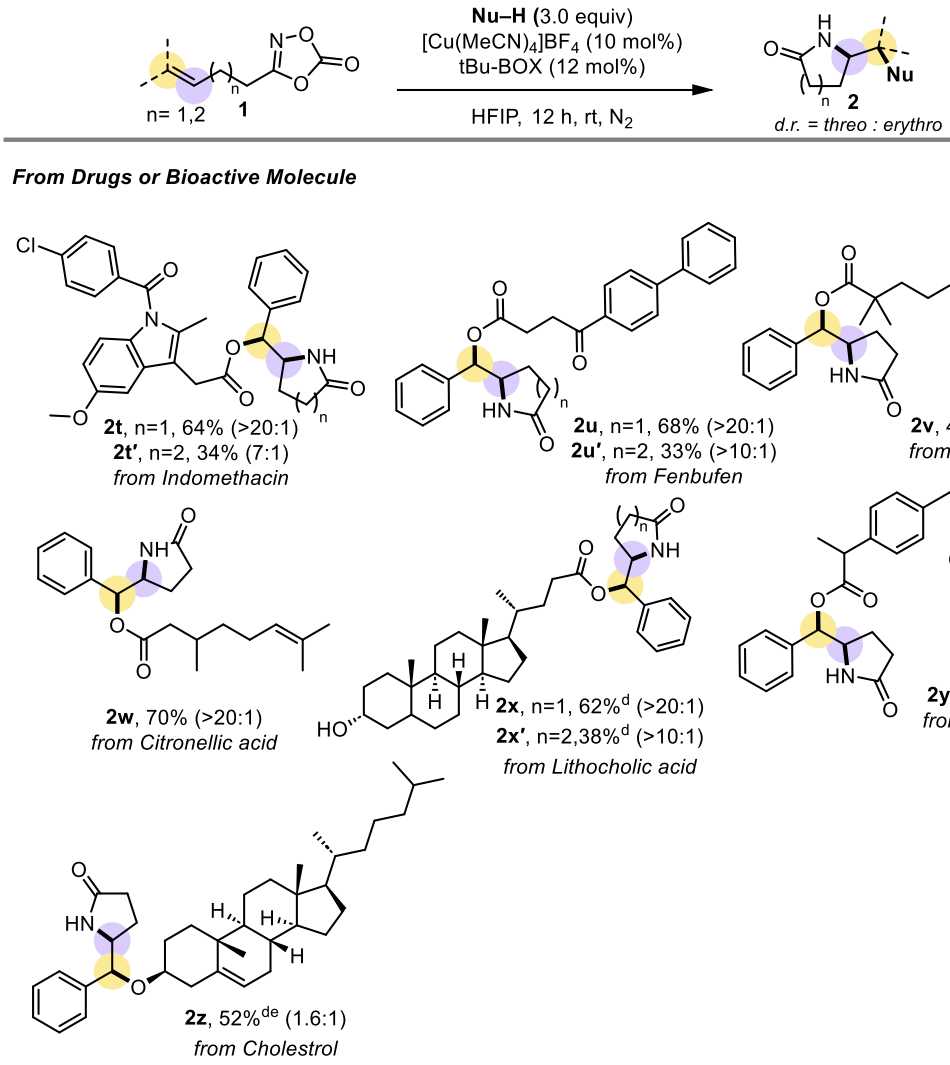


2s, n=1, 60%[g] (1:1.2)
2s′, n=2, 34% [g] (1:1.3)

[a]Reaction conditions: **1** (0.1 mmol), NuH (0.3 mmol), $[Cu(MeCN)_4]BF_4$ (10 mol%) and tBu-BOX (12 mol%) in HFIP under N_2 for 12 hours at room temperature. [b]Isolated yield. [c]d.r. were determined by ^1H NMR of the crude reaction mixture. [d]Run without

carboxylic acid. [e]TFE is used as solvent. [f]HFIP:H_2O (10:1) is used as solvent. [g]DCM is used as solvent.

Table 4.3 Substrate Scope for the Cu-Catalyzed Intramolecular Alkene Oxyamidation Involving Nucleophiles Derived from Bioactive Molecules[a-c]



[a]Reaction conditions: **1** (0.1 mmol), NuH (0.3 mmol), $[Cu(MeCN)_4]BF_4$ (10 mol%) and tBu-BOX (12 mol%) in HFIP under N_2 for 12 hours at room temperature. [b]Isolated yield. [c]d.r. were determined by ^1H NMR of the crude reaction mixture. [d]2,9-*n*-butylphenanthroline used as ligand. [e]DCM is used as solvent.

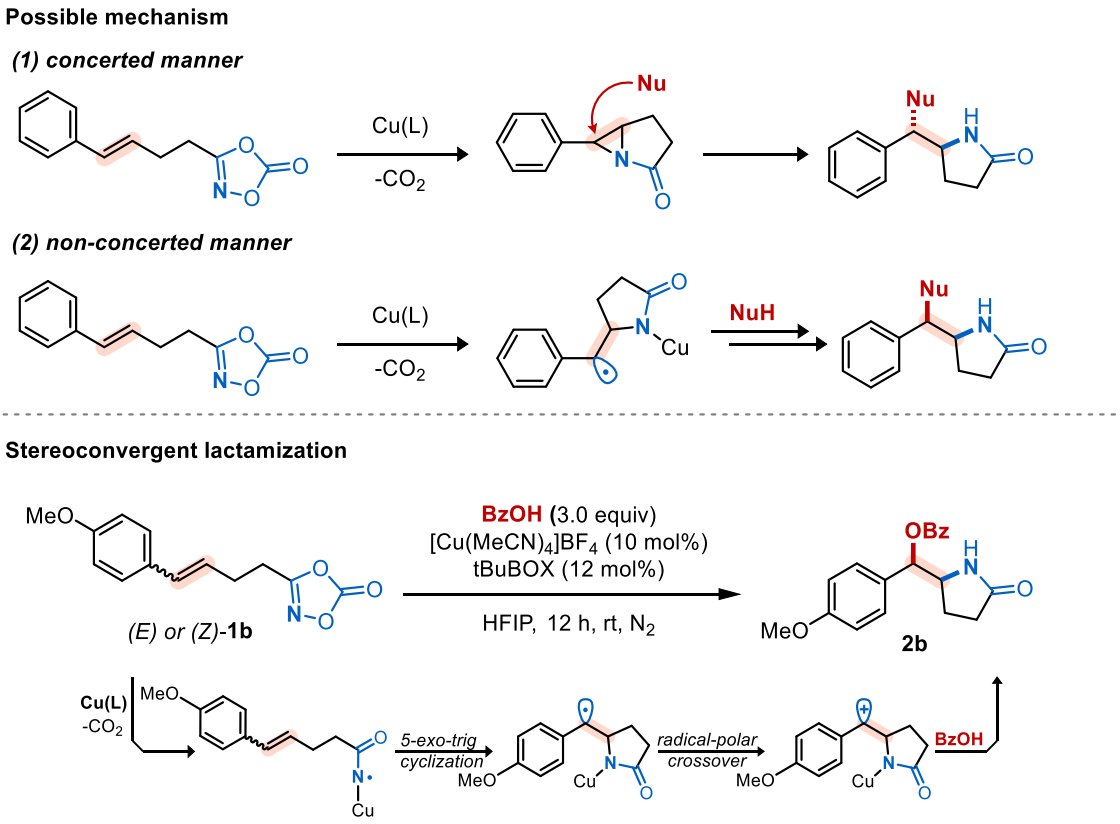
4.3 Mechanistic Studies

There are two possible pathways for the lactam formation (1) non-concerted pathway and (2) concerted aziridination followed by ring opening. Our previous study (Chapter 3) already showed that Cu-amidyl radical complex is the plausible intermediate when reacting the Cu(I) precursor with dioxazolones. Mechanistically, the *5-exo-trig* cyclization of the nitrene radical onto the alkene π-bond should produce an open-shell carboradical intermediate. The open-shell carboradical would undergo unhindered C–C rotation resulting in *cis*- and *trans* isomerization of the initial alkenes. As a result, both cis- and trams-alkenes should afford the same carboradicals after the electrophilic amidyl radical addition to the C–C π-bond, giving rise to the identical *γ*-lactam products in a stereoconvergent manner. As anticipated, the dioxazolones derived from *trans*- and *cis*-carboxylic acids reacted under the Cu-catalyzed conditions to furnish the identical *threo*-lactam **2b** in >90% yield. It was found that the lactamization of the (*Z*)-configured allyl dioxazolones **1b** gave slightly lower diastereoselectivity (>10: 1) compared to (*E*)-configured derivative (>20: 1).

A plausible mechanism using **1a** and benzoic acid as example was depicted in Figure 4.3. The reaction was initiated by a rate-limiting decarboxylation of dioxazolone to form the active Cu–amidyl radical species (**I**), followed by a rapid *5-exo-trig* cyclization to give the carboradical intermediate (**II**). Subsequent radical polar

crossover should generate the carbocation intermediate (**III**) which would attack by the benzoic acid to yield the γ-lactam product. Alternatively, the carboradical intermediate (**II**) may undergo radical displacement (radical reductive elimination) via **IV** to give the oxy-γ-lactam product.

Scheme 4.2 Possible Reaction Mechanism and Stereoconvergent Lactamization



Scheme 4.3 Proposed Transition State for the Diastereoselectivity Towards threo-Isomer

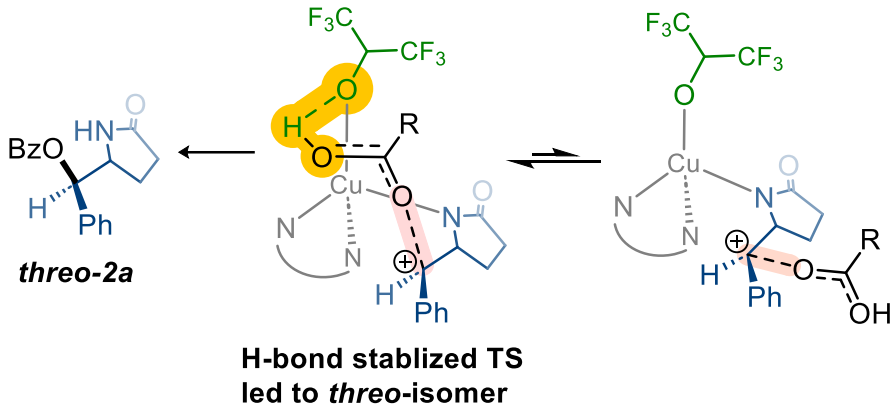
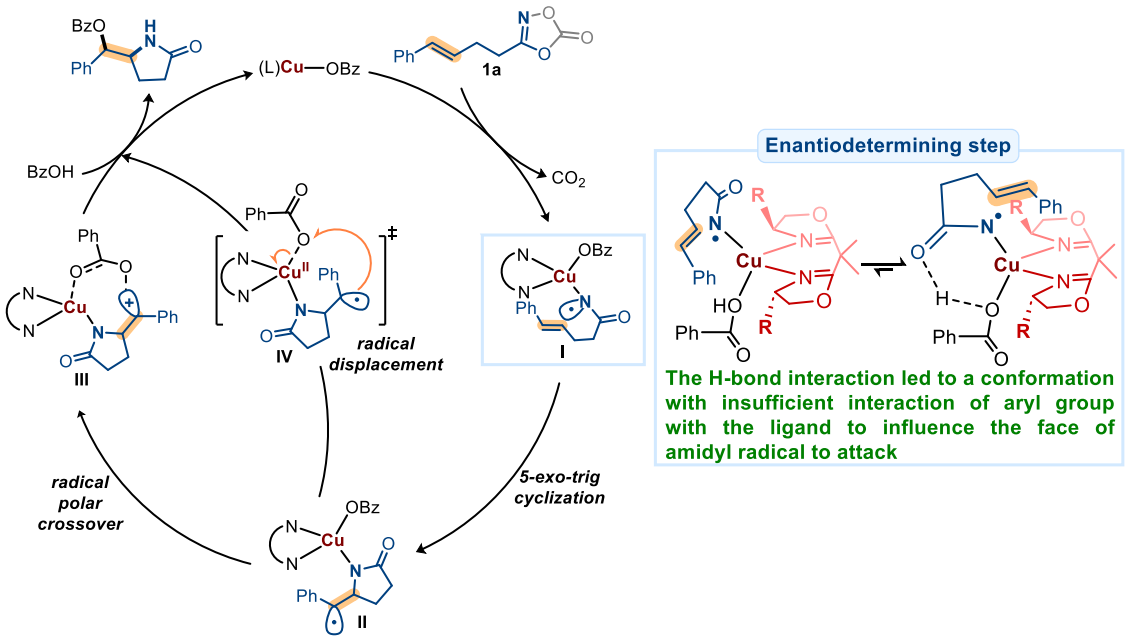


Figure 4.3 Plausible Mechanistic Cycle



4.4 Concluding Summary

In conclusion, a stereoselective copper-catalyzed intramolecular oxyamidation of alkenyl dioxazolones have been developed, and the *threo*-γ-lactams were obtained in excellent yield without significant Curtius-type rearrangement observed. Excellent diastereoselectivity of *threo*- isomers were obtained. The oxyamidation reaction has been extended to δ-lactams synthesis with remarkable diastereoselectivity. This study represents a new base metal-catalyzed C–N coupling for the easy transformation of olefin to lactams. The development of an enantio- and stereoselective catalytic oxyamidation is underway.

4.5 Experimental Section

4.5.1 General Experimental Section

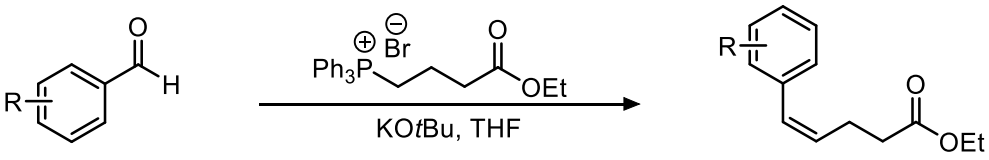
All the solvents and reagents were obtained from commercial sources and used without purification unless stated otherwise. HFIP was dried with activated 3Å molecular sieves (heated at 500 °C before use) and stored in a sealed tube with N_2 protection. All glassware was dried overnight at 150 °C prior to use. Analytical thin layer chromatography (TLC) was performed on precoated silica gel plates with aluminum backing. Preparative TLC was performed on 20 × 20 cm precoated silica gel with layer thickness of 0.5 mm. Visualization on TLC was achieved using UV light (254 nm) or treatment with an aqueous potassium permanganate solution followed by heating. Flash column chromatography was performed on a silica gel (Merck, 230-400 mesh) column. ^{1}H and ^{13}C NMR spectra were recorded on a Brüker DPX-400 MHz spectrometer or Brüker DPX-600 MHz spectrometer. The chemical shift (δ) values were given in ppm and are referenced to residual solvent peaks; carbon multiplicities were determined by DEPT-135 experiments. Coupling constants (*J*) were reported in hertz (Hz). The NMR yields were determined using dibromomethane or 1,1,2,2-tetrachloroethane as internal standard. Mass spectra and high-resolution mass spectra (HRMS) were obtained on a VG MICROMASS Fison VG platform, a Finnigan Model Mat 95 ST instrument, or a Bruker APEX 47e FT-ICR mass spectrometer. Single Crystal Data collection was

performed by a Bruker-AXS diffractometer (see crystallographic section for details). The structure was solved by SHELXT and refined by the full-matrix least-squares (SHELXL) method.

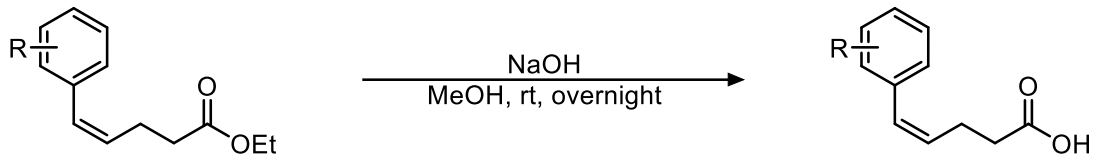
High performance liquid chromatography analyses were performed on an Agilent 1100 series HPLC equipped with a Chiralcel® OD-H *or* IC column (4.6 mm φ × 250 mmL) (UV detection at 210, 230, 250, 254 and 280 nm).

4.5.2 Experimental Procedures and Physical Characterization

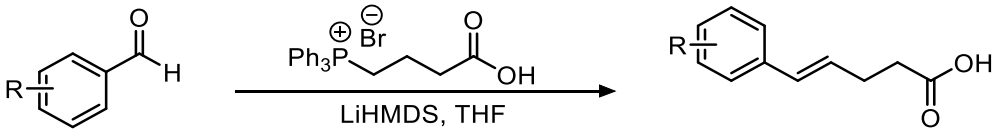
4.5.2.1 General Procedure for the Preparation of Alkenoic Acids[110]



A mixture of (4-ethoxy-4-oxobutyl)triphenylphosphonium bromide (4.3 g, 9.5 mmol) and potassium tert-butoxide (1.1 g, 9.5 mmol) in THF (20 mL) was stirred at 0 ℃ for 30 min. The resulting mixture was sirred at room temperature for an additional 1 hour. The solution was again cooled to 0 °C, and 4-substituted-benzaldehyde (7.9 mmol) was added dropwise. The solution was stirred at room temperature for 5 hours. The reaction mixture was quenched with H_2O, and then the aqueous layers were extracted with Et_2O (20 mL×3). The organic layers were washed with brine, dried over Na_2SO_4, and concentrated *in vacuo* followed by flash Column chromatography to afford ethyl (*Z*)-5-(4-substituted-phenyl)pent-4-enoatein.



A mixture of ethyl (*Z*)-5-(4-substituted-phenyl)pent-4-enoatein (2 mmol) and NaOH (0.2 g, 5 mmol) in MeOH (20 mL) was stirred at room temperature overnight. The reaction mixture was concentrated *in vacuo*. H_2O (50 mL) was added to the reaction mixture and the aqueous layer was extracted with EtOAc (3 x 15 mL). The remaining aqueous layer was acidified to pH 2 using HCl (1.0 M). The acidified aqueous layer was further extracted with ethyl acetate (3 x 20 mL). The combined organic extracts were dried with $MgSO_4$ and concentrated *in vacuo* to give the crude carboxylic acid, which was used for next step without further purification.

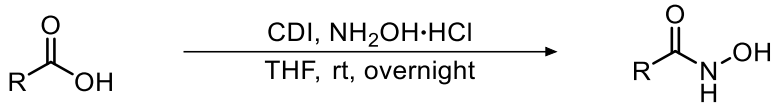


(3-carboxypropyl)triphenylphosphonium bromide (10.8 mmol, 1.08 equiv) was first suspended in THF (40 mL) at -20 °C. LiHMDS (20.16 mmol, 2.16 equiv) was added into the suspension in a dropwise manner and further stirred for 20 min. The mixture was then cooled to -78 °C and the corresponding aldehyde (10 mmol, 1.0 equiv) was added in dropwise. After stirring for 18 hours, H_2O (80 mL) was added to the reaction mixture and extracted with ethyl acetate (3 x 20 mL). The remaining aqueous layer was acidified to pH 2 using HCl (1.0 M). The acidified aqueous layer was further extracted with ethyl acetate (3 x 20 mL). The combined organic extracts were dried with $MgSO_4$

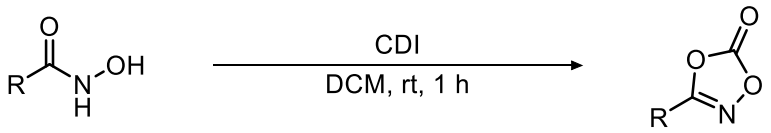
and concentrated *in vacuo*. The reaction crude was purified by flash chromatography (n-hexane/EtOAc = 1:1) to obtain corresponding (*E*)-alkenoic acid.

4.5.2.2 General Procedure for the Preparation of 1,4,2-Dioxazol-5-ones[41, 66i, 100]

Method A:



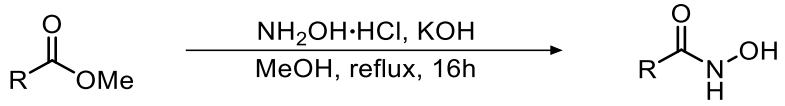
To a round bottom flask equipped with a magnetic stir bar, a solution of corresponding carboxylic acids (2 mmol) in dry THF (20 mL) was added. CDI (3 mmol) was then added to the solution, and the resulting mixture was stirred at room temperature. After stirring for 1 h, hydroxylamine hydrochloride (4 mmol) was added to the reaction mixture. The resulting mixture was then stirred at room temperature overnight and quenched by 5% $KHSO_4$(aq) (20 mL). The aqueous layer was extracted with EtOAc (3 x 20 mL). The combined organic extracts were dried over $MgSO_4$ and concentrated by rotary evaporation to obtain the corresponding hydroxamic acid for use without further purification.



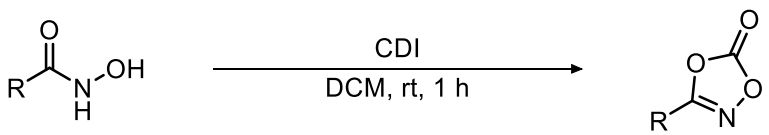
The crude hydroxamic acid and CDI (1.1 equiv) were dissolved in DCM (20 mL) and was stirred at room temperature for 1 h. The mixture was quenched with 1 M HCl

(20 mL), and the aqueous layer was extracted with DCM (3 x 10 mL). The combined organic extracts were dried over $MgSO_4$ and concentrated by rotary evaporation. The crude mixture was purified by flash chromatography (n-hexane/EtOAc = 10:1 to 8:2) to obtain corresponding 1,4,2-dioxazol-5-ones.

Method B:



To a round bottom flask equipped with a magnetic stir bar, a solution of corresponding ester (2.0 mmol) in dry MeOH (20 mL) was added. KOH (12.0 mmol) and hydroxylamine hydrochloride (6.0 mmol) were then added to the solution, and the resulting mixture was stirred under reflux and an N_2 atmosphere for 16 h. The reaction mixture was then cooled to room temperature and acidified with 1 N HCL to pH 4. The resultant liquid was then extracted with EtOAc (10 mL x 3). The combined organic layer was dried over $MgSO_4$ and concentrated by rotary evaporation to obtain the corresponding hydroxamic acid for use without further purification.

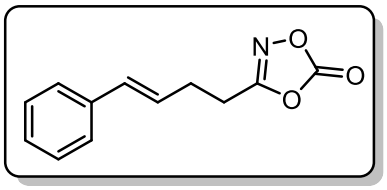


The crude hydroxamic acid and CDI (1.1 equiv) were dissolved in DCM (20 mL) and was stirred at room temperature for 1 h. The mixture was quenched with 1 M HCl

(20 mL), and the aqueous layer was extracted with DCM (3 x 10 mL). The combined organic extracts were dried over $MgSO_4$ and concentrated by rotary evaporation. The crude mixture was purified by flash chromatography (n-hexane/EtOAc = 10:1 to 8:2) to obtain corresponding 1,4,2-dioxazol-5-ones.

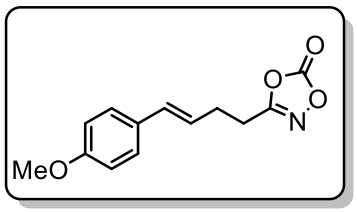
4.5.2.3 Physical Characterization of Substrates

(*E*)-3-(4-Phenylbut-3-en-1-yl)-1,4,2-dioxazol-5-one[106a]



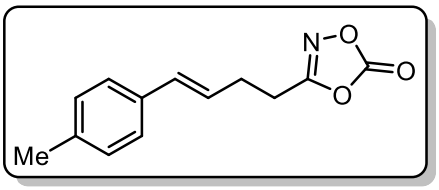
Prepared according to method **A**. White solid (78%); ^{1}H NMR (400 MHz, $CDCl_3$) δ 7.39 – 7.21 (m, 5H), 6.51 (d, *J* = 15.8 Hz, 1H), 6.17 (dt, *J* = 15.8, 6.9 Hz, 1H), 2.81 (t, *J* = 7.4 Hz, 2H), 2.64 (q, *J* = 7.5 Hz, 2H). ^{13}C NMR (151 MHz, $CDCl_3$) δ 166.0, 154.1, 136.6, 132.9, 128.7, 127.8, 126.3, 125.6, 27.8, 24.9.

(*E*)-3-(4-(4-Methoxyphenyl)but-3-en-1-yl)-1,4,2-dioxazol-5-one[106a]



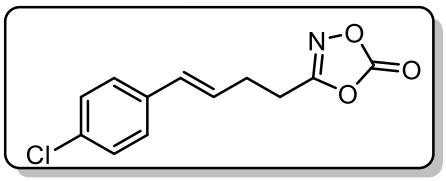
Prepared according to method **A**. White solid (88%); ^{1}H NMR (400 MHz, $CDCl_3$) δ 7.27 (d, *J* = 8.8 Hz, 2H), 6.84 (d, *J* = 8.8 Hz, 2H), 6.43 (d, *J* = 15.8 Hz, 1H), 6.00 (dt, *J* = 15.7, 6.9 Hz, 1H), 3.80 (s, 3H), 2.79 (t, *J* = 7.4 Hz, 2H), 2.61 (q, *J* = 7.1 Hz, 2H). ^{13}C NMR (101 MHz, $CDCl_3$) δ 166.2, 159.5, 154.3, 132.4, 129.5, 127.5, 123.4, 114.2, 55.5, 28.0, 25.2.

(*E*)-3-(4-(4-Methylphenyl)but-3-en-1-yl)-1,4,2-dioxazol-5-one[106a]



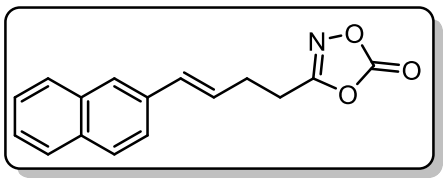
Prepared according to method **A**. White solid (80%);^{1}H NMR (400 MHz, Chloroform-*d*) δ 7.25 (d, *J* = 8.0 Hz, 2H), 7.13 (d, *J* = 7.8 Hz, 2H), 6.48 (d, *J* = 15.8 Hz, 1H), 6.11 (dt, *J* = 16.0, 6.9 Hz, 1H), 2.82 (t, *J* = 7.3 Hz, 2H), 2.64 (q, *J* = 7.2 Hz, 2H), 2.34 (s, 3H). ^{13}C NMR (151 MHz, $CDCl_3$) δ 166.1, 154.1, 137.6, 133.8, 132.7, 129.4, 126.2, 124.6, 27.8, 25.0, 21.2.

(*E*)-3-(4-(4-Chlorophenyl)but-3-en-1-yl)-1,4,2-dioxazol-5-one[106a]



Prepared according to method **A**. White solid (83%); ^{1}H NMR (400 MHz, CD_2Cl_2) δ 7.31 (s, 4H), 6.49 (d, *J* = 15.8 Hz, 1H), 6.20 (dt, *J* = 15.8, 6.9 Hz, 1H), 2.83 (t, *J* = 7.3 Hz, 2H), 2.64 (q, *J* = 7.2 Hz, 2H). ^{13}C NMR (101 MHz, $CDCl_3$) δ 165.9, 154.0, 135.1, 133.4, 131.7, 128.8, 127.5, 126.3, 27.7, 24.8.

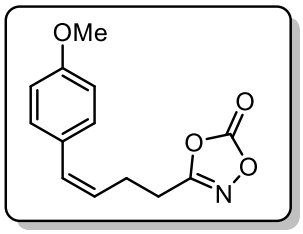
(*E*)-3-(4-(Naphthalen-2-yl)but-3-en-1-yl)-1,4,2-dioxazol-5-one[106a]



Prepared according to method **A**. White solid (88%);^{1}H NMR (600 MHz, $CDCl_3$) δ 7.86 – 7.78 (m, 3H), 7.72 (d, *J* = 1.8 Hz, 1H), 7.58 (dd, *J* = 8.5, 1.7 Hz, 1H), 7.52 – 7.43 (m, 2H),

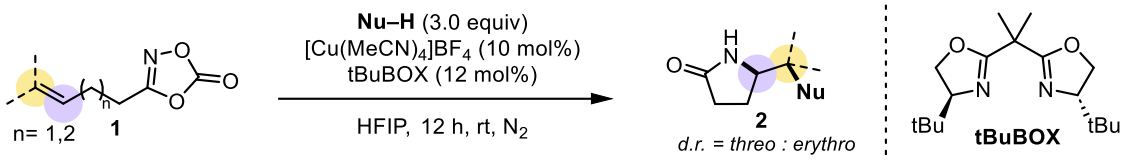
6.69 (d, *J* = 15.8 Hz, 1H), 6.32 (dt, *J* = 15.7, 6.9 Hz, 1H), 2.89 (t, *J* = 7.4 Hz, 2H), 2.73 (q, *J* = 7.3, 6.9 Hz, 2H). ^{13}C NMR (101 MHz, $CDCl_3$) δ 166.0, 154.1, 134.0, 133.6, 133.0, 133.0, 128.3, 127.80, 127.7, 126.4, 126.2, 126.0, 125.9, 123.3, 27.9, 25.0.

(*Z*)-3-(4-(4-Methoxyphenyl)but-3-en-1-yl)-1,4,2-dioxazol-5-one[100]



Prepared according to method **B**. Yellow liquid (72%); ^{1}H NMR (400 MHz, $CDCl_3$) δ 7.16 (d, *J* = 8.7 Hz, 2H), 6.90 – 6.81 (d, *J* = 8.7 Hz, 2H), 6.49 (d, *J* = 11.4 Hz, 1H), 5.53 – 5.42 (m, 1H), 3.79 (s, 3H), 2.76 – 2.64 (m, 4H). ^{13}C NMR (101 MHz, $CDCl_3$) δ 166.1, 158.8, 154.1, 131.4, 129.9, 129.1, 126.1, 113.9, 55.3, 25.1, 23.5.

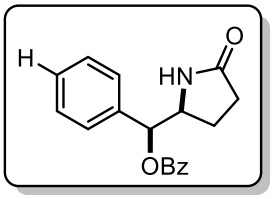
4.5.3 Experimental Procedure for Cu(I)-Catalyzed Oxyamidation



General procedure: All reactions were performed in glovebox under N_2. Cu catalyst (10 mol%) and ligand (12 mol%) were added to an oven-dried 8 mL vial equipped with a magnetic stir bar. Solvent (2 mL) was added, and the mixture was stirred at room temperature for 1-3 min. 1,4,2-Dioxazol-5-one **1** (0.1 mmol) and nucleophile (3.0 equiv) were added to the mixture, and the vial was capped. The reaction was stirred under the indicated time and temperature. Afterward, the reaction mixture was filtered through a pad of silica gel and washed with EtOAc (2 mL × 3). The filtrate was concentrated under vacuum, and the residue was purified by flash column chromatography (eluent: 10:10:1 Hexane/EtOAc/MeOH *or* 100:1:0.1 EtOAc/MeOH/NH_3) to obtain the desired product.

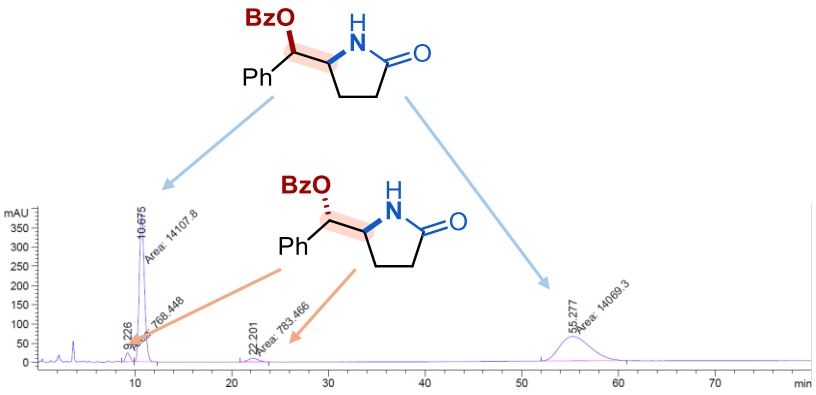
4.5.4 Physical Characterization of Products

threo-(5-Oxopyrrolidin-2-yl)(phenyl)methyl benzoate[100]



White solid (92%); ^{1}H NMR (400 MHz, $CDCl_3$); δ 8.06 (d, *J* = 7.32 Hz, 2H), 7.59 – 7.52 (m, 1H), 7.46 – 7.30 (m, 7H), 6.55 (s, 1H), 5.82 (d, *J* = 6.7 Hz, 1H), 4.12 (q, *J* = 4.92 Hz, 1H), 2.37 – 2.15 (m, 2H), 2.11 – 2.02 (m, 1H), 1.94 – 1.85 (m, 1H); ^{13}C NMR (100 MHz, $CDCl_3$); δ 178.5, 165.6, 136.9, 133.6, 129.9, 129.8, 129.0, 128.9, 128.7, 126.9, 79.1, 58.2, 29.9, 23.6.

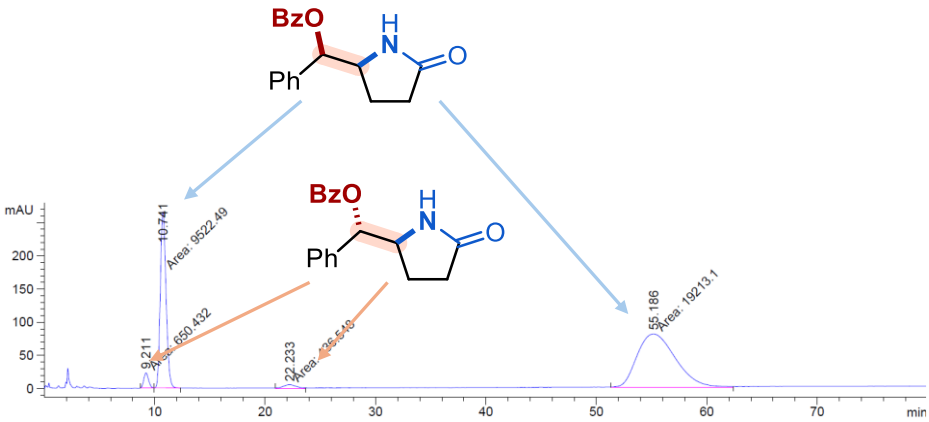
chiral compound



Signal 1: DAD1 C, Sig=210,8 Ref=360,100

Peak #	RetTime [min]	Type	Width [min]	Area [mAU*s]	Height [mAU]	Area %
1	9.226	MM	0.5459	768.44757	23.46008	2.5848
2	10.675	MM	0.6114	1.41078e4	384.60641	47.4546
3	22.201	MM	1.3145	783.46613	9.93401	2.6354
4	55.277	MM	3.6936	1.40693e4	63.48514	47.3252

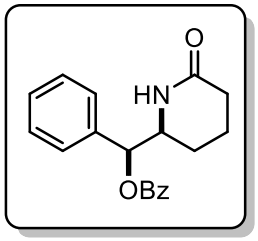
racemic compound



Signal 1: DAD1 C, Sig=210,8 Ref=360,100

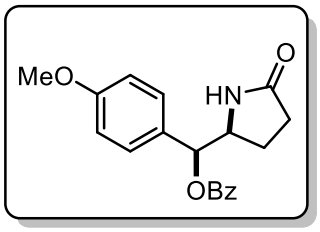
Peak #	RetTime [min]	Type	Width [min]	Area [mAU*s]	Height [mAU]	Area %
1	9.211	MM	0.4878	650.43170	22.22198	2.1810
2	10.741	MM	0.5988	9522.49121	265.04199	31.9305
3	22.233	MM	1.3701	436.54785	5.31049	1.4638
4	55.186	MM	3.9973	1.92131e4	80.10825	64.4247

***threo*- (6-Oxopiperidin-2-yl)(phenyl)methyl benzoate**



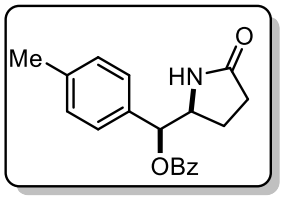
Yellow solid (40%); ^{1}H NMR (400 MHz, $CDCl_3$) δ 8.10 – 8.02 (m, 2H), 7.64 – 7.55 (m, 1H), 7.46 (t, *J* = 7.8 Hz, 2H), 7.44 – 7.34 (m, 4H), 7.37 – 7.25 (m, 1H), 6.16 (s, 1H), 5.76 (d, *J* = 8.1 Hz, 1H), 3.90 (td, *J* = 8.1, 4.5 Hz, 1H), 2.49 – 2.22 (m, 2H), 1.98 – 1.79 (m, 1H), 1.76 – 1.59 (m, 2H), 1.52 – 1.38 (m, 1H). ^{13}C NMR (151 MHz, $CDCl_3$) δ 172.1, 165.4, 136.7, 133.6, 129.7, 129.5, 129.0, 129.0, 128.6, 126.9, 79.5, 56.6, 31.5, 25.1, 19.6. **HRMS** (ESI) m/z calcd. for $C_{19}H_{19}NO_3$ $[M+Na]^+$: 332.1257, found: 332.1267.

***threo*-(4-Methoxyphenyl)(5-oxopyrrolidin-2-yl)methyl benzoate[100]**



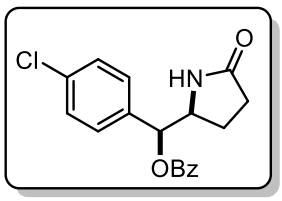
White solid (96%); ^{1}H NMR (400 MHz, $CDCl_3$); δ 8.06 (d, *J* = 7.4 Hz, 2H), 7.56 (t, *J* = 7.4 Hz, 1H), 7.44 (t, *J* = 7.7 Hz, 2H), 7.34 (d, *J* = 8.6 Hz, 2H), 6.88 (d, *J* = 8.6 Hz, 2H), 6.58 (s, 1H), 5.76 (d, *J* = 7.2 Hz, 1H), 4.13 (q, *J* = 7.3 Hz, 1H), 3.77 (s, 3H), 2.35 – 2.21 (m, 2H), 2.12 – 1.98 (m, 1H), 2.05 – 1.81 (m, 1H); ^{13}C NMR (100 MHz, $CDCl_3$); δ 178.4, 165.6, 160.0, 133.5, 129.9, 128.9, 128.7, 128.4, 114.4, 79.1, 58.1, 55.4, 29.8, 23.5.

***threo*-(5-Oxopyrrolidin-2-yl)(p-tolyl)methyl benzoate[100]**



White solid (90%); ^{1}H NMR (600 MHz, $CDCl_3$); δ 8.08 (d, *J* = 7.4 Hz, 2H), 7.60 (t, *J* = 7.5 Hz, 1H), 7.48 (t, *J* = 7.7 Hz, 2H), 7.32 (d, *J* = 7.8 Hz, 2H), 7.20 (d, *J* = 7.8 Hz, 2H), 6.34 (s, 1H), 5.83 (d, *J* = 6.8 Hz, 1H), 4.16 (td, *J* = 7.5, 5.1 Hz, 1H), 2.41 – 2.29 (m, 5H), 2.17 – 2.07 (m, 1H), 1.94 (ddt, *J* = 13.9, 10.0, 5.7 Hz, 1H); ^{13}C NMR (151 MHz, $CDCl_3$); δ 178.2, 165.4, 138.7, 133.7, 133.4, 129.7, 129.6, 128.6, 126.7, 79.0, 58.1, 29.7, 23.5, 21.2.

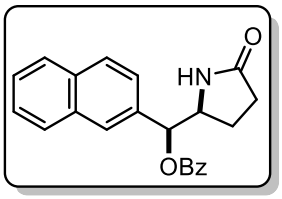
***threo*-(4-Chlorophenyl)(5-oxopyrrolidin-2-yl)methyl benzoate[106a]**



White solid (76%);^{1}H NMR (600 MHz, $CDCl_3$); δ 8.07 (d, *J* = 7.7 Hz, 2H), 7.61 (t, *J* = 7.3 Hz, 1H), 7.48 (t, *J* = 7.6 Hz, 2H),

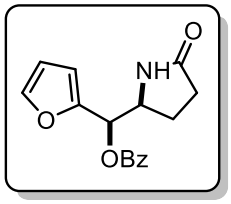
7.37 (s, 4H), 6.46 (s, 1H), 5.80 (d, *J* = 6.8 Hz, 1H), 4.13 (q, *J* = 7.0 Hz, 1H), 2.37 – 2.14 (m, 2H), 2.11 – 2.08 (m, 1H), 1.93 – 1.88 (m, 1H); ^{13}C NMR (151 MHz, $CDCl_3$) δ 178.1, 165.4, 135.3, 134.8, 133.6, 129.8, 129.3, 129.2, 128.7, 128.2, 78.5, 57.8, 29.6, 23.4.

threo-Naphthalen-2-yl(5-oxopyrrolidin-2-yl)methyl benzoate[106a]



White solid (80%);^{1}H NMR (600 MHz, $CDCl_3$) δ 8.03 – 8.01 (m, 2H), 7.80 – 7.73 (m, 4H), 7.55 – 7.50 (m, 1H), 7.43 – 7.38 (m, 5H), 6.13 (s, 1H), 5.92 (d, *J* = 6.7 Hz, 1H), 4.17 (td, *J* = 7.5, 5.0 Hz, 1H), 2.34 – 2.27 (m, 1H), 2.25 – 2.19 (m, 1H), 2.07 – 2.00 (m, 1H), 1.93 – 1.87 (m, 1H). ^{13}C NMR (101 MHz, $CDCl_3$) δ 178.2, 165.6, 134.3, 133.7, 133.5, 133.2, 129.9, 129.7, 129.1, 128.8, 128.3, 127.9, 126.8, 126.8, 126.4, 124.1, 79.4, 58.1, 29.9, 23.7.

Furan-2-yl(5-oxopyrrolidin-2-yl)methyl benzoate

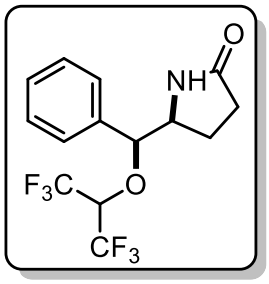


Yellow solid (70%); ***threo*** ^{1}H NMR (600 MHz, $CDCl_3$) δ 8.05 (m, 2H), 7.61 – 7.50 (m, 1H), 7.45 (td, *J* = 8.1, 2.1 Hz, 2H), 7.45 – 7.37 (m, 1H), 6.49 (d, *J* = 3.2 Hz, 1H), 6.37 (m, 2H), 5.95 (d, *J* = 6.4 Hz, 1H), 4.38 – 4.33 (m, 1H), 2.44 – 2.24 (m, 3H), 2.15 – 1.88 (m, 1H). ^{13}C NMR (101 MHz, $CDCl_3$) δ178.1, 165.4, 156.6, 149.6, 143.2, 133.6, 129.8, 128.6, 110.7, 110.6, 71.6, 55.6, 29.4, 23.4. ***erythro*** ^{1}H NMR (600 MHz, $CDCl_3$) δ 8.05 (m, 2H), 7.61 – 7.50

(m, 1H), 7.45 (td, *J* = 8.1, 2.1 Hz, 2H), 7.45 – 7.37 (m, 1H), 6.49 (d, *J* = 3.2 Hz, 1H), 6.37 (m, 2H), 6.05 (d, *J* = 5.9 Hz, 1H), 4.31 (dt, *J* = 8.7, 4.7 Hz, 1H), 2.44 – 2.24 (m, 3H), 2.15 – 1.88 (m, 1H). ^{13}C NMR (101 MHz, $CDCl_3$) δ 178.2, 165.4, 156.6, 149.3, 143.3, 133.6, 129.3, 128.6, 110.6, 110.5, 70.7, 55.7, 29.1, 23.0.

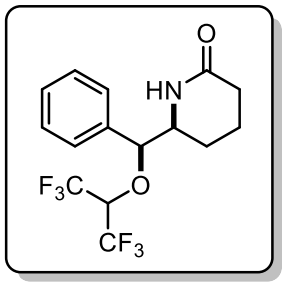
HRMS (ESI) m/z calcd. for $C_{16}H_{15}NO_4$ $[M+Na]^+$: 308.0899, found: 308.0902.

***threo*-5-(((1,1,1,3,3,3-Hexafluoropropan-2-yl)oxy)(phenyl)methyl)pyrrolidin-2-one[106a]**



White solid (90%); ^{1}H NMR (600 MHz, $CDCl_3$); δ 7.47 – 7.46(m, 3H), 7.35 (d, *J* = 2.4 Hz, 2H), 6.16 (s, 1H), 4.51 (d, *J* = 8.4 Hz, 1H), 4.04 – 3.98 (m, 2H), 2.39 – 2.26 (m, 2H), 1.87 – 1.79 (m, 1H), 1.69 – 1.60 (m, 1H); ^{13}C NMR (151 MHz, $CDCl_3$); δ 177.4, 133.3, 130.3, 129.3, 128.4, 123.0, 121.6, 121.1, 119.7, 88.9, 72.7, 72.5, 72.3, 72.1, 71.9, 58.4, 29.6, 23.4; ^{19}F NMR (565 MHz, $CDCl_3$) δ -72.0, -72.0, -72.1, -72.1, -73.4, -73.5, -73.5, -73.5.

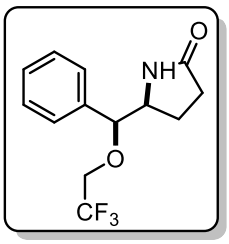
***threo*-6-(((1,1,1,3,3,3-Hexafluoropropan-2-yl)oxy)(phenyl)methyl)piperidin-2-one**



White Solid (70%); ^{1}H NMR (600 MHz, $CDCl_3$) δ 7.46 – 7.44 (m, 3H), 7.34 – 7.30 (dd, *J* = 6.3, 2.7 Hz, 2H), 6.42 (s, 1H), 4.49 (d, *J* = 9.0 Hz, 1H), 3.96 (hept, *J* = 5.8 Hz, 1H), 3.74 (td, *J* = 9.7, 4.6 Hz, 1H), 2.51 – 2.40 (m, 1H), 2.37 – 2.26 (m, 1H), 1.85 – 1.80 (m, 1H), 1.64 – 1.59 (m, 1H), 1.33 – 1.29 (m, 1H), 1.22 – 1.15 (m, 1H). ^{13}C NMR (151 MHz, $CDCl_3$) δ 171.7, 133.5, 130.4, 129.4, 128.4, 88.5, 72.2, 72.0, 57.4, 31.4, 25.0, 19.7. ^{19}F NMR (565 MHz, $CDCl_3$) δ -71.6, -71.6, -71.6, -71.7, -73.4, -73.4, -73.4, -73.4.

HRMS (ESI) m/z calcd. for $C_{15}H_{15}F_6NO_2$ $[M+Na]^+$: 378.0899, found: 378.0901.

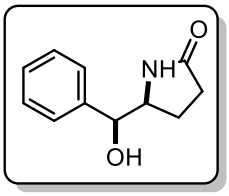
5-(Phenyl(2,2,2-trifluoroethoxy)methyl)pyrrolidin-2-one[106a]



White solid (78%);^{1}H NMR (600 MHz, $CDCl_3$) ***threo*** δ 7.51 – 7.37 (m, 3H), 7.37 – 7.30 (m, 2H), 6.13 (s, 1H), 4.24 (d, *J* = 8.0 Hz, 1H), 3.88 (q, *J* = 7.7, 1H), 3.75 – 3.69 (m, 1H), 3.65 – 3.60 (m, 1H), 2.41 – 2.25 (m, 2H), 1.89 – 1.83 (m, 1H), 1.78 – 1.72 (m, 1H). ^{13}C NMR (151 MHz, $CDCl_3$) δ 177.6, 135.7, 129.4, 129.1, 127.4, 126.6, 124.7, 122.9, 121.0, 87.3, 66.0, 65.8, 65.5, 65.3, 58.9, 29.8, 23.3. ^{19}F NMR (565 MHz, $CDCl_3$) δ -73.9 ***erythro*** δ 7.51 – 7.37 (m, 3H), 7.37 – 7.30 (m, 2H), 5.53 (s, 1H), 4.31 (d, *J* = 6.5 Hz, 1H), 3.95 – 3.91 (m, 1H),

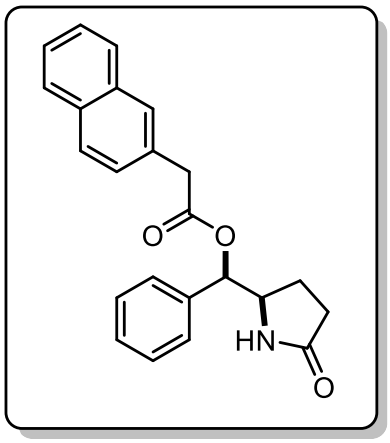
3.75 – 3.69 (m, 1H), 3.65 – 3.60 (m, 1H), 2.41 – 2.25 (m, 2H), 1.89 – 1.83 (m, 1H), 1.78 – 1.72 (m, 1H). ^{13}C NMR (151 MHz, $CDCl_3$) δ 178.0, 135.9, 129.4, 129.1, 127.6, 126.6, 124.7, 122.9, 121.0, 85.6, 66.0, 65.8, 65.5, 65.3, 58.3, 29.1, 23.4. ^{19}F NMR (565 MHz, $CDCl_3$) δ -73.9.

***threo*-5-(Hydroxy(phenyl)methyl)pyrrolidin-2-one[106a]**



White solid (70%);^{1}H NMR (600 MHz, $CDCl_3$) δ 7.43 – 7.33 (m, 5H), 6.33 (s, 1H), 4.49 (d, *J* = 7.6 Hz, 1H), 3.87 (q, *J* = 7.2 Hz, 1H), 2.83 (s, 1H), 2.41 – 2.27 (m, 2H), 1.92 – 1.82 (m, 1H), 1.85 – 1.76 (m, 1H). ^{13}C NMR (101 MHz, DMSO) δ 177.4, 142.5, 128.5, 127.9, 127.6, 76.3, 59.9, 30.2, 22.8.

***threo*-(5-Oxopyrrolidin-2-yl)(phenyl)methyl 2-(naphthalen-2-yl)acetate**

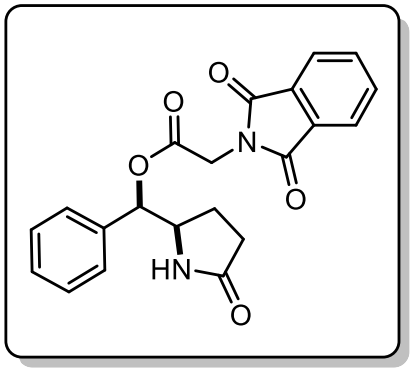


White solid (74%); ^{1}H NMR (600 MHz, $CDCl_3$) δ 7.84 – 7.80 (m, 1H), 7.79 (d, *J* = 8.4 Hz, 1H), 7.76 – 7.74 (m, 1H), 7.64 (s, 1H), 7.46 (qq, *J* = 4.0, 2.2 Hz, 2H), 7.33 (dd, *J* = 8.4, 1.8 Hz, 1H), 7.29 (dd, *J* = 4.9, 2.0 Hz, 3H), 7.23 (dt, *J* = 7.2, 3.6 Hz, 2H), 6.65 (s, 1H), 5.55 (d, *J* = 7.5 Hz, 1H), 3.95 (td, *J* = 7.8, 5.4 Hz, 1H), 3.88 – 3.79 (m, 2H), 2.23 (t, *J*

= 8.2 Hz, 2H), 1.92 (dq, *J* = 13.3, 8.0 Hz, 1H), 1.73 (dtd, *J* = 13.6, 8.2, 5.4 Hz, 1H). ^{13}C NMR (151 MHz, $CDCl_3$) δ 178.4, 170.5, 136.4, 133.4, 132.5, 131.0, 128.8, 128.8, 128.4, 128.2, 128.0, 127.7, 127.6, 127.2, 126.9, 126.3, 126.1, 125.9, 79.3, 57.9, 41.5, 29.7, 23.1.

HRMS (ESI) m/z calcd. for $C_{23}H_{21}NO_3$ $[M+Na]^+$: 382.1414, found: 382.1419.

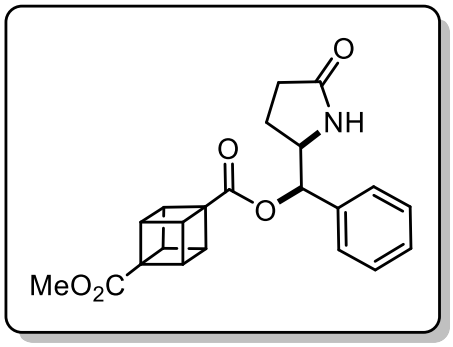
***threo*-(5-Oxopyrrolidin-2-yl)(phenyl)methyl 2-(1,3-dioxoisoindolin-2-yl)acetate**



Yellow solid (68%); ^{1}H NMR (600 MHz, $CDCl_3$) δ 7.88 (dd, *J* = 5.4, 3.1 Hz, 2H), 7.78 – 7.72 (m, 2H), 7.34 (ddd, *J* = 13.8, 7.7, 6.0 Hz, 3H), 7.30 – 7.27 (m, 2H), 6.93 (d, *J* = 6.5 Hz, 1H), 5.62 (d, *J* = 7.5 Hz, 1H), 4.60 – 4.41 (m, 2H), 4.03 (td, *J* = 7.8, 5.6 Hz, 1H), 2.40 – 2.26 (m, 2H), 1.98 (tdd, *J* = 16.2, 11.1, 6.7 Hz, 1H), 1.80 (ddt, *J* = 13.7, 9.7, 6.4 Hz, 1H). ^{13}C NMR (151 MHz, $CDCl_3$) δ 178.5, 177.3, 167.4, 166.5, 135.6, 134.4, 134.1, 132.1, 131.9, 129.1, 129.0, 126.9, 123.7, 123.5, 80.3, 58.0, 39.0, 29.8, 23.1.

HRMS (ESI) m/z calcd. for $C_{21}H_{18}N_2O_5$ $[M+Na]^+$: 401.1108, found: 401.1112.

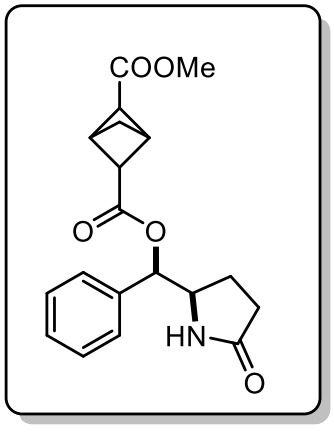
***threo*-Methyl 4-((5-oxopyrrolidin-2-yl)(phenyl)methyl) (1r,2R,3r,8S)-cubane-1,4-dicarboxylate**



White solid (62%); ^{1}H NMR (600 MHz, $CDCl_3$) δ 7.43 – 7.30 (m, 5H), 6.81 (s, 1H), 5.55 (d, *J* = 7.9 Hz, 1H), 4.25 (s, 6H), 4.06 (td, *J* = 8.0, 5.5 Hz, 1H), 3.73 (s, 3H), 2.39 – 2.26 (m, 2H), 2.04 – 1.95 (m, 1H), 1.81 (dddd, *J* = 13.2, 9.3, 7.3, 5.5 Hz, 1H). ^{13}C NMR (151 MHz, $CDCl_3$, *two carbon signals were merged together*) δ 178.6, 171.9, 170.3, 136.6, 128.9, 128.9, 127.0, 78.9, 57.9, 55.8, 55.7, 51.7, 47.1, 47.0, 33.5, 29.8, 29.7, 26.8, 23.3.

HRMS (ESI) m/z calcd. for $C_{22}H_{21}NO_5$ $[M+Na]^+$: 402.1317, found: 402.1325.

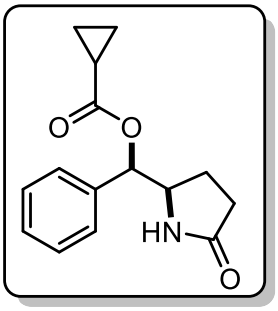
***threo*-2-Methyl 4-((5-oxopyrrolidin-2-yl)(phenyl)methyl) bicyclo[1.1.1]pentane-2,4-dicarboxylate**



White solid (63%); ^{1}H NMR (600 MHz, $CDCl_3$) δ 7.40 – 7.31 (m, 3H), 7.33 – 7.26 (m, 2H), 6.93 (s, 1H), 5.50 (d, *J* = 7.7 Hz, 1H), 4.02 (td, *J* = 7.9, 5.3 Hz, 1H), 3.68 (s, 3H), 2.33 (d, *J* = 6.2 Hz, 8H), 2.06 – 1.93 (m, 1H), 1.82 – 1.76 (m, 1H). ^{13}C NMR (151 MHz, $CDCl_3$) δ 178.8, 169.6, 168.1, 136.3, 129.0, 128.9, 126.8, 79.2, 58.0, 52.9, 52.7, 51.9, 37.7, 37.6, 29.8, 23.2.

HRMS (ESI) m/z calcd. for $C_{19}H_{21}NO_5$ $[M+Na]^+$: 366.1317, found: 366.1322.

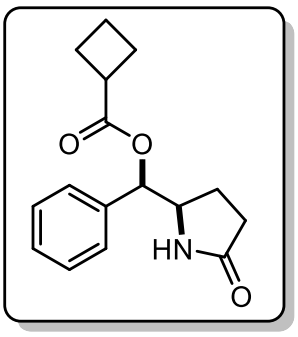
***threo*-(5-Oxopyrrolidin-2-yl)(phenyl)methyl cyclopropanecarboxylate**



Colorless liquid (70%); ^{1}H NMR (600 MHz, $CDCl_3$) δ 7.39 (dd, *J* = 8.5, 6.3 Hz, 2H), 7.37 – 7.33 (m, 3H), 6.31 (s, 1H), 5.57 (d, *J* = 7.3 Hz, 1H), 4.03 (td, *J* = 7.6, 5.2 Hz, 1H), 2.33 (qdd, *J* = 17.1, 9.7, 6.6 Hz, 2H), 2.03 (ddt, *J* = 14.5, 9.4, 7.2 Hz, 1H), 1.90 – 1.81 (m, 1H), 1.70 (tt, *J* = 8.2, 4.6 Hz, 1H), 1.03 (dtd, *J* = 14.0, 7.9, 7.2, 3.7 Hz, 1H), 0.97 (tt, *J* = 9.1, 3.3 Hz, 1H), 0.90 (dtt, *J* = 14.9, 8.8, 2.4 Hz, 2H). ^{13}C NMR (151 MHz, $CDCl_3$) δ 178.2, 173.9, 136.8, 128.8, 128.7, 126.8, 78.6, 57.9, 29.7, 23.3, 12.9, 9.0, 8.9.

HRMS (ESI) m/z calcd. for $C_{15}H_{17}NO_3$ $[M+Na]^+$: 282.1101, found: 282.1106.

***threo*-(5-Oxopyrrolidin-2-yl)(phenyl)methyl cyclobutanecarboxylate**

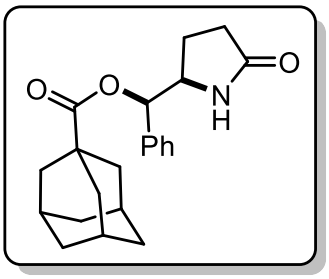


White solid (80%); ^{1}H NMR (600 MHz, $CDCl_3$) δ 7.42 – 7.31 (m, 5H), 6.26 (s, 1H), 5.55 (d, *J* = 7.3 Hz, 1H), 4.01 (td, *J* = 7.8, 5.2 Hz, 1H), 3.22 (p, *J* = 8.6 Hz, 1H), 2.39 – 2.25 (m, 3H), 2.28 – 2.19 (m, 3H), 2.08 – 1.94 (m, 2H), 1.94 – 1.80 (m, 2H).

^{13}C NMR (151 MHz, $CDCl_3$) δ 178.2, 174.3, 136.9, 128.8, 128.7, 126.8, 78.5, 57.9, 38.0, 29.7, 25.2, 25.1, 23.3, 18.4.

HRMS (ESI) m/z calcd. for $C_{16}H_{19}NO_3$ $[M+Na]^+$: 296.1257, found: 296.1264.

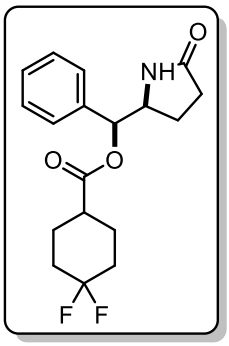
***threo*-(5-Oxopyrrolidin-2-yl)(phenyl)methyl (3r,5r,7r)-adamantane-1-carboxylate**



White solid (52%); ^{1}H NMR (600 MHz, $CDCl_3$) δ 7.41 – 7.30 (m, 5H), 5.74 (s, 1H), 5.54 (d, *J* = 6.8 Hz, 1H), 4.01 (td, *J* = 7.5, 5.4 Hz, 1H), 2.43 – 2.27 (m, 2H), 2.11 – 2.01 (m, 4H), 1.96 – 1.84 (m, 6H), 1.74 – 1.69 (m, 7H).^{13}C NMR (151 MHz, $CDCl_3$) δ 177.7, 176.3, 137.1, 128.9, 128.7, 126.5, 78.0, 58.0, 40.9, 38.8, 36.4, 29.7, 27.8, 23.3.

HRMS (ESI) m/z calcd. for $C_{22}H_{27}NO_3$ $[M+Na]^+$: 376.1883, found: 376.1887.

***threo*-(5-Oxopyrrolidin-2-yl)(phenyl)methyl 4,4-difluorocyclohexane-1-carboxylate**

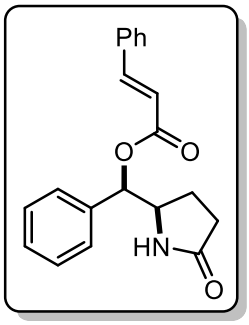


White solid (64%);^{1}H NMR (600 MHz, $CDCl_3$) δ 7.43 – 7.30 (m, 5H), 6.31 (s, 1H), 5.56 (d, *J* = 7.5 Hz, 1H), 4.03 (td, *J* = 7.7, 5.3 Hz, 1H), 2.54 – 2.47 (m, 1H), 2.38 – 2.27 (m, 2H), 2.17 – 2.08 (m, 1H), 2.08 – 1.99 (m, 4H), 1.91 – 1.72 (m, 4H). ^{13}C NMR (101 MHz,

$CDCl_3$) δ 177.9, 173.1, 136.6, 128.9, 126.7, 122.5, 79.0, 57.7, 40.6, 32.8, 32.7, 32.5, 32.5, 32.3, 32.2, 29.6, 25.2, 25.1, 24.9, 23.3. ^{19}F NMR (565 MHz, $CDCl_3$) δ -93.9, -94.3, -99.9, -100.3.

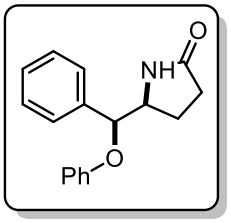
HRMS (ESI) m/z calcd. for $C_{18}H_{21}F_2NO_3$ $[M+Na]^+$: 360.1382, found: 360.1388.

***threo*-(5-Oxopyrrolidin-2-yl)(phenyl)methyl cinnamate[106b]**



White solid (70%); ^1H NMR (600 MHz, $CDCl_3$) δ 7.74 (d, *J* = 16.0 Hz, 1H), 7.56 (dd, *J* = 6.6, 2.9 Hz, 2H), 7.41 (dd, *J* = 9.7, 3.3 Hz, 7H), 7.38 – 7.30 (m, 1H), 6.52 (d, *J* = 16.0 Hz, 1H), 6.49 (s, 1H), 5.72 (d, *J* = 7.1 Hz, 1H), 4.10 (td, *J* = 7.7, 5.1 Hz, 1H), 2.41 – 2.26 (m, 2H), 2.12 – 2.02 (m, 1H), 1.94 – 1.86 (m, 1H). ^{13}C NMR (151 MHz, $CDCl_3$) δ 178.2, 165.9, 146.1, 136.8, 134.1, 130.6, 129.0, 128.9, 128.8, 128.3, 126.9, 117.3, 78.7, 58.0, 29.8, 23.4.

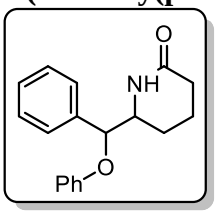
5-(Phenoxy(phenyl)methyl)pyrrolidin-2-one



Yellow solid (60%); ***erythro*** ^1H NMR (600 MHz, $CDCl_3$) δ 7.41 – 7.31 (m, 5H), 7.20 (t, *J* = 7.8 Hz, 2H), 6.91 (t, *J* = 7.3 Hz, 1H), 6.83 (d, *J* = 8.1 Hz, 2H), 6.15 (s, 1H), 4.98 (d, *J* = 6.0 Hz, 1H), 4.10 – 4.05 (m, 1H), 2.48 – 2.13 (m, 3H), 2.07 – 1.93 (m, 1H). ^{13}C NMR (101 MHz, $CDCl_3$)

δ 177.9, 157.4, 137.3, 129.4, 129.0, 128.6, 126.8, 121.4, 115.9, 82.1, 58.9, 29.3, 23.2. ***threo*** ^{1}H NMR (600 MHz, $CDCl_3$) δ 7.41 – 7.31 (m, 5H), 7.20 (t, *J* = 7.8 Hz, 2H), 6.91 (t, *J* = 7.3 Hz, 1H), 6.83 (d, *J* = 8.1 Hz, 2H), 5.76 (s, 1H) , 4.93 (d, *J* = 7.0 Hz, 1H), 4.02 (q, *J* = 13.6 Hz, 1H) 2.48 – 2.13 (m, 3H), 2.07 – 1.93 (m, 1H). ^{13}C NMR (101 MHz, $CDCl_3$) δ 178.3, 157.5, 137.3, 129.4, 129.0, 128.6, 126.9, 121.4, 115.9, 83.5, 59.5, 30.0, 23.4. **HRMS** (ESI) m/z calcd. for $C_{17}H_{17}NO_2$ $[M+Na]^+$: 290.1157, found: 290.1159.

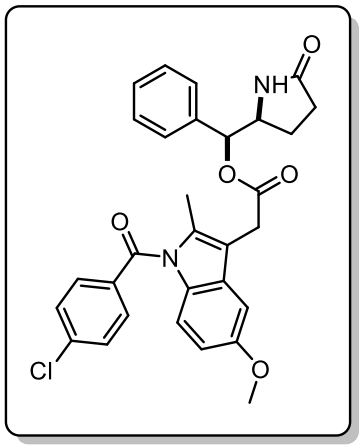
6-(Phenoxy(phenyl)methyl)piperidin-2-one



White solid (34%); ***threo*** ^{1}H NMR (600 MHz, $CDCl_3$) δ 7.39 – 7.34 (m, 4H), 7.34 – 7.30 (m, 1H), 7.17 (dt, *J* = 8.8, 7.6 Hz, 2H), 6.91 – 6.86 (m, 1H), 6.83 – 6.79 (m, 2H), 5.69 (s, 1H), 4.92 (d, *J* = 6.6 Hz, 1H), 3.90 – 3.83 (m, 1H), 2.47 – 2.14 (m, 4H), 1.93 – 1.81 (m, 1H), 1.76 – 1.61 (m, 1H). ^{13}C NMR (151 MHz, $CDCl_3$) δ 172.4, 157.3, 136.7, 129.5, 129.0, 128.8, 127.5, 121.4, 115.9, 82.1, 57.3, 31.6, 25.0, 19.2. ***erythro*** ^{1}H NMR (600 MHz, $CDCl_3$) δ 7.39 – 7.34 (m, 4H), 7.34 – 7.30 (m, 1H), 7.17 (dt, *J* = 8.8, 7.6 Hz, 2H), 6.91 – 6.86 (m, 1H), 6.83 – 6.79 (m, 2H), 6.52 (s, 1H), 4.84 (d, *J* = 8.4 Hz, 1H), 3.74 – 3.69 (m, 1H), 2.47 – 2.14 (m, 4H), 1.93 – 1.81 (m, 1H), 1.76 – 1.61 (m, 1H). ^{13}C NMR (151 MHz, $CDCl_3$) δ 171.9, 157.2, 137.3, 129.4, 128.9, 128.8, 127.0, 121.5, 115.9, 83.9, 58.1, 31.5, 25.0, 19.8.

HRMS (ESI) m/z calcd. for $C_{18}H_{19}NO_2$ $[M+Na]^+$: 304.1308, found: 304.1317.

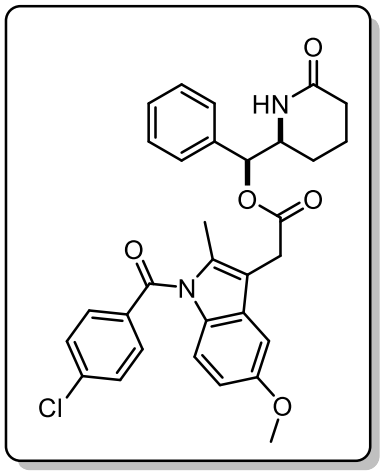
***threo*-(5-Oxopyrrolidin-2-yl)(phenyl)methyl 2-(1-(4-chlorobenzoyl)-5-methoxy-2-methyl-1H-indol-3-yl)acetate**



Yellow solid (64%); ^{1}H NMR (600 MHz, $CDCl_3$) δ 7.66 (d, *J* = 8.2 Hz, 2H), 7.48 (d, *J* = 8.3 Hz, 2H), 7.35 – 7.29 (m, 3H), 7.22 (p, *J* = 2.9 Hz, 2H), 6.90 (d, *J* = 9.0 Hz, 1H), 6.86 (d, *J* = 2.5 Hz, 1H), 6.72 – 6.66 (m, 2H), 5.54 (d, *J* = 7.7 Hz, 1H), 3.97 (td, *J* = 7.9, 5.4 Hz, 1H), 3.75 (s, 3H), 3.73 (s, 2H), 2.33 (s, 3H), 2.30 – 2.18 (m, 2H), 1.99 – 1.90 (m, 1H), 1.79 – 1.69 (m, 1H). ^{13}C NMR (151 MHz, $CDCl_3$) δ 178.3, 169.8, 168.3, 156.1, 139.3, 136.3, 135.9, 133.8, 131.2, 131.1, 130.8, 130.4, 129.2, 129.1, 128.9, 128.8, 126.9, 115.1, 114.9, 112.2, 111.9, 111.5, 101.1, 79.4, 57.9, 55.7, 30.4, 29.6, 23.1, 13.3.

HRMS (ESI) m/z calcd. for $C_{30}H_{27}ClN_2O_5$ $[M+H]^+$: 531.1687, found: 531.1691.

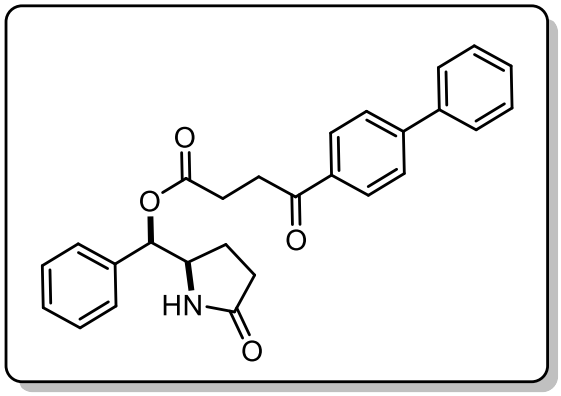
***threo*-(6-Oxopiperidin-2-yl)(phenyl)methyl 2-(1-(4-chlorobenzoyl)-5-methoxy-2-methyl-1H-indol-3-yl)acetate**



White solid (34%); ^{1}H NMR (400 MHz, CD_2Cl_2) δ 7.57 (d, *J* = 8.5 Hz, 2H), 7.41 (d, *J* = 8.5 Hz, 2H), 7.23 (q, *J* = 3.2 Hz, 3H), 7.14 (dd, *J* = 6.6, 2.9 Hz, 2H), 6.85 (d, *J* = 8.9 Hz, 1H), 6.79 (d, *J* = 2.6 Hz, 1H), 6.58 (dd, *J* = 9.0, 2.6 Hz, 1H), 5.83 (s, 1H), 5.36 (d, *J* = 8.4 Hz, 1H), 3.67 (d, *J* = 2.3 Hz, 5H), 3.57 (td, *J* = 9.2, 5.0 Hz, 1H), 2.22 (d, *J* = 6.1 Hz, 4H), 2.07 (ddd, *J* = 17.4, 10.7, 6.0 Hz, 1H), 1.75 – 1.66 (m, 1H), 1.43 – 1.33 (m, 1H), 1.29 – 1.18 (m, 2H). ^{13}C NMR (151 MHz, $CDCl_3$) δ 178.3, 169.8, 168.3, 156.1, 139.3, 136.3, 135.9, 133.8, 131.2, 131.1, 130.8, 130.4, 129.2, 129.1, 128.9, 128.8, 126.9, 115.1, 114.9, 112.2, 111.9, 111.5, 101.1, 79.4, 57.9, 55.7, 30.4, 29.6, 23.1, 13.3.

HRMS (ESI) m/z calcd. for $C_{31}H_{29}ClN_2O_5$ $[M+Na]^+$: 567.1657, found: 567.1672.

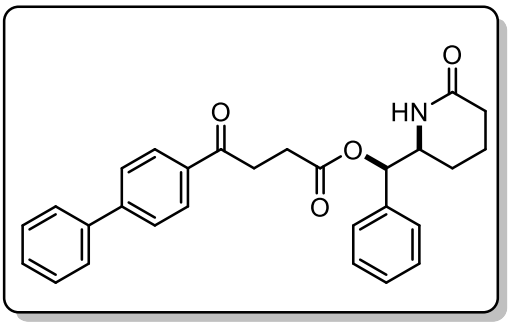
***threo*-(5-Oxopyrrolidin-2-yl)(phenyl)methyl 4-([1,1'-biphenyl]-4-yl)-4-oxobutanoate**



White solid (68%); ^{1}H NMR (600 MHz, $CDCl_3$) δ 8.04 (d, *J* = 8.3 Hz, 2H), 7.68 (d, *J* = 8.3 Hz, 2H), 7.62 (dd, *J* = 7.5, 1.7 Hz, 2H), 7.46 (q, *J* = 8.7, 8.1 Hz, 3H), 7.40 – 7.32 (m, 5H), 6.74 (s, 1H), 5.63 (d, *J* = 7.9 Hz, 1H), 4.05 (td, *J* = 7.9, 5.7 Hz, 1H), 3.41 (ddd, *J* = 18.2, 8.2, 5.5 Hz, 1H), 3.37 – 3.26 (m, 1H), 2.89 (ddd, *J* = 16.8, 8.3, 5.4 Hz, 1H), 2.73 (dt, *J* = 16.9, 5.9 Hz, 1H), 2.41 – 2.26 (m, 2H), 1.96 (dddd, *J* = 13.7, 9.8, 8.0, 5.8 Hz, 1H), 1.81 (dddd, *J* = 13.2, 9.7, 7.2, 5.7 Hz, 1H). ^{13}C NMR (151 MHz, $CDCl_3$) δ 197.9, 178.2, 172.0, 146.1, 139.8, 136.5, 135.0, 129.0, 128.9, 128.8, 128.8, 128.3, 127.3, 127.3, 127.1, 79.1, 58.1, 33.6, 29.9, 28.5, 23.4.

HRMS (ESI) m/z calcd. for $C_{27}H_{25}NO_4$ $[M+Na]^+$: 450.1681, found: 450.1685.

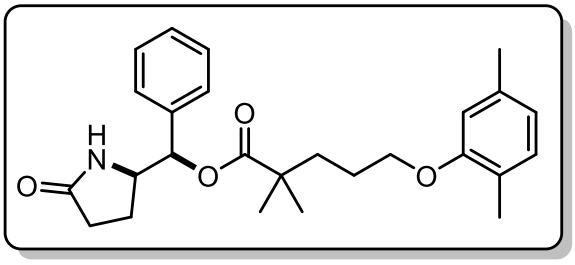
***threo*-(6-Oxopiperidin-2-yl)(phenyl)methyl 4-([1,1'-biphenyl]-4-yl)-4-oxobutanoate**



White solid (33%); ^{1}H NMR (600 MHz, $CDCl_3$) δ 8.05 (d, *J* = 8.2 Hz, 2H), 7.68 (d, *J* = 8.2 Hz, 2H), 7.62 (d, *J* = 7.5 Hz, 3H), 7.47 (t, *J* = 7.5 Hz, 2H), 7.44 – 7.27 (m, 6H), 6.34 (s, 1H), 5.54 (d, *J* = 8.4 Hz, 1H), 3.75 (td, *J* = 9.3, 4.7 Hz, 1H), 3.42 – 3.27 (m, 2H), 2.89 – 2.87 (m, 1H), 2.78 – 2.76 (m, 1H), 2.45 – 2.38 (m, 1H), 2.38 – 2.23 (m, 1H), 1.92 – 1.84 (m, 1H), 1.54 – 1.53 (m, 1H), 1.37 – 1.35 (m, 1H). ^{13}C NMR (151 MHz, $CDCl_3$) δ 197.5, 172.1, 172.0, 146.1, 139.8, 136.7, 135.0, 129.0, 128.9, 128.9, 128.7, 128.3, 127.3, 127.3, 127.0, 79.5, 56.5, 33.5, 31.5, 28.5, 25.0, 19.6.

HRMS (ESI) m/z calcd. for $C_{28}H_{27}NO_4$ $[M+Na]^+$: 464.1832, found: 464.1840.

***threo*-(5-Oxopyrrolidin-2-yl)(phenyl)methyl 5-(2,5-dimethylphenoxy)-2,2-dimethylpentanoate**

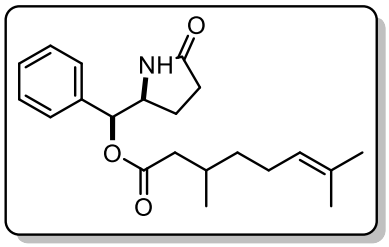


White solid (48%); ^{1}H NMR (400 MHz, $CDCl_3$) δ 7.40 – 7.26 (m, 5H), 7.00 (d, *J* = 7.5 Hz, 1H), 6.67 (d, *J* = 7.5 Hz, 1H), 6.60 (s, 1H), 5.96 (s, 1H), 5.51 (d, *J* = 7.3 Hz, 1H), 4.01 (td, *J* = 7.8, 5.4 Hz, 1H), 3.87

(ddt, *J* = 15.0, 9.1, 4.7 Hz, 2H), 2.30 (s, 3H), 2.17 (s, 3H), 2.05 – 1.96 (m, 2H), 1.87 – 1.79 (m, 2H), 1.71 – 1.55 (m, 4H), 1.24 (d, *J* = 9.0 Hz, 6H). ^{13}C NMR (101 MHz, $CDCl_3$) δ 177.8, 176.5, 156.9, 136.8, 136.5, 130.3, 128.8, 126.8, 123.6, 120.9, 112.2, 78.8, 67.9, 57.7, 42.2, 37.1, 29.6, 25.3, 25.1, 24.9, 23.3, 21.4, 15.8.

HRMS (ESI) m/z calcd. for $C_{26}H_{33}NO_4$ $[M+Na]^+$: 446.2307, found: 446.2310.

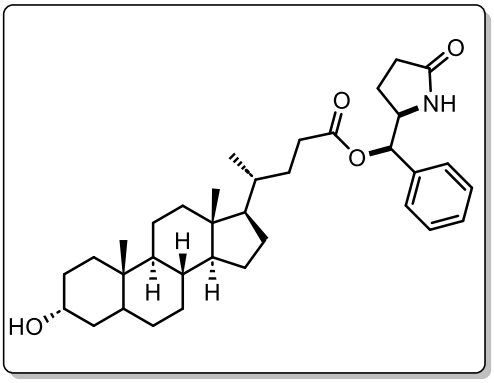
***threo*-(5-Oxopyrrolidin-2-yl)(phenyl)methyl 3,7-dimethyloct-6-enoate**



Colorless liquid (70%); ^{1}H NMR (600 MHz, $CDCl_3$) δ 7.36 (dd, *J* = 7.9, 6.1 Hz, 2H), 7.32 (td, *J* = 8.2, 7.7, 4.2 Hz, 3H), 5.95 (s, 1H), 5.53 (dd, *J* = 7.4, 3.5 Hz, 1H), 5.04 (dddq, *J* = 7.0, 5.2, 3.4, 1.7 Hz, 1H), 3.99 (td, *J* = 7.7, 5.3 Hz, 1H), 2.40 – 2.23 (m, 3H), 2.17 (ddd, *J* = 14.6, 8.3, 5.6 Hz, 1H), 2.05 – 1.88 (m, 4H), 1.86 – 1.76 (m, 1H), 1.67 (s, 3H), 1.57 (d, *J* = 8.2 Hz, 3H), 1.29 (m, 1H), 1.23 – 1.14 (m, 1H), 0.88 (dd, *J* = 8.1, 6.6 Hz, 3H). ^{13}C NMR (151 MHz, $CDCl_3$) δ 177.8, 172.1, 136.8, 131.7, 128.8, 128.8, 126.9, 124.1, 78.7, 57.7, 41.8, 36.7, 30.1, 29.6, 25.7, 25.4, 23.4, 19.6, 17.7.

HRMS (ESI) m/z calcd. for $C_{21}H_{29}NO_3$ $[M+Na]^+$: 366.2048, found: 366.2050.

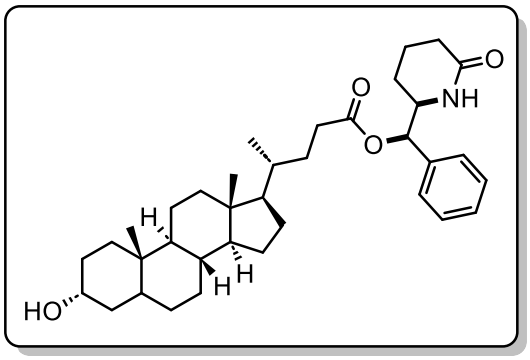
***threo*-(5-Oxopyrrolidin-2-yl)(phenyl)methyl (4R)-4-((3R,8R,9S,10S,13R,14S,17R)-3-hydroxy-10,13-dimethylhexadecahydro-1H-cyclopenta[a]phenanthren-17-yl)pentanoate**



White solid (62%); ^{1}H NMR (600 MHz, $CDCl_3$) δ 7.36 (dd, *J* = 7.8, 6.2 Hz, 2H), 7.32 (tt, *J* = 7.9, 1.8 Hz, 3H), 5.99 (d, *J* = 3.4 Hz, 1H), 5.53 (d, *J* = 7.4 Hz, 1H), 4.00 (m, 1H), 3.62 (m, 1H), 2.46 – 2.18 (m, 4H), 2.06 – 1.96 (m, 1H), 1.93 (dt, *J* = 12.6, 3.3 Hz, 1H), 1.88 – 1.70 (m, 3H), 1.65 (s, 3H), 1.59 – 1.47 (m, 3H), 1.36 (dtd, *J* = 23.0, 15.8, 15.0, 11.4 Hz, 7H), 1.29 – 1.17 (m, 4H), 1.17 – 1.00 (m, 4H), 0.99 – 0.83 (m, 9H), 0.60 (s, 3H), 0.59 (s, 3H). ^{13}C NMR (151 MHz, CDCl3) δ 177.8, 173.1, 136.8, 128.8, 128.8, 126.9, 126.9, 78.6, 71.9, 57.7, 56.5, 55.9, 42.7, 42.1, 40.4, 40.2, 36.5, 35.8, 35.4, 35.2, 34.6, 31.2, 30.9, 30.8, 30.6, 29.7, 28.2, 27.2, 26.8, 26.4, 24.2, 23.4, 20.8, 18.2, 12.0.

HRMS (ESI) m/z calcd. for $C_{35}H_{51}NO_4$ $[M+Na]^+$: 572.3716, found: 572.3721

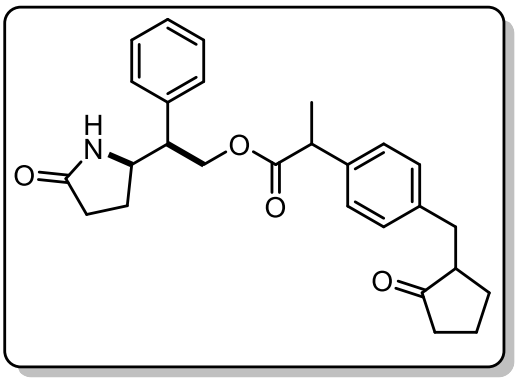
***threo*-(6-Oxopiperidin-2-yl)(phenyl)methyl (4R)-4-((3R,8R,9S,10S,13R,14S,17R)-3-hydroxy-10,13-dimethylhexadecahydro-1H-cyclopenta[a]phenanthren-17-yl)pentanoate**



Colorless liquid (38%);^{1}H NMR (600 MHz, $CDCl_3$) δ 7.40 – 7.28 (m, 5H), 6.06 (s, 1H), 5.45 (d, *J* = 8.6 Hz, 1H), 3.72 (td, *J* = 9.2, 4.6 Hz, 1H), 3.67 – 3.58 (m, 1H), 2.39 (ddt, *J* = 25.3, 15.3, 5.3 Hz, 2H), 2.35 – 2.16 (m, 6H), 1.94 (dd, *J* = 12.1, 3.2 Hz, 1H), 1.91 – 1.70 (m, 6H), 1.68 – 1.62 (m, 2H), 1.58 – 1.47 (m, 3H), 1.46 – 1.30 (m, 9H), 1.30 – 1.17 (m, 3H), 1.16 – 0.92 (m, 6H), 0.89 (dd, *J* = 6.5, 3.1 Hz, 3H), 0.60 (d, *J* = 8.8 Hz, 3H). ^{13}C NMR (151 MHz, $CDCl_3$) δ 173.0, 172.0, 136.9, 128.9, 128.8, 127.0, 127.0, 79.2, 71.9, 56.5, 56.3, 55.9, 42.7, 42.1, 40.4, 40.2, 36.5, 35.8, 35.4, 35.3, 35.2, 34.6, 31.4, 31.2, 30.7, 30.6, 28.2, 27.2, 26.4, 24.9, 24.2, 23.4, 20.8, 19.6, 18.2, 12.0.

HRMS (ESI) m/z calcd. for $C_{36}H_{53}NO_4$ $[M+Na]^+$: 586.3867, found: 586.3876

2-(5-Oxopyrrolidin-2-yl)-2-phenylethyl2-(4-((2-oxocyclopentyl)methyl)phenyl) propanoate

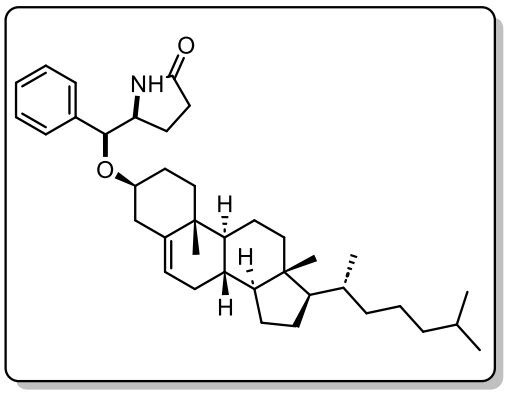


Yellow solid (70%); ***threo*** ^{1}H NMR (600 MHz, $CDCl_3$) δ 7.35 (m, 2H), 7.31 – 7.12 (m, 6H), 7.04 (dd, *J* = 7.5, 2.0 Hz, 1H), 5.62 (d, *J* = 17.1 Hz, 1H), 5.49 (d, *J* = 7.5 Hz, 1H), 3.90 (qdd, *J* = 7.6, 5.2, 2.7 Hz, 1H), 3.77 (ddq, *J* = 29.3, 14.8, 7.1 Hz, 1H), 3.15 (td, *J* = 14.3, 4.1 Hz, 1H), 2.58 – 2.48 (m, 1H), 2.41 – 2.31 (m, 3H), 2.29 – 2.23 (m, 1H), 2.18 – 2.07 (m, 4H), 2.07 – 1.87 (m, 2H), 1.77 (ddddd, *J* = 17.0, 12.7, 10.6, 8.2, 6.4 Hz, 1H), 1.67 – 1.50 (m, 2H), 1.48 (dd, *J* = 9.5, 7.2 Hz, 3H). ^{13}C NMR (151 MHz, $CDCl_3$) δ 178.3, 173.5, 139.5, 136.6, 136.3, 129.5, 129.2, 129.1, 128.8, 128.8, 128.6, 127.7, 127.6, 127.5, 126.8, 126.6, 78.9, 58.0, 51.0, 45.2, 38.2, 35.2, 29.7, 29.3, 23.1, 20.6, 18.0. ***erythro*** ^{1}H NMR (600 MHz, $CDCl_3$) δ 7.35 (t, *J* = 7.8 Hz, 2H), 7.31 – 7.12 (m, 6H), 7.04 (dd, *J* = 7.5, 2.0 Hz, 1H), 6.40 (s, 1H), 5.49 (t, *J* = 7.6 Hz, 1H), 3.90 (qdd, *J* = 7.6, 5.2, 2.7 Hz, 1H), 3.77 (ddq, *J* = 29.3, 14.8, 7.1 Hz, 1H), 3.15 (td, *J* = 14.3, 4.1 Hz, 1H), 2.58 – 2.48 (m, 1H), 2.41 – 2.31 (m, 3H), 2.29 – 2.23 (m, 1H), 2.18 – 2.07 (m, 4H), 2.07 – 1.87 (m, 2H), 1.77 (ddddd, *J* = 17.0, 12.7, 10.6, 8.2, 6.4 Hz, 1H), 1.67 – 1.50 (m, 2H), 1.48 (dd, *J* = 9.5, 7.2 Hz, 3H). ^{13}C NMR (151 MHz, $CDCl_3$) δ 177.9, 173.2, 139.5, 136.6, 136.3, 129.5, 129.2, 129.1,

128.8, 128.8, 128.6, 127.7, 127.6, 127.5, 126.8, 126.6, 78.8, 57.9, 51.0, 45.1, 38.2, 35.2, 29.4, 29.2, 23.1, 20.6, 18.0.

HRMS (ESI) m/z calcd. for $C_{26}H_{29}NO_4$ $[M+Na]^+$: 442.1989, found: 442.1999.

5-((((3*S*,8*S*,9*S*,10*R*,13*R*,14*S*,17*R*)-10,13-Dimethyl-17-((R)-6-methylheptan-2-yl)-2,3,4,7,8,9,10,11,12,13,14,15,16,17-tetradecahydro-1H-cyclopenta[a]phenanthren-3-yl)oxy)(phenyl)methyl)pyrrolidin-2-one

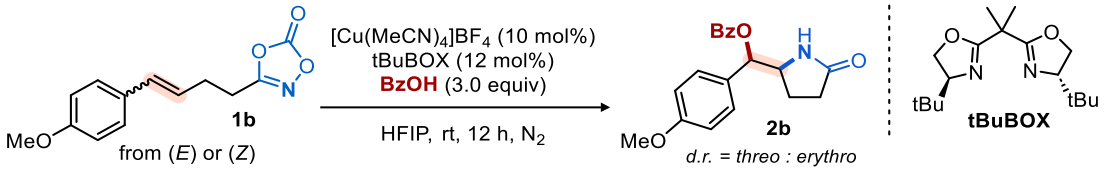


White solid (52%); ***threo*** ^{1}H NMR (600 MHz, $CDCl_3$) δ 7.41 – 7.30 (m, 5H), 6.07 (s, 1H), 5.37 (d, *J* = 7.1 Hz, 1H), 4.19 (d, *J* = 8.2 Hz, 1H), 3.83 – 3.71 (m, 1H), 3.11 (tq, *J* = 11.2, 5.7, 4.5 Hz, 1H), 2.44 – 2.17 (m, 3H), 2.15 – 1.71 (m, 6H), 1.59 – 1.30 (m, 8H), 1.29 – 1.02 (m, 9H), 1.00 (d, *J* = 3.1 Hz, 4H), 0.98 – 0.78 (m, 14H), 0.67 (s, 3H). ^{13}C NMR (151 MHz, $CDCl_3$) δ 178.2, 140.7, 139.1, 128.6, 127.4, 127.3, 121.9, 83.3, 81.5, 71.8, 59.5, 56.8, 56.2, 50.1, 42.3, 39.8, 39.5, 37.3, 36.8, 36.2, 35.8, 31.9, 31.7, 30.2, 29.6, 28.2, 24.3, 23.8, 23.5, 22.8, 22.6, 21.0, 19.4, 18.7, 11.9. ***erythro*** ^{1}H NMR (600 MHz, $CDCl_3$) δ 7.41 – 7.30 (m, 5H), 5.33 (d, *J* = 5.1 Hz, 1H), 5.19 (d, *J* = 5.1 Hz, 1H), 4.28 (d, *J* = 6.6 Hz, 1H), 3.83 – 3.71 (m, 1H), 3.11 (tq, *J* = 11.2, 5.7, 4.5 Hz, 1H), 2.44 – 2.17 (m, 3H), 2.15 – 1.71 (m, 6H), 1.59 – 1.30 (m, 8H), 1.29 – 1.02 (m, 9H), 1.00 (d, *J* = 3.1 Hz, 4H), 0.98 – 0.78 (m, 14H), 0.67 (s, 3H). ^{13}C NMR (151 MHz, $CDCl_3$) δ177.7, 140.5, 138.8, 128.4, 127.4, 127.3, 121.7, 83.0, 81.5, 71.8, 59.0, 56.7, 56.1, 50.1, 42.3, 39.8, 38.5, 37.3, 36.8, 36.2, 35.8, 31.8, 31.7, 30.2,

29.4, 28.0, 24.3, 23.8, 23.5, 22.8, 22.6, 21.0, 19.4, 18.7, 11.9. **HRMS** (ESI) m/z calcd. for $C_{38}H_{57}NO_2$ $[M+H]^+$: 560.4468, found: 560.4479.

4.5.5 Mechanistic Studies

4.5.5.1 Stereoconvergent Study

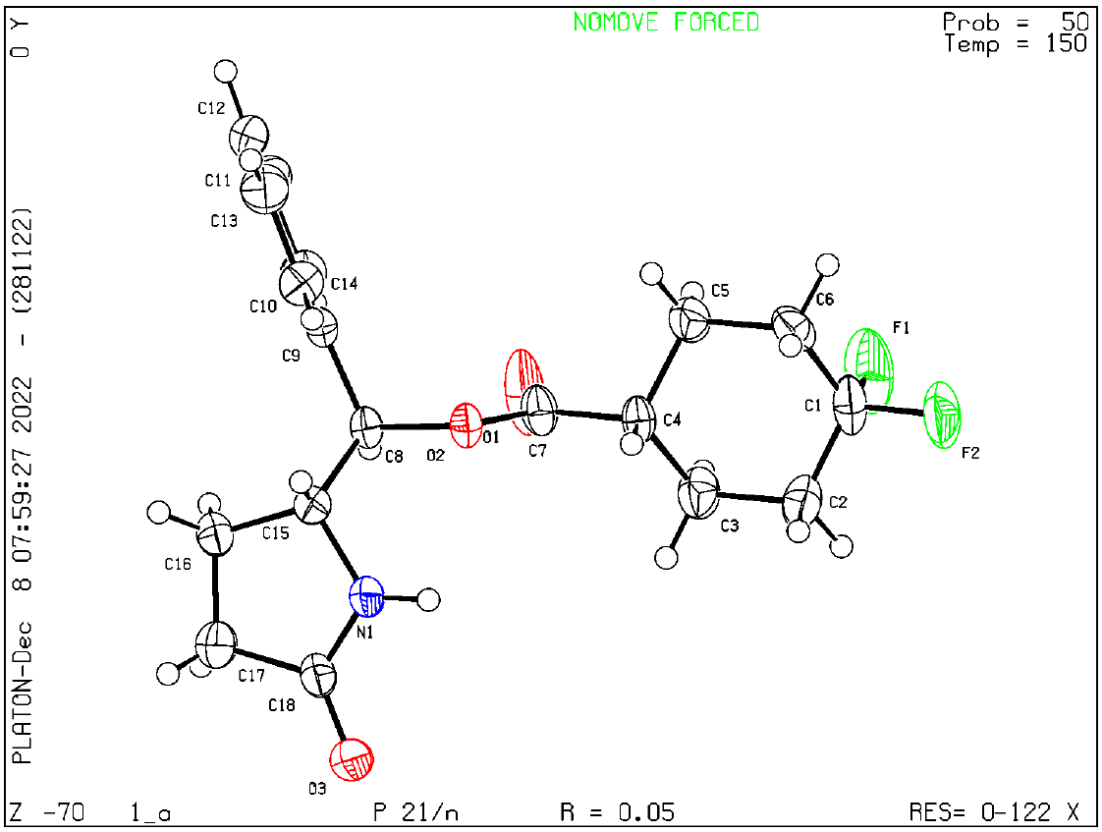


Procedure: In a glovebox, $[Cu(MeCN)_4]BF_4$ (10.0 mol%), tBuBOX (12.0 mol%) and HFIP (1.0 mL) were added to an oven-dried 8 mL vial. The resultant mixture was stirred at room temperature for 2 min and (*E*) or (*Z*) 3-(4-(4-methoxyphenyl)but-3-en-1-yl)-1,4,2-dioxazol-5-one **1b** (0.1 mmol) with benzoic acid (3.0 equiv) were added to the vial. The reaction mixture was allowed to stir at room temperature for 12 hours. After stirring at room temperature for 12 h, the reaction mixture was filtered through a pad of silica gel and washed with EtOAc (2 mL × 3). The mixture was concentrated under vacuum. The d.r. were determined by ^{1}H NMR of the crude reaction mixture.

By comparing the ^{1}H NMR spectral characteristics of the *threo*-**2b** (δ_H 5.76 ppm) and *erythro*-**2b** (δ_H 5.93 ppm) isomers, the diastereoselectivity (*threo*: *erythro*) >20:1 *d.r.* was registered with the use of (*E*)-**1b**, while *threo*: *erythro* = >10: 1 was registered with the use of (*Z*)-**1b**. This result shows that the lactamization is proceeded in a non-concerted mechanism.

4.5.6 Single Crystal X-Ray Diffraction Data

Figure 4.4 Molecular Structure of 2q



CCDC 2226006

Table 4.4 Crystal Data and Structure Refinement for 2q

Identification code	CCDC 2226006
Empirical formula	$C_{18}H_{21}F_2NO_3$
Formula weight	337.36
Temperature/K	150(2)
Crystal system	monoclinic
Space group	P 21/n
a/Å	15.008(3)
b/Å	5.8037(8)
c/Å	19.710(3)
α/°	90
β/°	92.325(6)
γ/°	90
Volume/Å^3	1715.3(5)
Z	4
ρ_{calc}g/cm^3	1.306
μ/mm^{-1}	0.103
F(000)	712.0
Crystal size/mm^3	0.1 x 0.04 x 0.02
Radiation	MoKα (λ = 0.71073)
2Θ range for data collection/°	2.068 to 25.996
Index ranges	$-18 \leq h \leq 18$, $-7 \leq k \leq 7$, $-24 \leq l \leq 24$
Reflections collected	19789
Independent reflections	3368 [R_{int} = 0.1195, R_{sigma} = 0.0960]
Data/restraints/parameters	1850/0/218
Goodness-of-fit on F^2	1.020
Final R indexes [I>=2σ (I)]	R_1 = 0.0511, wR_2 = 0.1021
Final R indexes [all data]	R_1 = 0.1208, wR_2 = 0.1308
Largest diff. peak/hole / e Å^{-3}	0.218/-0.220

Table 4.5 Fractional Atomic Coordinates and Equivalent Isotropic Displacement Parameters (Å^2) for 2q.

U_{eq} is defined as 1/3 of the trace of the orthogonalized U_{IJ}tensor

Atom	*x*	*y*	*z*	U(eq)
C1	0.8781(2)	0.7029(4)	0.68516(14)	0.0448(8)
C2	0.7801(2)	0.6764(5)	0.68043(14)	0.0453(8)
C3	0.7534(2)	0.4666(4)	0.63751(14)	0.0434(8)
C4	0.79338(18)	0.4809(4)	0.56787(12)	0.0298(6)
C5	0.89485(19)	0.5014(4)	0.57524(15)	0.0411(7)
C6	0.92199(19)	0.7090(4)	0.61909(15)	0.0437(8)
C7	0.76814(19)	0.2694(4)	0.52793(13)	0.0346(7)
C8	0.69416(17)	0.1178(4)	0.42799(12)	0.0273(6)
C9	0.76320(17)	0.0349(4)	0.38069(12)	0.0265(6)
C10	0.8032(2)	-0.1778(4)	0.39111(14)	0.0408(7)
C11	0.8705(2)	-0.2509(5)	0.35039(16)	0.0482(8)
C12	0.8987(2)	-0.1148(5)	0.29884(16)	0.0472(8)
C13	0.8581(2)	0.0946(5)	0.28680(15)	0.0483(8)
C14	0.79103(19)	0.1693(4)	0.32751(13)	0.0366(7)
C15	0.60878(17)	0.2038(4)	0.39222(13)	0.0312(6)
C16	0.55203(18)	0.0041(4)	0.36232(14)	0.0393(7)
C17	0.4597(2)	0.0379(6)	0.38829(18)	0.0643(10)
C18	0.4680(2)	0.2260(4)	0.44031(14)	0.0381(7)
F1	0.91514(15)	0.5235(3)	0.72358(9)	0.0838(8)
F2	0.90022(13)	0.8977(3)	0.72266(9)	0.0700(6)
N1	0.55028(15)	0.3093(3)	0.44033(11)	0.0361(6)
O1	0.78025(17)	0.0753(3)	0.54788(10)	0.0684(8)
O2	0.72904(11)	0.3160(2)	0.46725(8)	0.0287(4)
O3	0.40836(13)	0.2950(3)	0.47693(10)	0.0491(6)

Table 4.6 Anisotropic Displacement Parameters (Å^2) for 2q.

The anisotropic displacement factor exponent takes the form: $-2\pi^2[h^2a^{*2}U_{11}+2hka^*b^*U_{12}+\ldots]$

Atom	U_{11}	U_{22}	U_{33}	U_{23}	U_{13}	U_{12}
C1	0.060(2)	0.0341(16)	0.0380(18)	-0.0081(13)	-0.0216(16)	0.0018(14)
C2	0.059(2)	0.0453(17)	0.0316(16)	-0.0080(13)	0.0036(15)	-0.0100(15)
C3	0.051(2)	0.0417(16)	0.0373(18)	-0.0027(13)	0.0014(15)	-0.0119(14)
C4	0.0386(17)	0.0254(13)	0.0245(14)	0.0019(10)	-0.0084(12)	-0.0020(11)
C5	0.0365(19)	0.0383(15)	0.0481(18)	-0.0104(13)	-0.0035(15)	0.0019(13)
C6	0.0298(17)	0.0373(16)	0.063(2)	-0.0108(14)	-0.0096(15)	-0.0017(13)
C7	0.0430(18)	0.0293(14)	0.0304(15)	0.0023(11)	-0.0119(13)	0.0004(12)
C8	0.0306(16)	0.0244(13)	0.0265(14)	-0.0022(10)	-0.0037(12)	-0.0034(11)
C9	0.0273(16)	0.0265(13)	0.0252(14)	-0.0030(11)	-0.0042(12)	-0.0022(11)
C10	0.047(2)	0.0304(15)	0.0444(17)	0.0016(13)	-0.0001(15)	0.0025(13)
C11	0.050(2)	0.0363(17)	0.059(2)	-0.0096(15)	0.0014(17)	0.0090(14)
C12	0.0366(19)	0.0517(19)	0.053(2)	-0.0259(16)	0.0019(16)	-0.0008(15)
C13	0.048(2)	0.0554(19)	0.0421(19)	-0.0008(15)	0.0068(16)	-0.0112(16)
C14	0.0391(18)	0.0337(15)	0.0371(16)	0.0012(13)	0.0033(14)	-0.0003(12)
C15	0.0288(16)	0.0342(14)	0.0307(15)	-0.0059(11)	-0.0001(12)	0.0023(12)
C16	0.0341(18)	0.0453(16)	0.0379(17)	-0.0113(13)	-0.0066(13)	0.0011(13)
C17	0.043(2)	0.072(2)	0.078(3)	-0.0465(19)	0.0061(19)	-0.0102(17)
C18	0.0330(18)	0.0399(16)	0.0408(18)	-0.0128(13)	-0.0063(14)	-0.0007(13)
F1	0.1194(19)	0.0696(13)	0.0578(13)	0.0034(10)	-0.0531(13)	0.0161(12)
F2	0.0739(15)	0.0644(12)	0.0698(13)	-0.0347(10)	-0.0201(11)	-0.0100(10)
N1	0.0303(14)	0.0371(12)	0.0407(14)	-0.0152(11)	-0.0014(11)	-0.0031(10)
O1	0.118(2)	0.0255(11)	0.0569(14)	0.0049(10)	-0.0514(14)	-0.0024(11)
O2	0.0353(11)	0.0251(9)	0.0250(10)	-0.0028(7)	-0.0071(8)	0.0001(8)
O3	0.0347(12)	0.0551(13)	0.0578(14)	-0.0238(11)	0.0073(11)	-0.0069(10)

Table 4.7 Bond Lengths for 2q

Bond	Length/Å	Bond	Length/Å
C1–F2	1.384(3)	C8–C15	1.521(3)
C1–F1	1.390(3)	C9–C14	1.384(3)
C1–C2	1.479(4)	C9–C10	1.384(3)
C1–C6	1.483(4)	C10–C11	1.383(4)
C2–C3	1.527(3)	C11–C12	1.367(4)
C3–C4	1.522(4)	C12–C13	1.375(4)
C4–C7	1.499(3)	C13–C14	1.383(4)
C4–C5	1.529(4)	C15–N1	1.454(3)
C5–C6	1.529(3)	C15–C16	1.541(3)
C7–O1	1.205(3)	C16–C17	1.509(4)
C7–O2	1.338(3)	C17–C18	1.499(4)
C8–O2	1.471(3)	C18–O3	1.239(3)
C8–C9	1.501(3)	C18–N1	1.326(3)

Table 4.8 Bond Angles for 2q

Bond	Angle/°	Bond	Angle/°
F2–C1–F1	103.8(2)	C14–C9–C10	118.2(3)
F2–C1–C2	109.6(2)	C14–C9–C8	121.8(2)
F1–C1–C2	109.3(3)	C10–C9–C8	120.0(2)
F2–C1–C6	110.1(2)	C11–C10–C9	120.7(3)
F1–C1–C6	108.3(2)	C12–C11–C10	120.6(3)
C2–C1–C6	115.0(2)	C11–C12–C13	119.4(3)
C1–C2–C3	110.8(2)	C12–C13–C14	120.3(3)
C4–C3–C2	110.6(2)	C13–C14–C9	120.8(3)
C7–C4–C3	109.2(2)	N1–C15–C8	110.8(2)
C7–C4–C5	110.1(2)	N1–C15–C16	103.1(2)
C3–C4–C5	110.2(2)	C8–C15–C16	111.9(2)
C4–C5–C6	110.9(2)	C17–C16–C15	105.8(2)
C1–C6–C5	111.1(2)	C18–C17–C16	106.0(2)
O1–C7–O2	122.4(2)	O3–C18–N1	125.2(2)
O1–C7–C4	124.3(2)	O3–C18–C17	126.3(3)

O2–C7–C4	113.33(19)	N1–C18–C17	108.5(3)
O2–C8–C9	109.7(2)	C18–N1–C15	115.7(2)
O2–C8–C15	105.21(18)	C7–O2–C8	116.46(17)
C9–C8–C15	114.0(2)	C14–C9–C10	118.2(3)

Table 4.9 Hydrogen Atom Coordinates (Å) and Isotropic Displacement Parameters (Å2) for 2q

Atom	*x*	*y*	*z*	U(eq)
H2A	0.75284	0.816586	0.659806	0.054
H2B	0.757222	0.65871	0.72656	0.054
H3A	0.774611	0.324681	0.660878	0.052
H3B	0.687631	0.458607	0.632155	0.052
H4	0.768964	0.619718	0.543475	0.036
H5A	0.919789	0.517983	0.529763	0.049
H5B	0.91978	0.359148	0.596261	0.049
H6A	0.987532	0.70933	0.62717	0.052
H6B	0.905121	0.852666	0.594714	0.052
H8	0.679422	-0.00939	0.459883	0.033
H10	0.784108	-0.27459	0.426596	0.049
H11	0.89751	-0.39703	0.358294	0.058
H12	0.94581	-0.16439	0.271595	0.057
H13	0.876342	0.188364	0.250353	0.058
H14	0.763683	0.314534	0.318891	0.044
H15	0.623026	0.316127	0.355749	0.037
H16A	0.550506	0.008881	0.312078	0.047
H16B	0.576858	-0.14618	0.377533	0.047
H17A	0.417432	0.083013	0.350778	0.077
H17B	0.438138	-0.10593	0.40904	0.077
H1	0.568302	0.421235	0.46771	0.043

Chapter 5 Conclusion

Selective transition-metal-catalyzed direct C–H amidation represents a powerful tool for introducing nitrogen atoms at a specific place on the hydrocarbon. Due to the natural abundance and environmental sustainability, using earth-abundant metal catalysts for organic transformations is currently of interest. In this thesis, we demonstrated using Fe and Cu for regioselective intramolecular C(sp^2)–H / C(sp^3)–H amidation.

Chapter 2 describes the development of ferrocenium-catalyzed C(aryl)–H amidation utilizing the Fe(IV)–amidyl radical intermediate. Taking advantage of the strong Cp-Fe linkages, the 17-electron ferrocenium complexes catalyzed facile intramolecular aryl C–H amidation with 1,4,2-dioxazol-5-one as amidyl radical precursors. The ferrocenium-catalyzed reaction affords 3,4-dihydroquinolin-2(1*H*)-ones in excellent yields and selectivity. Experimental and computational studies revealed that the intramolecular arene amidation took place by electrophilic arene addition by reactive Fe(IV)-amidyl radical species. A recyclable heterogeneous amidation catalyst has been prepared by grafting ferrocene onto commercially available silica, and comparable catalytic activities with the homogeneous system were observed.

Differentiating different C(sp^3)–H bonds on the hydrocarbon substrates remains a formidable challenge, especially in designing a catalytic system targeting the stronger C–H on the same carbon chain. *Chapter 3* explores the ligand-controlled Cu-catalyzed regioselective C(sp^3)–H amidation for the synthesis of γ-/δ-lactams. This reaction features a regioselective C(sp^3)–H amidation by controlling 1,5-/1,6-HAT of the copper–amidyl radical intermediate. Combined with experimental and computational studies, the regioselectivity is sterically controlled in which the 2,9-diphenylphenanthroline would favor a smaller ring transition state resulting in γ-lactam formation where 2-bromophenanthroline would favor the δ-lactam.

Chapter 4 describes the development of intramolecular oxyamidation of alkene using the 1,4,2-dioxazol-5-ones as nitrene precursor. With the use of Cu(I) salt and tBuBOX as ligand, intramolecular oxyamidation of alkenyl dioxazolones furnish the *threo*-γ-lactams via *5-exo-trig* cyclization. Up to >20: 1 diastereoselectivities were registered, and successful coupling of different O-nucleophiles led to syn-1,2-additon products. This reaction involving a mixture of E-/Z-alkenes was found to be stereoconverging. This implies that the oxyamidation reactions should proceed via a non-concerted pathway. The reaction can be extended to δ-lactam synthesis via a *6-exo-trig* cyclization.

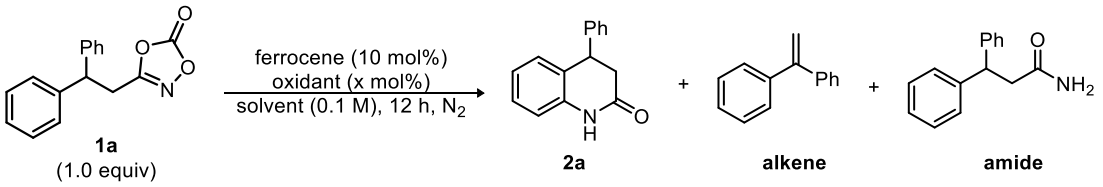
Appendices

A.1 Supplementary Information of Chapter 2

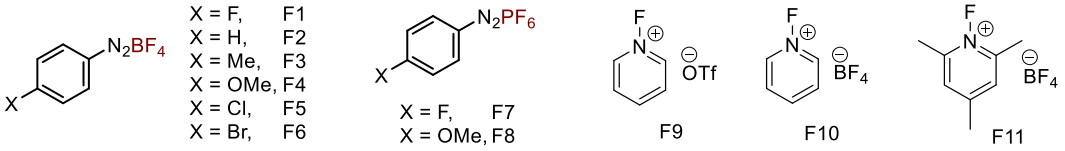
Experimental Optimization of Ferrocenium-Catalyzed C(sp^2)–H Amidation

General procedure: All reactions were performed in a glovebox under an N_2 atmosphere. Catalyst and oxidants were added to an oven-dried 8 mL vial A equipped with a magnetic stir bar. Dry solvent (1 mL) was then added to the vial A and stirred at room temperature for 15 min. 3-(2,2-diphenylethyl)-1,4,2-dioxazol-5-one **1a** (0.2 mmol) was dissolved in dry solvent (1 mL) and transferred to reaction vial A. After stirred at indicated temperature for 12 h, the reaction crude was filtered through a pad of silica gel and washed with EtOAc (2 x 5 mL). The resultant mixture was concentrated under vacuum. The NMR yield was obtained by ^{1}H NMR spectroscopic analysis using $CDCl_3$ as solvent with CH_2Br_2 as internal standard.

Table A1 Optimization of Ferrocene-Catalyzed Arene C–H Amidation[a,b]

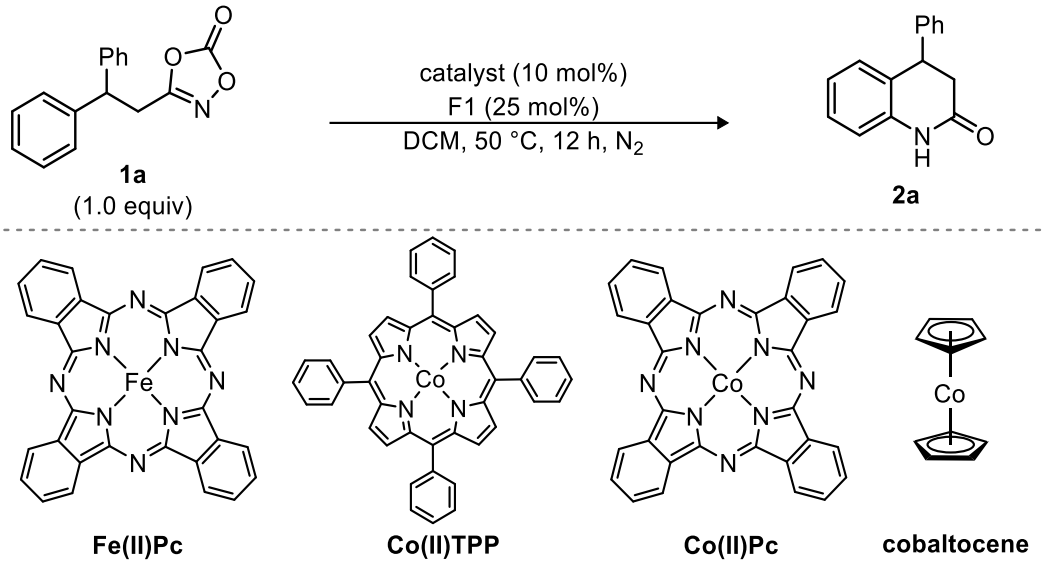


entry	solvent	T (°C)	oxidant (x mol %)	2a (%)	alkene (%)	amide (%)
1	DCE	50	F1 (15)	67	11	12
2	MeCN	50	F1 (15)	n.d.	n.d.	n.d.
3	THF	50	F1 (15)	16	<5	<5
4	TFE	50	F1 (15)	31	15	6
5	HFIP	50	F1 (15)	n.d.	n.d.	n.d.
6	DCM	50	F1 (15)	74	11	15
7	Acetone	50	F1 (15)	n.d	n.d.	n.d.
8	DMA	50	F1 (15)	n.d.	n.d.	n.d.
9	Toluene	50	F1 (15)	n.d.	n.d.	n.d.
10	$CHCl_3$	50	F1 (15)	65	12	14
11	DCM/TFE (1:1)	50	F1 (15)	n.d.	n.d.	n.d.
12	DCE/TFE (1:1)	50	F1 (15)	n.d.	n.d.	n.d.
13[c]	DCM	50	F1 (15)	n.d.	n.d.	n.d.
14	DCM	50	F1 (0)	n.d.	n.d.	n.d.
15[d]	DCM	50	F1 (0)	n.d	n.d.	n.d.
16	DCM	rt	F1 (15)	24	<5	<5
17	DCM	40	F1 (15)	57	<5	<5
18	DCM	60	F1 (15)	59	13	12
19	DCM	50	F1 (25)	92	<5	<5
20	DCM	50	F1 (50)	77	<5	<5
21	DCM	50	F1 (100)	82	<5	<5
22	DCM	50	F2 (25)	84	11	10
23	DCM	50	F3 (25)	75	8	7
24	DCM	50	F4 (25)	85	<5	<5
25	DCM	50	F5 (25)	83	7	7
26	DCM	50	F6 (25)	72	<5	<5
27	DCM	50	F7 (25)	29	12	23
28	DCM	50	F8 (25)	28	10	21
29	DCM	50	F9 (25)	10	<5	<5
30	DCM	50	F10 (25)	5	<5	<5
31	DCM	50	F11 (25)	43	8	6
32[e]	DCM	50	F1 (25)	93	<5	<5
33[f]	DCM	50	F1 (25)	91	<5	<5
34	DCM	50	NFSI (25)	n.d.	n.d.	n.d.
35	DCM	50	Selectfluor® (25)	44	11	22
36	DCM	50	$KMnO_4$ (25)	n.d.	n.d.	n.d.
37	DCM	50	MnO_2 (25)	n.d.	n.d.	n.d.
38	DCM	50	I_2 (25)	n.d.	n.d.	n.d.
39	DCM	50	$Cu(OAc)_2$ (25)	n.d.	n.d.	n.d.
40	DCM	50	AgOAc (25)	n.d.	n.d.	n.d.
41	DCM	50	H_2O_2 (25)	n.d.	n.d.	n.d.



[a]Reaction conditions: **1a** (0.2 mmol), ferrocene (10 mol%), oxidant (x mol%), solvent (2 mL) at T °C for 12 h under N_2; [b]NMR yield using CH_2Br_2 as the internal standard; [c]No catalyst; [d]No catalyst and no oxidant; [e]T=12 h under Air; [f]T=16 h under Air.

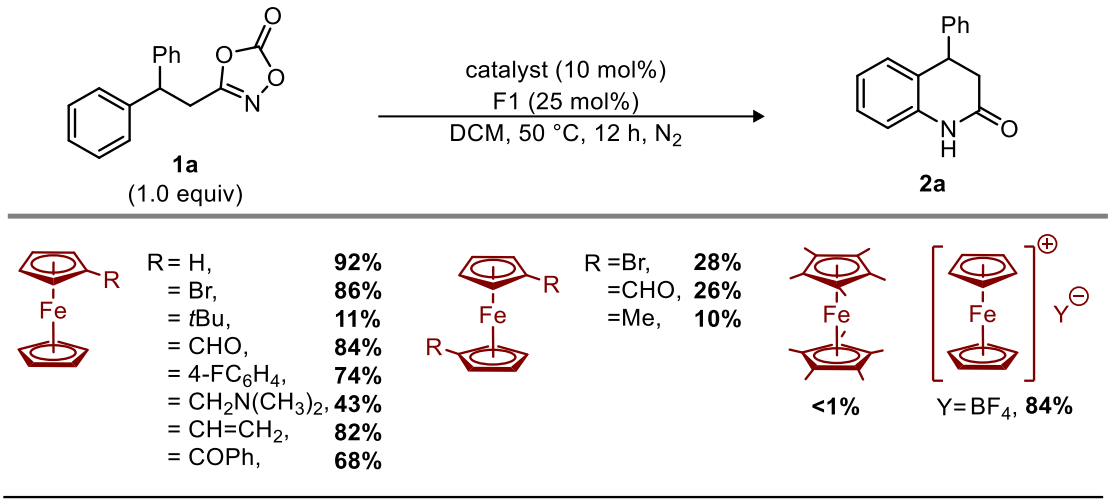
Table A2 Catalyst Screening[a]



entry	catalyst	yield (%)
1	**ferrocene**	**85**
2	$Fe(OAc)_2$	n.d.
3	$FeSO_4 \cdot 7H_2O$	n.d.
4	$Cu(OAc)_2$	n.d.
5	$CuCl_2$	n.d.
6	CuBr	n.d.
7	CuCl	n.d.
8	$Co(OAc)_2 \cdot 4H_2O$	n.d.
9	$CoCl_2 \cdot 6H_2O$	n.d.
10	$Co(acac)_2$	n.d.
11	Co(salen)	n.d.
12	$Mn(acac)_2$	n.d.
13	Fe(II)Pc	n.d.
14	Co(II)TPP	n.d.
15	Co(II)Pc	n.d.
16	cobaltocene	n.d.

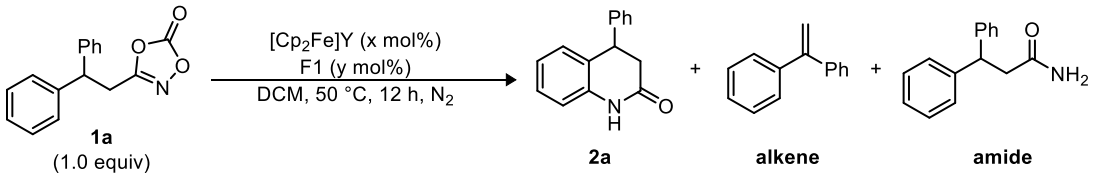
[a]Reaction conditions: **1a** (0.2 mmol), catalyst (10 mol%), F1 oxidant (25 mol%) in DCM (2 mL) at 50 °C for 12 h under N_2; Isolated yield.

Table A3 Ferrocene Derivatives Screening[a,b]

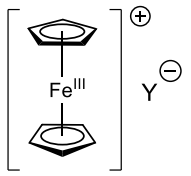


[a]Reaction conditions: **1a** (0.2 mmol), ferrocene derivatives (10 mol%), F1 oxidant (25 mol%), DCM (2 mL) at 50 °C for 12 h under N_2; [b]NMR yield using CH_2Br_2 as the internal standard.

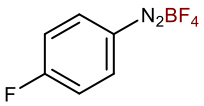
Table A4 Effects of Anion of Fe-Catalyzed C–H Amidation[a]



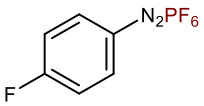
entry	[Y]	(x mol %)	F1 (y mol %)	2a (%)	alkene (%)	amide (%)
1	BF_4	2.5	0	69	17	9
2	BF_4	5	0	67	16	13
3	BF_4	10	0	64	16	15
4	BF_4	25	0	51	12	16
5	BF_4	50	0	42	10	22
6	BF_4	100	0	36	11	20
7	BF_4	10	15	87	<5	<5
8	BF_4	10	25	86	<5	<5
9[b]	BF_4	10	0	47	13	18
10	PF_6	10	0	23	18	20
11	PF_6	10	25	21	<5	<5
12[b]	PF_6	10	0	30	15	13
13	PF_6	25	0	24	19	12
14	PF_6	50	0	26	16	15
15	PF_6	100	0	22	15	19
16[c]	PF_6	10	0	21	14	17



[Cp2Fe]Y



F1

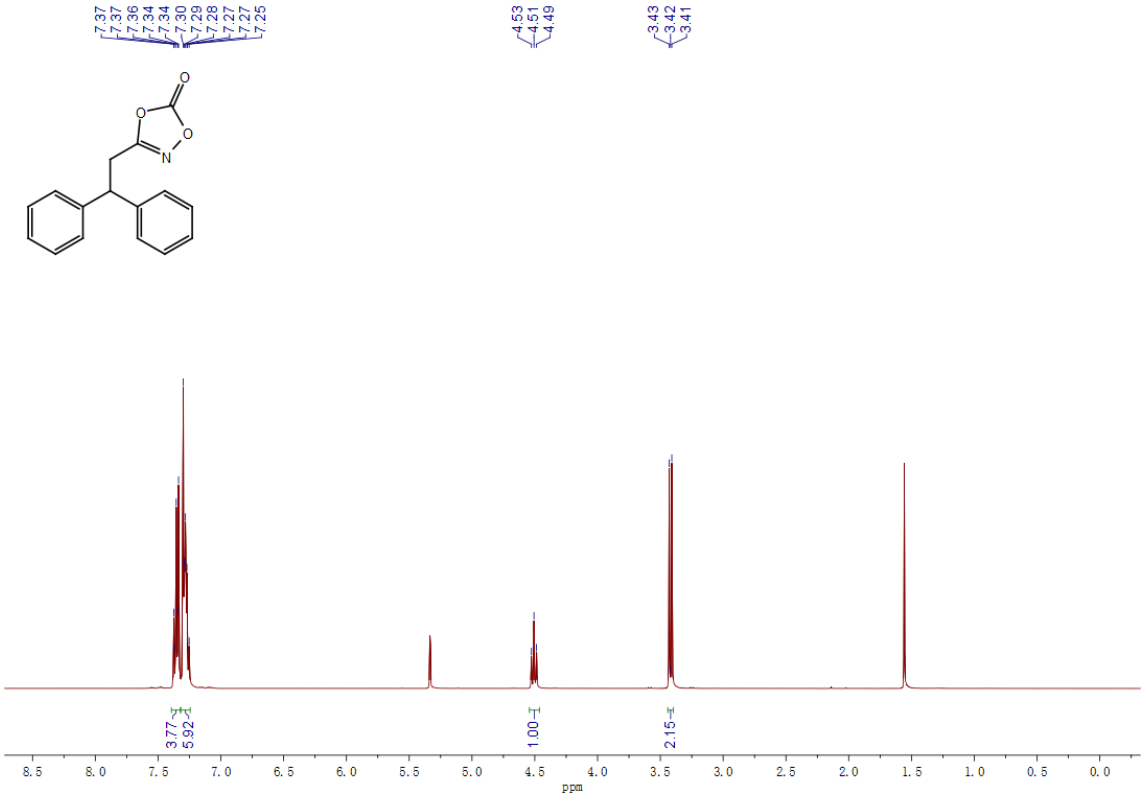


F7

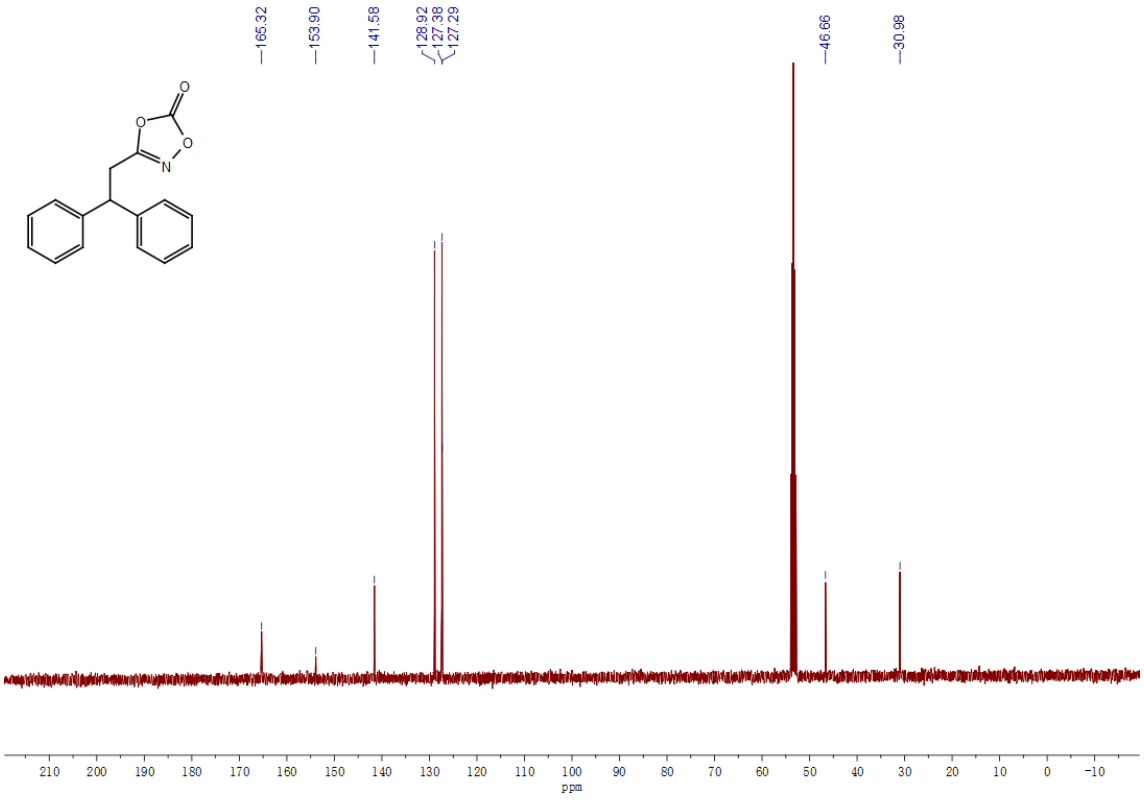
[a]Reaction conditions: **1a** (0.2 mmol), [Cp_2Fe]Y (x mol%), F1 (y mol%) in DCM (2 mL) at 50 °C for 12 h under N_2; NMR yield using CH_2Br_2 as the internal standard; [b]TBA[BF4] (25 mol%) added; [c]F7 (25 mol%) added.

A.2 NMR Spectra of Chapter 2

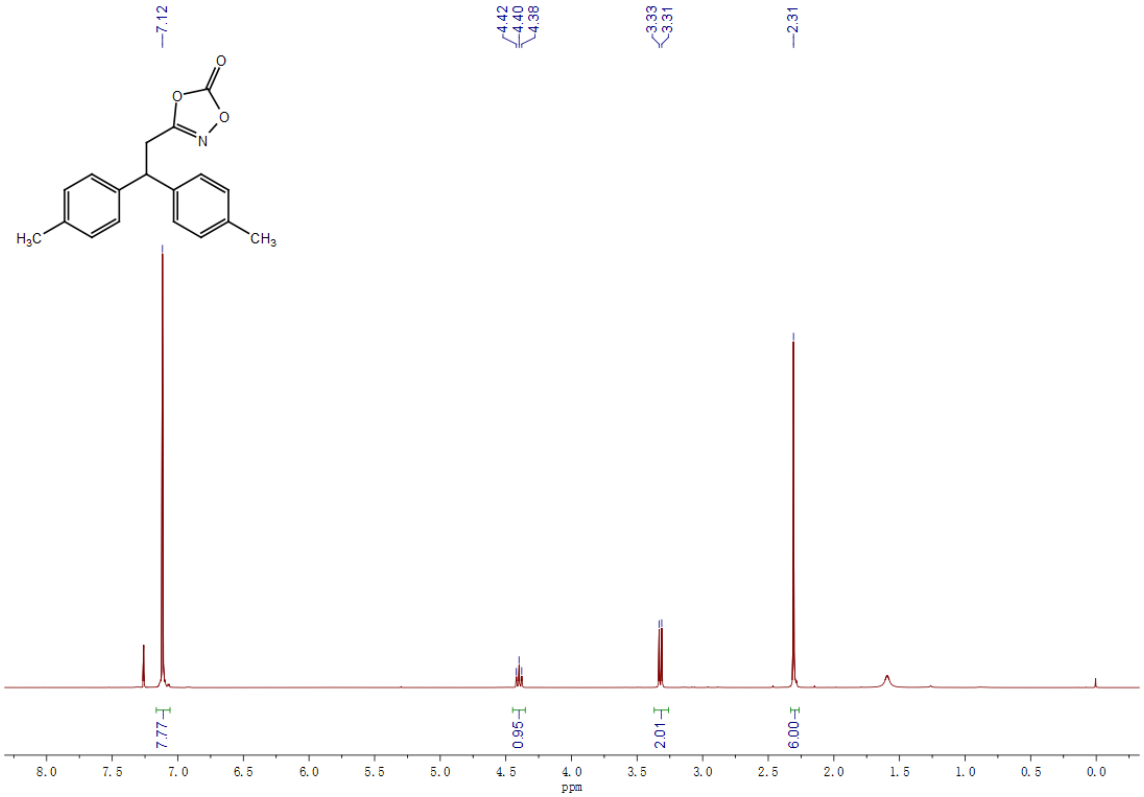
^{1}H NMR of 1a



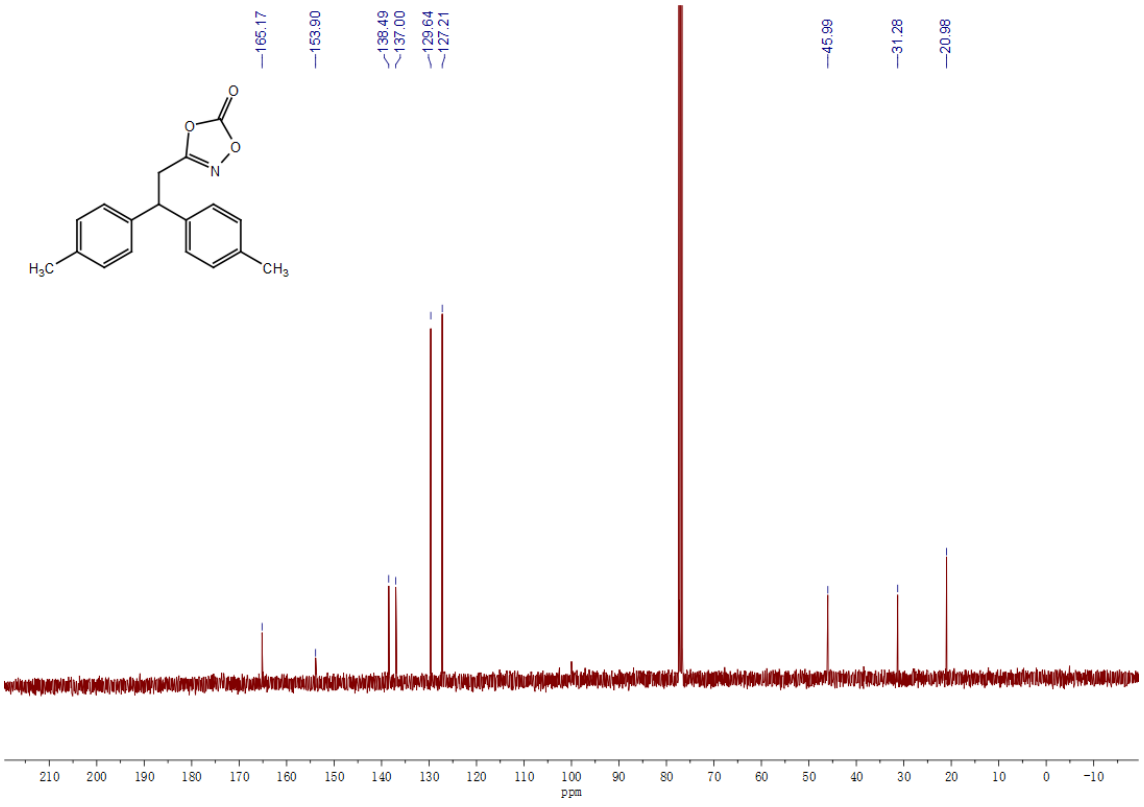
^{13}C NMR of 1a



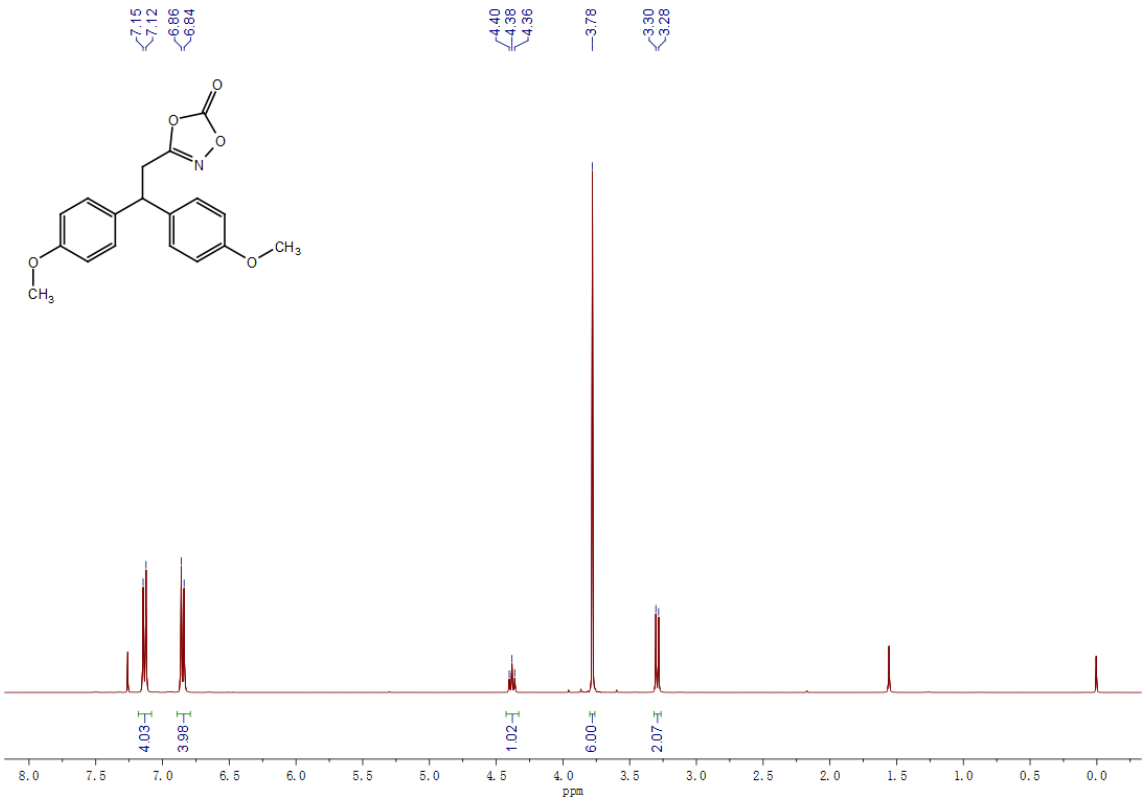
^{1}H NMR of 1b



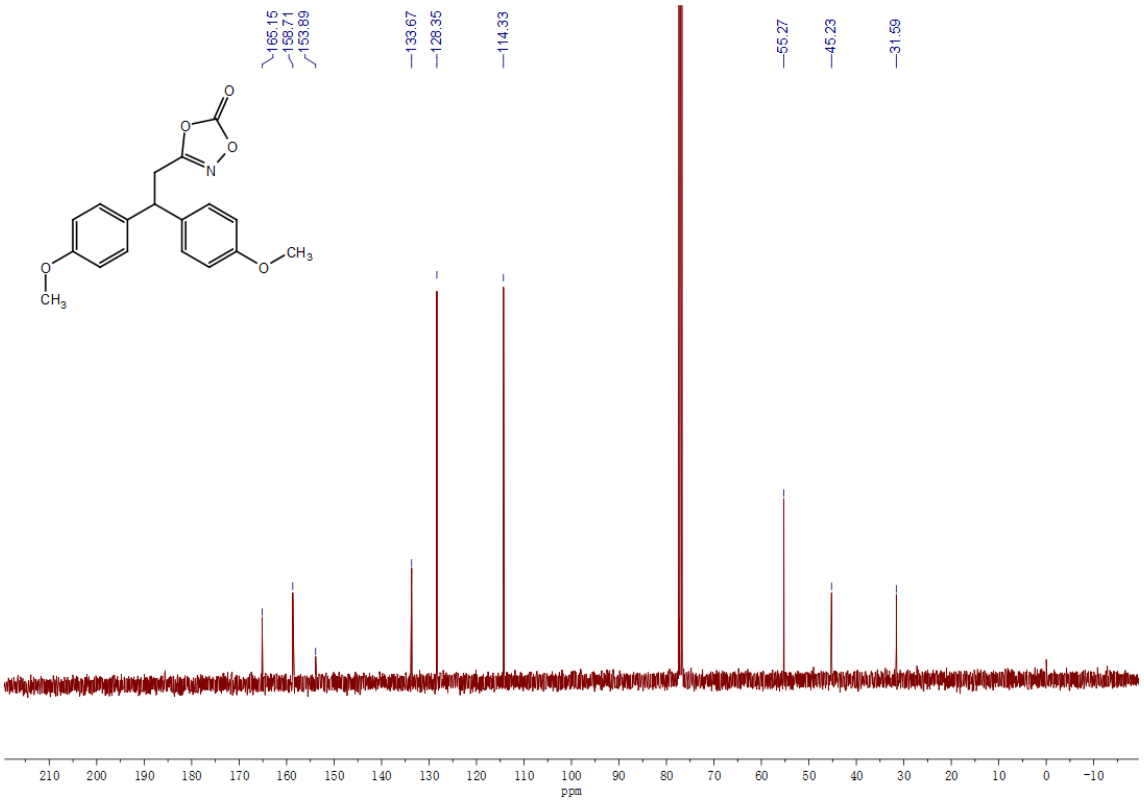
^{13}C NMR of 1b



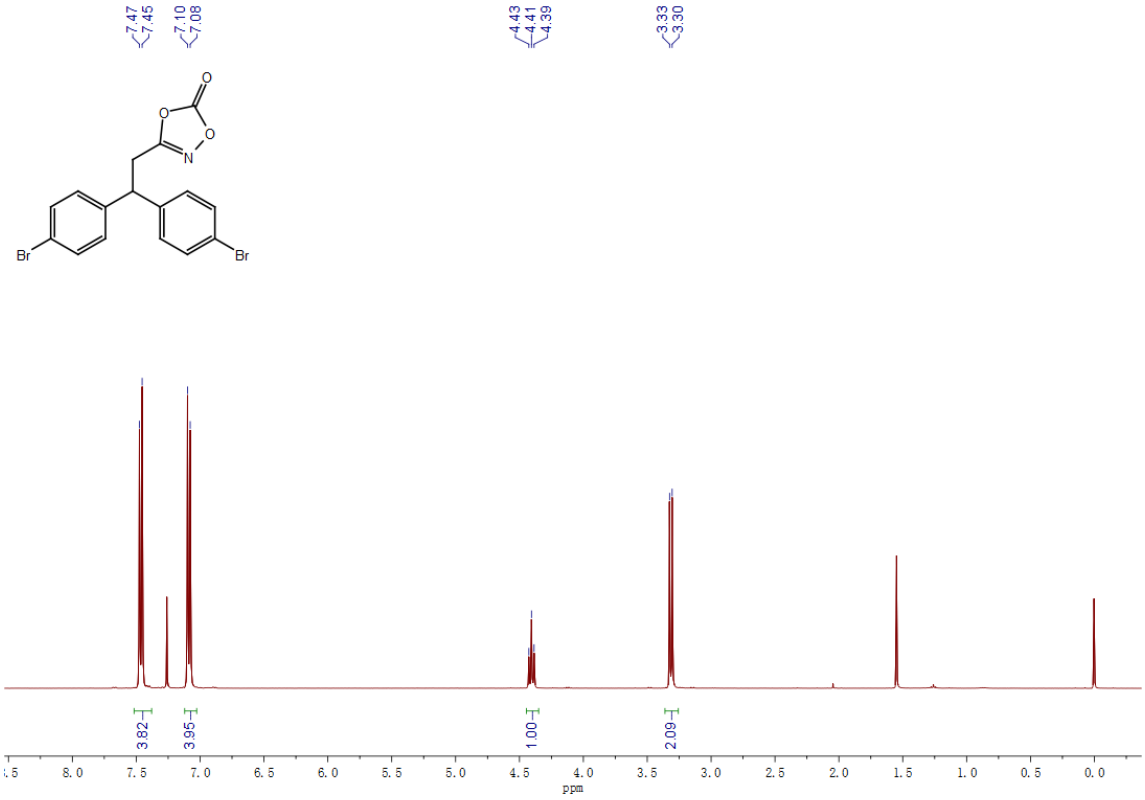
^{1}H NMR of 1c



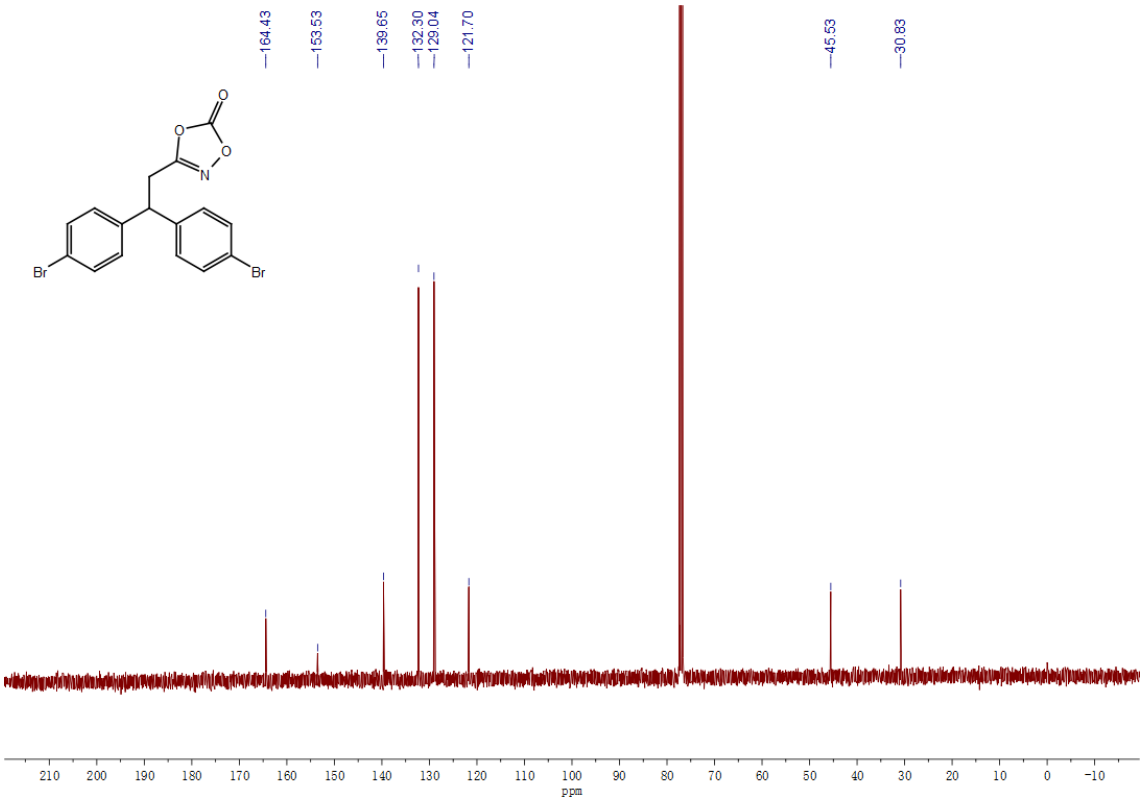
^{13}C NMR of 1c



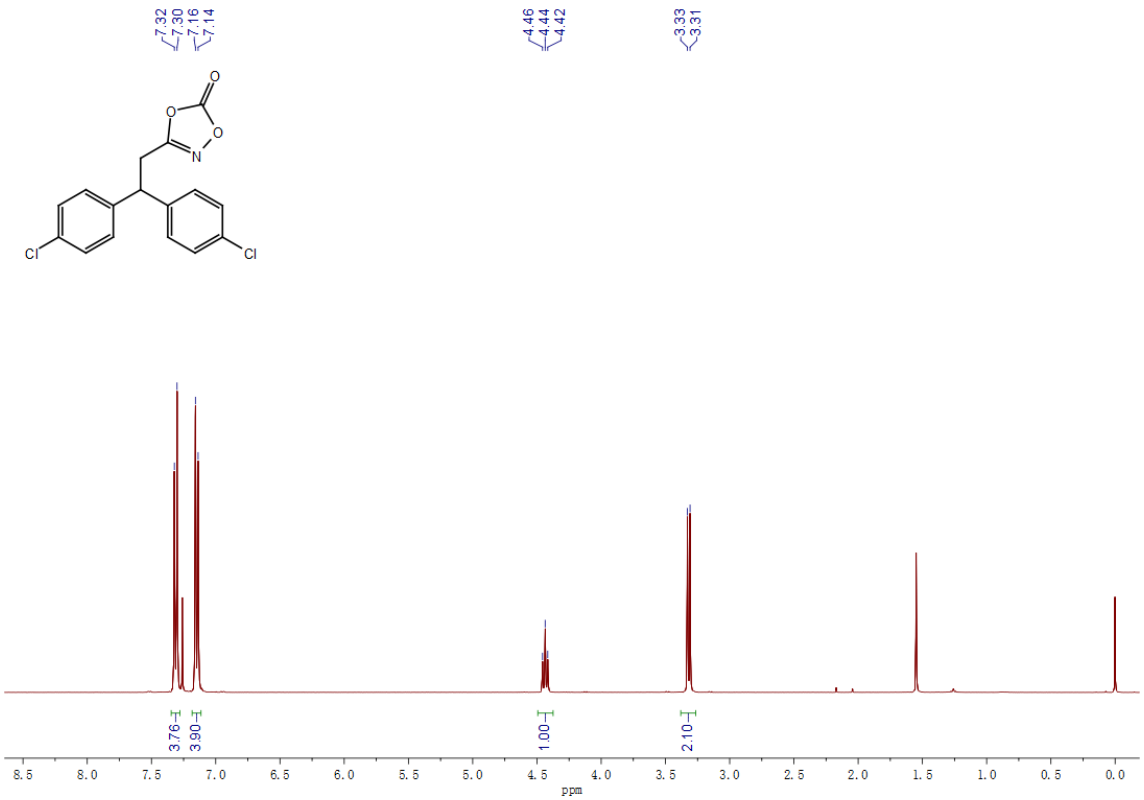
^{1}H NMR of 1d



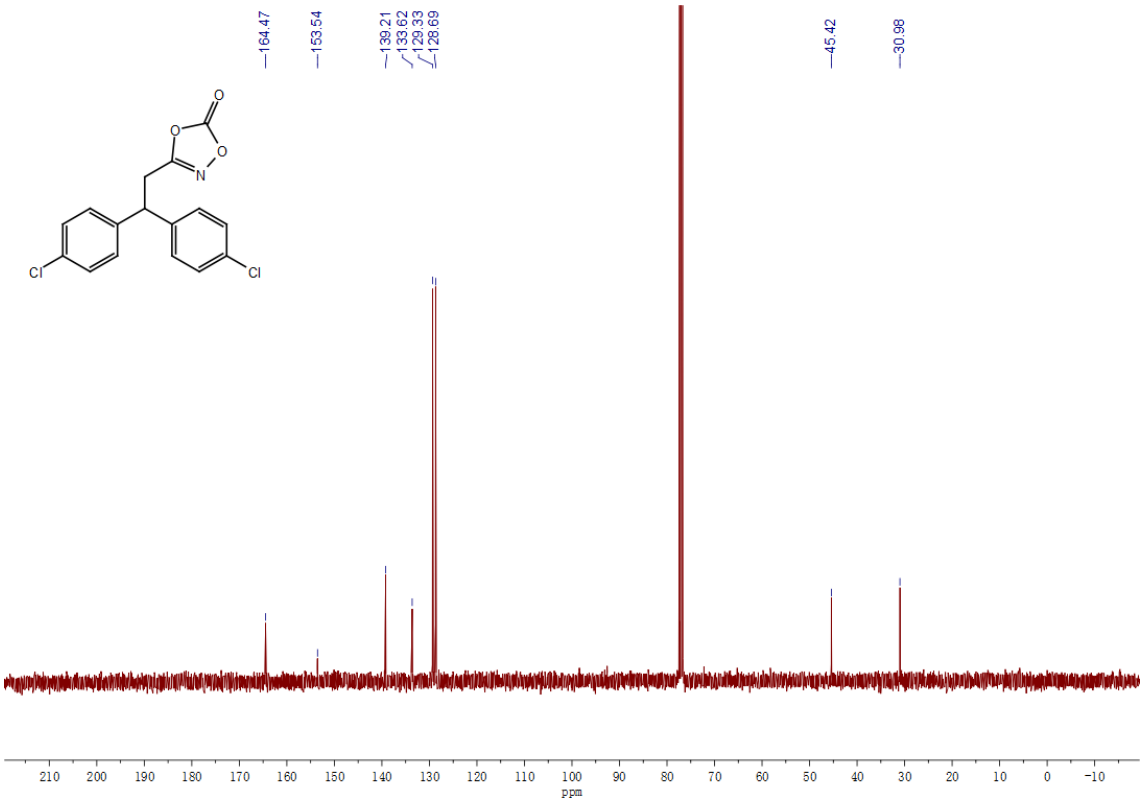
^{13}C NMR of 1d



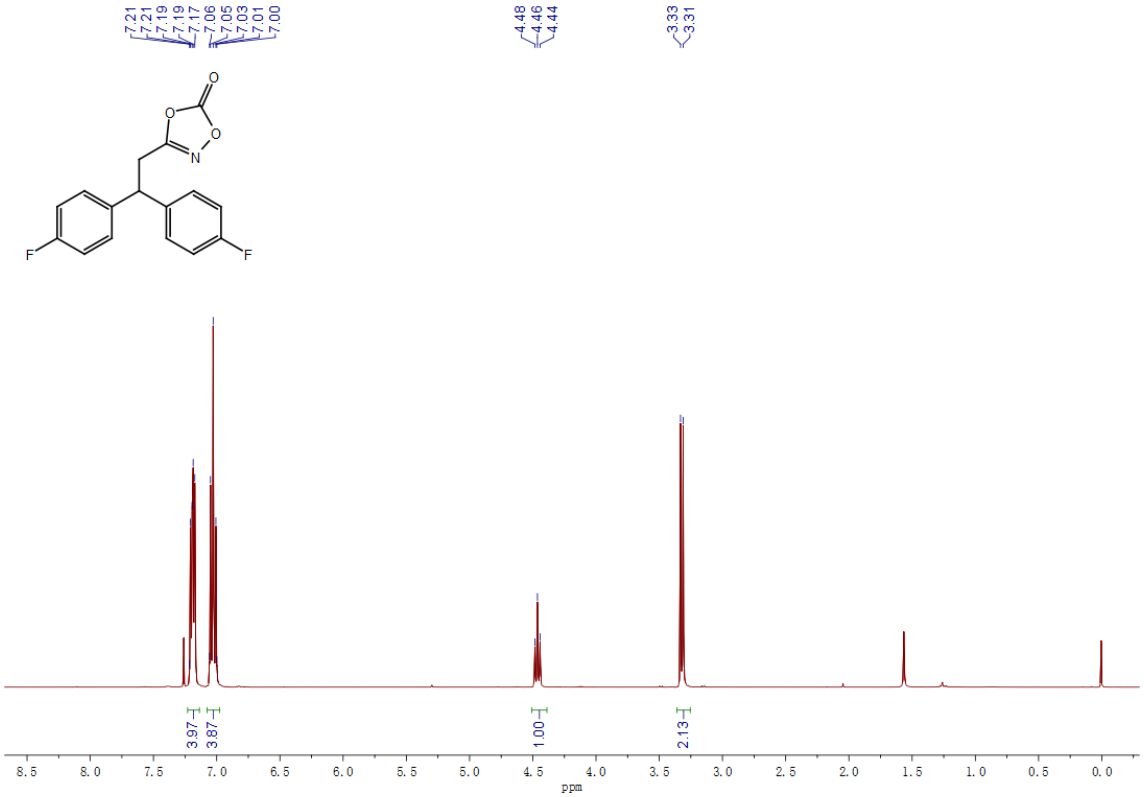
^{1}H NMR of 1e



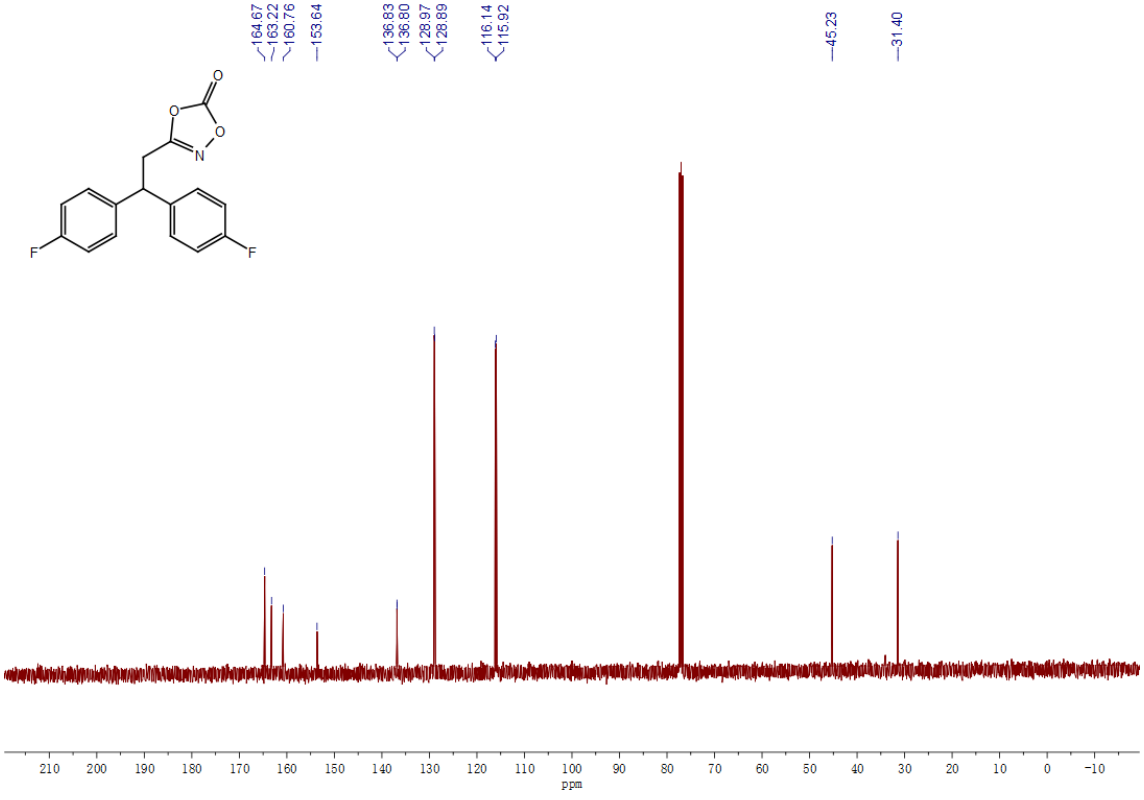
^{13}C NMR of 1e



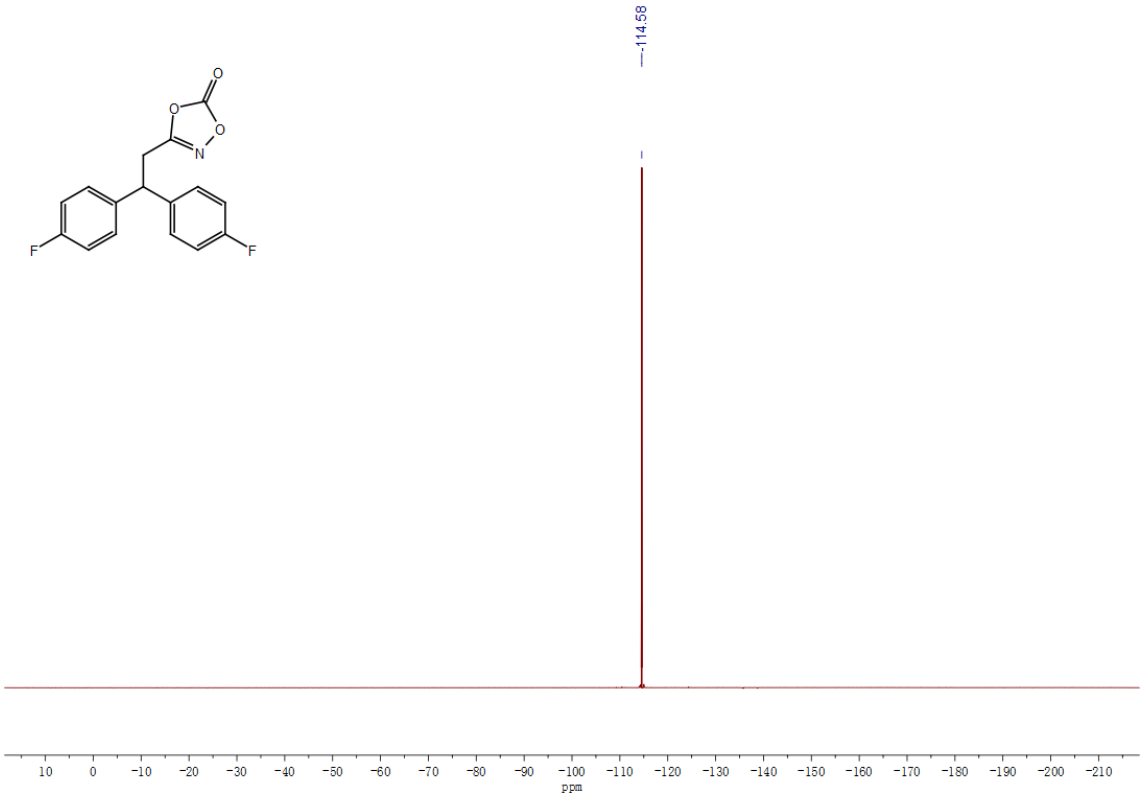
^{1}H NMR of 1f



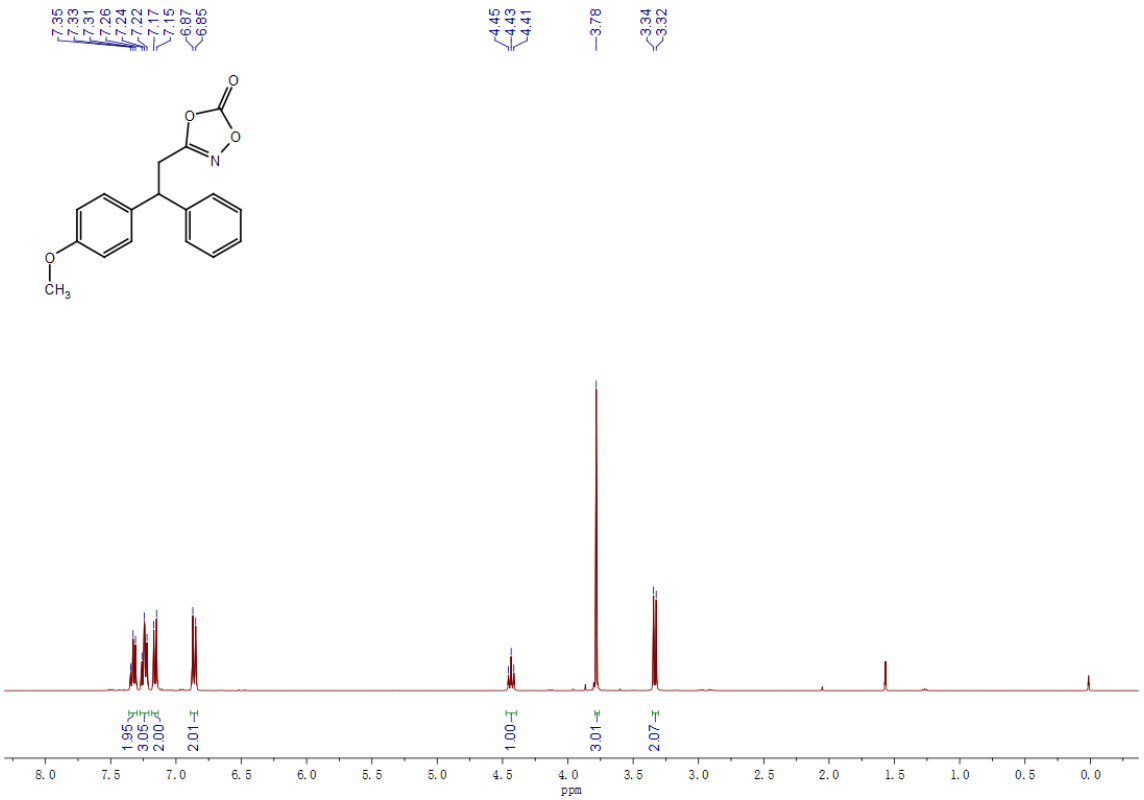
^{13}C NMR of 1f



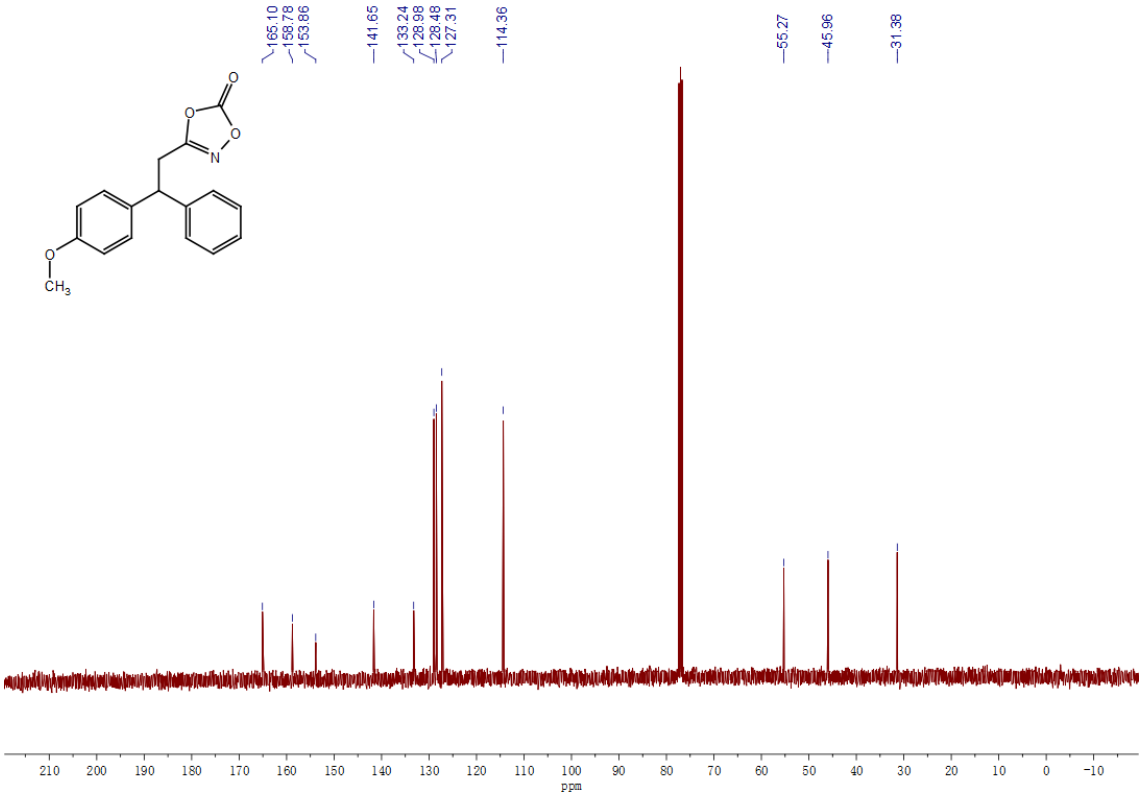
^{19}F NMR of 1f


-114.58
10
0
-10
-20
-30
-40
-50
-60
-70
-80
-90
-100
-110
-120
-130
-140
-150
-160
-170
-180
-190
-200
-210
ppm

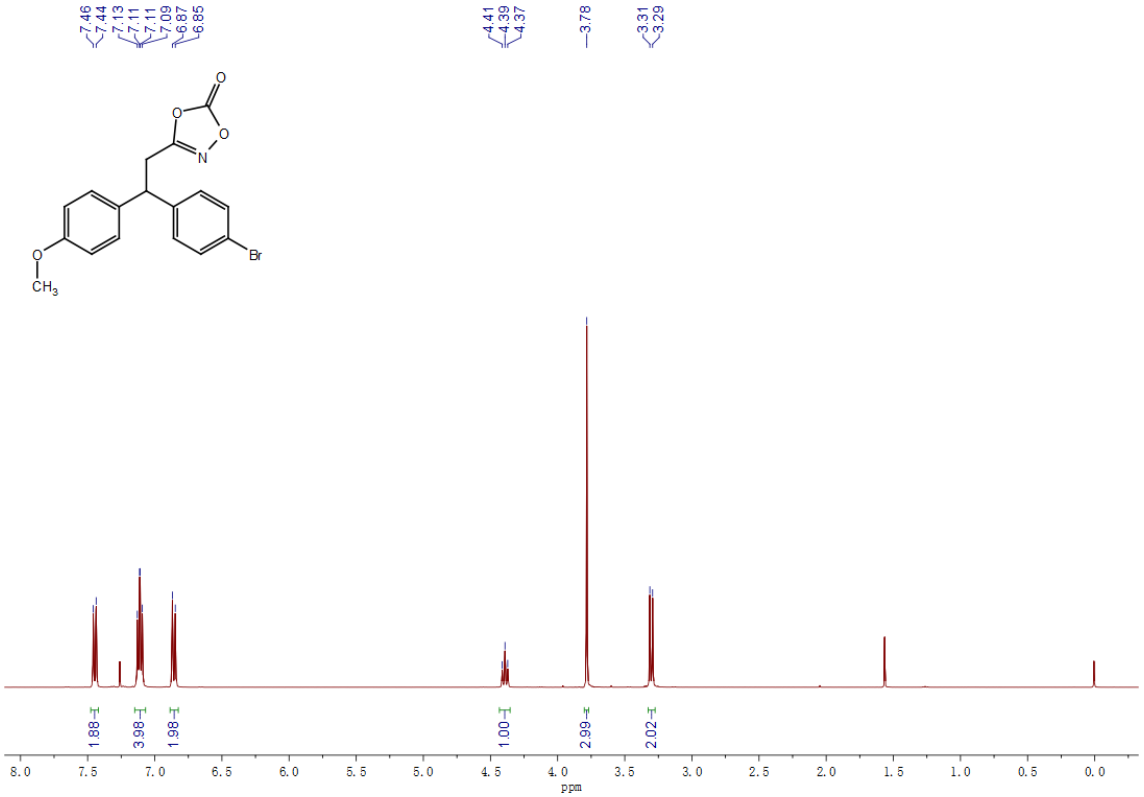
^{1}H NMR of 1g



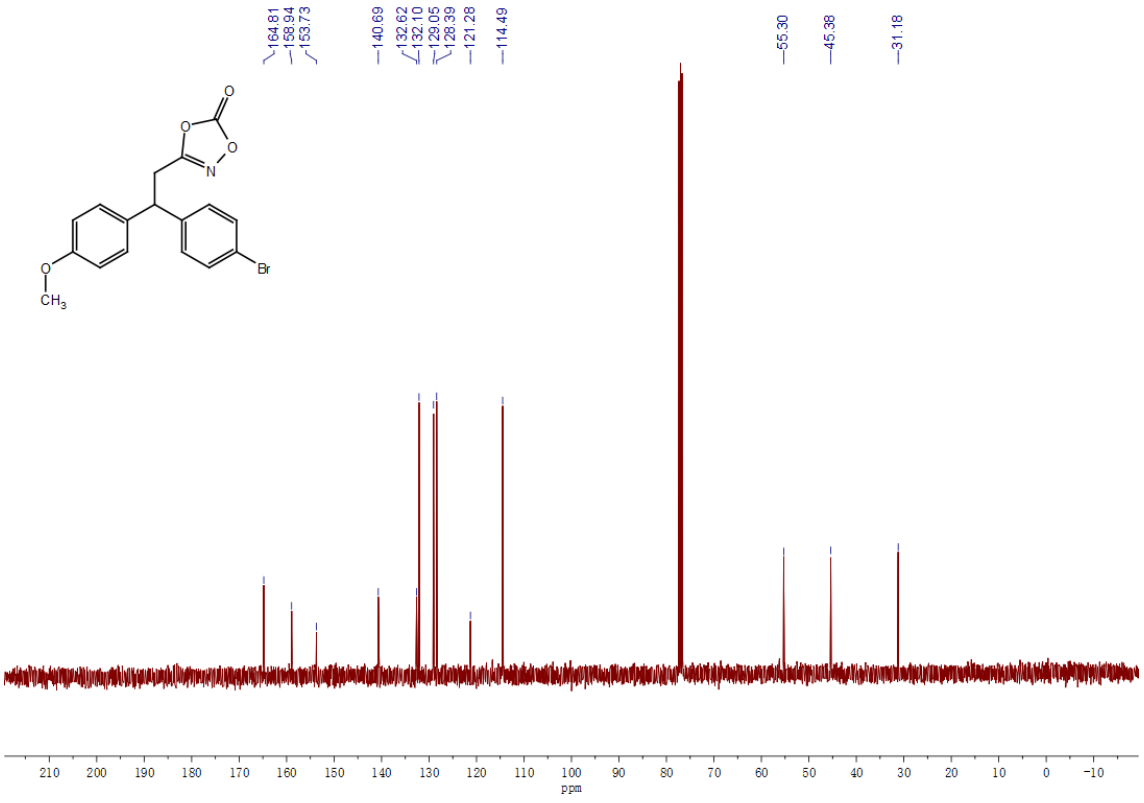
^{13}C NMR of 1g



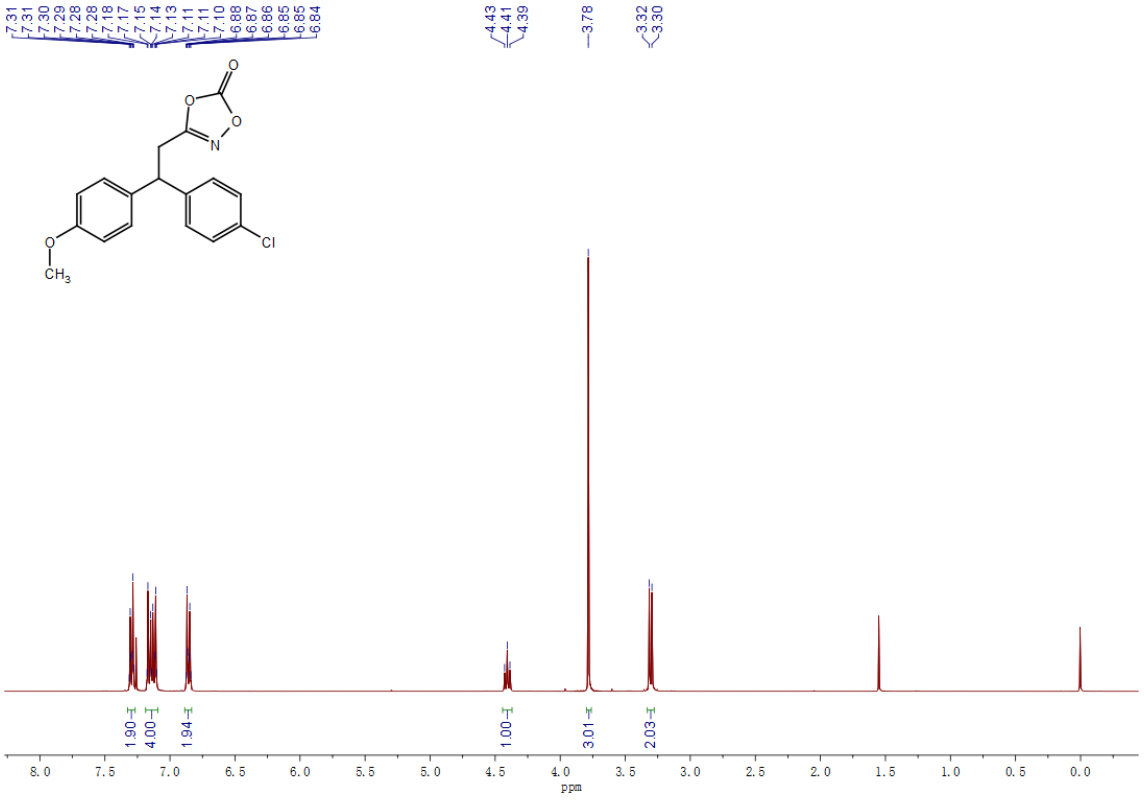
^{1}H NMR of 1h



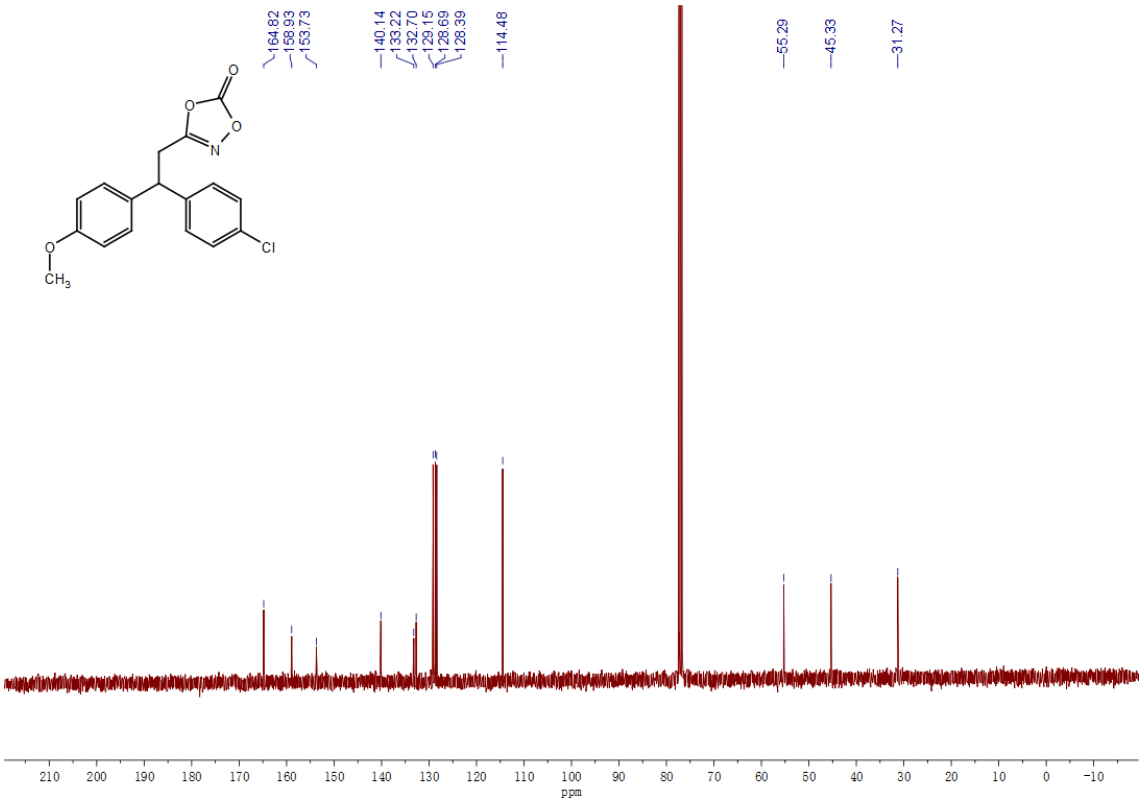
^{13}C NMR of 1h



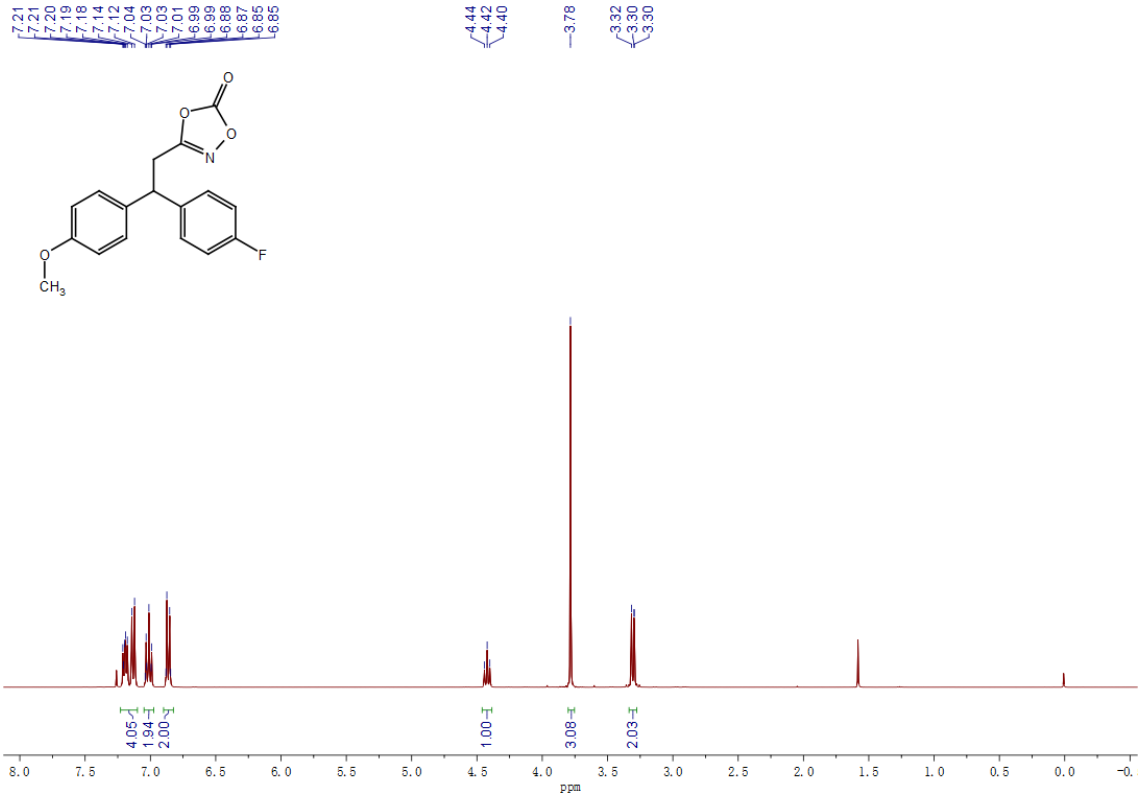
^{1}H NMR of 1i



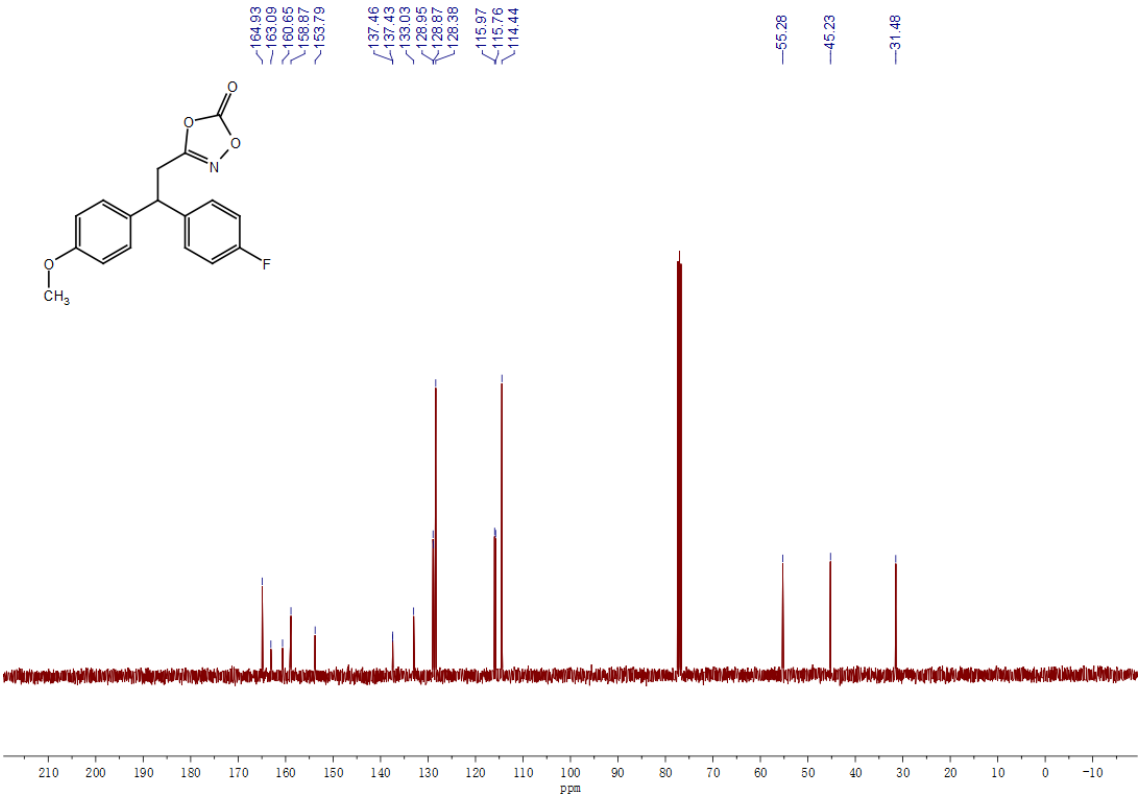
^{13}C NMR of 1i



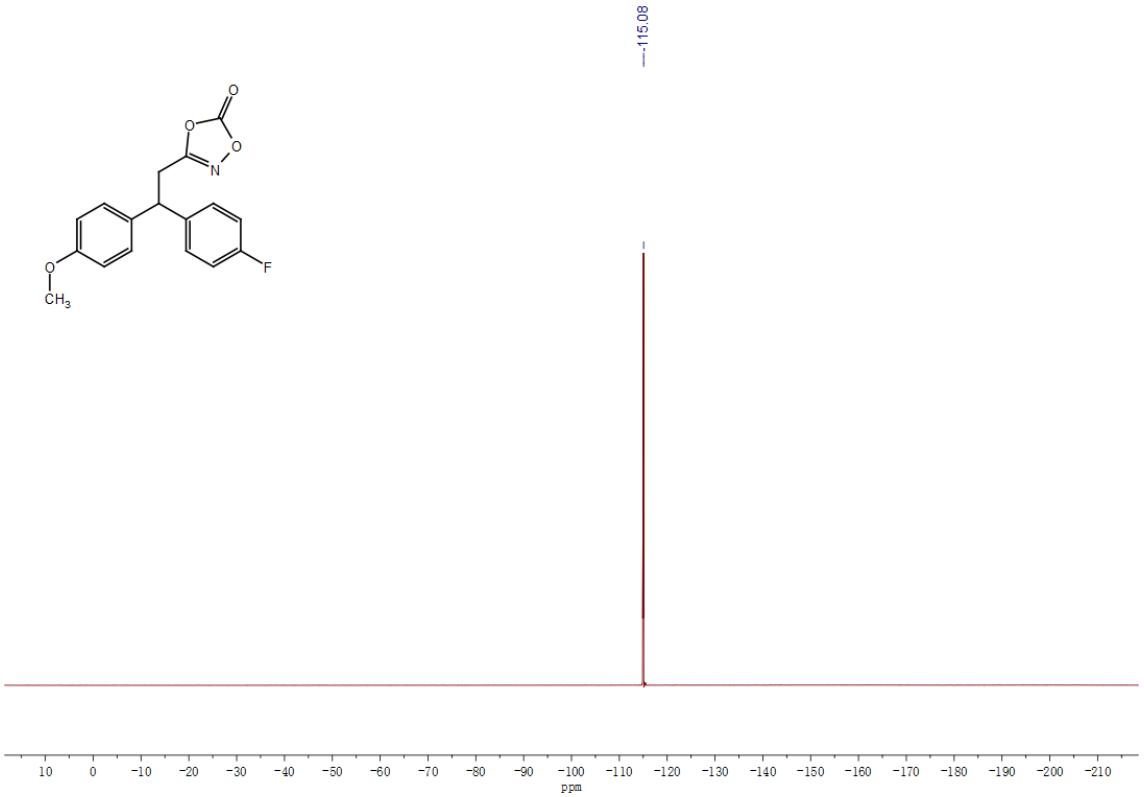
^{1}H NMR of 1j



^{13}C NMR of 1j



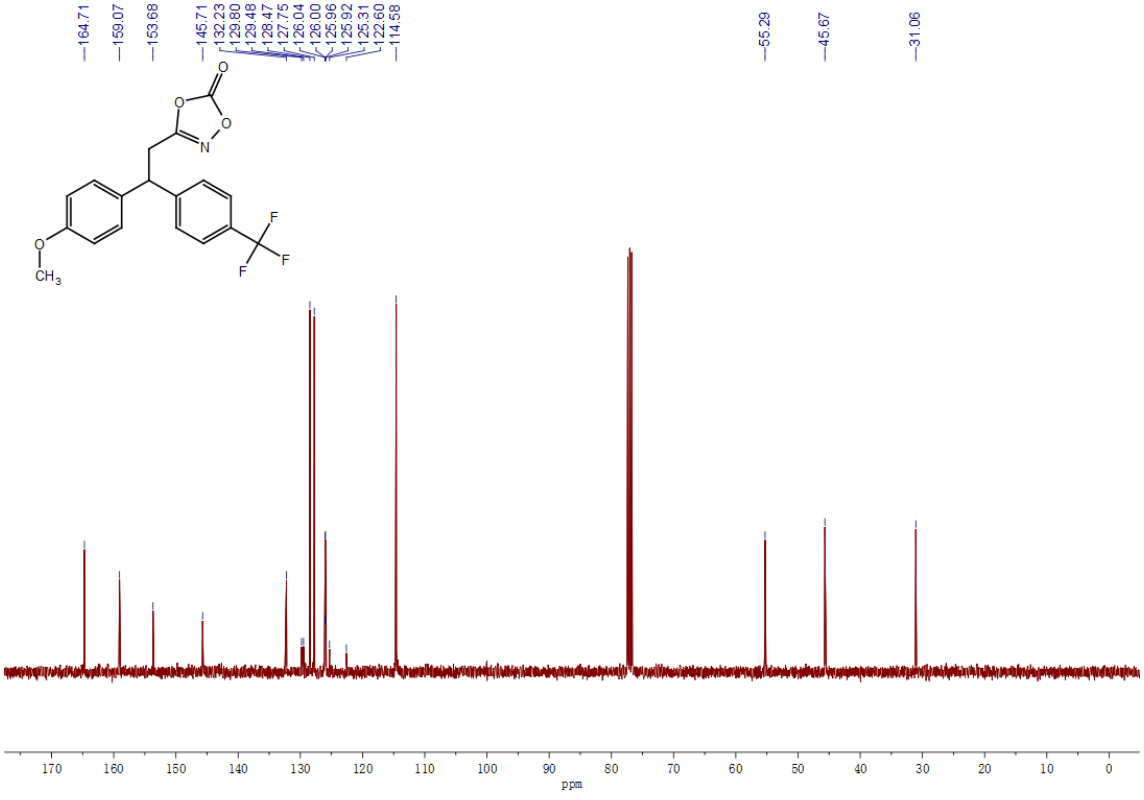
^{19}F NMR of 1j


-115.08
O
O
O
N
O
CH3
F
10
0
-10
-20
-30
-40
-50
-60
-70
-80
-90
-100
-110
-120
-130
-140
-150
-160
-170
-180
-190
-200
-210
ppm

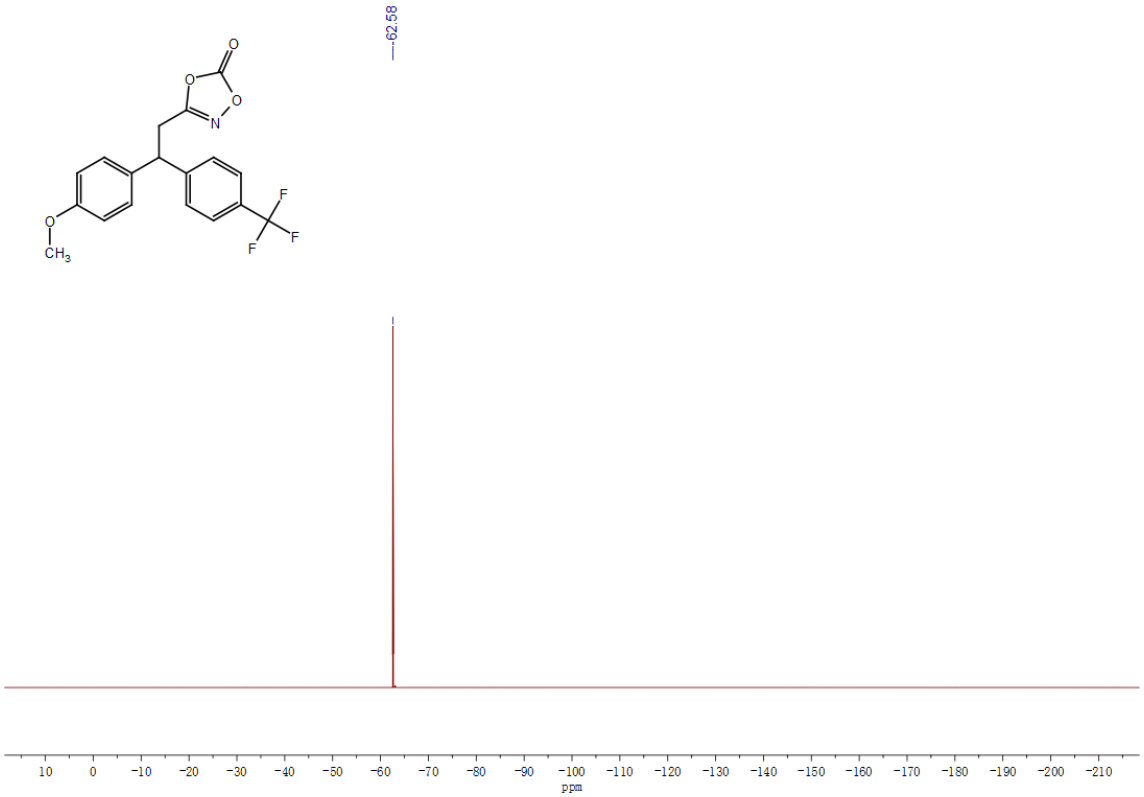
^{1}H NMR of 1k



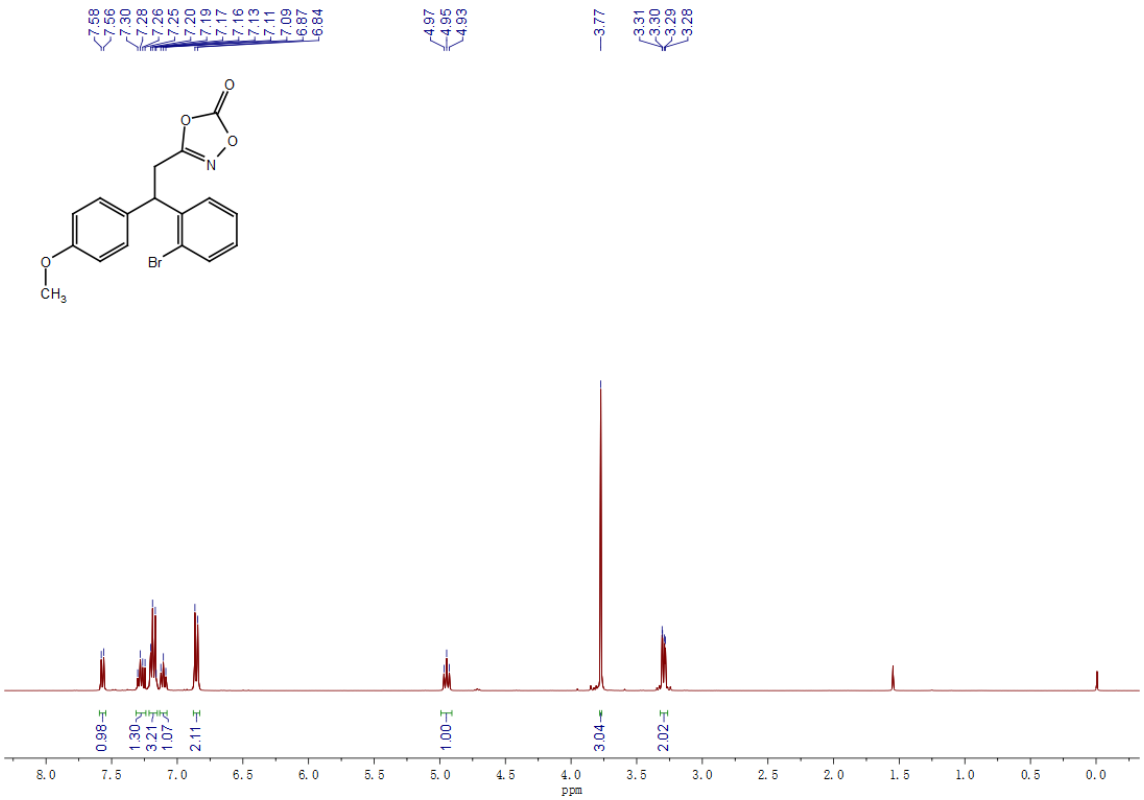
^{13}C NMR of 1k



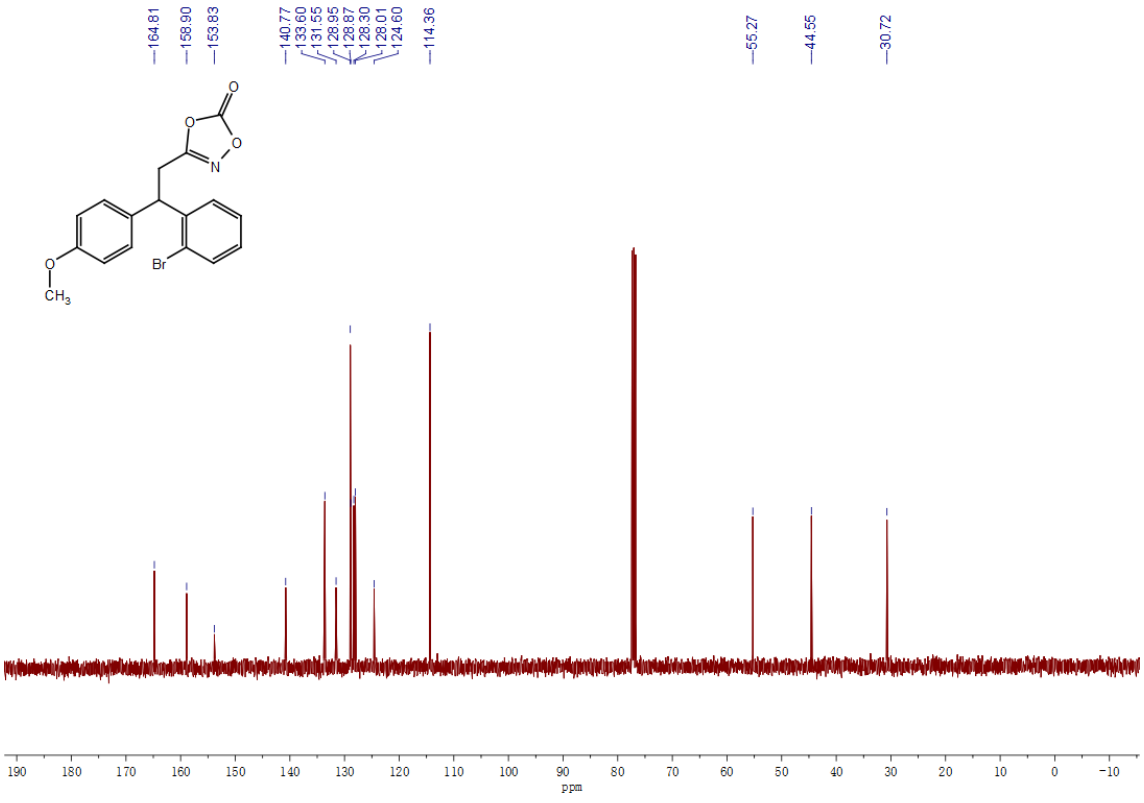
^{19}F NMR of 1k


-62.58
10 0 -10 -20 -30 -40 -50 -60 -70 -80 -90 -100 -110 -120 -130 -140 -150 -160 -170 -180 -190 -200 -210
ppm

^{1}H NMR of 1l



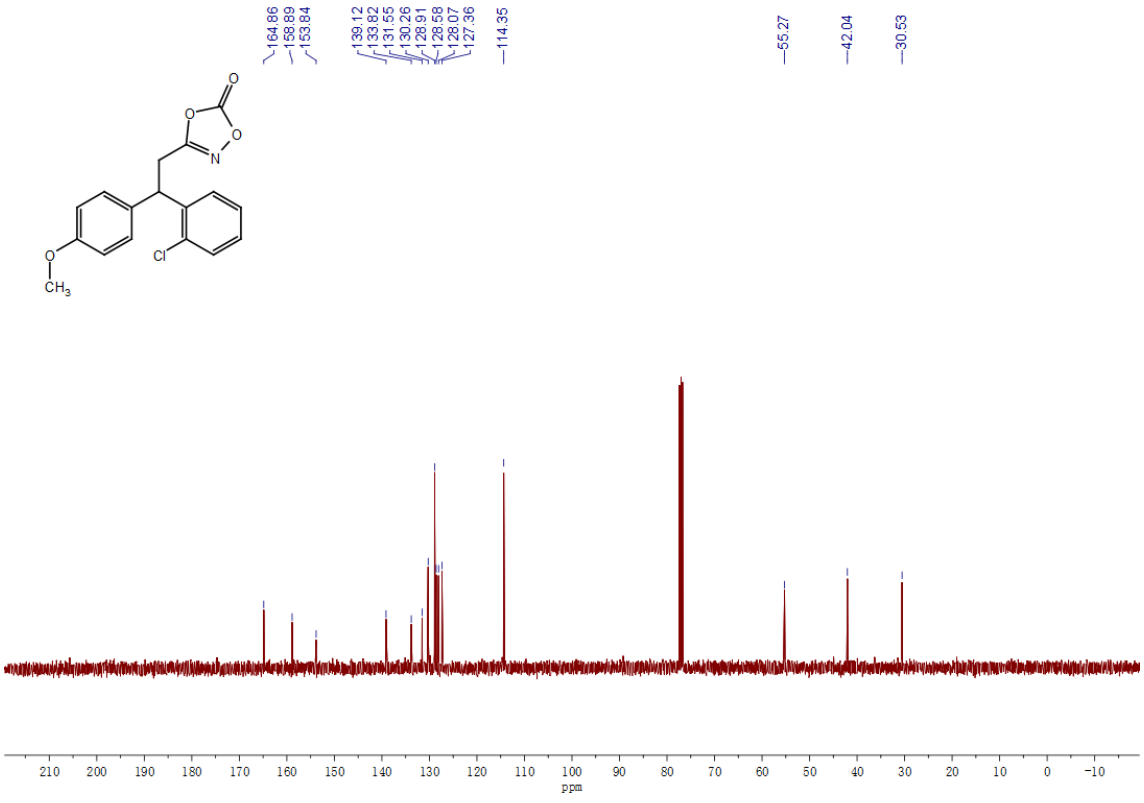
^{13}C NMR of 1l



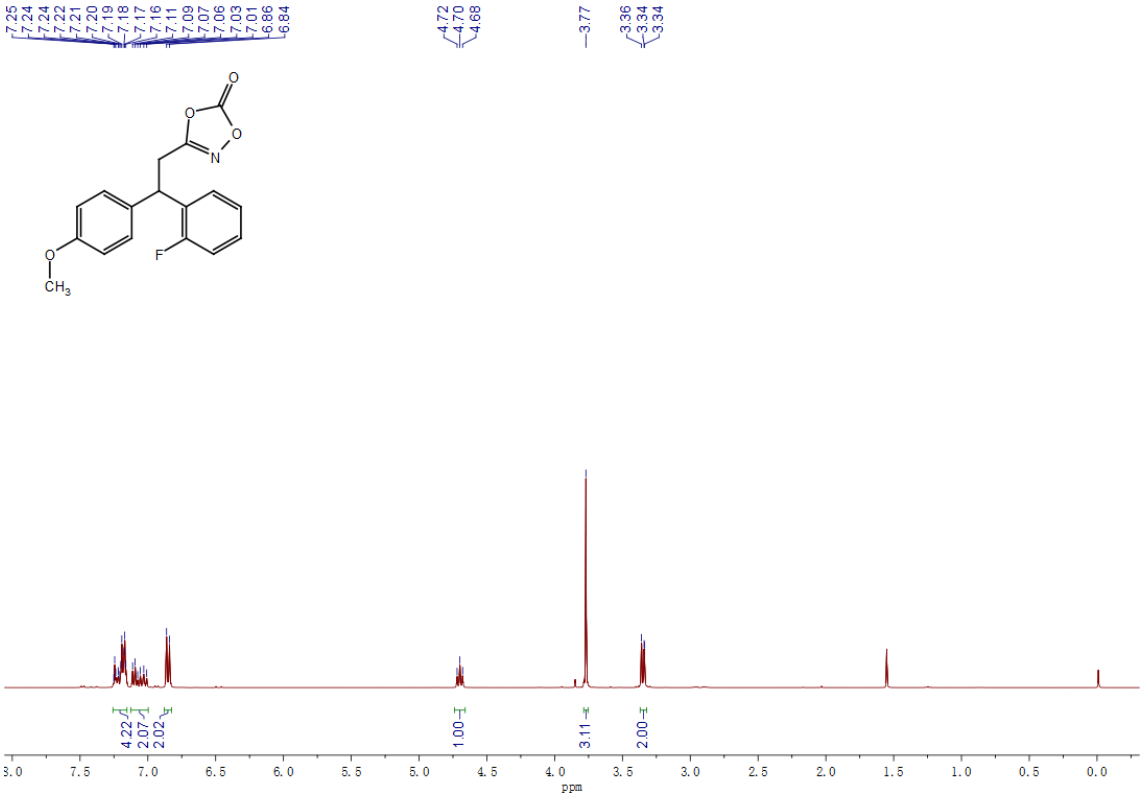
^{1}H NMR of 1m



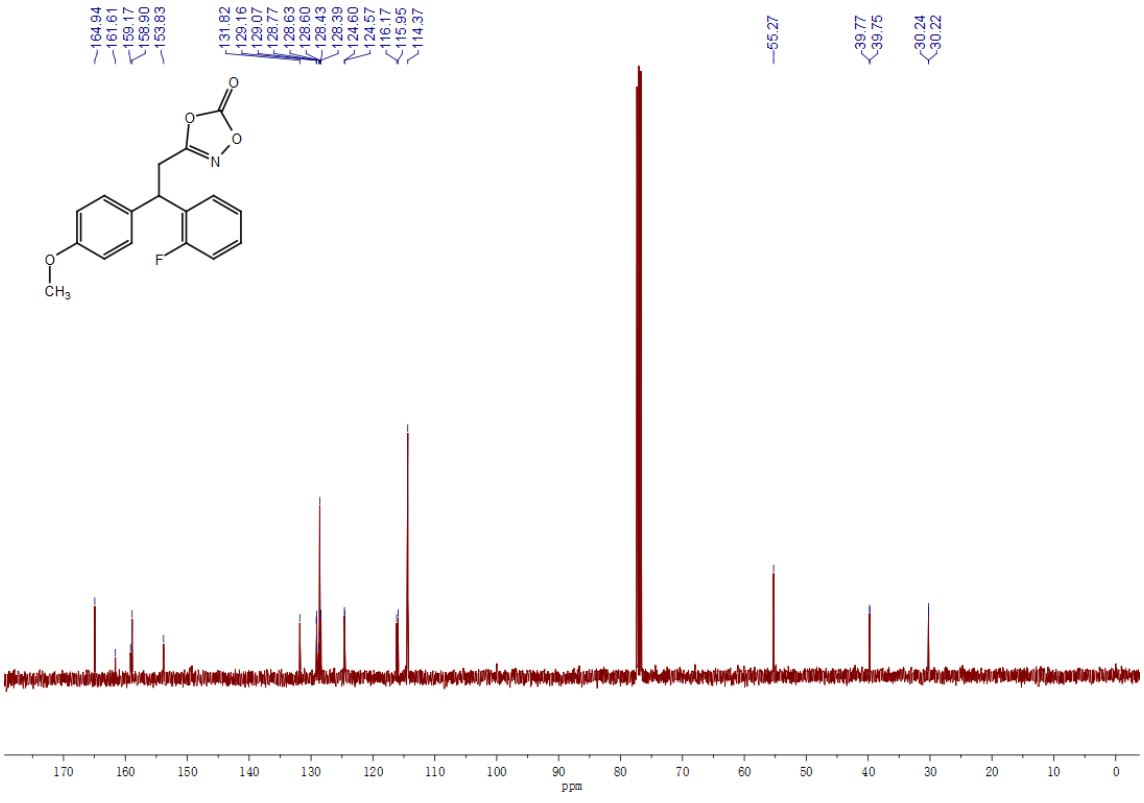
^{13}C NMR of 1m



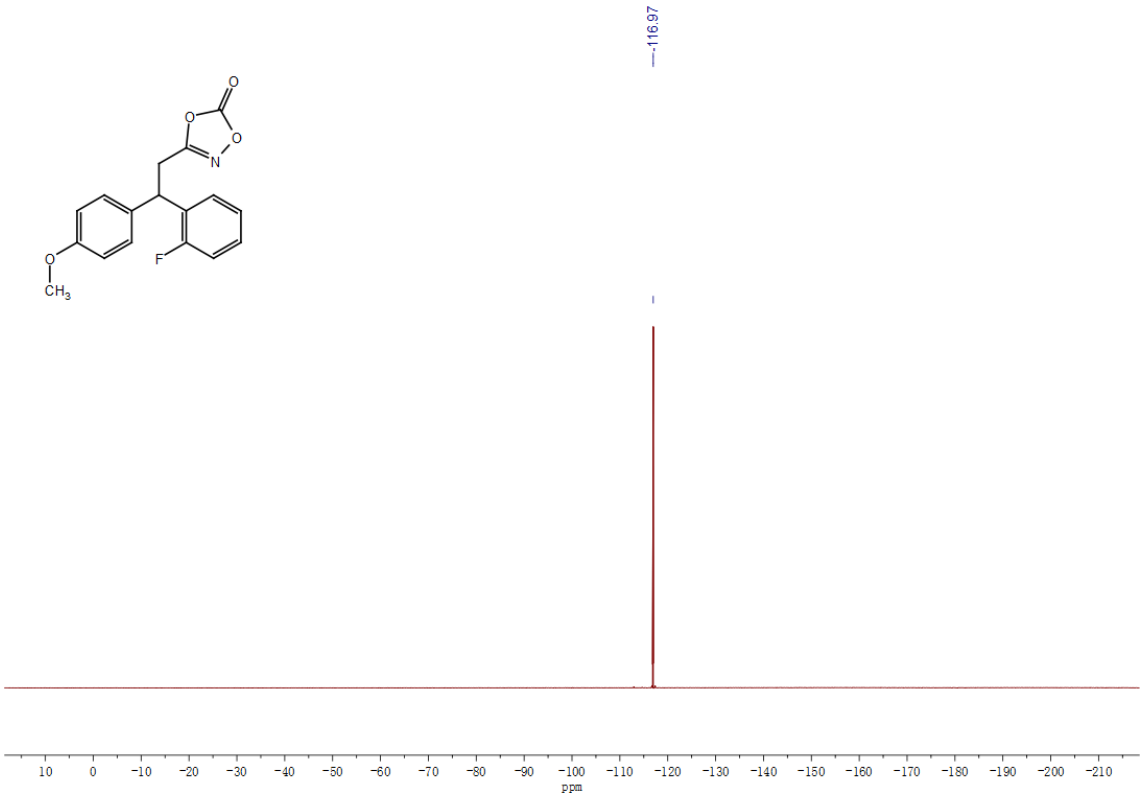
^{1}H NMR of 1n



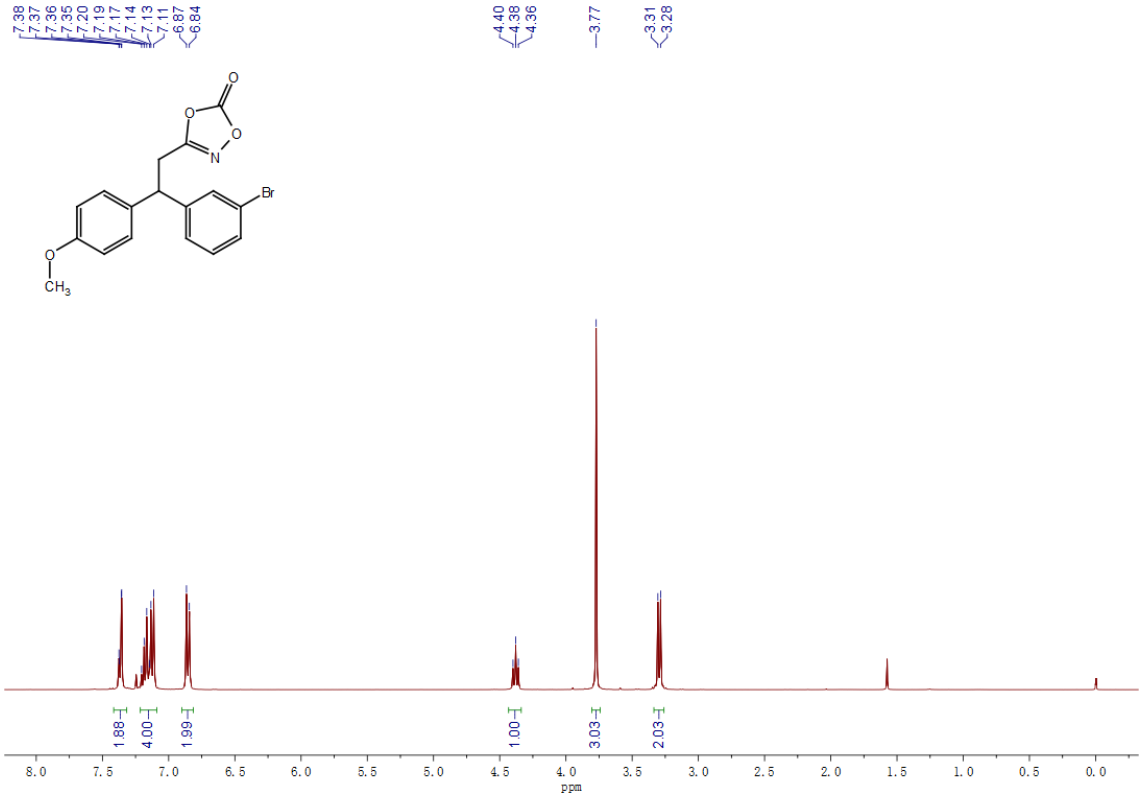
^{13}C NMR of 1n



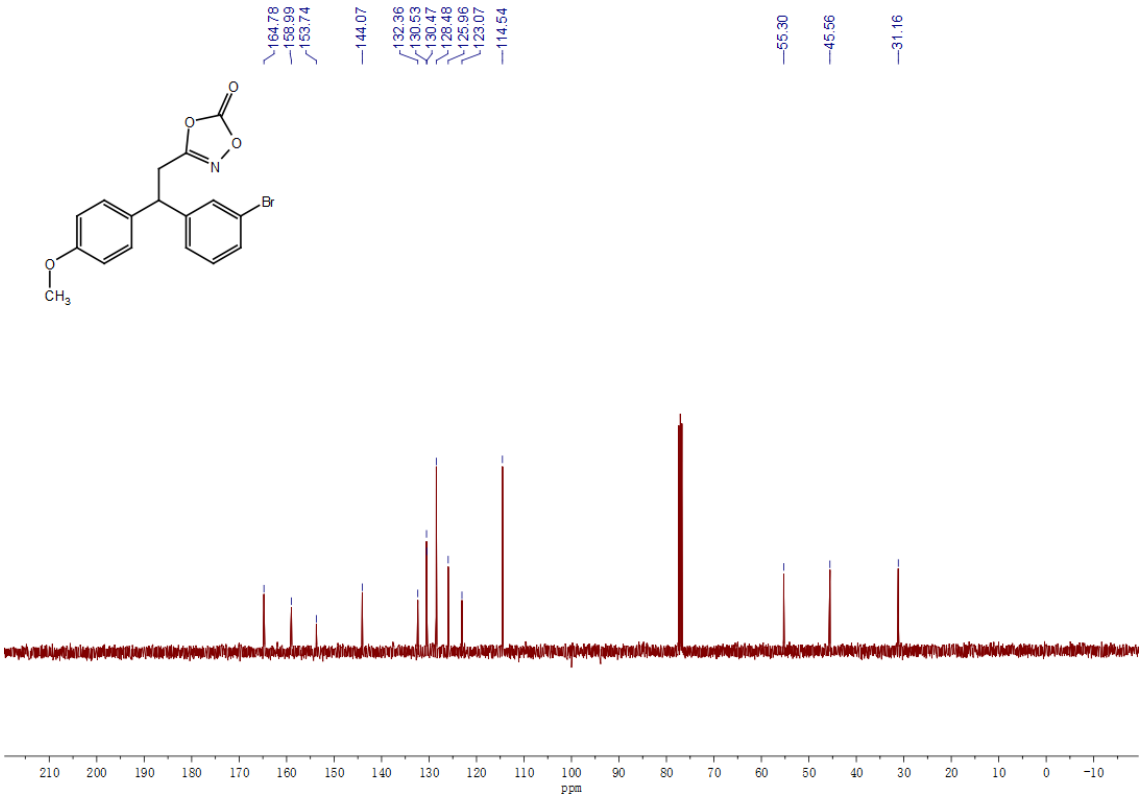
^{19}F NMR of 1n


-116.97
O
O
O
N
O
F
O
CH3
10
0
-10
-20
-30
-40
-50
-60
-70
-80
-90
-100
-110
-120
-130
-140
-150
-160
-170
-180
-190
-200
-210
ppm

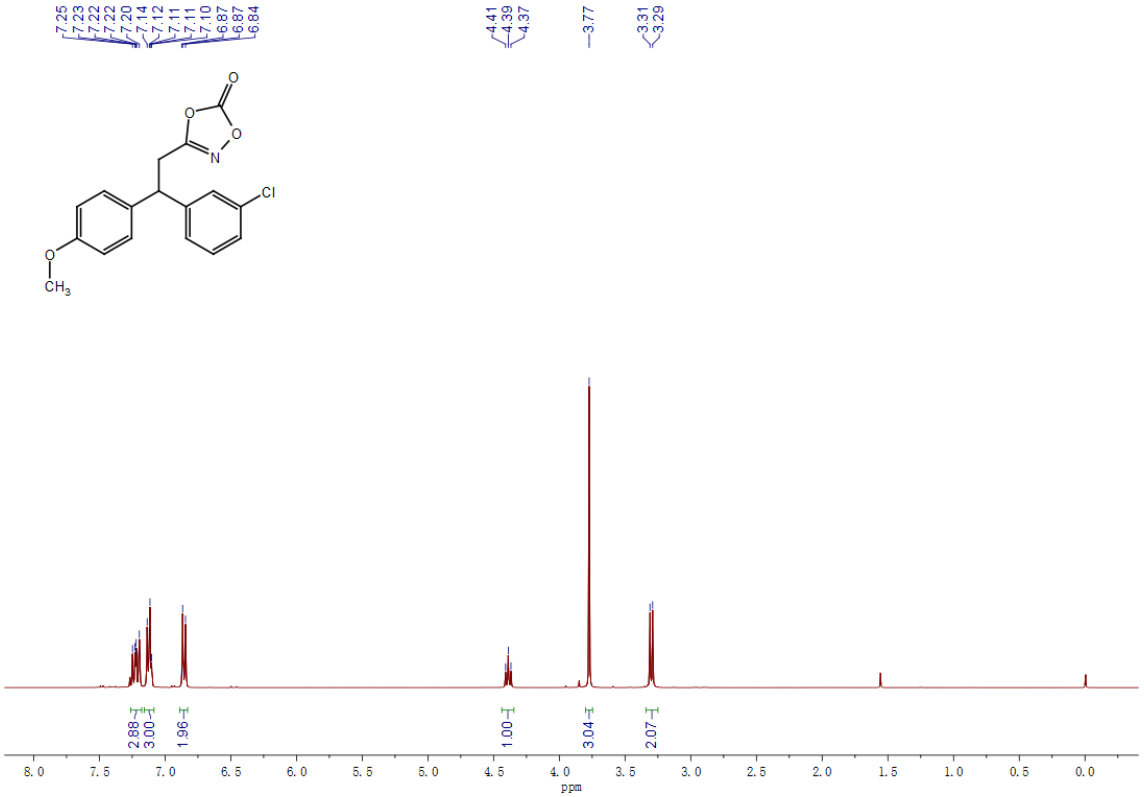
^{1}H NMR of 1o



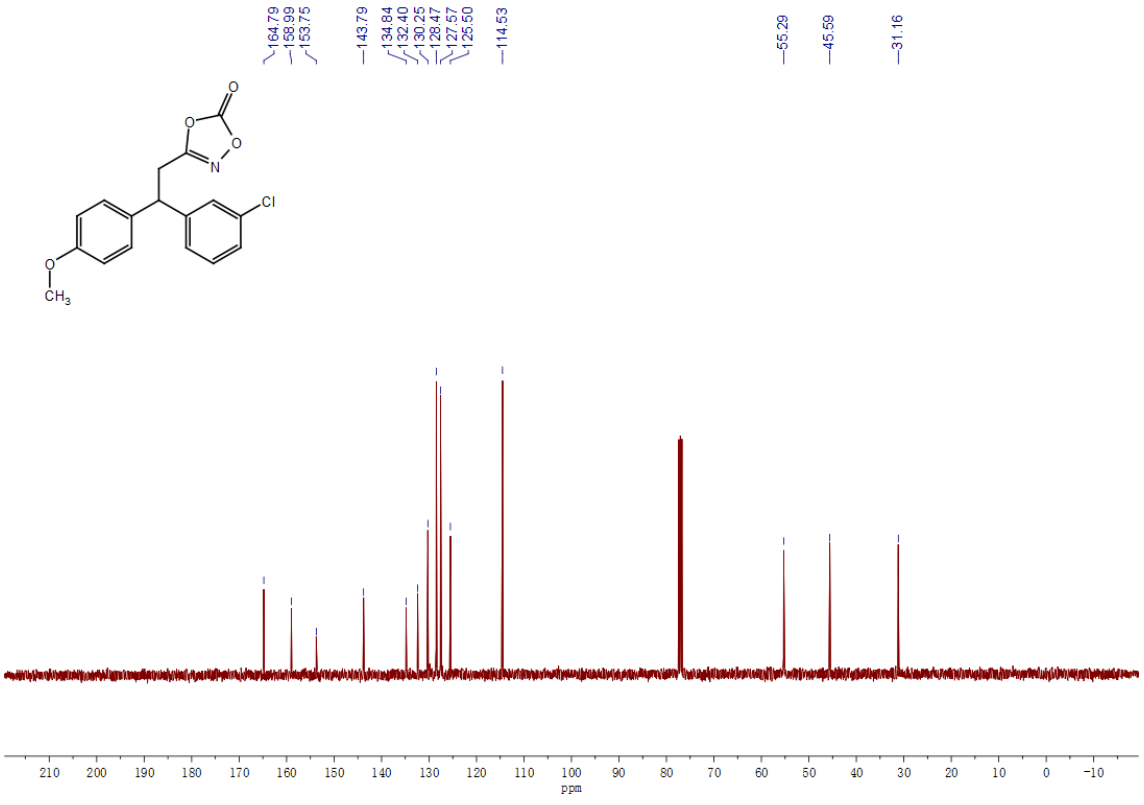
^{13}C NMR of 1o



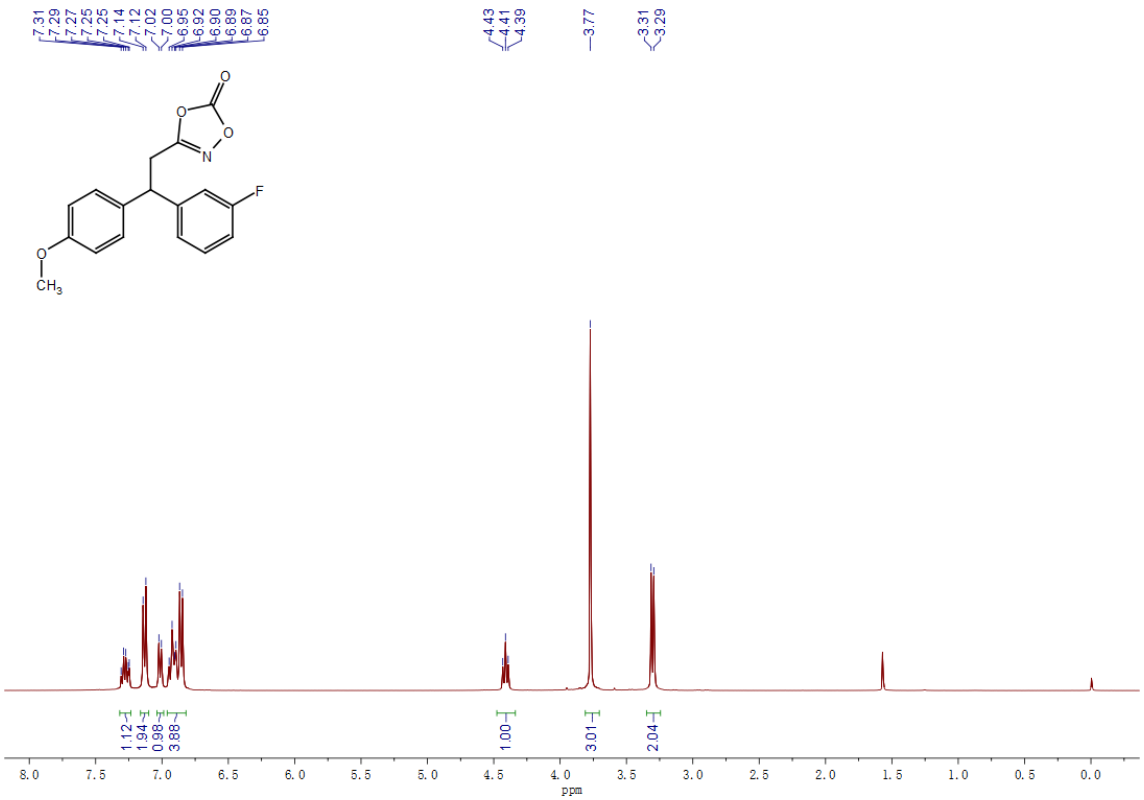
^{1}H NMR of 1p



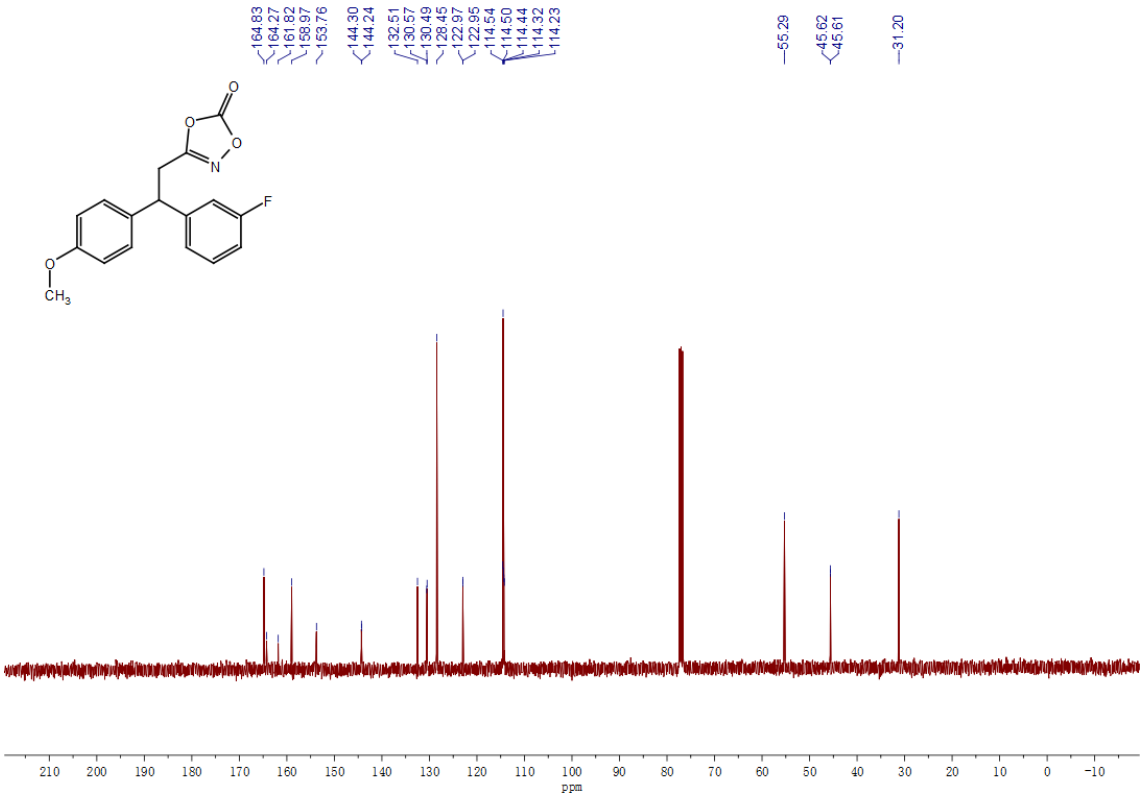
^{13}C NMR of 1p



^{1}H NMR of 1q



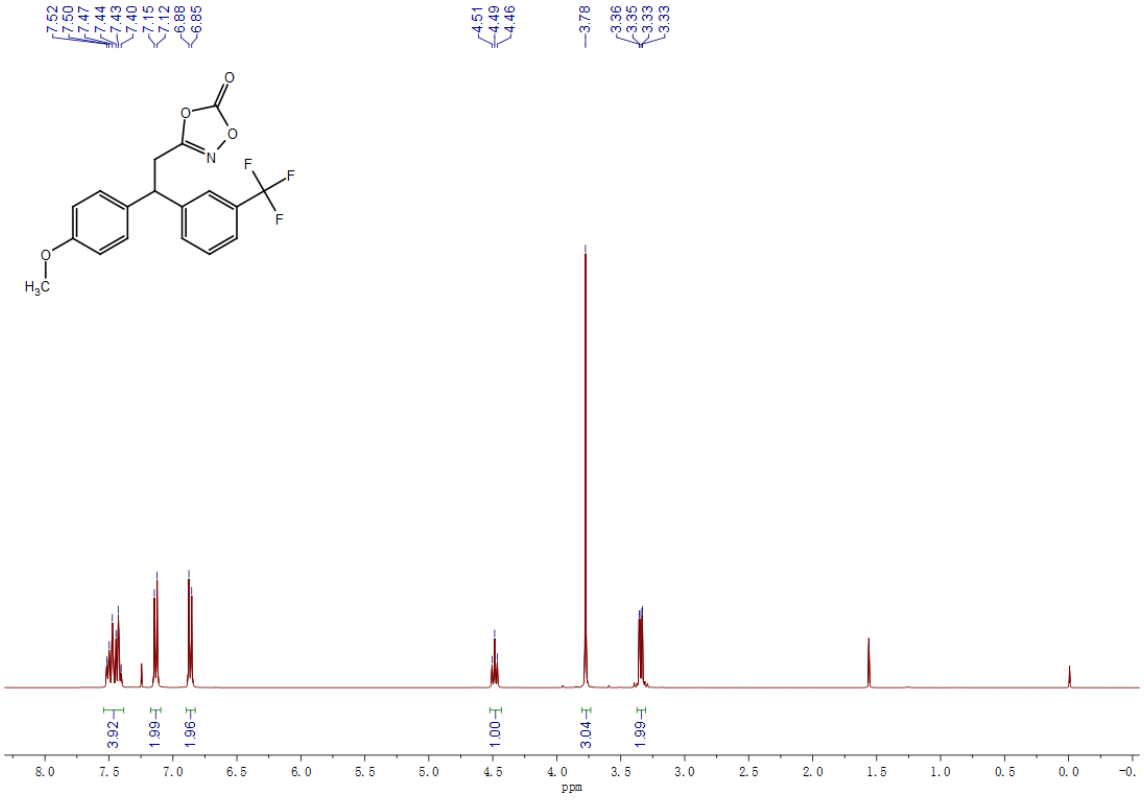
^{13}C NMR of 1q



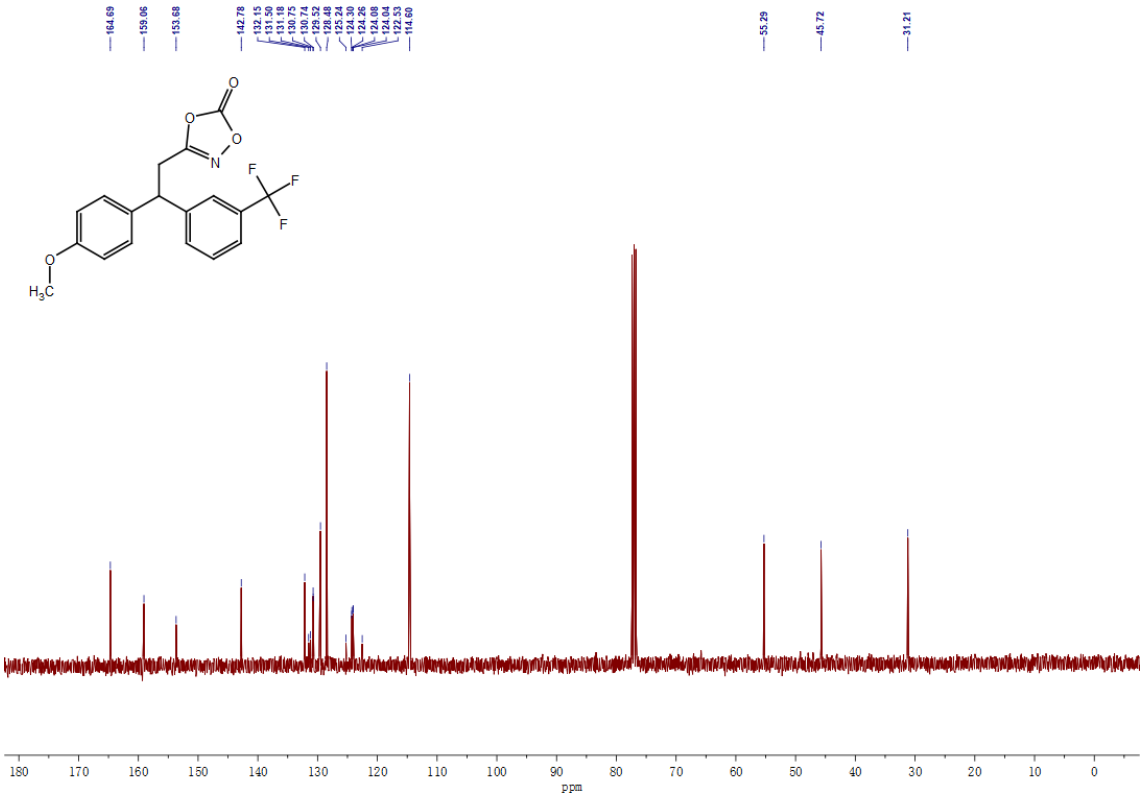
^{19}F NMR of 1q


-111.85
O
O
O
N
F
O
CH3
10
0
-10
-20
-30
-40
-50
-60
-70
-80
-90
-100
-110
-120
-130
-140
-150
-160
-170
-180
-190
-200
-210
ppm

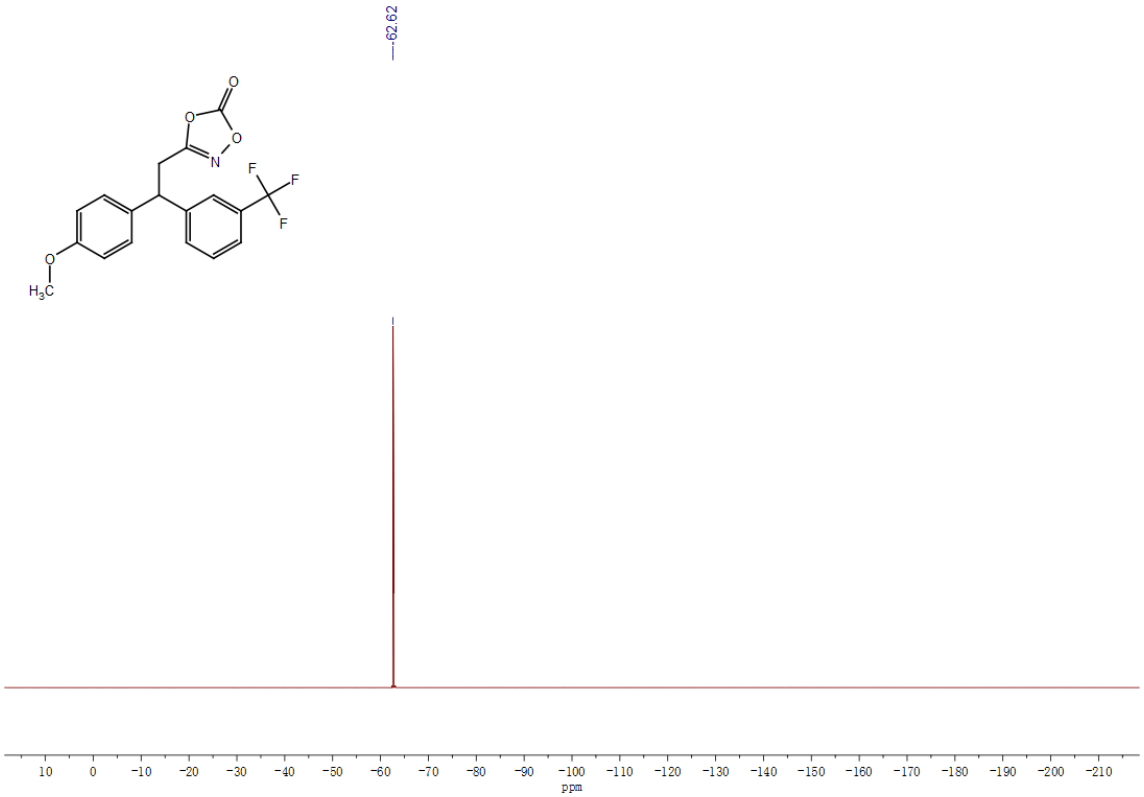
^{1}H NMR of 1r



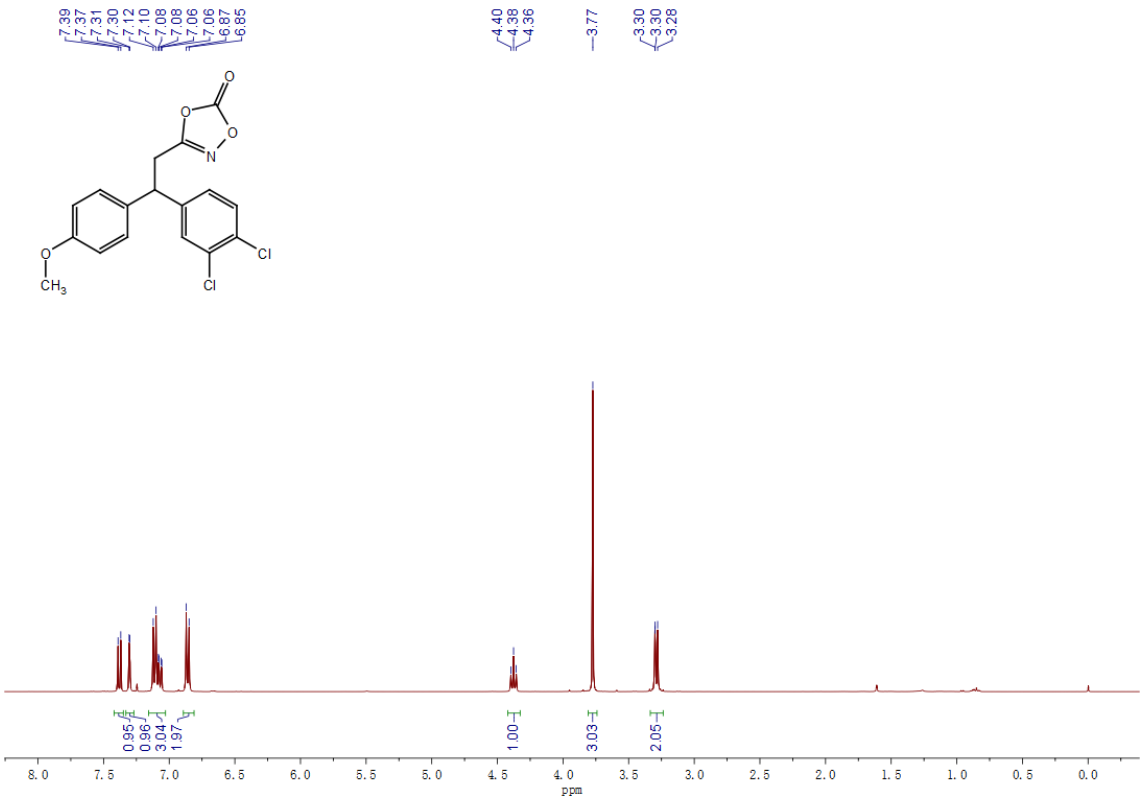
^{13}C NMR of 1r



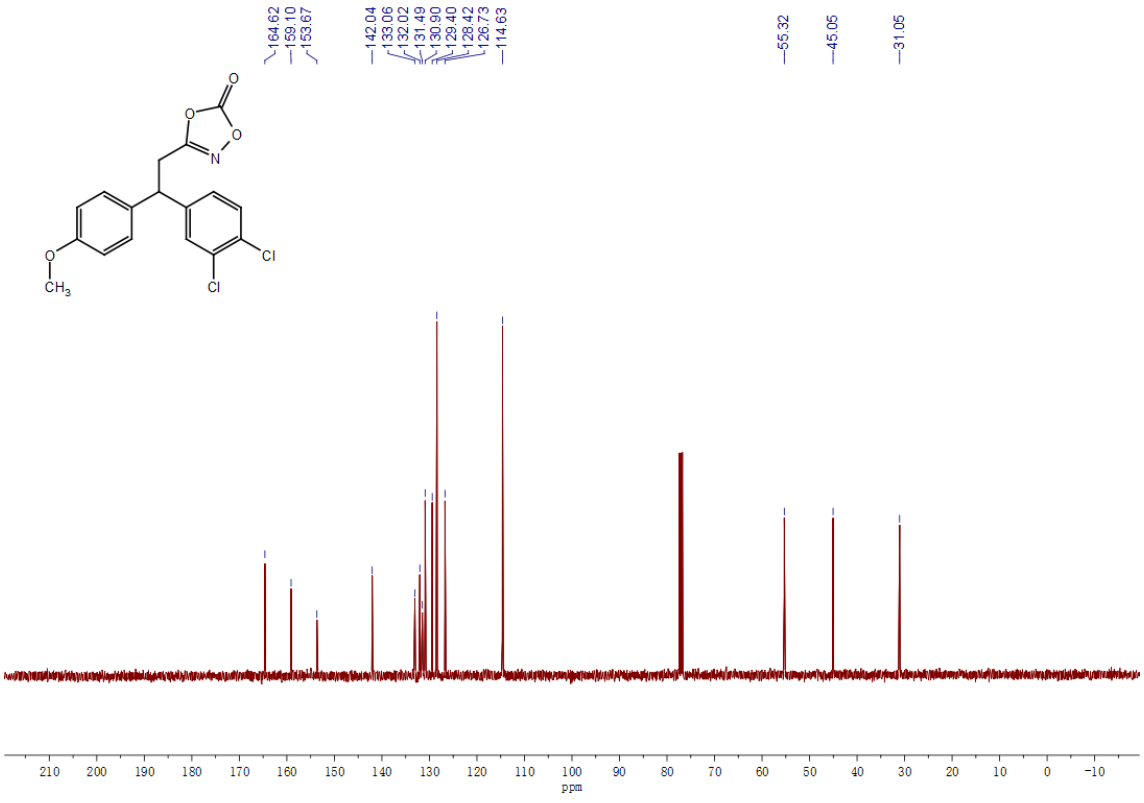
^{19}F NMR of 1r


-62.62
O
O
O
N
O
F
F
F
O
H3C
10
0
-10
-20
-30
-40
-50
-60
-70
-80
-90
-100
-110
-120
-130
-140
-150
-160
-170
-180
-190
-200
-210
ppm

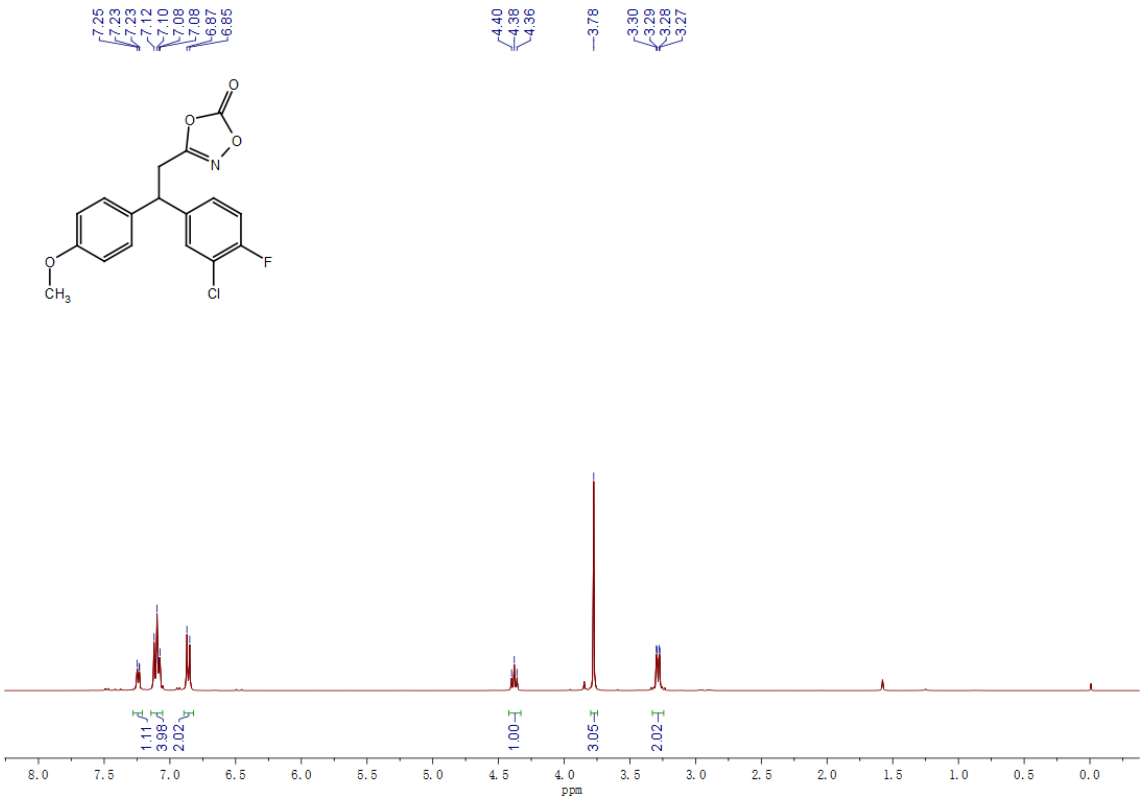
^{1}H NMR of 1s



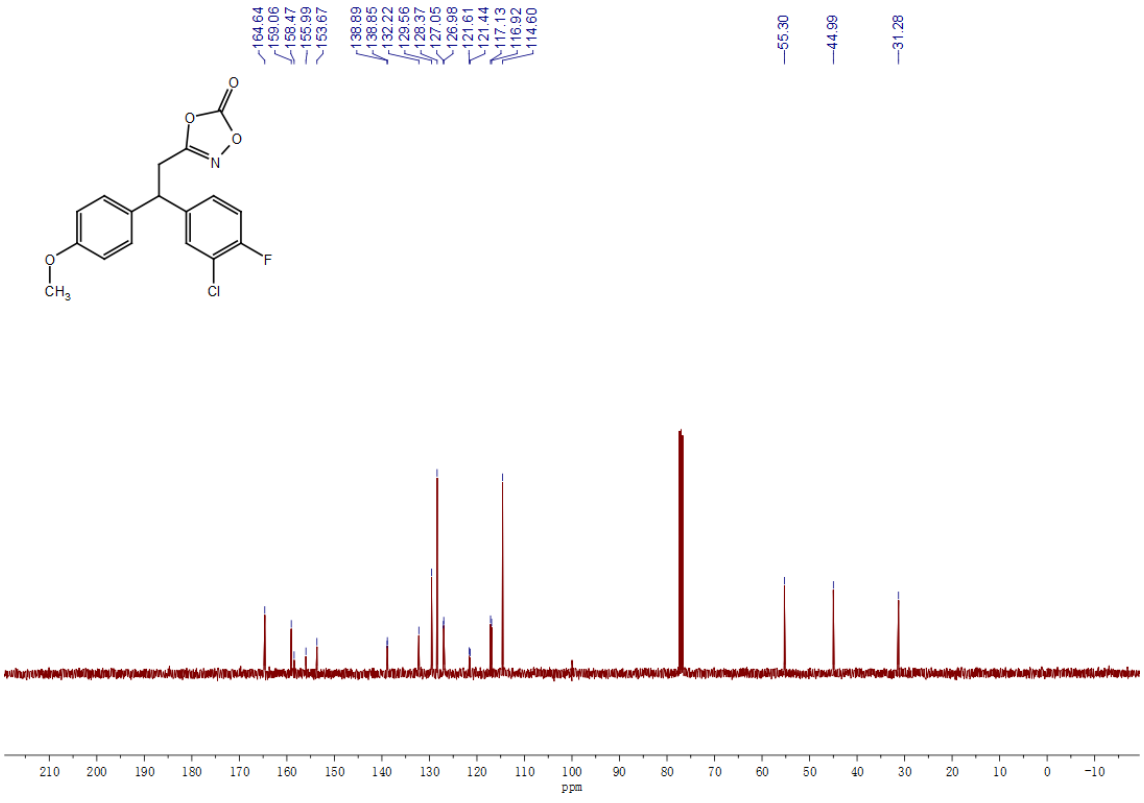
^{13}C NMR of 1s



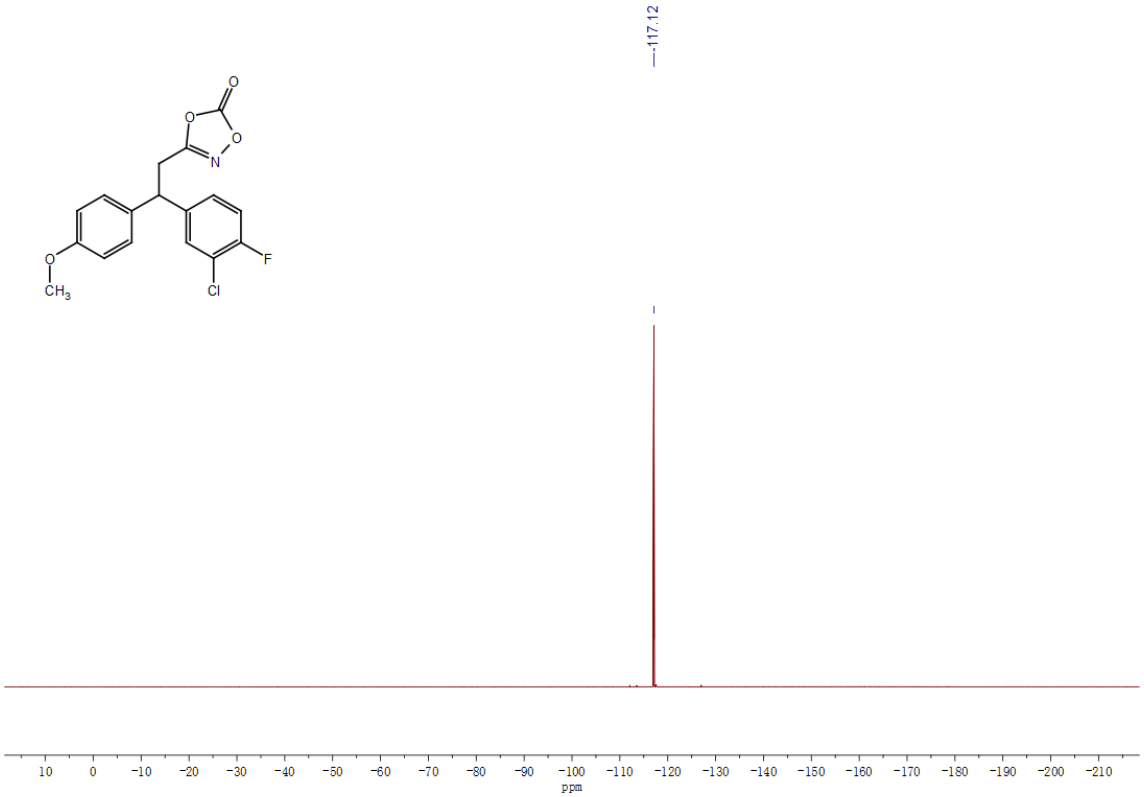
^{1}H NMR of 1t



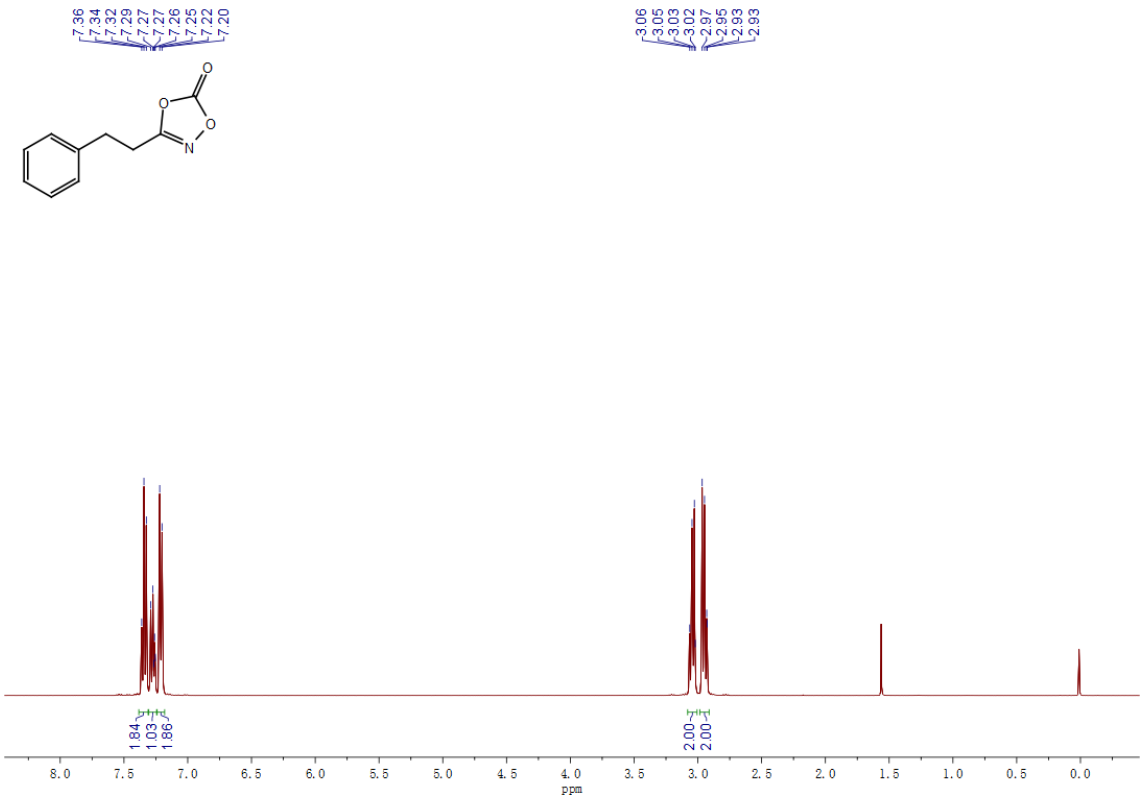
^{13}C NMR of 1t



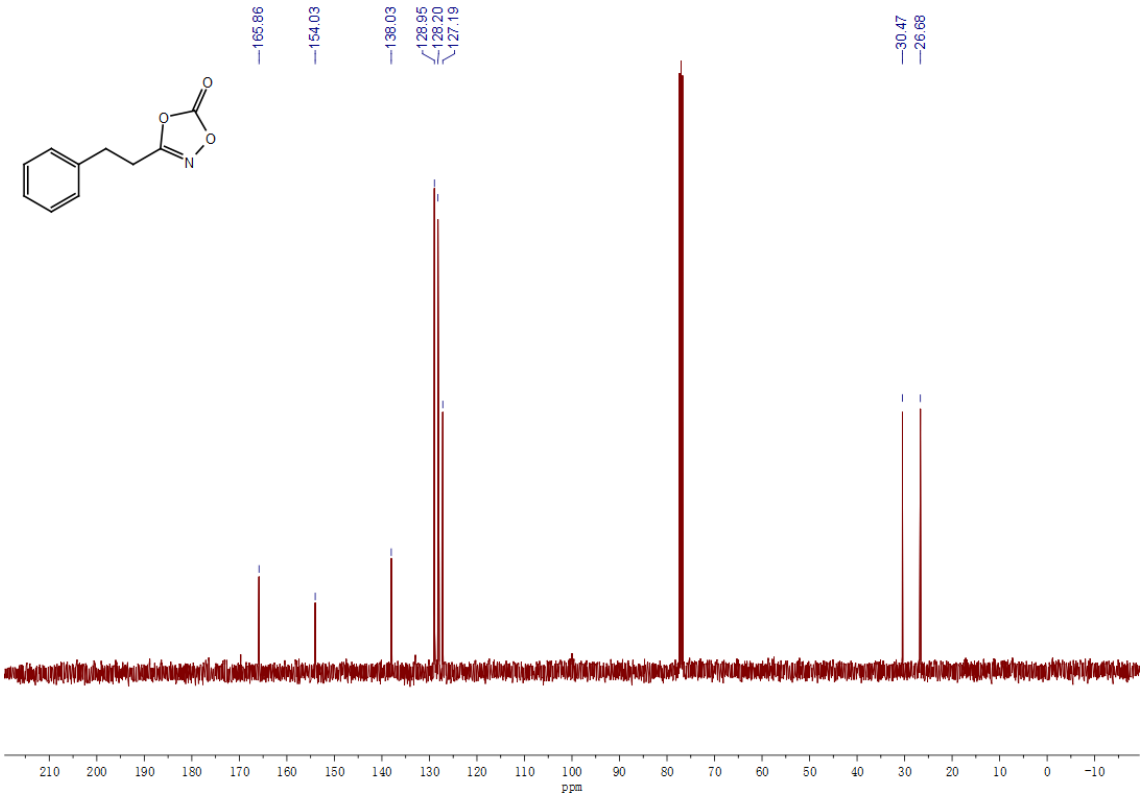
^{19}F NMR of 1t


-117.12
O
O
O
N
O
O
CH3
Cl
F
10
0
-10
-20
-30
-40
-50
-60
-70
-80
-90
-100
-110
-120
-130
-140
-150
-160
-170
-180
-190
-200
-210
ppm

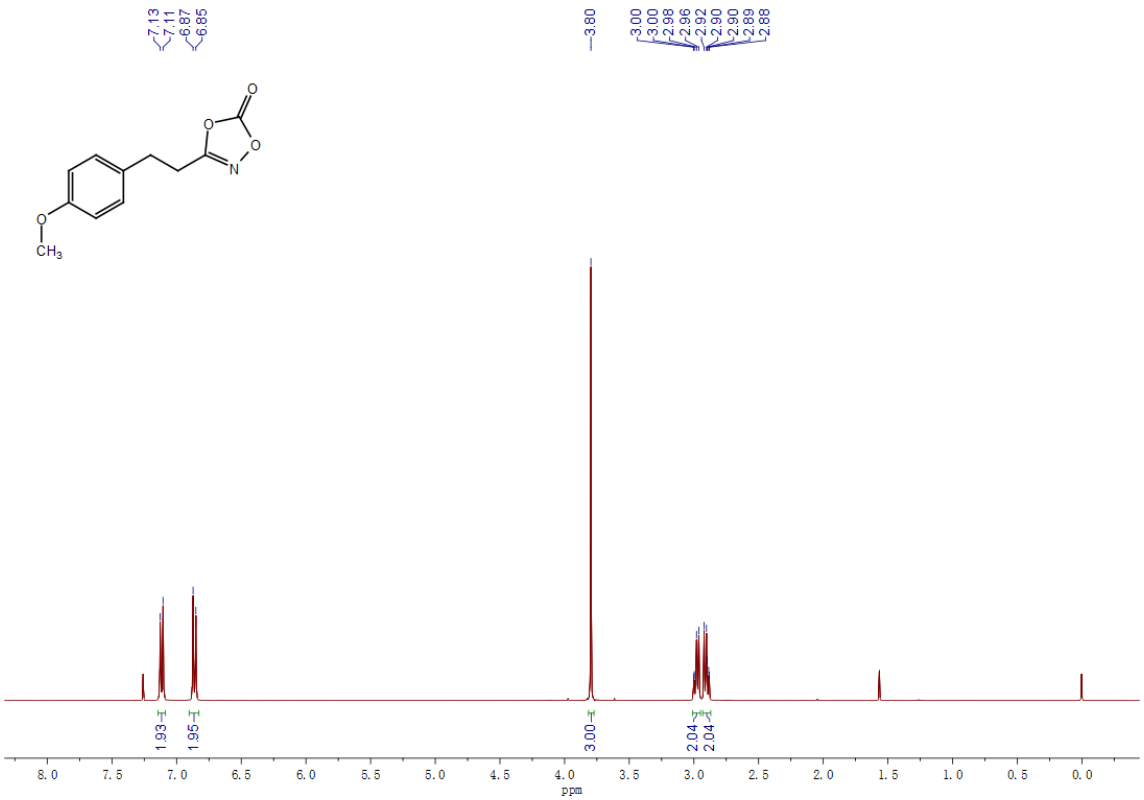
^{1}H NMR of 1u



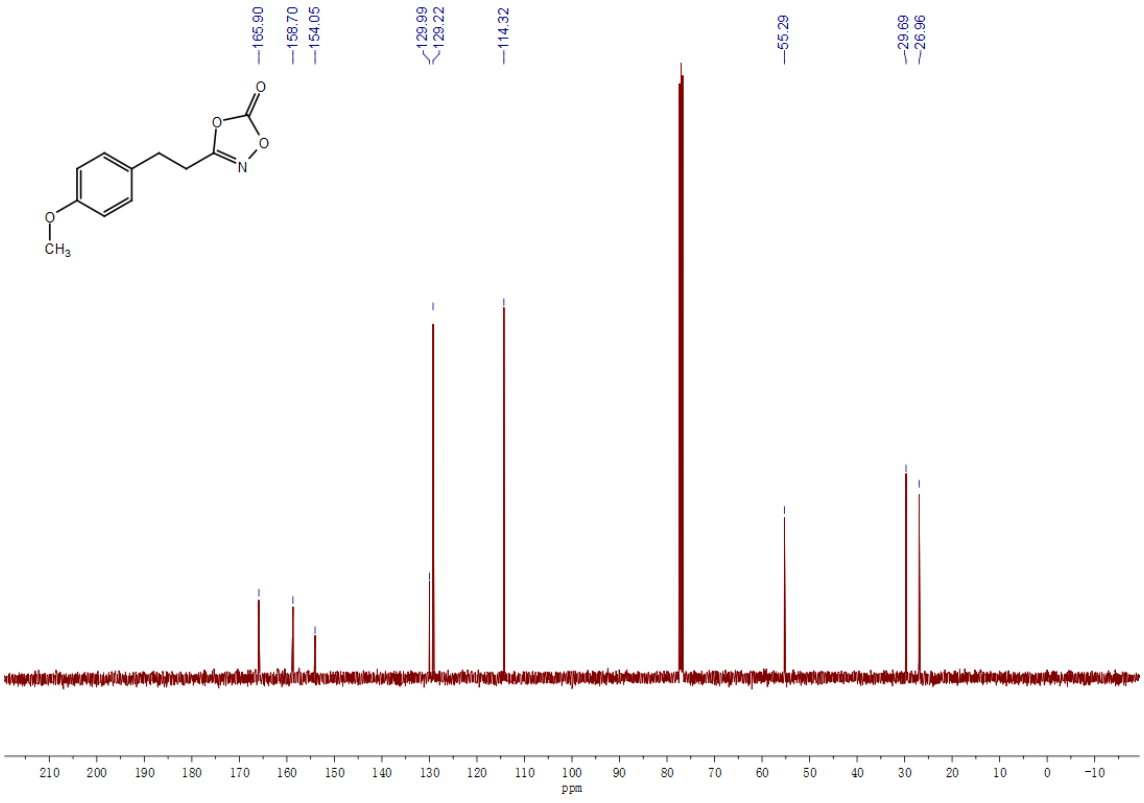
^{13}C NMR of 1u



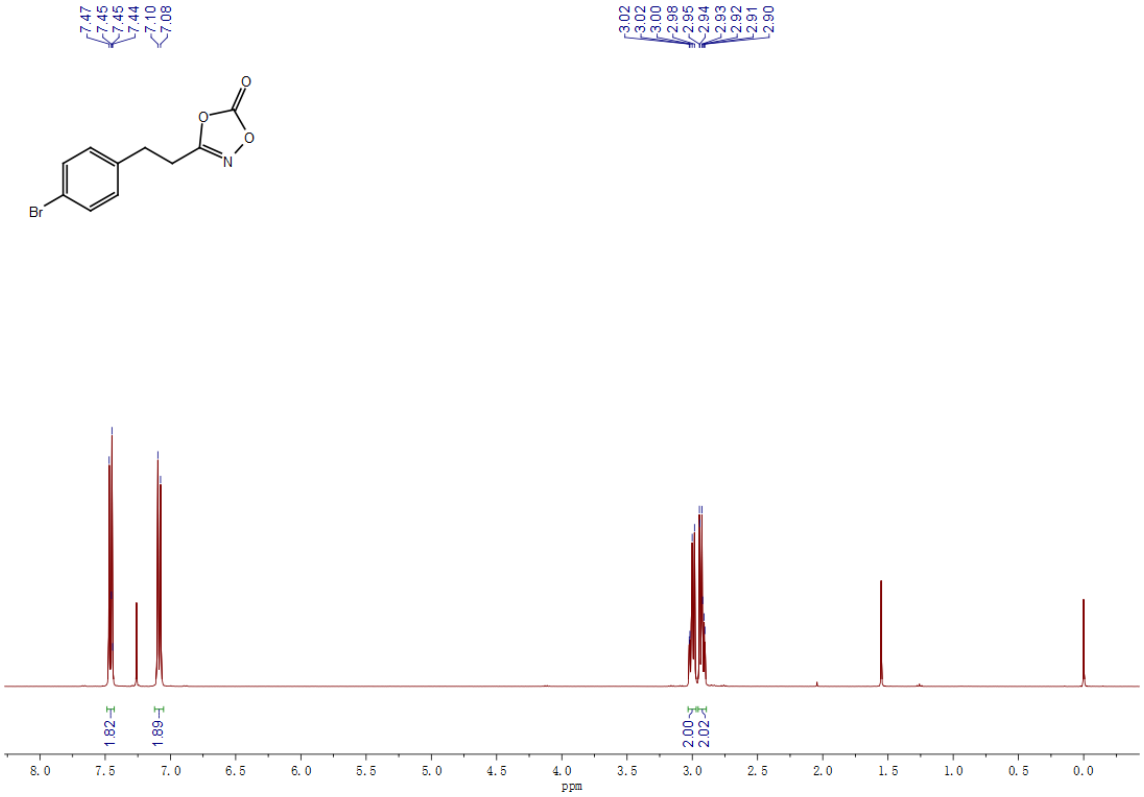
^{1}H NMR of 1v



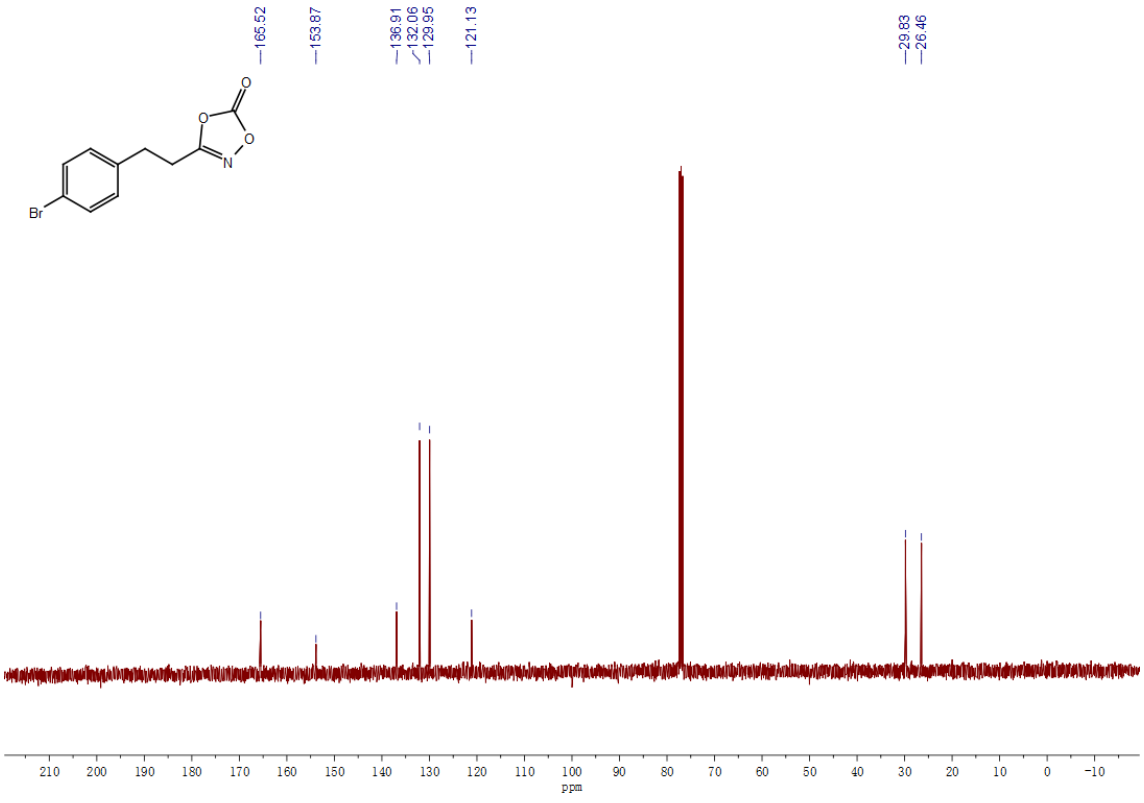
^{13}C NMR of 1v



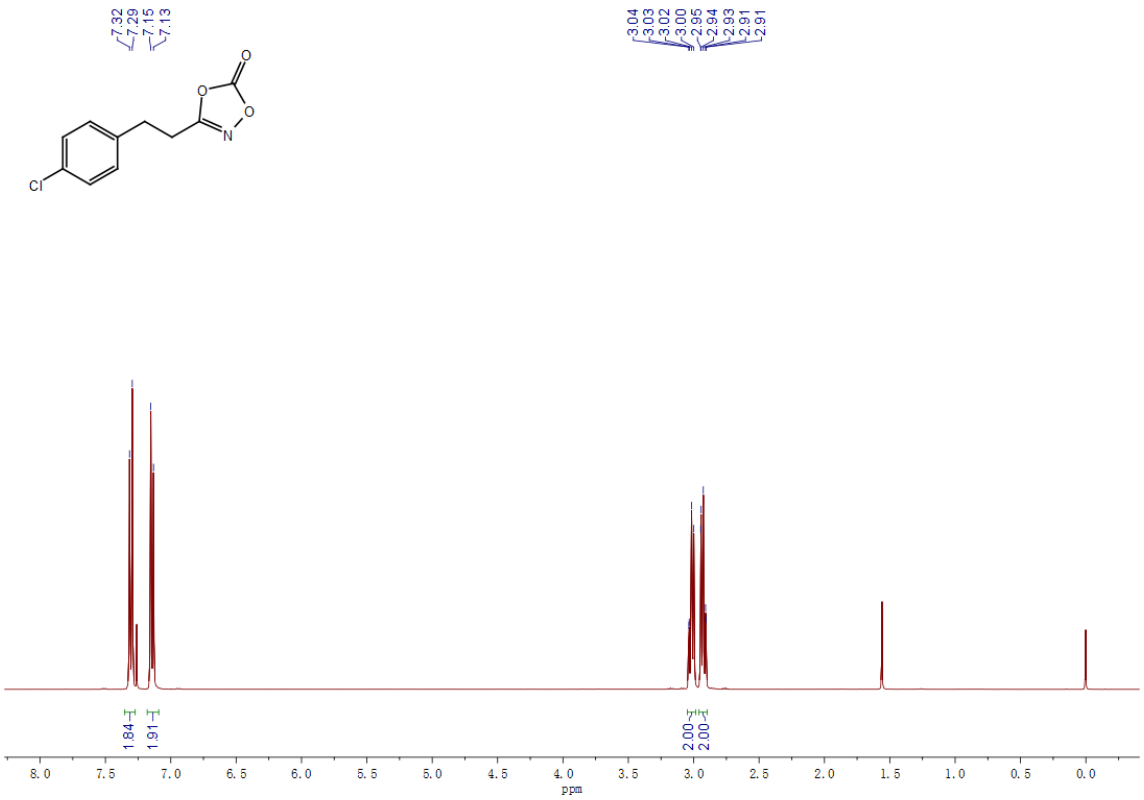
^{1}H NMR of 1w



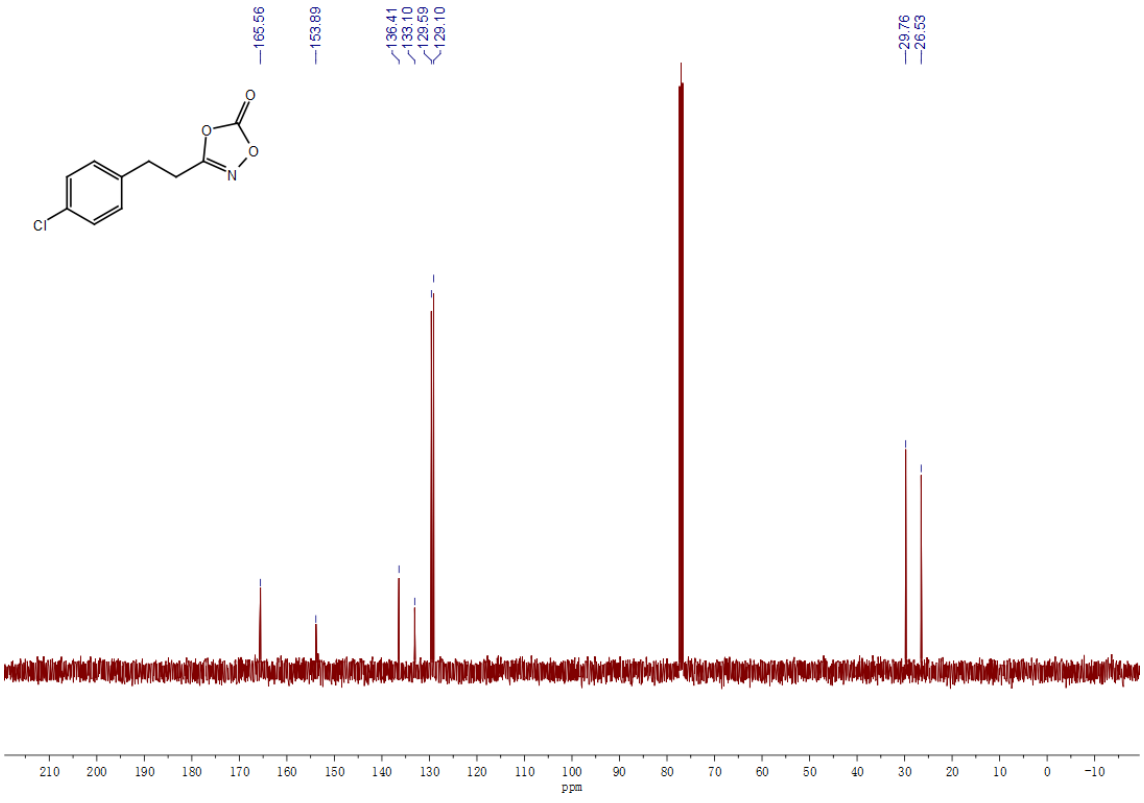
^{13}C NMR of 1w



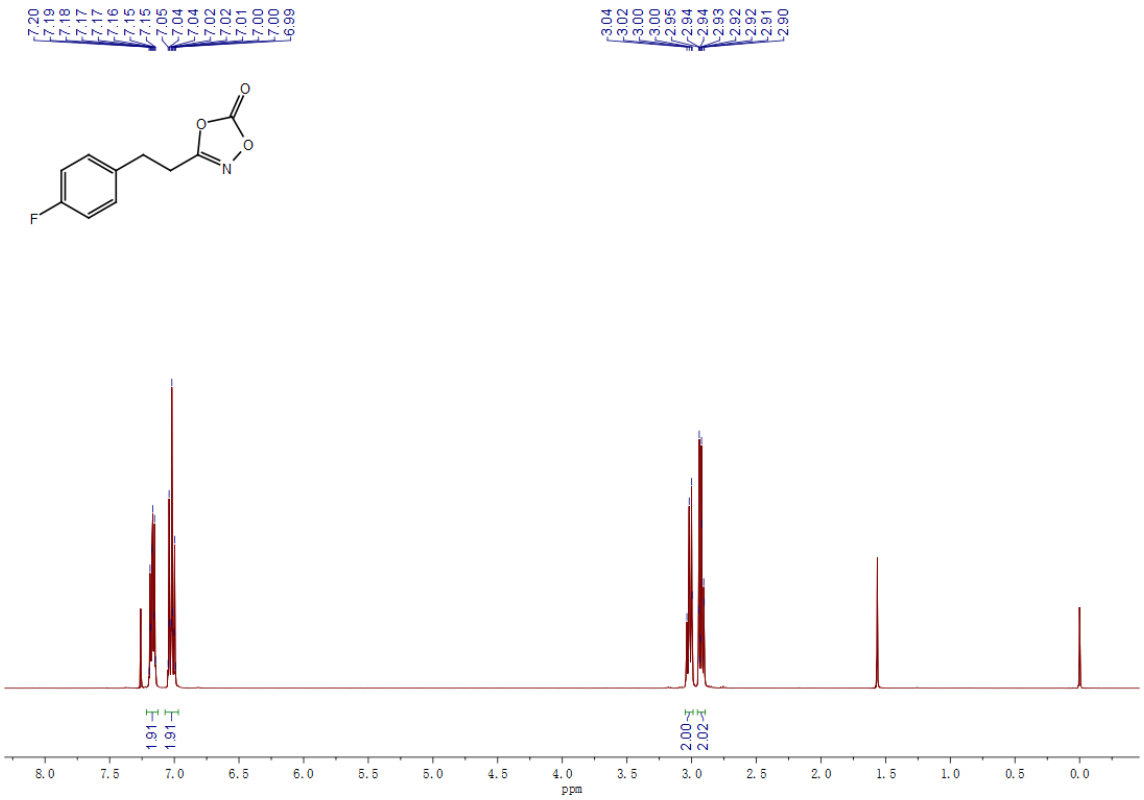
^{1}H NMR of 1x



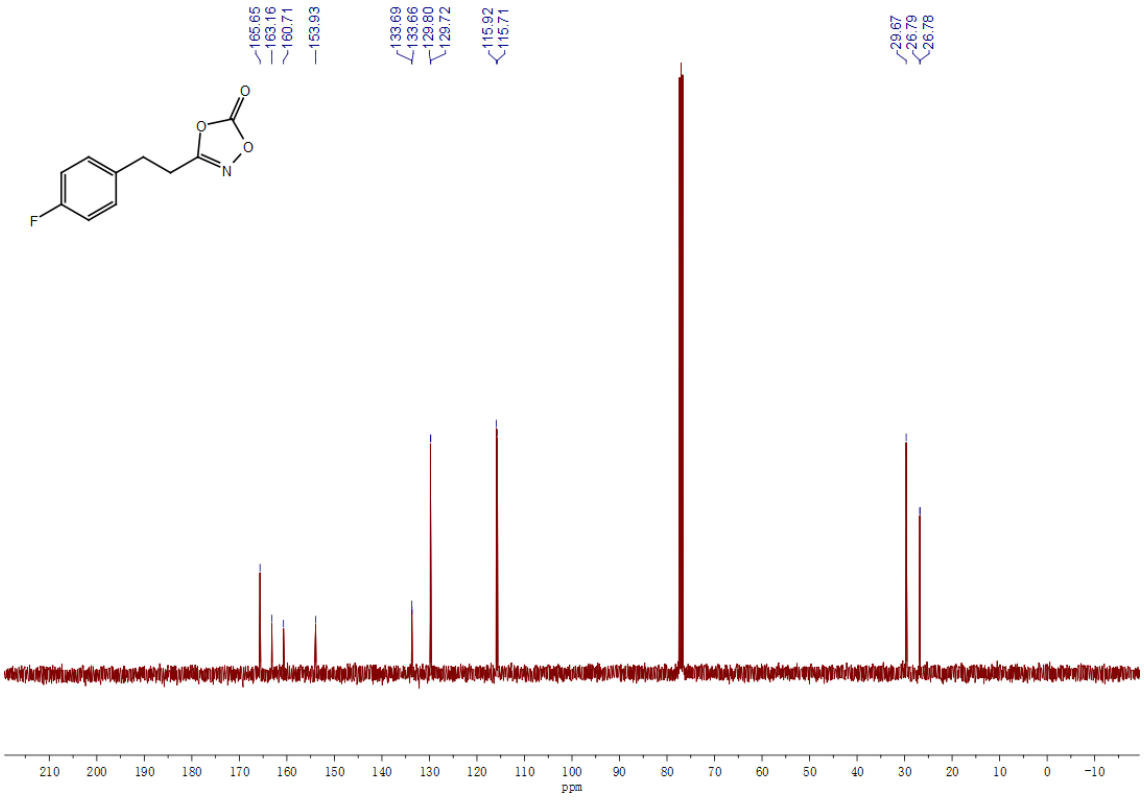
^{13}C NMR of 1x



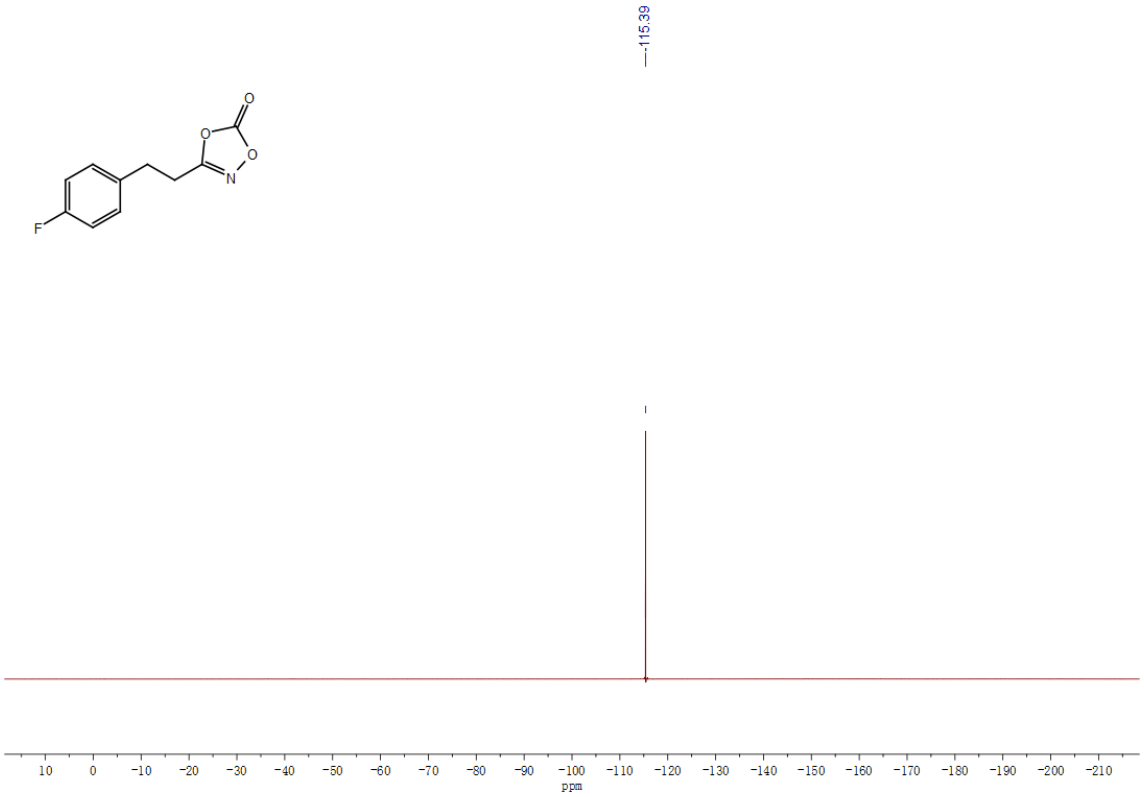
^{1}H NMR of 1y



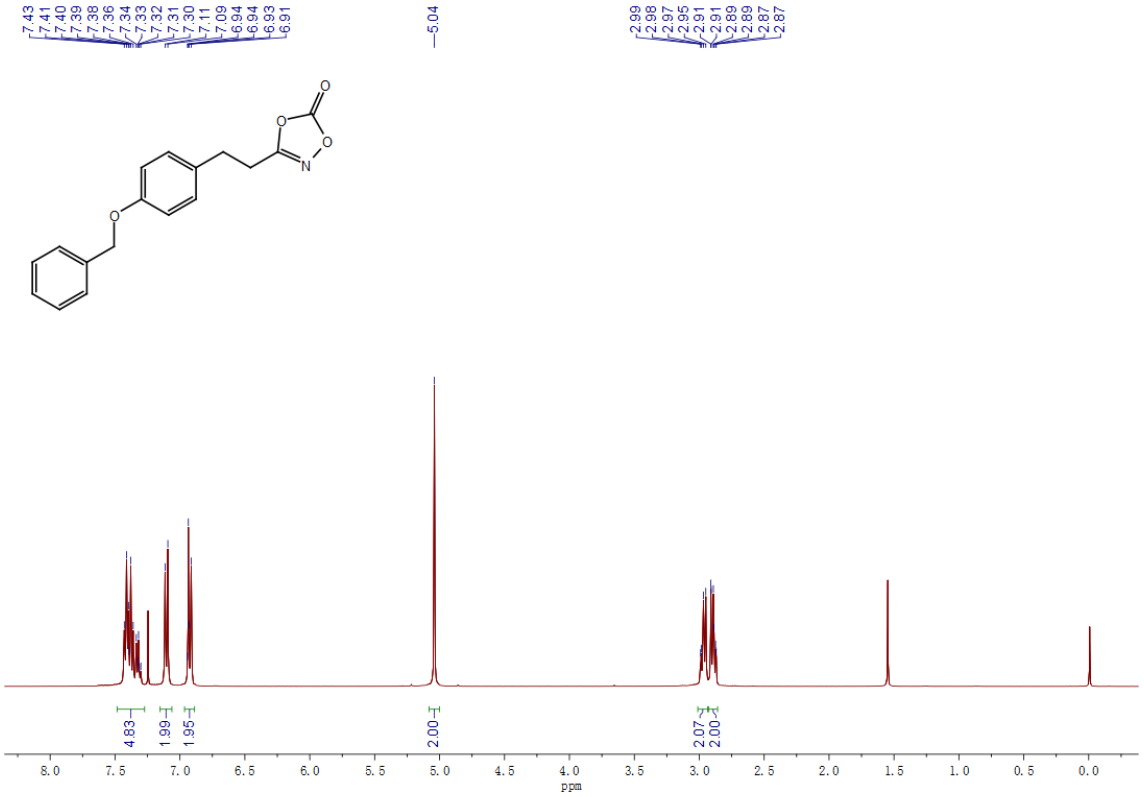
^{13}C NMR of 1y



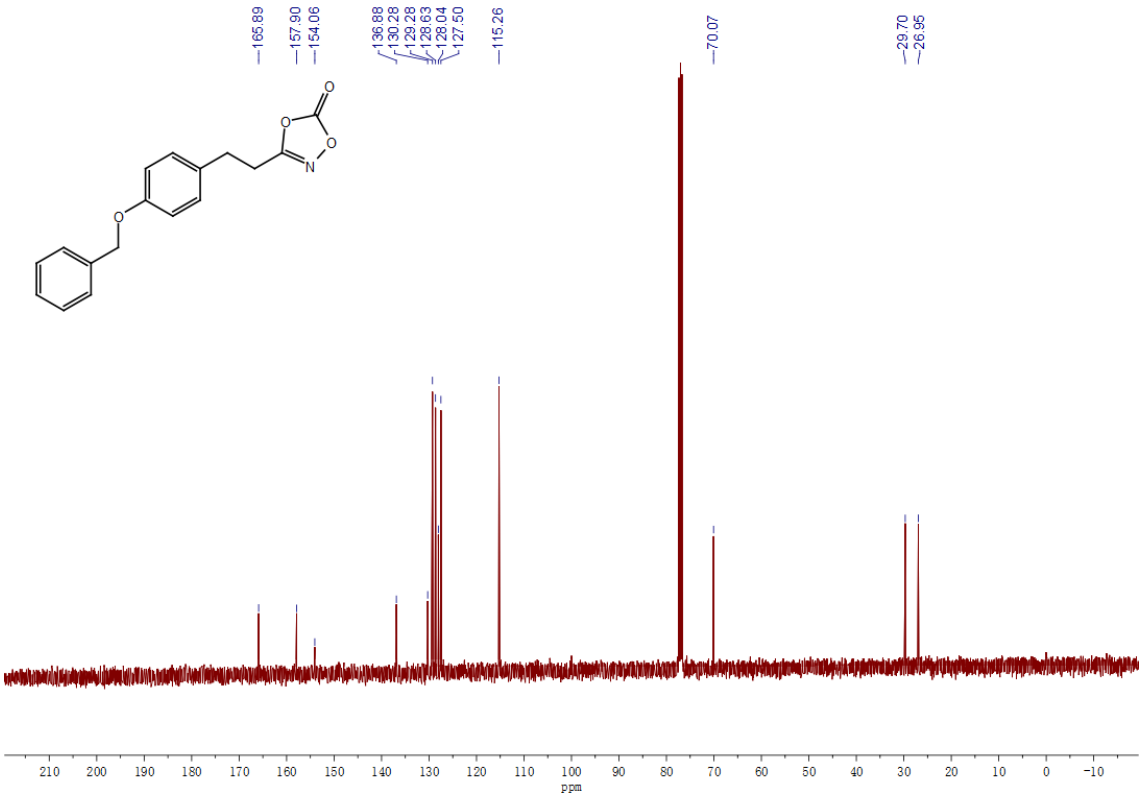
^{19}F NMR of 1y


-115.39
O
O
O
N
F
10
0
-10
-20
-30
-40
-50
-60
-70
-80
-90
-100
-110
-120
-130
-140
-150
-160
-170
-180
-190
-200
-210
ppm

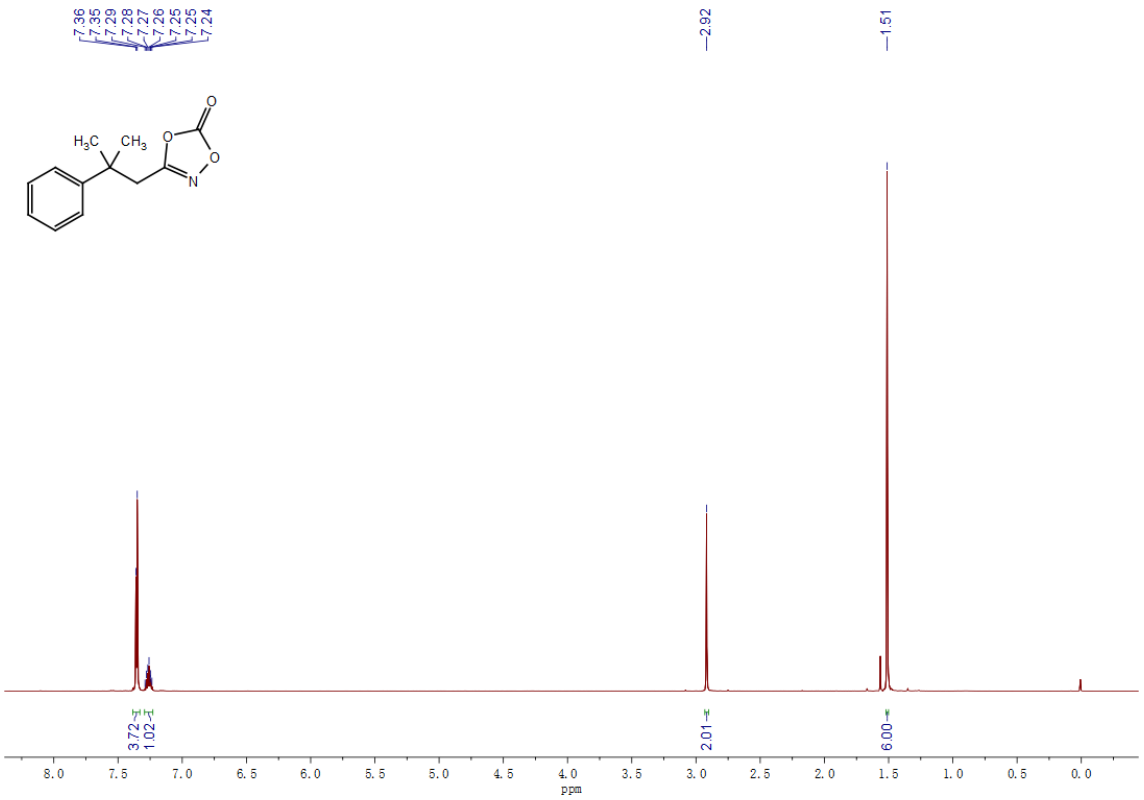
^{1}H NMR of 1z



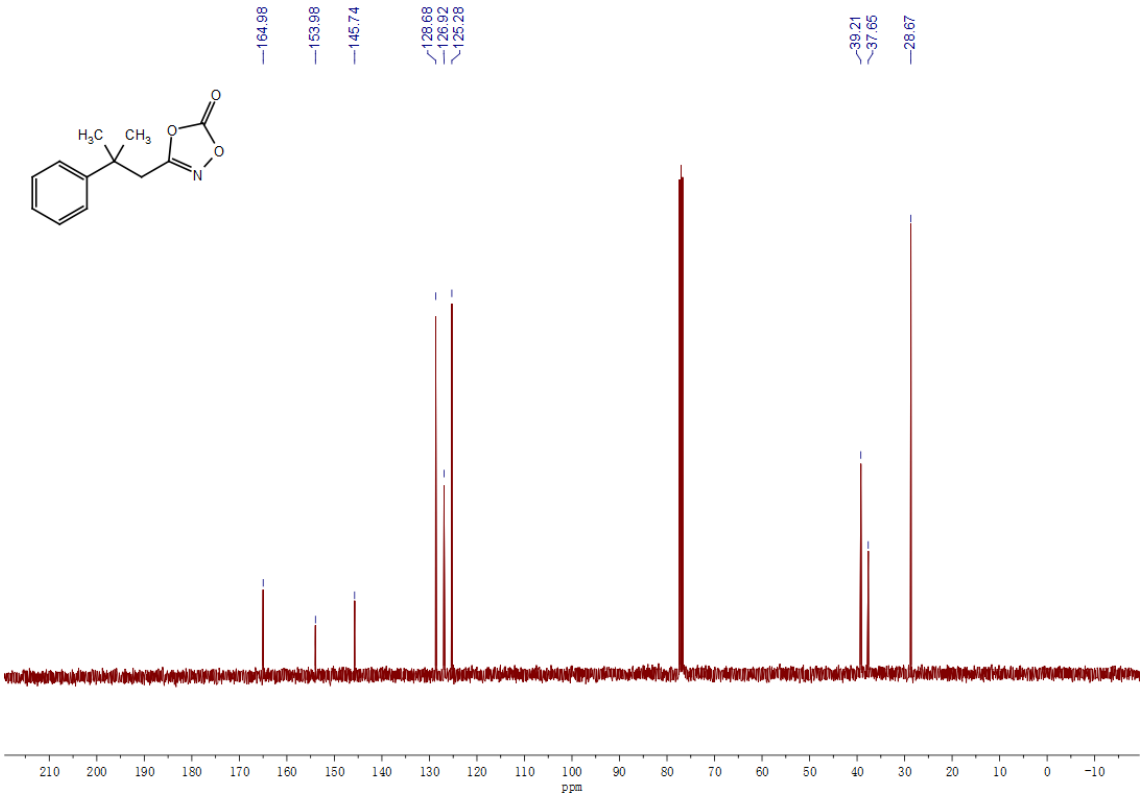
^{13}C NMR of 1z



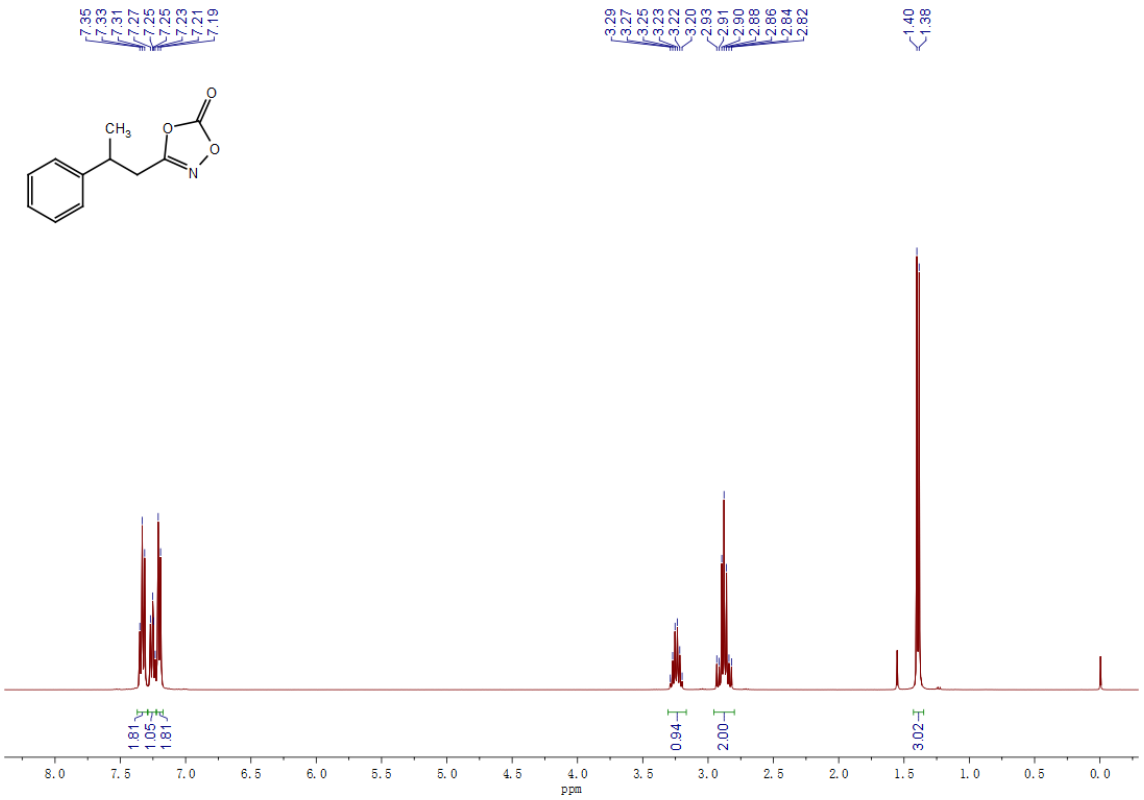
^{1}H NMR of 1za



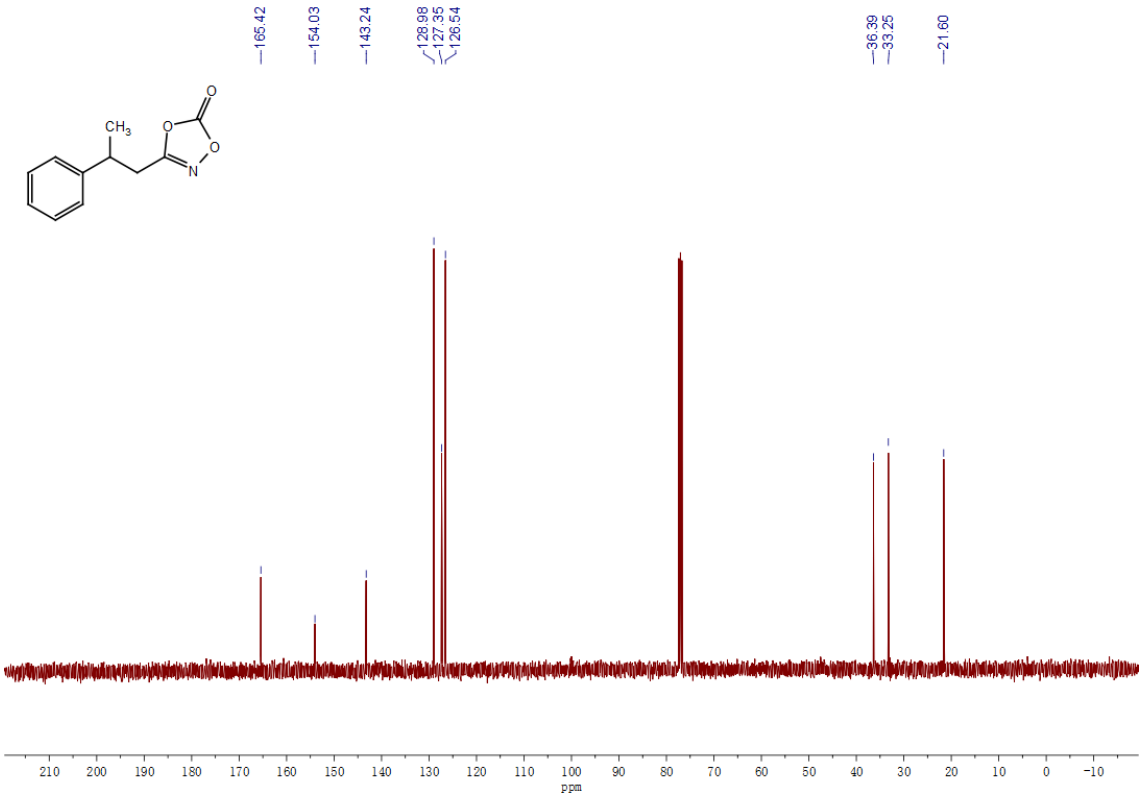
^{13}C NMR of 1za



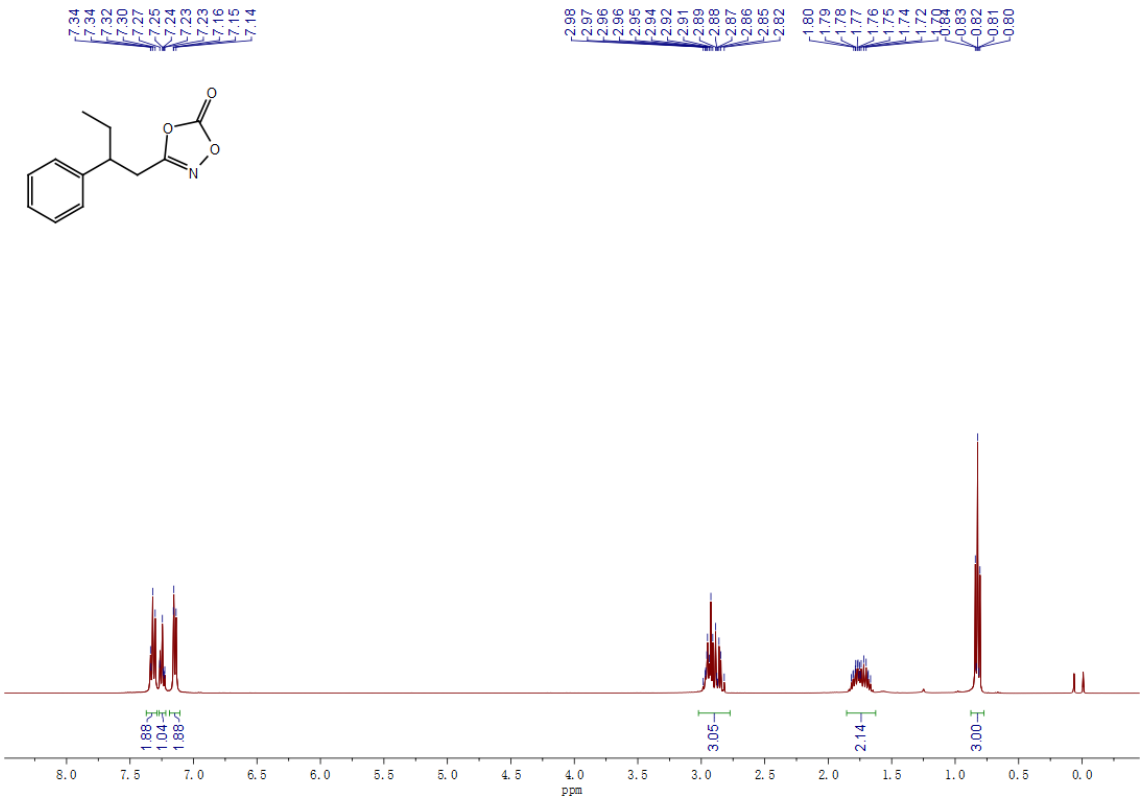
^{1}H NMR of 1zb



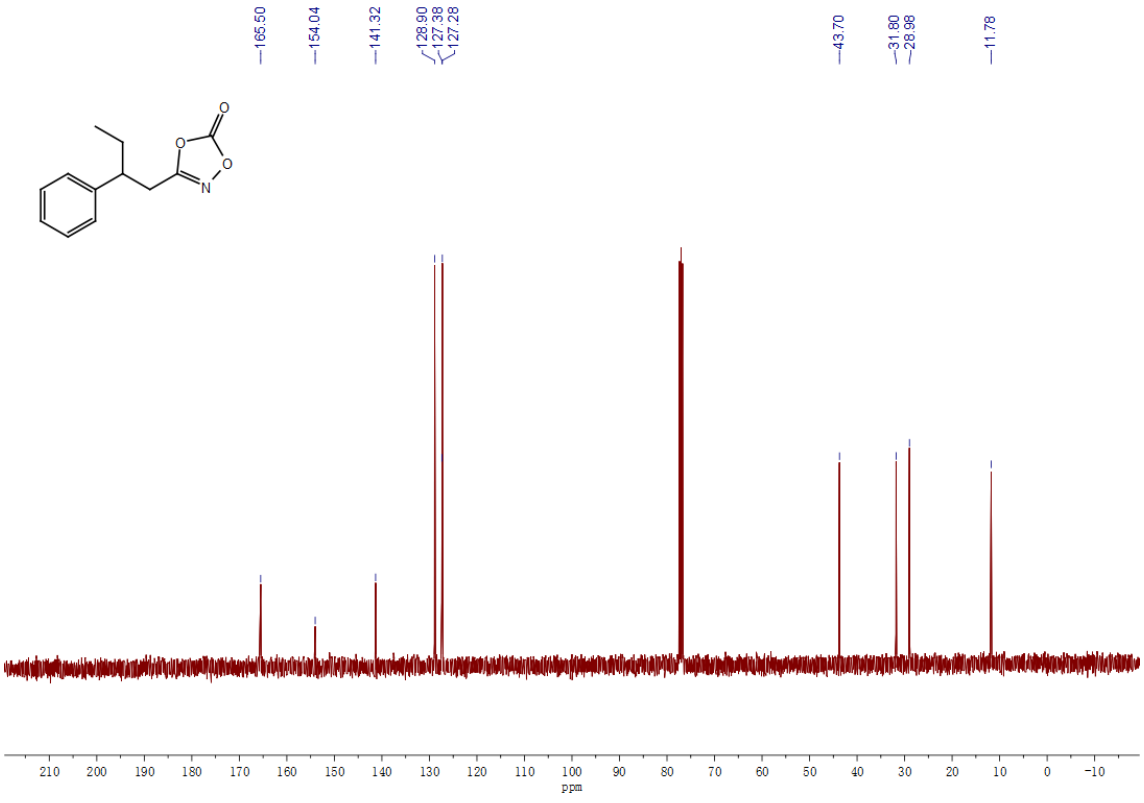
^{13}C NMR of 1zb



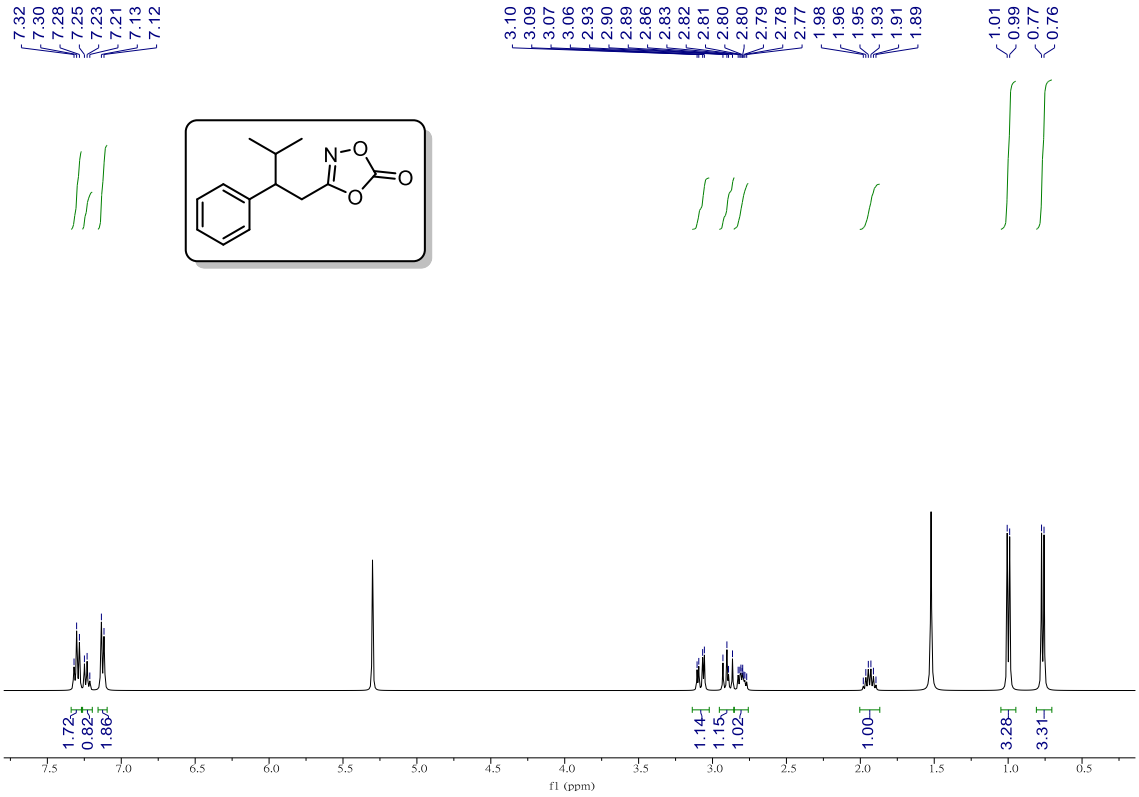
^{1}H NMR of 1zc



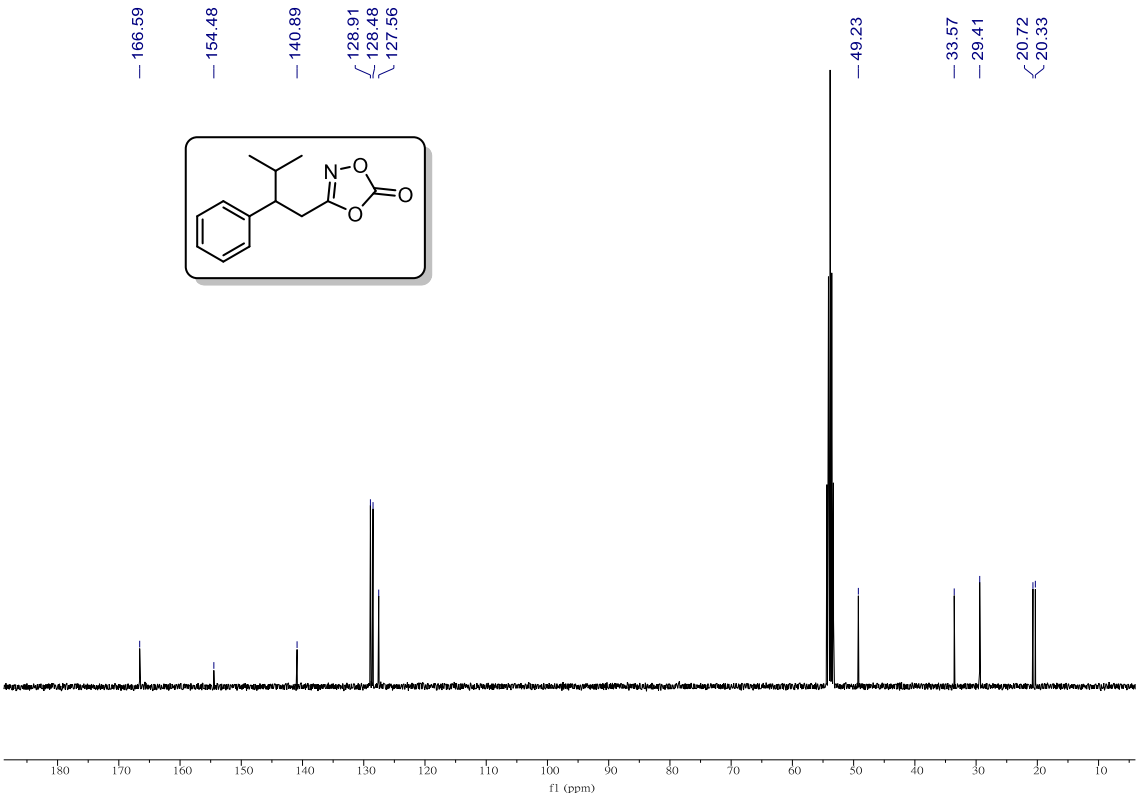
^{13}C NMR of 1zc



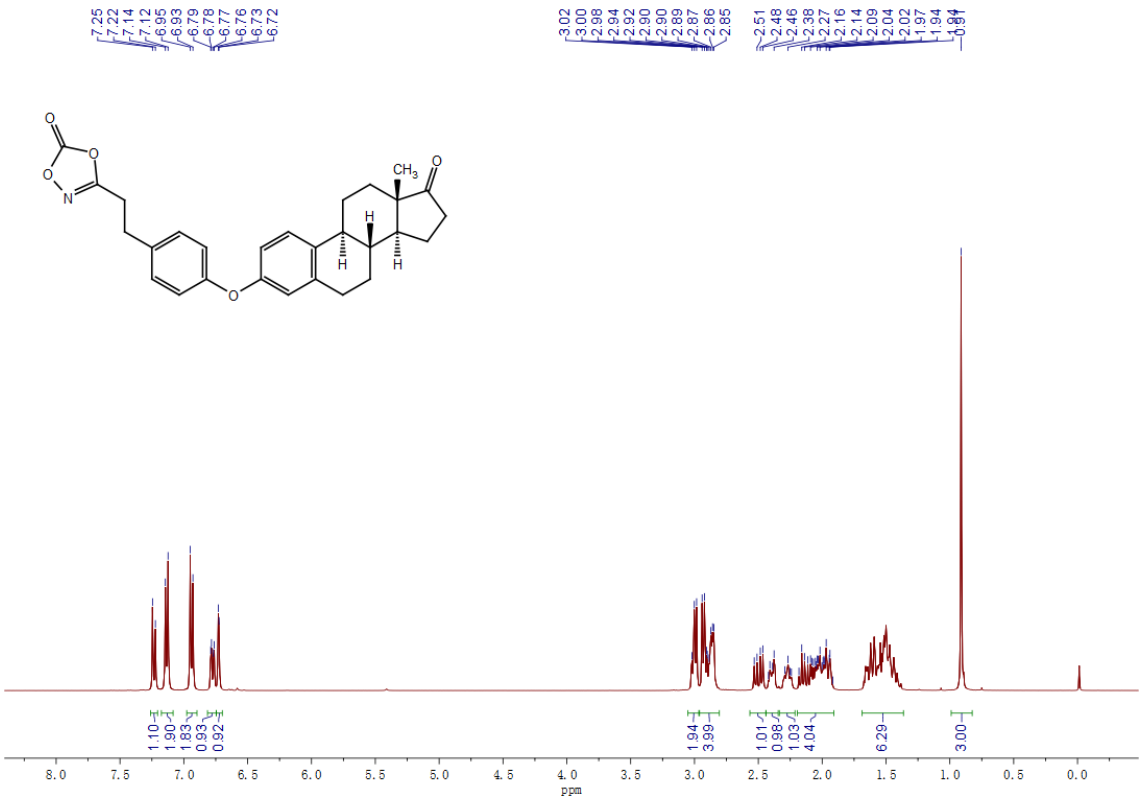
^{1}H NMR of 1zd



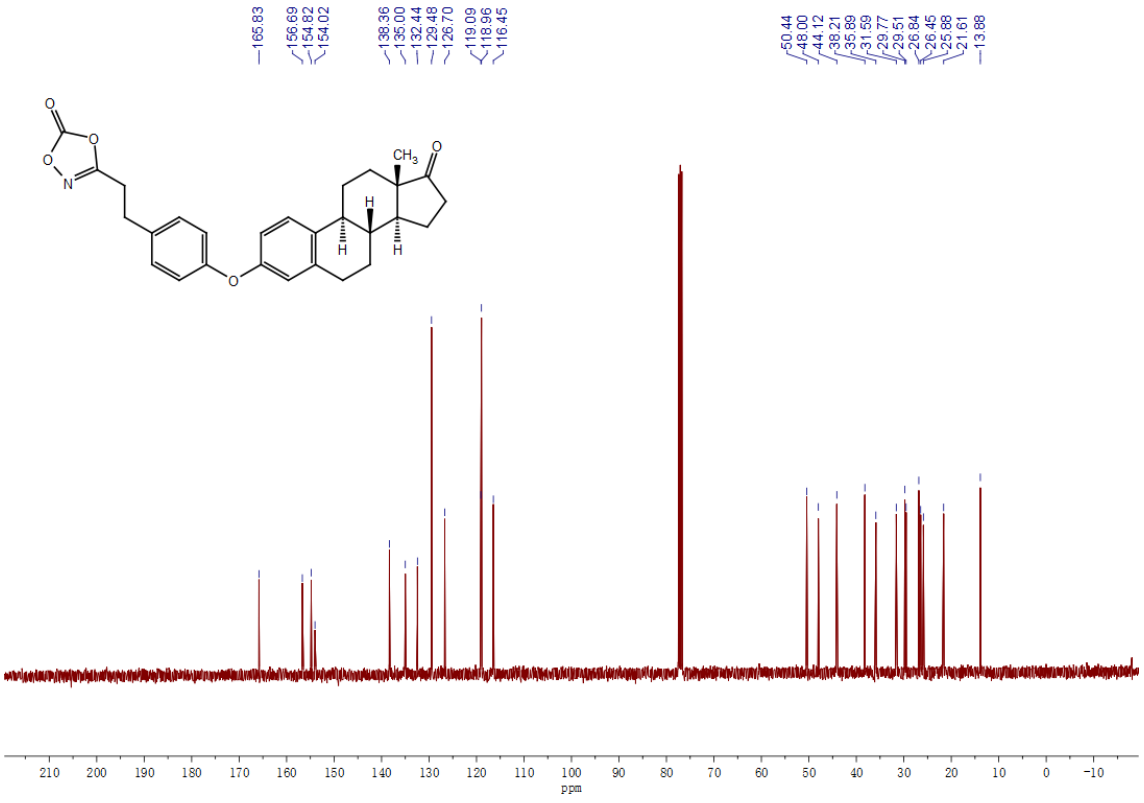
^{13}C NMR of 1zd



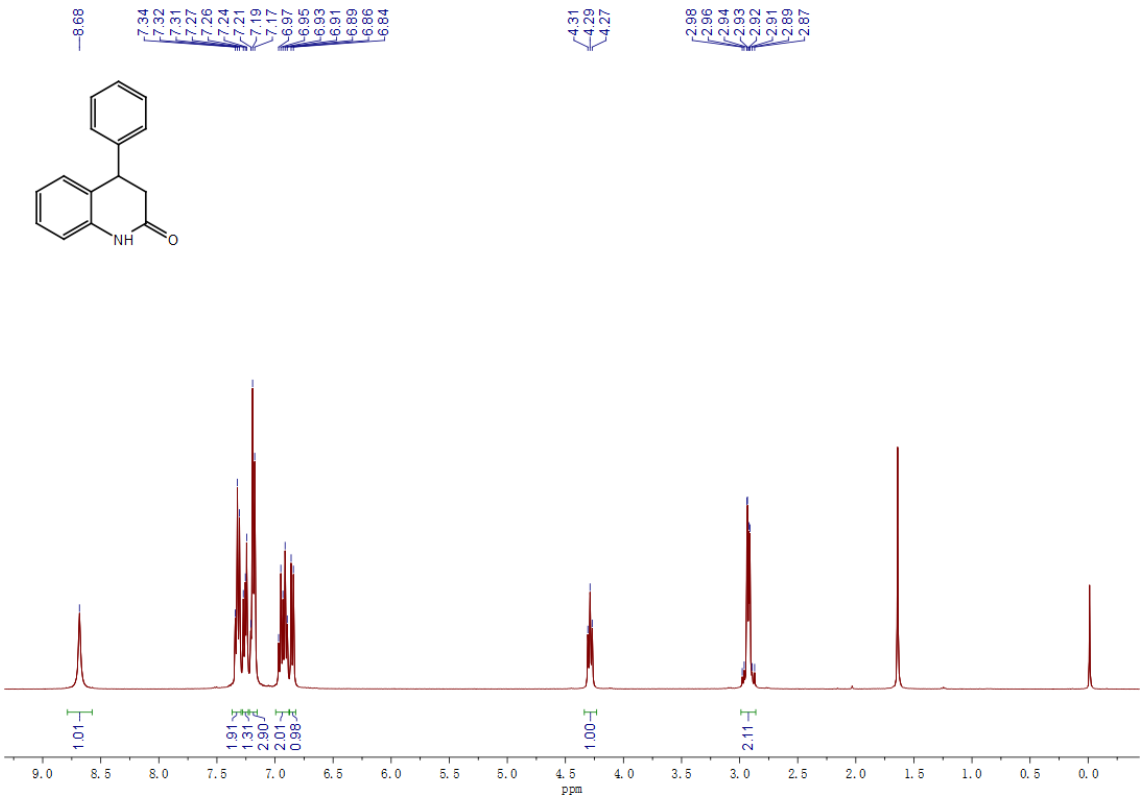
^{1}H NMR of 1ze



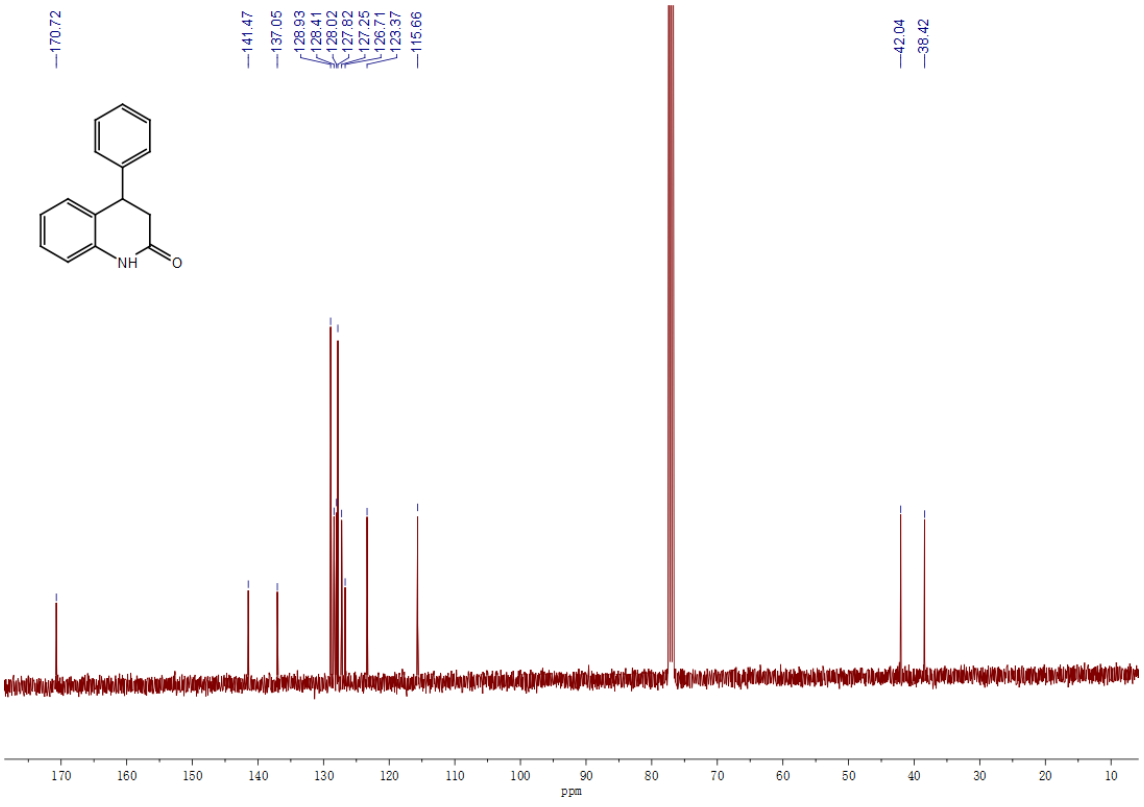
^{13}C NMR of 1ze



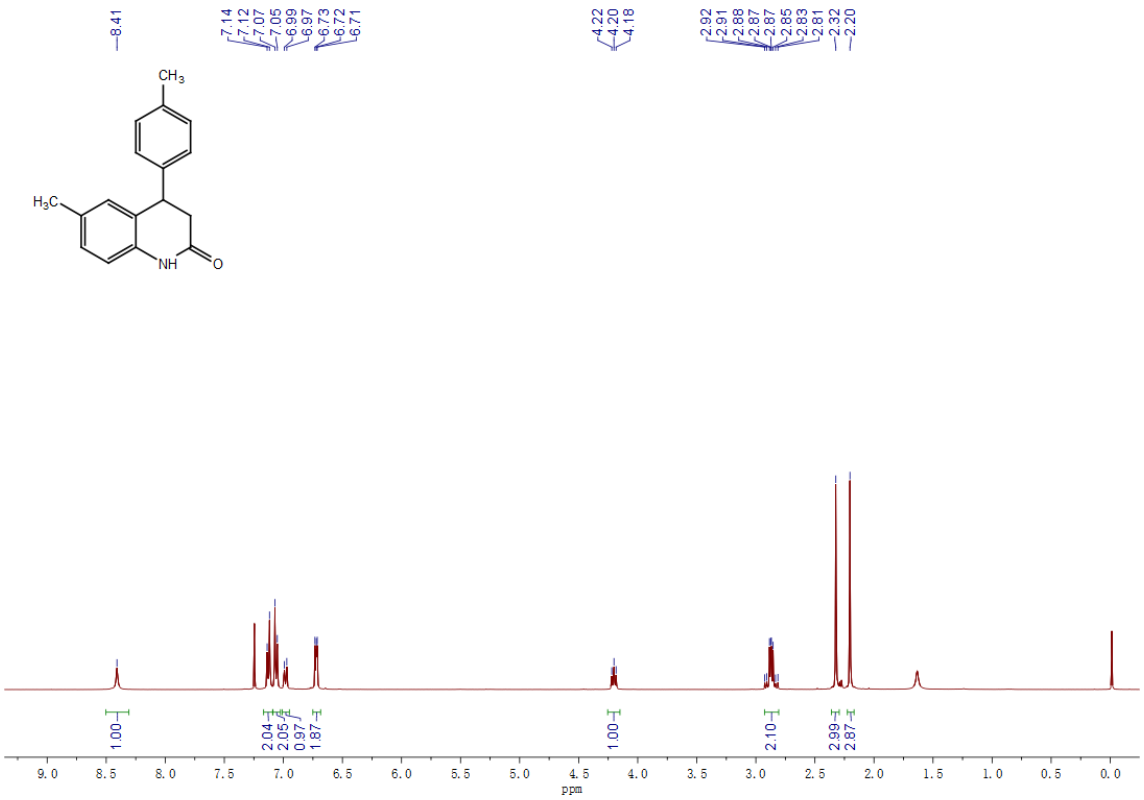
^{1}H NMR of 2a



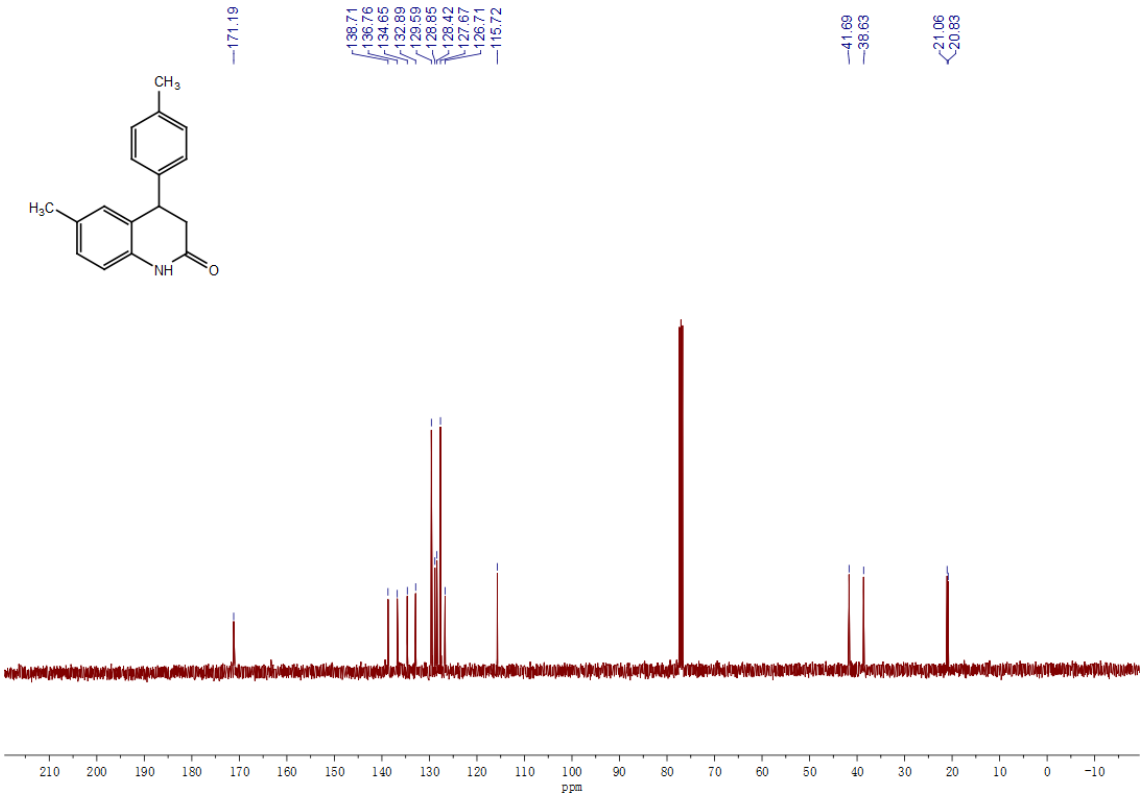
^{13}C NMR of 2a



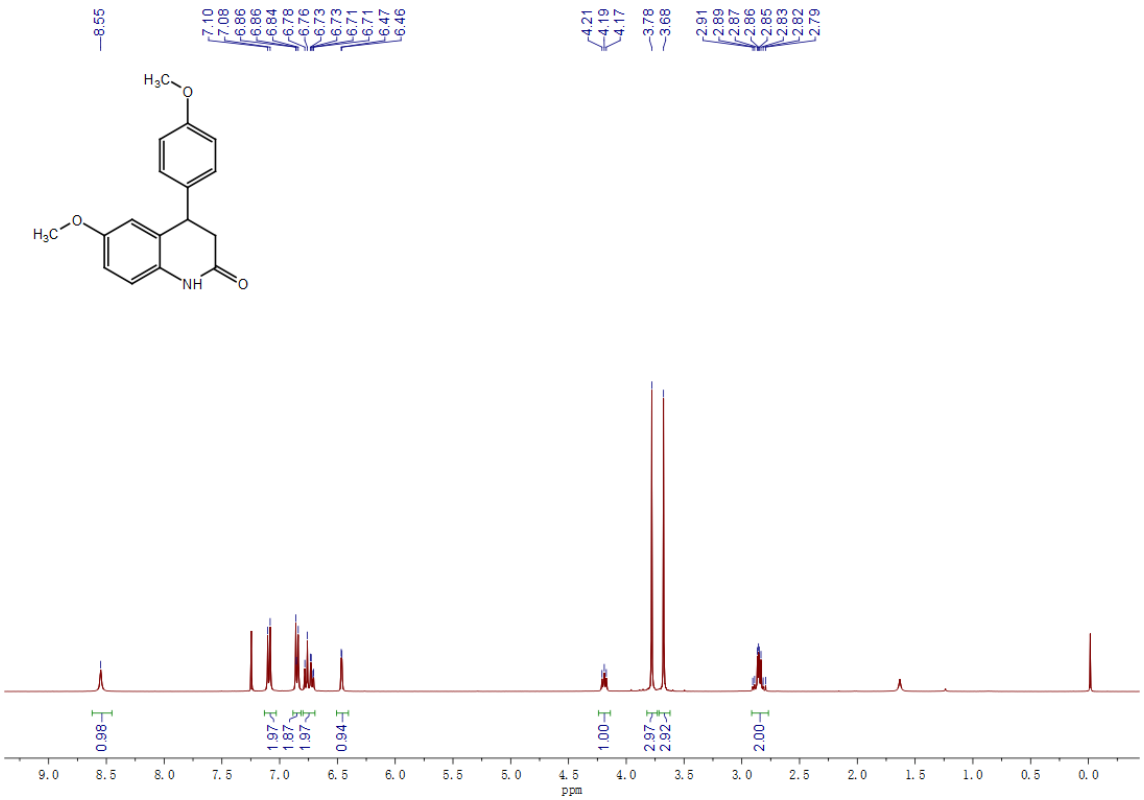
^{1}H NMR of 2b



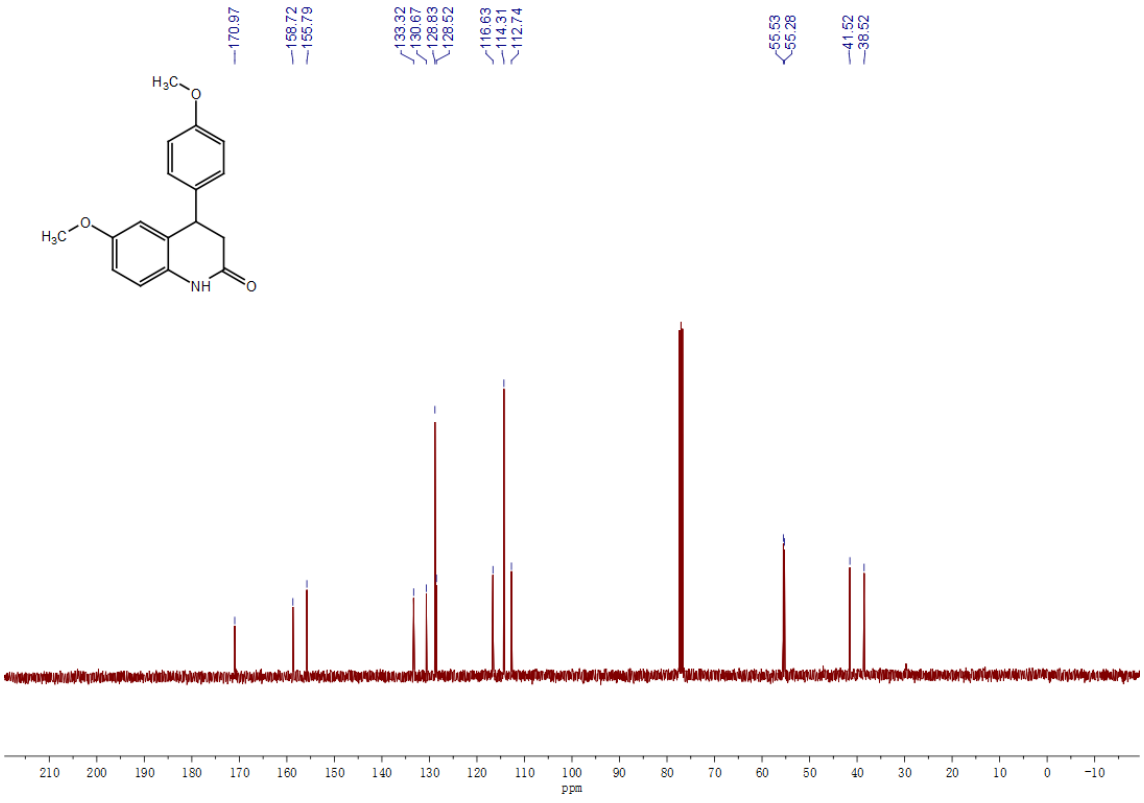
^{13}C NMR of 2b



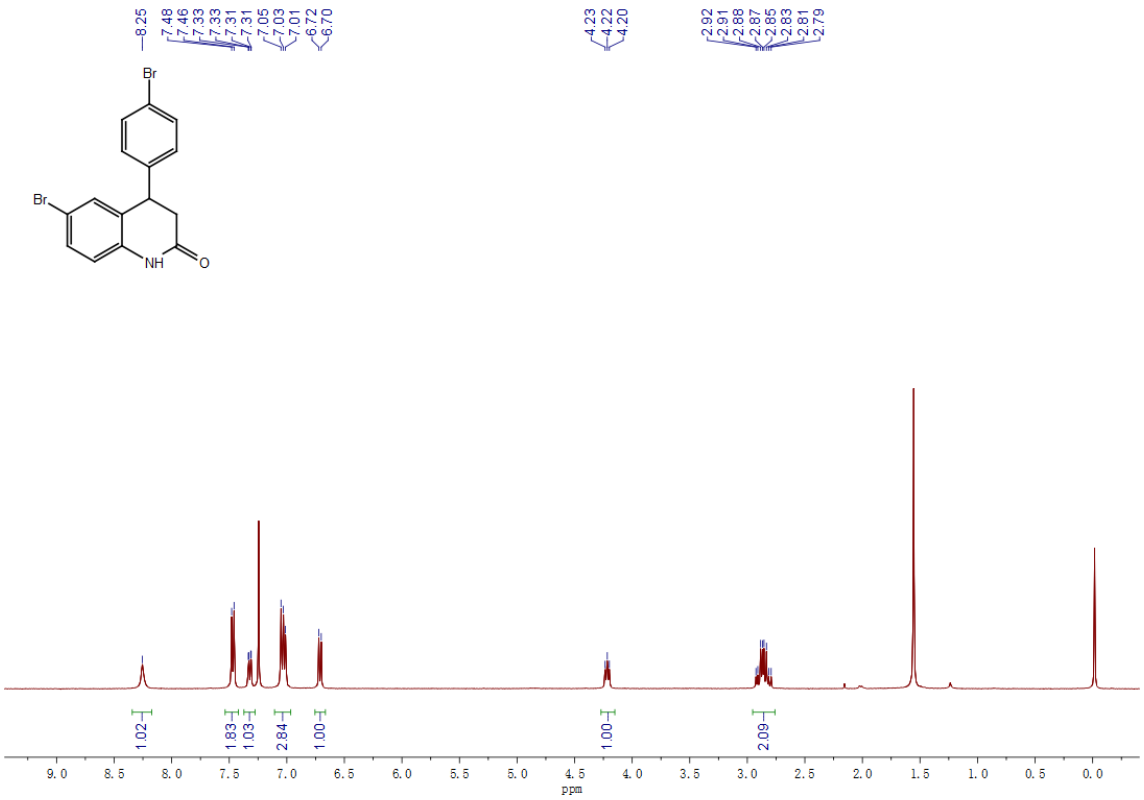
^{1}H NMR of 2c



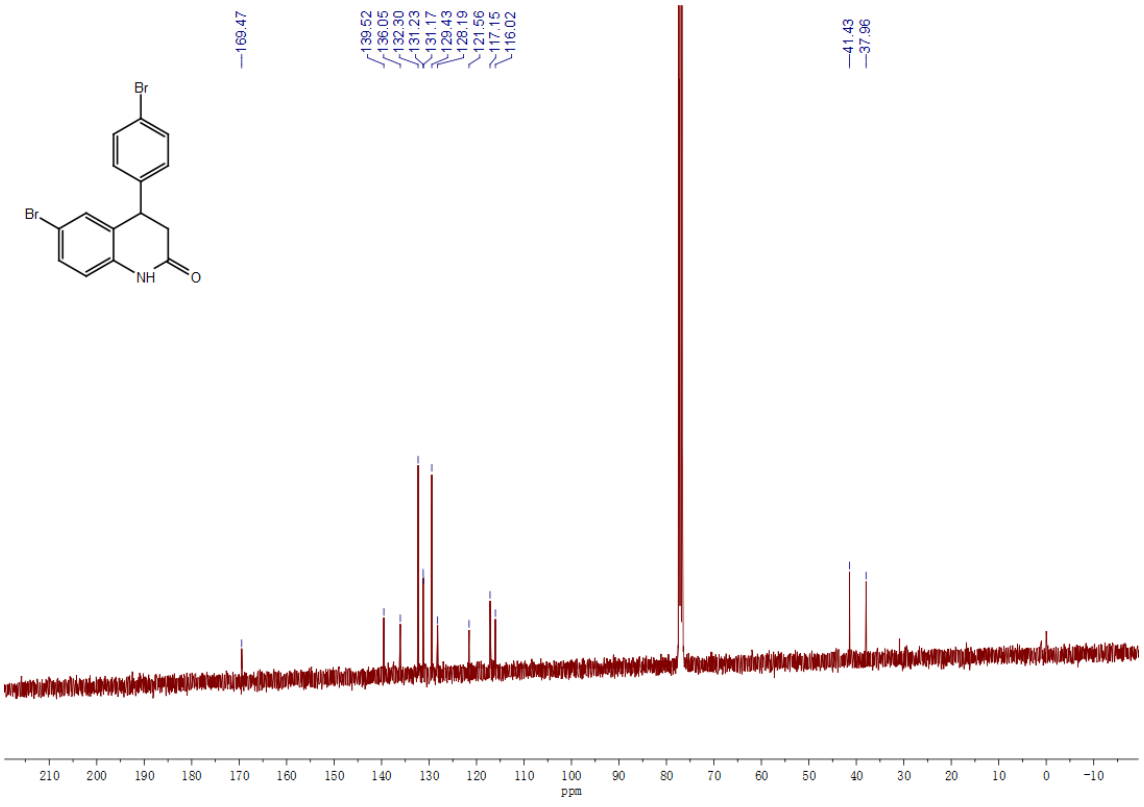
^{13}C NMR of 2c



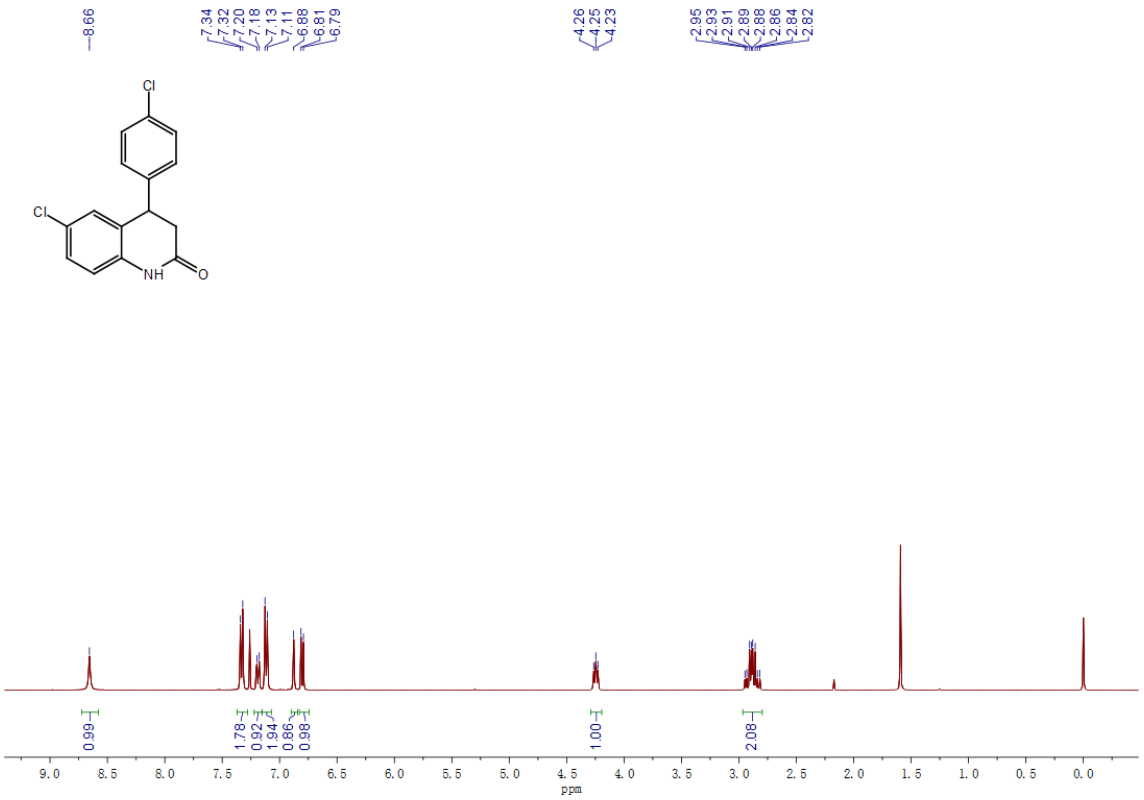
^{1}H NMR of 2d



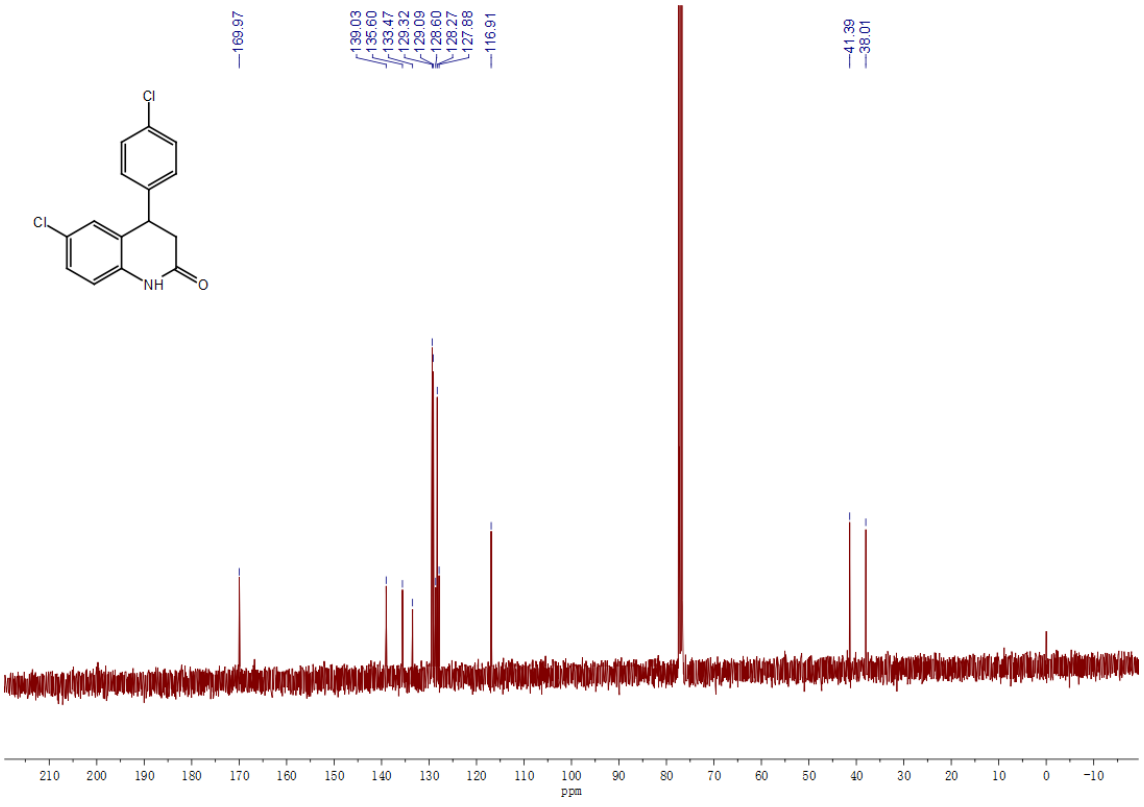
^{13}C NMR of 2d



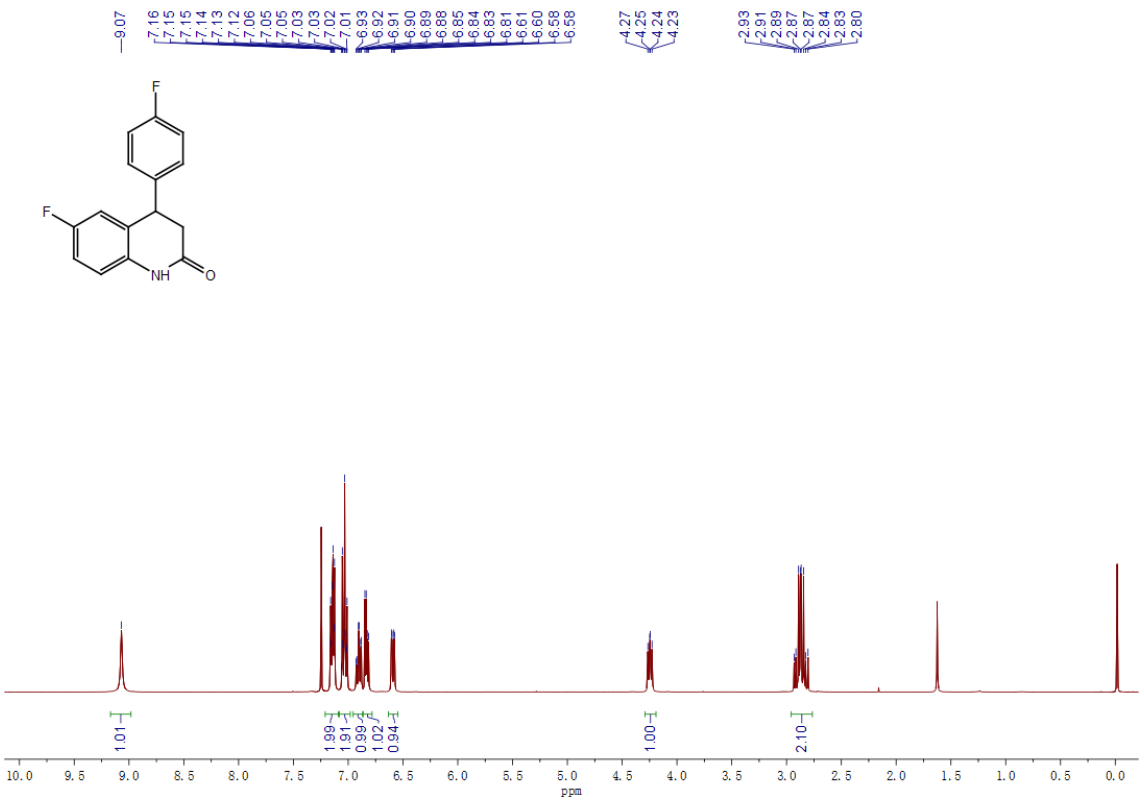
^{1}H NMR of 2e



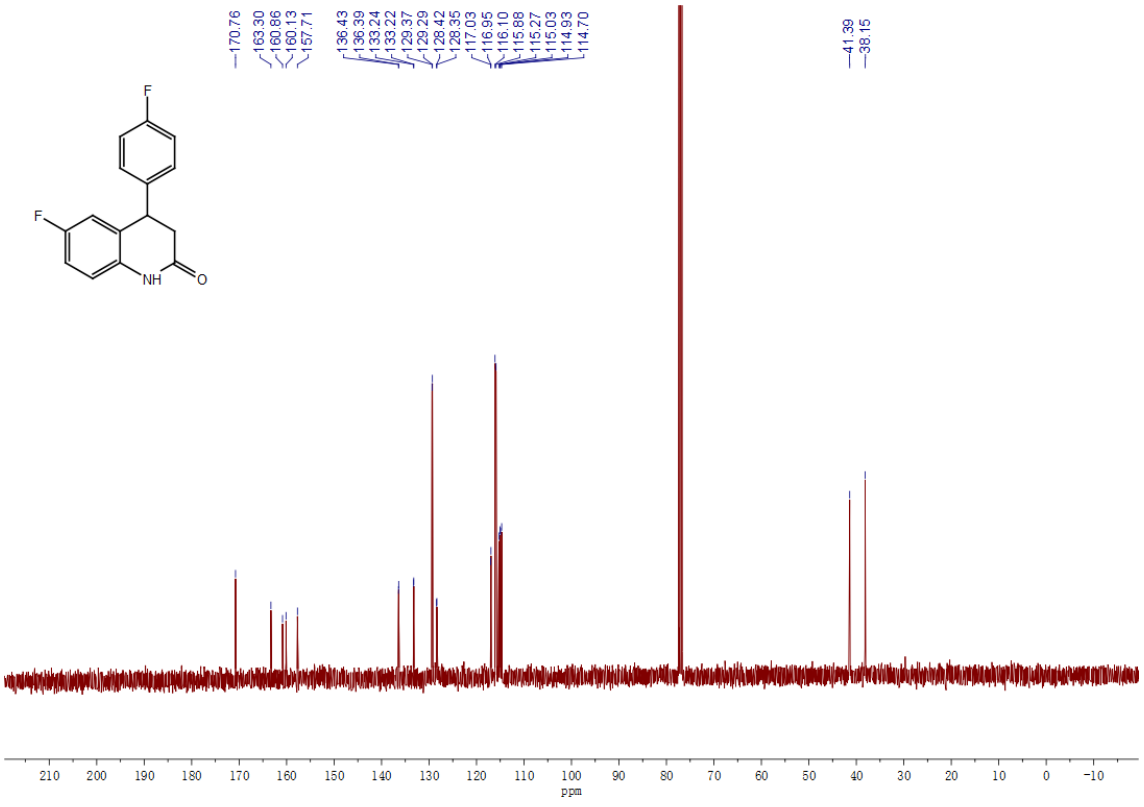
^{13}C NMR of 2e



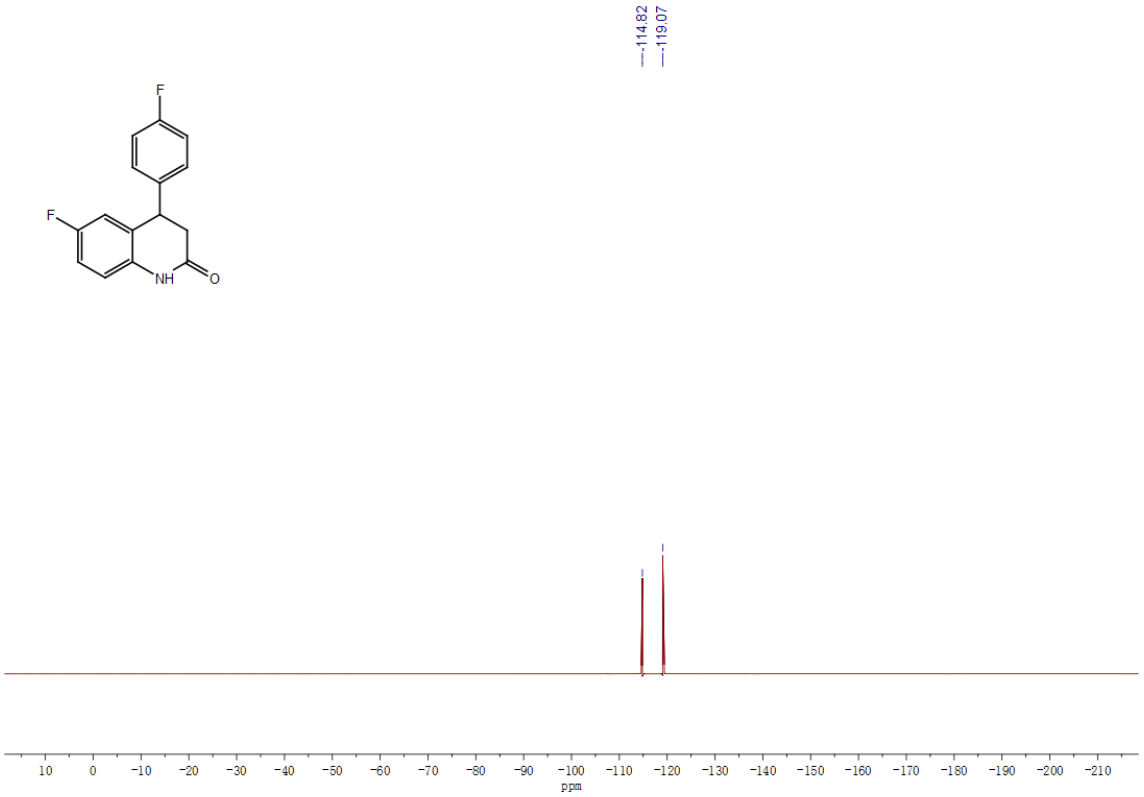
^{1}H NMR of 2f



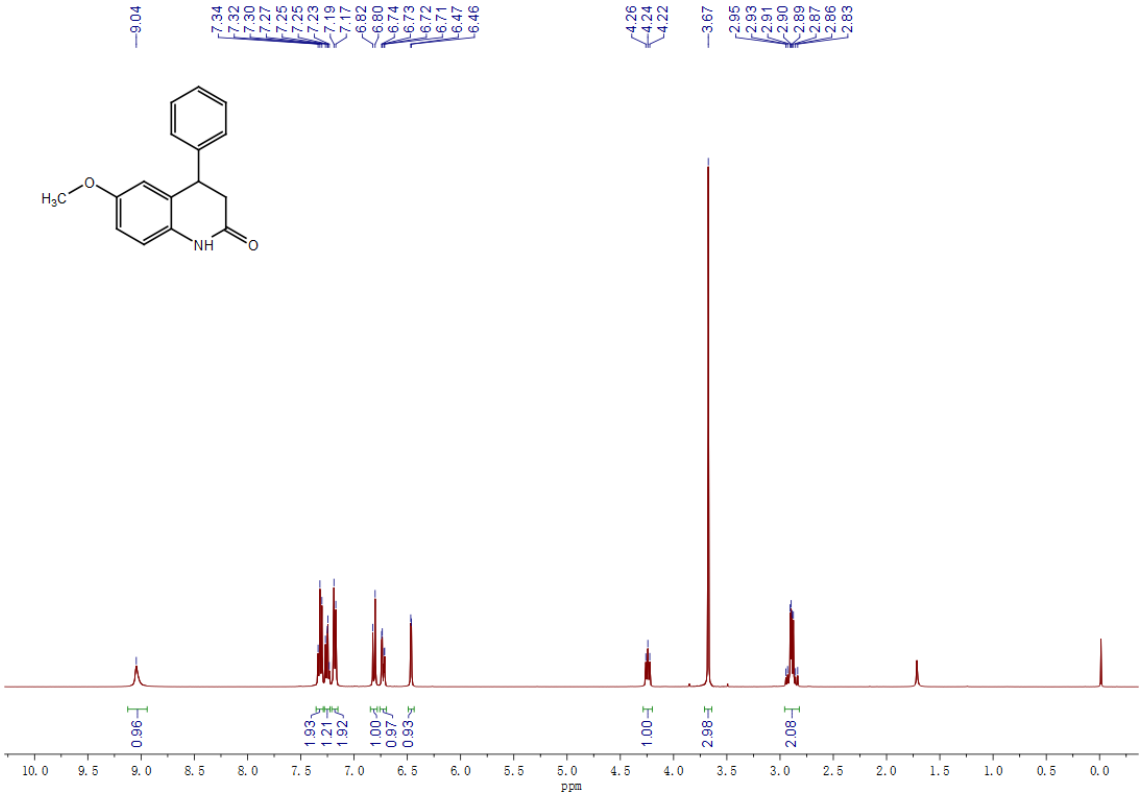
^{13}C NMR of 2f



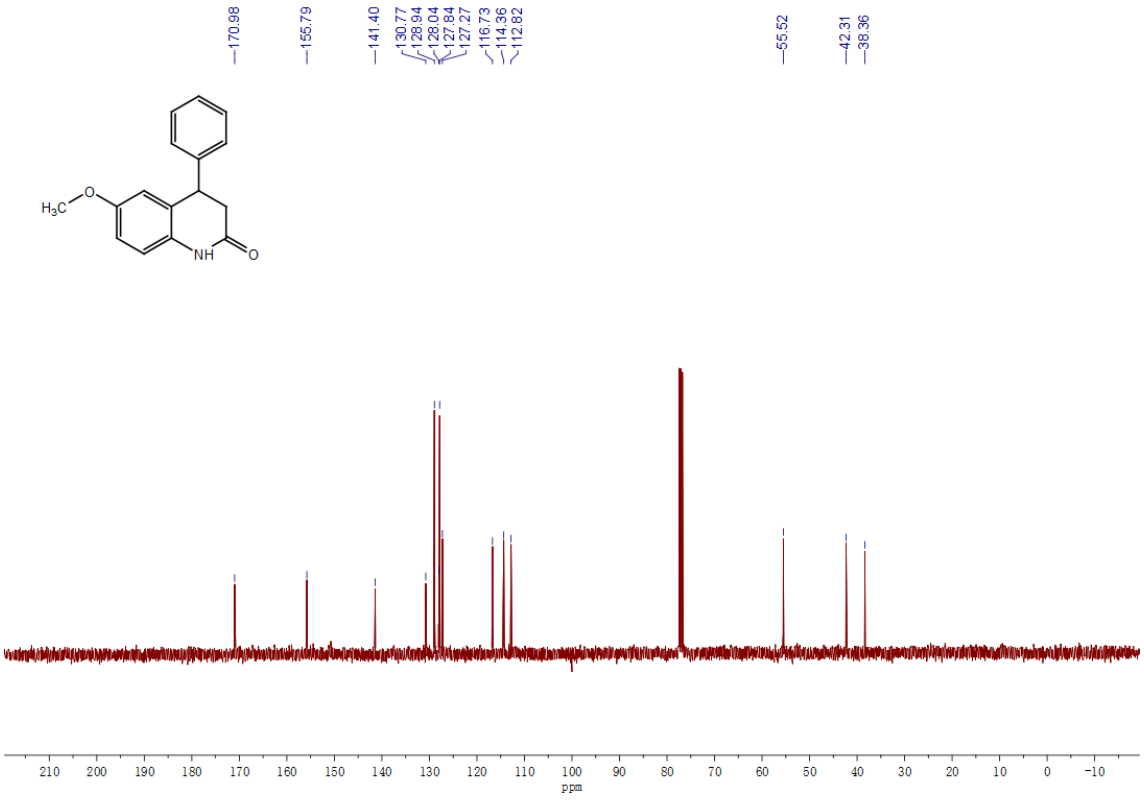
^{19}F NMR of 2f


-114.82
-119.07
F
F
NH
O
10
0
-10
-20
-30
-40
-50
-60
-70
-80
-90
-100
-110
-120
-130
-140
-150
-160
-170
-180
-190
-200
-210
ppm

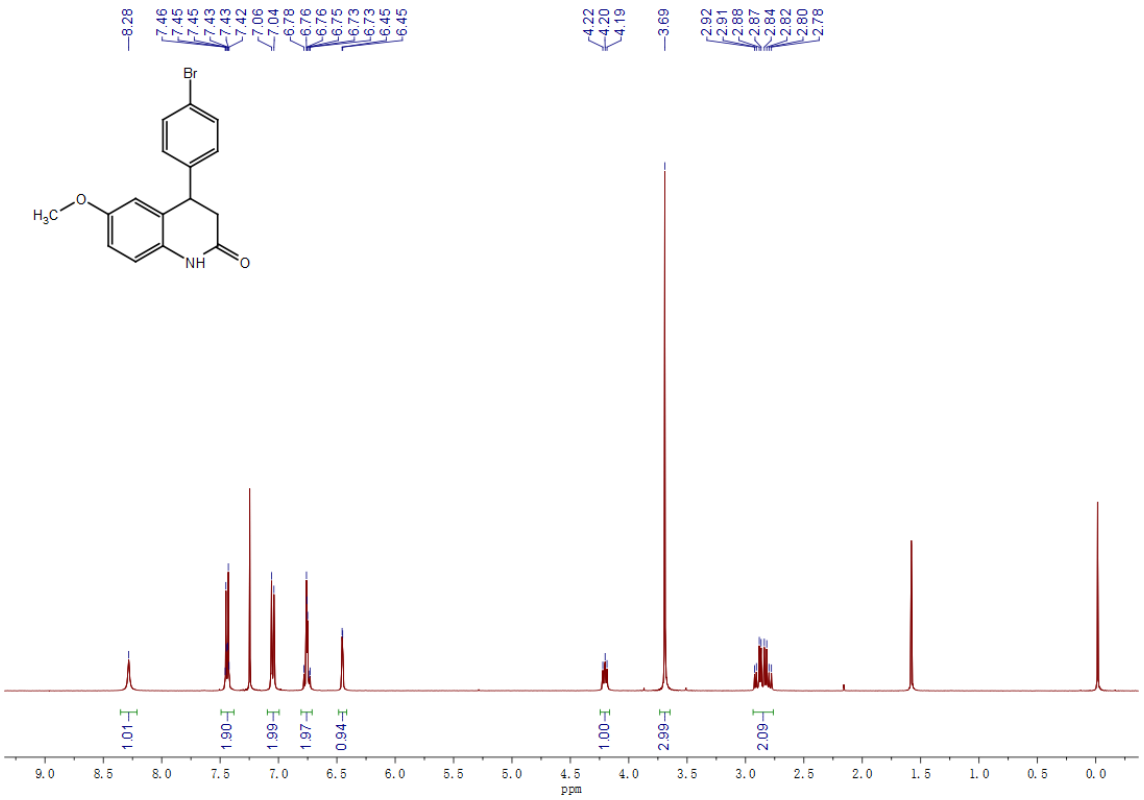
^{1}H NMR of 2g



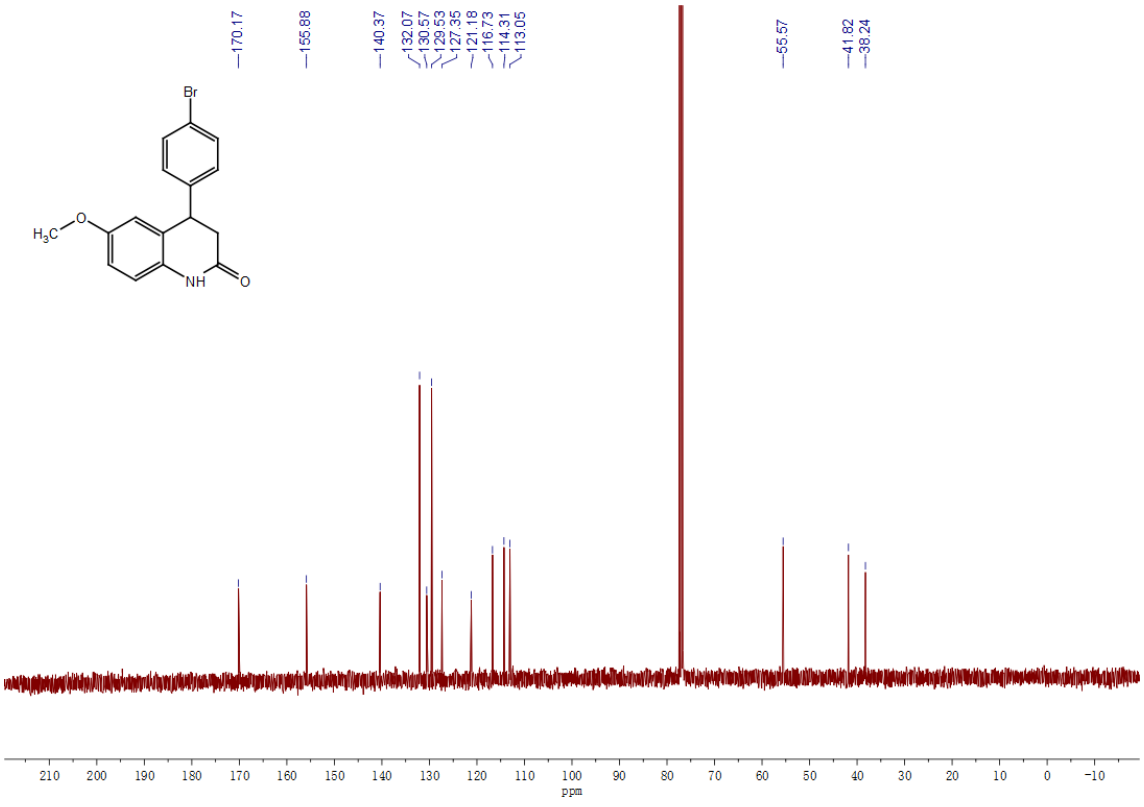
^{13}C NMR of 2g



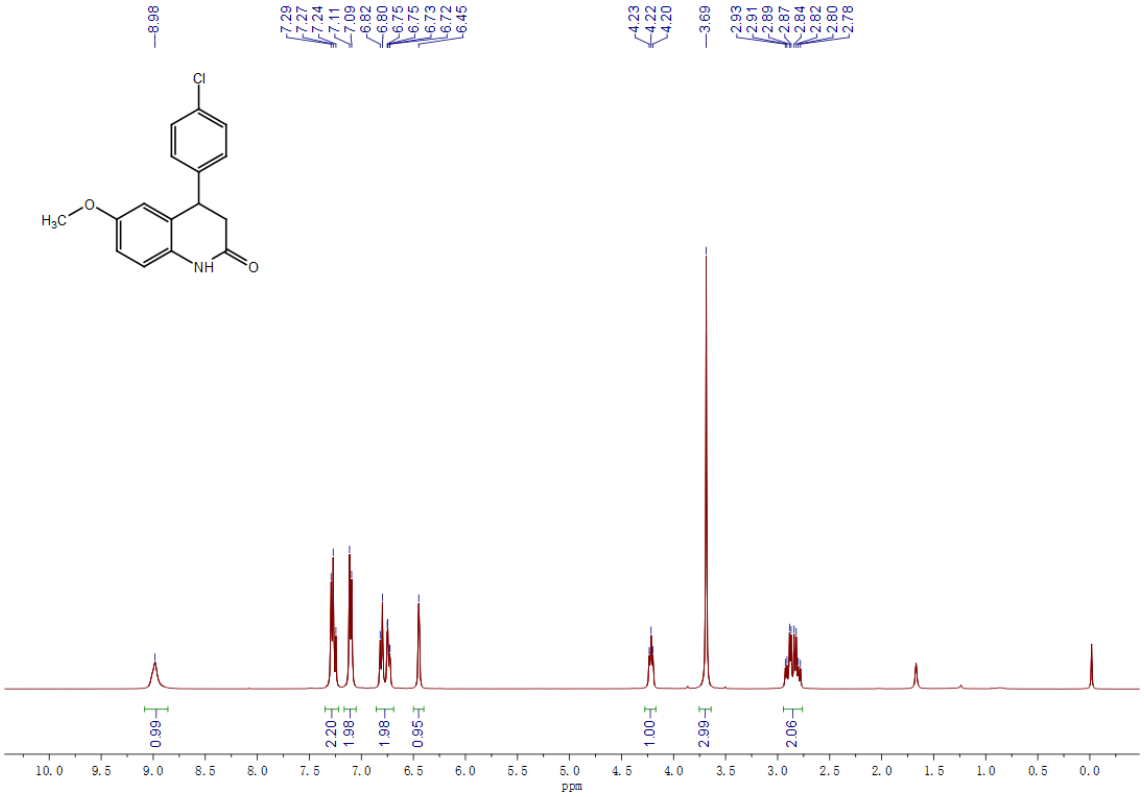
^{1}H NMR of 2h



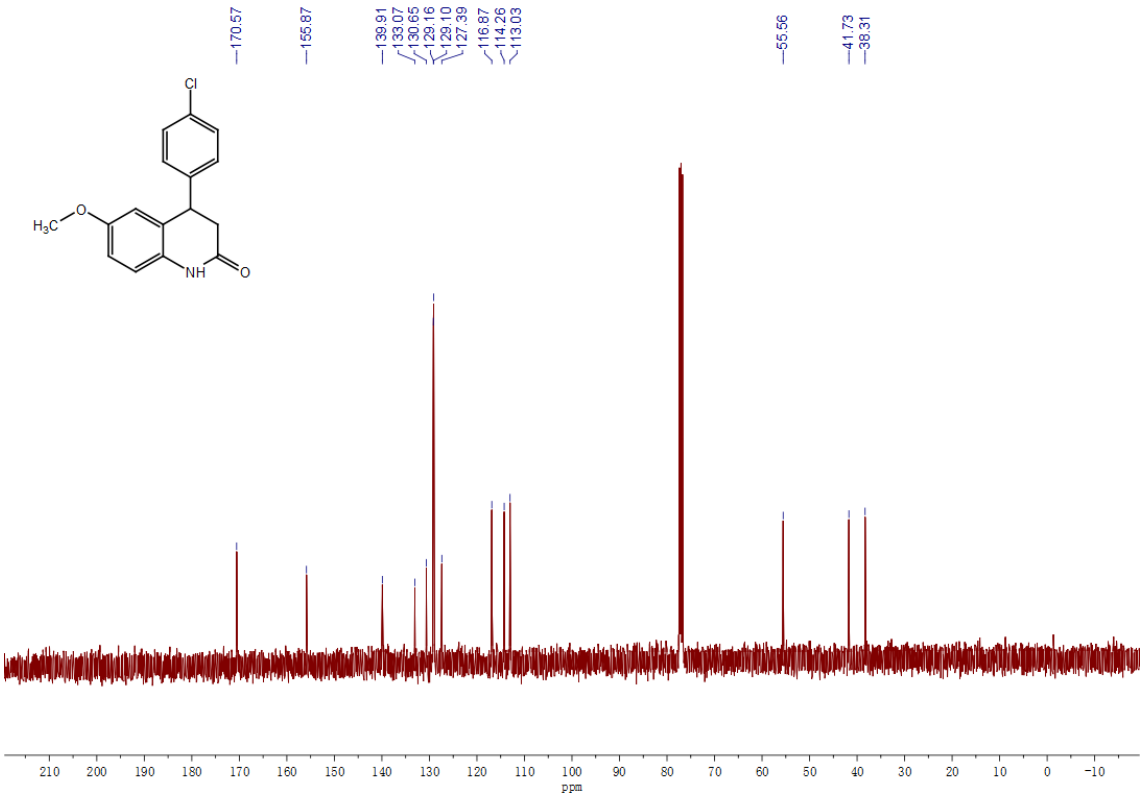
^{13}C NMR of 2h



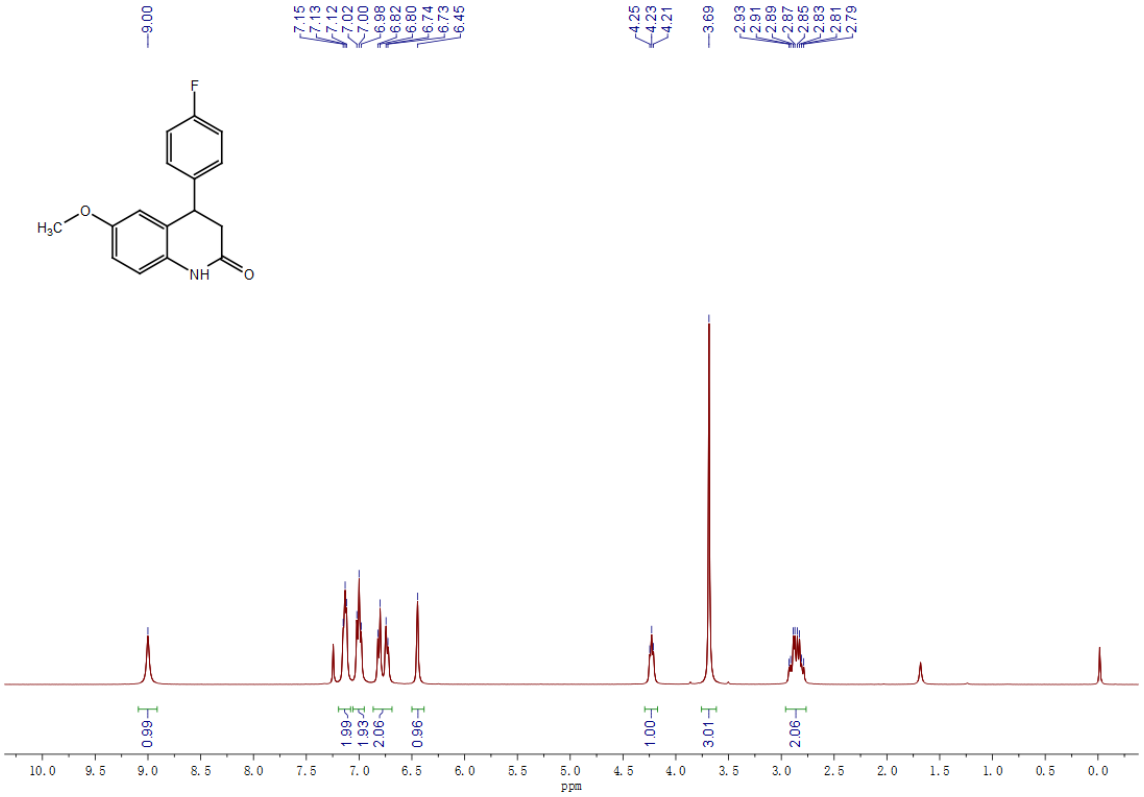
^{1}H NMR of 2i



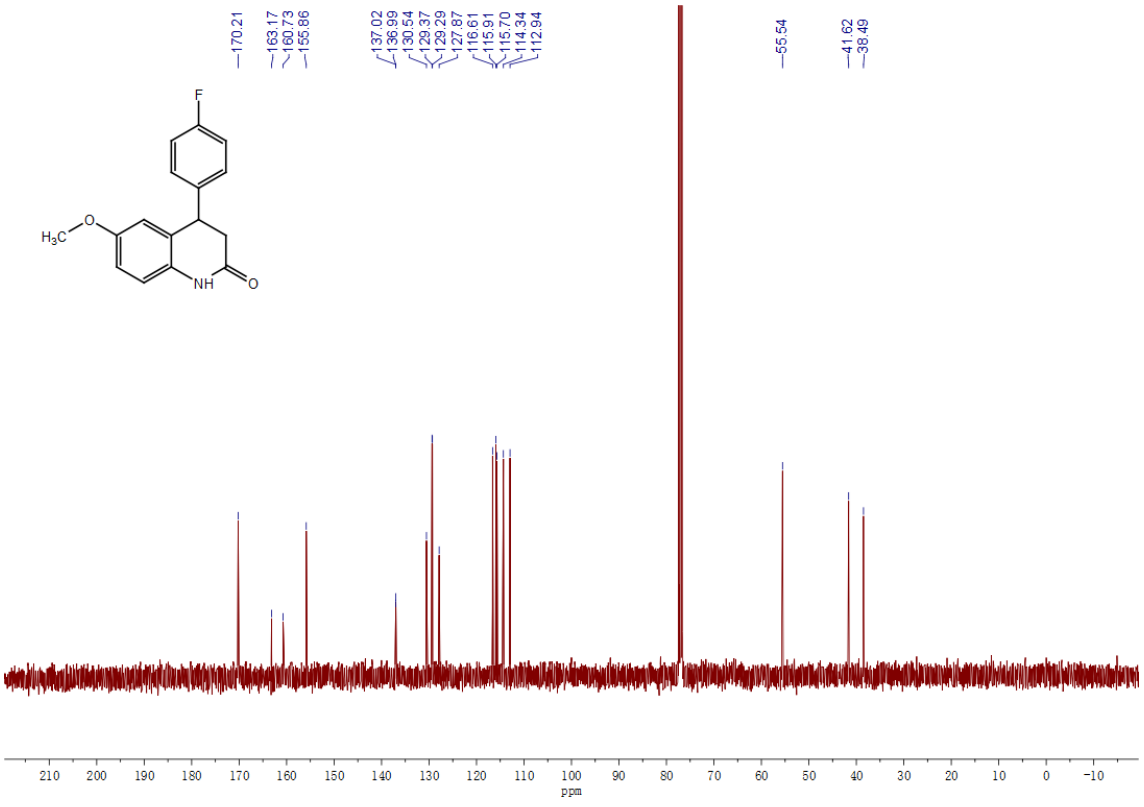
^{13}C NMR of 2i



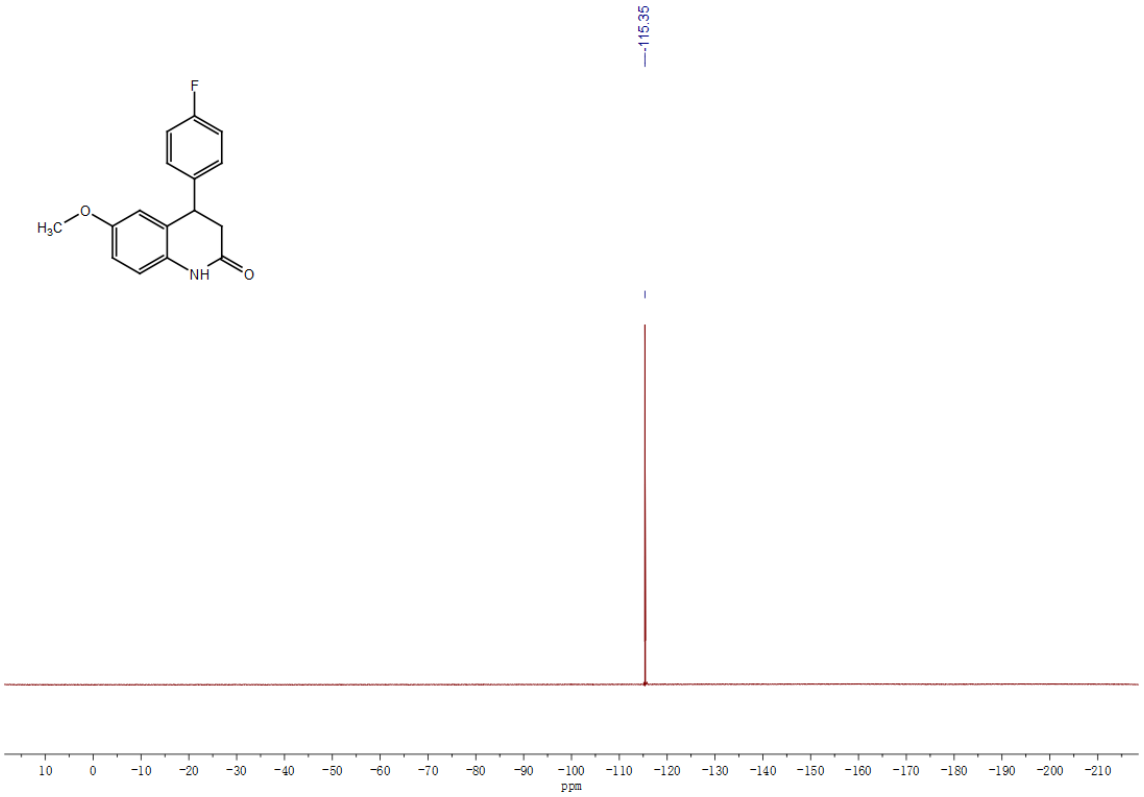
^{1}H NMR of 2j



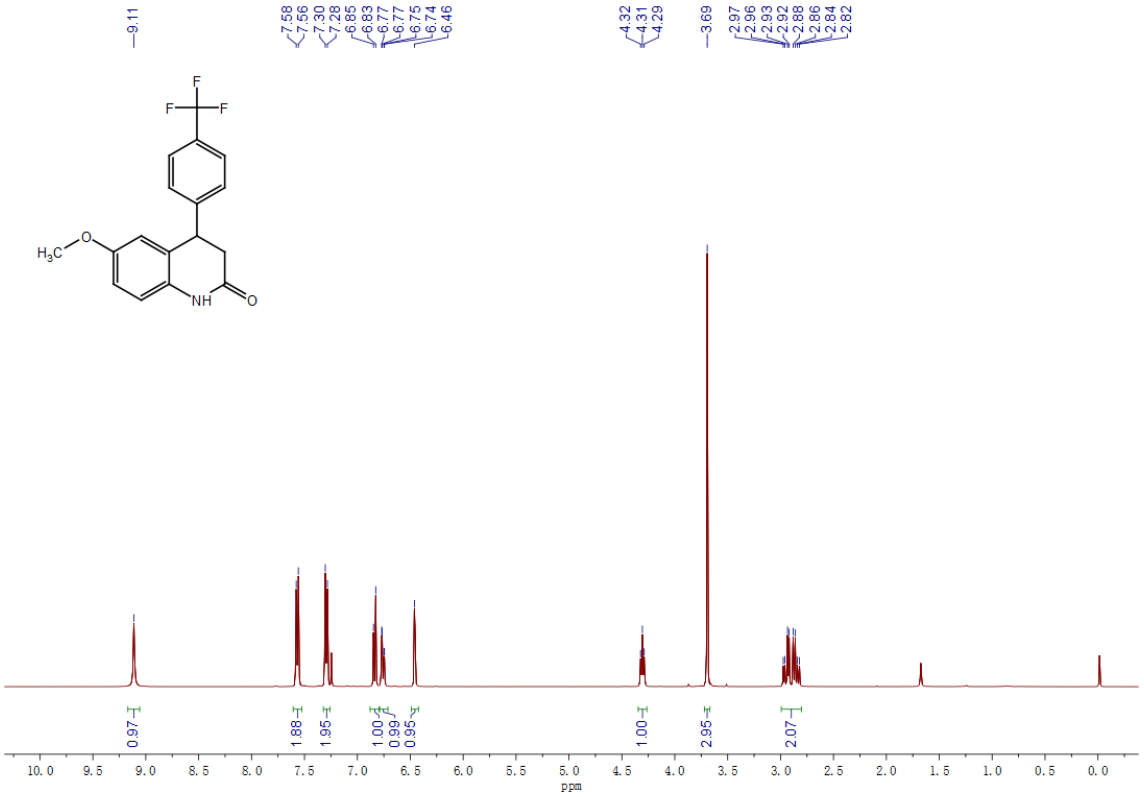
^{13}C NMR of 2j



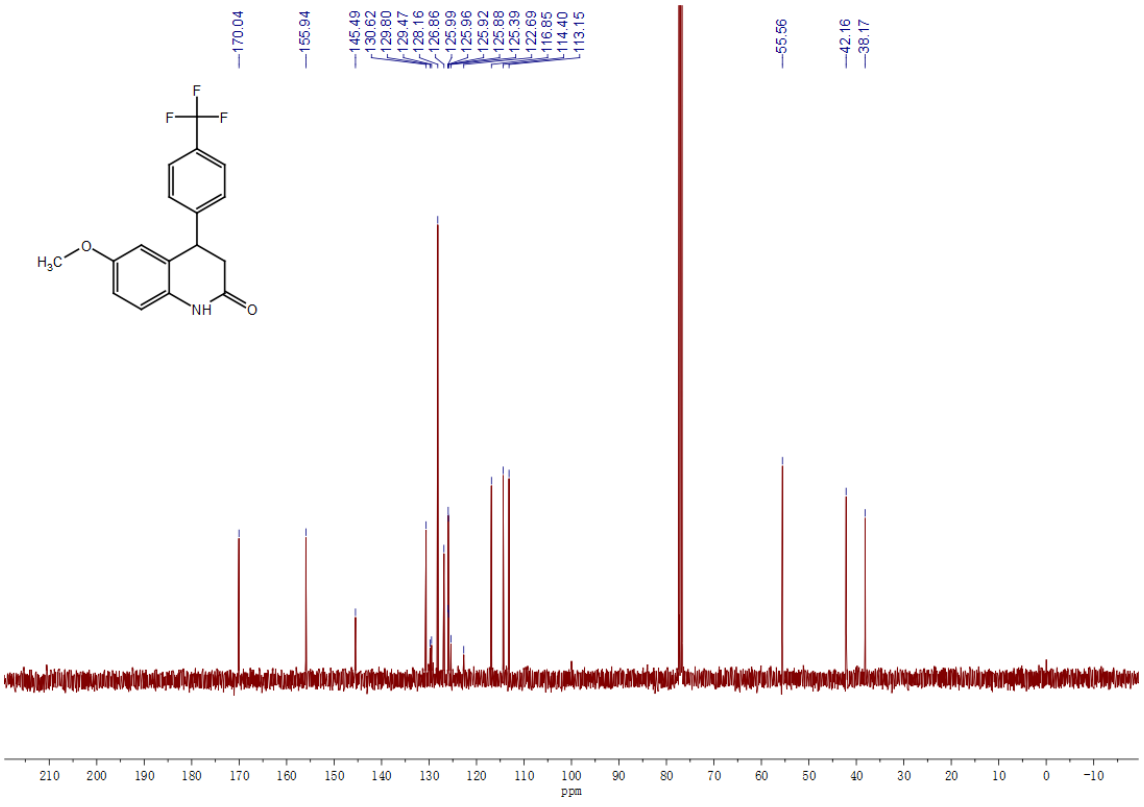
^{19}F NMR of 2j


-115.35
F
H3C
O
NH
O
10
0
-10
-20
-30
-40
-50
-60
-70
-80
-90
-100
-110
-120
-130
-140
-150
-160
-170
-180
-190
-200
-210
ppm

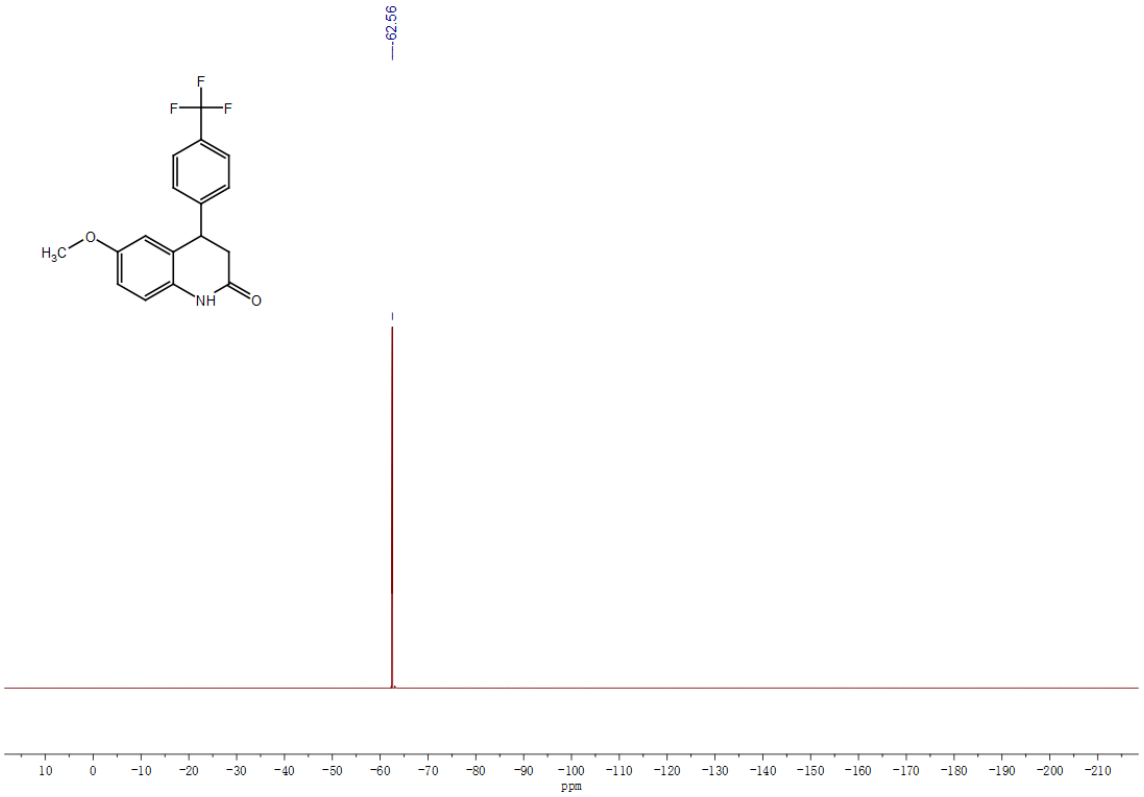
^{1}H NMR of 2k



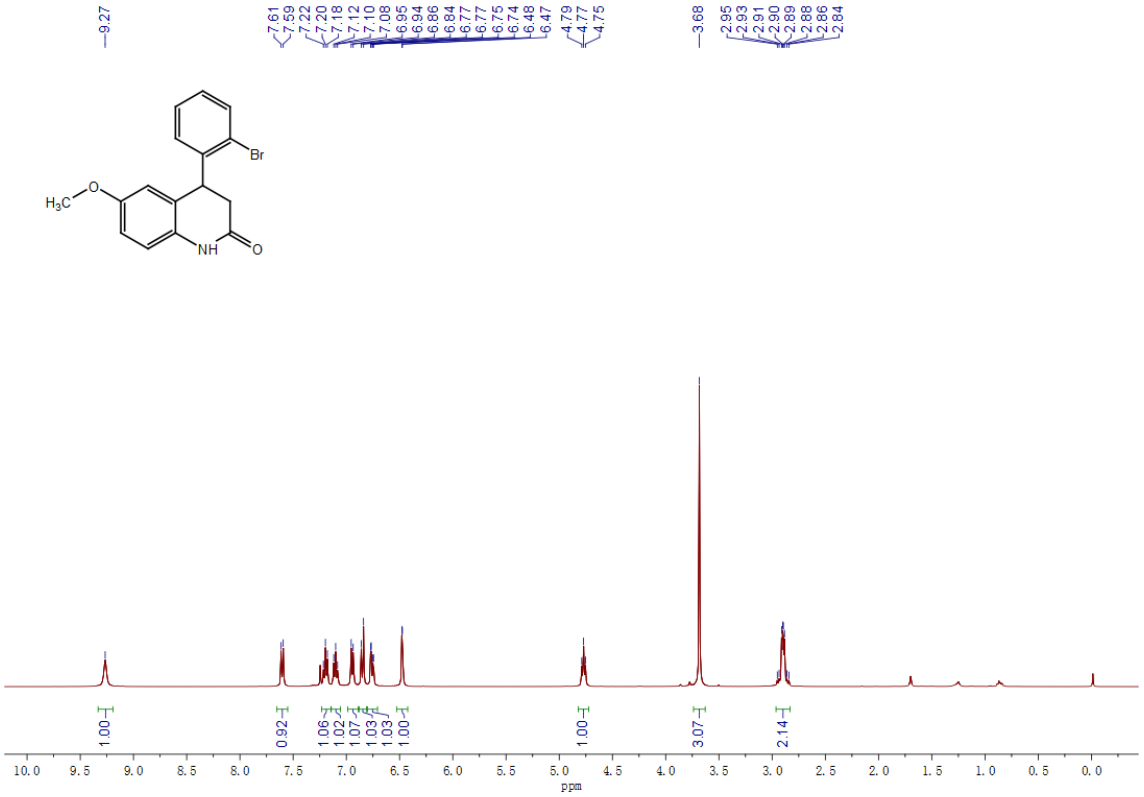
^{13}C NMR of 2k



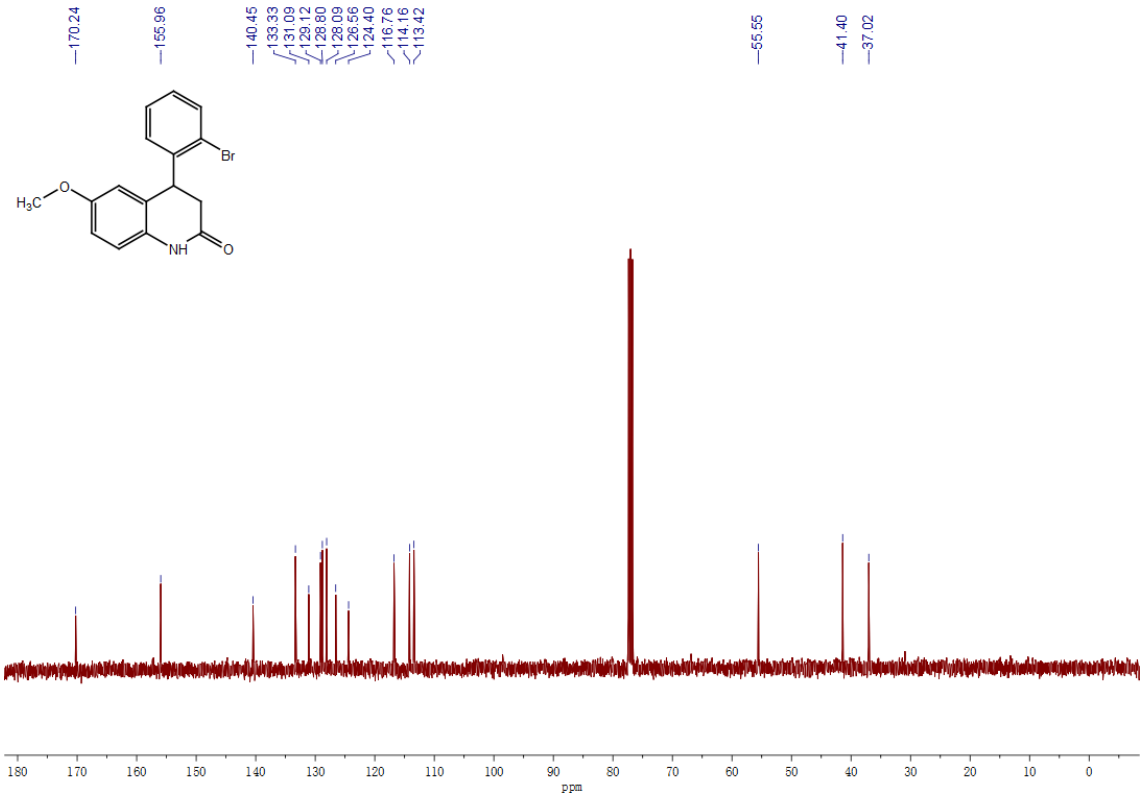
^{19}F NMR of 2k


-62.56
F
F
F
H3C
O
NH
O
10
0
-10
-20
-30
-40
-50
-60
-70
-80
-90
-100
-110
-120
-130
-140
-150
-160
-170
-180
-190
-200
-210
ppm

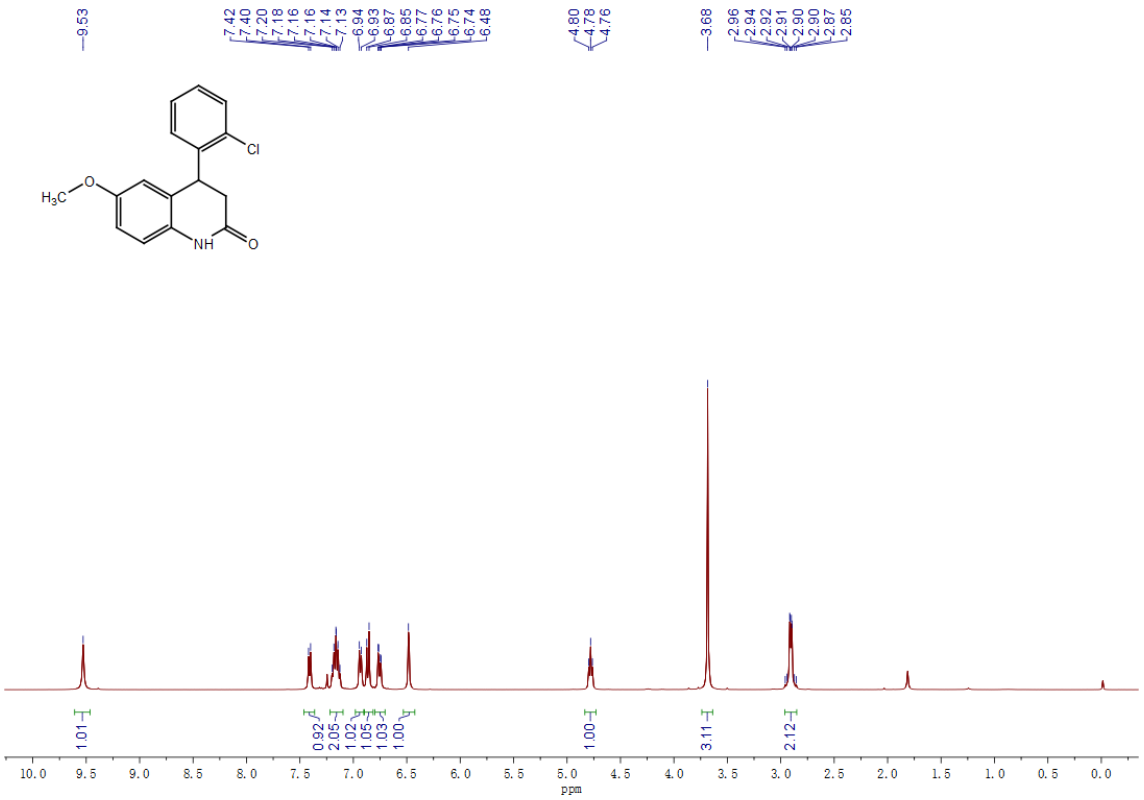
^{1}H NMR of 2l



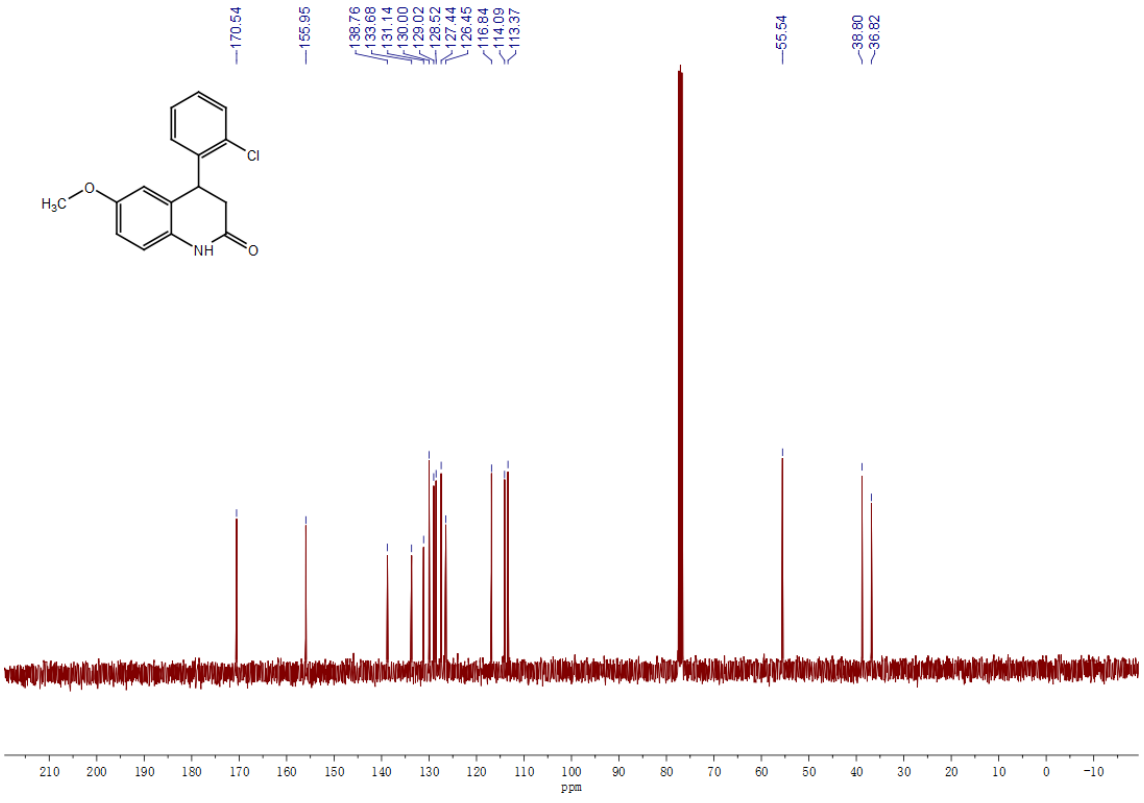
^{13}C NMR of 2l



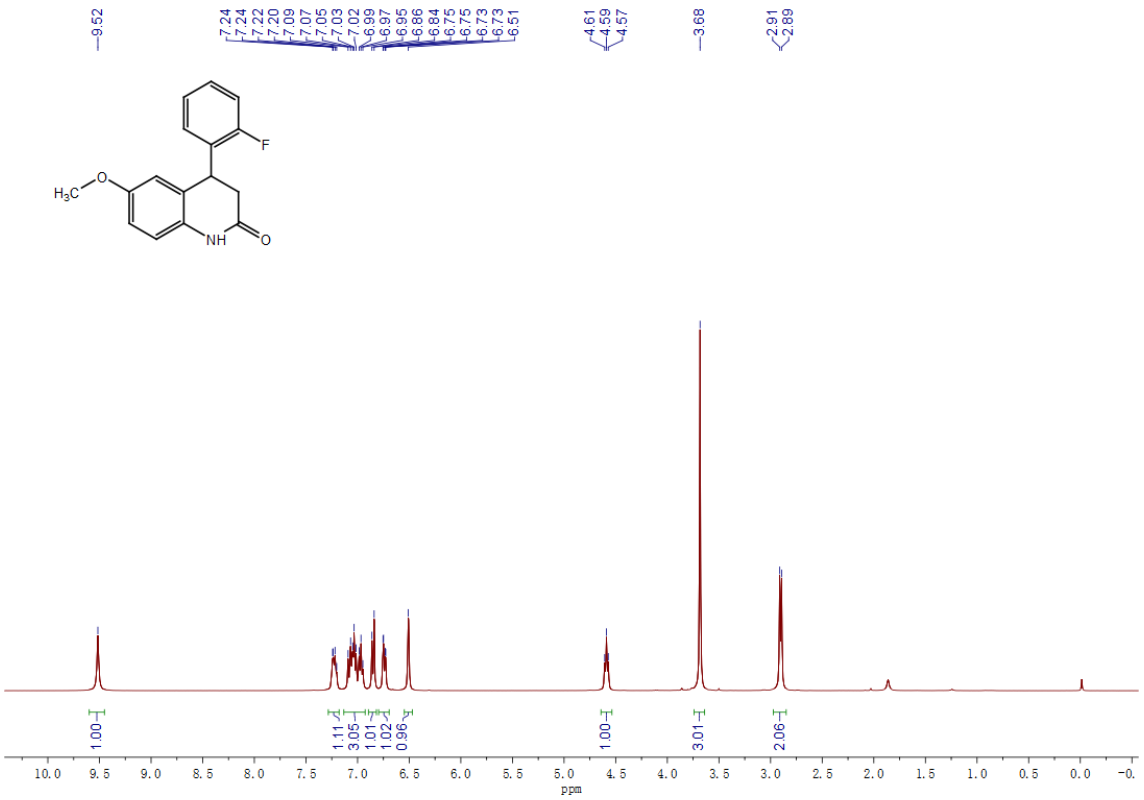
^{1}H NMR of 2m



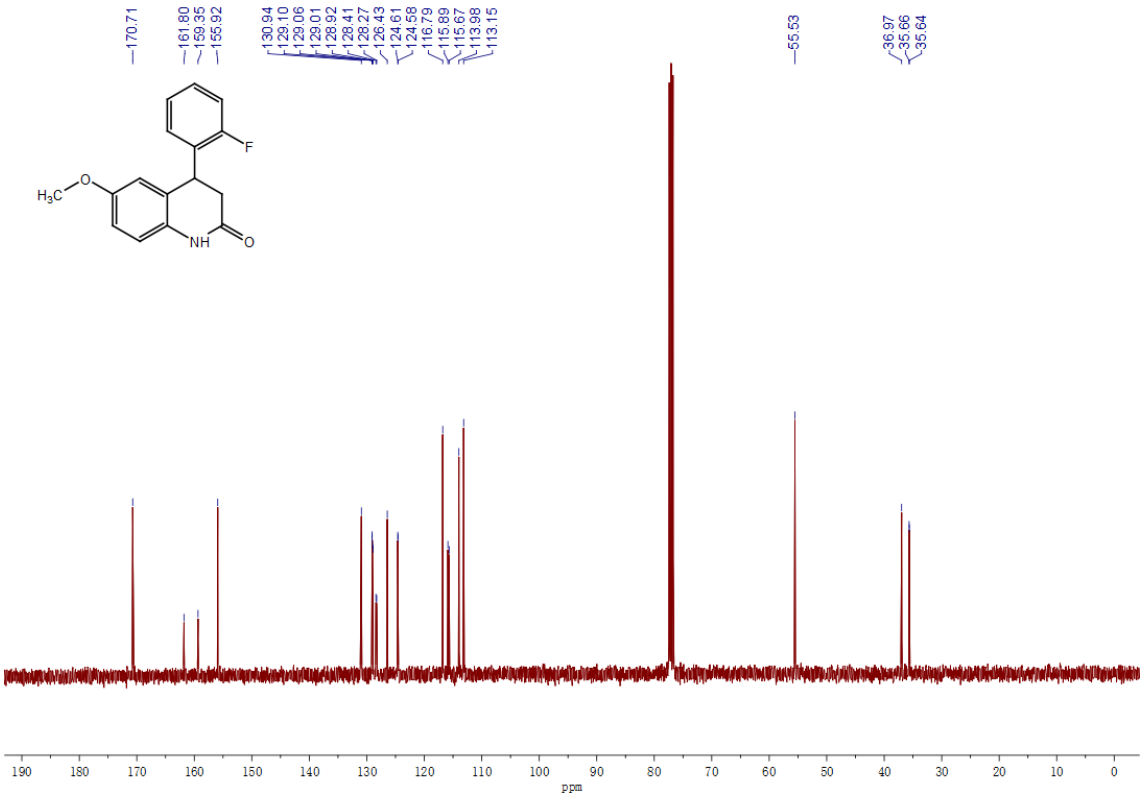
^{13}C NMR of 2m



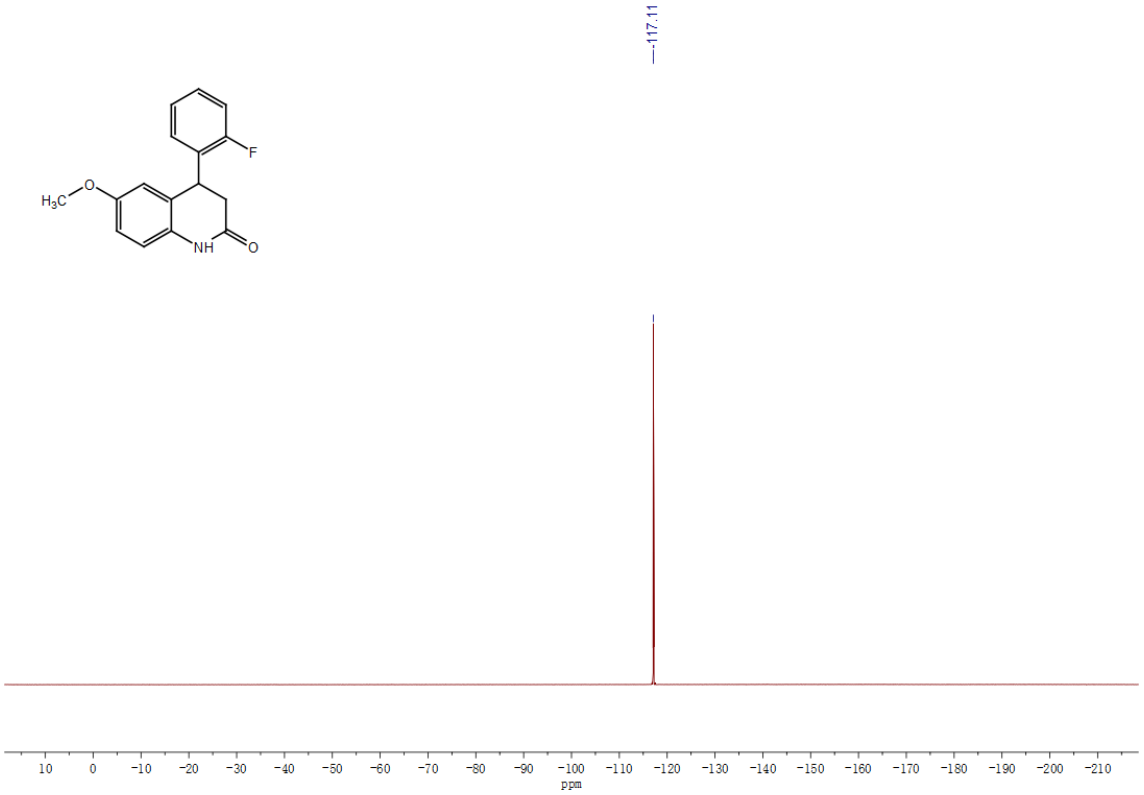
^{1}H NMR of 2n



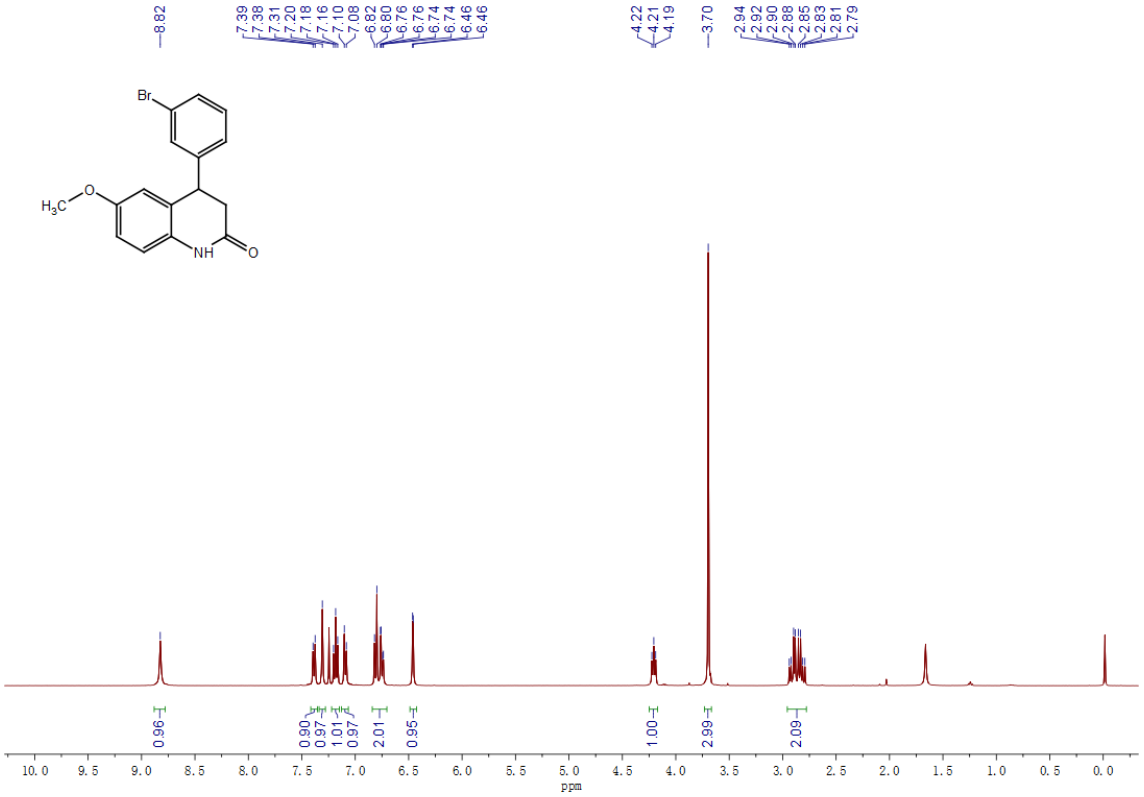
^{13}C NMR of 2n



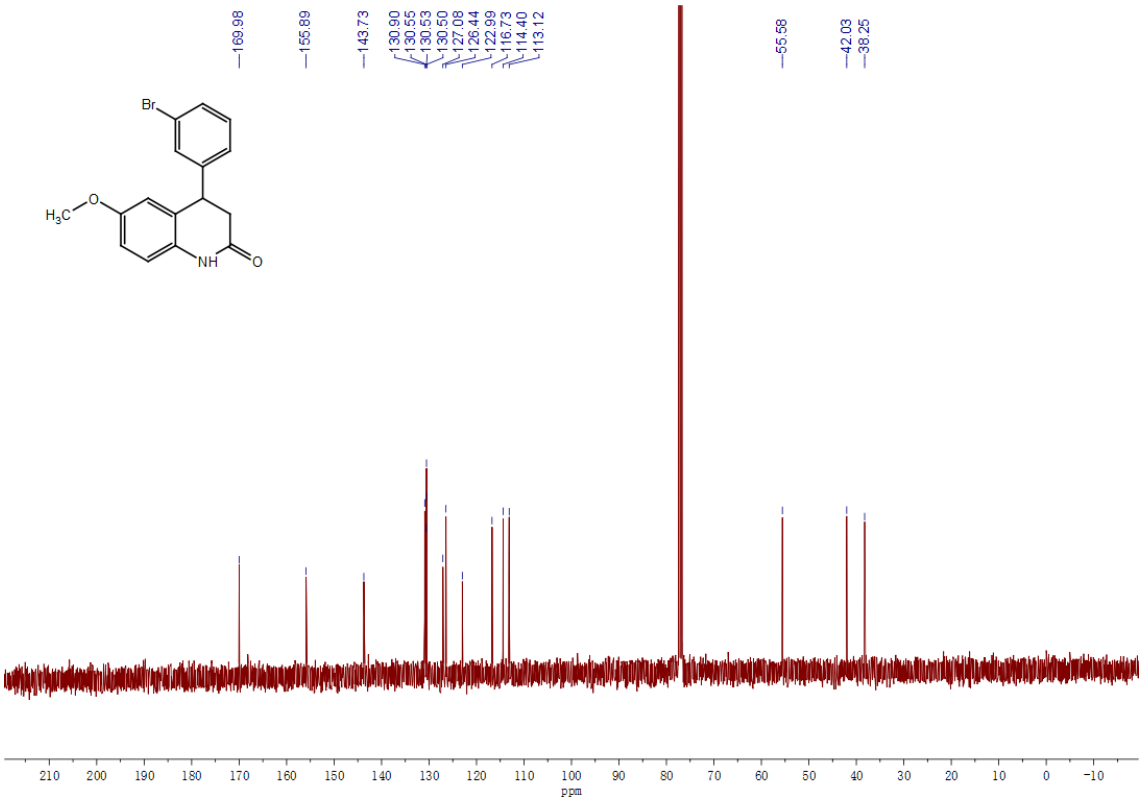
^{19}F NMR of 2n


-117.11
F
H3C
O
NH
O
10
0
-10
-20
-30
-40
-50
-60
-70
-80
-90
-100
-110
-120
-130
-140
-150
-160
-170
-180
-190
-200
-210
ppm

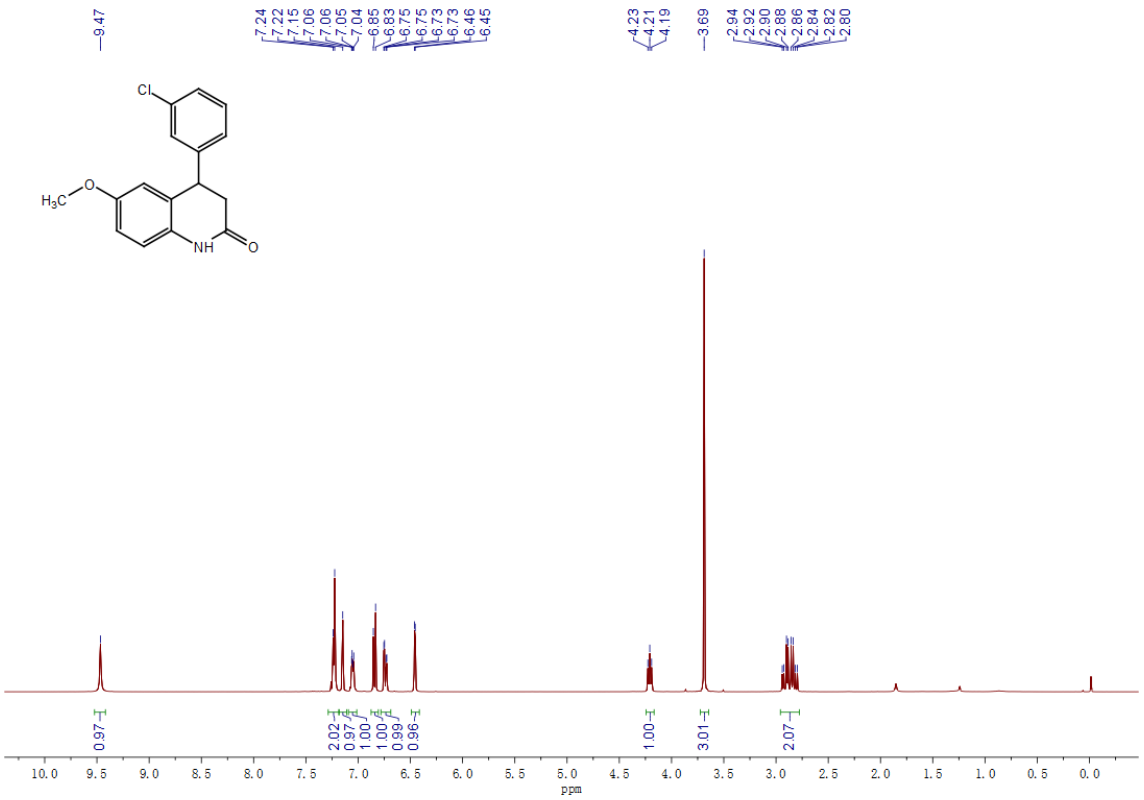
^{1}H NMR of 2o



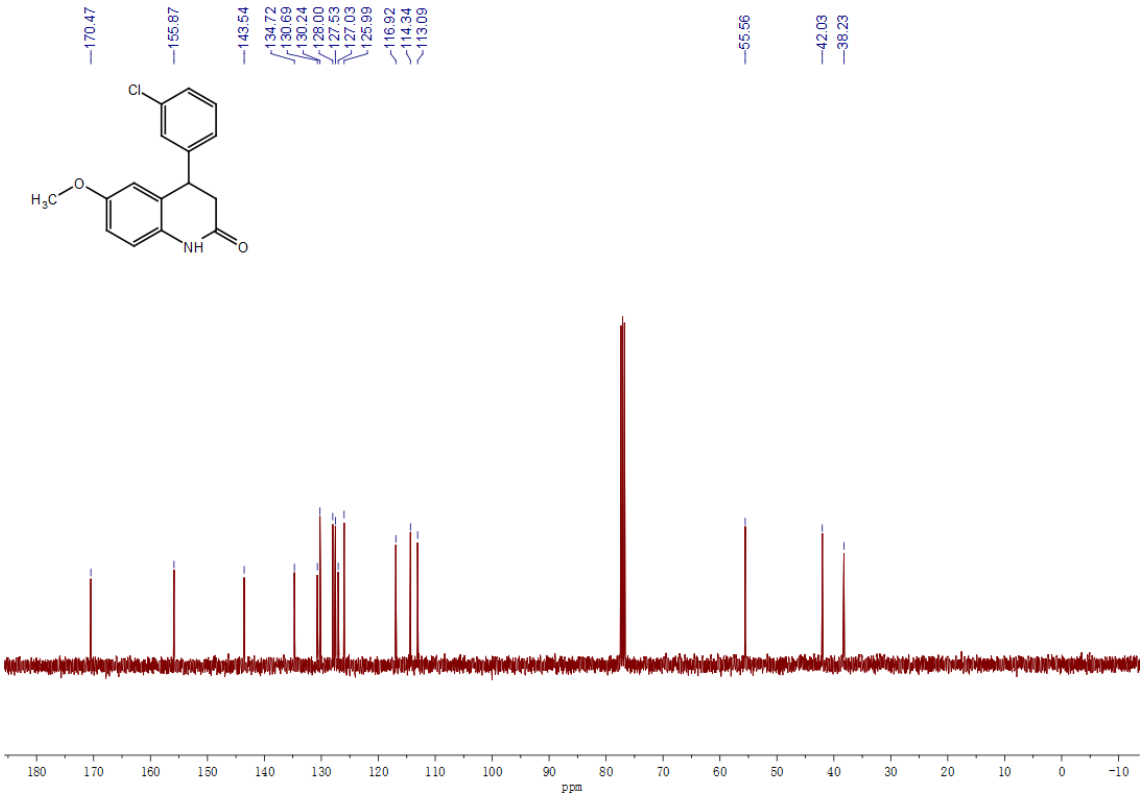
^{13}C NMR of 2o



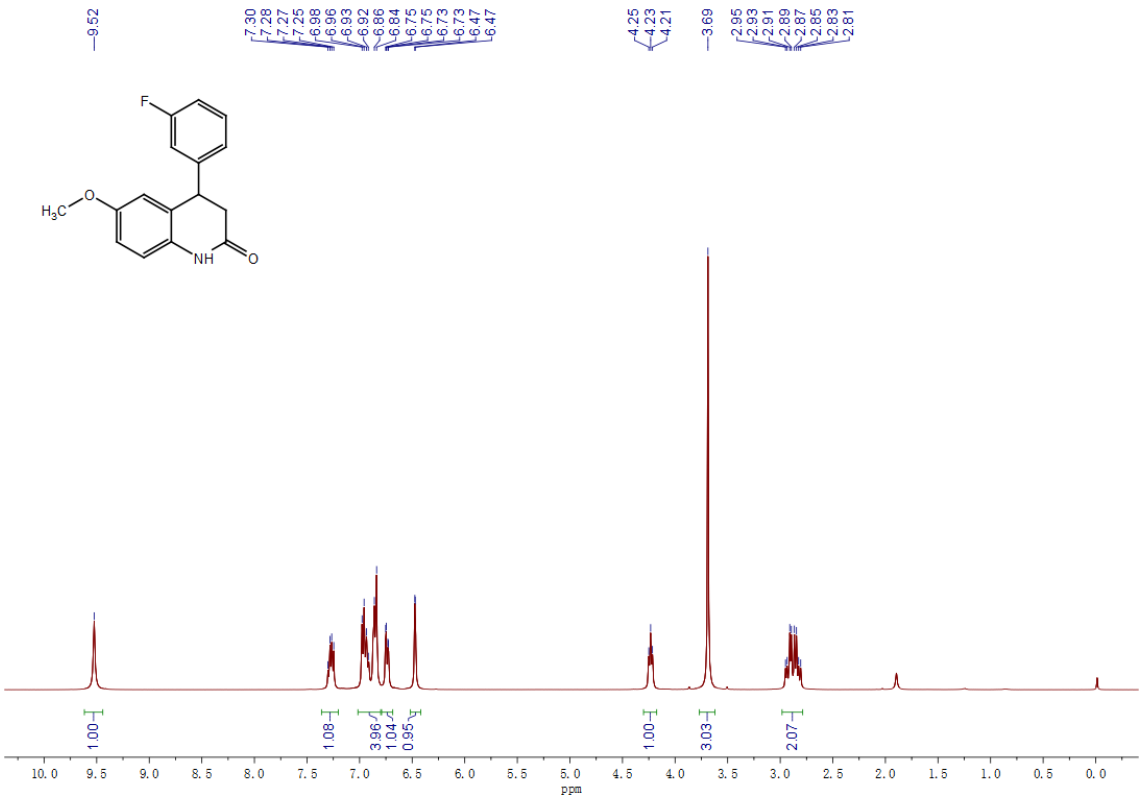
^{1}H NMR of 2p



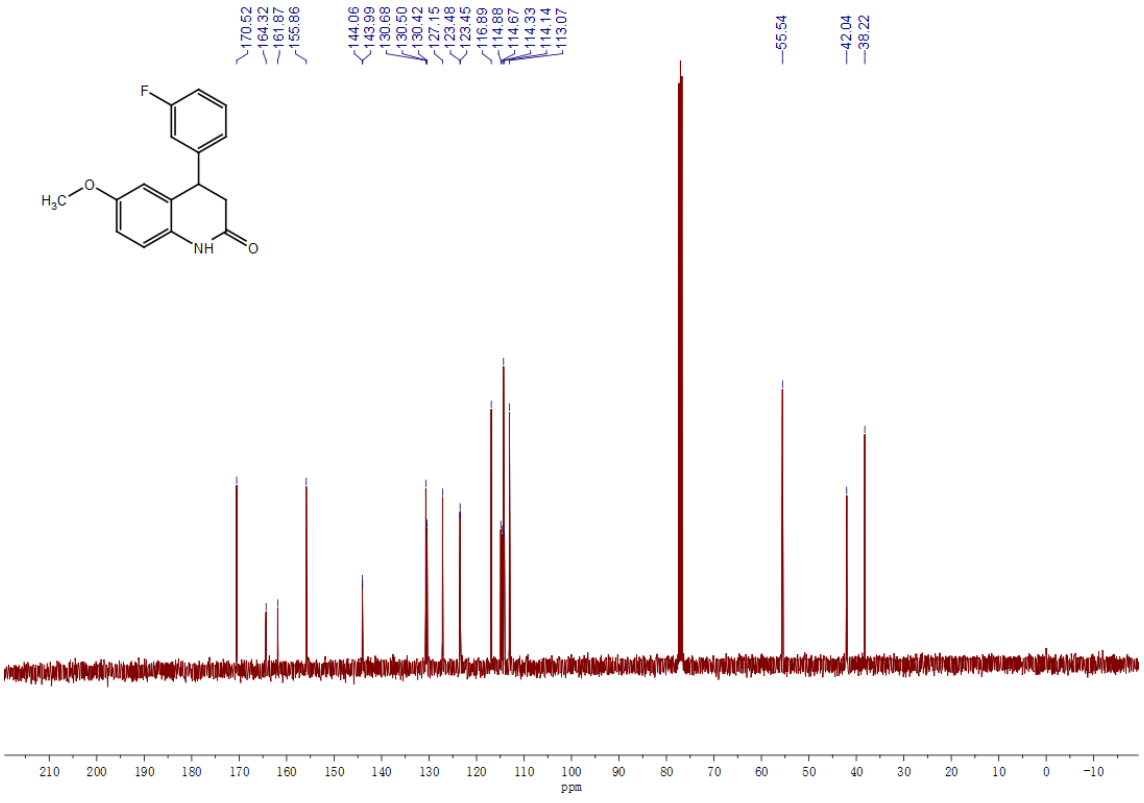
^{13}C NMR of 2p



^{1}H NMR of 2q



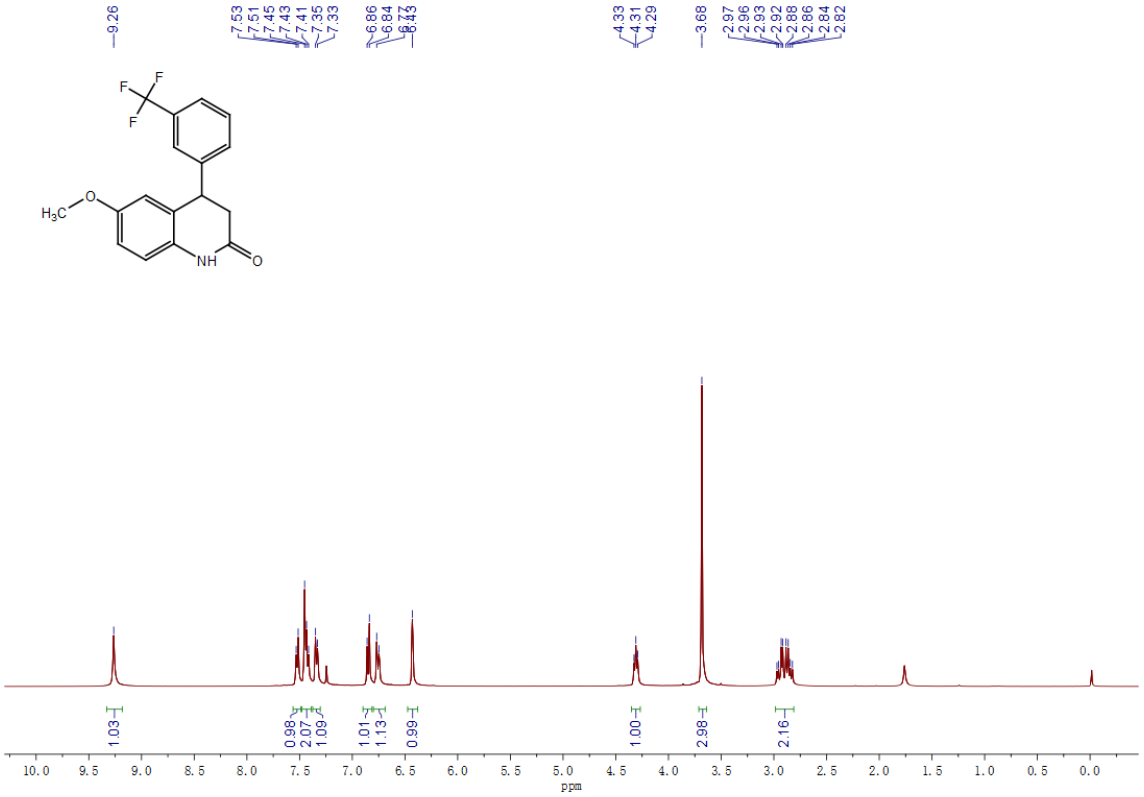
^{13}C NMR of 2q



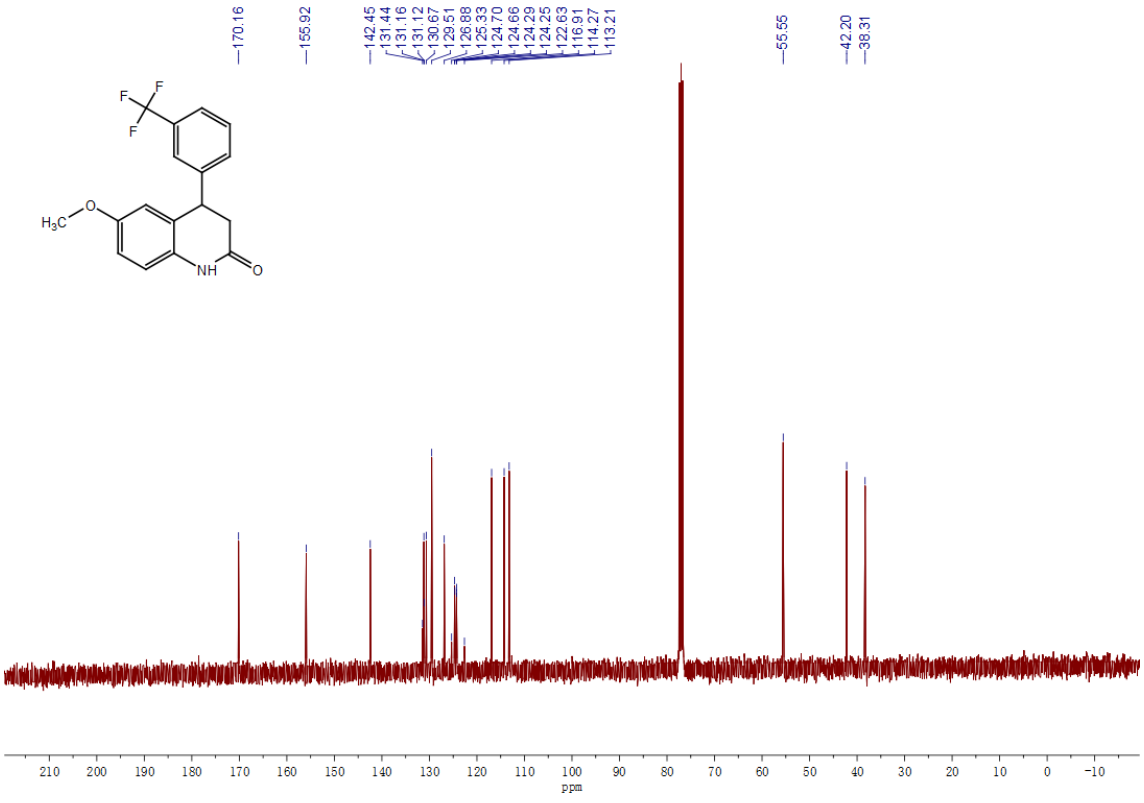
^{19}F NMR of 2q


-112.24
F
O
H_3C
NH
O
10
0
-10
-20
-30
-40
-50
-60
-70
-80
-90
-100
-110
-120
-130
-140
-150
-160
-170
-180
-190
-200
-210
ppm

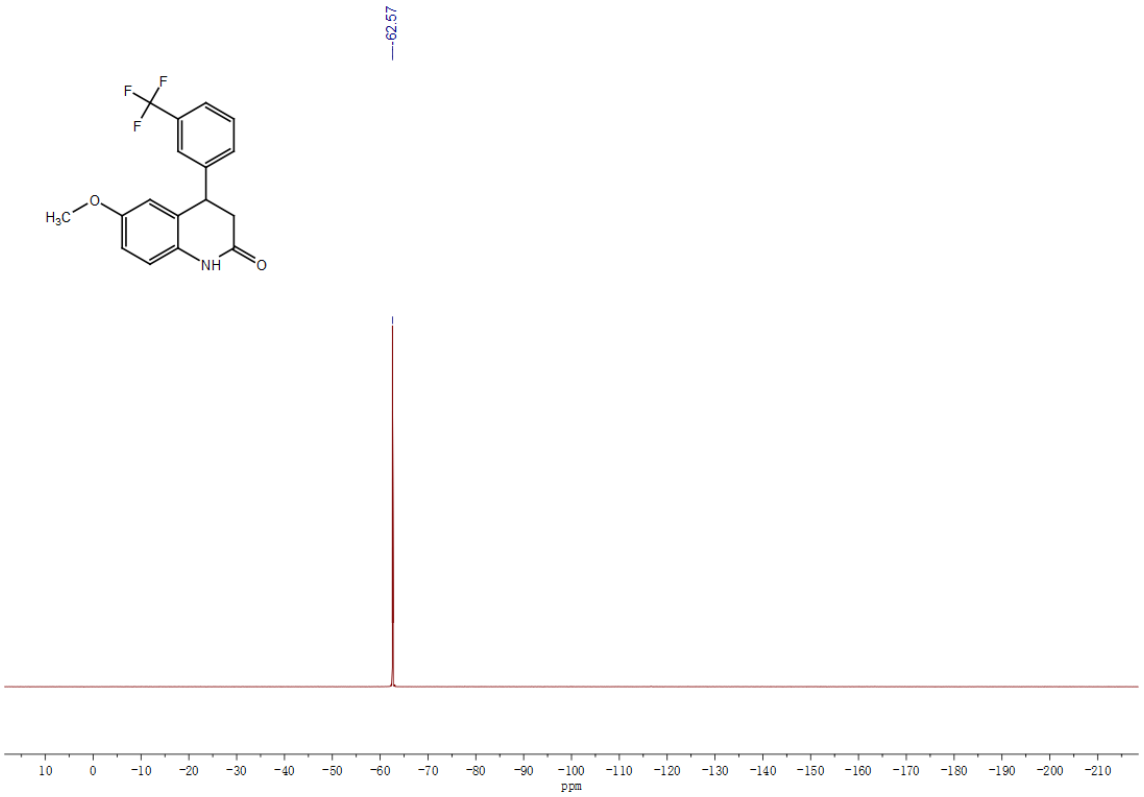
^{1}H NMR of 2r



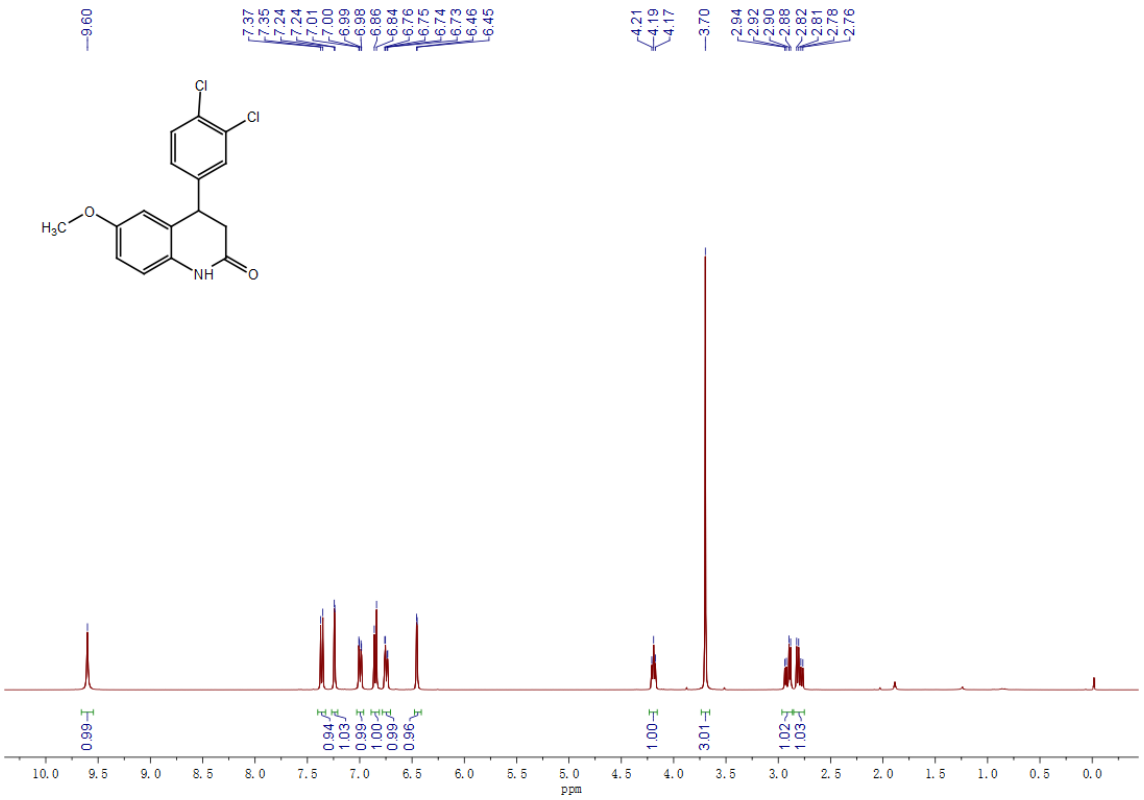
^{13}C NMR of 2r



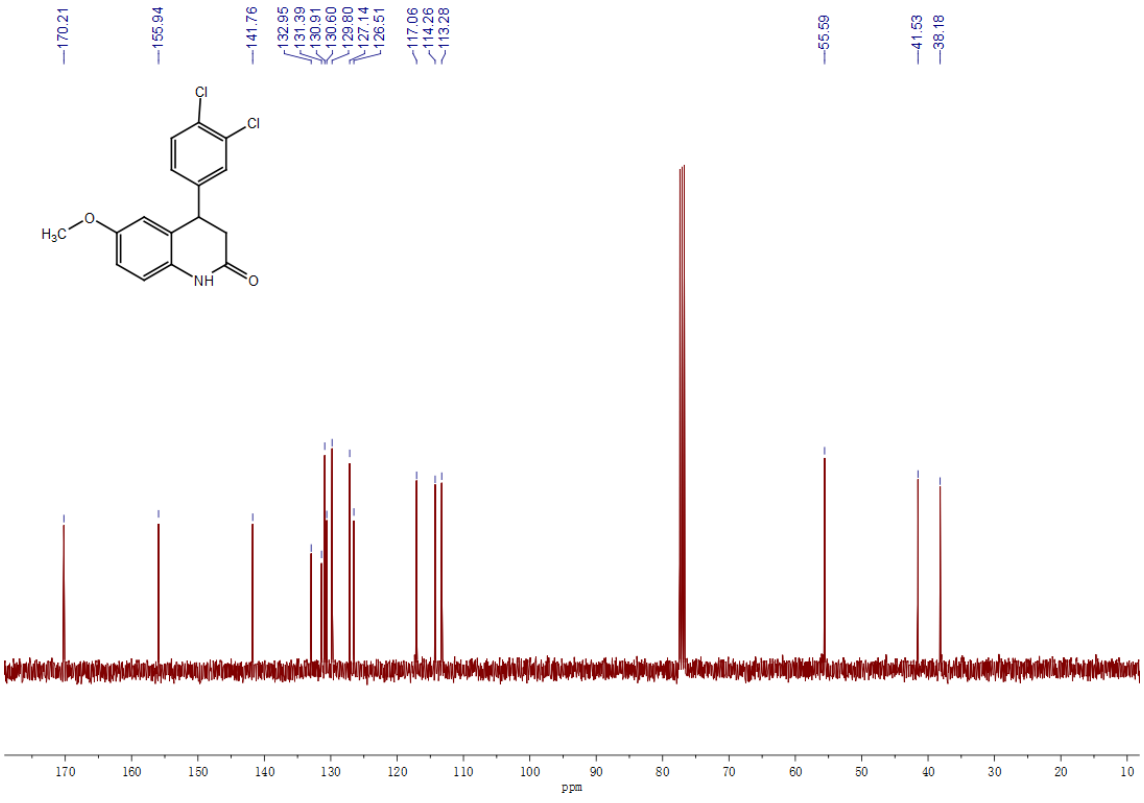
^{19}F NMR of 2r


-62.57
F
F
F
H3C
O
NH
O
10
0
-10
-20
-30
-40
-50
-60
-70
-80
-90
-100
-110
-120
-130
-140
-150
-160
-170
-180
-190
-200
-210
ppm

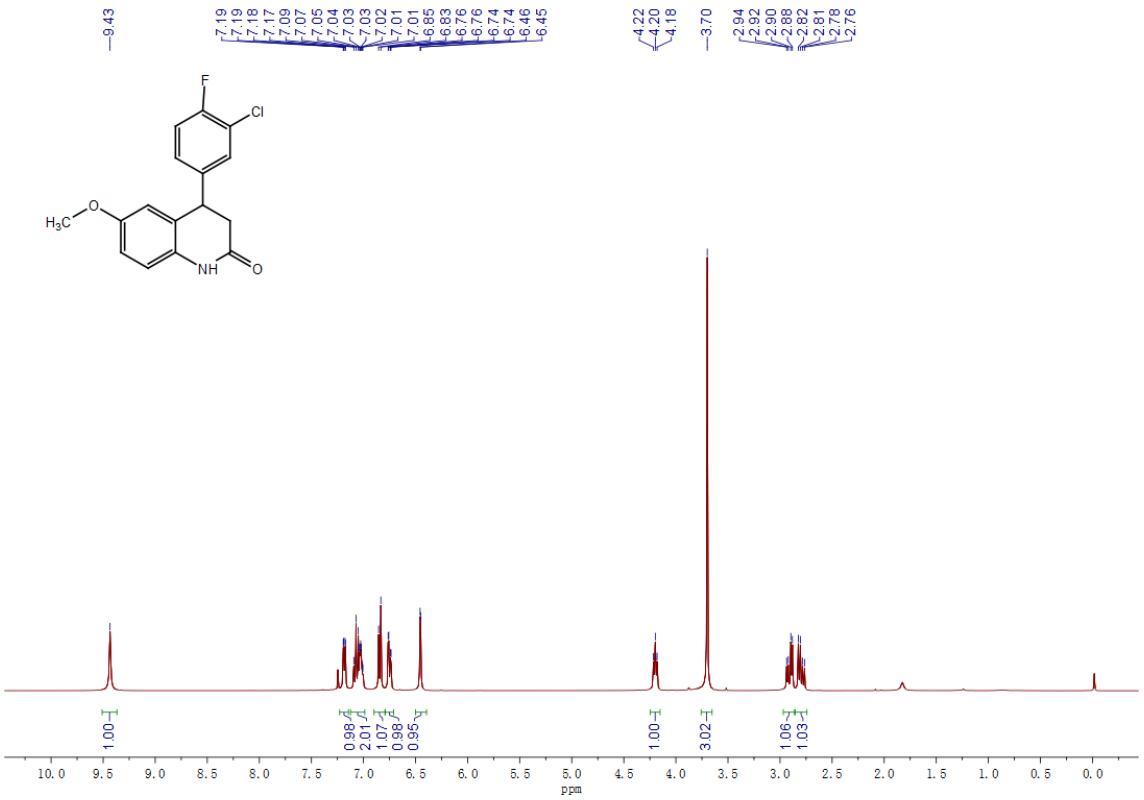
^{1}H NMR of 2s



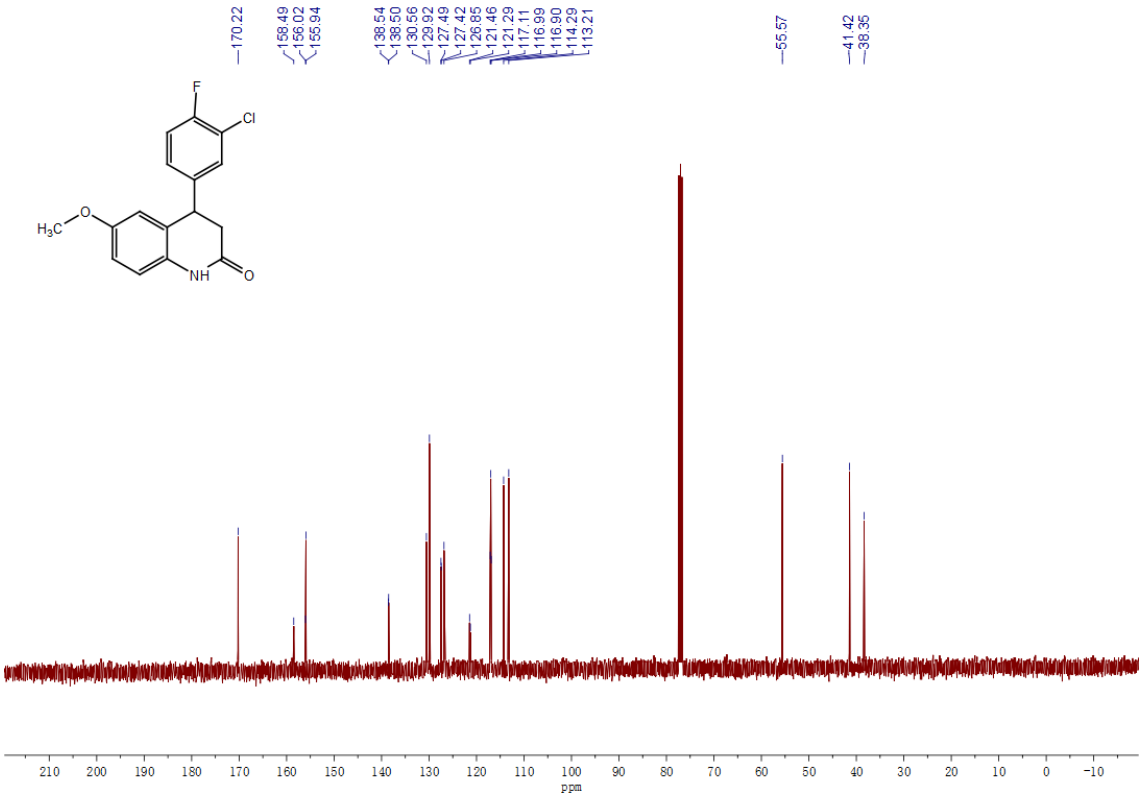
^{13}C NMR of 2s



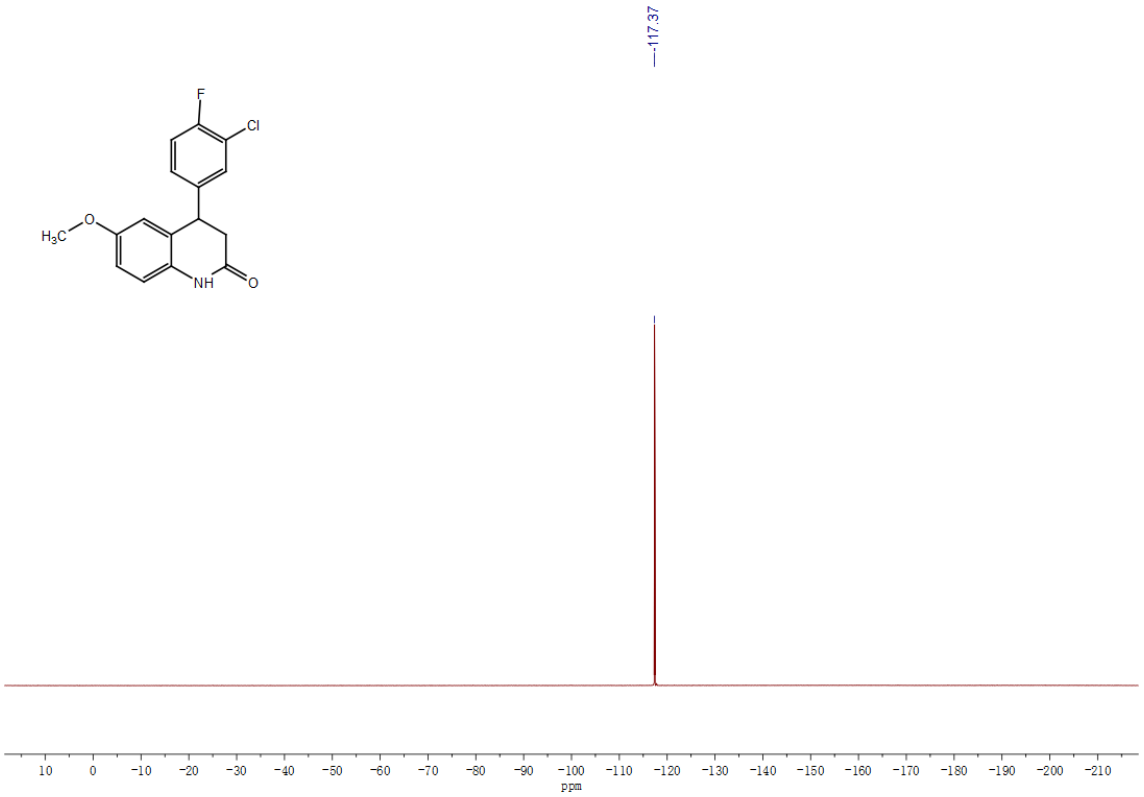
^{1}H NMR of 2t



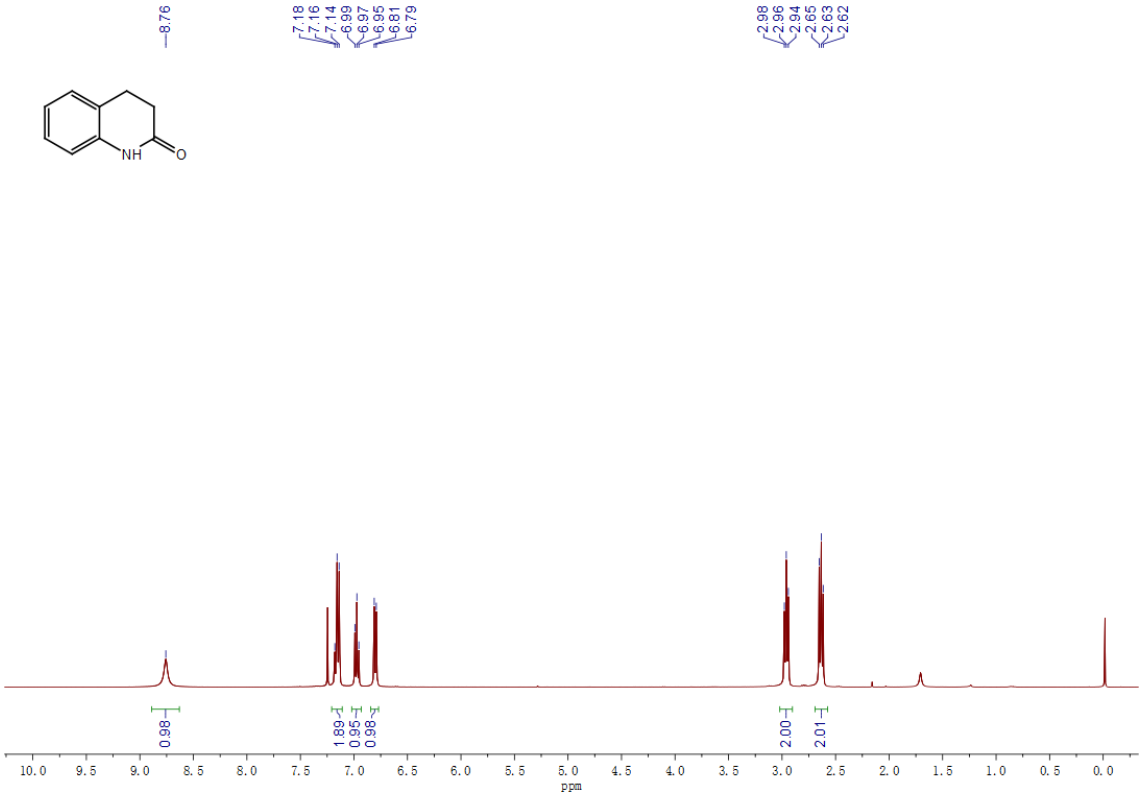
^{13}C NMR of 2t



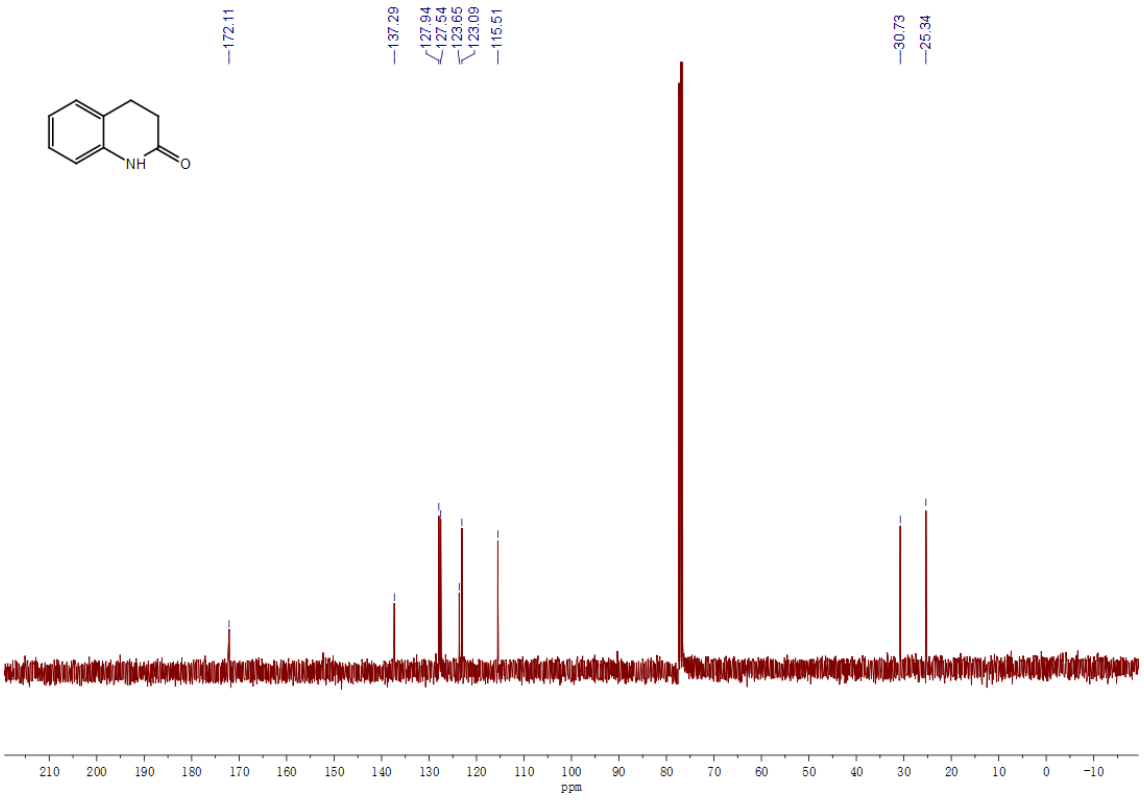
^{19}F NMR of 2t


-117.37
F
Cl
H3C
O
NH
O
10
0
-10
-20
-30
-40
-50
-60
-70
-80
-90
-100
-110
-120
-130
-140
-150
-160
-170
-180
-190
-200
-210
ppm

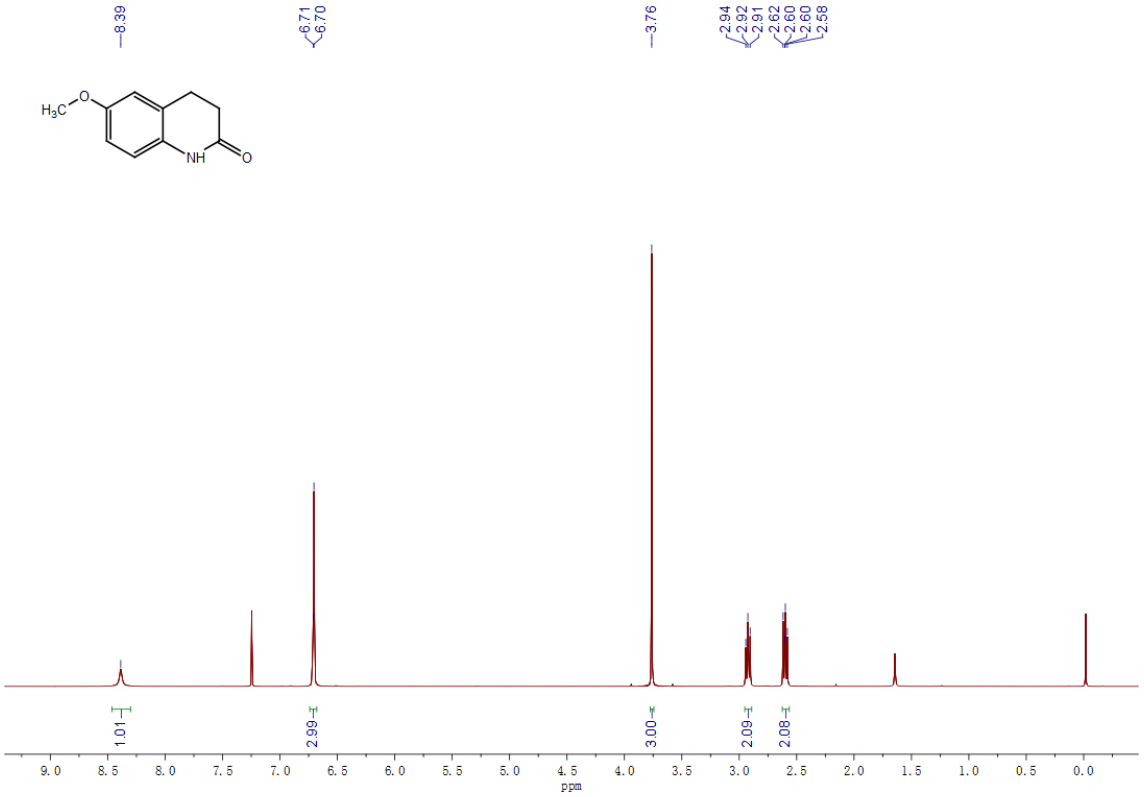
^{1}H NMR of 2u



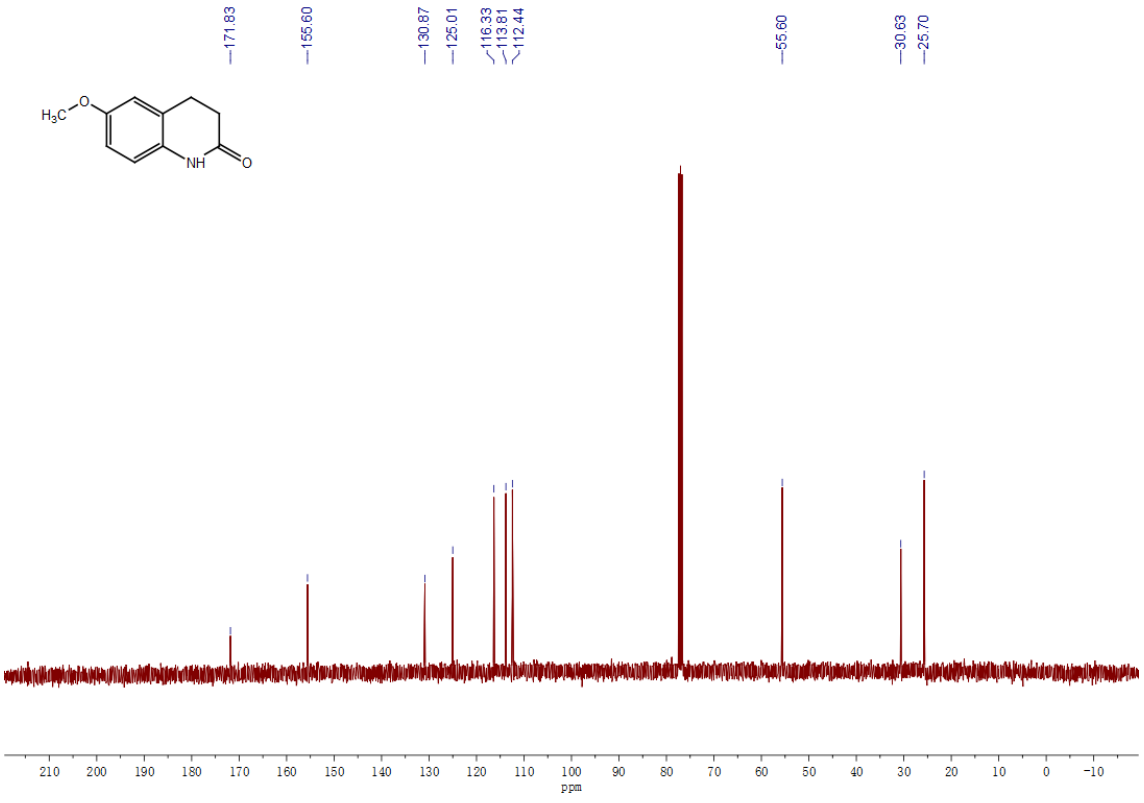
^{13}C NMR of 2u



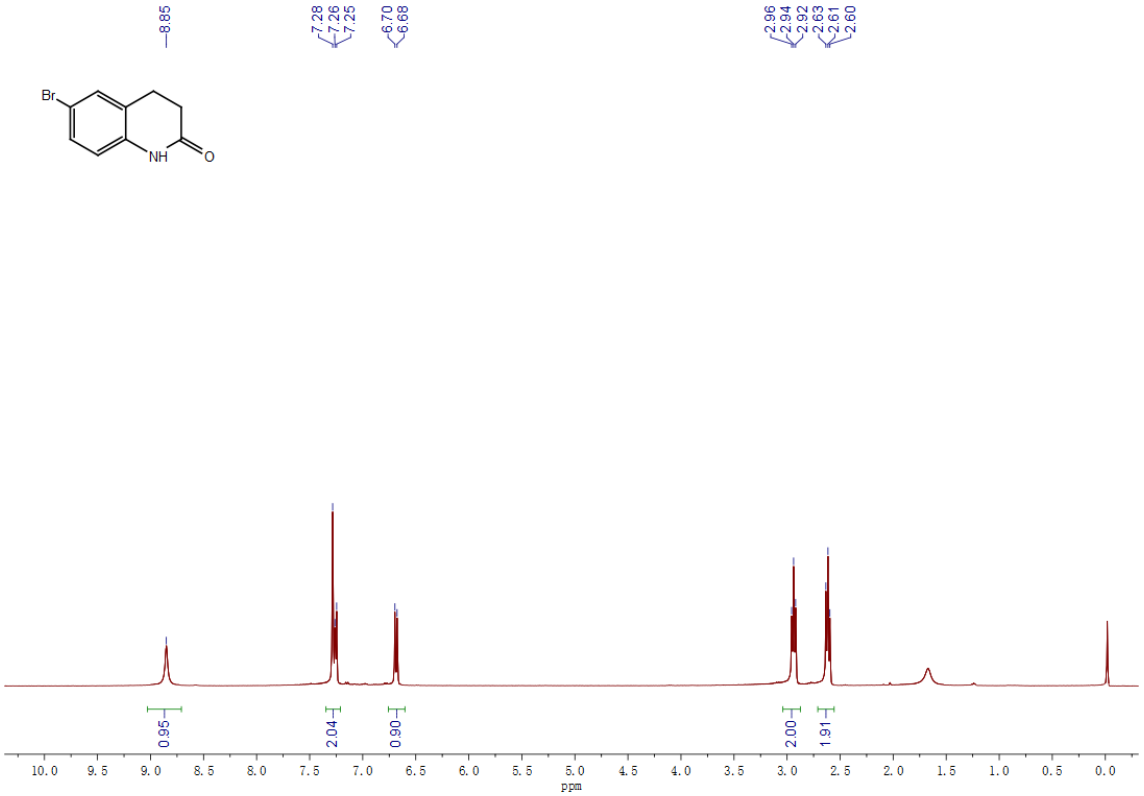
^{1}H NMR of 2v



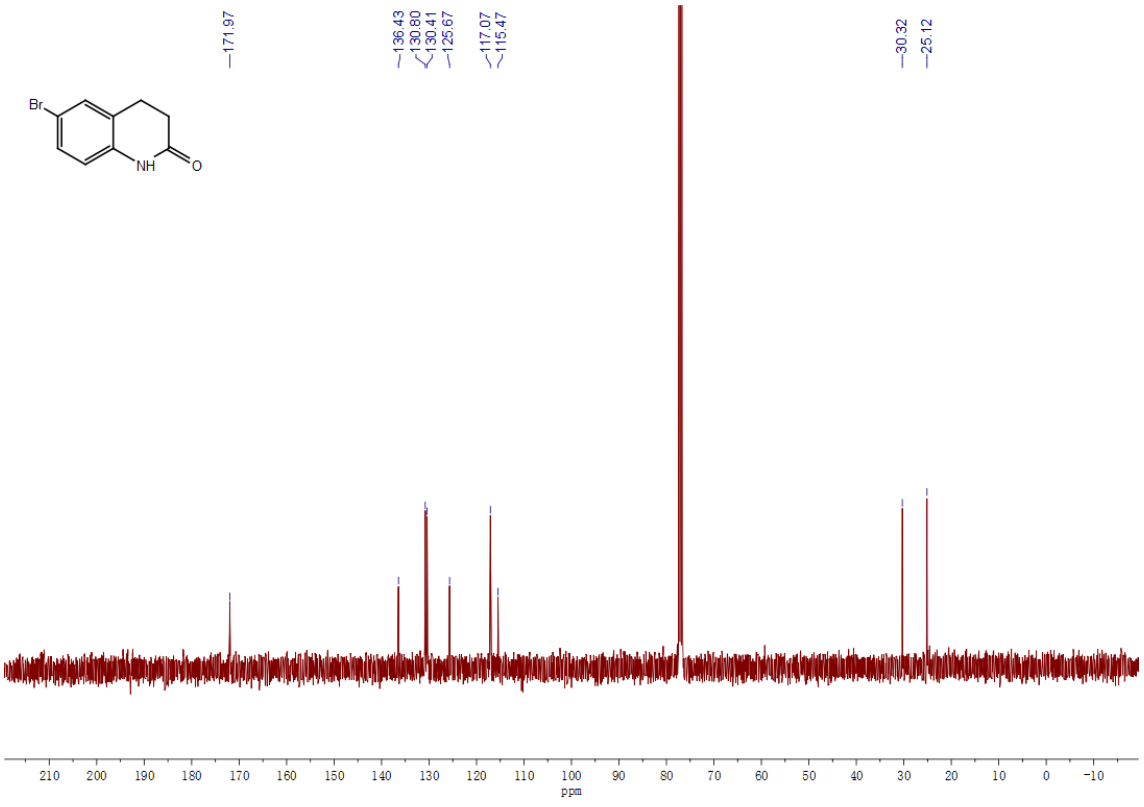
^{13}C NMR of 2v



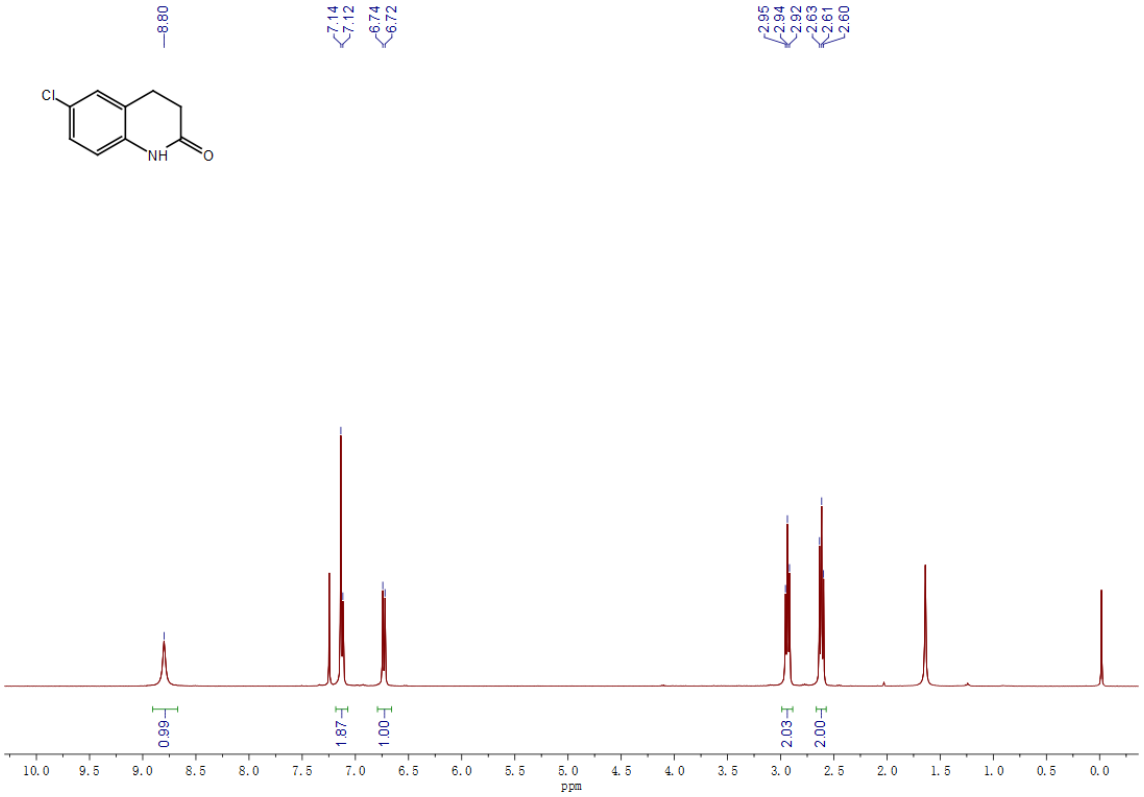
^{1}H NMR of 2w



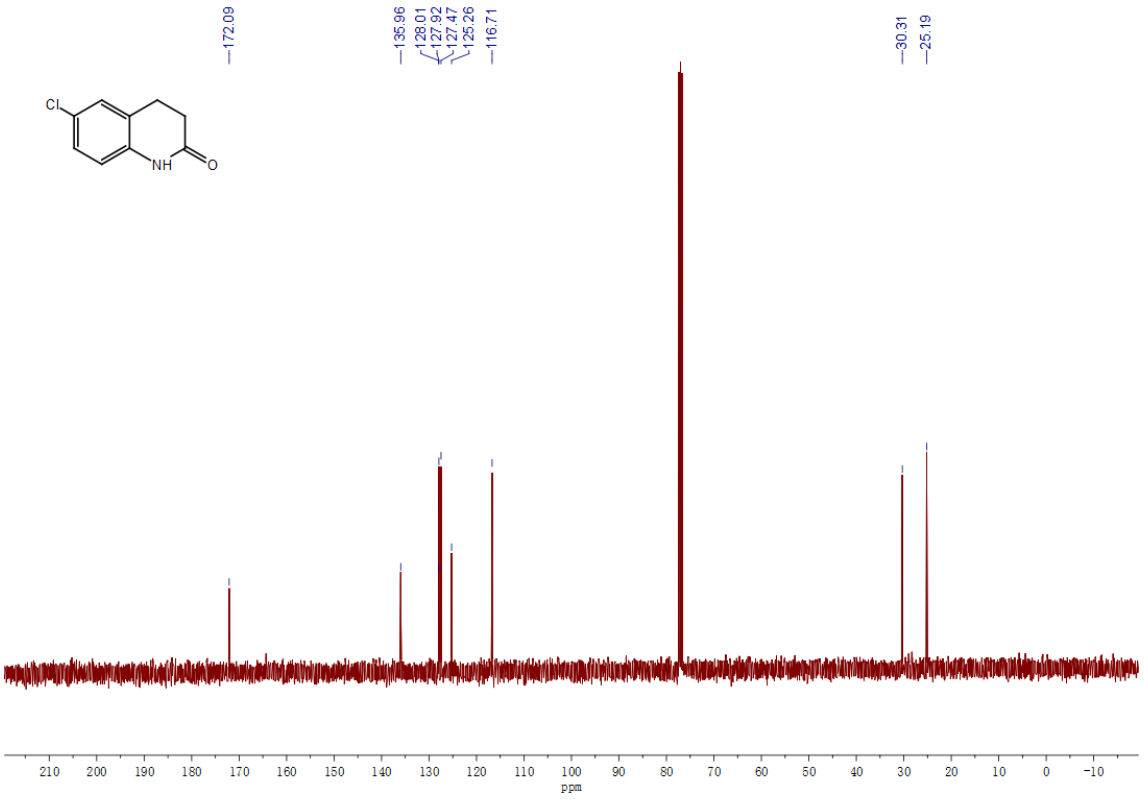
^{13}C NMR of 2w



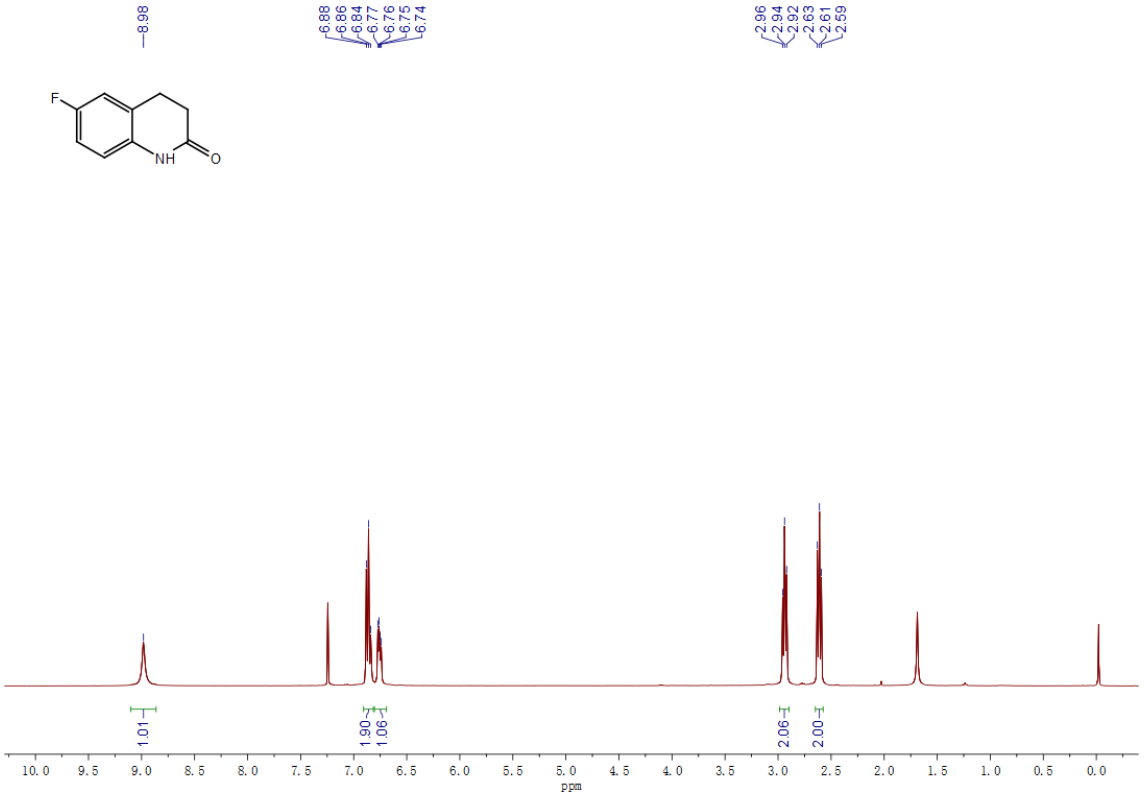
^{1}H NMR of 2x



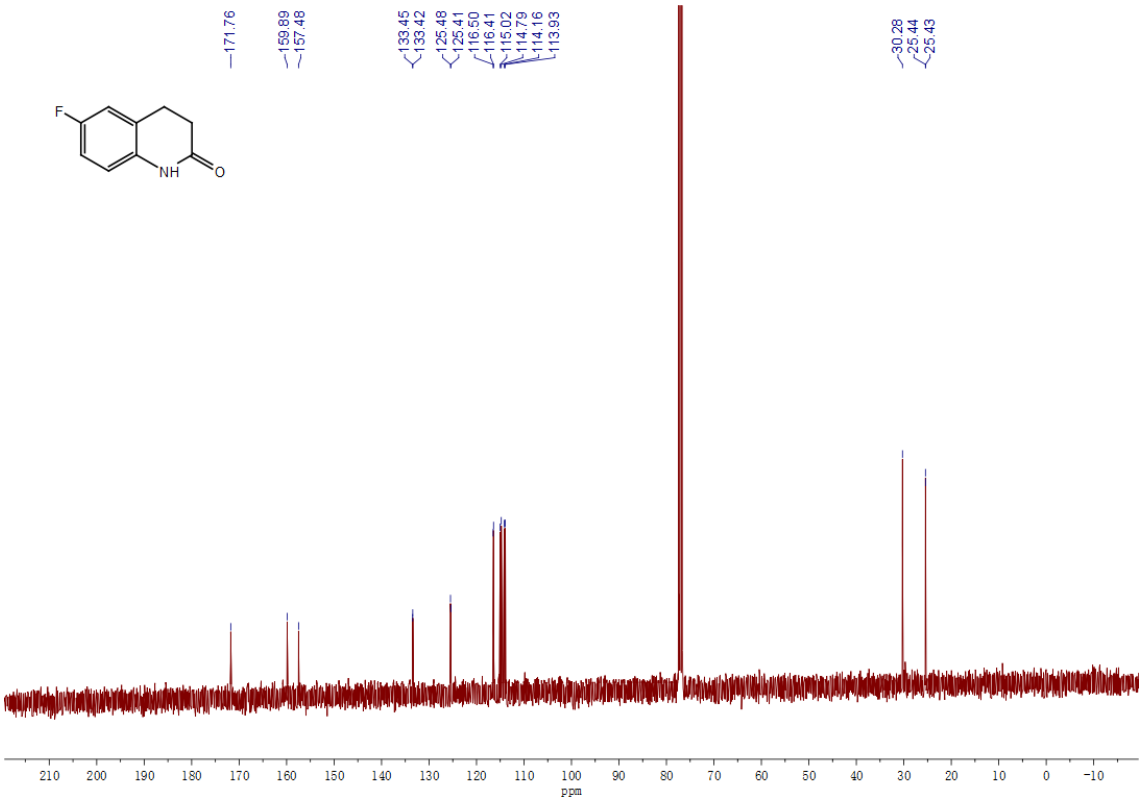
^{13}C NMR of 2x



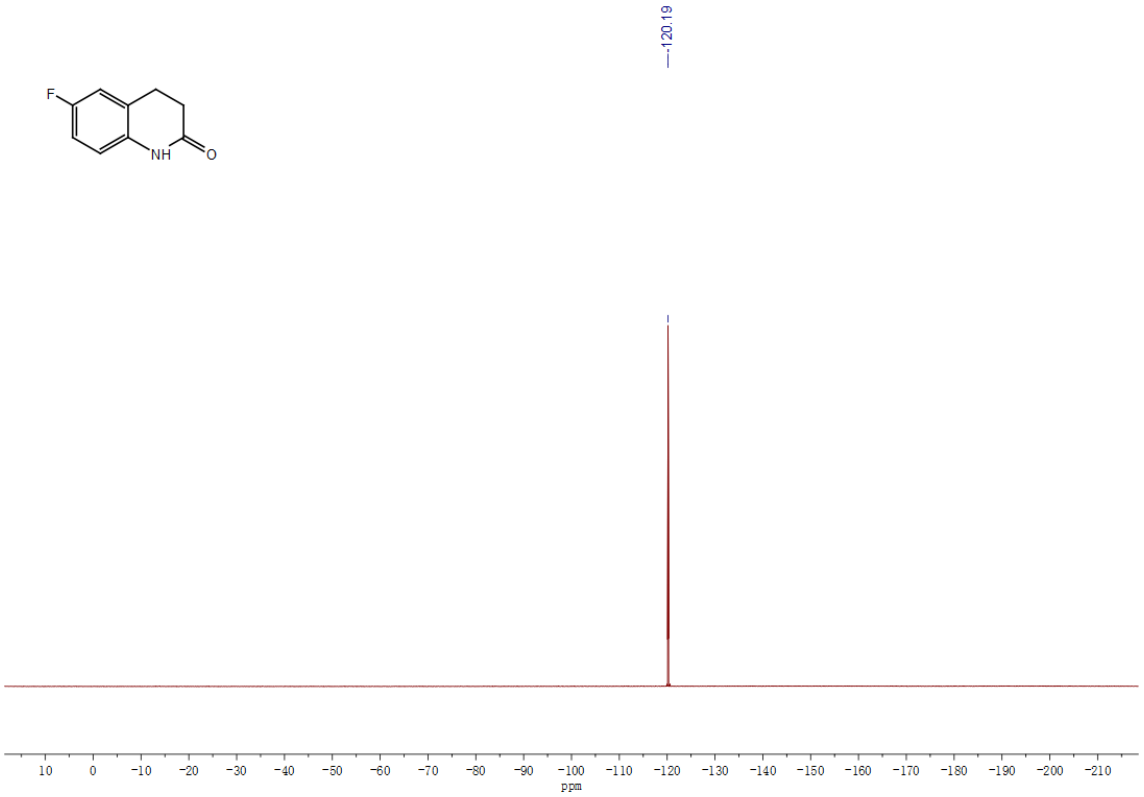
^{1}H NMR of 2y



^{13}C NMR of 2y



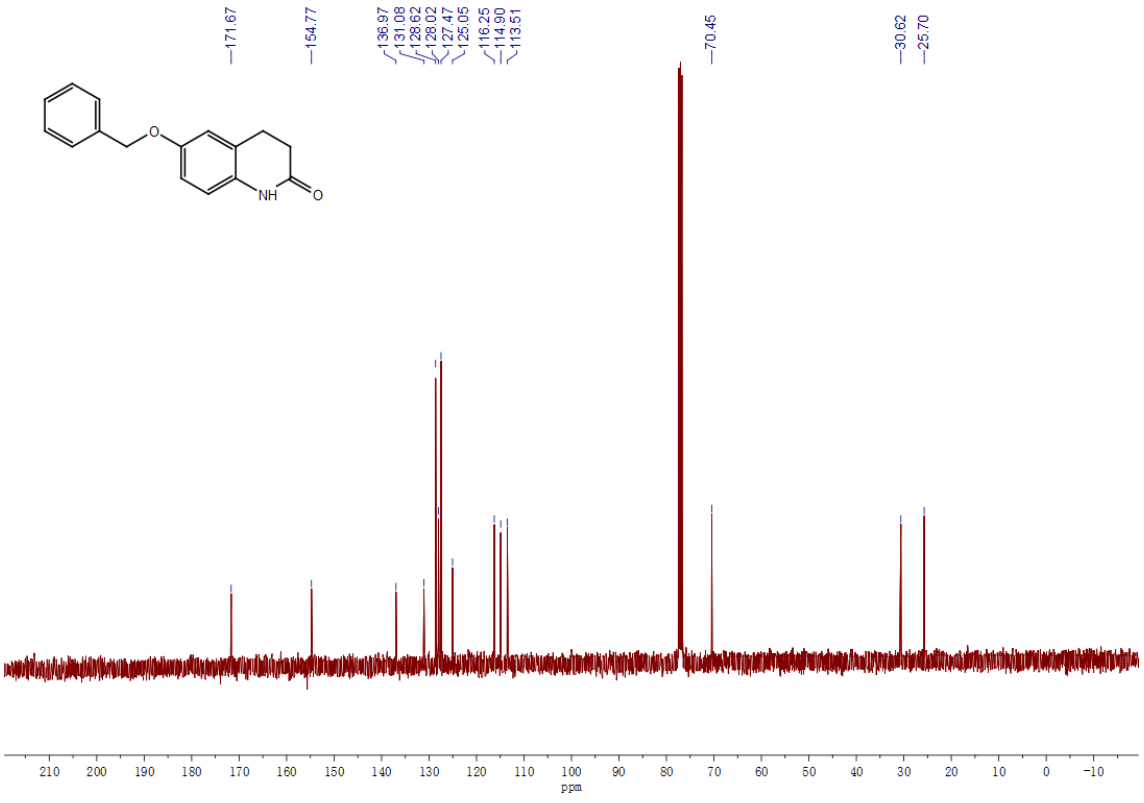
^{19}F NMR of 2y


-120.19
F
NH
O
10
0
-10
-20
-30
-40
-50
-60
-70
-80
-90
-100
-110
-120
-130
-140
-150
-160
-170
-180
-190
-200
-210
ppm

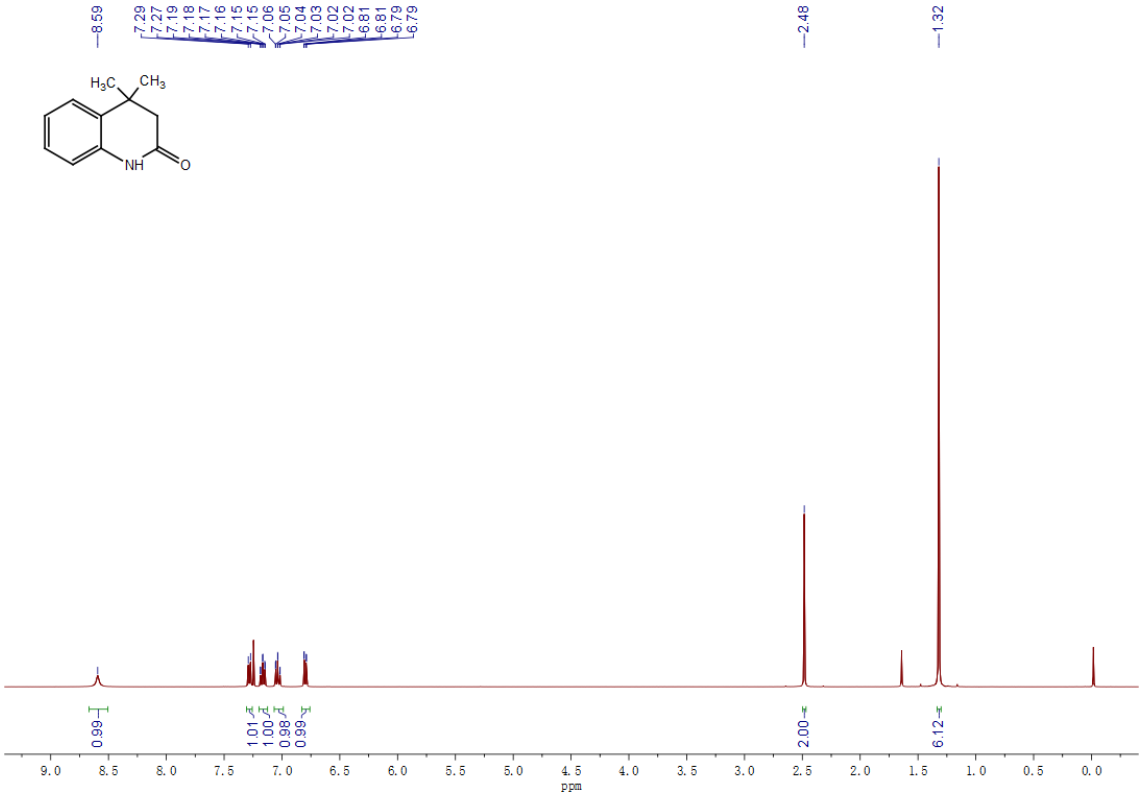
^{1}H NMR of 2z



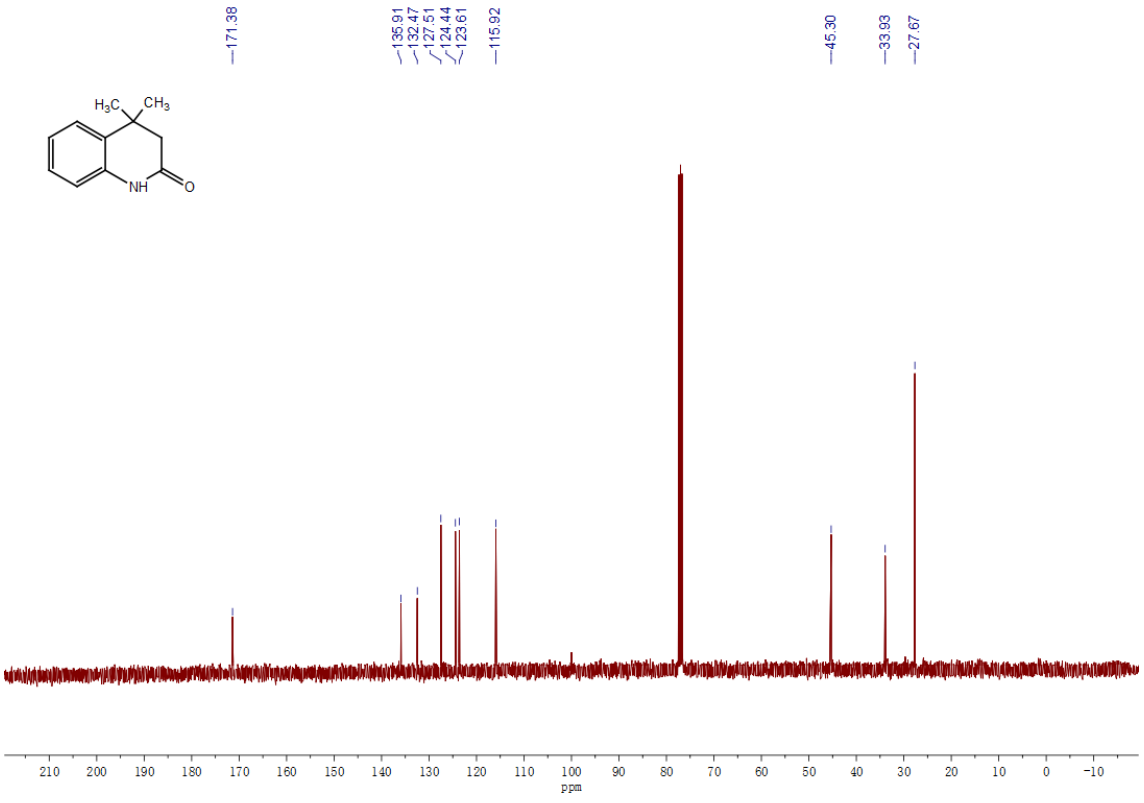
^{13}C NMR of 2z



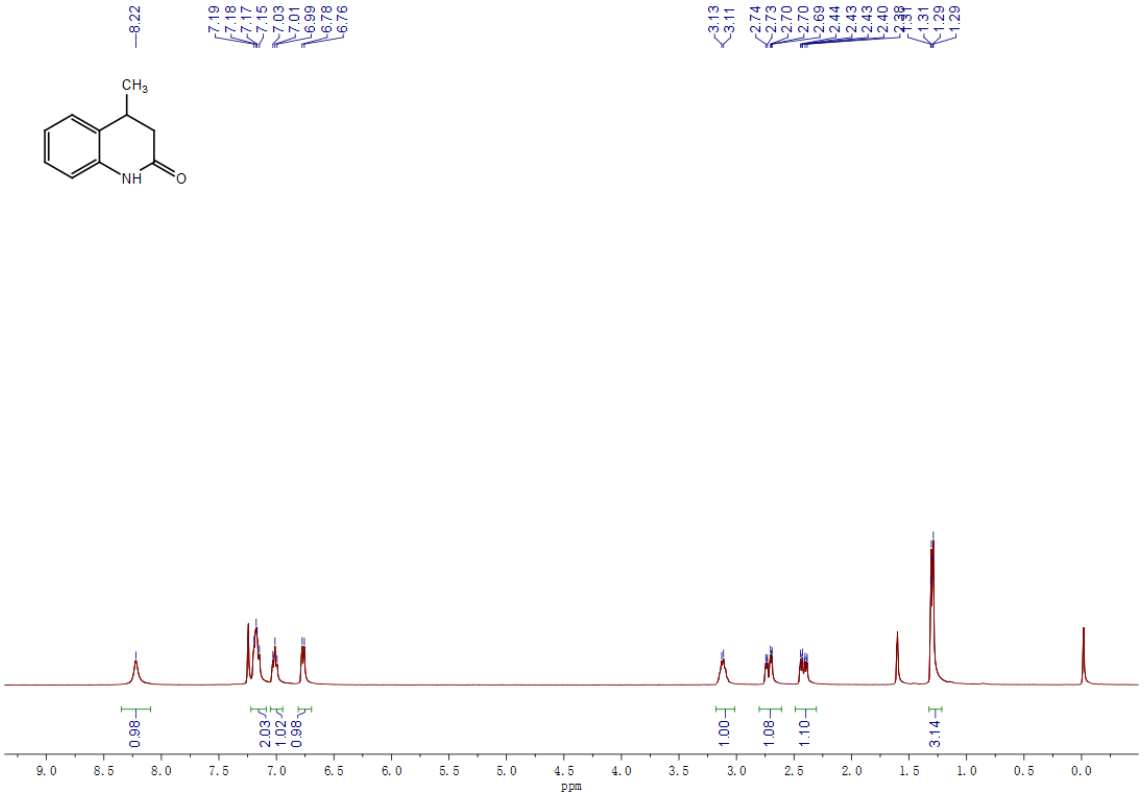
^{1}H NMR of 2za



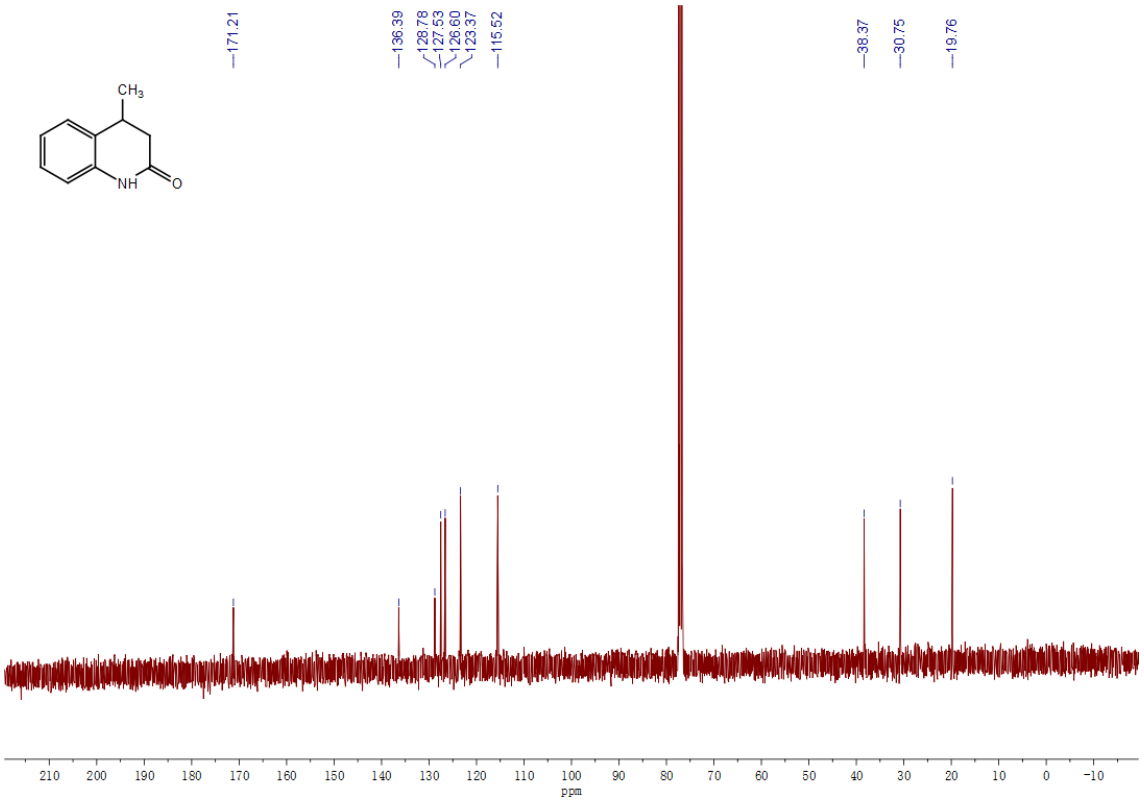
^{13}C NMR of 2za



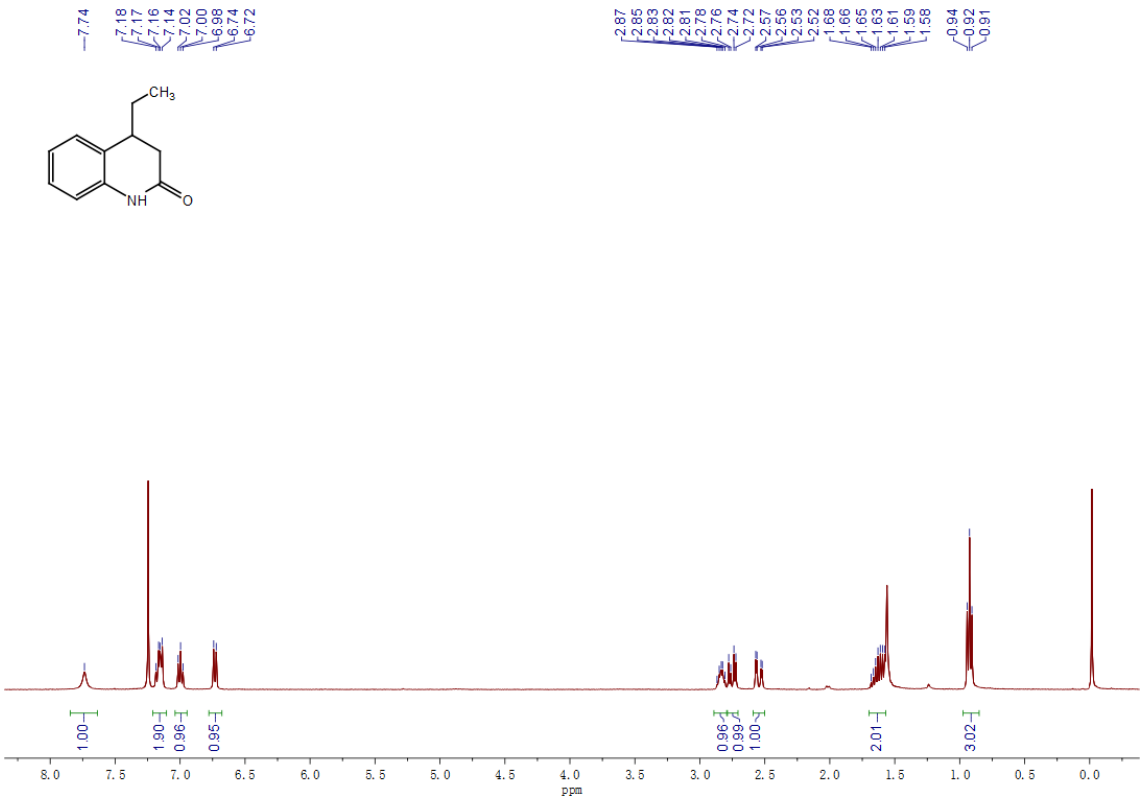
^{1}H NMR of 2zb



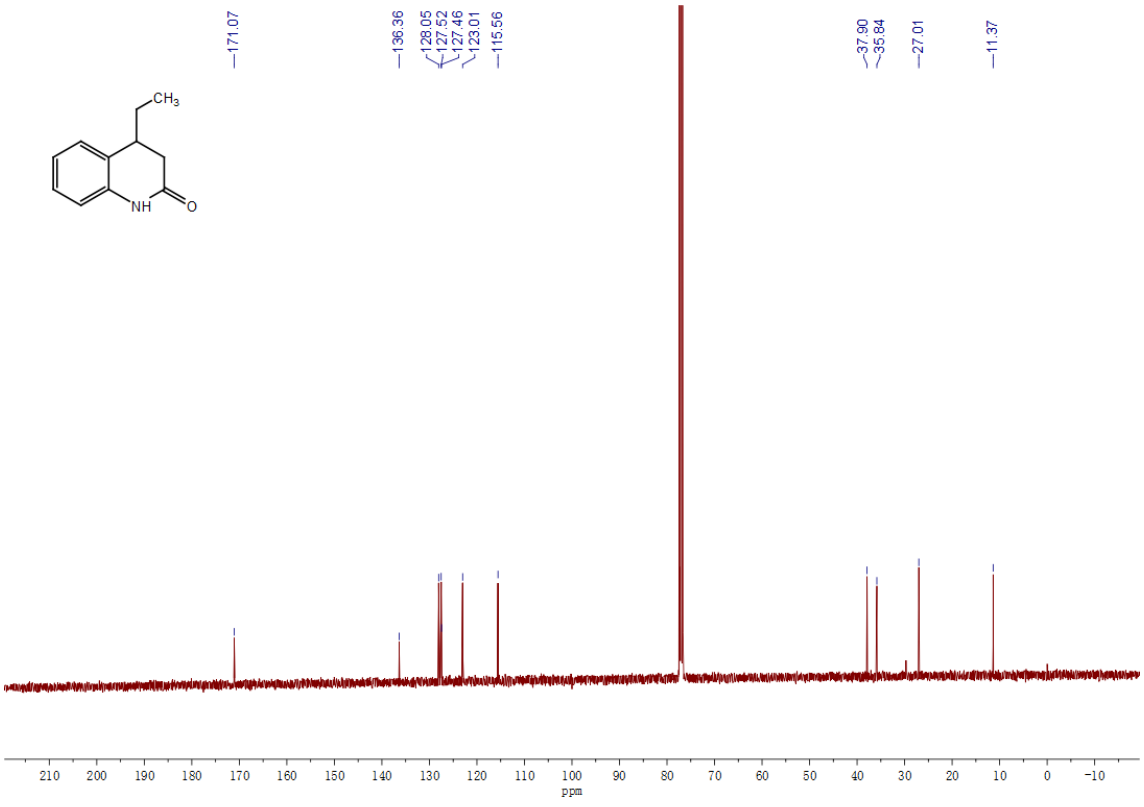
^{13}C NMR of 2zb



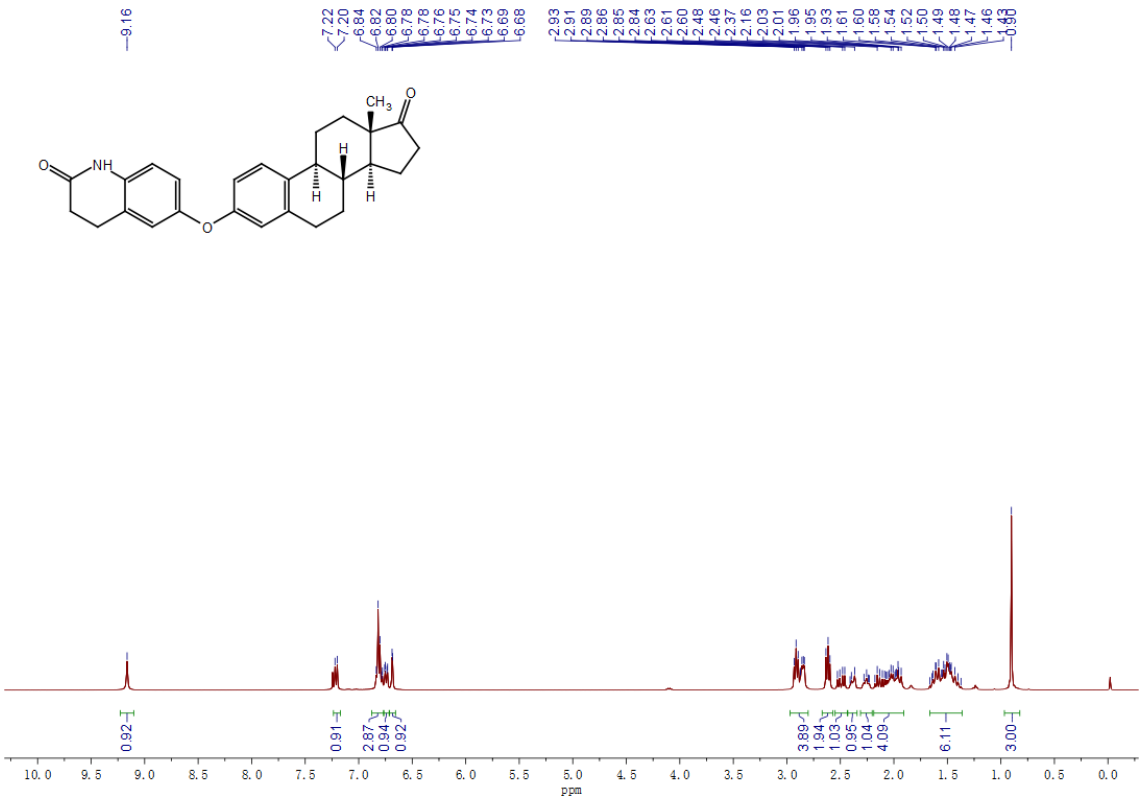
^{1}H NMR of 2zc



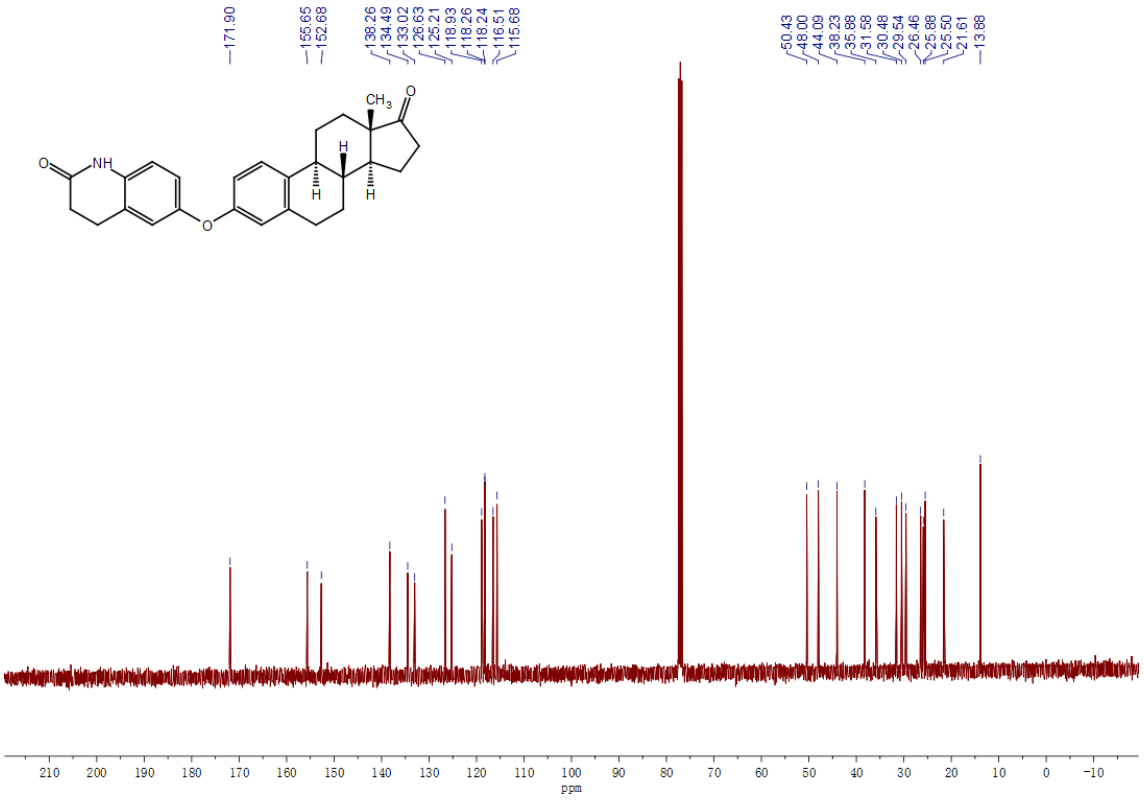
^{13}C NMR of 2zc



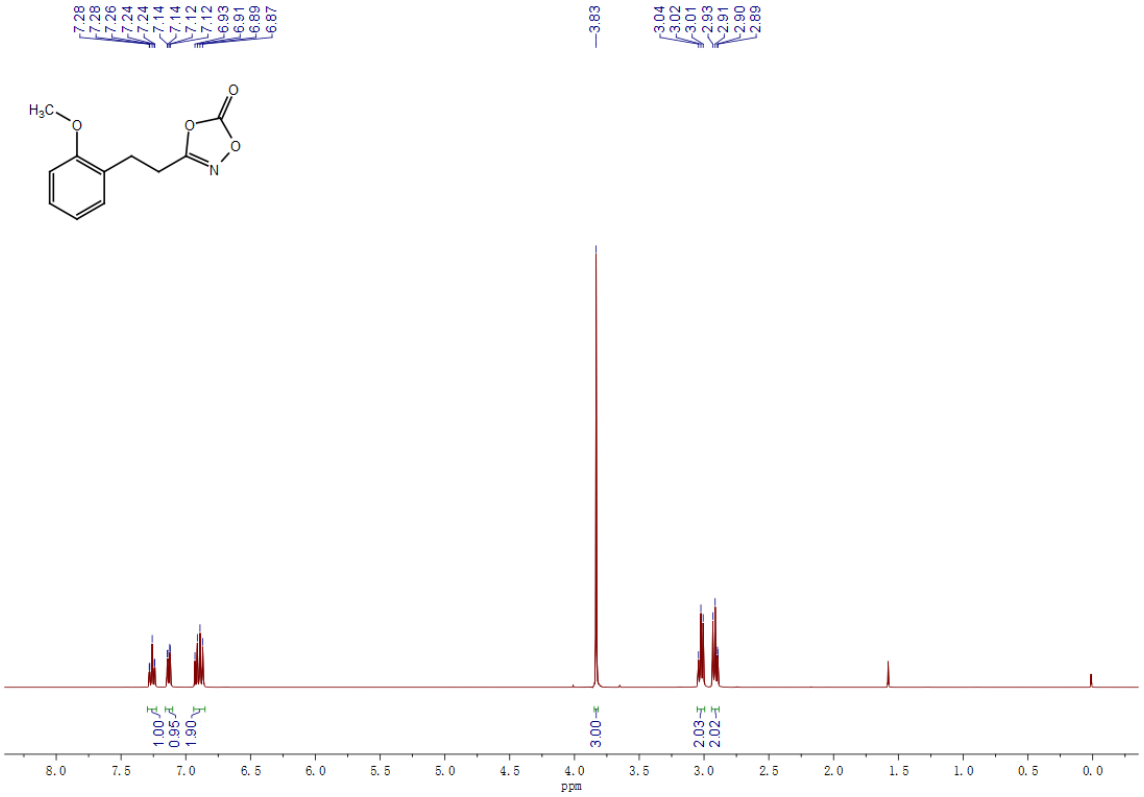
^{1}H NMR of 2ze



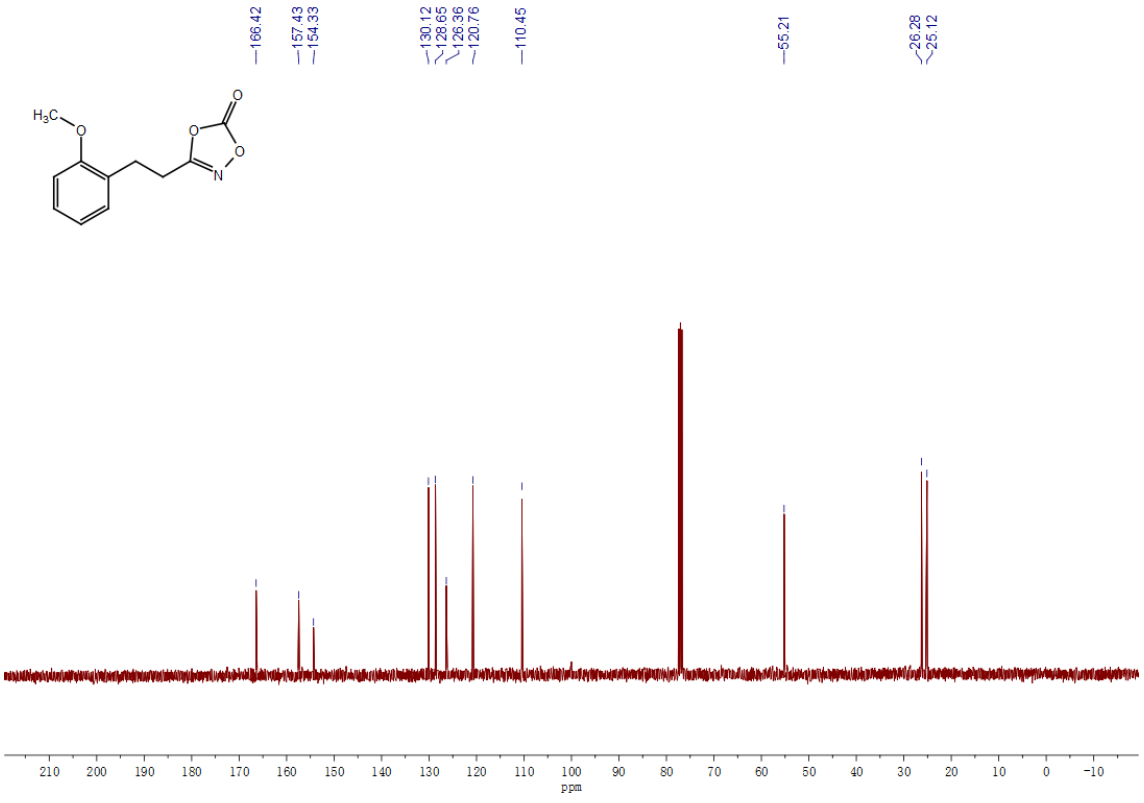
^{13}C NMR of 2ze



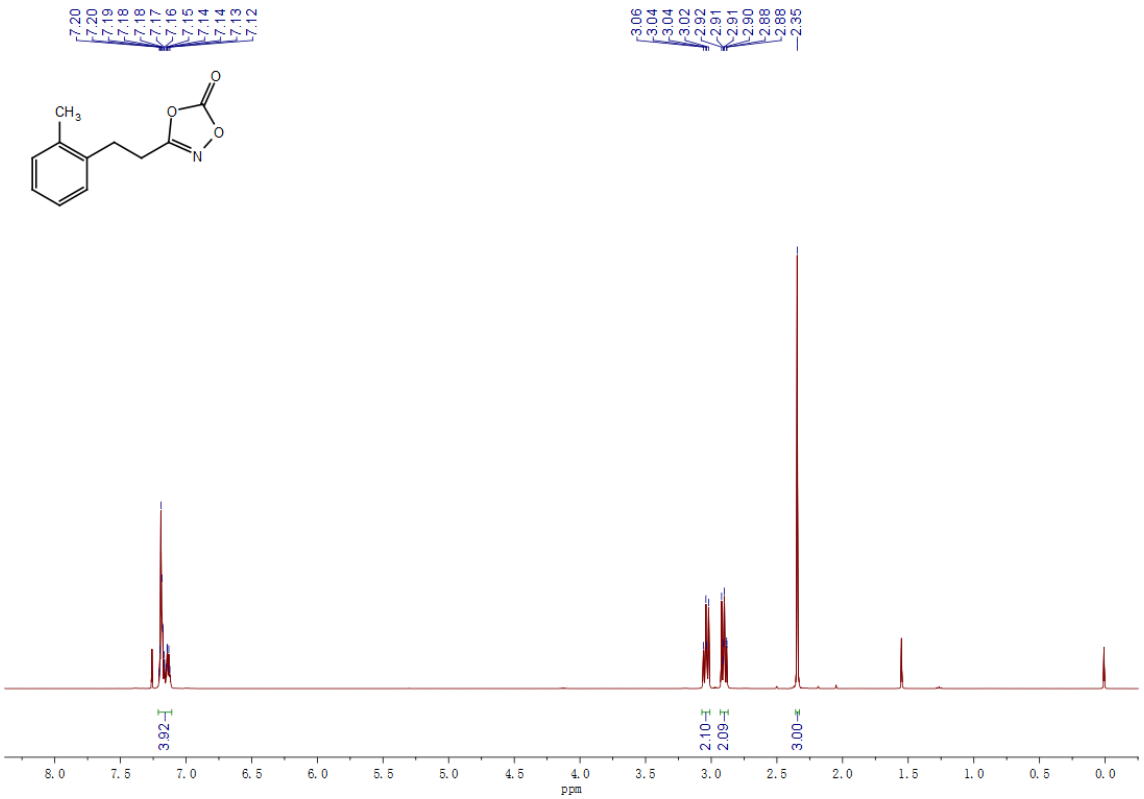
^{1}H NMR of 3a



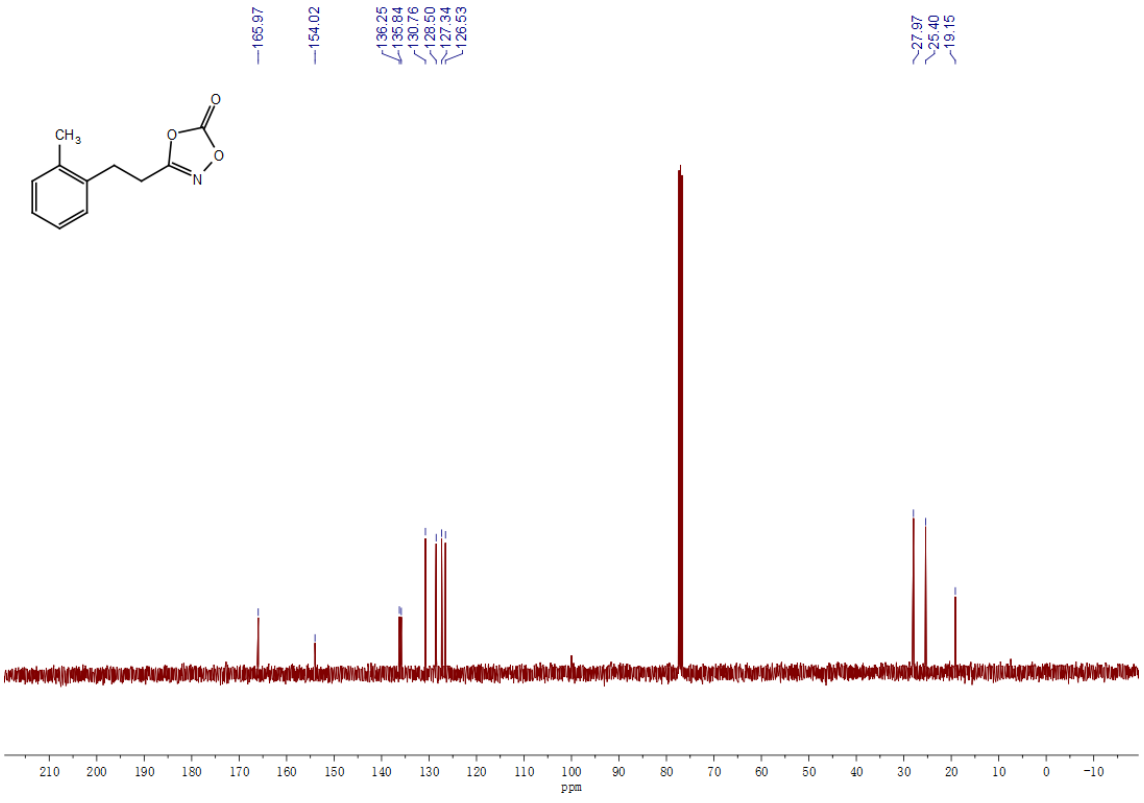
^{13}C NMR of 3a



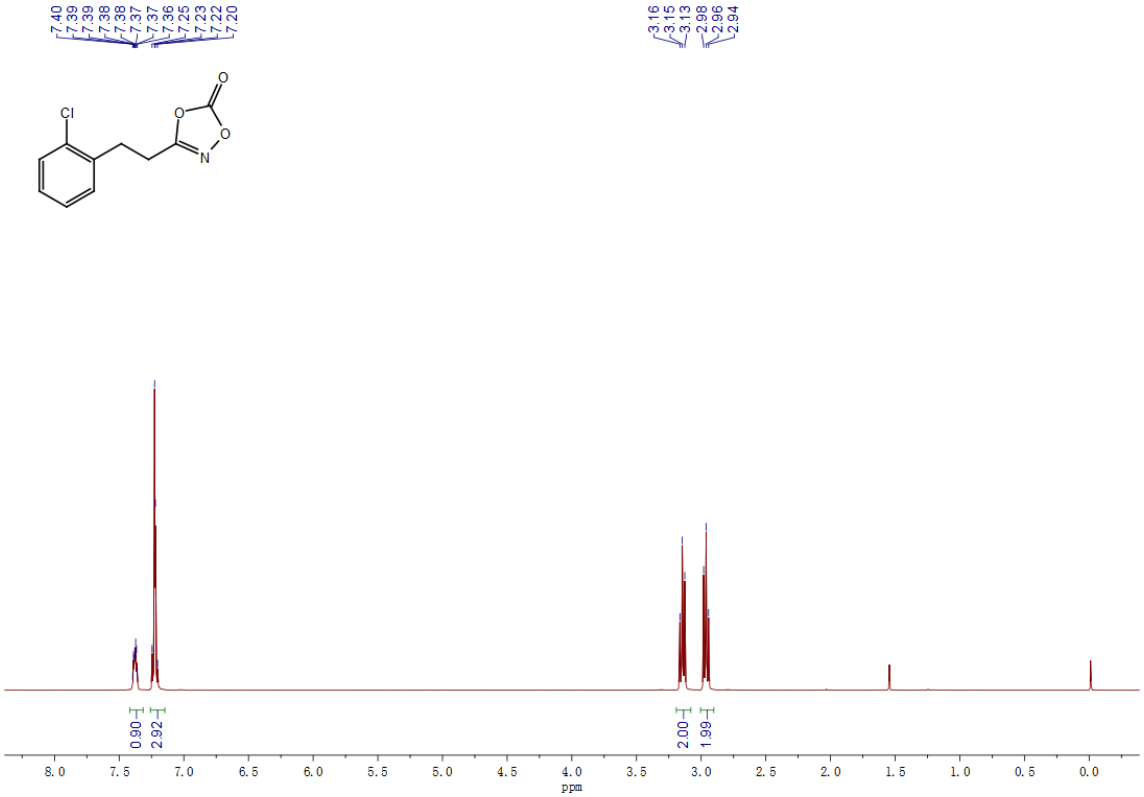
^{1}H NMR of 3b



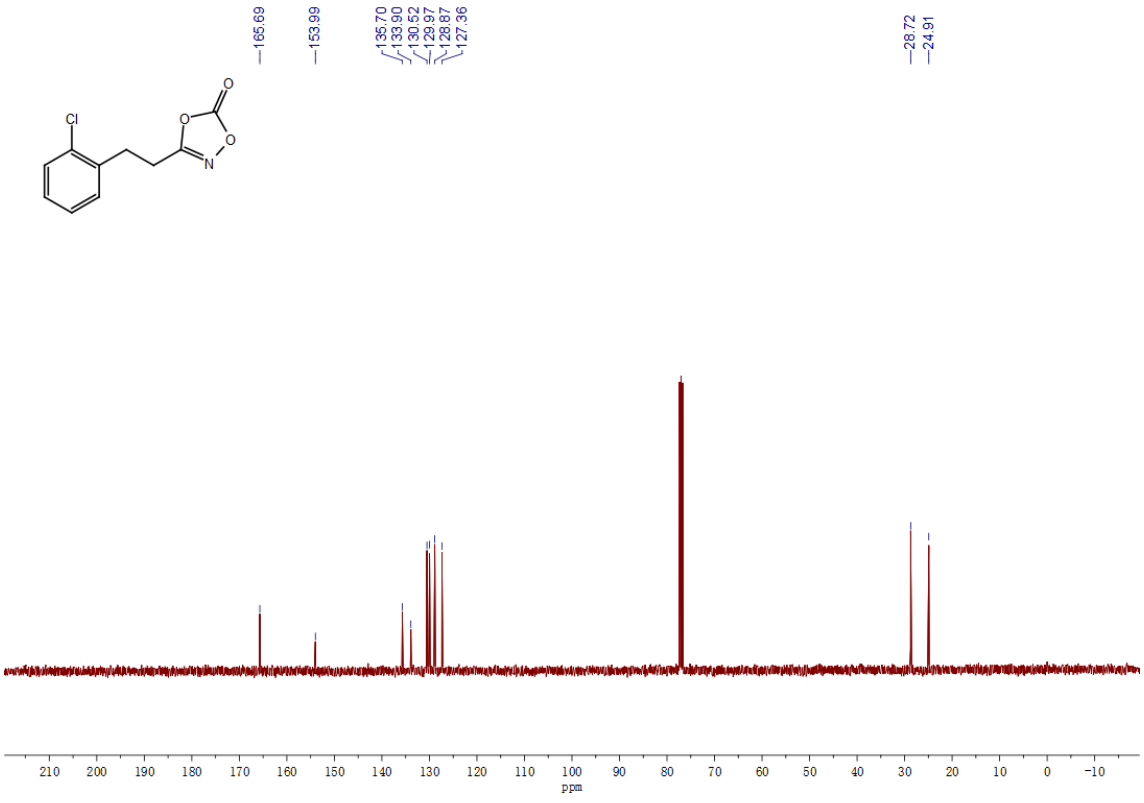
^{13}C NMR of 3b



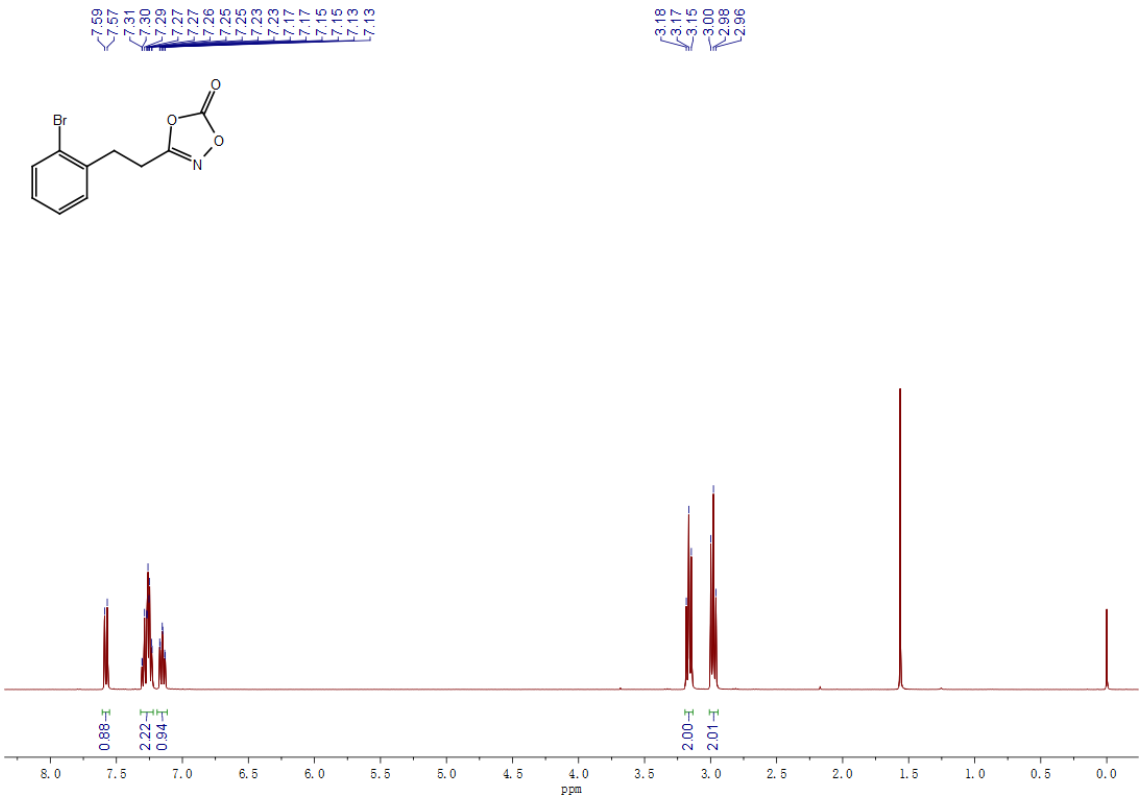
^{1}H NMR of 3c



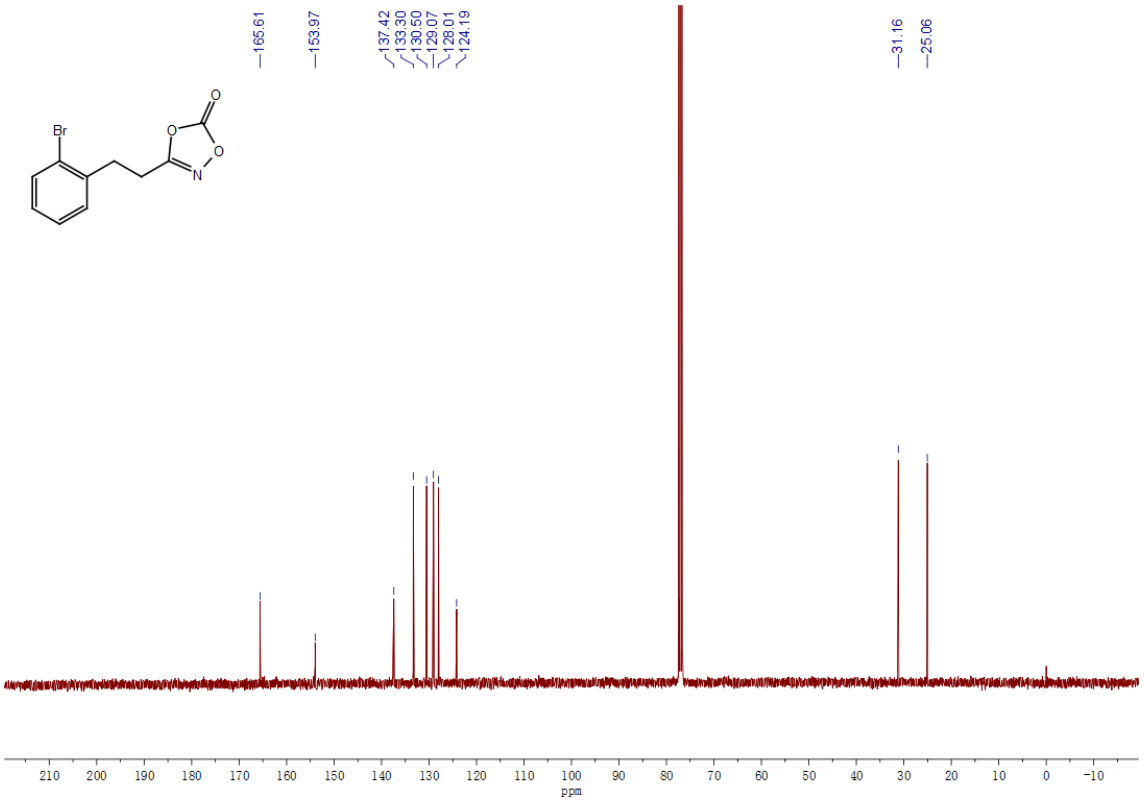
^{13}C NMR of 3c



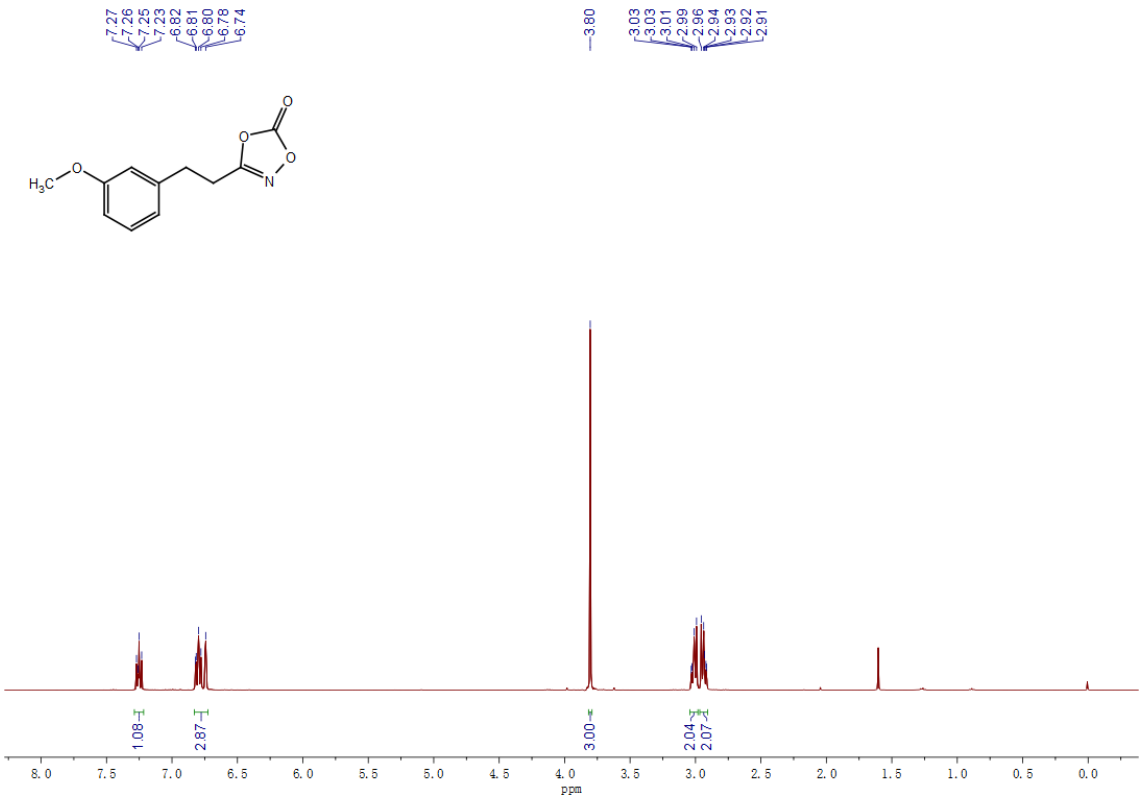
^{1}H NMR of 3d



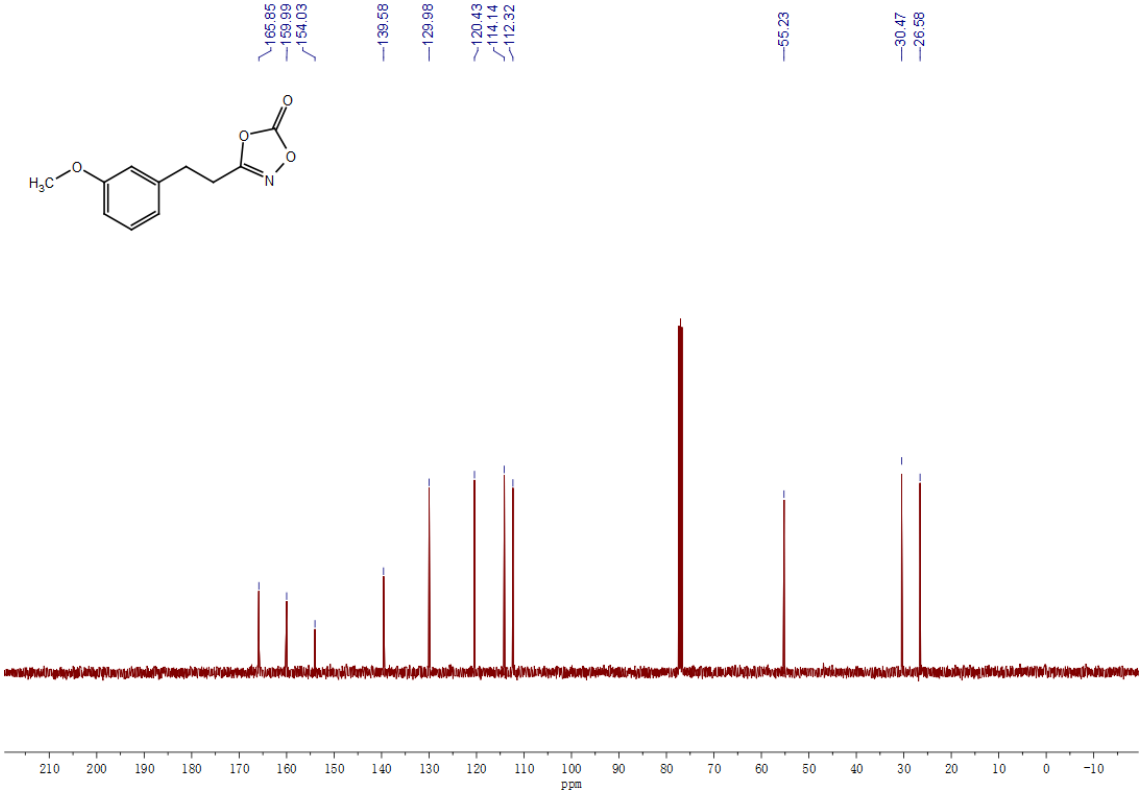
^{13}C NMR of 3d



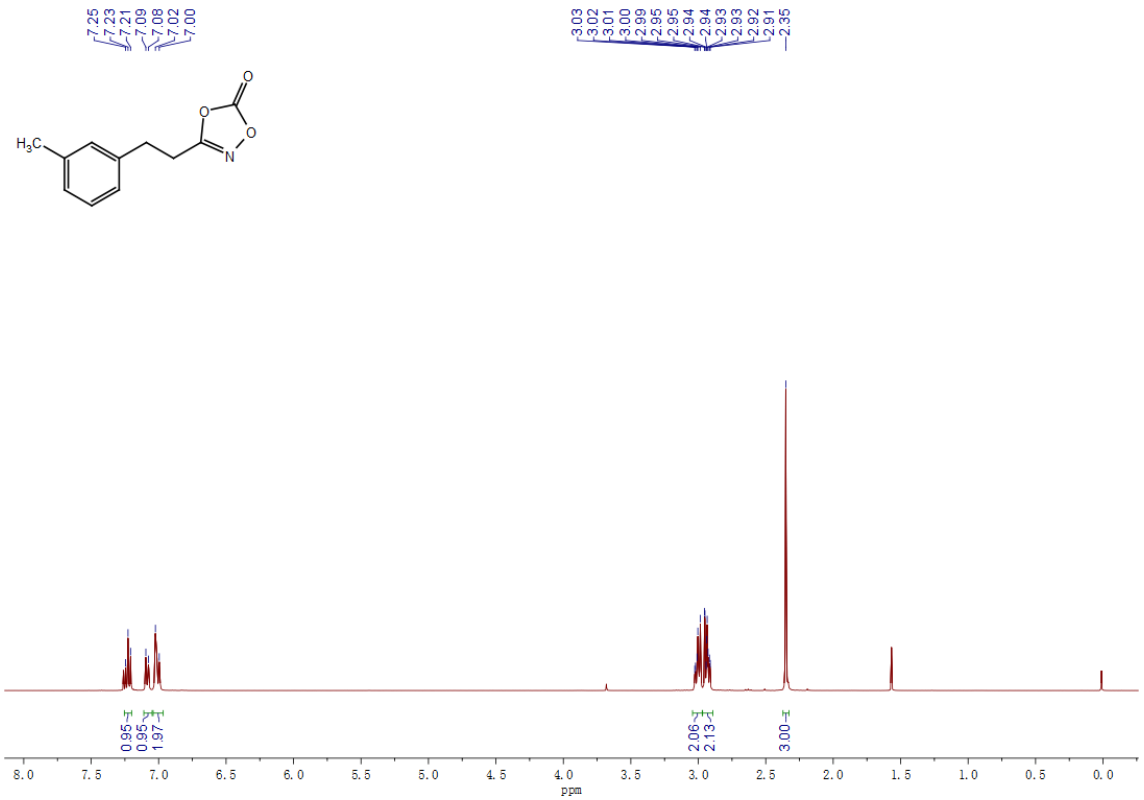
^{1}H NMR of 5a



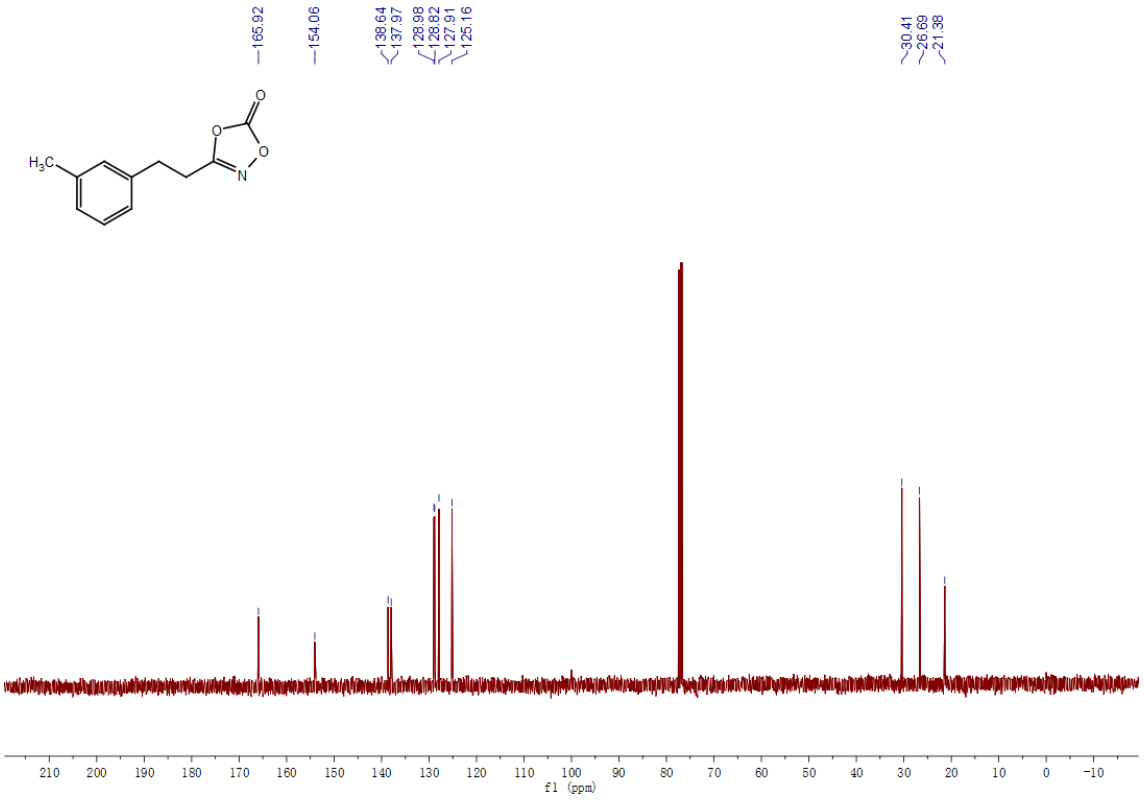
^{13}C NMR of 5a



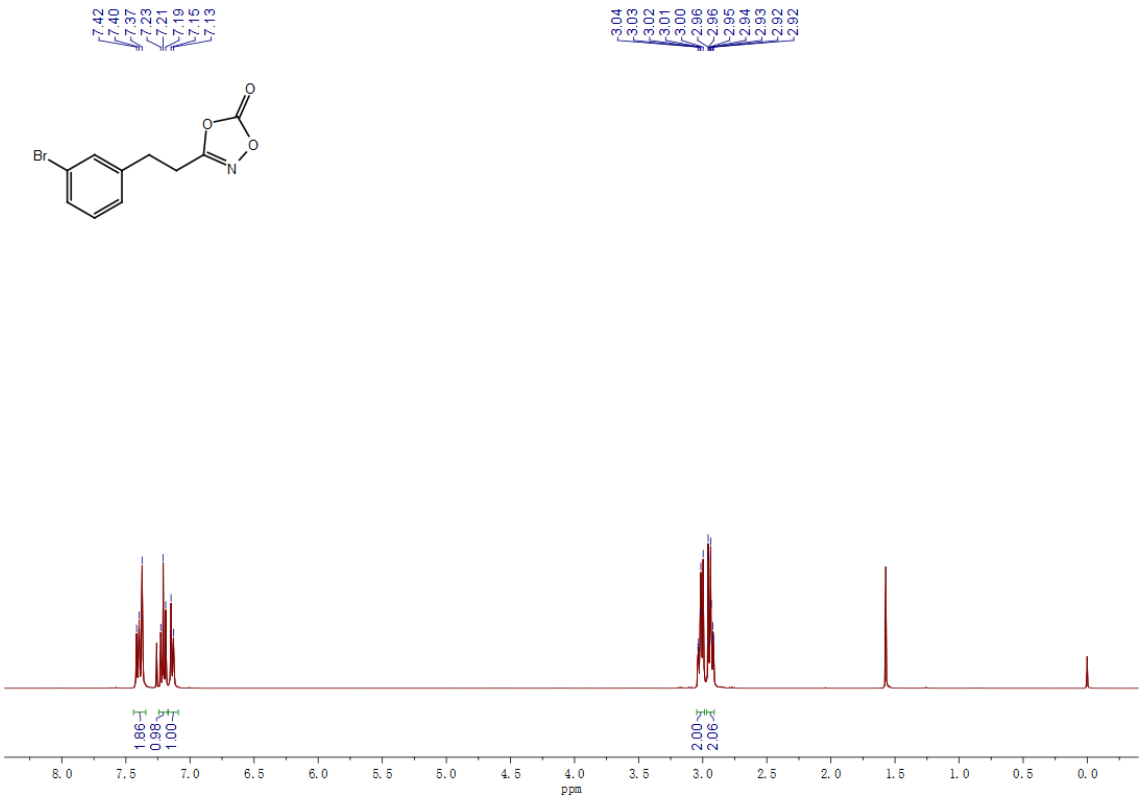
^{1}H NMR of 5b



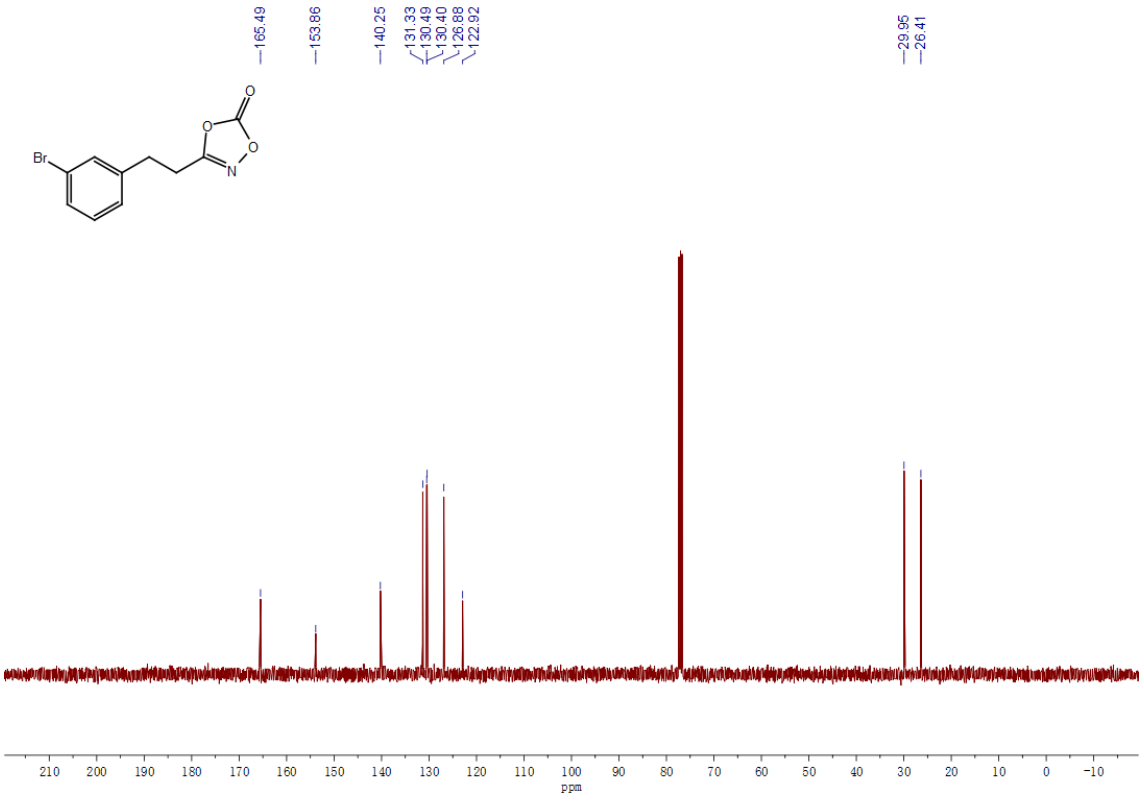
^{13}C NMR of 5b



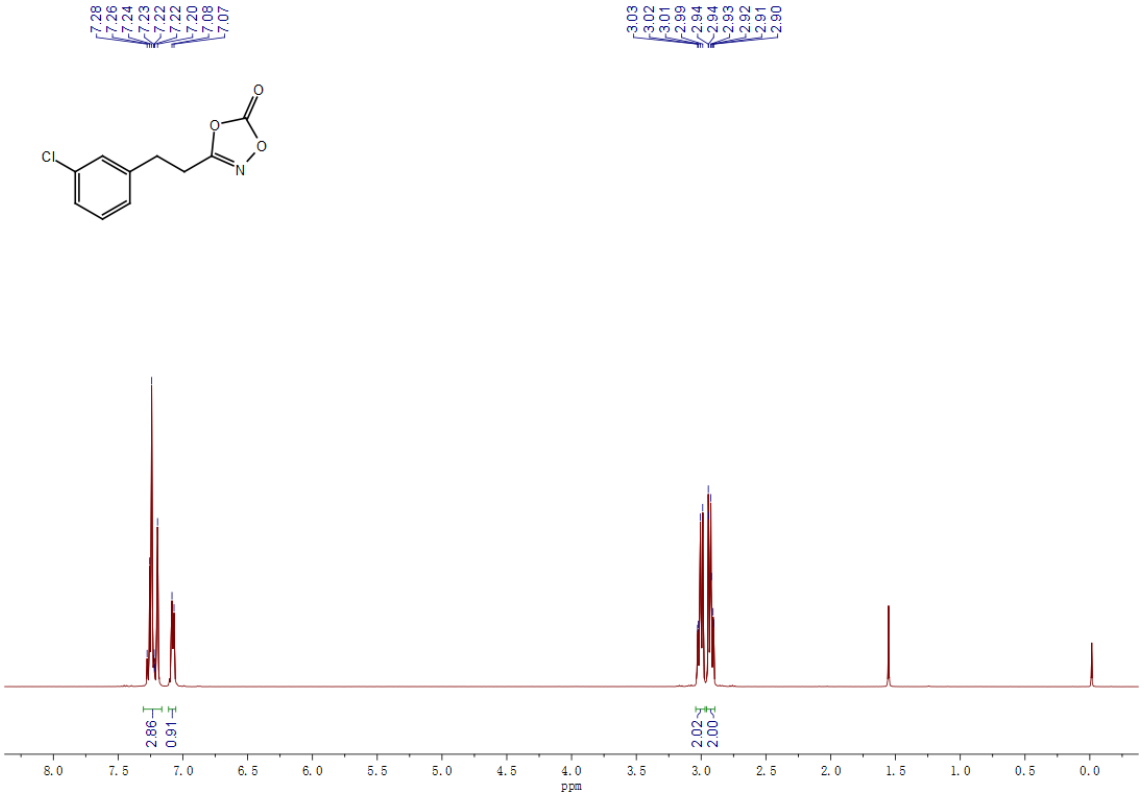
^{1}H NMR of 5c



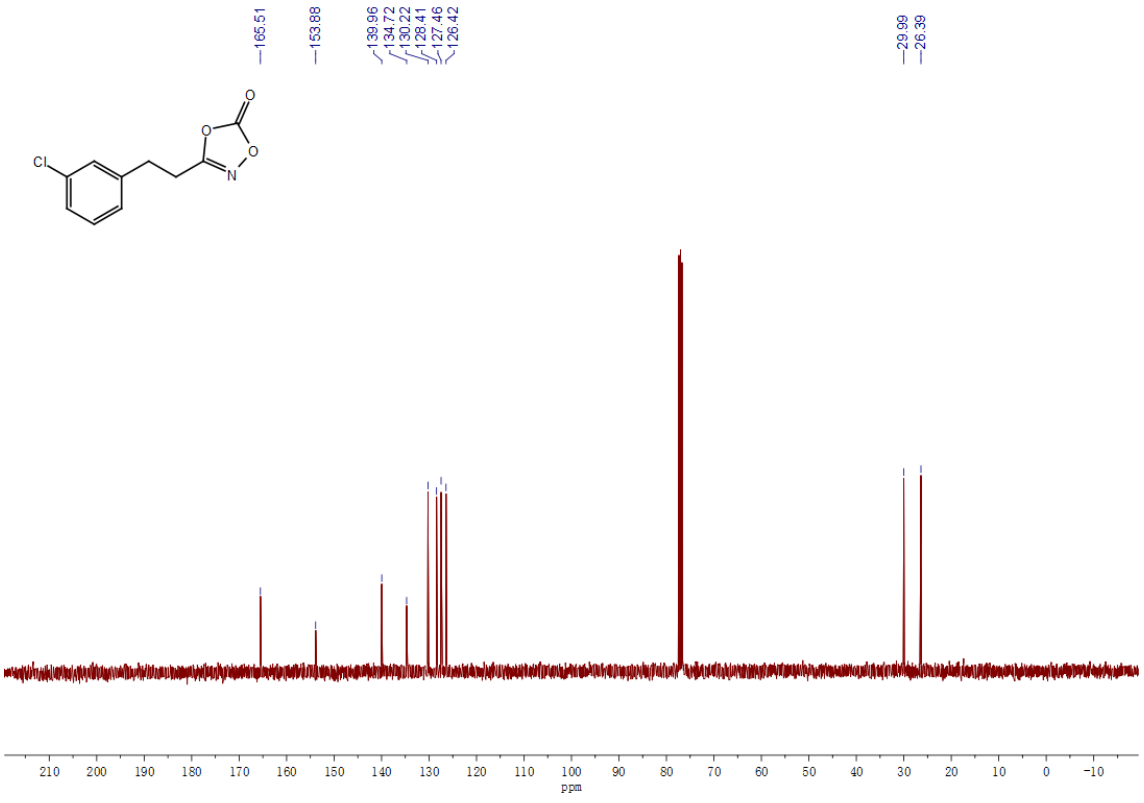
^{13}C NMR of 5c



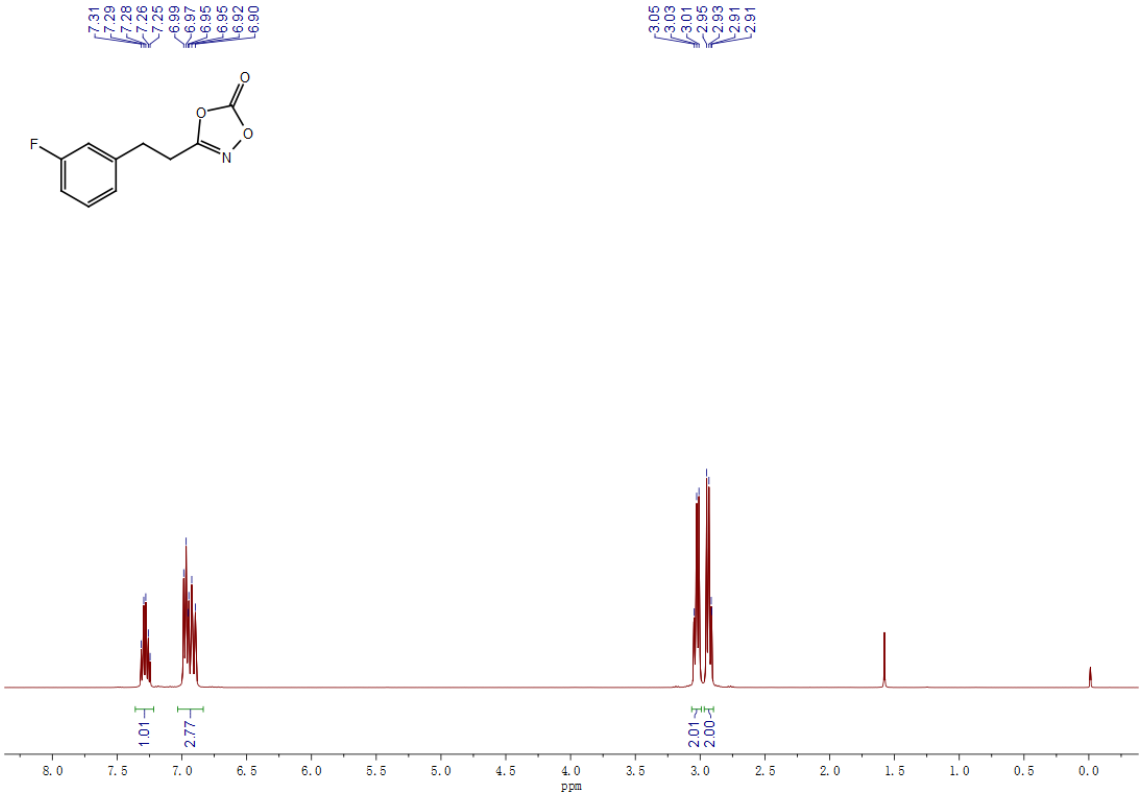
^{1}H NMR of 5d



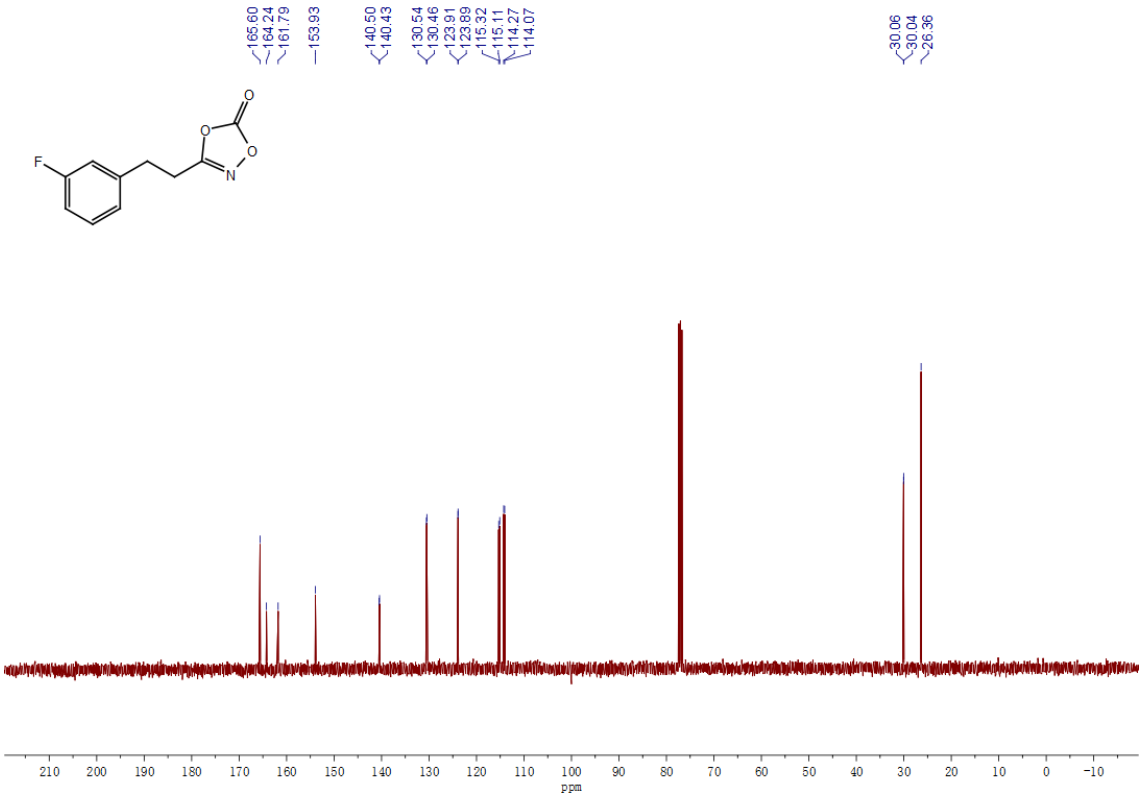
^{13}C NMR of 5d



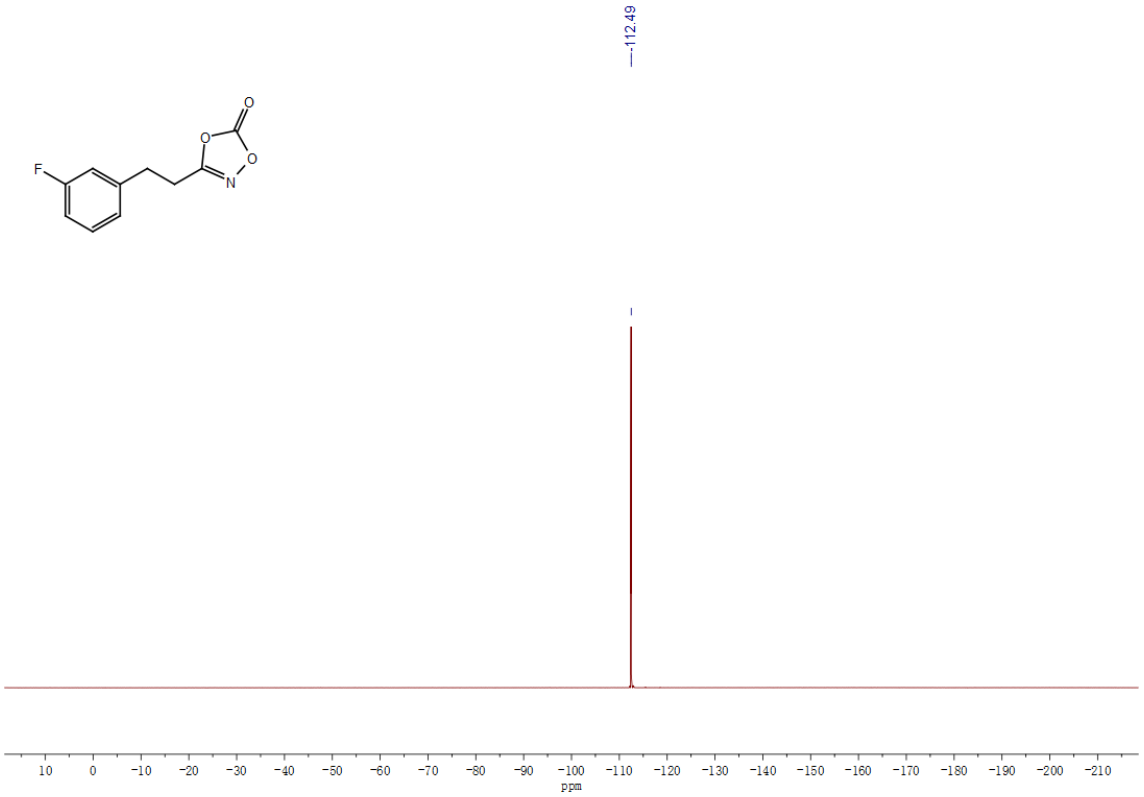
^{1}H NMR of 5e



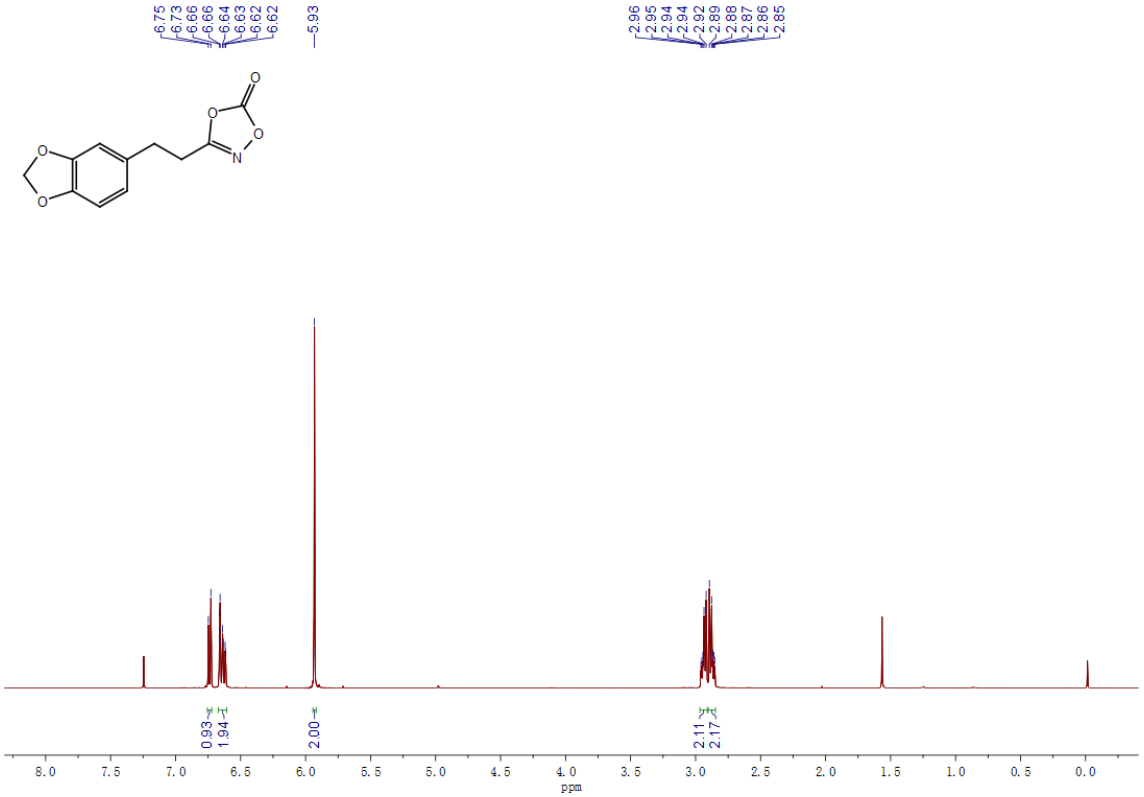
^{13}C NMR of 5e



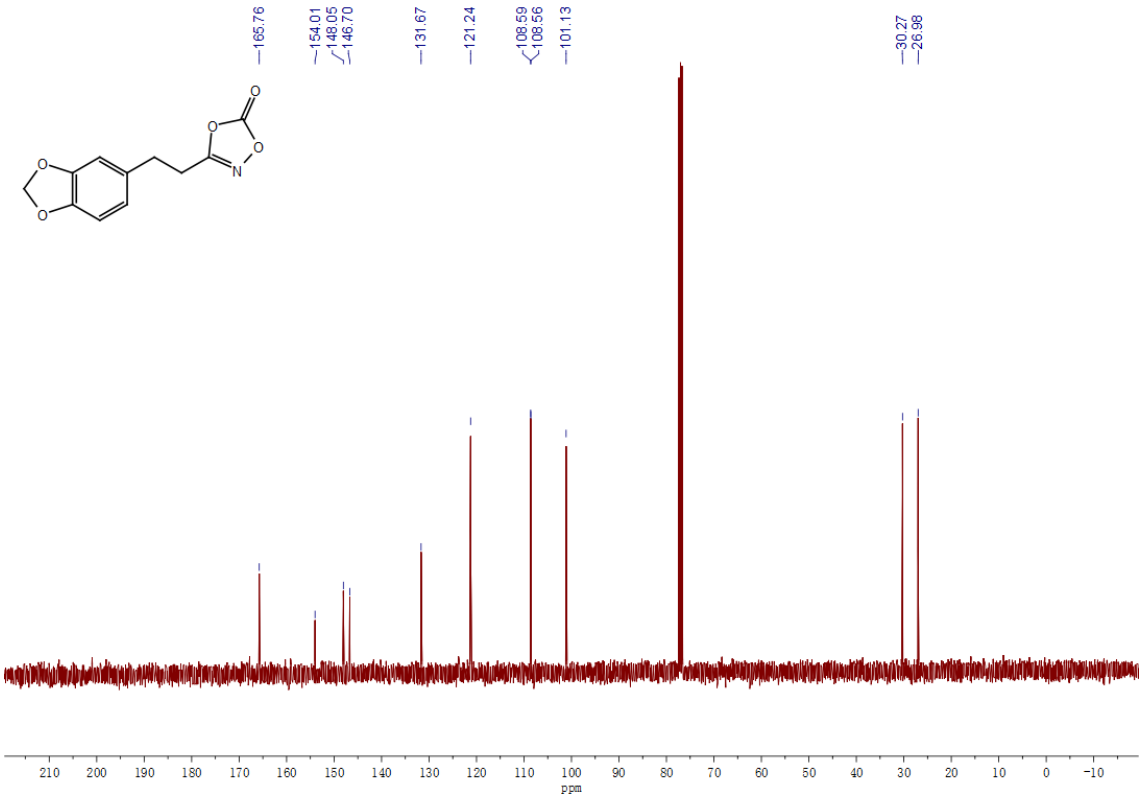
^{19}F NMR of 5e


-112.49
F
O
O
O
N
10
0
-10
-20
-30
-40
-50
-60
-70
-80
-90
-100
-110
-120
-130
-140
-150
-160
-170
-180
-190
-200
-210
ppm

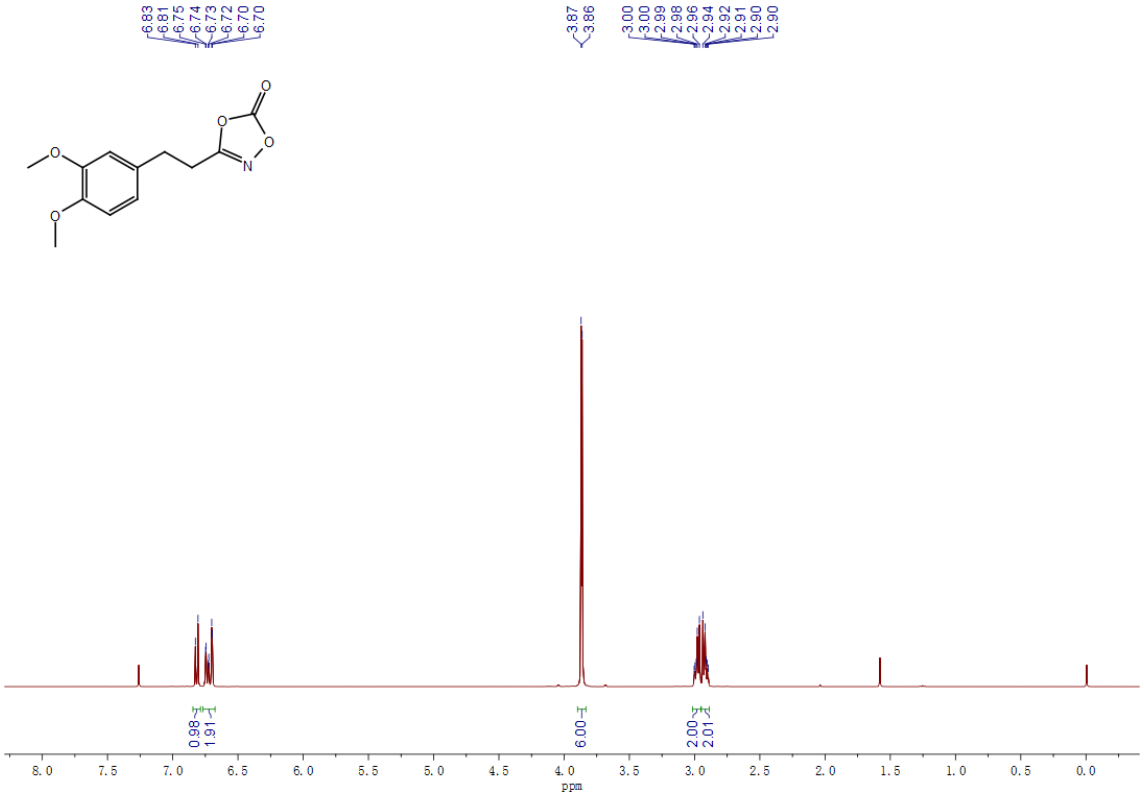
^{1}H NMR of 7a



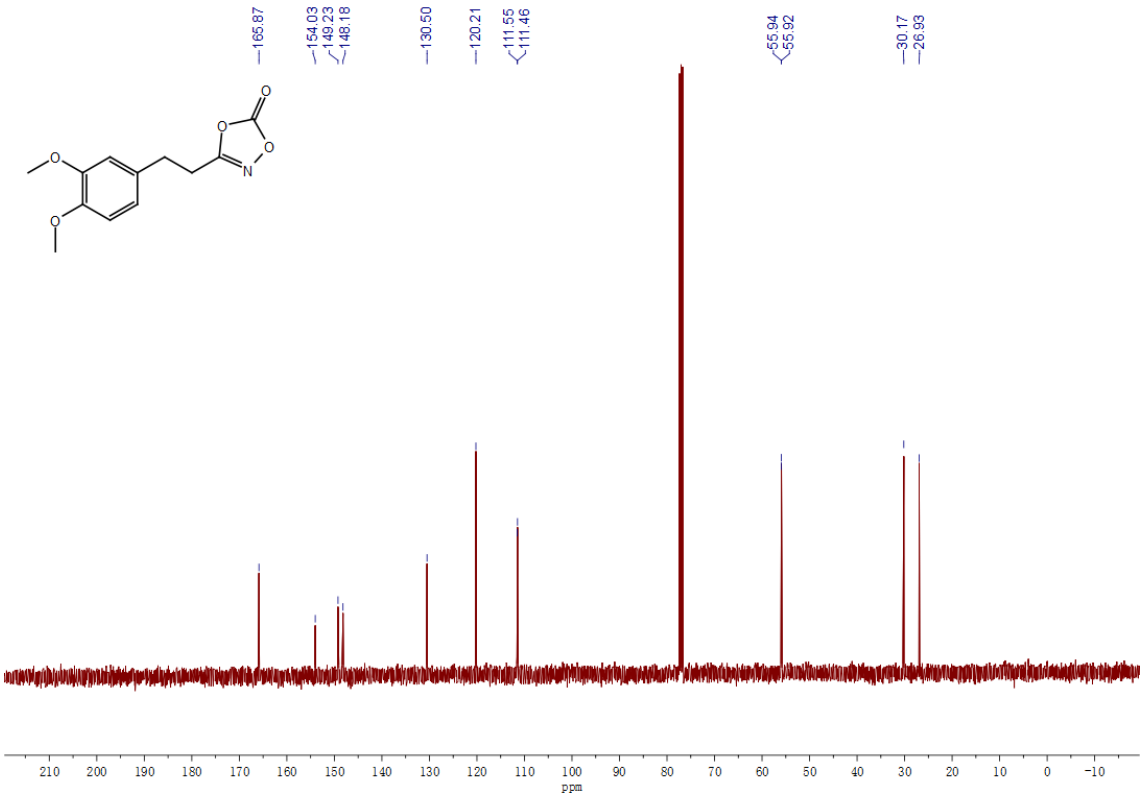
^{13}C NMR of 7a



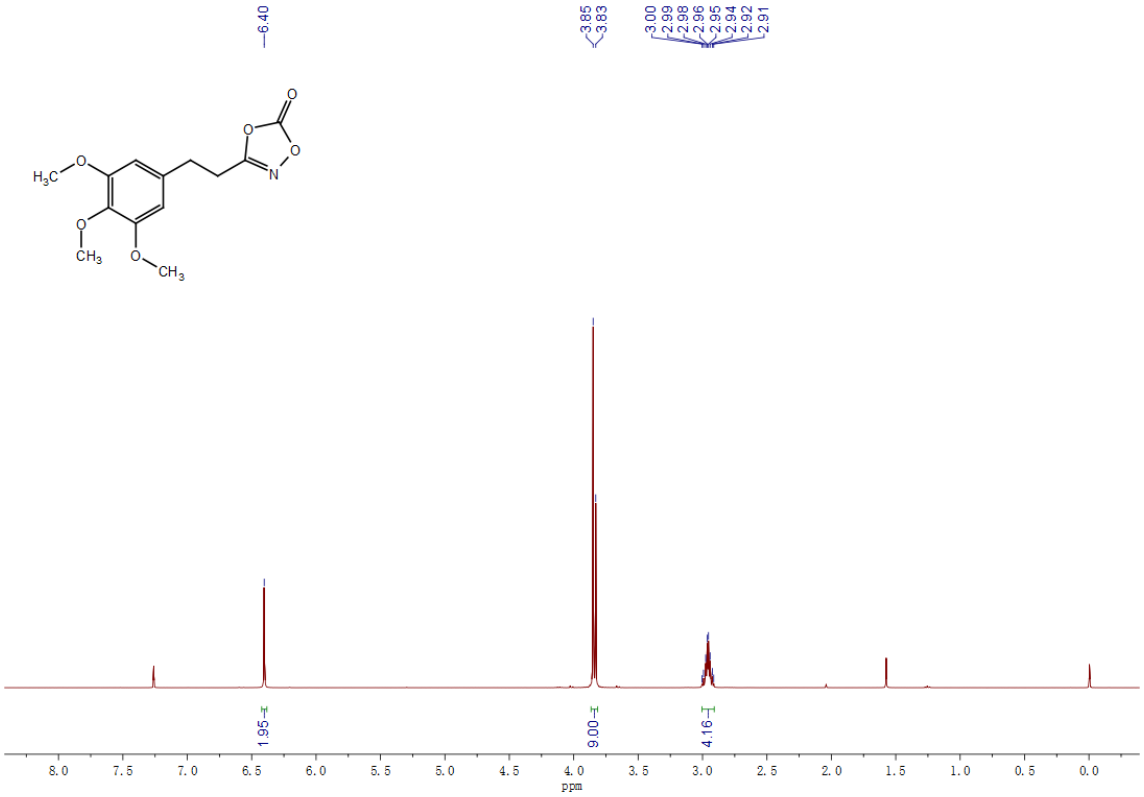
^{1}H NMR of 7b



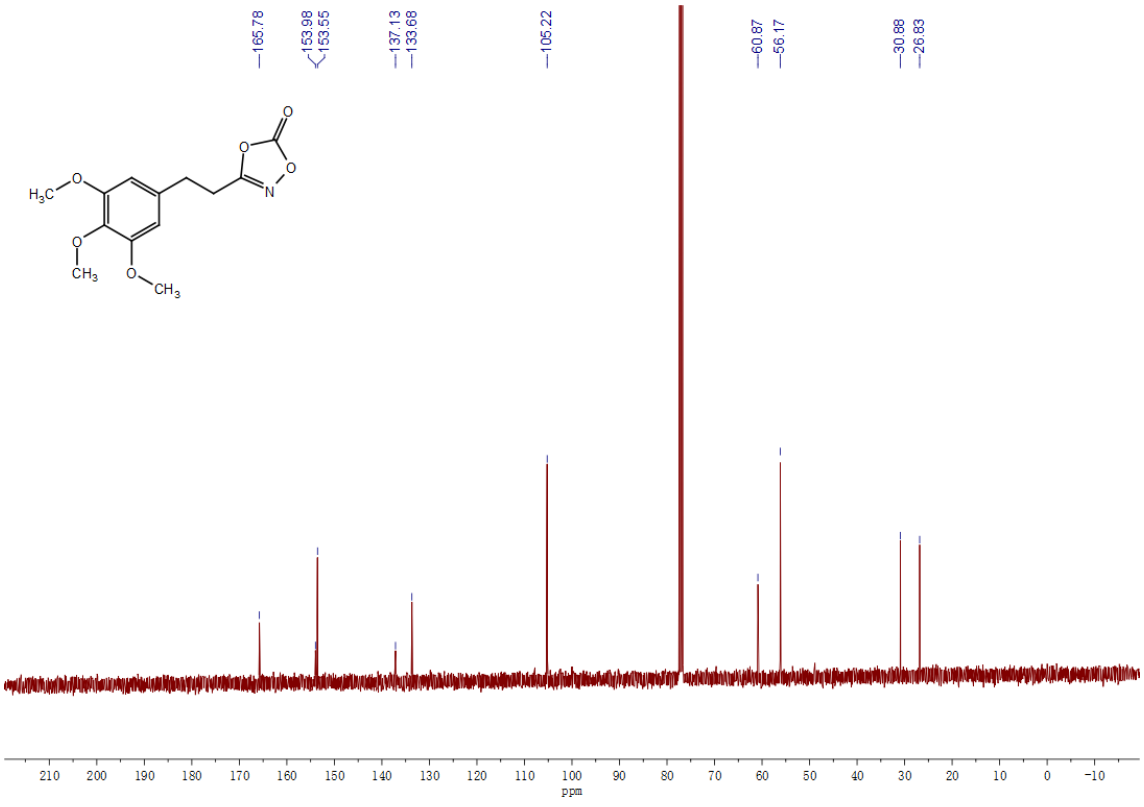
^{13}C NMR of 7b



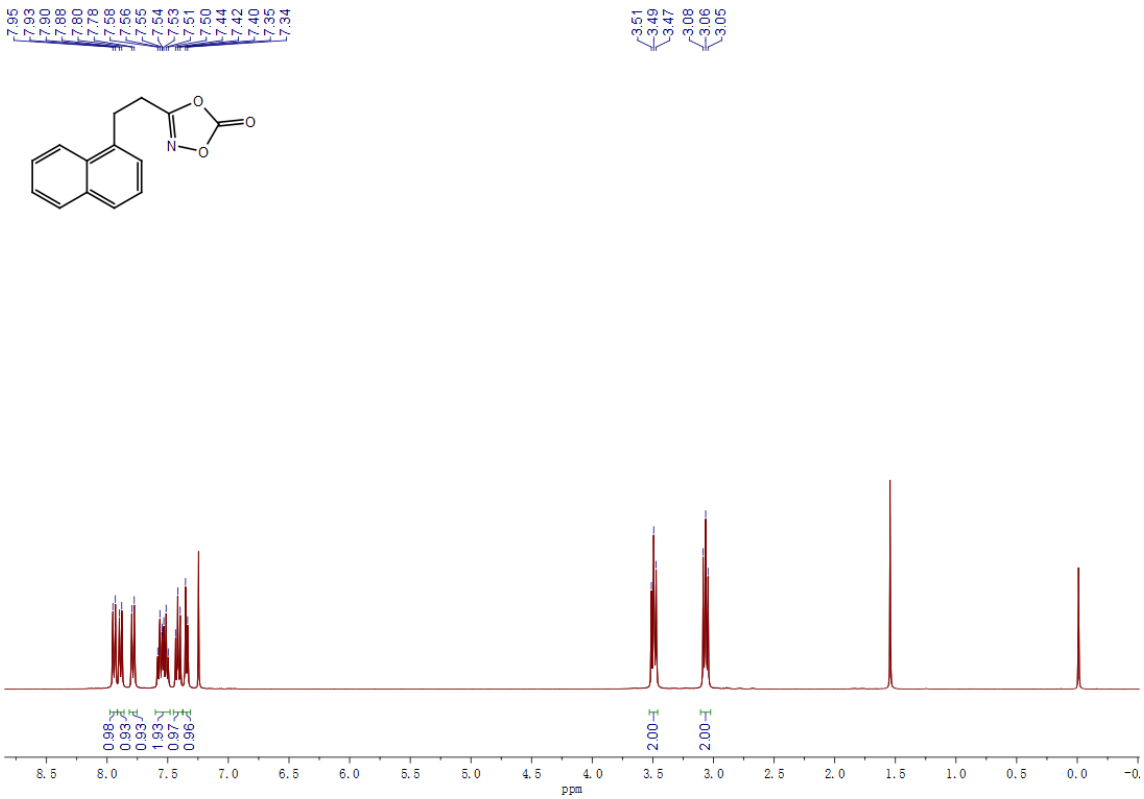
^{1}H NMR of 7c



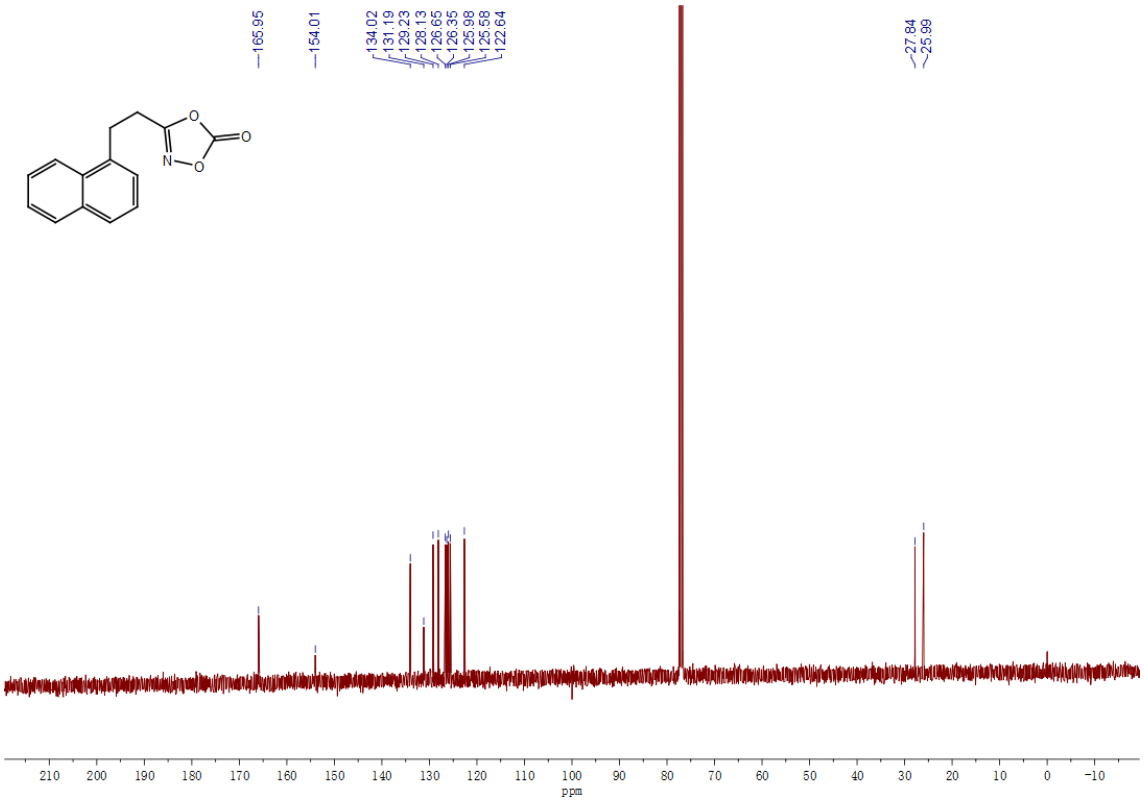
^{13}C NMR of 7c



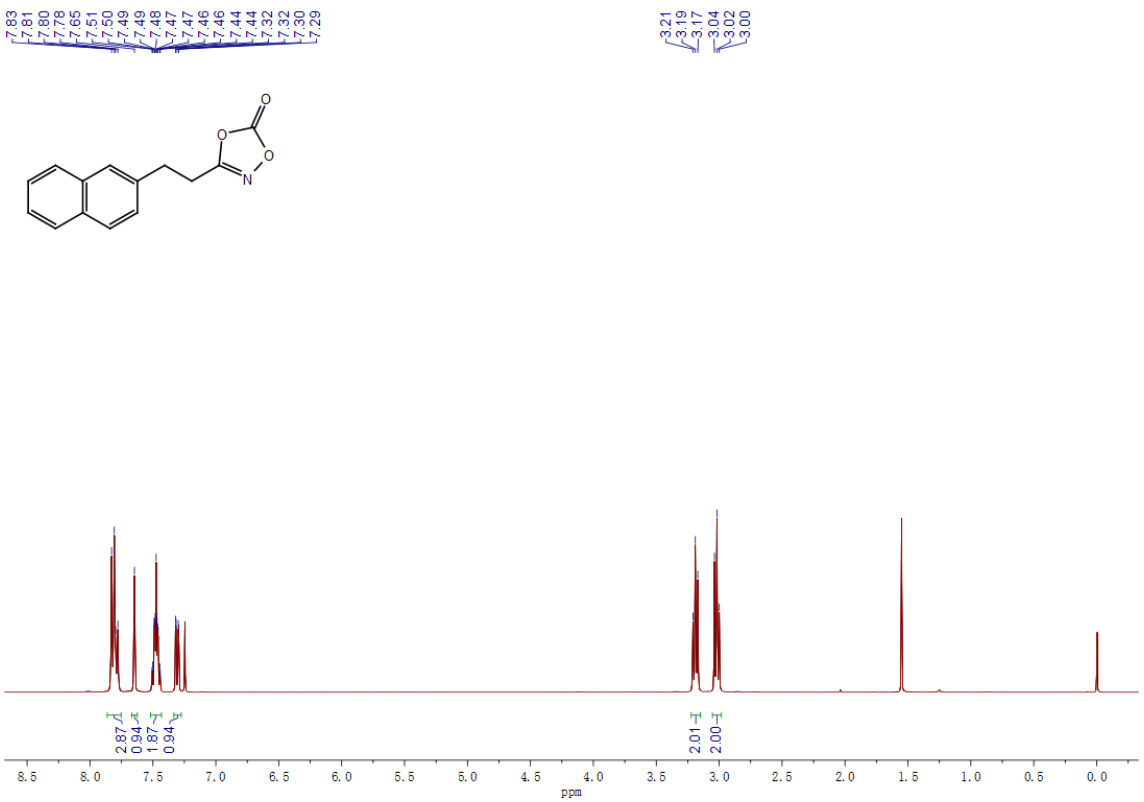
^{1}H NMR of 7d



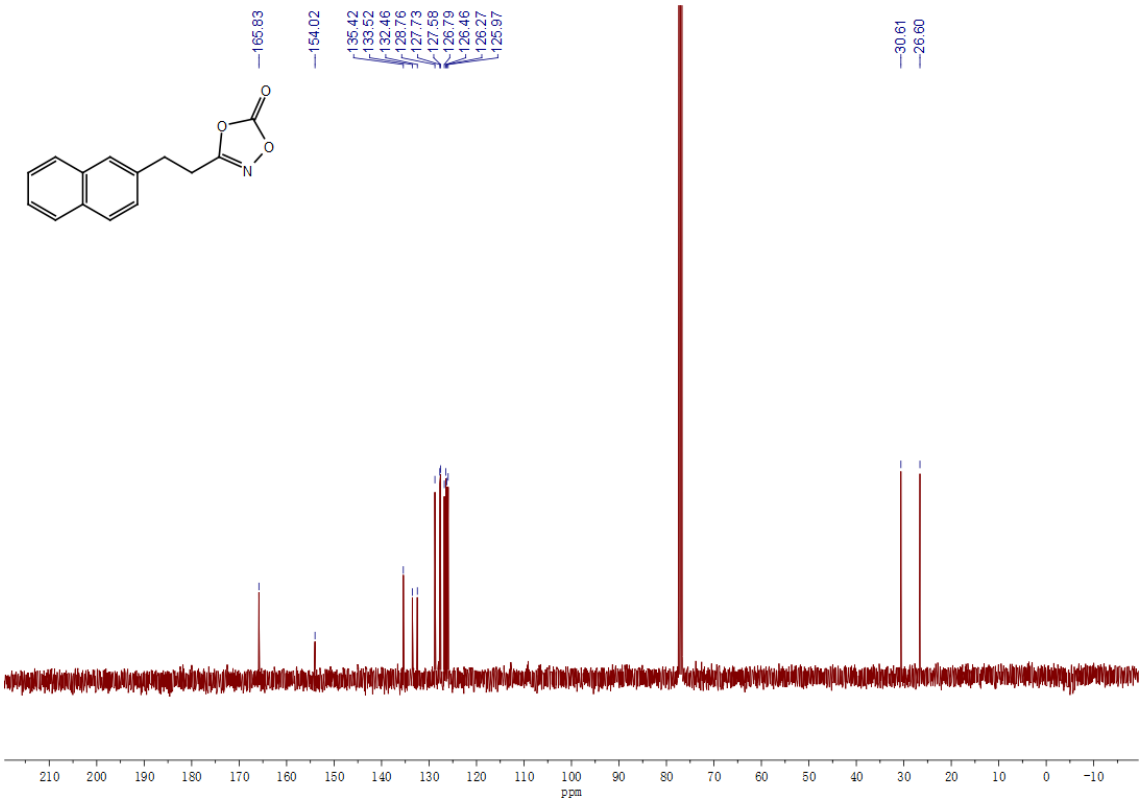
^{13}C NMR of 7d



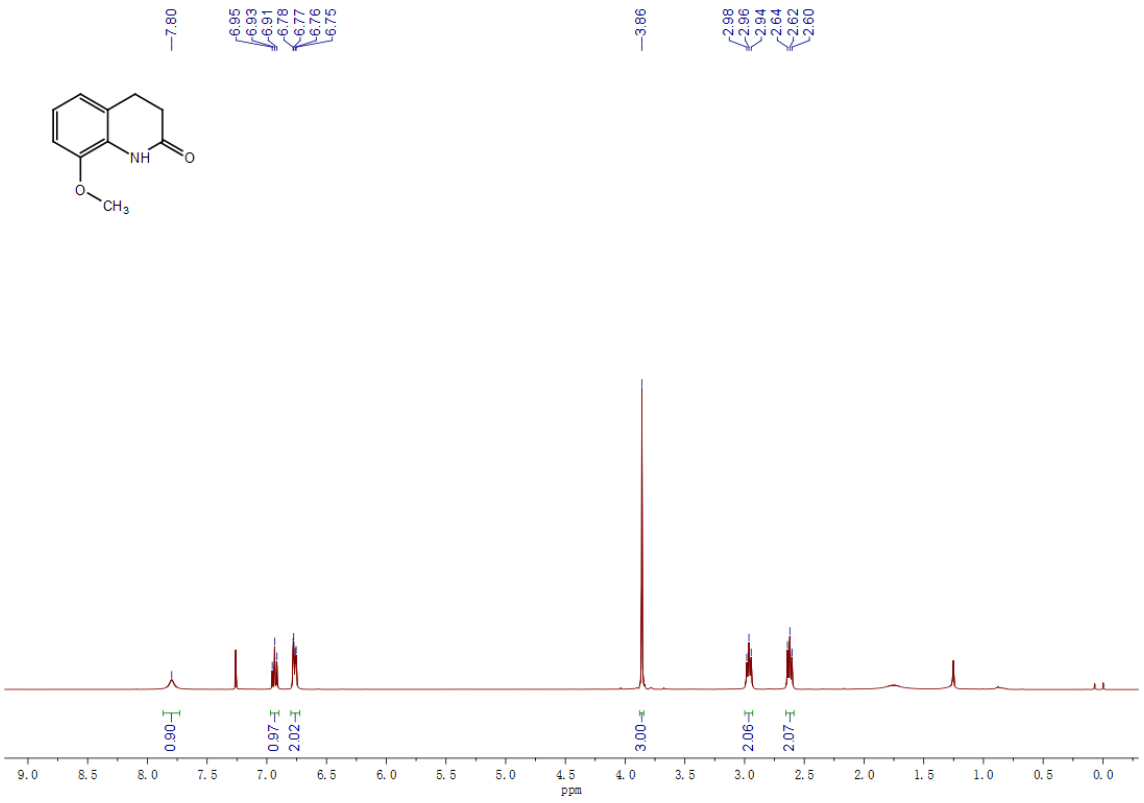
^{1}H NMR of 7e



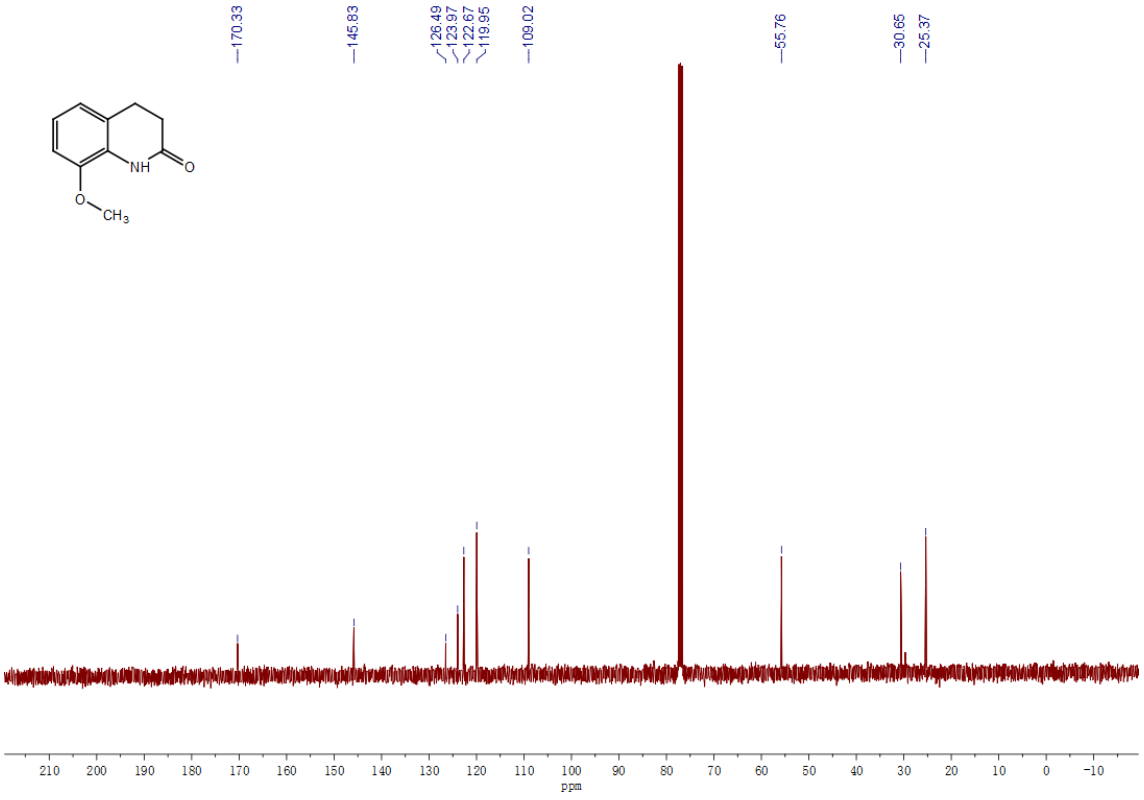
^{13}C NMR of 7e



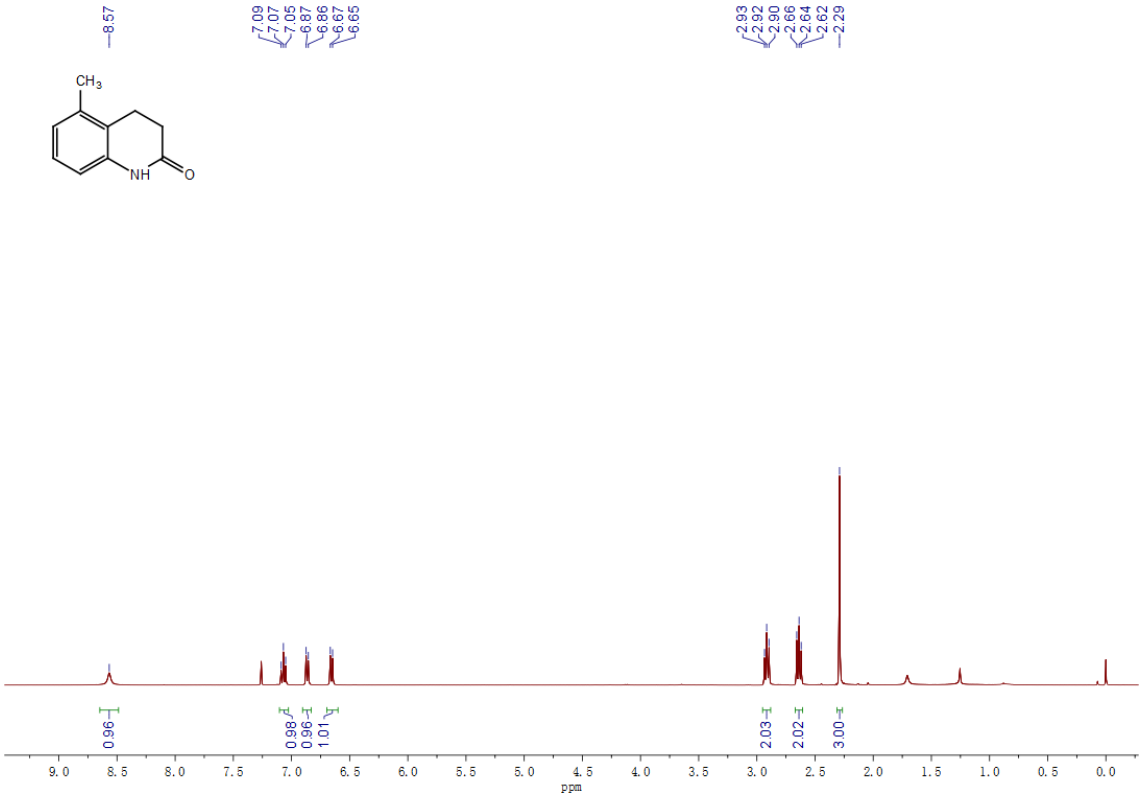
^{1}H NMR of 4a



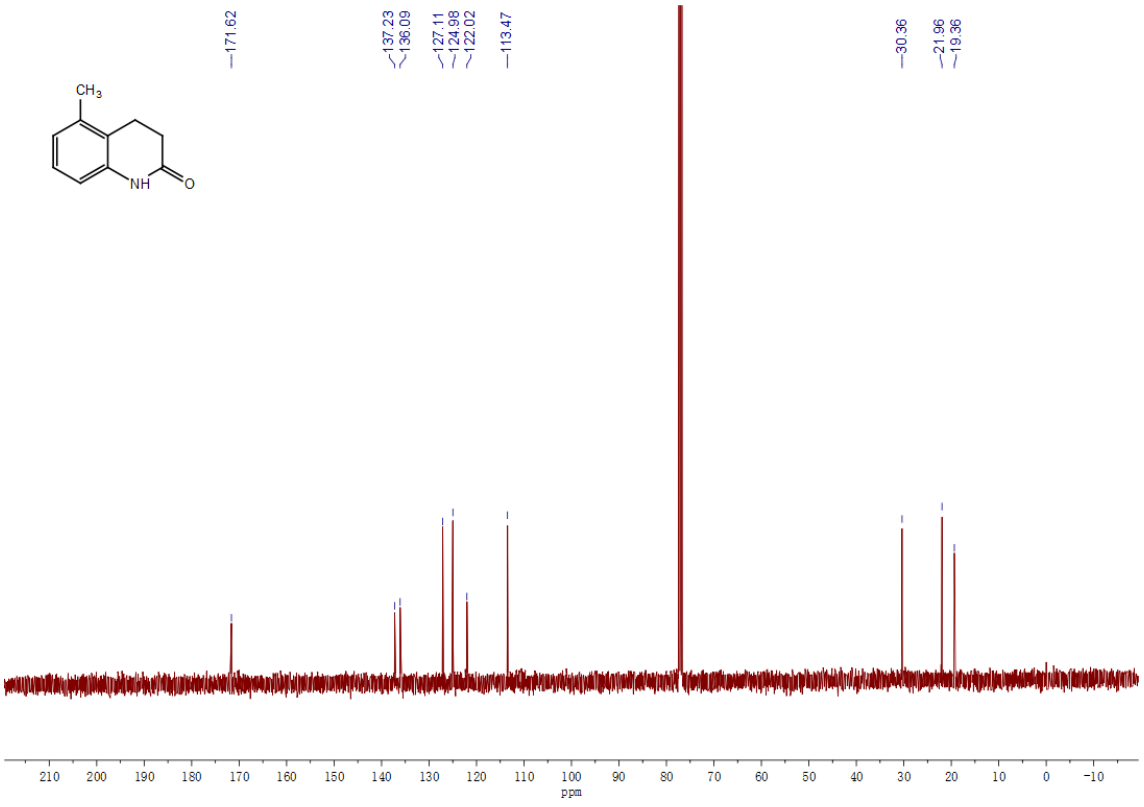
^{13}C NMR of 4a



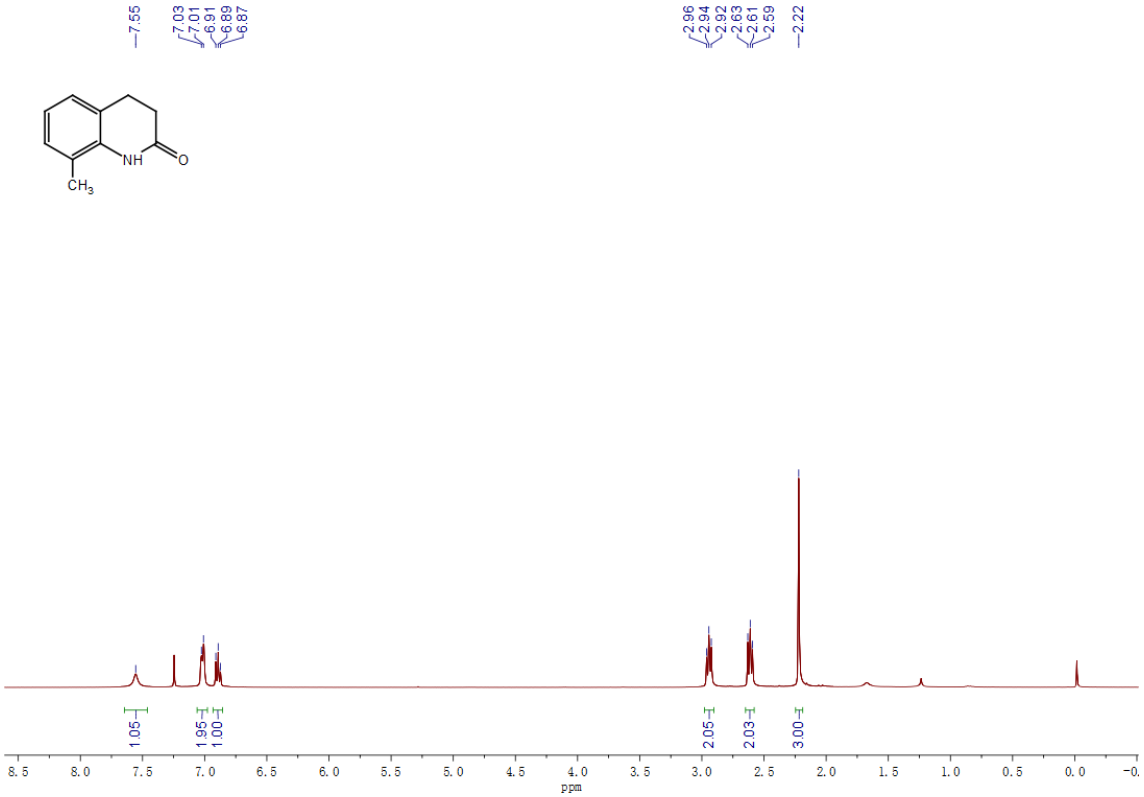
^{1}H NMR of 4b’



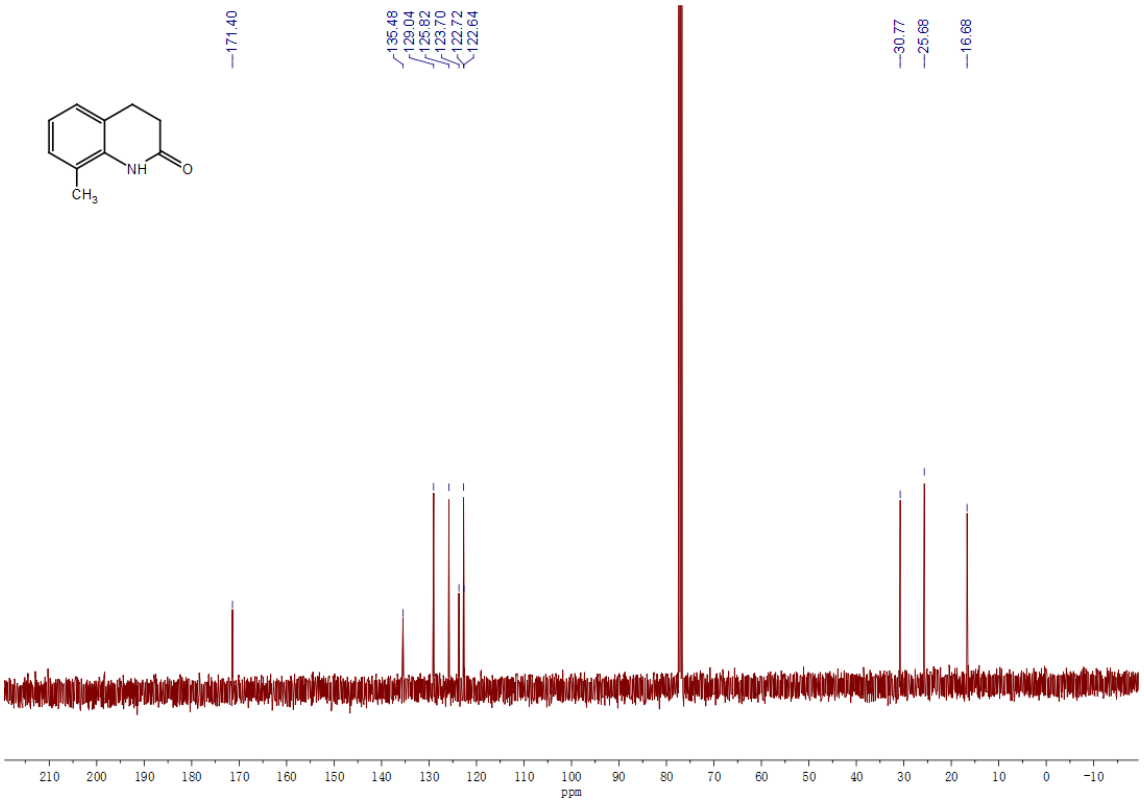
^{13}C NMR of 4b’



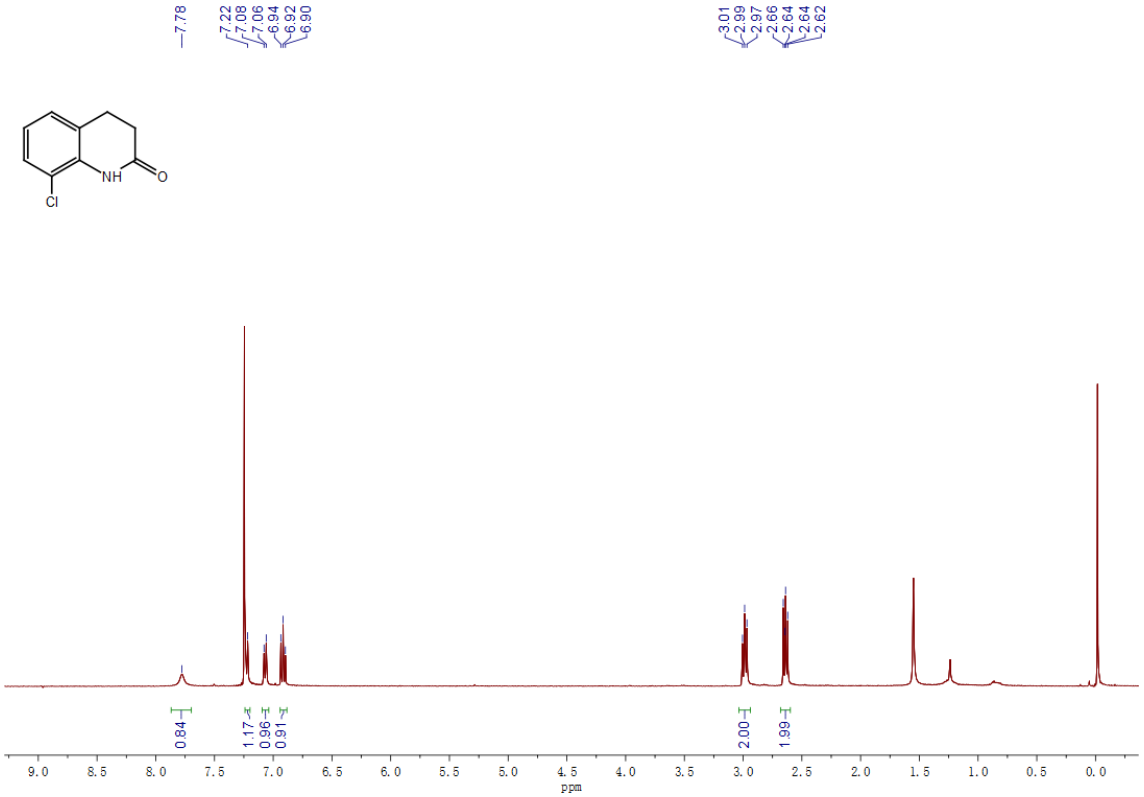
^{1}H NMR of 4b



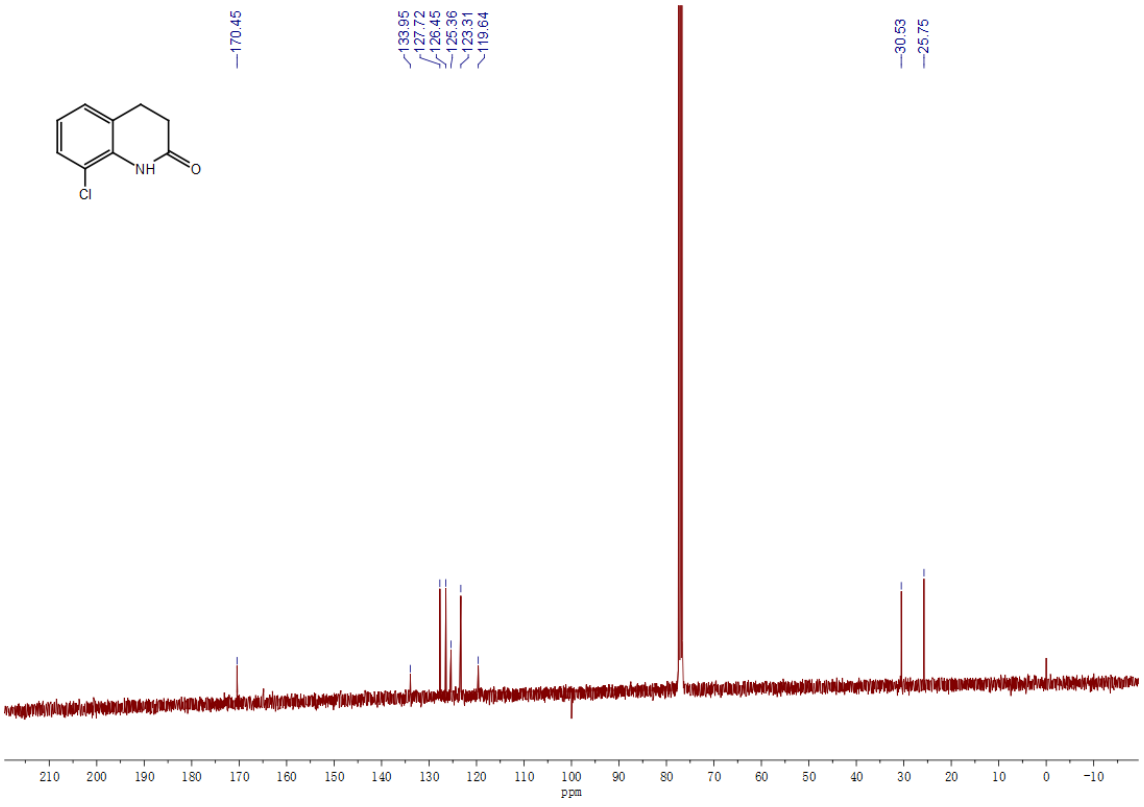
^{13}C NMR of 4b



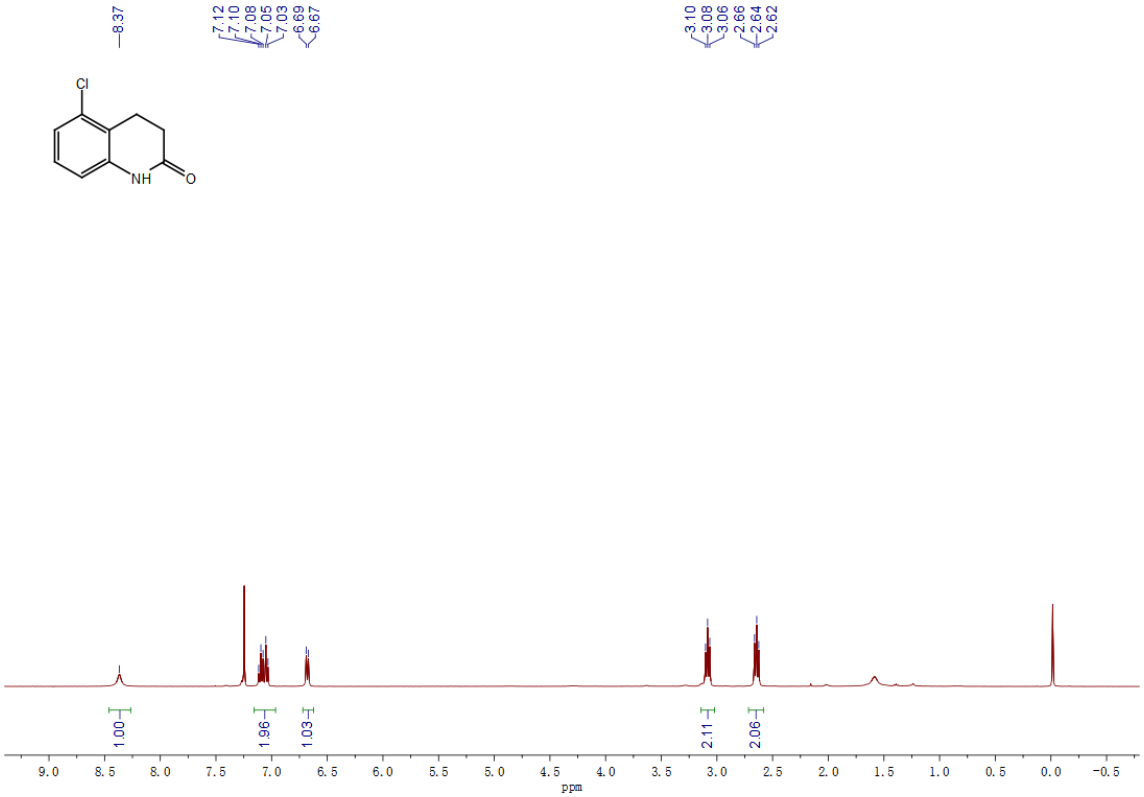
^{1}H NMR of 4c



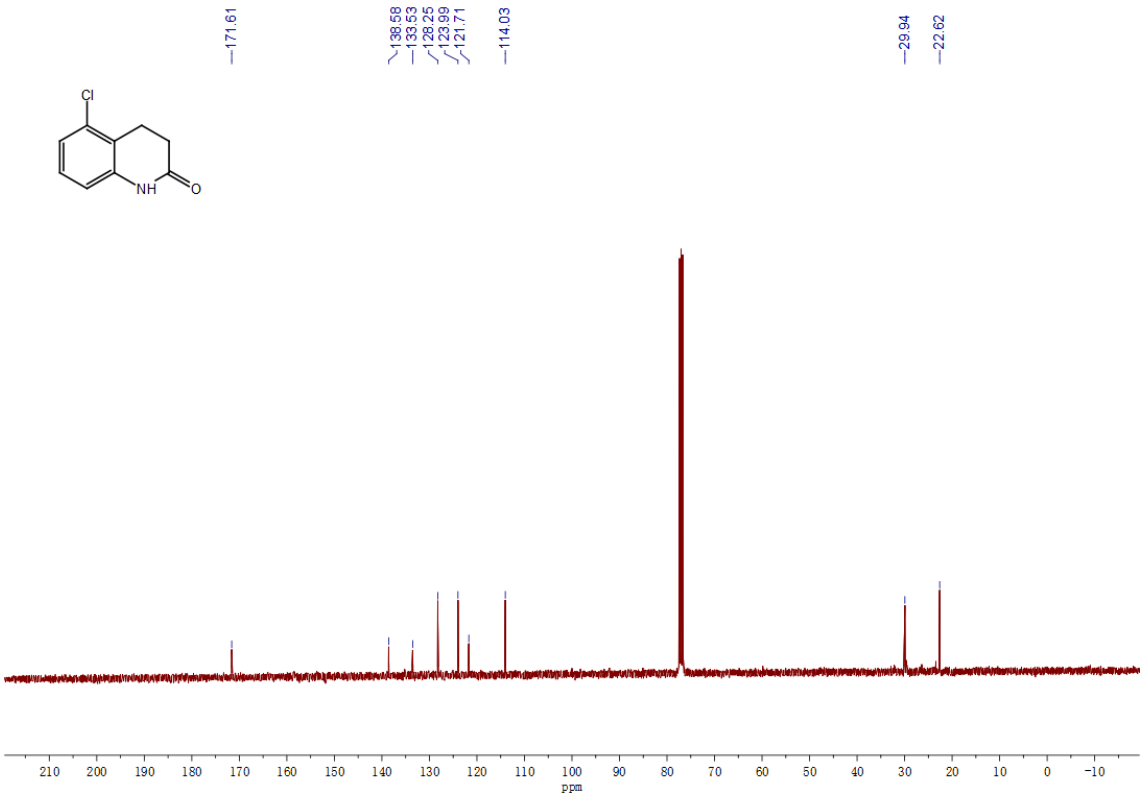
^{13}C NMR of 4c



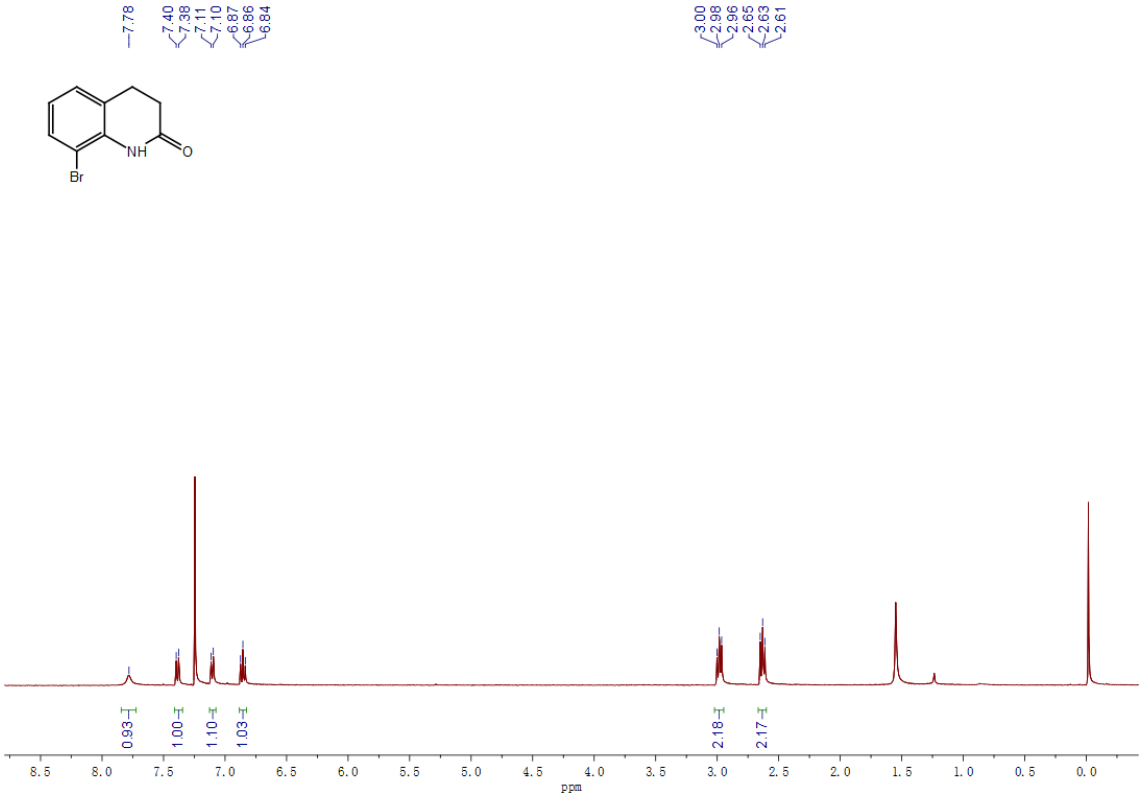
^{1}H NMR of 4c’



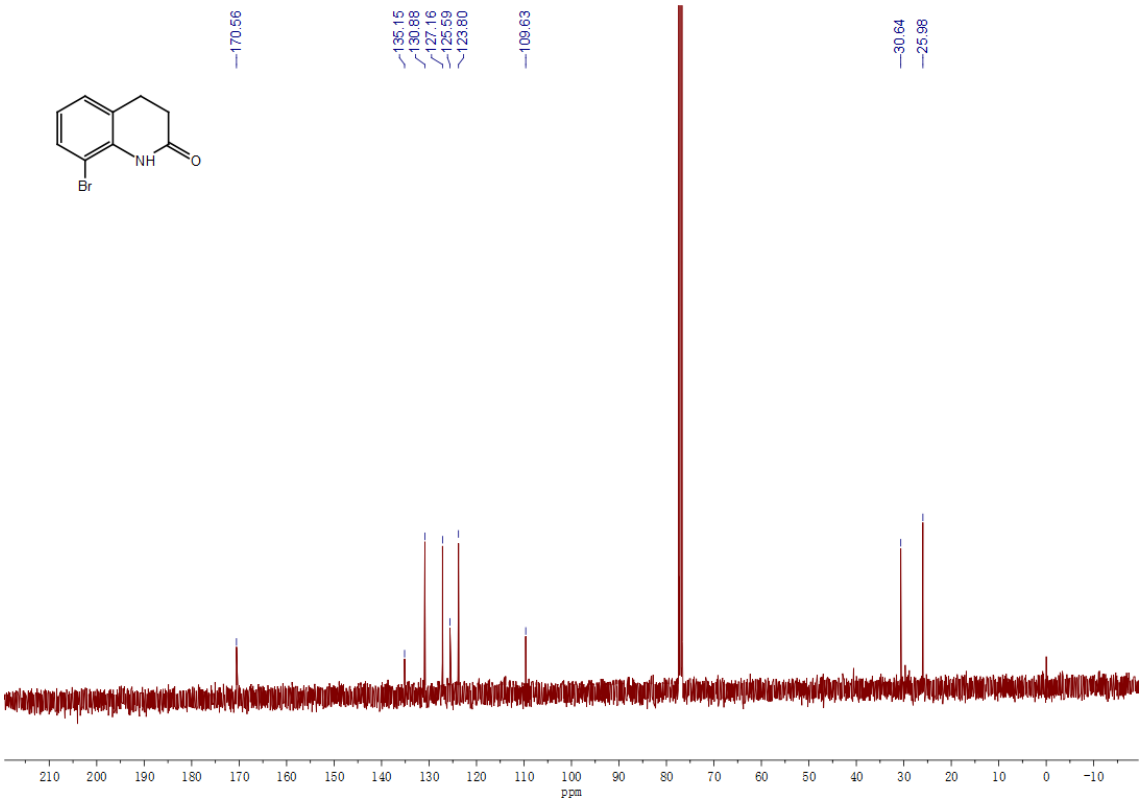
^{13}C NMR of 4c’



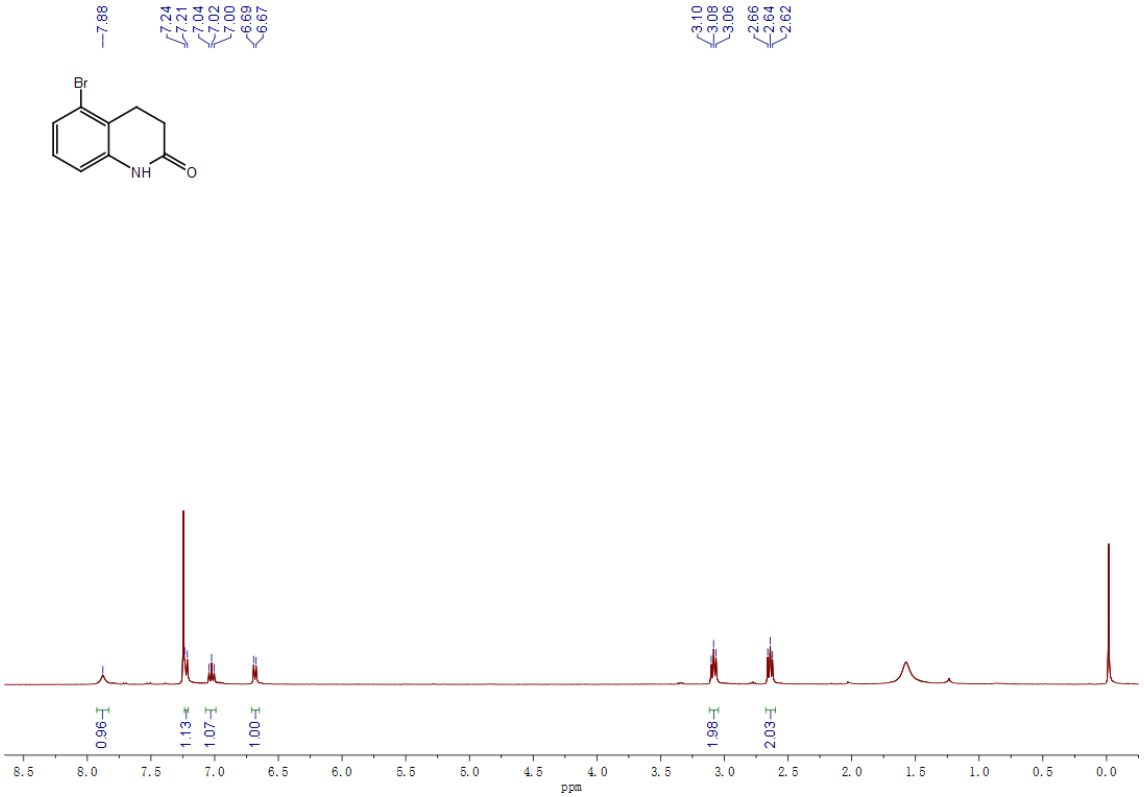
^{1}H NMR of 4d



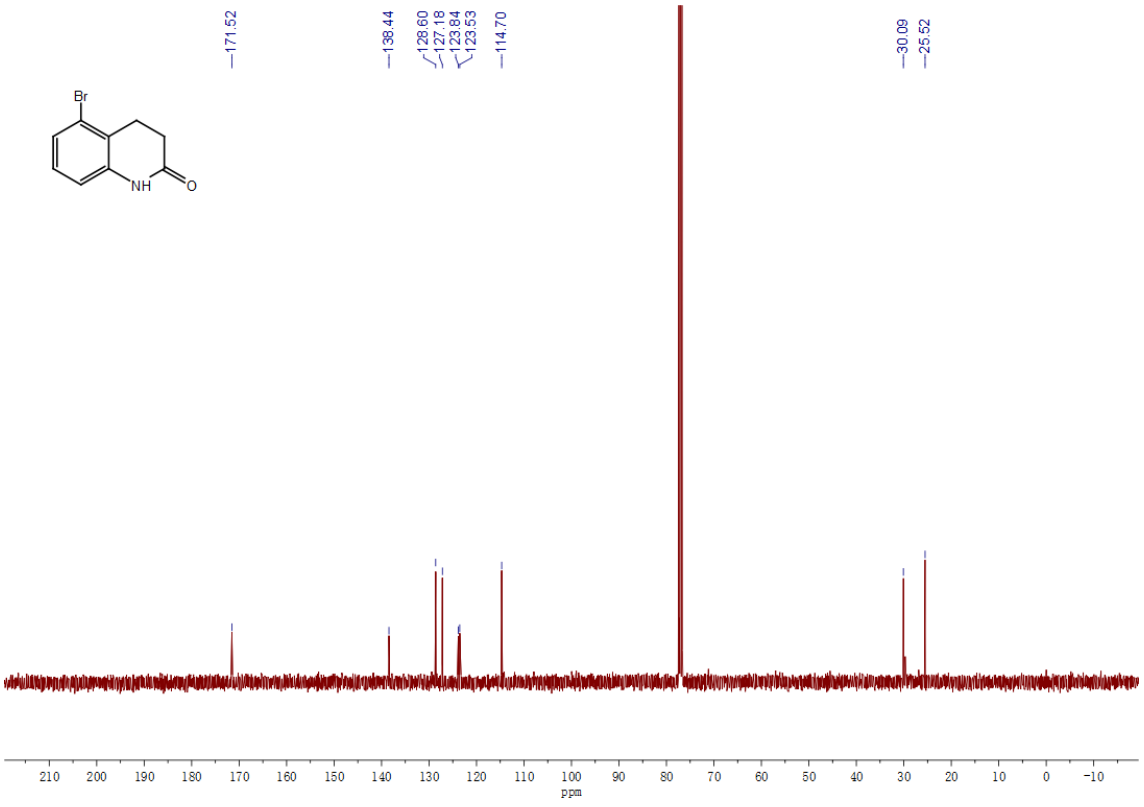
^{13}C NMR of 4d



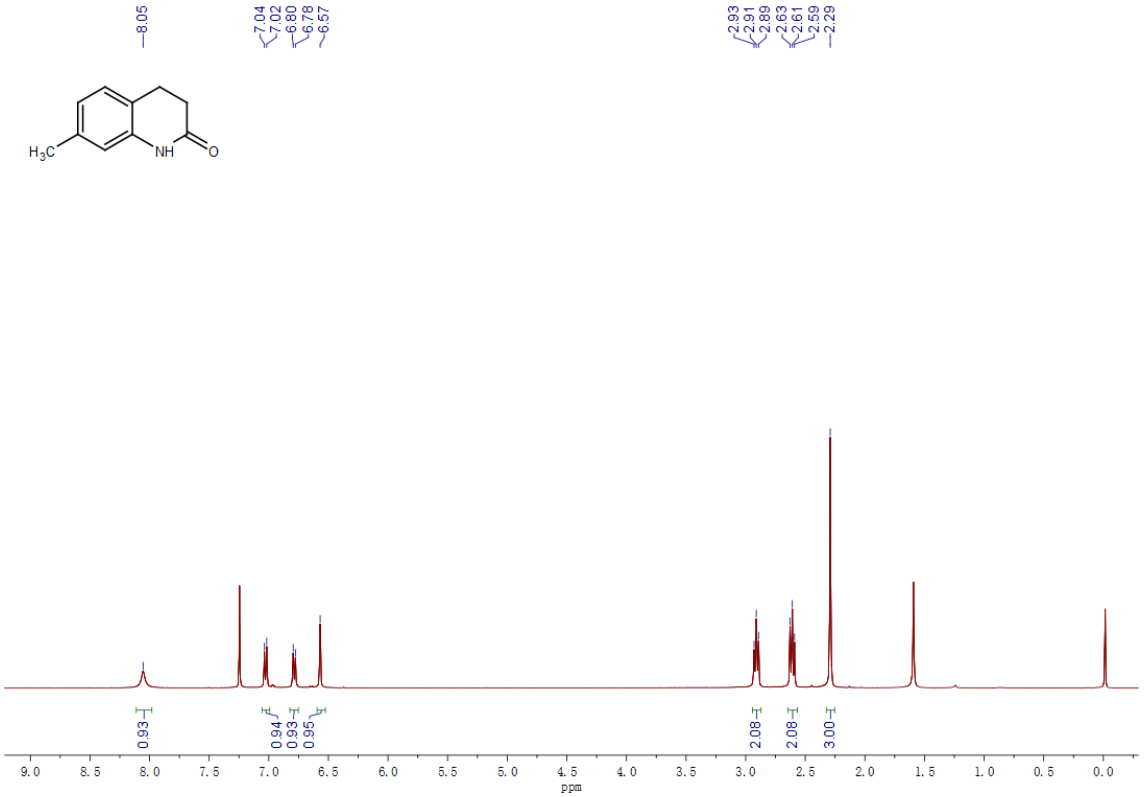
^{1}H NMR of 4d’



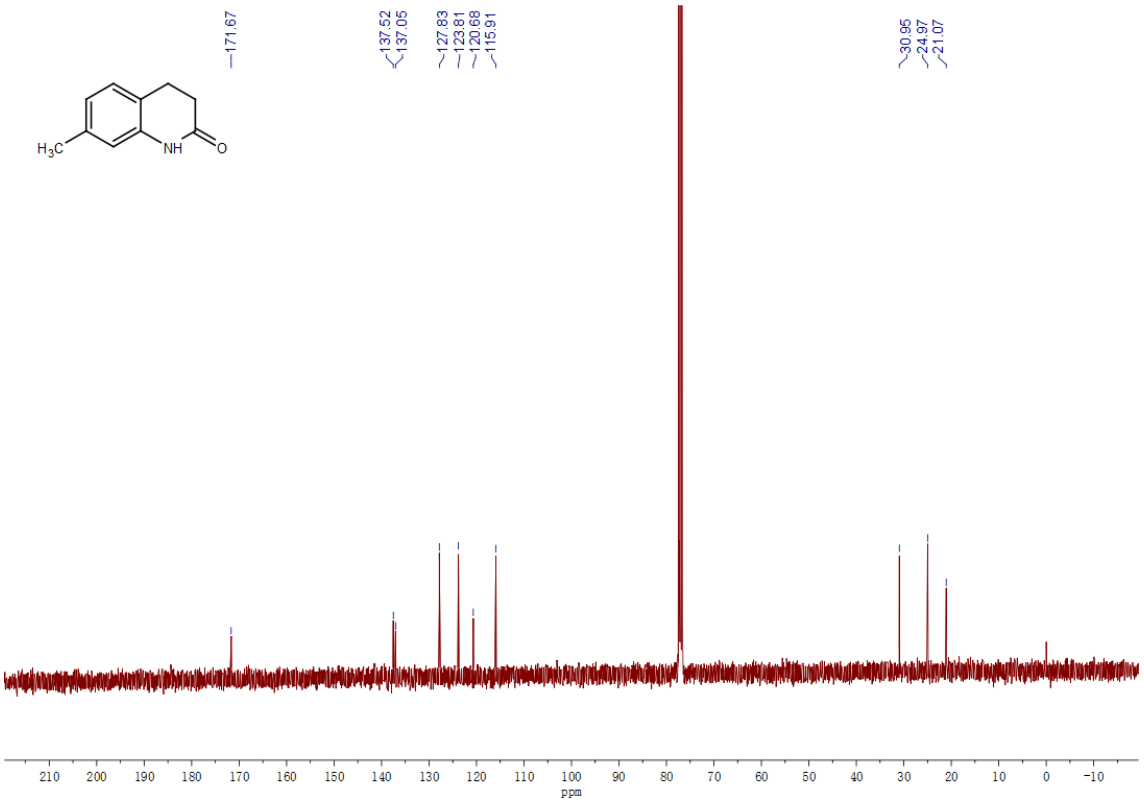
^{13}C NMR of 4d’



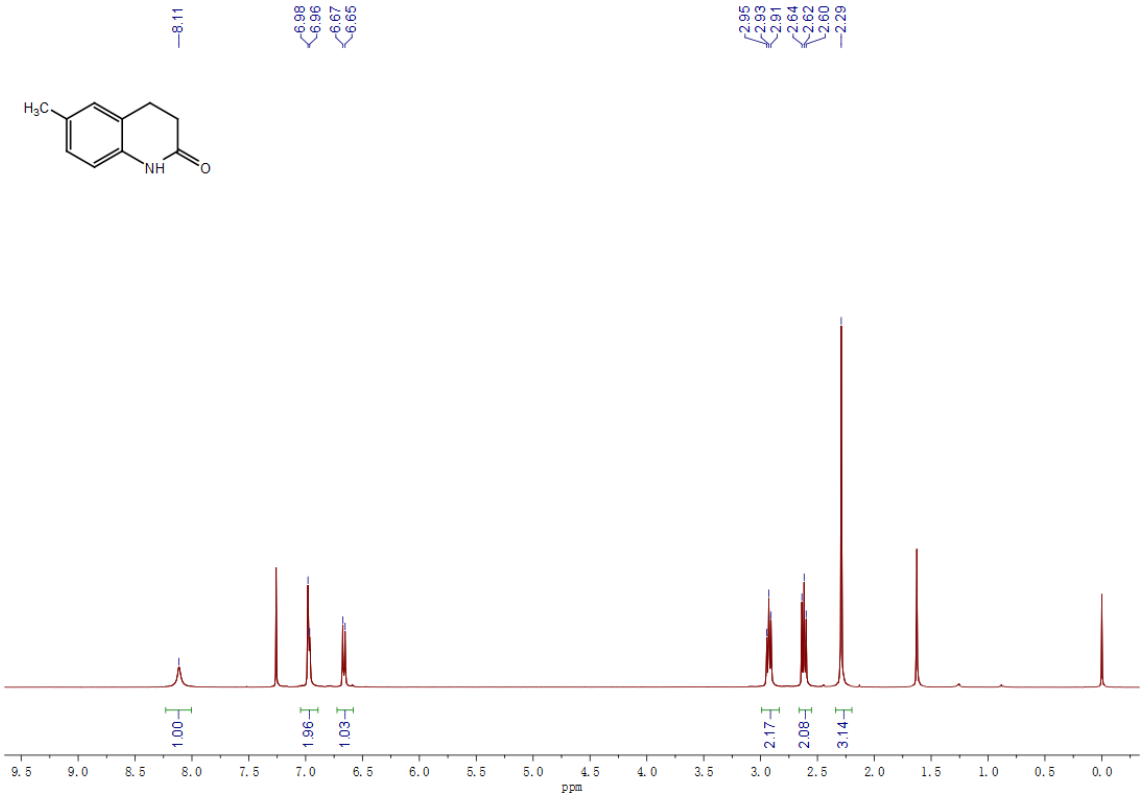
^{1}H NMR of 6b



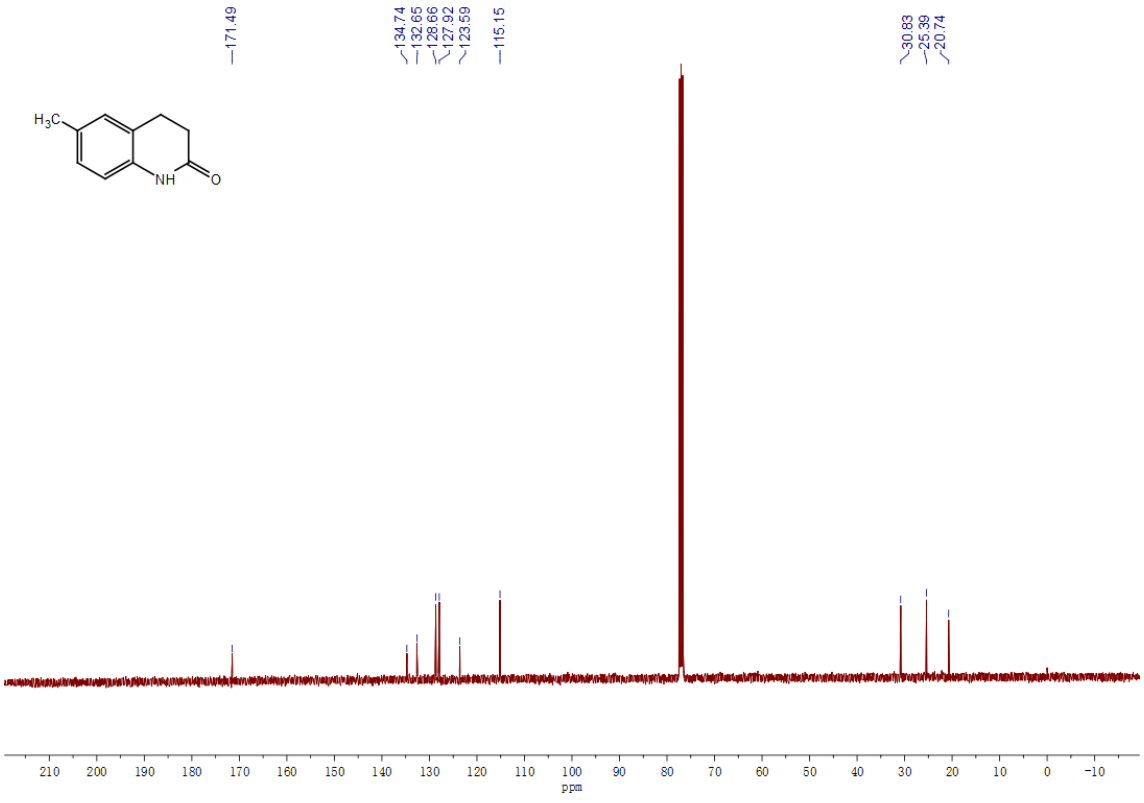
^{13}C NMR of 6b



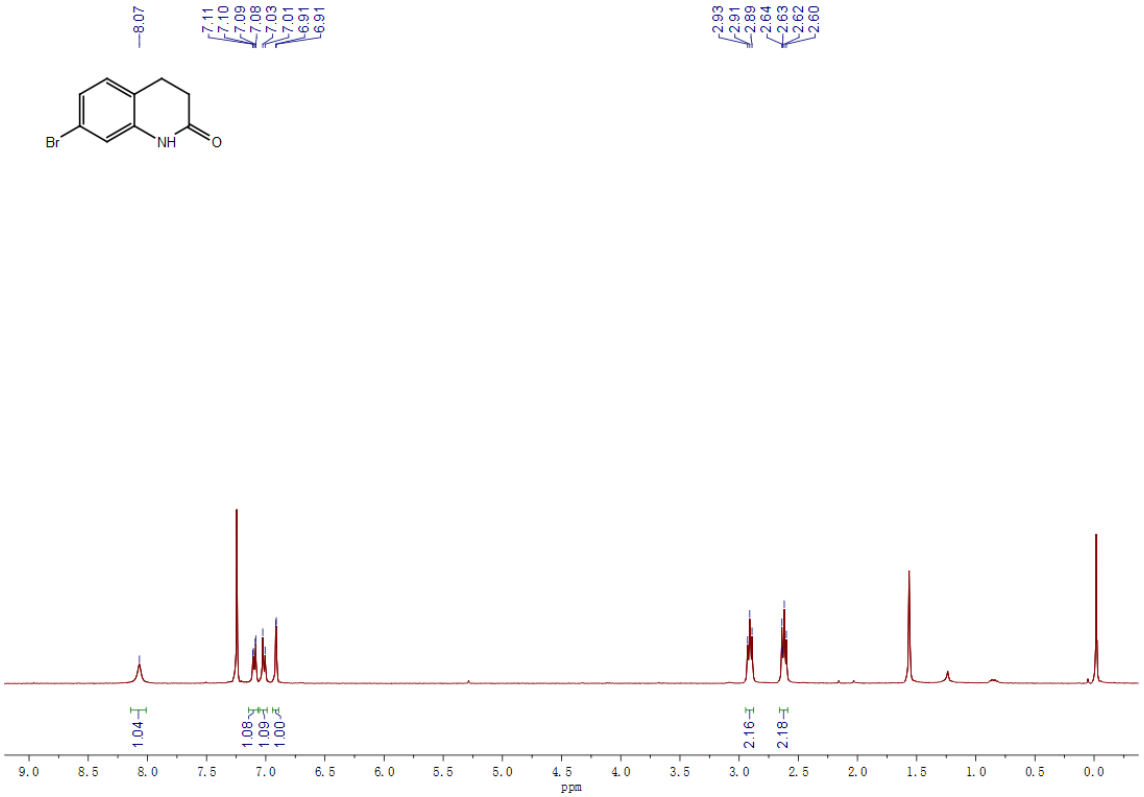
^{1}H NMR of 6b’



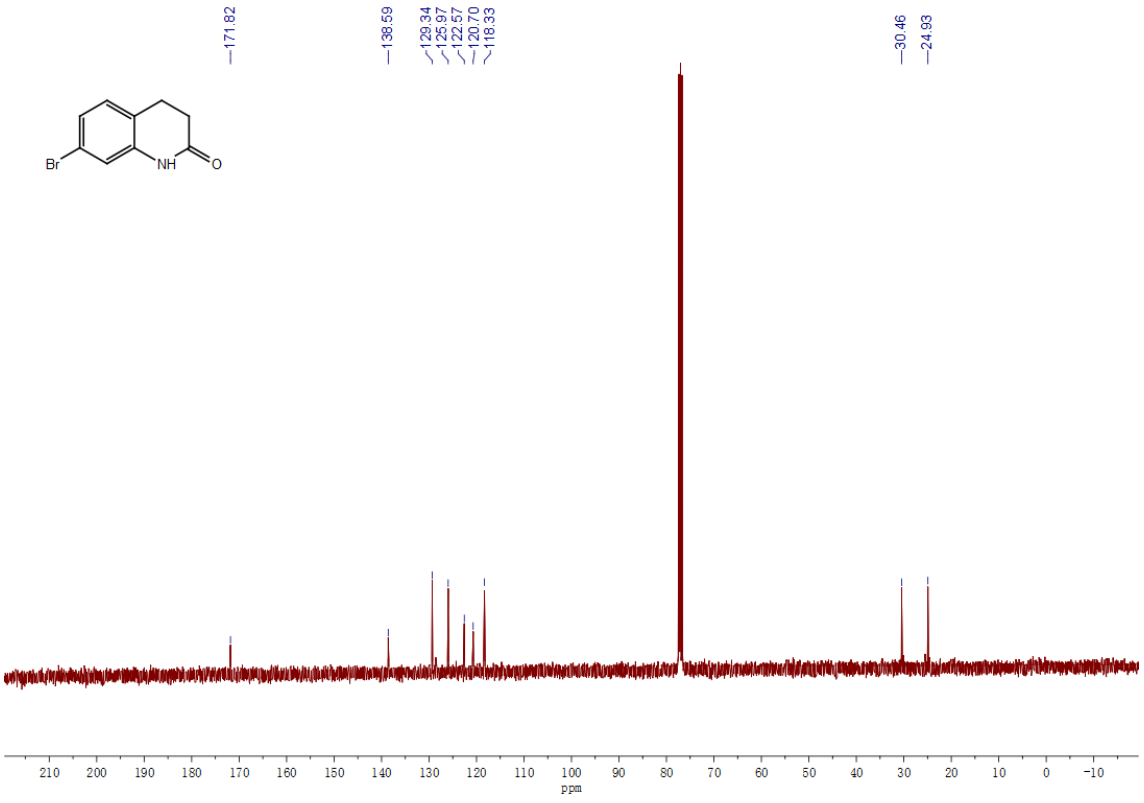
^{13}C NMR of 6b’



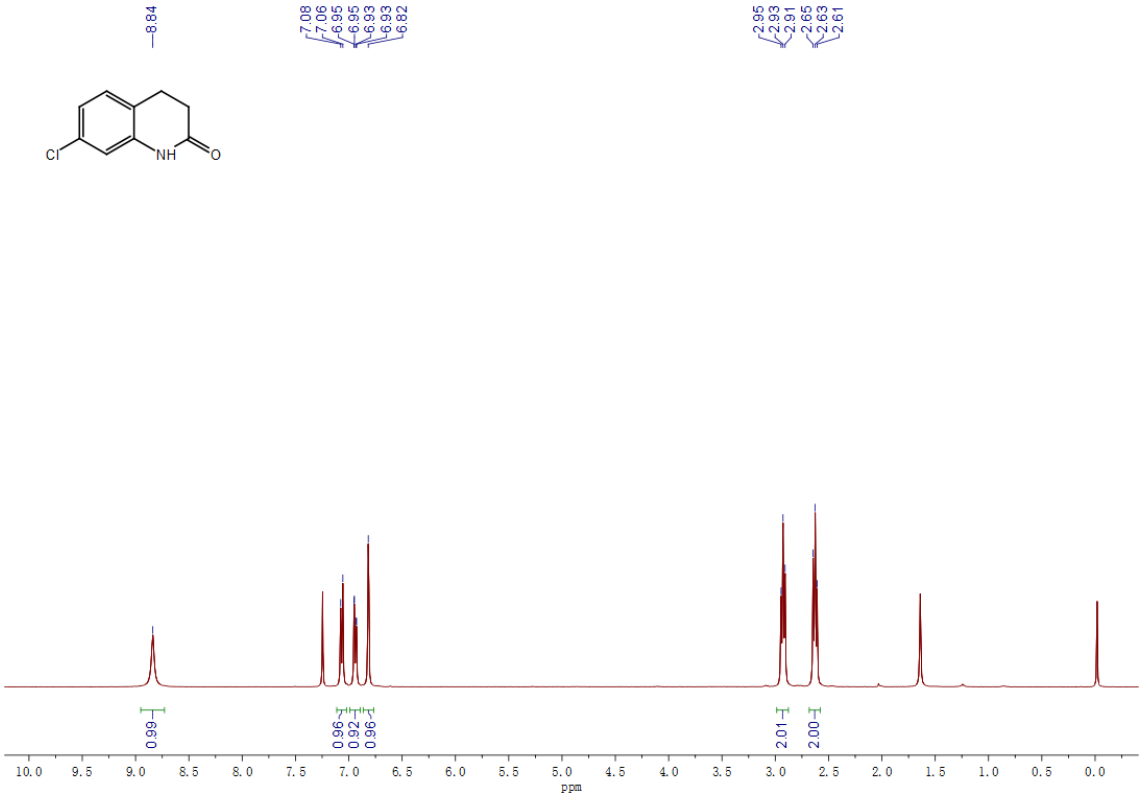
^{1}H NMR of 6c



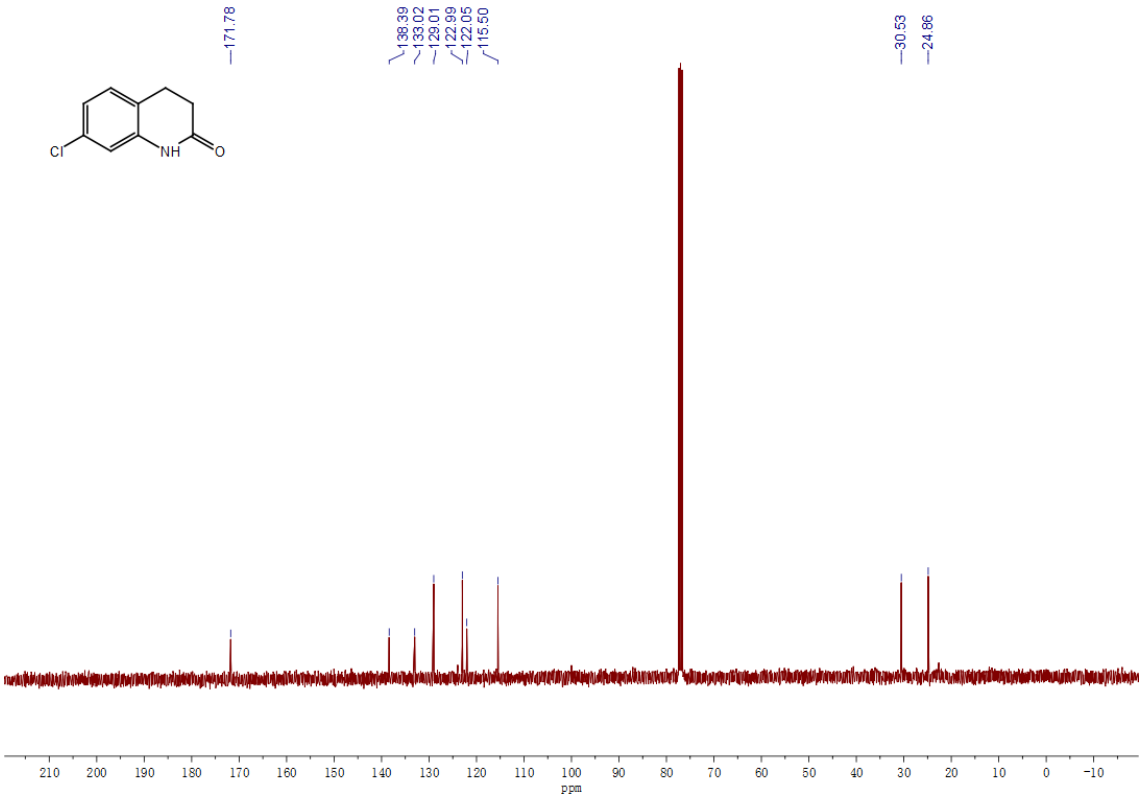
^{13}C NMR of 6c



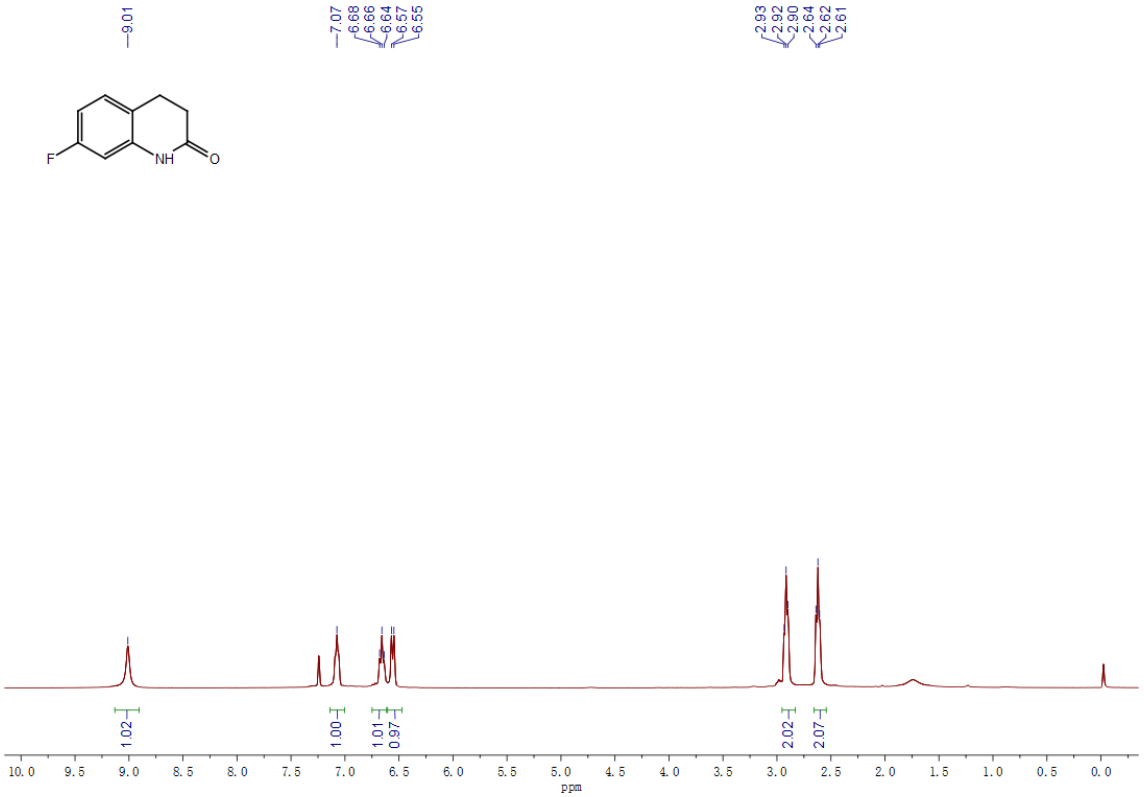
^{1}H NMR of 6d



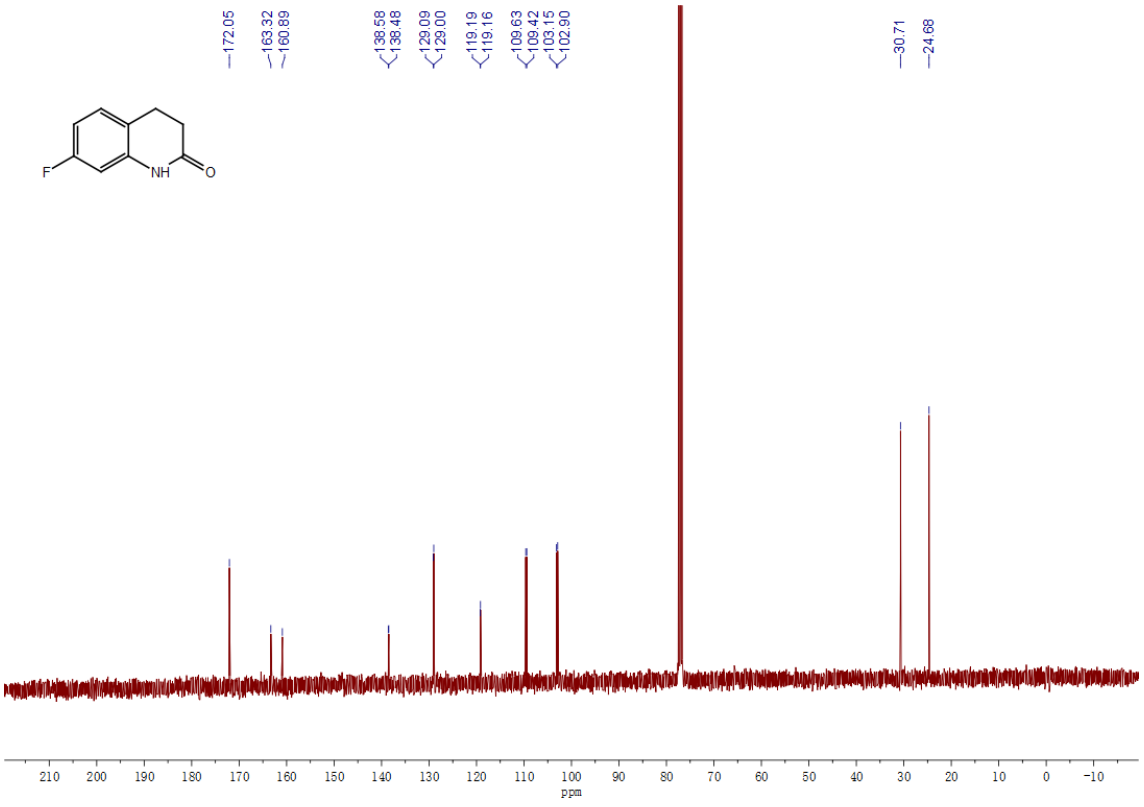
^{13}C NMR of 6d



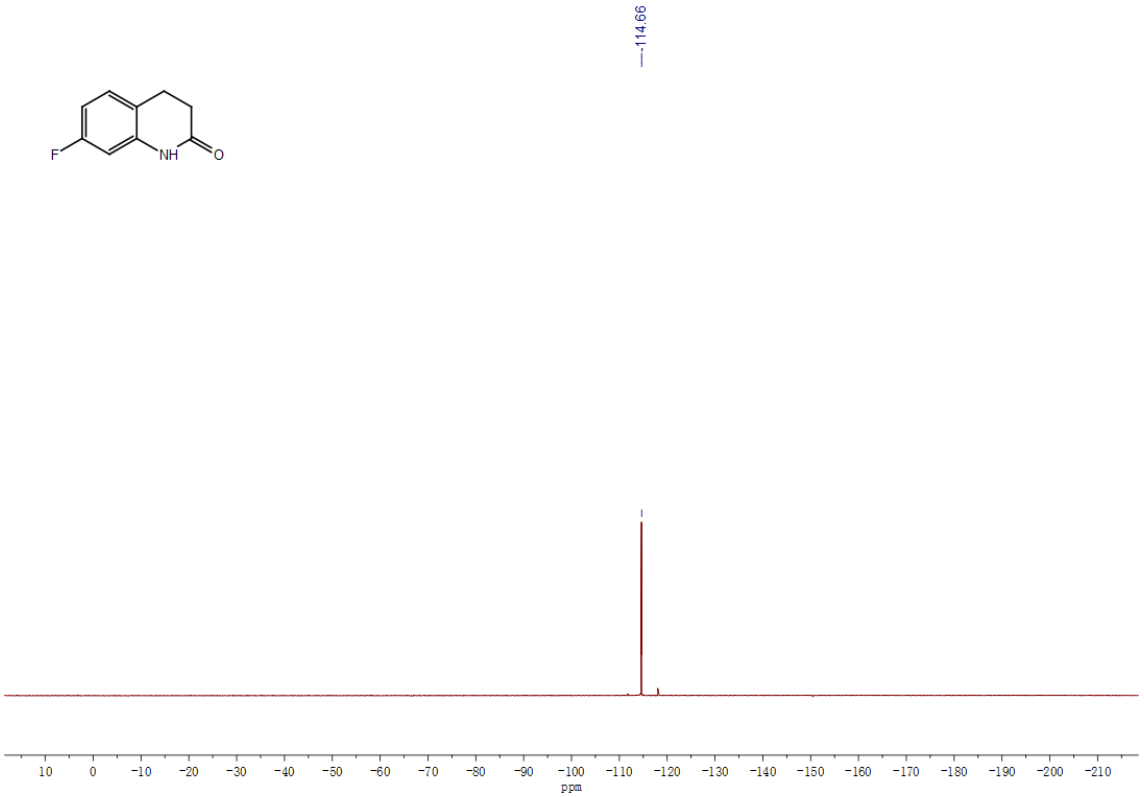
^{1}H NMR of 6e



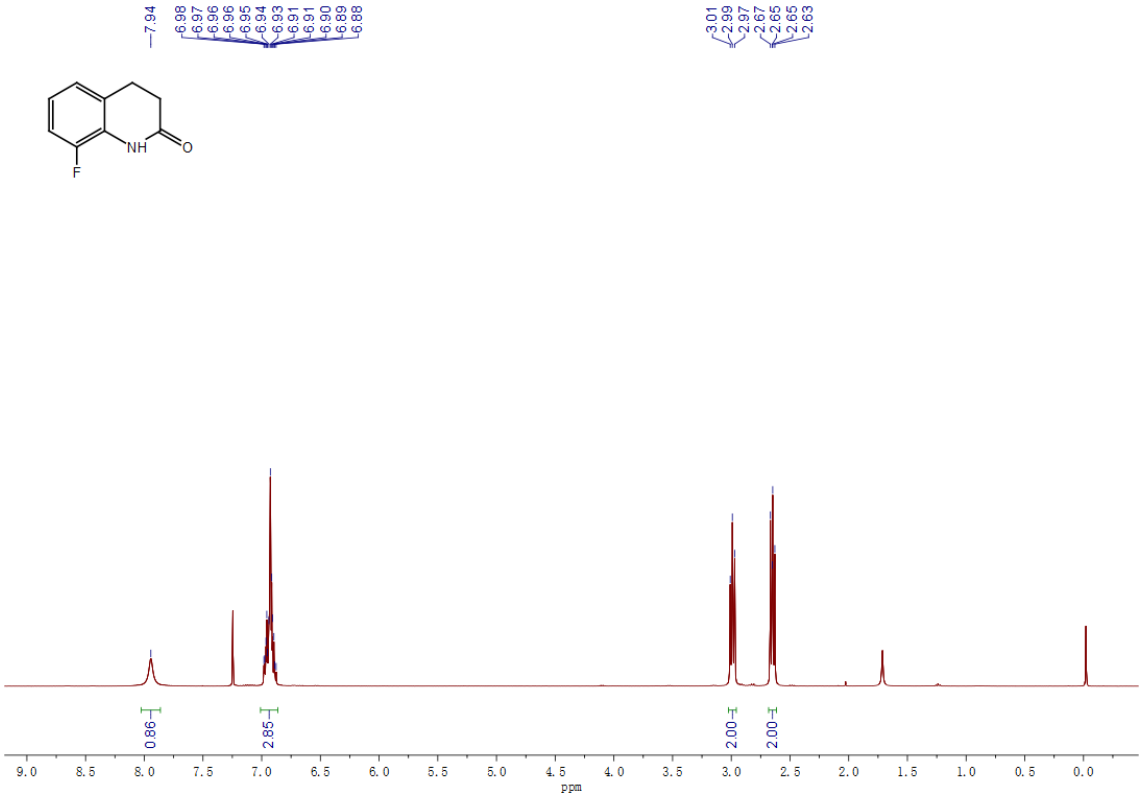
^{13}C NMR of 6e



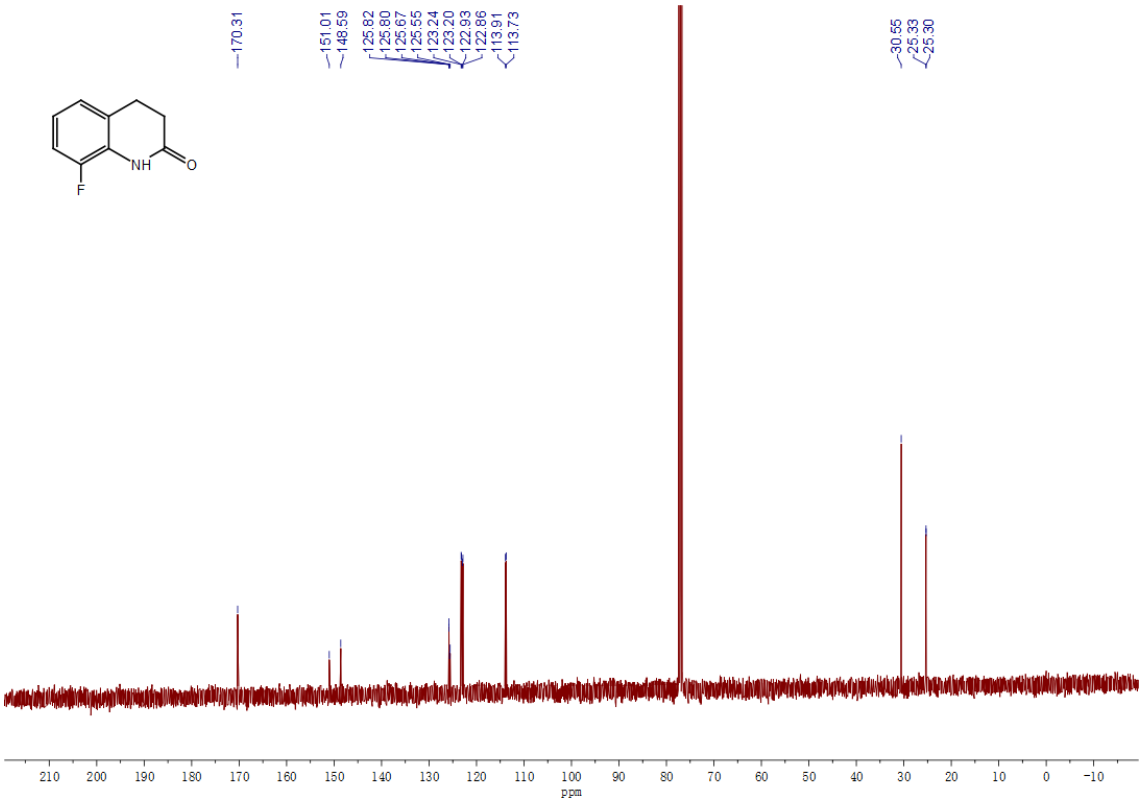
^{19}F NMR of 6e


-114.66
F
NH
O
10
0
-10
-20
-30
-40
-50
-60
-70
-80
-90
-100
-110
-120
-130
-140
-150
-160
-170
-180
-190
-200
-210
ppm

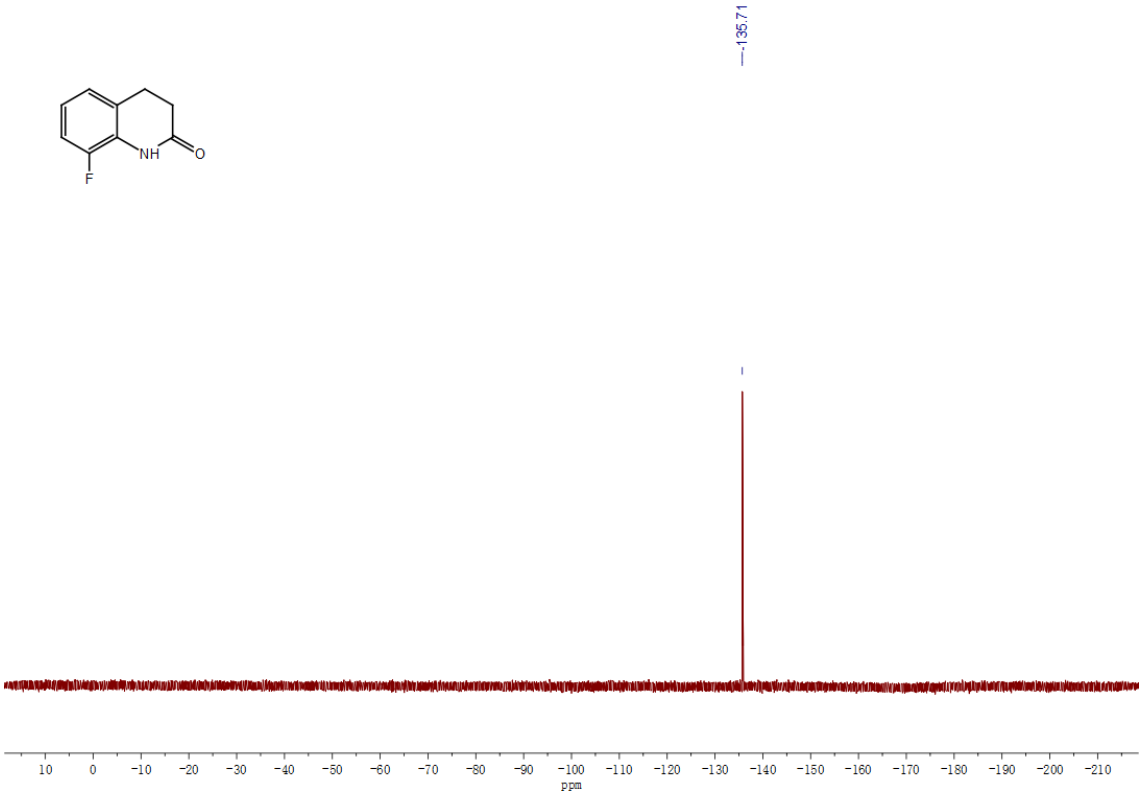
^{1}H NMR of 6e”



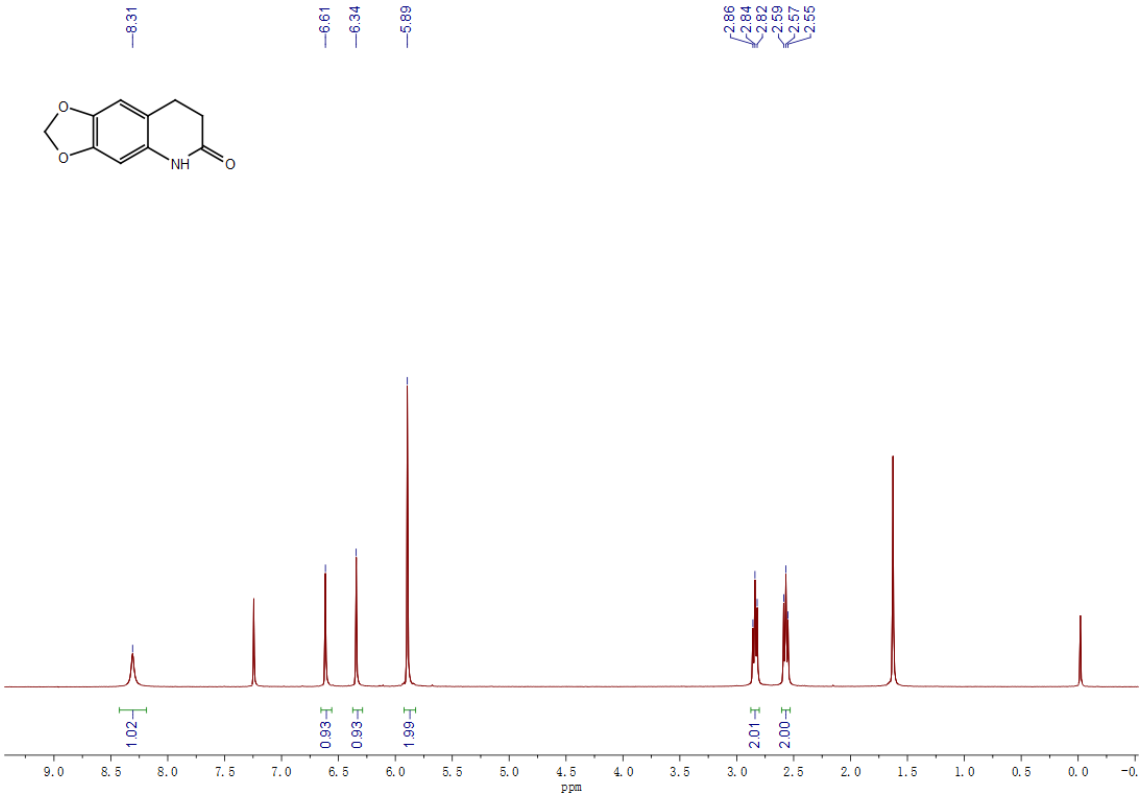
^{13}C NMR of 6e”



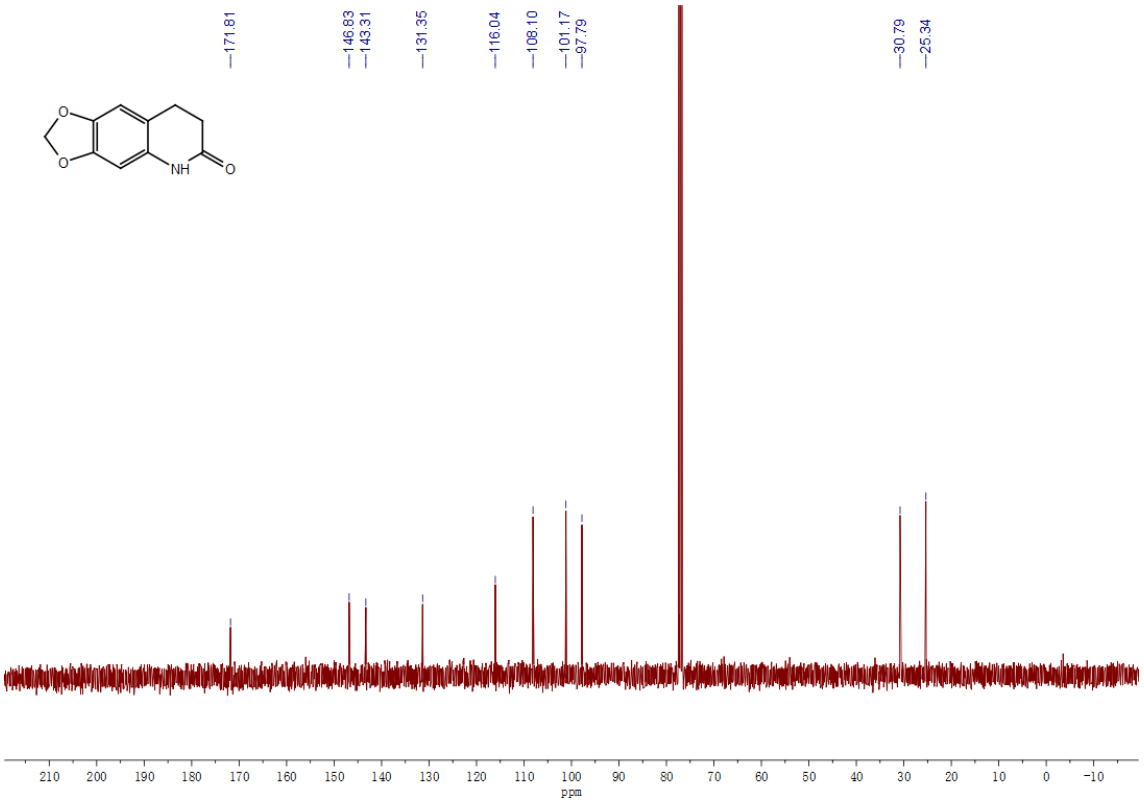
^{19}F NMR of 6e”


-135.71
NH
O
F
10
0
-10
-20
-30
-40
-50
-60
-70
-80
-90
-100
-110
-120
-130
-140
-150
-160
-170
-180
-190
-200
-210
ppm

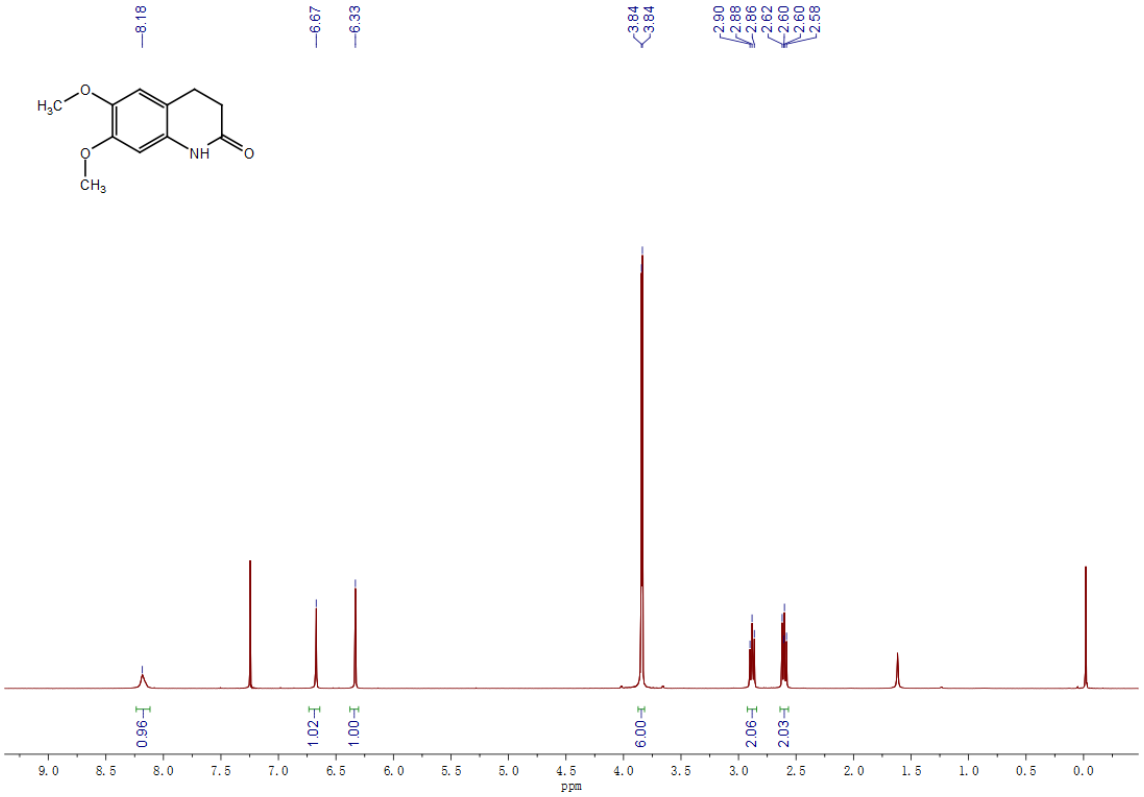
^{1}H NMR of 8a



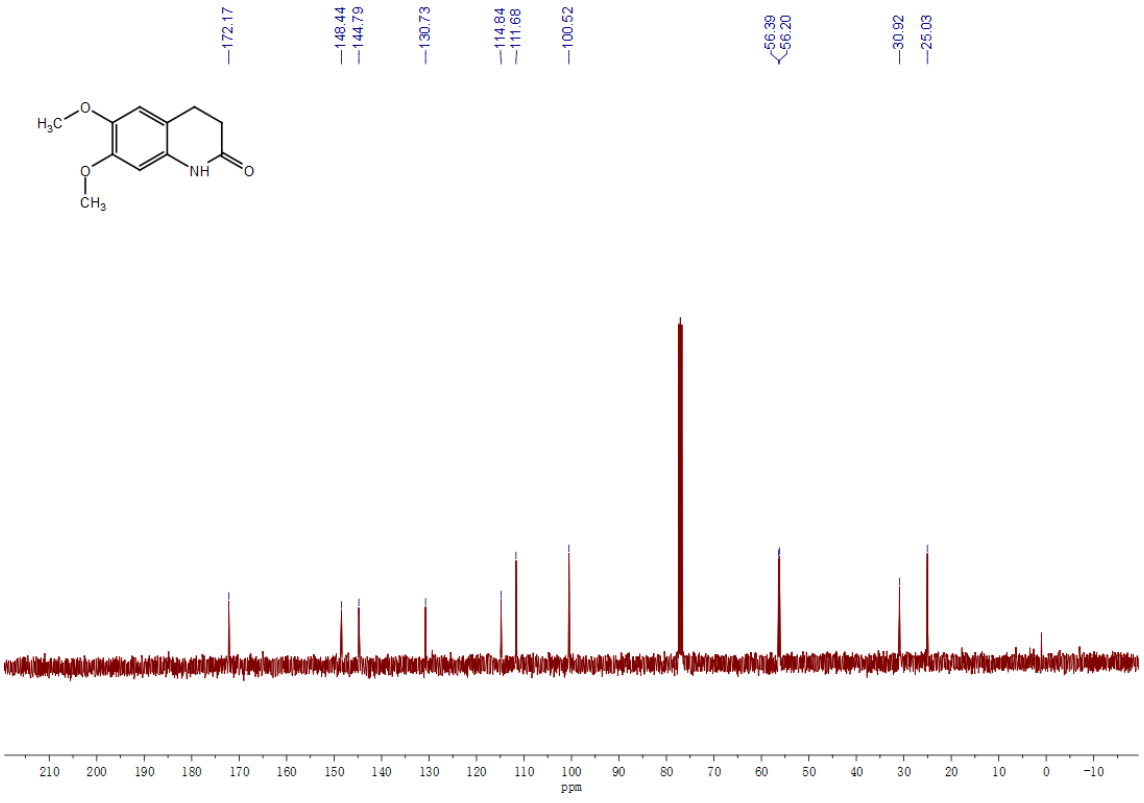
^{13}C NMR of 8a



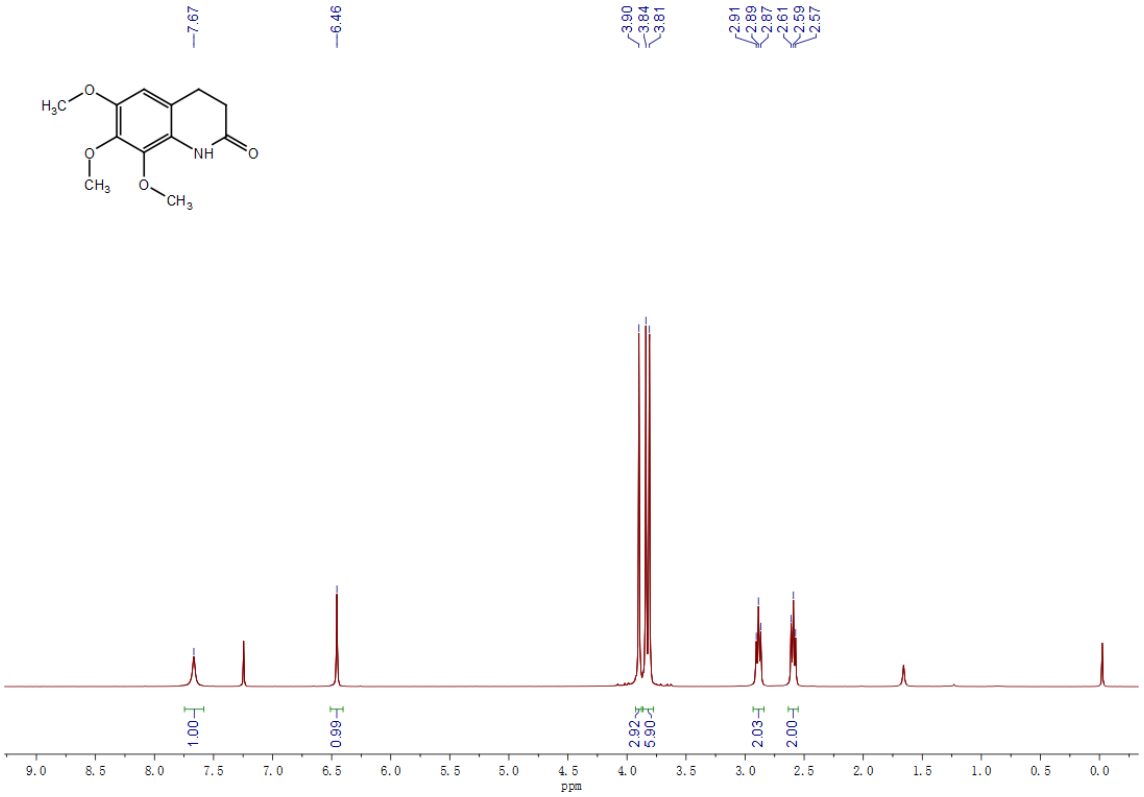
^{1}H NMR of 8b



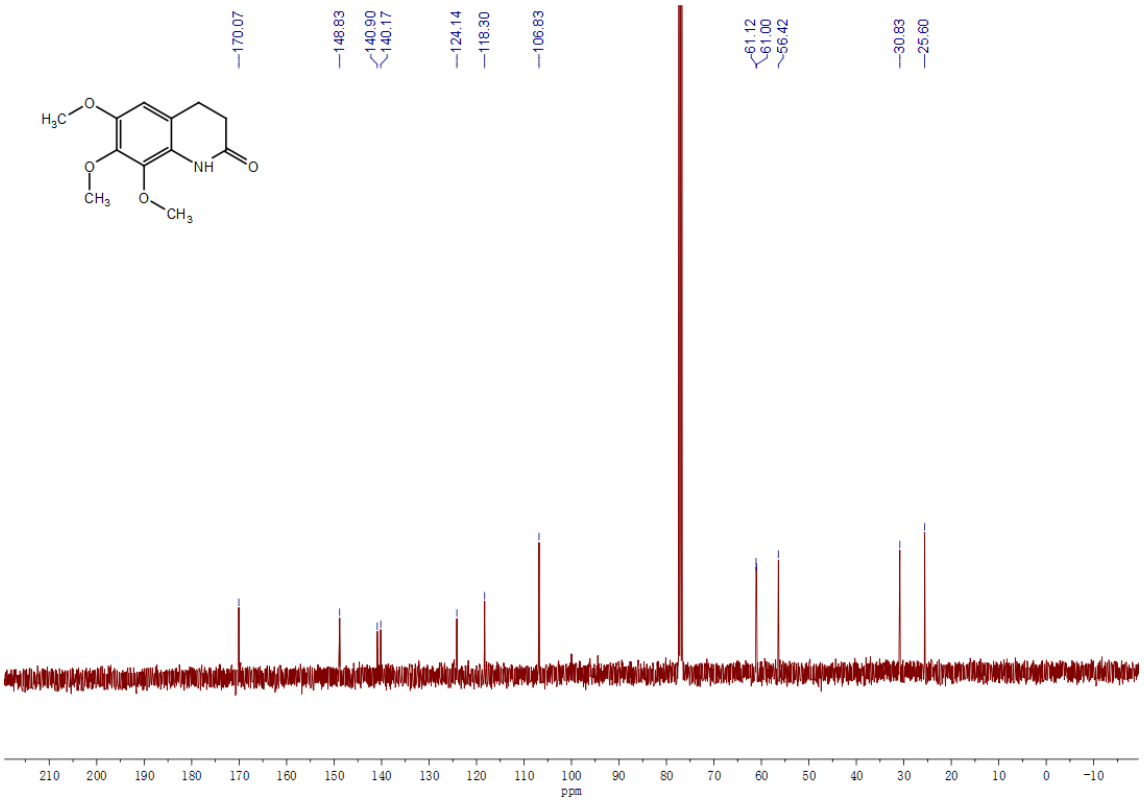
^{13}C NMR of 8b



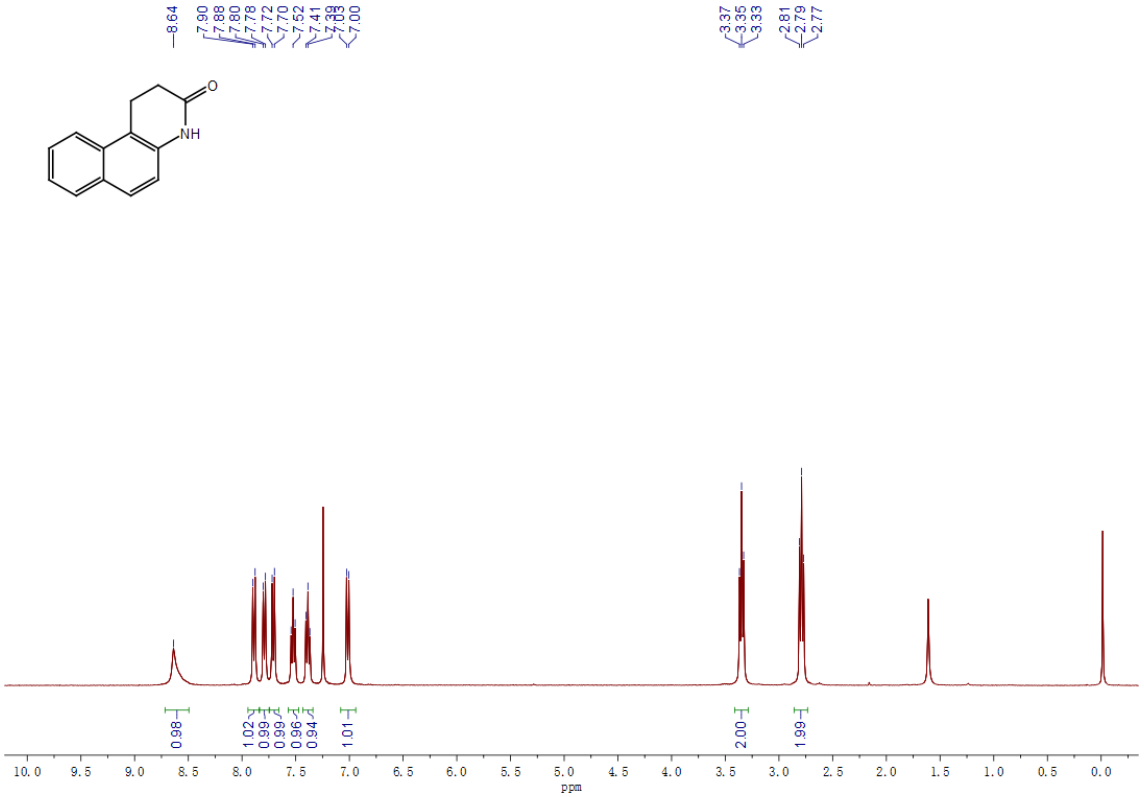
^{1}H NMR of 8c



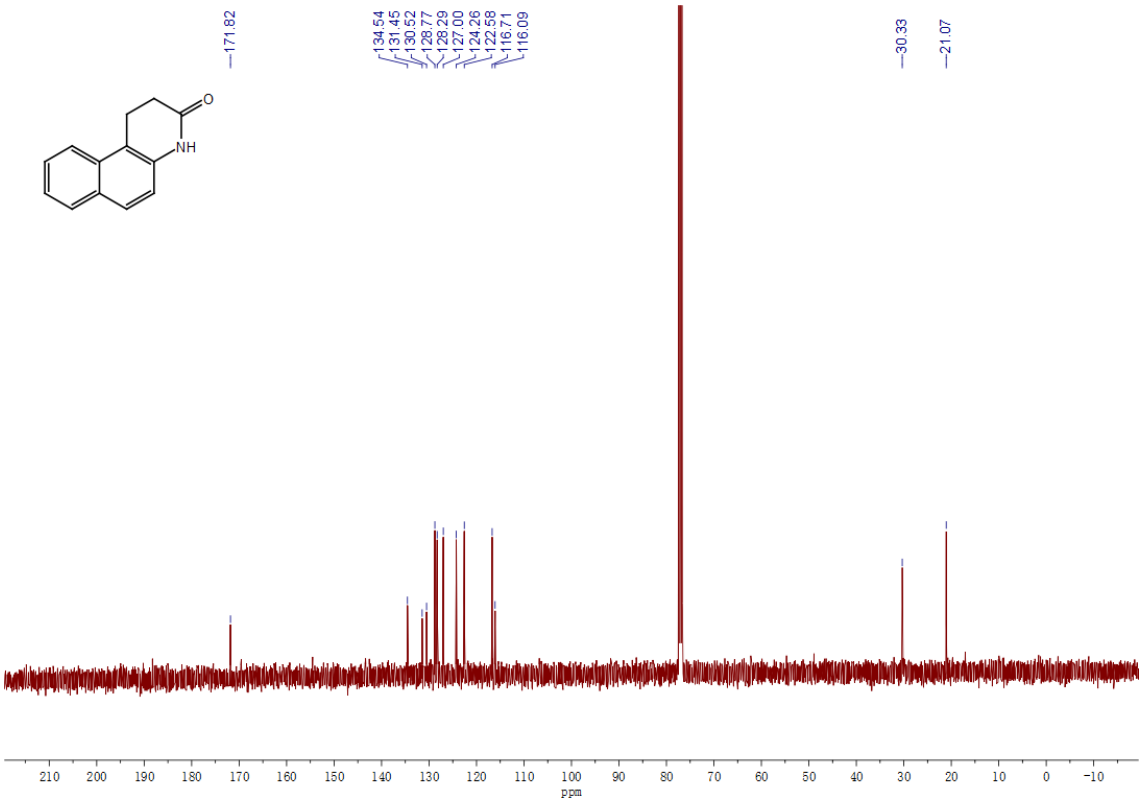
^{13}C NMR of 8c



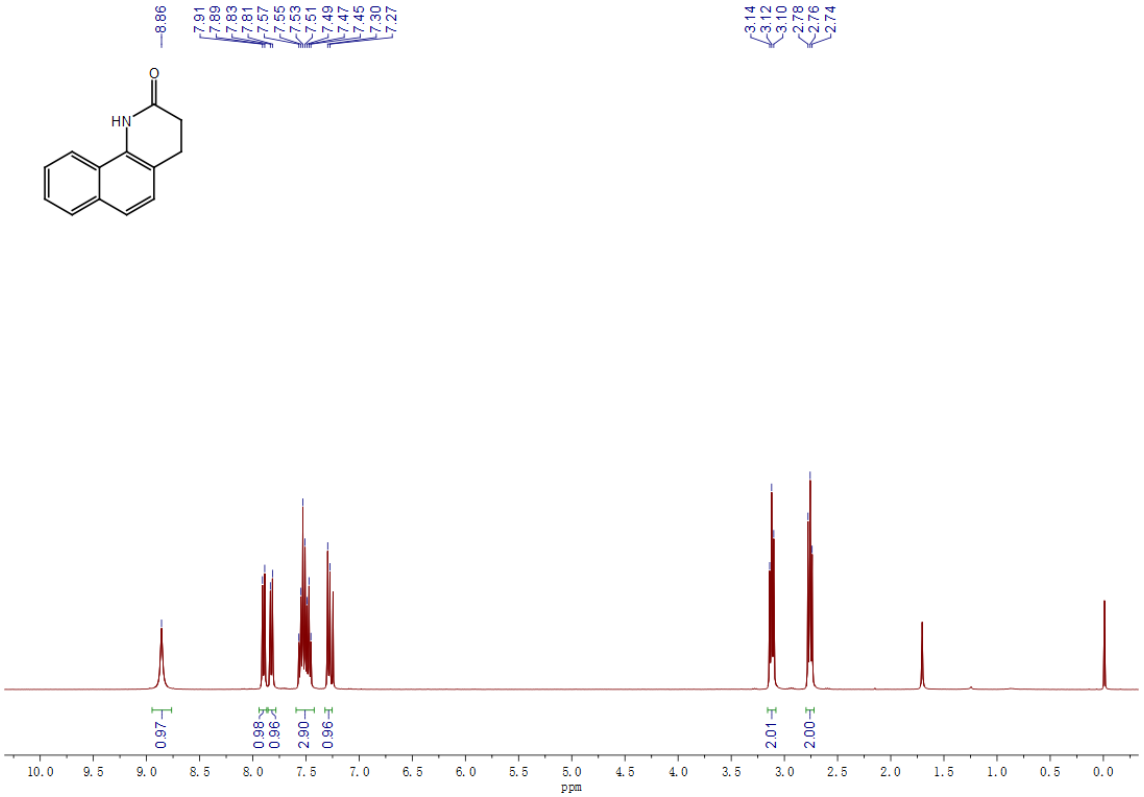
^{1}H NMR of 8d



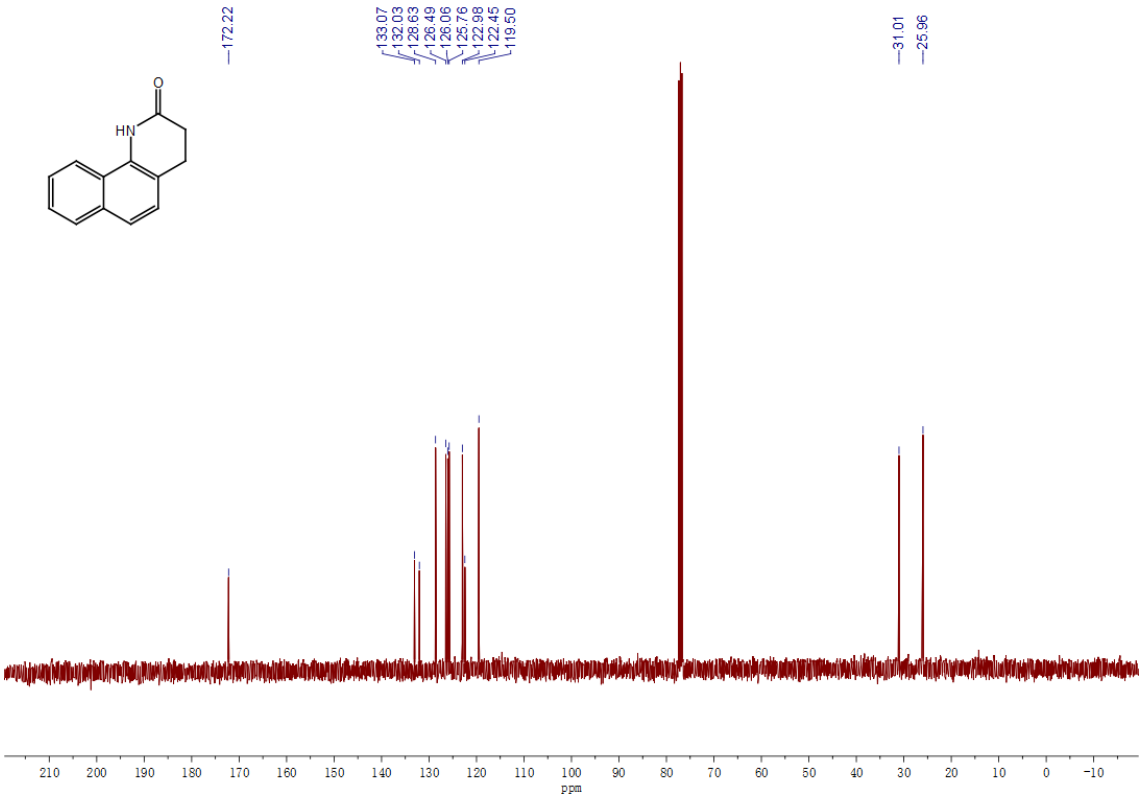
^{13}C NMR of 8d



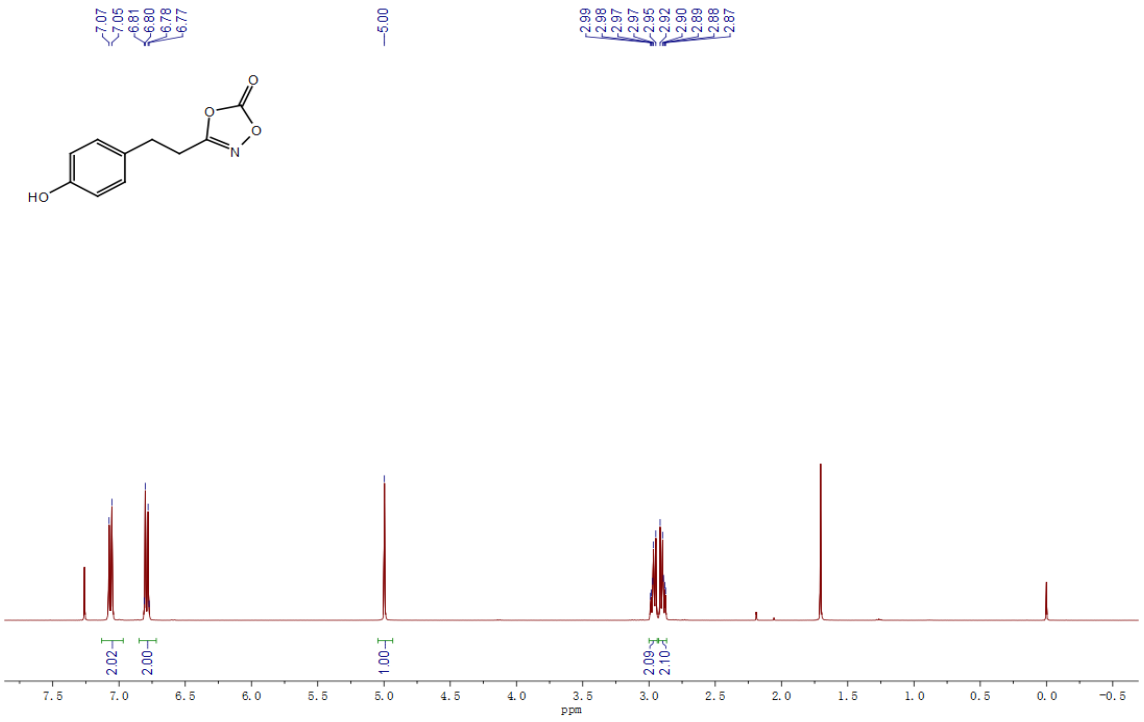
^{1}H NMR of 8e



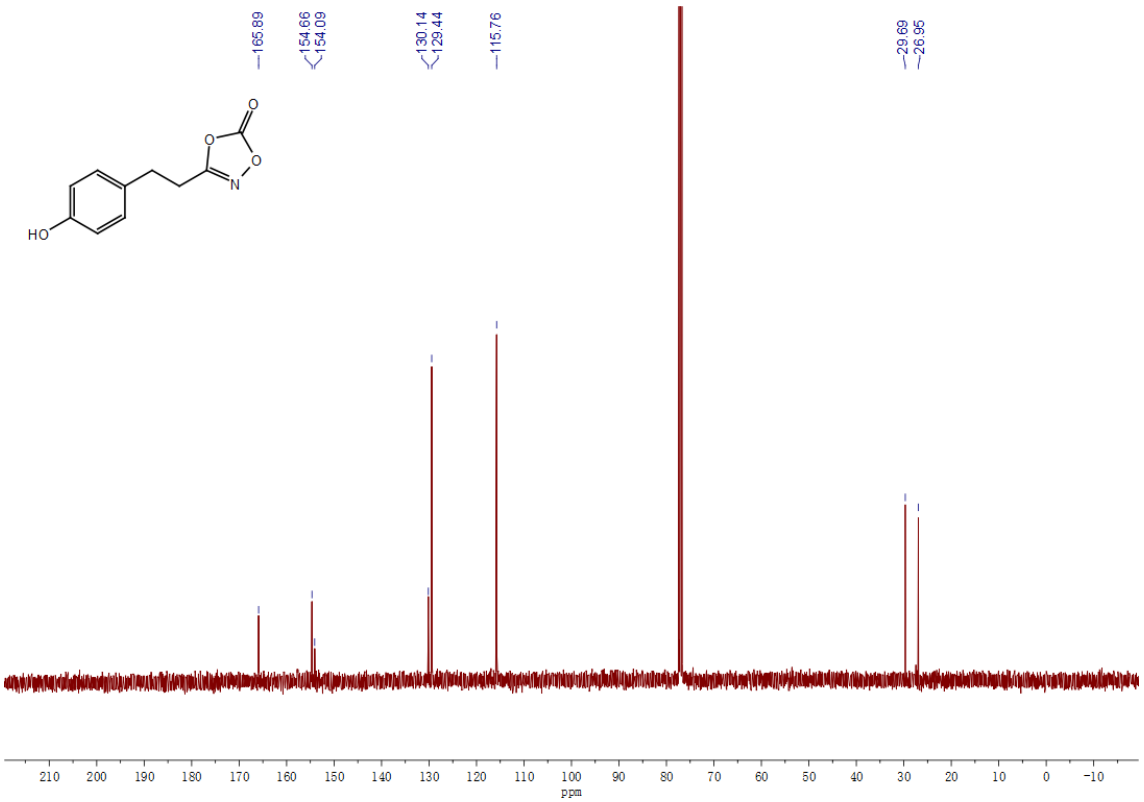
^{13}C NMR of 8e



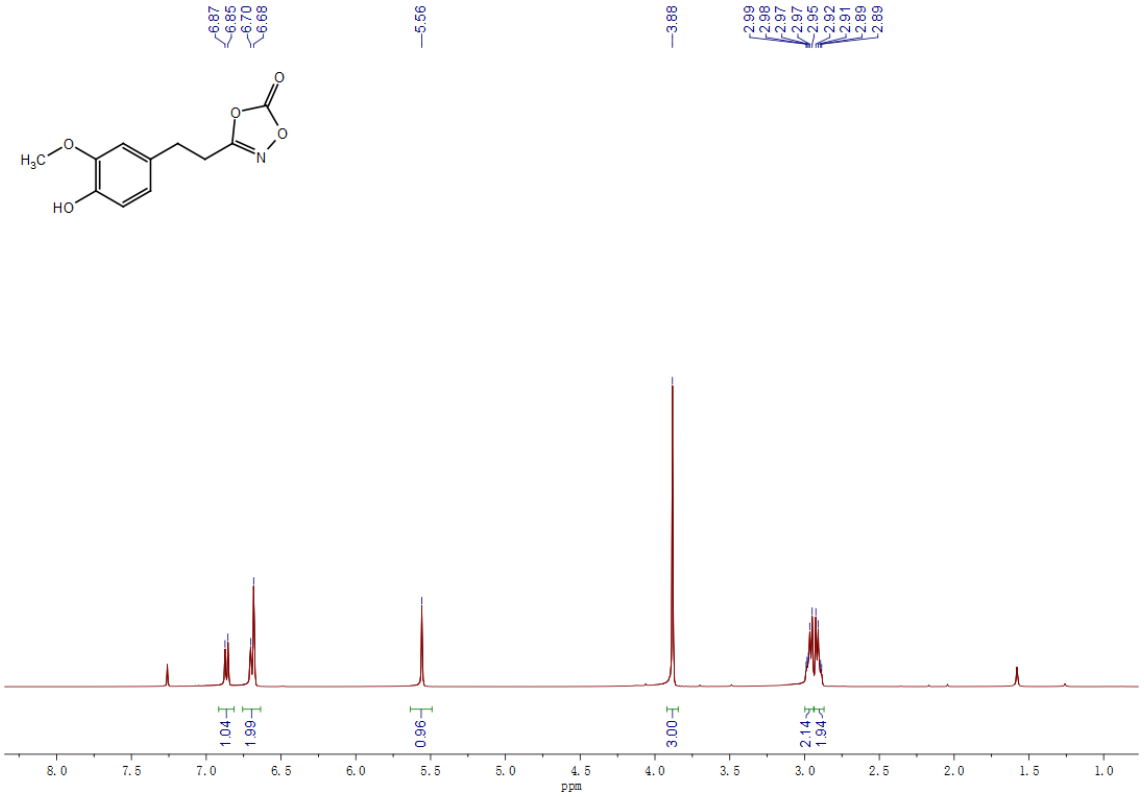
^{1}H NMR of 9a



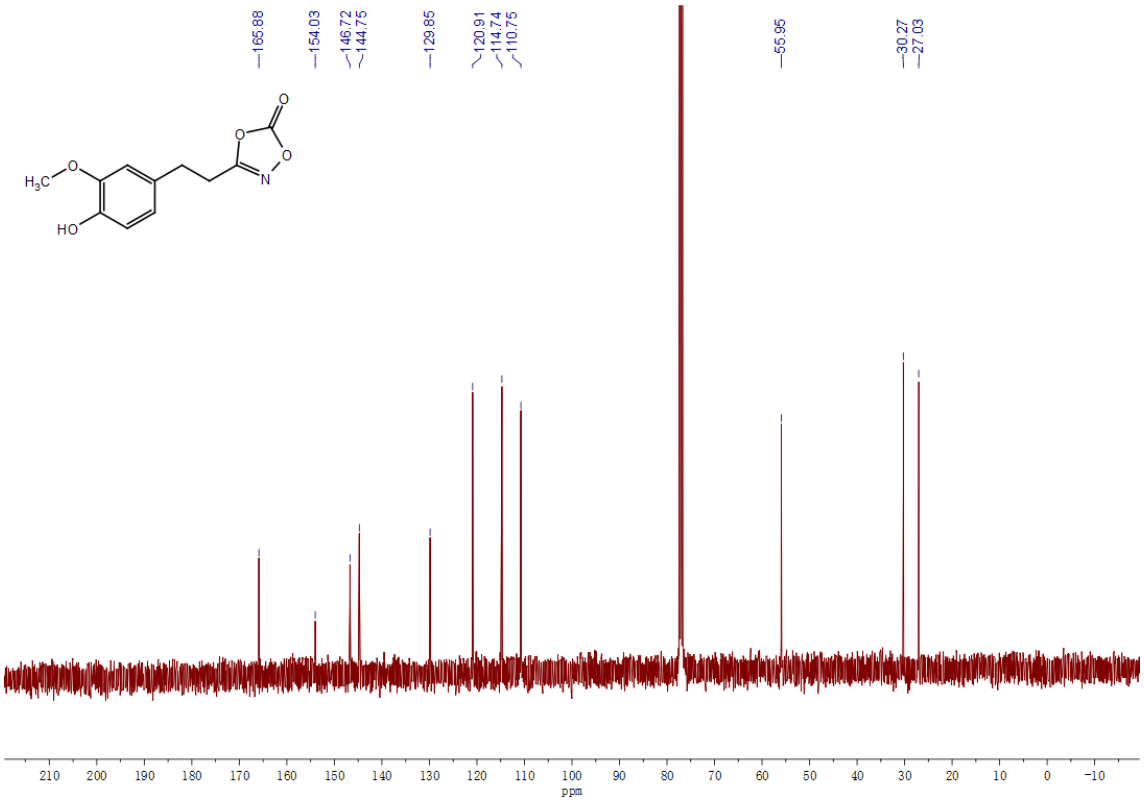
^{13}C NMR of 9a



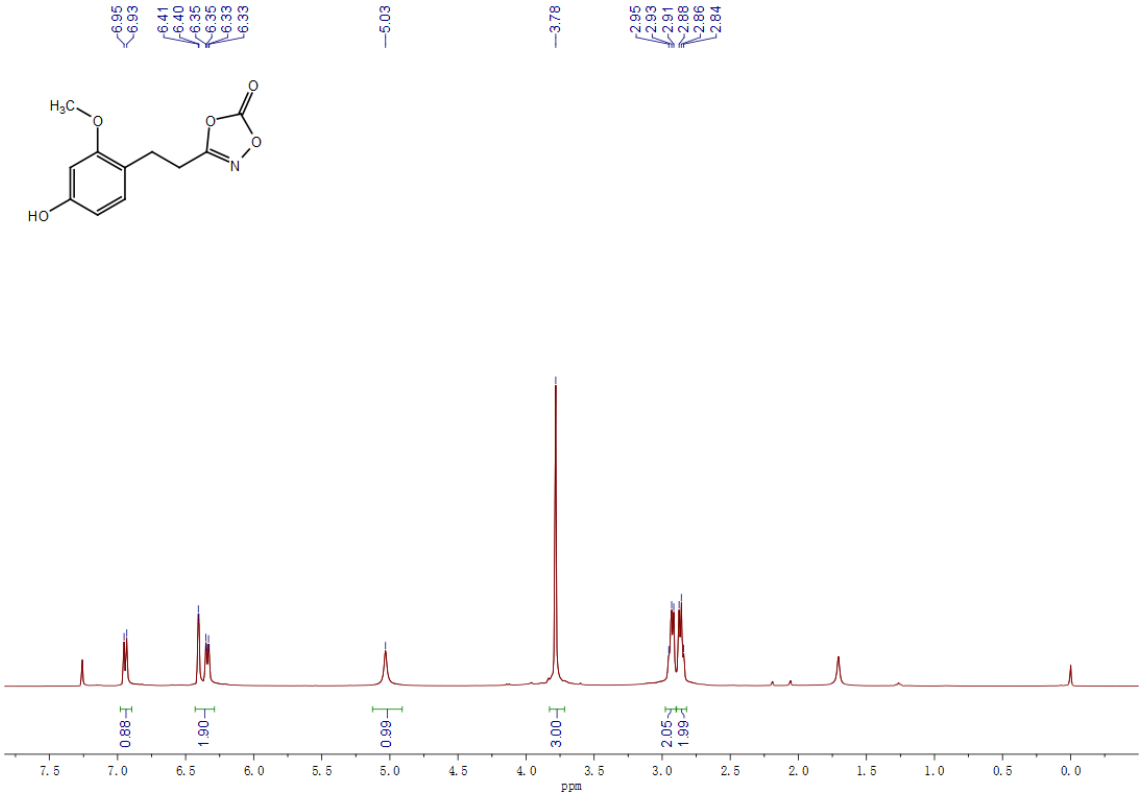
^{1}H NMR of 9b



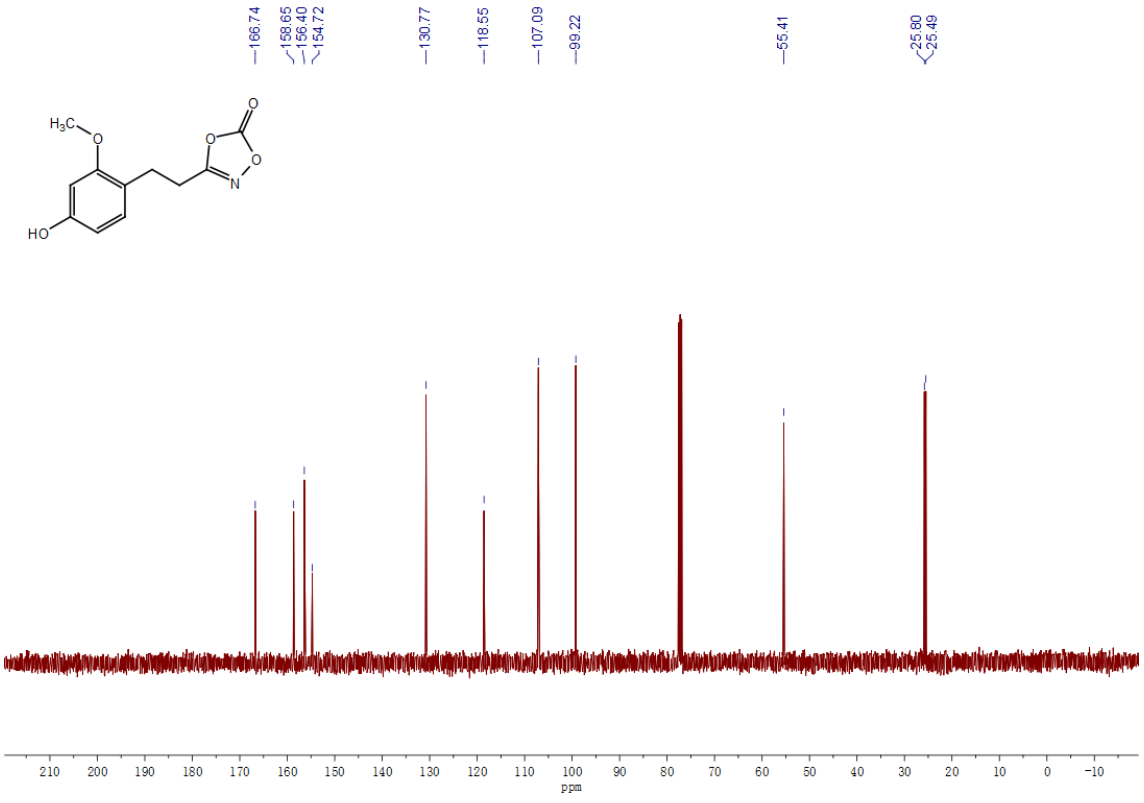
^{13}C NMR of 9b



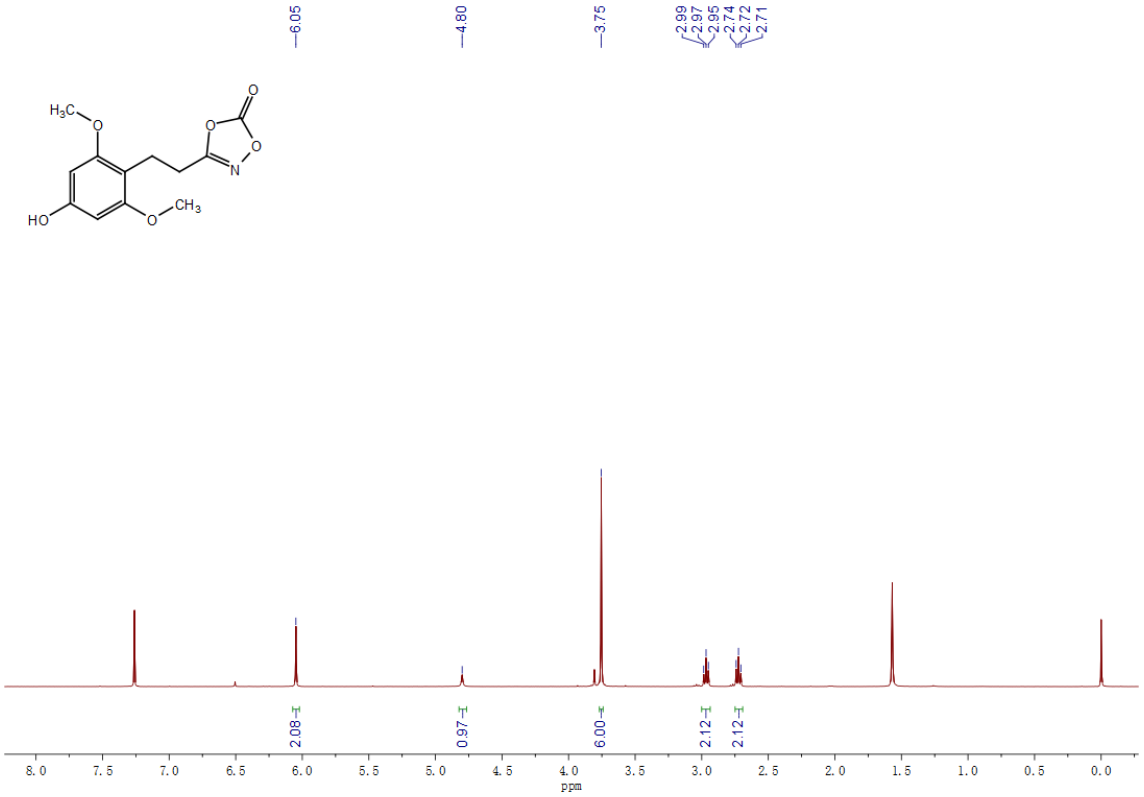
^{1}H NMR of 9c



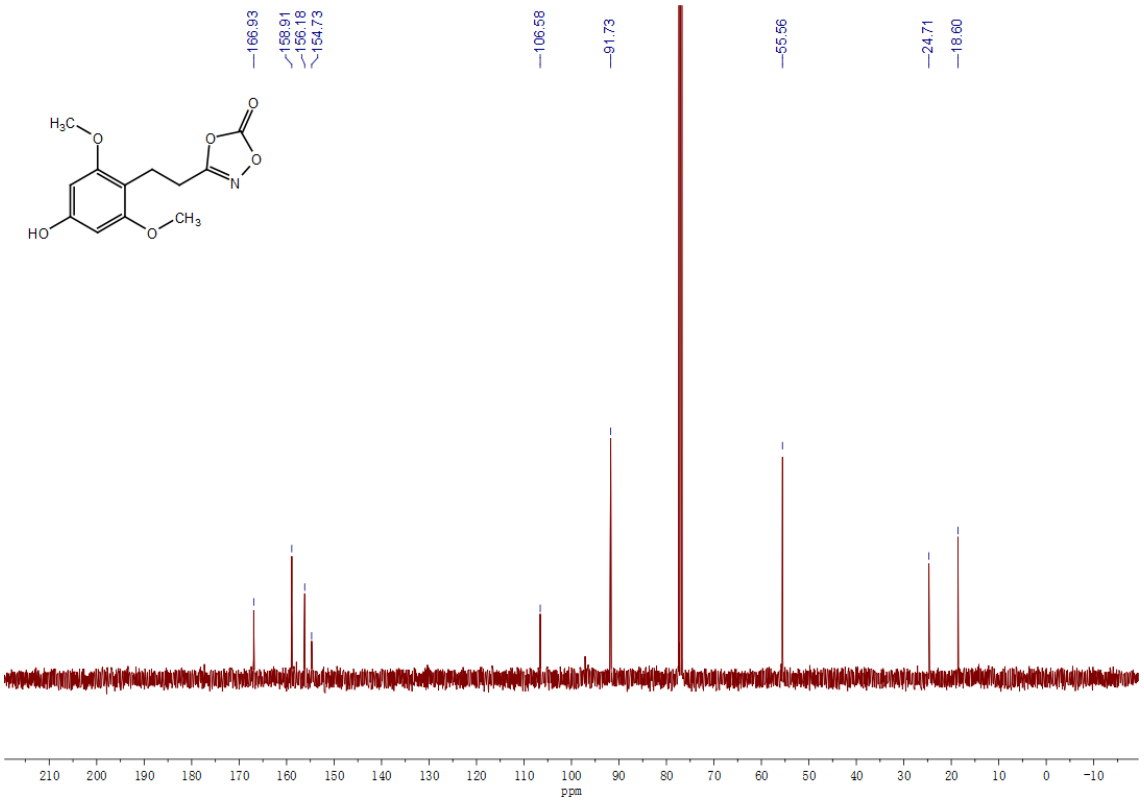
^{13}C NMR of 9c



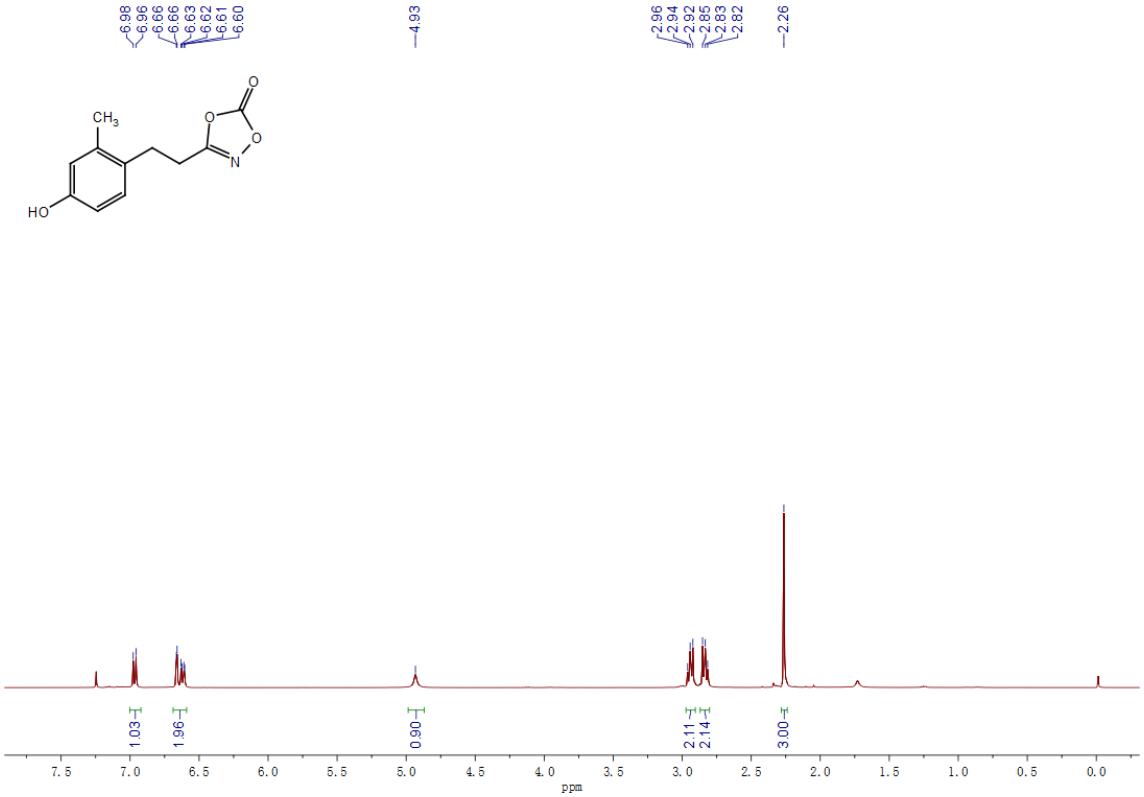
^{1}H NMR of 9d



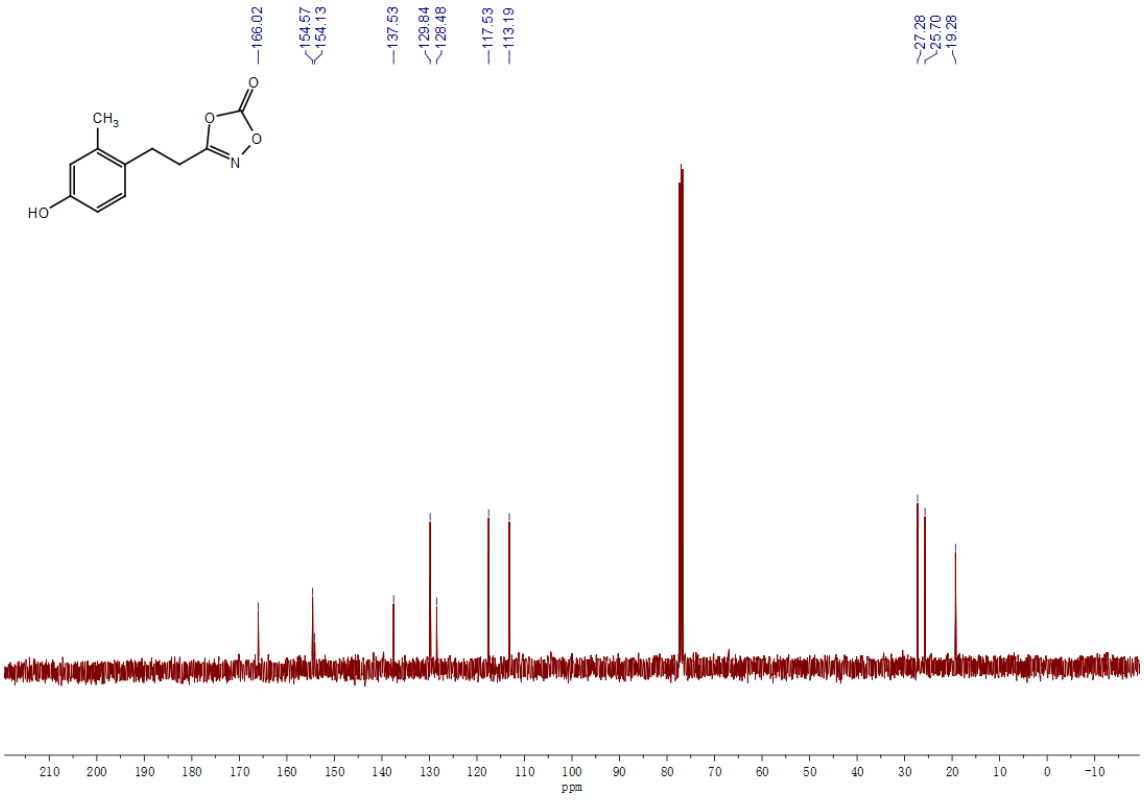
^{13}C NMR of 9d



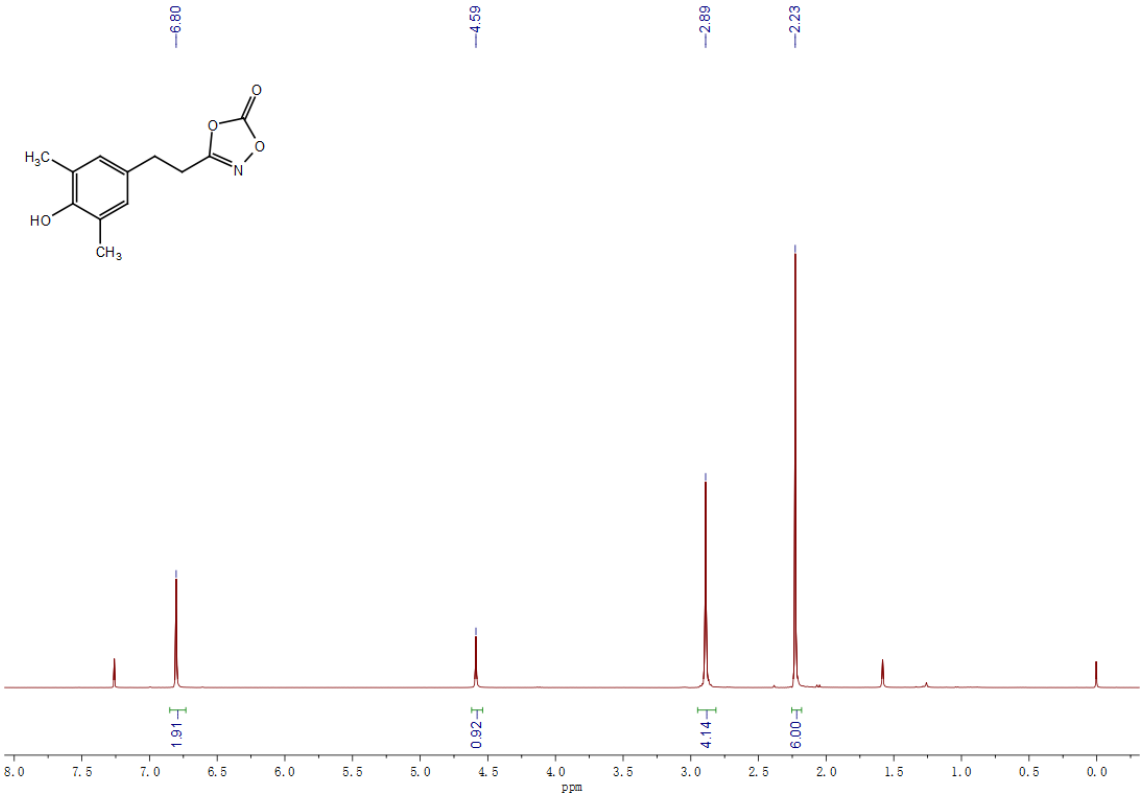
^{1}H NMR of 9e



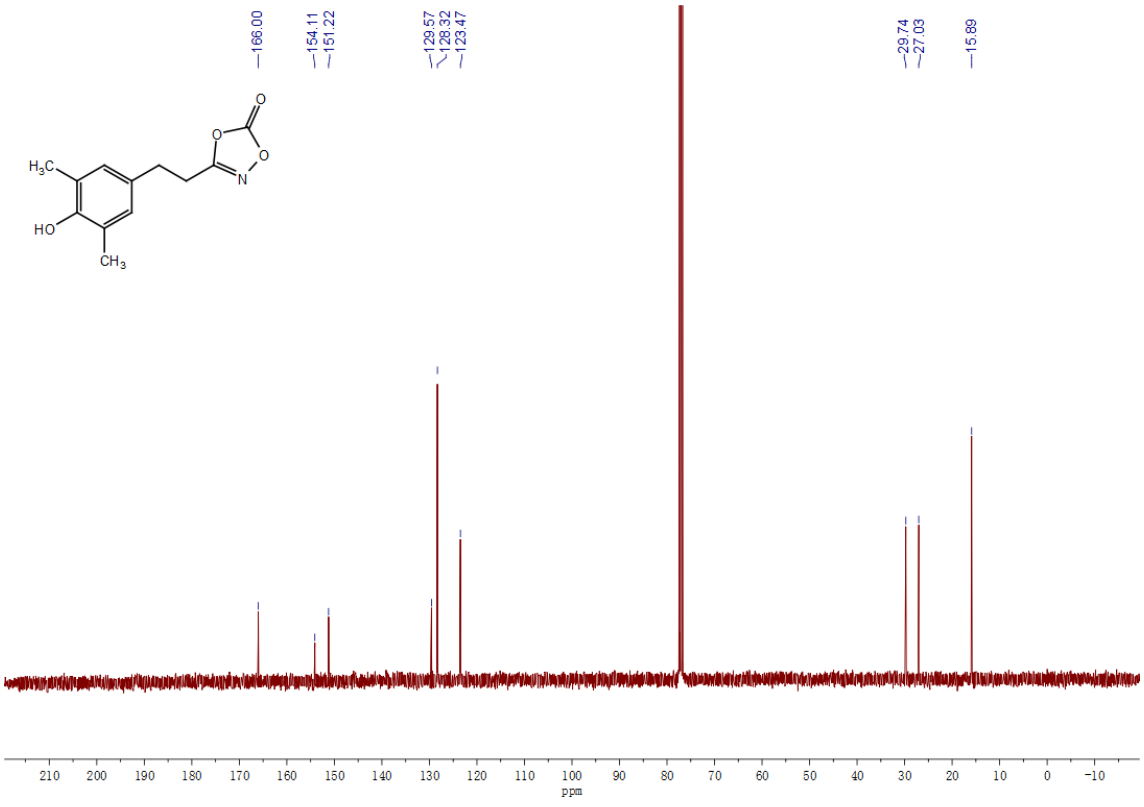
^{13}C NMR of 9e



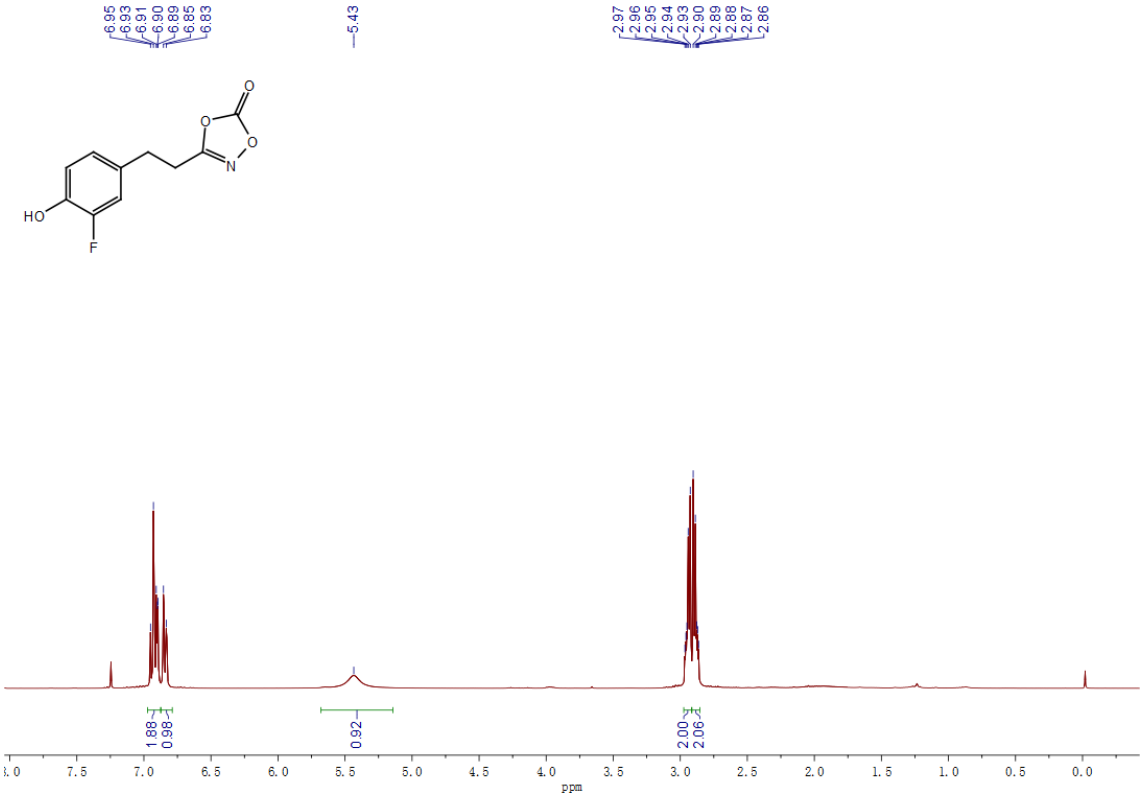
^{1}H NMR of 9f



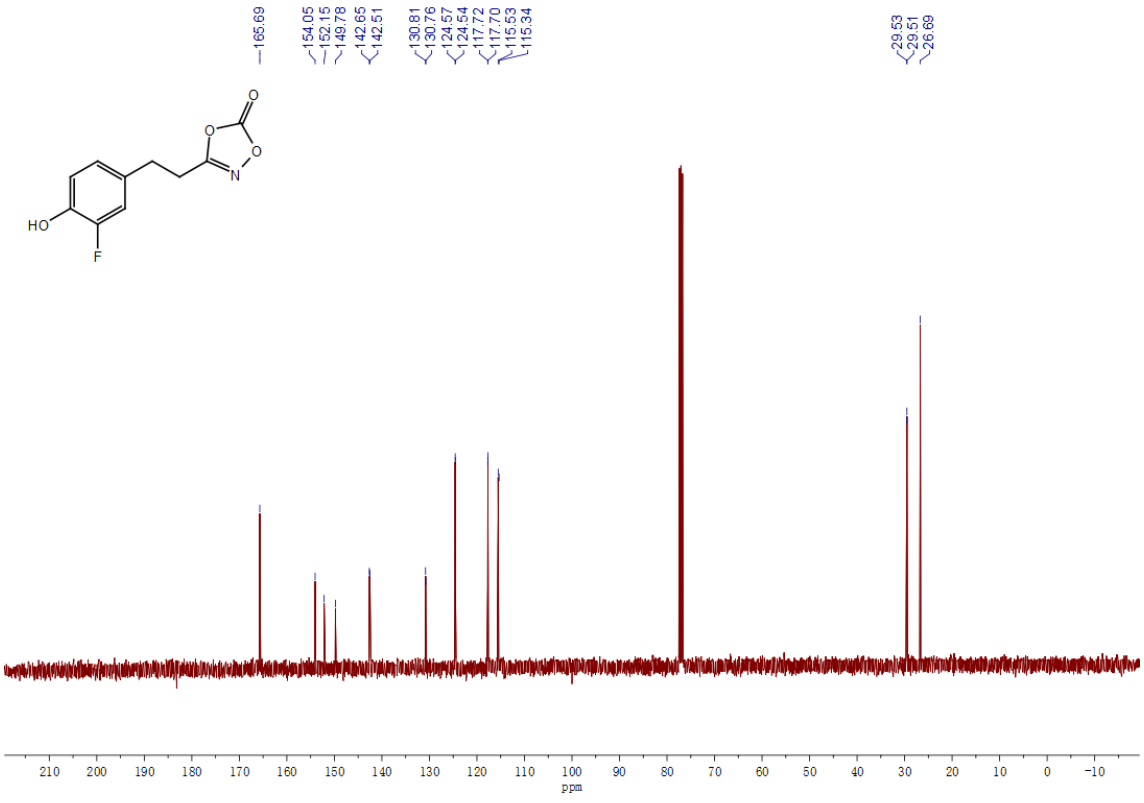
^{13}C NMR of 9f



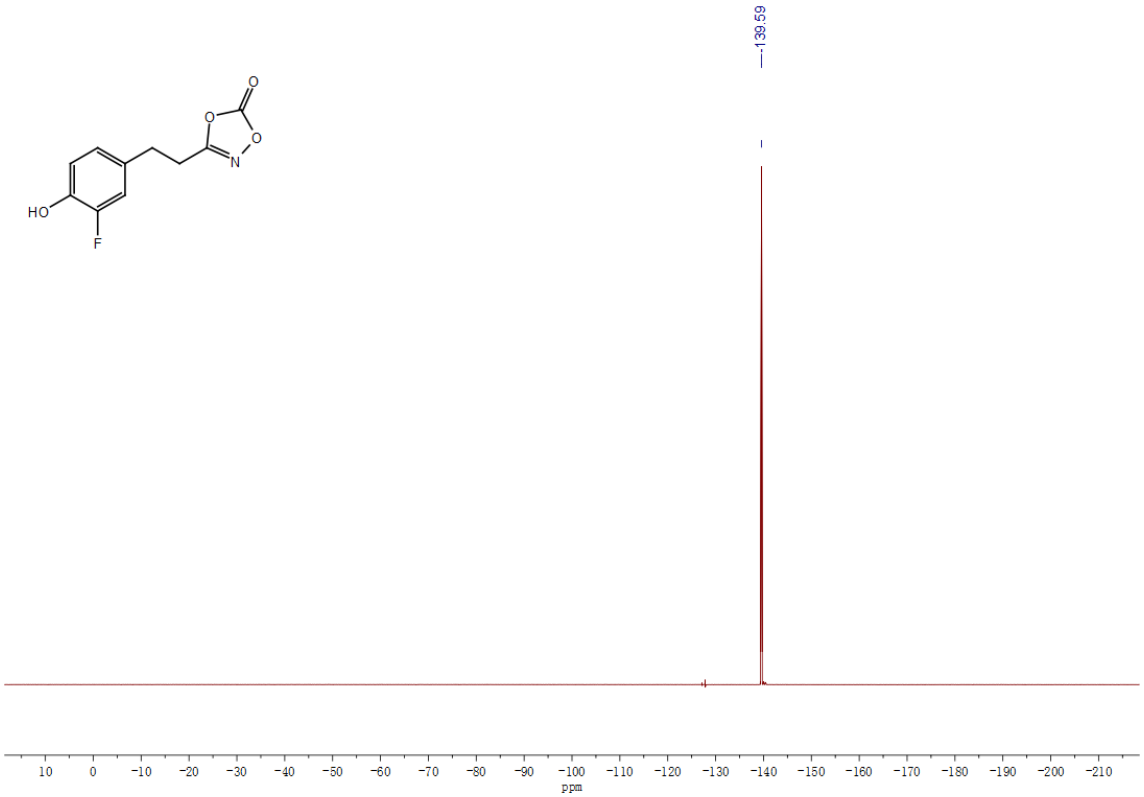
^{1}H NMR of 9g



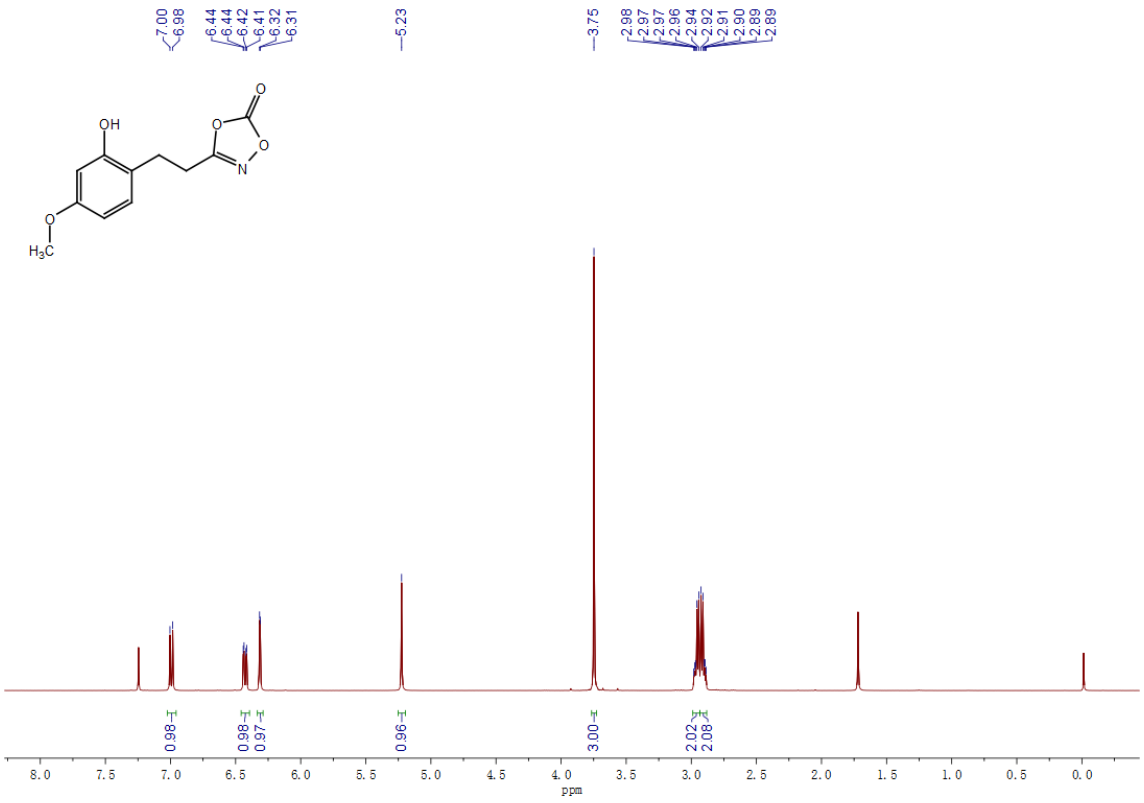
^{13}C NMR of 9g



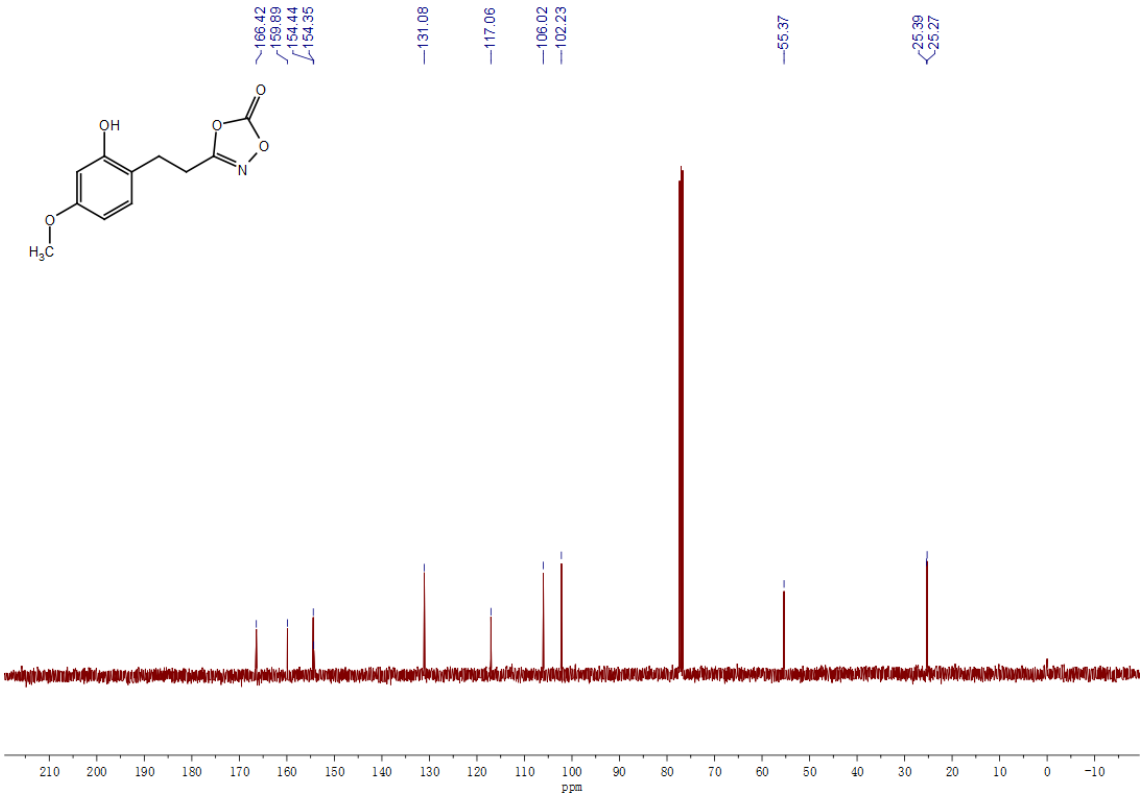
^{19}F NMR of 9g


-139.59
HO
F
O
O
O
N
10
0
-10
-20
-30
-40
-50
-60
-70
-80
-90
-100
-110
-120
-130
-140
-150
-160
-170
-180
-190
-200
-210
ppm

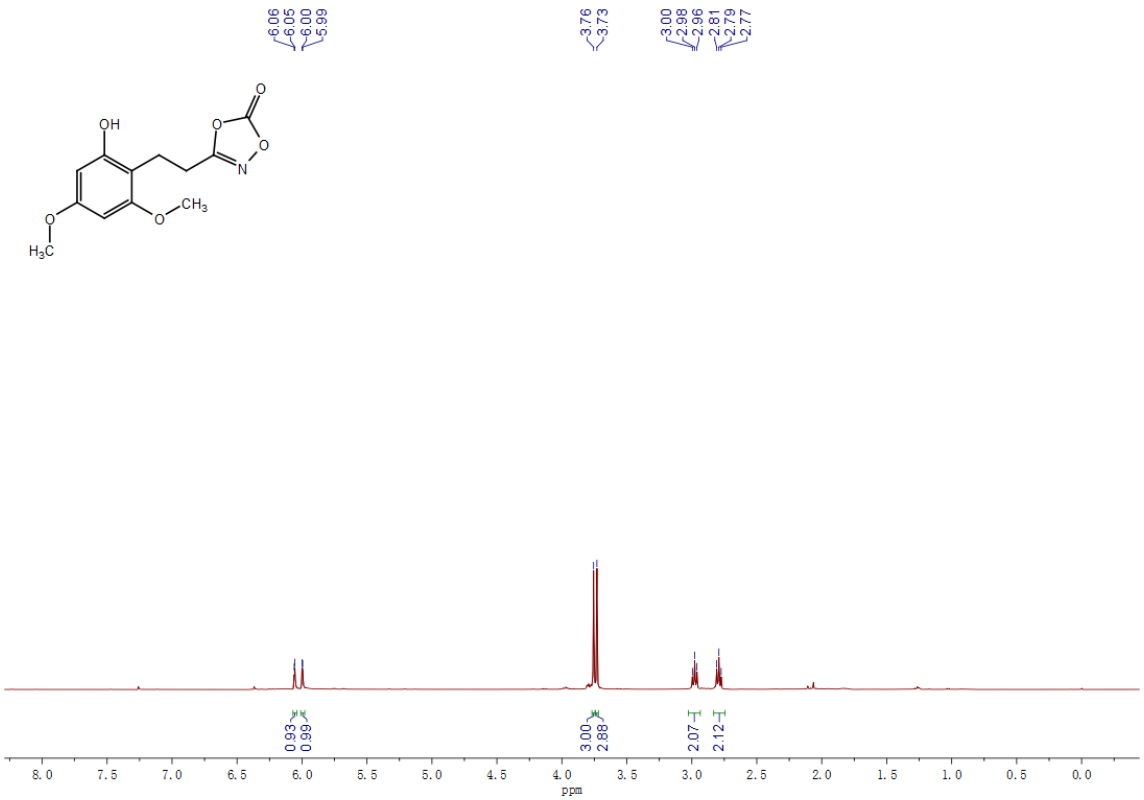
^{1}H NMR of 9h



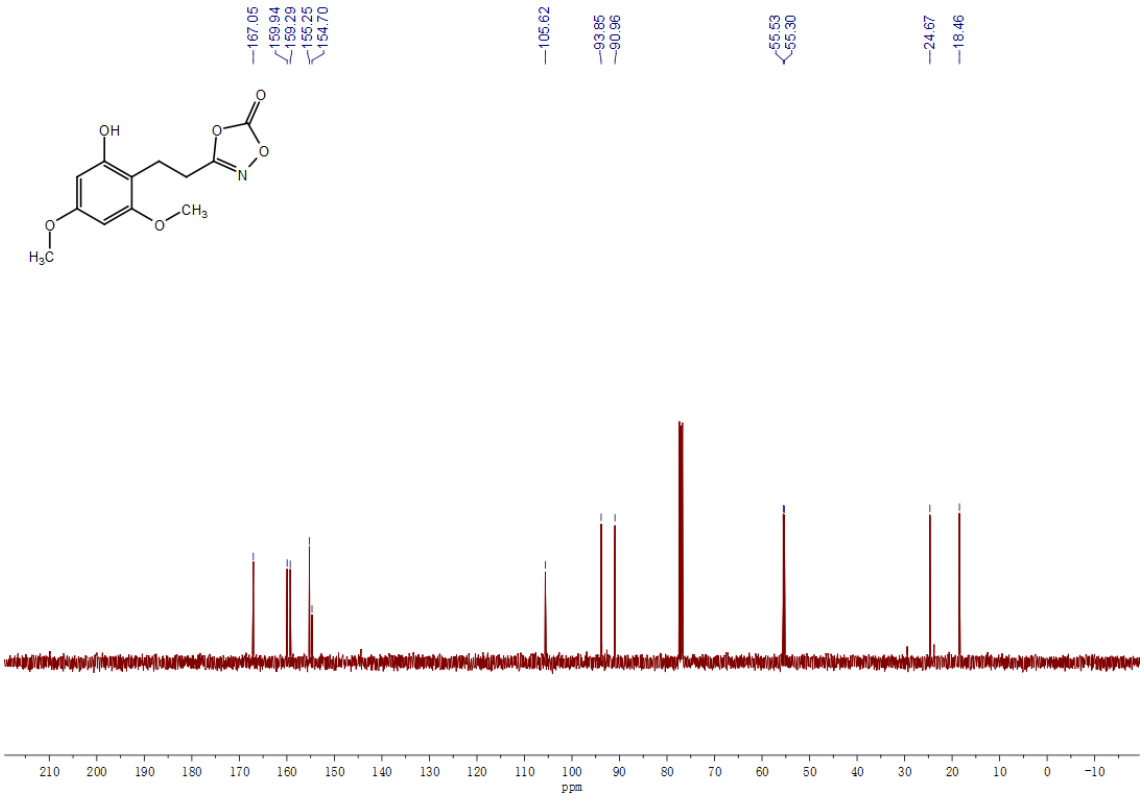
^{13}C NMR of 9h



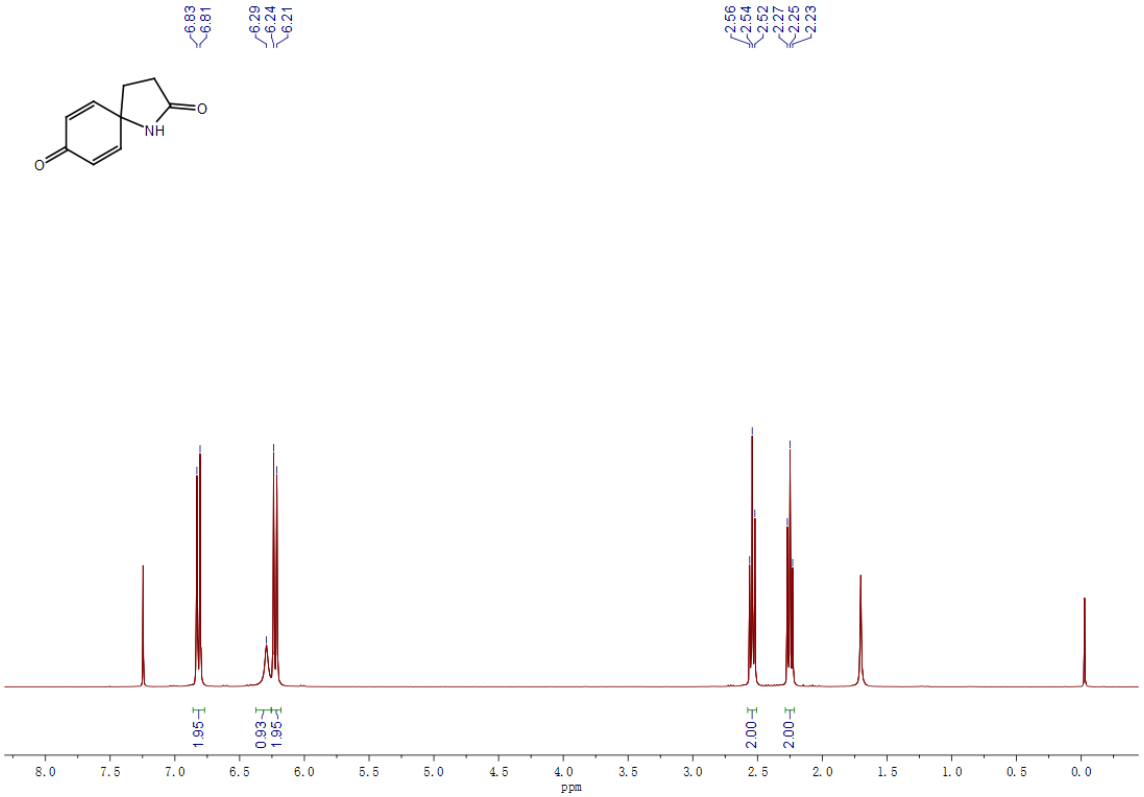
^{1}H NMR of 9i



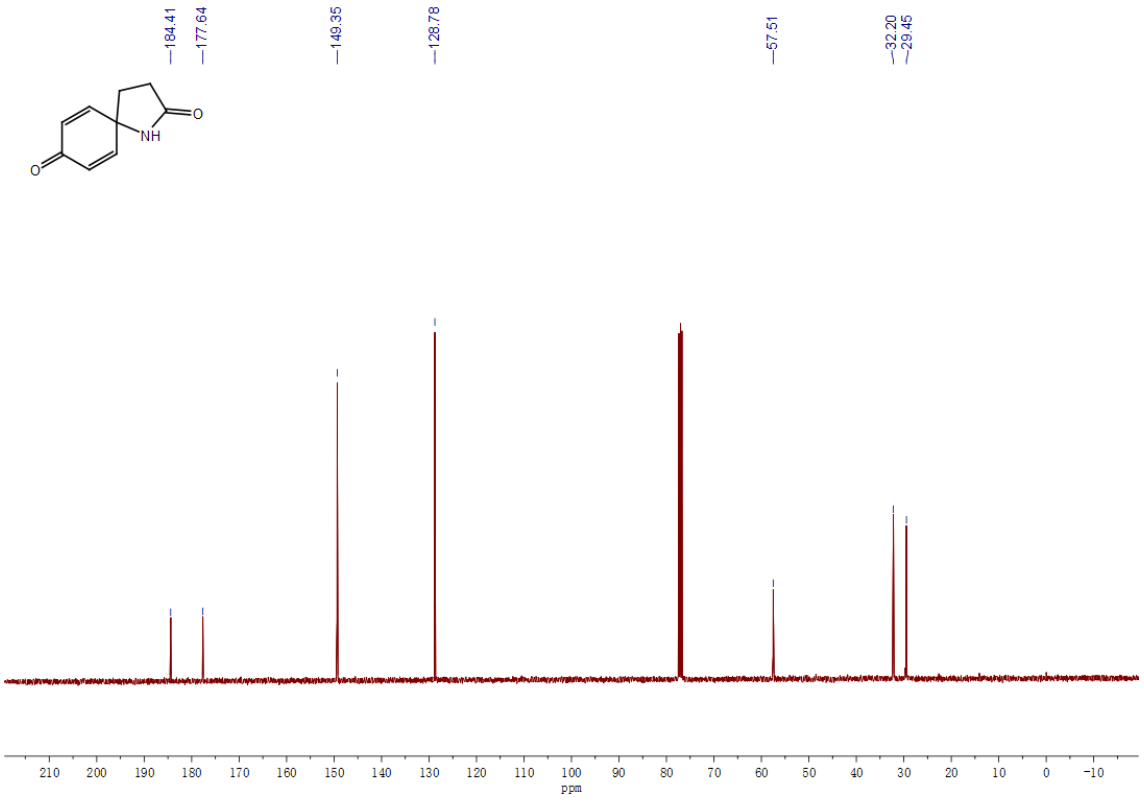
^{13}C NMR of 9i



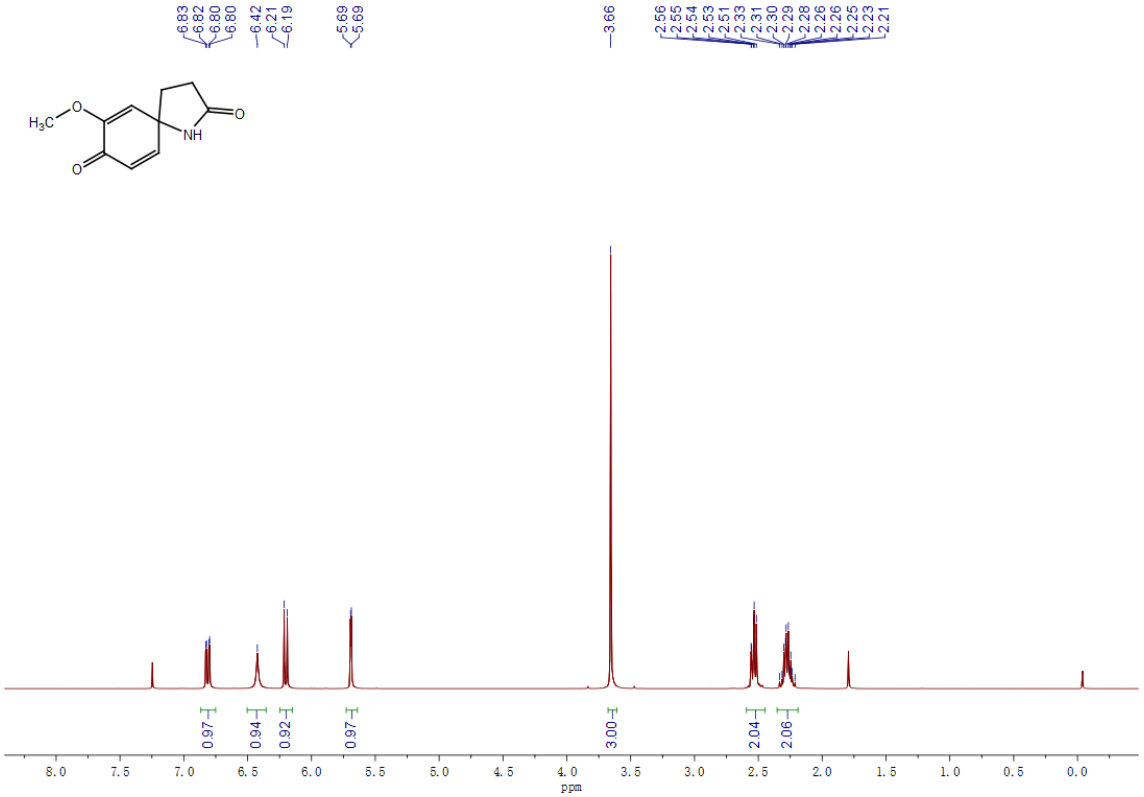
^{1}H NMR of 10a



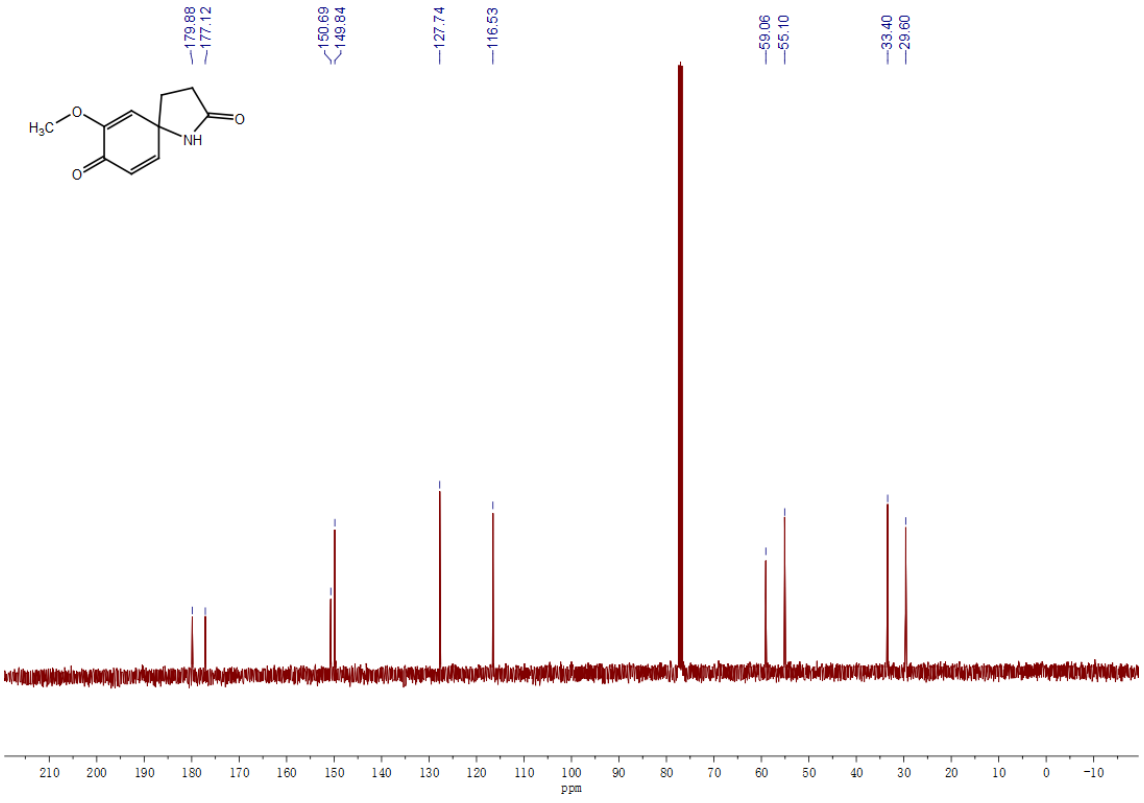
^{13}C NMR of 10a



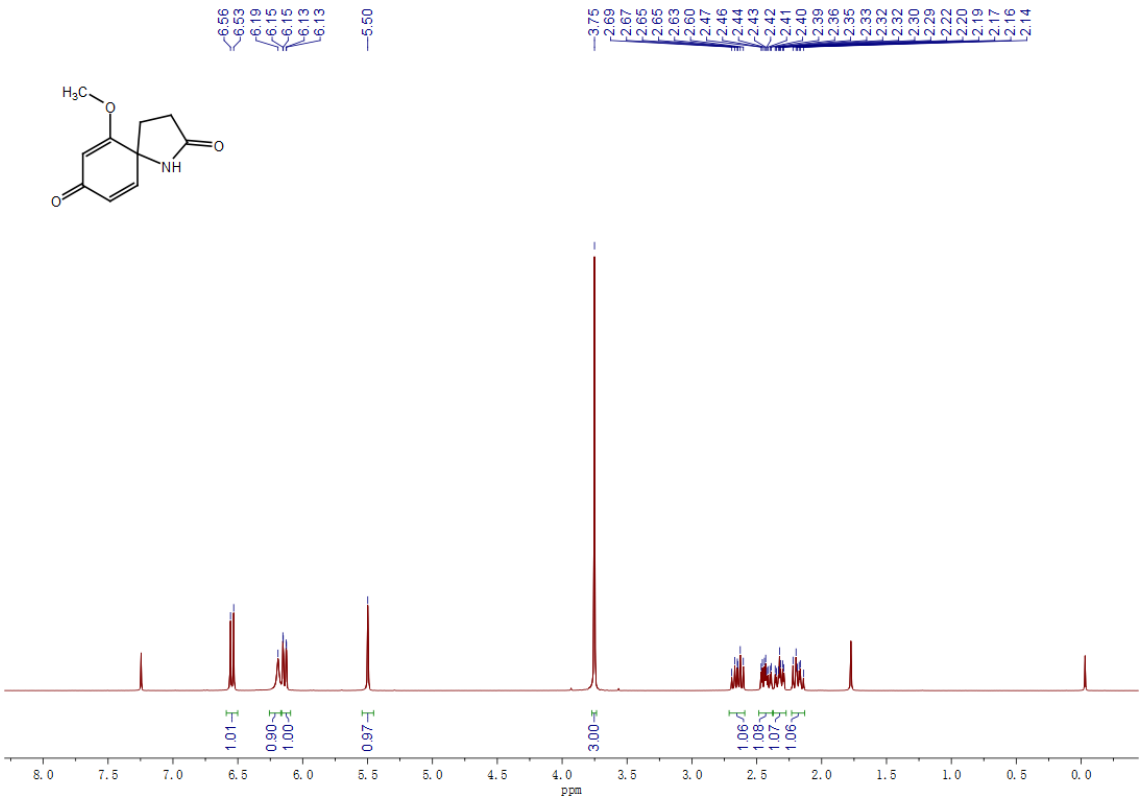
^{1}H NMR of 10b



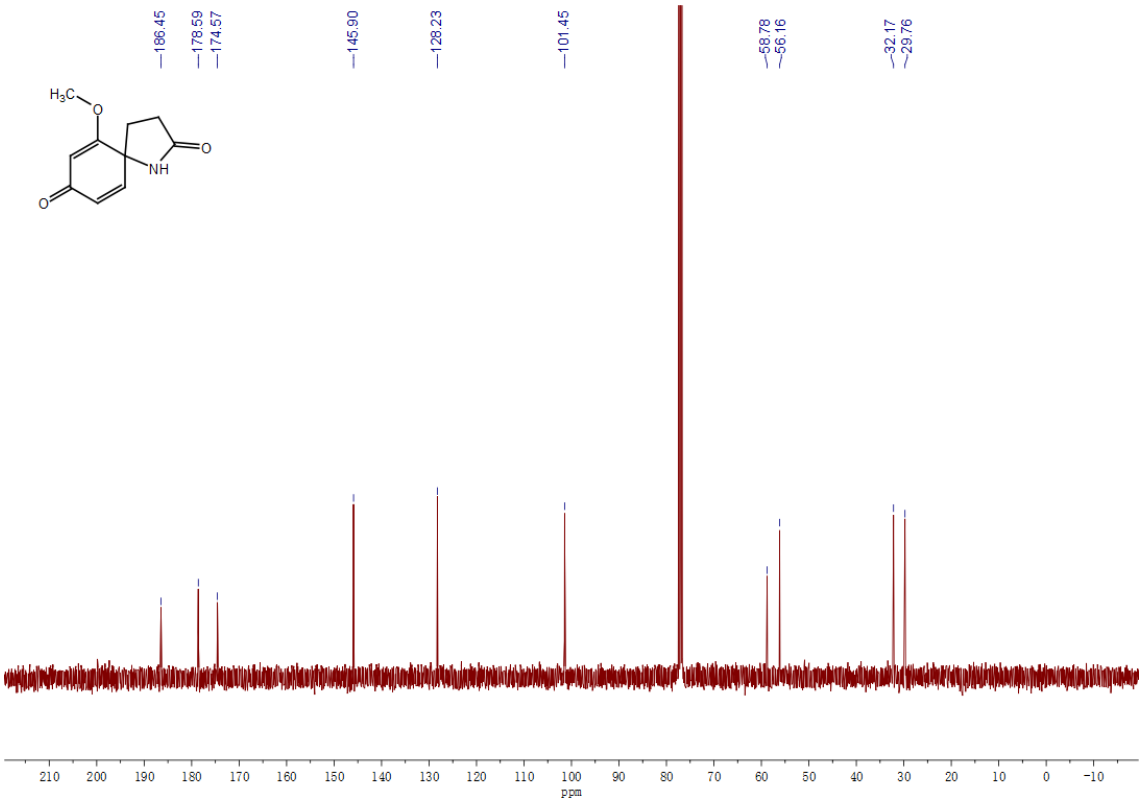
^{13}C NMR of 10b



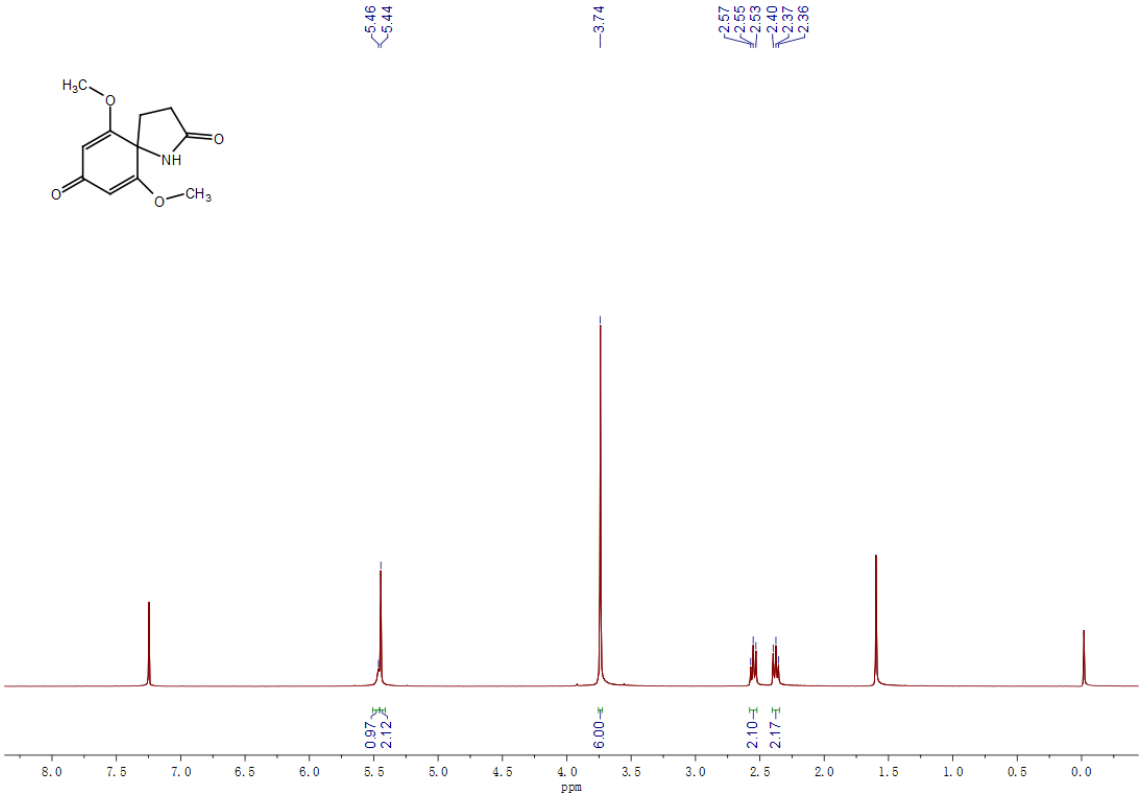
^{1}H NMR of 10c



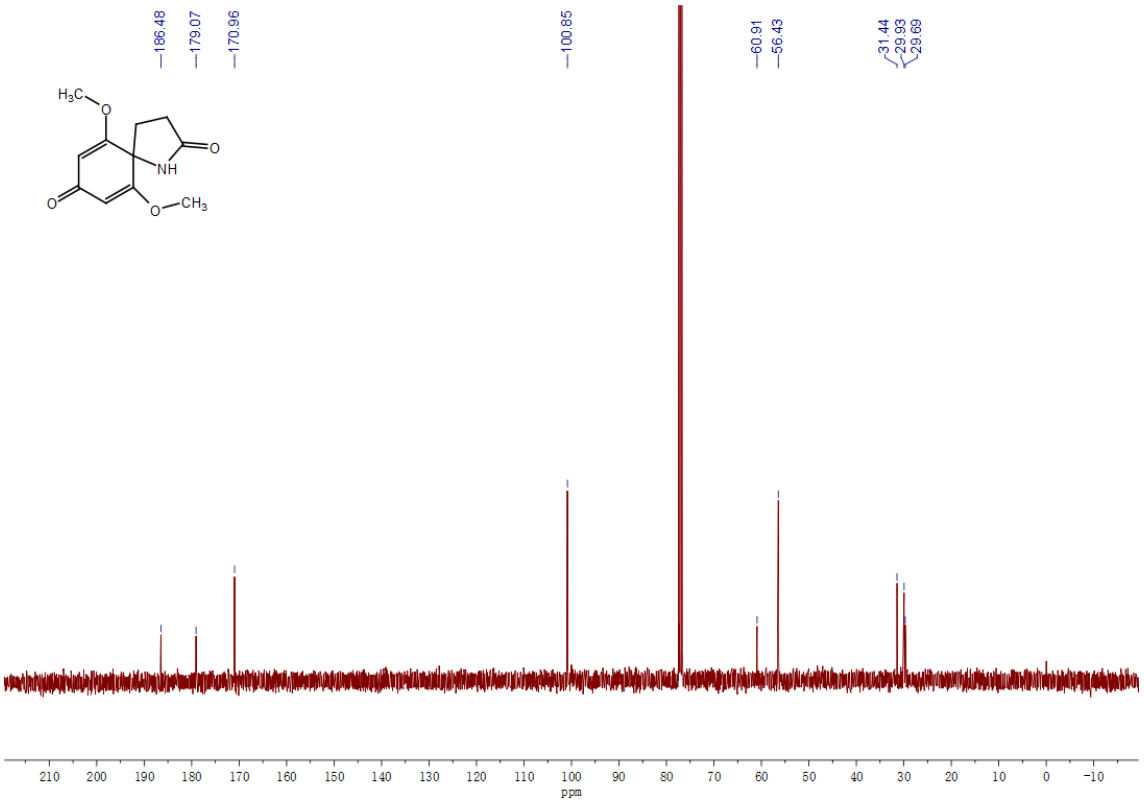
^{13}C NMR of 10c



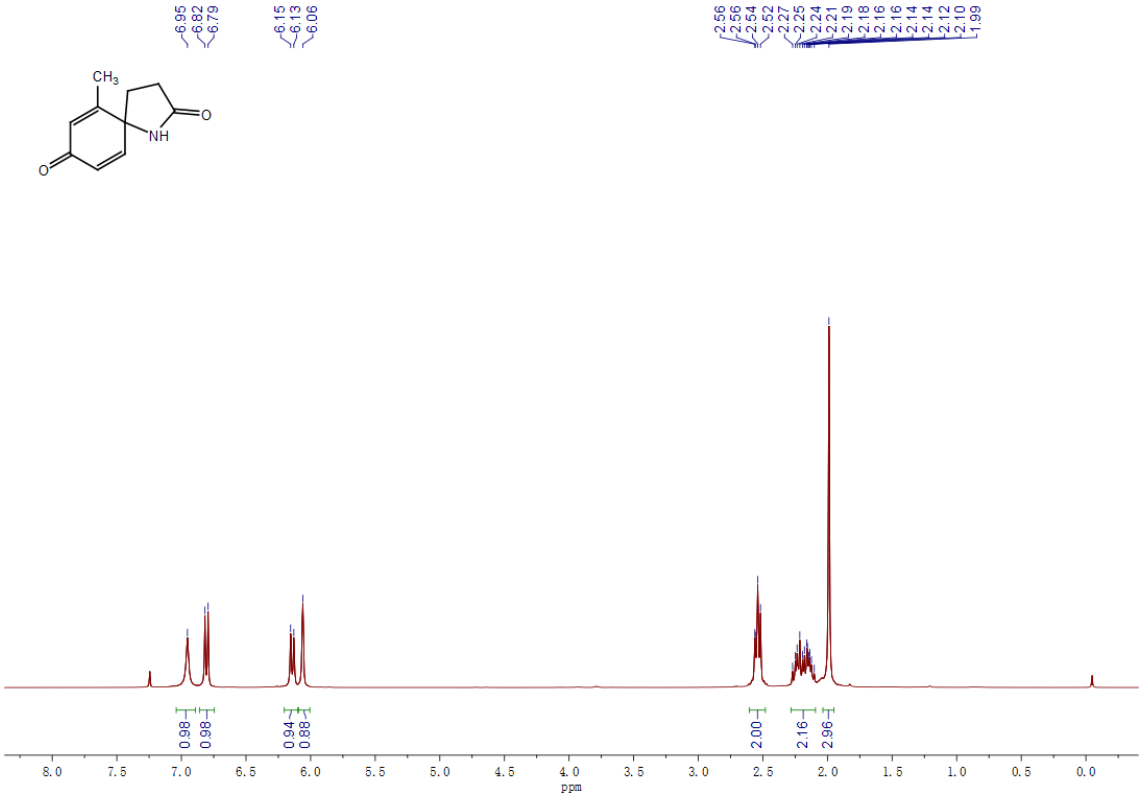
^{1}H NMR of 10d



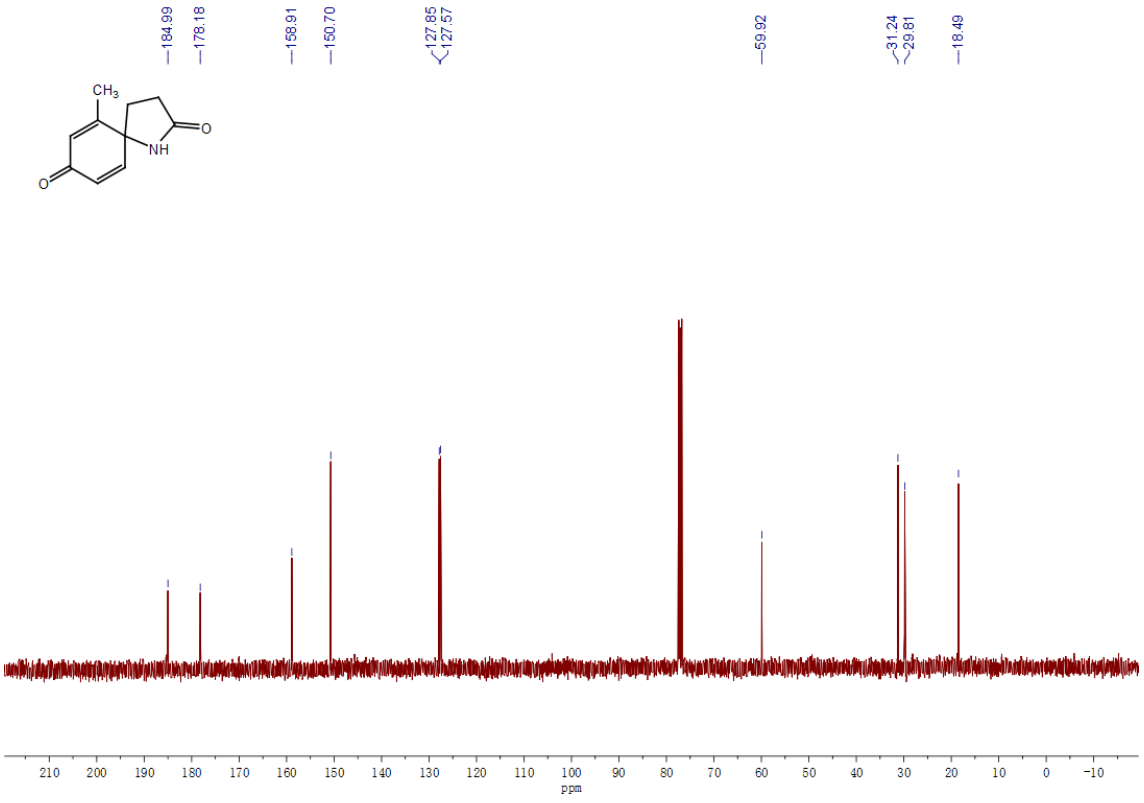
^{13}C NMR of 10d



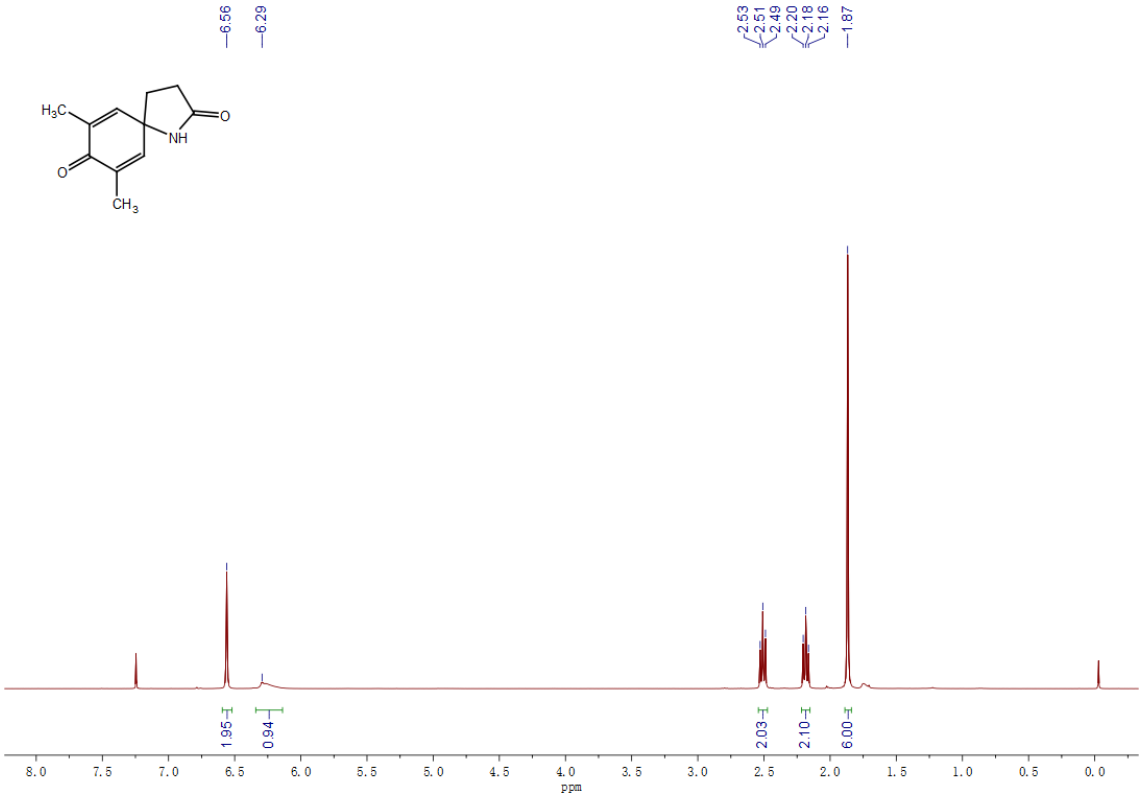
^{1}H NMR of 10e



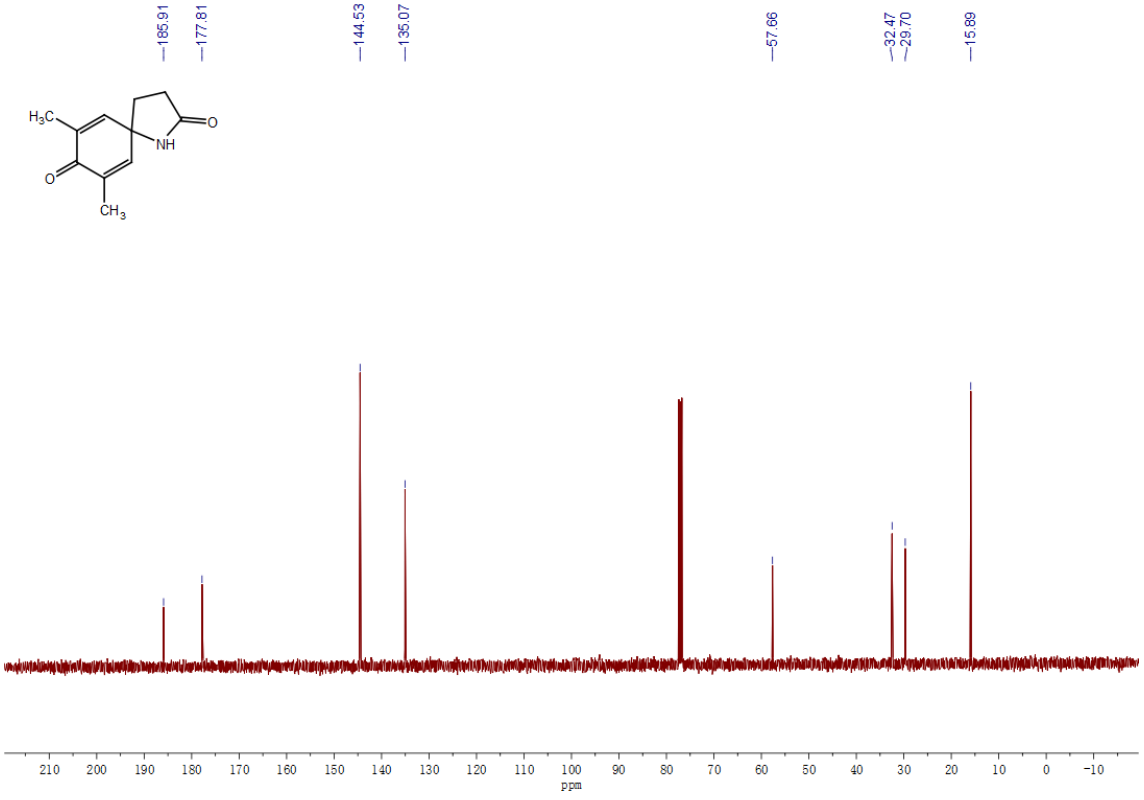
^{13}C NMR of 10e



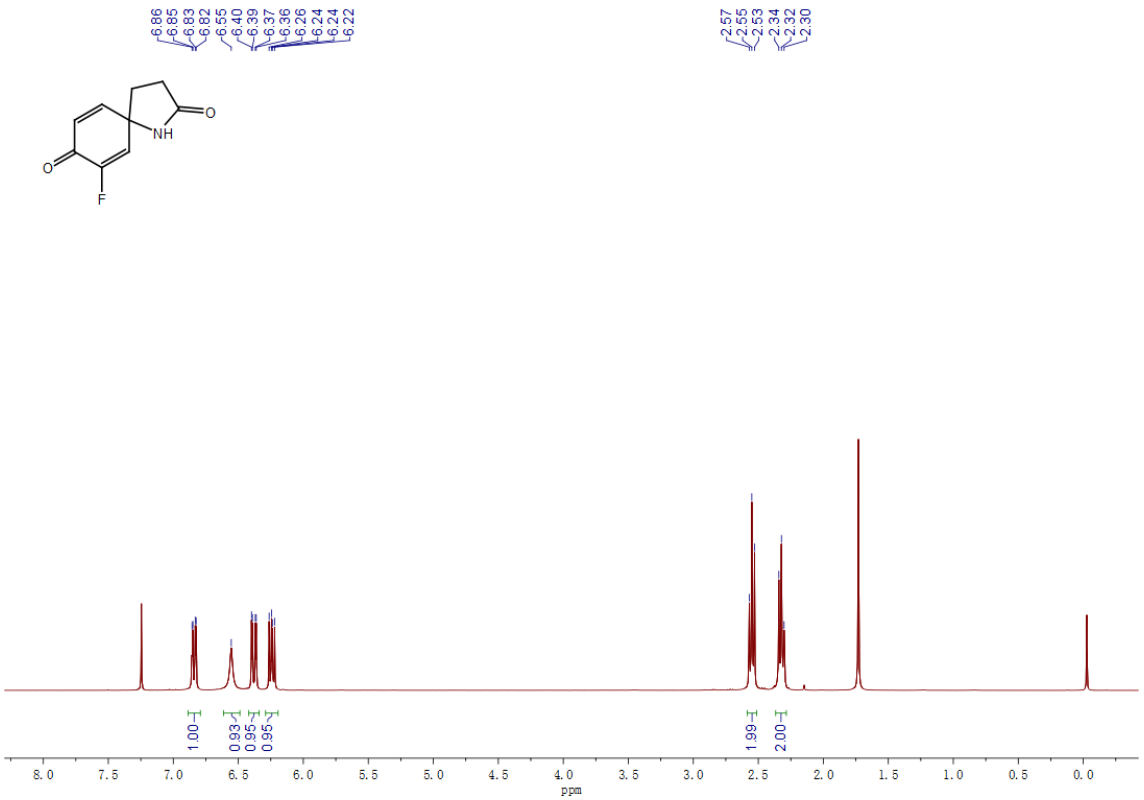
^{1}H NMR of 10f



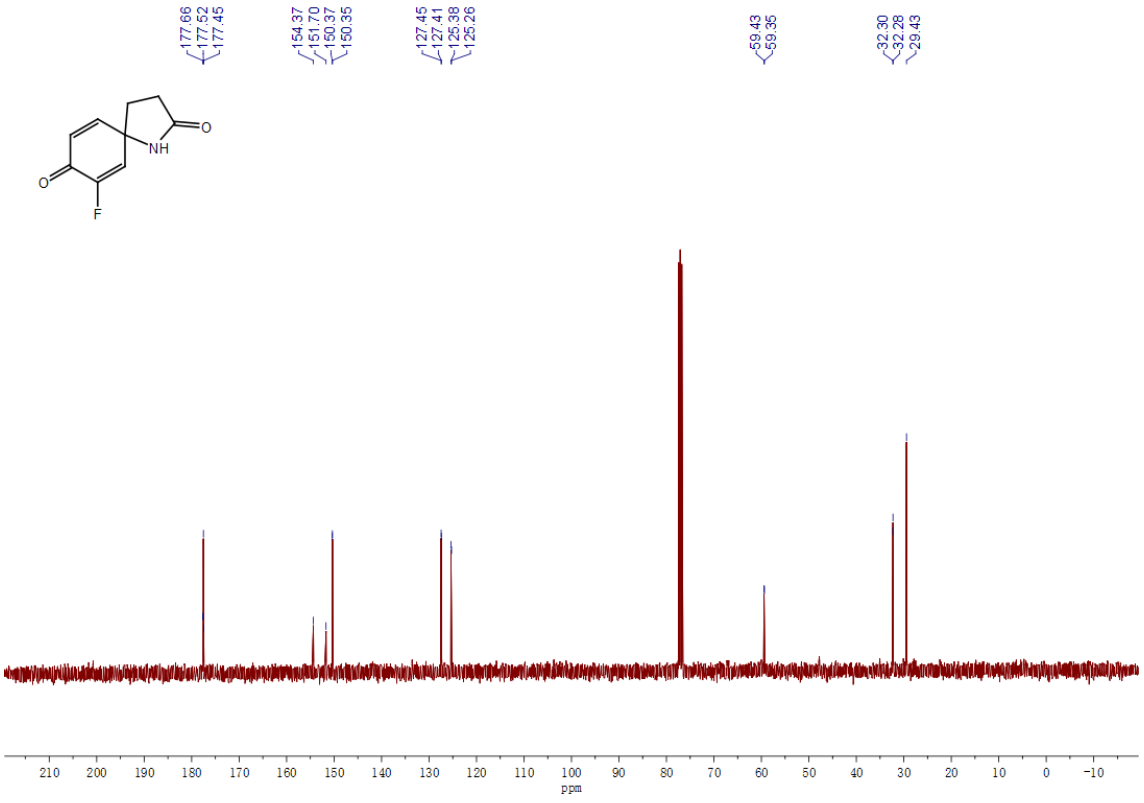
^{13}C NMR of 10f



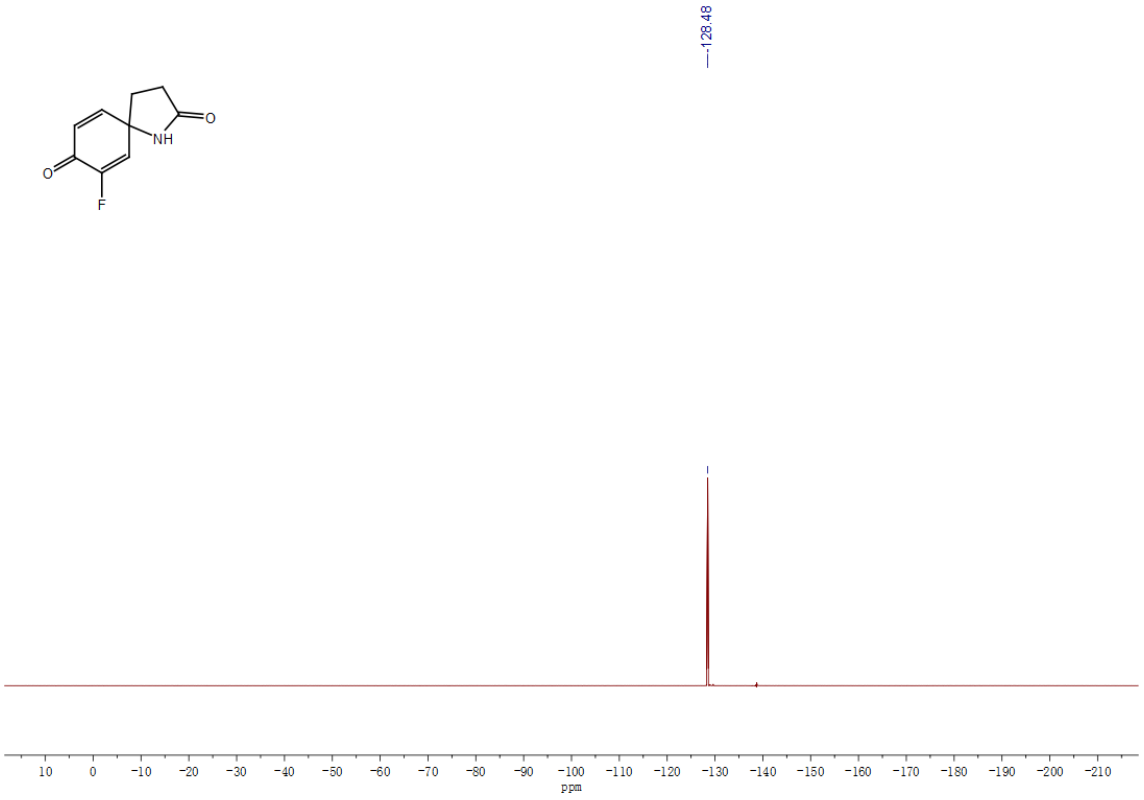
^{1}H NMR of 10g



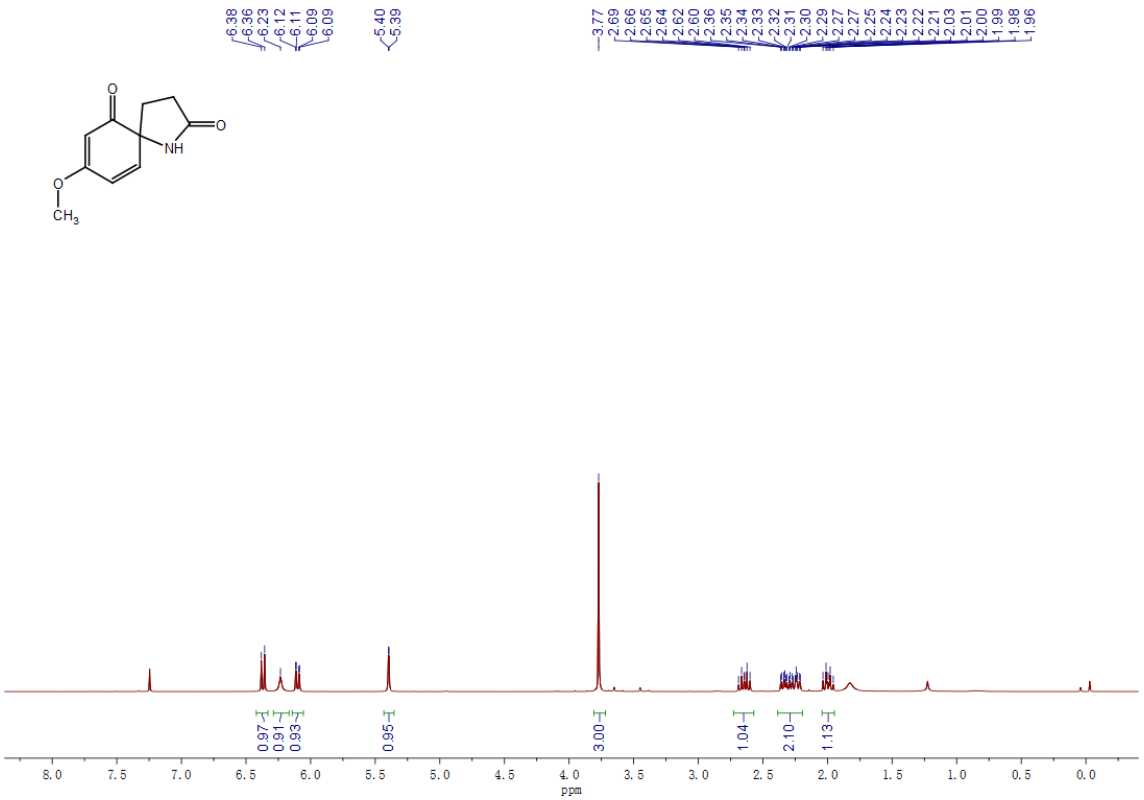
^{13}C NMR of 10g



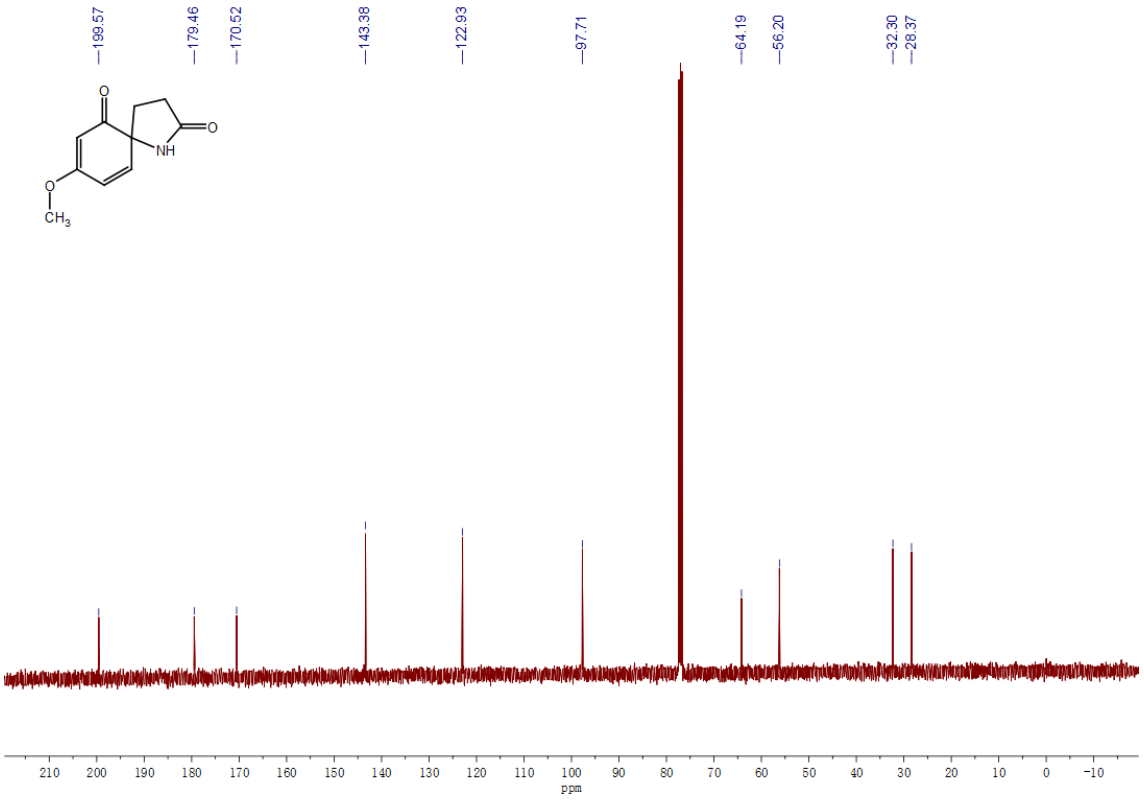
^{19}F NMR of 10g



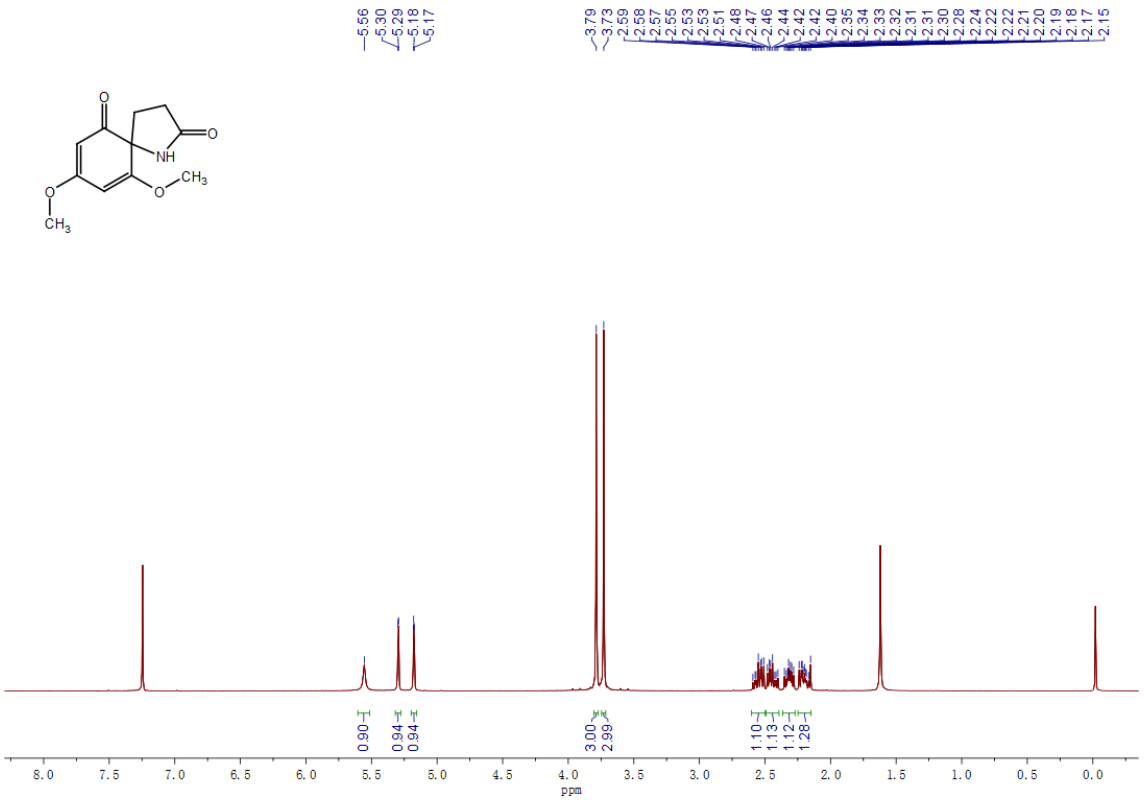
^{1}H NMR of 11a



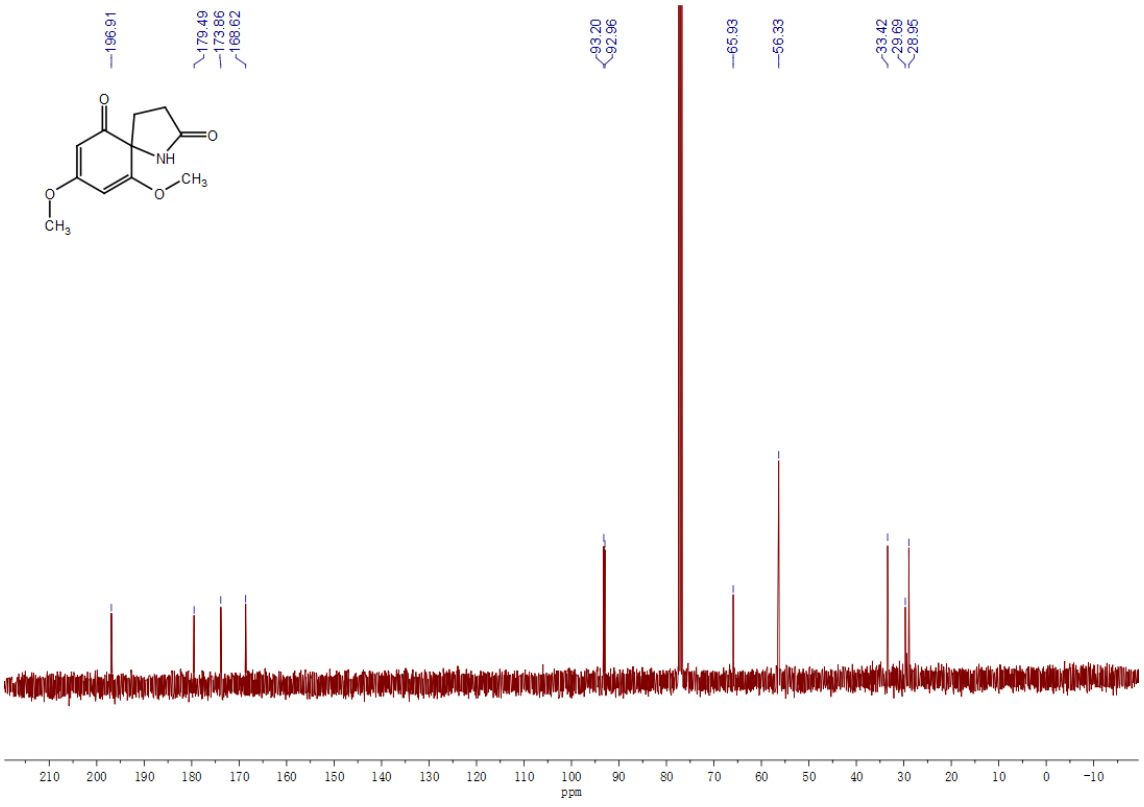
^{13}C NMR of 11a



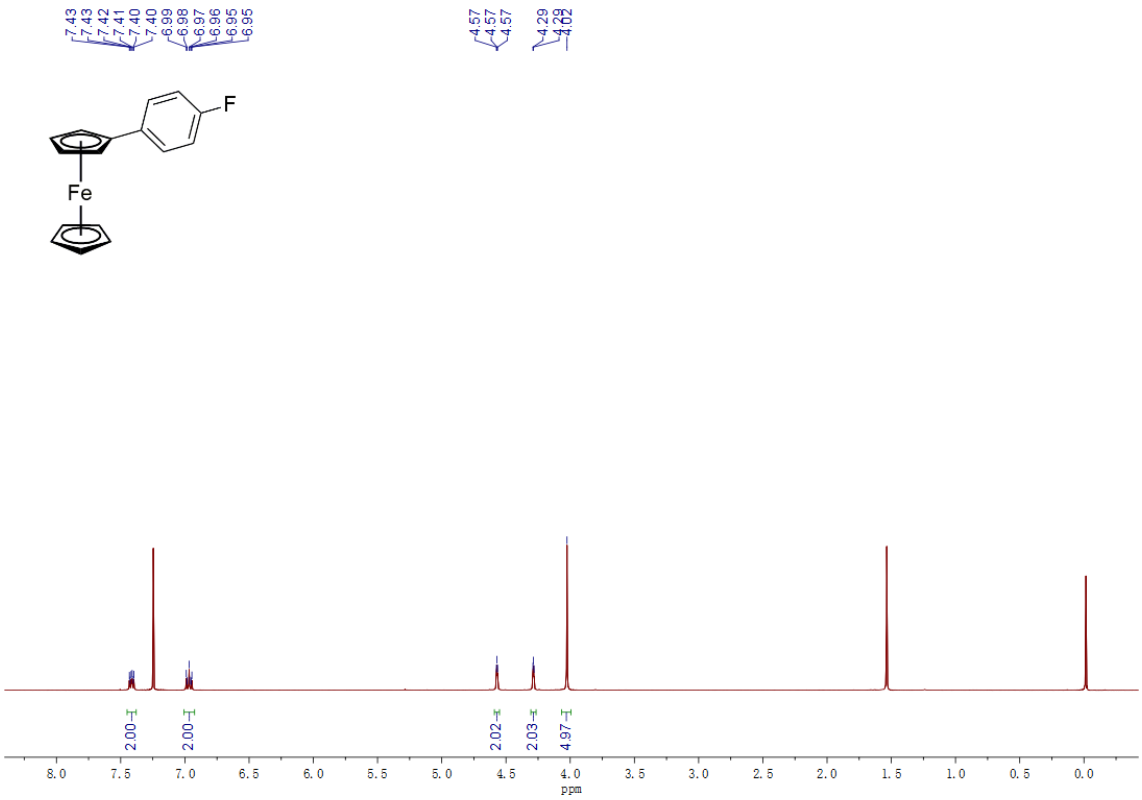
^{1}H NMR of 11b



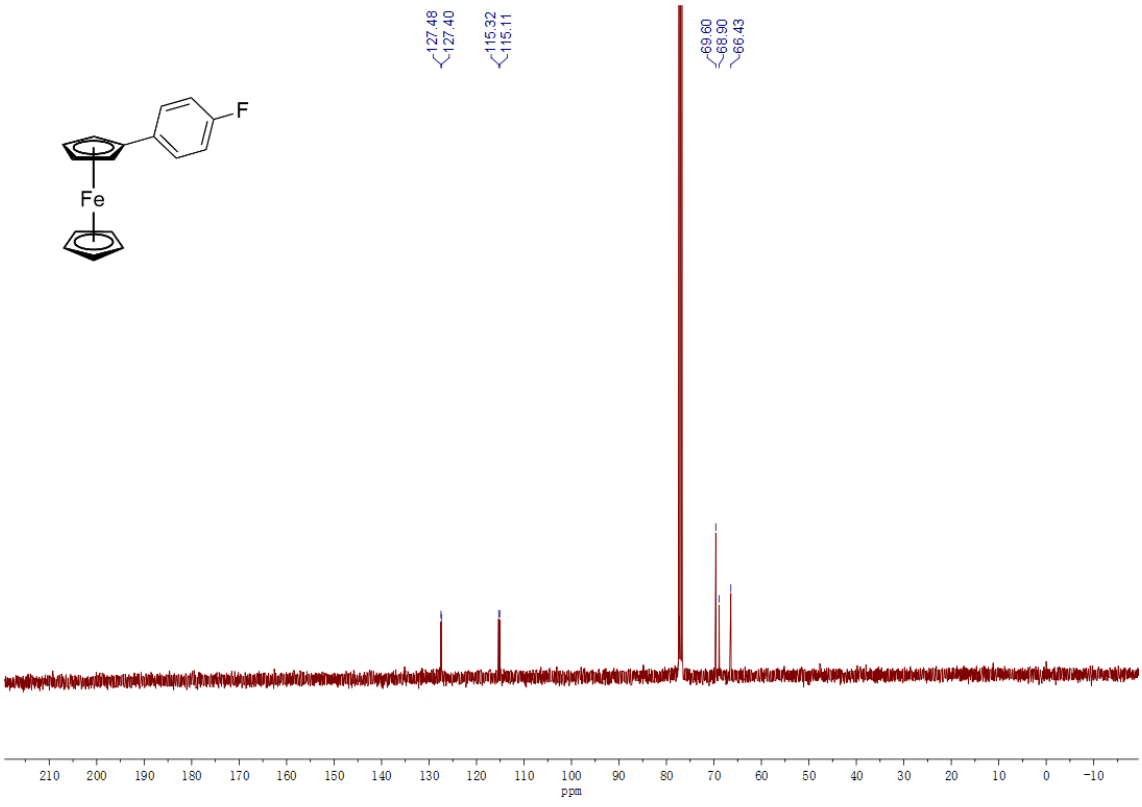
^{13}C NMR of 11b



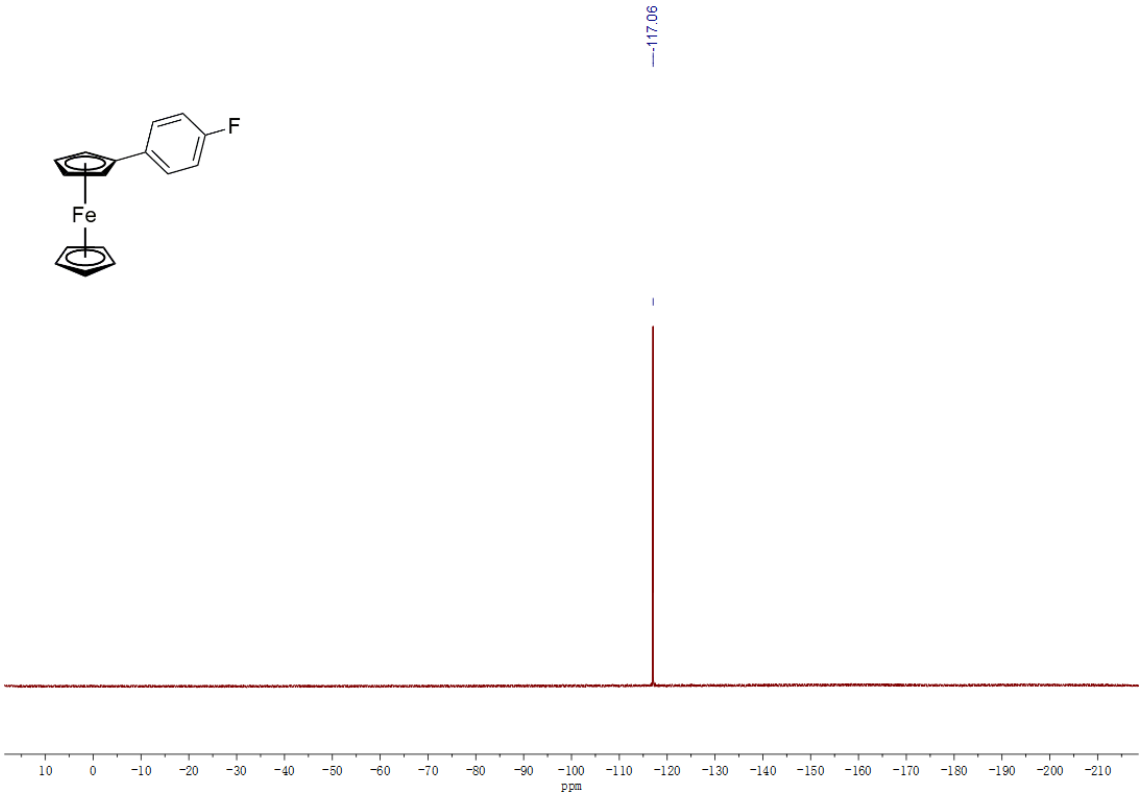
^{1}H NMR of (4-Fluorophenyl)ferrocene



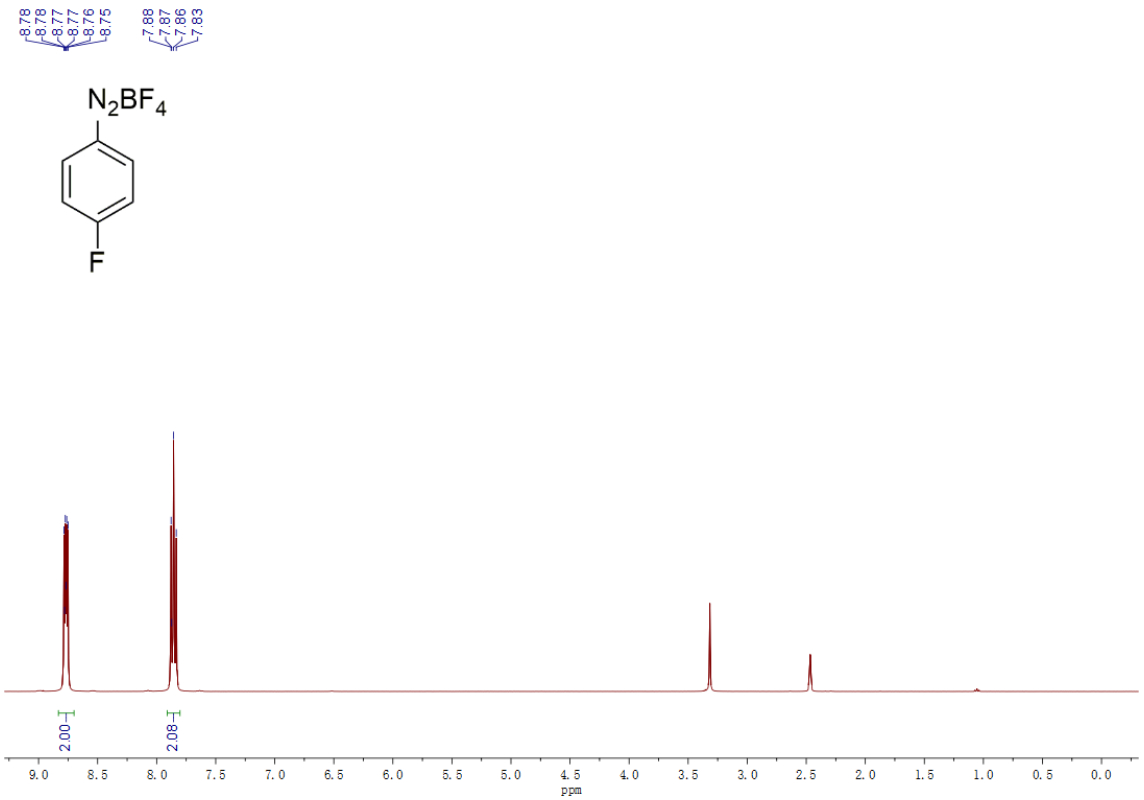
^{13}C NMR of (4-Fluorophenyl)ferrocene



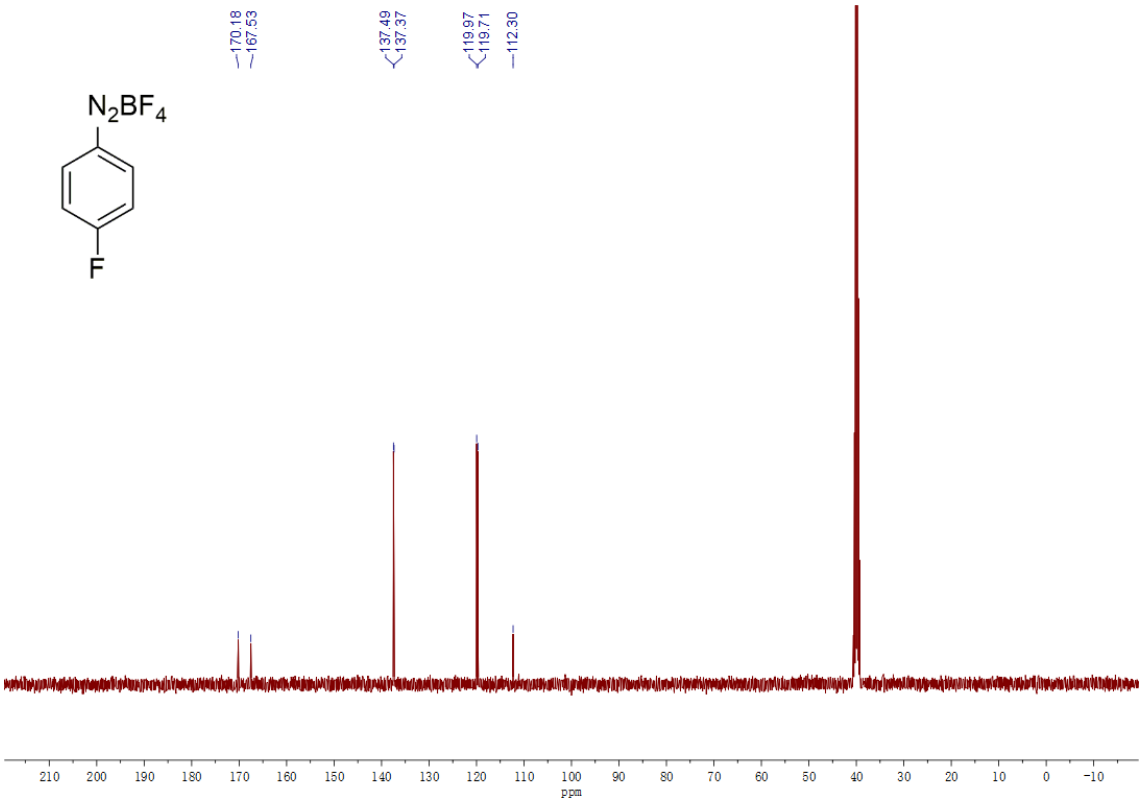
^{19}F NMR of (4-Fluorophenyl)ferrocene



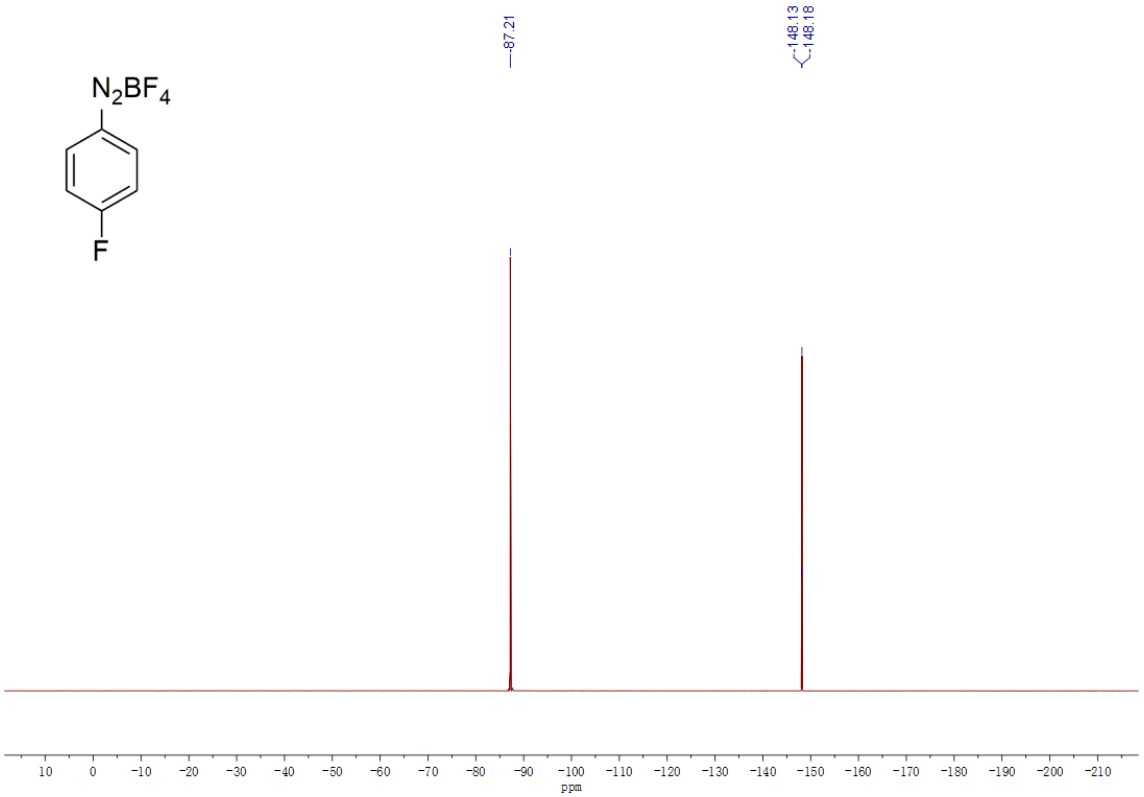
^{1}H NMR of F1



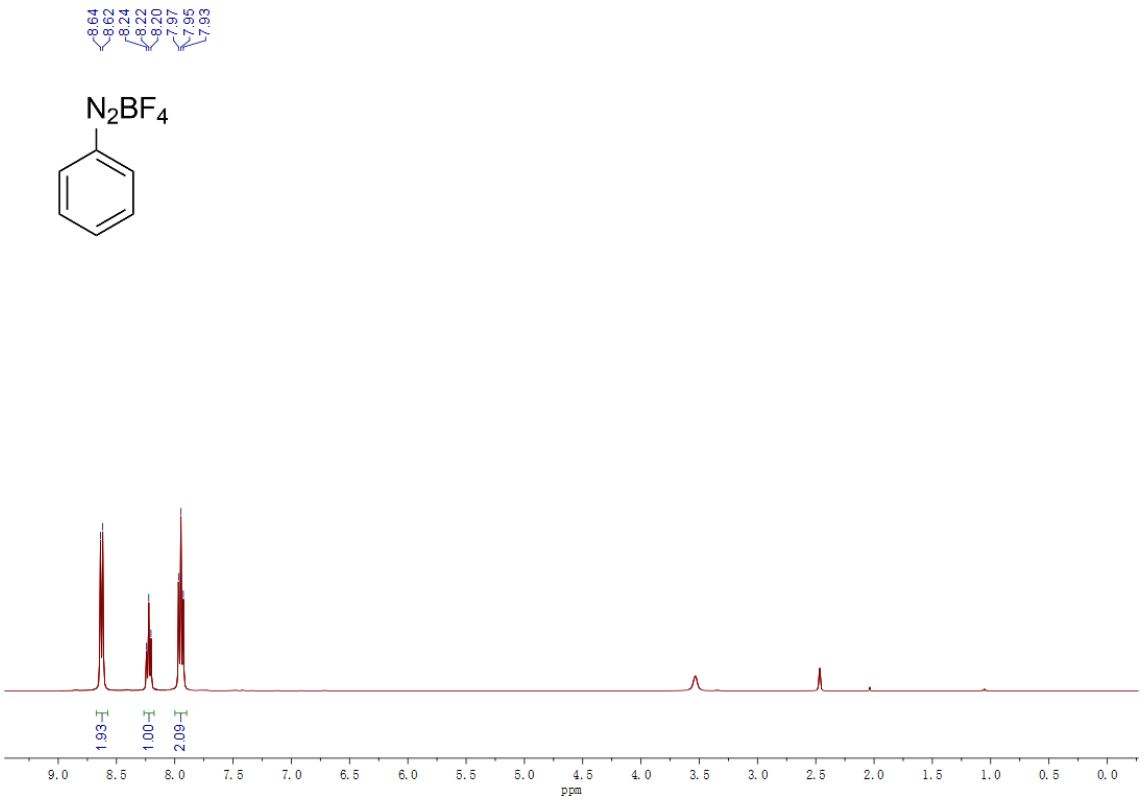
^{13}C NMR of F1



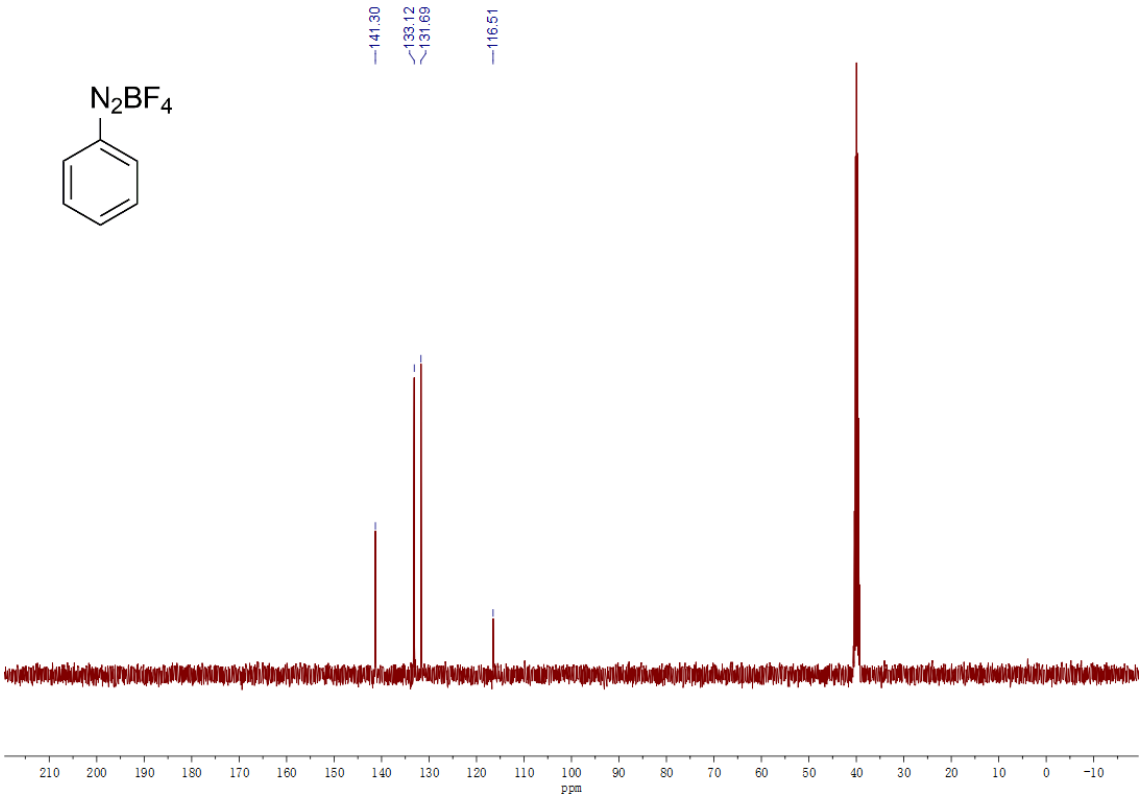
^{19}F NMR of F1


N2BF4
F
-87.21
-148.13
-148.18
10 0 -10 -20 -30 -40 -50 -60 -70 -80 -90 -100 -110 -120 -130 -140 -150 -160 -170 -180 -190 -200 -210
ppm

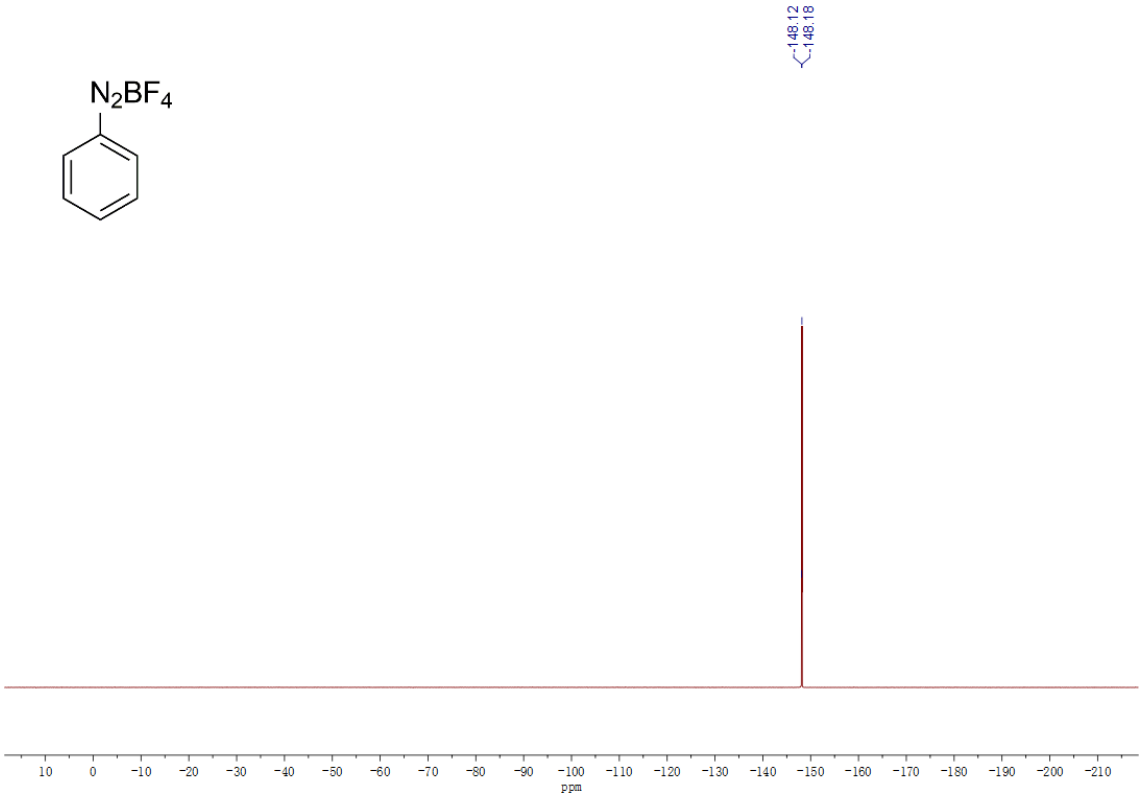
^{1}H NMR of F2



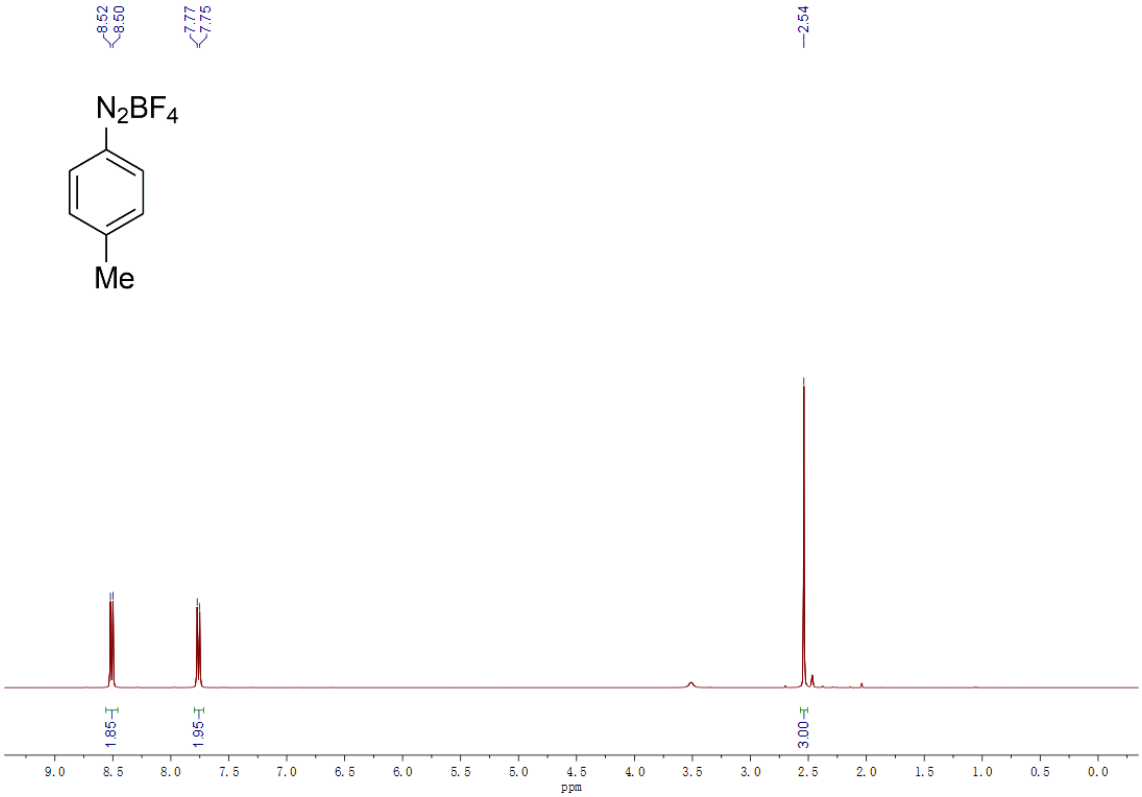
^{13}C NMR of F2



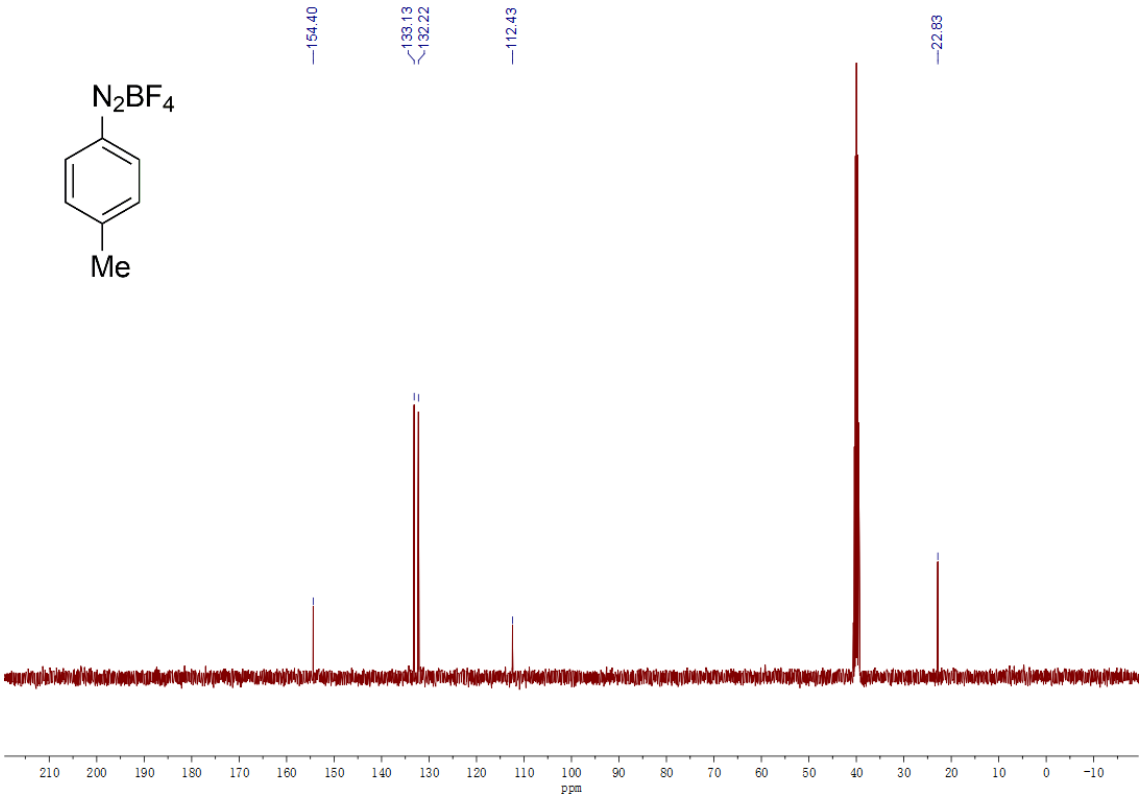
^{19}F NMR of F2


N2BF4
-148.12
-148.18
10 0 -10 -20 -30 -40 -50 -60 -70 -80 -90 -100 -110 -120 -130 -140 -150 -160 -170 -180 -190 -200 -210
ppm

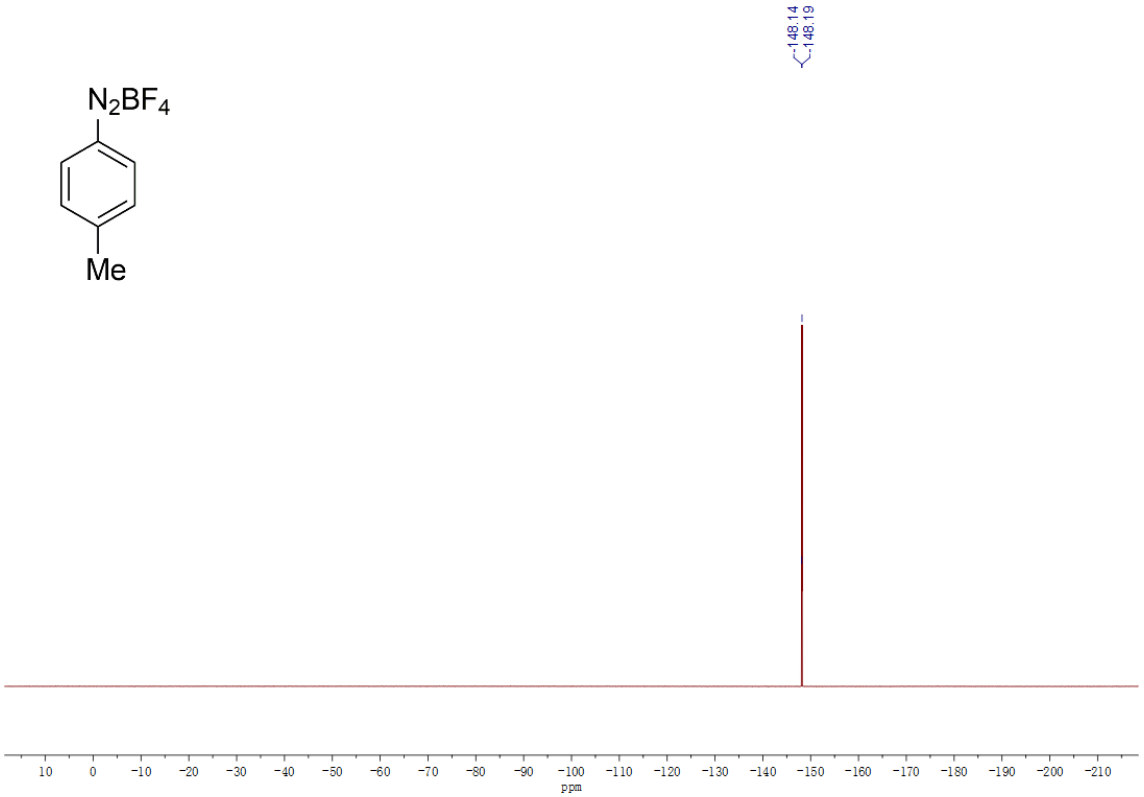
^{1}H NMR of F3



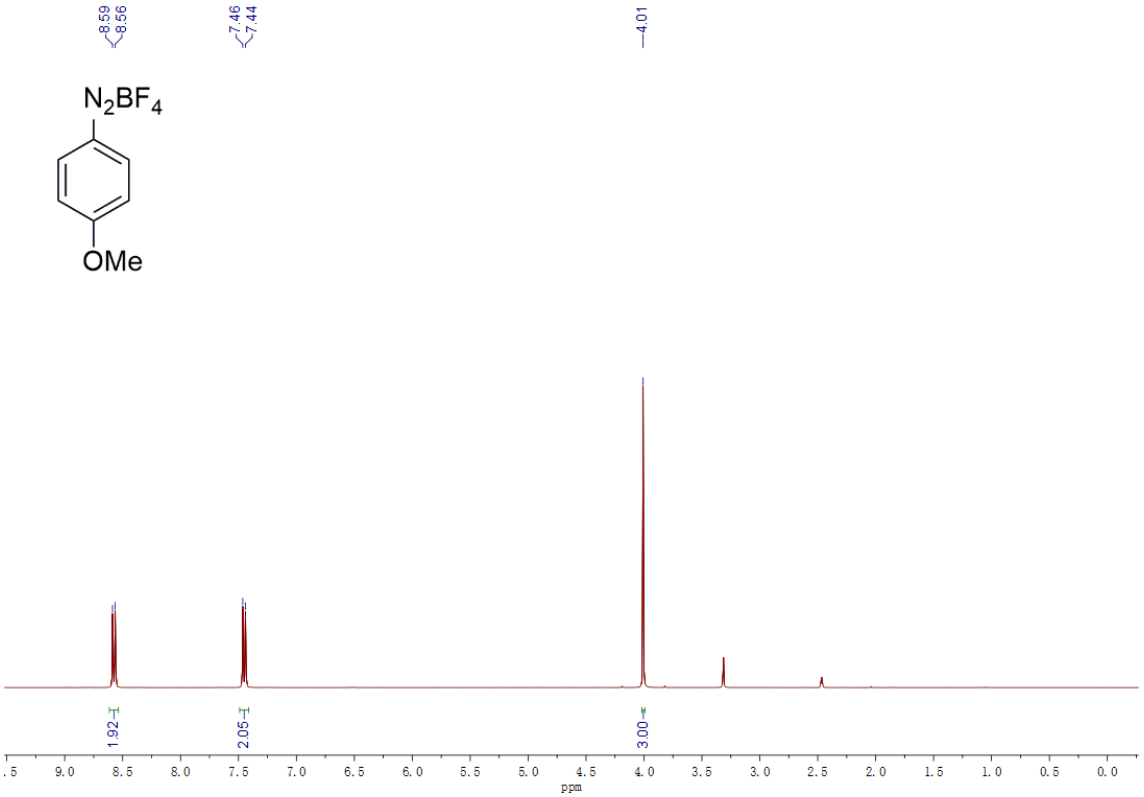
^{13}C NMR of F3



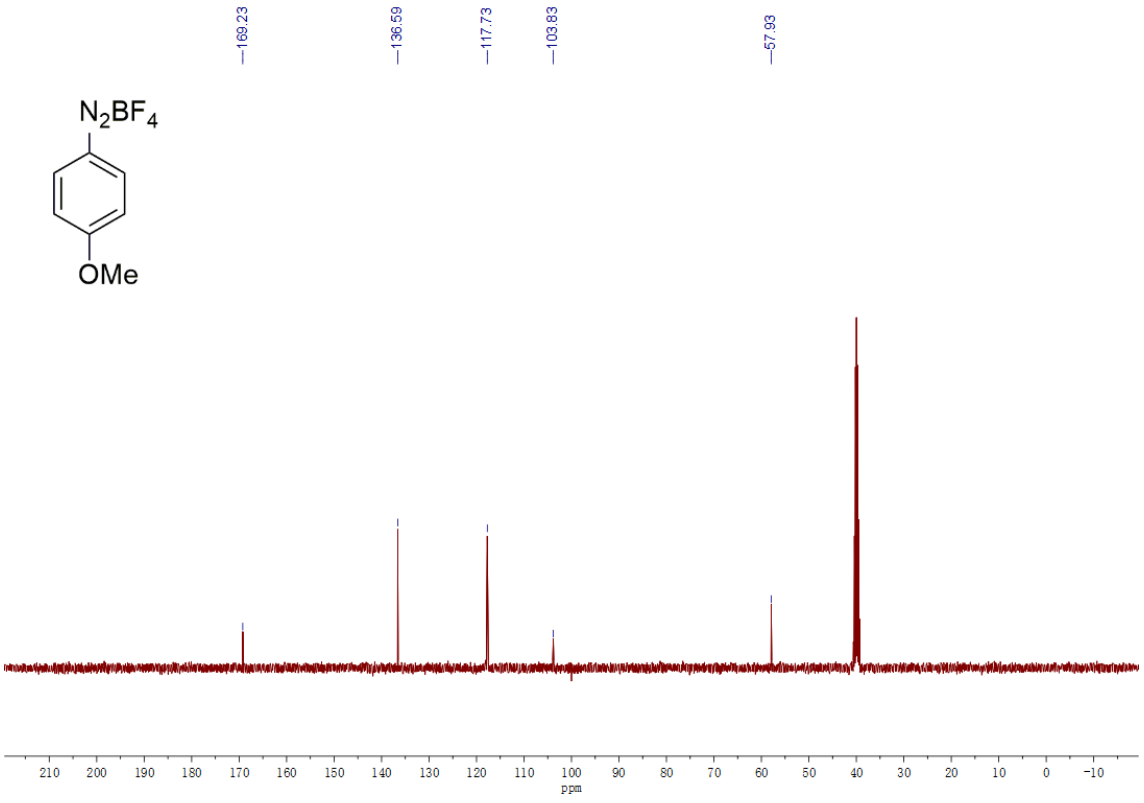
^{19}F NMR of F3


-148.14
-148.19
N2BF4
Me
10 0 -10 -20 -30 -40 -50 -60 -70 -80 -90 -100 -110 -120 -130 -140 -150 -160 -170 -180 -190 -200 -210
ppm

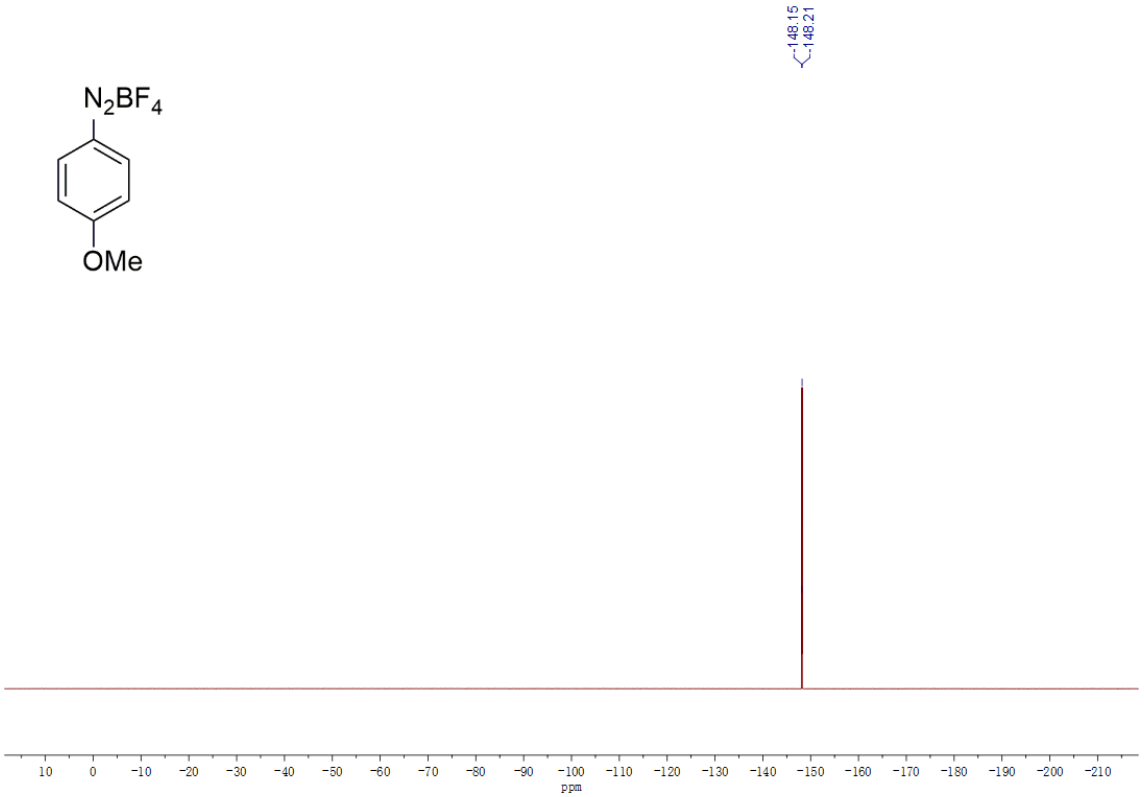
^{1}H NMR of F4



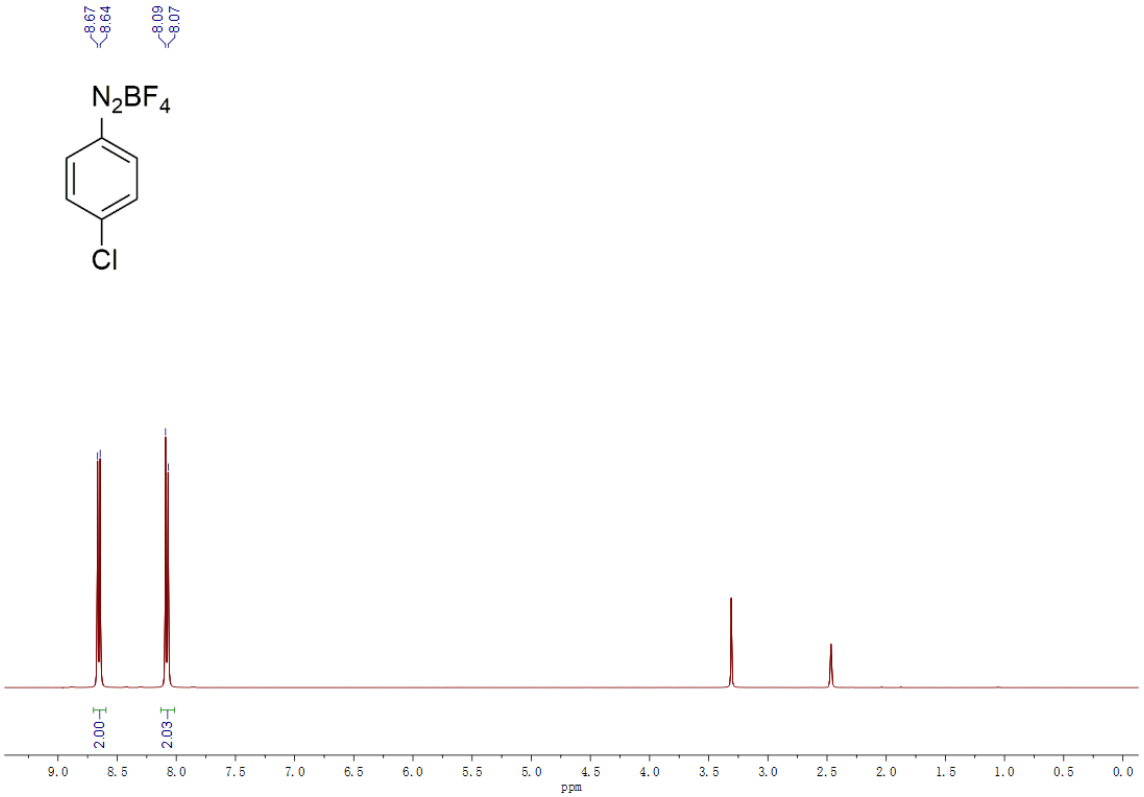
^{13}C NMR of F4



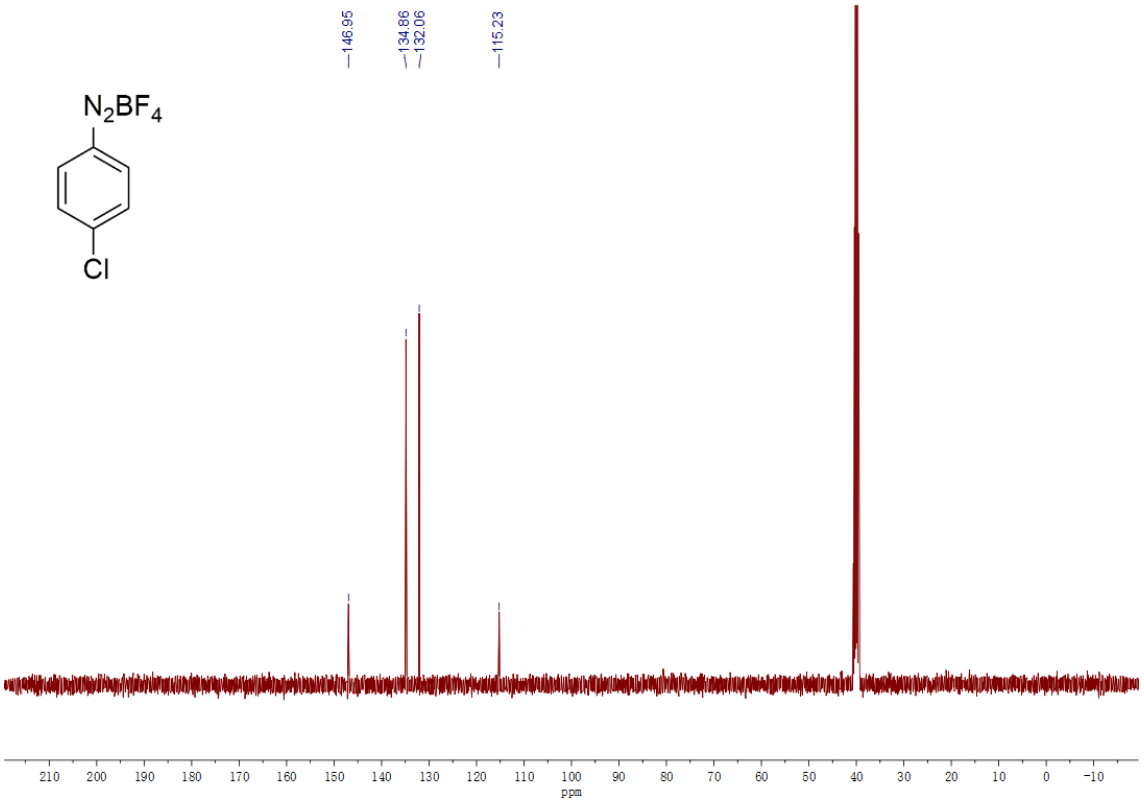
^{19}F NMR of F4


-148.15
-148.21
N2BF4
OMe
10 0 -10 -20 -30 -40 -50 -60 -70 -80 -90 -100 -110 -120 -130 -140 -150 -160 -170 -180 -190 -200 -210
ppm

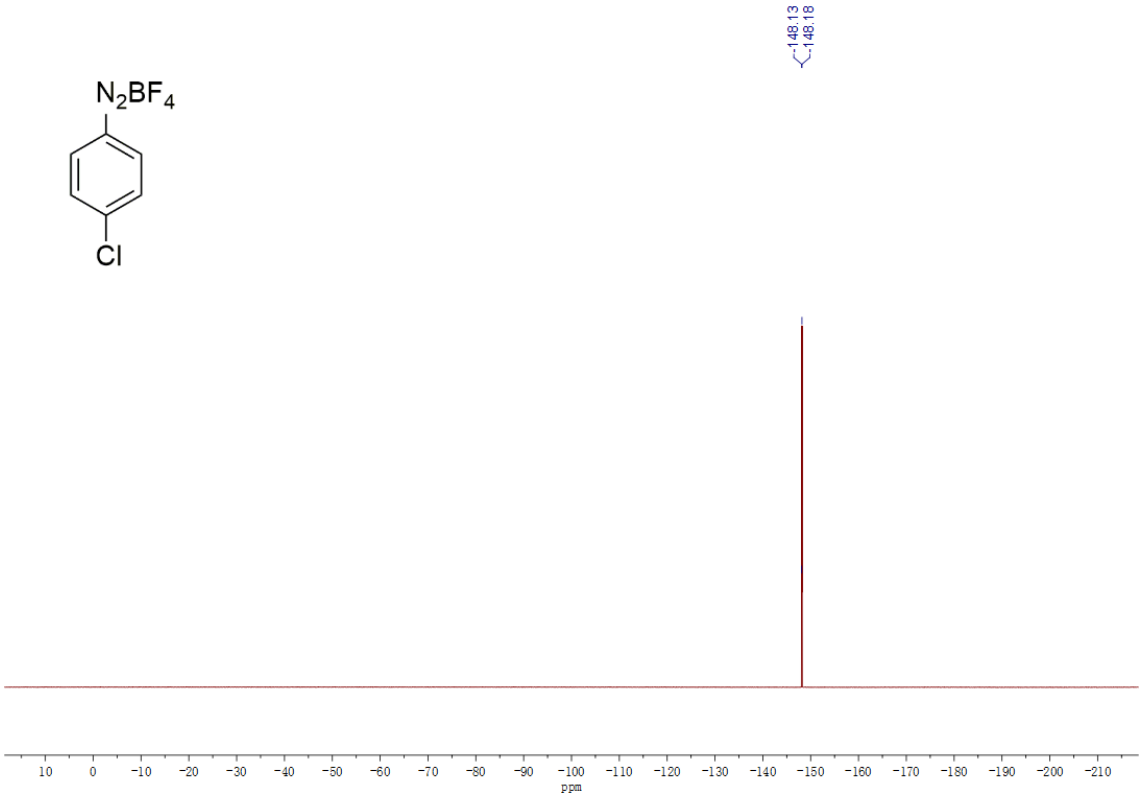
^{1}H NMR of F5



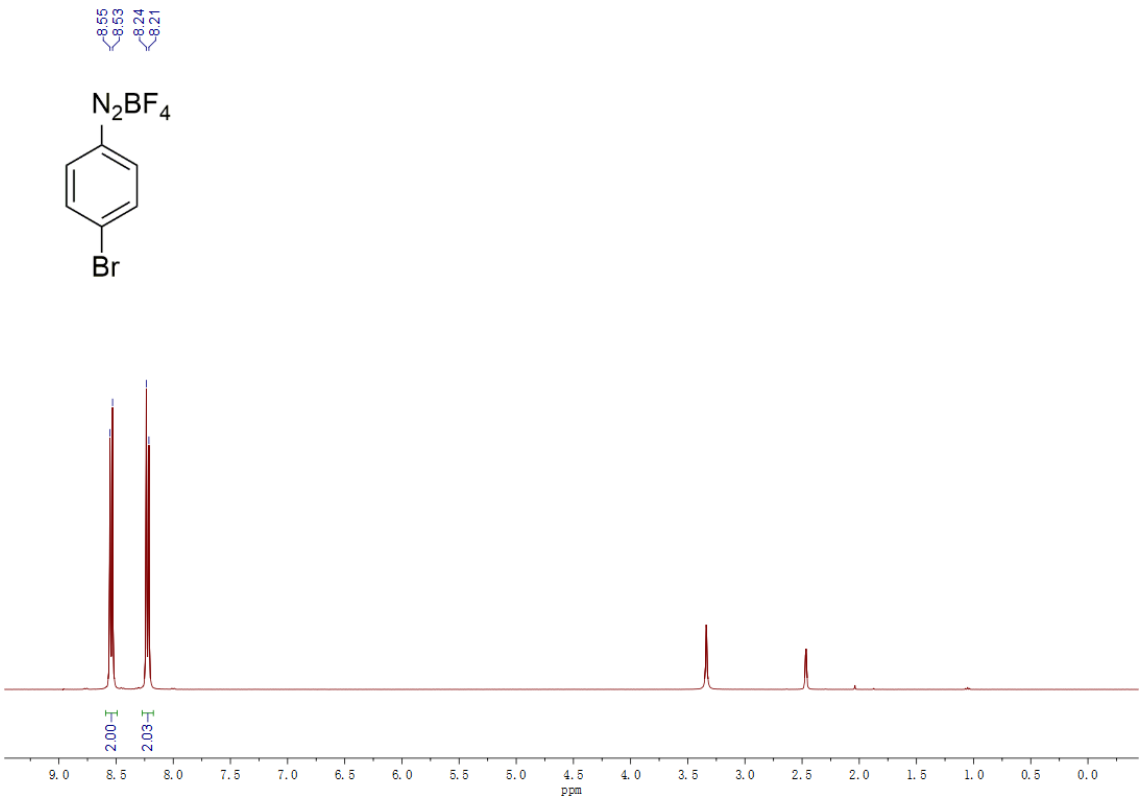
^{13}C NMR of F5



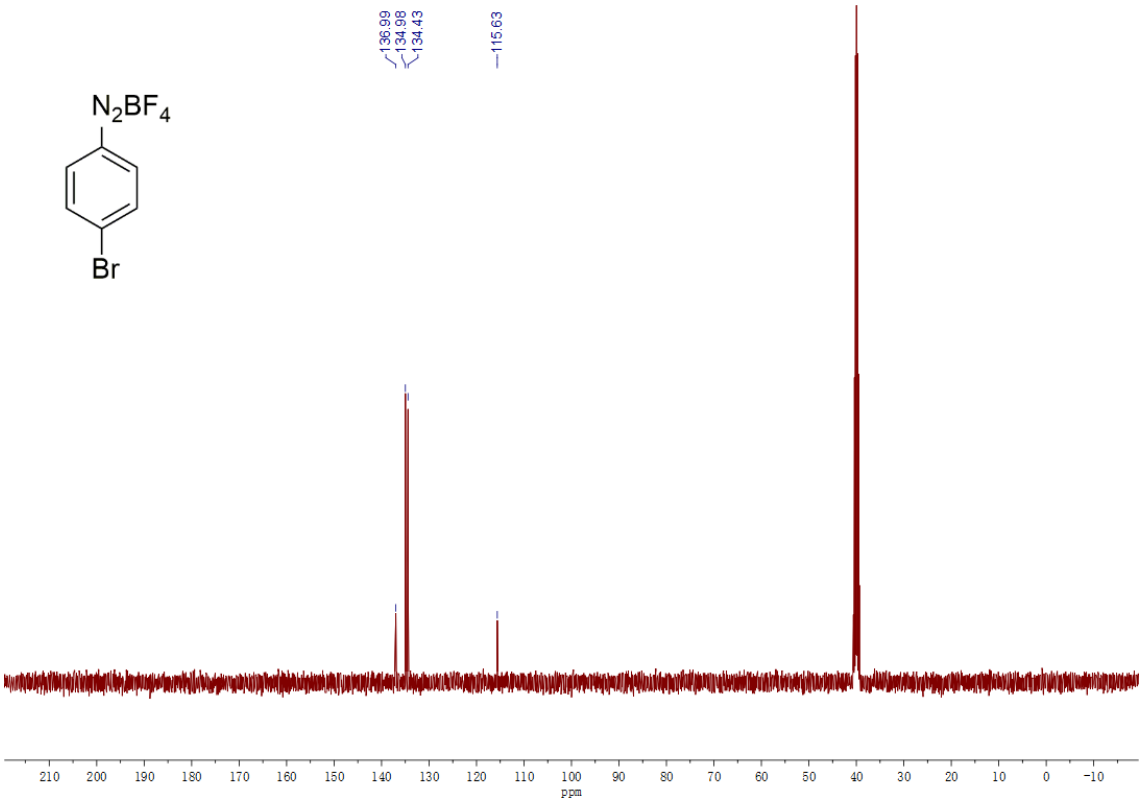
^{19}F NMR of F5


N2BF4
Cl
-148.13
-148.18
10 0 -10 -20 -30 -40 -50 -60 -70 -80 -90 -100 -110 -120 -130 -140 -150 -160 -170 -180 -190 -200 -210
ppm

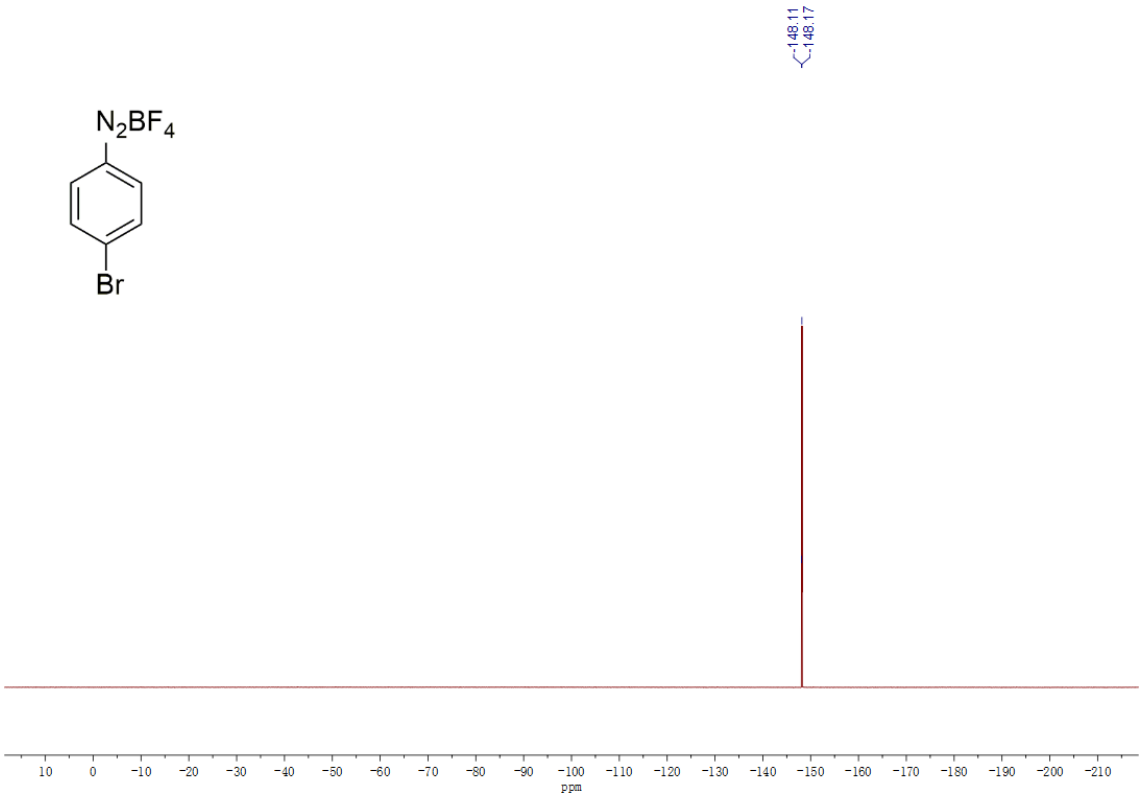
^{1}H NMR of F6



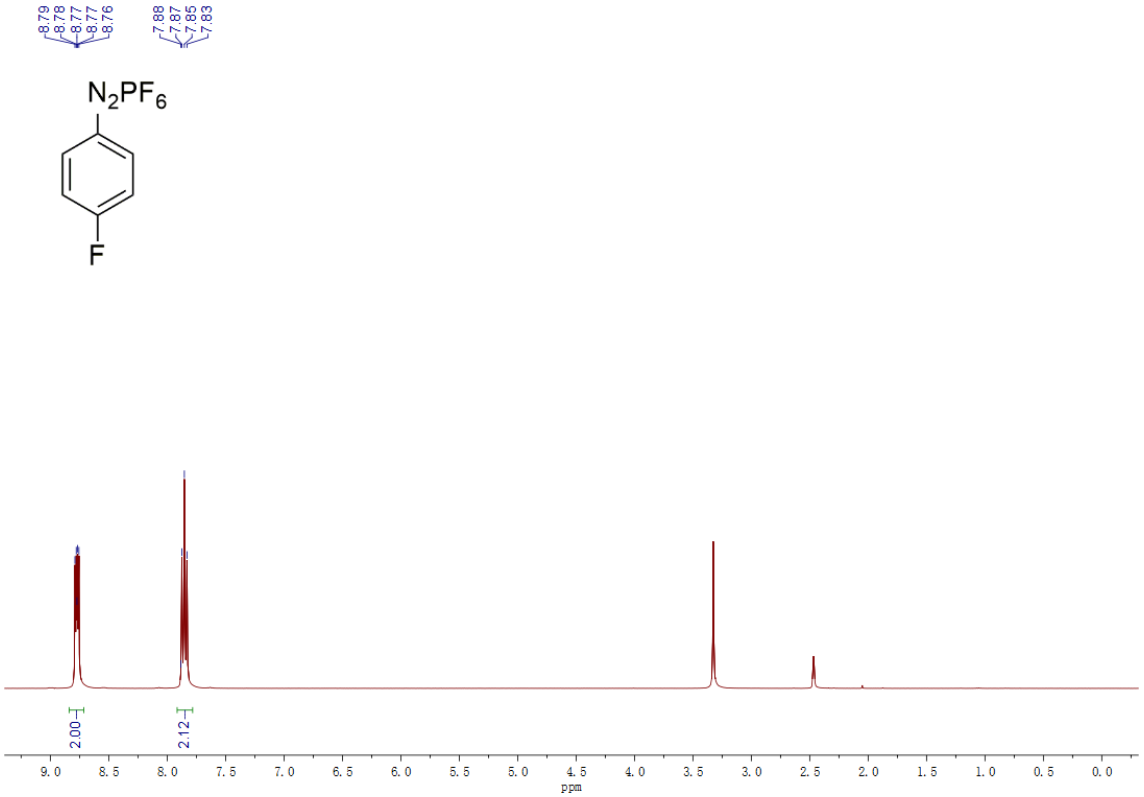
^{13}C NMR of F6



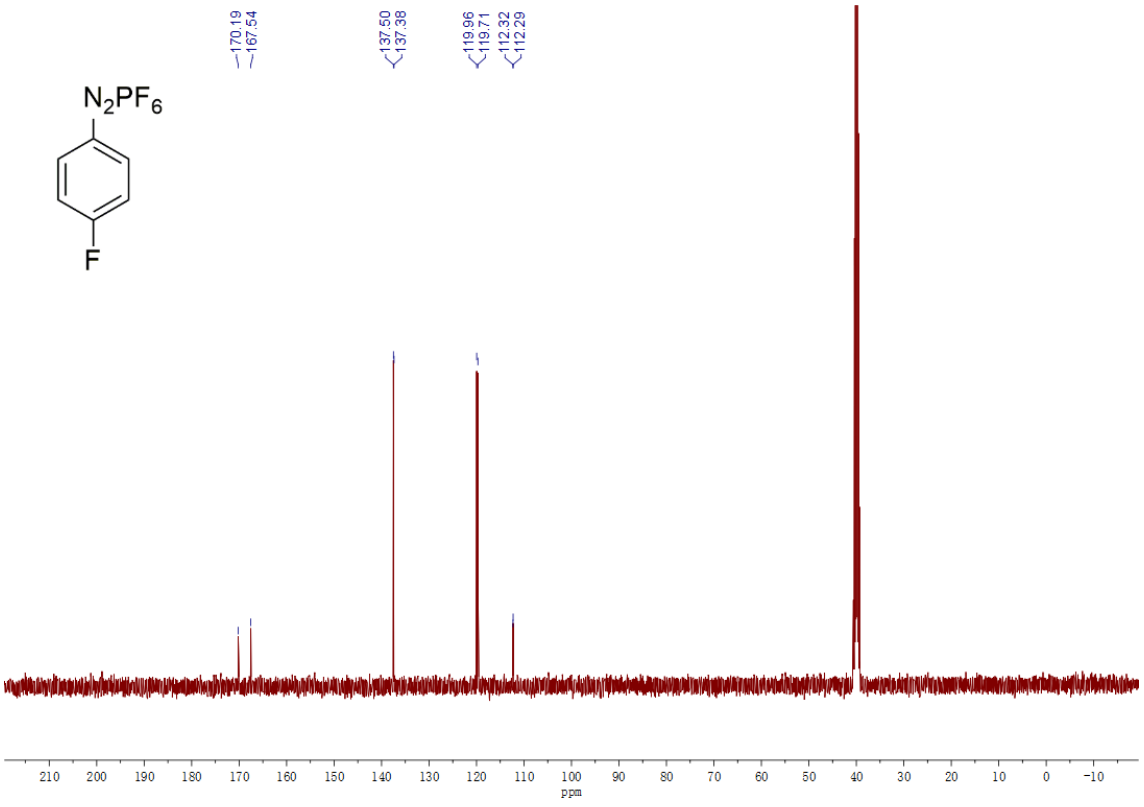
^{19}F NMR of F6


-148.11
-148.17
N2BF4
Br
10 0 -10 -20 -30 -40 -50 -60 -70 -80 -90 -100 -110 -120 -130 -140 -150 -160 -170 -180 -190 -200 -210
ppm

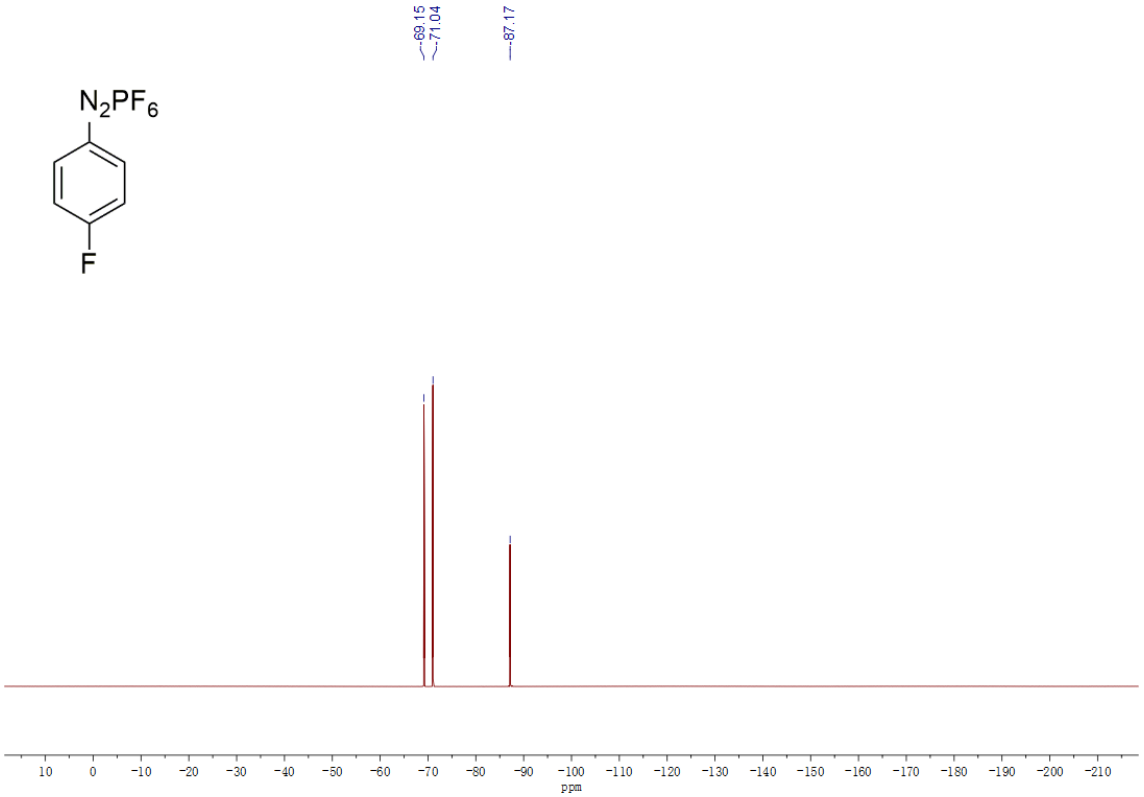
^{1}H NMR of F7



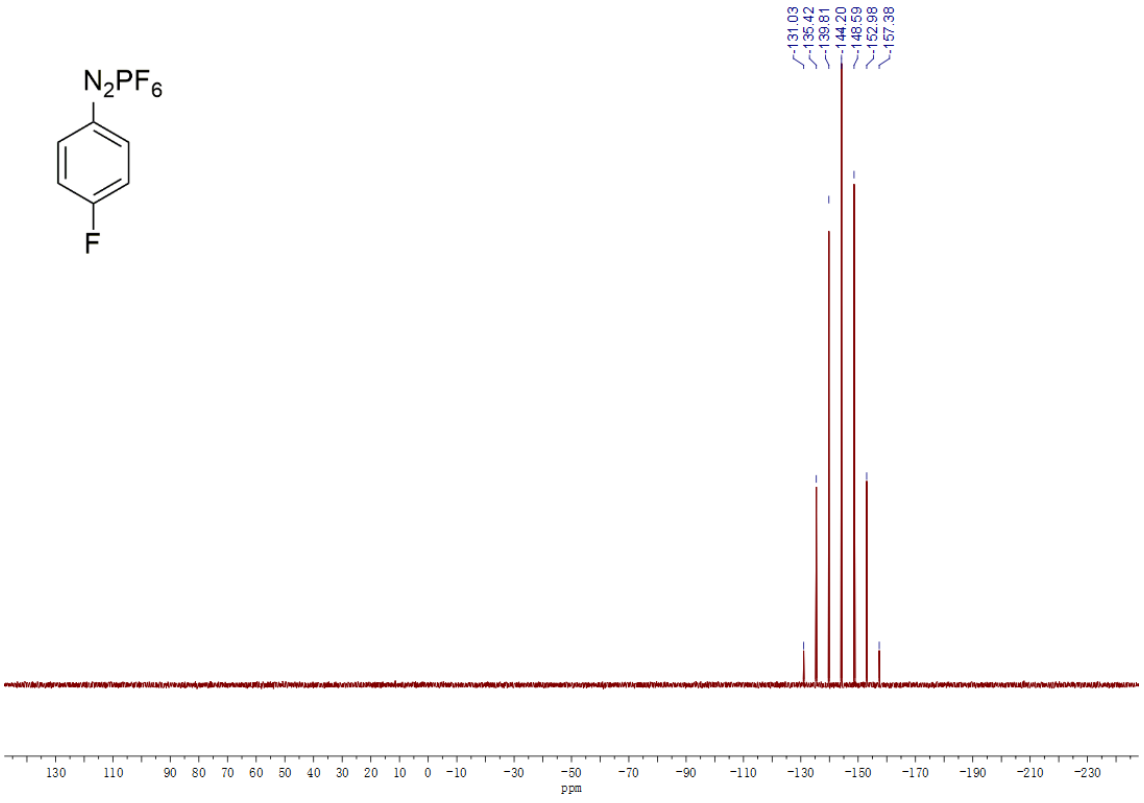
^{13}C NMR of F7



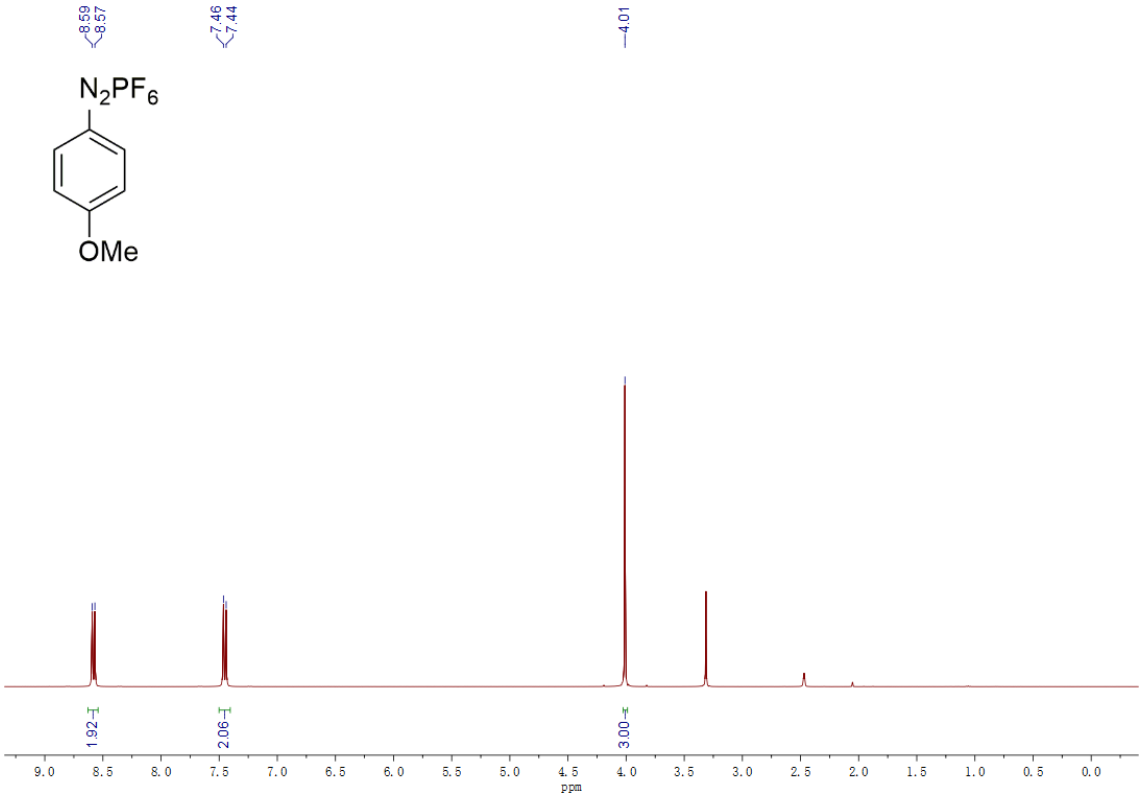
^{19}F NMR of F7



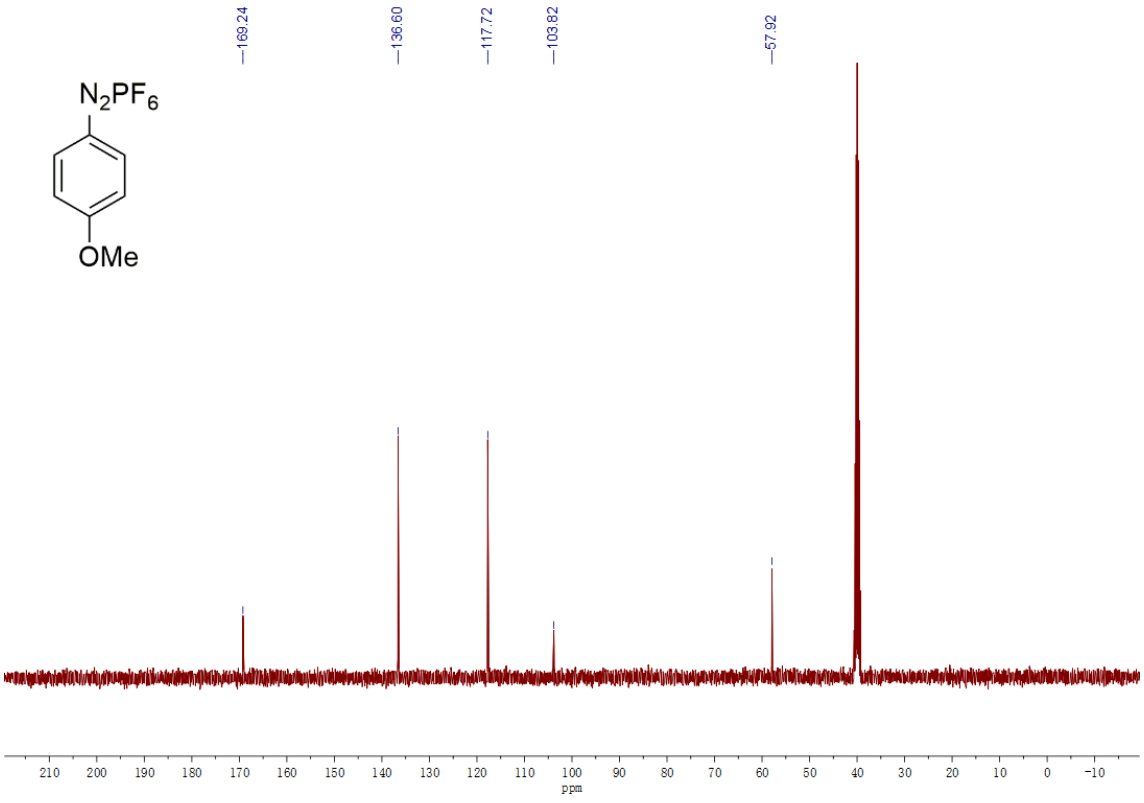
^{31}P NMR of F7



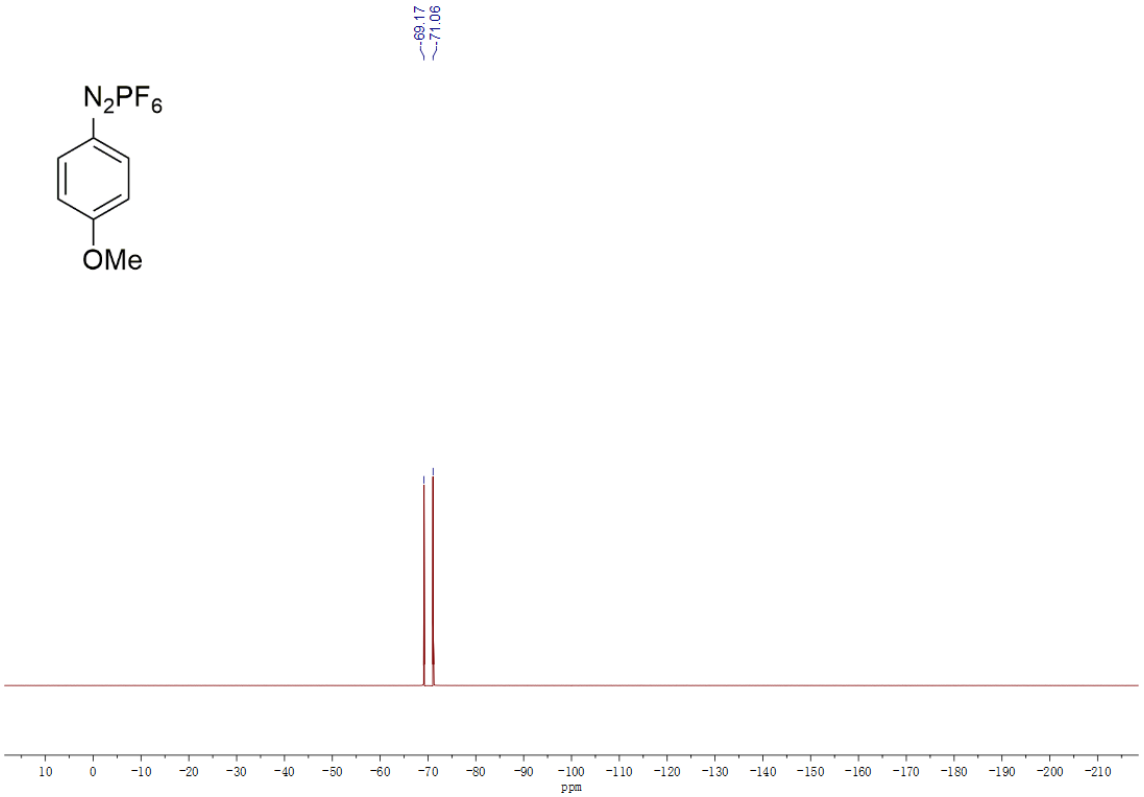
^{1}H NMR of F8



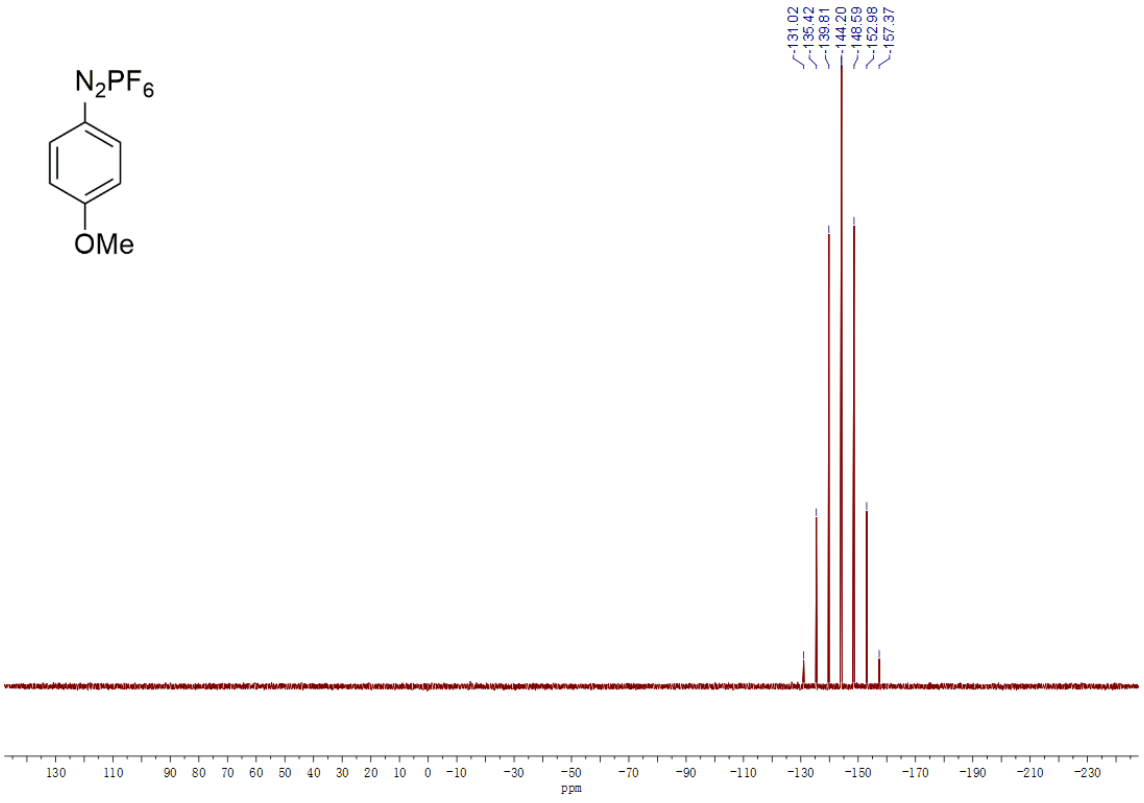
^{13}C NMR of F8



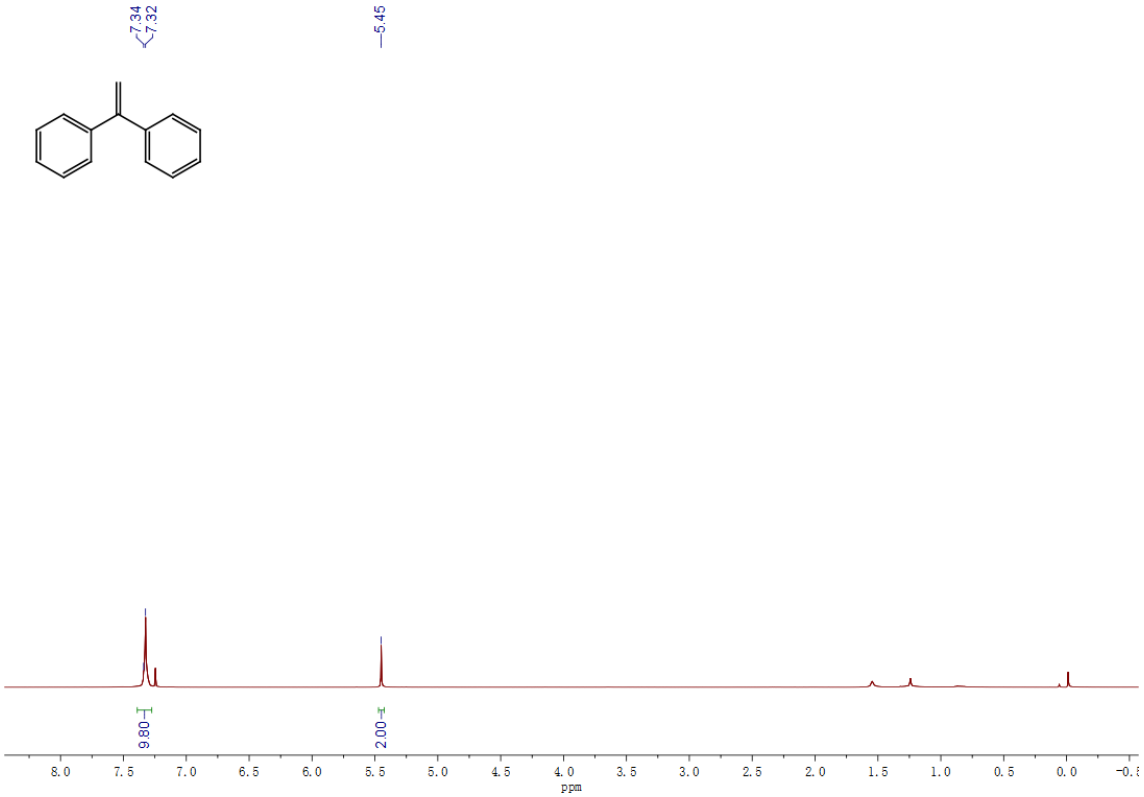
^{19}F NMR of F8



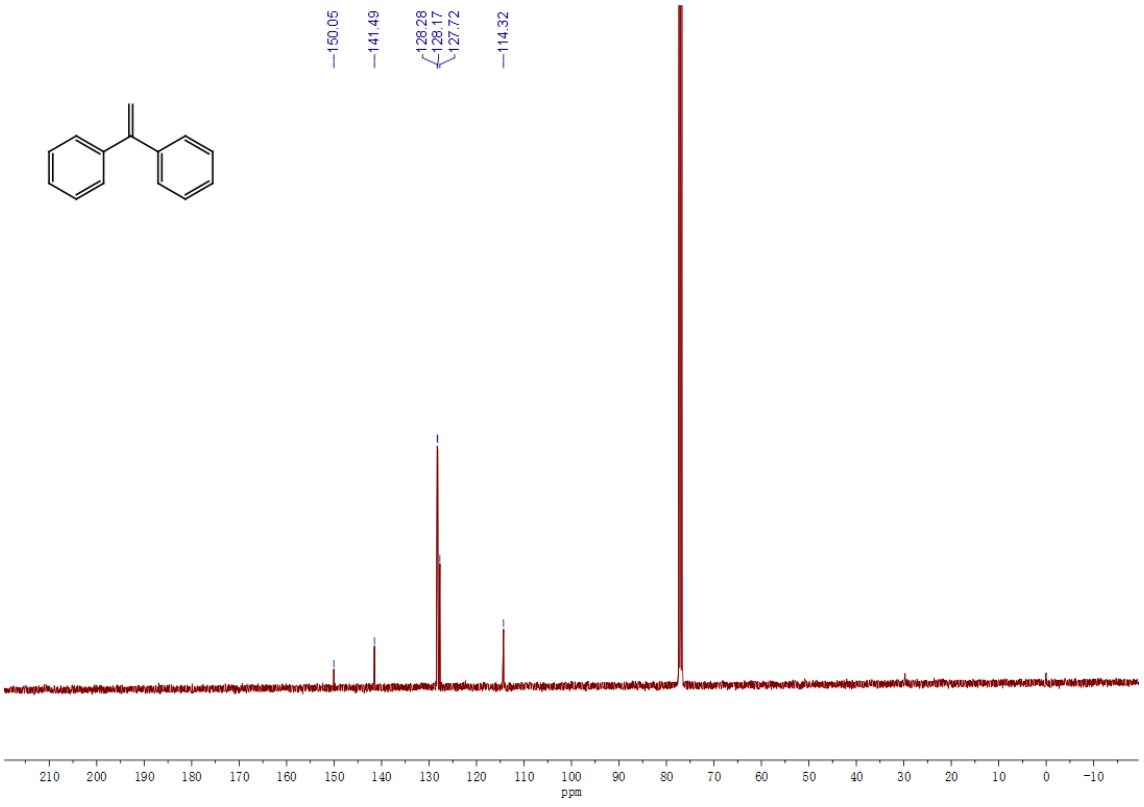
^{31}P NMR of F8



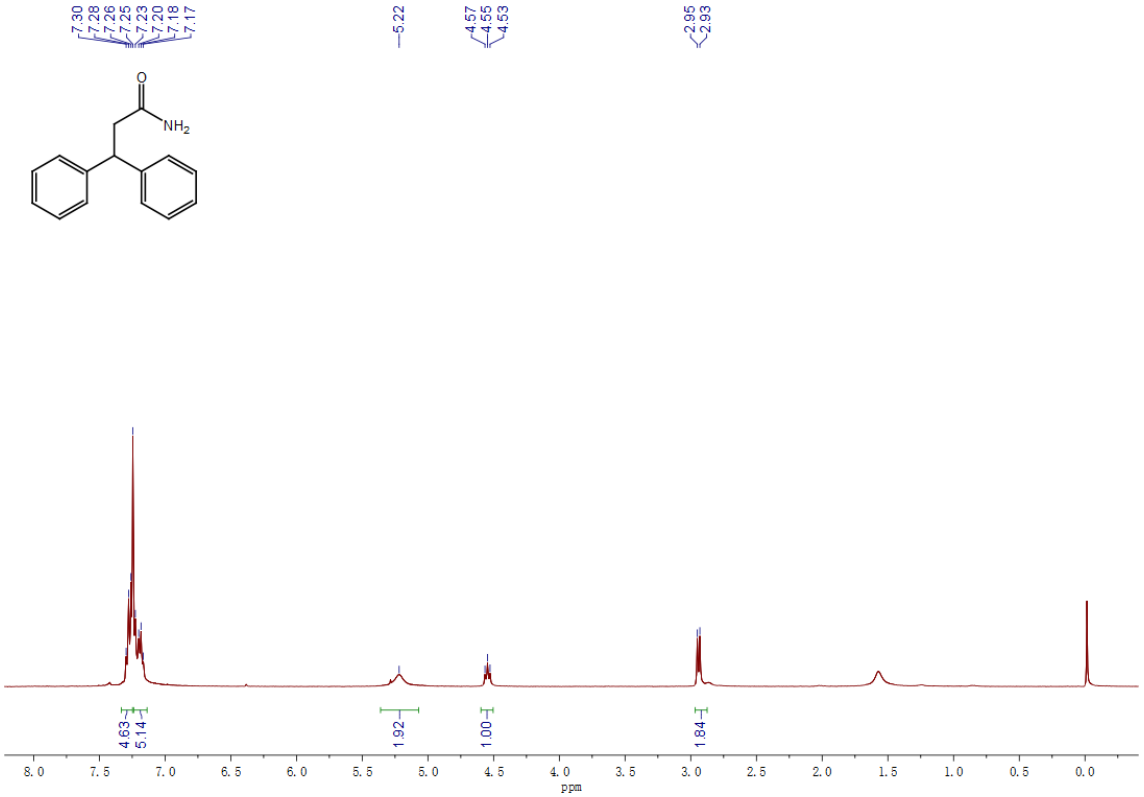
^{1}H NMR of ethene-1,1-diyldibenzene



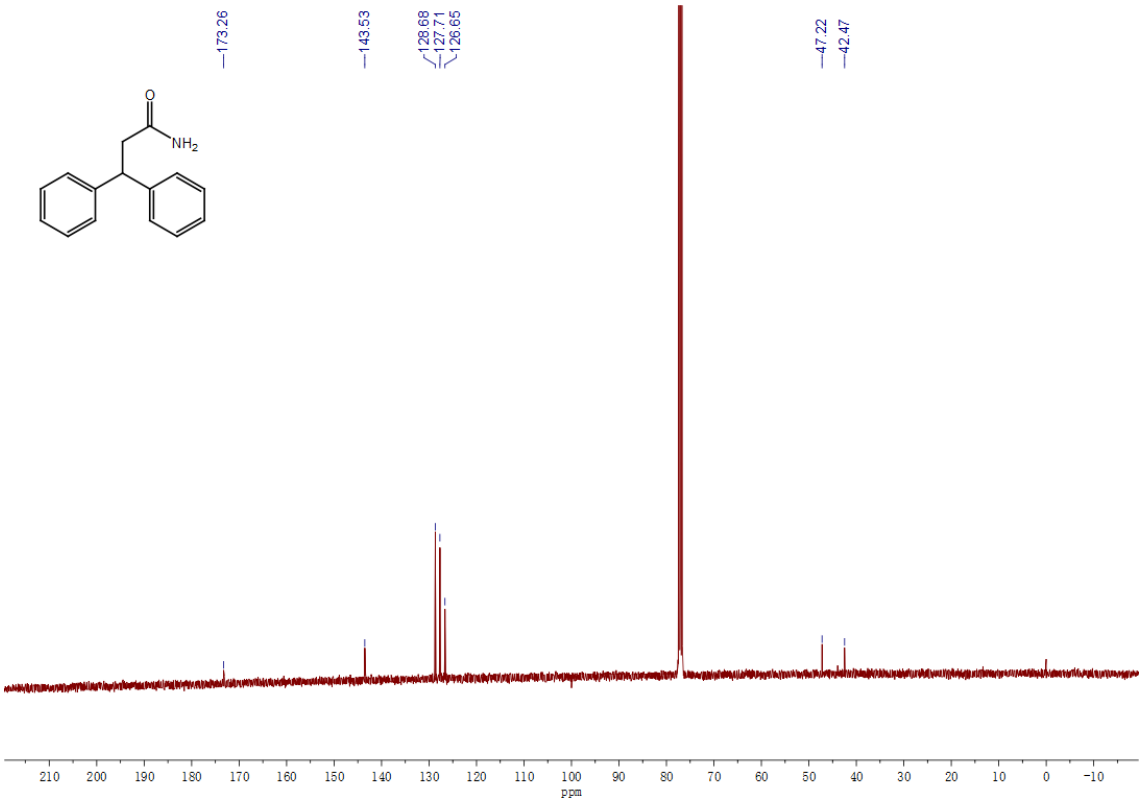
^{13}C NMR of ethene-1,1-diyldibenzene



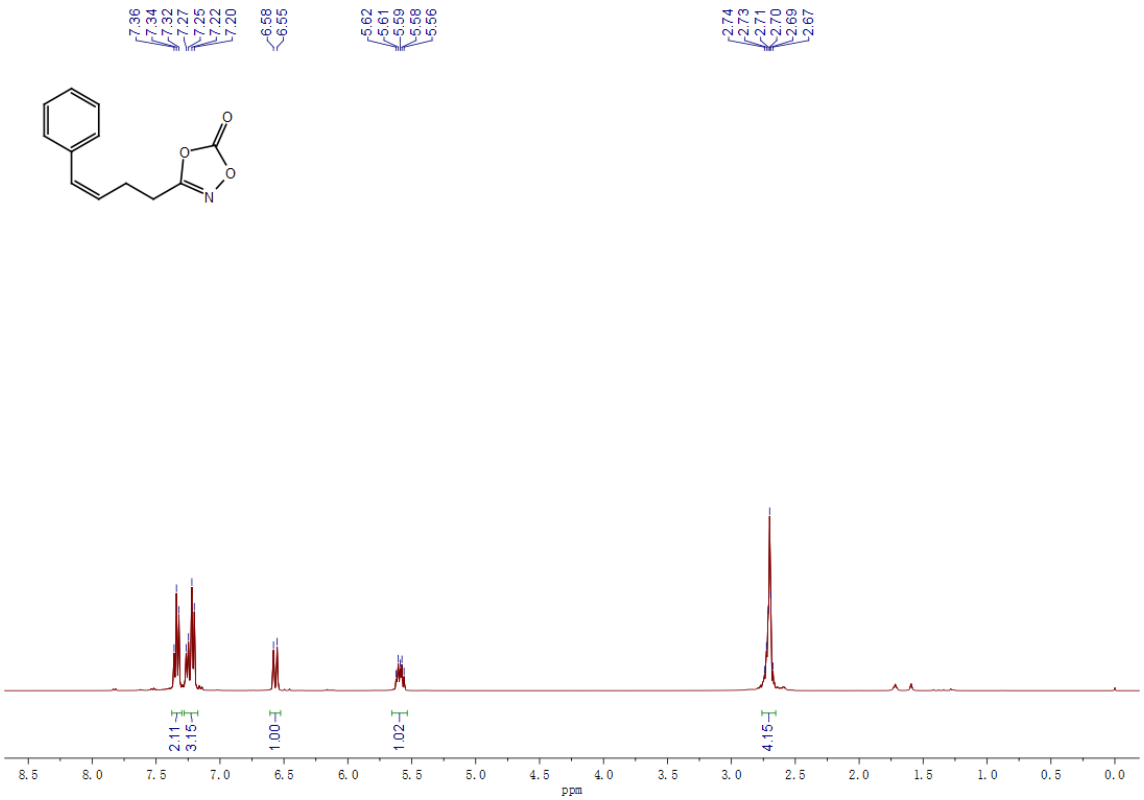
^{1}H NMR of 3,3-diphenylpropanamide



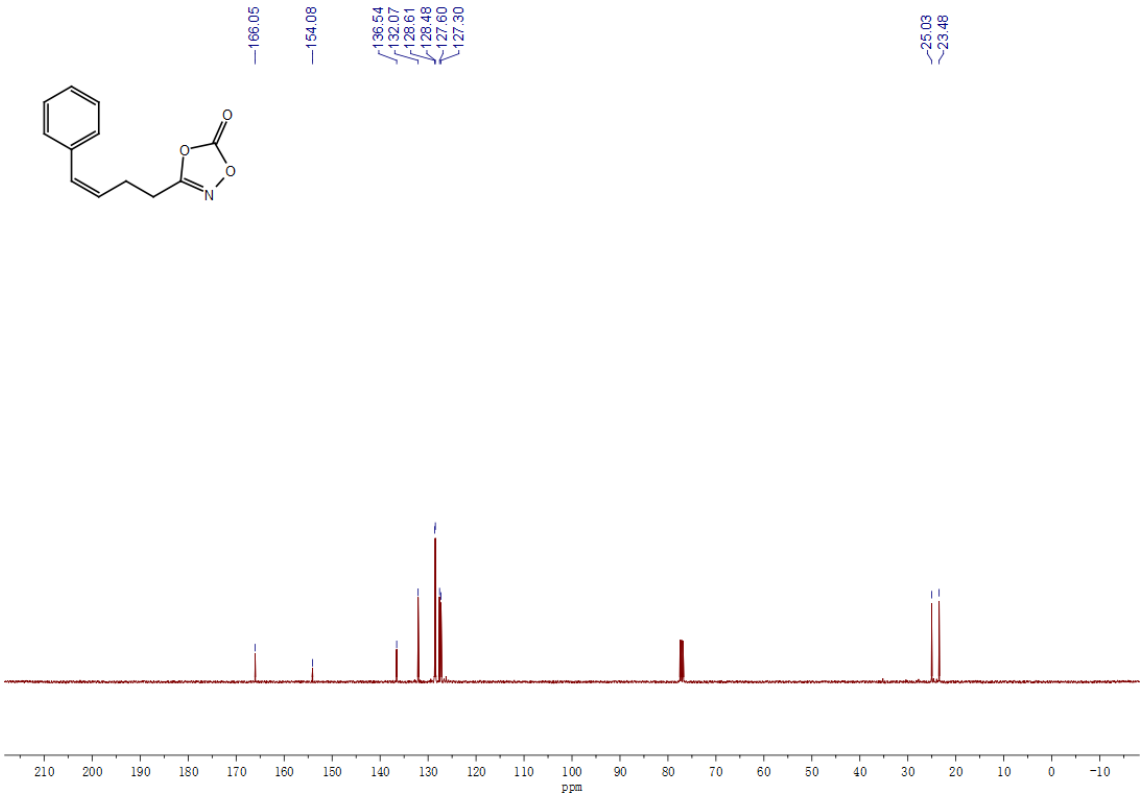
^{13}C NMR of 3,3-diphenylpropanamide



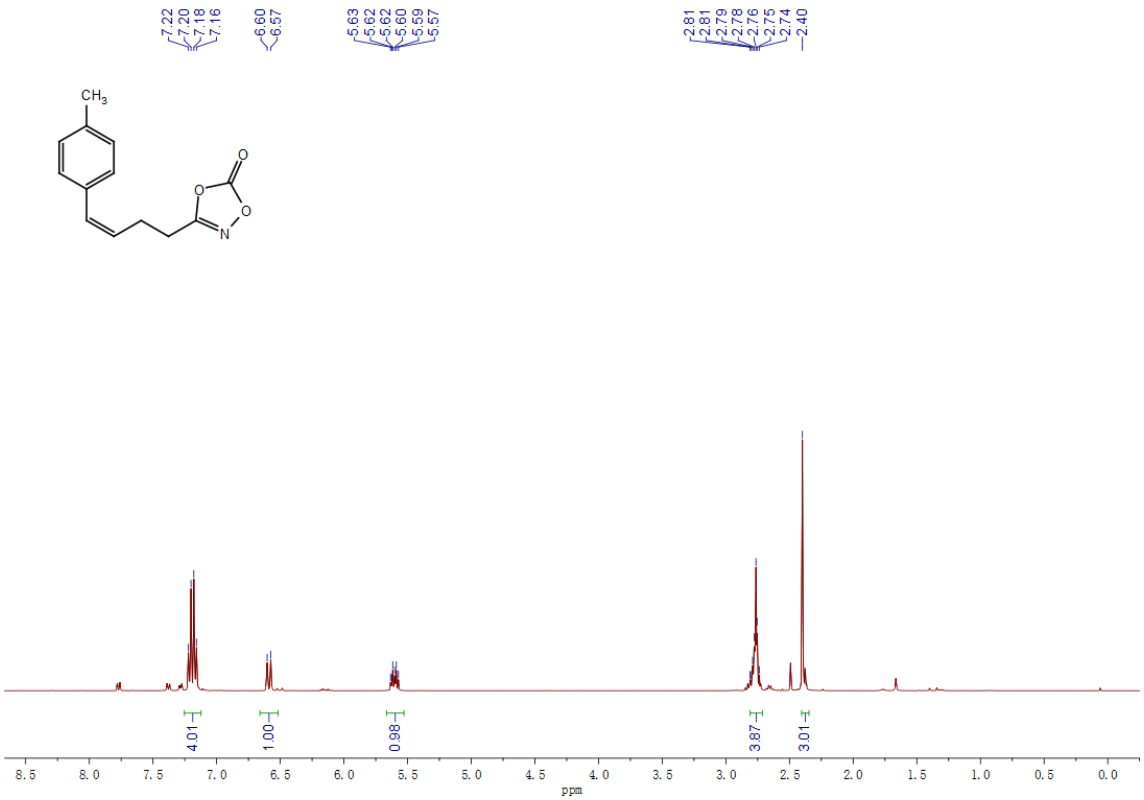
^{1}H NMR of 12a



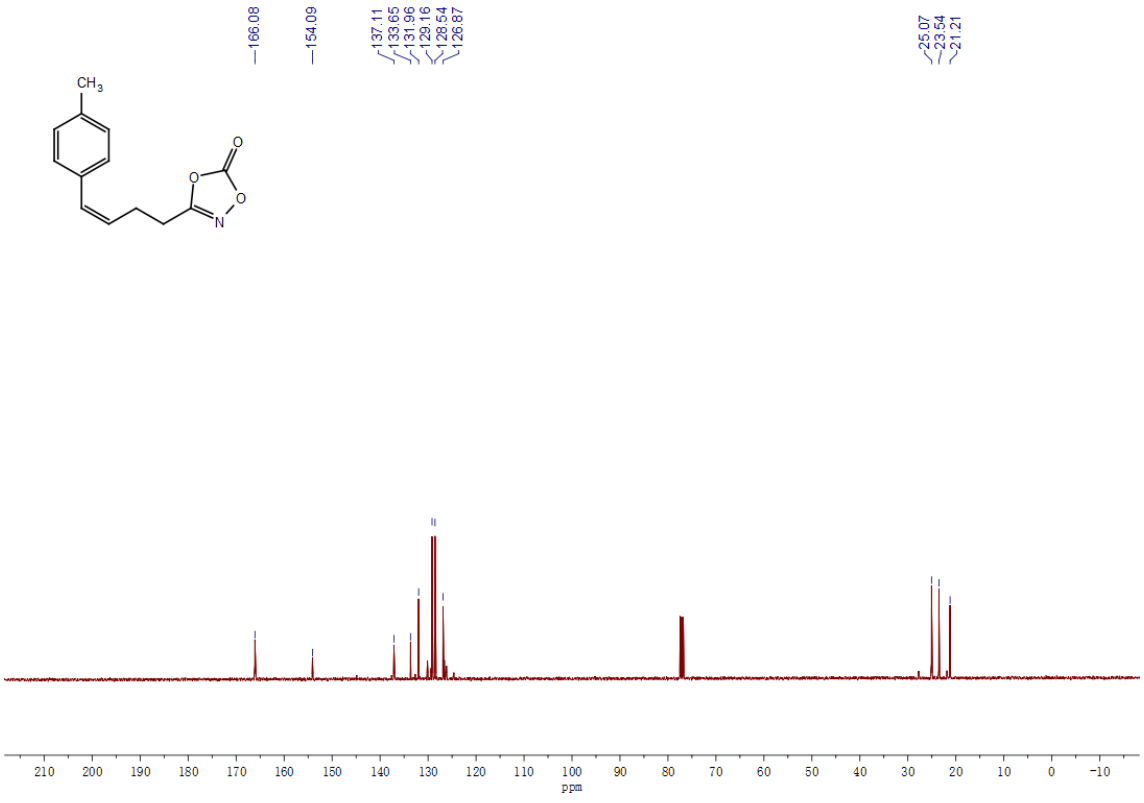
^{13}C NMR of 12a



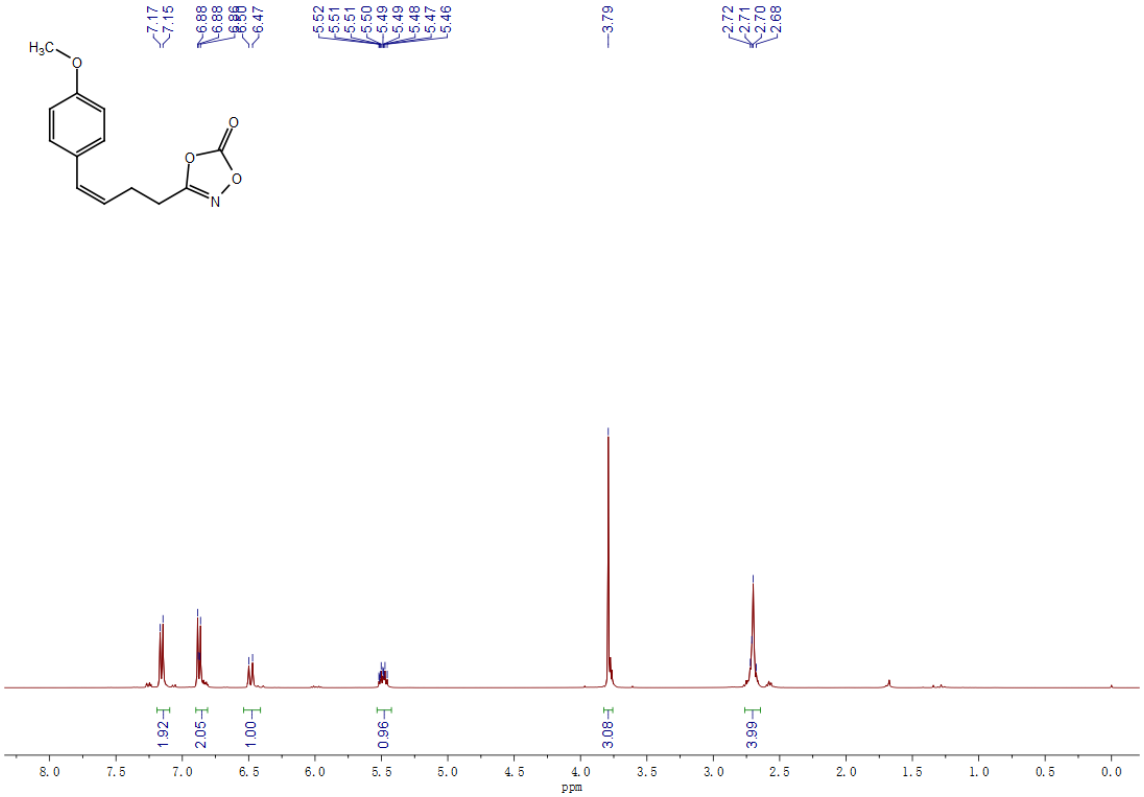
^{1}H NMR of 12b



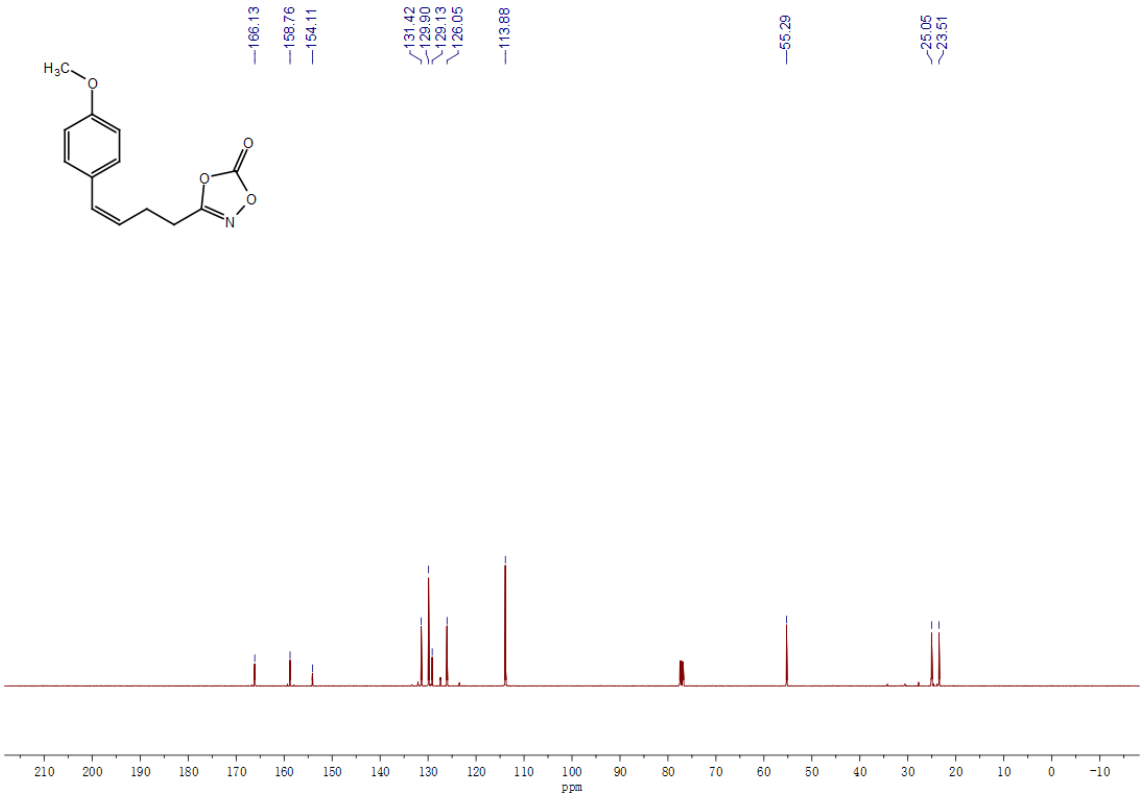
^{13}C NMR of 12b



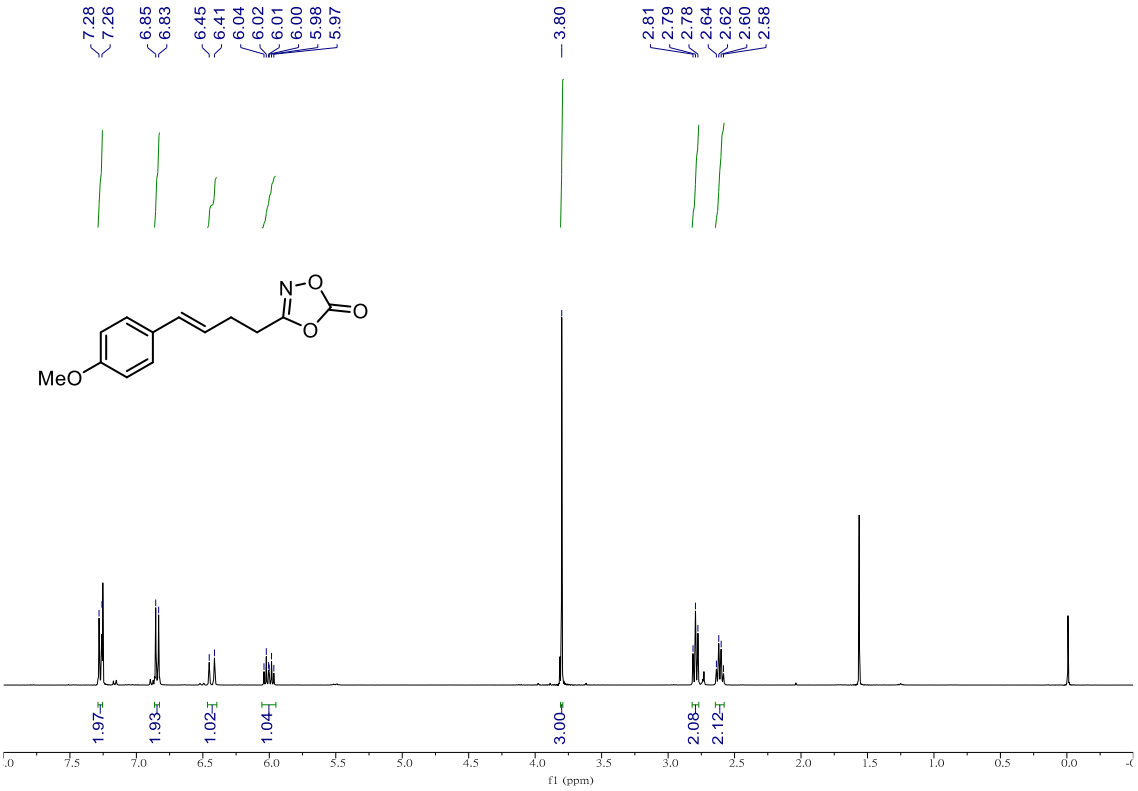
^{1}H NMR of (Z)-12c



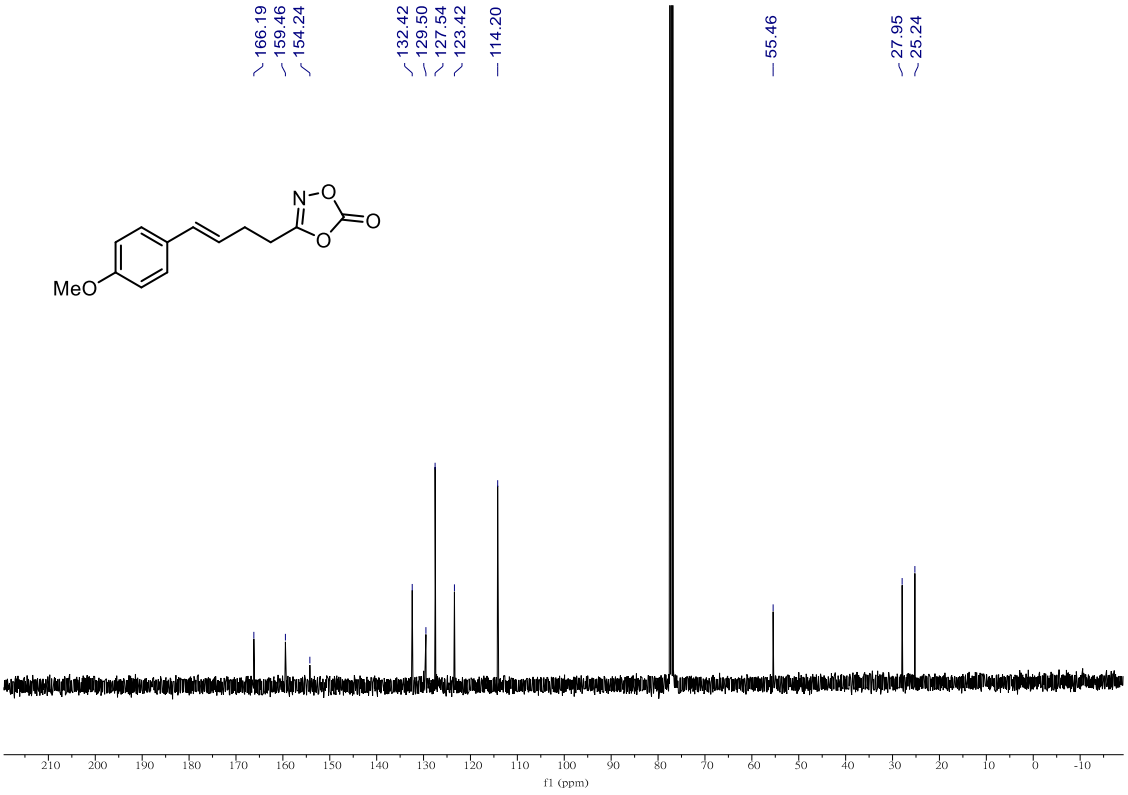
^{13}C NMR of (Z)-12c



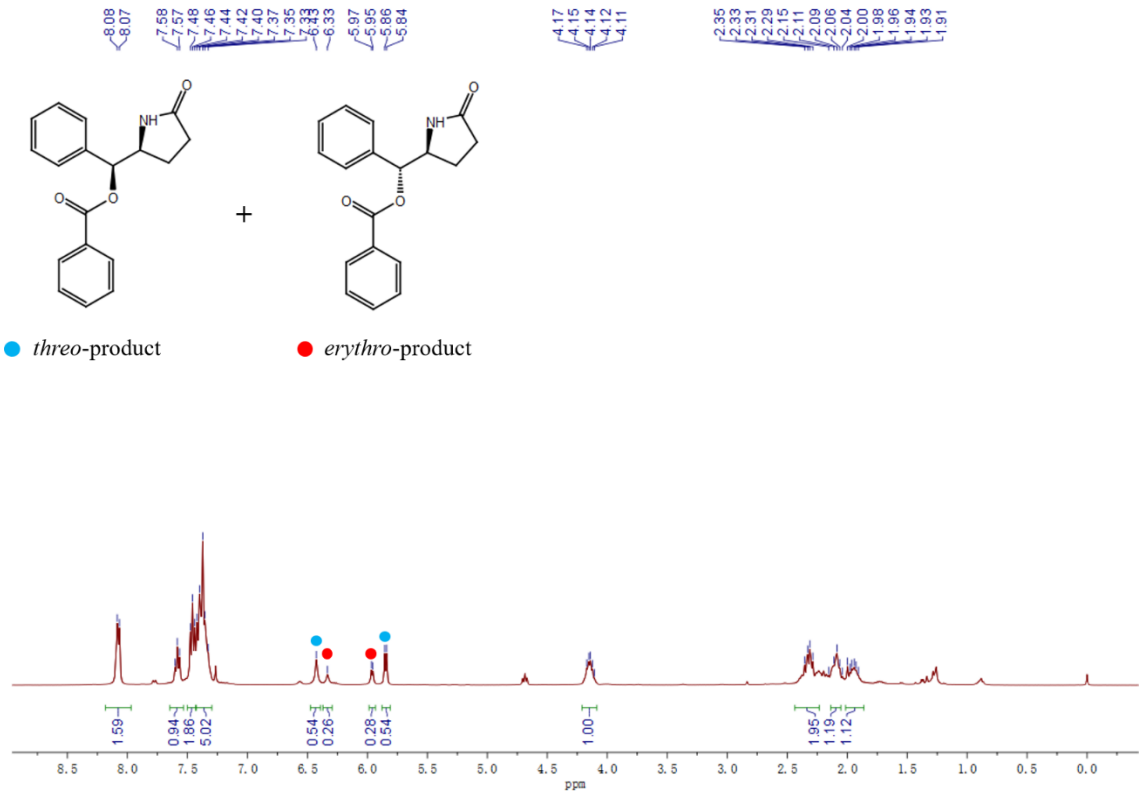
^{1}H NMR of (E)-12c



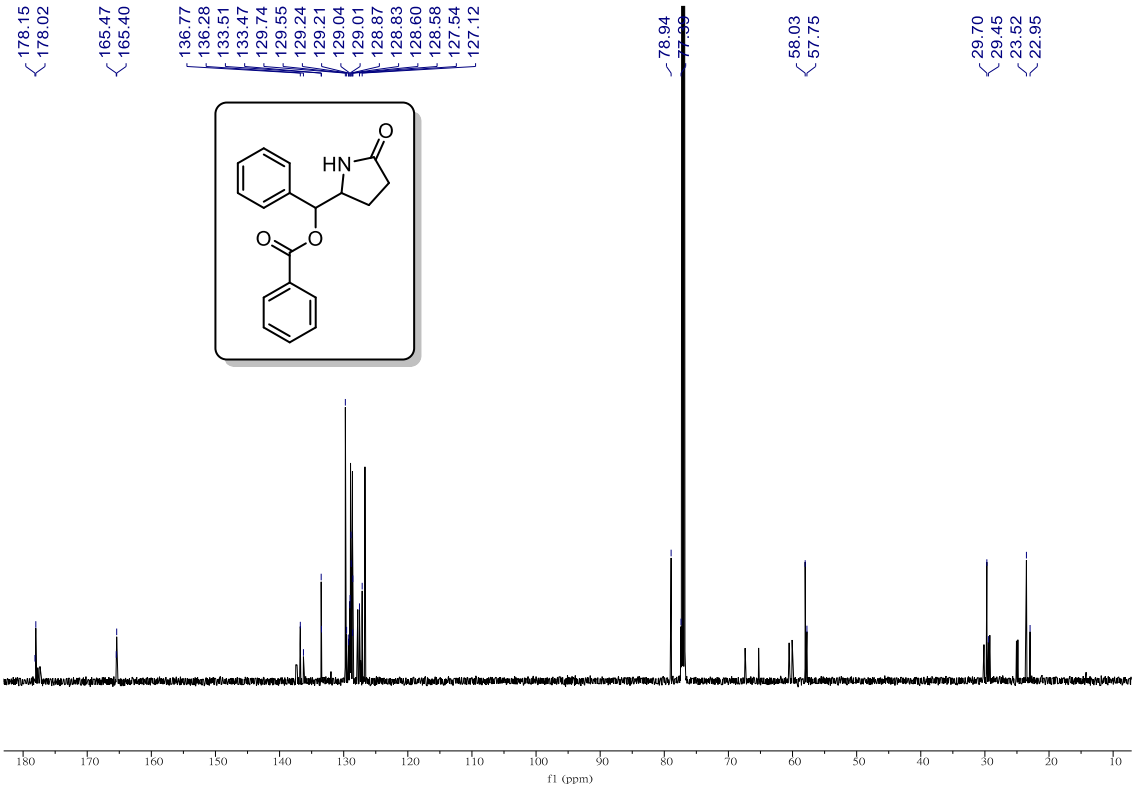
^{13}C NMR of (E)-12c



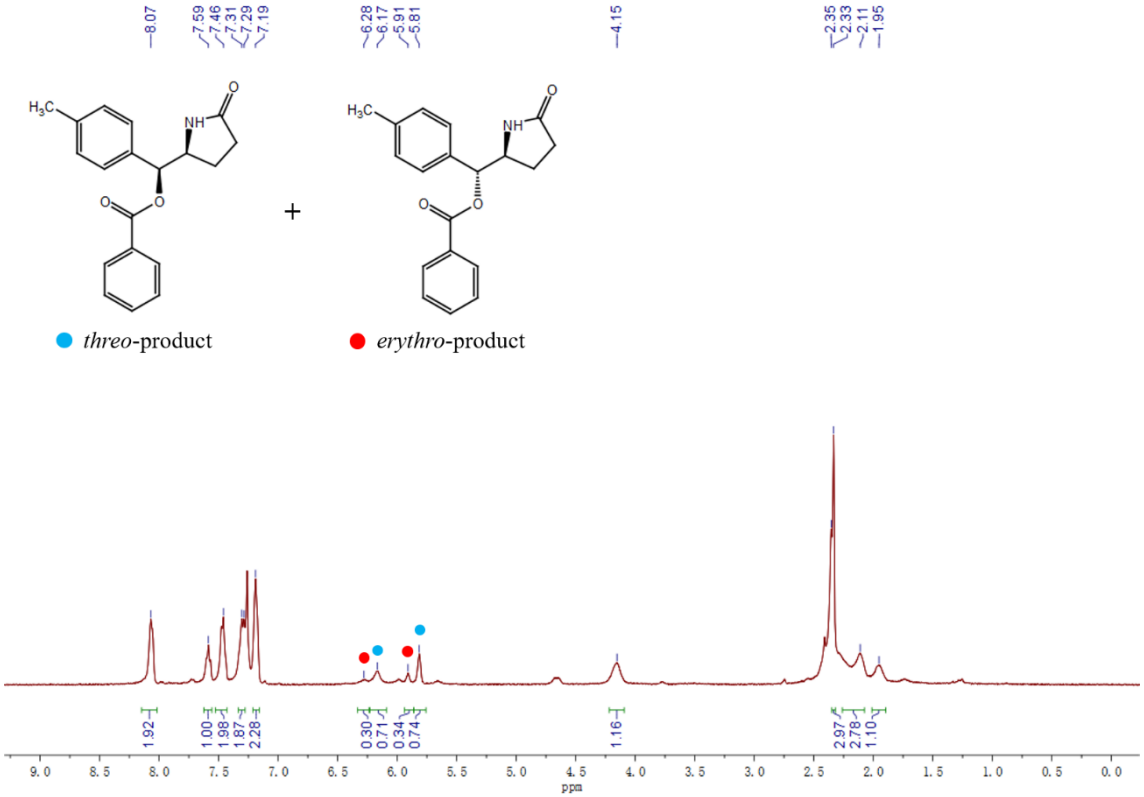
^{1}H NMR of 13a



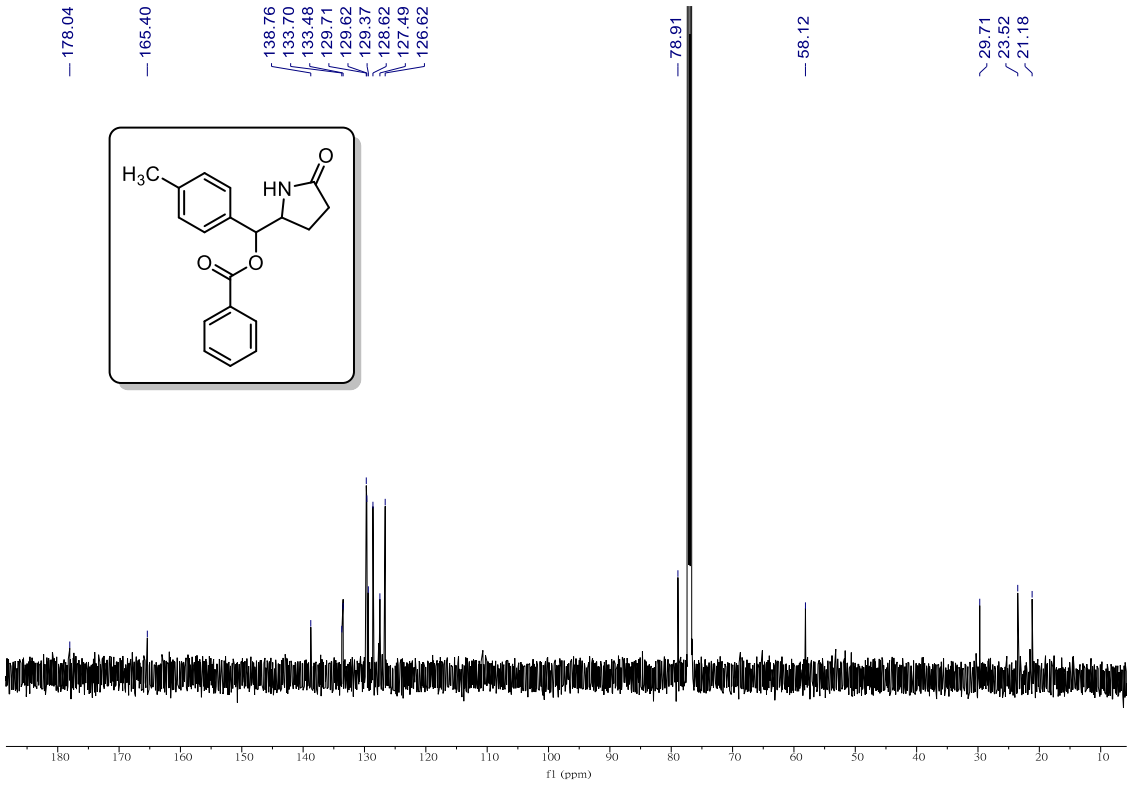
^{13}C NMR of 13a



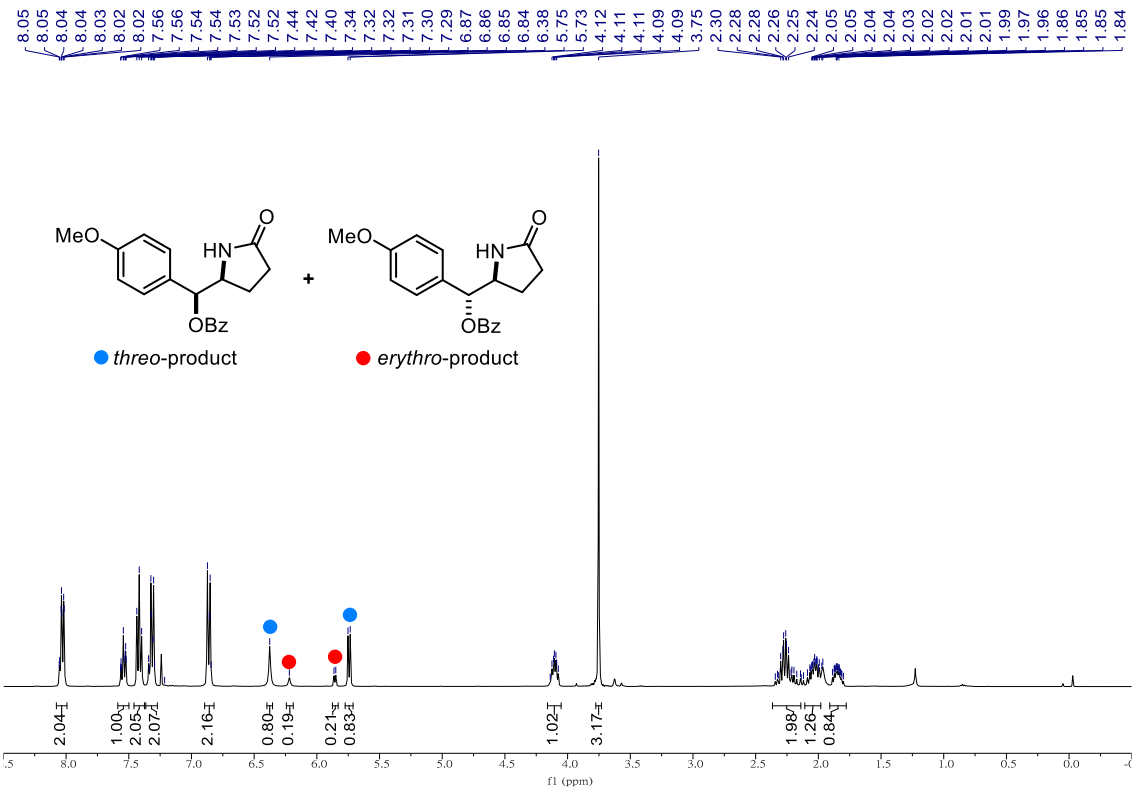
^{1}H NMR of 13b



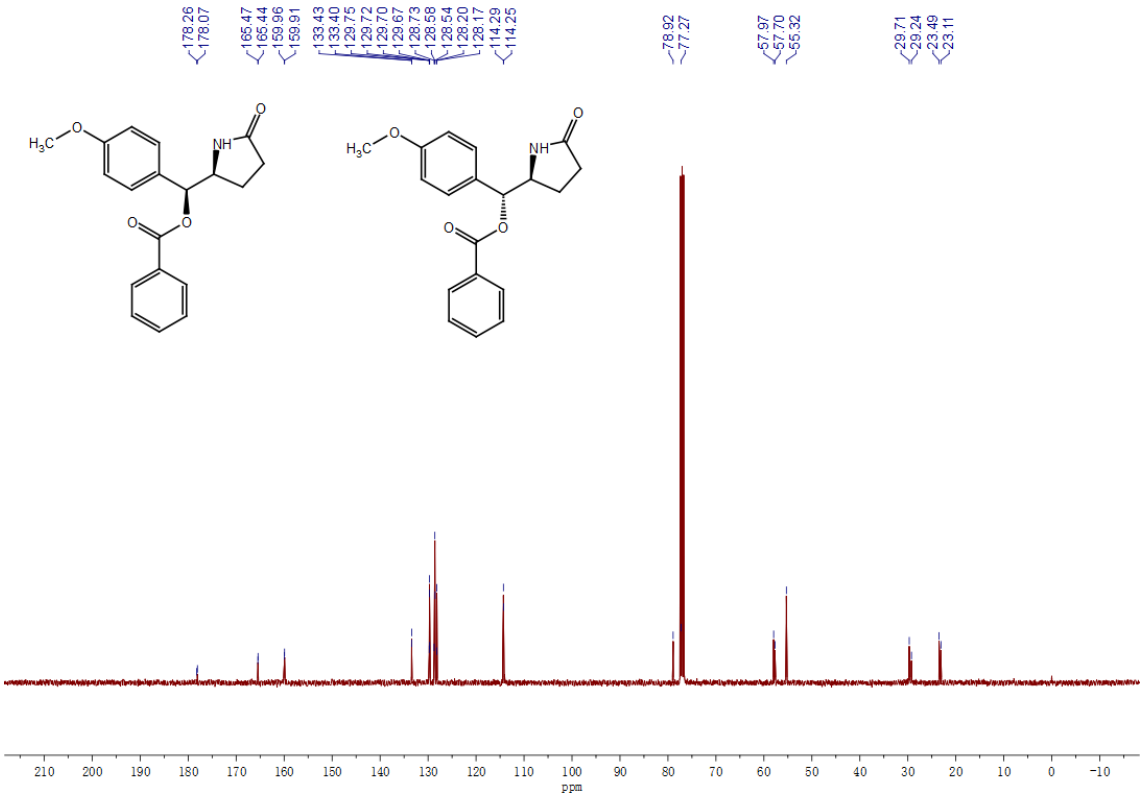
^{13}C NMR of 13b



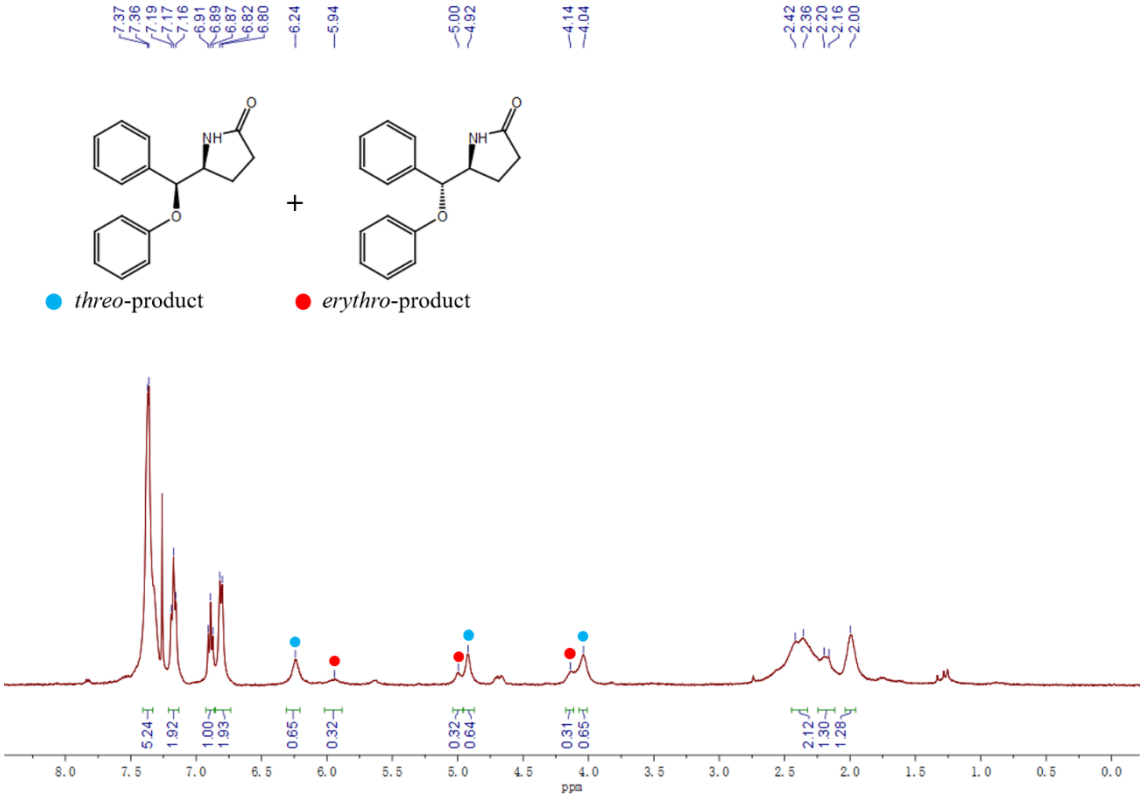
^{1}H NMR of 13c



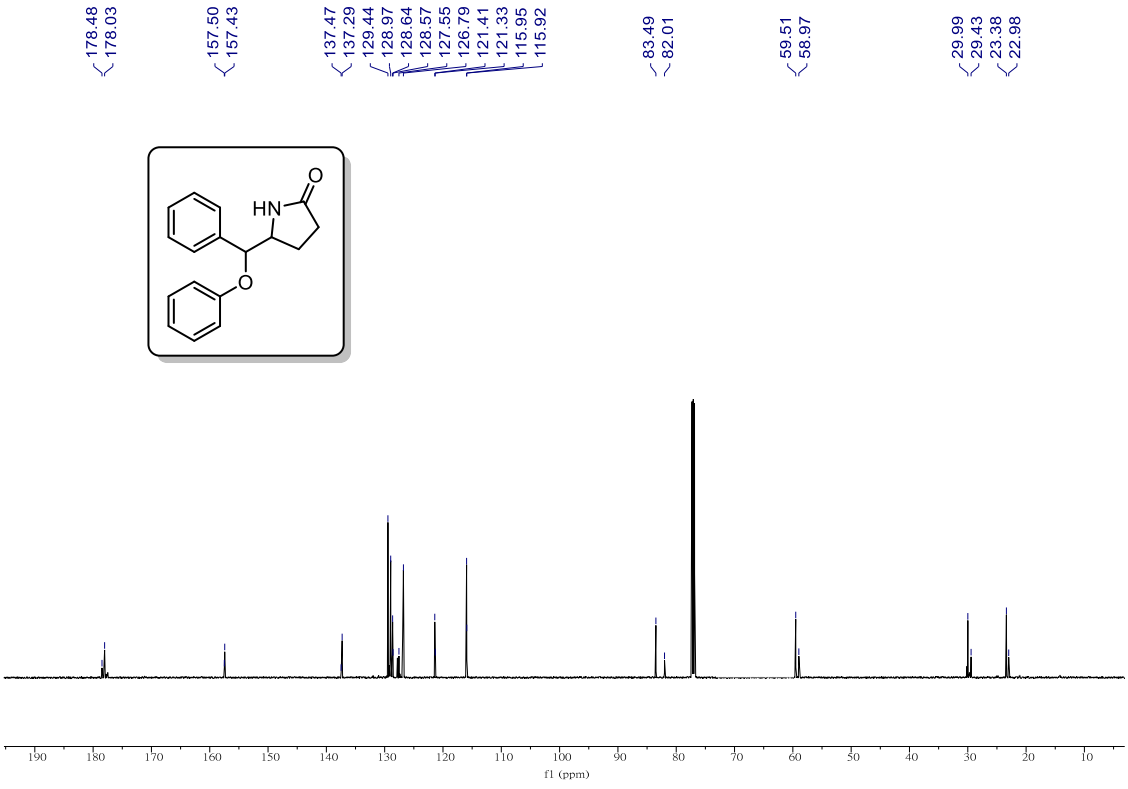
^{13}C NMR of 13c



^{1}H NMR of 13d



^{13}C NMR of 13d

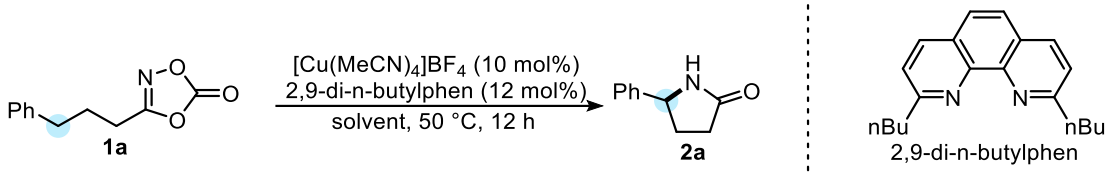


A.4 Supplementary Information of Chapter 3

Experimental Optimization of Cu-catalyzed C(sp^3)–H Amidation for the Synthesis of γ-Lactam

General procedure: All reactions were performed in a glovebox under an N_2 atmosphere. Cu catalyst (10 mol%) and ligand (12 mol%) were added to an oven-dried 8 mL vial equipped with a magnetic stir bar. Solvent (2 mL) was added to the resultant mixture and stirred at specified temperature for 3 min. 3-(3-phenylpropyl)-1,4,2-dioxazol-5-one **1a** (0.2 mmol, 42 mg) was then added to the solution and capped. After stirring at room temperature for 12 h, the reaction mixture was filtered through a pad of silica gel and washed with EtOAc (2 mL × 3). The mixture was concentrated under vacuum. The NMR yield was obtained by ^{1}H NMR spectroscopic analysis using $CDCl_3$ (0.7 mL) as solvent with CH_2Br_2 (0.2 mmol, 13.96 uL) as internal standard.

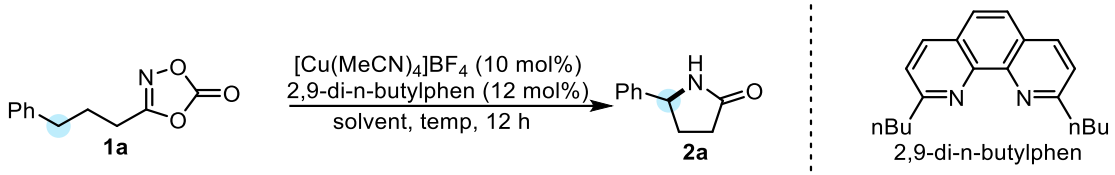
Table A5 Effect of Solvents[a]



entry	solvent	yield of **2a**[b] (%)
1	toluene	9
2	dioxane	27
3	THF	14
4	DCE	10
5	DCM	40
6	acetone	24
7	MeCN	40
8	MeOH	10
9	**TFE**	**76**
10	**HFIP**	**83**

[a]**1a** (0.2 mmol), Cu catalyst (10 mol%), ligand (12 mol%), solvent (2 mL), 50 °C, 12 h, N_2. [b]^{1}H NMR yield using CH_2Br_2 as internal standard.

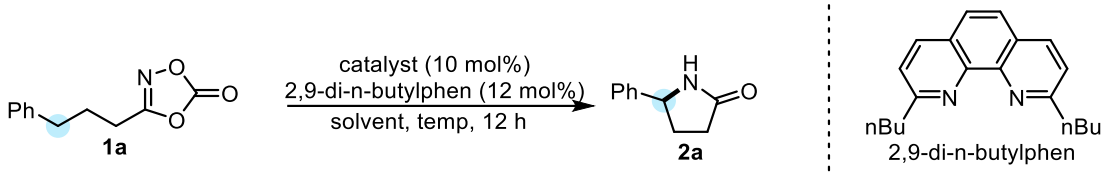
Table A6 Effect of Solvents and Temperature[a]



entry	solvent	Temperature (°C)	yield of **2a**[b] (%)
1	DCE	rt	<1
2	DCE	50	10
3	**TFE**	**rt**	**90**
4	TFE	50	76
5	**HFIP**	**rt**	**93**
6	HFIP	50	83
7	dioxane	rt	<1
8	dioxane	50	27
9	**NFTB**	**rt**	**60**

[a]**1a** (0.2 mmol), Cu catalyst (10 mol%), ligand (12 mol%), solvent (2 mL), 12 h, N_2. [b]^{1}H NMR yield using CH_2Br_2 as internal standard.

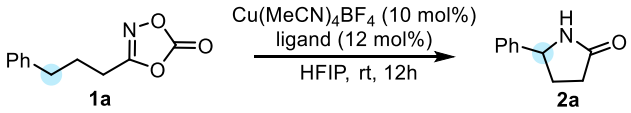
Table A7 Effect of Copper Salt[a]

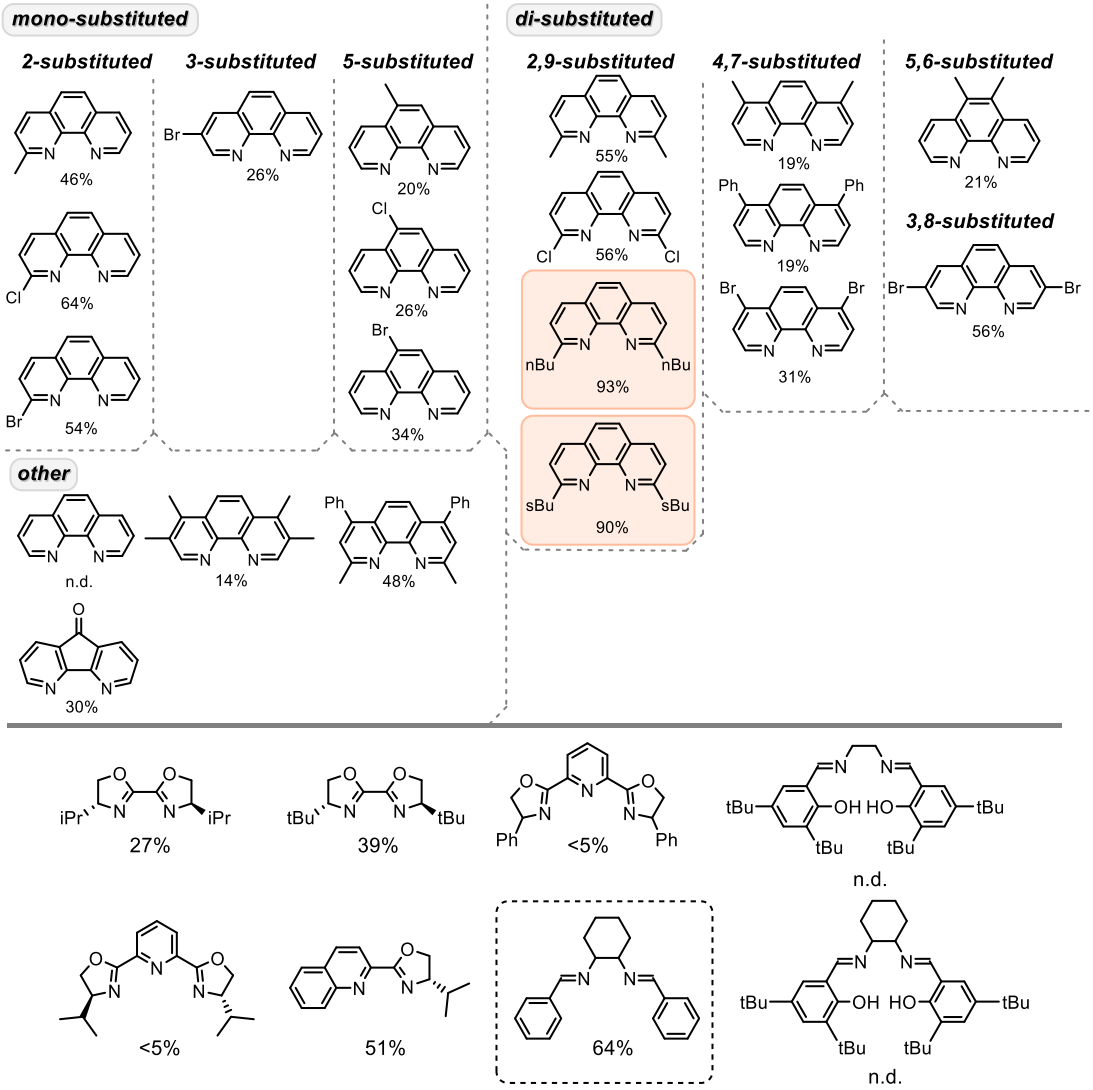


entry	catalyst	solvent	temp/ °C	yield of **2a**[b] (%)
1	$[Cu(MeCN)_4]BF_4$	DCE	50	10
2	$[Cu(MeCN)_4]PF_6$	DCE	50	24
3	**$[Cu(MeCN)_4]BF_4$**	**TFE**	**50**	**76**
4	$[Cu(MeCN)_4]PF_6$	TFE	50	28
5	**$[Cu(MeCN)_4]BF_4$**	**HFIP**	**rt**	**93**
6	$[Cu(MeCN)_4]PF_6$	HFIP	rt	75
7	**$Cu(OAc)_2$**	**HFIP**	**rt**	**79**
8	Cu_2O	HFIP	rt	n.r.
9	CuCN	HFIP	rt	6
10	CuF_2	HFIP	rt	n.r.
11	$CuCl_2$	HFIP	rt	n.r.
12	$CuSO_4\,5H_2O$	HFIP	rt	n.r.
13	$Cu(OTf)_2$	HFIP	rt	85
14	CuOAc	HFIP	rt	84
15	$[Cu(OTf)]_2\,C_6H_6$	HFIP	rt	87
16	CuI	HFIP	rt	n.r.

[a]**1a** (0.2 mmol), Cu catalyst (10 mol%), ligand (12 mol%), solvent (2 mL), 12 h, N_2. [b]^{1}H NMR yield using CH_2Br_2 as internal standard, isolated yield in parentheses

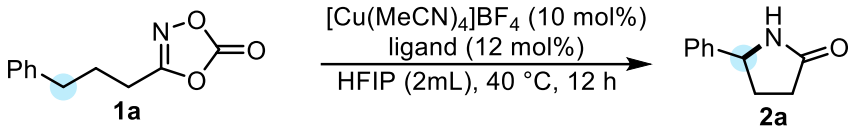
Table A8 Effect of Ligands[a-b]

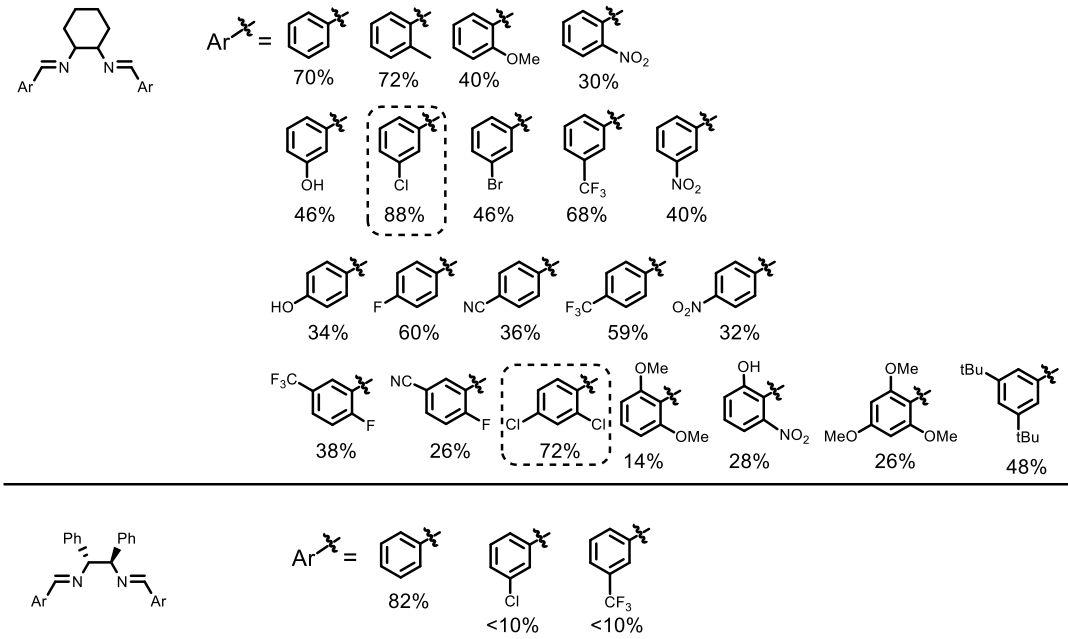




[a]**1a** (0.2 mmol), Cu catalyst (10 mol%), ligand (12 mol%), solvent (2 mL), 12 h, N_2. [b]^{1}H NMR yield using CH_2Br_2 as internal standard.

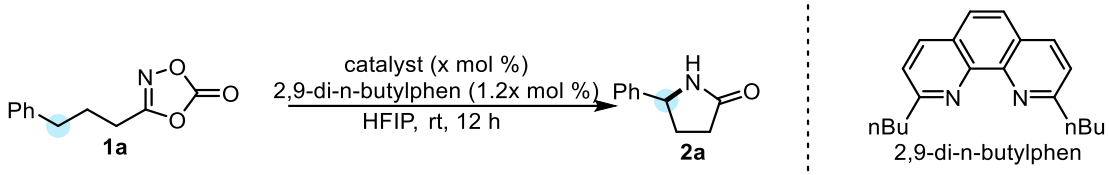
Table A9 Effect of Ligands[a-b]





[a]**1a** (0.2 mmol), Cu catalyst (10 mol%), ligand (12 mol%), solvent (2 mL), 40 °C, 12 h, N_2. [b]^{1}H NMR yield using CH_2Br_2 as internal standard.

Table A10 Effect of Catalyst Loading[a]



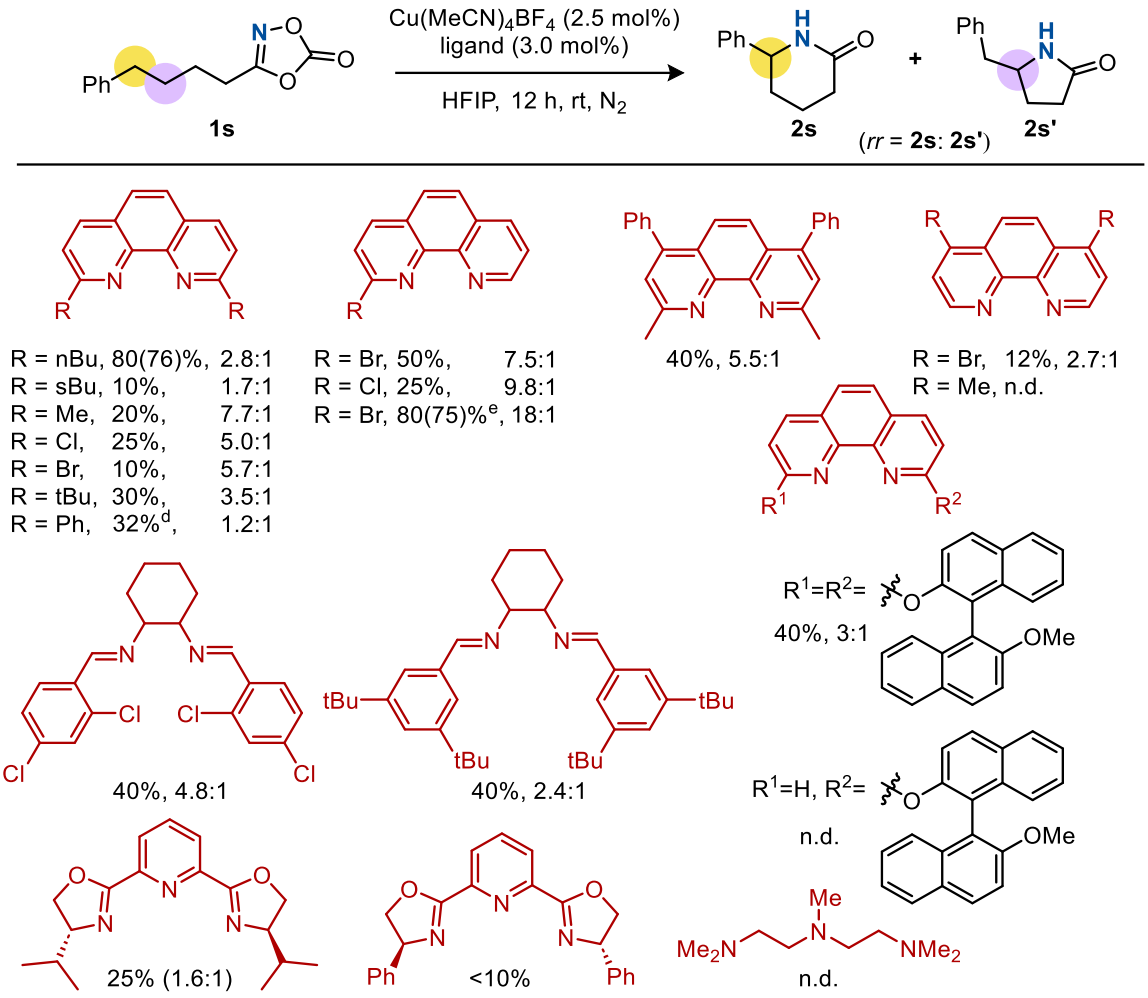
entry	catalyst (mol%)	yield of **2a**[b] (%)
1	$[Cu(MeCN)_4]BF_4$ (0.025 mol%)	n.r.
2	$[Cu(MeCN)_4]BF_4$ (0.25 mol%)	30
3	**$[Cu(MeCN)_4]BF_4$ (2.5 mol%)**	**99**
4	**$[Cu(MeCN)_4]BF_4$ (10 mol%)**	**93**

[a]**1a** (0.2 mmol), [Cu] catalyst (x mol%), ligand (1.2x mol%), HFIP (2 mL), 12 h, N_2. [b]^{1}H NMR yield using CH_2Br_2 as internal standard.

Experimental Optimization of Cu-Catalyzed Regioselective δ-/ γ-Lactam Synthesis

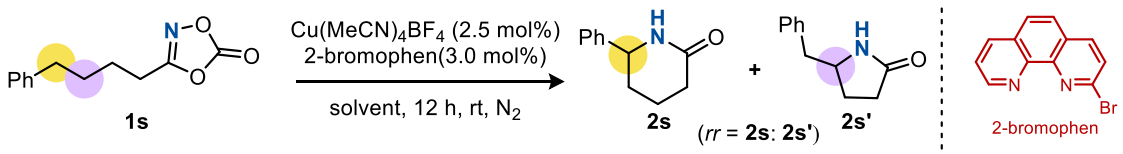
General procedure: All reactions were performed in a glovebox under an N_2 atmosphere. Cu catalyst (2.5 mol%) and ligand (3.0 mol%) were added to an oven-dried 8 mL vial equipped with a magnetic stir bar. Solvent (2 mL) was added to the resultant mixture and stirred at specified temperature for 3 min. 3-(4-phenylbutyl)-1,4,2-dioxazol-5-one **1s** (0.2 mmol) was then added to the solution and capped. After stirring at room temperature for 12 h, the reaction mixture was filtered through a pad of silica gel and washed with EtOAc (2 mL × 3). The mixture was concentrated under vacuum. The NMR yield was obtained by ^{1}H NMR spectroscopic analysis using $CDCl_3$ (0.7 mL) as solvent with CH_2Br_2 (0.2 mmol, 13.96 uL) as internal standard.

Table A11 Effect of Ligands on δ- versus γ-Lactamization Regioselectivity[a-c]



[a]Reaction conditions: **1s** (0.2 mmol), $[Cu(MeCN)_4]BF_4$ (2.5 mol%), and ligand (3.0 mol%) in HFIP under N_2 for 12 hours at room temperature. [b] ^1H NMR yield; Isolated yield in parentheses; Combined yield of **2** and **2′**. [c]Regioselectivity (*rr*) were determined by ^1H NMR of the crude reaction mixture. [d]Reaction run in 10 mol% catalyst and 12 mol% ligand. [e]Reaction run in HFIP: toluene = 4: 1.

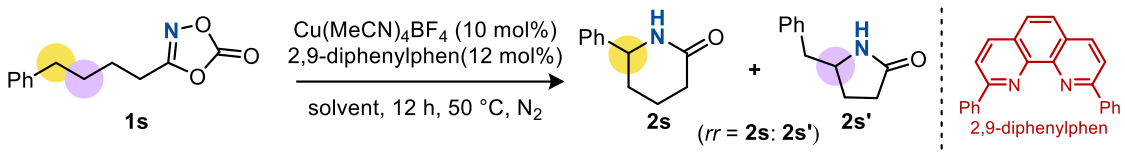
Table A12 Effect of Solvents on δ- versus γ-Lactamization Regioselectivity Using 2-Bromophenanthroline Ligand[a]



entry	solvent	combined yield[b] (%)	δ vs γ[c]
1	TFE	20	>20: 1
2	HFIP	50	7.5: 1
3	NFTB	20	4: 1
4	HFIP: toluene (1: 1)	50.	>20: 1
5	HFIP: toluene (2: 1)	50	>20: 1
6	HFIP: toluene (3: 1)	57	>20: 1
7	**HFIP: toluene (4: 1)**	**78(75)**	**18: 1**

[a]Reaction conditions: **1s** (0.2 mmol), $[Cu(MeCN)_4]BF_4$ (10 mol%), and 2,9-diphenylphenanthroline (12 mol%) in specified solvent under N_2 for 12 hours at 50 °C. [b] ^1H NMR yield; Isolated yield in parentheses; Combined yield of **2** and **2′**. [c]Regioselectivity (*rr*) was determined by ^1H NMR of the crude reaction mixture.

Table A13 Effect of Solvents on δ- versus γ-Lactamization Regioselectivity Using 2,9-Diphenylphenanthroline Ligand[a]

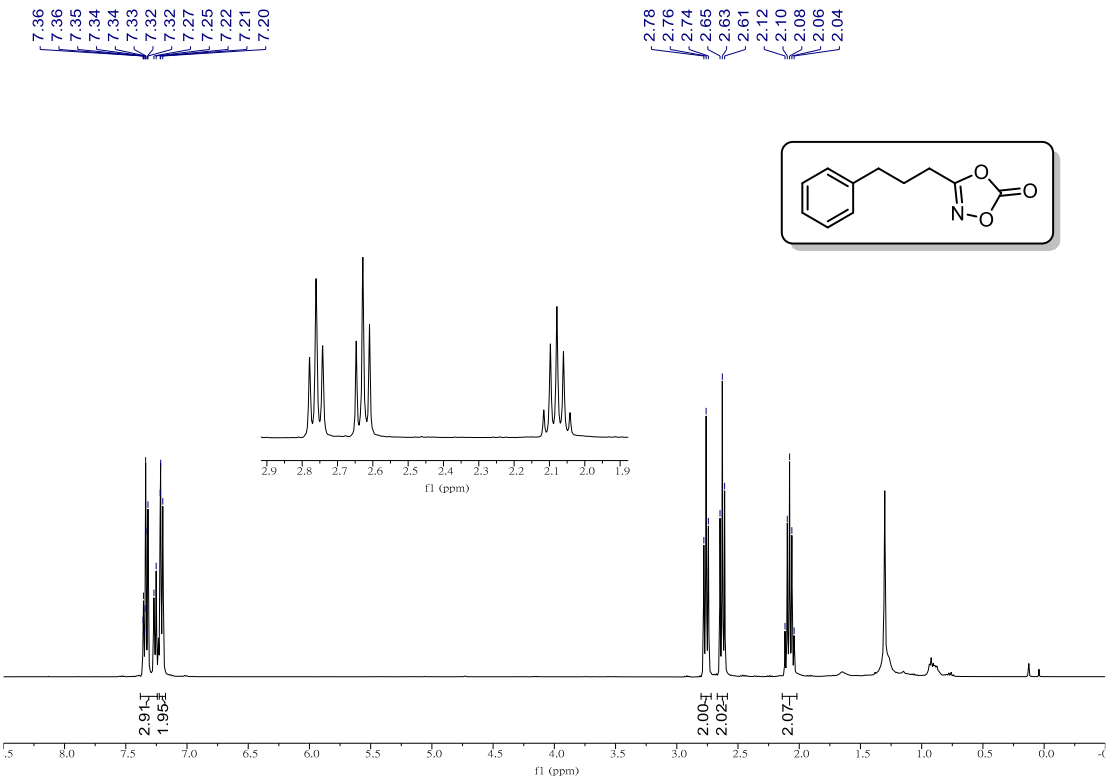


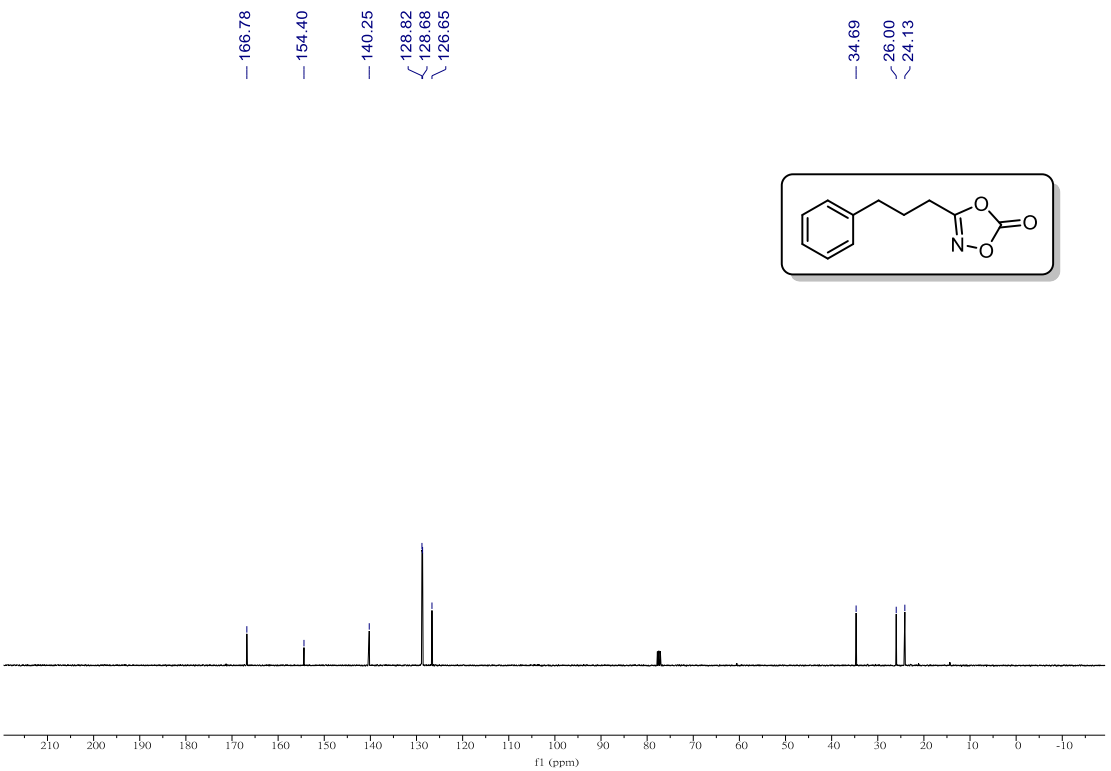
entry	solvent	combined yield[b] (%)	δ vs γ[c]
1	MeCN	12	>20: 1
2	DCM	n.d.	-
3	dioxane	17	>20: 1
4	PhCl	n.d.	-
5	TFE	40	3.2: 1
6	HFIP	32	1.2: 1
7	NFTB	40	1: 3.1
8	**NFTB: toluene (1: 1)**	**55(51)[d]**	**1: 3.6**
9	NFTB: toluene (4: 1)	35[d]	1: 5.2

[a]Reaction conditions: **1s** (0.2 mmol), $[Cu(MeCN)_4]BF_4$ (10 mol%), and 2,9-diphenylphenanthroline (12 mol%) in specified solvent under N_2 for 12 hours at 50 °C. [b] ^1H NMR yield; Isolated yield in parentheses; Combined yield of **2** and **2′**. [c]Regioselectivity (*rr*) was determined by ^1H NMR of the crude reaction mixture. [d]Reaction run at room temperature.

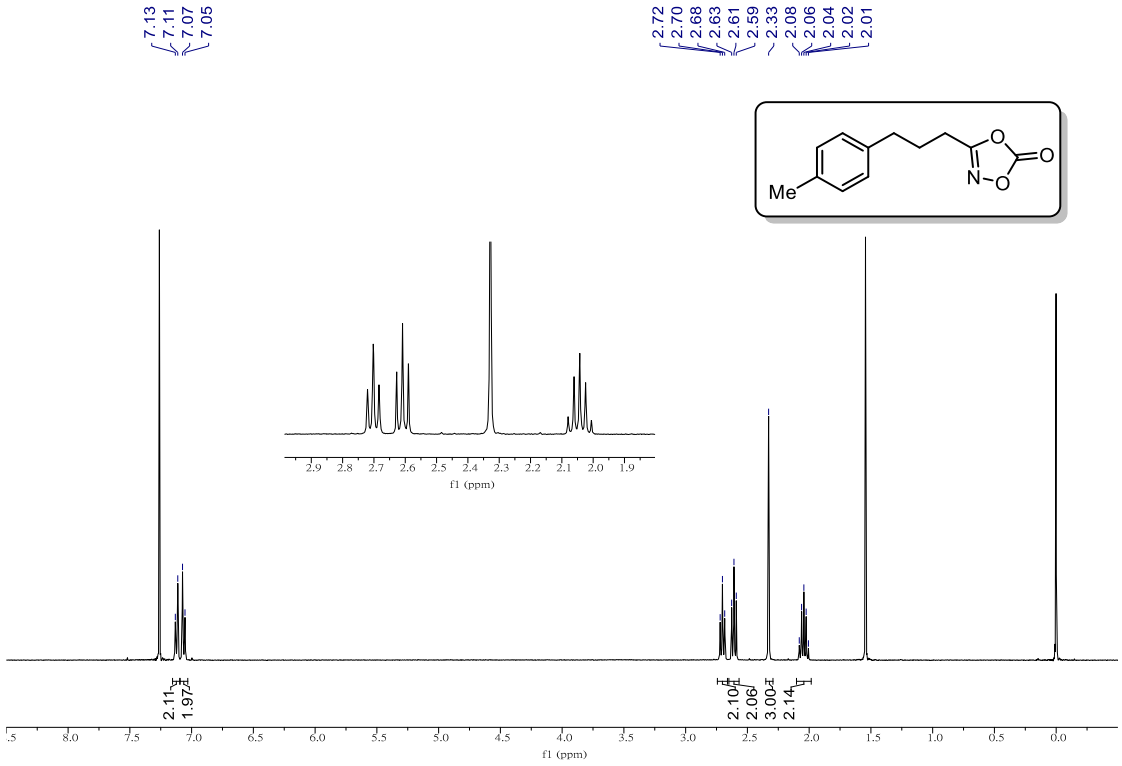
A.4 NMR Spectra of Chapter 3

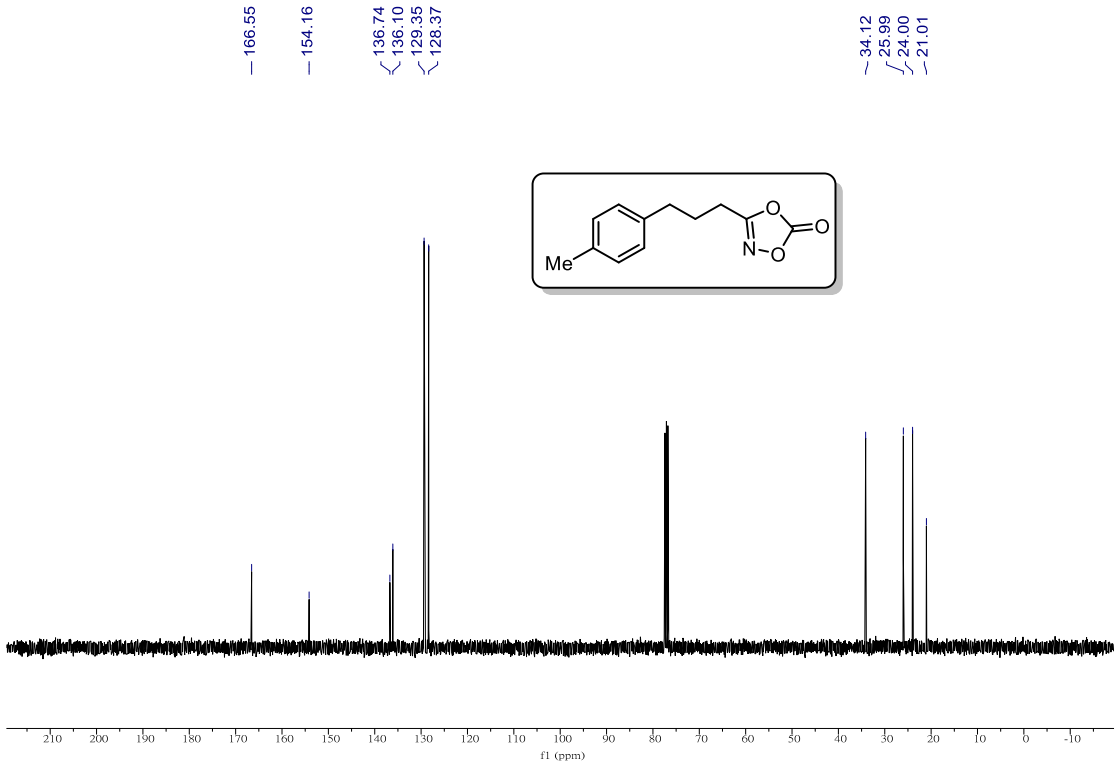
3-(3-Phenylpropyl)-1,4,2-dioxazol-5-one



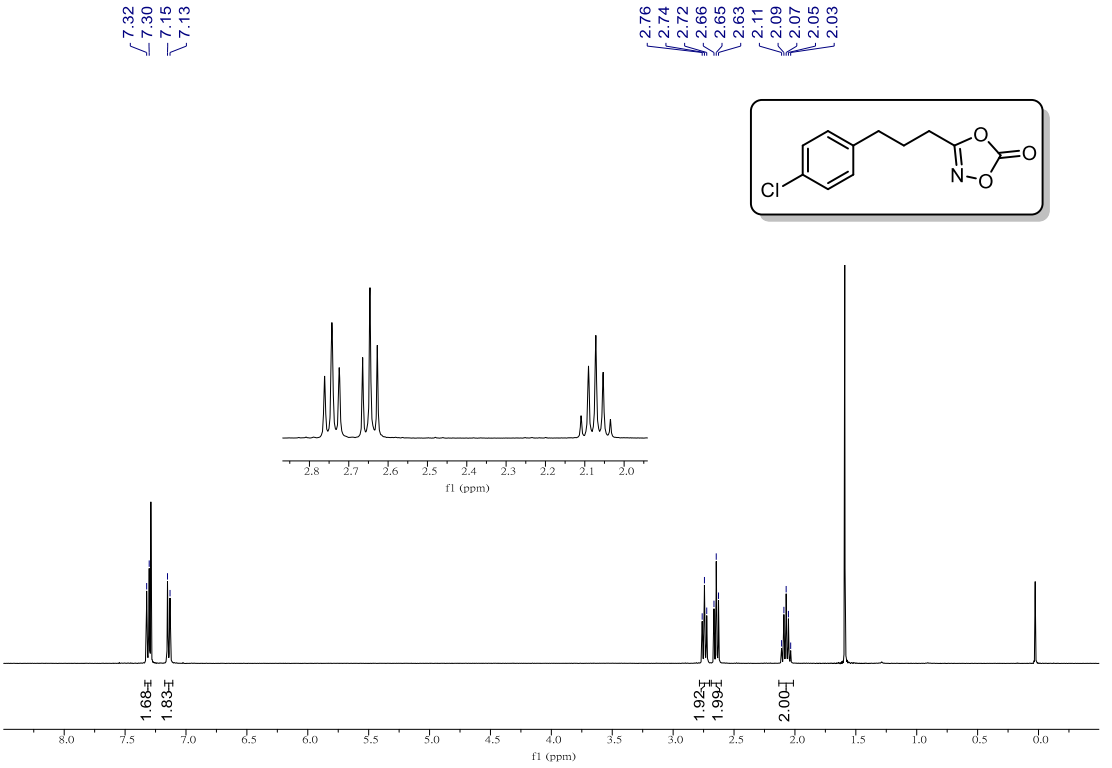


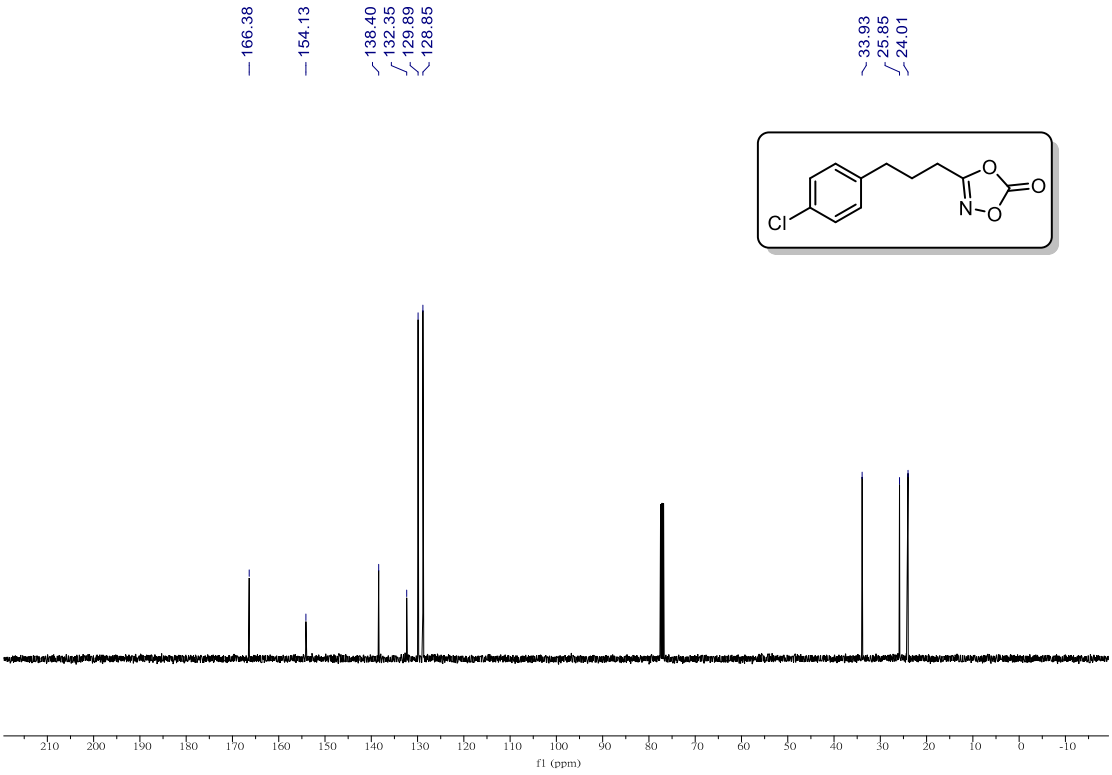
3-(3-(p-Tolyl)propyl)-1,4,2-dioxazol-5-one



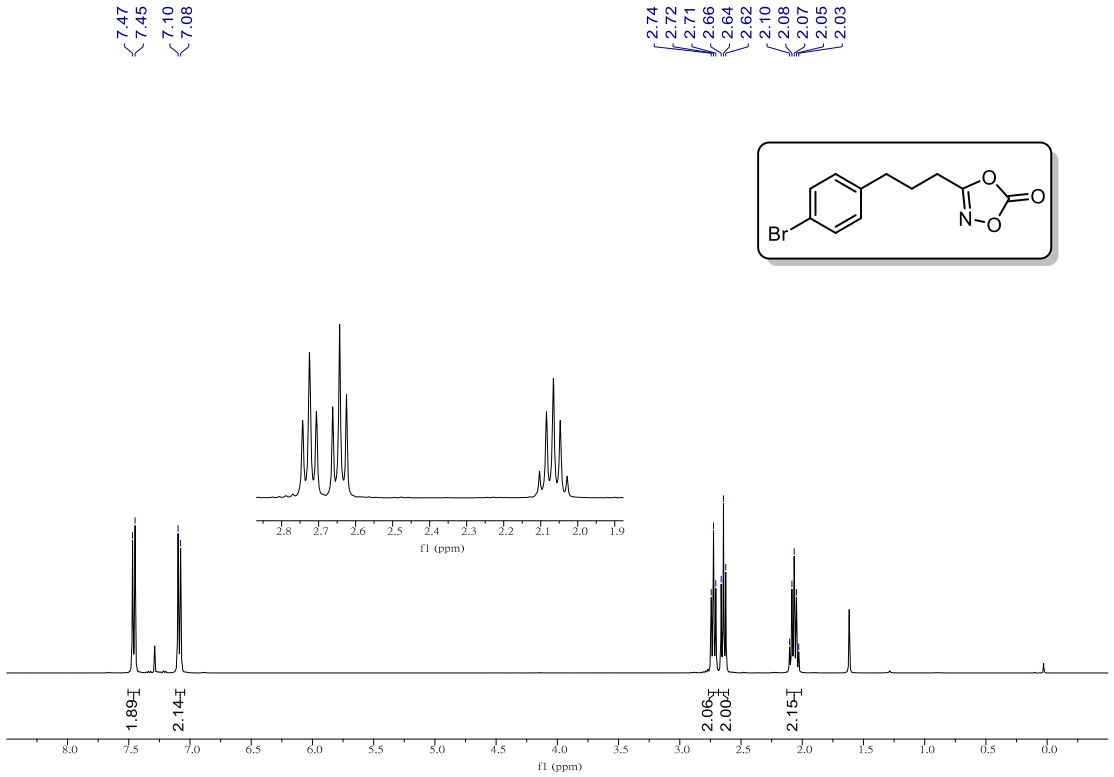


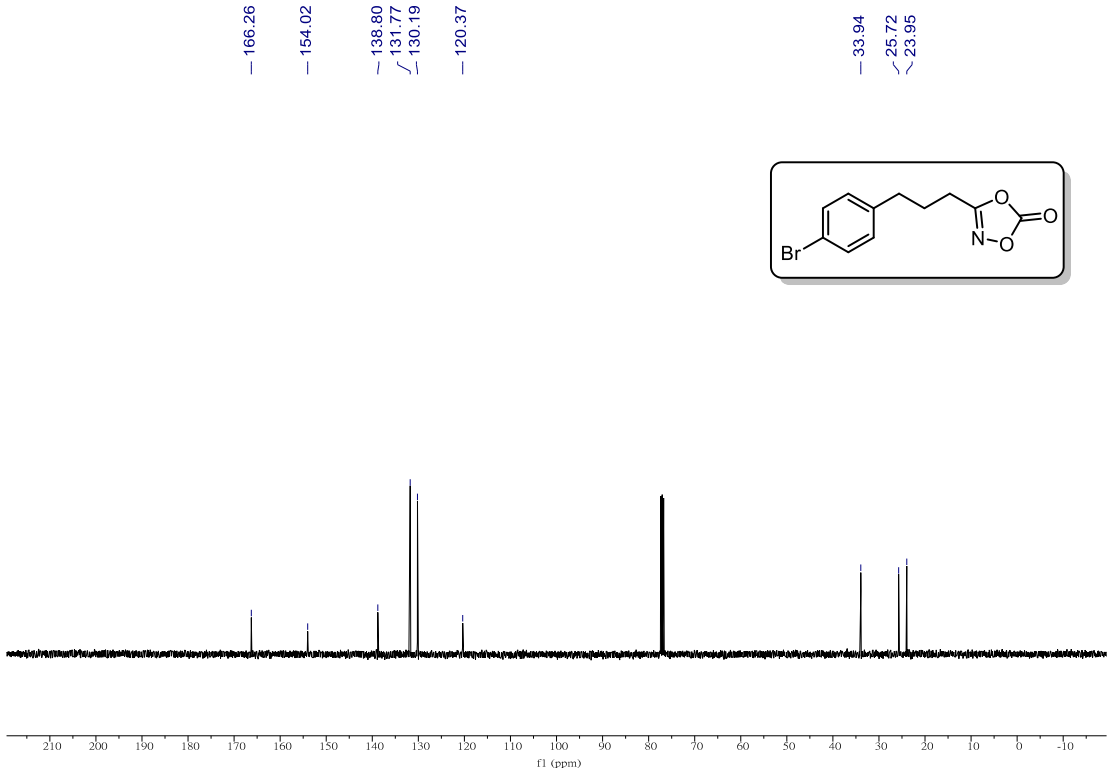
3-(3-(4-Chlorophenyl)propyl)-1,4,2-dioxazol-5-one



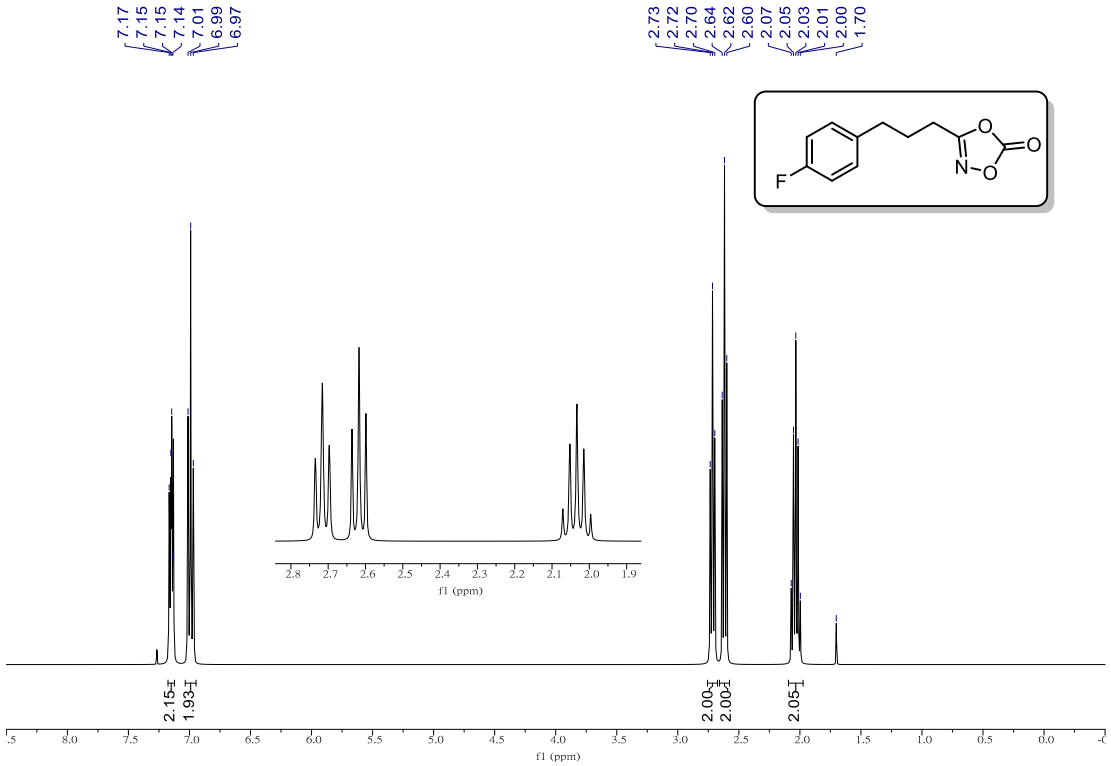


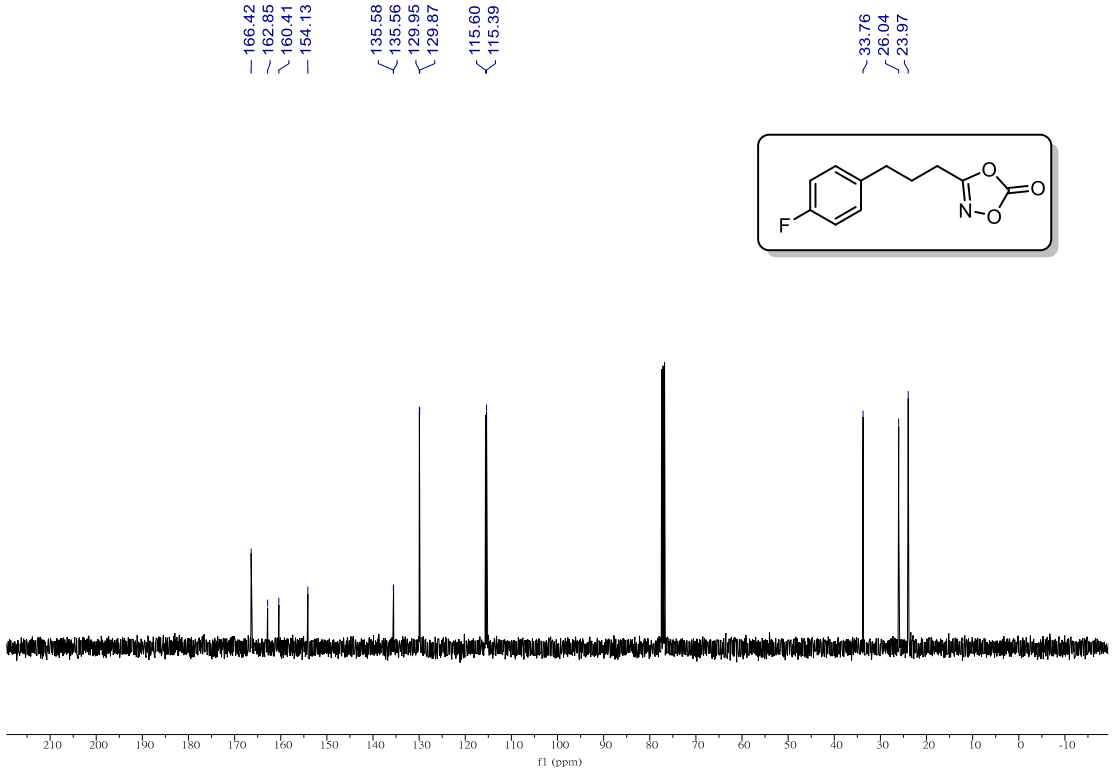
3-(3-(4-Bromophenyl)propyl)-1,4,2-dioxazol-5-one

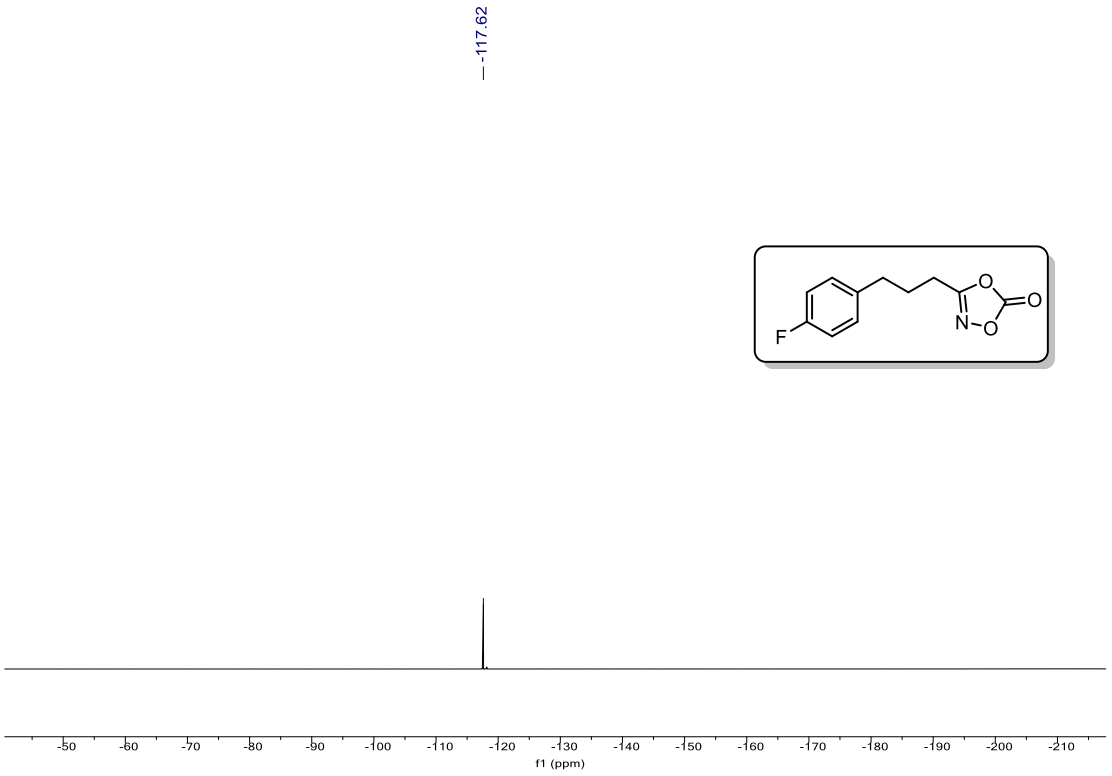




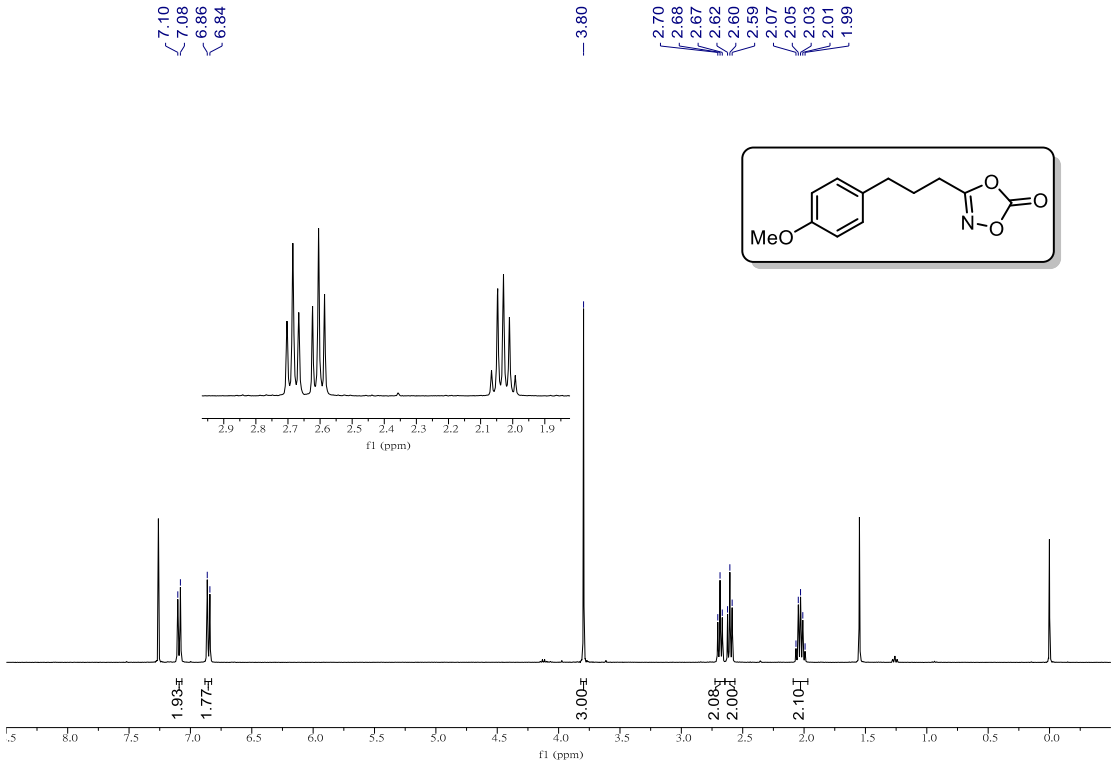
3-(3-(4-Fluorophenyl)propyl)-1,4,2-dioxazol-5-one

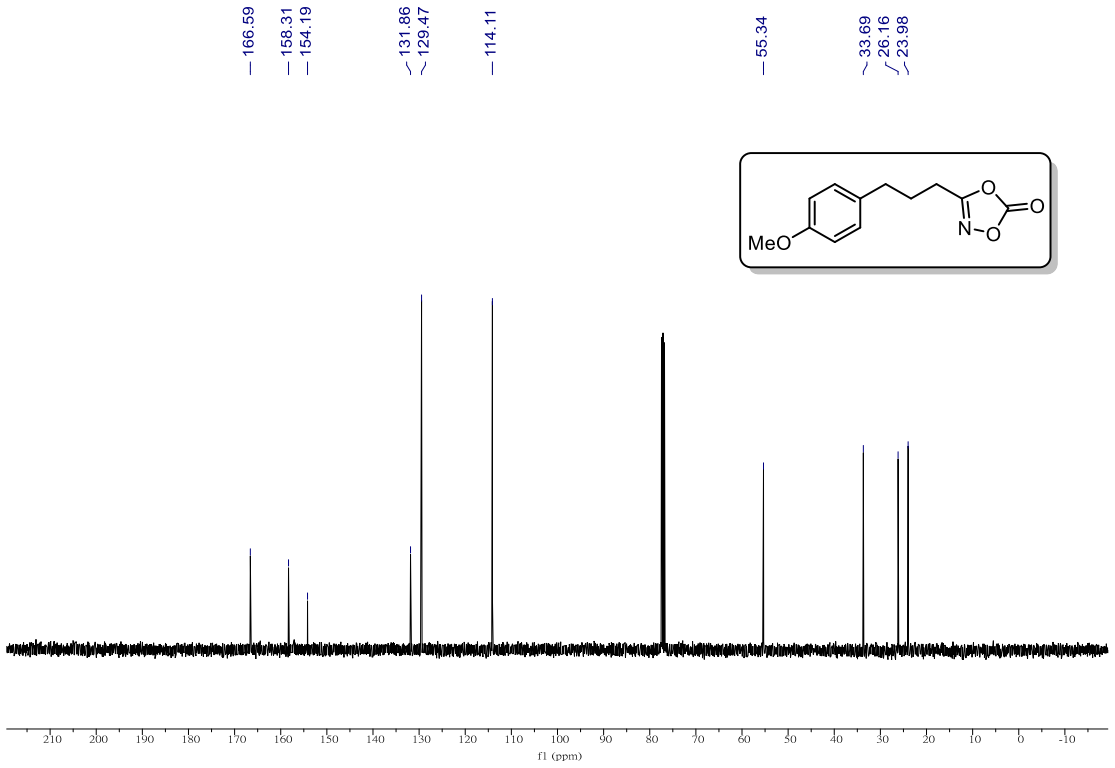




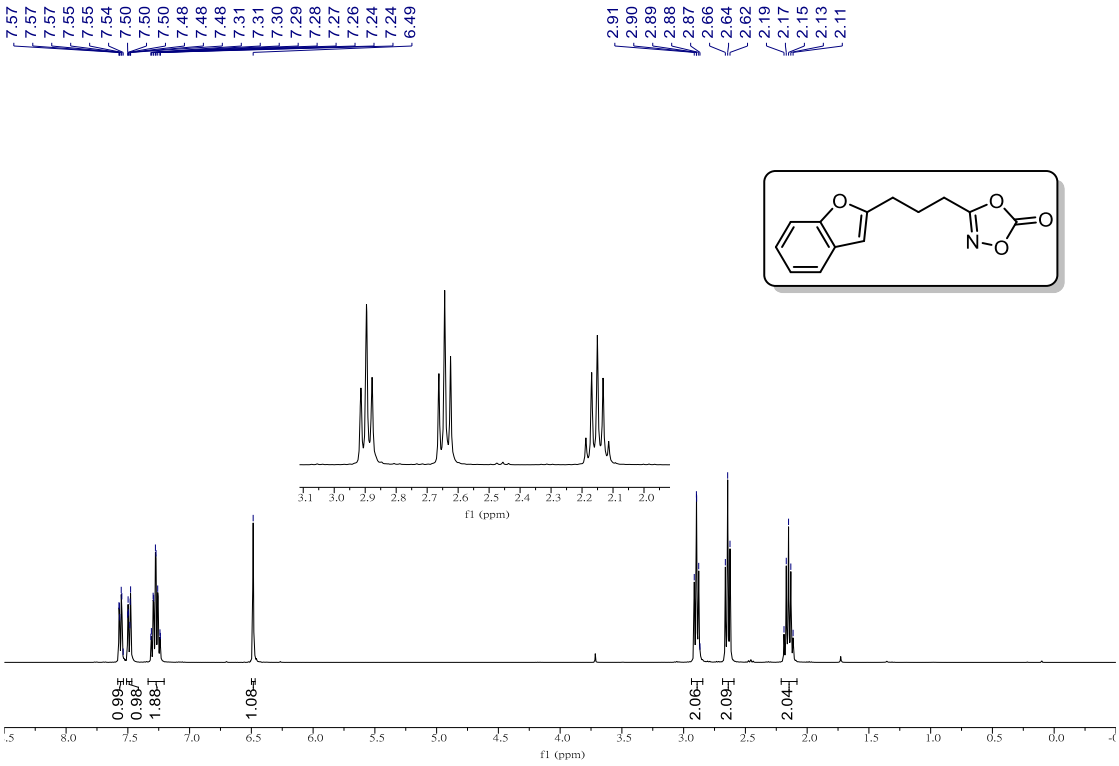

-117.62
F
O
O
N
O
-50
-60
-70
-80
-90
-100
-110
-120
-130
-140
-150
-160
-170
-180
-190
-200
-210
f1 (ppm)

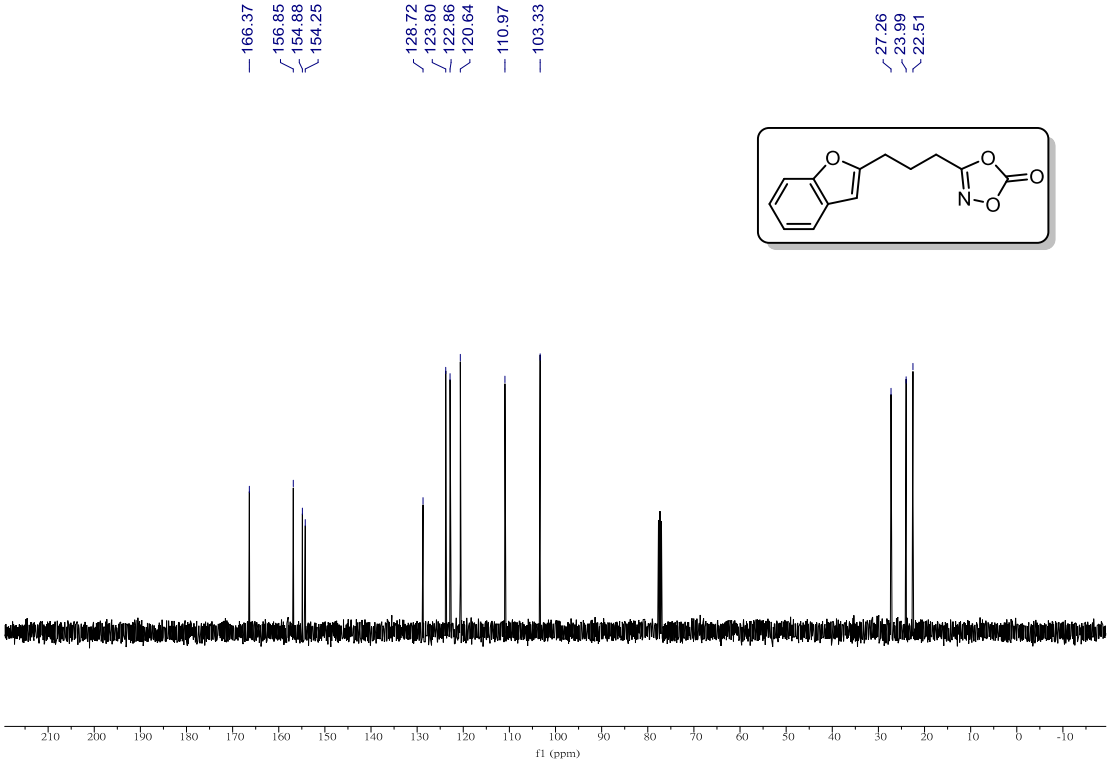
3-(3-(4-Methoxyphenyl)propyl)-1,4,2-dioxazol-5-one



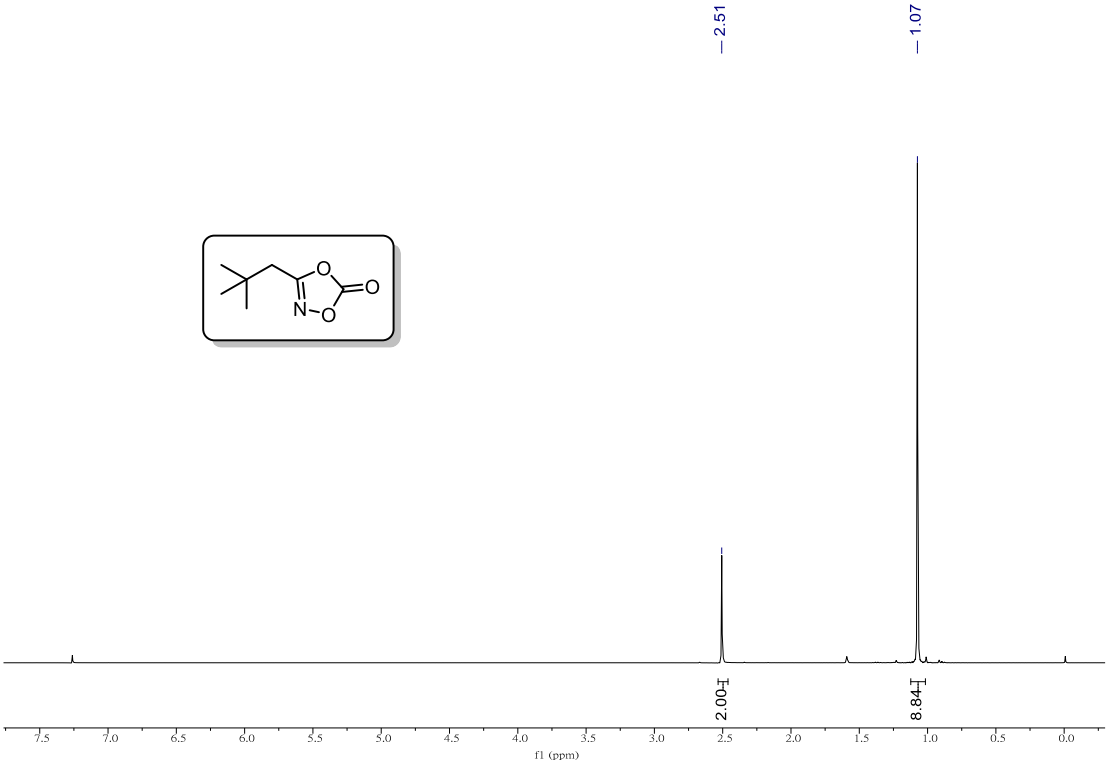


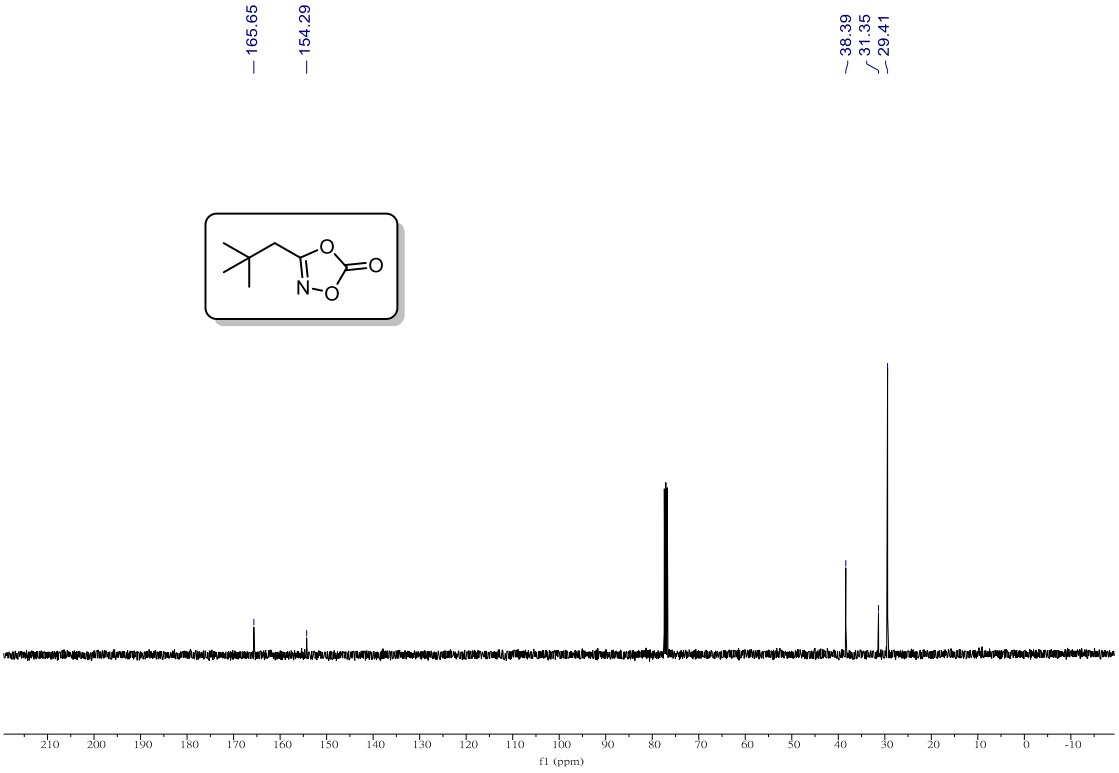
3-(3-(Benzofuran-2-yl)propyl)-1,4,2-dioxazol-5-one



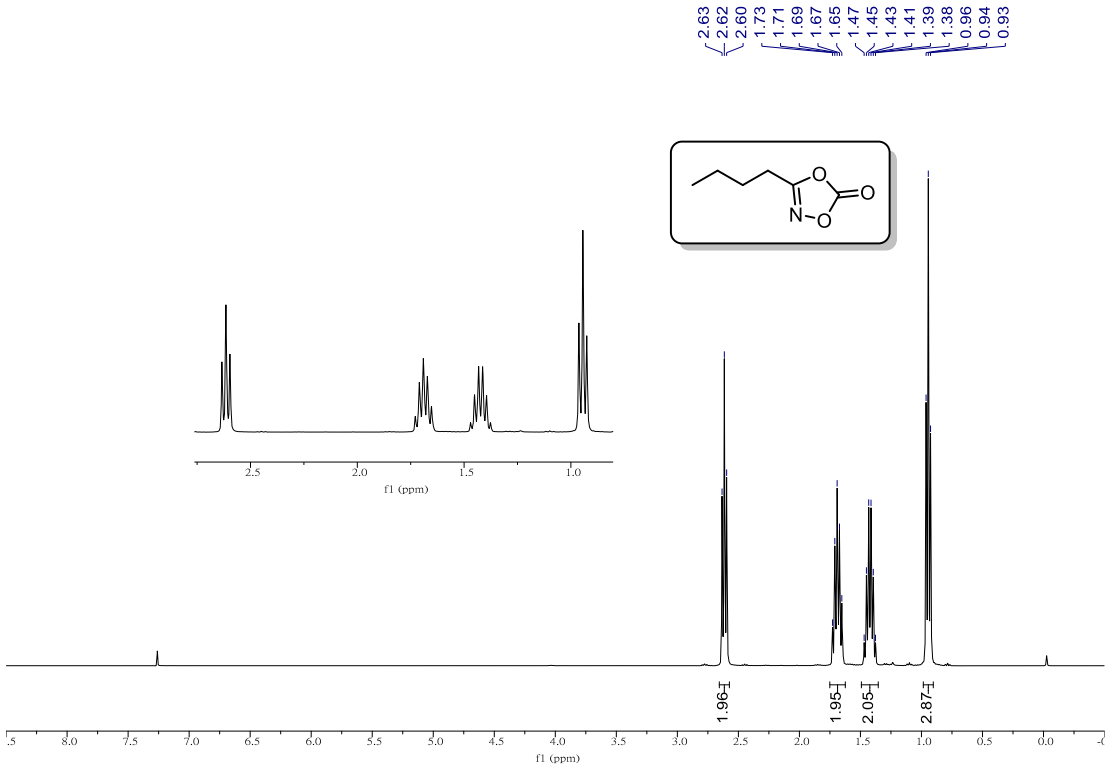


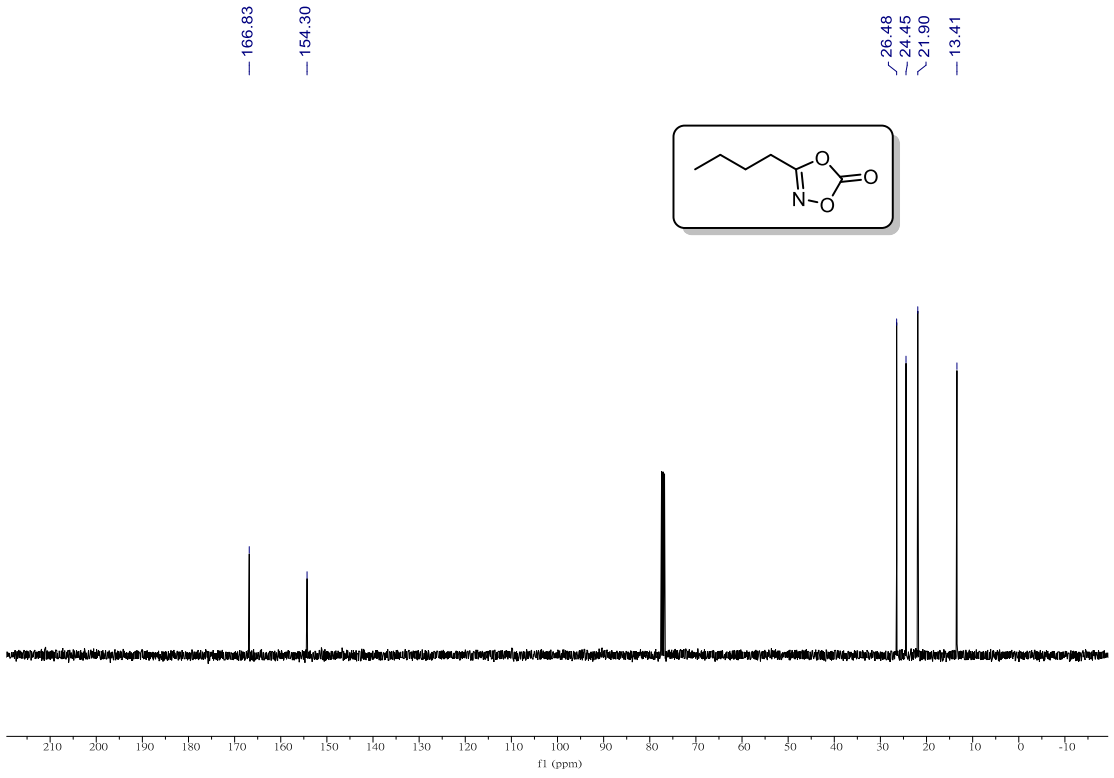
3-Neopentyl-1,4,2-dioxazol-5-one



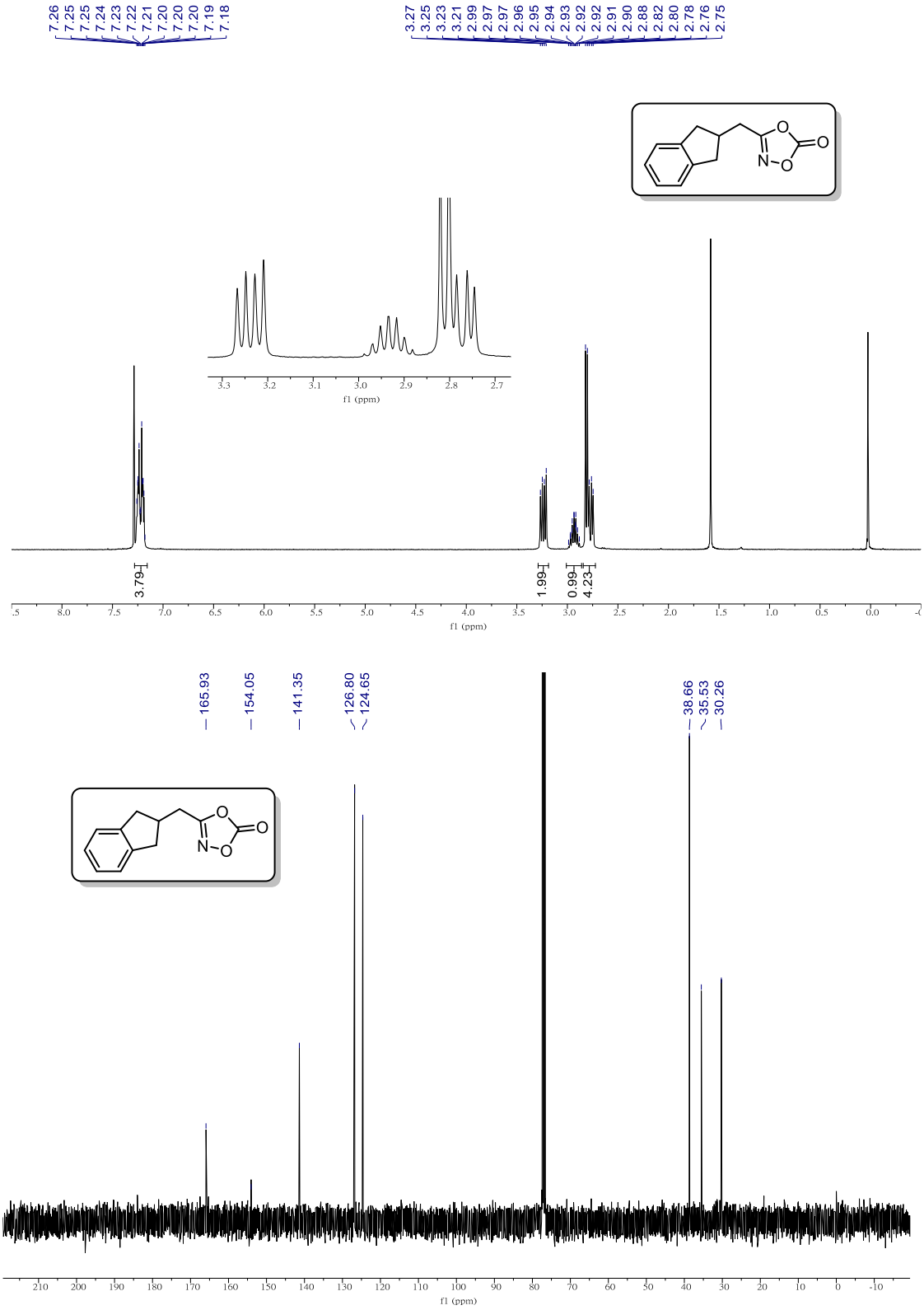


3-Butyl-1,4,2-dioxazol-5-one

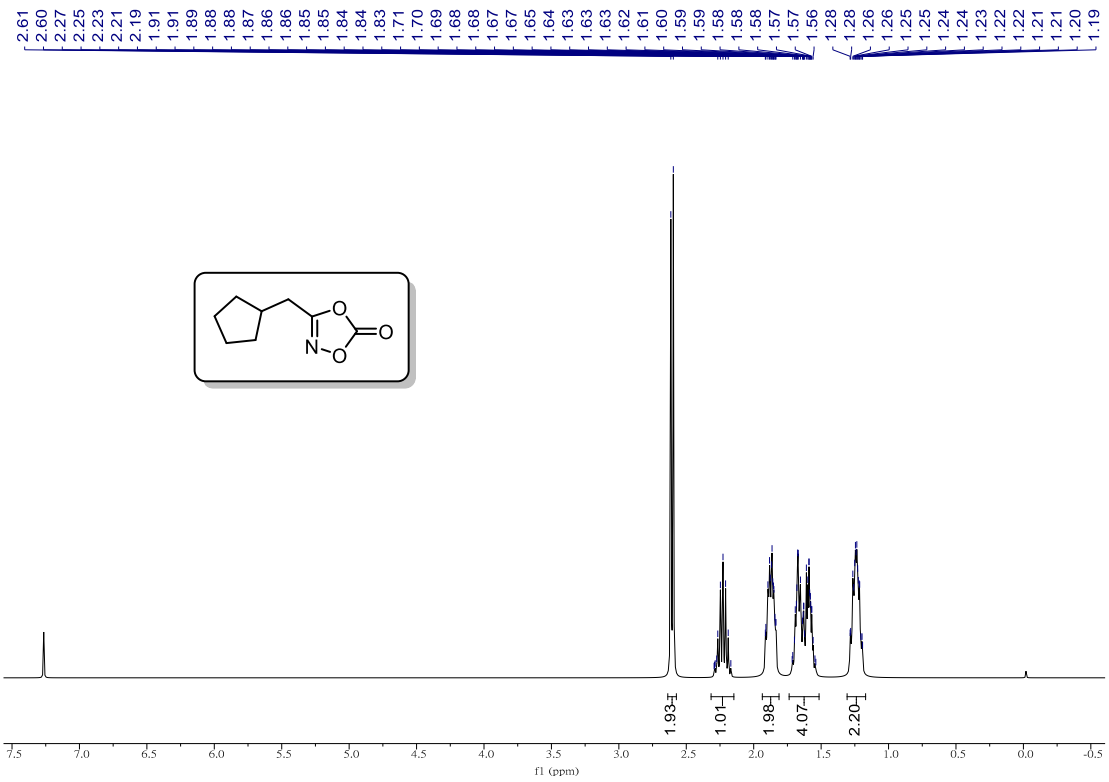


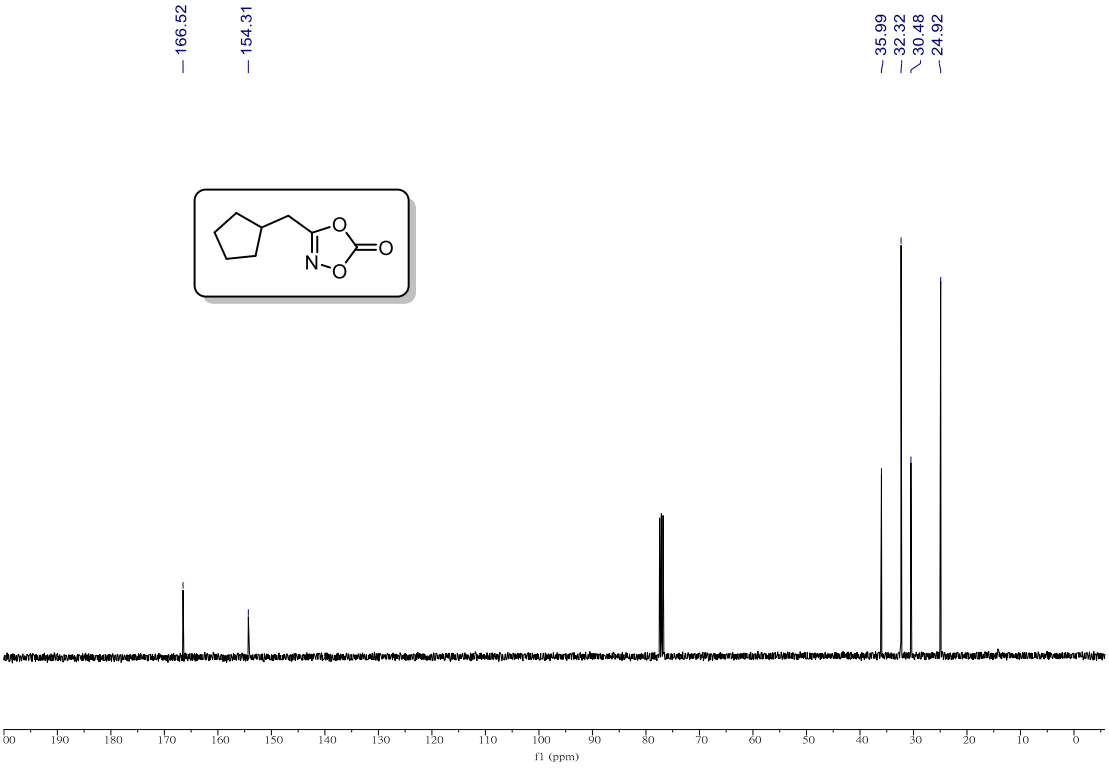


3-((2,3-Dihydro-1H-inden-2-yl)methyl)-1,4,2-dioxazol-5-one

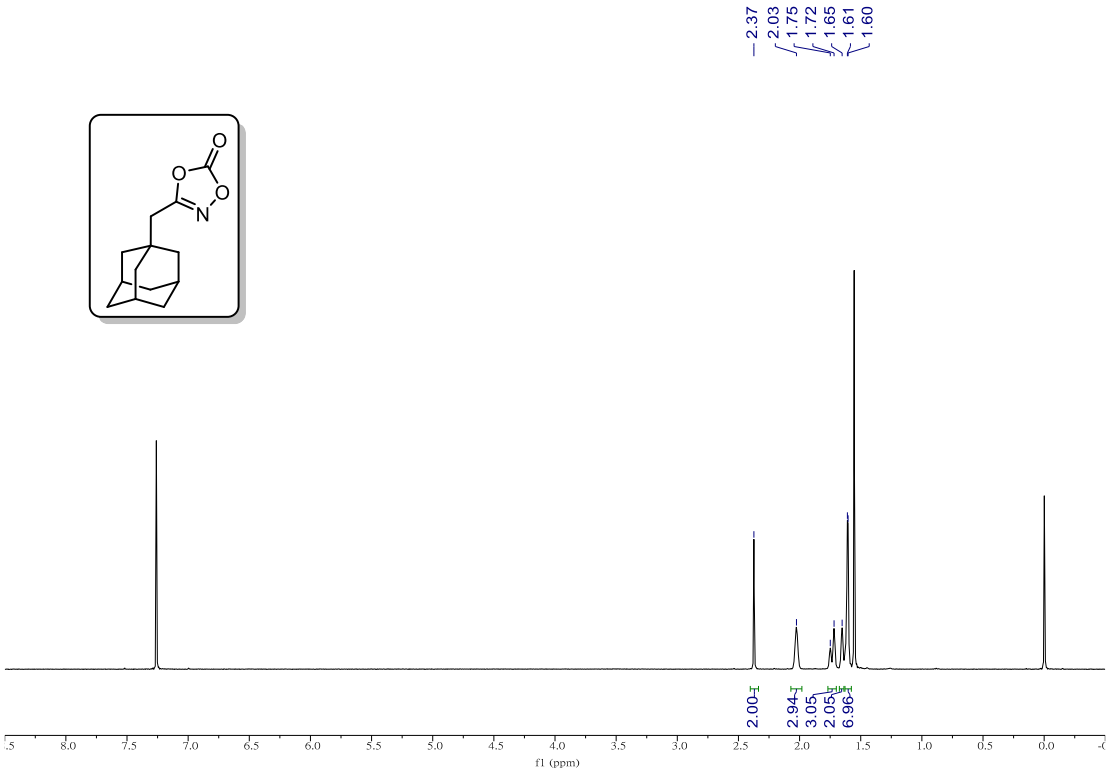


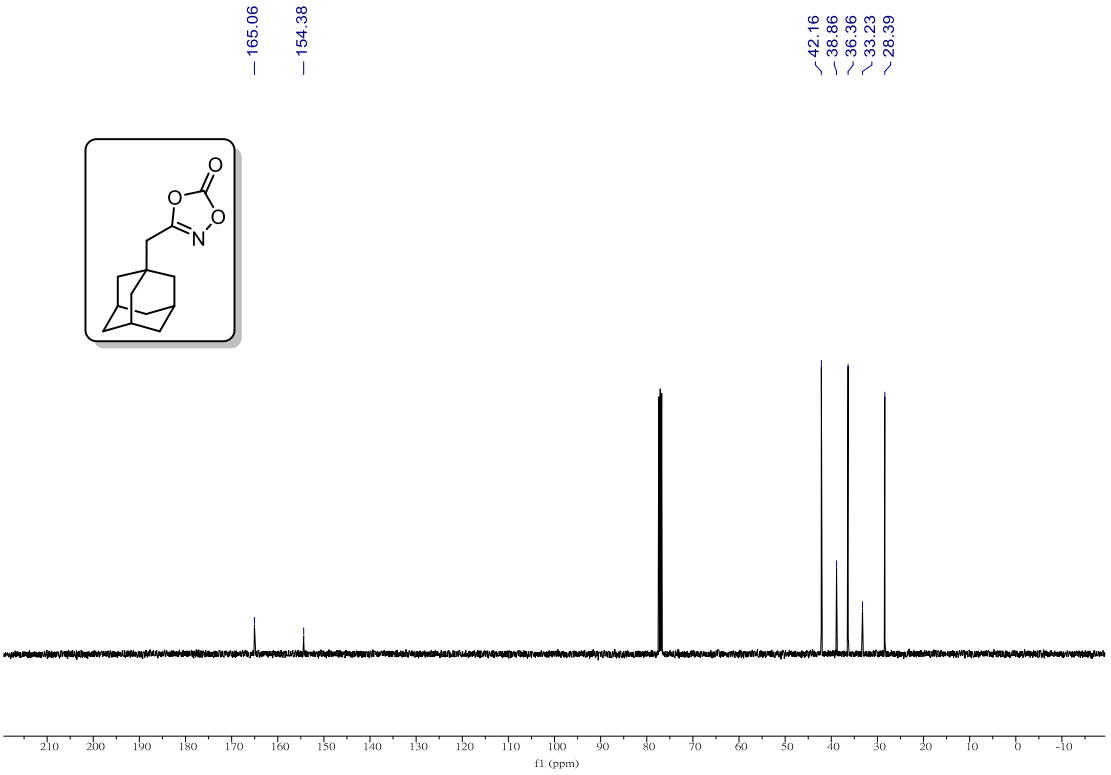
3-(Cyclopentylmethyl)-1,4,2-dioxazol-5-one



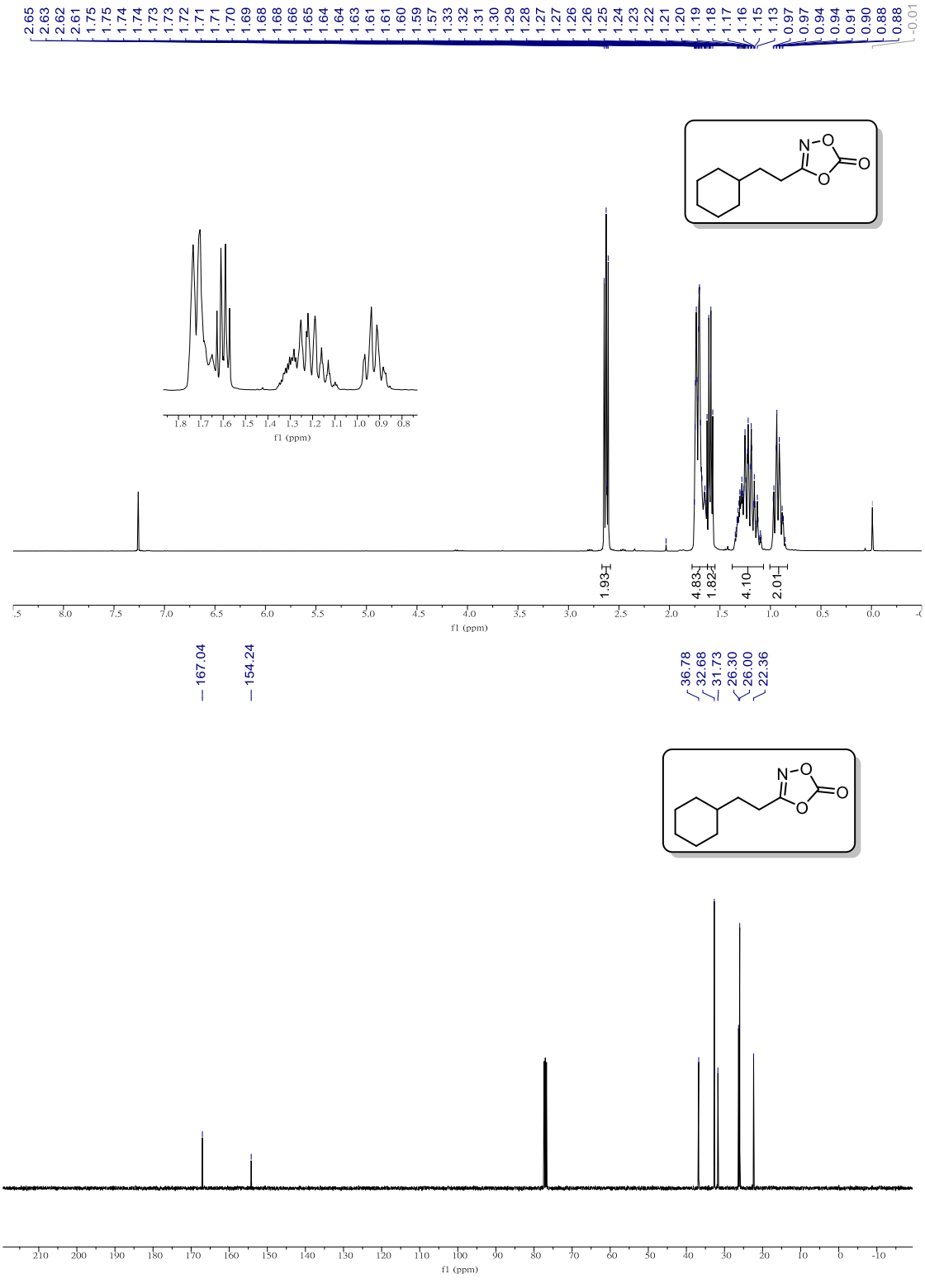


3-(((3r,5r,7r)-Adamantan-1-yl)methyl)-1,4,2-dioxazol-5-one

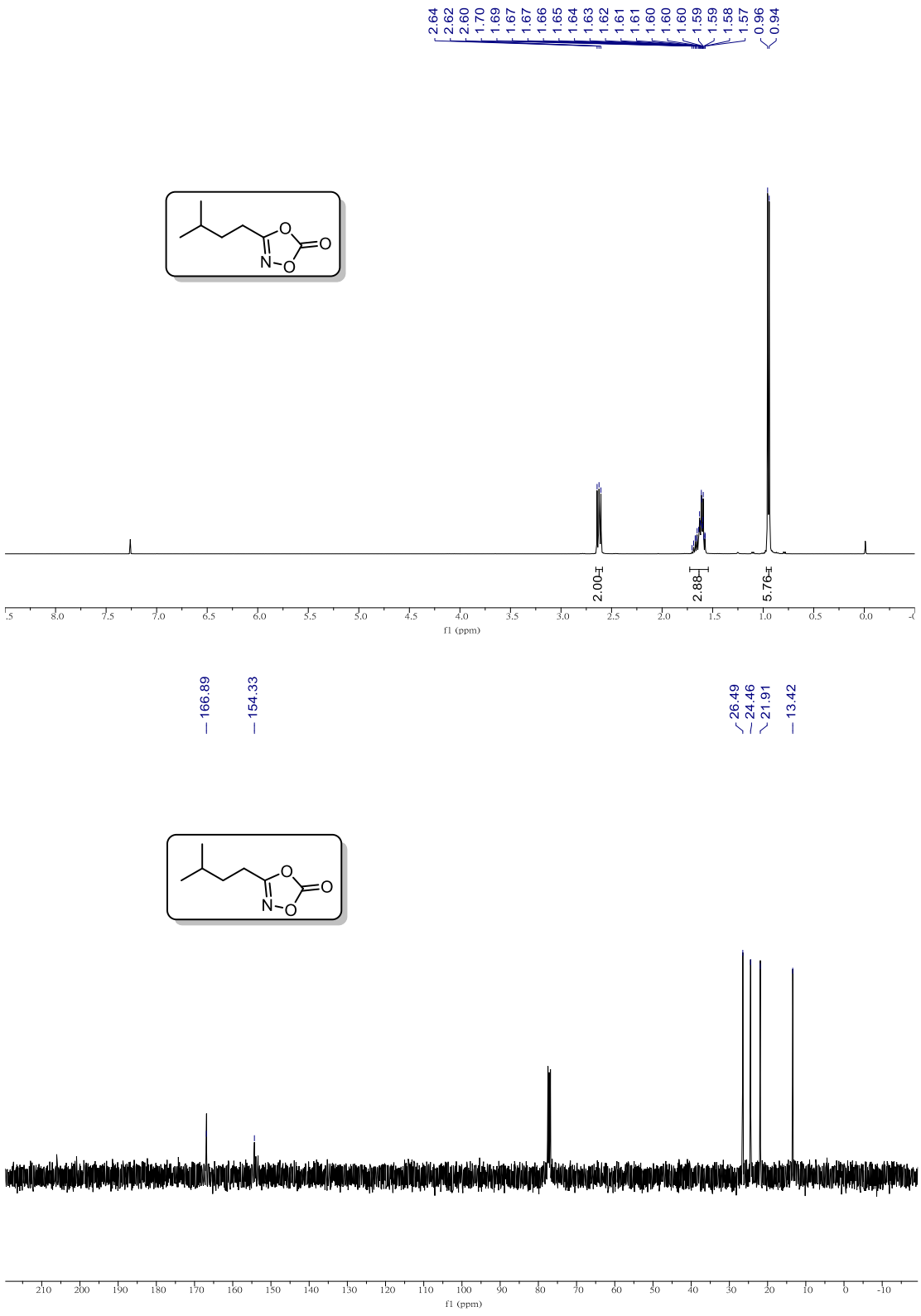




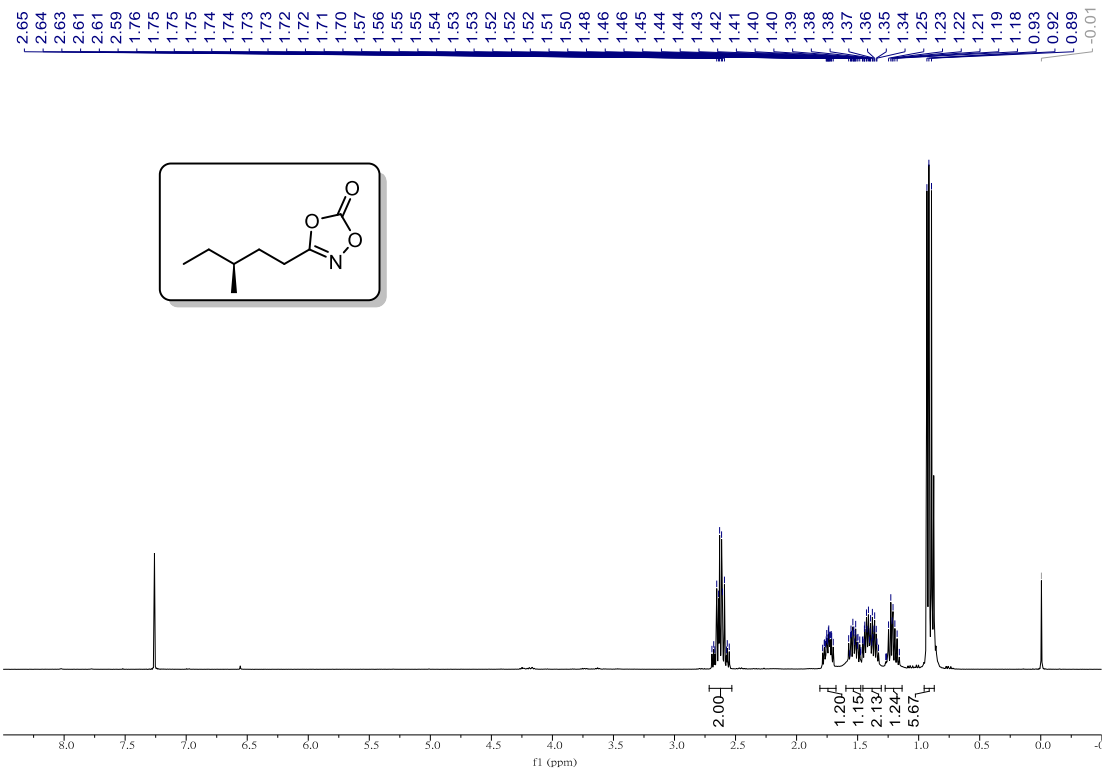
3-(2-Cyclohexylethyl)-1,4,2-dioxazol-5-one

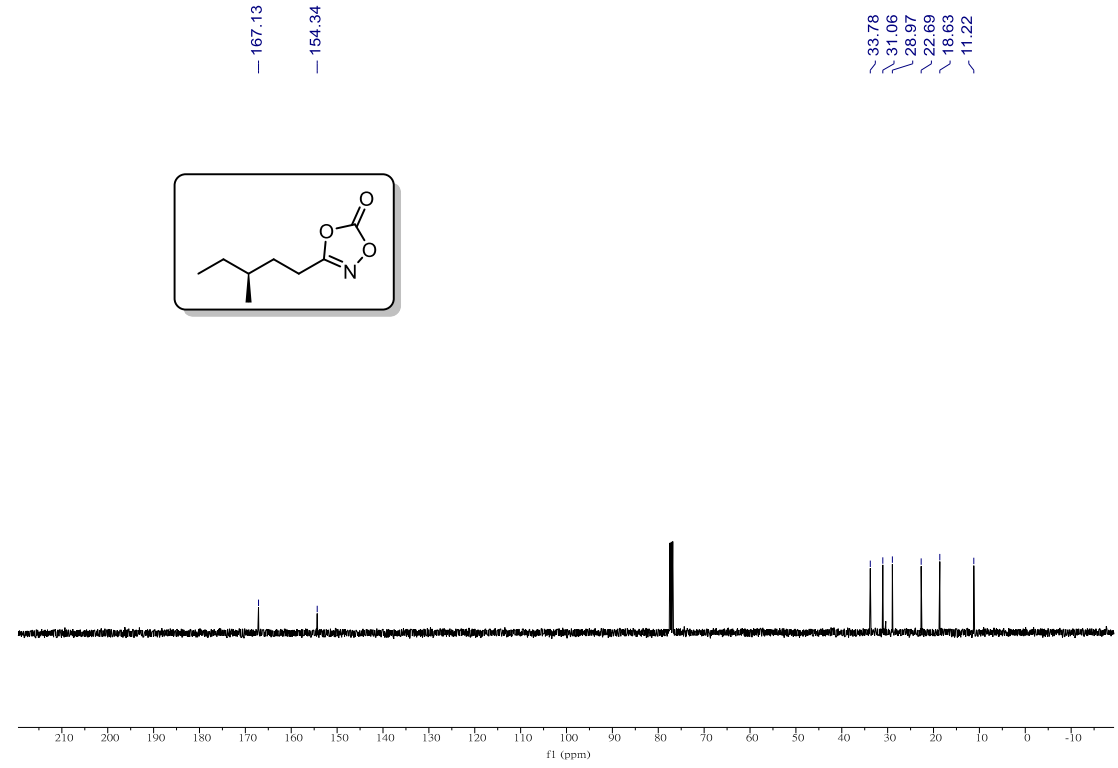


3-Isopentyl-1,4,2-dioxazol-5-one

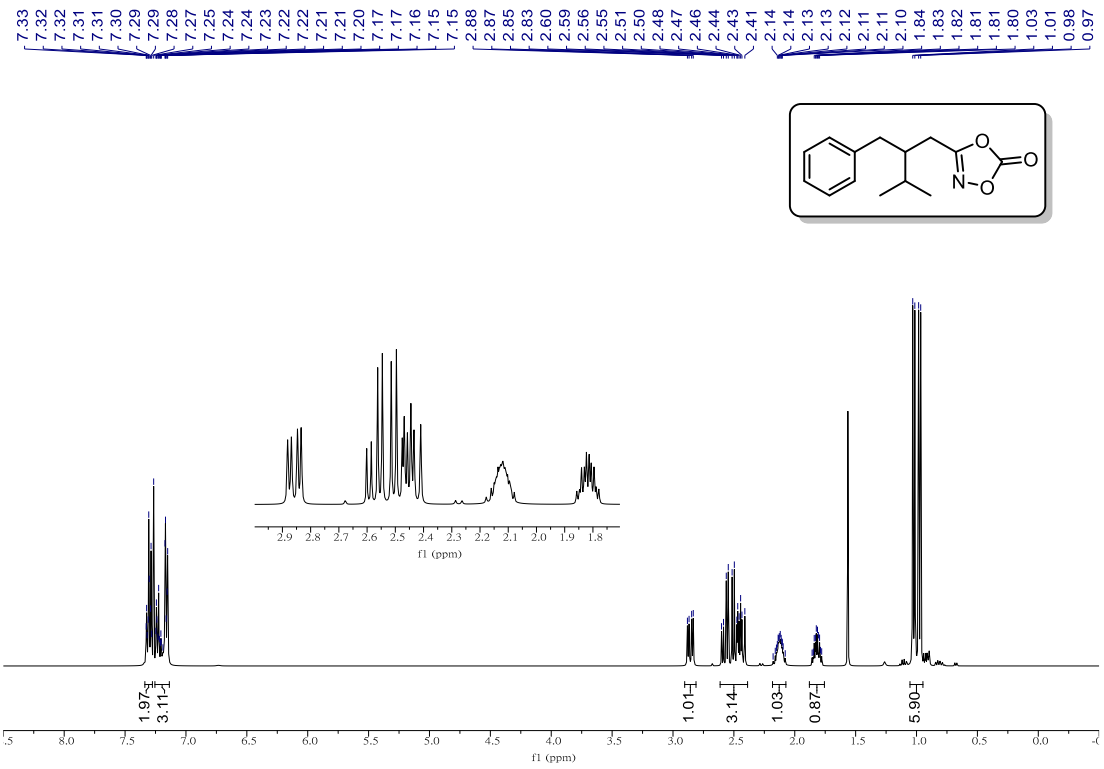


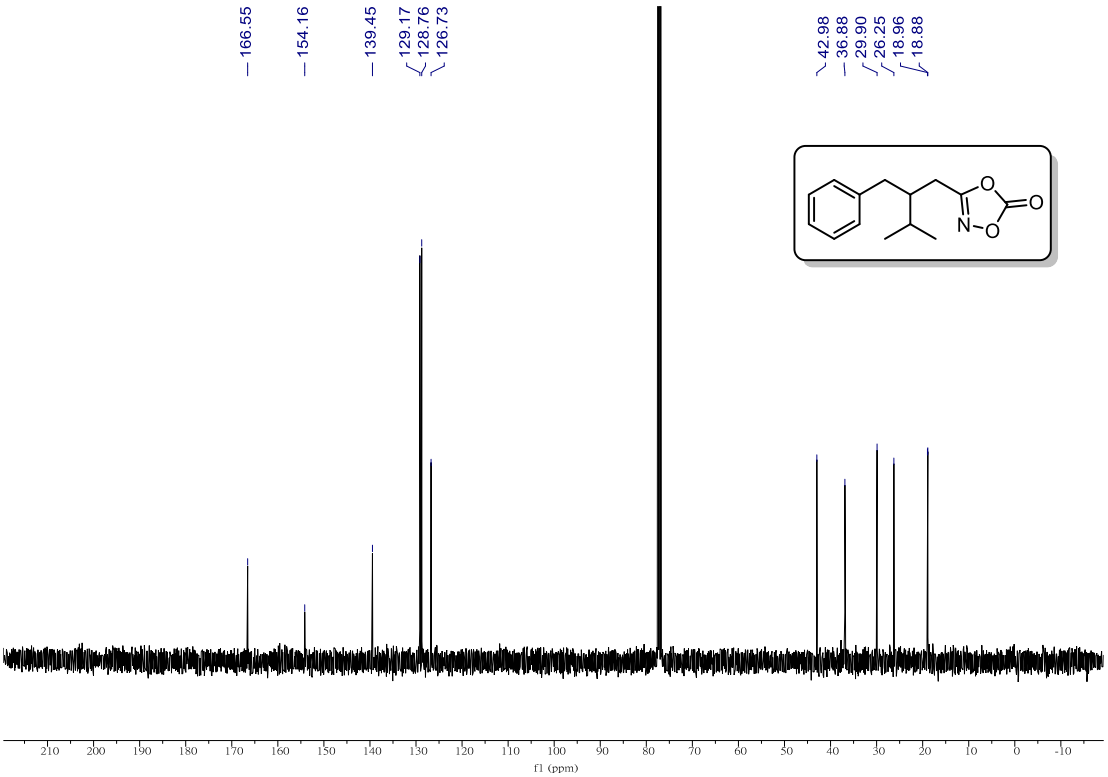
(S)-3-(3-Methylpentyl)-1,4,2-dioxazol-5-one



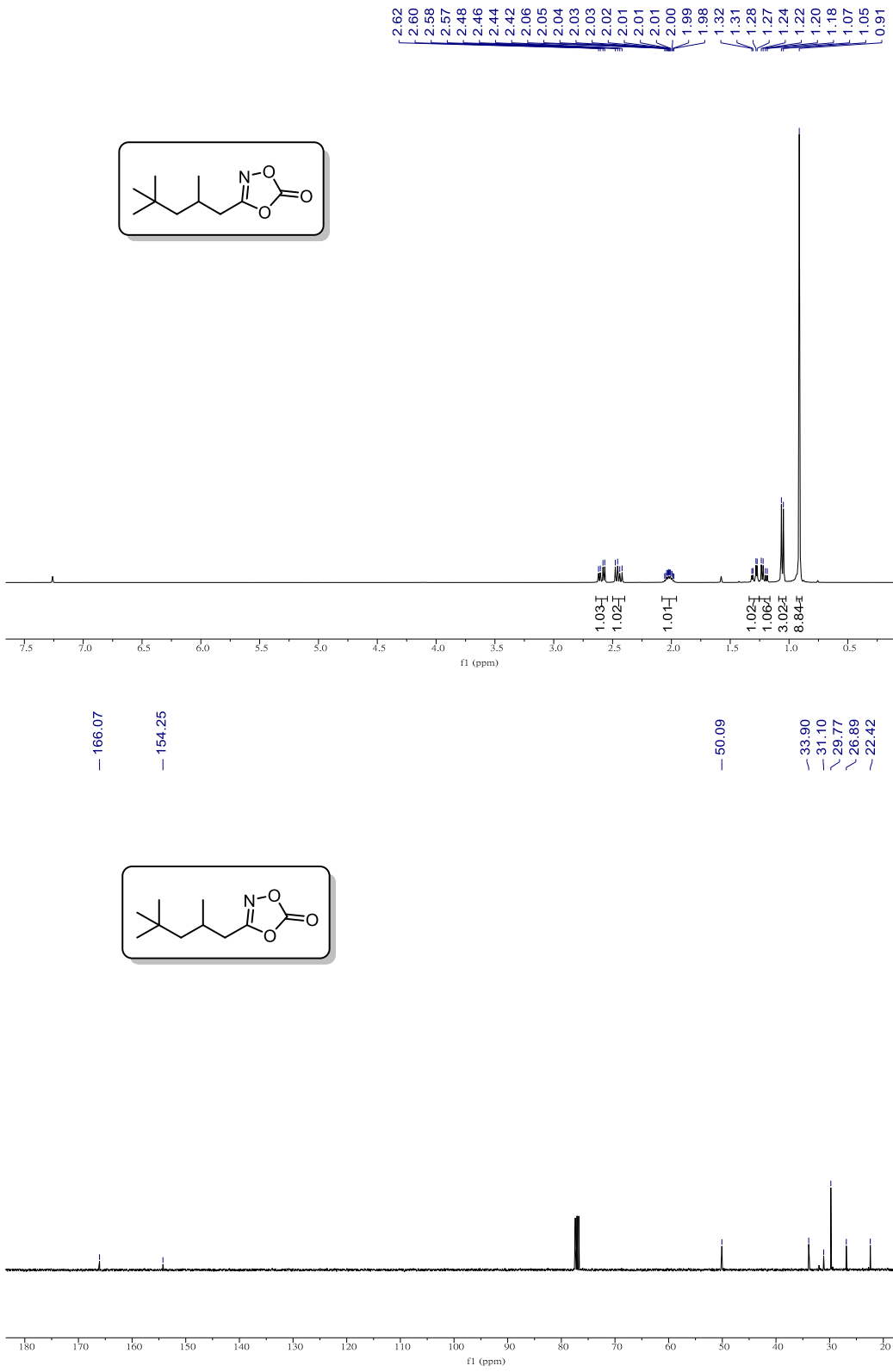


3-(2-Benzyl-3-methylbutyl)-1,4,2-dioxazol-5-one

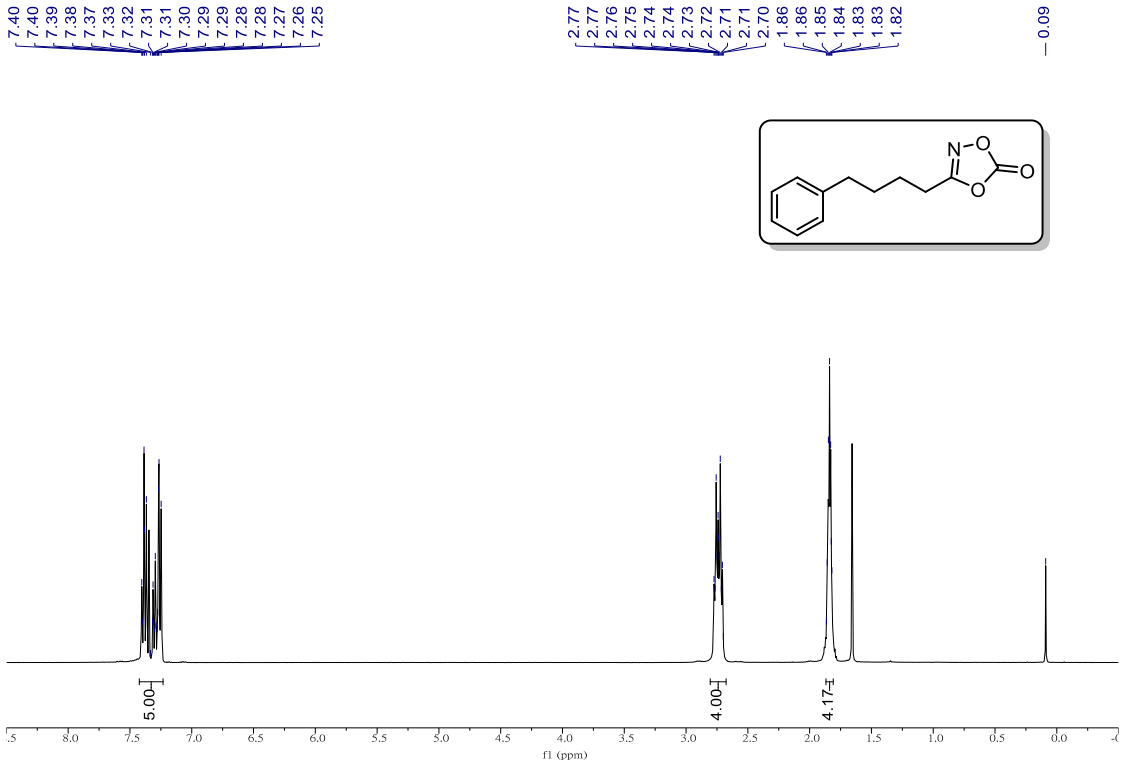


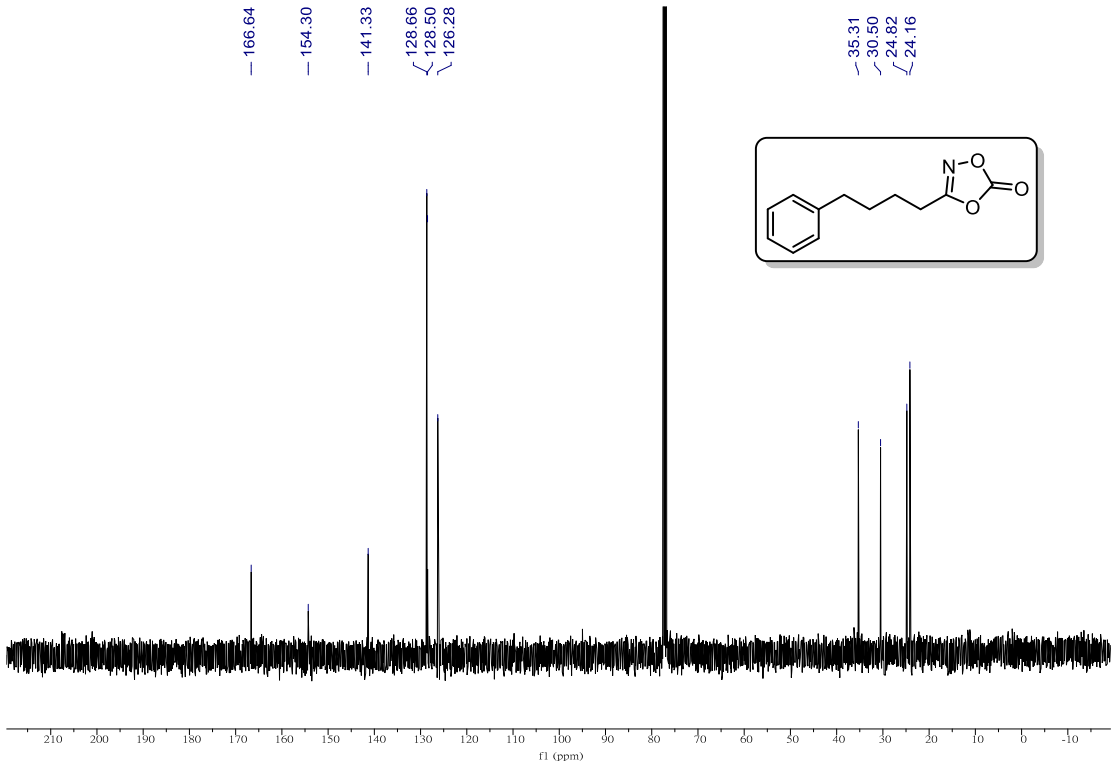


3-(2,4,4-Trimethylpentyl)-1,4,2-dioxazol-5-one

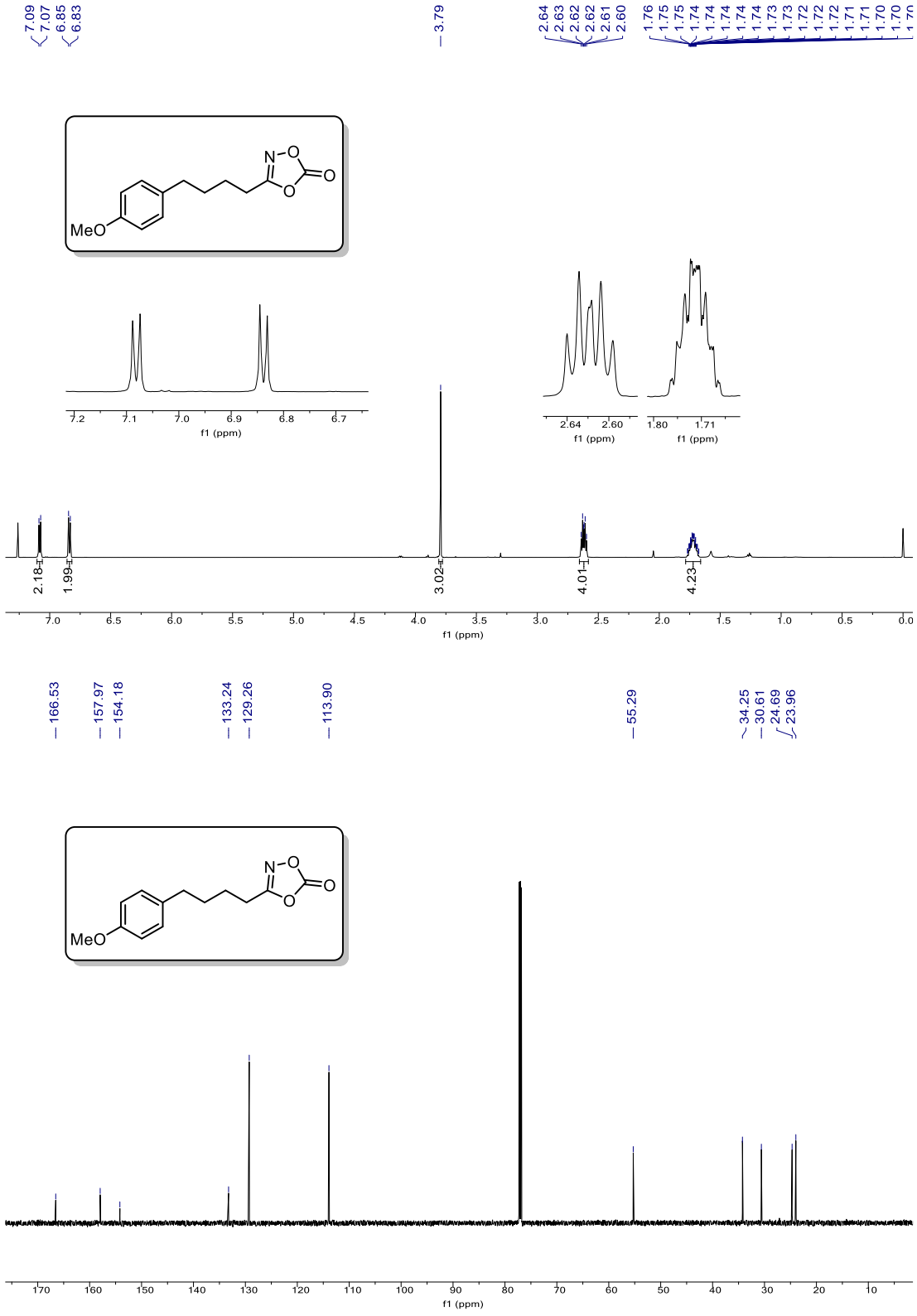


3-(4-Phenylbutyl)-1,4,2-dioxazol-5-one

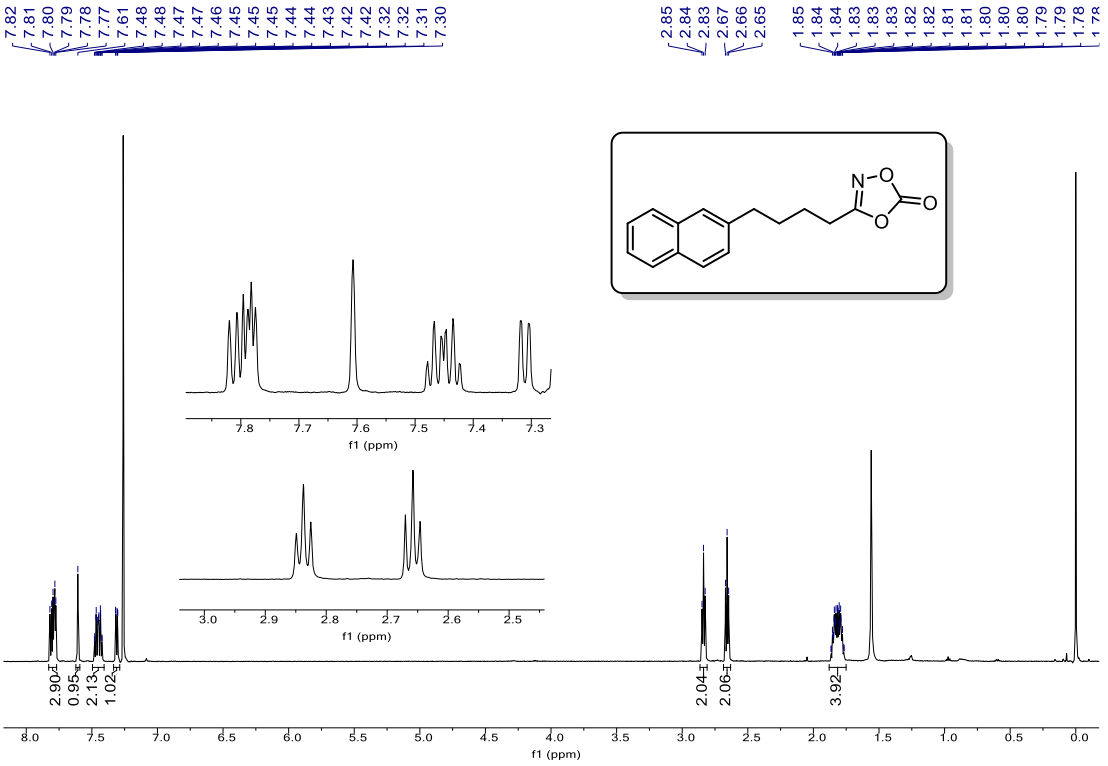


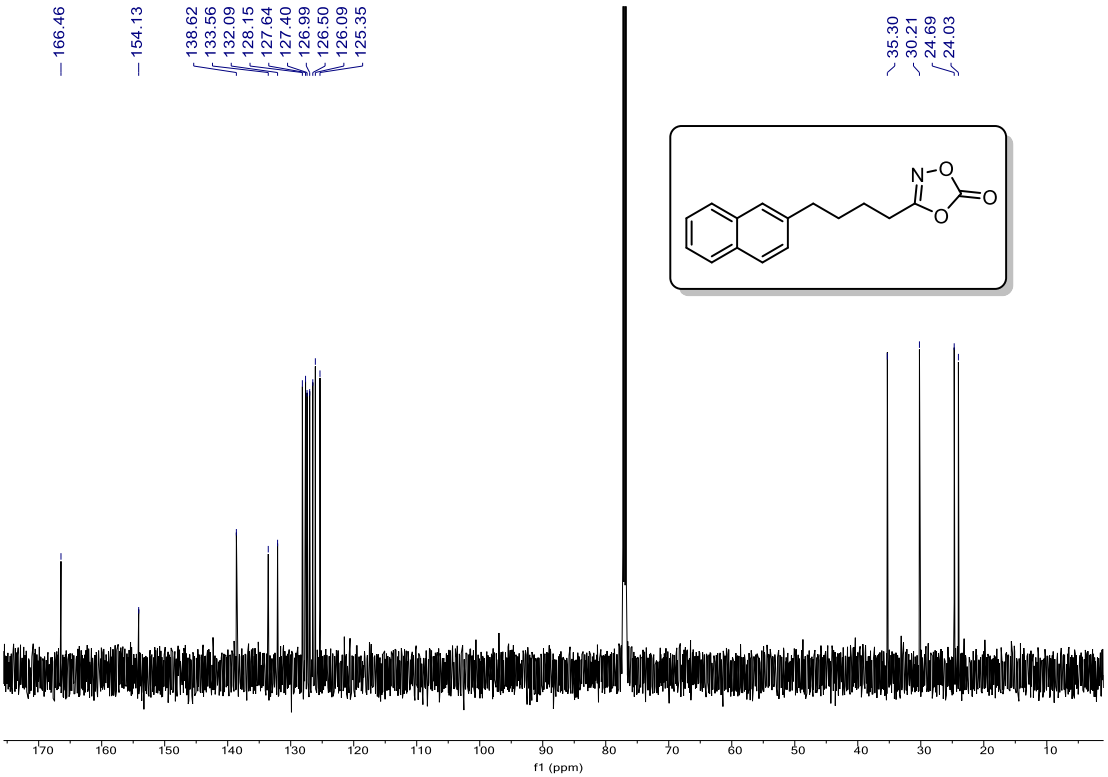


3-(4-(4-Methoxyphenyl)butyl)-1,4,2-dioxazol-5-one

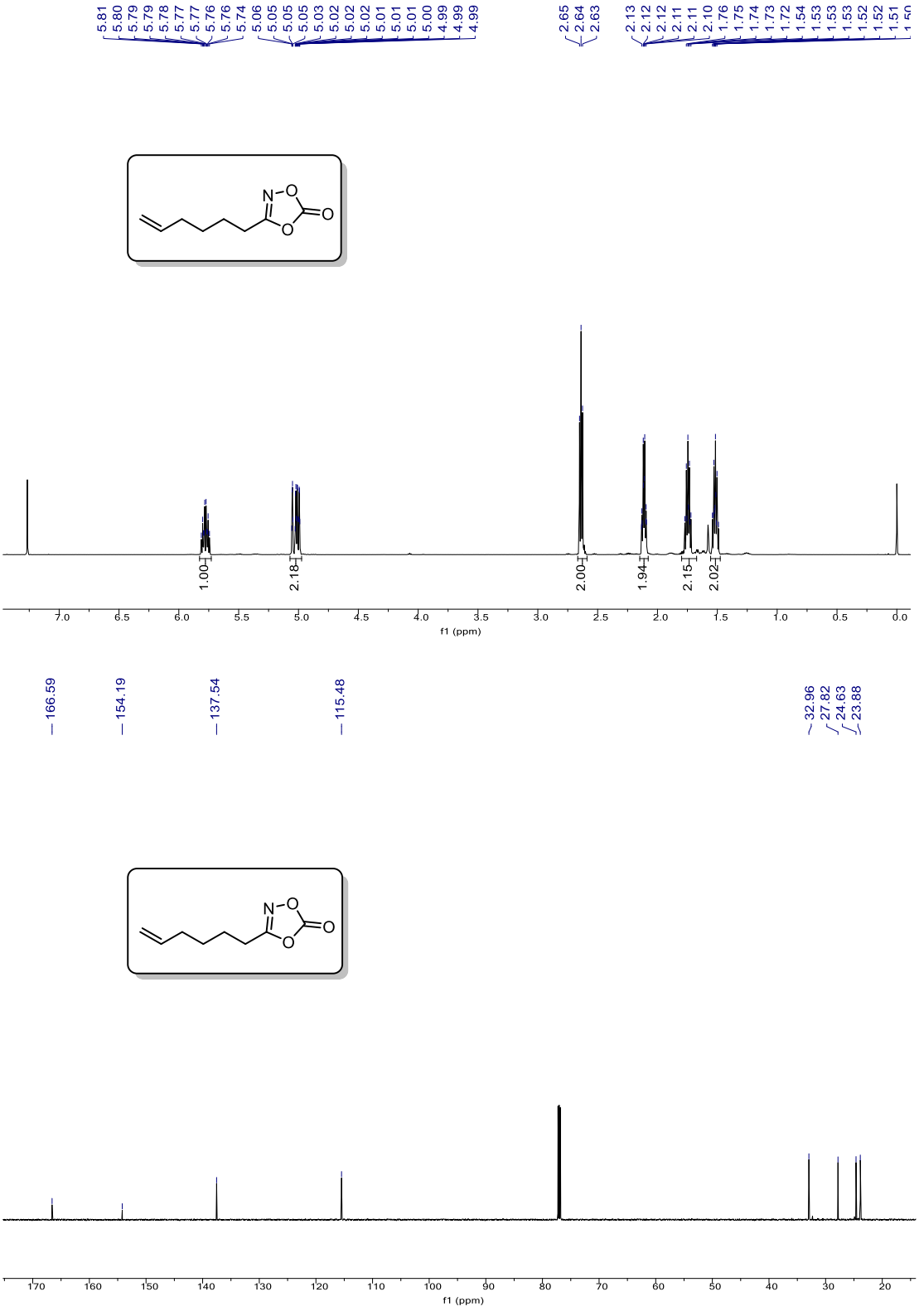


3-(4-(Naphthalen-2-yl)butyl)-1,4,2-dioxazol-5-one



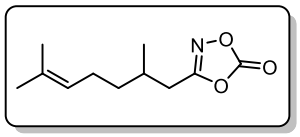


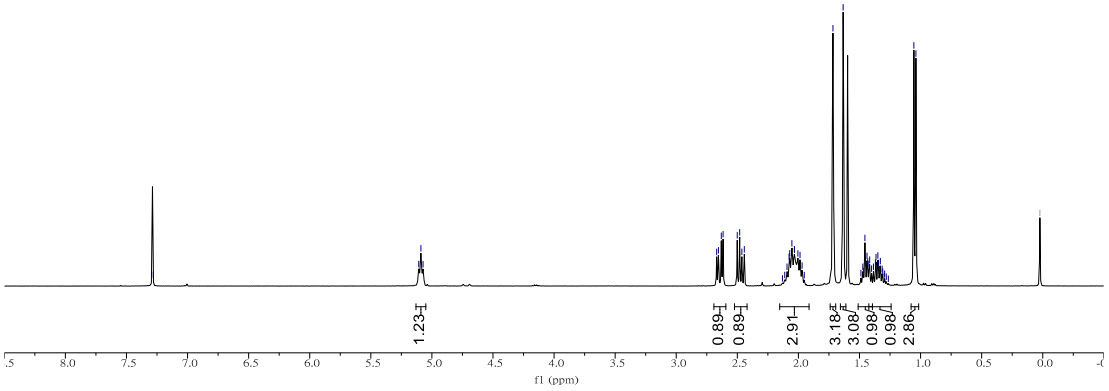
3-(Hex-5-en-1-yl)-1,4,2-dioxazol-5-one



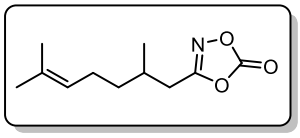
3-(2,6-Dimethylhept-5-en-1-yl)-1,4,2-dioxazol-5-one

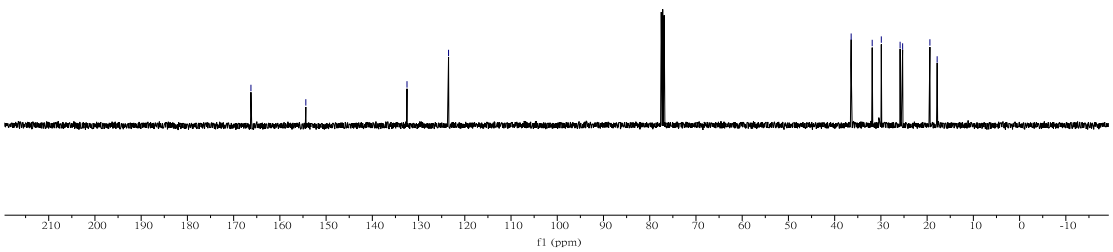




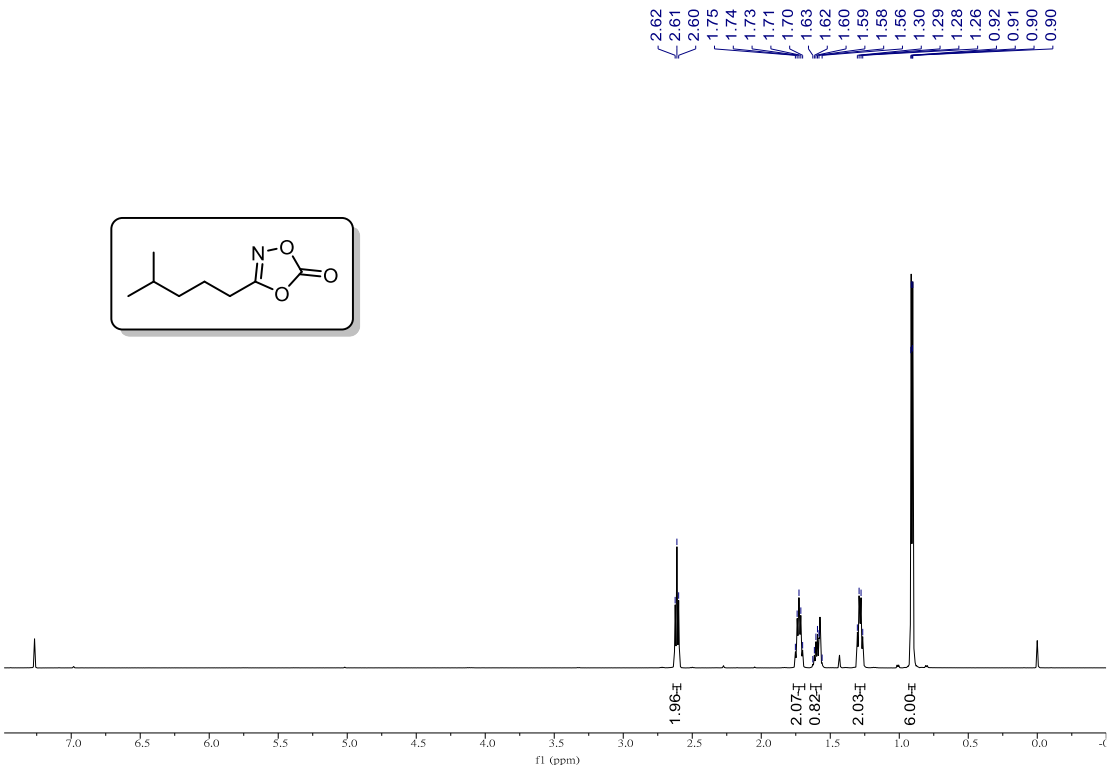


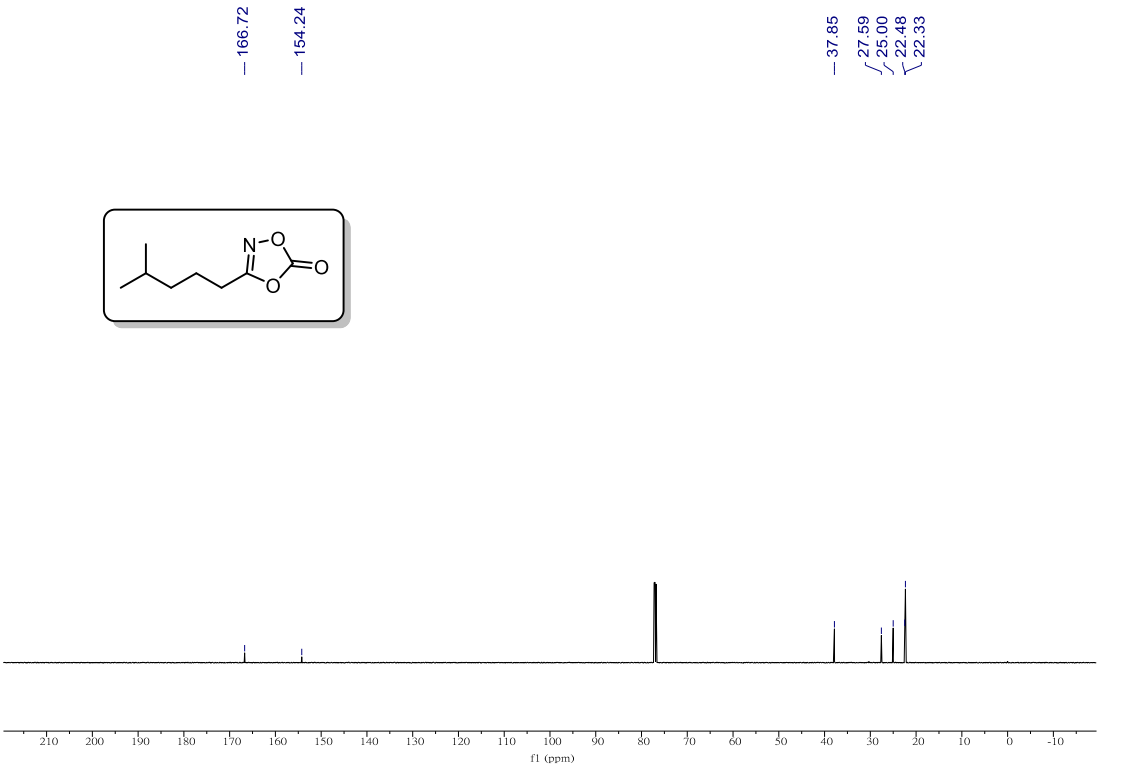






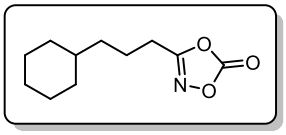
3-(4-Methylpentyl)-1,4,2-dioxazol-5-one

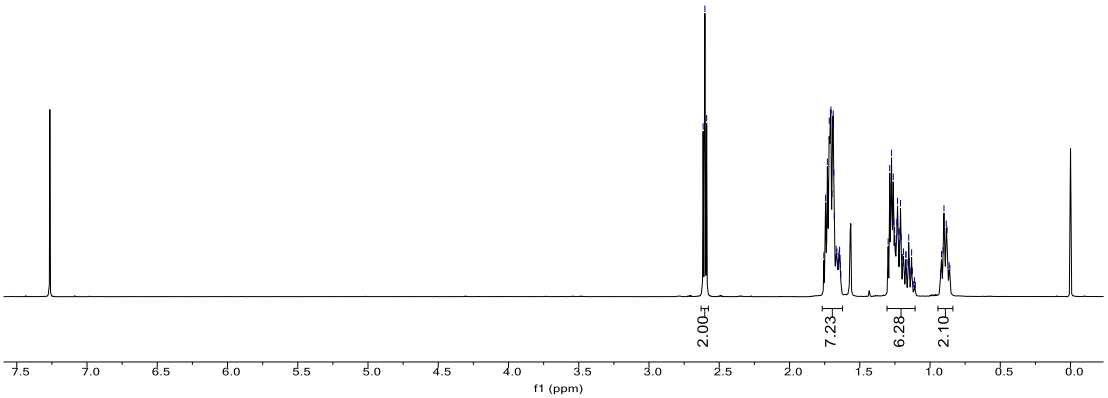


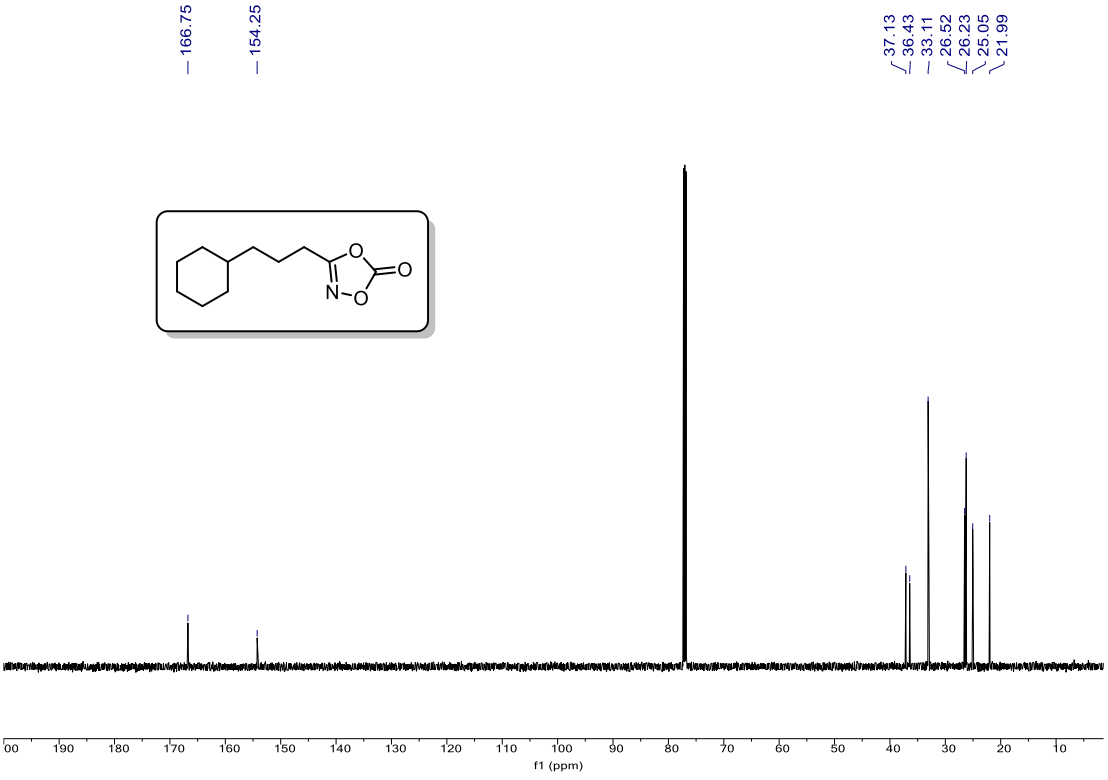


3-(3-Cyclohexylpropyl)-1,4,2-dioxazol-5-one



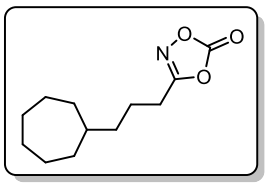


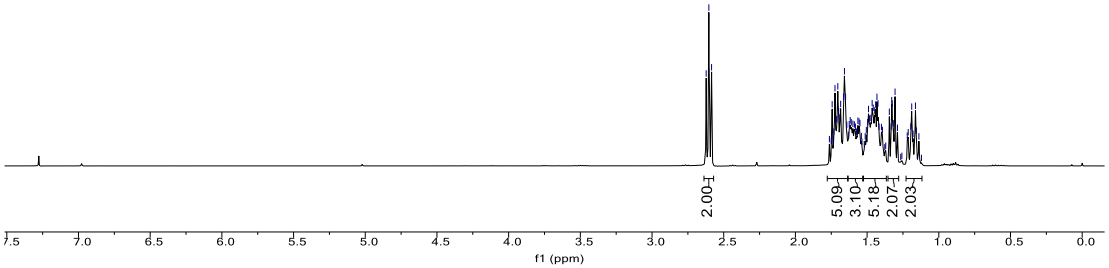




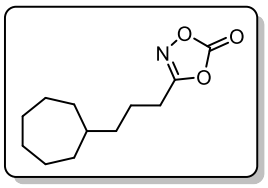
3-(3-Cycloheptylpropyl)-1,4,2-dioxazol-5-one

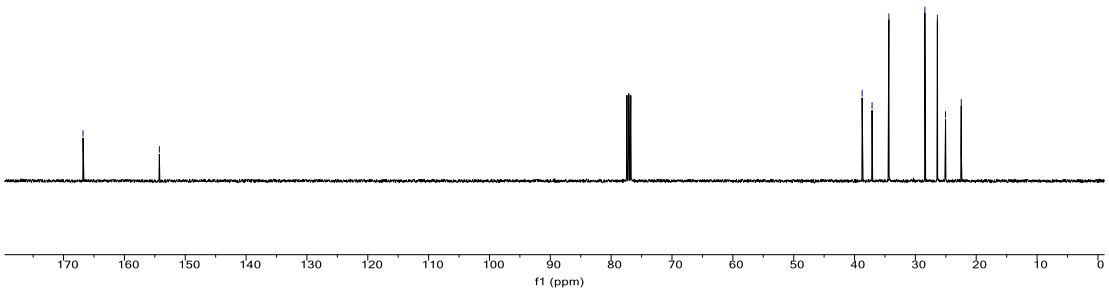




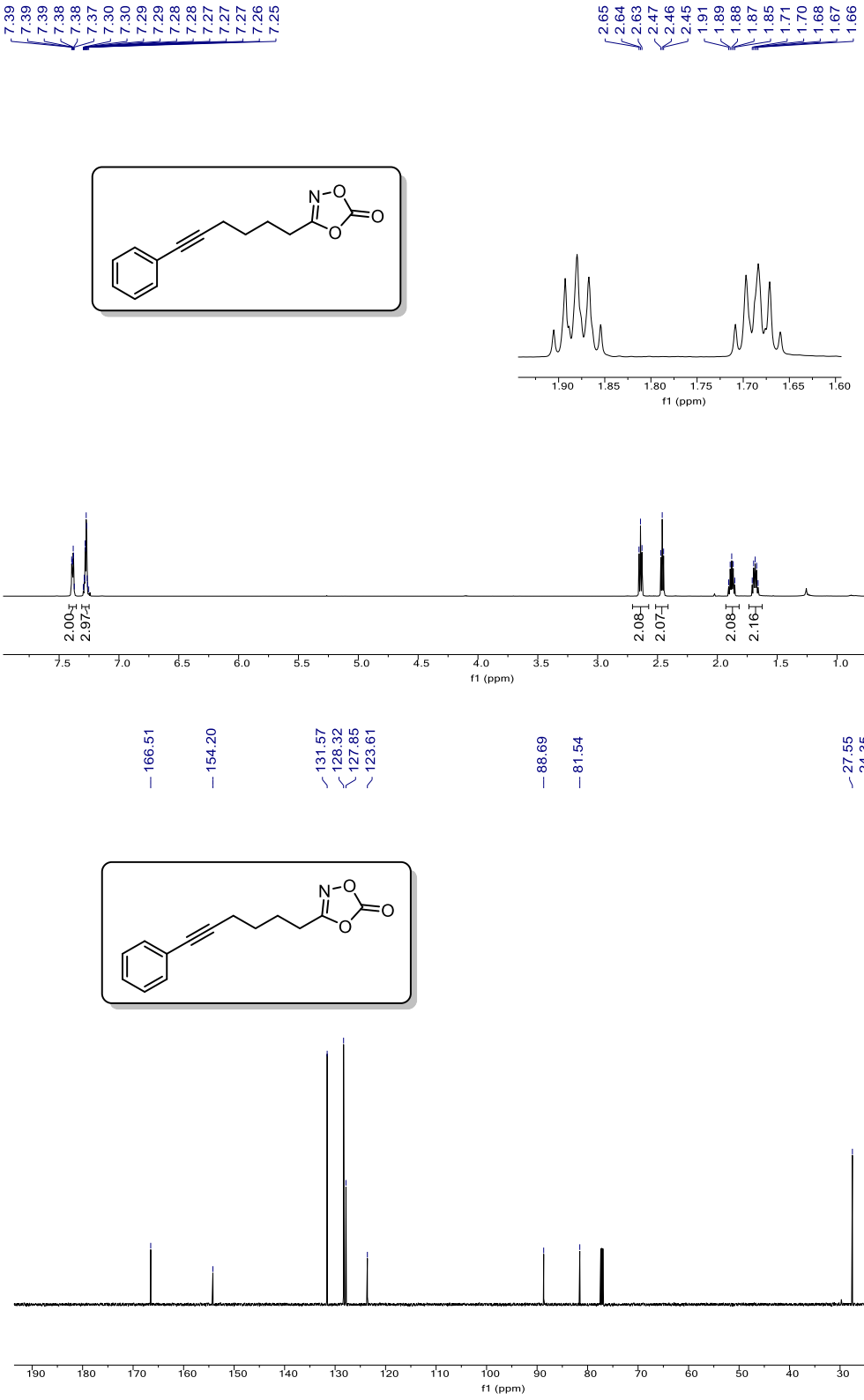




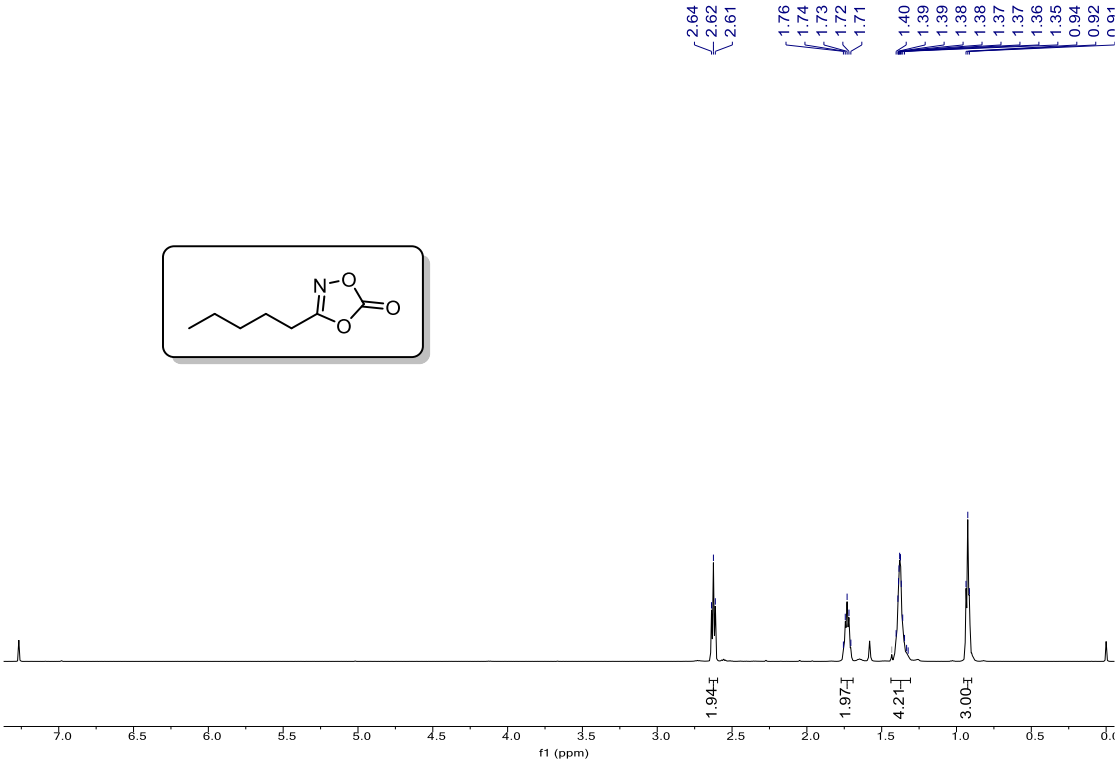




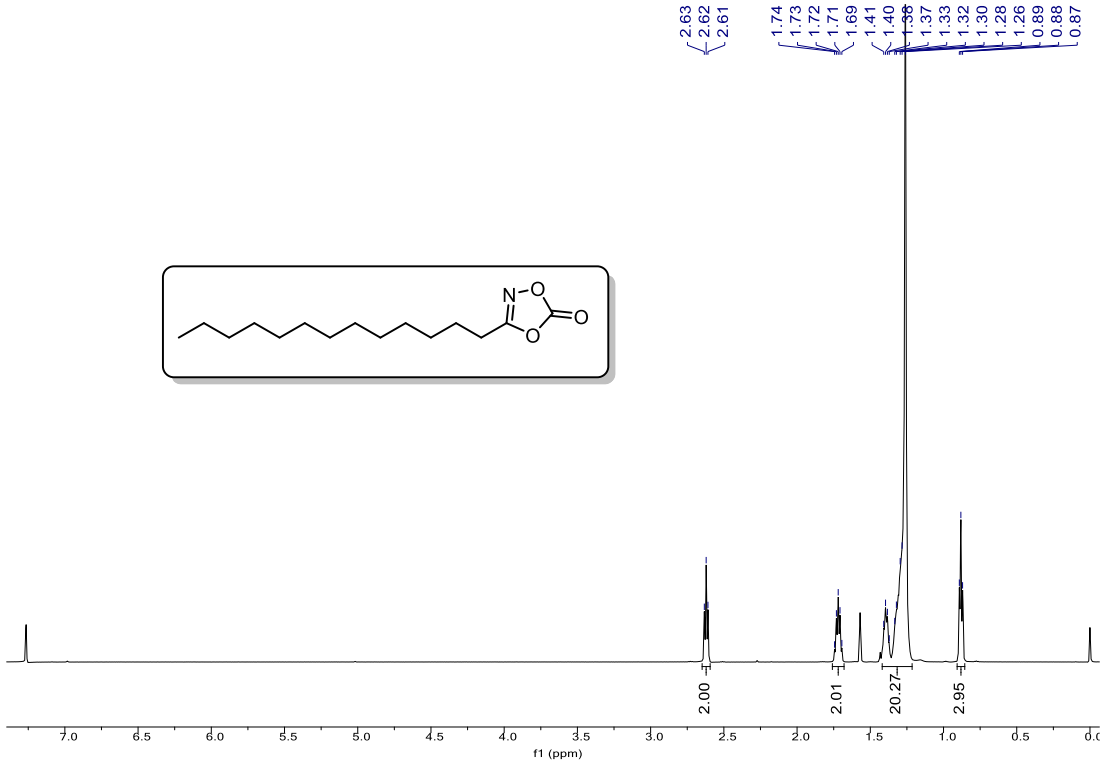
3-(6-Phenylhex-5-yn-1-yl)-1,4,2-dioxazol-5-one

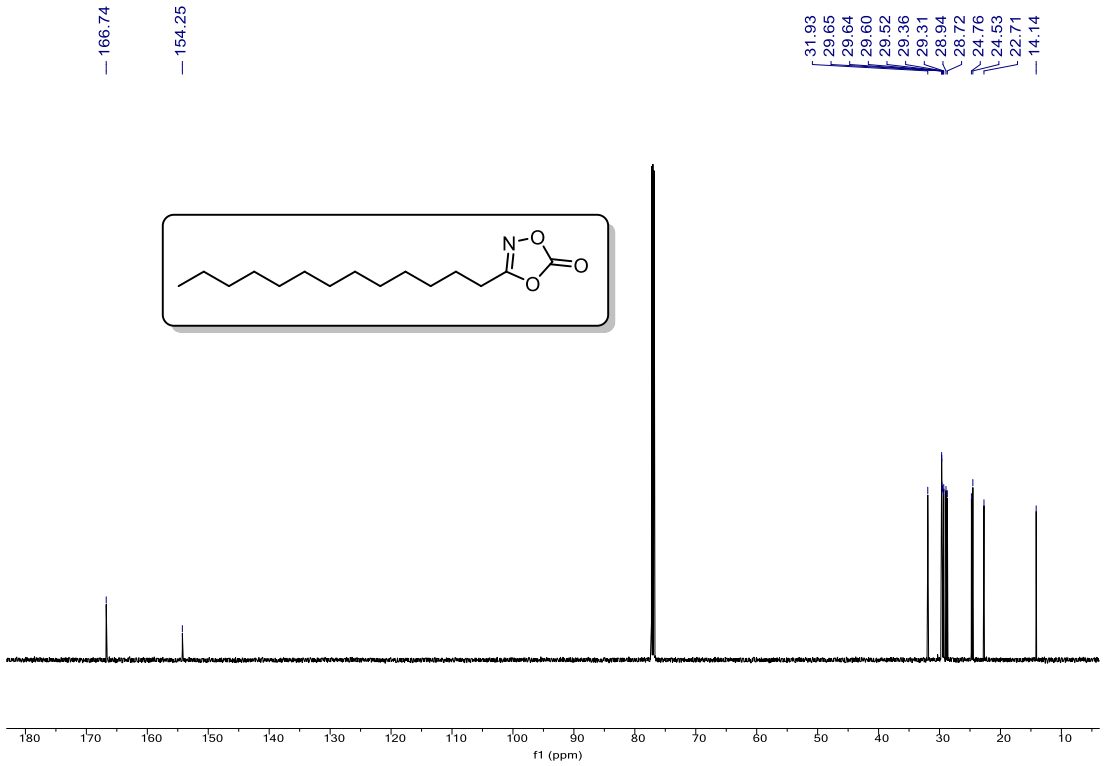


3-Pentyl-1,4,2-dioxazol-5-one

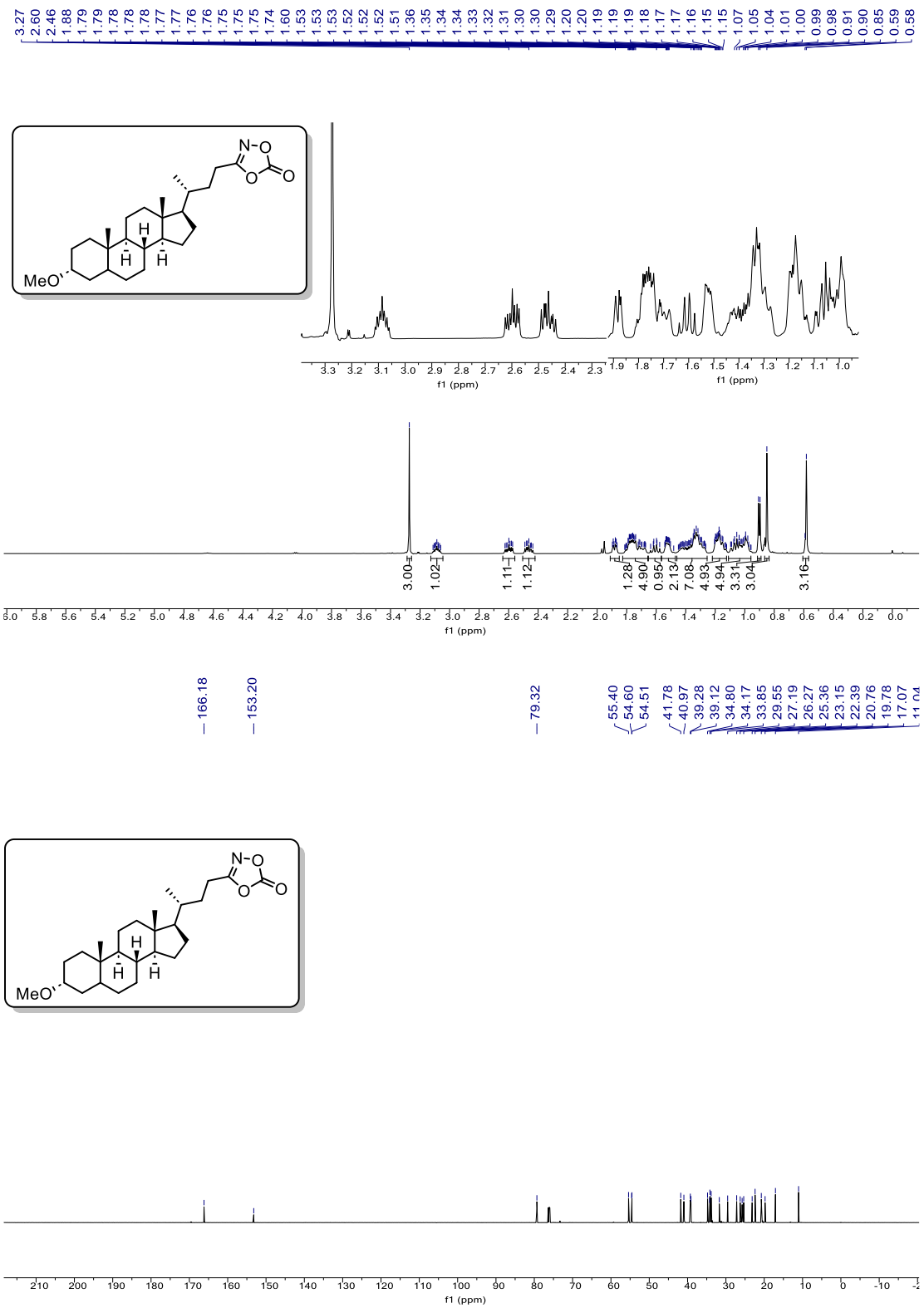


3-Tridecyl-1,4,2-dioxazol-5-one

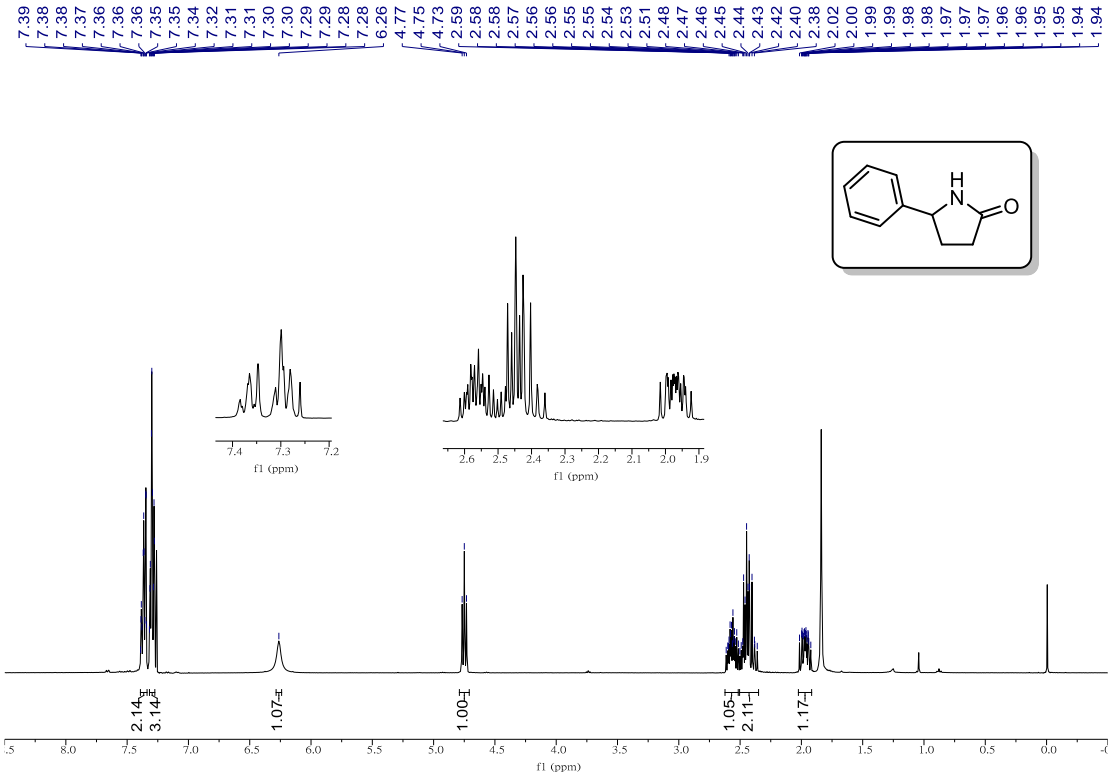


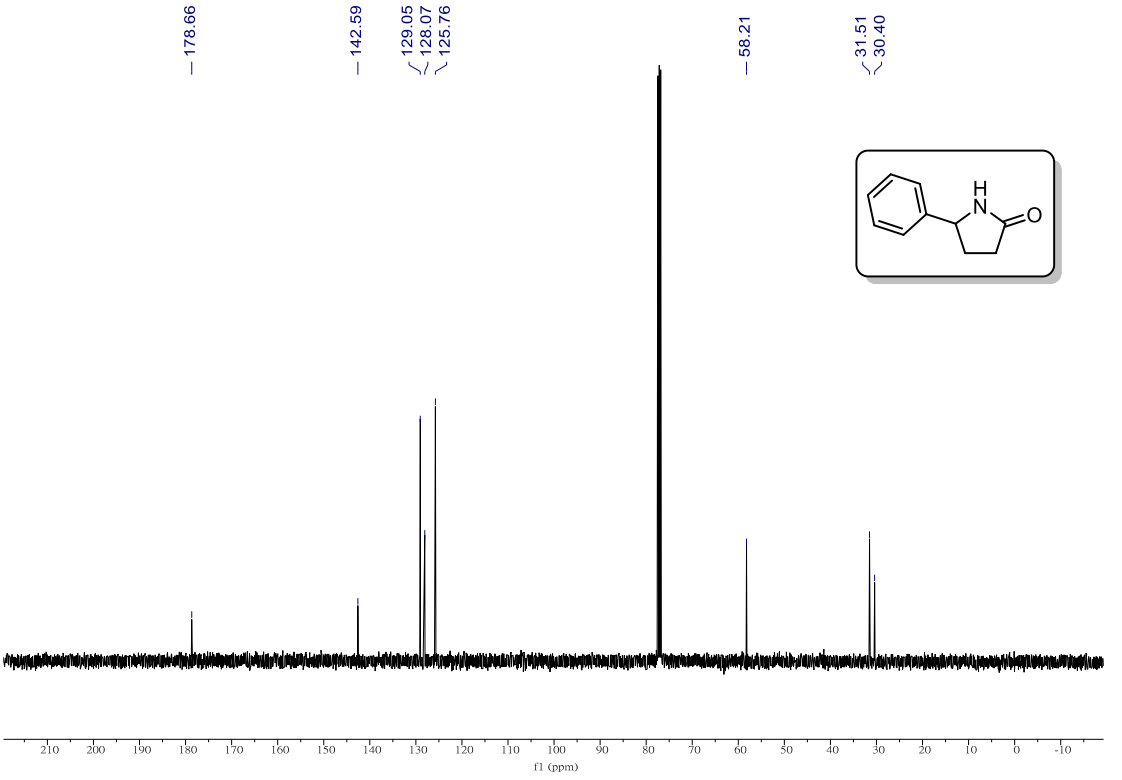


3-((3R)-3-((3R,8R,9S,10S,13R,14S,17R)-3-Methoxy-10,13-dimethylhexadecahydro-1H-cyclopenta[a]phenanthren-17-yl)butyl)-1,4,2-dioxazol-5-one

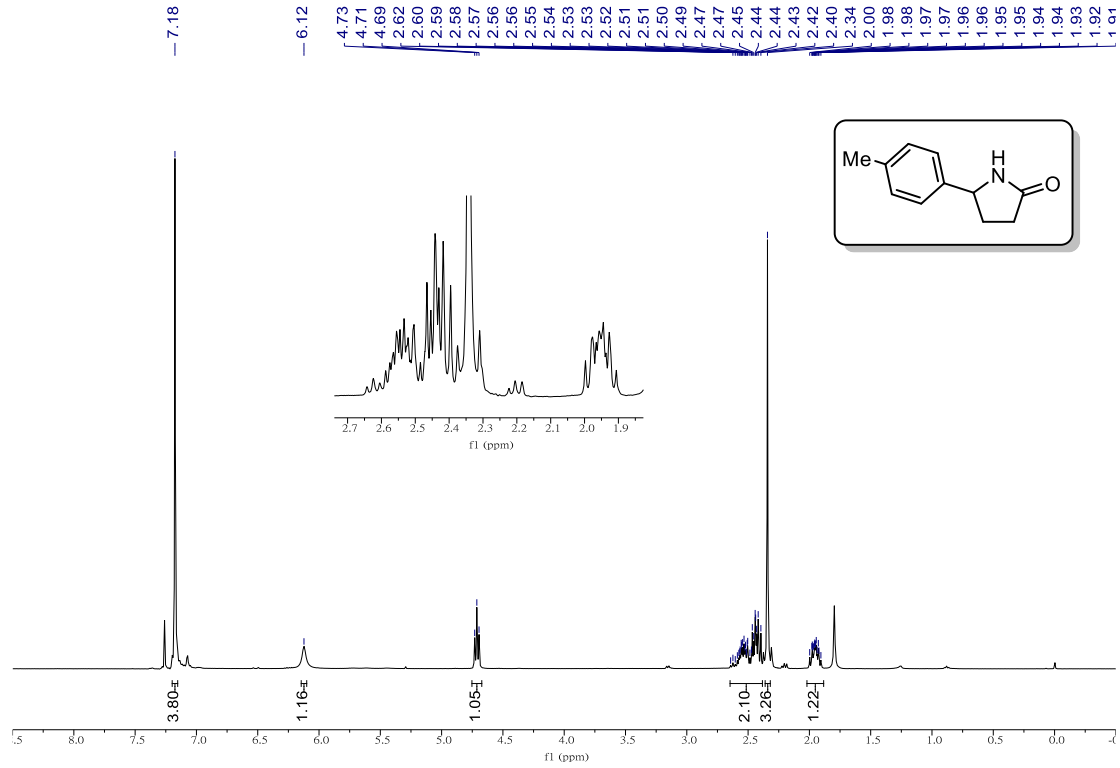


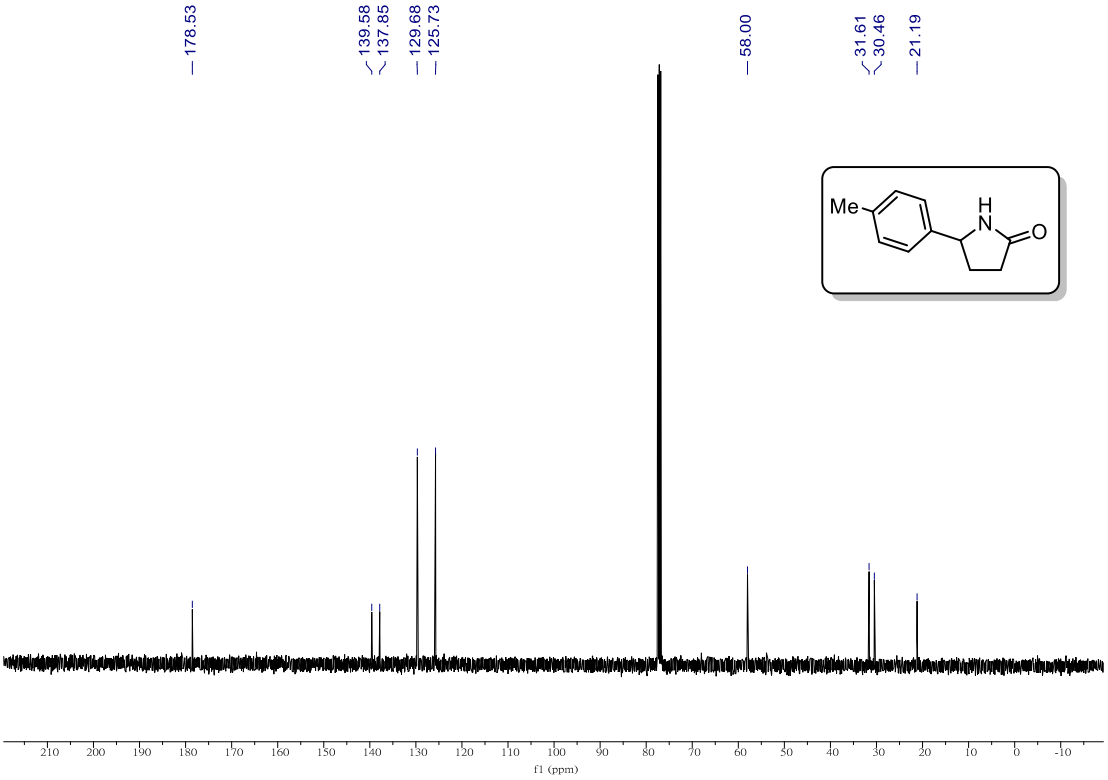
5-Phenylpyrrolidin-2-one



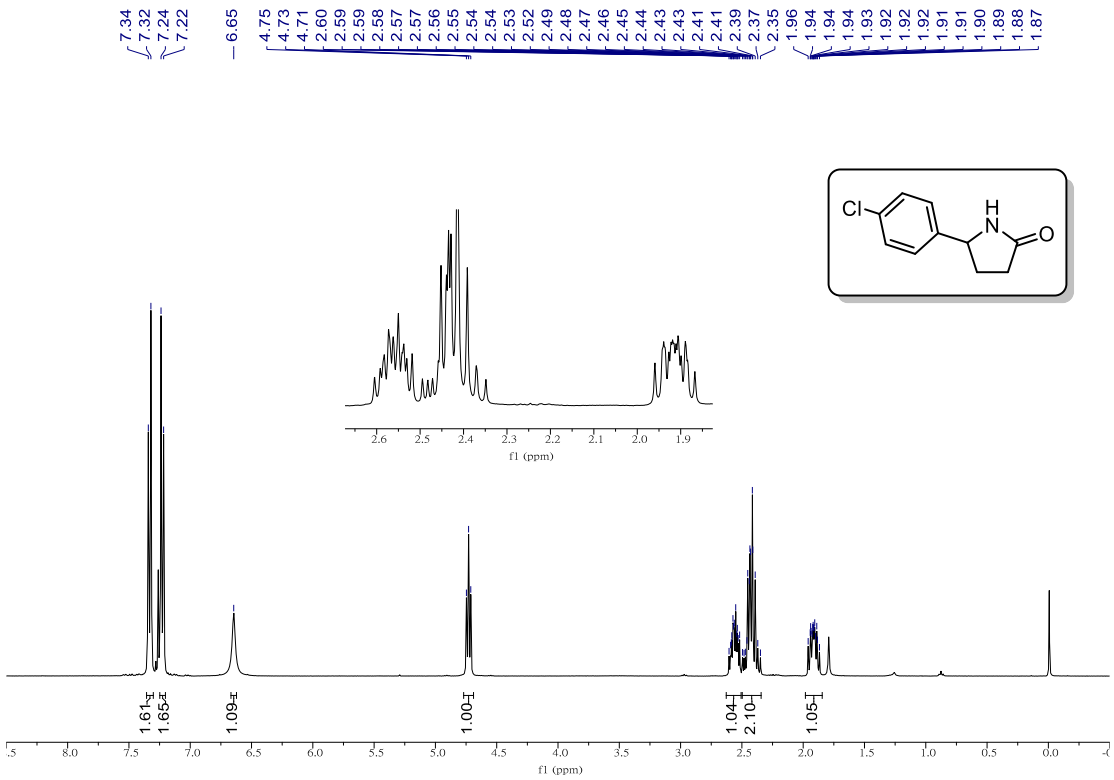


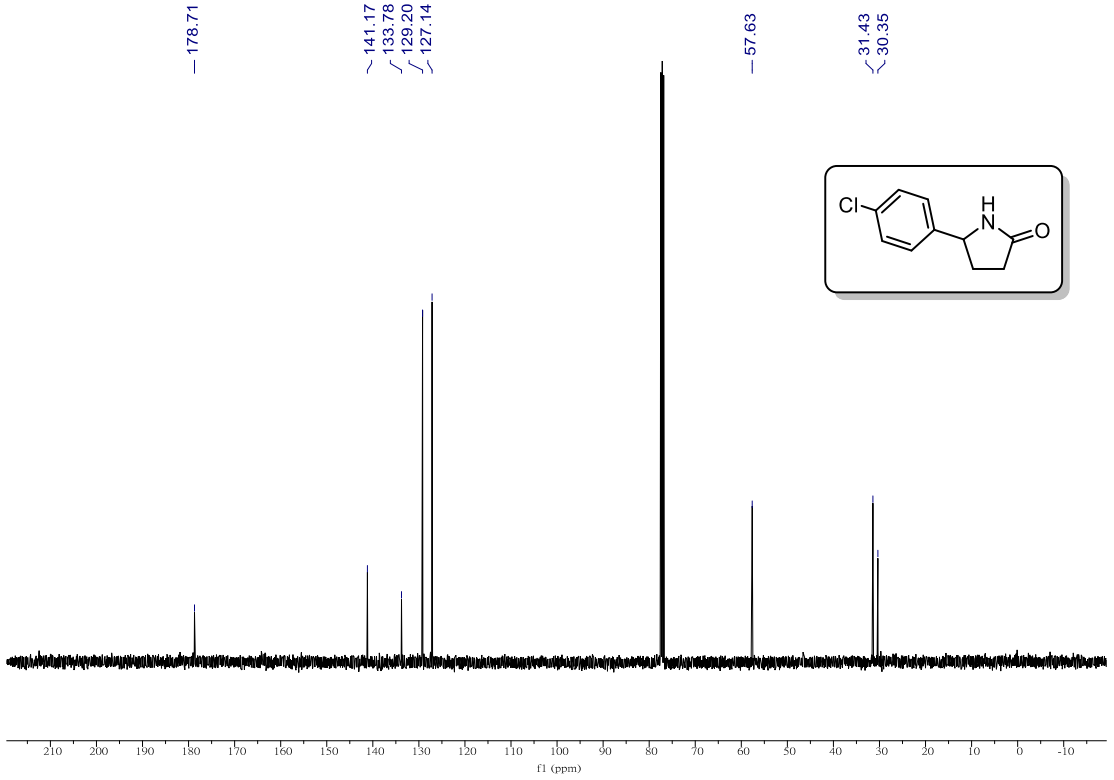
5-(p-Tolyl)pyrrolidin-2-one



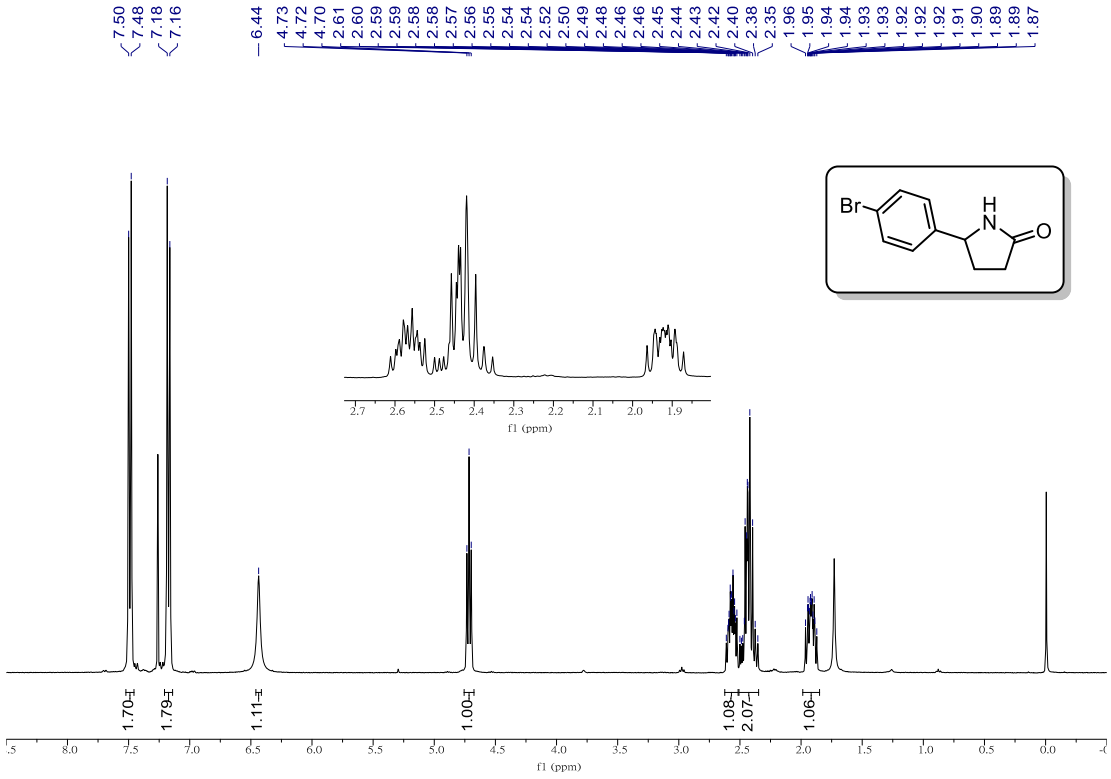


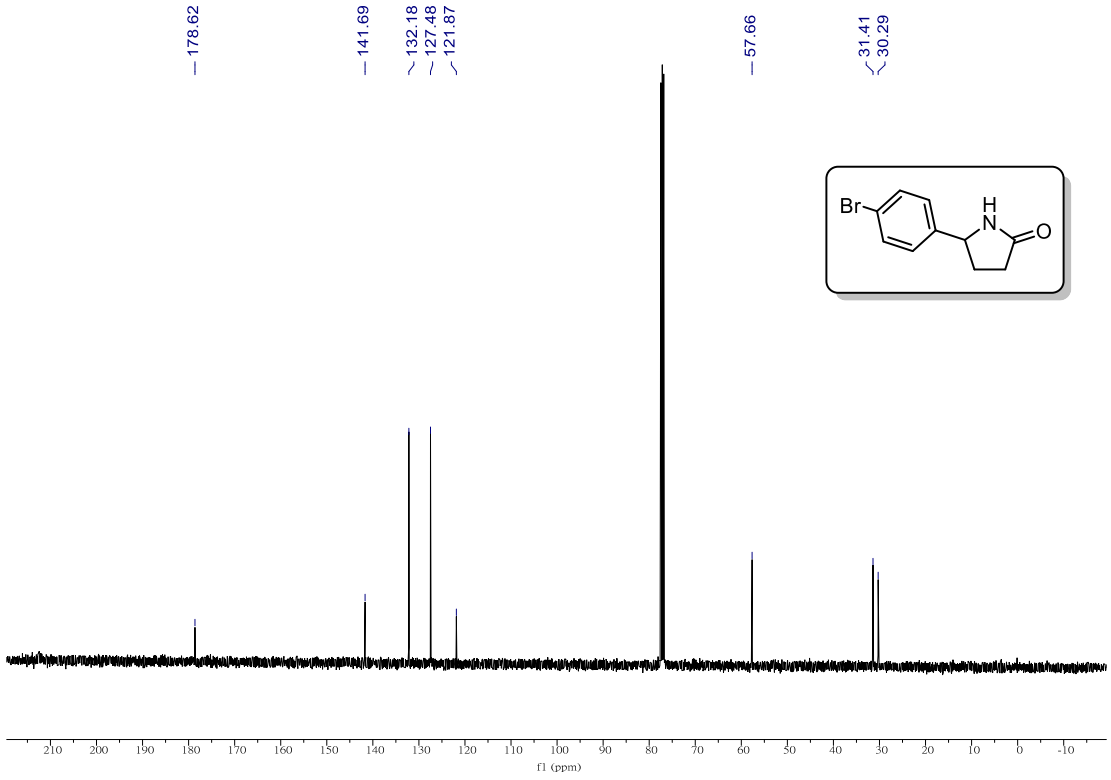
5-(4-Chlorophenyl)pyrrolidin-2-one



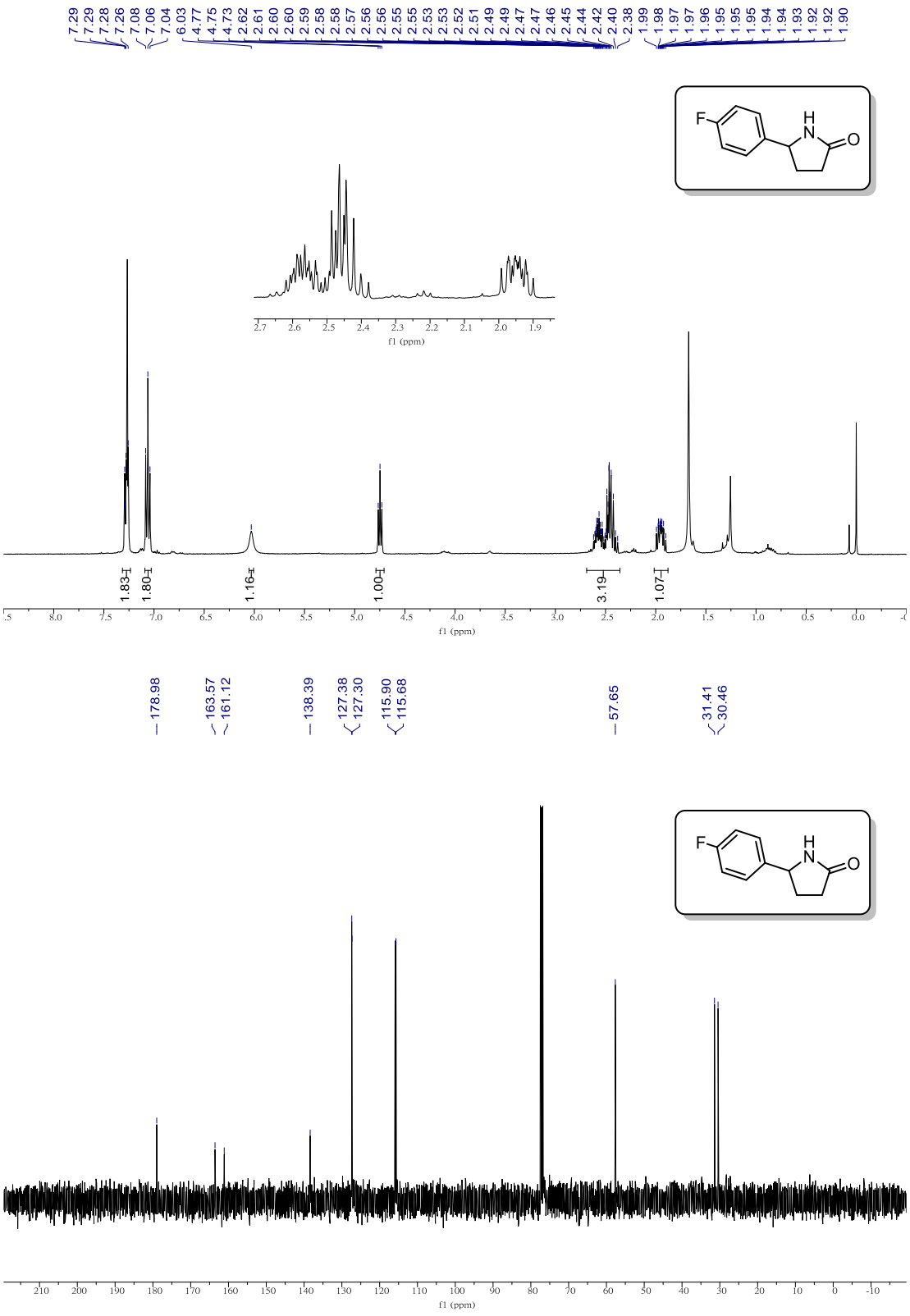


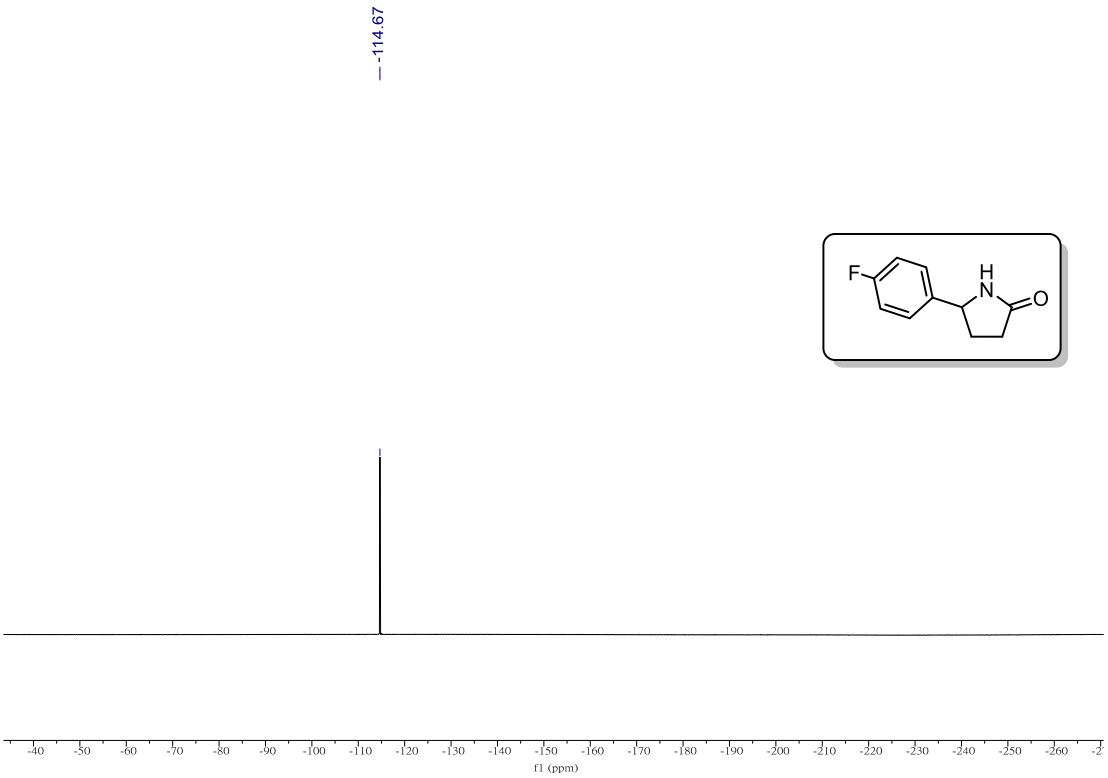
5-(4-Bromophenyl)pyrrolidin-2-one



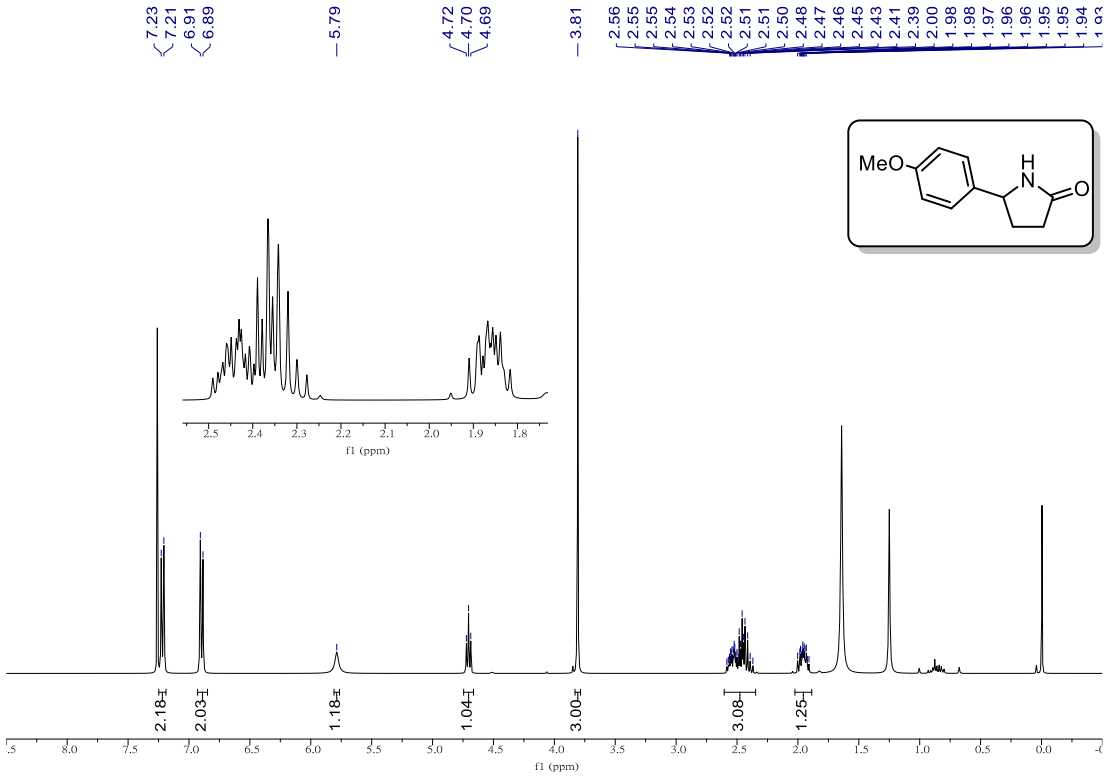


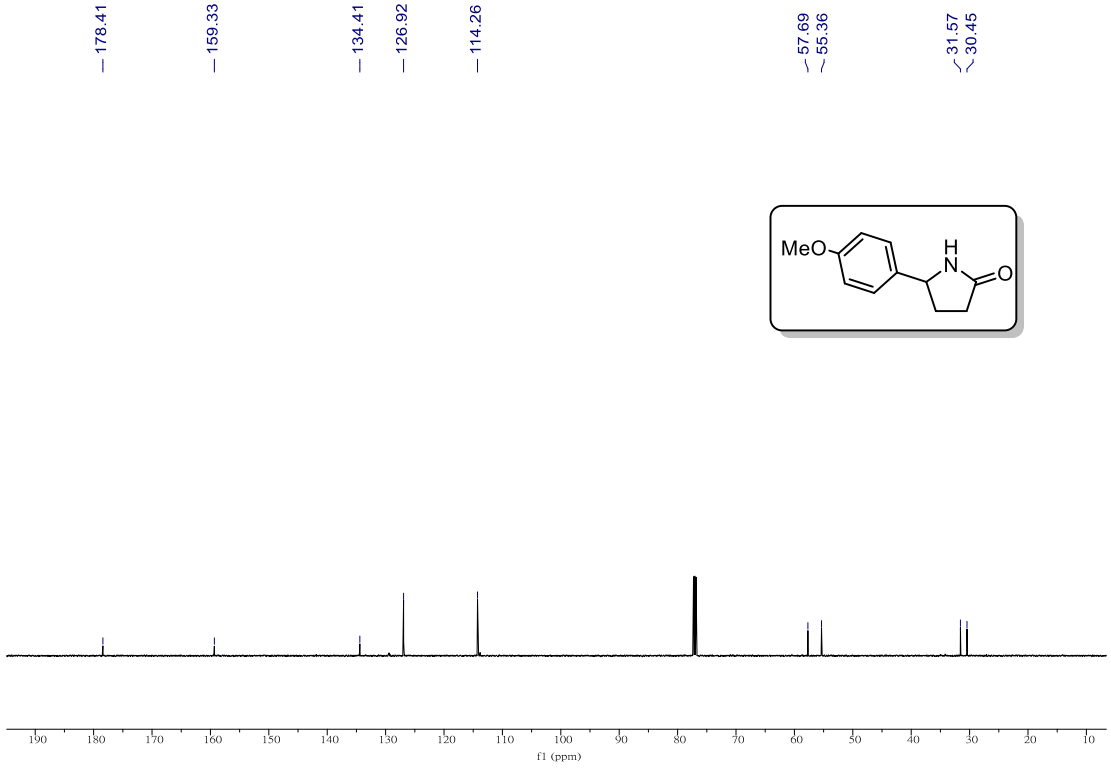
5-(4-Fluorophenyl)pyrrolidin-2-one



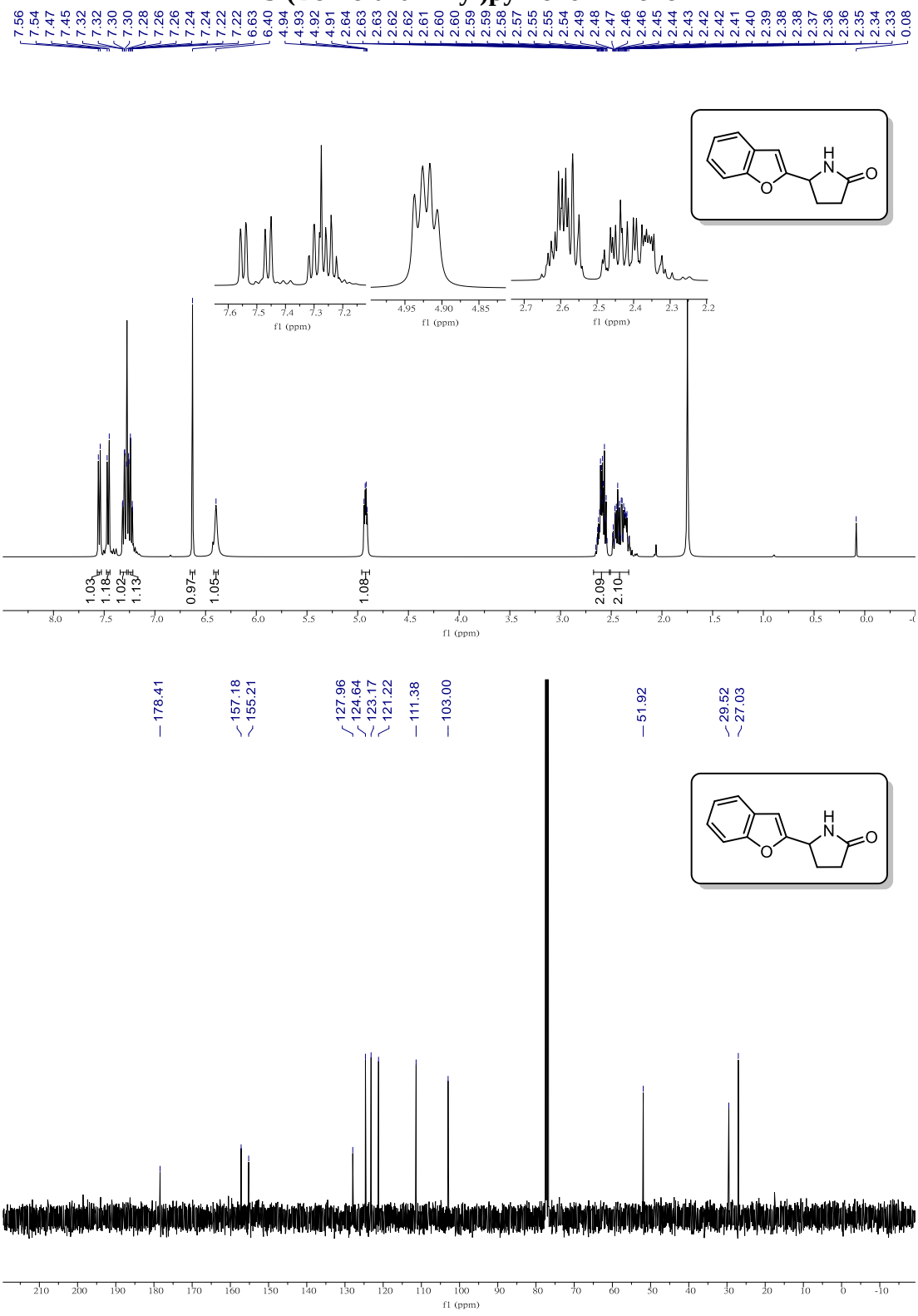

-114.67
F
H
N
O
-40
-50
-60
-70
-80
-90
-100
-110
-120
-130
-140
-150
-160
-170
-180
-190
-200
-210
-220
-230
-240
-250
-260
f1 (ppm)

5-(4-Methoxyphenyl)pyrrolidin-2-one

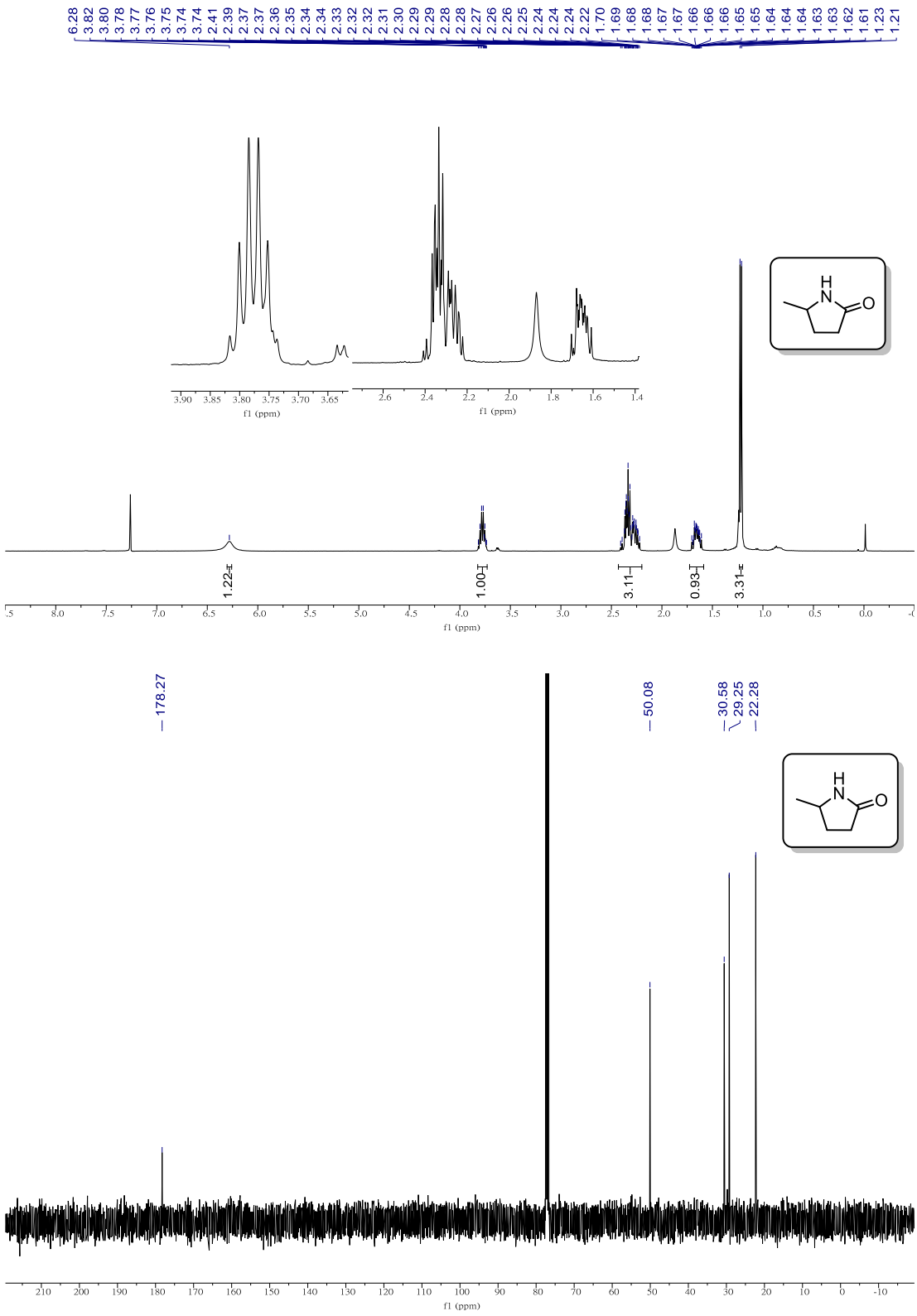




5-(Benzofuran-2-yl)pyrrolidin-2-one

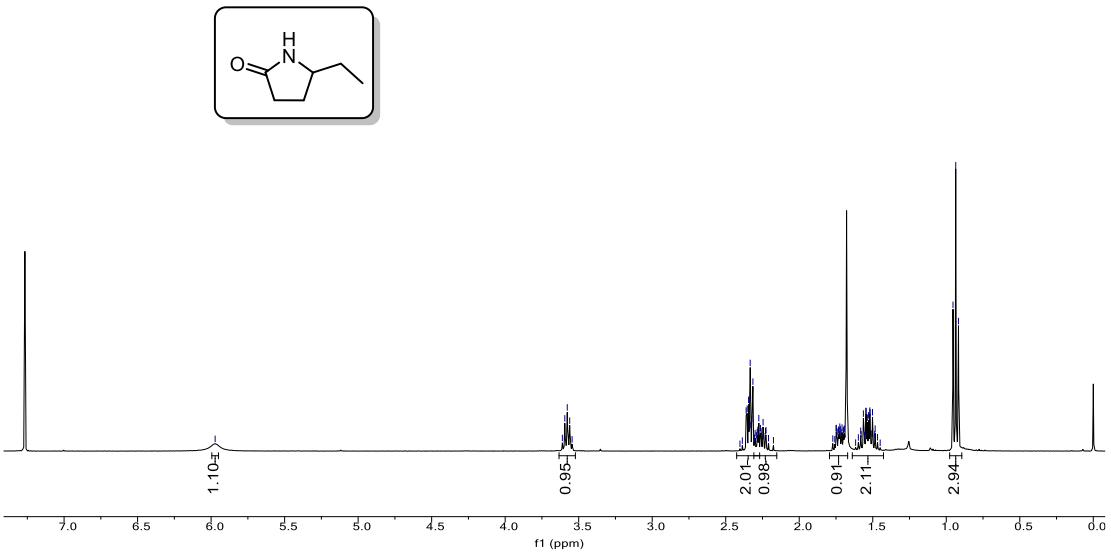


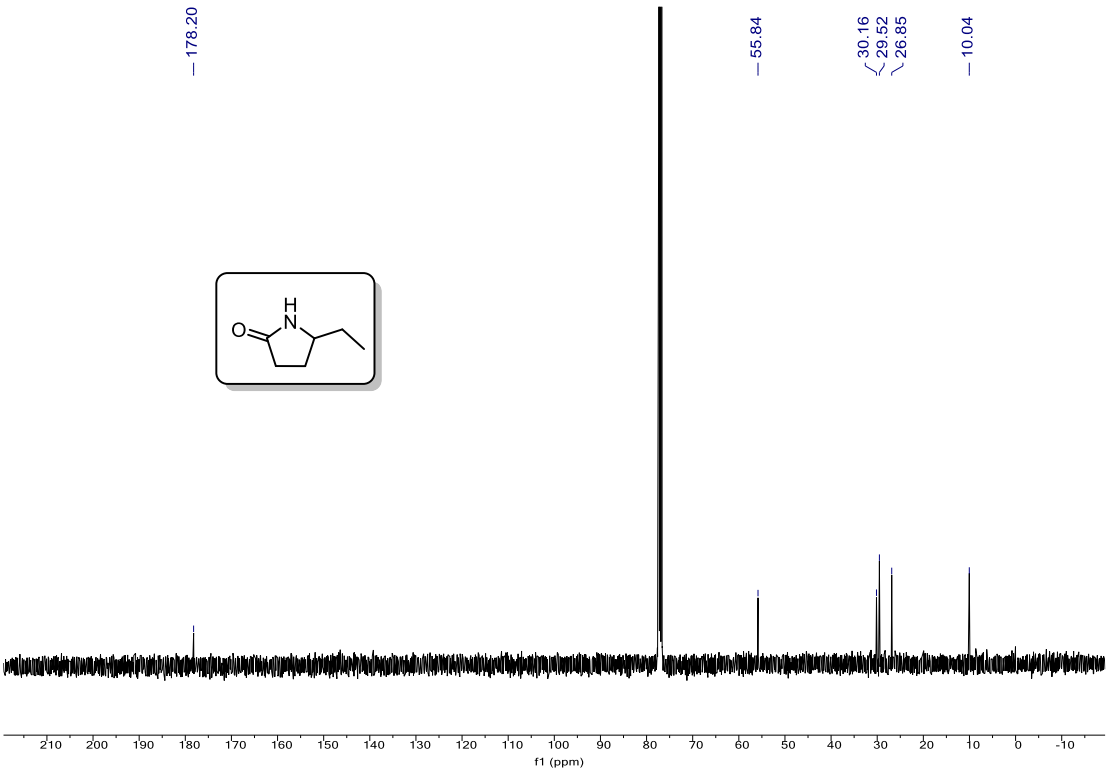
5-Methylpyrrolidin-2-one



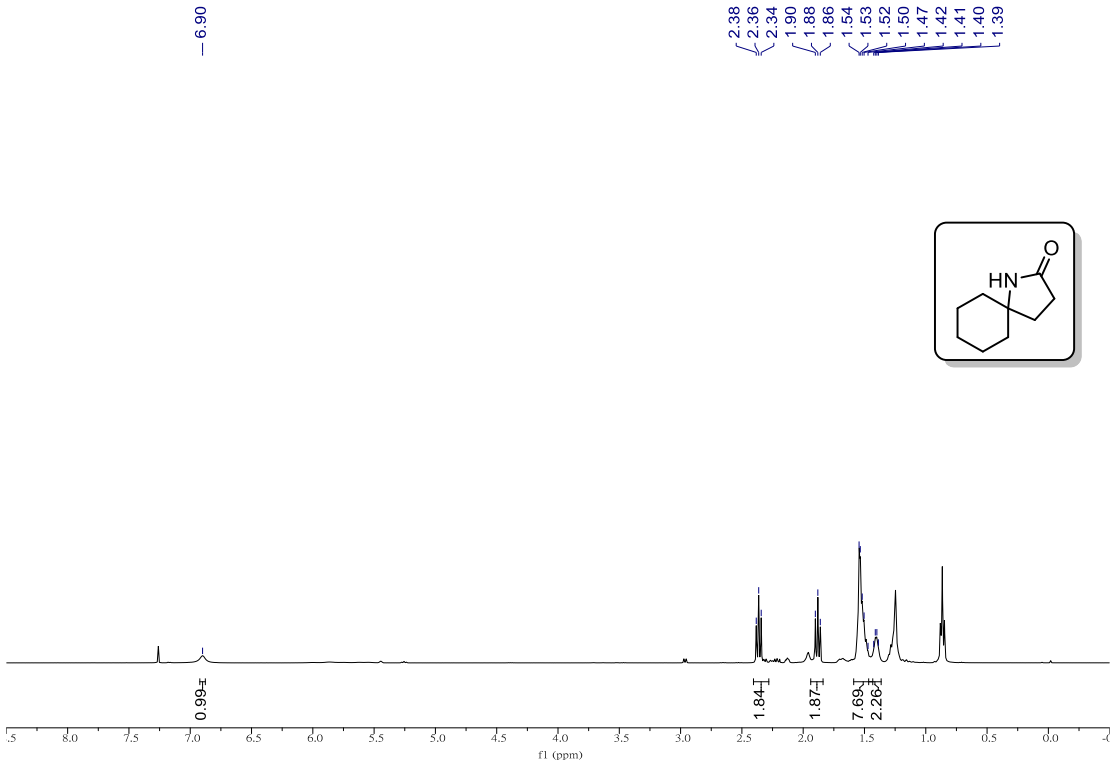
5-Ethylpyrrolidin-2-one

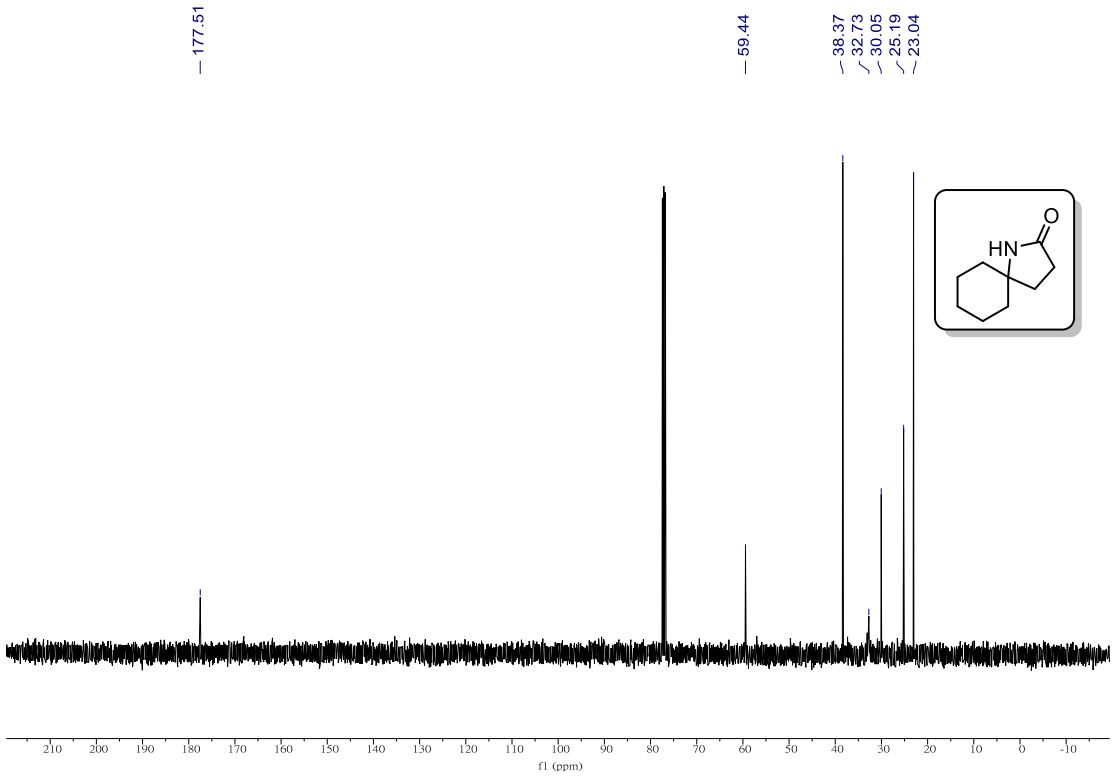




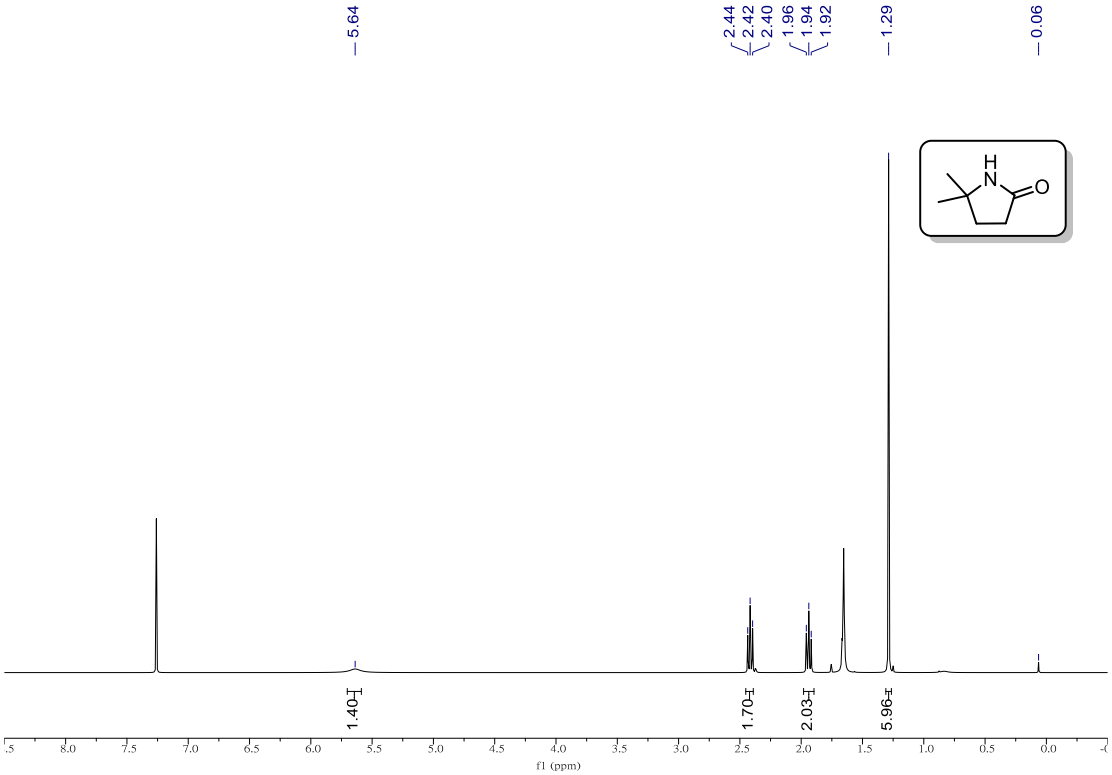


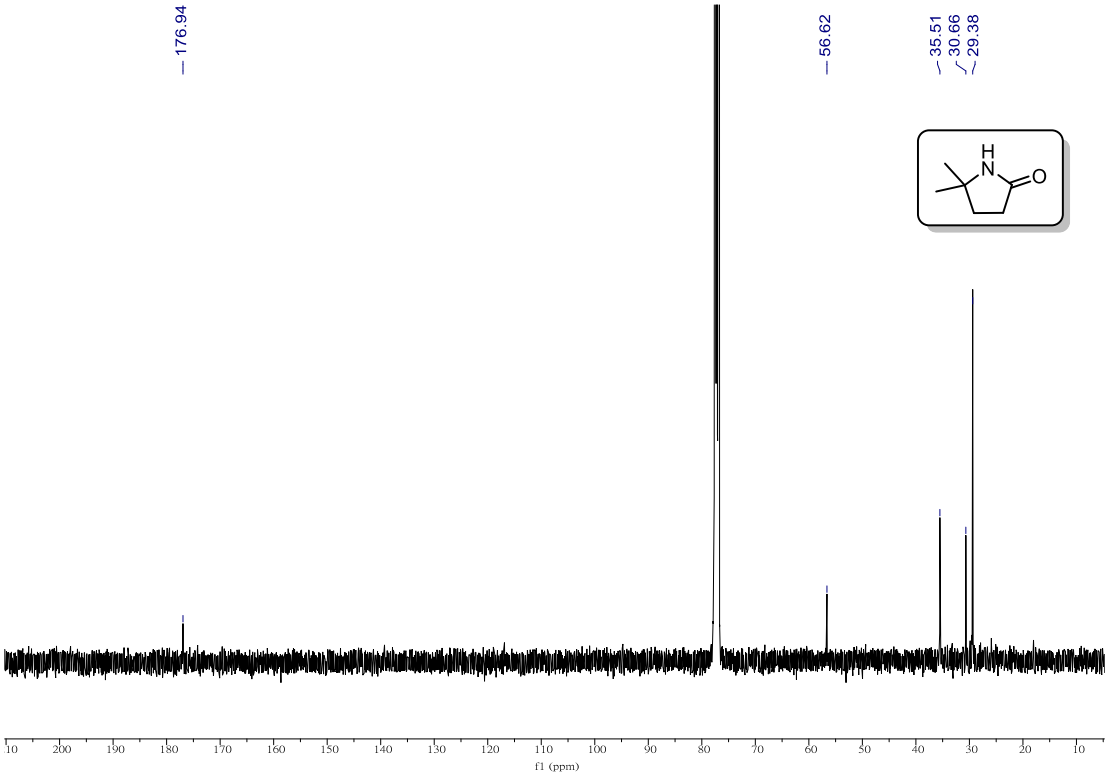
1-Azaspiro[4.5]decan-2-one



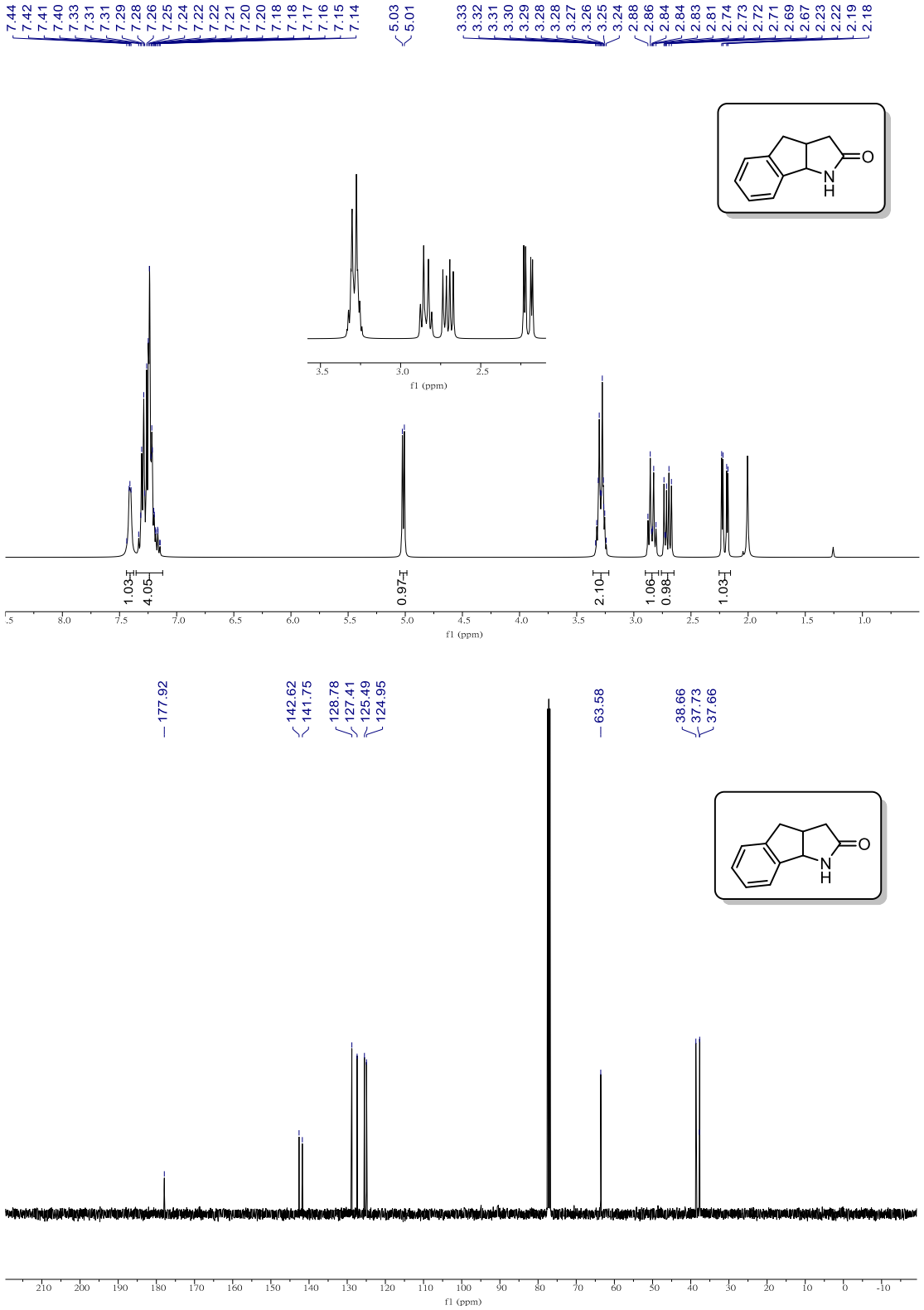


5,5-Dimethylpyrrolidin-2-one



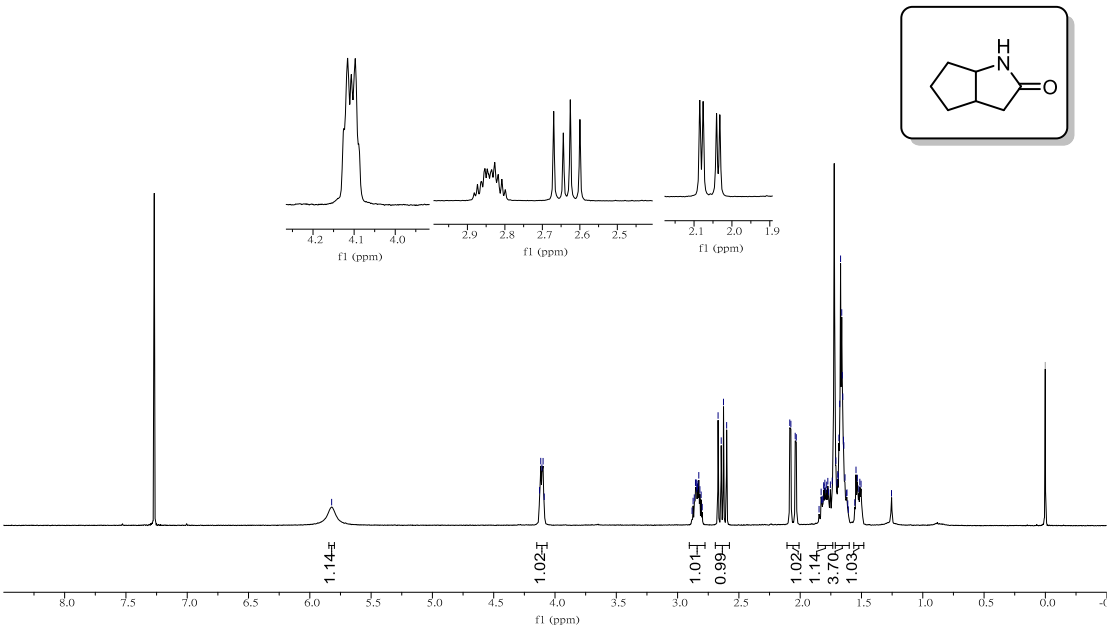


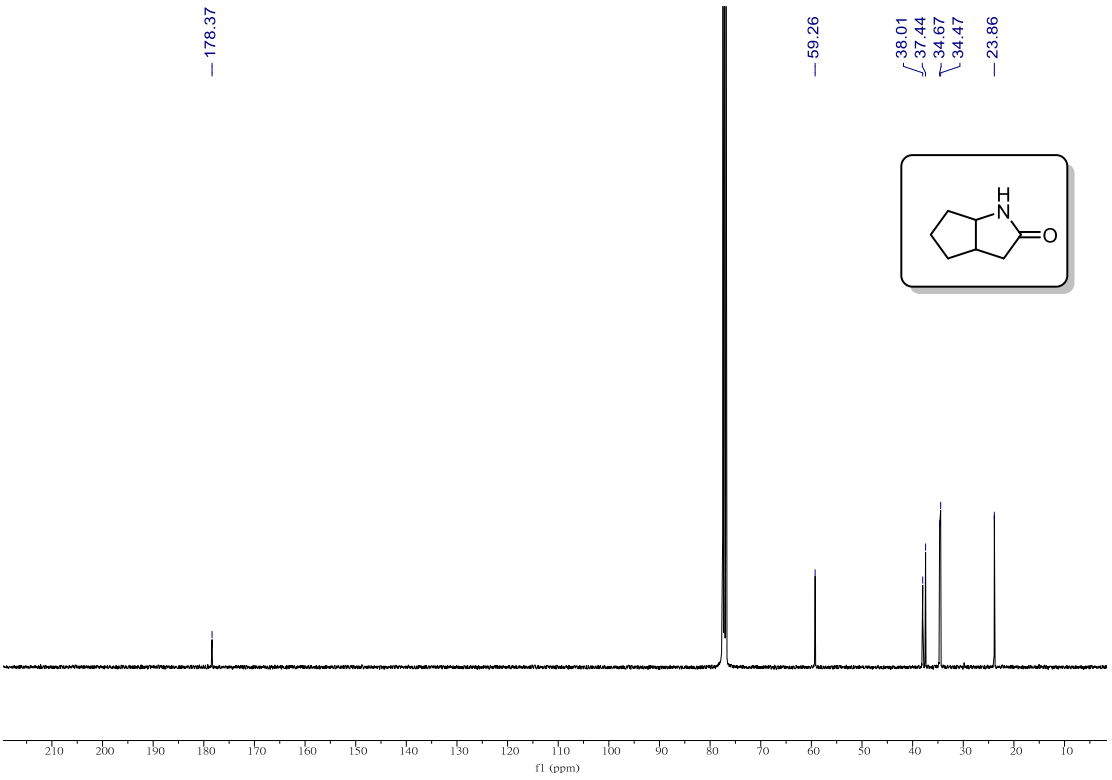
3,3a,4,8b-Tetrahydroindeno[1,2-b]pyrrol-2(1H)-one



Hexahydrocyclopenta[b]pyrrol-2(1H)-one

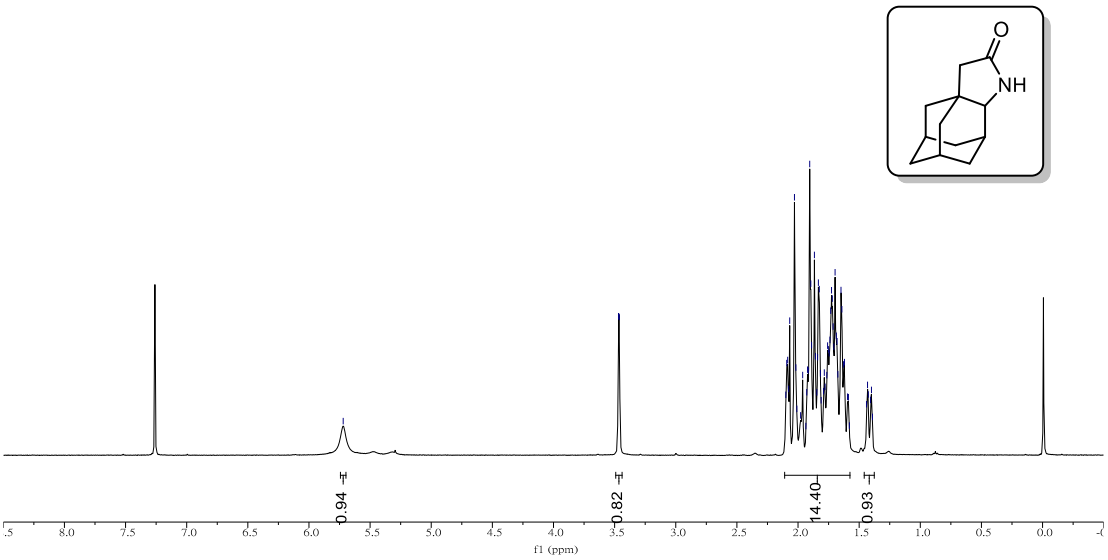




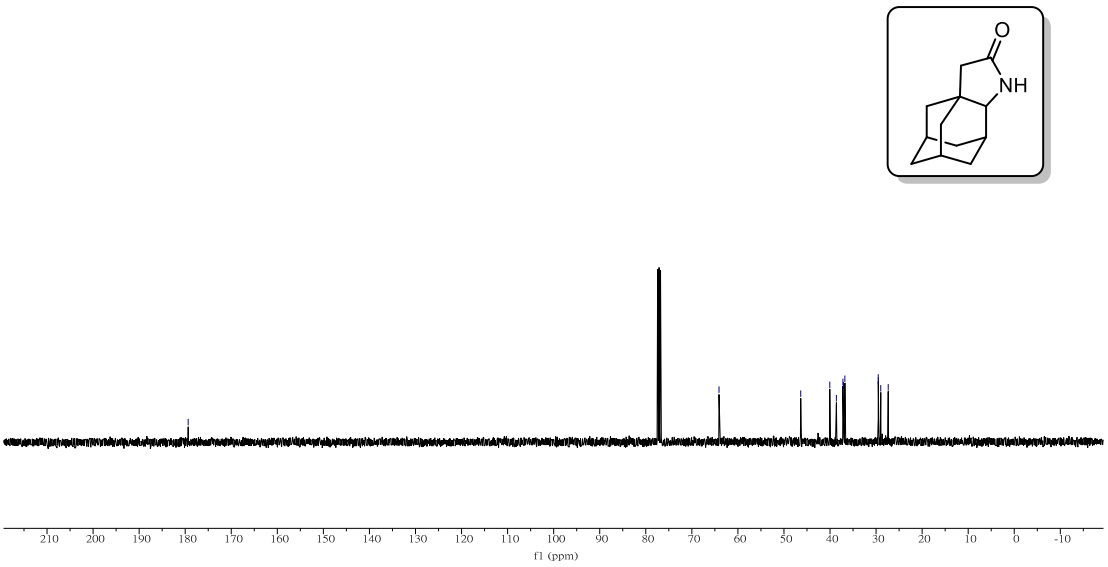


(3ar,5R,7S,9s)-Octahydro-3a,7:5,9-dimethanocycloocta[b]pyrrol-2(3H)-one

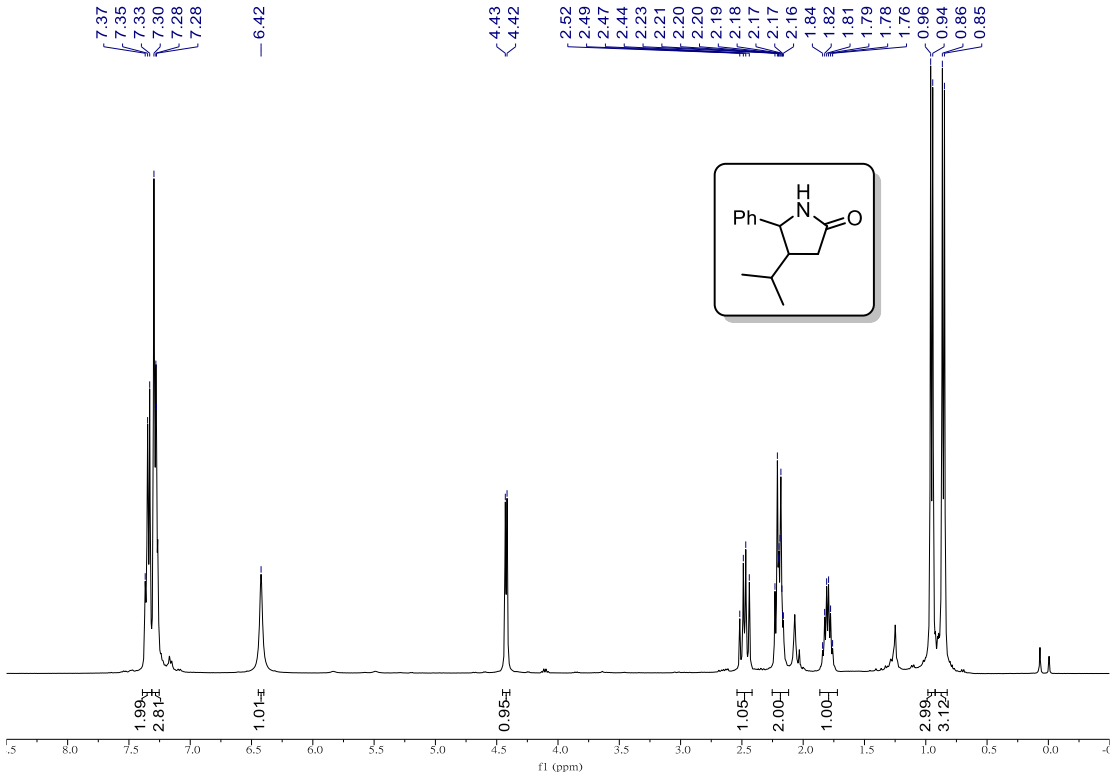


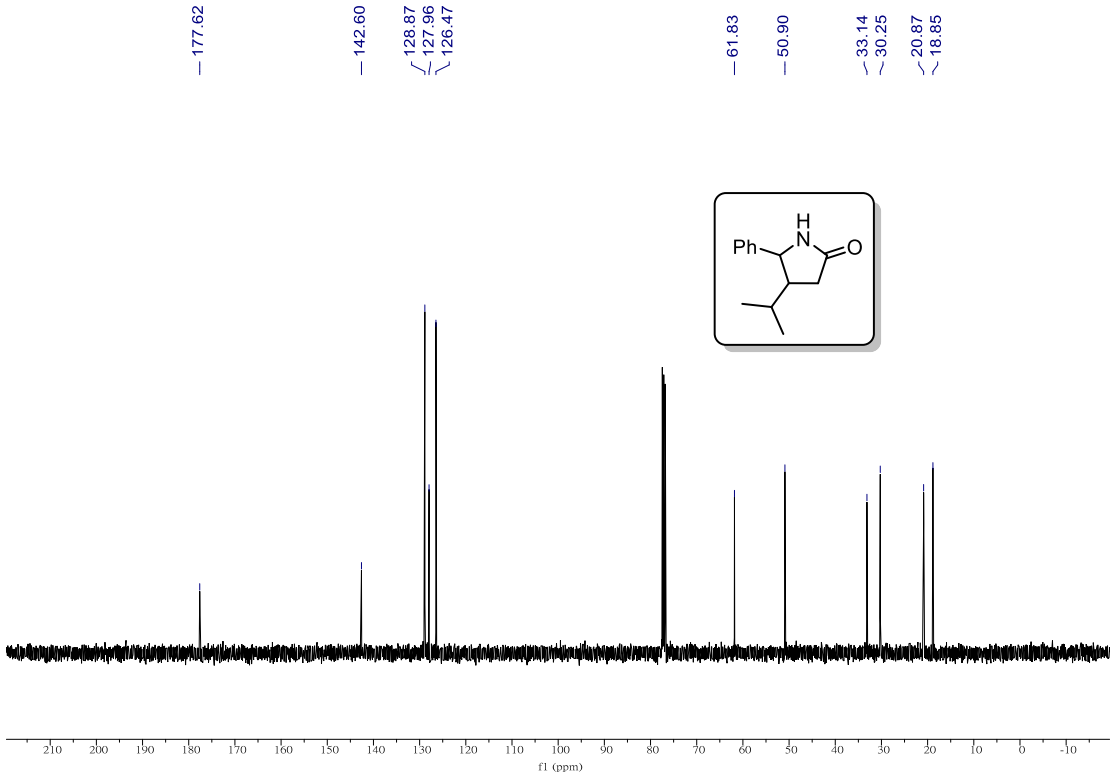




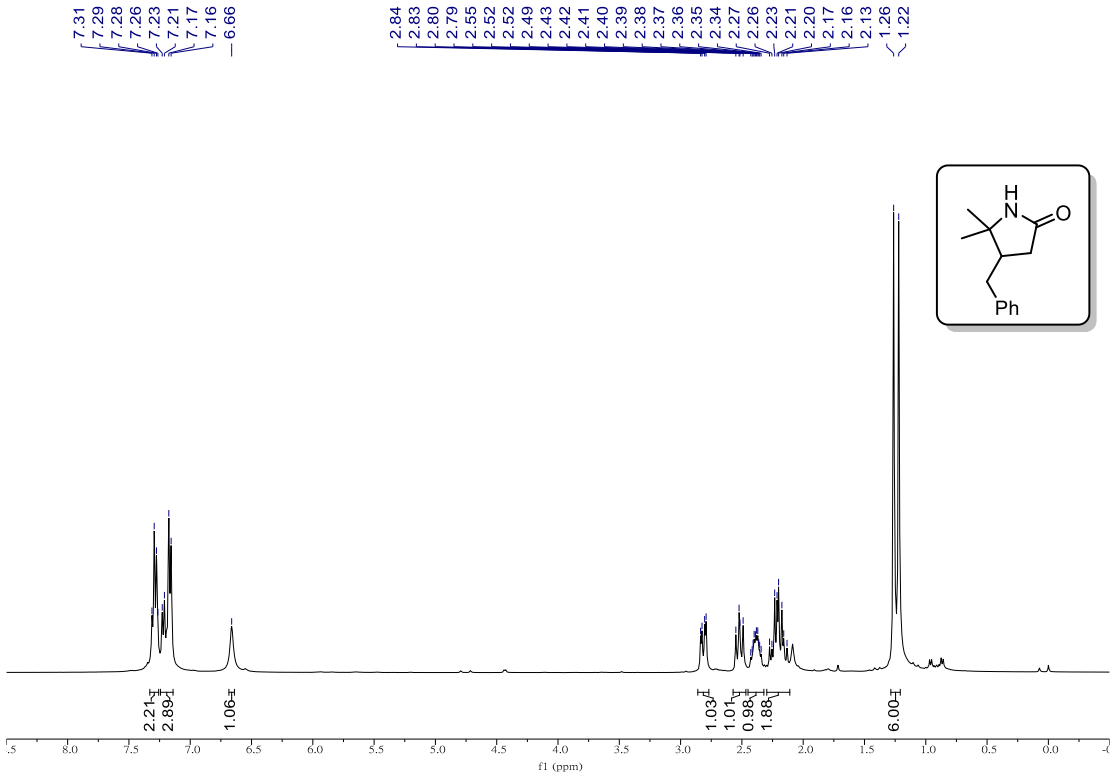


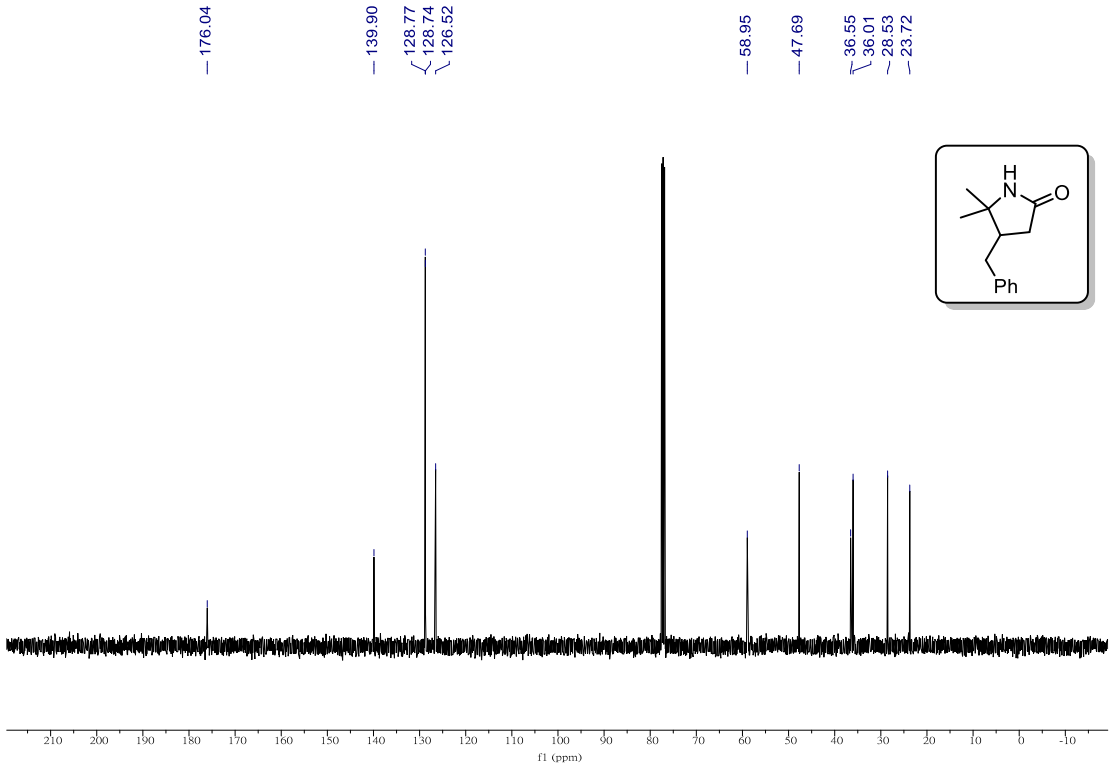
4-Isopropyl-5-phenylpyrrolidin-2-one



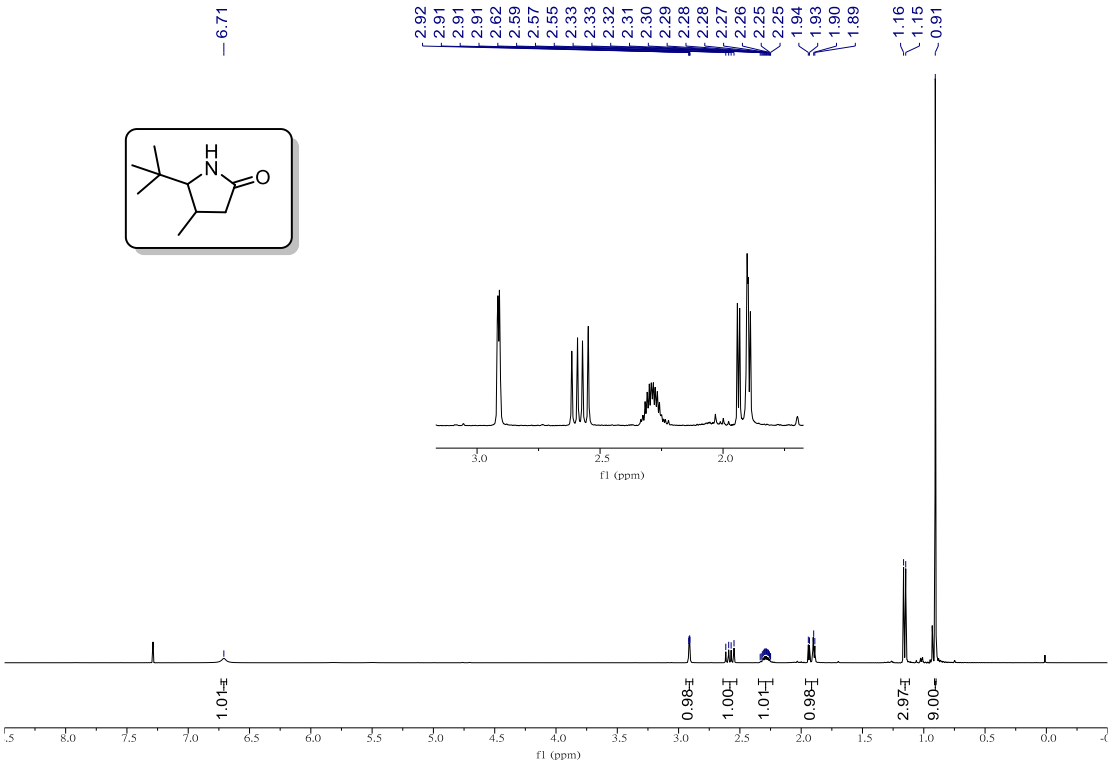


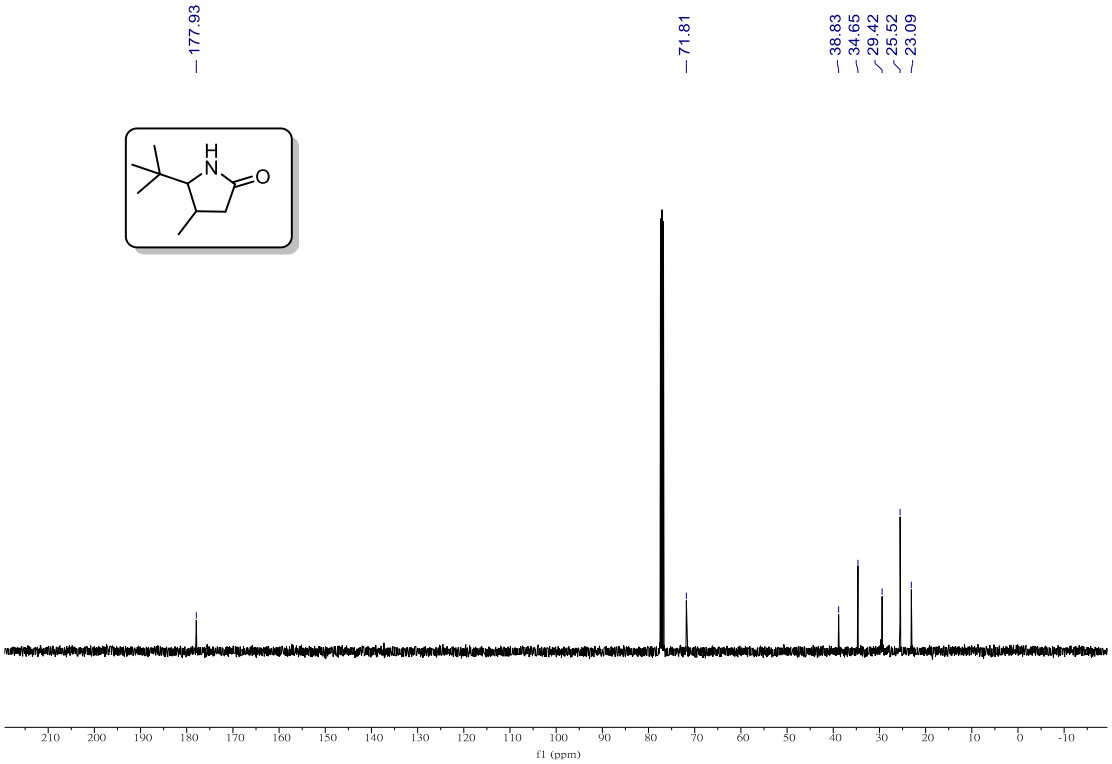
4-Benzyl-5,5-dimethylpyrrolidin-2-one



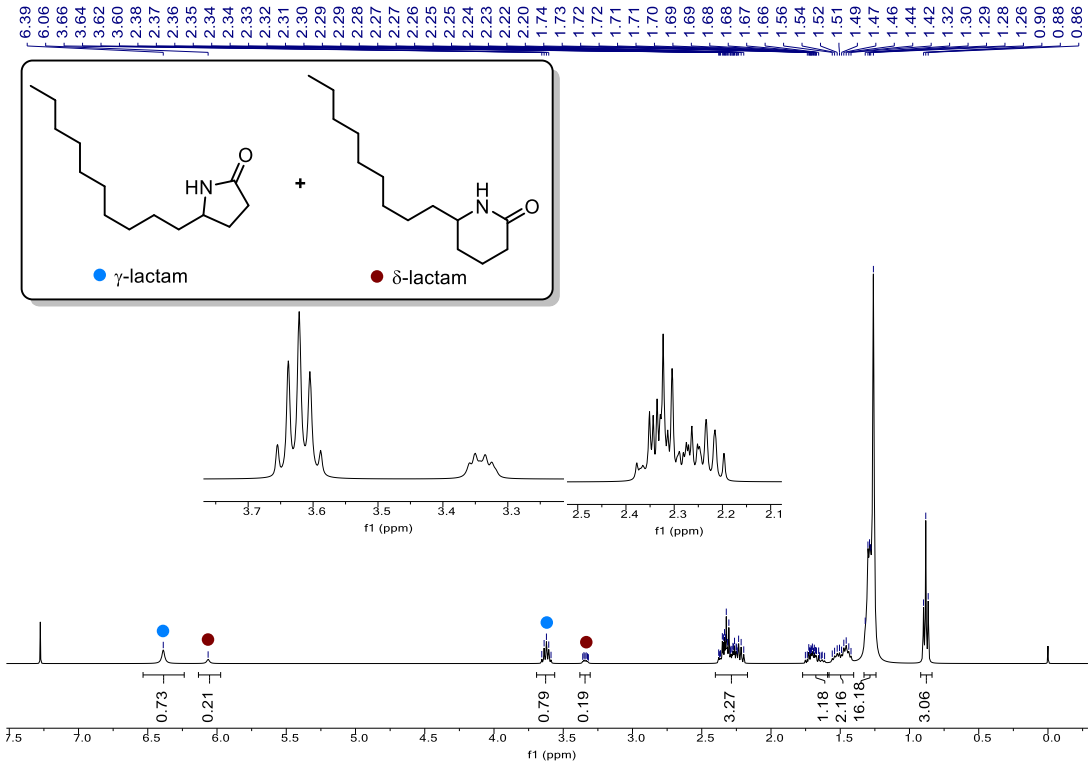


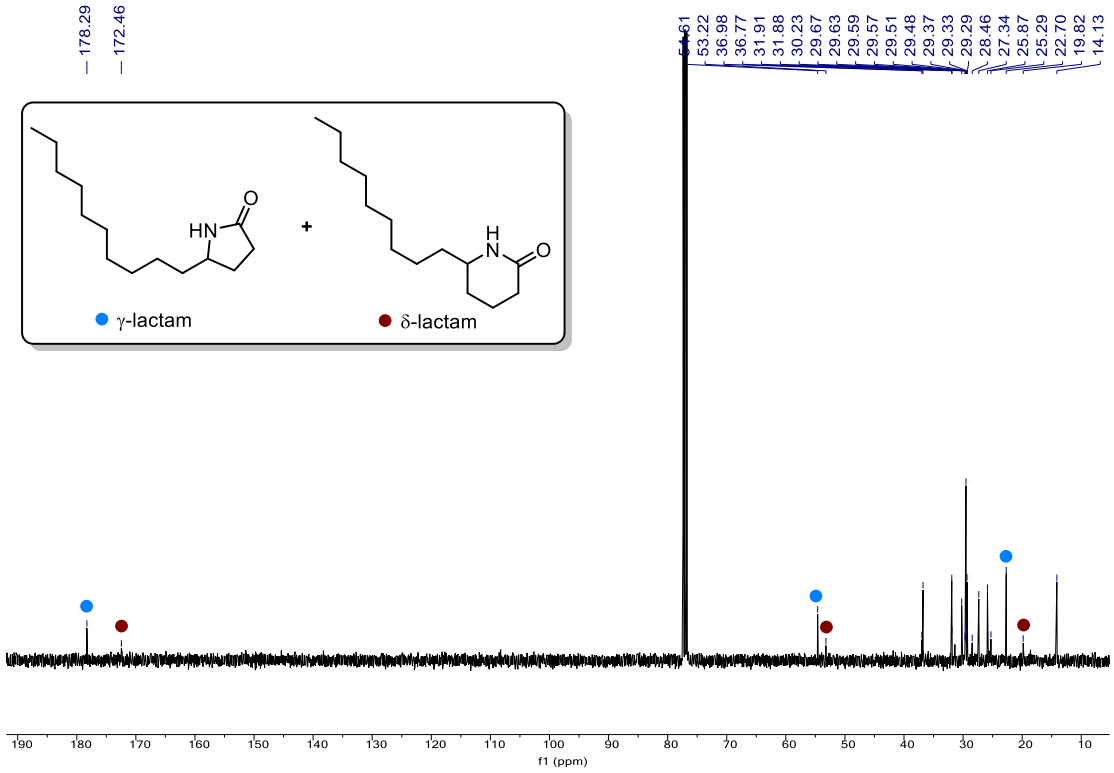
5-(tert-Butyl)-4-methylpyrrolidin-2-one



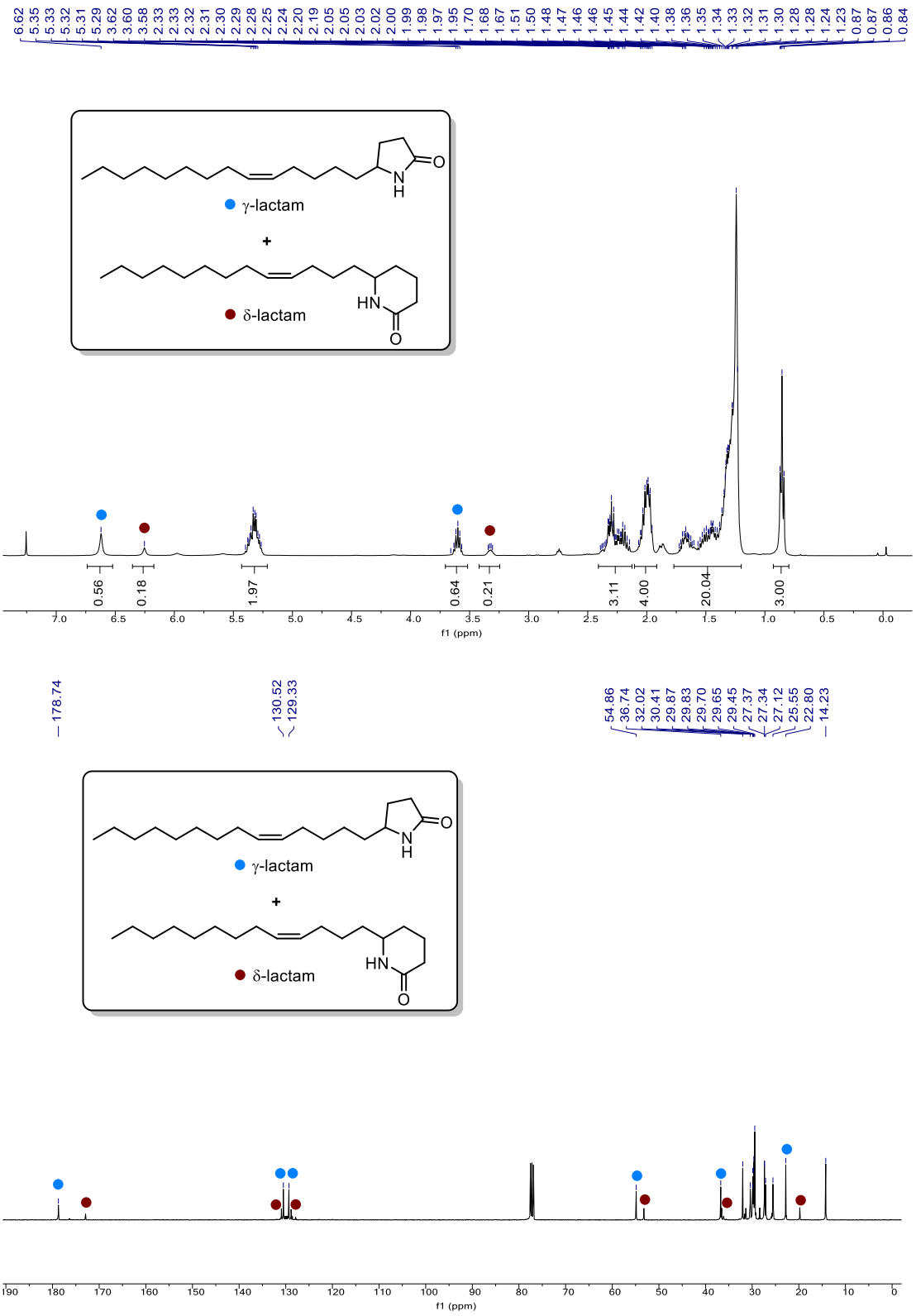


5-Decylpyrrolidin-2-one & 6-nonylpiperidin-2-one

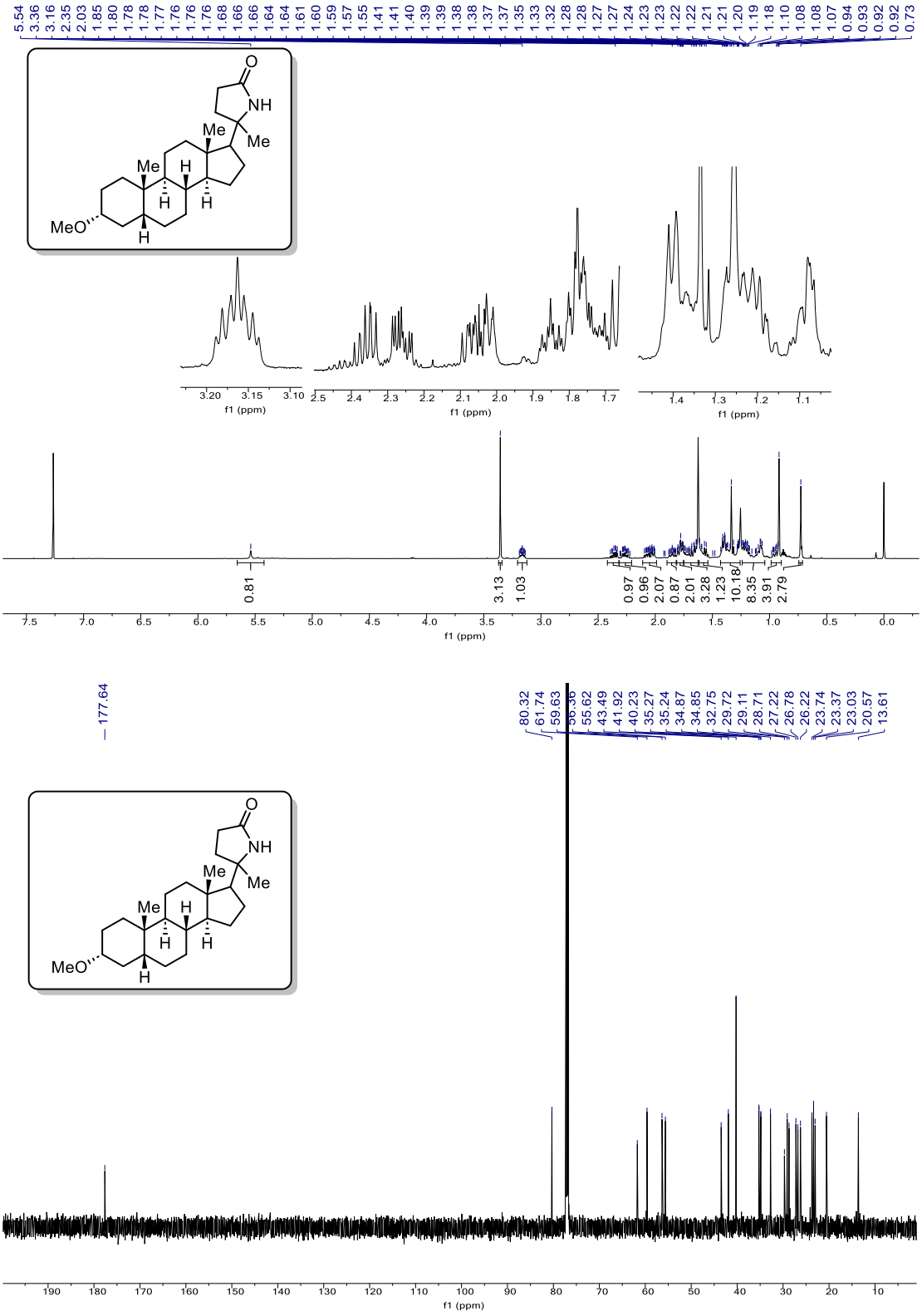




(Z)-5-(Tetradec-5-en-1-yl)pyrrolidin-2-one

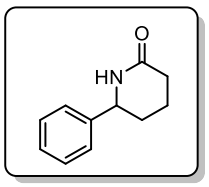


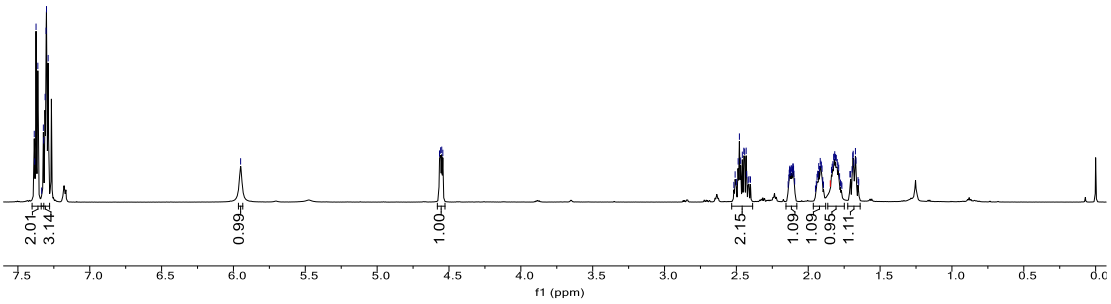
5-((3R,5R,8R,9S,10S,13S,14S)-3-Methoxy-10,13-dimethylhexadecahydro-1H-cyclopenta[a]phenanthren-17-yl)-5-methylpyrrolidin-2-one



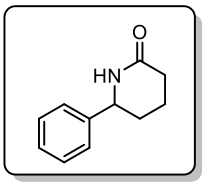
6-Phenylpiperidin-2-one

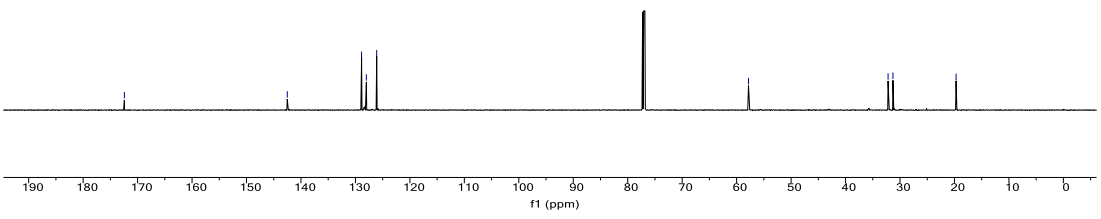




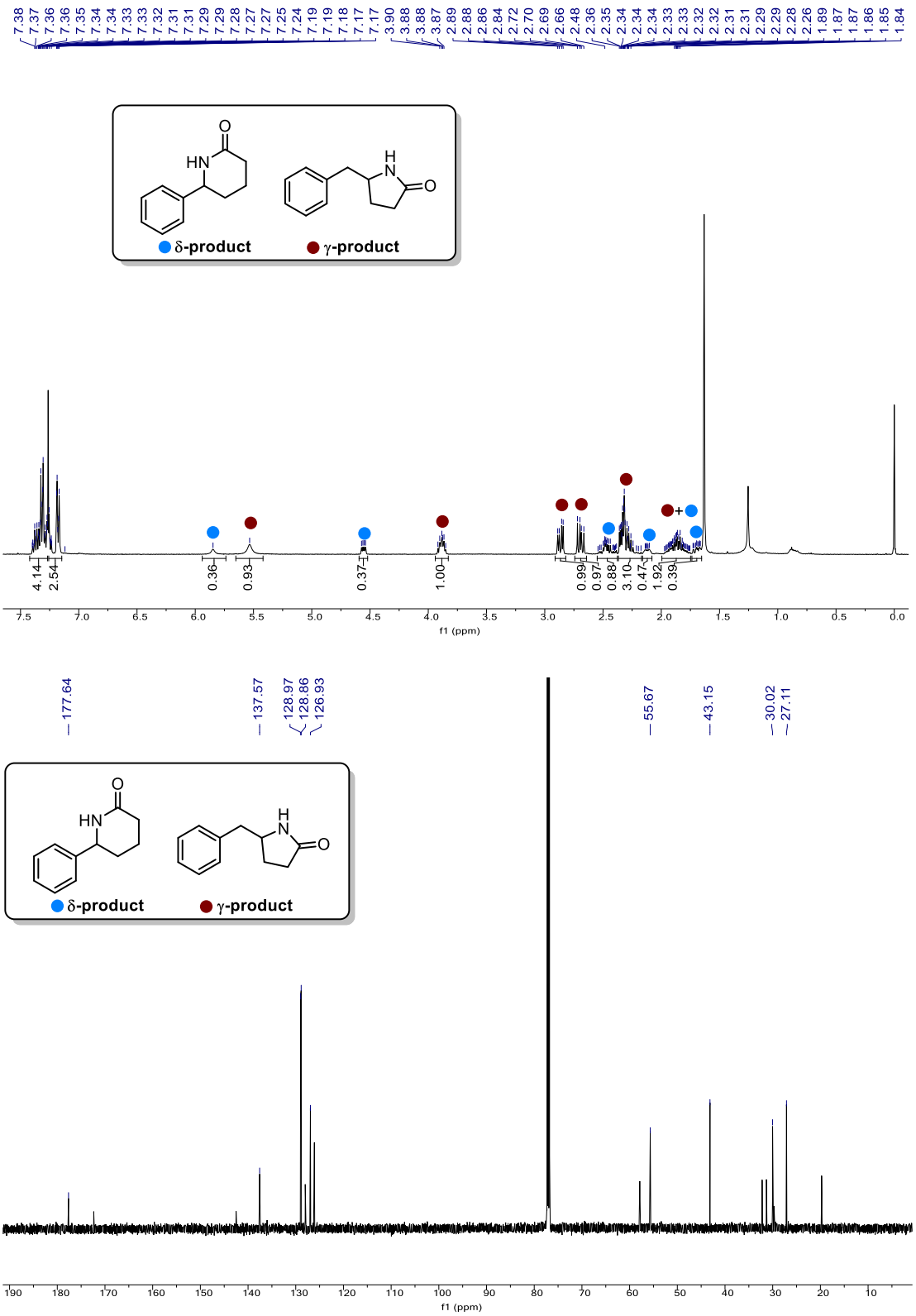






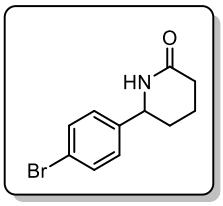


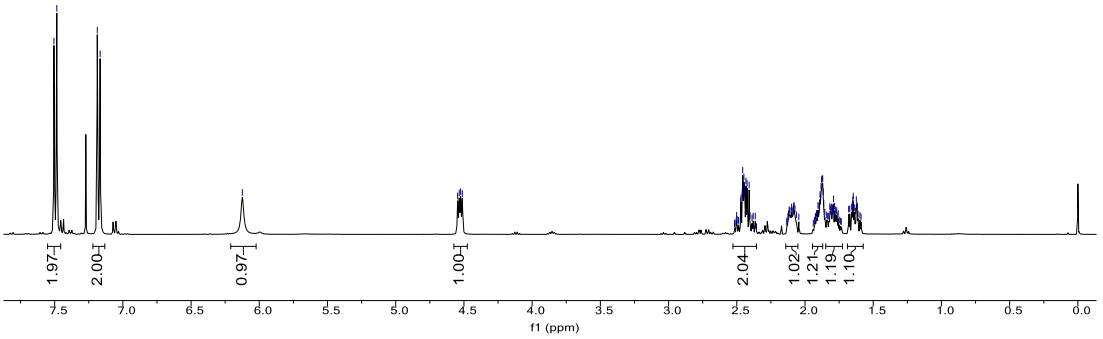
5-Benzylpyrrolidin-2-one

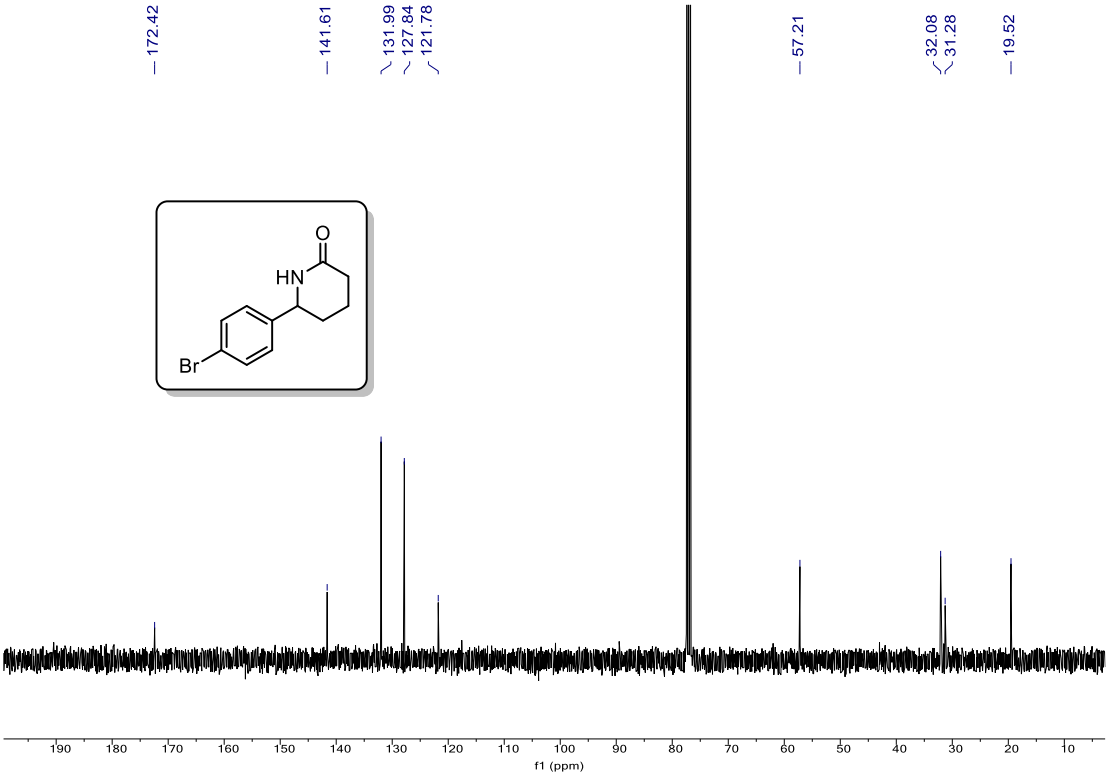


6-(4-Bromophenyl)piperidin-2-one

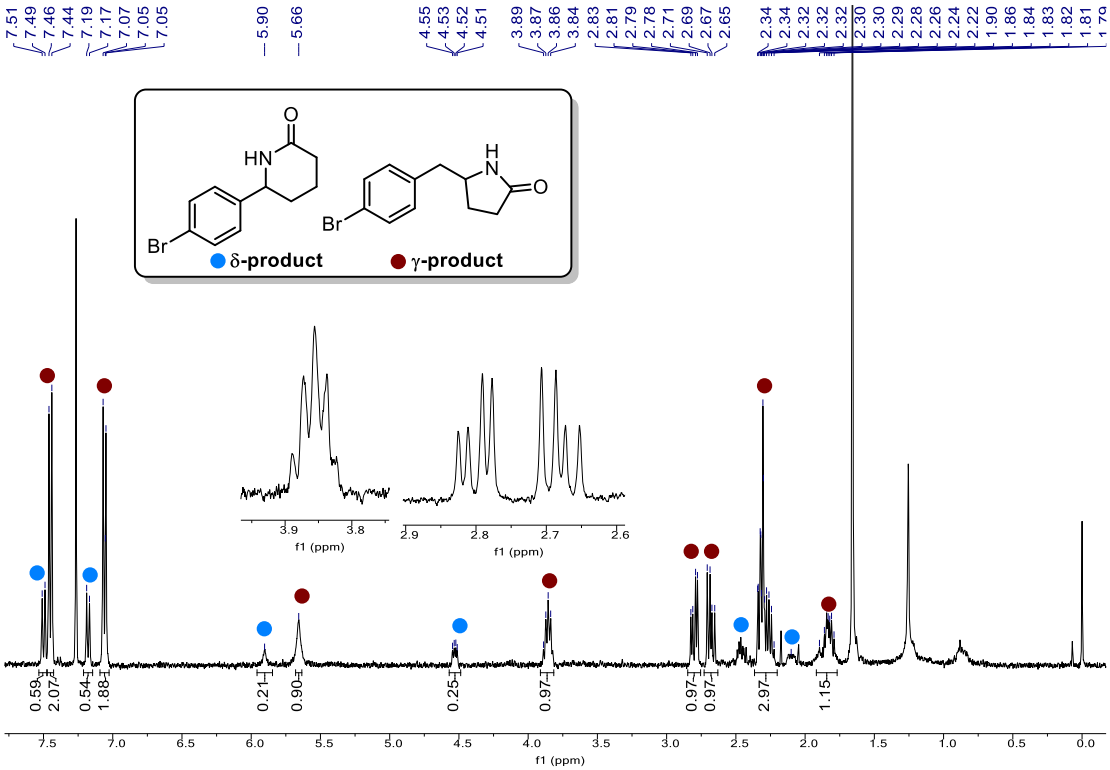


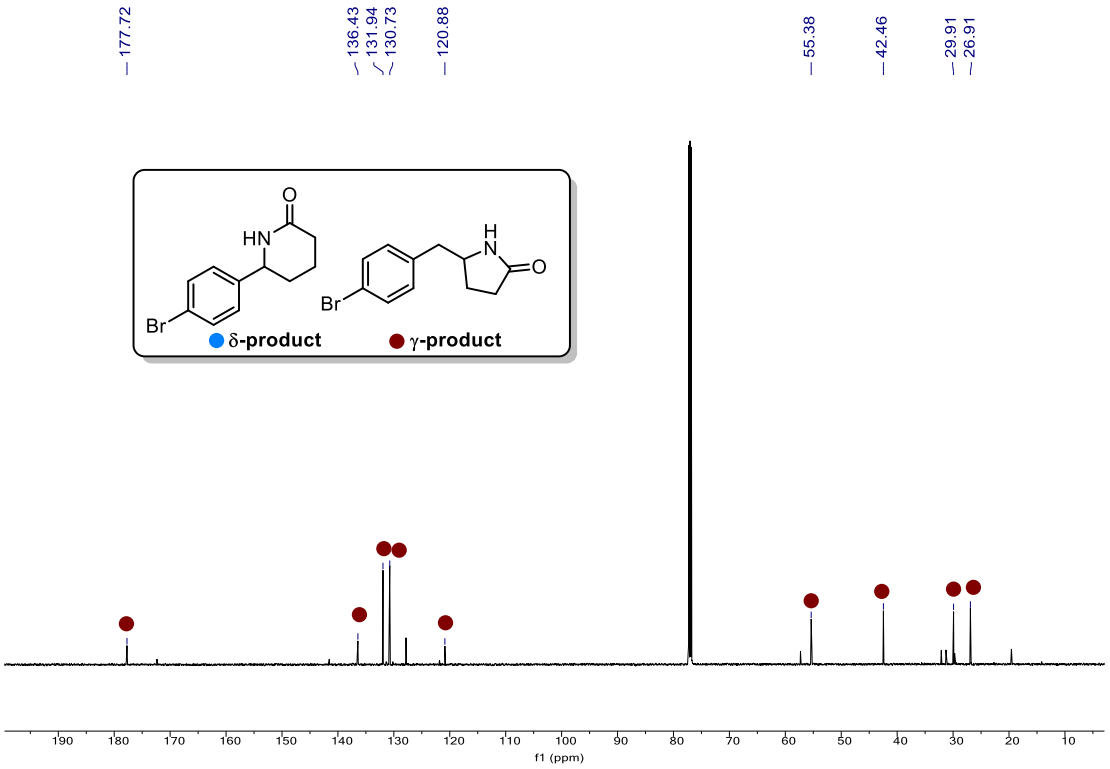






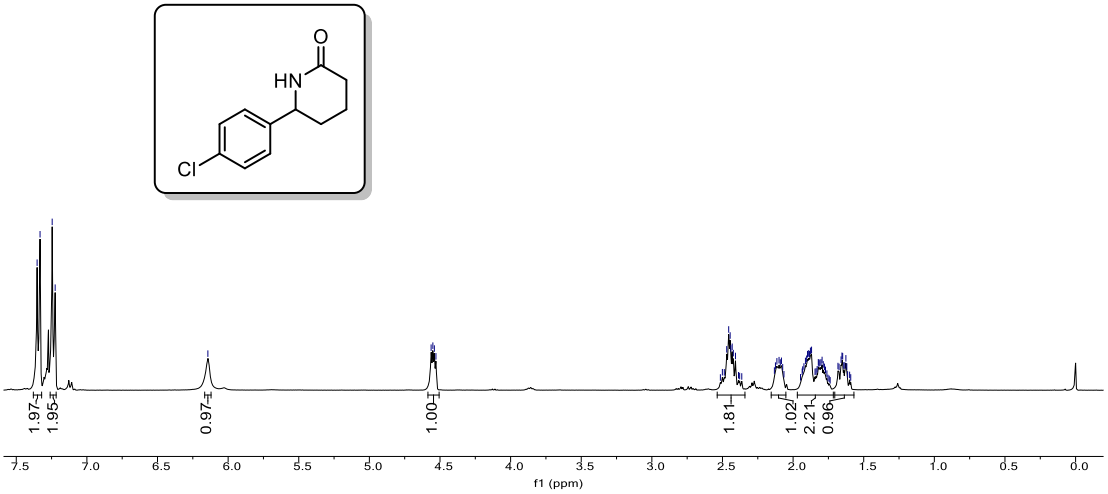
5-(4-Bromobenzyl)pyrrolidin-2-one



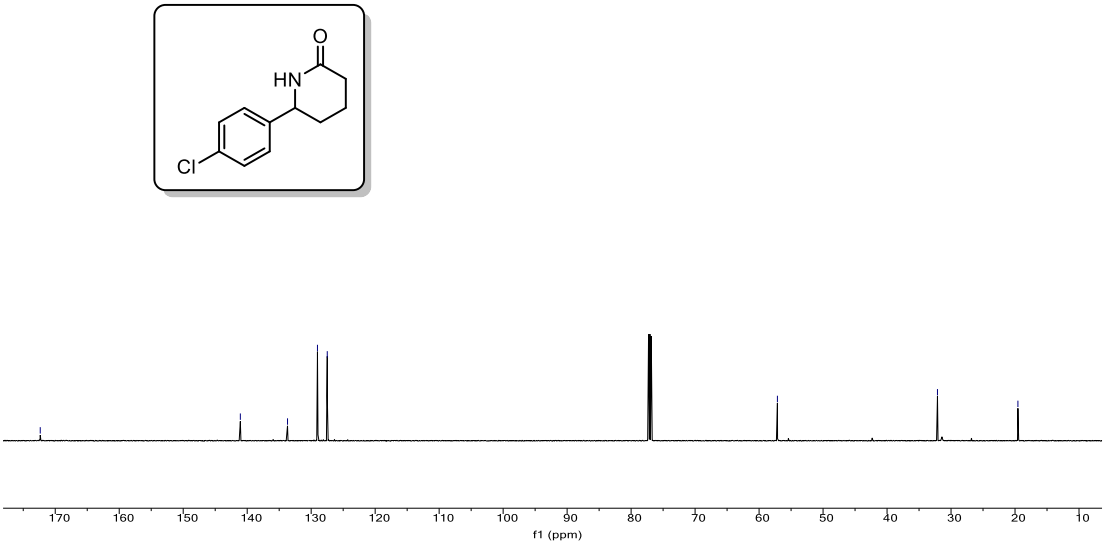


6-(4-Chlorophenyl)piperidin-2-one

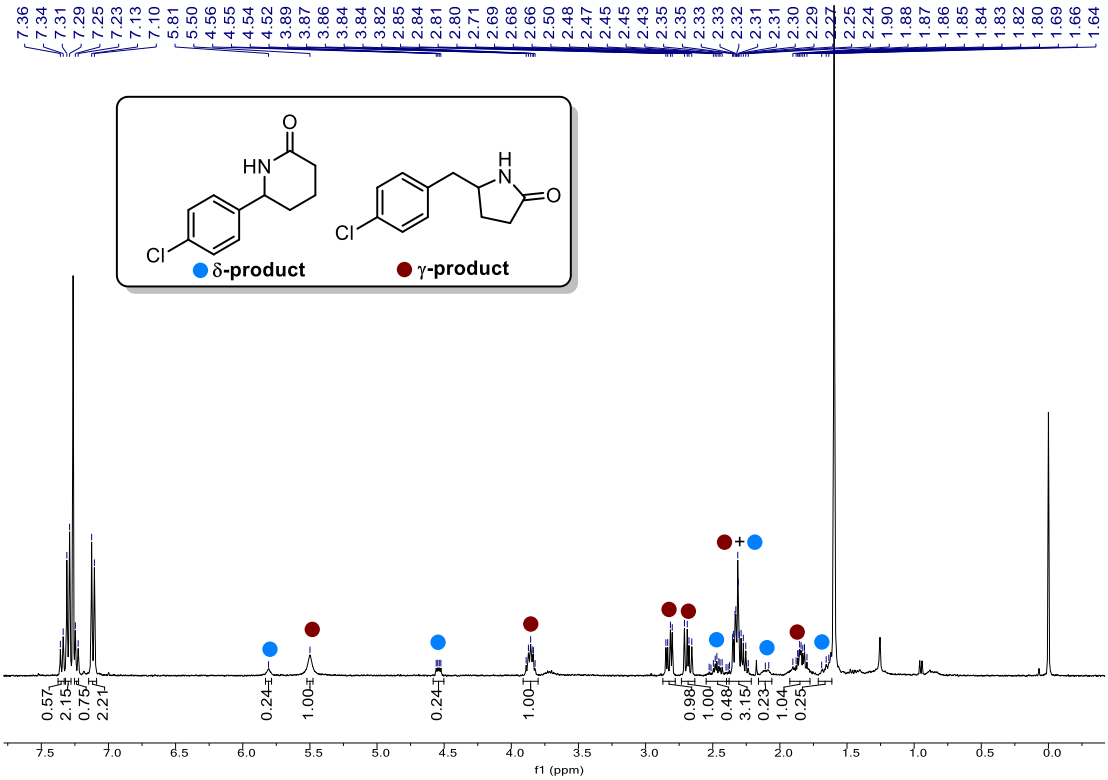


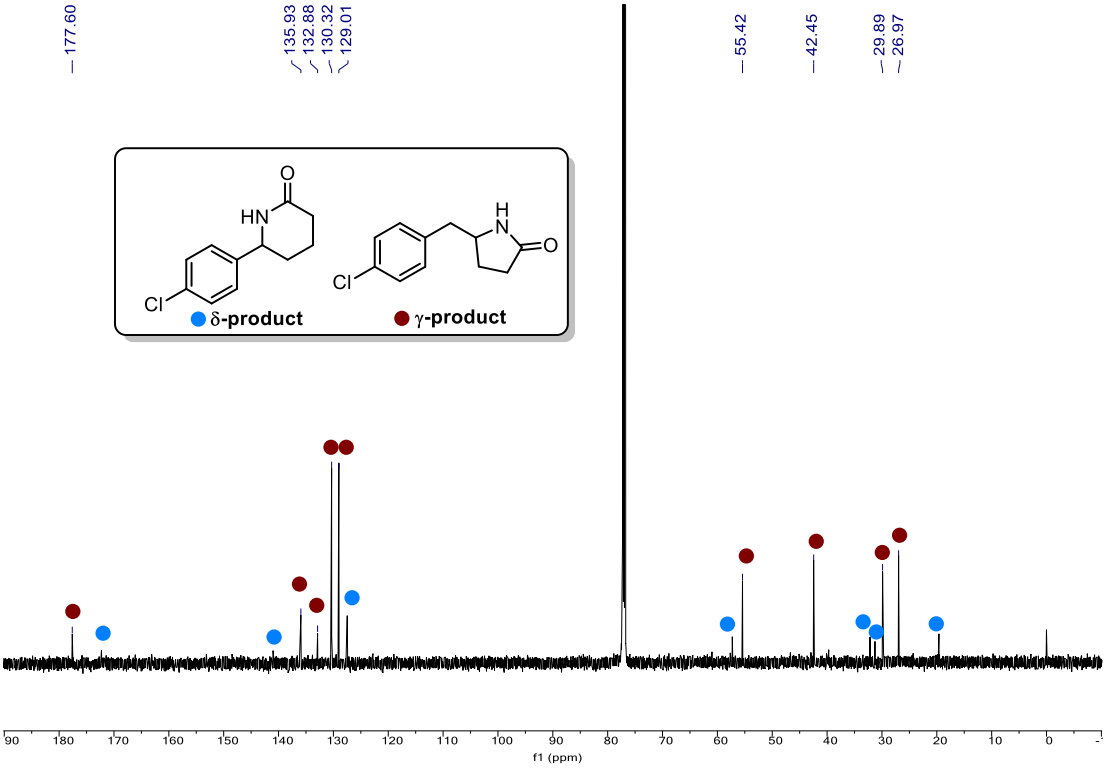




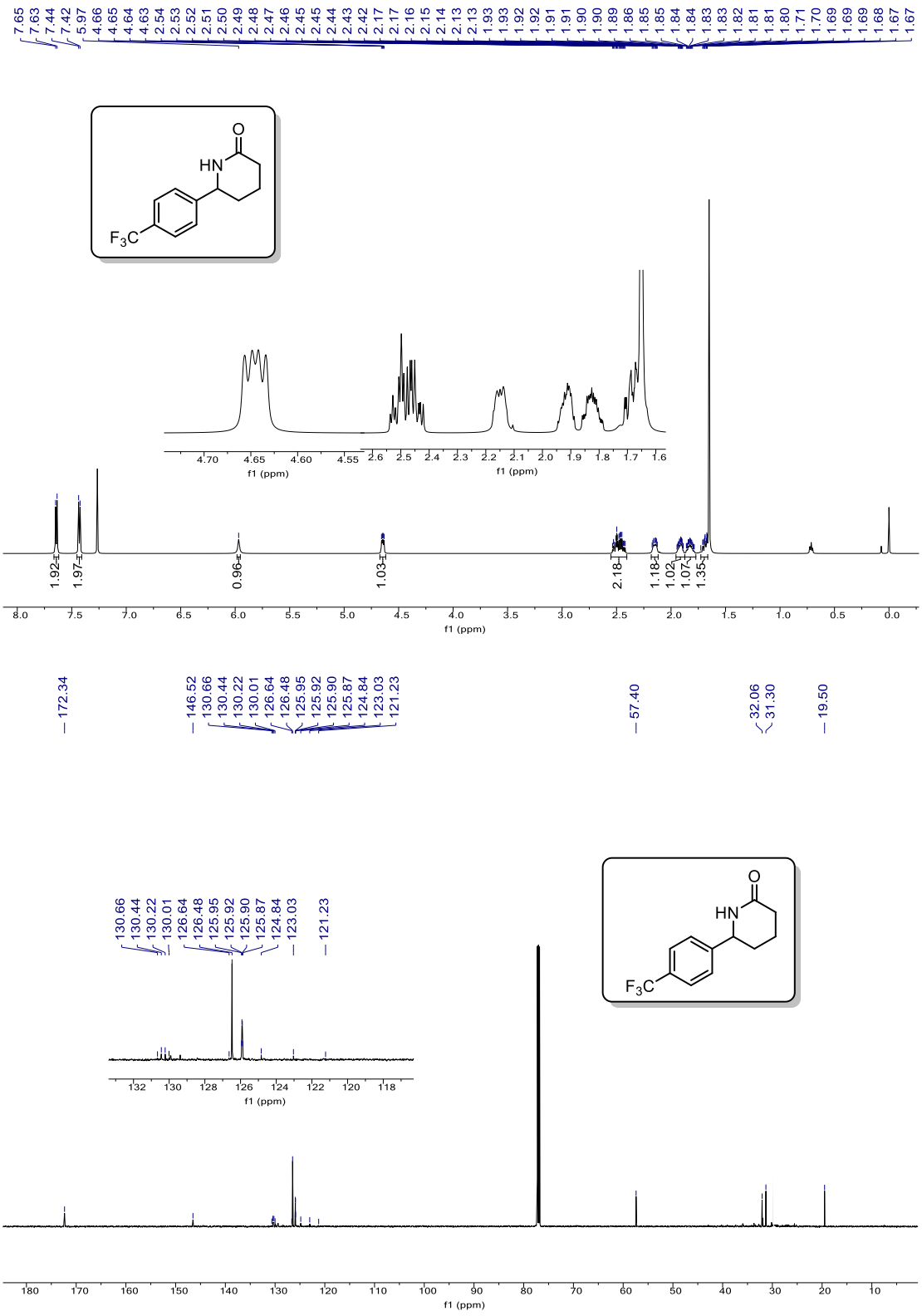


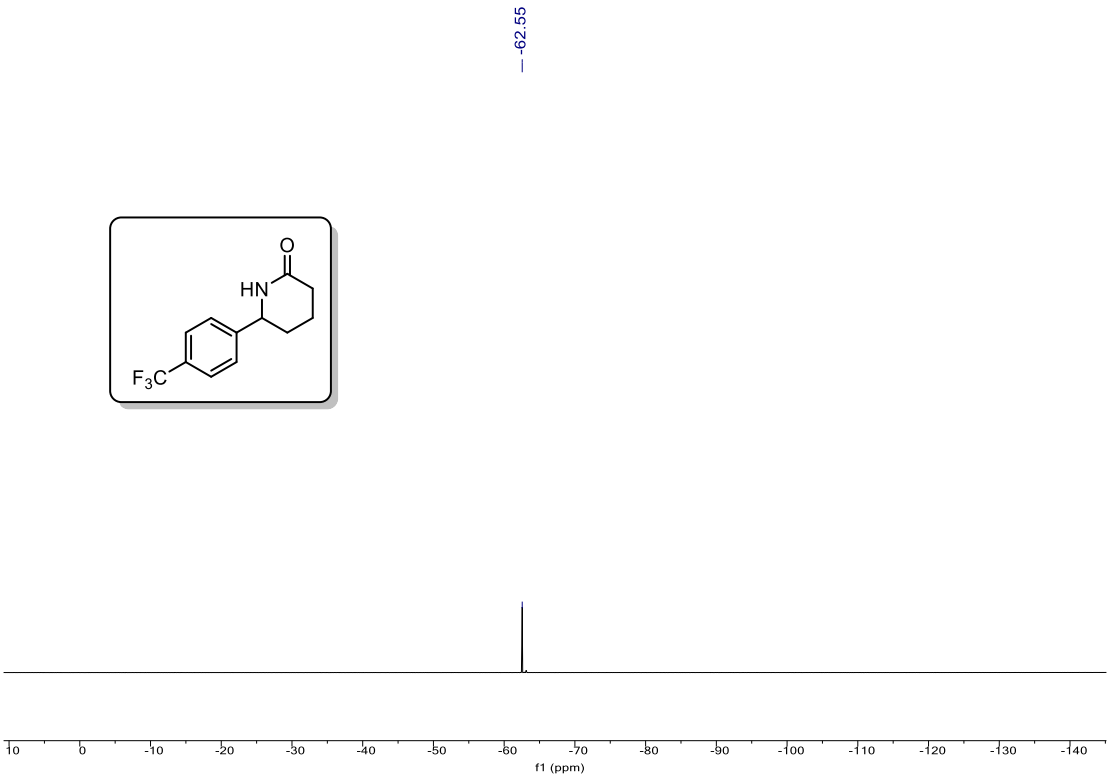
5-(4-Chlorobenzyl)pyrrolidin-2-one



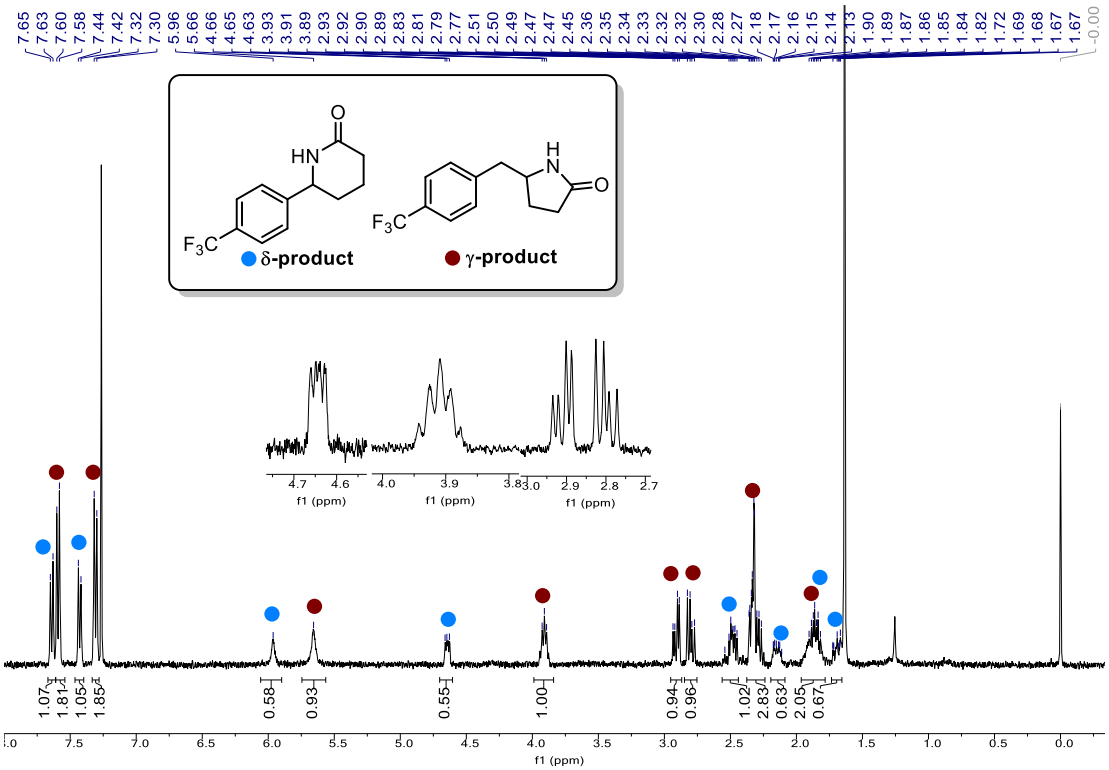


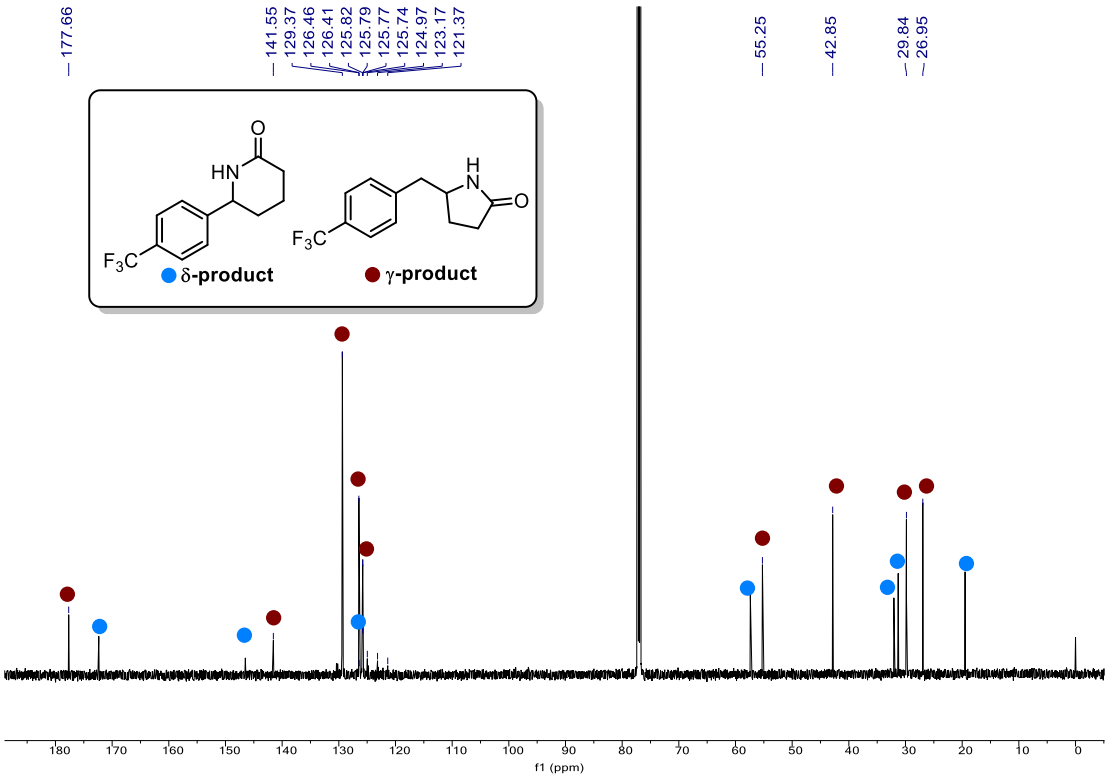
6-(4-(Trifluoromethyl)phenyl)piperidin-2-one

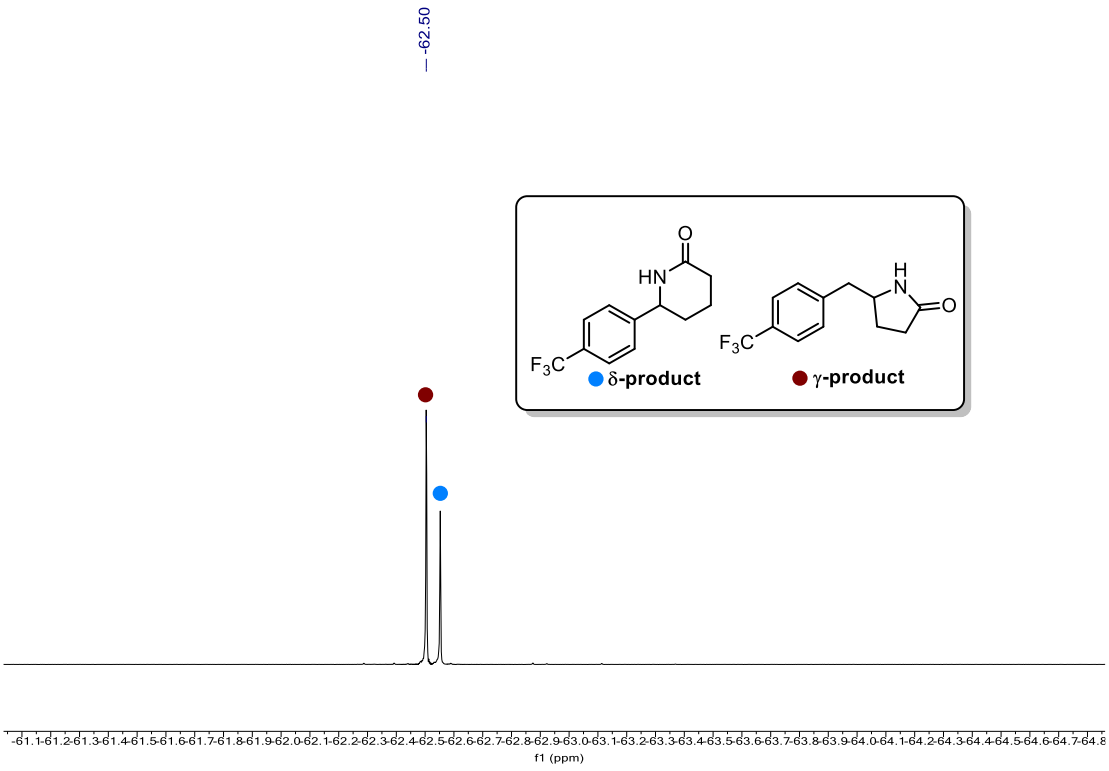



-62.55
O
HN
F3C
10
0
-10
-20
-30
-40
-50
-60
-70
-80
-90
-100
-110
-120
-130
-140
f1 (ppm)

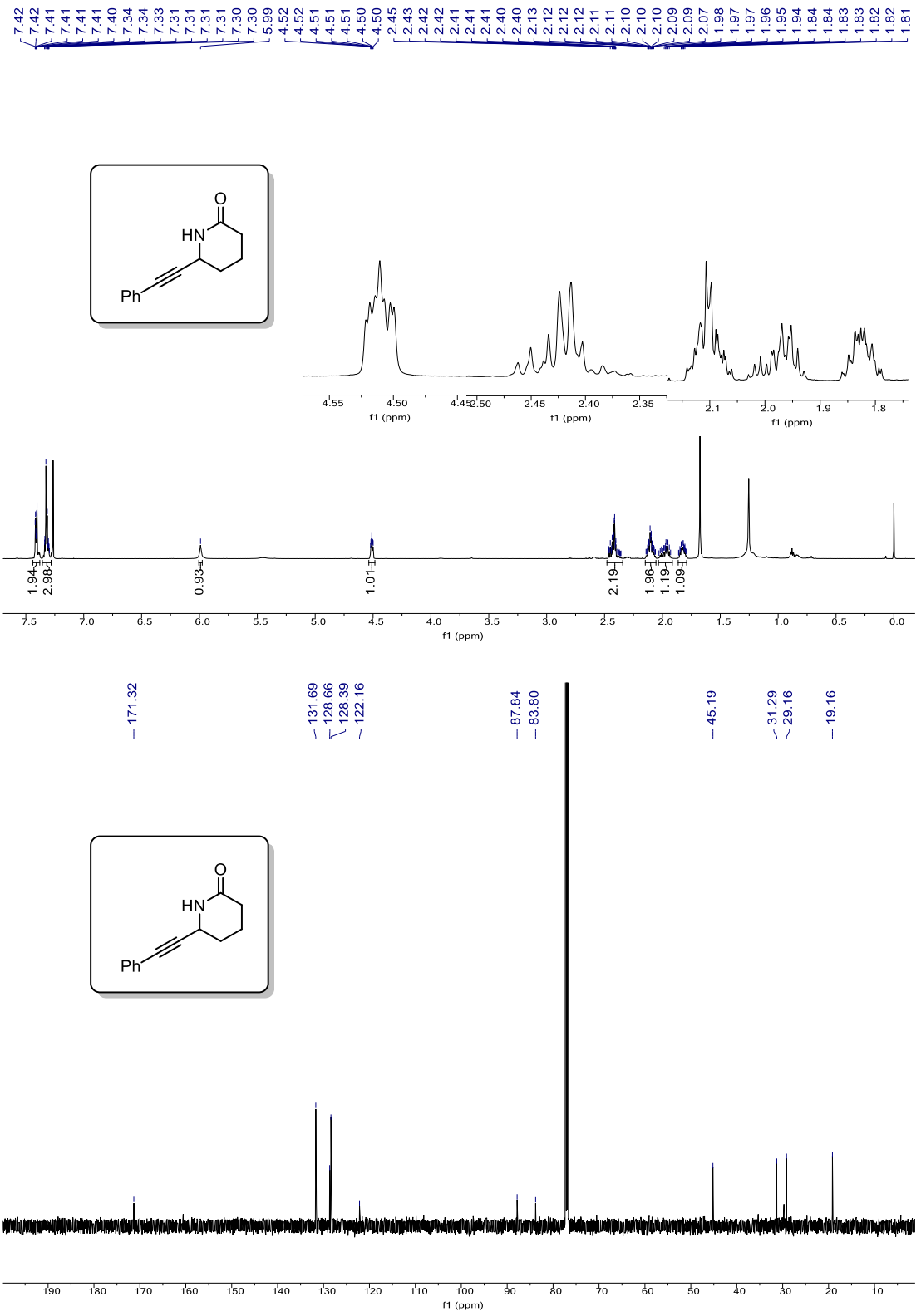
5-(4-(Trifluoromethyl)benzyl)pyrrolidin-2-one



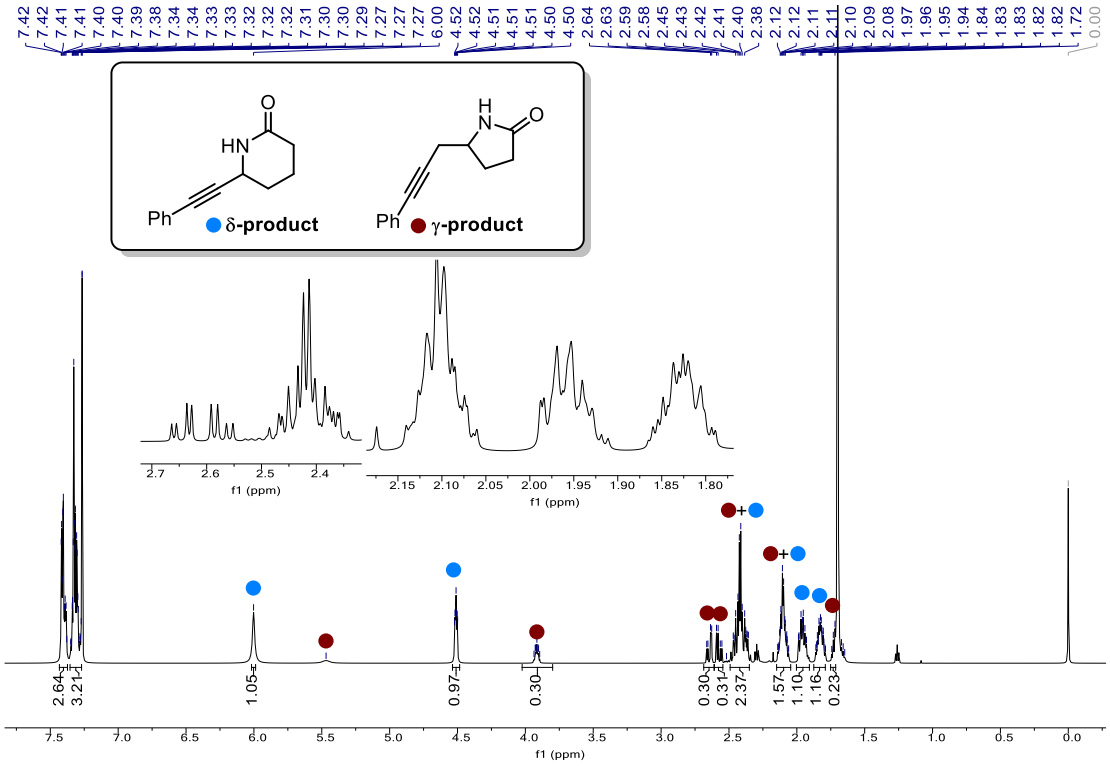


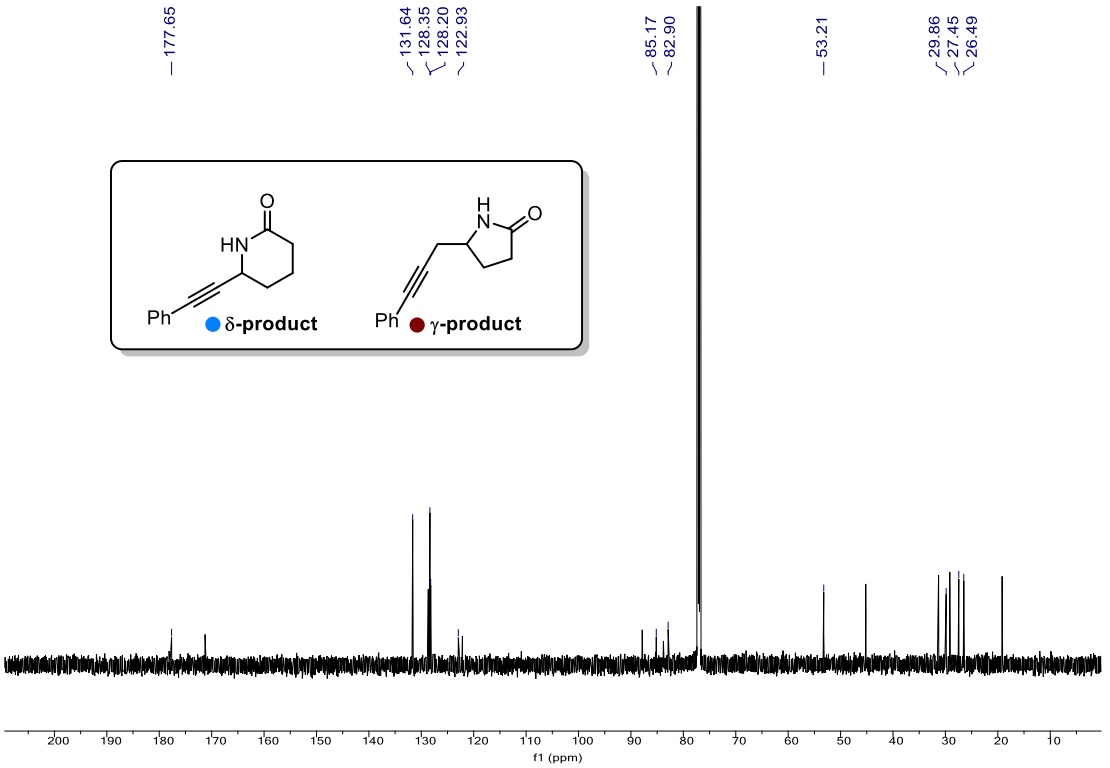

-62.50
HN
O
F3C
δ-product
H
N
O
F3C
γ-product
f1 (ppm)

6-(Phenylethynyl)piperidin-2-one

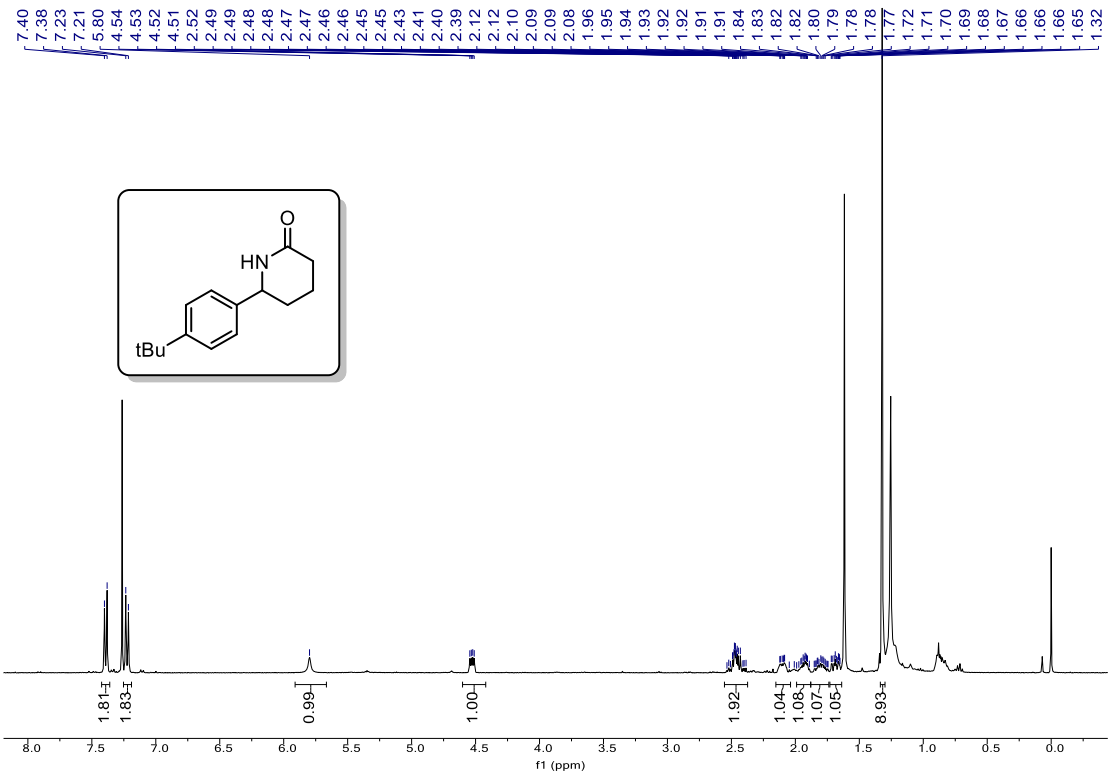


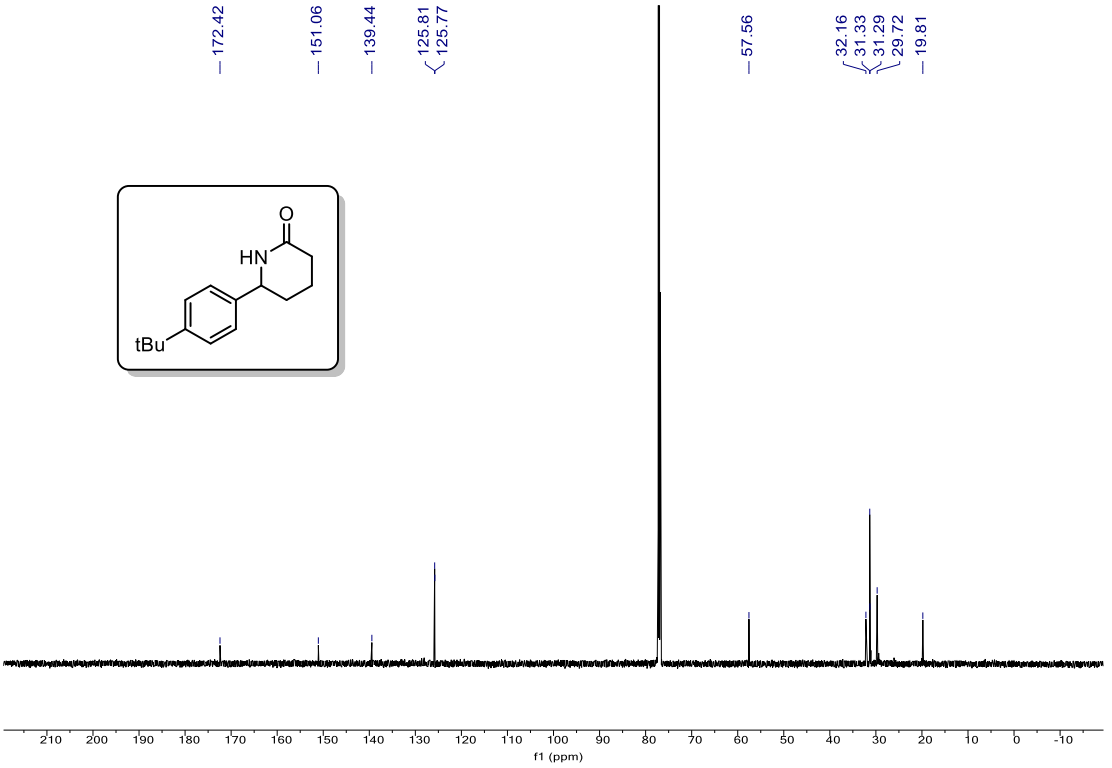
5-(3-Phenylprop-2-yn-1-yl)pyrrolidin-2-one



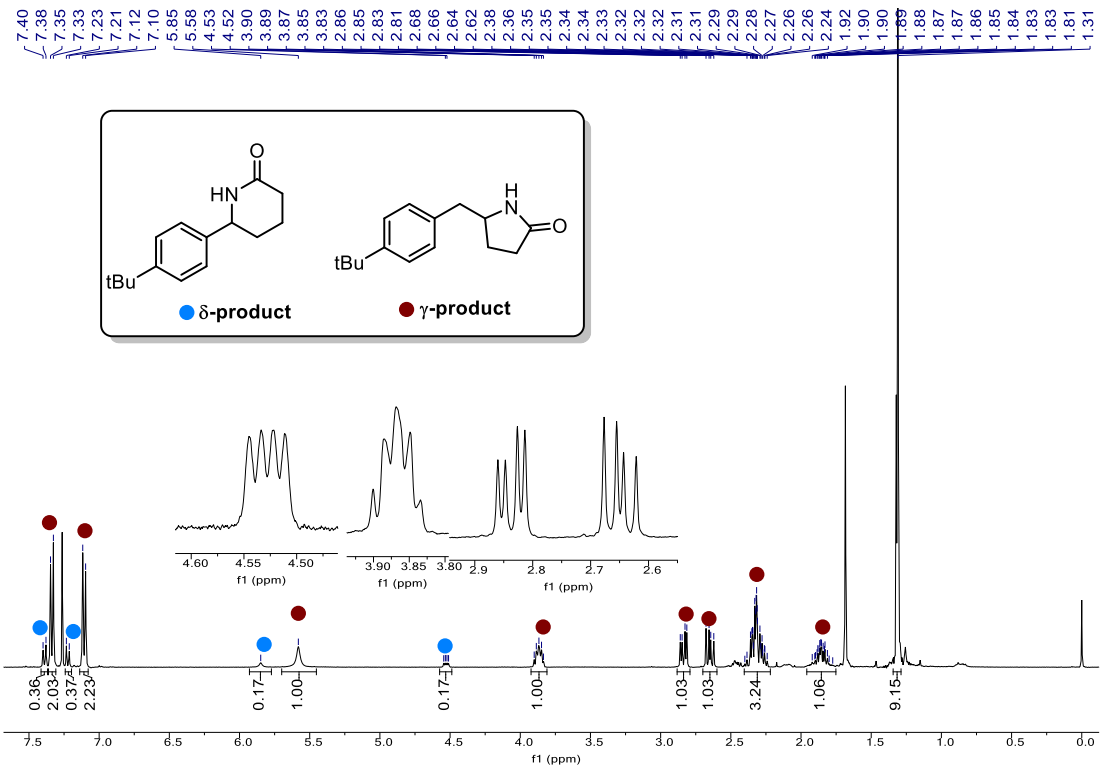


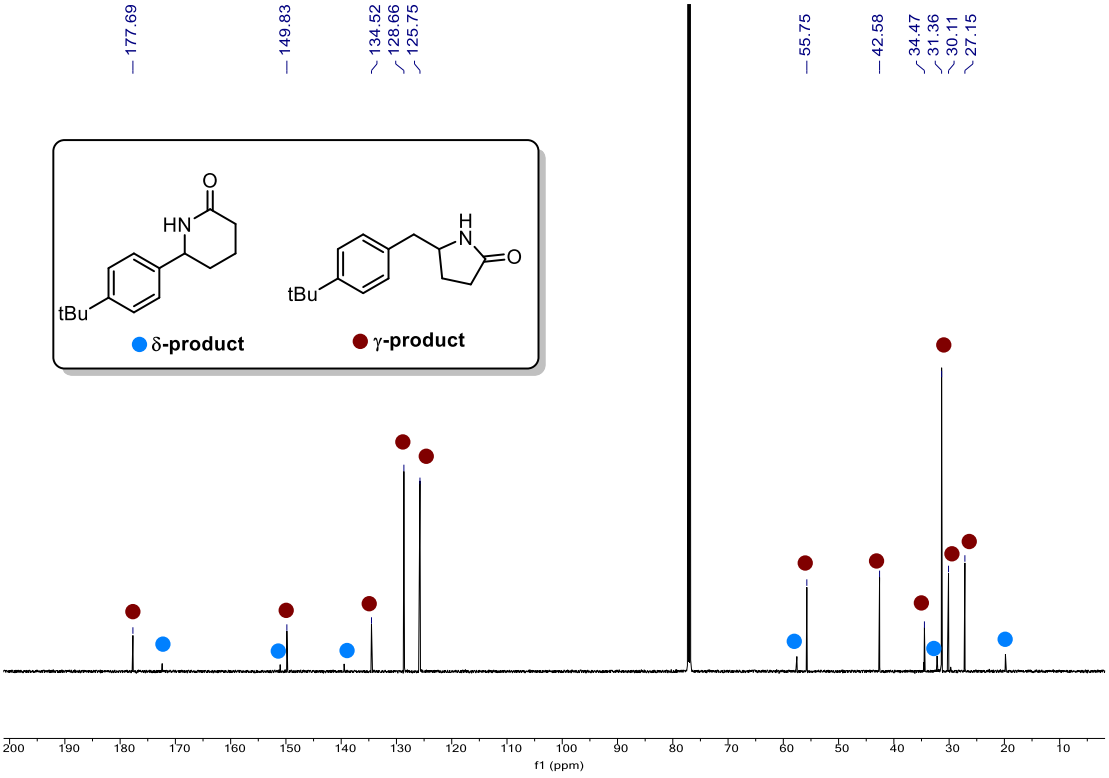
6-(4-(tert-Butyl)phenyl)piperidin-2-one



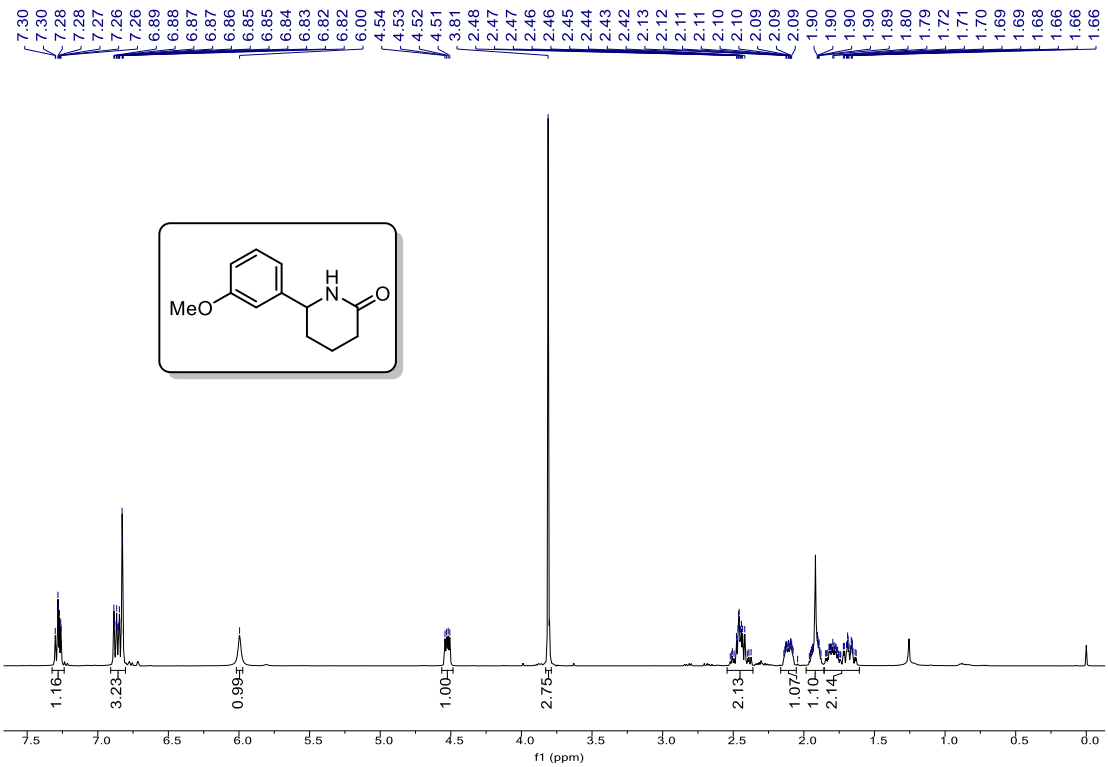


5-(4-(*tert*-Butyl)benzyl)pyrrolidin-2-one



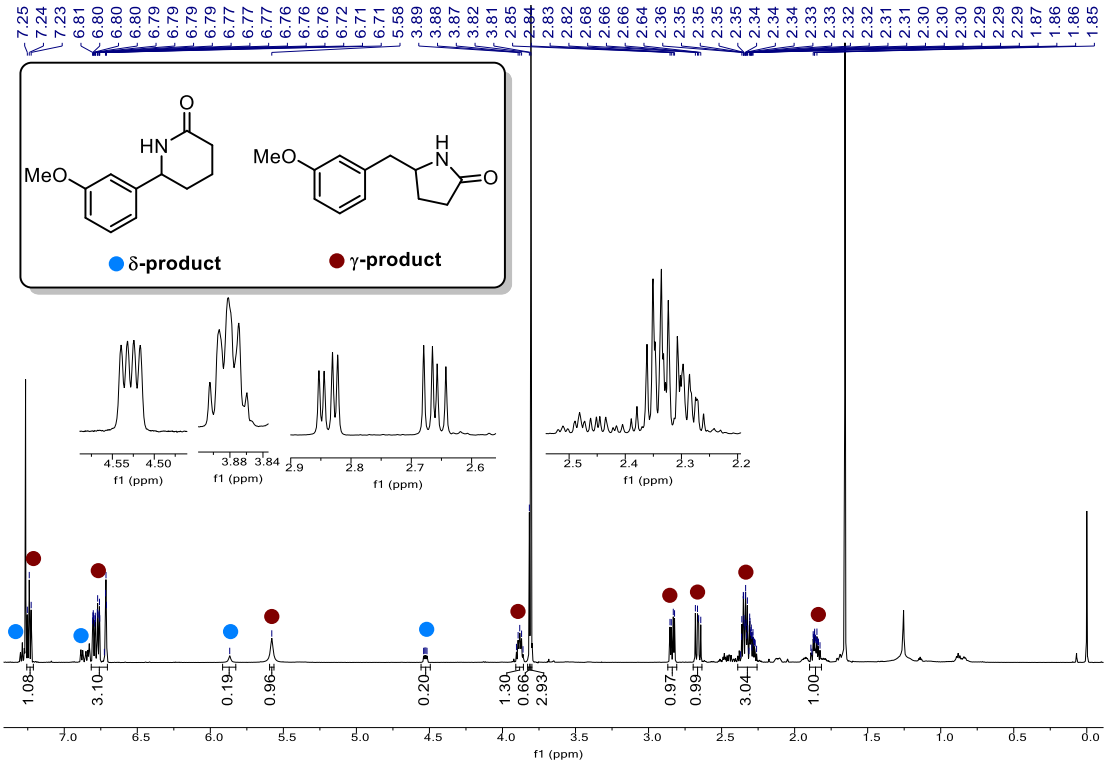


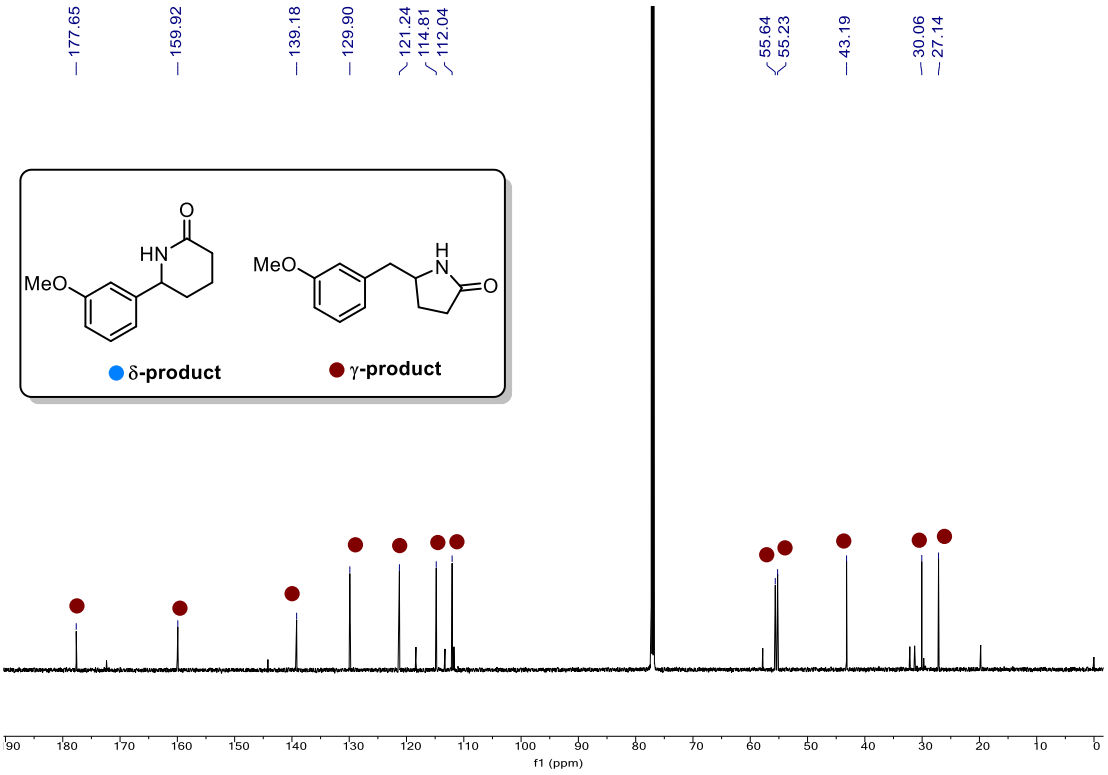
6-(3-Methoxyphenyl)piperidin-2-one



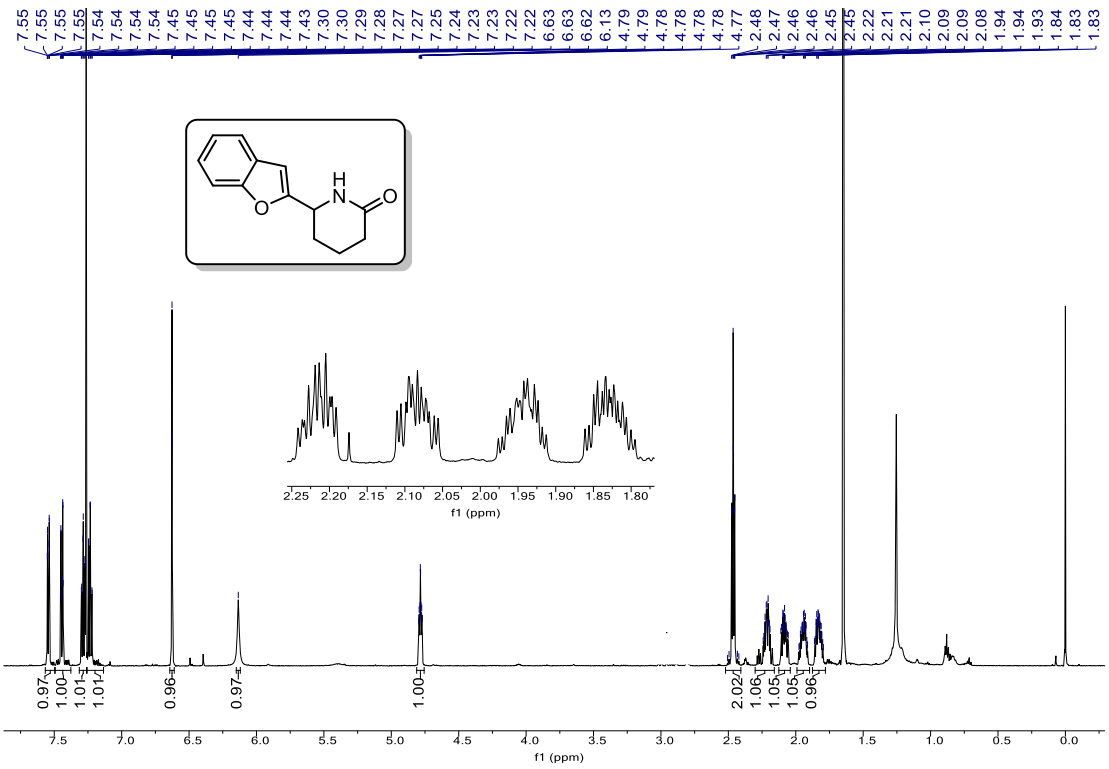


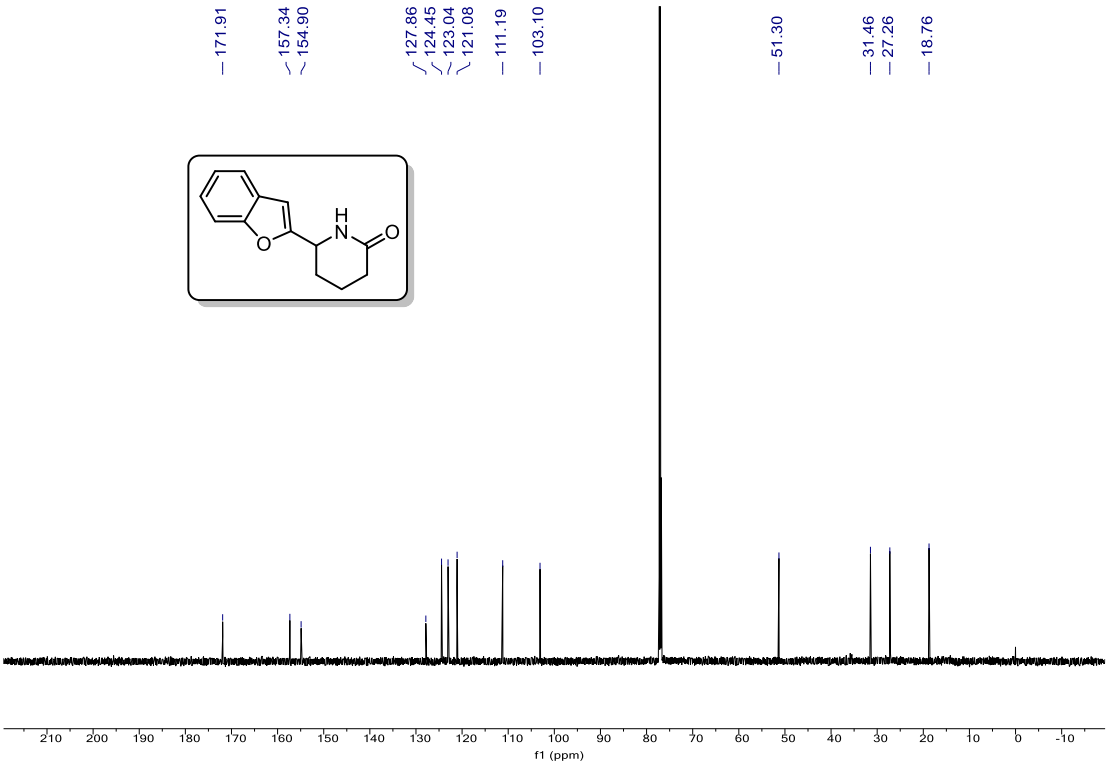
5-(3-Methoxybenzyl)pyrrolidin-2-one



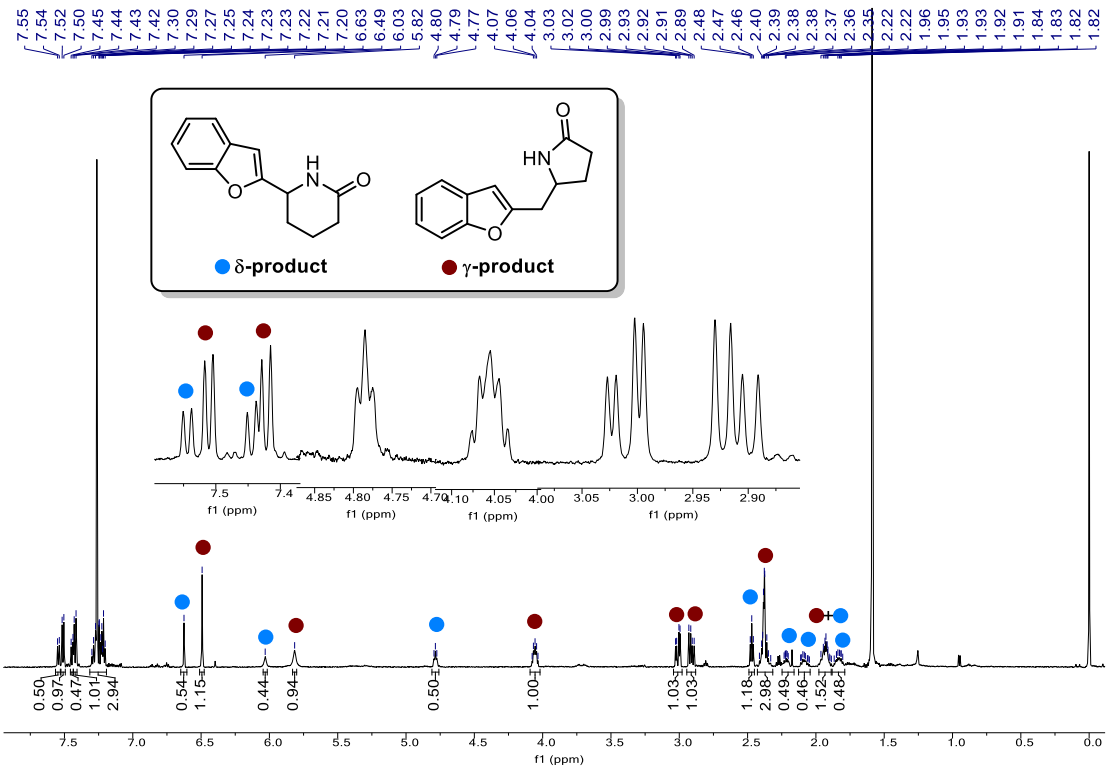


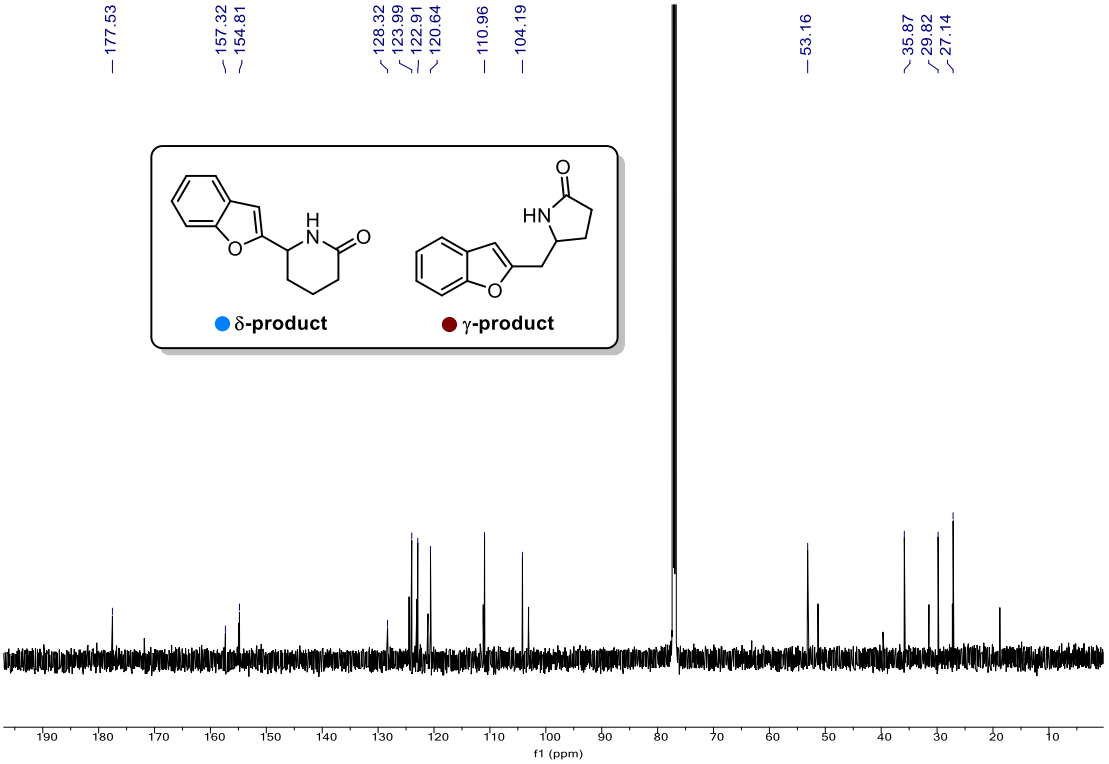
6-(Benzofuran-2-yl)piperidin-2-one



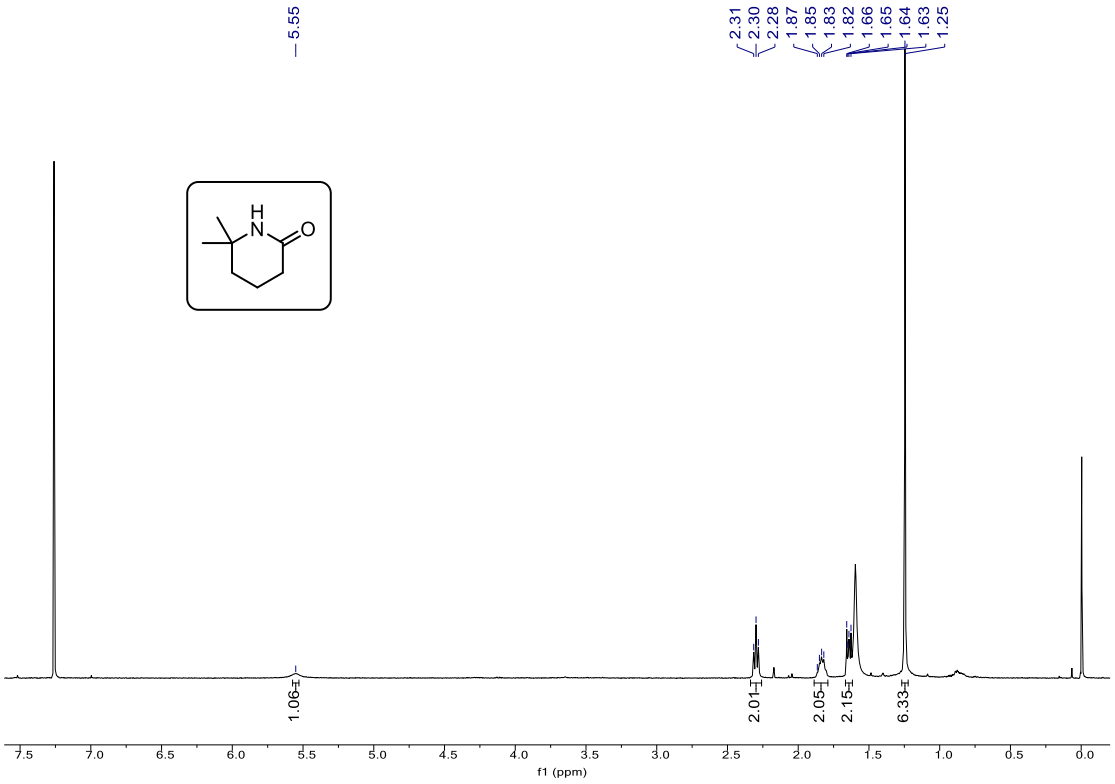


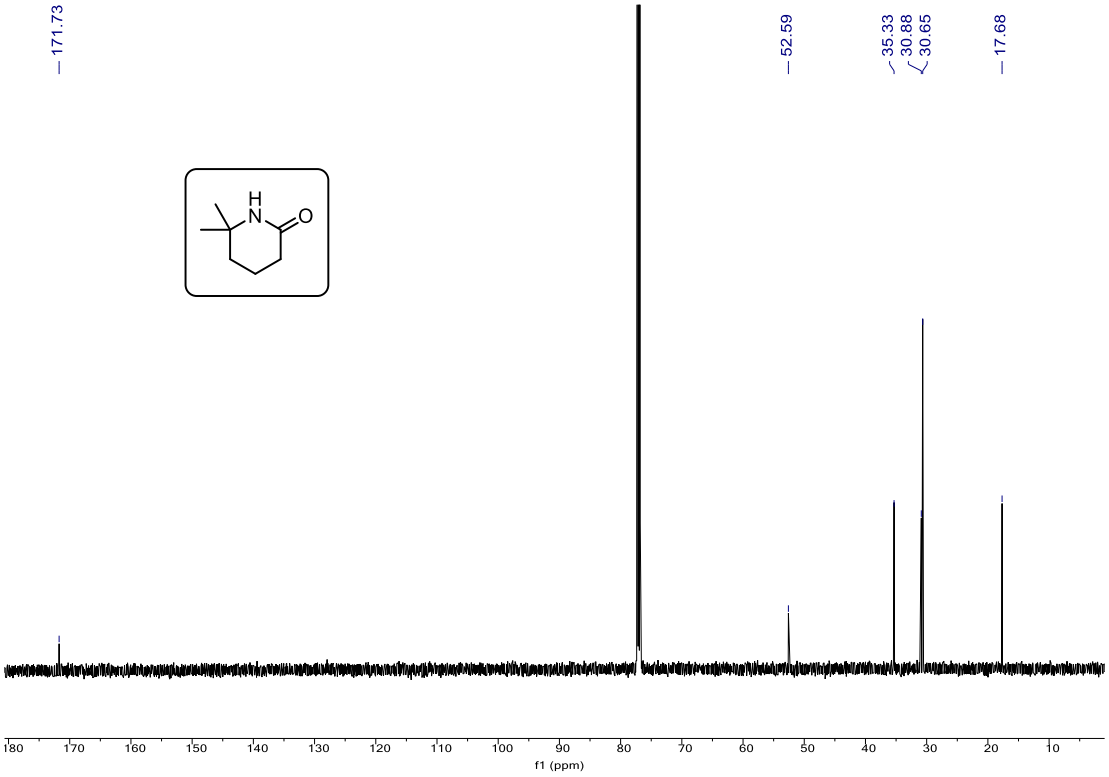
5-(Benzofuran-2-ylmethyl)pyrrolidin-2-one



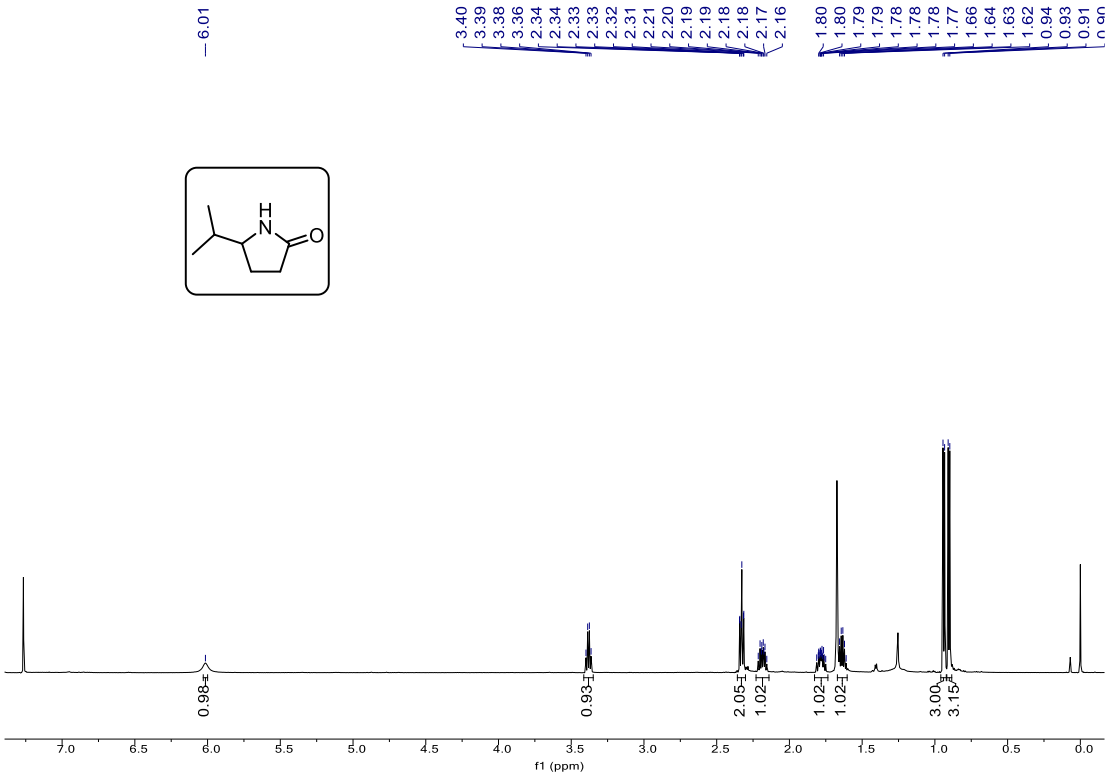


6,6-Dimethylpiperidin-2-one



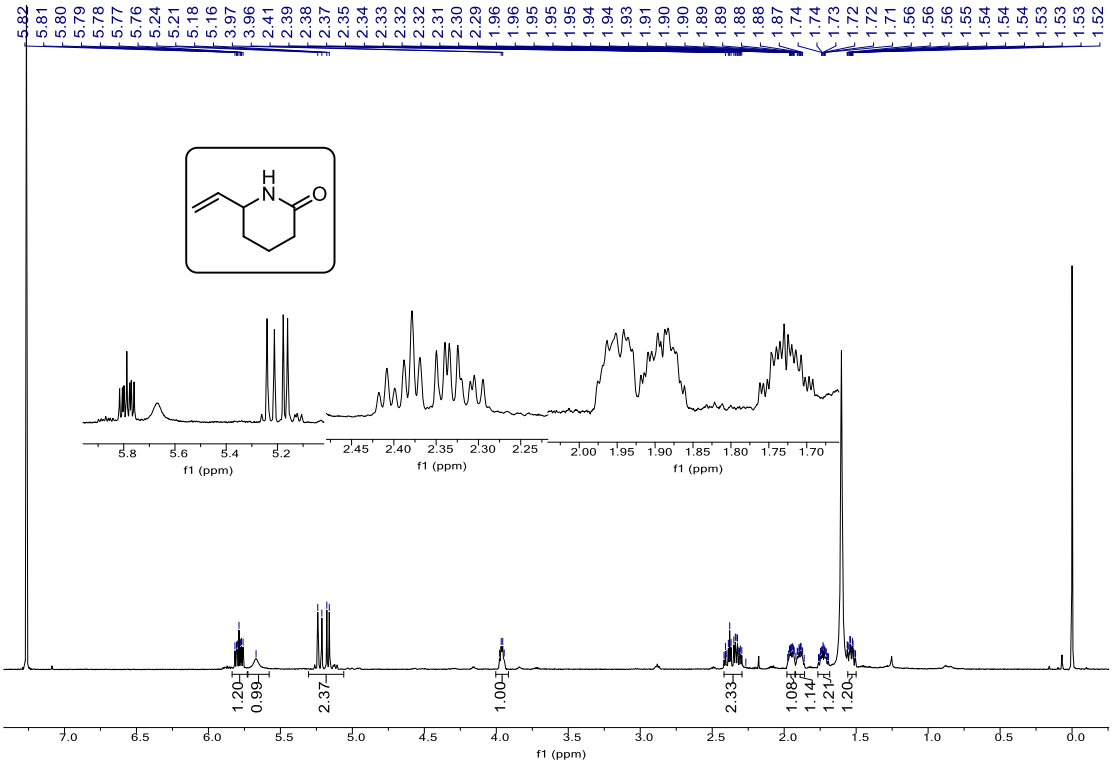


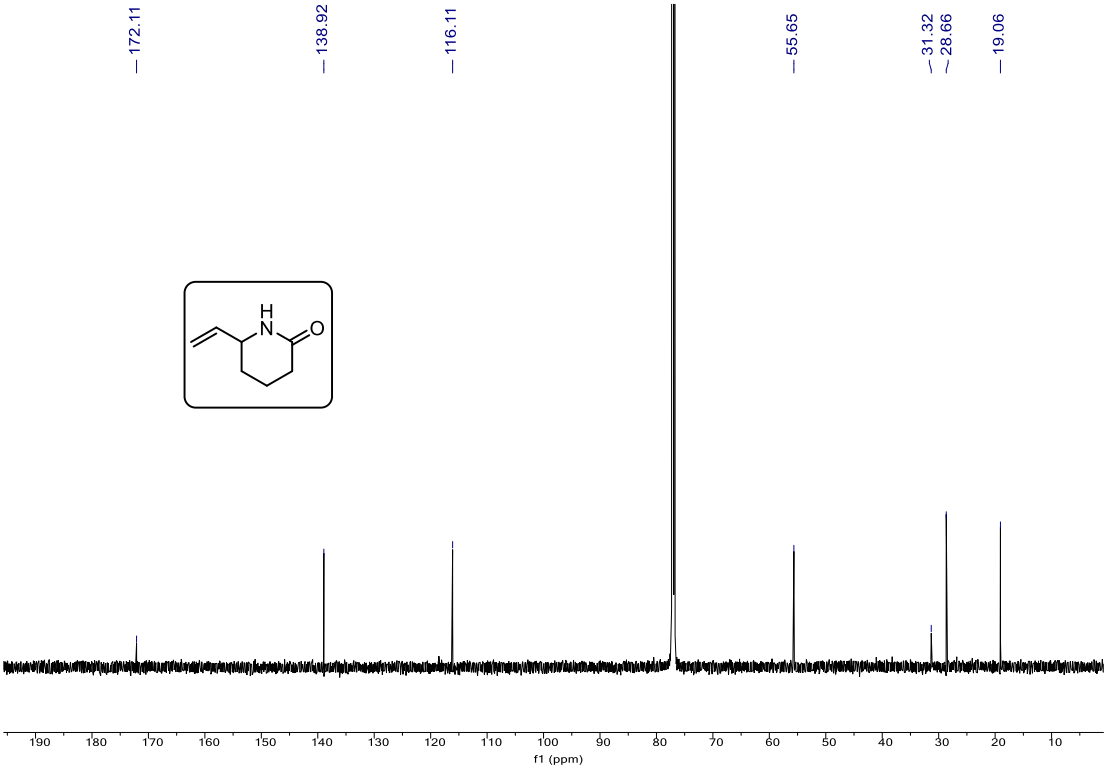
5-Isopropylpyrrolidin-2-one



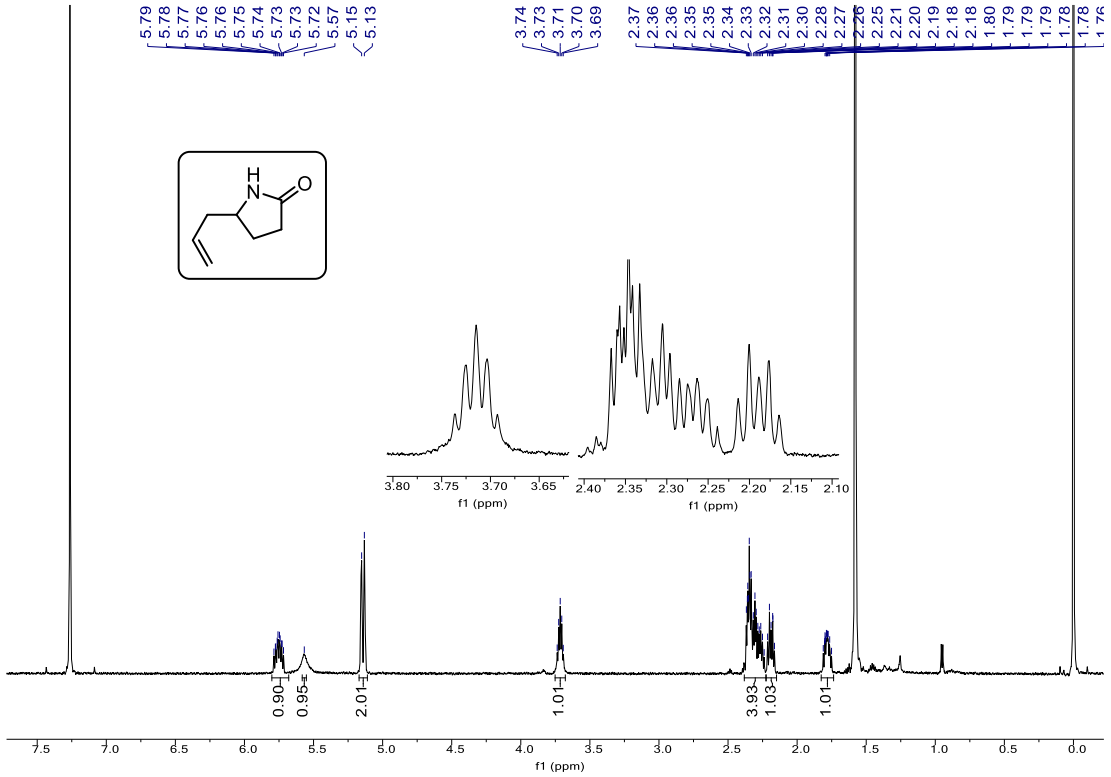


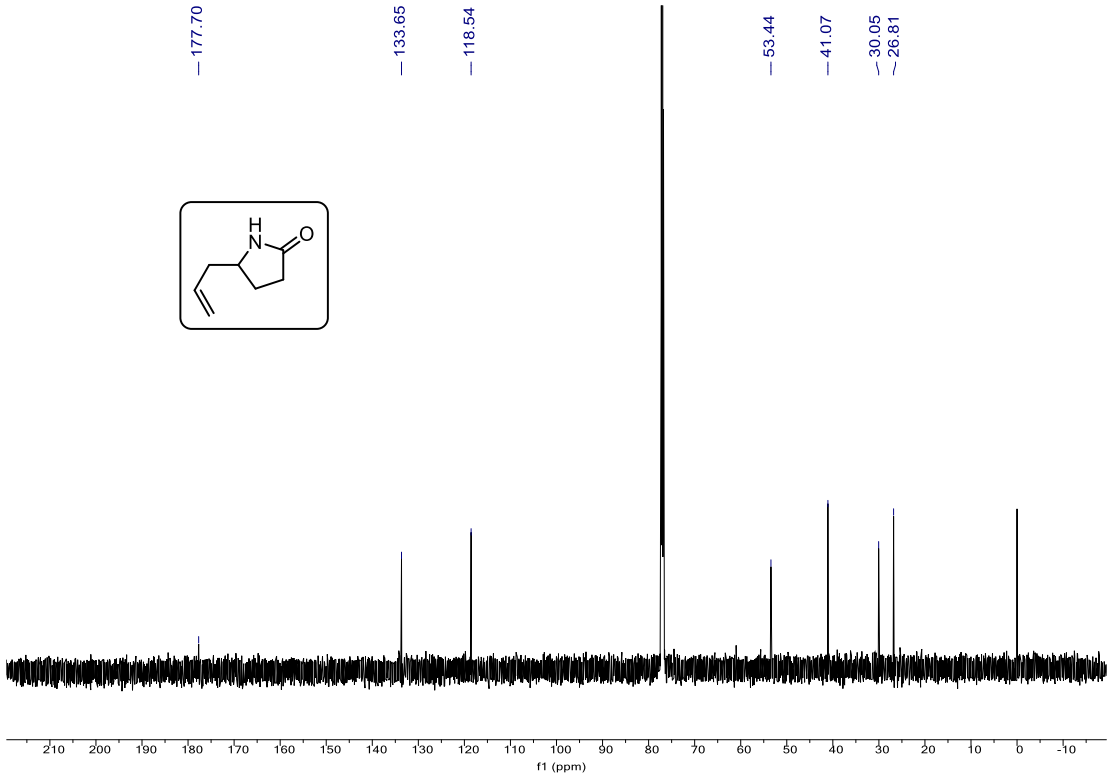
6-Vinylpiperidin-2-one



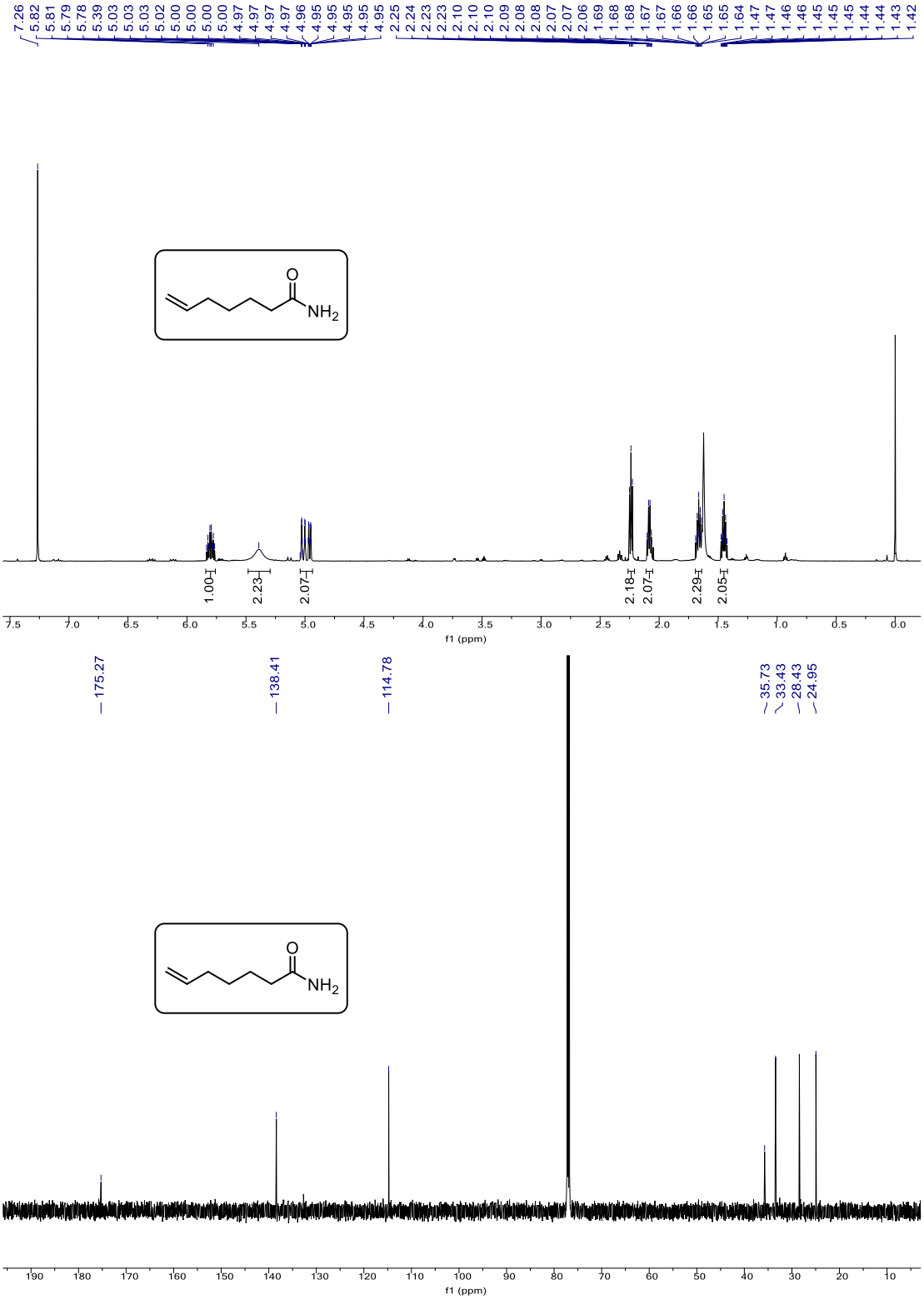


5-Allylpyrrolidin-2-one

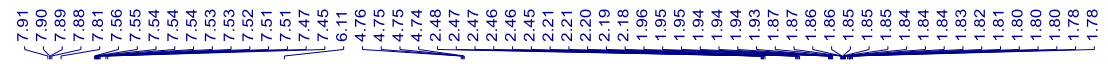


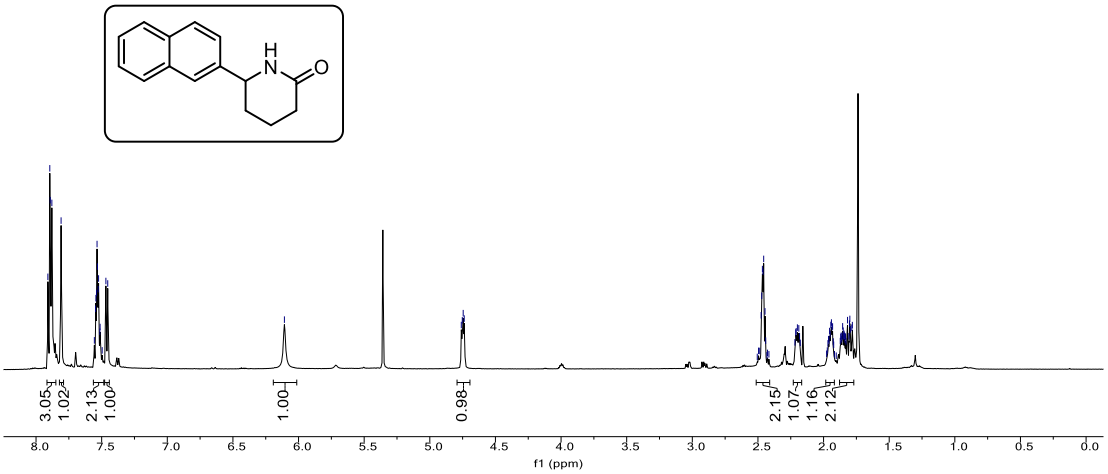


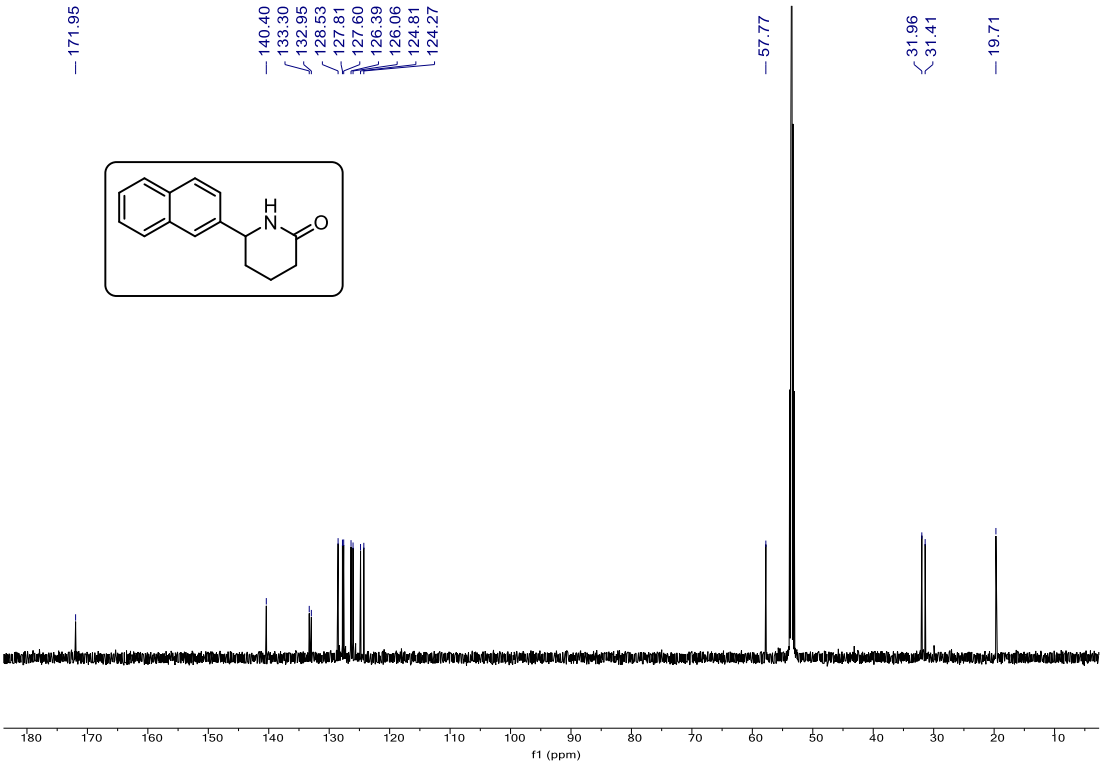
Hept-6-enamide



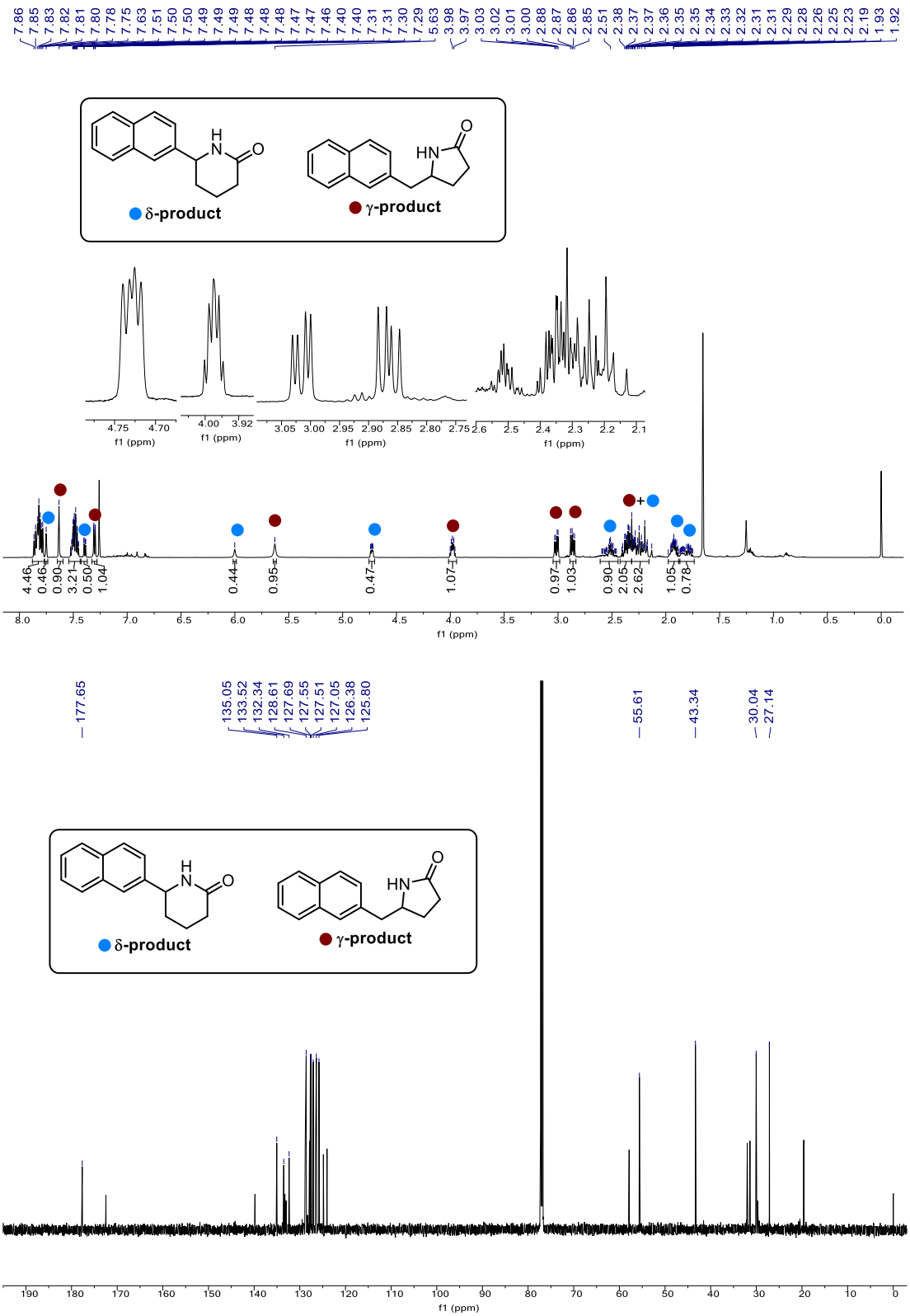
6-(Naphthalen-2-yl)piperidin-2-one



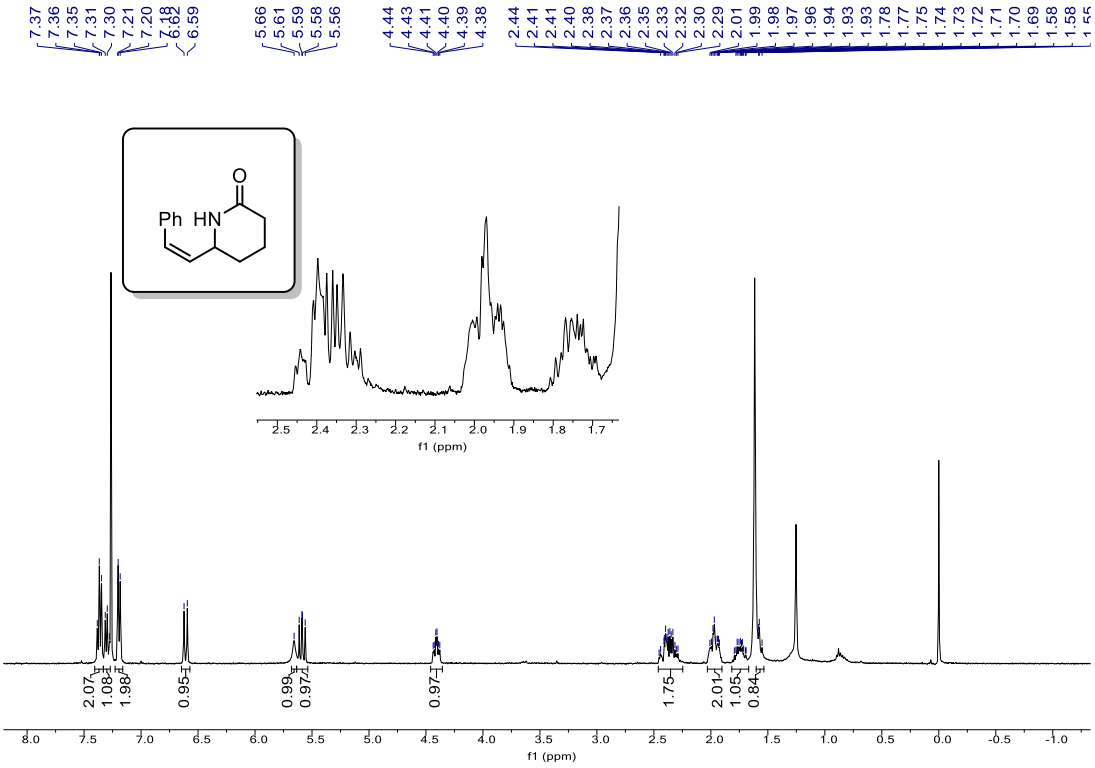


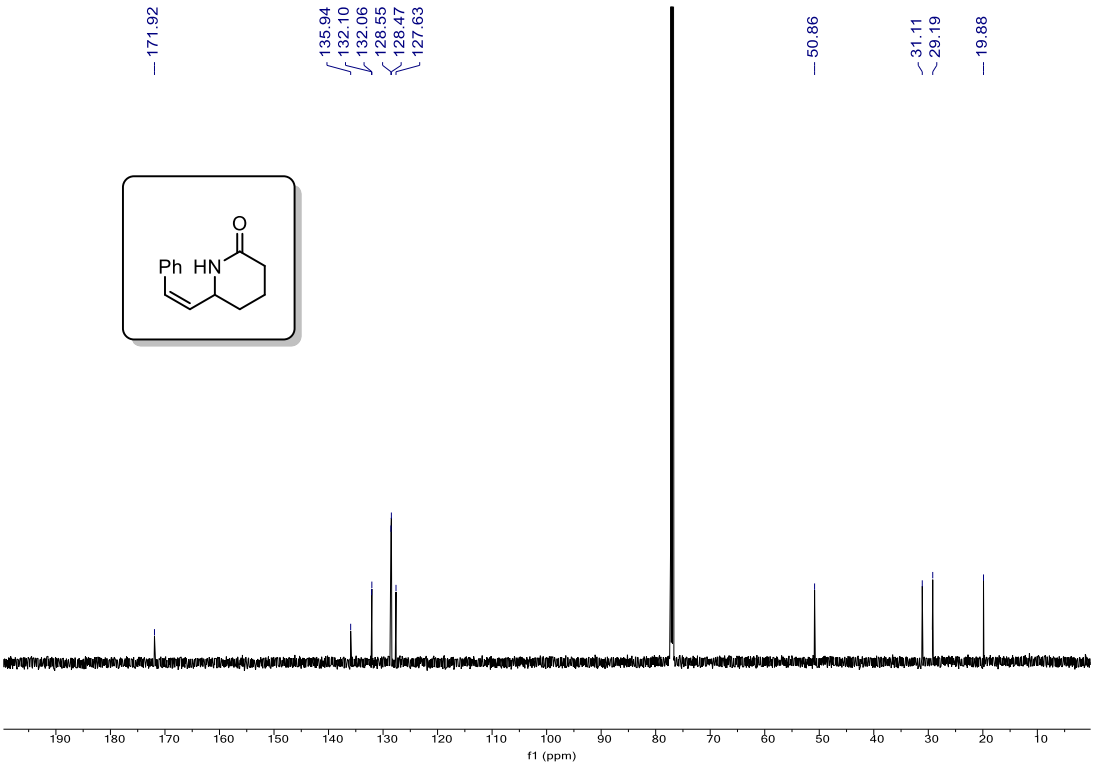


5-(Naphthalen-2-ylmethyl)pyrrolidin-2-one

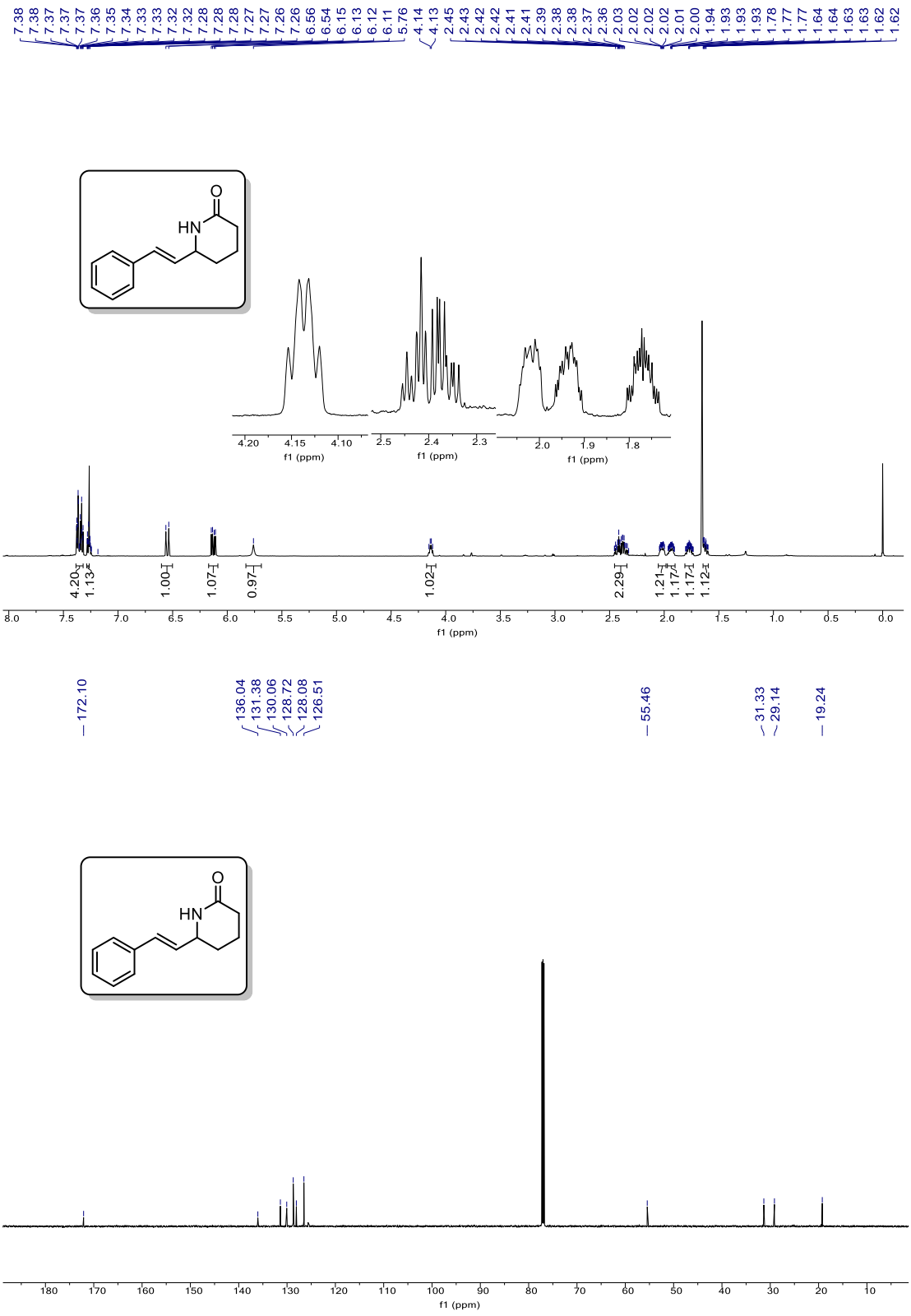


(*Z*)-6-Styrylpiperidin-2-one

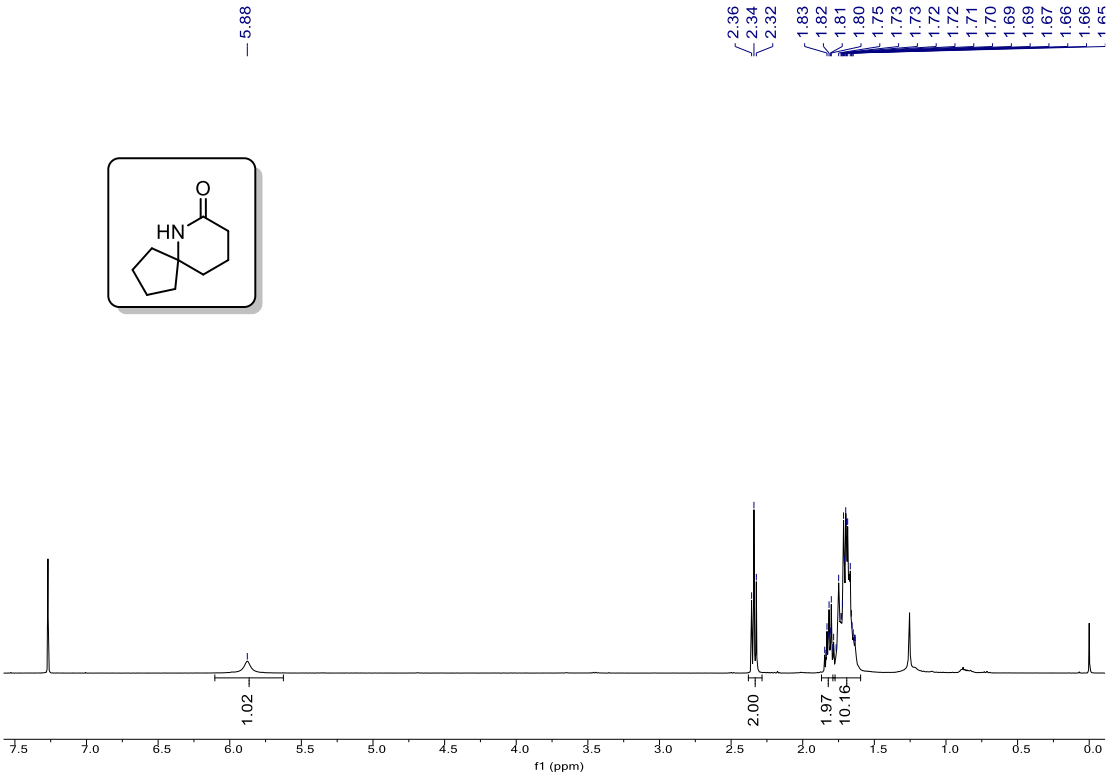


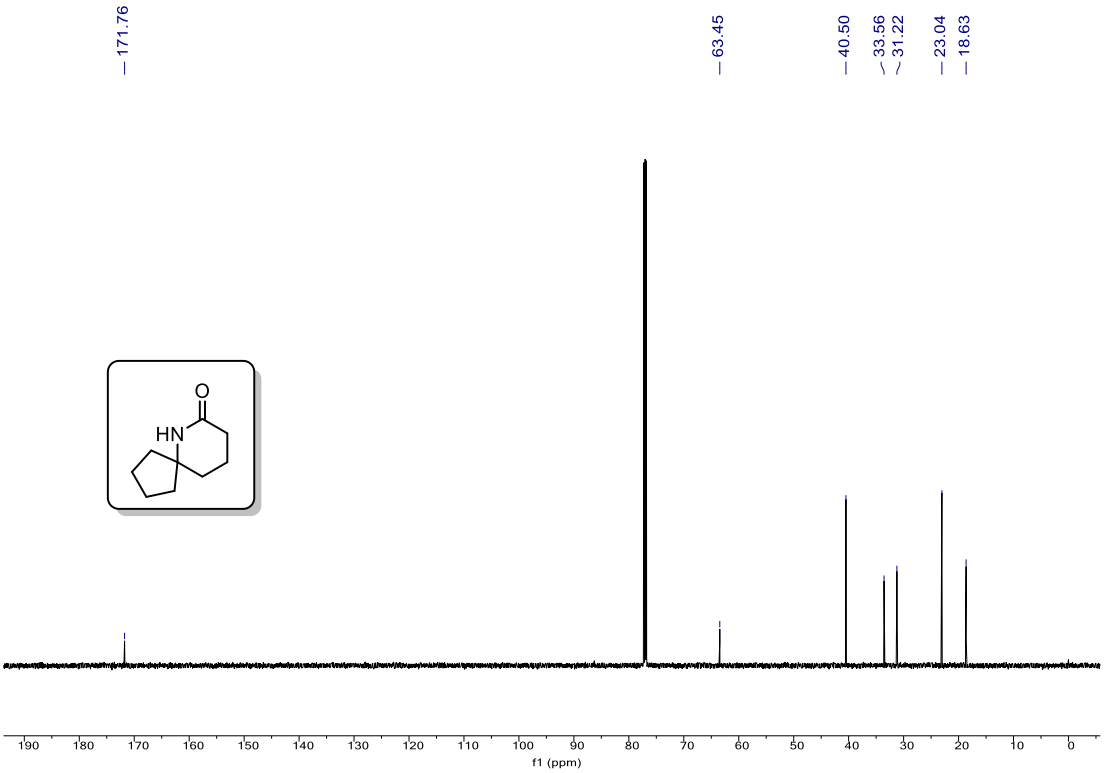


(*E*)-6-Styrylpiperidin-2-one



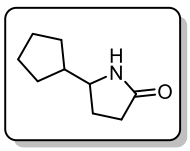
6-Azaspiro[4.5]decan-7-one

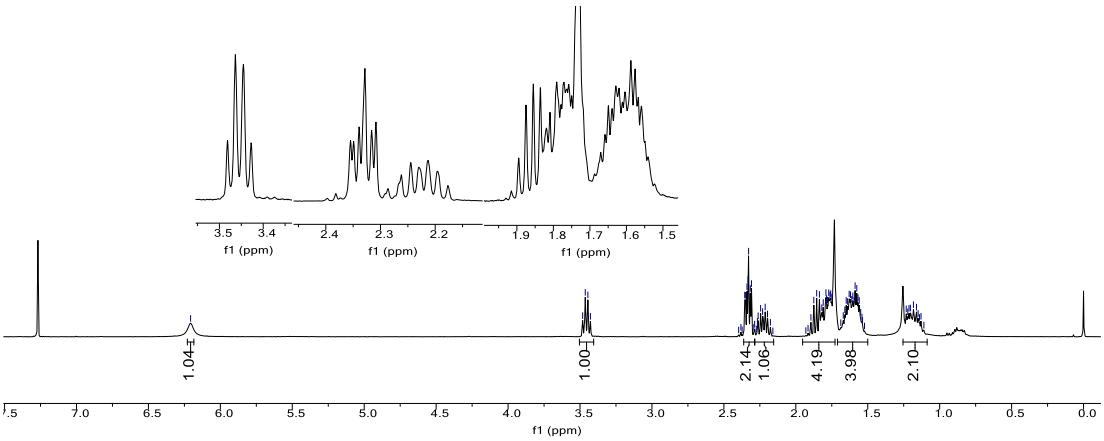


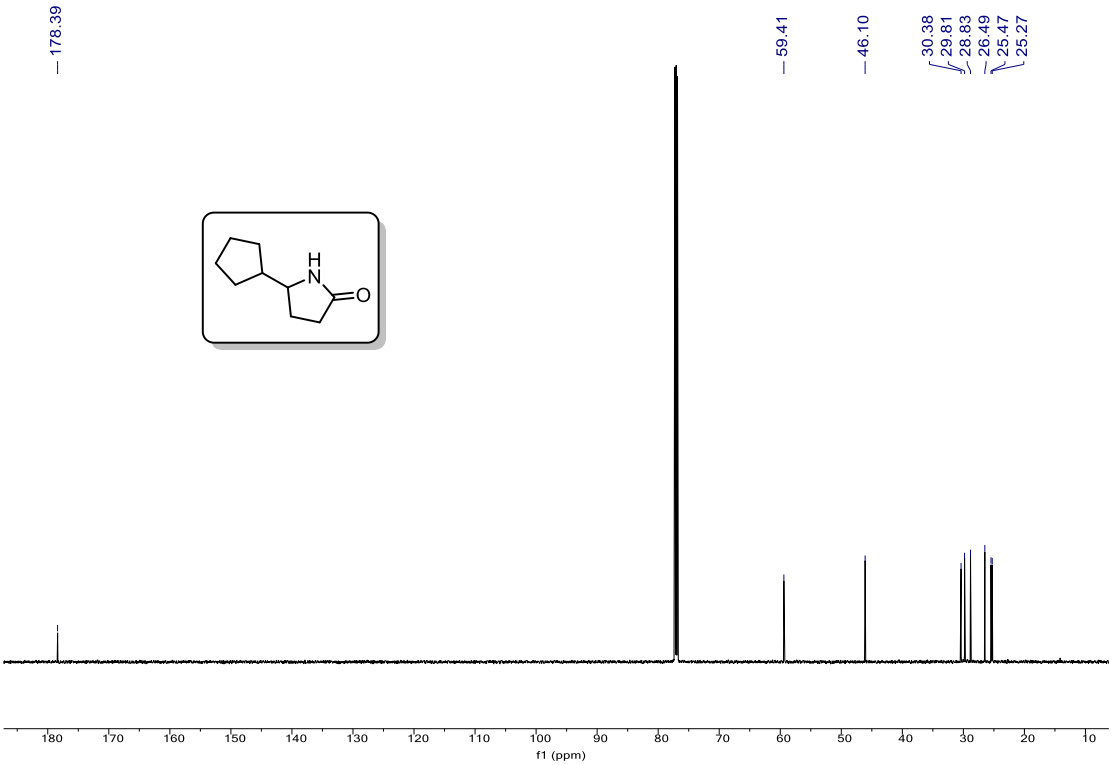


5-Cyclopentylpyrrolidin-2-one

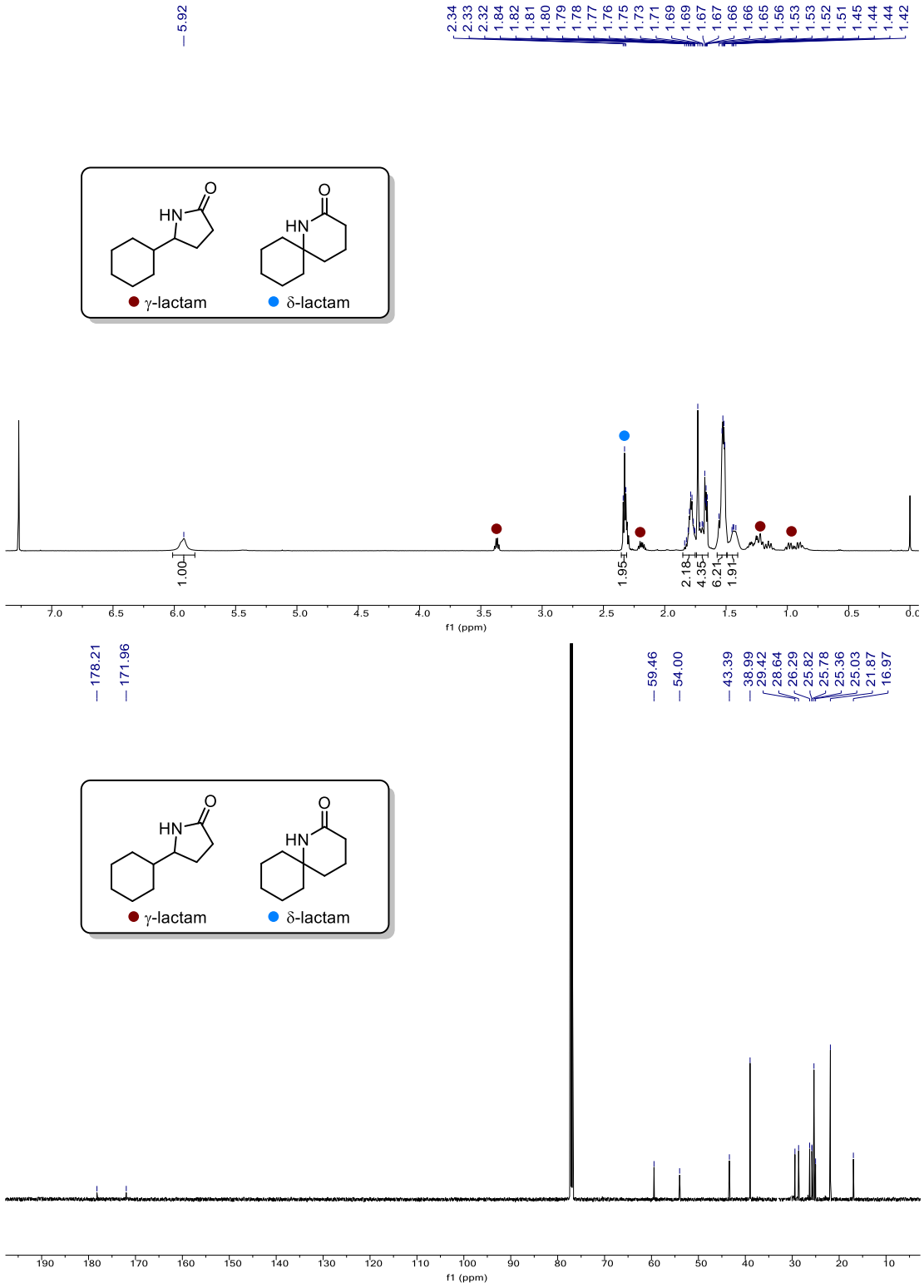




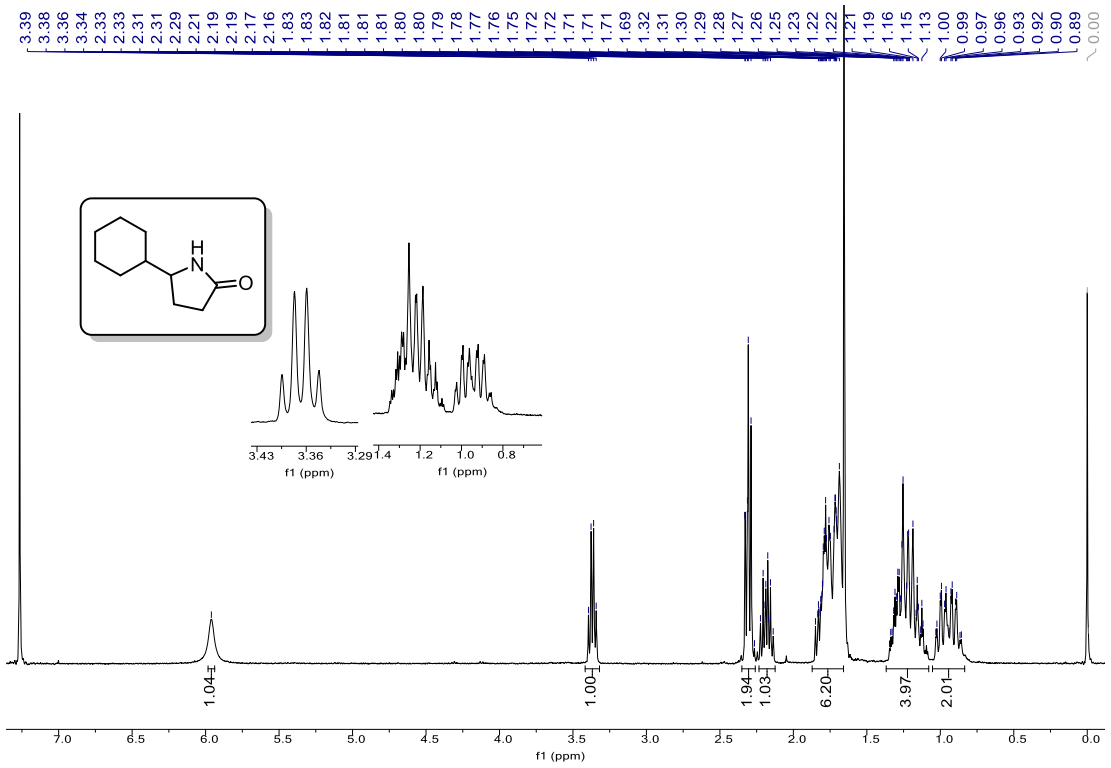


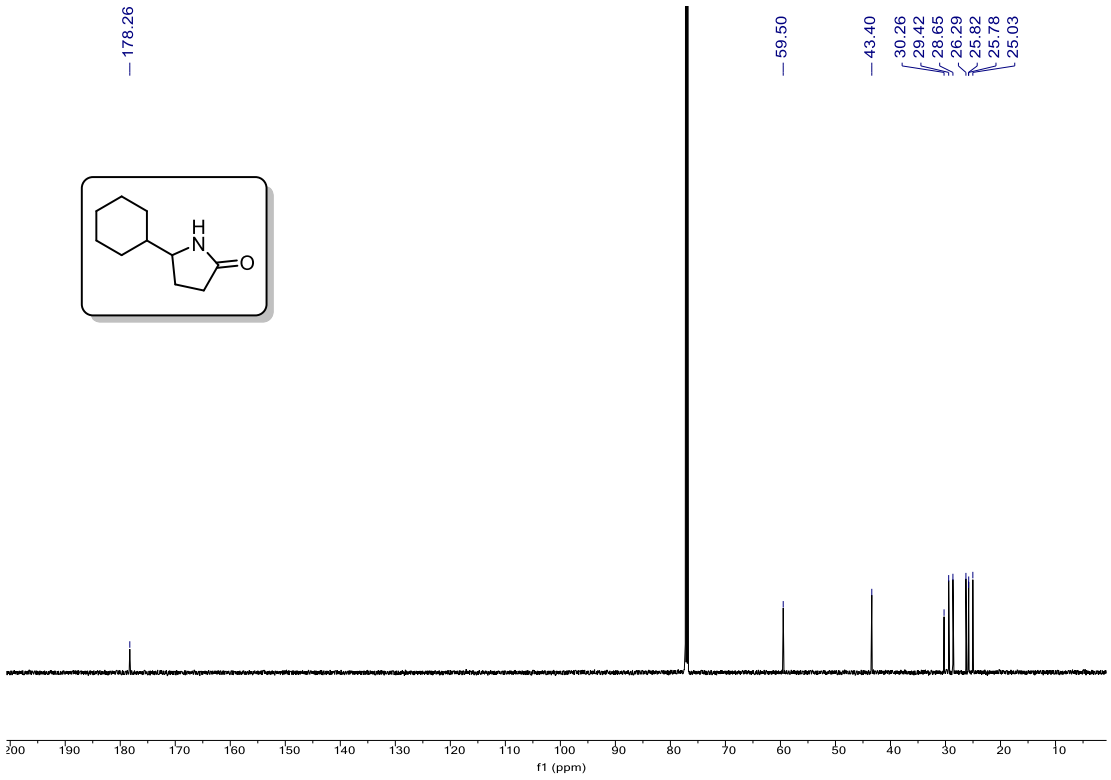


1-Azaspiro[5.5]undecan-2-one

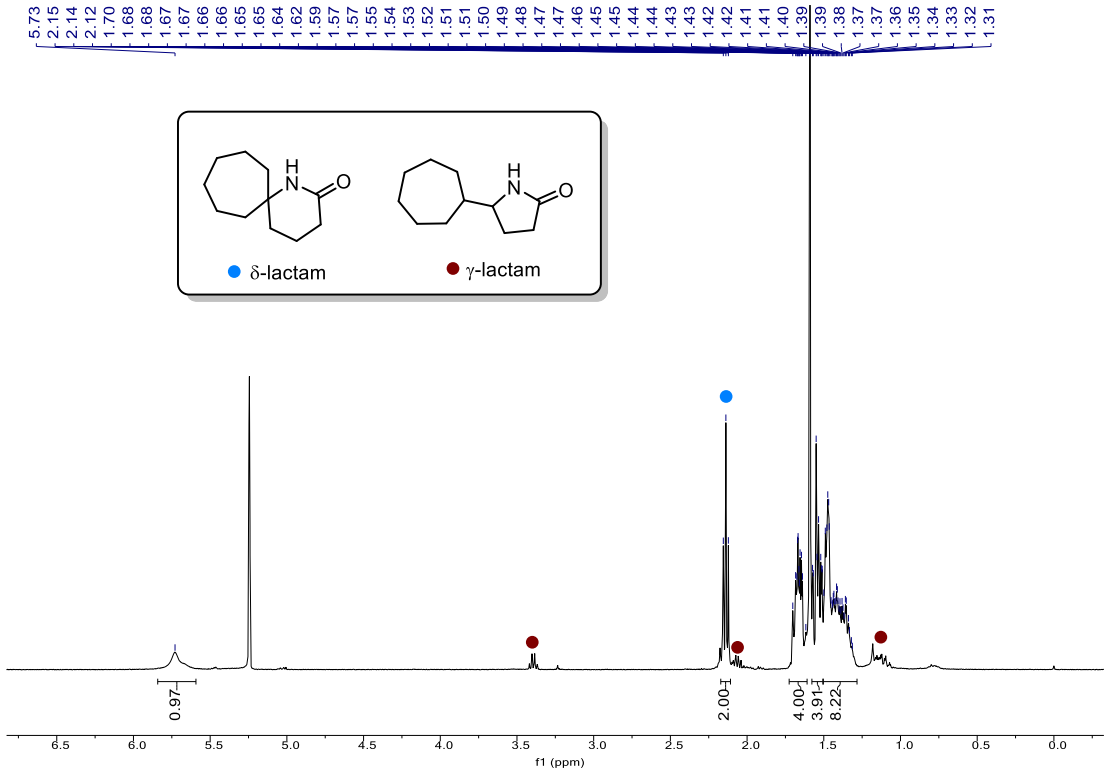


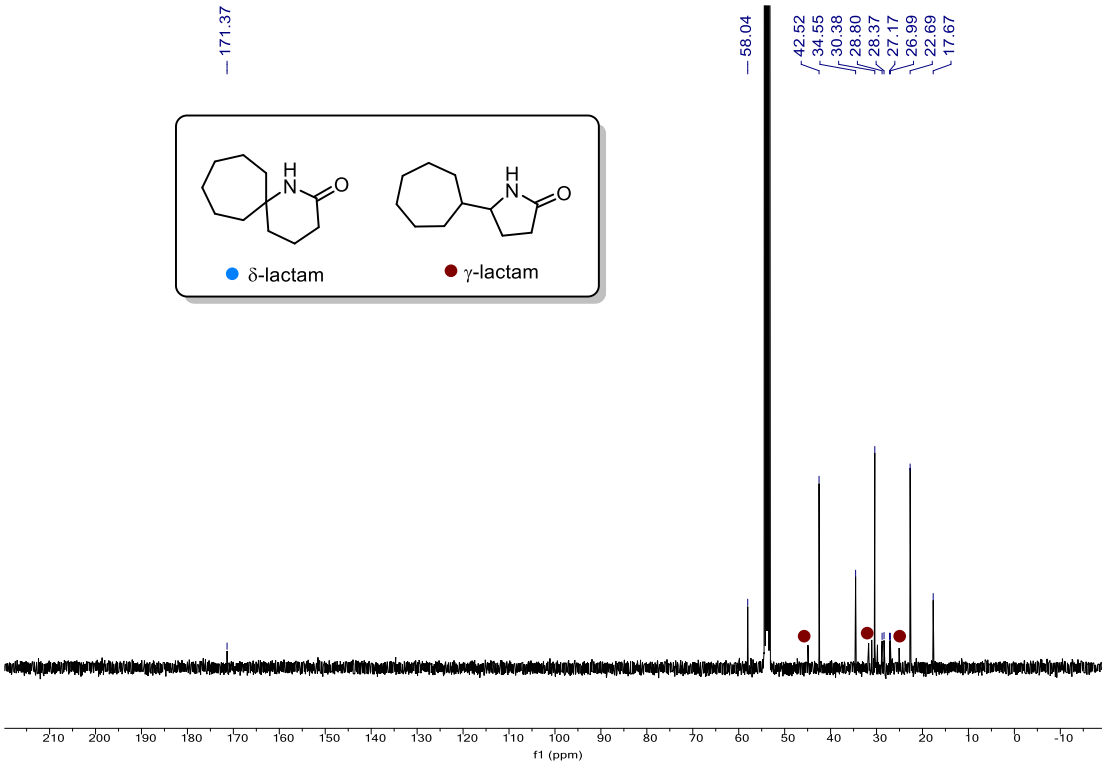
5-Cyclohexylpyrrolidin-2-one



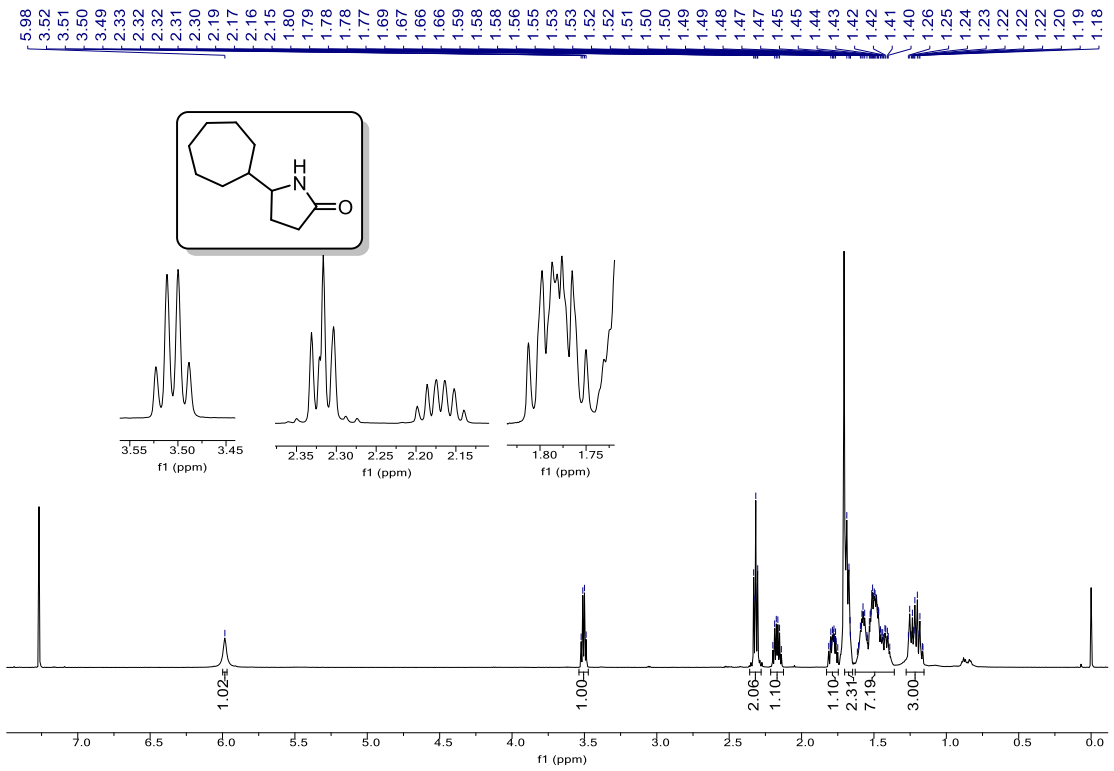


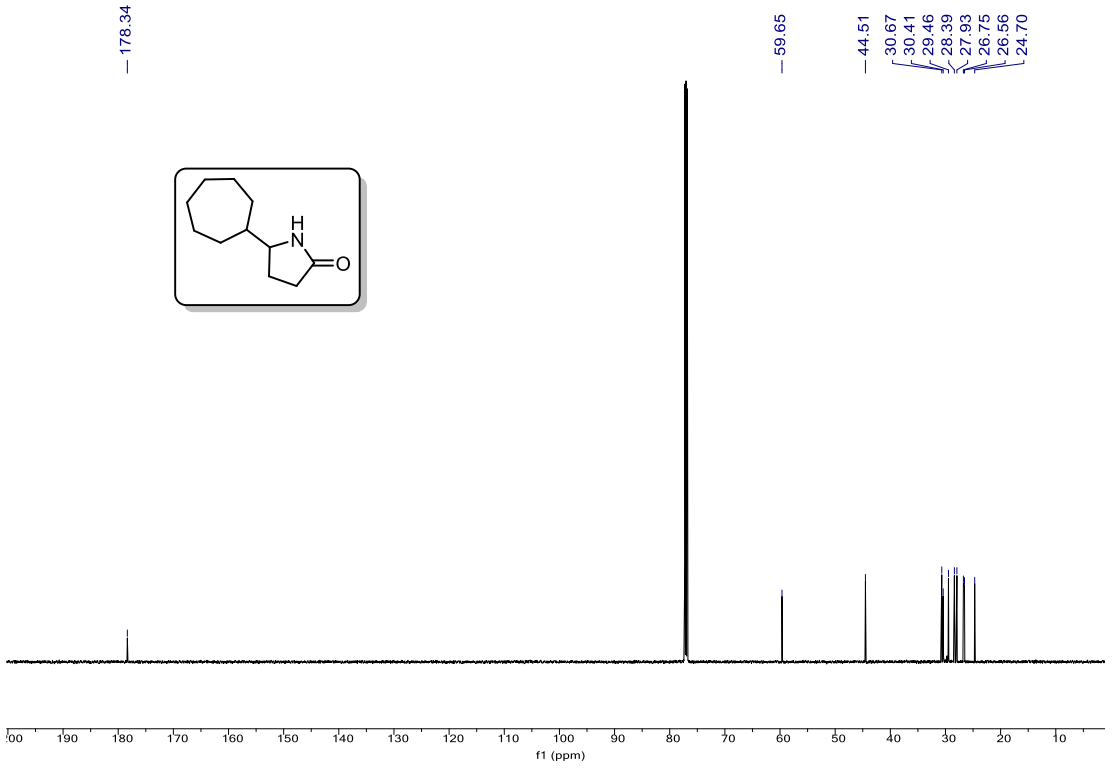
1-Azaspiro[5.6]dodecan-2-one



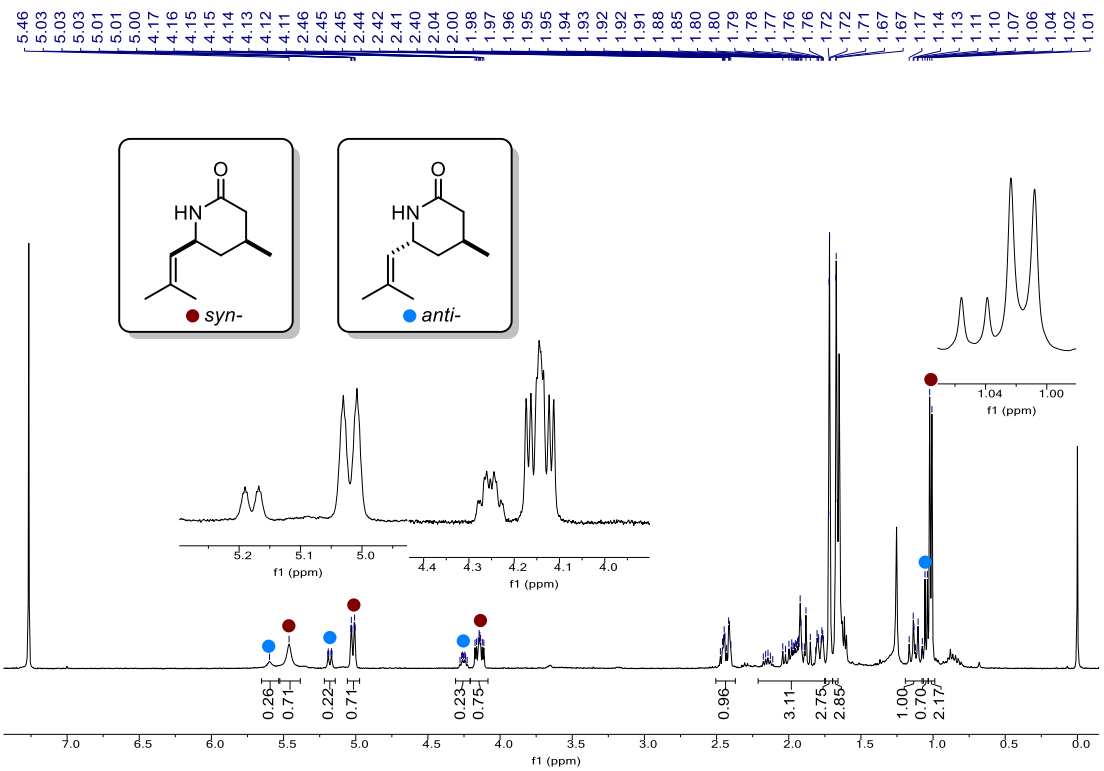


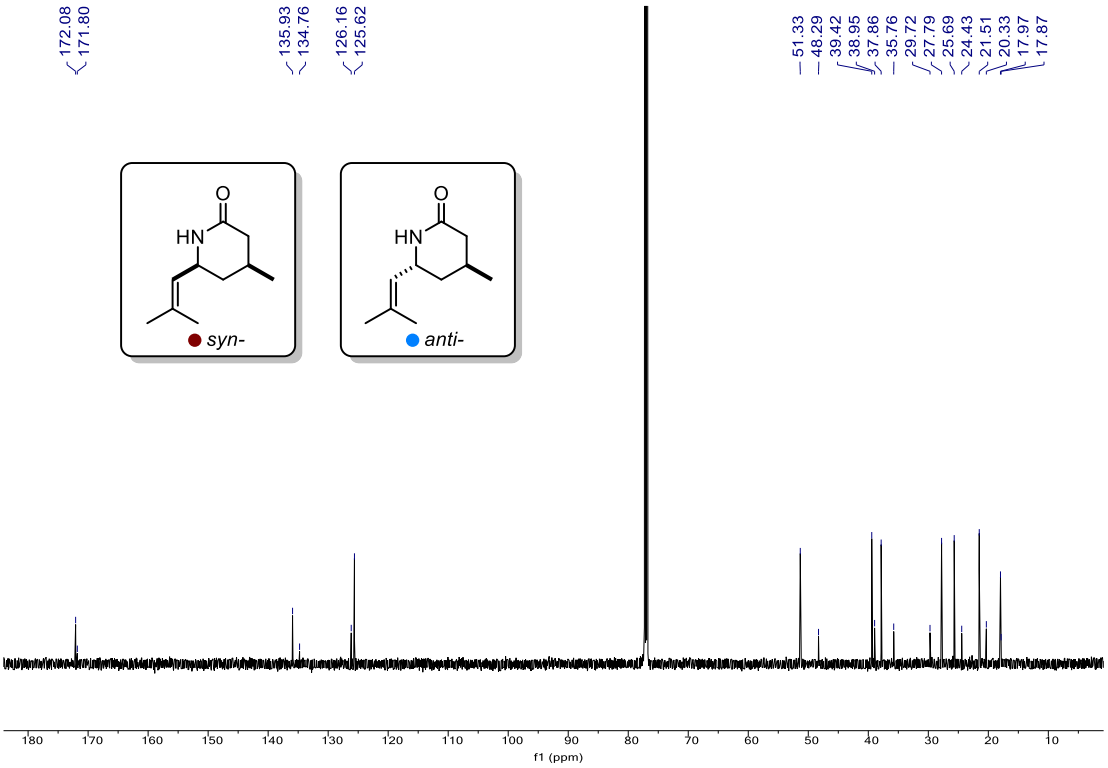
5-Cycloheptylpyrrolidin-2-one



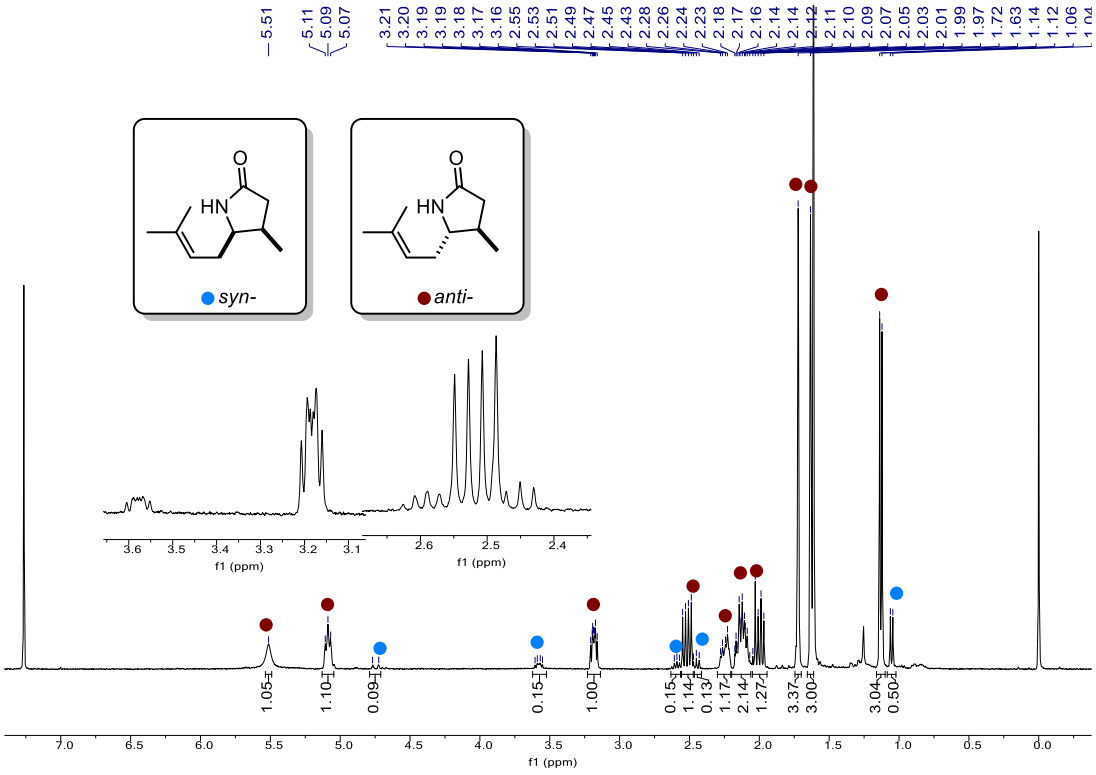


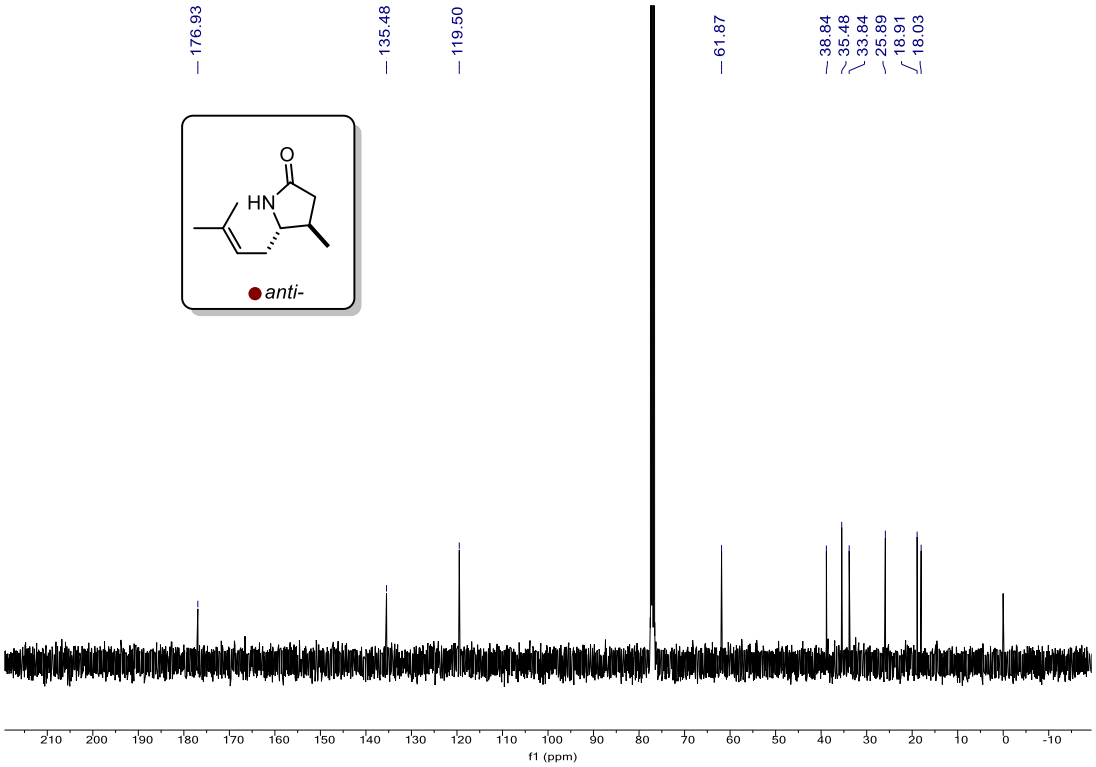
4-Methyl-6-(2-methylprop-1-en-1-yl)piperidin-2-one



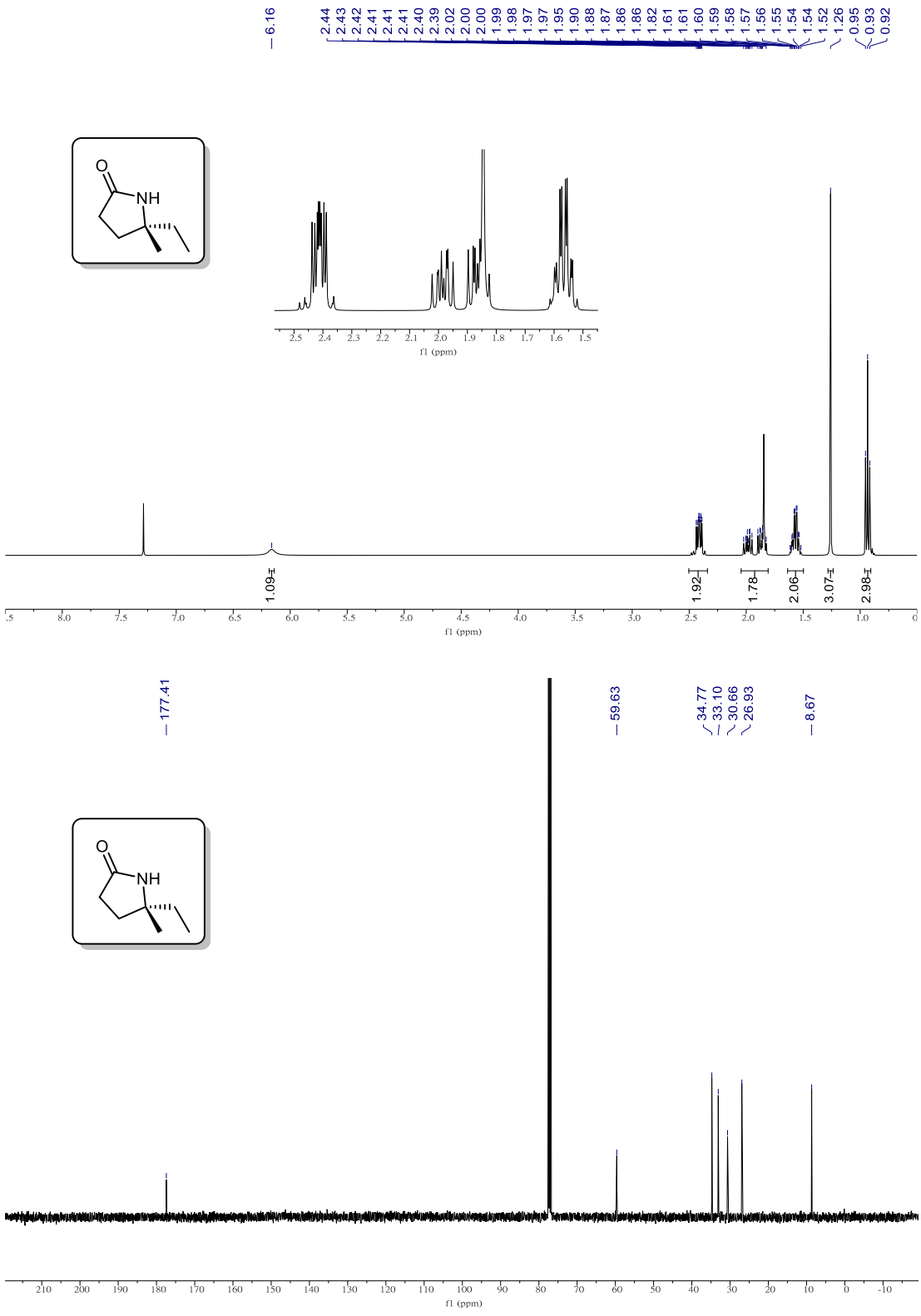


(±)-*trans*-4-Methyl-5-(3-methylbut-2-en-1-yl)pyrrolidin-2-one

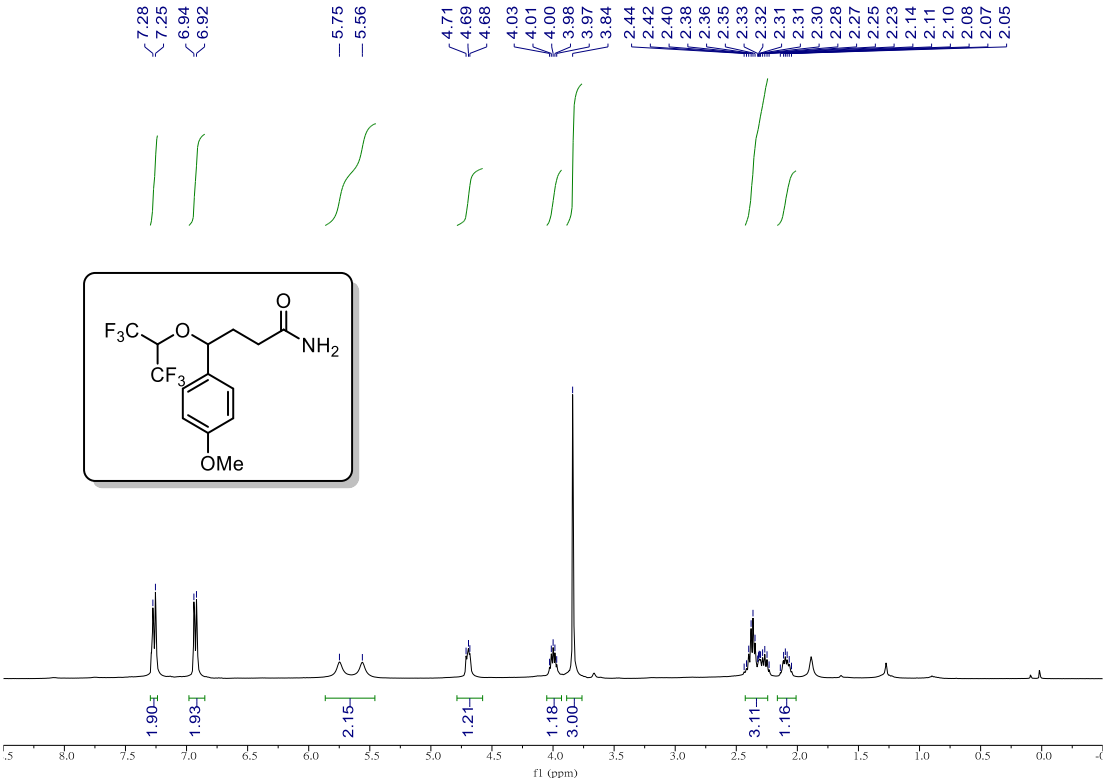


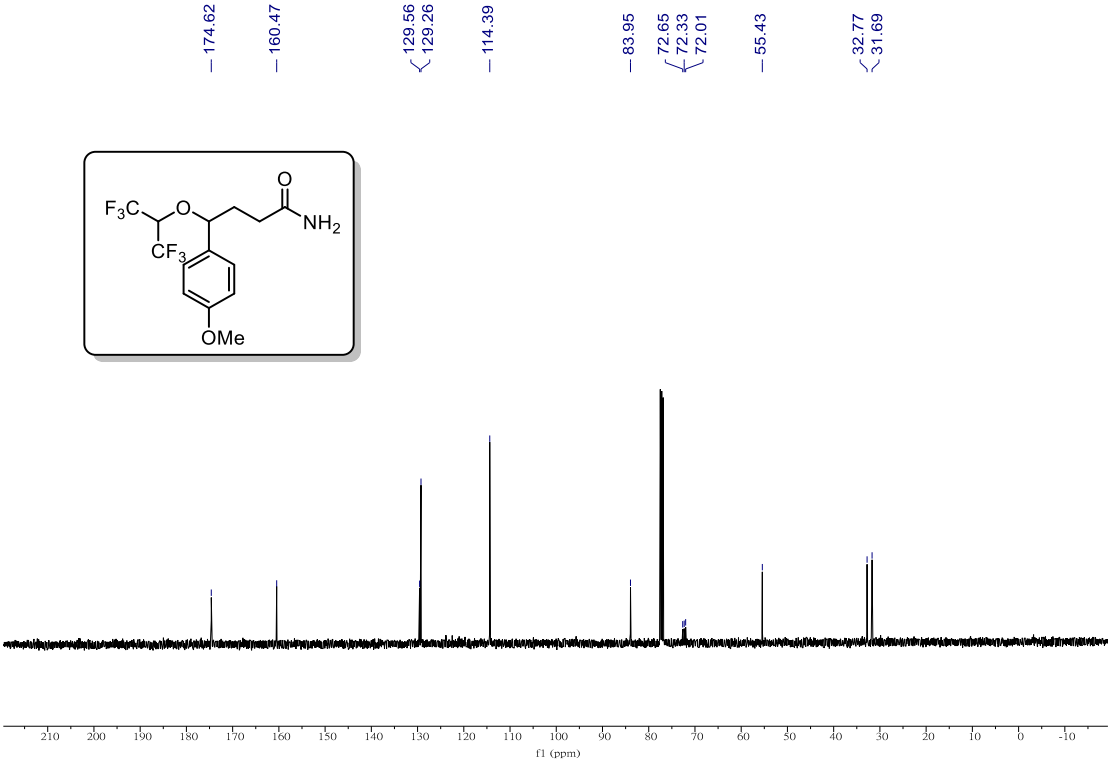


(*R*)-5-Ethyl-5-methylpyrrolidin-2-one

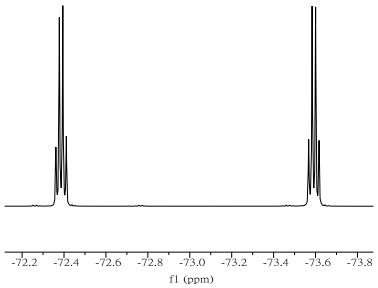


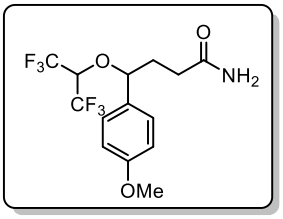
4-((1,1,1,3,3,3-Hexafluoropropan-2-yl)oxy)-4-(4-methoxyphenyl)butanamide

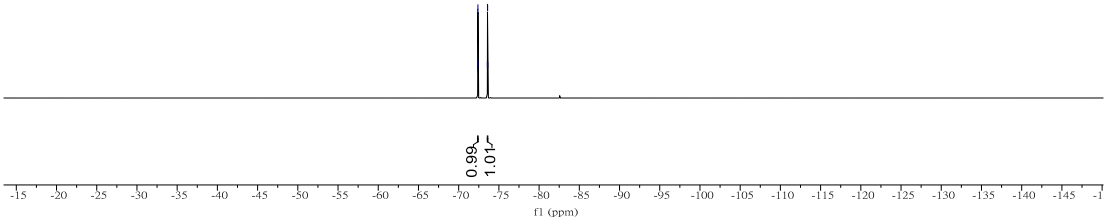




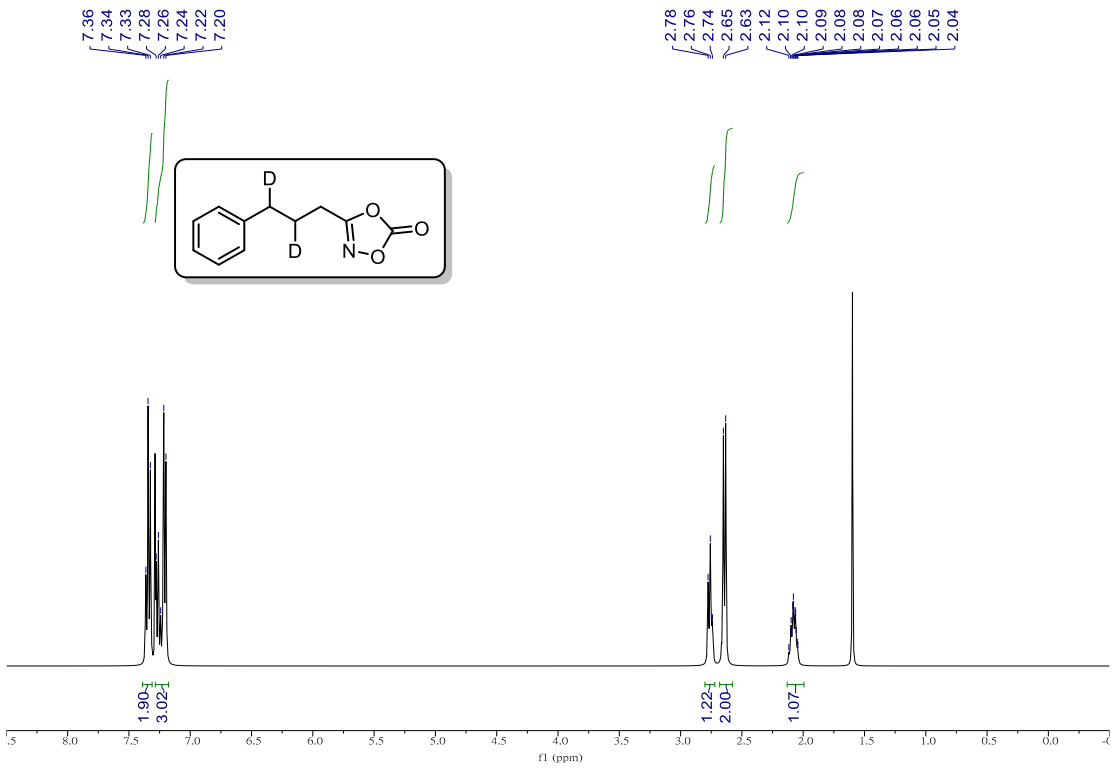

-72.36
-72.38
-72.39
-72.41
-73.57
-73.58
-73.60
-73.62

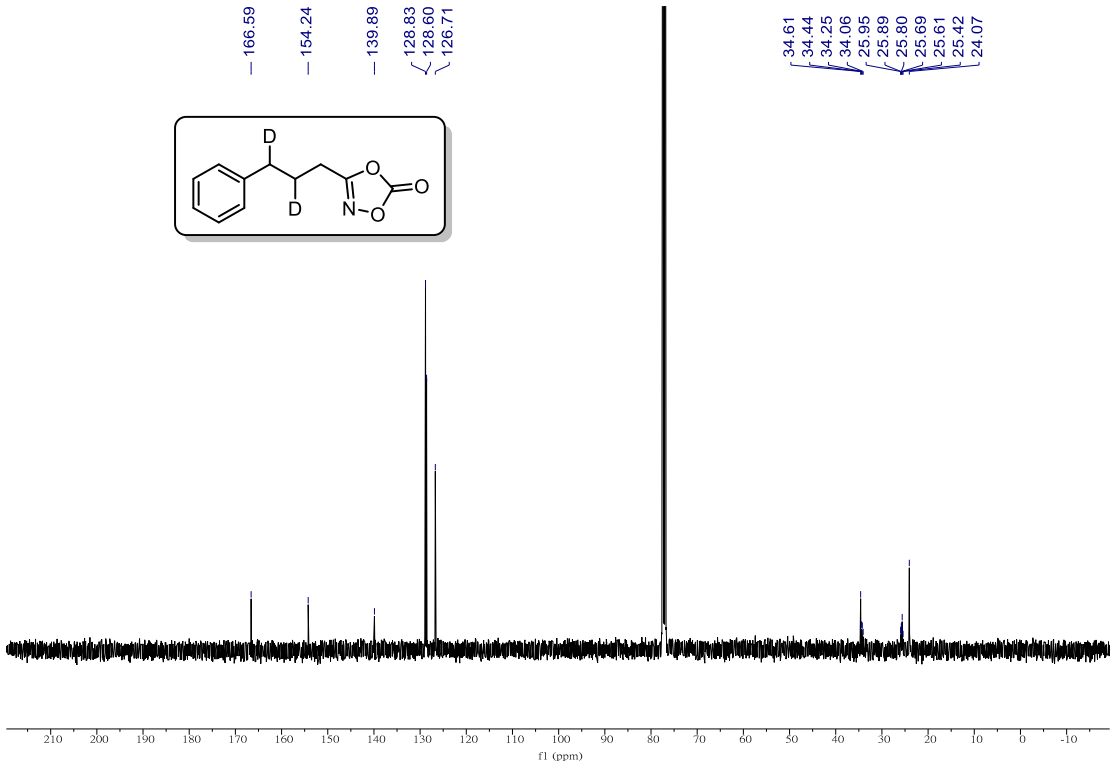

-72.2
-72.4
-72.6
-72.8
-73.0
-73.2
-73.4
-73.6
-73.8
f1 (ppm)


F3C
O
CF3
O
NH2
OMe

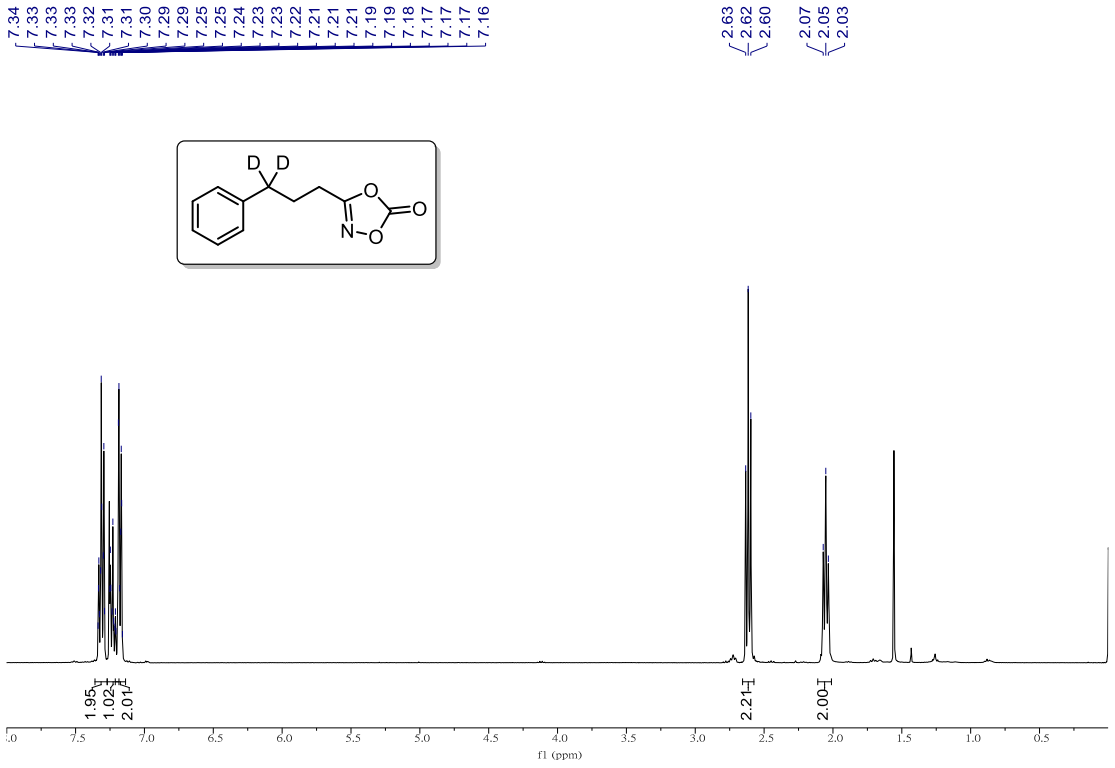

0.99
1.01
-15
-20
-25
-30
-35
-40
-45
-50
-55
-60
-65
-70
-75
-80
-85
-90
-95
-100
-105
-110
-115
-120
-125
-130
-135
-140
-145
f1 (ppm)

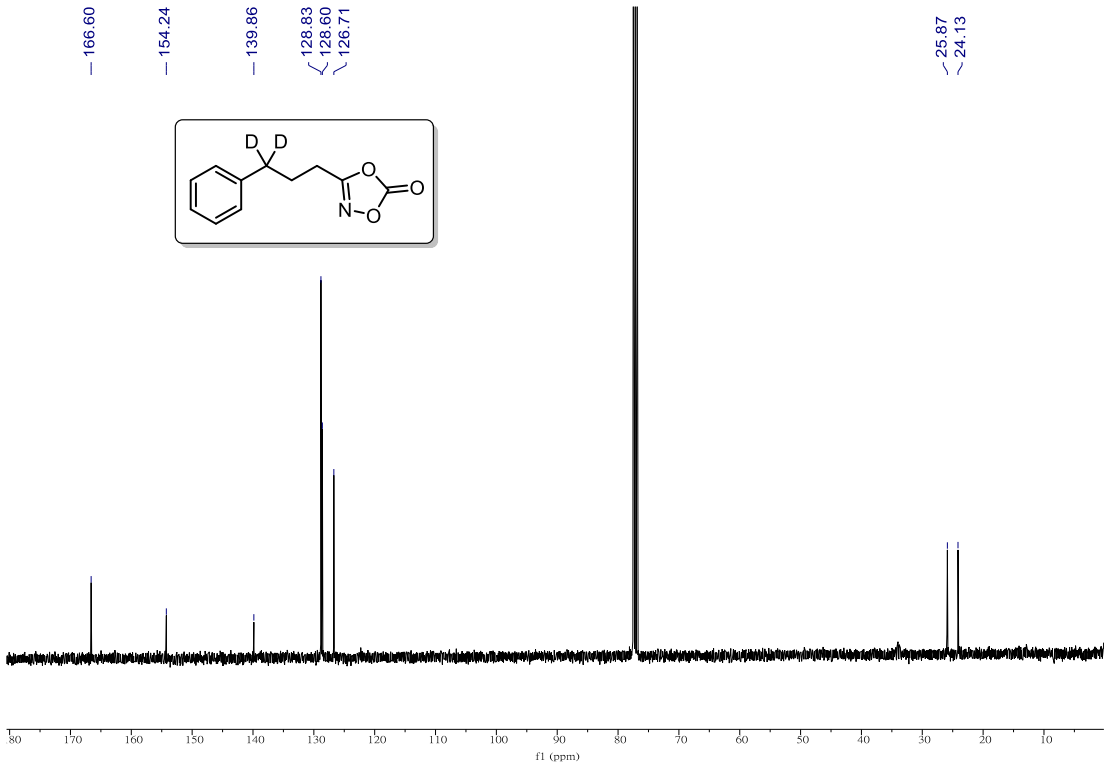
3-(3-Phenylpropyl)-1,4,2-dioxazol-5-one-d$_2$ (1a-*d*$_2$-2)



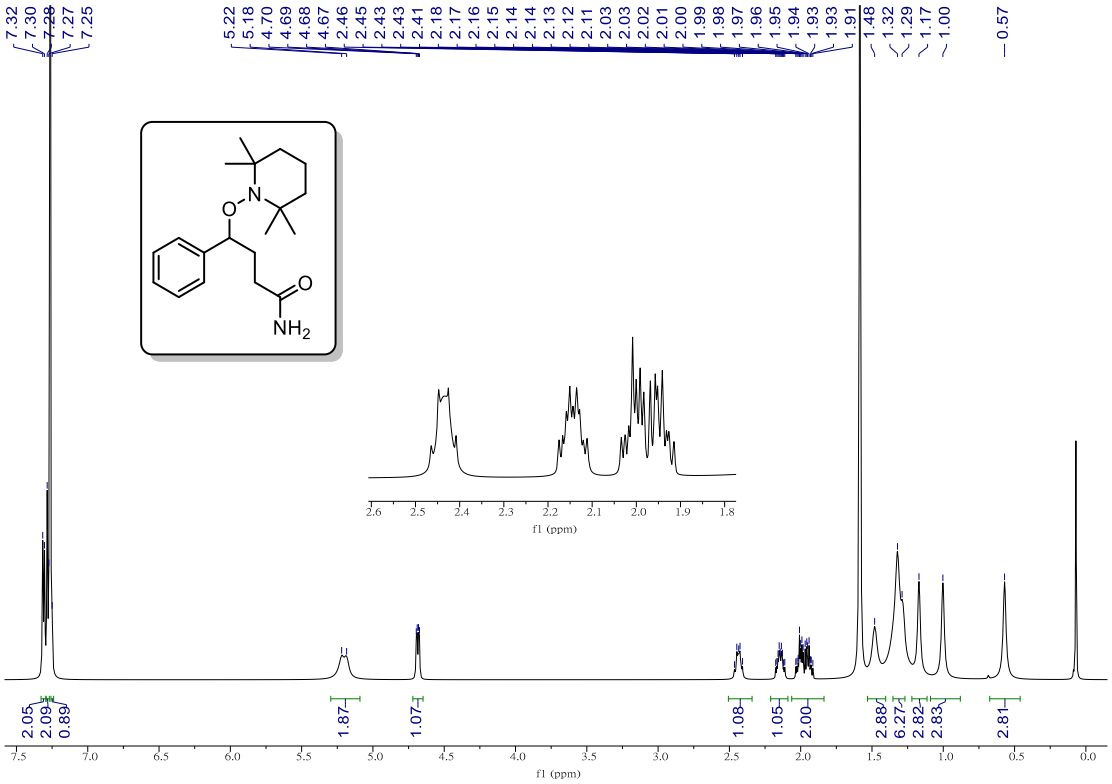


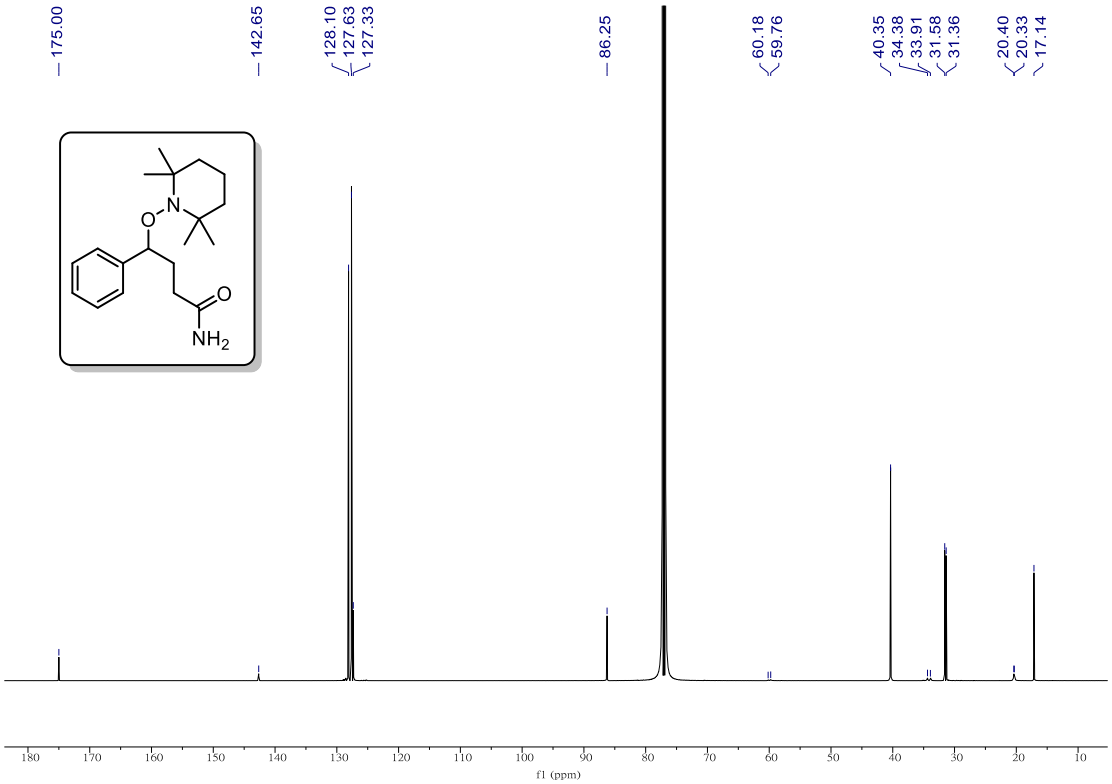
3-(3-Phenylpropyl)-1,4,2-dioxazol-5-one-d$_2$ (1a-*d*$_2$-1)





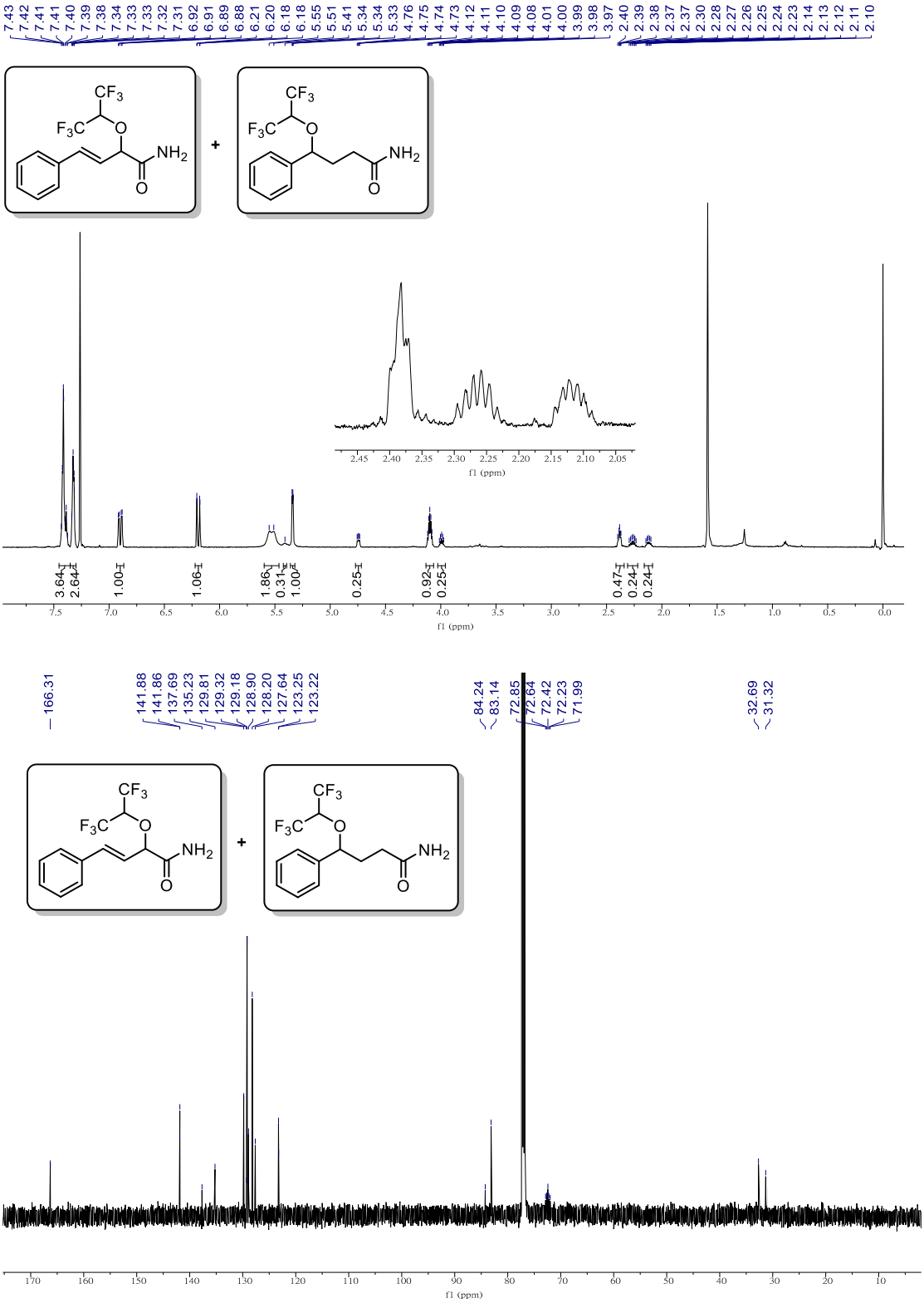
4-Phenyl-4-((2,2,6,6-tetramethylpiperidin-1-yl)oxy)butanamide

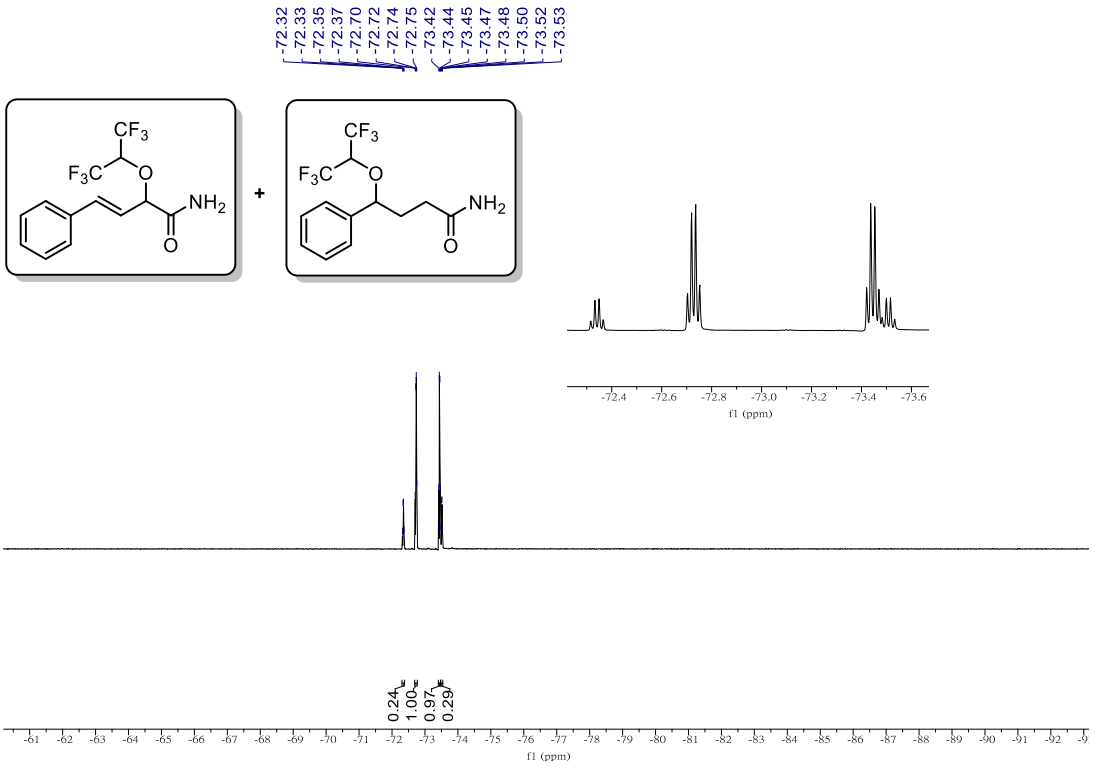




(*E*)-2-((1,1,1,3,3,3-Hexafluoropropan-2-yl)oxy)-4-phenylbut-3-enamide &

4-((1,1,1,3,3,3-Hexafluoropropan-2-yl)oxy)-4-phenylbutanamide



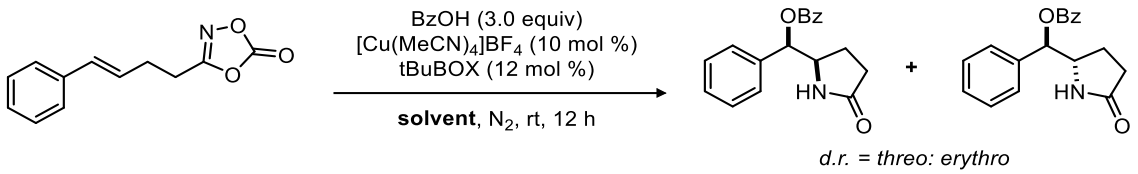

-72.32
-72.33
-72.35
-72.37
-72.70
-72.72
-72.74
-72.75
-73.42
-73.44
-73.45
-73.47
-73.48
-73.50
-73.52
-73.53
CF3
F3C
O
NH2
O
+
CF3
F3C
O
NH2
O
-72.4
-72.6
-72.8
-73.0
-73.2
-73.4
-73.6
f1 (ppm)
0.24
1.00
0.97
0.29
-61
-62
-63
-64
-65
-66
-67
-68
-69
-70
-71
-72
-73
-74
-75
-76
-77
-78
-79
-80
-81
-82
-83
-84
-85
-86
-87
-88
-89
-90
-91
-92
f1 (ppm)

A.5 Supplementary Information of Chapter 4

Experimental Optimization of Cu-Catalyzed Intramolecular Oxyamidation of 1,4,2-Dioxazol-5-ones

General procedure : All reactions were performed in a glovebox under an N_2 atmosphere. Cu catalyst (10 mol%) and ligand (12 mol%) were added to an oven-dried 8 mL vial equipped with a magnetic stir bar. Solvent (2 mL) was added to the resultant mixture and stirred at specified temperature for 3 min. (*E*)-3-(4-Phenylbut-3-en-1-yl)-1,4,2-dioxazol-5-one **1a** (0.1 mmol) and benzoic acid (3.0 equiv) was then added to the solution and capped. After stirring at room temperature for 12 h, the reaction mixture was filtered through a pad of silica gel and washed with EtOAc (2 mL × 3). The mixture was concentrated under vacuum. The NMR yield was obtained by ^{1}H NMR spectroscopic analysis using $CDCl_3$ (0.7 mL) as solvent with CH_2Br_2 (0.2 mmol, 13.96 uL) as internal standard.

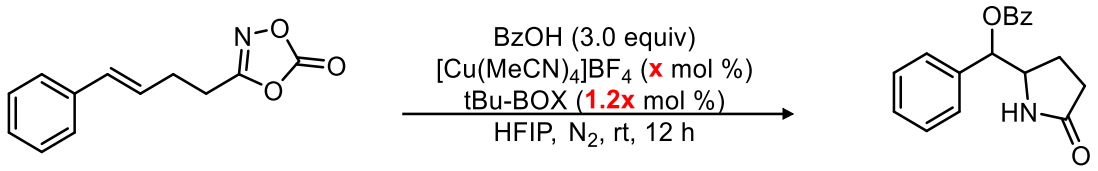
Table A14 Effect of Solvent with tBuBOX Ligand[a]



entry	solvent	yield[b]	d.r.[c]
1	TFE	19[d]	7:1
2	**HFIP**	**96(92)[e]**	**>20:1**
3	NFTB	76	12:1
4	EtOH	n.d.	-
5	toluene	n.d.	-
6	DCM	47	2.3:1
7	HFIP:DCM 1:1	84(80)[e]	>10:1

[a]Reaction conditions: **1a** (0.1 mmol), BzOH (3.0 equiv), Cu catalyst (10 mol%), and tBuBOX (12 mol%) in solvent under N_2 for 12 hours at room temperature. [b]^{1}H NMR yield (internal standard: dibromomethane), isolated yield in parentheses. [c]d.r. were determined by ^{1}H NMR of the crude reaction mixture. [d]77% of TFE adduct was obtained. [e]30% enantiomeric excess was obtained.

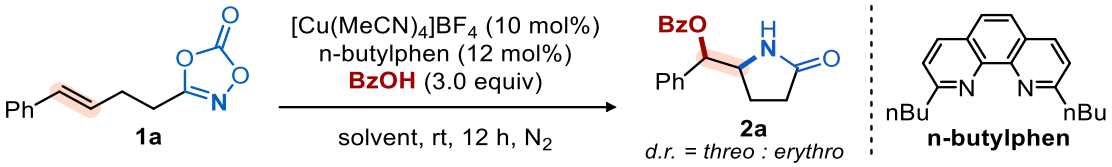
Table A15 Effect of Catalyst Loading[a]



entry	catalyst loading/ x mol%	yield[b]	d.r.[c]
1	**10.0 mol%**	**96(92)**	**>20:1**
2	5.0 mol%	60	>20:1
3	2.5 mol%	40	>20:1
4	1.0 mol%	12	>20:1
5	0.5 mol%	<5	>20:1

[a]Reaction conditions: **1a** (0.1 mmol), BzOH (3.0 equiv), Cu catalyst (x mol%), and tBuBOX(1.2x mol%) in HFIP under N_2 for 12 hours at room temperature. [b]^{1}H NMR yield (internal standard: dibromomethane), isolated yield in parentheses. [c]d.r. were determined by ^{1}H NMR of the crude reaction mixture.

Table A16 Effect of Solvents with 2,9-*n*-Butylphenanthroline Ligand[a]

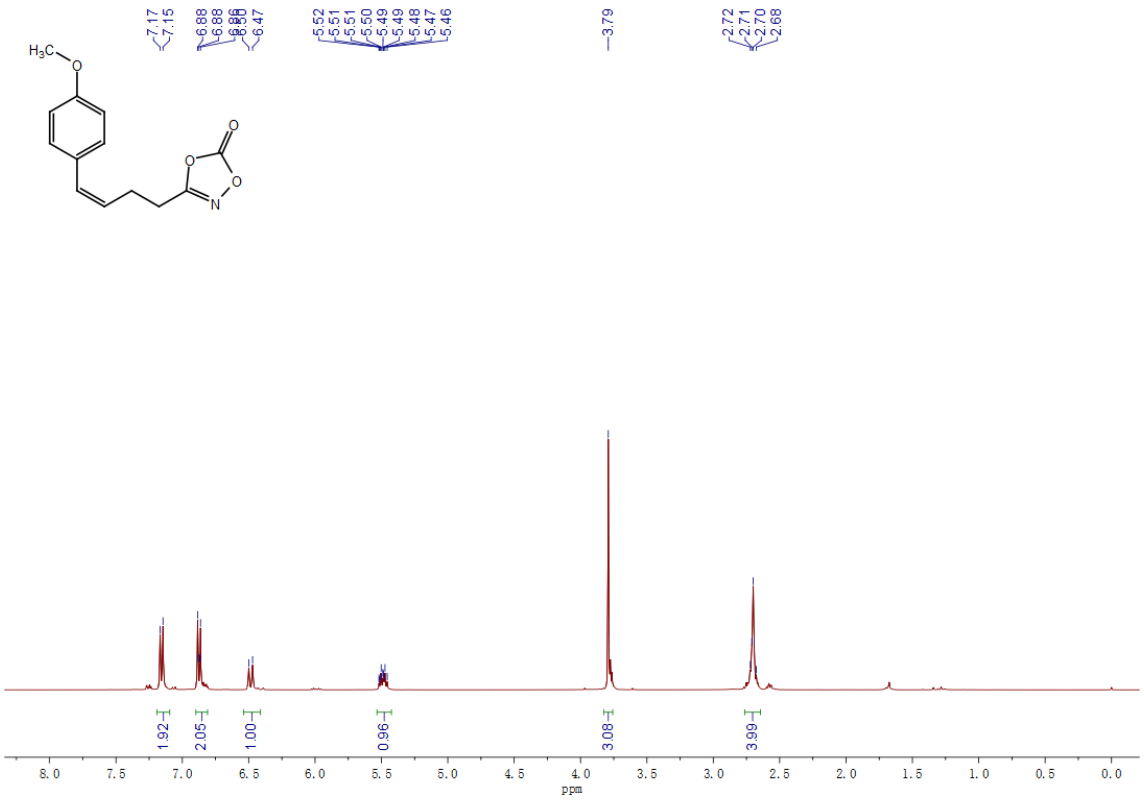


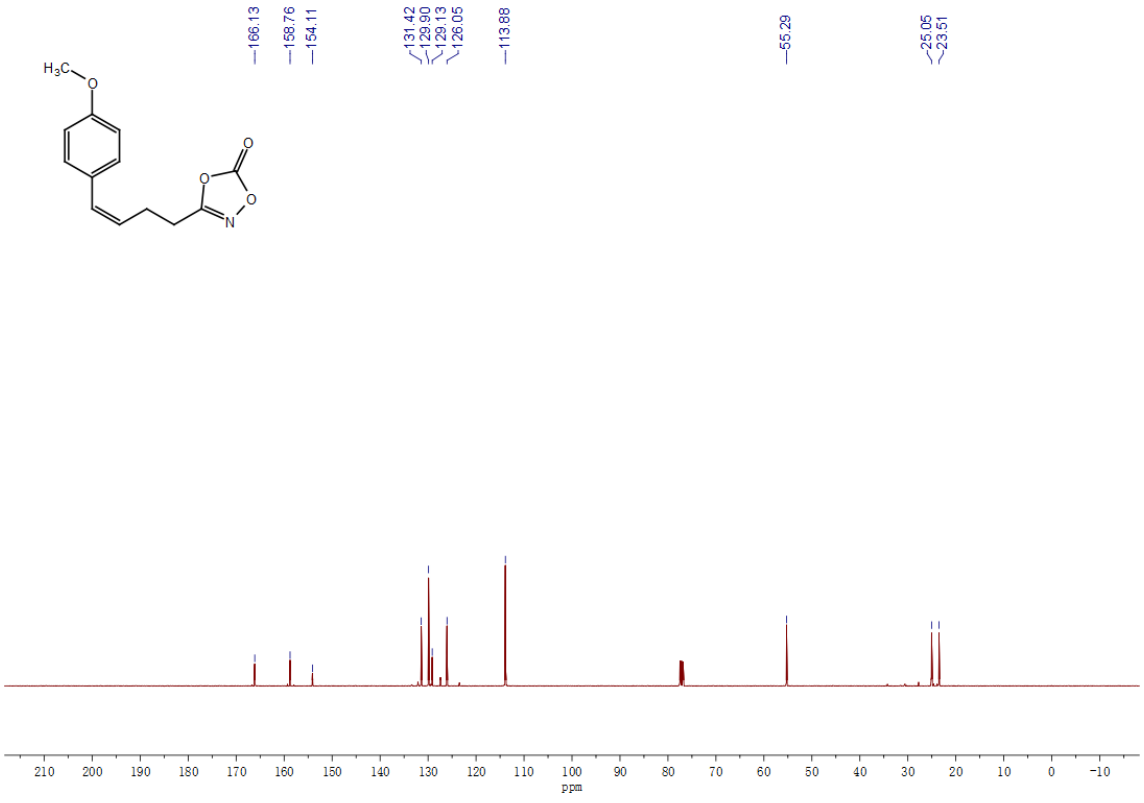
entry	solvent	yield of **2a** (%)[b]	d.r.[c]
1	DCM	47	2:1
2	DCE	38	2:1
3	MeCN	n.d.	-
4	PhCl	n.d.	-
5	$PhCF_3$	22	1:1
6	toluene	17	1.3:1
7	TFE	18	10:1
8	HFIP	80	17:1
9	HFIP	n.d.[d]	-

[a]Reaction conditions: **1a** (0.1 mmol), BzOH (3.0 equiv), Cu catalyst (10 mol%), and 2,9-n-butylphenanthroline (12 mol%) in solvent under N_2 for 12 hours at room temperature. [b]^{1}H NMR yield (internal standard: dibromomethane), isolated yield in parentheses. [c]d.r. were determined by ^{1}H NMR of the crude reaction mixture. [d]Reaction run without Cu catalyst.

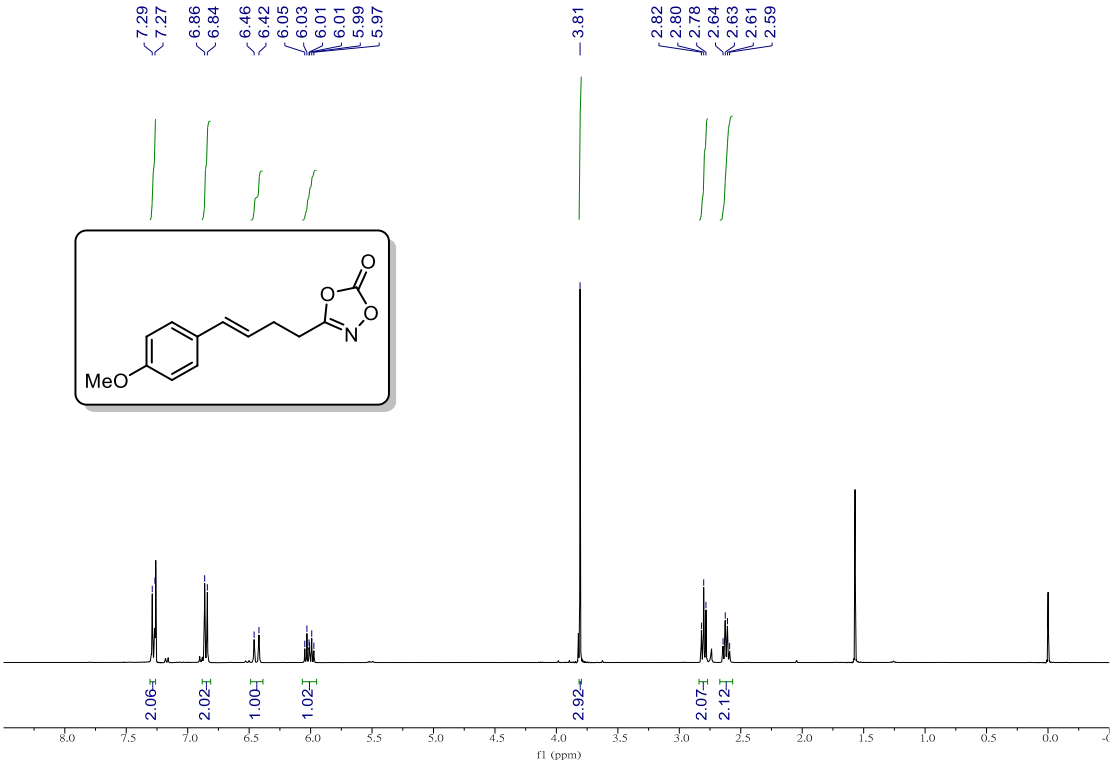
A.6 NMR Spectra of Chapter 4

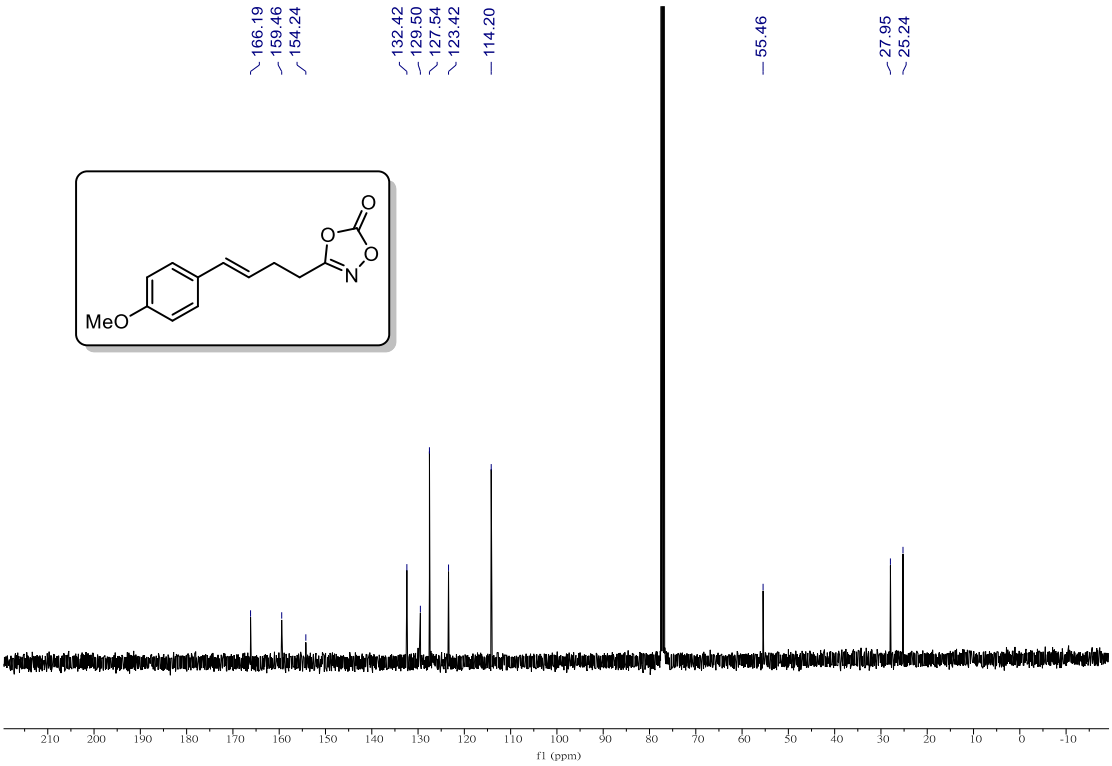
(Z)-3-(4-(4-Methoxyphenyl)but-3-en-1-yl)-1,4,2-dioxazol-5-one



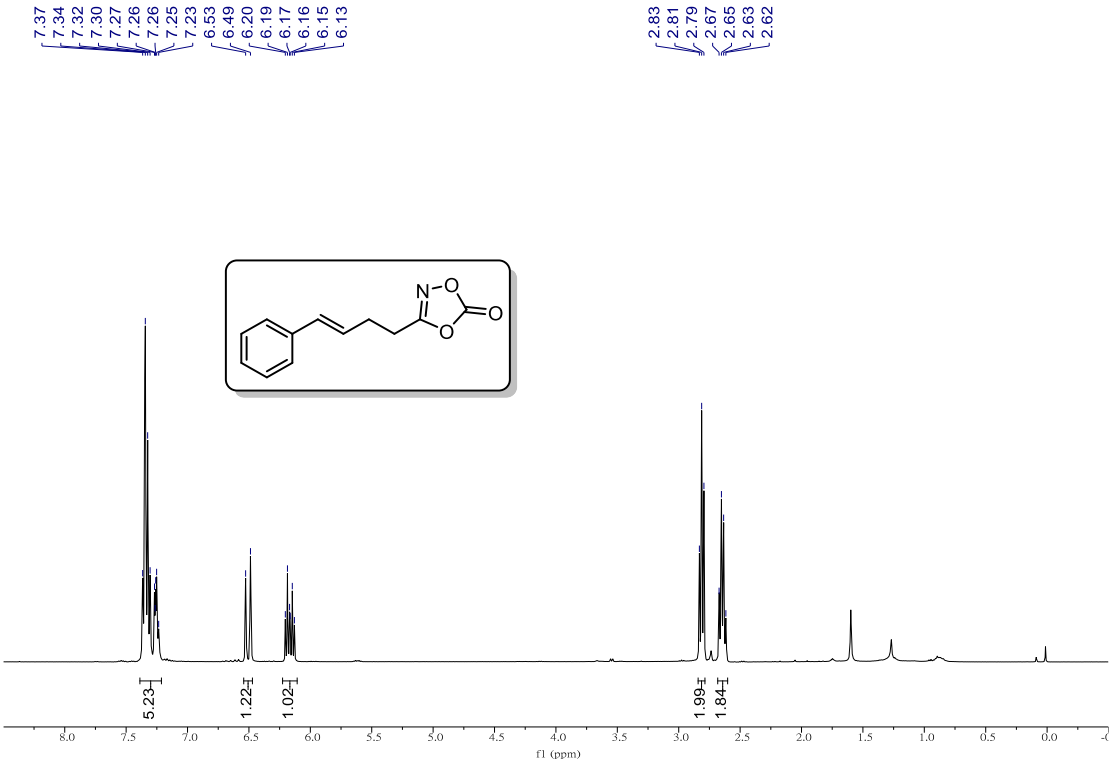


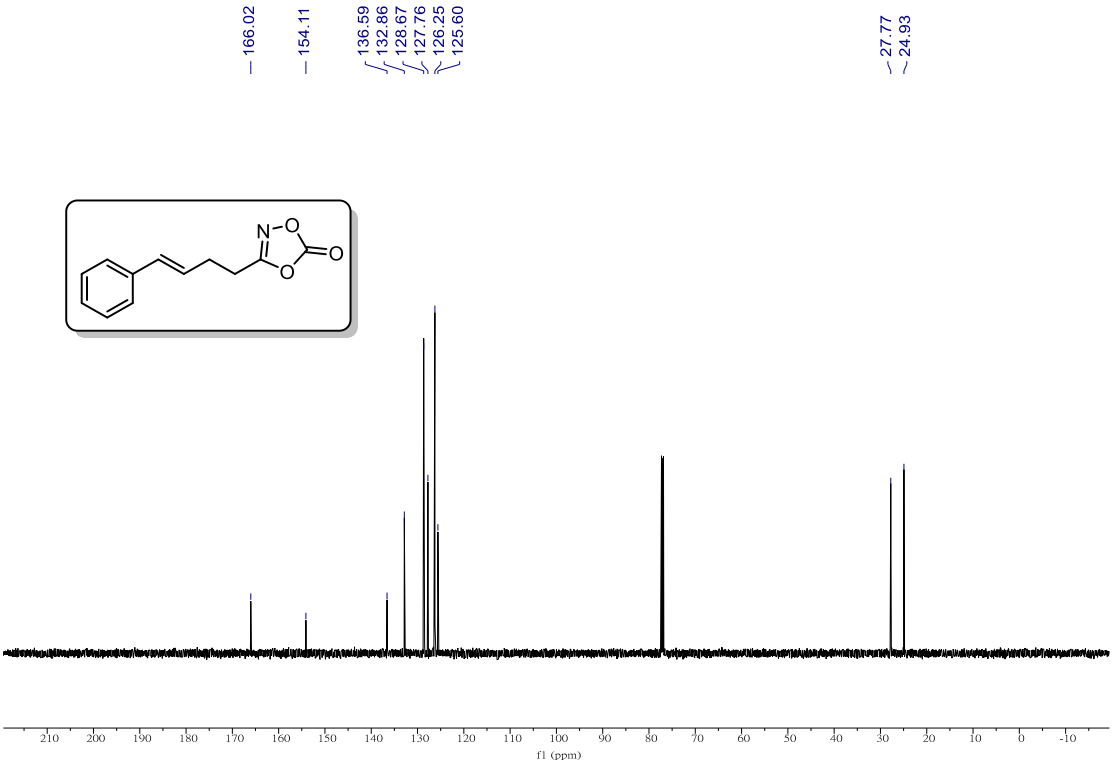
(*E*)-3-(4-(4-Methoxyphenyl)but-3-en-1-yl)-1,4,2-dioxazol-5-one



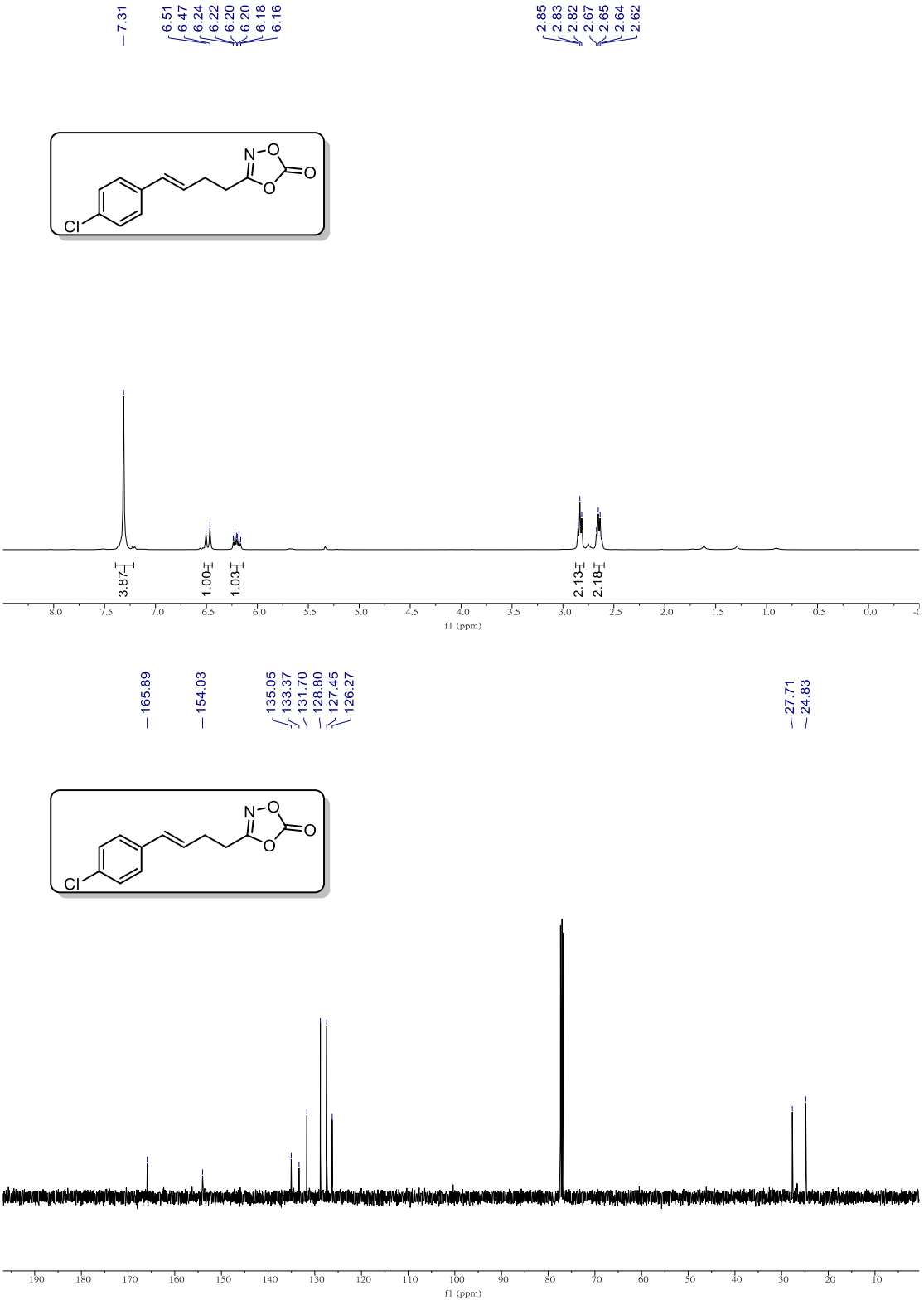


(*E*)-3-(4-Phenylbut-3-en-1-yl)-1,4,2-dioxazol-5-one

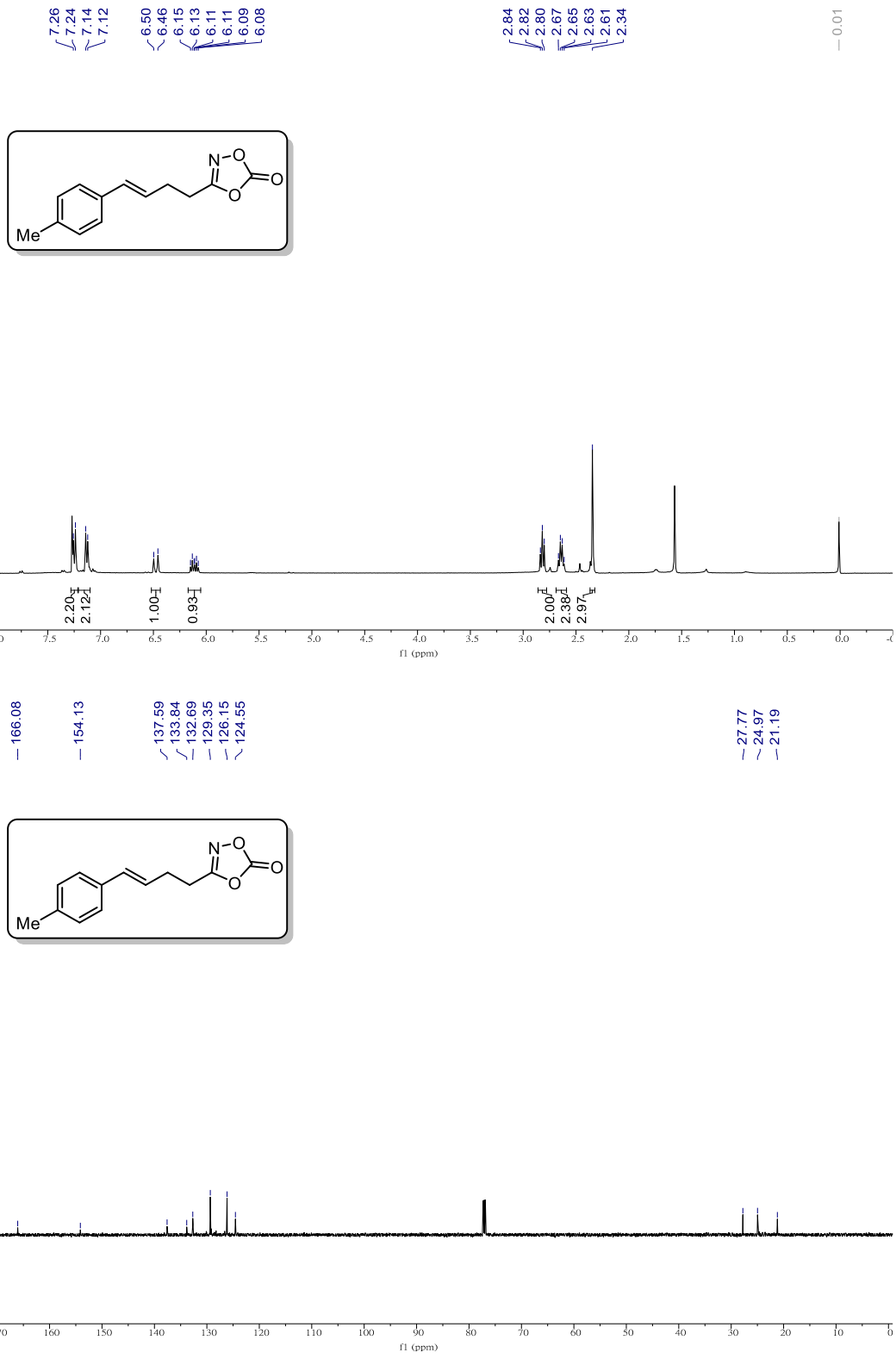




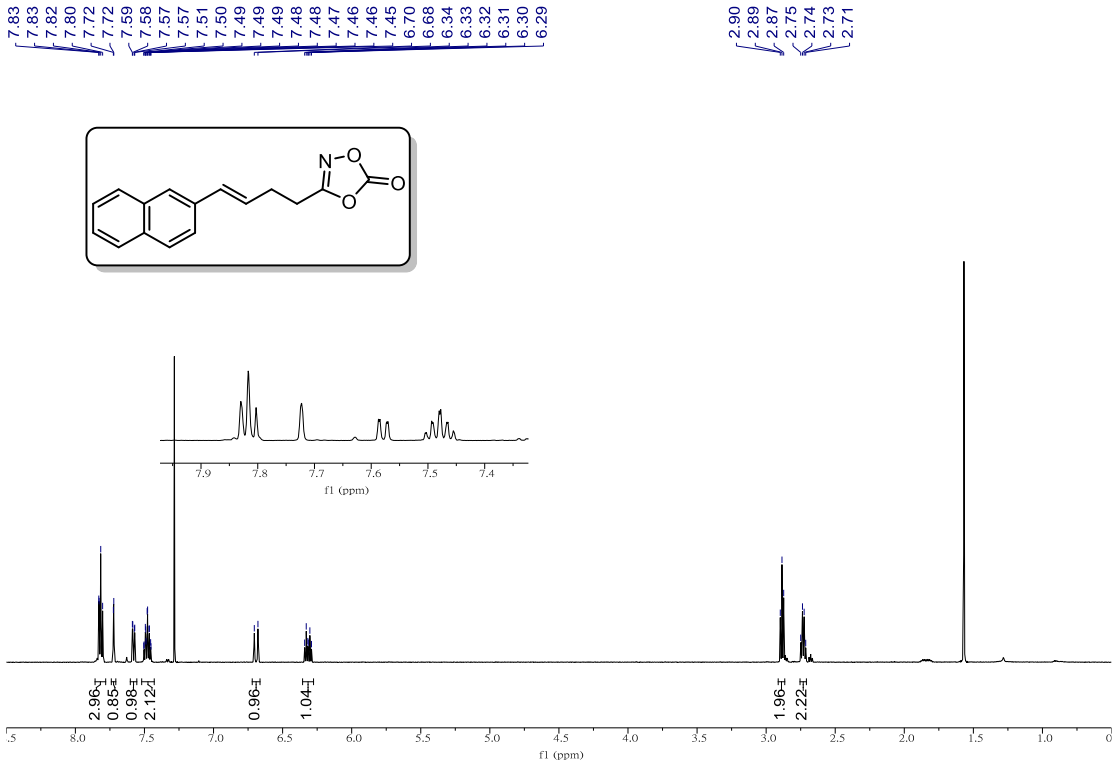
(*E*)-3-(4-(4-Chlorophenyl)but-3-en-1-yl)-1,4,2-dioxazol-5-one

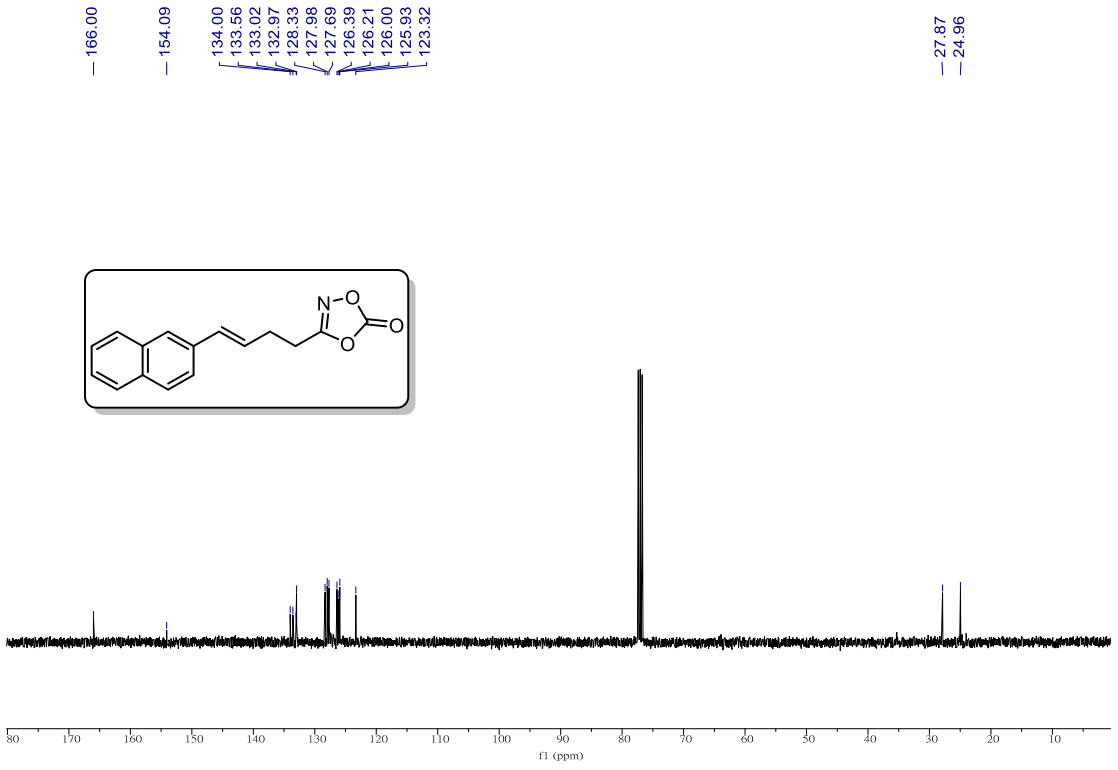


(*E*)-3-(4-(p-Tolyl)but-3-en-1-yl)-1,4,2-dioxazol-5-one

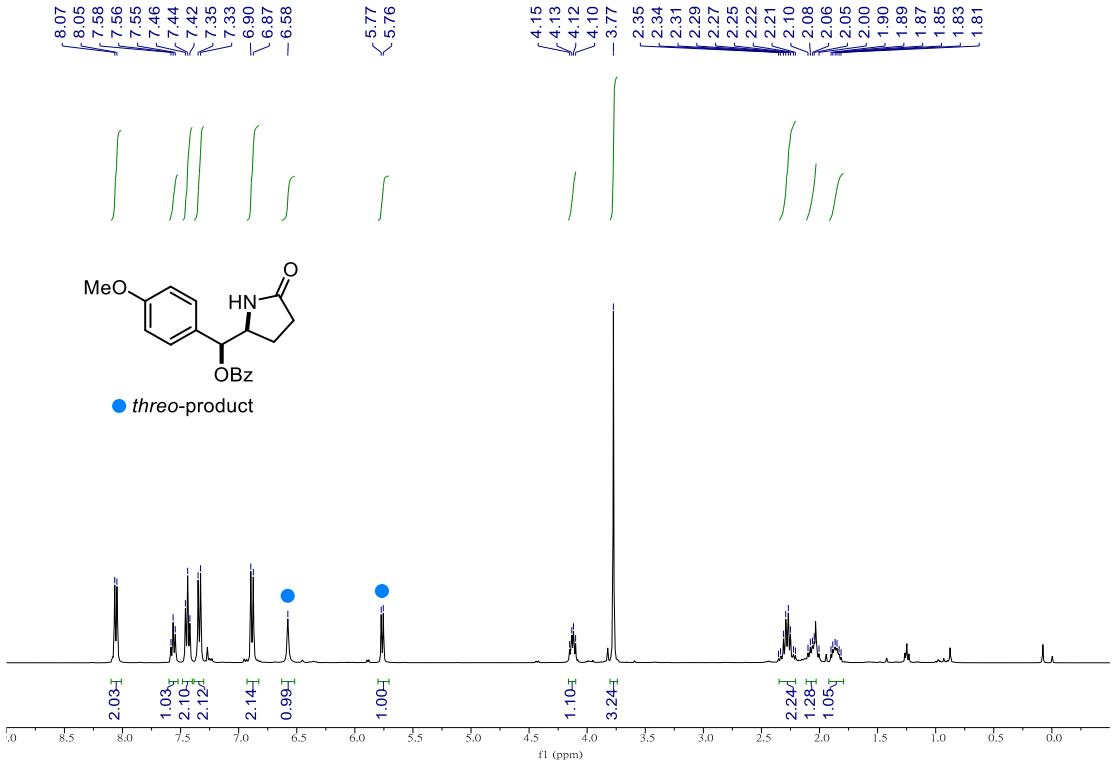


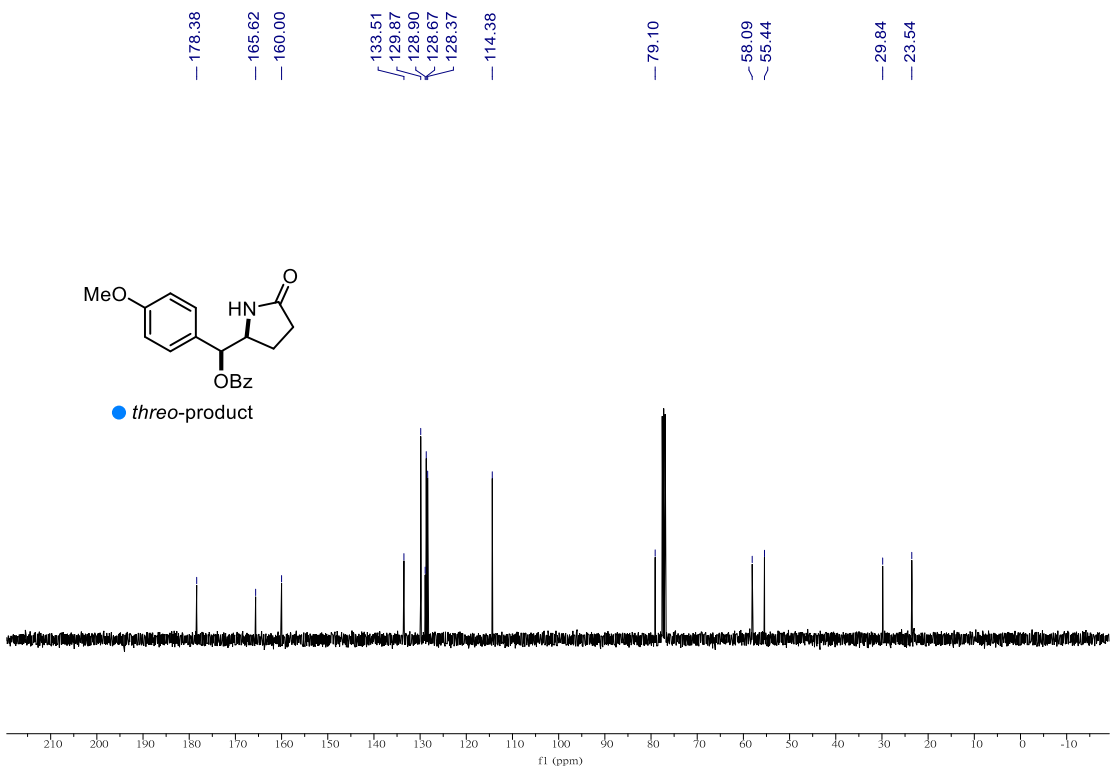
(*E*)-3-(4-(Naphthalen-2-yl)but-3-en-1-yl)-1,4,2-dioxazol-5-one



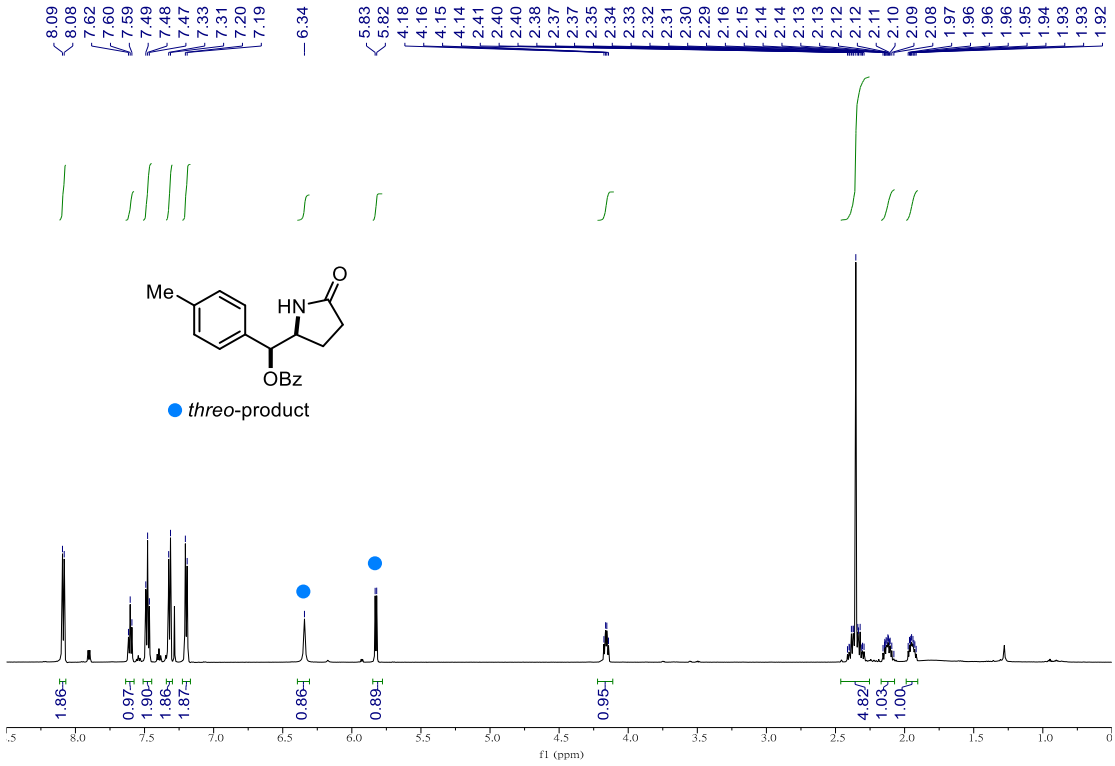


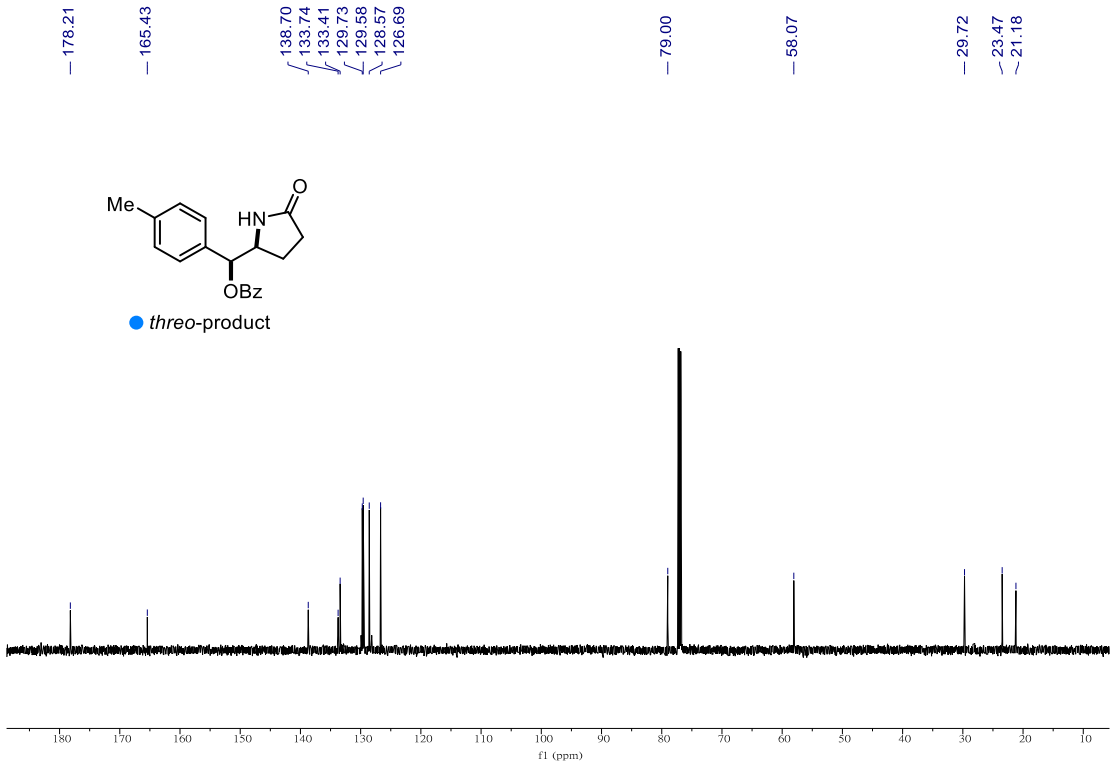
(4-Methoxyphenyl)(5-oxopyrrolidin-2-yl)methyl benzoate



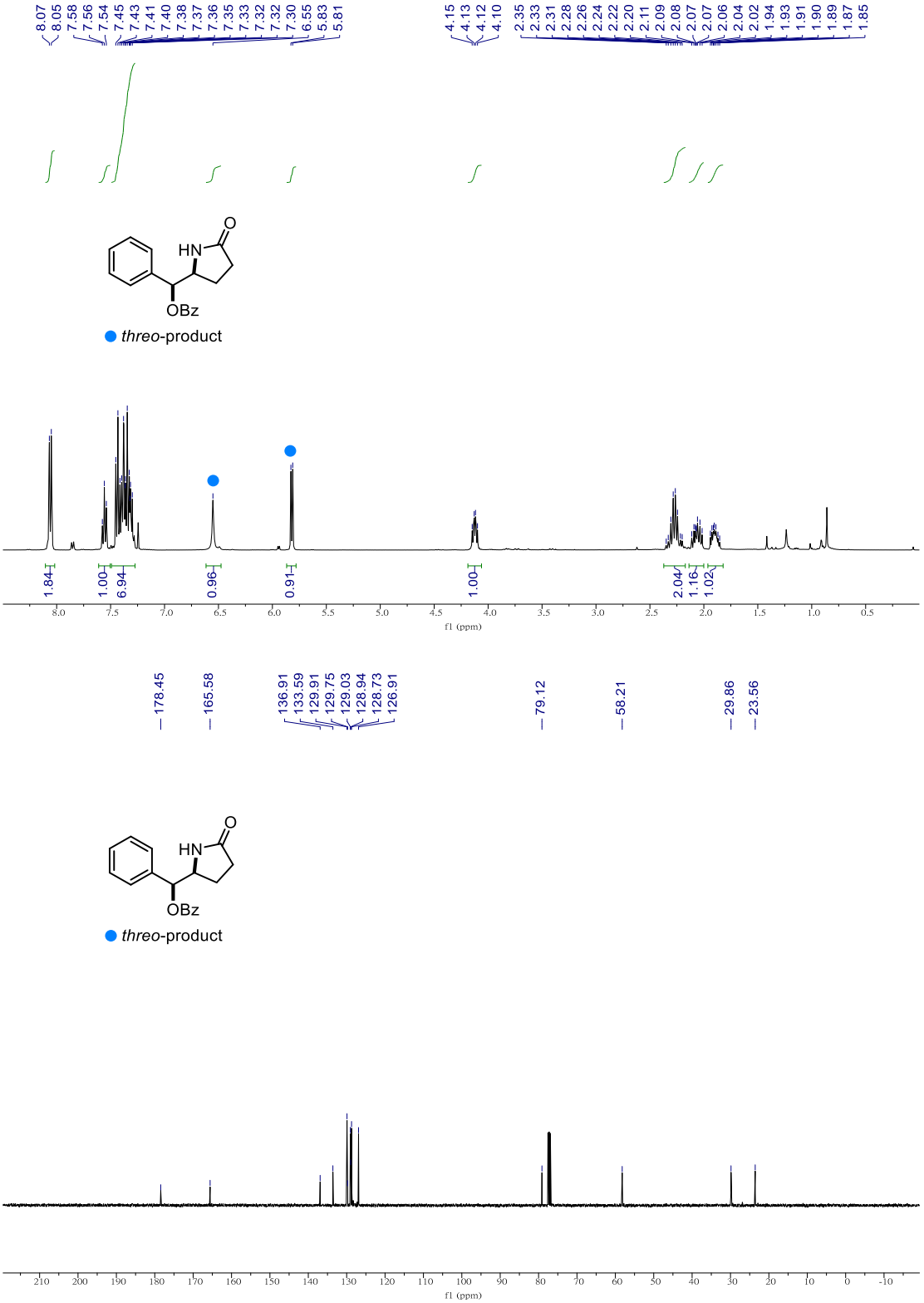


(5-Oxopyrrolidin-2-yl)(p-tolyl)methyl benzoate



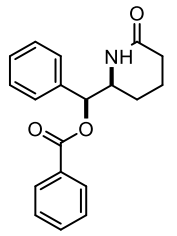


(5-Oxopyrrolidin-2-yl)(phenyl)methyl benzoate

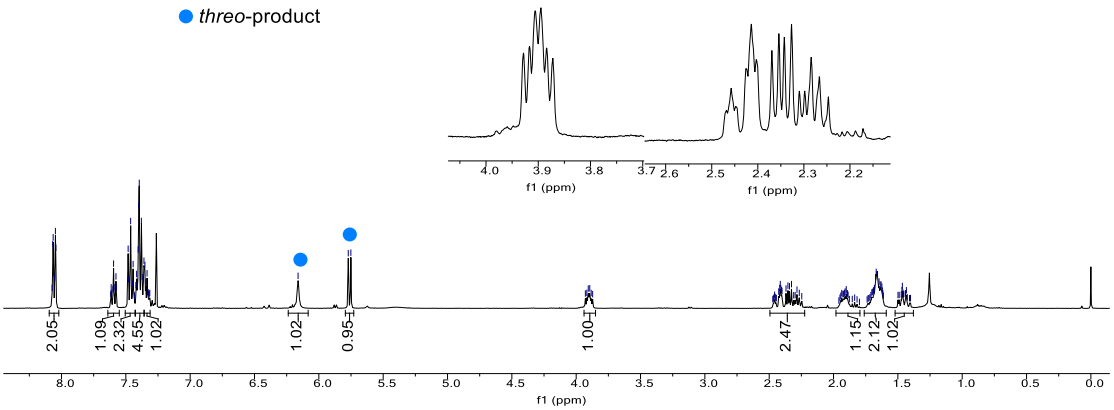


(6-Oxopiperidin-2-yl)(phenyl)methyl benzoate

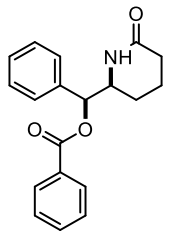




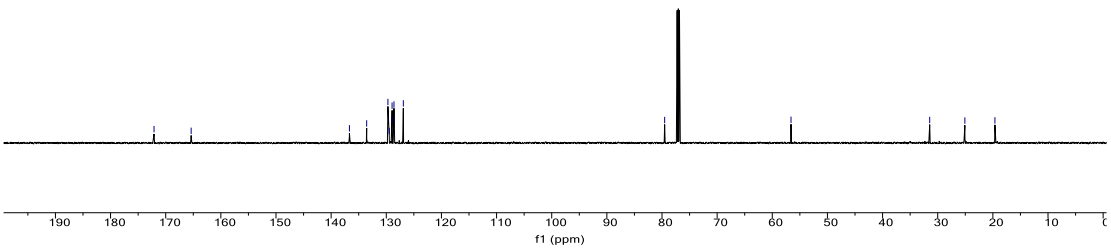
● *threo*-product



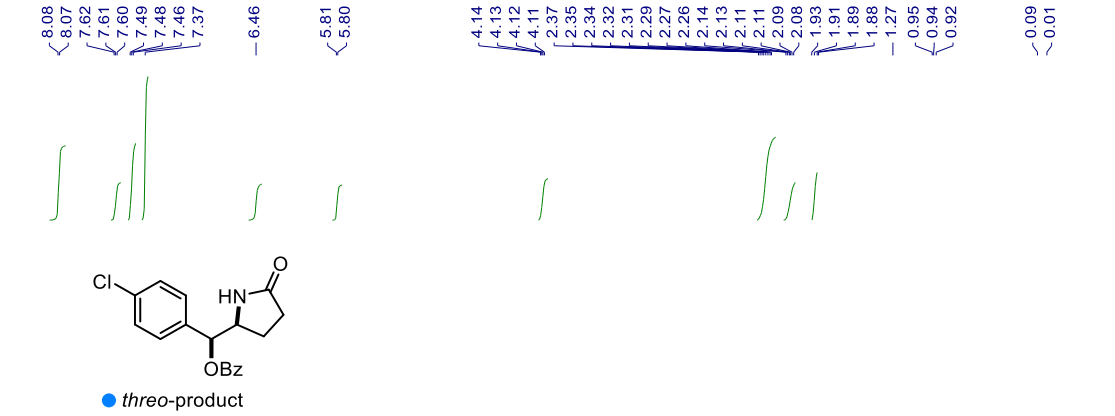




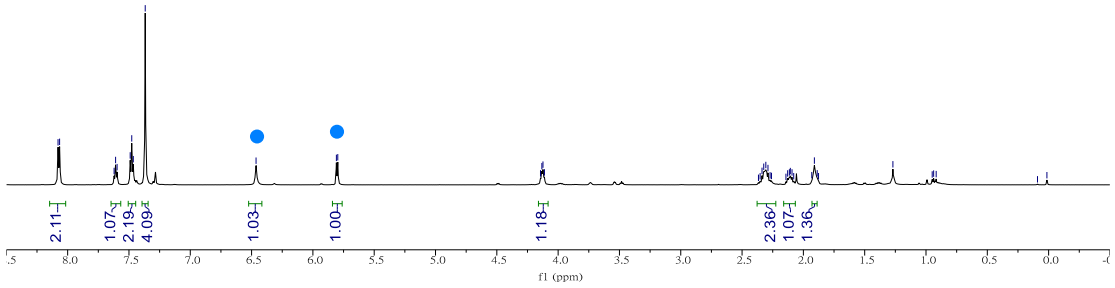
● *threo*-product



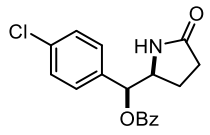
(4-Chlorophenyl)(5-oxopyrrolidin-2-yl)methyl benzoate



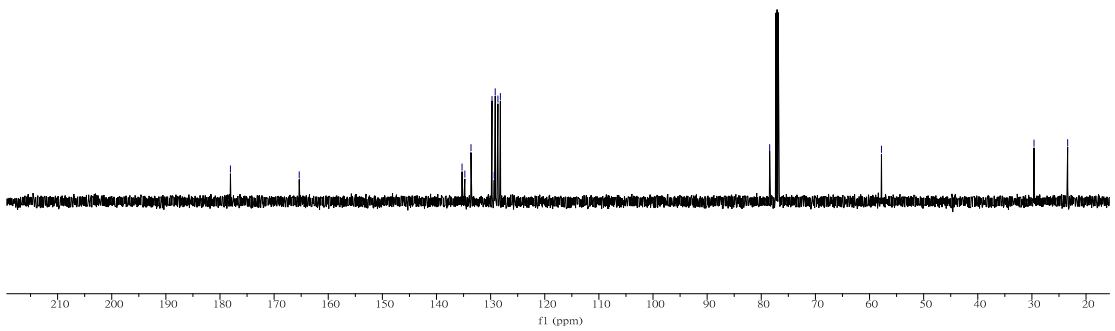
● *threo*-product





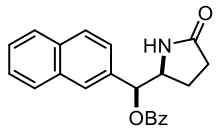


● *threo*-product

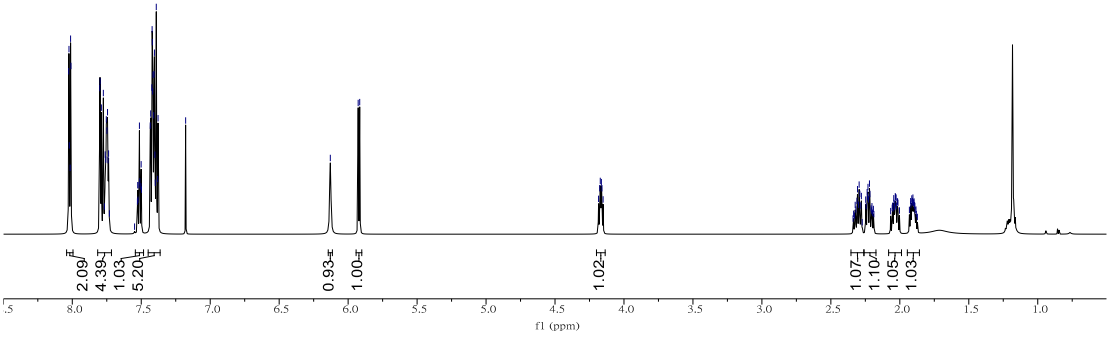


Naphthalen-2-yl(5-oxopyrrolidin-2-yl)methyl benzoate

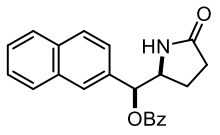




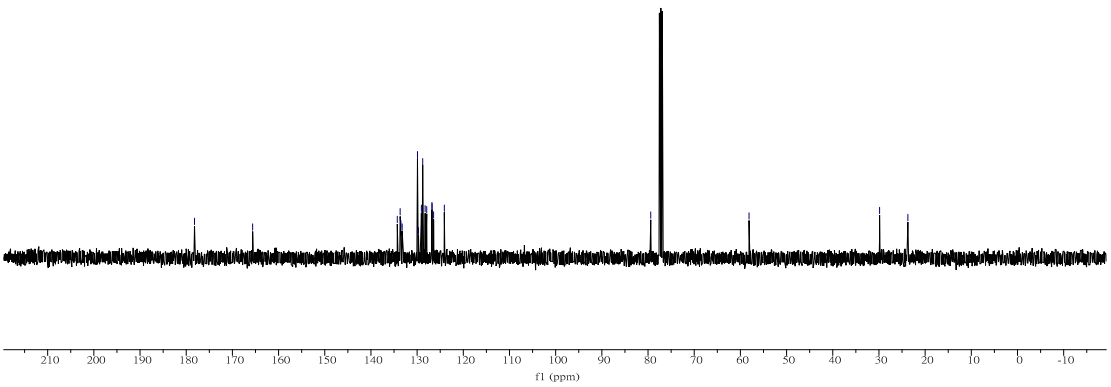
● *threo*-product



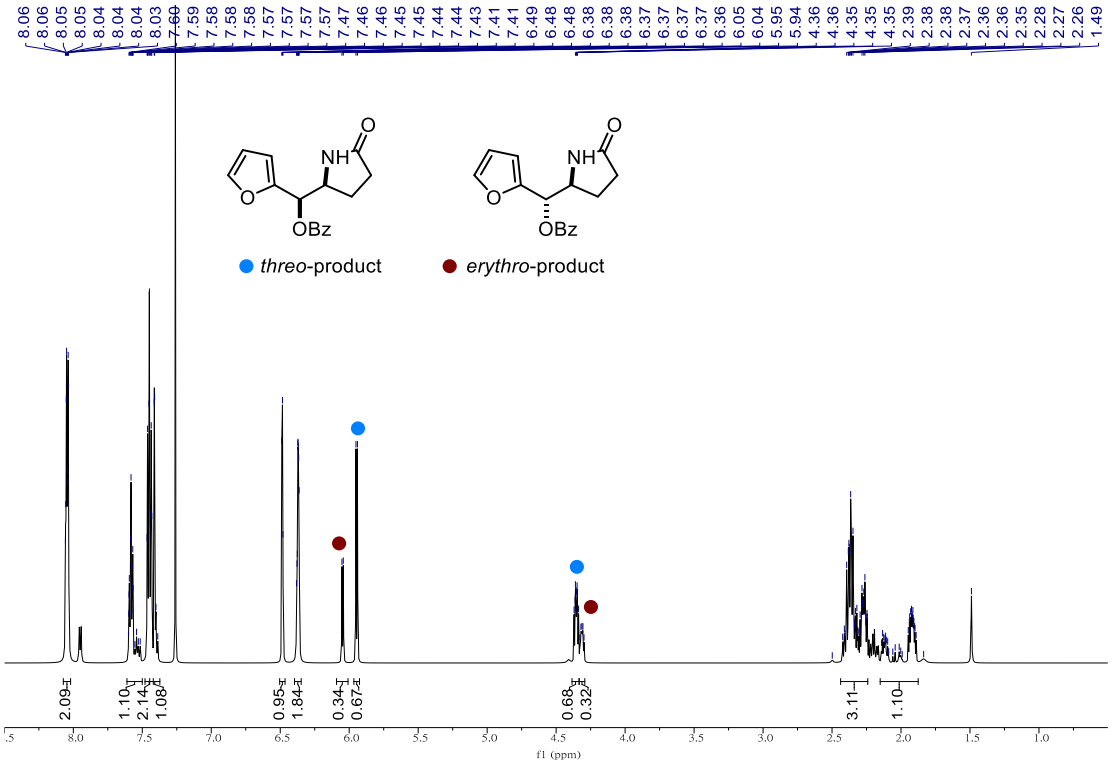


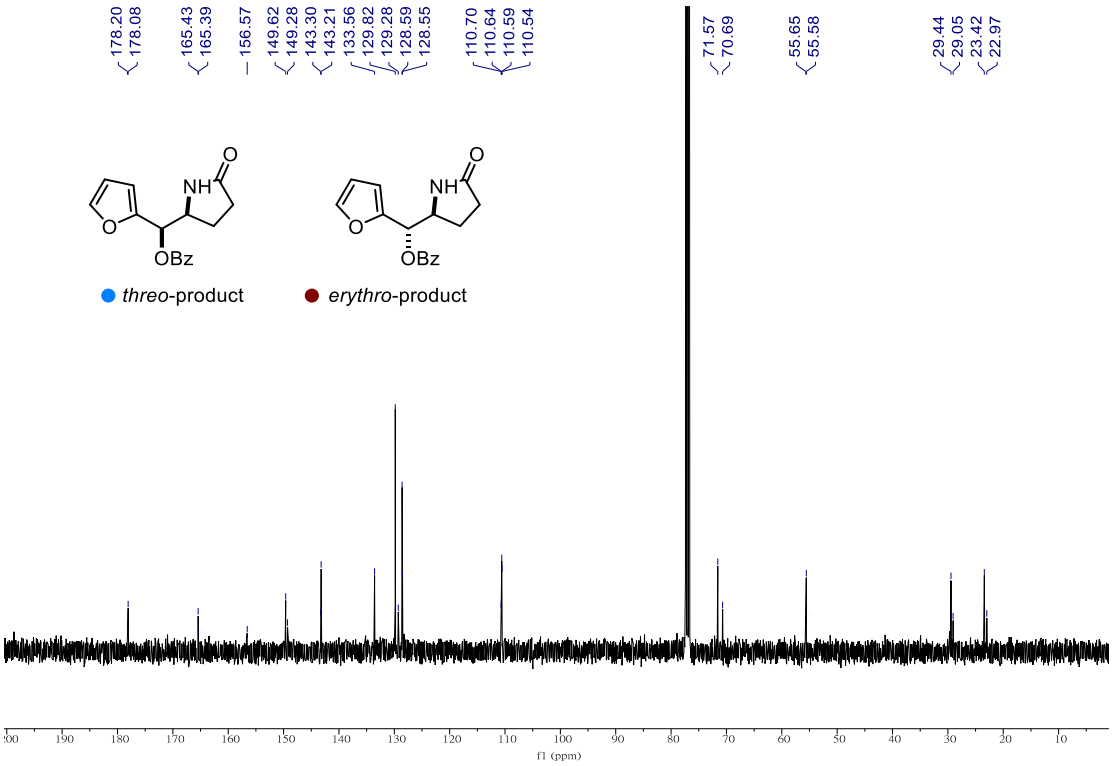


● *threo*-product

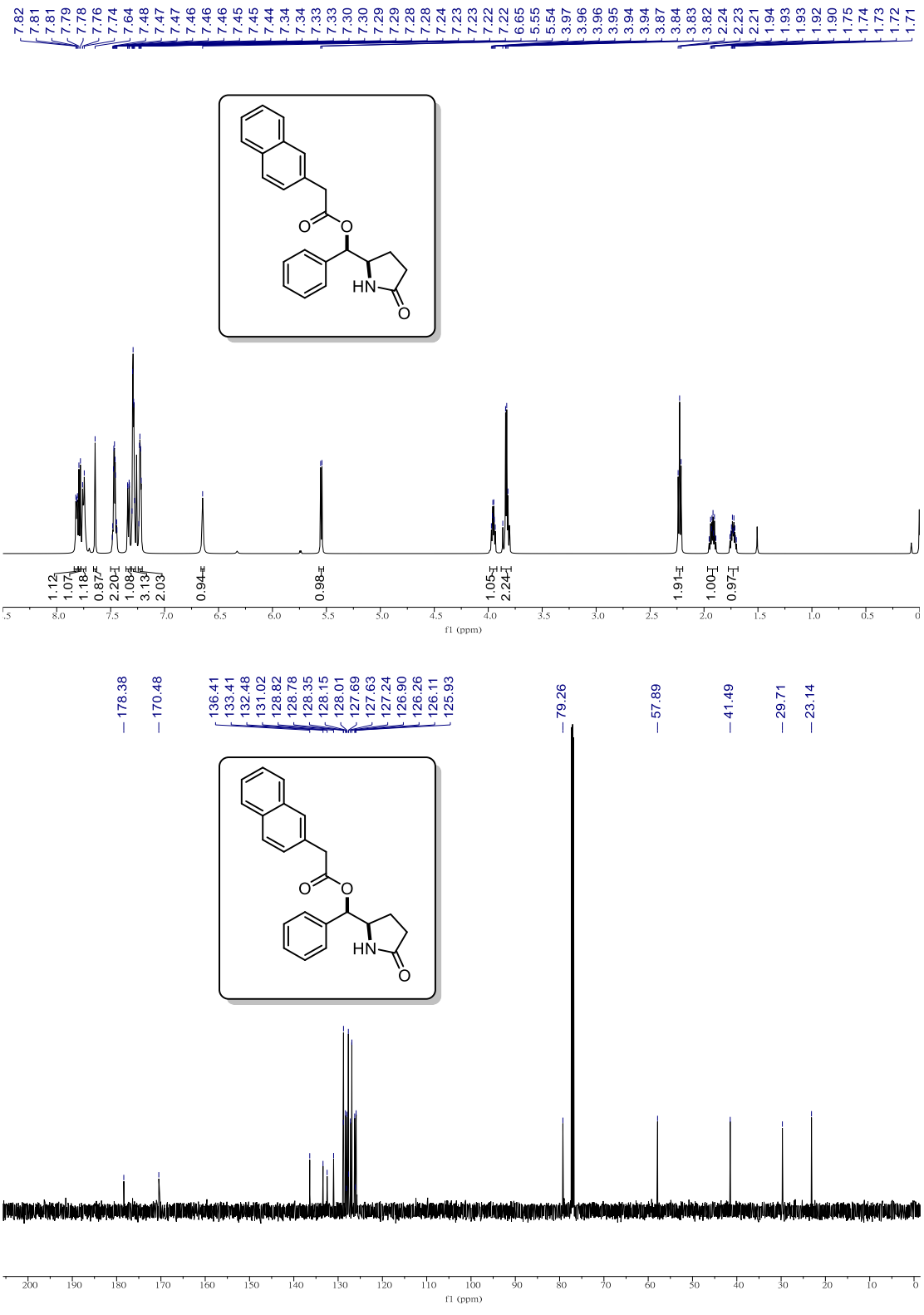


Furan-2-yl(5-oxopyrrolidin-2-yl)methyl benzoate

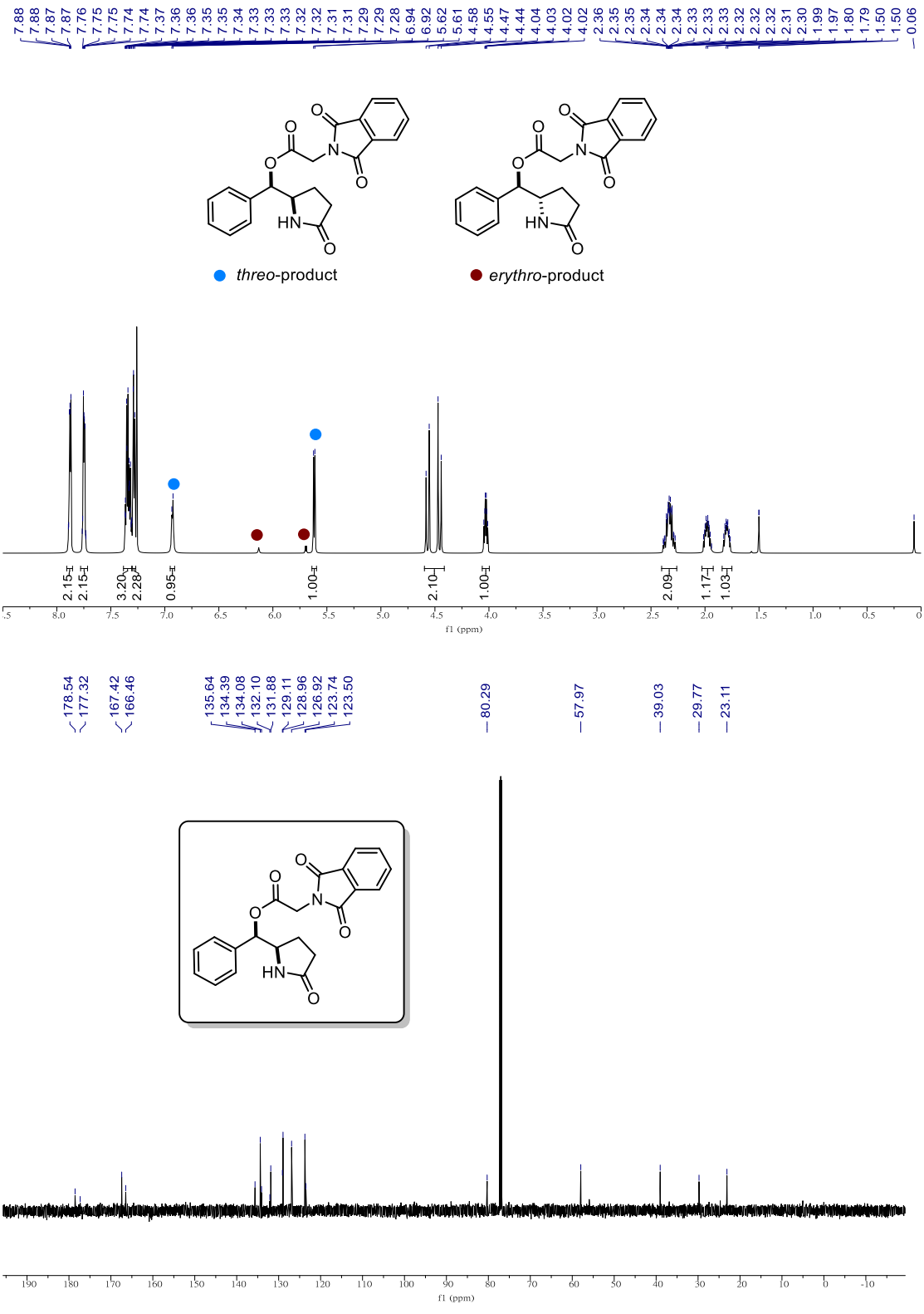




(5-Oxopyrrolidin-2-yl)(phenyl)methyl 2-(naphthalen-2-yl)acetate

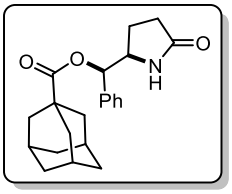


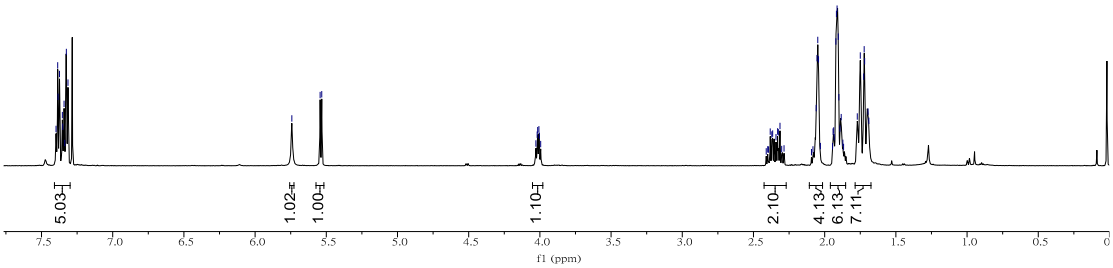
(5-Oxopyrrolidin-2-yl)(phenyl)methyl 2-(1,3-dioxoisoindolin-2-yl)acetate

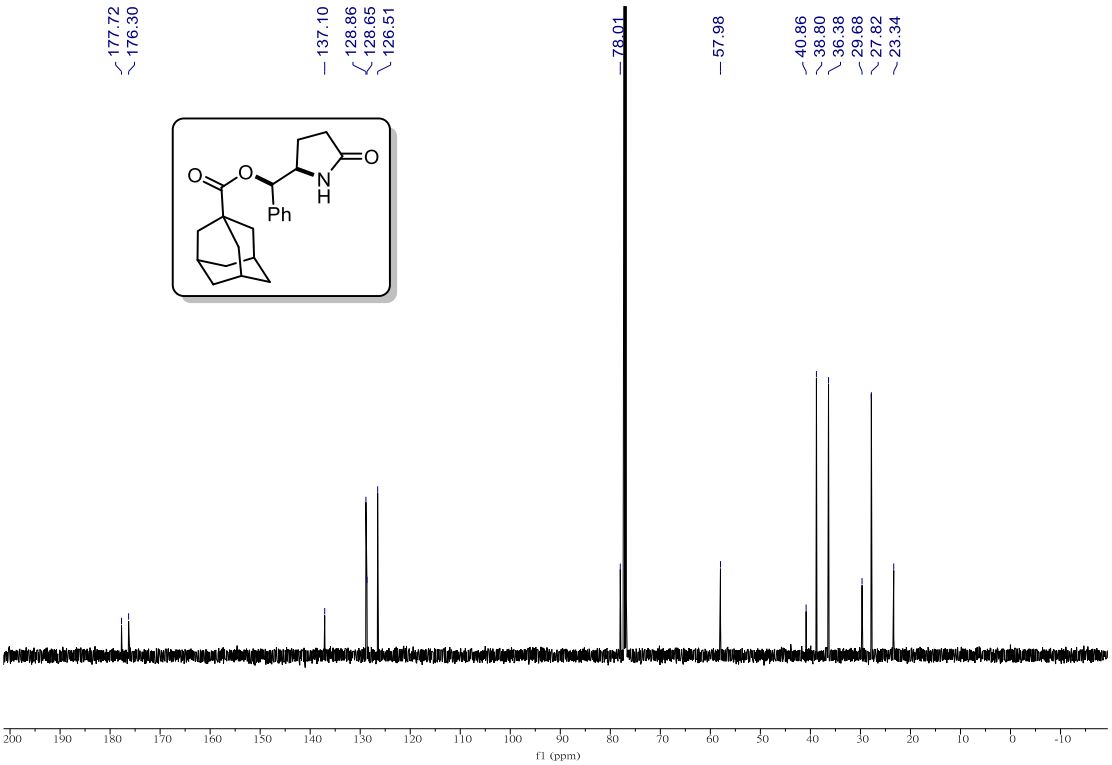


(5-Oxopyrrolidin-2-yl)(phenyl)methyl (3r,5r,7r)-adamantane-1-carboxylate

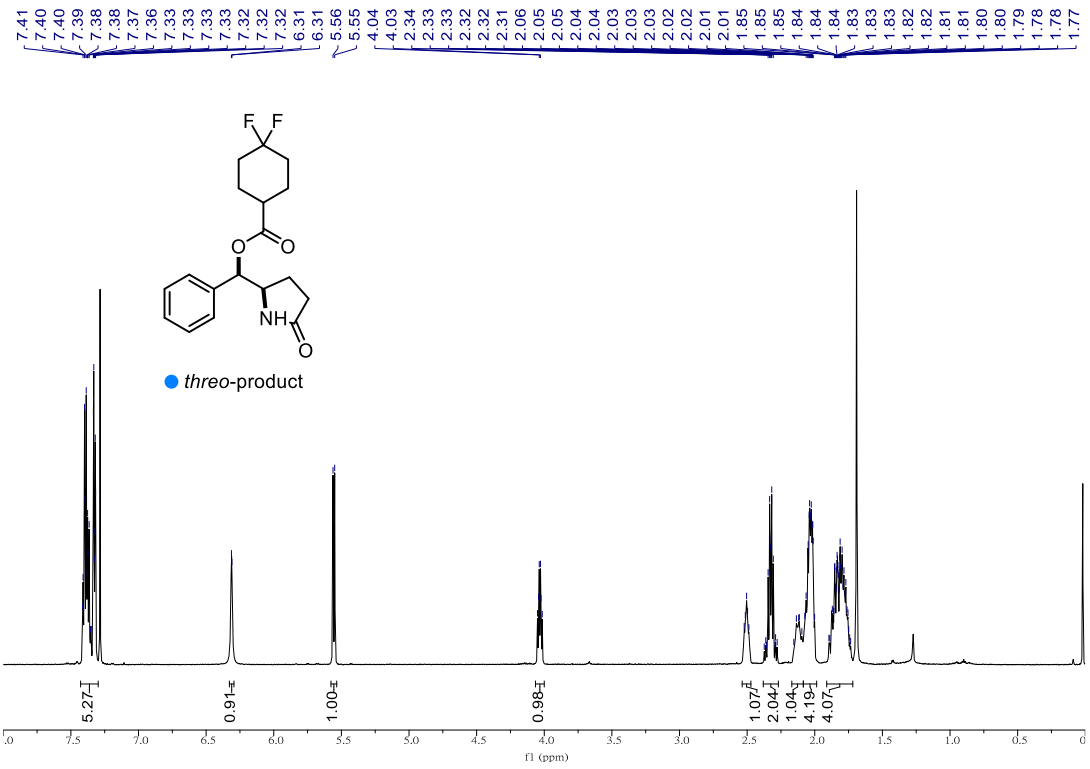


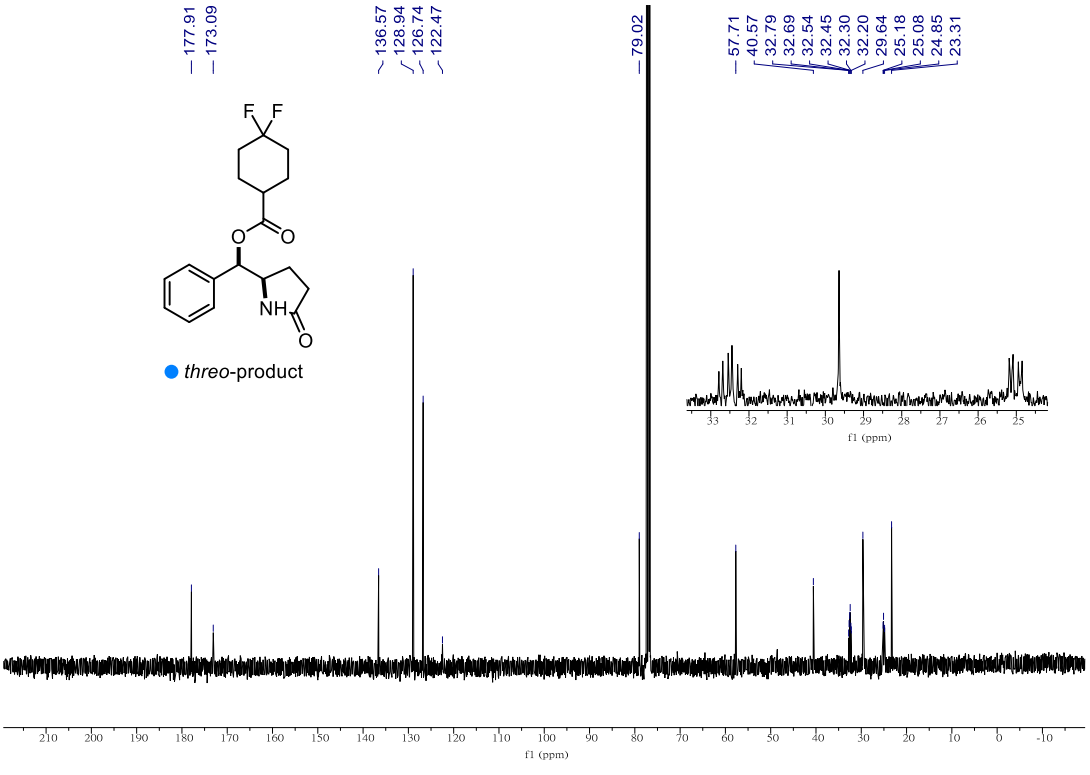


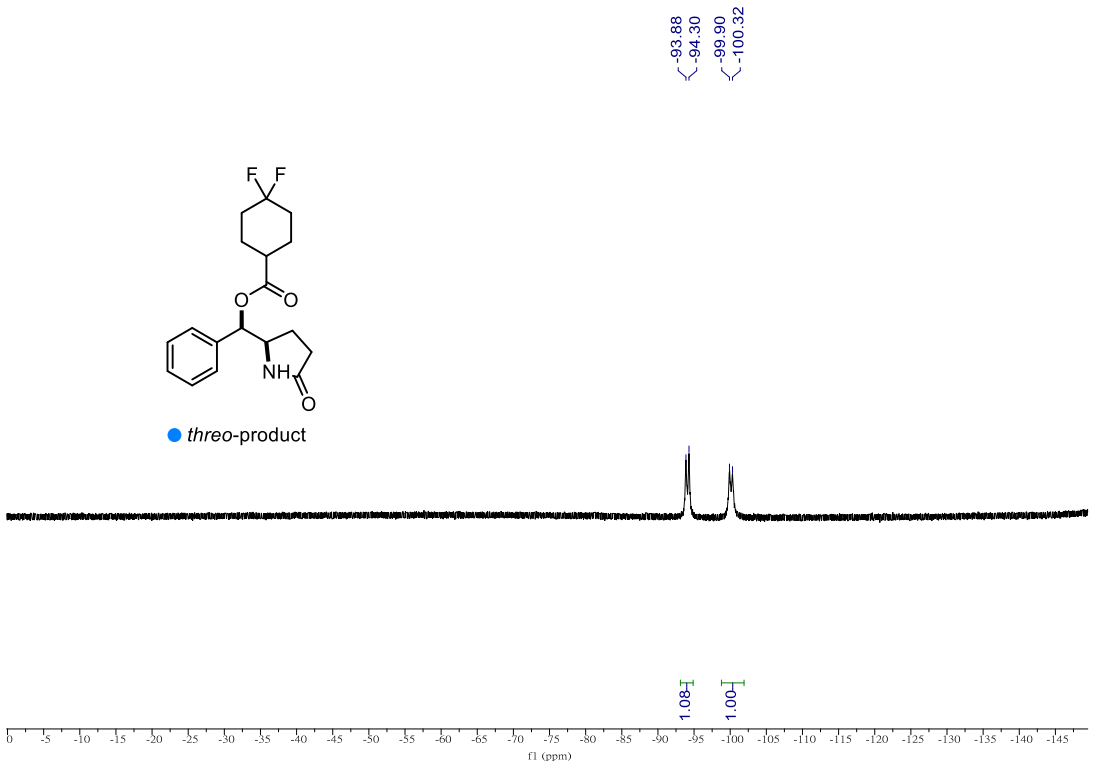




(5-Oxopyrrolidin-2-yl)(phenyl)methyl 4,4-difluorocyclohexane-1-carboxylate

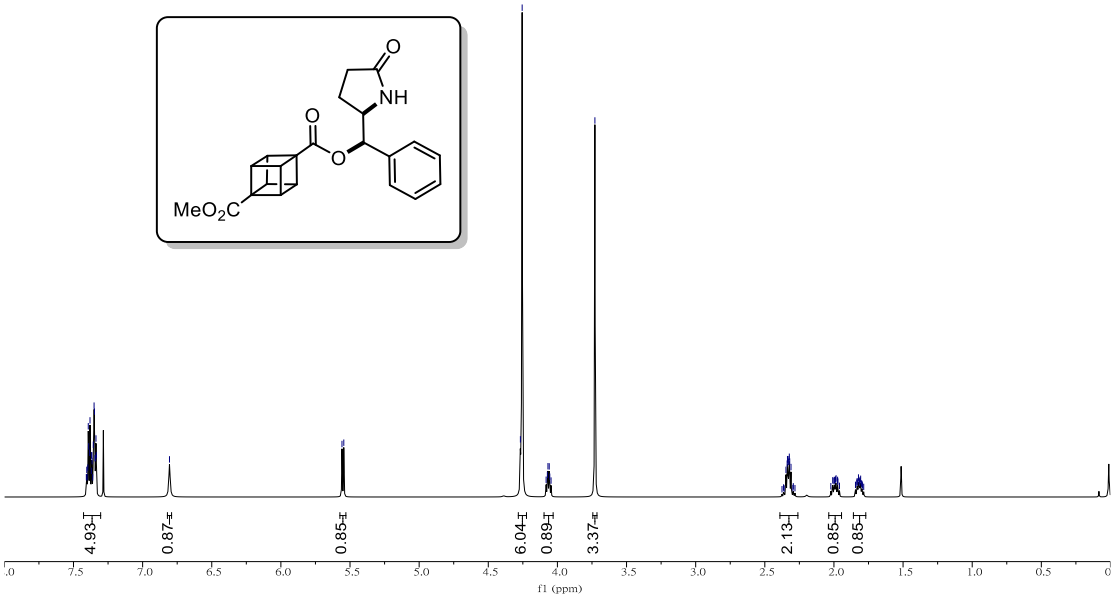




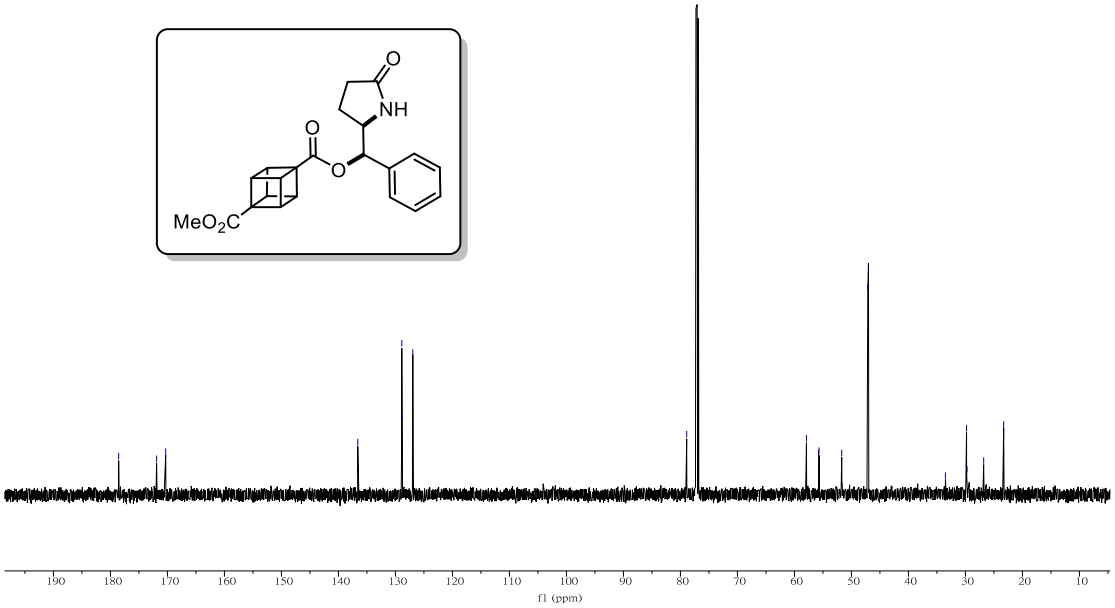

-93.88
-94.30
-99.90
-100.32
F F
O O
NH
O
threo-product
1.08
1.00
0 -5 -10 -15 -20 -25 -30 -35 -40 -45 -50 -55 -60 -65 -70 -75 -80 -85 -90 -95 -100 -105 -110 -115 -120 -125 -130 -135 -140 -145
f1 (ppm)

Methyl 4-((5-oxopyrrolidin-2-yl)(phenyl)methyl) (1r,2R,3r,8S)-cubane-1,4-dicarboxylate

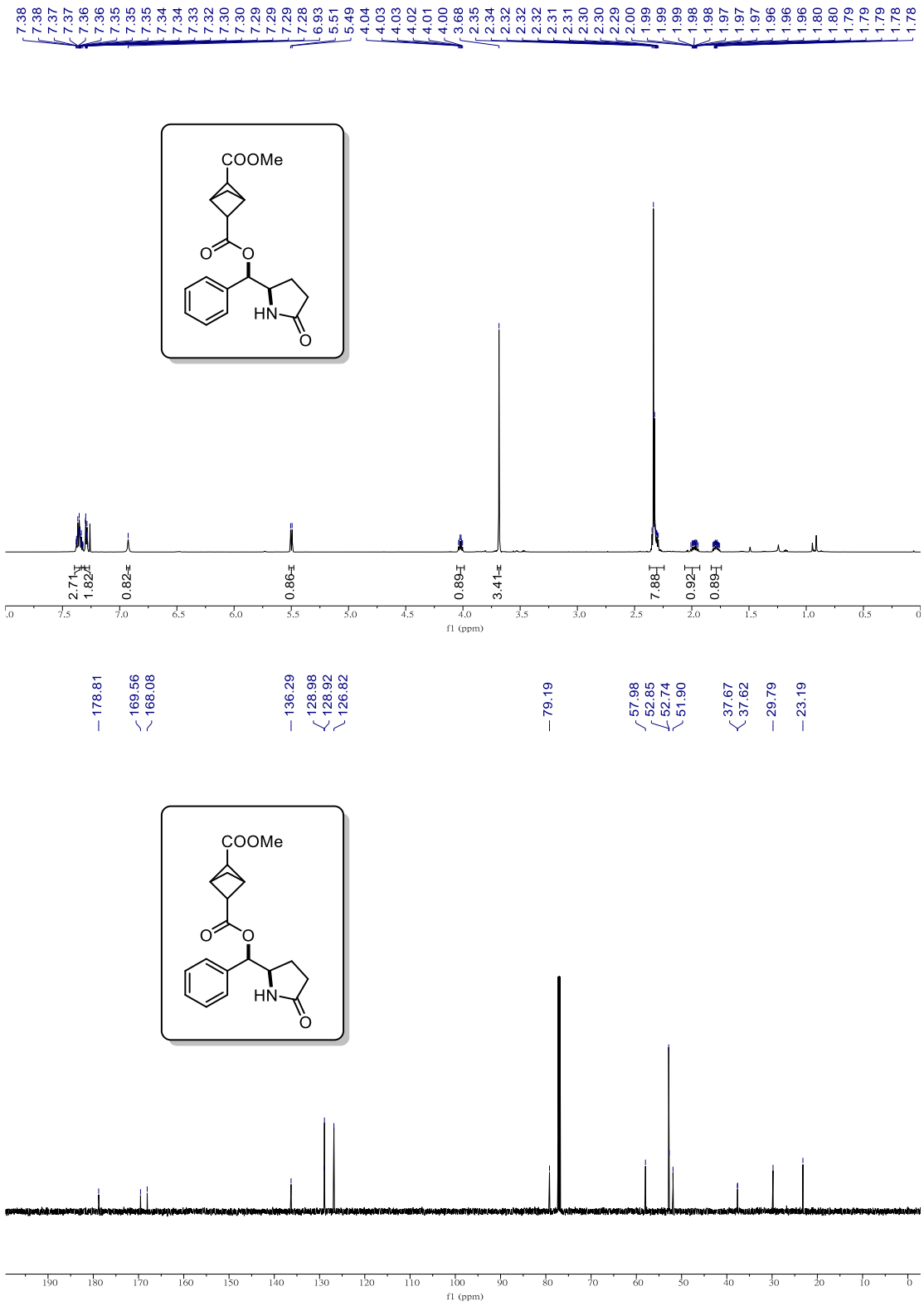






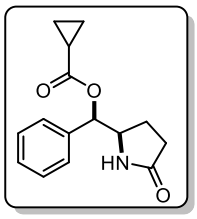


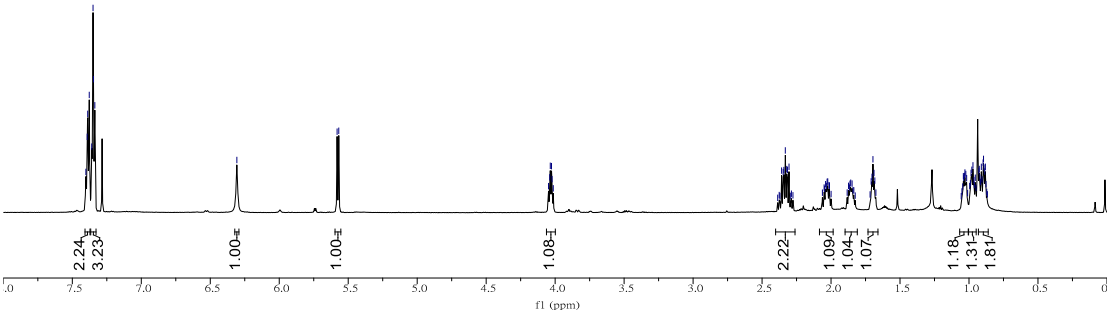
2-Methyl 4-((5-oxopyrrolidin-2-yl)(phenyl)methyl) bicyclo[1.1.1]pentane-2,4-dicarboxylate



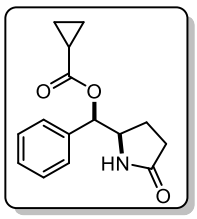
(5-Oxopyrrolidin-2-yl)(phenyl)methyl cyclopropanecarboxylate

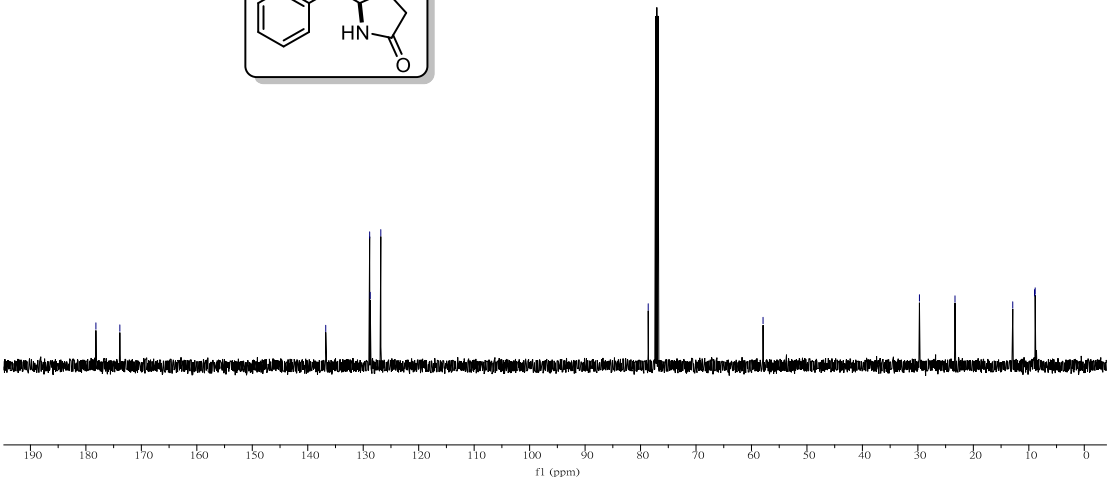




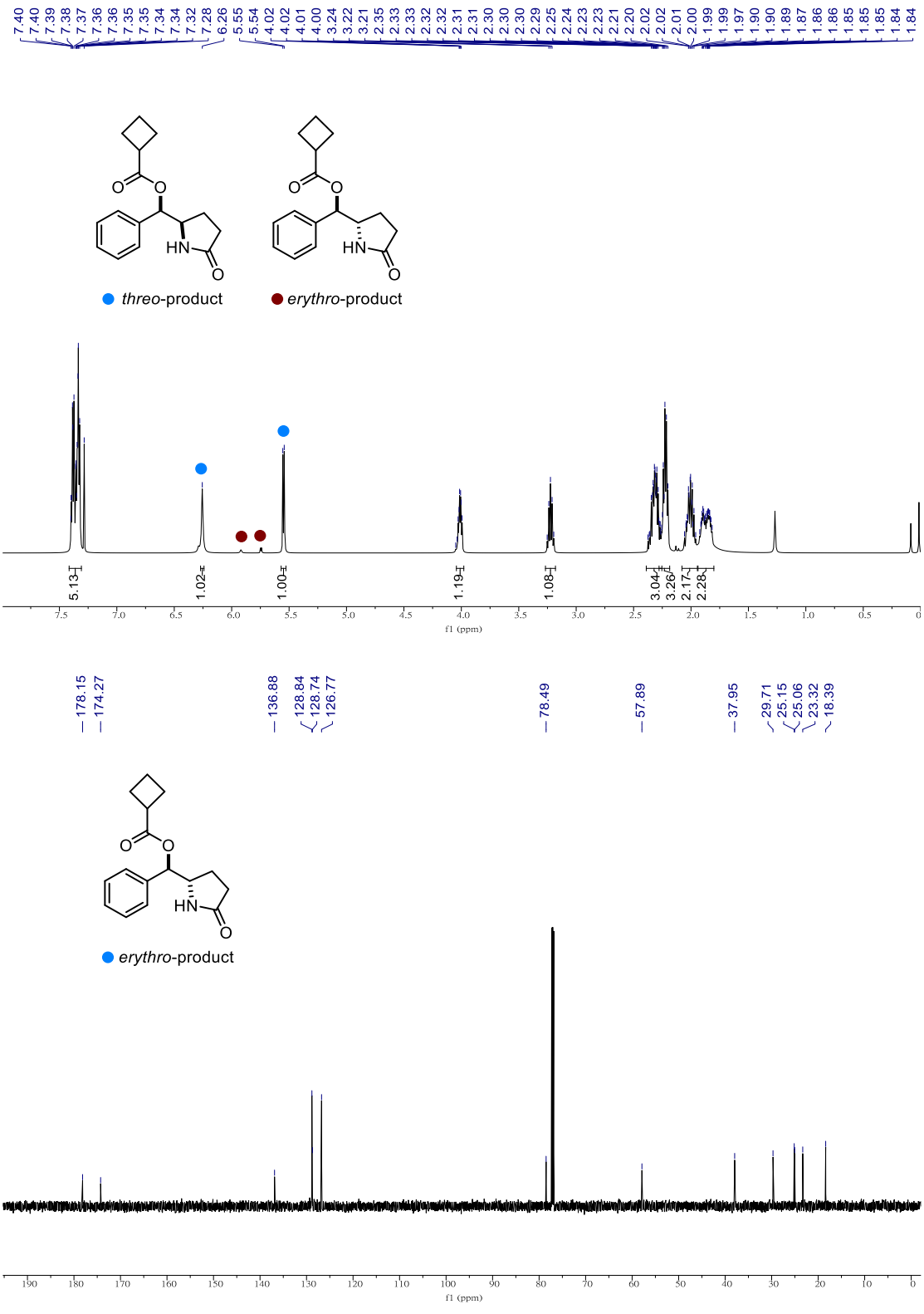




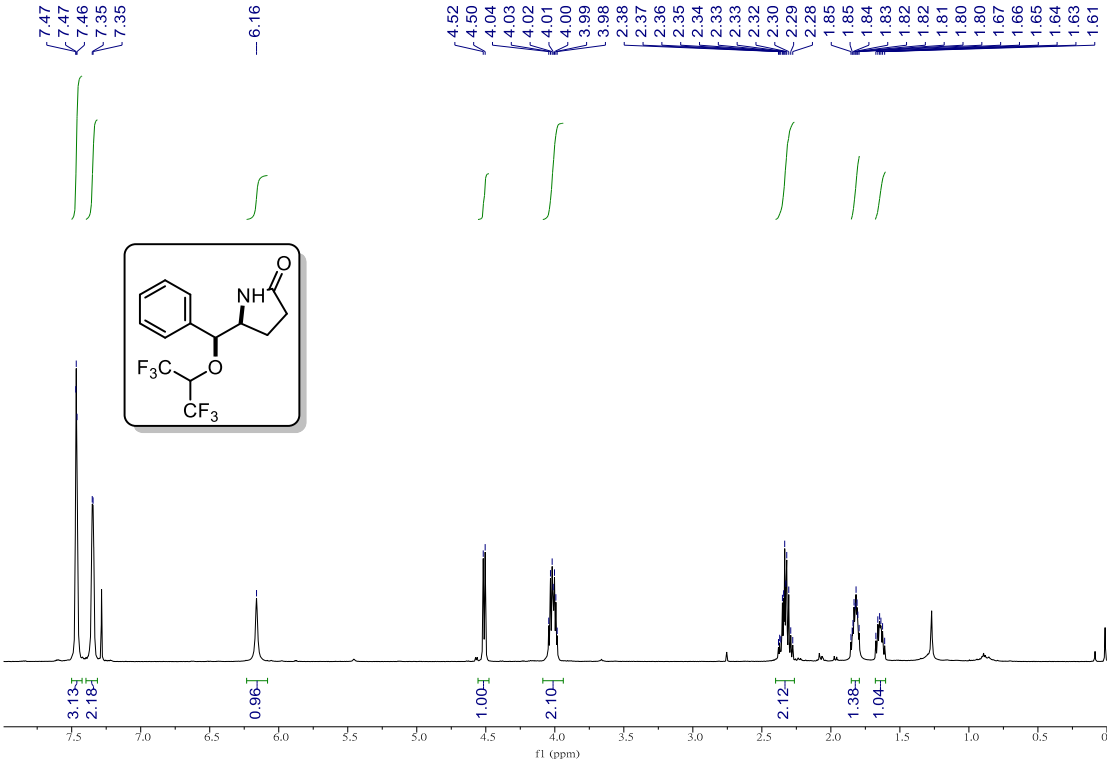


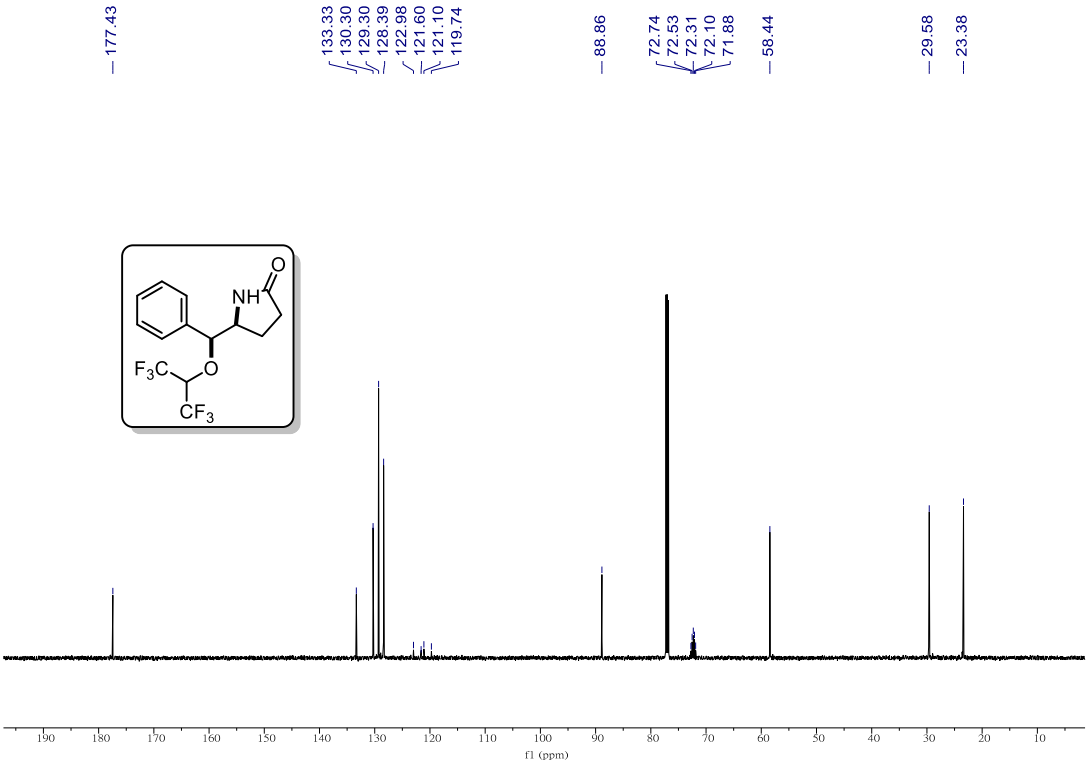


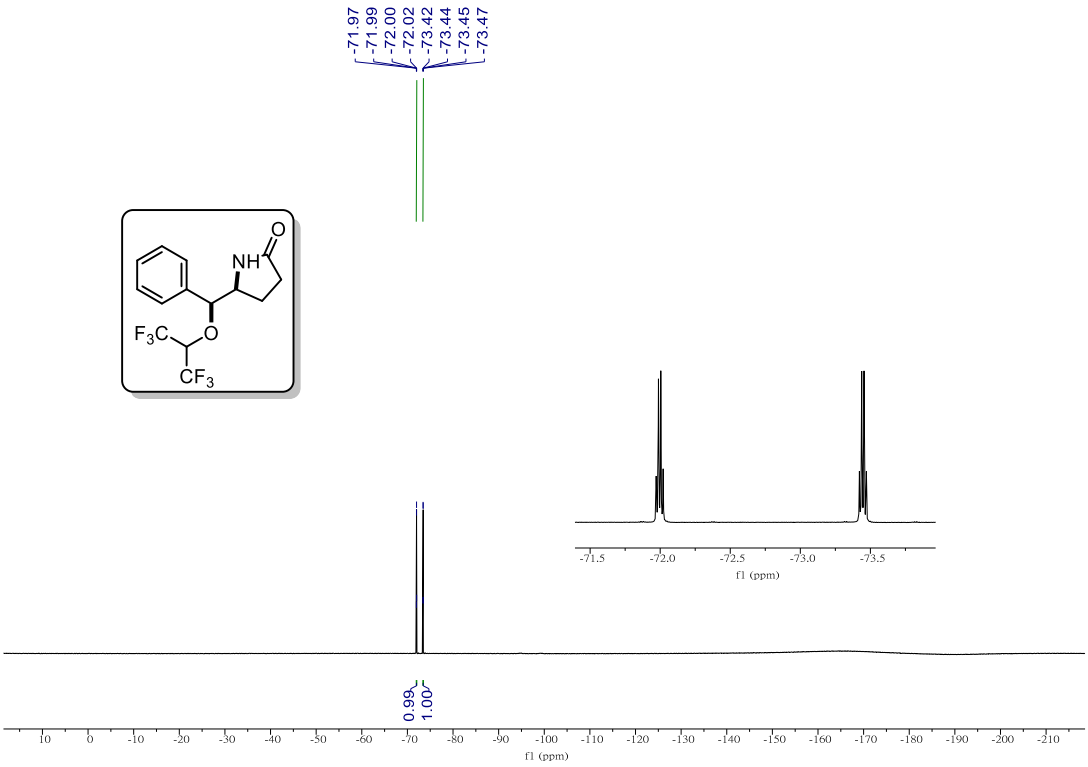
(5-Oxopyrrolidin-2-yl)(phenyl)methyl cyclobutanecarboxylate



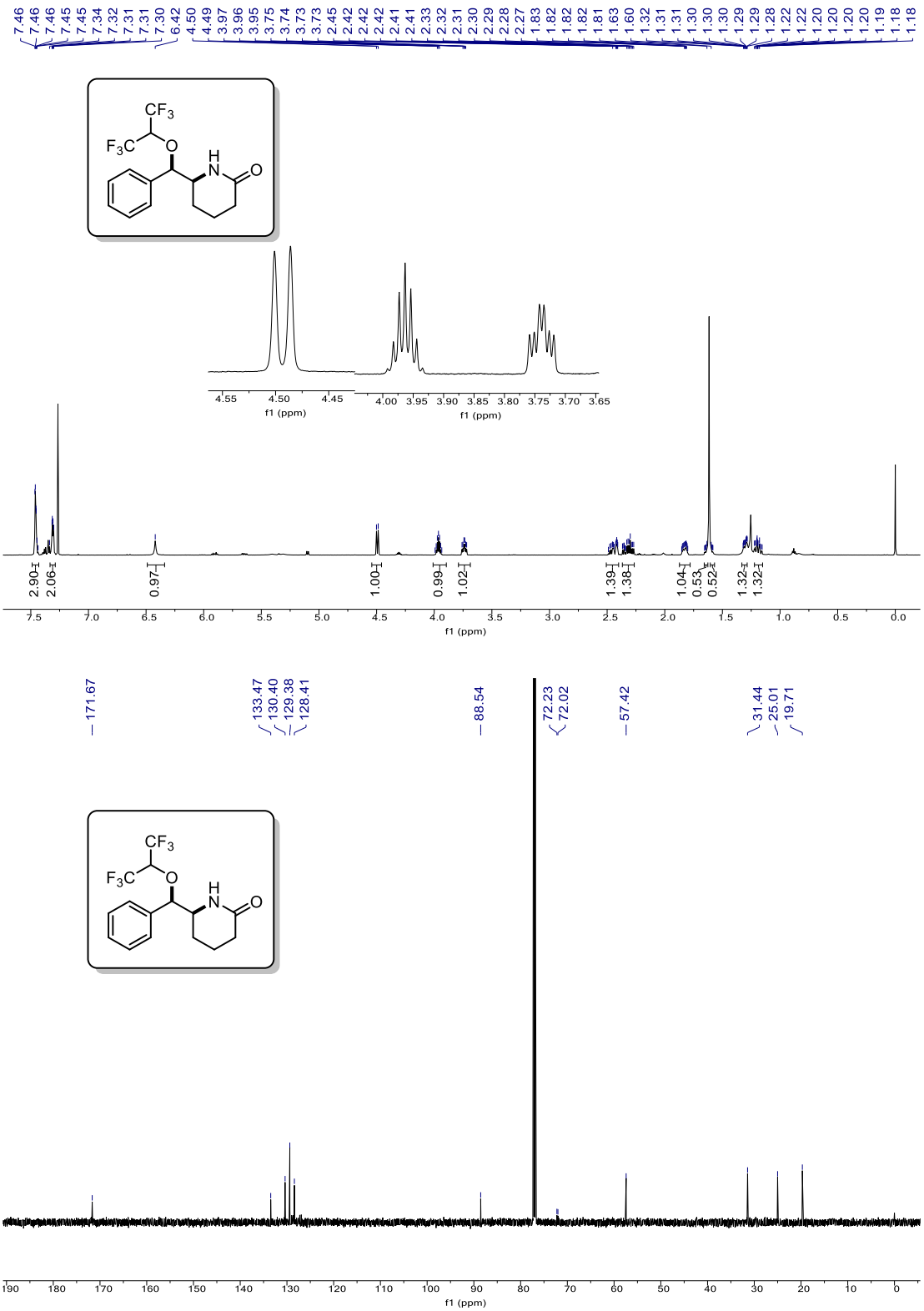
5-(((1,1,1,3,3,3-Hexafluoropropan-2-yl)oxy)(phenyl)methyl)pyrrolidin-2-one

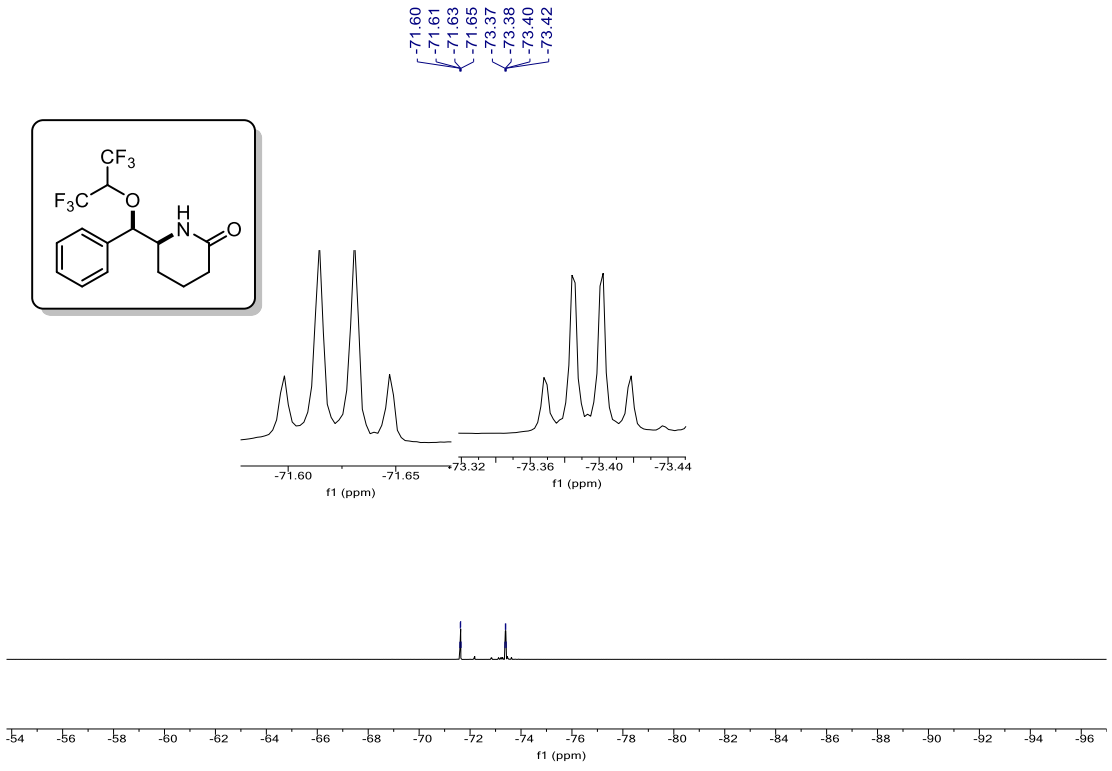




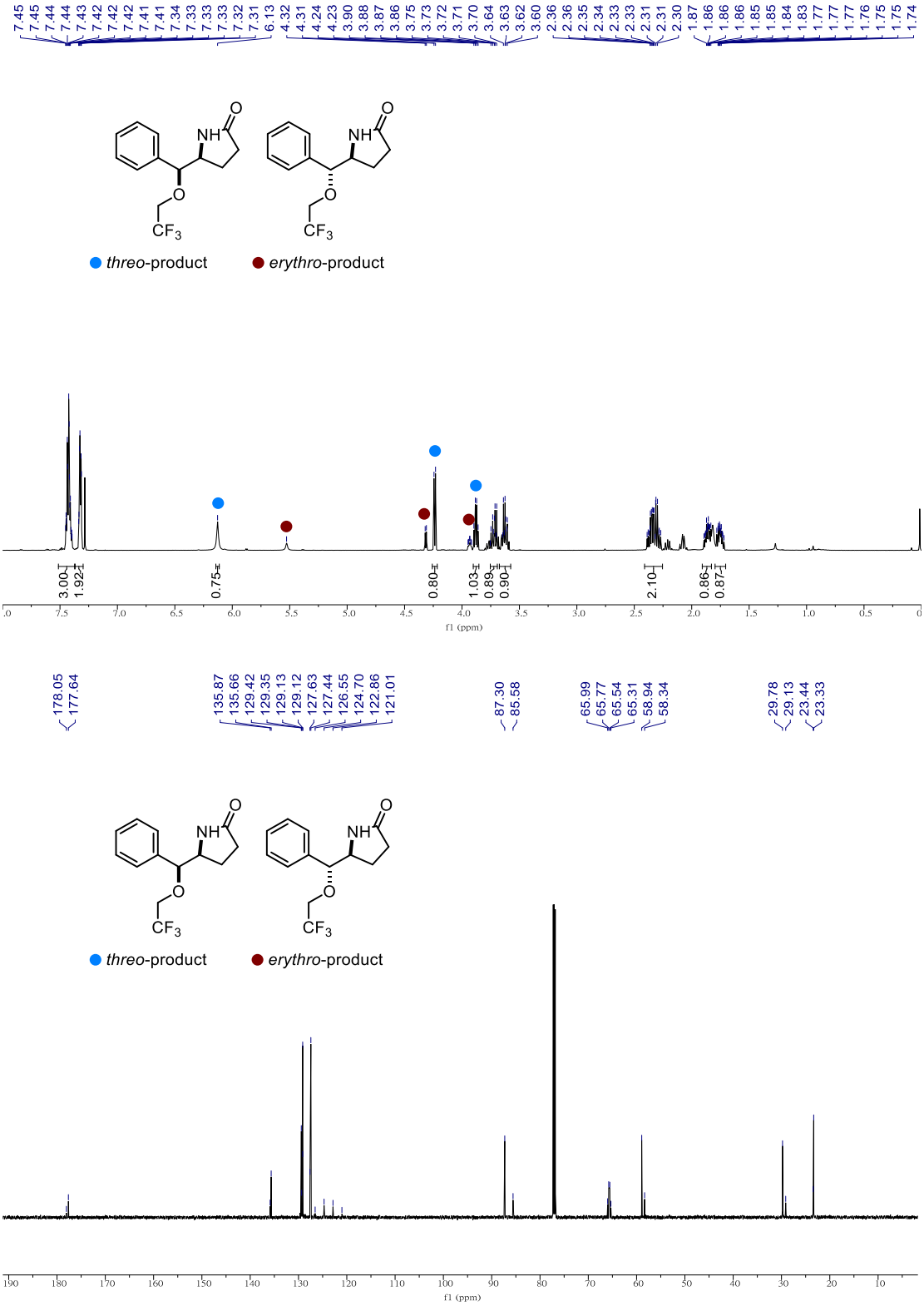

-71.97
-71.99
-72.00
-72.02
-73.42
-73.44
-73.45
-73.47
O
NH
F3C
O
CF3
-71.5
-72.0
-72.5
-73.0
-73.5
f1 (ppm)
0.99
1.00
10
0
-10
-20
-30
-40
-50
-60
-70
-80
-90
-100
-110
-120
-130
-140
-150
-160
-170
-180
-190
-200
-210
f1 (ppm)

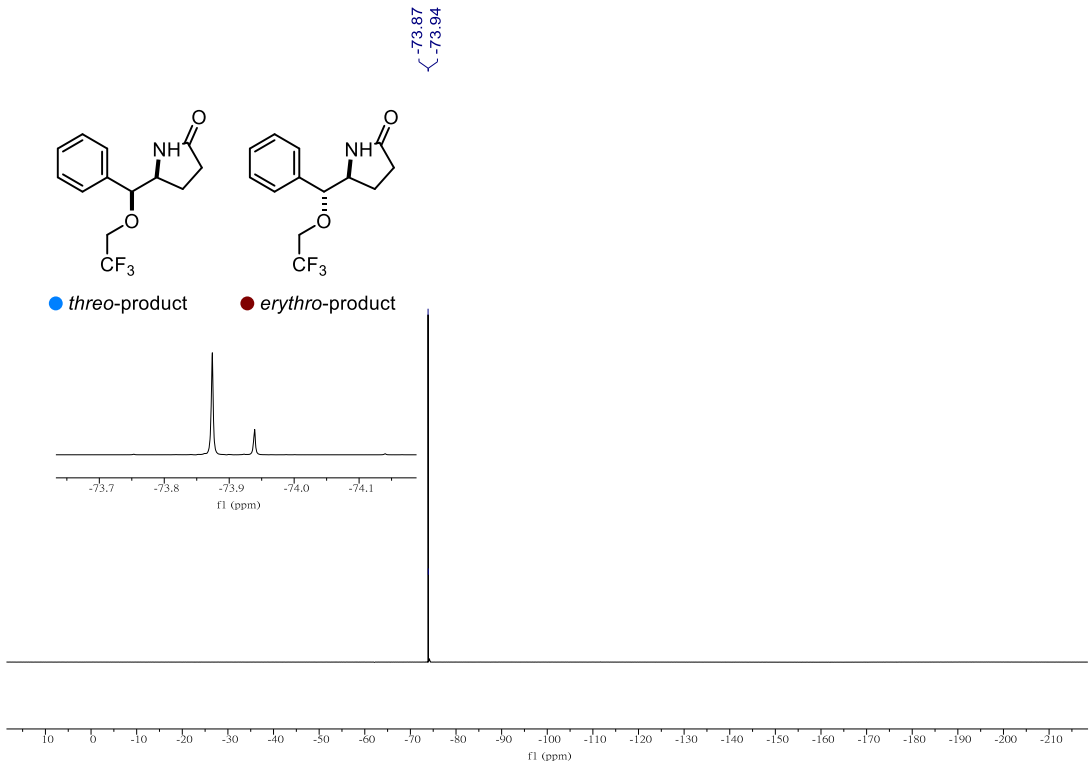
6-(((1,1,1,3,3,3-Hexafluoropropan-2-yl)oxy)(phenyl)methyl)piperidin-2-one



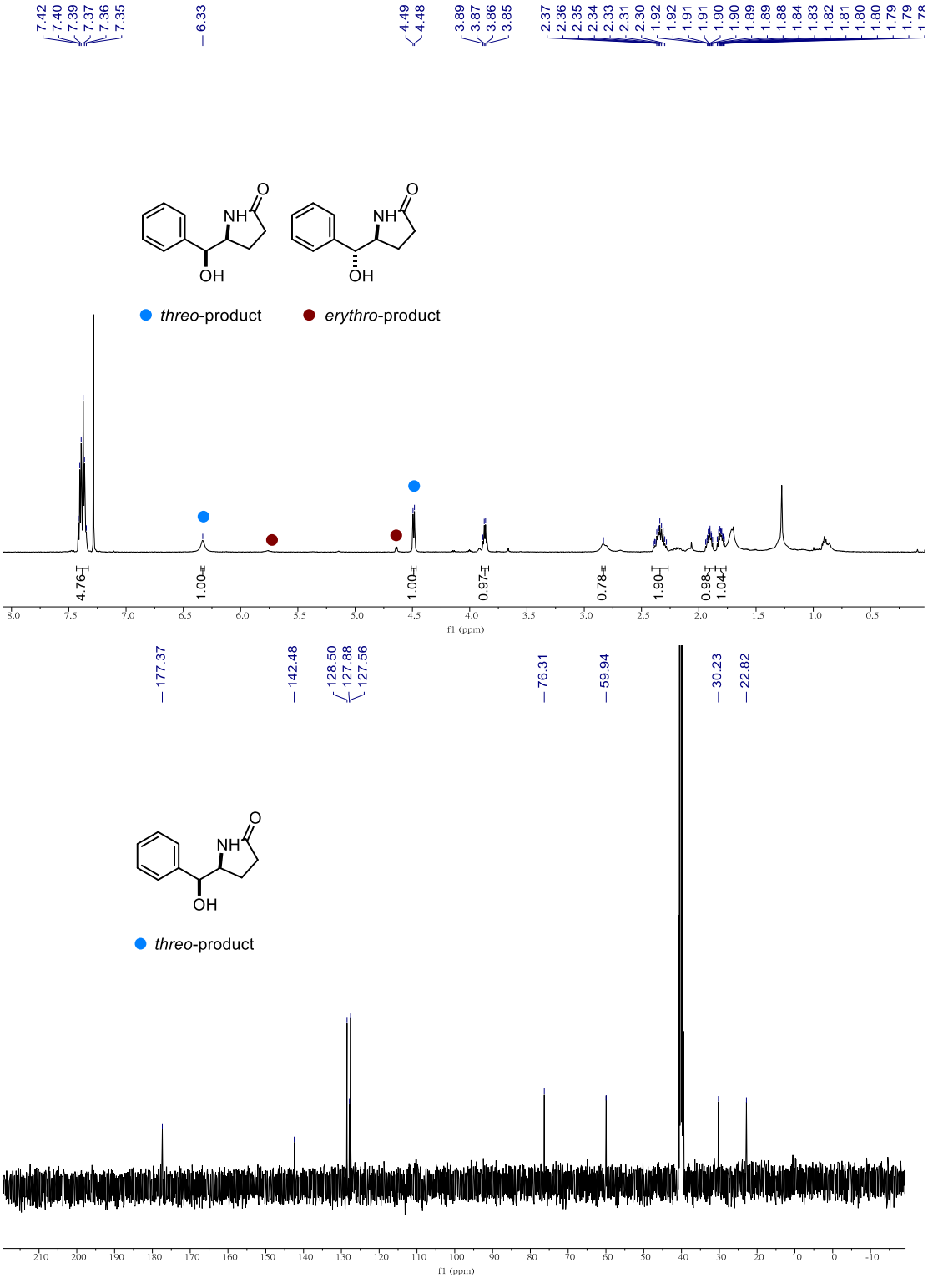

-71.60
-71.61
-71.63
-71.65
-73.37
-73.38
-73.40
-73.42
CF3
F3C
O
H
N
O
-71.60
-71.65
f1 (ppm)
-73.32
-73.36
-73.40
-73.44
f1 (ppm)
-54
-56
-58
-60
-62
-64
-66
-68
-70
-72
-74
-76
-78
-80
-82
-84
-86
-88
-90
-92
-94
-96
f1 (ppm)

5-(Phenyl(2,2,2-trifluoroethoxy)methyl)pyrrolidin-2-one

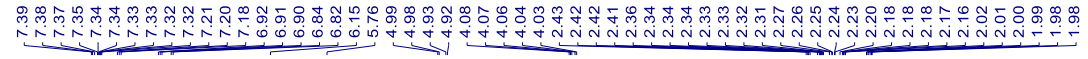


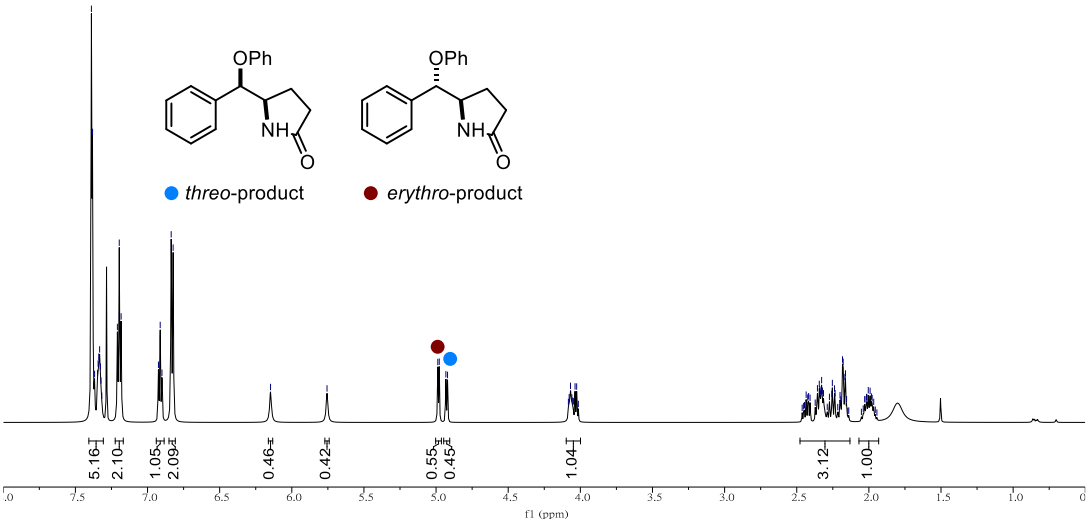

-73.87
-73.94
NH
O
O
CF3
NH
O
O
CF3
threo-product
erythro-product
-73.7
-73.8
-73.9
-74.0
-74.1
f1 (ppm)
10
0
-10
-20
-30
-40
-50
-60
-70
-80
-90
-100
-110
-120
-130
-140
-150
-160
-170
-180
-190
-200
-210
f1 (ppm)

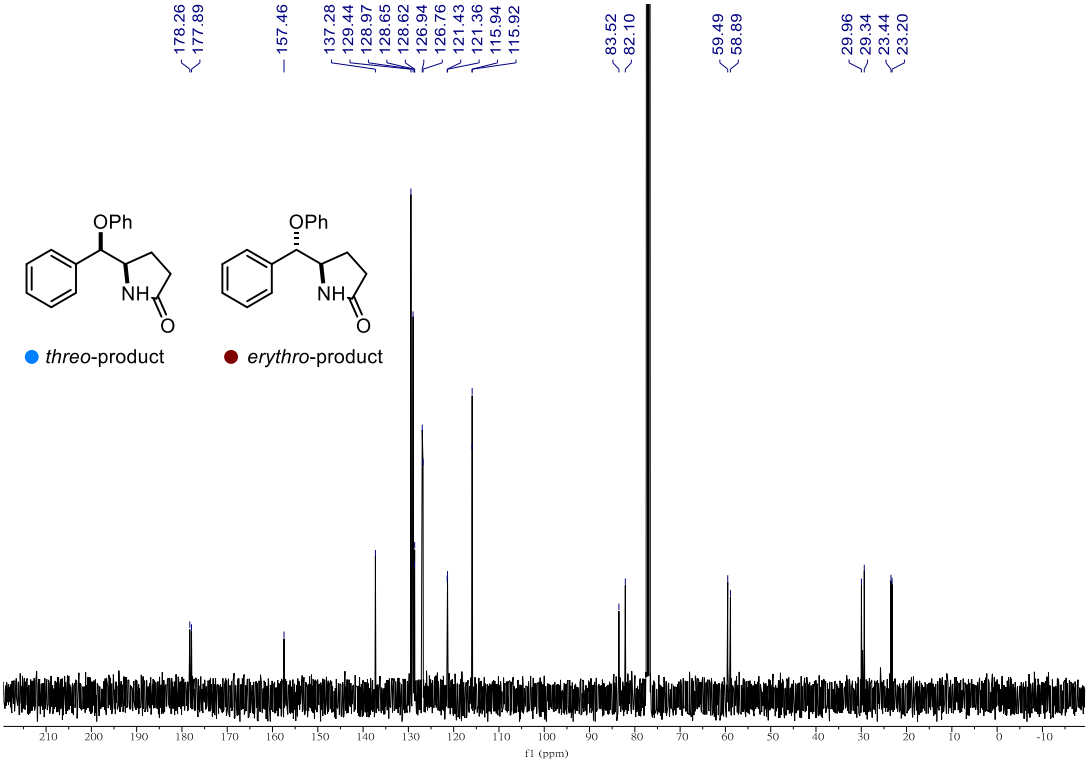
5-(Hydroxy(phenyl)methyl)pyrrolidin-2-one



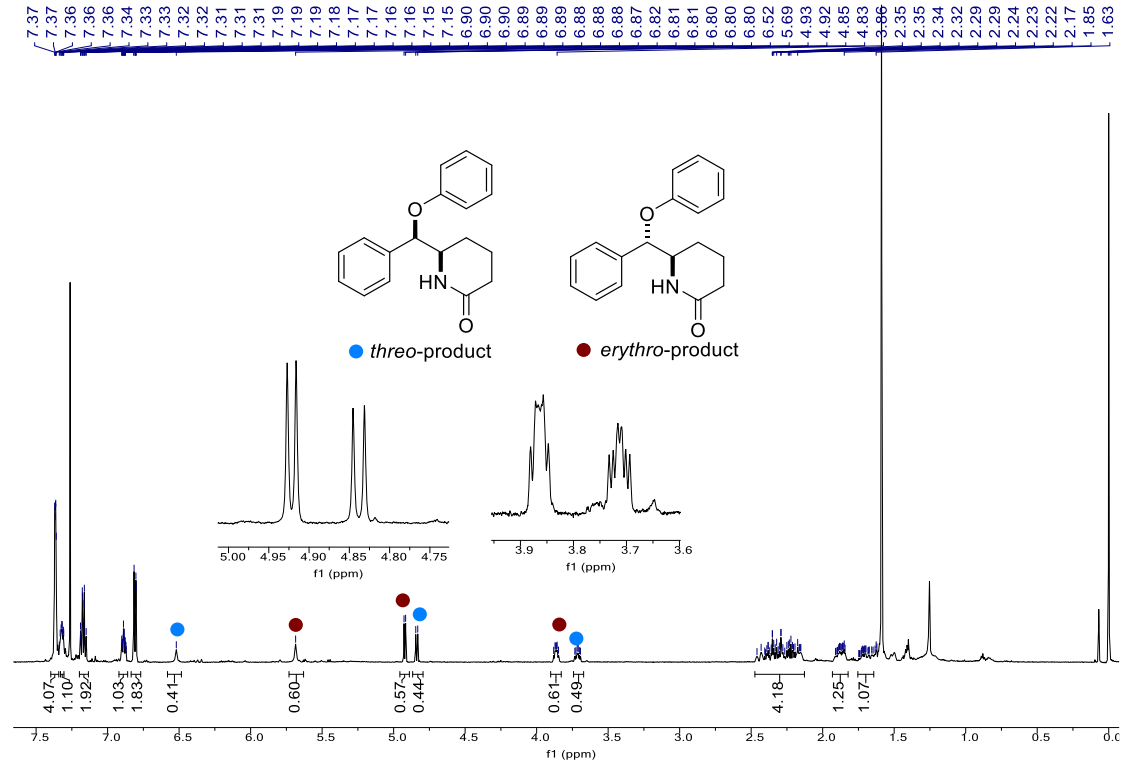
5-(Phenoxy(phenyl)methyl)pyrrolidin-2-one

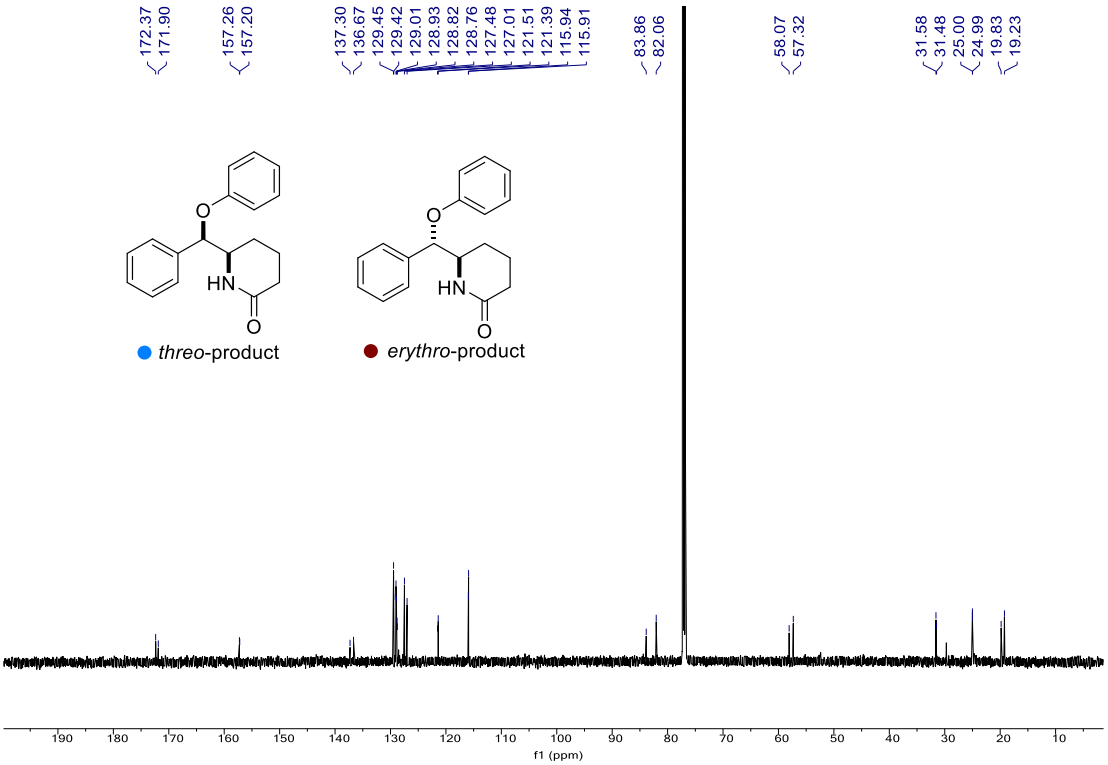






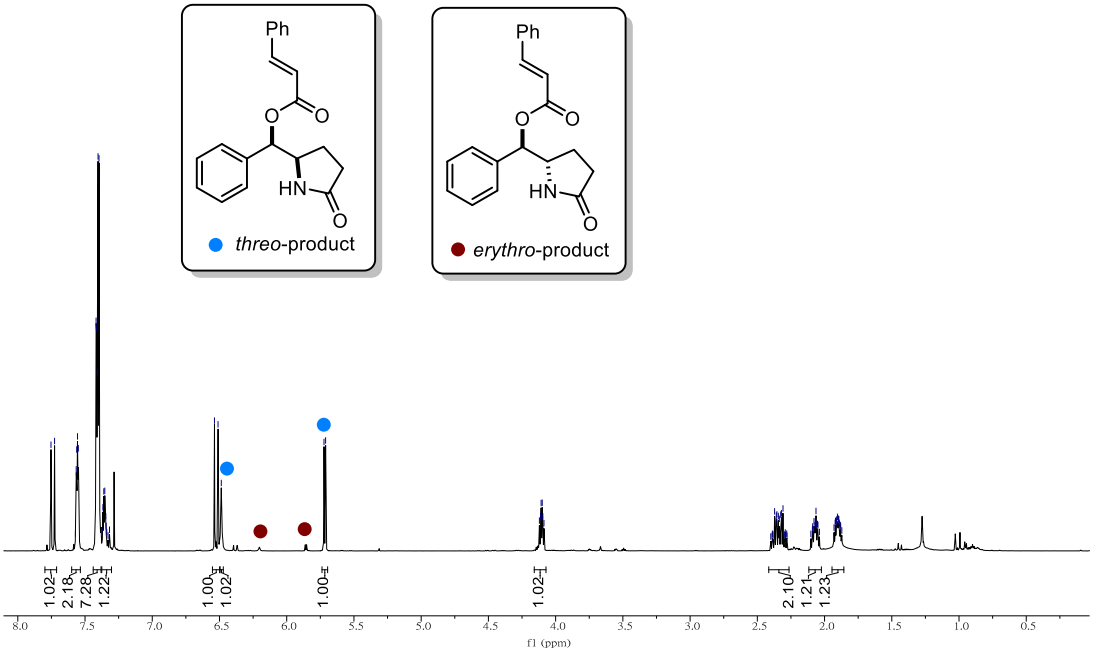
6-(Phenoxy(phenyl)methyl)piperidin-2-one



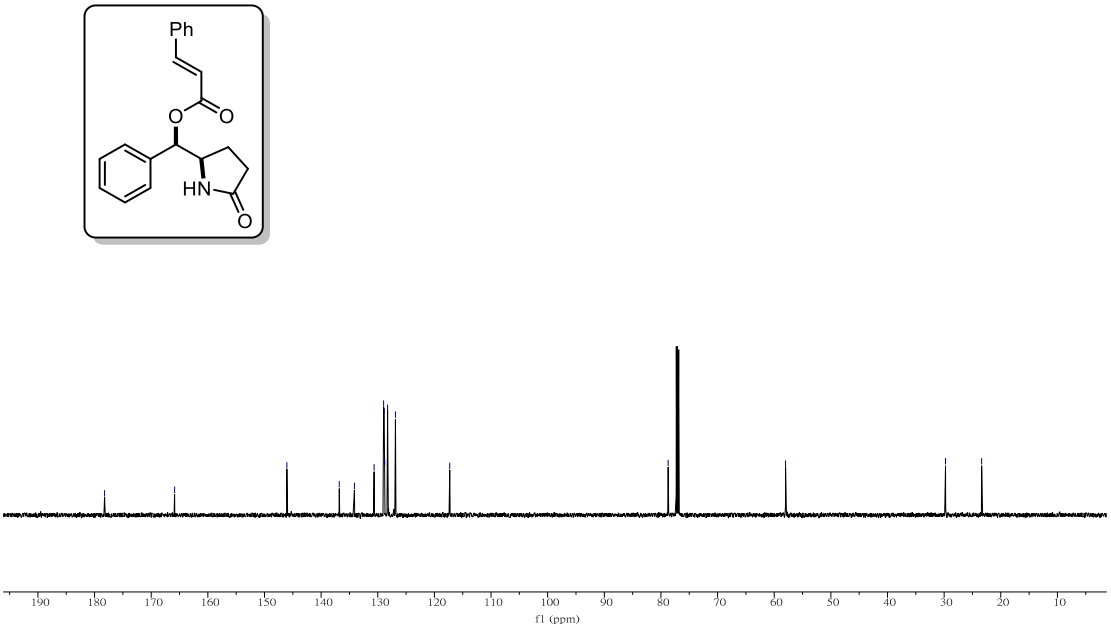


(5-Oxopyrrolidin-2-yl)(phenyl)methyl cinnamate

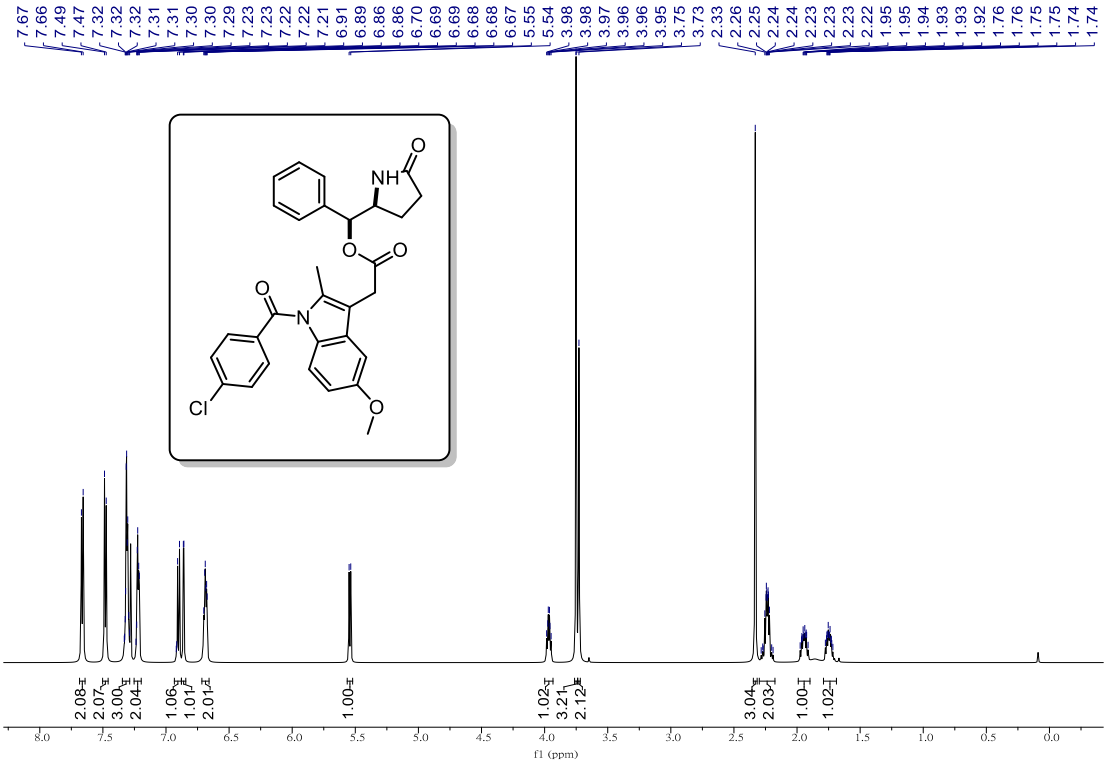


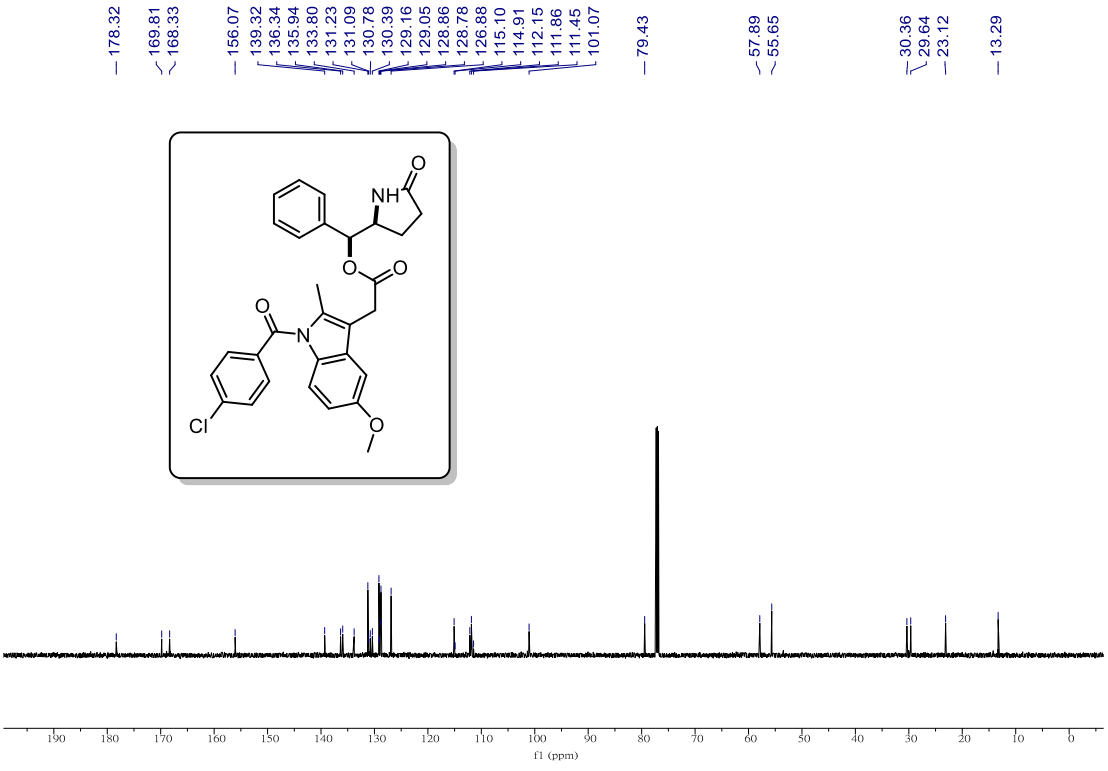




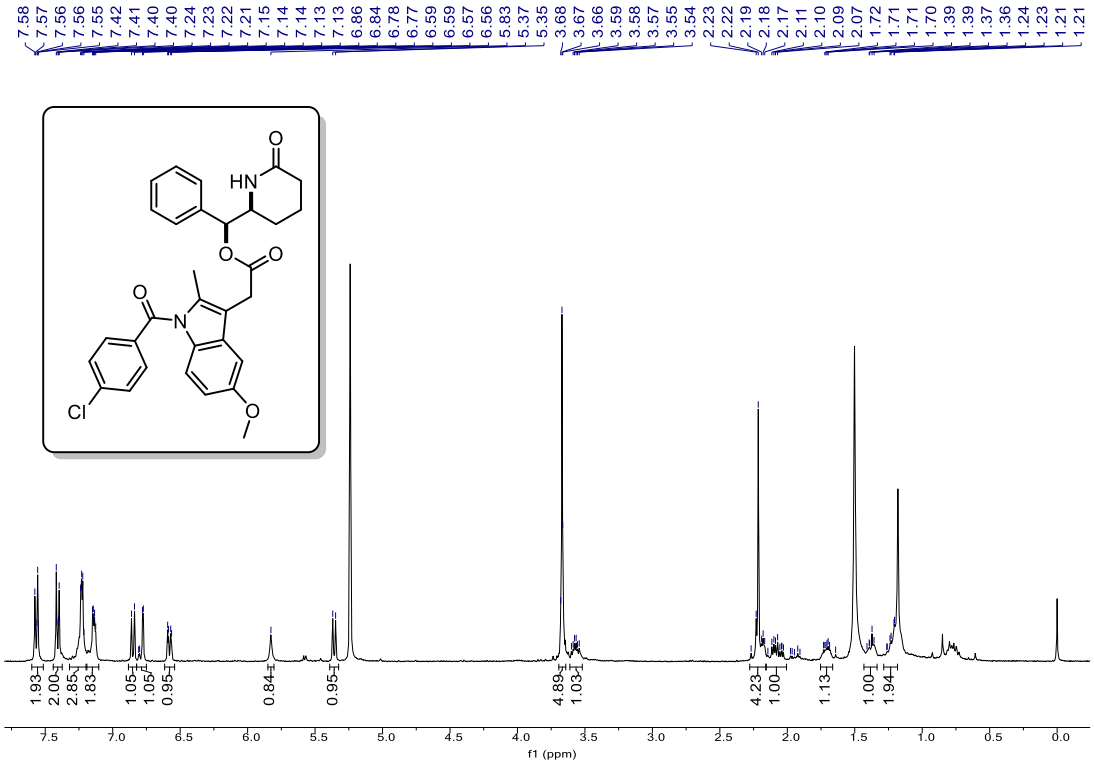


(5-Oxopyrrolidin-2-yl)(phenyl)methyl 2-(1-(4-chlorobenzoyl)-5-methoxy-2-methyl-1H-indol-3-yl)acetate

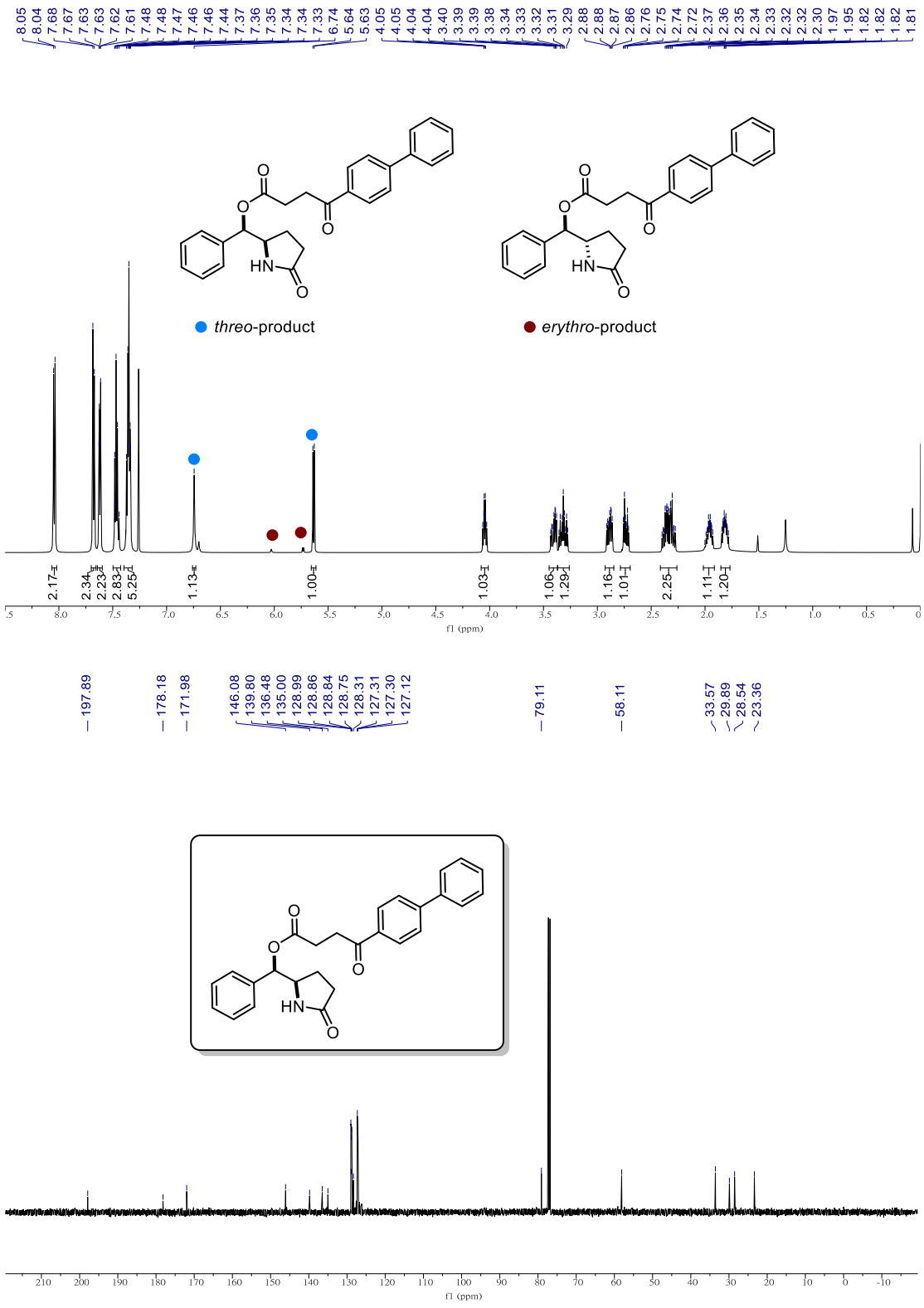




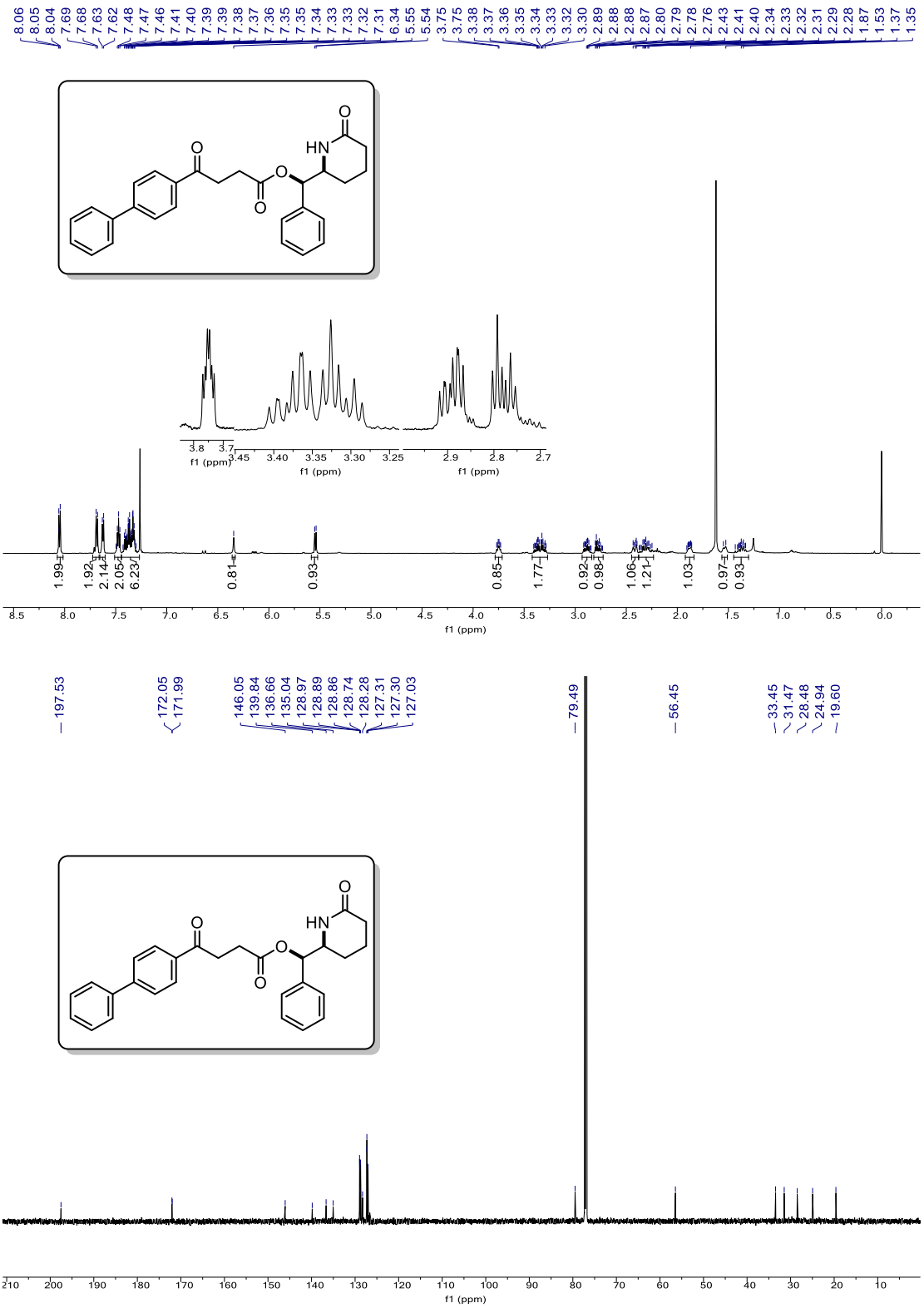
(6-Oxopiperidin-2-yl)(phenyl)methyl 2-(1-(4-chlorobenzoyl)-5-methoxy-2-methyl-1H-indol-3-yl)acetate



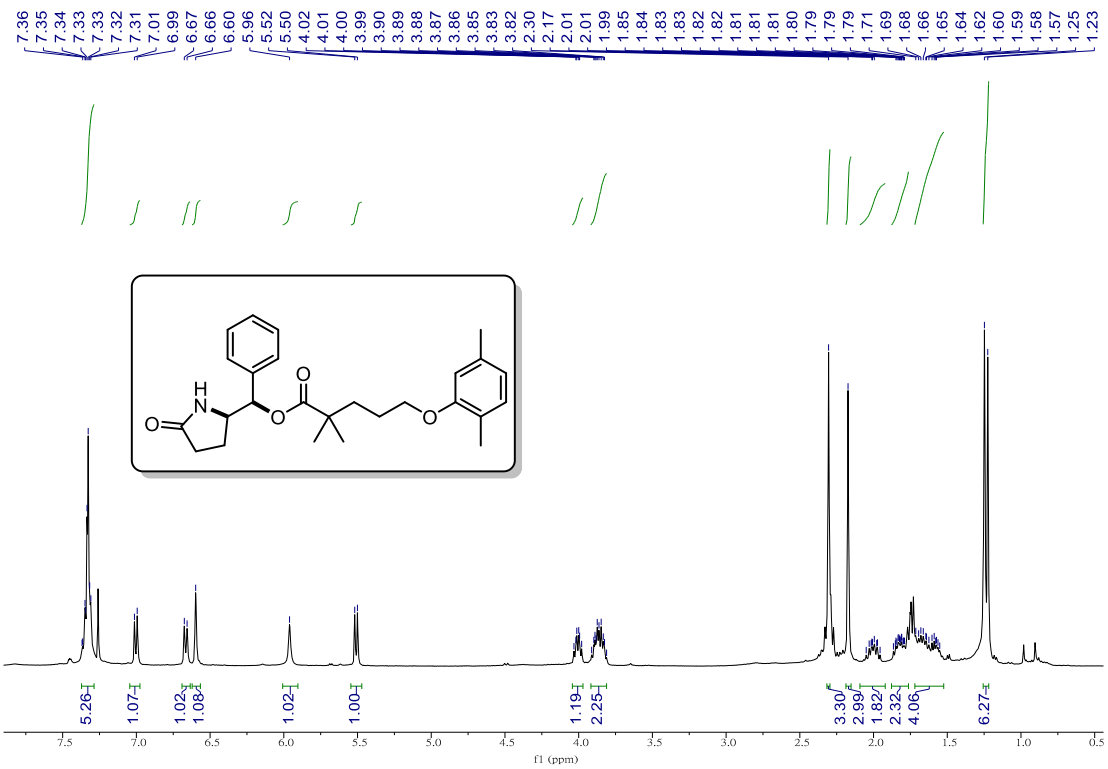
(5-Oxopyrrolidin-2-yl)(phenyl)methyl 4-([1,1'-biphenyl]-4-yl)-4-oxobutanoate

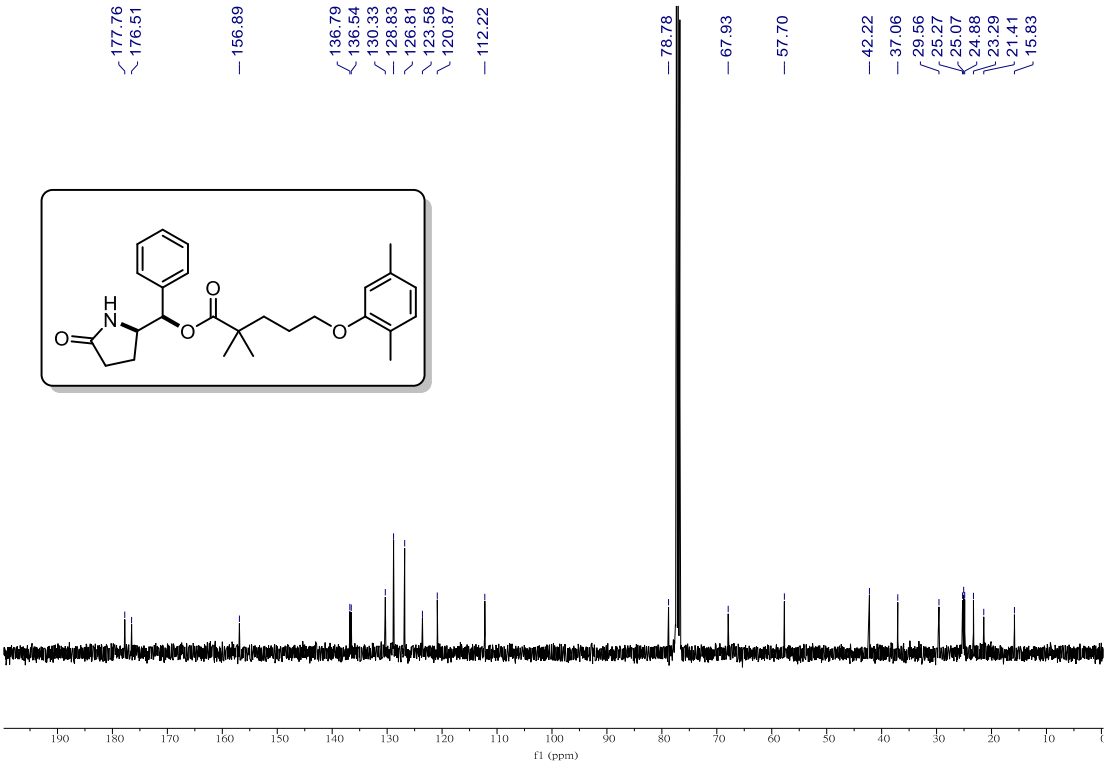


6-Oxopiperidin-2-yl)(phenyl)methyl 4-([1,1'-biphenyl]-4-yl)-4-oxobutanoate



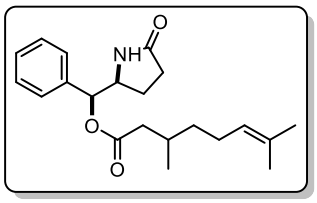
(5-Oxopyrrolidin-2-yl)(phenyl)methyl 5-(2,5-dimethylphenoxy)-2,2-dimethylpentanoate

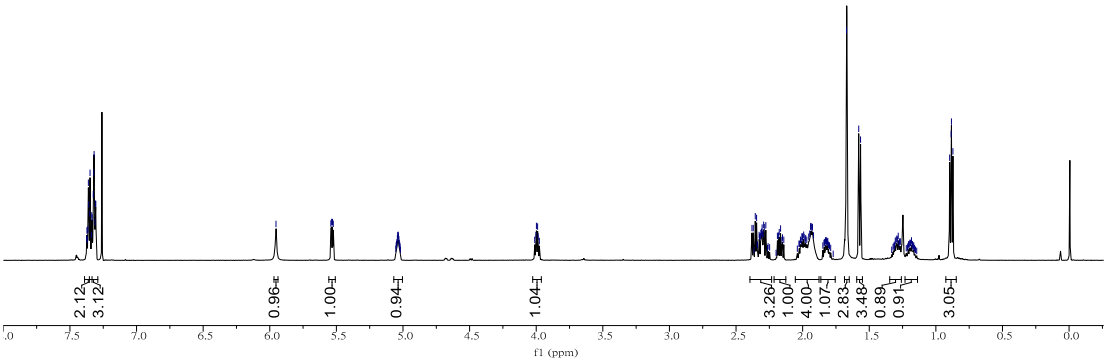


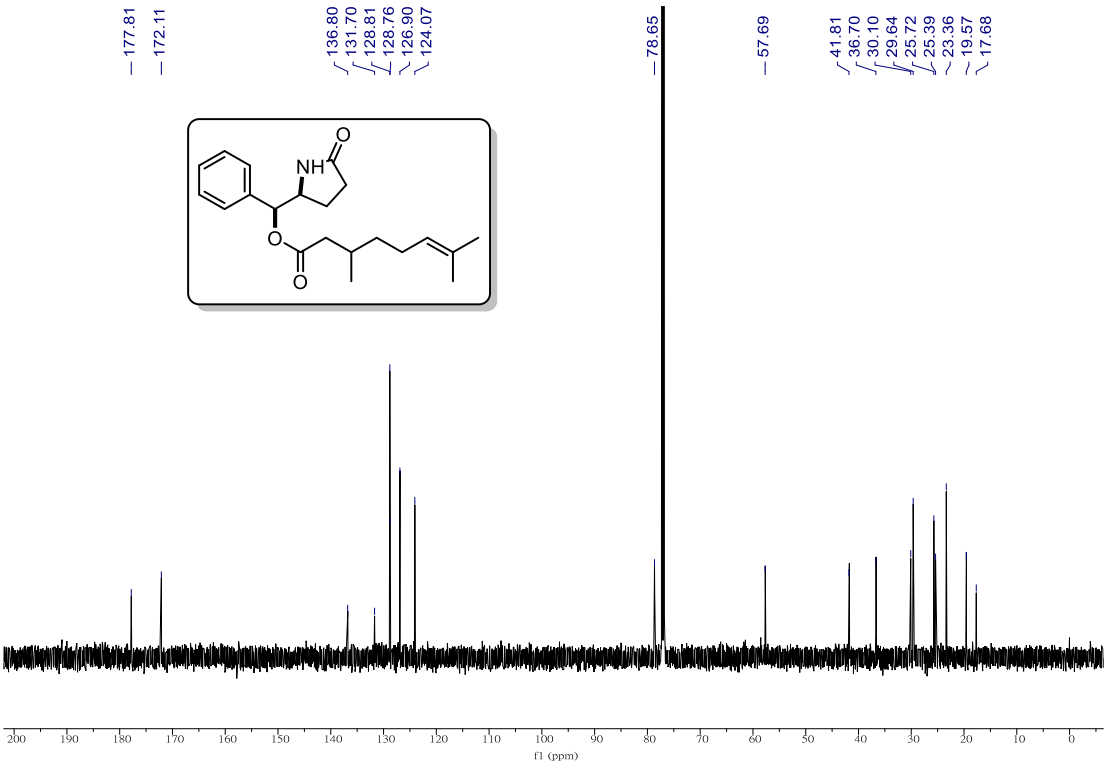


(5-Oxopyrrolidin-2-yl)(phenyl)methyl 3,7-dimethyloct-6-enoate

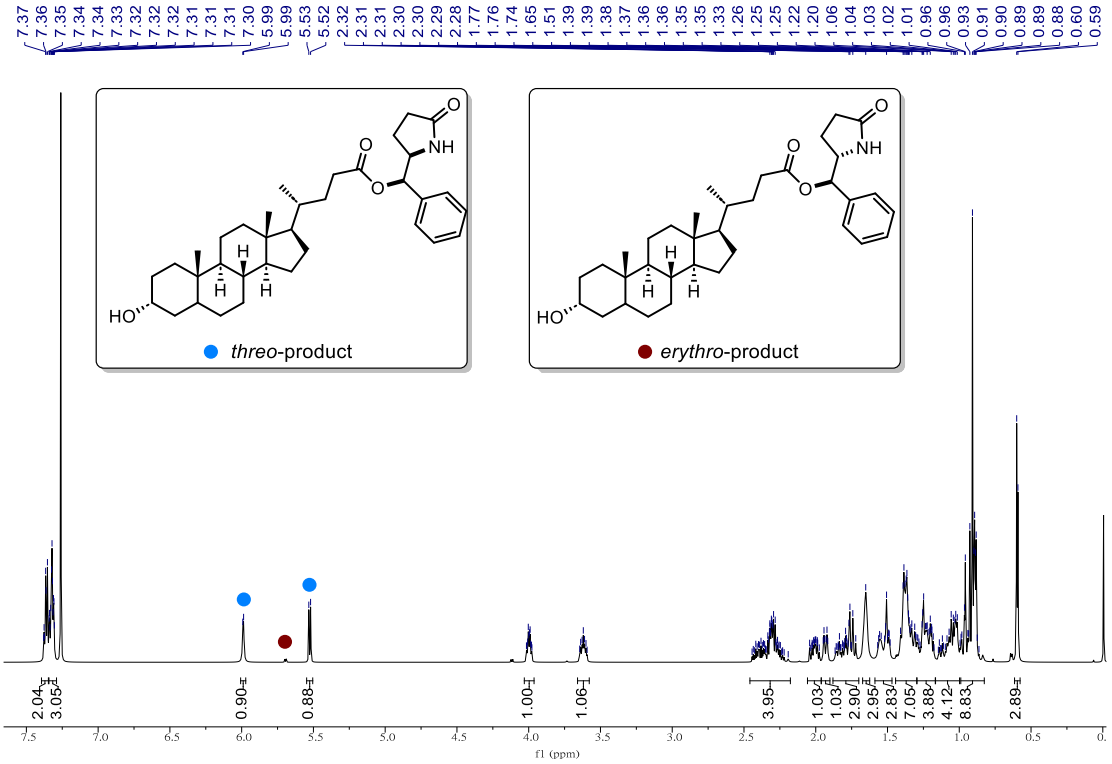


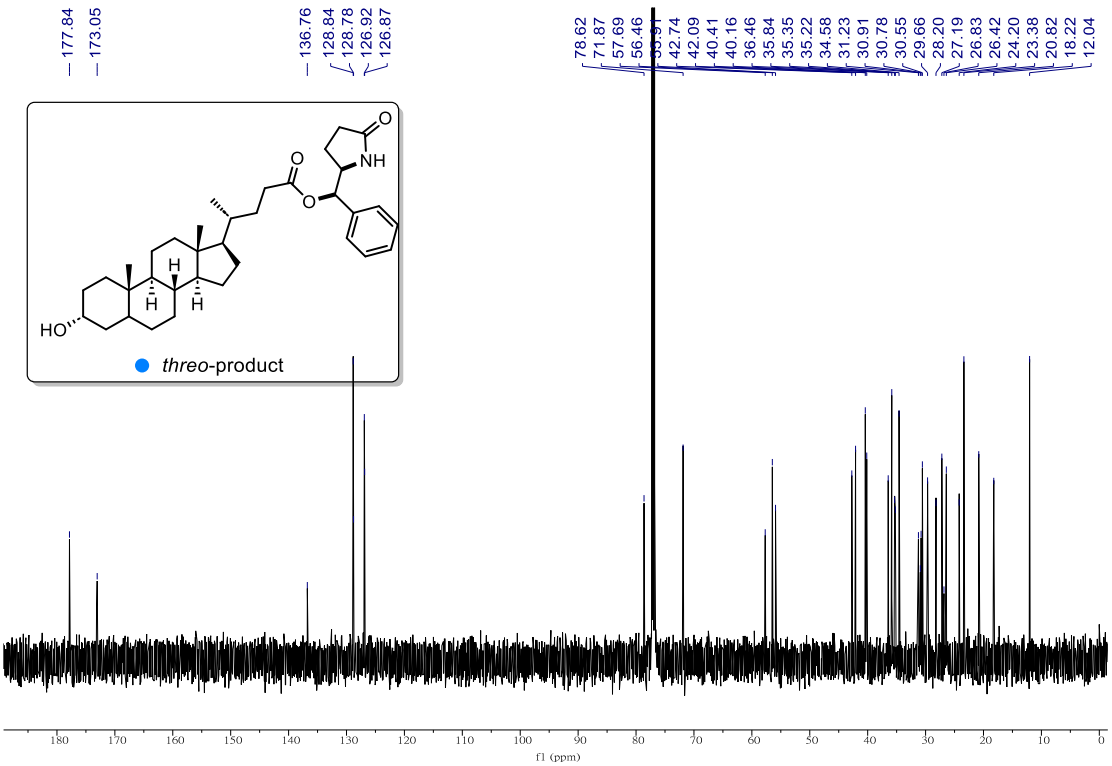




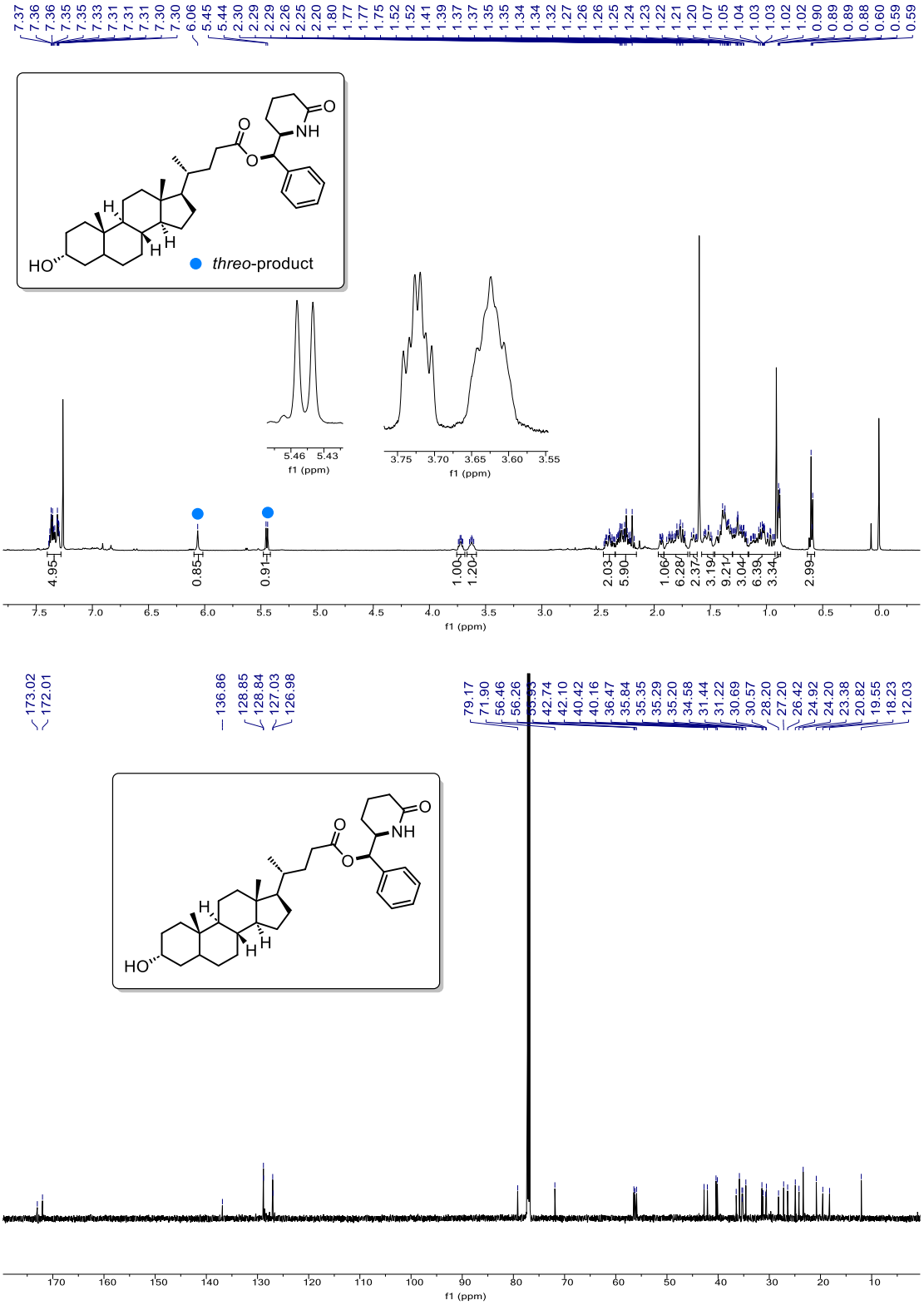


(5-Oxopyrrolidin-2-yl)(phenyl)methyl (4R)-4-((3R,8R,9S,10S,13R,14S,17R)-3-hydroxy-10,13-dimethylhexadecahydro-1H-cyclopenta[a]phenanthren-17-yl)pentanoate

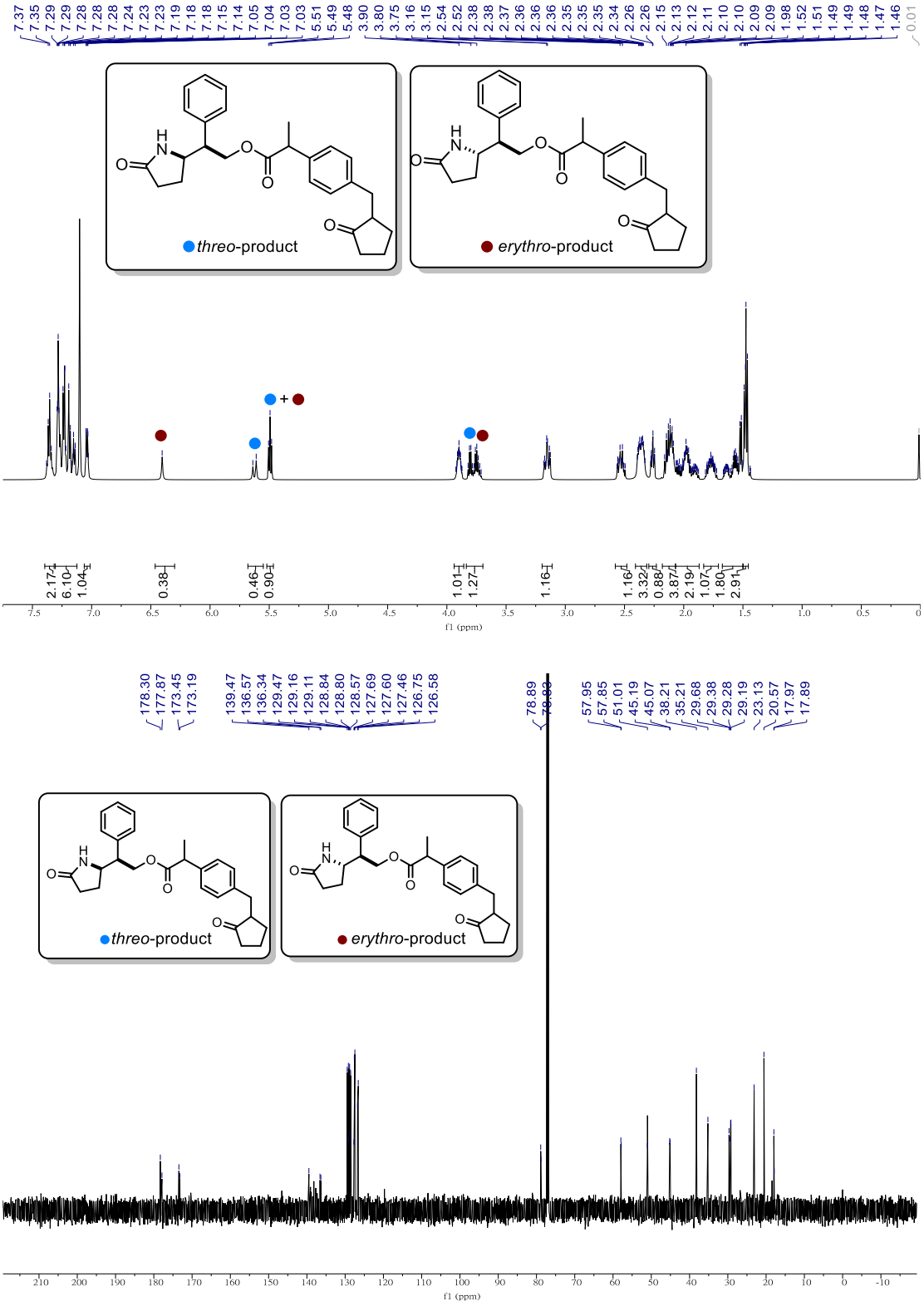




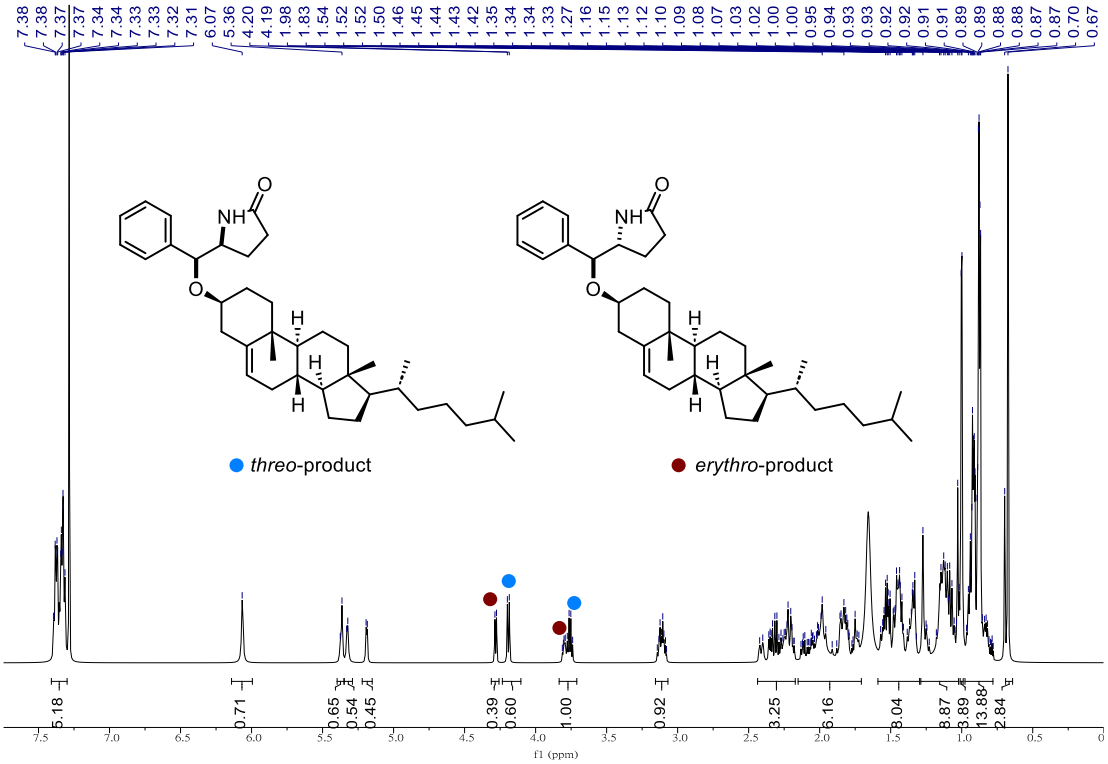
(6-Oxopiperidin-2-yl)(phenyl)methyl (4R)-4-((3R,8R,9S,10S,13R,14S,17R)-3-hydroxy-10,13-dimethylhexadecahydro-1H-cyclopenta[a]phenanthren-17-yl)pentanoate

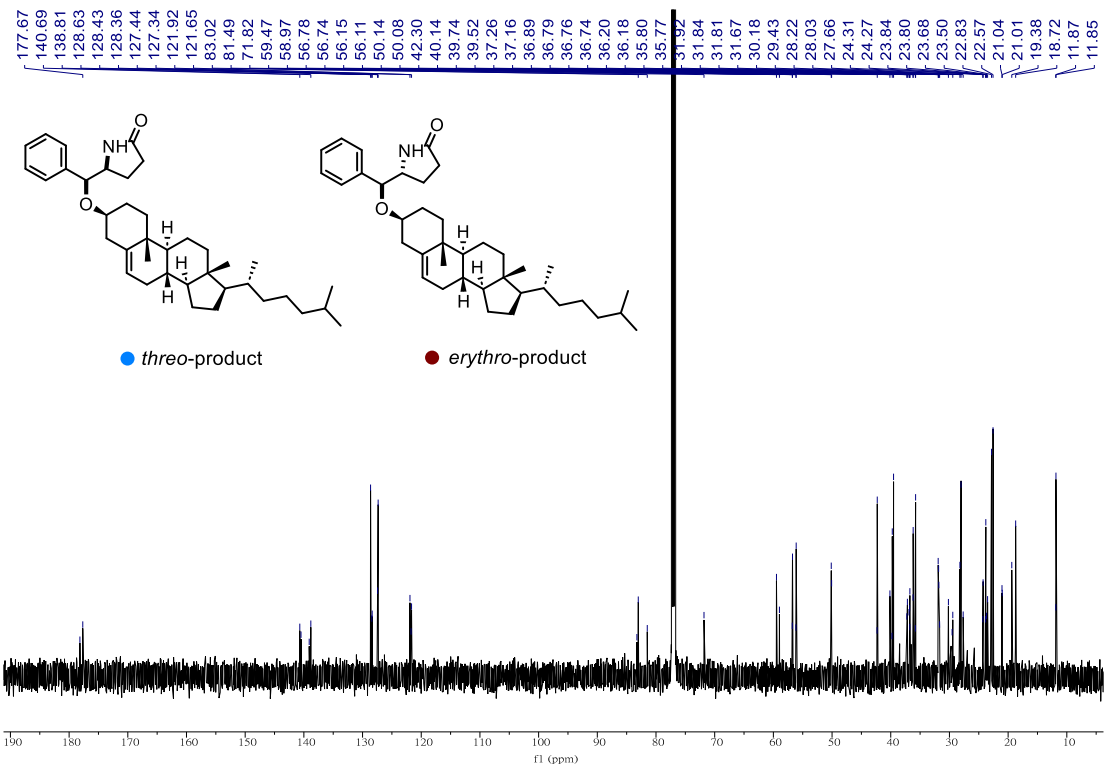


2-(5-Oxopyrrolidin-2-yl)-2-phenylethyl 2-(4-((2-oxocyclopentyl)methyl)phenyl)propanoate



5-((((3S,8S,9S,10R,13R,14S,17R)-10,13-Dimethyl-17-((R)-6-methylheptan-2-yl)-2,3,4,7,8,9,10,11,12,13,14,15,16,17-tetradecahydro-1H-cyclopenta[a]phenanthren-3-yl)oxy)(phenyl)methyl)pyrrolidin-2-one





References

(1) (a) Pattabiraman, V. R.; Bode, J. W. Rethinking amide bond synthesis. *Nature* **2011**, *480*, 471–479. (b) Du, B.; Chan, C.-M.; Au, C.-M.; Yu, W.-Y. Transition Metal-Catalyzed Regioselective Direct C–H Amidation: Interplay between Inner- and Outer-Sphere Pathways for Nitrene Cross-Coupling Reactions. *Acc. Chem. Res.* **2022**, *55*, 2123–2137.

(2) (a) Boström, J.; Brown, D. G.; Young, R. J.; Keserü, G. M. Expanding the medicinal chemistry synthetic toolbox. *Nat. Rev. Drug Discov* **2018**, *17*, 709–727. (b) Brown, D. G.; Boström, J. Analysis of Past and Present Synthetic Methodologies on Medicinal Chemistry: Where Have All the New Reactions Gone? *J. Med. Chem.* **2015**, *59*, 4443–4458. (c) Roughley, S. D.; Jordan, A. M. The Medicinal Chemist's Toolbox: An Analysis of Reactions Used in the Pursuit of Drug Candidates. *J. Med. Chem.* **2011**, *54*, 3451–3479.

(3) Afanasyev, O. I.; Kuchuk, E.; Usanov, D. L.; Chusov, D. Reductive Amination in the Synthesis of Pharmaceuticals. *Chem. Rev.* **2019**, *119*, 11857-11911.

(4) Ullmann, F. Ueber eine neue Bildungsweise von Diphenylaminderivaten. *Chem. Ber.* **1903**, *36*, 2382-2384.

(5) (a) Guram, A. S.; Buchwald, S. L. Palladium-Catalyzed Aromatic Aminations with in situ Generated Aminostannanes. *J. Am. Chem. Soc.* **1994**, *116*, 7901–7902. (b) Paul, F.; Patt, J.; Hartwig, J. F. Palladium-catalyzed formation of carbon-nitrogen bonds. Reaction intermediates and catalyst improvements in the hetero cross-coupling of aryl halides and tin amides. *J. Am. Chem. Soc.* **1994**, *116*, 5969–5970.

(6) Ruiz-Castillo, P.; Buchwald, S. L. Applications of Palladium-Catalyzed C–N Cross-Coupling Reactions. *Chem. Rev.* **2016**, *116*, 12564–12649.

(7) (a) Hamann, B. C.; Hartwig, J. F. Sterically Hindered Chelating Alkyl Phosphines Provide Large Rate Accelerations in Palladium-Catalyzed Amination of Aryl Iodides,

Bromides, and Chlorides, and the First Amination of Aryl Tosylates. *J. Am. Chem. Soc.* **1998**, *120*, 7369–7370. (b) Shen, Q.; Ogata, T.; Hartwig, J. F. Highly Reactive, General and Long-Lived Catalysts for Palladium-Catalyzed Amination of Heteroaryl and Aryl Chlorides, Bromides, and Iodides: Scope and Structure–Activity Relationships. *J. Am. Chem. Soc.* **2008**, *130*, 6586–6596. (c) Shen, Q.; Shekhar, S.; Stambuli, J. P.; Hartwig, J. F. Highly Reactive, General, and Long-Lived Catalysts for Coupling Heteroaryl and Aryl Chlorides with Primary Nitrogen Nucleophiles. *Angew. Chem. Int. Ed.* **2005**, *44*, 1371-1375.

(8) Park, Y.; Kim, Y.; Chang, S. Transition Metal-Catalyzed C–H Amination: Scope, Mechanism, and Applications. *Chem. Rev.* **2017**, *117*, 9247–9301.

(9) Blanksby, S. J.; Ellison, G. B. Bond Dissociation Energies of Organic Molecules. *Acc. Chem. Res.* **2003**, *36*, 255–263.

(10) (a) Collet, F.; Dodd, R. H.; Dauban, P. Catalytic C–H amination: recent progress and future directions. *Chem. Commun.* **2009**, 5061–5074. (b) Jazzar, R.; Hitce, J.; Renaudat, A.; Sofack-Kreutzer, J.; Baudoin, O. Functionalization of Organic Molecules by Transition-Metal-Catalyzed C(sp³) H Activation. *Chem. Eur. J.* **2010**, *16*, 2654-2672. (c) Hong, S. Y.; Hwang, Y.; Lee, M.; Chang, S. Mechanism-Guided Development of Transition-Metal-Catalyzed C–N Bond-Forming Reactions Using Dioxazolones as the Versatile Amidating Source. *Acc. Chem. Res.* **2021**, *54*, 2683-2700.

(11) (a) Breslow, R.; Gellman, S. H. Tosylamidation of cyclohexane by a cytochrome P-450 model. *Chem. Commun.* **1982**, 1400-1401. (b) Breslow, R.; Gellman, S. H. Intramolecular Nitrene C–H Insertions Mediated by Transition-metal Complexes as Nitrogen Analogues of Cytochrome P-450 Reactions. *J. Am. Chem. Soc.* **1983**, *105*, 6729–6730. (c) Mahy, J. P.; Bedi, G.; Battioni, P.; Mansuy, D. Allylic amination of

alkenes by tosyliminoiodobenzene: manganese porphyrins as suitable catalysts. *Tetrahedron Lett.* **1988**, *29*, 1927-1930.

(12) (a) Huang, J.-S.; Che, C.-M.; Poon, C.-K. Synthesis and spectroscopy of tert-butylimido complexes of osmium(VI) and ruthenium(VI) porphyrins. *J. Chem. Soc., Chem. Commun.* **1992**, 161. (b) Au, S.-M.; Fung, W.-H.; Cheng, M.-C.; Che, C.-M.; Peng, S.-M. Synthesis, characterisation and reactivity of novel bis(tosyl)imidoruthenium(vi) porphyrin complexes; X-ray crystal structure of a tosylamidoruthenium(iv) porphyrin. *Chem. Commun.* **1997**, 1655-1656.

(13) Au, S.-M.; Huang, J.-S.; Yu, W.-Y.; Fung, W.-H.; Che, C.-M. Aziridination of Alkenes and Amidation of Alkanes by Bis(tosylimido)ruthenium(VI) Porphyrins. A Mechanistic Study. *Journal of the American Chemical Society.* **1999**, *121*, 9120-9132.

(14) Au, S.-M.; Zhang, S.-B.; Fung, W.-H.; Yu, W.-Y.; Che, C.-M.; Cheung, K.-K. Ruthenium-mediated amidation of saturated C–H bonds and crystal structure of a bis(tosyl)amidoruthenium(III) complex of 1,4,7-trimethyl-1,4,7-triazacyclononane. *Chem. Commun.* **1998**, 2677-2678.

(15) Sze-Man Au; Jie-Sheng Huang; Chi-Ming Che, a.; Yu, W.-Y. Amidation of Unfunctionalized Hydrocarbons Catalyzed by Ruthenium Cyclic Amine or Bipyridine Complexes. *J. Org. Chem.* **2000**, *65*, 7858–7864.

(16) (a) Jung, H.; Kweon, J.; Suh, J.-M.; Lim, M. H.; Kim, D.; Chang, S. Mechanistic snapshots of rhodium-catalyzed acylnitrene transfer reactions. *Science* **2023**, *381*, 525-532. (b) Sun, J.; Abbenseth, J.; Verplancke, H.; Diefenbach, M.; De Bruin, B.; Hunger, D.; Würtele, C.; Van Slageren, J.; Holthausen, M. C.; Schneider, S. A platinum(ii) metallonitrene with a triplet ground state. *Nature Chemistry* **2020**, *12*, 1054-1059. (c) Mindiola, D. J. Oxidatively Induced Abstraction Reactions. A Synthetic Approach to

Low-Coordinate and Reactive Early Transition Metal Complexes Containing Metal−Ligand Multiple Bonds. *Acc. Chem. Res.* **2006**, *39*, 813-821.

(17) (a) Walroth, R. C.; Lukens, J. T.; Macmillan, S. N.; Finkelstein, K. D.; Lancaster, K. M. Spectroscopic Evidence for a 3d¹⁰ Ground State Electronic Configuration and Ligand Field Inversion in [Cu(CF₃)₄]^{1–}. *J. Am. Chem. Soc.* **2016**, *138*, 1922-1931. (b) Hoffmann, R.; Alvarez, S.; Mealli, C.; Falceto, A.; Cahill, T. J.; Zeng, T.; Manca, G. From Widely Accepted Concepts in Coordination Chemistry to Inverted Ligand Fields. *Chem. Rev.* **2016**, *116*, 8173-8192. (c) Cundari, T. R.; Dinescu, A.; Kazi, A. B. Bonding and Structure of Copper Nitrenes. *Inorg. Chem.* **2008**, *47*, 10067-10072.

(18) Yosra M. Badiei; Ammani Krishnaswamy; Marie M. Melzer, a.; Warren*, T. H. Transient Terminal Cu−Nitrene Intermediates from Discrete Dicopper Nitrenes. *J. Am. Chem. Soc.* **2006**, *128*, 15056–15057.

(19) Badiei, Y. M.; Dinescu, A.; Dai, X.; Palomino, R. M.; Heinemann, F. W.; Cundari, T. R.; Warren, T. H. Copper–Nitrene Complexes in Catalytic C H Amination. *Angew. Chem. Int. Ed.* **2008**, *47*, 9961-9964.

(20) Aguila, M. J. B.; Badiei, Y. M.; Warren, T. H. Mechanistic Insights into C–H Amination via Dicopper Nitrenes. *J. Am. Chem. Soc.* **2013**, *135*, 9399–9406.

(21) (a) Corona, T.; Ribas, L.; Rovira, M.; Farquhar, E. R.; Ribas, X.; Ray, K.; Company, A. Characterization and Reactivity Studies of a Terminal Copper–Nitrene Species. *Angew. Chem. Int. Ed.* **2016**, *55*, 14005-14008. (b) Kundu, S.; Miceli, E.; Farquhar, E.; Pfaff, F. F.; Kuhlmann, U.; Hildebrandt, P.; Braun, B.; Greco, C.; Ray, K. Lewis Acid Trapping of an Elusive Copper–Tosylnitrene Intermediate Using Scandium Triflate. *J. Am. Chem. Soc.* **2012**, *134*, 14710–14713.

(22) Dielmann, F.; Andrada, D. M.; Frenking, G.; Bertrand, G. Isolation of Bridging and Terminal Coinage Metal–Nitrene Complexes. *J. Am. Chem. Soc.* **2014**, *136*, 3800−3802.

(23) Carsch, K. M.; Dimucci, I. M.; Iovan, D. A.; Li, A.; Zheng, S.-L.; Titus, C. J.; Lee, S. J.; Irwin, K. D.; Nordlund, D.; Lancaster, K. M.; et al. Synthesis of a copper-supported triplet nitrene complex pertinent to copper-catalyzed amination. *Science* **2019**, *365*, 1138-1143.

(24) (a) Christine G. Espino; Paul M. Wehn; Jessica Chow; DuBois, J. Synthesis of 1,3-Difunctionalized Amine Derivatives through Selective C−H Bond Oxidation. *J. Am. Chem. Soc.* **2001**, *123*, 6935-6936. (b) Espino, C. G.; Bois, J. D. A Rh-Catalyzed C−H Insertion Reaction for the Oxidative Conversion of Carbamates to Oxazolidinones. *Angew. Chem. Int. Ed.* **2001**, *40*, 598-600.

(25) (a) Roizen, J. L.; Harvey, M. E.; DuBois, J. Metal-Catalyzed Nitrogen-Atom Transfer Methods for the Oxidation of Aliphatic C–H Bonds. *Acc. Chem. Res.* **2012**, *45*, 911-922. (b) Wehn, P. M.; Lee, J.; Bois, J. D. Stereochemical Models for Rh-Catalyzed Amination Reactions of Chiral Sulfamates. *Org. Lett.* **2003**, *5*, 4823-4826. (c) Kim, M.; Mulcahy, J. V.; Espino, C. G.; Bois, J. D. Expanding the Substrate Scope for C−H Amination Reactions: Oxidative Cyclization of Urea and Guanidine Derivatives. *Org. Lett.* **2006**, *8*, 1073-1076.

(26) Nguyen, Q.; Sun, K.; Driver, T. G. Rh2(II)-Catalyzed Intramolecular Aliphatic C–H Bond Amination Reactions Using Aryl Azides as the N-Atom Source. *J. Am. Chem. Soc.* **2012**, *134*, 7262-7265.

(27) Espino, C. G.; Fior, K. W.; Kim, M.; Bois, J. D. Expanding the Scope of C−H Amination through Catalyst Design. *J. Am. Chem. Soc.* **2004**, *126*, 15378-15379.

(28) (a) Olson, D. E.; Maruniak, A.; Malhotra, S.; Trost, B. M.; Bois, J. D. Synthesis and Reactivity of Unique Heterocyclic Structures en Route to Substituted Diamines. *Org. Lett.*

2011, *13*, 3336–3339. (b) Kurokawa, T.; Kim, M.; Bois, J. D. Synthesis of 1,3-Diamines Through Rhodium-Catalyzed C-H Insertion. *Angew. Chem.* **2009**, *121*, 2815-2817.

(29) (a) Bois, J. D. Rhodium-Catalyzed C–H Amination. An Enabling Method for Chemical Synthesis. *Org. Process Res. Dev.* **2011**, *15*, 758–762. (b) Fiori, K. W.; Espino, C. G.; Brodsky, B. H.; Bois, J. D. A mechanistic analysis of the Rh-catalyzed intramolecular C–H amination reaction. *Tetrahedron* **2009**, *65*, 3042-3051.

(30) (a) Liang, C.; Collet, F.; Robert-Peillard, F.; Müller, P.; Dodd, R. H.; Dauban, P. Toward a Synthetically Useful Stereoselective C−H Amination of Hydrocarbons. *J. Am. Chem. Soc.* **2008**, *130*, 343-350. (b) Collet, F.; Lescot, C.; Liang, C.; Dauban, P. Studies in catalytic C–H amination involving nitrene C–H insertion. *Dalton Trans.* **2010**, *39*, 10401-10413.

(31) Bess, E. N.; Deluca, R. J.; Tindall, D. J.; Oderinde, M. S.; Roizen, J. L.; Du Bois, J.; Sigman, M. S. Analyzing Site Selectivity in Rh₂(esp)₂-Catalyzed Intermolecular C–H Amination Reactions. *J. Am. Chem. Soc.* **2014**, *136*, 5783-5789.

(32) Brunard, E.; Boquet, V.; Elslande, E. V.; Saget, T.; Dauban, P. Catalytic Intermolecular C(sp3)–H Amination: Selective Functionalization of Tertiary C–H Bonds vs Activated Benzylic C–H Bonds. *J. Am. Chem. Soc.* **2021**, *143*, 6407–6412.

(33) Brunard, E.; Boquet, V.; Saget, T.; Carrizo, E. D. S.; Sircoglou, M.; Dauban, P. Catalyst-Controlled Intermolecular Homobenzylic C(sp3)–H Amination for the Synthesis of β-Arylethylamines. *J. Am. Chem. Soc.* **2024**, *146*, 5843−5854.

(34) Alderson, J. M.; Corbin, J. R.; Schomaker, J. M. Tunable, Chemo- and Site-Selective Nitrene Transfer Reactions through the Rational Design of Silver(I) Catalysts. *Acc. Chem. Res.* **2017**, *50*, 2147−2158.

(35) (a) and, Y. C.; He, C. Efficient Aziridination of Olefins Catalyzed by a Unique Disilver(I) Compound. *J. Am. Chem. Soc.* **2003**, *125*, 16202-16203. (b) Cui, Y.; He, C. A Silver-Catalyzed Intramolecular Amidation of Saturated C-H Bonds. *Angew. Chem. Int. Ed.* **2004**, *43*, 4210-4212. (c) Li, Z.; Capretto, D. A.; Rahaman, R.; He, C. Silver-Catalyzed Intermolecular Amination of C-H Groups. *Angew. Chem. Int. Ed.* **2007**, *46*, 5184-5186.

(36) Llaveria, J.; Beltrán, Á.; Díaz-Requejo, M. M.; Matheu, M. I.; Castillón, S.; Pérez, P. J. Efficient Silver-Catalyzed Regio- and Stereospecific Aziridination of Dienes. *Angew. Chem. Int. Ed.* **2010**, *49*, 7092-7095.

(37) (a) Rigoli, J. W.; Weatherly, C. D.; Alderson, J. M.; Vo, B. T.; Schomaker, J. M. Tunable, Chemoselective Amination via Silver Catalysis. *J. Am. Chem. Soc.* **2013**, *135*, 17238-17241. (b) Ju, M.; Weatherly, C. D.; Guzei, I. A.; Schomaker, J. M. Chemo- and Enantioselective Intramolecular Silver-Catalyzed Aziridinations. *Angew. Chem. Int. Ed.* **2017**, *56*, 9944-9948. (c) Huang, M.; Corbin, J. R.; Dolan, N. S.; Fry, C. G.; Vinokur, A. I.; Guzei, I. A.; Schomaker, J. M. Synthesis, Characterization, and Variable-Temperature NMR Studies of Silver(I) Complexes for Selective Nitrene Transfer. *Inorg. Chem.* **2017**, *56*, 6725-6733. (d) Weatherly, C.; Alderson, J. M.; Berry, J. F.; Hein, J. E.; Schomaker, J. M. Catalyst-Controlled Nitrene Transfer by Tuning Metal:Ligand Ratios: Insight into the Mechanisms of Chemoselectivity. *Organometallics* **2017**, *36*, 1649-1661. (e) Rigoli, J. W.; Weatherly, C. D.; Vo, B. T.; Neale, S.; Meis, A. R.; Schomaker, J. M. Chemoselective Allene Aziridination via Ag(I) Catalysis. *Org. Lett.* **2012**, *15*, 290-293.

(38) Scriven, E. F. V.; Turnbull, K. Azides: their preparation and synthetic uses. *Chem. Rev.* **1988**, *88*, 297-368.

(39) Park, Y.; Park, K. T.; Kim, J. G.; Chang, S. Mechanistic Studies on the Rh(III)-Mediated Amido Transfer Process Leading to Robust C–H Amination with a New Type of Amidating Reagent. *J. Am. Chem. Soc.* **2015**, *137*, 4534–4542.

(40) Hong, S. Y.; Park, Y.; Hwang, Y.; Kim, Y. B.; Baik, M.-H.; Chang, S. Selective formation of γ-lactams via C-H amidation enabled by tailored iridium catalysts. *Science* **2018**, *359*, 1016-1021.

(41) Xing, Q.; Chan, C.-M.; Yeung, Y.-W.; Yu, W.-Y. Ruthenium(II)-Catalyzed Enantioselective γ-Lactams Formation by Intramolecular C–H Amidation of 1,4,2-Dioxazol-5-ones. *J. Am. Chem. Soc.* **2019**, *141*, 3849-3853.

(42) (a) Park, Y.; Chang, S.; Park, Y.; Chang, S. Asymmetric formation of γ-lactams via C–H amidation enabled by chiral hydrogen-bond-donor catalysts. *Nature Catalysis* **2019**, *2*, 219-227. (b) Wang, H.; Park, Y.; Bai, Z.; Chang, S.; He, G.; Chen, G. Iridium-Catalyzed Enantioselective C(sp³)–H Amidation Controlled by Attractive Noncovalent Interactions. *J. Am. Chem. Soc.* **2019**, *141*, 7194-7201.

(43) Kwart, H.; Khan, A. A. Copper-Catalyzed Decomposition of Benzenesulfonyl Azide in Cyclohexene Solution. *J. Am. Chem. Soc.* **1967**, *89*, 1951-1953.

(44) Carr, D.; Seden, T. P.; Turner, R. W. A convenient synthesis of N-Arylsulphonyl sulphoximines. *Tetrahedron Lett.* **1969**, *10*, 477-478.

(45) Díaz-Requejo, M. M.; Belderraín, T. R.; Nicasio, M. C.; Trofimenko, S.; Pérez, P. J. Cyclohexane and Benzene Amination by Catalytic Nitrene Insertion into C−H Bonds with the Copper-Homoscorpionate Catalyst TpBr3Cu(NCMe). *J. Am. Chem. Soc.* **2003**, *125*, 12078-12079.

(46) Barman, D. N.; Nicholas, K. M. Copper-Catalyzed Intramolecular C–H Amination. *Eur. J. Org. Chem.* **2011**, *2011*, 908-911.

(47) Barman, D. N.; Nicholas, K. M. Ligand-assisted, copper-catalyzed enantioselective benzylic amination. *Tetrahedron Lett.* **2010**, *51*, 1815-1818.

(48) (a) III, R. T. G.; Warren, T. H. Copper-Catalyzed sp3 C–H Amination. *Organometallics* **2012**, *31*, 7728-7752. (b) Dauban, P.; Sanière, L.; Tarrade, A.; Dodd, R. H. Copper-Catalyzed Nitrogen Transfer Mediated by Iodosylbenzene PhIO. *J. Am. Chem. Soc.* **2001**, *123*, 7707-7708. (c) Bagchi, V.; Paraskevopoulou, P.; Das, P.; Chi, L.; Wang, Q.; Choudhury, A.; Mathieson, J. S.; Cronin, L.; Pardue, D. B.; Cundari, T. R.; et al. A Versatile Tripodal Cu(I) Reagent for C–N Bond Construction via Nitrene-Transfer Chemistry: Catalytic Perspectives and Mechanistic Insights on C–H Aminations/Amidinations and Olefin Aziridinations. *J. Am. Chem. Soc.* **2014**, *136*, 11362-11381.

(49) Overman, L. E.; Tomasi, A. L. Enantioselective Total Synthesis of Hispidospermidin. *J. Am. Chem. Soc.* **1998**, *120*, 4039-4040.

(50) Xing, Q.; Jiang, D.; Zhang, J.; Guan, L.; Li, T.; Zhao, Y.; Di, M.; Chen, H.; Che, C.; Zhu, Z. Combining visible-light induction and copper catalysis for chemo-selective nitrene transfer for late-stage amination of natural products. *Communications Chemistry* **2022**, *5*, 79.

(51) Zhang, L.; Deng, L. C-H bond amination by iron-imido/nitrene species. *Chin. Sci. Bull.* **2012**, *57*, 2352–2360.

(52) Yan, S.-Y.; Wang, Y.; Shu, Y.-J.; Liu, H.-H.; Zhou, X.-G. Nitrene transfer reaction catalyzed by substituted metallophthalocyanines. *J. Mol. Catal. A: Chem.* **2006**, *248*, 148-151.

(53) Liu, Y.; Che, C.-M. [FeIII(F20-tpp)Cl] Is an Effective Catalyst for Nitrene Transfer Reactions and Amination of Saturated Hydrocarbons with Sulfonyl and Aryl Azides as

Nitrogen Source under Thermal and Microwave-Assisted Conditions. *Chem. Eur. J.* **2010**, *16*, 10494-10501.

(54) McIntosh, J. A.; Coelho, P. S.; Farwell, C. C.; Wang, Z. J.; Lewis, J. C.; Brown, T. R.; Arnold, F. H. Enantioselective Intramolecular C-H Amination Catalyzed by Engineered Cytochrome P450 Enzymes In Vitro and In Vivo. *Angew. Chem. Int. Ed.* **2013**, *52*, 9309-9312.

(55) Singh, R.; Bordeaux, M.; Fasan, R. P450-Catalyzed Intramolecular sp3 C–H Amination with Arylsulfonyl Azide Substrates. *ACS Catalysis* **2014**, *4*, 546-552.

(56) Wang, P.; Deng, L. Recent Advances in Iron-Catalyzed C—H Bond Amination via Iron Imido Intermediate. *Chin. J. Chem* . **2018**, *36*, 1222-1240.

(57) Liu, P.; Wong, E. L.-M.; Yuen, A. W.-H.; Che, C.-M. Highly Efficient Alkene Epoxidation and Aziridination Catalyzed by Iron(II) Salt + 4,4′,4″-Trichloro-2,2′:6′,2″-terpyridine/4,4″-Dichloro-4′-O-PEG-OCH3-2,2′:6′,2″-terpyridine. *Org. Lett.* **2008**, *10*, 3275-3278.

(58) (a) King, E. R.; Betley, T. A. C−H Bond Amination from a Ferrous Dipyrromethene Complex. *Inorg. Chem.* **2009**, *48*, 2361-2363. (b) King, E. R.; Hennessy, E. T.; Betley, T. A. Catalytic C−H Bond Amination from High-Spin Iron Imido Complexes. *J. Am. Chem. Soc.* **2011**, *133*, 4917-4923.

(59) Hennessy, E. T.; Betley, T. A. Complex N-Heterocycle Synthesis via Iron-Catalyzed, Direct C–H Bond Amination. *Science* **2013**, *340*, 591-595.

(60) (a) Welsch, M. E.; Snyder, S. A.; Stockwell, B. R. Privileged scaffolds for library design and drug discovery. *Curr. Opin. Chem. Biol.* **2010**, *14*, 347-361. (b) Bariwal, J.; Eycken, E. V. d. C–N bond forming cross-coupling reactions: an overview. *Chem. Soc. Rev.* **2013**, *42*, 9283-9303. (c) Shin, K.; Kim, H.; Chang, S. Transition-Metal-Catalyzed C–N Bond Forming Reactions Using Organic Azides as the Nitrogen Source: A Journey

for the Mild and Versatile C–H Amination. *Acc. Chem. Res.* **2015**, *48*, 1040–1052. (d) Brown, D. G.; Boström, J. Analysis of Past and Present Synthetic Methodologies on Medicinal Chemistry: Where Have All the New Reactions Gone? *J. Med. Chem.* **2016**, *59*, 4443-4458. (e) Ju, M.; Schomaker, J. M. Nitrene Transfer Catalysts for Enantioselective C–N Bond Formation. *Nat. Rev. Chem.* **2021**, *5*, 580-594.

(61) (a) Zard, S. Z. Recent progress in the generation and use of nitrogen-centred radicals. *Chem. Soc. Rev.* **2008**, *37*, 1603-1618. (b) Dequirez, G.; Pons, V.; Dauban, P. Nitrene Chemistry in Organic Synthesis: Still in Its Infancy? *Angew. Chem. Int. Ed.* **2012**, *51*, 7384-7395. (c) Kuijpers, P. F.; Vlugt, J. I. v. d.; Schneider, S.; Bruin, B. d. Nitrene Radical Intermediates in Catalytic Synthesis. *Chem. Eur. J.* **2017**, *23*, 13819-13829. (d) Park, Y.; Kim, Y.; Chang, S. Transition Metal-Catalyzed C–H Amination: Scope, Mechanism, and Applications. *Chem. Rev.* **2017**, *117*, 9247-9301. (e) Kwon, K.; Simons, R. T.; Nandakumar, M.; Roizen, J. L. Strategies to Generate Nitrogen-centered Radicals That May Rely on Photoredox Catalysis: Development in Reaction Methodology and Applications in Organic Synthesis. *Chem. Rev.* **2021**, *122*, 2353-2428. (f) Holmberg-Douglas, N.; Nicewicz, D. A. Photoredox-Catalyzed C–H Functionalization Reactions. *Chem. Rev.* **2021**, *122*, 1925-2016. (g) Pratley, C.; Fenner, S.; Murphy, J. A. Nitrogen-Centered Radicals in Functionalization of sp2 Systems: Generation, Reactivity, and Applications in Synthesis. *Chem. Rev.* **2022**, *122*, 8181–8260.

(62) (a) Song, L.; Zhang, L.; Luo, S.; Cheng, J.-P. Visible-Light Promoted Catalyst-Free Imidation of Arenes and Heteroarenes. *Chem. Eur. J.* **2014**, *20*, 14231-14234. (b) Kim, H.; Kim, T.; Lee, D. G.; Roh, S. W.; Lee, C. Nitrogen-centered radical-mediated C–H imidation of arenes and heteroarenes via visible light induced photocatalysis. *Chem. Commun.* **2014**, *50*, 9273-9276. (c) Allen, L. J.; Cabrera, P. J.; Lee, M.; Sanford, M. S. N-Acyloxyphthalimides as Nitrogen Radical Precursors in the Visible Light

Photocatalyzed Room Temperature C–H Amination of Arenes and Heteroarenes. *J. Am. Chem. Soc.* **2014**, *136*, 5607-5610.

(63) Greulich, T. W.; Daniliuc, C. G.; Studer, A. N-Aminopyridinium Salts as Precursors for N-Centered Radicals – Direct Amidation of Arenes and Heteroarenes. *Org. Lett.* **2014**, *17*, 254-257.

(64) (a) Qin, Q.; Yu, S. Visible-Light-Promoted Redox Neutral C–H Amidation of Heteroarenes with Hydroxylamine Derivatives. *Org. Lett.* **2014**, *16*, 3504-3507. (b) Davies, J.; Svejstrup, T. D.; Reina, D. F.; Sheikh, N. S.; Leonori, D. Visible-Light-Mediated Synthesis of Amidyl Radicals: Transition-Metal-Free Hydroamination and N-Arylation Reactions. *J. Am. Chem. Soc.* **2016**, *138*, 8092-8095. (c) Cecere, G.; König, C. M.; Alleva, J. L.; MacMillan, D. W. C. Enantioselective Direct α-Amination of Aldehydes via a Photoredox Mechanism: A Strategy for Asymmetric Amine Fragment Coupling. *J. Am. Chem. Soc.* **2013**, *135*, 11521-11524. (d) Jung, H.; Keum, H.; Kweon, J.; Chang, S. Tuning Triplet Energy Transfer of Hydroxamates as the Nitrene Precursor for Intramolecular C(sp3)–H Amidation. *J. Am. Chem. Soc.* **2020**, *142*, 5811-5818. (e) Keum, H.; Jung, H.; Jeong, J.; Kim, D.; Chang, S. Visible-Light Induced C(sp2)−H Amidation with an Aryl–Alkyl σ-Bond Relocation via Redox-Neutral Radical–Polar Crossover. *Angew. Chem. Int. Ed.* **2021**, *60*, 25235-25240. (f) Roos, C. B.; Demaerel, J.; Graff, D. E.; Knowles, R. R. Enantioselective Hydroamination of Alkenes with Sulfonamides Enabled by Proton-Coupled Electron Transfer. *J. Am. Chem. Soc.* **2020**, *142*, 5974-5979. (g) Miller, D. C.; Choi, G. J.; Orbe, H. S.; Knowles, R. R. Catalytic Olefin Hydroamidation Enabled by Proton-Coupled Electron Transfer. *J. Am. Chem. Soc.* **2015**, *137*, 13492-13495.

(65) (a) Vliet, K. M. v.; Bruin, B. d. Dioxazolones: Stable Substrates for the Catalytic Transfer of Acyl Nitrenes. *ACS Catalysis* **2020**, *10*, 4751–4769. (b) Hong, S. Y.; Hwang,

Y.; Lee, M.; Chang, S. Mechanism-Guided Development of Transition-Metal-Catalyzed C–N Bond-Forming Reactions Using Dioxazolones as the Versatile Amidating Source. *Acc. Chem. Res.* **2021**, *54*, 2683–2700.

(66) (a) Jung, H.; Schrader, M.; Kim, D.; Baik, M.-H.; Park, Y.; Chang, S. Harnessing Secondary Coordination Sphere Interactions That Enable the Selective Amidation of Benzylic C–H Bonds. *J. Am. Chem. Soc.* **2019**, *141*, 15356-15366. (b) Zhou, Z.; Chen, S.; Hong, Y.; Winterling, E.; Tan, Y.; Hemming, M.; Harms, K.; Houk, K. N.; Meggers, E. Non-C2-Symmetric Chiral-at-Ruthenium Catalyst for Highly Efficient Enantioselective Intramolecular C(sp3)–H Amidation. *J. Am. Chem. Soc.* **2019**, *141*, 19048-19057. (c) Sun, W.; Ling, C.-H.; Au, C.-M.; Yu, W.-Y. Ruthenium-Catalyzed Intramolecular Arene C(sp2)–H Amidation for Synthesis of 3,4-Dihydroquinolin-2(1H)-ones. *Org. Lett.* **2021**, *23*, 3310-3314. (d) Park, Y.; Park, K. T.; Kim, J. G.; Chang, S. Mechanistic Studies on the Rh(III)-Mediated Amido Transfer Process Leading to Robust C–H Amination with a New Type of Amidating Reagent. *J. Am. Chem. Soc.* **2015**, *137*, 4534-4572. (e) Lee, M.; Heo, J.; Kim, D.; Chang, S. On the Origin of Rh-Catalyzed Selective Ring-Opening Amidation of Substituted Cyclopropanols to Access β2-Amino Ketones. *J. Am. Chem. Soc.* **2022**, *144*, 3667-3675. (f) Lyu, X.; Zhang, J.; Kim, D.; Seo, S.; Chang, S. Merging NiH Catalysis and Inner-Sphere Metal-Nitrenoid Transfer for Hydroamidation of Alkynes. *J. Am. Chem. Soc.* **2021**, *143*, 5867-5877. (g) Du, B.; Ouyang, Y.; Chen, Q.; Yu, W.-Y. Thioether-Directed NiH-Catalyzed Remote γ-C(sp3)–H Hydroamidation of Alkenes by 1,4,2-Dioxazol-5-ones. *J. Am. Chem. Soc.* **2021**, *143*, 14962-14968. (h) Mahato, S. K.; Ohara, N.; Khake, S. M.; Chatani, N. Iridium(III)-Catalyzed Direct Intermolecular Chemoselective α-Amidation of Masked Aliphatic Carboxylic Acids with Dioxazolones via Nitrene Transfer. *ACS Catalysis* **2021**, *11*, 7126-7131. (i) Hong, S. Y.; Park, Y.; Hwang, Y.; Kim, Y. B.; Baik, M.-H.; Chang, S. Selective

formation of γ-lactams via C–H amidation enabled by tailored iridium catalysts. *Science* **2018**, *359*, 1016-1021. (j) Hong, S. Y.; Kim, D.; Chang, S. Catalytic Access to Carbocation Intermediates via Nitrenoid Transfer Leading to Allylic Lactams. *Nature Catalysis* **2020**, *4*, 79-88. (k) Kim, S.; Kim, D.; Hong, S. Y.; Chang, S. Tuning Orbital Symmetry of Iridium Nitrenoid Enables Catalytic Diastereo- and Enantioselective Alkene Difunctionalizations. *J. Am. Chem. Soc.* **2021**, *143*, 3993-4004. (l) Zhou, Y.; Engl, O. D.; Bandar, J. S.; Chant, E. D.; Buchwald, S. L. CuH-Catalyzed Asymmetric Hydroamidation of Vinylarenes. *Angew. Chem. Int. Ed.* **2018**, *57*, 6672-6675. (m) Vliet, K. M. v.; Polak, L. H.; Siegler, M. A.; Vlugt, J. I. v. d.; Guerra, C. F.; Bruin, B. d. Efficient Copper-Catalyzed Multicomponent Synthesis of N-Acyl Amidines via Acyl Nitrenes. *J. Am. Chem. Soc.* **2019**, *141*, 15240-15249. (n) Liu, X.; Li, W.; Jiang, W.; Lu, H.; Liu, J.; Lin, Y.; Cao, H. Cu(II)-Catalyzed C–H Amidation/Cyclization of Azomethine Imines with Dioxazolones via Acyl Nitrenes: A Direct Access to Diverse 1,2,4-Triazole Derivatives. *Org. Lett.* **2022**, *24*, 613-618. (o) Bizet, V.; Buglioni, L.; Bolm, C. Light-Induced Ruthenium-Catalyzed Nitrene Transfer Reactions: A Photochemical Approach towards N-Acyl Sulfimides and Sulfoximines. *Angew. Chem.* **2014**, *126*, 5745-5748. (p) Burman, J. S.; Harris, R. J.; Farr, C. M. B.; Bacsa, J.; Blakey, S. B. Rh(III) and Ir(III)Cp* Complexes Provide Complementary Regioselectivity Profiles in Intermolecular Allylic C–H Amidation Reactions. *ACS Catalysis* **2019**, *9*, 5474-5479.

(67) (a) Zhao, X.; Liang, S.; Fan, X.; Yang, T.; Yu, W. Iron-Catalyzed Intramolecular C–H Amination of α-Azidyl Amides. *Org. Lett.* **2019**, *21*, 1559-1563. (b) Shing, K.-P.; Liu, Y.; Cao, B.; Chang, X.-Y.; You, T.; Che, C.-M. N-Heterocyclic Carbene Iron(III) Porphyrin-Catalyzed Intramolecular C(sp3)–H Amination of Alkyl Azides. *Angew. Chem. Int. Ed.* **2018**, *57*, 11947-11951. (c) V., A.; Prasanthi, G.; Begum, S.; Srivastava, H. K.; Tiwari, S. K.; Singh, R. Iron-Catalyzed Arene C–H Amidation Using Functionalized

Hydroxyl Amines at Room Temperature. *ACS Catalysis* **2018**, *8*, 8369-8375. (d) Liu, J.; Wu, K.; Shen, T.; Liang, Y.; Zou, M.; Zhu, Y.; Li, X.; Li, X.; Jiao, N. Fe-Catalyzed Amination of (Hetero)Arenes with a Redox-Active Aminating Reagent under Mild Conditions. *Chem. Eur. J.* **2017**, *23*, 563-567. (e) Liang, S.; Zhao, X.; Yang, T.; Yu, W. Iron–Phosphine Complex-Catalyzed Intramolecular C(sp3)–H Amination of Azides. *Org. Lett.* **2020**, *22*, 1961-1965. (f) Legnani, L.; Cerai, G. P.; Morandi, B. Direct and Practical Synthesis of Primary Anilines through Iron-Catalyzed C–H Bond Amination. *ACS Catalysis* **2016**, *6*, 8162-8165. (g) Anugu, R. R.; Munnuri, S.; Falck, J. R. Picolinate-Directed Arene meta-C–H Amination via FeCl3 Catalysis. *J. Am. Chem. Soc.* **2020**, *142*, 5266-5271. (h) Alt, I. T.; Plietker, B. Iron-Catalyzed Intramolecular C(sp2)−H Amination. *Angew. Chem. Int. Ed.* **2016**, *55*, 1519-1522. (i) Alt, I. T.; Guttroff, C.; Plietker, B. Iron-Catalyzed Intramolecular Aminations of C(sp3)−H Bonds in Alkylaryl Azides. *Angew. Chem. Int. Ed.* **2017**, *56*, 10582-10586. (j) Shi, P.; Tu, Y.; Kong, D.; Wu, P.; Ma, D.; Bolm, C. Iron-Catalyzed Intramolecular Arene C(sp2)−H Amidations under Mechanochemical Conditions. *Angew. Chem. Int. Ed.* **2022**, *61*, e202204874. (k) Kweon, J.; Kim, D.; Kang, S.; Chang, S. Access to β-Lactams via Iron-Catalyzed Olefin Oxyamidation Enabled by the π-Accepting Phthalocyanine Ligand. *J. Am. Chem. Soc.* **2022**, *144*, 1872-1880. (l) Kweon, J.; Chang, S. Highly Robust Iron Catalyst System for Intramolecular C(sp3)−H Amidation Leading to γ-Lactams. *Angew. Chem. Int. Ed.* **2021**, *60*, 2909-2914.

(68) (a) Mandal, R.; Garai, B.; Sundararaju, B. Weak-Coordination in C–H Bond Functionalizations Catalyzed by 3d Metals. *ACS Catalysis* **2022**, *12*, 3452-3506. (b) Arevalo, R.; Chirik, P. J. Enabling Two-Electron Pathways with Iron and Cobalt: From Ligand Design to Catalytic Applications. *J. Am. Chem. Soc.* **2019**, *141*, 9106-9123.

(69) Leest, N. P. v.; Vlugt, J. I. v. d.; Bruin, B. d. Catalytic Chemoselective Sulfimidation with an Electrophilic [CoIII(TAML)]−-Nitrene Radical Complex**. *Chem. Eur. J.* **2021**, *27*, 371-378.

(70) (a) Bayly, S. R.; Beer, P. D.; Chen, G. Z. Ferrocene Sensors. In *Ferrocenes: Ligands, Materials and Biomolecules*, Stepnicka, P. Ed.; Wiley, Hoboken, 2008; pp 218-318. (b) Zanello, P. Electrochemical and X-ray Structural Aspects of
Transition Metal Complexes Containing Redox-Active Ferrocene
Ligands. In *Ferrocenes*, Togni, A., Hayashi, T., Eds. Eds.; Wiley-VCH, 1994; pp 317-430. (c) Togni, A.; Bieler, N.; Burckhardt, U.; Köllner, C.; Pioda, G.; Schneider, R.; Schnyder, A.; Togni, A.; Bieler, N.; Burckhardt, U.; et al. Recent studies in asymmetric catalysis using ferrocenyl ligands. *Pure Appl. Chem.* **1999**, *71*, 1531-1537. (d) Connelly, N. G.; Geiger, W. E. Chemical Redox Agents for Organometallic Chemistry. *Chem. Rev.* **1996**, *96*, 877-910. (e) Long, N. J. Organometallic Compounds for Nonlinear Optics—The Search for En-light-enment! *Angew. Chem. Int. Ed. Engl.* **1995**, *34*, 21-38. (f) Arrayás, R. G.; Adrio, J.; Carretero, J. C. Recent Applications of Chiral Ferrocene Ligands in Asymmetric Catalysis. *Angew. Chem. Int. Ed.* **2006**, *45*, 7674-7715. (g) and, D. R. v. S.; Metzler-Nolte*, N. Bioorganometallic Chemistry of Ferrocene. *Chem. Rev.* **2004**, *104*, 5931-5986.

(71) Foo, K.; Sella, E.; Thomé, I.; Eastgate, M. D.; Baran, P. S. A Mild, Ferrocene-Catalyzed C–H Imidation of (Hetero)Arenes. *J. Am. Chem. Soc.* **2014**, *136*, 5279-5282.

(72) (a) Mosconi, D.; Blanco, M.; Gatti, T.; Calvillo, L.; Otyepka, M.; Bakandritsos, A.; Menna, E.; Agnoli, S.; Granozzi, G. Arene CH insertion catalyzed by ferrocene covalently heterogenized on graphene acid. *Carbon* **2019**, *143*, 318-328. (b) Broadhead, G. D.; Pauson, P. L. Ferrocene derivatives. Part II. Arylation. *J. Chem. Soc.* **1955**, 367-370.

(73) Hwang, Y.; Park, Y.; Kim, Y. B.; Kim, D.; Chang, S. Revisiting Arene C(sp2)−H Amidation by Intramolecular Transfer of Iridium Nitrenoids: Evidence for a Spirocyclization Pathway. *Angew. Chem. Int. Ed.* **2018**, *57*, 13565.

(74) Athavale, S. V.; Gao, S.; Liu, Z.; Mallojjala, S. C.; Hirschi, J. S.; Arnold, F. H. Biocatalytic, Intermolecular C−H Bond Functionalization for the Synthesis of Enantioenriched Amides. *Angew. Chem. Int. Ed.* **2021**, *60*, 24864-24869.

(75) McKittrick, M. W.; Jones, C. W. Toward Single-Site, Immobilized Molecular Catalysts: Site-Isolated Ti Ethylene Polymerization Catalysts Supported on Porous Silica. *J. Am. Chem. Soc.* **2004**, *126*, 3052-3053.

(76) Liu, J.; Ye, W.; Wang, S.; Zheng, J.; Tang, W.; Li, X. Synthesis of Lactams via Ir-Catalyzed C–H Amidation Involving Ir-Nitrene Intermediates. *J. Org. Chem.* **2020**, *85*, 4430–4440.

(77) Jahn, U.; Hartmann, P.; Dix, I.; Jones, Peter G. Lithium Malonate Enolates as Precursors for Radical Reactions − Convenient Induction of Radical Cyclizations with either Radical or Cationic Termination. *Eur. J. Org. Chem.* **2001**, *2001*, 3333-3355.

(78) Khobragade, D. A.; Mahamulkar, S. G.; Pospíšil, L.; Císařová, I.; Rulíšek, L.; Jahn, U. Acceptor-Substituted Ferrocenium Salts as Strong, Single-Electron Oxidants: Synthesis, Electrochemistry, Theoretical Investigations, and Initial Synthetic Application. *Chem. Eur. J.* **2012**, *18*, 12267-12277.

(79) Erb, W.; Hellal, A.; Albini, M.; Rouden, J.; Blanchet, J. An Easy Route to (Hetero)arylboronic Acids. *Chem. Eur. J.* **2014**, *20*, 6608-6612.

(80) (a) Saldívar-González, F. I.; Lenci, E.; Trabocchi, A.; Medina-Franco, J. L. Exploring the chemical space and the bioactivity profile of lactams: a chemoinformatic study. *RSC Advances* **2019**, *9*, 27105-27116. (b) Caruano, J.; Muccioli, G. G.; Robiette, R. Biologically active γ-lactams: synthesis and natural sources. *Organic and*

Biomolecular Chemistry **2016**, *14*, 10134–10156. (c) Lepikhina, A.; Bakulina, O.; Dar'in, D.; Krasavin, M. The first solvent-free synthesis of privileged γ- and δ-lactams via the Castagnoli–Cushman reaction. *RSC Advances* **2016**, *6*, 83808-83813. (d) Weinreb, S. M. Product Class 10: γ-Lactams and Larger Ring Lactams. In *Category 3, Compounds with Four and Three Carbon Heteroatom Bonds*, Vol. 21; Georg Thieme Verlag KG, 2005; pp 647-712..

(81) (a) Du, B.; Chan, C.-M.; Au, C.-M.; Yu, W.-Y. Transition Metal-Catalyzed Regioselective Direct C–H Amidation: Interplay between Inner- and Outer-Sphere Pathways for Nitrene Cross-Coupling Reactions. *Acc. Chem. Res.* **2022**, *55*, 2123-2137. (b) Dutta, S.; Chatterjee, S.; Al-Thabaiti, S. A.; Bawaked, S.; Mokhtar, M.; Maiti, D. C–H activation: A strategic approach toward lactams using transition metals. *Chem Catalysis* **2022**, *2*, 1046-1083. (c) Rogge, T.; Kaplaneris, N.; Chatani, N.; Kim, J.; Chang, S.; Punji, B.; Schafer, L. L.; Musaev, D. G.; Wencel-Delord, J.; Roberts, C. A.; et al. C–H activation. *Nat. Rev. Methods Primers* **2021**, *1*, . (d) Trowbridge, A.; Walton, S. M.; Gaunt, M. J. New Strategies for the Transition-Metal Catalyzed Synthesis of Aliphatic Amines. *Chem. Rev.* **2020**, *120*, 2613–2692. (e) Hayashi, H.; Uchida, T. Nitrene Transfer Reactions for Asymmetric C–H Amination: Recent Development. *Eur. J. Org. Chem.* **2020**, *2020*, 909-916. (f) Ye, L.-W.; Shu, C.; Gagosz, F. Recent progress towards transition metal-catalyzed synthesis of γ-lactams. *Organic & Biomolecular Chemistry* **2014**, *12*, 1833-1845. (g) Ramirez, T. A.; Zhao, B.; Shi, Y. Recent advances in transition metal-catalyzed sp3 C–H amination adjacent to double bonds and carbonyl groups. *Chem. Soc. Rev.* **2012**, *41*, 931-942. (h) Newhouse, T.; Baran, P. S. If C-H Bonds Could Talk: Selective C-H Bond Oxidation. *Angew. Chem. Int. Ed.* **2011**, *50*, 3362-3374. (i) Zalatan, D. N.; Bois, J. D. Metal-Catalyzed Oxidations of C–H to C–N Bonds. In *C-H Activation*, Yu, J.-Q., Shi, Z. Eds.; Springer Berlin Heidelberg, 2009; pp 347-378. (j) Collet, F.; Dodd,

R. H.; Dauban, P. Catalytic C–H amination: recent progress and future directions. *Chem. Commun.* **2009**, 5061-5074. (k) Davies, H. M. L.; Manning, J. R. Catalytic C–H functionalization by metal carbenoid and nitrenoid insertion. *Nature* **2008**, *451*, 417–424.

(82) Jeong, J.; Jung, H.; Kim, D.; Chang, S. Multidimensional Screening Accelerates the Discovery of Rhodium Catalyst Systems for Selective Intra- and Intermolecular C–H Amidations. *ACS Catalysis* **2022**, *12*, 8127-8138.

(83) (a) Huang, F.; Tian, X.; Hou, F.; Xu, Y.; Lu, G. Electrostatic repulsion-controlled regioselectivity in nitrene-mediated allylic C–H amidations. *Organic Chemistry Frontiers* **2021**, *8*, 6038-6047. (b) Jung, H.; Choi, J.; Kim, D.; Lee, J. H.; Ihee, H.; Kim, D.; Chang, S. Photoinduced Group Transposition via Iridium-Nitrenoid Leading to Amidative Inner-Sphere Aryl Migration. *Angew. Chem. Int. Ed.* **2024**, *63*, e202408123. (c) Tufano, E.; Lee, E.; Barilli, M.; Casali, E.; Oštrek, A.; Jung, H.; Morana, M.; Kang, J.; Kim, D.; Chang, S.; et al. Iridium Acylnitrenoid-Initiated Biomimetic Cascade Cyclizations: Stereodefined Access to Polycyclic δ-Lactams. *J. Am. Chem. Soc.* **2023**, *145*, 24724-24735. (d) Wang, Q.; Jung, H.; Kim, D.; Chang, S. Iridium-Catalyzed Migratory Terminal C(sp3)–H Amidation of Heteroatom-Substituted Internal Alkenes via Olefin Chain Walking. *J. Am. Chem. Soc.* **2023**, *145*, 24940-24951.

(84) Yang, Z.-L.; Xu, X.-L.; Chen, X.-R.; Mao, Z.-F.; Zhou, Y.-F. Silver-Catalyzed Acyl Nitrene Transfer Reactions Involving Dioxazolones: Direct Assembly of N-Acylureas. *Eur. J. Org. Chem.* **2021**, *2021*, 648-652.

(85) Pradhan, S.; Kweon, J.; Sahoo, M. K.; Jung, H.; Heo, J.; Kim, Y. B.; Kim, D.; Park, J.-W.; Chang, S. A Formal γ-C–H Functionalization of Carboxylic Acids Guided by Metal-Nitrenoids as an Unprecedented Mechanistic Motif. *J. Am. Chem. Soc.* **2023**, *145*, 28251–28263.

(86) (a) Ping, L.; Chung, D. S.; Bouffard, J.; Lee, S.-G. Transition metal-catalyzed site- and regio-divergent C–H bond functionalization. *Chem. Soc. Rev.* **2017**, *46*, 4299-4328. (b) Théveau, L.; Schneider, C.; Fruit, C.; Hoarau, C. Orthogonal Palladium-Catalyzed Direct C−H Bond Arylation of Heteroaromatics with Aryl Halides. *ChemCatChem* **2016**, *8*, 3183-3194. (c) Tiwari, V. K.; Kapur, M. Catalyst-controlled positional-selectivity in C–H functionalizations. *Organic & Biomolecular Chemistry* **2019**, *17*, 1007-1026. (d) Liao, K.; Yang, Y.-F.; Li, Y.; Sanders, J. N.; Houk, K. N.; Musaev, D. G.; Davies, H. M. L. Design of catalysts for site-selective and enantioselective functionalization of non-activated primary C–H bonds. *Nature Chemistry* **2018**, *10*, 1048-1055. (e) Mao, J.-H.; Wang, Y.-B.; Yang, L.; Xiang, S.-H.; Wu, Q.-H.; Cui, Y.; Lu, Q.; Lv, J.; Li, S.; Tan, B. Organocatalyst-controlled site-selective arene C–H functionalization. *Nature Chemistry* **2021**, *13*, 982-991.

(87) (a) Clark, J. R.; Feng, K.; Sookezian, A.; White, M. C. Manganese-catalysed benzylic C(sp3)–H amination for late-stage functionalization. *Nature Chemistry* **2018**, *10*, 583-591. (b) Álvarez, M.; Molina, F.; Pérez, P. J. Carbene-Controlled Regioselective Functionalization of Linear Alkanes under Silver Catalysis. *J. Am. Chem. Soc.* **2022**, *144*, 23275-23279. (c) Caballero, A.; Díaz-Requejo, M. M.; Belderraín, T. R.; Nicasio, M. C.; Trofimenko, S.; Pérez, P. J. Highly Regioselective Functionalization of Aliphatic Carbon−Hydrogen Bonds with a Perbromohomoscorpionate Copper(I) Catalyst. *J. Am. Chem. Soc.* **2003**, *125*, 1446–1447. (d) Bakhoda, A. G.; Jiang, Q.; Badiei, Y. M.; Bertke, J. A.; Cundari, T. R.; Warren, T. H. Copper-Catalyzed C(sp3)−H Amidation: Sterically Driven Primary and Secondary C−H Site-Selectivity. *Angew. Chem. Int. Ed.* **2019**, *58*, 3421 –3425. (e) Lee, J.; Jin, S.; Kim, D.; Hong, S. H.; Chang, S. Cobalt-Catalyzed Intermolecular C–H Amidation of Unactivated Alkanes. *J. Am. Chem. Soc.* **2021**, *143*, 5191−5200.

(88) (a) Ju, M.; Huang, M.; Vine, L. E.; Dehghany, M.; Roberts, J. M.; Schomaker, J. M. Tunable catalyst-controlled syntheses of β- and γ-amino alcohols enabled by silver-catalysed nitrene transfer. *Nature Catalysis* **2019**, *2*, 899–908. (b) Fu, Y.; Zerull, E. E.; Schomaker, J. M.; Liu, P. Origins of Catalyst-Controlled Selectivity in Ag-Catalyzed Regiodivergent C–H Amination. *J. Am. Chem. Soc.* **2022**, *144*, 2735−2746. (c) Corbin, J. R.; Schomaker, J. M. Tunable differentiation of tertiary C–H bonds in intramolecular transition metal-catalyzed nitrene transfer reactions. *Chem. Commun.* **2017**, *53*, 4346-4349. (d) Huang, M.; Yang, T.; Paretsky, J. D.; Berry, J. F.; Schomaker, J. M. Inverting Steric Effects: Using "Attractive" Noncovalent Interactions To Direct Silver-Catalyzed Nitrene Transfer. *J. Am. Chem. Soc.* **2017**, *139*, 17376-17386. (e) Dolan, N. S.; Scamp, R. J.; Yang, T.; Berry, J. F.; Schomaker, J. M. Catalyst-Controlled and Tunable, Chemoselective Silver-Catalyzed Intermolecular Nitrene Transfer: Experimental and Computational Studies. *J. Am. Chem. Soc.* **2016**, *138*, 14658-14667. (f) Alderson, J. M.; Phelps, A. M.; Scamp, R. J.; Dolan, N. S.; Schomaker, J. M. Ligand-Controlled, Tunable Silver-Catalyzed C–H Amination. *J. Am. Chem. Soc.* **2014**, *136*, 16720-16723.

(89) (a) Herbort, J. H.; Bednar, T. N.; Chen, A. D.; RajanBabu, T. V.; Nagib, D. A. γ C–H Functionalization of Amines via Triple H-Atom Transfer of a Vinyl Sulfonyl Radical Chaperone. *J. Am. Chem. Soc.* **2022**, *144*, 13366−13373. (b) Stateman, L. M.; Nakafuku, K. M.; Nagib, D. A. Remote C–H Functionalization via Selective Hydrogen Atom Transfer. *Synthesis* **2018**, *50*, 1569-1586. (c) Choi, G. J.; Zhu, Q.; Miller, D. C.; Gu, C. J.; Knowles, R. R. Catalytic alkylation of remote C–H bonds enabled by proton-coupled electron transfer. *Nature* **2016**, *539*, 268-271. (d) Chu, J. C. K.; Rovis, T. Amide-directed photoredox-catalysed C–C bond formation at unactivated sp3 C–H bonds. *Nature* **2016**, *539*, 272-275. (e) Stateman, L. M.; Dare, R. M.; Paneque, A. N.; Nagib, D. A. Aza-heterocycles via copper-catalyzed, remote C–H desaturation of amines. *Chem* **2022**, *8*,

210-224. (f) Nakafuku, K. M.; Zhang, Z.; Wappes, E. A.; Stateman, L. M.; Chen, A. D.; Nagib, D. A. Enantioselective radical C–H amination for the synthesis of β-amino alcohols. *Nature Chemistry* **2020**, *12*, 697-704. (g) Jin, W.; Yu, S. Photoinduced and Palladium-Catalyzed Remote Desaturation of Amide Derivatives. *Org. Lett.* **2021**, *23*, 6931–6935. (h) Wan, Y.; Ramírez, E.; Ford, A.; Zhang, H. K.; Norton, J. R.; Li, G. Cooperative Fe/Co-Catalyzed Remote Desaturation for the Synthesis of Unsaturated Amide Derivatives. *J. Am. Chem. Soc.* **2024**, *146*, 4985–4992. (i) Wan, Y.; Adda, A. K.; Qian, J.; Vaccaro, D. A.; He, P.; Li, G.; Norton, J. R. Hydrogen Atom Transfer (HAT)-Mediated Remote Desaturation Enabled by Fe/Cr–H Cooperative Catalysis. *J. Am. Chem. Soc.* **2024**, *146*, 4795–4802. (j) Zhou, S.; Zhang, Z.-J.; Yu, J.-Q. Copper-catalysed dehydrogenation or lactonization of C(sp3)–H bonds. *Nature* **2024**, *629*, 363-369. (k) Tan, Y.; Chen, S.; Zhou, Z.; Hong, Y.; Ivlev, S.; Houk, K. N.; Meggers, E. Intramolecular C(sp3)–H Bond Oxygenation by Transition-Metal Acylnitrenoids. *Angew. Chem. Int. Ed.* **2020**, *59*, . (l) Guo, W.; Wang, Q.; Zhu, J. Visible light photoredox-catalysed remote C–H functionalisation enabled by 1,5-hydrogen atom transfer (1,5-HAT). *Chem. Soc. Rev.* **2021**, *50*, 7359-7377.

(90) Laohapaisan, P.; Roy, I.; Nagib, D. A. Chiral pyrrolidines via an enantioselective Hofmann-Löffler-Freytag reaction. *Chem Catalysis* **2024**, 101149.

(91) (a) Badiei, Y. M.; Dinescu, A.; Dai, X.; Palomino, R. M.; Heinemann, F. W.; Cundari, T. R.; Warren, T. H. Copper-Nitrene Complexes in Catalytic C H Amination. *Angew. Chem. Int. Ed.* **2008**, *47*, 9961-9964. (b) Aguila, M. J. B.; Badiei, Y. M.; Warren, T. H. Mechanistic Insights into C–H Amination via Dicopper Nitrenes. *J. Am. Chem. Soc.* **2013**, *135*, 9399-9406.

(92) Kim, S.; Song, S. L.; Zhang, J.; Kim, D.; Hong, S.; Chang, S. Regio- and Enantioselective Catalytic δ-C–H Amidation of Dioxazolones Enabled by Open-Shell Copper-Nitrenoid Transfer. *J. Am. Chem. Soc.* **2023**, *145*, 16238–16248.

(93) Pradhan, S.; Kweon, J.; Sahoo, M. K.; Jung, H.; Heo, J.; Kim, Y. B.; Kim, D.; Park, J.-W.; Chang, S. A Formal γ-C–H Functionalization of Carboxylic Acids Guided by Metal-Nitrenoids as an Unprecedented Mechanistic Motif. *J. Am. Chem. Soc.* **2023**, *145*, 28251-28263.

(94) (a) Jiang, X.; Ji, G. A self-consistent and cross-checked scale of spin-delocalization substituent constants, the. sigma. JJ. bul. scale. *J. Org. Chem.* **1992**, *57*, 6051-6056. (b) Fisher, T. H.; Meierhoefer, A. W. Substituent effects in free-radical reactions. A study of 4-substituted 3-cyanobenzyl free radicals. *J. Org. Chem.* **2002**, *43*, 224-228. (c) Dinçtürk, S.; Jackson, R. A. Free radical reactions in solution. Part 7. Substituent effects on free radical reactions: comparison of the σ˙ scale with other measures of radical stabilization. *J. Chem. Soc., Perkin Trans. 2*, **1981**, .

(95) Kamlet, M. J.; Abboud, J. L. M.; Abraham, M. H.; Taft, R. W. Linear solvation energy relationships. 23. A comprehensive collection of the solvatochromic parameters, .pi.*, .alpha., and .beta., and some methods for simplifying the generalized solvatochromic equation. *J. Org. Chem.* **1983**, *48*, 2877-2887.

(96) (a) Motiwala, H. F.; Armaly, A. M.; Cacioppo, J. G.; Coombs, T. C.; Koehn, K. R. K.; Verrill M. Norwood, I.; Aubé, J. HFIP in Organic Synthesis. *Chem. Rev.* **2022**, *122*, 12544–12747. (b) Wencel-Delord, J.; Colobert, F. A remarkable solvent effect of fluorinated alcohols on transition metal catalysed C–H functionalizations. *Organic Chemistry Frontiers* **2016**, *3*, 394-400. (c) Sinha, S. K.; Bhattacharya, T.; Maiti, D. Role of hexafluoroisopropanol in C–H activation. *React. Chem. Eng.* **2019**, *4*, 244-253. (d) Maciuk, S.; Wood, S. H.; Patel, V. K.; Shapland, P. D. P.; Tomkinson, N. C. O. Peracid

Oxidation of Unactivated sp3 C−H Bonds: An Important Solvent Effect. *Chem. Eur. J.* **2023**, *29*, e202204007. (e) Bhattacharya, T.; Ghosh, A.; Maiti, D. Hexafluoroisopropanol: the magical solvent for Pd-catalyzed C–H activation. *Chem. Sci.* **2021**, *12*, 3857-3870.

(97) (a) Menger, F. M.; D'Angelo, L. L. Does the conformation of hydrocarbon chains depend on solvation?Article link copied! *J. Am. Chem. Soc.* **1988**, *110*, 8241-8242. (b) Dyson, P. J.; Jessop, P. G. Solvent effects in catalysis: rational improvements of catalysts via manipulation of solvent interactions. *Catal. Sci. Technol.* **2016**, *6*, 3302-3316. (c) Breslow, R. Determining the Geometries of Transition States by Use of Antihydrophobic Additives in Water. *Acc. Chem. Res.* **2004**, *37*, 471-478. (d) John H. Conway, J.; Rovis, T. Regiodivergent Iridium(III)-Catalyzed Diamination of Alkenyl Amides with Secondary Amines: Complementary Access to γ- or δ-Lactams. *J. Am. Chem. Soc.* **2017**, *140*, 135–138.

(98) Filler, R.; Schure, R. M. Highly acidic perhalogenated alcohols. A new synthesis of perfluoro-tert-butyl alcohol. *J. Org. Chem.* **2002**, *32*, 1217-1219.

(99) (a) Charton, M. Steric effects. III. Bimolecular nucleophilic substitution. *J. Am. Chem. Soc.* **1975**, *97*, 3694-3697. (b) Charton, M. Steric effects. II. Base-catalyzed ester hydrolysis. *J. Am. Chem. Soc.* **1975**, *97*, 3691-3693. (c) Charton, M. Steric effects. I. Esterification and acid-catalyzed hydrolysis of esters. *J. Am. Chem. Soc.* **1975**, *97*, 1552-1556. (d) Charton, M. Nature of the ortho effect. II. Composition of the Taft steric parameters. *J. Am. Chem. Soc.* **1969**, *91*, 615-618.

(100) Sun, W.; Au, C.-M.; Wong, K.-W.; Chan, K. L.; Ngai, C. K.; Lee, H. K.; Lin, Z.; Yu, W.-Y. Intramolecular Arene C(sp²)–H Amidation Enabled by Ferrocenium-Mediated Decomposition of 1,4,2-Dioxazol-5-ones as Amidyl Radical Precursors. *ACS Catalysis* **2023**, *13*, 11389-11398.

(101) Oña Burgos, P.; Fernández, I.; Iglesias, M. J.; García-Granda, S.; López Ortiz, F. Phosphinamide-Directed Benzylic Lithiation. Application to the Synthesis of Peptide Building Blocks. *Org. Lett.* **2008**, *10*, 537-540.

(102) Fisher, T. H.; Meierhoefer, A. W. Substituent effects in free-radical reactions. A study of 4-substituted 3-cyanobenzyl free radicals. *J. Org. Chem.* **1978**, *43*, 224-228.

(103) (a) Hofmann, R. J.; Vlatković, M.; Wiesbrock, F.; Hofmann, R. J.; Vlatković, M.; Wiesbrock, F. Fifty Years of Hydrosilylation in Polymer Science: A Review of Current Trends of Low-Cost Transition-Metal and Metal-Free Catalysts, Non-Thermally Triggered Hydrosilylation Reactions, and Industrial Applications. *Polymers* **2017**, *9*, 534. (b) Franke, R.; Selent, D.; Börner, A. Applied Hydroformylation. *Chem. Rev.* **2012**, *112*, 5675–5732. (c) Shimizu, Y.; Kanai, M. Recent progress in copper-catalyzed difunctionalization of unactivated carboncarbon multiple bonds. *Tetrahedron Lett.* **2014**, *55*, 3727-3737. (d) Sauer, G. S.; Lin, S. An Electrocatalytic Approach to the Radical Difunctionalization of Alkenes. *ACS Catalysis* **2018**, *8*, 5175–5187.

(104) (a) Vitaku, E.; Smith, D. T.; Njardarson, J. T. Analysis of the Structural Diversity, Substitution Patterns, and Frequency of Nitrogen Heterocycles among U.S. FDA Approved Pharmaceuticals. *J. Med. Chem.* **2014**, *57*, 10257–10274. (b) Y.-Y. Yeung; Xuri Gao; Corey, E. J. A General Process for the Haloamidation of Olefins. Scope and Mechanism. *J. Am. Chem. Soc.* **2006**, *128*, 9644–9645. (c) Qian, B.; Chen, S.; Wang, T.; Zhang, X.; Bao, H. Iron-Catalyzed Carboamination of Olefins: Synthesis of Amines and Disubstituted β-Amino Acids. *J. Am. Chem. Soc.* **2017**, *139*, 13076–13082. (d) Minatti, A.; Muñiz, K. Intramolecular aminopalladation of alkenes as a key step to pyrrolidines and related heterocycles. *Chem. Soc. Rev.* **2007**, *36*, 1142-1152. (e) Gockel, S. N.; Buchanan, T. L.; Hull, K. L. Cu-Catalyzed Three-Component Carboamination of Alkenes. *J. Am. Chem. Soc.* **2017**, *140*, 58–61. (f) Falk, E.; Makai, S.; Delcaillau, T.; Gürtler, L.;

Morandi, B. Design and Scalable Synthesis of N-Alkylhydroxylamine Reagents for the Direct Iron-Catalyzed Installation of Medicinally Relevant Amines. *Angew. Chem. Int. Ed.* **2020**, *59*, 21064-21071.

(105) (a) Bruncko, M.; Schlingloff, G.; Sharpless, K. B. N-Bromoacetamide—A New Nitrogen Source for the Catalytic Asymmetric Aminohydroxylation of Olefins. *Angew. Chem. Int. Ed. Engl.* **1997**, *36*, 1483-1486. (b) Herranz, E.; Biller, S. A.; Sharpless, K. B. Osmium-catalyzed vicinal oxyamination of olefins by N-chloro-N-argentocarbamates. *J. Am. Chem. Soc.* **2002**, *100*, 3596–3598. (c) Li, G.; Angert, H. H.; Sharpless, K. B. N-Halocarbamate Salts Lead to More Efficient Catalytic Asymmetric Aminohydroxylation. *Angew. Chem. Int. Ed. Engl.* **1996**, *35*, 2813-2817. (d) Rudolph, J.; Sennhenn, P. C.; Vlaar, C. P.; Sharpless, K. B. Smaller Substituents on Nitrogen Facilitate the Osmium-Catalyzed Asymmetric Aminohydroxylation. *Angew. Chem. Int. Ed. Engl.* **1996**, *35*, 2810-2813. (e) Sharpless, K. B.; Patrick, D. W.; Truesdale, L. K.; Biller, S. A. New reaction. Stereospecific vicinal oxyamination of olefins by alkyl imido osmium compounds. *J. Am. Chem. Soc.* **2002**, *97*, 2305–2307.

(106) (a) Hong, S. Y.; Chang, S. Stereodefined Access to Lactams via Olefin Difunctionalization: Iridium Nitrenoids as a Motif of LUMO-Controlled Dipoles. *J. Am. Chem. Soc.* **2019**, *141*, 10399–10408. (b) Kim, S.; Kim, D.; Hong, S. Y.; Chang, S. Tuning Orbital Symmetry of Iridium Nitrenoid Enables Catalytic Diastereo- and Enantioselective Alkene Difunctionalizations. *J. Am. Chem. Soc.* **2021**, *143*, 3993–4004. (c) Kweon, J.; Kim, D.; Kang, S.; Chang, S. Access to β-Lactams via Iron-Catalyzed Olefin Oxyamidation Enabled by the π-Accepting Phthalocyanine Ligand. *J. Am. Chem. Soc.* **2022**, *144*, 1872–1880.

(107) (a) Burg, F.; Rovis, T. Rh(III)-Catalyzed Intra- and Intermolecular 3,4-Difunctionalization of 1,3-Dienes via Rh(III)-π-Allyl Amidation with 1,4,2-

Dioxazolones. *ACS Catalysis* **2022**, *12*, 9690–9697. (b) Burg, F.; Rovis, T. Diastereoselective Three-Component 3,4-Amino Oxygenation of 1,3-Dienes Catalyzed by a Cationic Heptamethylindenyl Rhodium(III) Complex. *J. Am. Chem. Soc.* **2021**, *143*, 17964–17969. (c) Li, X.; Song, H.; Yu, S.; Mi, R.; Li, X.-X. Rhodium-Catalyzed Enantioselective 1,4-Oxyamination of Conjugated gem-Difluorodienes via Coupling with Carboxylic Acids and Dioxazolones. *Angew. Chem. Int. Ed.* **2023**, *62*, e202305669.

(108) Lei, H.; John H. Conway, J.; Cook, C. C.; Rovis, T. Ligand Controlled Ir-Catalyzed Regiodivergent Oxyamination of Unactivated Alkenes. *J. Am. Chem. Soc.* **2019**, *141*, 11864–11869.

(109) Donohoe, T. J.; Callens, C. K. A.; Thompson, A. L. Tethered Aminohydroxylation (TA) Reaction of Amides. *Org. Lett.* **2009**, *11*, 2305–2307.

(110) (a) Tan, C. K.; Zhou, L.; Yeung, Y.-Y. Aminothiocarbamate-Catalyzed Asymmetric Bromolactonization of 1,2-Disubstituted Olefinic Acids. *Org. Lett.* **2011**, *13*, 2738–2741. (b) Feng, Y.; Yang, C.; Deng, Q.; Xiong, R.; Zhang, X.; Xiong, Y. Synthesis of Antitricyclic Morpholine Derivatives through Iodine(III)-Mediated Intramolecular Umpolung Cycloaddition of Olefins. *J. Org. Chem.* **2020**, *85*, 4500–4506.